

UNCLASSIFIED

2a. SECURITY CLASSIFICATION AUTHORITY			3. DISTRIBUTION / AVAILABILITY OF REPORT Approved for public release; distribution is unlimited			
2b. DECLASSIFICATION / DOWNGRADING SCHEDULE						
4. PERFORMING ORGANIZATION REPORT NUMBER(S)			5. MONITORING ORGANIZATION REPORT NUMBER(S) TR 89-08			
6a. NAME OF PERFORMING ORGANIZATION Department of Meteorology Naval Postgraduate School		6b. OFFICE SYMBOL (If applicable)		7a. NAME OF MONITORING ORGANIZATION Naval Environmental Prediction Research Facility		
6c. ADDRESS (City, State, and ZIP Code) Monterey, CA 93943-5000			7b. ADDRESS (City, State, and ZIP Code) Monterey, CA 93943-5006			
8a. NAME OF FUNDING / SPONSORING ORGANIZATION Commander, Naval Oceanography Command		8b. OFFICE SYMBOL (If applicable)		9. PROCUREMENT INSTRUMENT IDENTIFICATION NUMBER NPS Block Funding V4P1		
8c. ADDRESS (City, State, and ZIP Code) J.C. Stennis Space Center, MS 39529-5000			10. SOURCE OF FUNDING NUMBERS			
			PROGRAM ELEMENT NO	PROJECT NO	TASK NO	
			WORK UNIT ACCESSION NO			
11. TITLE (Include Security Classification) Forecasters Handbook for Central America and Adjacent Waters (U)						
12. PERSONAL AUTHOR(S) Williams, F.R.; Jung, G.H.; Renard, R.J.						
13a. TYPE OF REPORT Final		13b. TIME COVERED FROM 6/86 TO 3/89		14. DATE OF REPORT (Year, Month, Day) 1989, September		
				15. PAGE COUNT 508		
16. SUPPLEMENTARY NOTATION						
17. COSATI CODES			18. SUBJECT TERMS (Continue on reverse if necessary and identify by block number)			
FIELD	GROUP	SUB-GROUP				
04	02		Central America meteorology Temporale Atemporalado			
			Central America oceanography Satellite case studies			
			Pacific Ocean Tropical storms Hurricanes Caribbean			
19. ABSTRACT (Continue on reverse if necessary and identify by block number)						
<p>This handbook describes the analysis and forecasting of both atmospheric and oceanic conditions important to air/sea operations over Central America and adjacent waters. Central America is defined herein to include Guatemala, Belize, El Salvador, Honduras, Nicaragua, Costa Rica and Panama. Case studies using satellite imagery are presented for the rainy season, dry season, and hurricane season. Sections also are included on general climatology and coastal geographic influences.</p>						
20. DISTRIBUTION / AVAILABILITY OF ABSTRACT <input checked="" type="checkbox"/> UNCLASSIFIED/UNLIMITED <input type="checkbox"/> SAME AS RPT <input type="checkbox"/> DTIC USERS			21. ABSTRACT SECURITY CLASSIFICATION UNCLASSIFIED			
22a. NAME OF RESPONSIBLE INDIVIDUAL Fett, Robert W., contract monitor			22b. TELEPHONE (Include Area Code) (408) 647-4728		22c. OFFICE SYMBOL	

90 01 09 14I

Contents

Foreword	iii
Preface	v
Acknowledgments	vii
Record of Changes	ix
1 TROPICAL METEOROLOGY OF CENTRAL AMERICA	1-1
1.1 General Introduction	1-1
1.2 Regional Climatologies	1-3
1.2.1 Rainy Season and Dry Season Charts	1-3
1.2.2 General Climatology	1-22
1.3 National Climatologies	1-29
1.3.1 Guatemala	1-32
1.3.2 Belize	1-36
1.3.3 Honduras	1-40
1.3.4 El Salvador	1-44
1.3.5 Nicaragua	1-48
1.3.6 Costa Rica	1-56
1.3.7 Panama	1-60
2 THE RAINY SEASON	2-1
2.1 General	2-1
2.2 Tropical Waves	2-1
2.3 Case Studies during the Rainy Season	2-11
2.3.1 Case I - Tropical Waves (3 - 7 October 1988)	2-13
2.3.2 Case II - Tropical Waves (1 - 6 August 1988)	2-51
2.3.3 Arc Cloud (2 October 1988)	2-88
2.4 Analysis & Forecasting "Thumb Rules" for the Rainy Season	2-99

3	THE DRY SEASON	3-1
3.1	General	3-1
3.2	Fronts or "Shear Lines"	3-1
3.2.1	Frontal Passage over Coastal Honduras	3-4
3.2.2	Frontal Passage over Belize	3-7
3.2.3	Atemporalado—with a Forecasting Index	3-10
3.3	Case Studies during the Dry Season	3-14
3.3.1	Case III - Cold Front Passage (12 - 15 December 1988)	3-14
3.3.2	Case IV - Cold Front Passage (14 - 17 March 1988)	3-39
3.3.3	Strong Surge during the Dry Season	3-70
3.4	Analysis & Forecasting "Thumb Rules" for the Dry Season	3-90
4	COASTAL OCEANOGRAPHIC INFLUENCES	4-1
4.1	Geological Structure of Central America and the Adjacent Ocean Basins . .	4-1
4.2	The Pacific Coast of Central America	4-15
4.3	The Caribbean Coast of Central America	4-30
5	HURRICANES AND TROPICAL STORMS	5-1
5.1	General (including Track "Thumb Rules")	5-1
5.2	Case Studies during Hurricanes	5-4
5.2.1	Case V - Hurricane Joan (14 - 25 October 1988)	5-4
5.2.2	Case VI - Hurricane Gilbert (9 - 14 September 1988)	5-70
	REFERENCES	R-1
	APPENDICES	
A	TROPICAL ANALYSIS	A-1
B	OPERATIONAL CLIMATIC DATA SUMMARIES	B-1
C	TRACKS OF NORTH ATLANTIC TROPICAL CYCLONES	C-1
D	MEAN TRACKS OF EASTERN NORTH PACIFIC OCEAN TROPICAL CYCLONES	D-1

FOREWORD

The Forecasters Handbook for Central America and Adjacent Waters was developed under the continuing effort of the Naval Environmental Prediction Research Facility (NEPRF) to improve the quality of operational weather forecasting support in all parts of the world.

While several sources exist concerning the environment of tropical Central America, including the land mass of Central America, the western Caribbean Sea and eastern North Pacific Ocean, the purpose of this document is to accumulate and suitably present the most pertinent information available for use by Fleet forecasters who are unfamiliar with the region.

It is intended that this document be responsive to current requirements of U. S. Navy operating forces; therefore, it has been assembled in loose-leaf form. Users are urged to submit to this Command their comments and suggestions regarding contents and changes thereto.

The Forecasters Handbook for Central America and Adjacent Waters was prepared through the efforts of Adjunct Professor Forrest R. Williams (CDR, USN, retired) of the Meteorology Department of the Naval Postgraduate School (NPS), Monterey, California, Dr. Glenn H. Jung, Professor Emeritus of the Oceanography Department, NPS and Dr. Robert J. Renard, Chairman and Professor of the Meteorology Department, NPS. Mr. Robert W. Fett (NEPRF) served as Project Coordinator. The project leading to the development of this handbook was sponsored by the Naval Environmental Prediction Research Facility and the Naval Postgraduate School. Funding for the printing of the handbook was provided by Commander Naval Oceanography Command.

William L. Shutt
Commander, U. S. Navy
Commanding Officer

Accession For	
NTIS	CF 11
DTIC	198
Unannounced	
Justification	
By	
Distribution	
Date	
Dist	
A-1	

PREFACE

This handbook is published to provide meteorological (and oceanographic) guidance, as well as regional familiarization, to naval personnel (embarked in Fleet units or ashore) supporting naval operations in the vicinity of Central America.

In the event of limited planning or preparation time prior to operations, it is recommended that forecasters first read Section 1 (Tropical Meteorology of Central America)—which includes an introduction to regional climatology—and then, depending on the time of the year, proceed directly to Section 2 (The Rainy Season), for operations during May to October, or to Section 3 (The Dry Season), for operations during November to April.

Naturally, for operations occurring during the *official* Atlantic hurricane season (June through November), Section 5 (Hurricanes and Tropical Storms) is very useful. As depicted in Appendix C, hurricanes occur in other months as well.

During the rainy season, diurnal rain showers dominate the weather over Central America, enhanced by sea-breeze convection, the passing of tropical waves, the 2-3 day rainy periods known locally as “Temporals” and the infrequent passing of hurricanes or tropical storms. The forecaster also must be aware of the monsoon trough, normally found *just* west of the Pacific coast. The dry season evolves as convection *slowly* “tapers off” (except along selected segments of the Caribbean coast), followed by the intermittent arrival of cold fronts (often called shear lines or “Atemporalados”) from the Gulf of Mexico. Only the stronger fronts (or surges) penetrate equatorward of the Honduras-Nicaragua border.

The following publications should be acquired before deployment—the first is a U. S. Navy document, while the last three are U. S. Air Force documents—(see References for publishers):

1. U. S. Navy Climatic Study of the Caribbean and Gulf of Mexico, Vol. 1,
2. Seasons in Review: GOES Satellite Photos over Central America,
3. Local and Regional Influences on the Meteorology of Central America and
4. Caribbean Basin—Climatology Study.

The case studies of Section 3 identify the *dry season* skill of the 24-h low-level wind prognosis of the Navy Operational Global Atmospheric Prediction System (NOGAPS) model 3.0,—i.e., the Navy’s spectral model 3.0. Modifications to the model’s radiation package are expected to improve *rainy season* prognosis by mid 1989, with improved model resolution to follow in late 1989.

ACKNOWLEDGMENTS

Appreciation is extended to Project Manager Kenneth R. Walters of the USAF Environmental Tactical Applications Center, Scott Air Force Base, Illinois for his unselfish assistance in providing extensive reference material—as well as for his zeal in promoting U. S. Navy–U. S. Air Force cooperation.

The Authors are also indebted to the National Hurricane Center (NHC)—especially to Mr. Mark Zimmer, Supervisor of the Tropical Satellite Analysis Center, for his ready response to requests for information and data available from daily operations at NHC.

A special thanks is extended to TSgt Colin Sells, USAF, who welcomed, escorted and briefed one of the authors during a 5-day visit to the 25th Weather Detachment, Fifth Weather Wing, Howard Air Force Base, Panama.

Appreciation is also extended to LT Dennis Miller, Officer in Charge of the Naval Oceanography Command Detachment, Key West, Florida for his hospitality and informativeness while providing tours of the detachment for two of the authors.

The authors are indebted to Professor James Sadler of the Department of Meteorology, University of Hawaii for his provision of gridded data from the Comprehensive Ocean-Atmospheric Data Set (COADS).

Thanks also to Professors Russell Elsberry and Chih-Pei Chang, Department of Meteorology, Naval Postgraduate School (NPS) for sharing their expertise in tropical meteorology.

Special thanks to Professor Carlyle Wash, Department of Meteorology, NPS for his support in the acquisition of both the *hardcopy* printer used with the satellite Digital Weather Information Processing System and the laser printer used in preparing the handbook, and to Dr. Lang Chou, Department of Meteorology, NPS for his efforts in restoring the hardware of the word processing system used by the authors to print the Handbook.

The Handbook could not have been completed without the genuine assistance provided by Meteorology Department staff, including Michael McDermet, Ellen Saunders, Benjamin Borelli and Joelle Cardinalli.

Finally, appreciation is extended to Meteorologist Dennis Perryman of the Naval Environmental Prediction Research Facility for proofreading the handbook.

RECORD OF CHANGES

[illegible]

1. TROPICAL METEOROLOGY OF CENTRAL AMERICA

1.1 General Introduction

This Handbook describes the analysis and forecasting of both atmospheric and oceanic conditions important to air/sea operations over Central America and adjacent waters.

Central America, as addressed in this handbook, includes the following seven nations, commencing with the nation located farthest west: Guatemala, Belize, El Salvador, Honduras, Nicaragua, Costa Rica and Panama (Figs. 1.1, 1.2).

Central America, lying between 7°N and 19°N, has its weather primarily influenced by features carried by the low-level "easterlies"¹ for most of the year, yet it is susceptible to the penetration of cold fronts (shear lines or "Atemporalados"²) during the Northern Hemisphere winter. While the time of the "rainy season" cannot be generalized for all of Central America, Portig (1976) depicts the rainy season for the North Pacific portion of Central America from about May through October, while it is a month later for the North Atlantic portion, i.e., from about June through November—despite appreciable rain in December.

While the threat of tropical storms or hurricanes is small, it cannot be dismissed, since all of the countries³ have experienced tropical cyclones, especially northeastern Honduras and Nicaragua, and Belize.

¹ Meteorological convention dictates that wind direction is the direction **from** which the wind is blowing i.e., easterly winds blow **from** the east (toward the west).

² See Subsubsection 3.2.3.

³ Panama and Costa Rica, minimally.

1.2 Regional Climatologies

1.2.1 Rainy Season and Dry Season Charts

While the appendices have extensive excerpts from more complete climatological references, the following sets of charts portray the features of the "rainy season" (August)⁴ and the "dry season" (February).

Figures 1.3 and 1.4, from Sadler et al. (1987)⁵, depict the resultant surface wind direction and speed, for August and February, respectively. The migration of surface convergence over the North Pacific Ocean, from near 10°N in August southward to near 5°N in February, is obvious.

Figures 1.5 and 1.6, from Sadler and Wann (1984), depict the mean 200 mb (upper tropospheric) flow⁶ for August and February, respectively. In August, the mean position of the Tropical Upper Tropospheric Trough (TUTT) extends eastward from just north of Belize separating the subtropical ridge (in the northern Gulf of Mexico) and the subequatorial ridge (extending from southern Guatemala through Nicaragua, eastward). The greater geopotential heights found in the subequatorial ridge correlate well with the enhanced convection associated with the more northerly August position of surface convergence (called, by some, the Intertropical Convergence Zone (ITCZ)). However, the mean 200 mb flow in February is southwesterly, increasing from an average 10 kt south of Panama to 40 kt just north of Belize.

Figures 1.7 and 1.8 from Sadler et al. (1987) depict averaged sea-level pressure for August and February, despite the preference of streamline/isotach analysis over pressure (or contour) analysis in the tropics (see Appendix A). It is immediately obvious that the lowest average sea-level pressure (for this large (synoptic) scale) is found over Panama and Costa Rica in both the rainy and dry seasons.

⁴These representative months have been rather arbitrarily selected. See Subsection 1.2.2 for further explanation. While Portig (1976) divides Central America into 14 rainfall regimes, USAFETAC (1985) supports the selection of these months, but includes "transitional" months between the rainy and dry seasons for Nicaragua, as well as a secondary rainfall maximum for Panama in October.

⁵Only the last 80 years, 1900 - 1979, have been used from the Comprehensive Ocean-Atmosphere Data Set (COADS). COADS is a continuing cooperative effort to compile global ship observations (initially for the period 1850 - 1979) between the National Oceanic and Atmospheric Administration (NOAA)—its Environmental Research Laboratories, National Climatic Data Center (NCDC) and Cooperative Institute for Research in Environmental Sciences (CIRES)—and the National Science Foundation's National Center for Atmospheric Research (NCAR). Details of how the ship observations were collected, evaluated and compiled are contained in Woodruff et al. (1987).

⁶The period of record is 1960 - 1973, consisting of 175,000 PIREP and RAWIN observations per month.

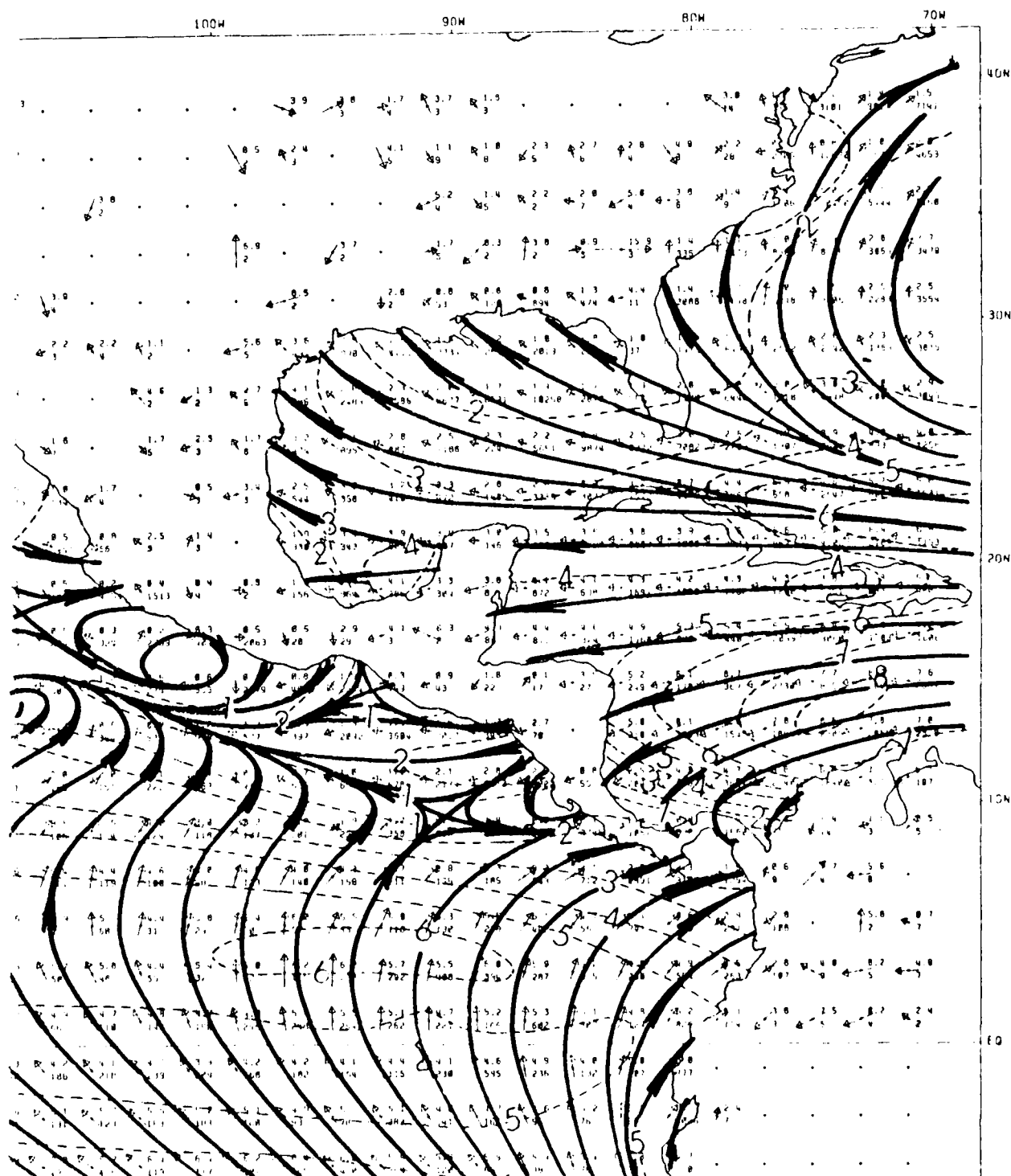


Figure 1.3: Surface Wind Direction / Speed (2° by 2°) Grid, August (Sadler et al., 1987)
 The resultant direction is depicted by streamlines and the resultant speed in m/sec by dashed lines. (Data plots contain (1) upper number: monthly average wind speed and (2) lower number: number of observations within each 2° square arrow shaft length is proportional to wind speed.)

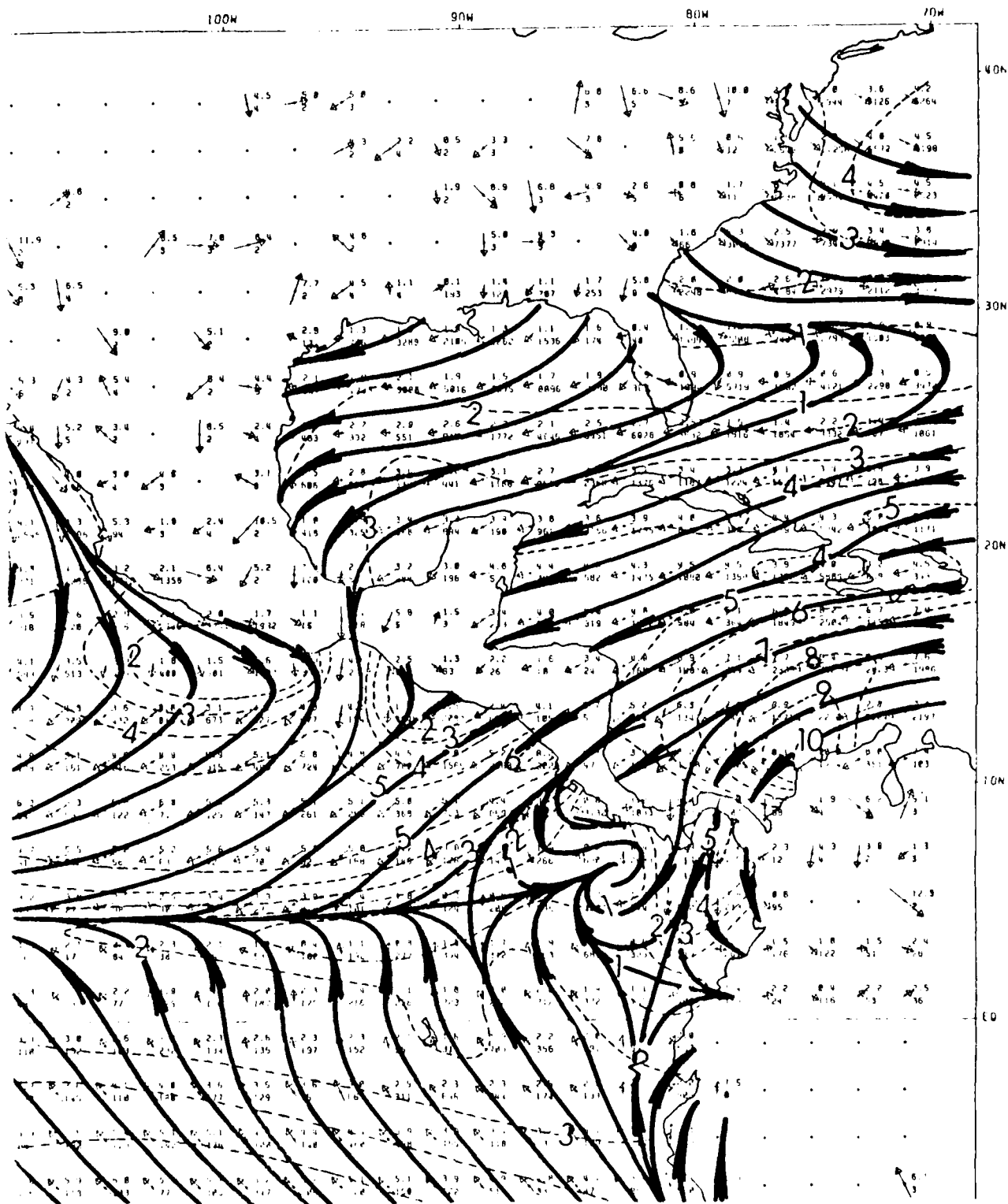


Figure 1.4: Surface Wind Direction / Speed (2° by 2°) Grid, February (Sadler et al., 1987)
 The resultant direction is depicted by streamlines and the resultant speed in m/sec by dashed lines. (Data plots contain (1) upper number: monthly average wind speed and (2) lower number: number of observations within each 2° square - arrow shaft length is proportional to wind speed.)

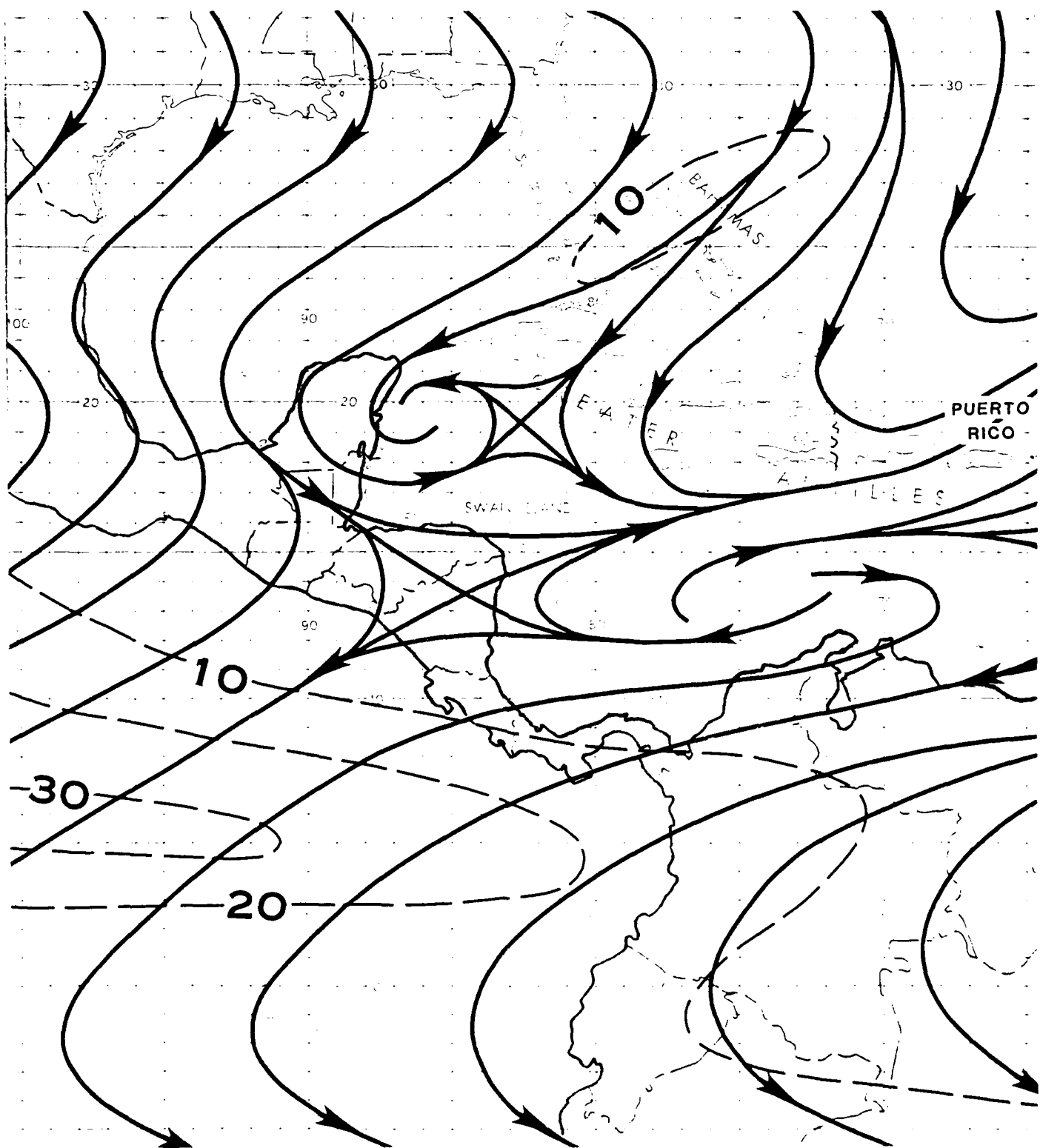


Figure 1.5: Mean 200 mb Flow, August (Sadler and Wann, 1984)
 Streamlines (solid, with arrows indicating direction of flow) and isotachs (dashed) in knots

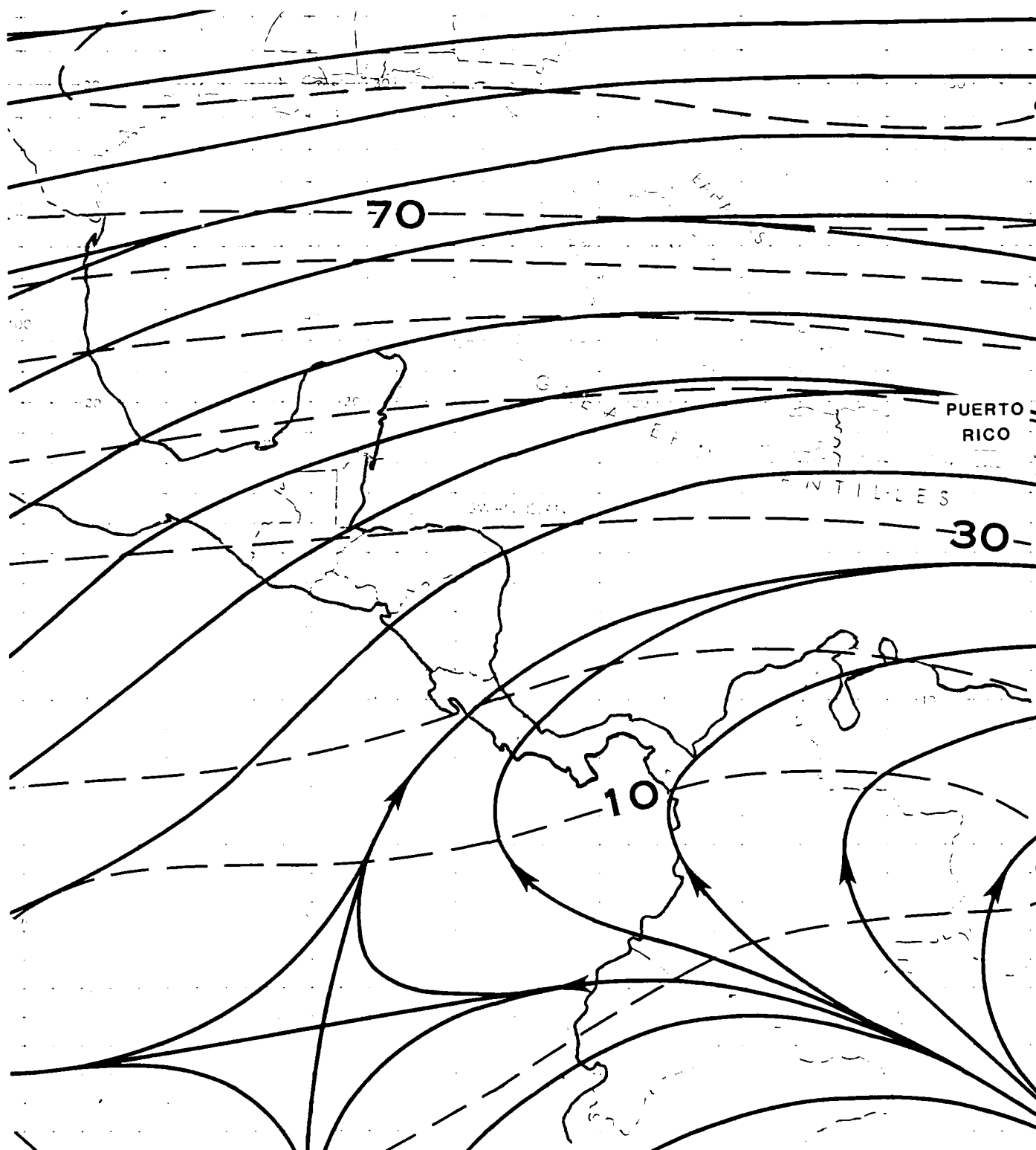


Figure 1.6: Mean 200 mb Flow, February (Sadler and Wann, 1984)
Streamlines (solid, with arrows indicating direction of flow) and isotachs (dashed) in knots

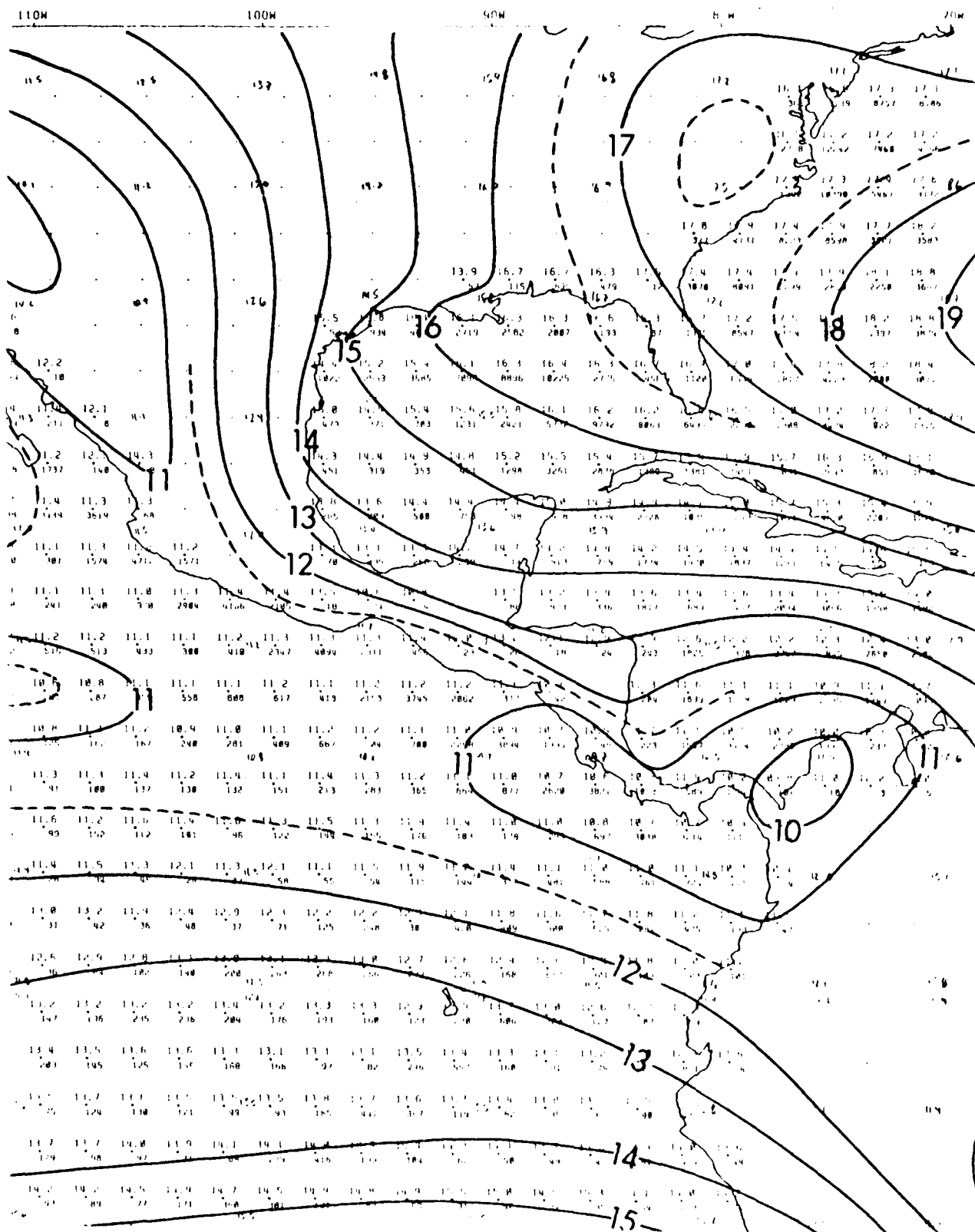


Figure 1.7: Mean sea-level Pressure, August (Sadler et al., 1987)
 The isobars are labeled in millibars (or hectopascals (hPa)) with the leading 10 omitted.
 Selected one-half millibar intervals are shown as dashed lines.

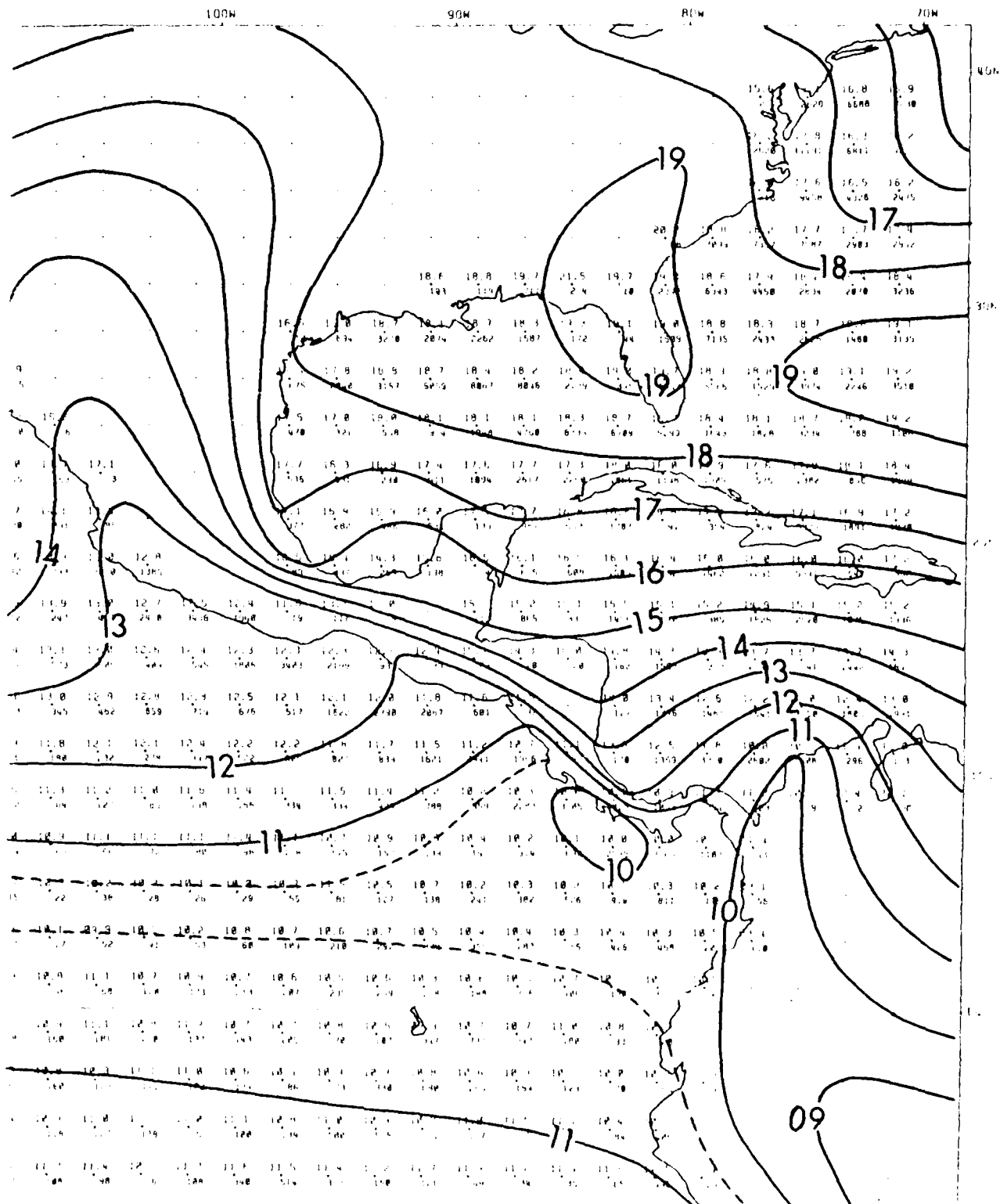


Figure 1.8: Mean sea-level Pressure, February (Sadler et al., 1987)
 The isobars are labeled in millibars (or hectopascals (hPa)) with the leading 10 omitted.
 Selected one-half millibar intervals are shown as dashed lines.

Figures 1.9 and 1.10 (NOCD, Asheville, 1985) depict the mean scalar wind speed for August and February. Note that the sea-level pressure figures, (1.7 and 1.8), and these figures of mean surface wind speed are from *different* references. The strength of the wind is greatest off the Caribbean coast of Columbia—a region known by oceanographers as the “Columbian Basin”. Recalling, again, that these are *average* winds, note the strength of the trade winds in February, reaching into the North Pacific Ocean after crossing the relatively flat southern Nicaragua, as contrasted to the very light winds southwest of the mountainous Costa Rica.

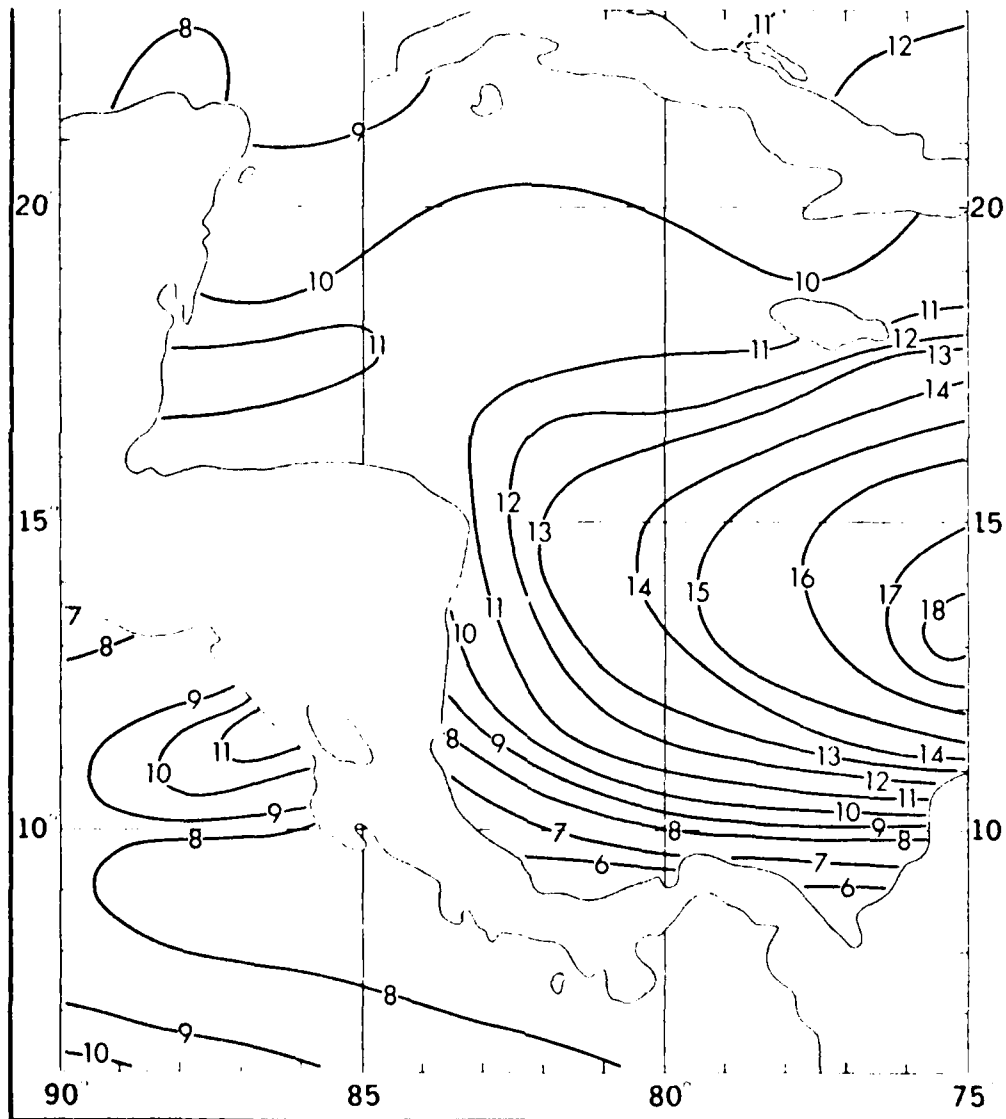


Figure 1.9: Mean Scalar Surface Wind Speed (kt), August (NOCD, Asheville, 1985)

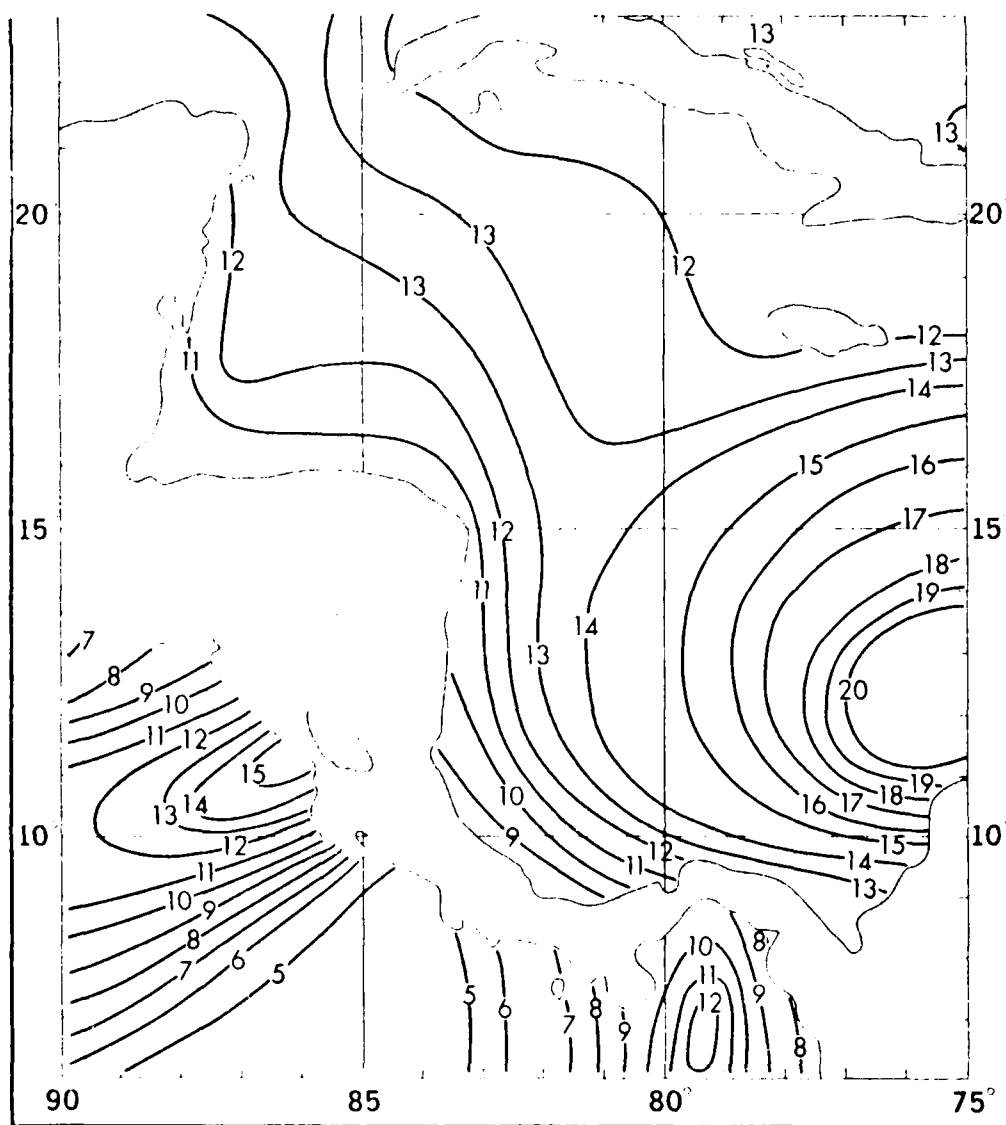


Figure 1.10: Mean Scalar Surface Wind Speed (kt), February (NOCD, Asheville, 1985)

Figures 1.11 and 1.12 (NOCD, Asheville, 1985) depict isopleths showing the percentage frequencies of wave heights ≥ 3 feet (solid lines) and ≥ 8 feet (dashed lines) for August and February. In agreement with the wind speed depicted in Figs. 1.9 and 1.10, large wave heights are more often found over the Columbian Basin, regardless of season. While wave heights surrounding Central America are generally high more often on the Caribbean side (the windward side) in February, note that wave heights on the North Pacific Ocean side are smaller in the lee of mountainous Costa Rica, but much larger west of Nicaragua.

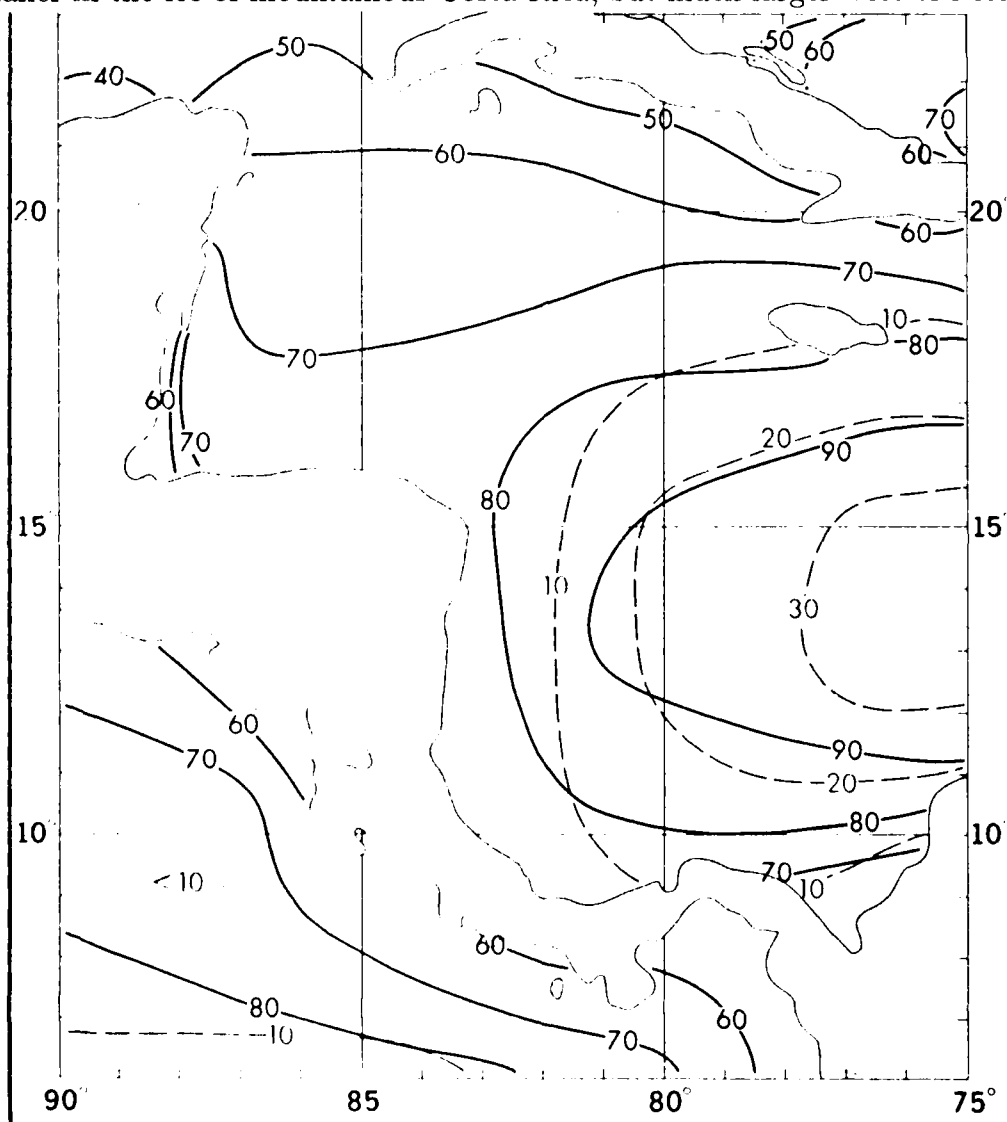


Figure 1.11: Wave-height Isopleths (Percent Frequency) August (NOCD, Asheville, 1985)
Solid line - Wave height ≥ 3 feet; Dashed line - Wave height ≥ 8 feet.
The wave height is the higher of sea or swell for observations containing both wave trains.
Sea is defined as waves generated by local winds.

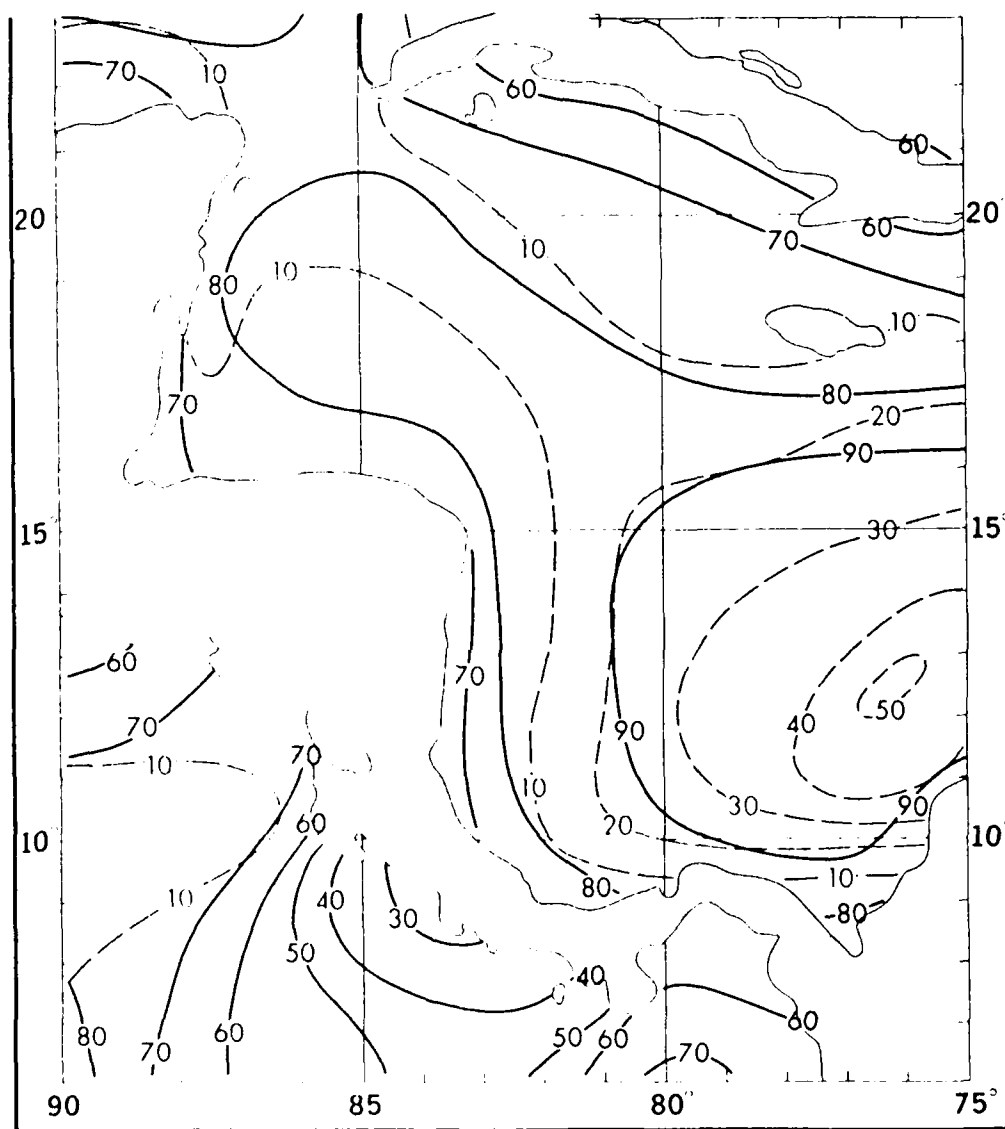


Figure 1.12: Wave-height Isopleths (Percent Frequency) February (NOCD, Asheville, 1985)
 Solid line - Wave height ≥ 3 feet; Dashed line - Wave height ≥ 8 feet.
 The wave height is the higher of sea or swell for observations containing both wave trains.
 Sea is defined as waves generated by local winds.

Figures 1.13 and 1.14 (Sadler and Wann, 1984) depict the mean monthly cloudiness over Central America and the adjacent waters during the period 1965–1973. The analysis was derived from operational nephanalyses⁷ with isopleths labeled in “octas”⁸ (eighths) of total cloud cover. There is no satisfactory “ground truth” monthly average cloud analyses to which this analysis can be compared. However, the patterns of cloudiness and the positions of the maximum and minimum areas of cloudiness are essentially identical to other *satellite* derived analyses—although there is an average difference of about 1 octa between different satellite analyses.

It is readily apparent that average monthly cloudiness over much of Central America decreases from $\sim 5/8$ in August (the rainy season, Fig. 1.13) to $\sim 3/8$ in February (the dry season, Fig. 1.14).

Figures 1.15 and 1.16 (Sadler et al., 1987), depict the mean sea-surface temperature (SST) during the months of August and February. During August, monthly SST in the waters surrounding Central America is generally between 28°C and 29°C. Again, note that the higher winds blowing from land toward the North Pacific Ocean, west of Nicaragua in February, lead to mixing of the upper layer of the ocean and to cooler temperatures ($\sim 26^\circ\text{C}$) than found in the North Pacific Ocean west of Costa Rica ($\sim 28^\circ\text{C}$) where winds are weaker.

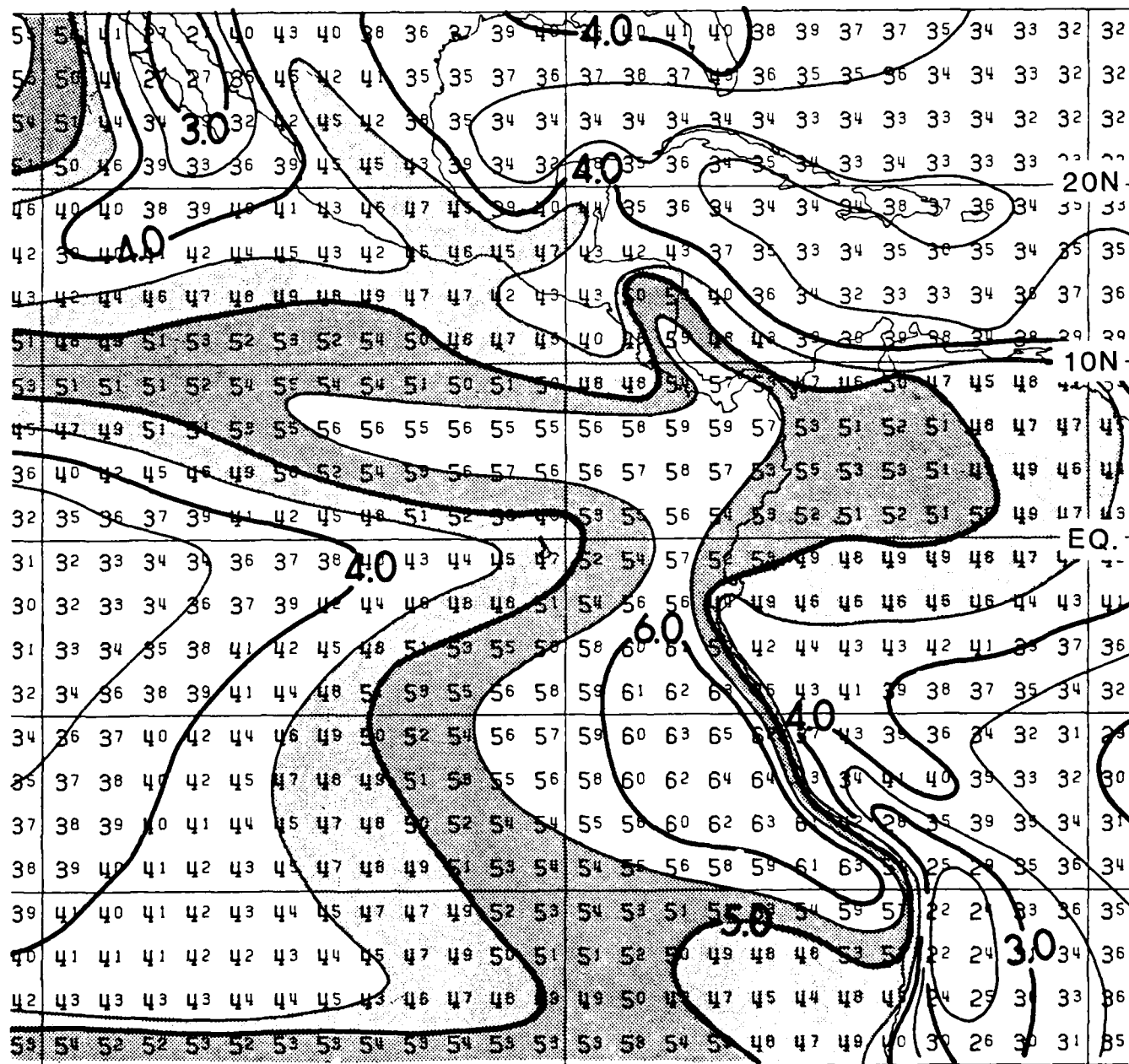
⁷Nephanalysis is a mapped analysis of the cloud distribution or “the analysis of a **synoptic chart** in terms of the types and amount of clouds and precipitation” (Huschke, 1959).

⁸Sadler emphasized the spelling of these labels so as to differentiate them from the fraction of cloud cover in “oktas” used by the World Meteorological Organization for *ground* based estimates.

120W

90W

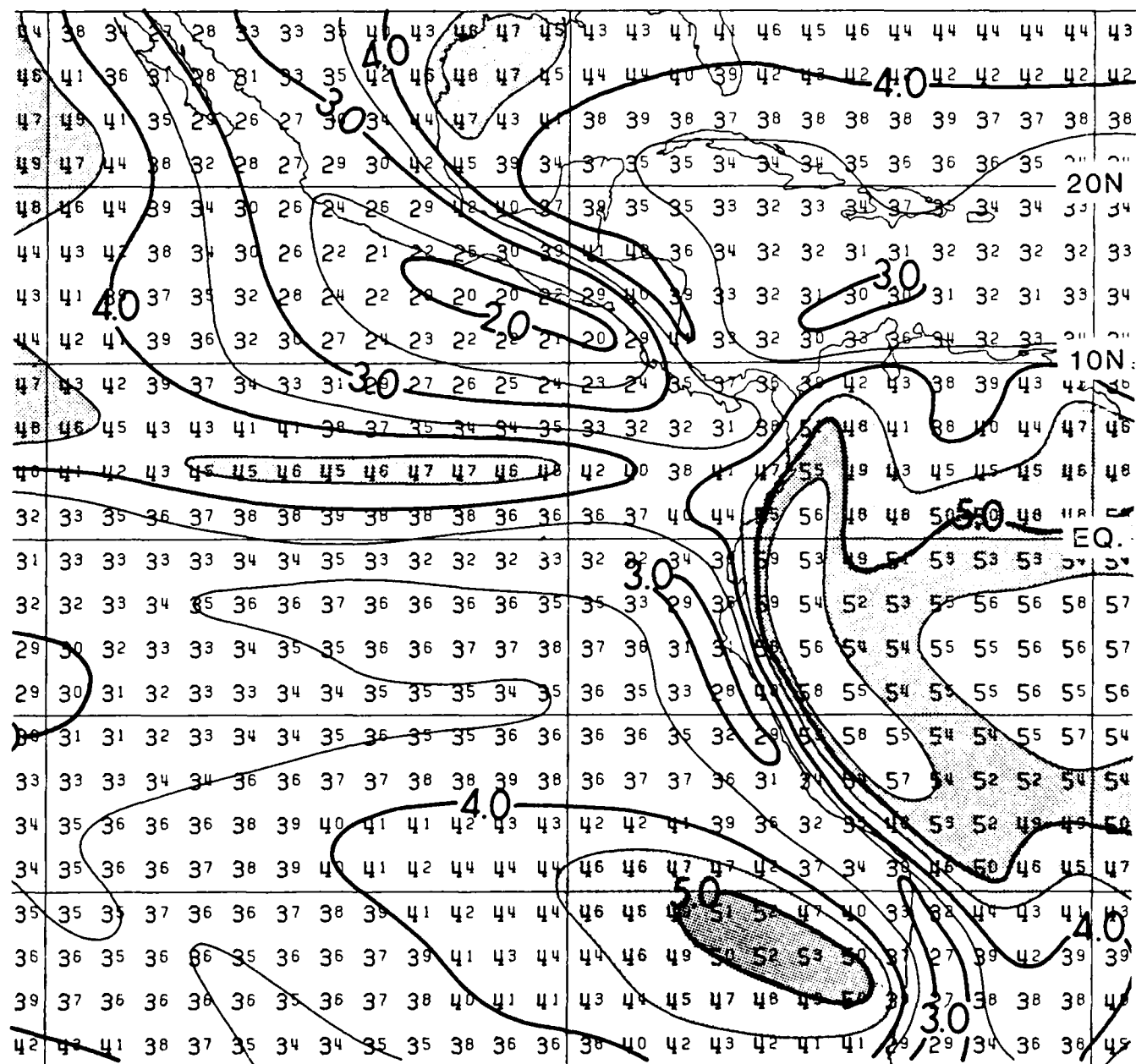
60W



120W

90W

60W



120W

90W

60W

Figure 1.14: Mean Monthly Cloudiness in Octas, February (Sadler and Wann, 1984)
The average cloud cover is plotted for each 2.5° latitude-longitude square.

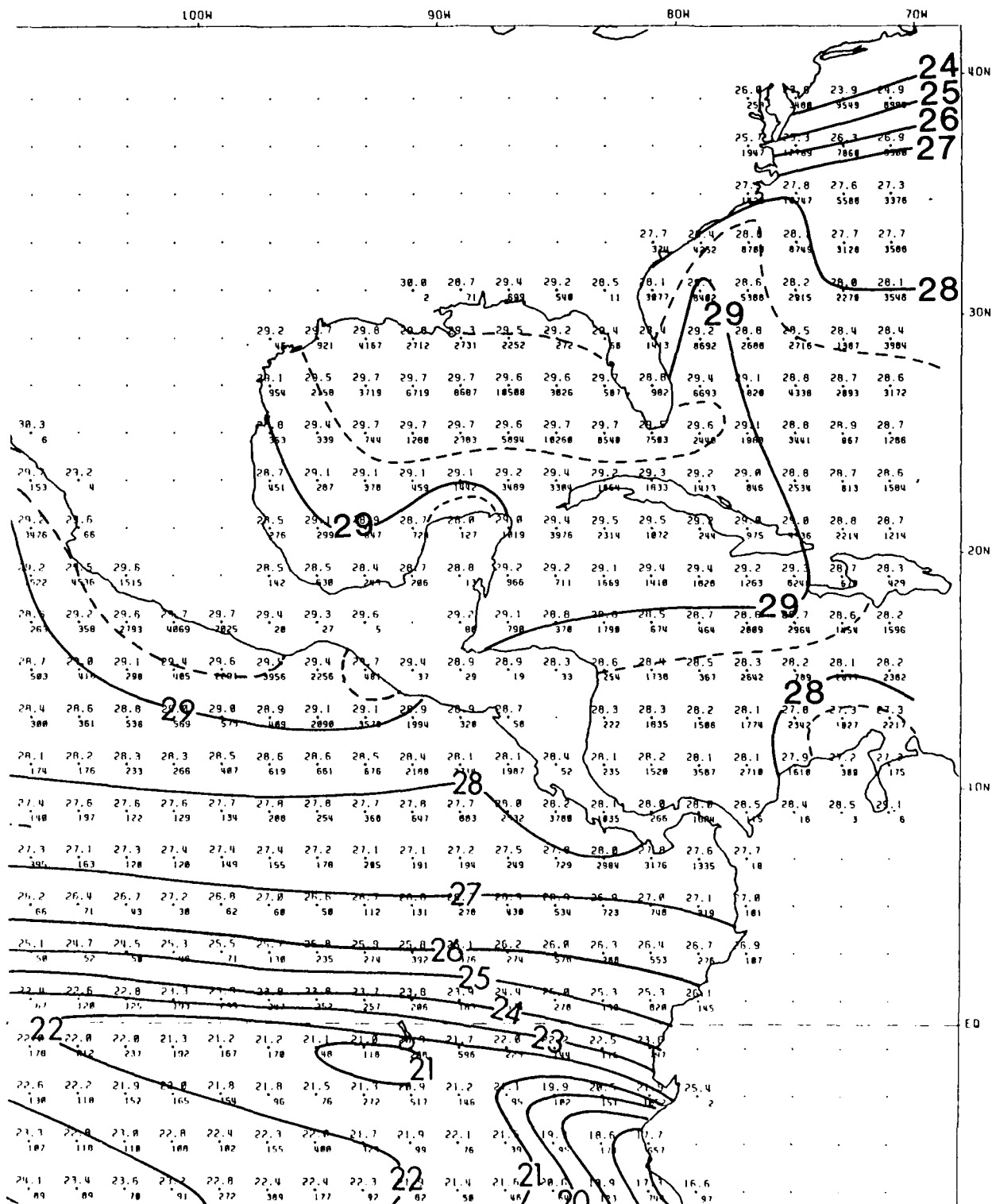


Figure 1.15: Mean Sea-Surface Temperature, August (Sadler et al., 1987)
 The isotherms are labeled in degrees Celsius. Where needed, one-half degree intervals are shown as dashed lines.

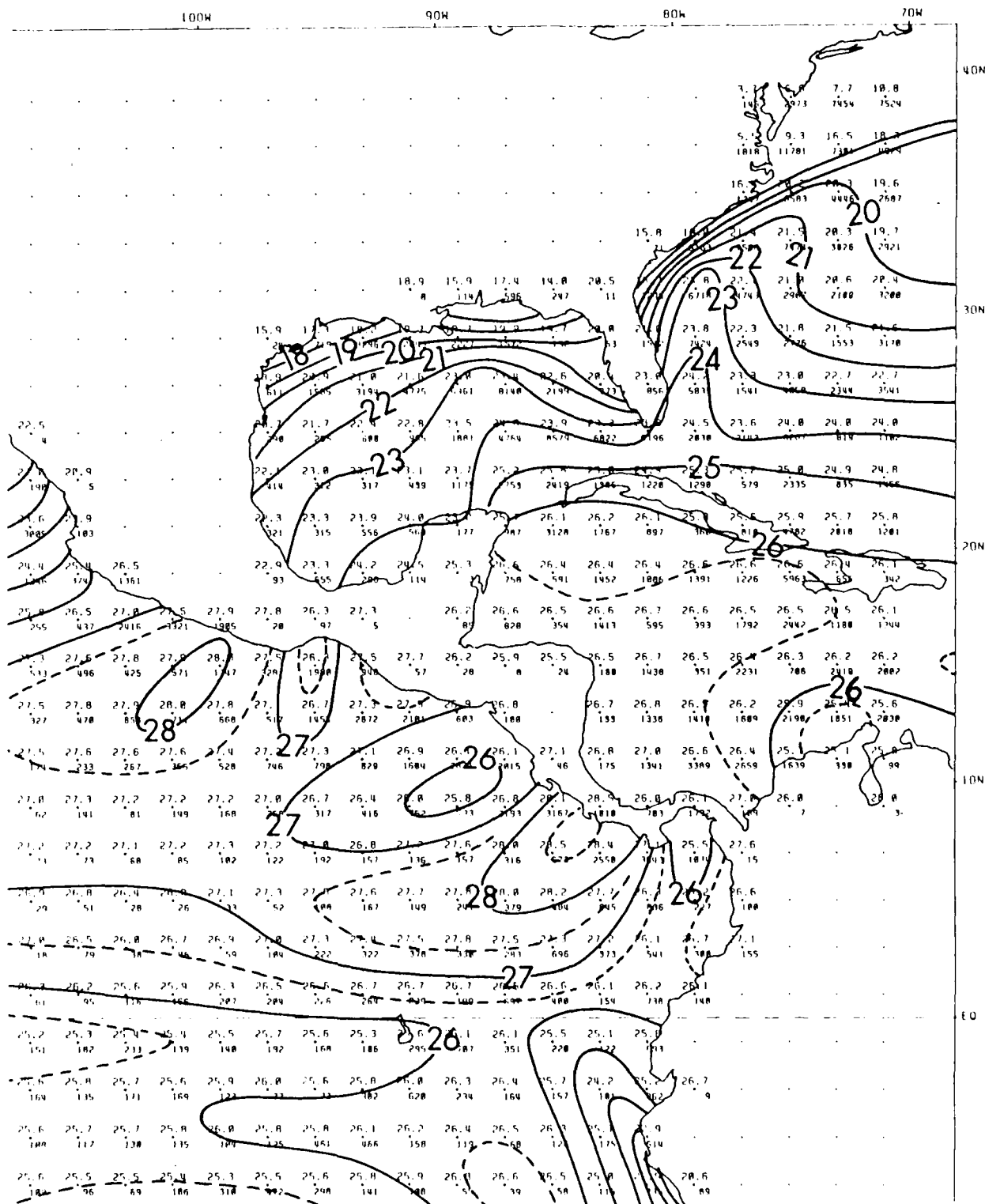


Figure 1.16: Mean Sea-Surface Temperature, February (Sadler et al., 1987)
 The isotherms are labeled in degrees Celsius. Where needed, one-half degree intervals are shown as dashed lines.

Finally, to assist mid-latitude meteorologists to adapt to the tropical setting of Central America, a *mean* sounding will be presented. While the International Civil Aviation Organization (ICAO) sounding⁹ with sea-level temperature of 15°C, as well as 500 mb height of 5574 m and temperature of -21.2°C, is so commonly used in extratropical applications, the mean atmosphere of Central America is obviously much warmer (and much more moist) with typically higher heights for constant pressure surfaces.

Jordan (1958) prepared a mean sounding from ten years of data from three stations: Miami, Florida; San Juan, Puerto Rico; and Swan Island¹⁰. The *annual* sounding is considered less useful and will not be presented since it provides a rather nonexistent sounding between the rainy and dry seasons.

Table 1.1 depicts the mean pressure, height, temperature and specific humidity of the four months¹¹, July through October, typical of the rainy season. To avoid the effects of daytime radiation, Jordan averaged only night time soundings—0300 GMT, as obtained operationally during the 1946–1955 period. Figure 1.17 presents a plot of this mean tropical sounding for the four summer months. Unlike the so familiar ICAO (or “U. S. Standard Atmosphere”) *extratropical* mean sounding, there is a dewpoint temperature sounding, available from the specific humidity data provided in Table 1.1.

⁹Identical with the U. S. Standard Atmosphere up to a height of 32 km.

¹⁰Swan Island is located at 17°N, 84°W in the western Caribbean Sea, ~100 miles north of eastern Honduras (see Fig. 1.21).

¹¹Defined by Jordan to be the “hurricane season”.

Table 1.1: Mean Tropical Atmosphere (West Indies) during Rainy Season (Jordan, 1958)

Pressure (mb)	Height (m)	Temperature (°C)	Specific Humidity (g/kg)
80	17883	-69.8	
100	16568	-73.5	
125	15260	-72.2	
150	14177	-67.6	
175	13236	-61.5	
200	12396	-55.2	
250	10935	-43.3	
300	9682	-33.2	
350	8581	-24.8	
400	7595	-17.7	
450	6703	-11.9	1.4
500	5888	-6.9	2.1
550	5138	-2.5	3.2
600	4442	1.4	3.6
650	3792	5.1	4.6
700	3182	8.6	5.8
750	2609	11.8	7.1
800	2063	14.6	8.4
850	1547	17.3	11.0
900	1054	19.8	13.0
950	583	23.0	15.3
1000	132	26.0	17.6

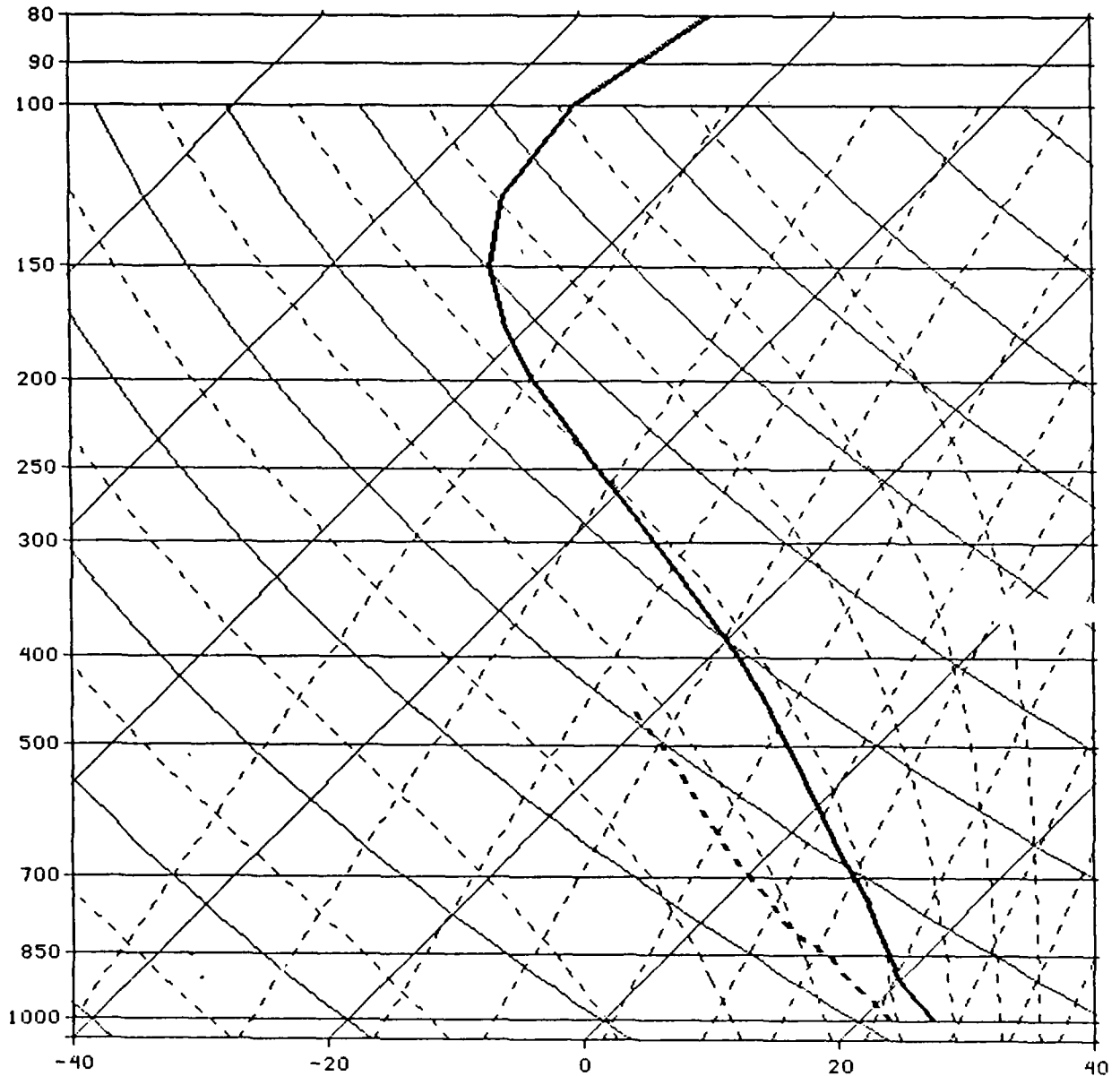


Figure 1.17: Mean Tropical Atmosphere (West Indies) during Rainy Season (Jordan, 1958) The temperature (heavy solid line) and dewpoint temperature (heavy dashed line) are plotted on a "Skew T, Log P" thermodynamic diagram, with isobars (thin solid horizontal lines), "skewed" isotherms (thin solid lines) sloping from lower left to upper right, dry adiabats (thin solid lines) sloping from lower right to upper left, pseudoadiabats (thin dashed lines) sloping from lower right to upper left, and mixing ratio lines (thin dashed lines) sloping from lower left to upper right.

1.2.2 General Climatology (Portig, 1976)

The following outline contains summary statements gleaned from Portig (1976) concerning the various climatological elements for Central America. (The reader is cautioned that these summaries do not refer to the figures (from other sources) presented in the previous subsection.)

Wind

Because wind is among the climatological elements most affected by local influences in the near Equatorial portion of Central America, one cannot use the geostrophic or gradient approximation for the wind. Using earlier data based primarily on ship observations (yet, not so complete as COADS), Portig (1976) states that mean streamlines from September (rainy season) and December (dry season) have the greatest month-to-month mutual deviations (see Fig. 1.18 below)¹². While the more northerly direction of the December winds is obvious, he notes that "in no month is there any (average) *southerly* component of the wind over the open Caribbean Sea".

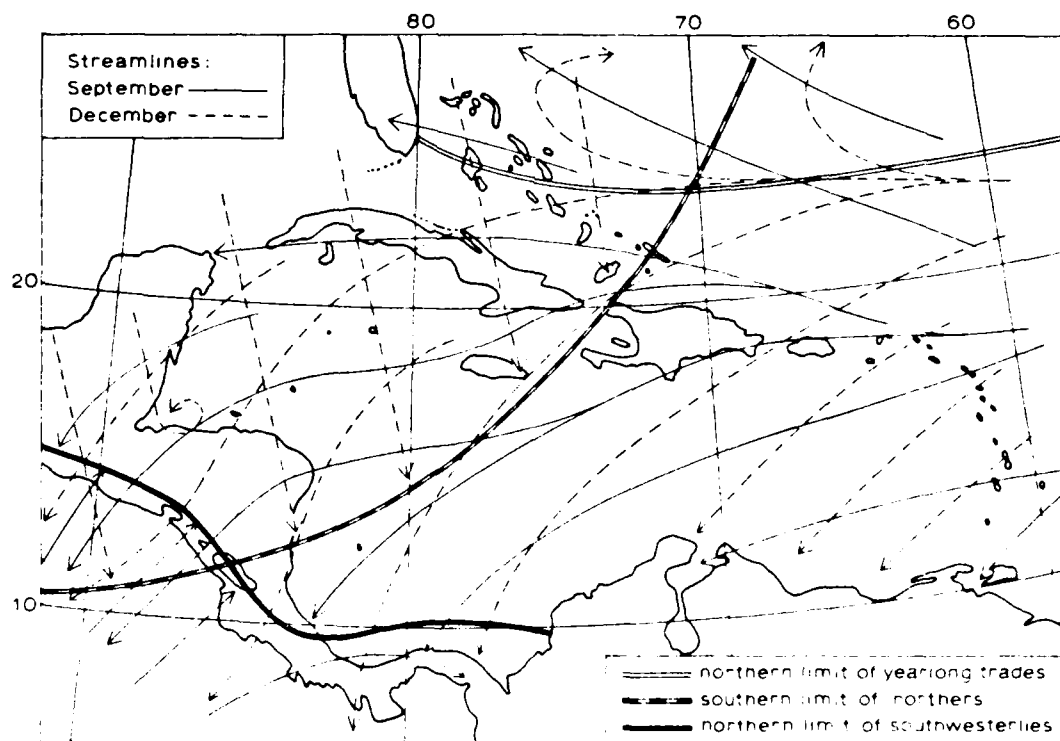


Figure 1.18: Mean Streamlines. Over the North Pacific coast of Central America two wind regimes alternate in September (Portig, 1976)

¹²The dashed lines from the north-northwest over the western Caribbean Sea indicate the presence of "northers", **intermittently** present with the north-northeasterly tradewinds during December. Northers are defined as "...strong, cold winds...associated with the southward movement of a cold anticyclone." (Huschke, 1959). However, other sources document northers reaching **Panama**.

Although hurricanes do occur in the region, they affect individual stations so seldom that their presence is not evident in wind statistics compiled over many years.

Not only do *inland* stations have a high percentage of calms, but there are periods (of hours) during which the wind speed is zero. Balloon records have revealed layers, several thousand meters thick, having no horizontal motion.

Stations have distinct diurnal variations, with the expected higher wind speeds in the afternoon and early evening. Stations with extensive land mass behind them, such as along the North Pacific coast, experience "sea breeze fronts". However, local orographic effects, "northers" and trade winds have their particular months (as well as time of day) of dominance.

Barometric Pressure

Relative maxima in mean pressure are found in December (or January) and in July. More importantly, the atmospheric pressure displays the familiar **double** wave every day, with minima near 0400L¹³ and 1600L, and maxima near 1000L and 2200L. At San Salvador, the magnitude of this twice daily pressure variation is as large as 4.2 mb in March.

Cloudiness

Central America is often under a canopy of cirrus (often tenuous), and even well-experienced observers often have difficulty in locating the edges of thin cirrus. However, tropical clouds show a high correlation with geographic features, such that not only mountain ranges but also coastlines are often identified in satellite imagery. The largest annual range of cloudiness over ocean areas (i.e., clearer in February/March, cloudier in September) is observed in the North Pacific Ocean, off the coast of Central America. Maximum cloud cover is also found along the east coast of Central America, from Belize to Panama.

Sunshine

Mean monthly sunshine, in percentage of the possible, shows a tendency for stations to have their sunshine extremes out of phase and a month or so earlier than rainfall extremes. That is, minimum sunshine occurs one month before the rainfall maximum, and maximum sunshine occurs one month before the rainfall minimum.

Temperature

Since Central America is tropical and primarily maritime, temperature changes are small. Portig (1976) found that the *hourly* temperature variations from observations in a well ventilated shelter depend mostly on cloud cover.

¹³L = Local Time

In most of Central America (except for the Caribbean coasts of Honduras and northern Nicaragua), the monsoon temperature variation dominates with the highest temperatures just before the onset of the summer rains. On land, the average temperature of the *warmest* month (at sea level) is less than 29°C, except at some island locations on the Pacific side of Central America where the mean April temperature rises to 31°C (e.g., in Amapala, a Honduran island in the Gulf of Fonseca¹⁴). Conversely, at sea level the average temperature of the *coldest* month is 19°C. The annual temperature range for most of Honduras is more than 4°C, dropping to less than 4°C at the coast, and to about 1.5°C at the Panama Canal. (The temperature range of stations at higher elevations is generally of the same magnitude as for nearby lowlands.)

Cold winter air invasions from North America affect the absolute temperature minima. While lowland temperatures almost never drop below 15°C southeast of a line running from Puerto Rico to Costa Rica, the lowland temperatures in Central America northwest of this line reach an absolute minima of approximately 7°C. Such low temperatures usually occur due to the combined effects of cold air intrusion and nocturnal cooling. The highest mountains of Guatemala and Costa Rica have experienced *below freezing* air temperatures.

The diurnal temperature range exceeds the annual temperature range, although the diurnal range is reduced by the nearness to sea. Also, the dry season has a larger daily temperature variation than the rainy season, in general.

Moisture

Most Central American climatological summaries do not include dewpoint temperatures; however, Appendix B contains average **monthly** relative humidity, vapor pressure and dewpoint temperature for selected stations. Although the strong influence of nearby oceans and warm temperatures dictates relatively high moisture for Central America, it is noted that moisture *can* drop to sufficiently low values where hygrometers become inaccurate.

Rainfall

Portig (1976) states that "the most important meteorological element in the tropics is the rainfall". Although Central America is practically always under the influence of maritime air masses, seasonal variation of precipitation are surprisingly high (see Fig. 1.19). While much of the variation can be attributed to orographic effects, significant differences in the timing of the rainfall seasons exists over short distances.

Areas of *lesser* rainfall (less than 100 cm (~40 in) include regions of elevated plains of central Guatemala, Honduras and northwestern Nicaragua, plus very small parts of the North Pacific coast west of the Gulf of Fonseca and southwest of Panama City.

¹⁴See Subsection 1.3 for geographical locations within respective countries.

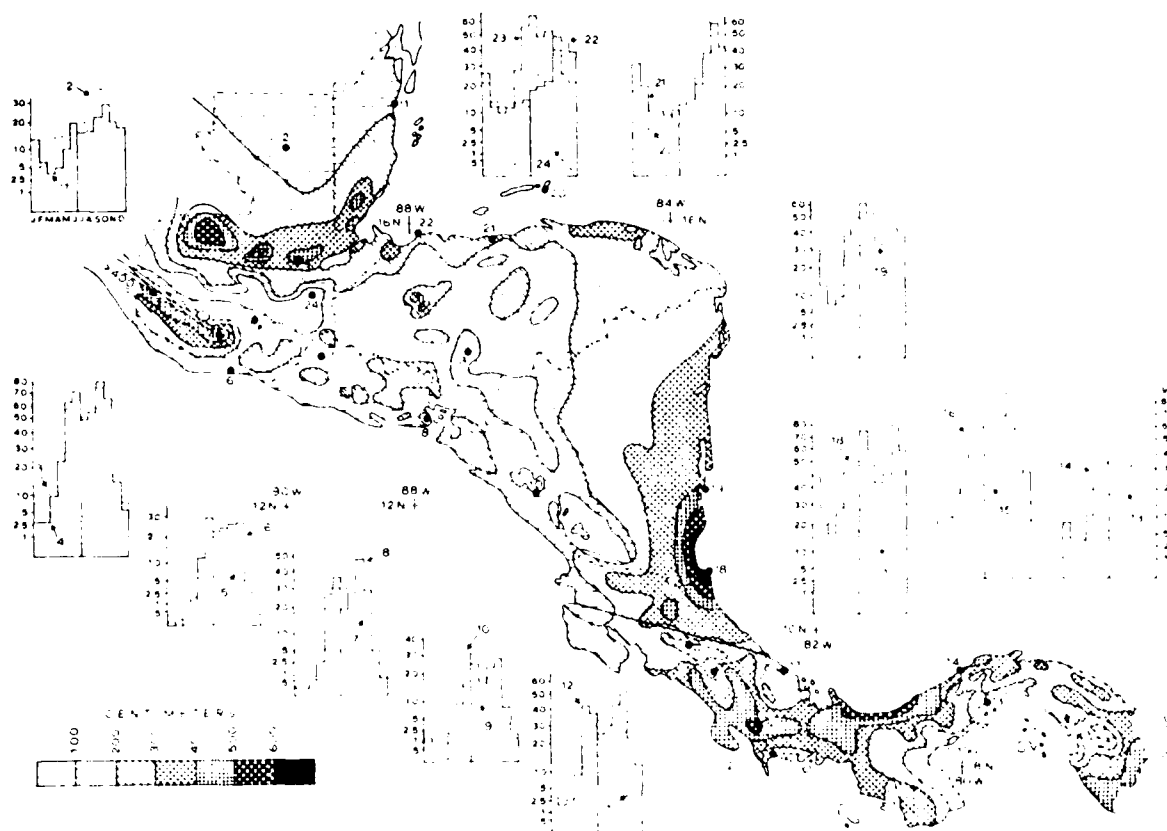


Figure 1.19: Mean annual rainfall (cm) in Central America (Portig, 1976). Numbers (1 through 24) locate the following stations: 1-Belize City, 2-Flores, 3-Santa Teresa, 4-San Andrés Osuna, 5-Guatemala City, 6-San José, G., 7-Taxis Junction, 8-Cutuco, 9-Tegucigalpa, 10-Managua, 11-San José, C. R., 12-Villa Mills, 13-Panama City, 14-Colón, 15-Puerto Armuelles, 16-Caracol, 17-Guabito, 18-San Juan del Norte, 19-Bluefields, 20-Guanaja, 21-La Ceiba, 22-Puerto Cortés, 23-Sepacuite, 24-Zacapa.

In contrast, areas of excessive rainfall are found in the mountains of Guatemala and the mountains connecting Costa Rica and Panama. The tops of lesser mountains and the slopes of the higher mountains receive large rainfall totals, while crests above 2,500 m receive less than half that falling on the slopes.

The other areas receiving excessive rains include the Caribbean coast near southern Belize to Puerto Barrios, Guatemala, the Caribbean coast of Nicaragua at and south of Bluefields, the Caribbean coast of Panama near the Gulf of Los Mosquitos, the southeast corner of Panama, and the *southern* coast of Costa Rica.

While most of the rain-bearing disturbances come from the Caribbean, leading to larger rainfall on the Caribbean side, the reader must keep in mind that diurnal sea breezes provide their rainfall production ashore on the North Pacific Ocean side as well, with winds from the south or west. Drier areas, such as west of the Gulf of Fonseca, are believed to be partly caused by katabatic winds¹⁵. Also, the drier eastern side of the Peninsula of Azuero, Panama may be shielded from disturbances of North Pacific origin by the mountain range on the western half of the peninsula.

¹⁵Winds blowing down an incline, the opposite of anabatic wind (Huschke, 1959).

With only a couple of exceptions, all of Central America has two rainfall maxima, with generally higher totals on the Caribbean Sea side. The main dry season occurs in winter or early spring and is much more intense (drier) on the North Pacific Ocean side of Central America.

With the drier winter and spring, the North Pacific Ocean side has appreciable accumulation from June through October, yet with a relative minimum during the two summer months of July and August. This relative minimum is locally labeled the "varanillo" (little summer). While all months have a diurnal rainfall maximum between sunset and midnight, June and September have an additional rainfall accumulation¹⁶ in the early afternoon (1200L-1600L). Thus the North Pacific side maxima are in June and September.

Again, while the Caribbean side has a not-so-dry late winter (as does the North Pacific Ocean side), the general pattern of its maxima consists of a summer maximum near June or July and another relative maximum in December.

Thunderstorms

While thunderstorms are a common occurrence in Central America, the two regions of maximum thunderstorm activity are (1) the Gulf of Fonseca (116 storm days¹⁷ per year on Amapala) and (2) the center of the Canal Zone (196 storm days at Madden Dam). The minima are 37 at Chimax, in central Guatemala and a questionable **three** at Belize City.

Visibility

Portig (1976) reports that fog practically never occurs at sea and at coastal stations, but that inland stations occasionally have shallow fog in the morning that is rapidly dissipated by the sun. (However, one of the authors observed **heavy** coastal morning fog during a winter (dry season) approach to the Caribbean side of the Panama Canal in February 1963.)

The dry season has many days with haze, providing a real hazard for aircraft. However, **above** the haze, the trade wind inversion provides unlimited visibility. Furthermore, the Pacific side of Central America has the "best" and the "worst" visibilities, i.e., the Pacific side has a larger variation in visibility, than the Caribbean side.

Overall Weather

In winter and spring, i.e., the dry season, the steadily blowing trades produce generally fine weather. Of course, the incursions of cold air from North America (or the Gulf of Mexico) interrupt this fine weather, with less effect equatorward of Nicaragua. (GOES imagery, examined during 1988, verified these statements.)

¹⁶From Portig(1976) data which is predominantly from San Salvador.

¹⁷While Portig (1976) does not define *storm day*, Huschke (1959) defines a *thunderstorm day* as "...an **observational day** during which thunder is heard at the station. Precipitation need not occur".

Most of the winter rain for northern Honduras comes from the long-lasting rain and drizzle accompanying cold fronts reaching the mountains. Again these cold fronts tend to be dry on the Pacific Ocean side because of the foehn¹⁸ effect. The cold north wind is called norte, norther, or tehuntepeco. While it can become destructively strong, it is often welcomed during the monotonous dry season. As mentioned earlier, the lowest temperatures occur when the wind subsides and cooling by nocturnal radiation follows.

While the first norther of the seasons tends to bring a distinct weather change, subsequent incursions become less potent. Accordingly, Portig (1976) states that it is difficult to determine the exact number of northers per season. Estimates run from 30–40 per year or less.

Chapel (1927), who has defined northers by wind rather than through weather patterns, studied the average conditions of six northers reaching Colon, Panama, noting that the wind nearly doubled in strength on the day of arrival, with a pressure rise **only** on the day of arrival, but with increased rainfall amounts for three days after arrival. While no rain may fall when a cold front passes, heavy downpours can occur where the front finally stalls. Such heavy rainfalls can be found on the Caribbean coastal area of southeastern Nicaragua.

However, the rainy season has more synoptically driven events than does the dry season. In the rainy season, they are manifest as hurricanes, tropical depressions, waves in the easterlies or even displaced fragments of the Intertropical Convergence Zone (ITCZ). Rainfall from hurricanes is considered beneficial in many areas, but hurricanes are **not** responsible for the rainfall maximum in the fall. Portig (1976) reports that "tropical lows or depressions occur at varying intensities all over region, and occasionally in the dry season"; moreover, personal communication¹⁹ in 1986 revealed that development of a tropical depression near the Canal in December 1985 required immediate measures to control the water level of the Canal, before the depression moved slowly toward the northwest.

Local developments

Portig (1976) defines the "temporal" as a longlasting rain, with no, or little, electrical activity. While categorizing them as "local" is debatable, they are typical of two areas: the north coast of Honduras (caused by invasions of cold air from the north during the winter (dry season) and the Pacific Ocean coast of all of Central America. While continued research is needed, the temporals along the Pacific Ocean coast may often be tropical depressions moving slowly westward. Portig (1976) suggests that they may transform from "temporal"-lows into hurricanes, and vice versa. While the Pacific temporal may have hurricane-like spiral bands, its winds are generally light and moderate, without lightning and thunder, but its rainfall, covering a relatively large area, can cause water damage.

¹⁸Foehn—A warm, dry wind on the lee side of a mountain range, the warmth and dryness of the air being due to adiabatic compression upon descending the mountain slopes (Huschke, 1959).

¹⁹Conversation between Joe Corelli, Hydrologist of the Panama Canal Commission and one of the authors.

Portig (1976) further reports that "it is not possible to clearly distinguish between the temporals and temporal-like situations ('tiempo atemporalado' as the man on the street says), but a fair estimate calls for one or two temporals a year for each location on the North Pacific coast of Central America". The greatest probability is in September or October, with a secondary maximum in June.

As a local phenomena, the sea breeze may be strong enough at times to overcome the large-scale wind regime, blowing from the west in a typical trade wind area. For example, in western Panama, it can reach 30 km inland.

Squalls are frequent, and over water thunderstorms frequently generate waterspouts. Tornadoes are less frequent than waterspouts, and hail is rare, even in locations experiencing many thunderstorms. Hail has fallen on the Pacific Ocean side of Guatemala and in Panama, and snow falls on elevations above 3400 m in Guatemala (Portig, 1976).

1.3 National Climatologies

Following closer examination of Central America and its topography, this section will discuss the climate and terrain of each country. On the following two pages, Fig. 1.20 (The Diagram Group, 1985) with its shading, and Spanish names for mountain ranges and volcanoes, provides a better perspective of terrain elevation, while Fig. 1.21 (The Diagram Group, 1985) with its *larger* scale (compared to Fig. 1.1) displays the national boundaries of the seven countries more clearly.

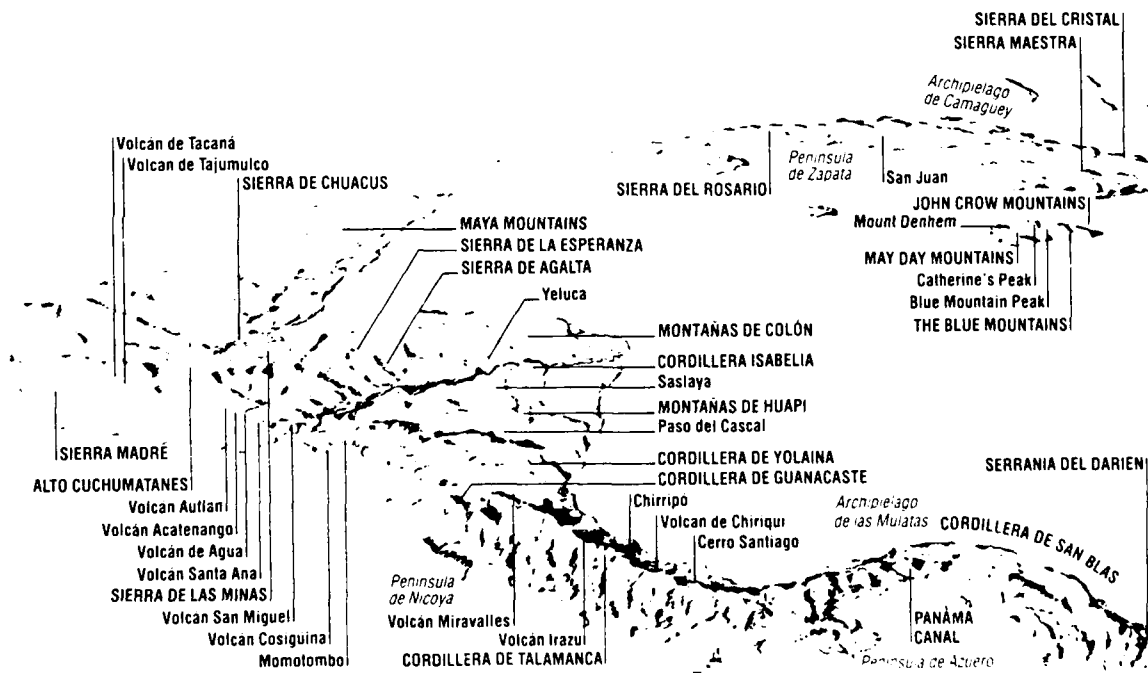


Figure 1.20: Topography of Central America (The Diagram Group, 1985)

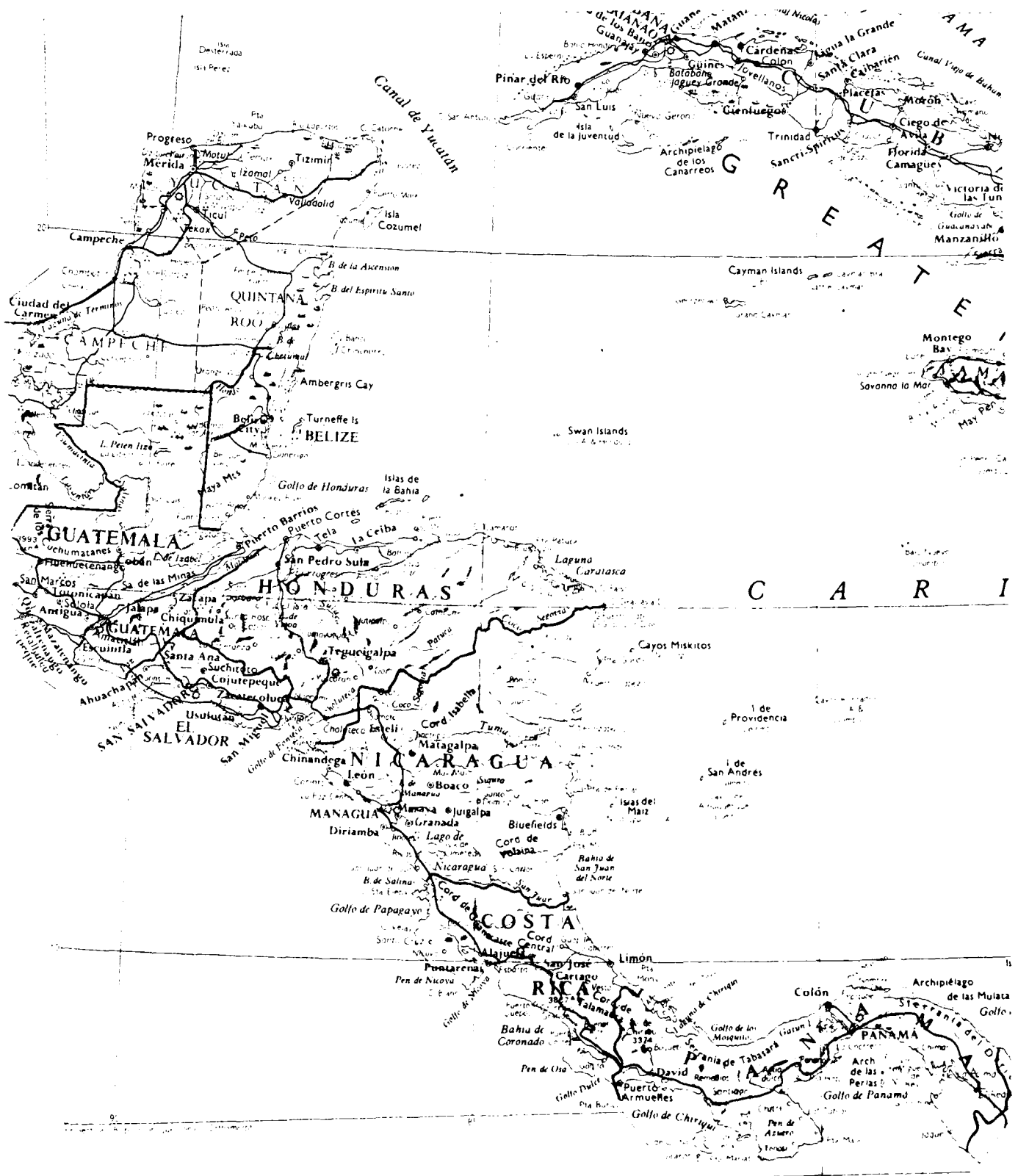


Figure 1.21: Seven Countries of Central America (The Diagram Group, 1985)

1.3.1 Guatemala

Land

While having the most people of any nation in Central America, Guatemala is the third largest nation, equivalent to the size of Tennessee. In addition to bordering Mexico on the north and west, its Pacific coastline is located to the southwest. On its eastern border (starting from the north) is Belize, followed by a short Caribbean coastline, and then finally Honduras and El Salvador.

As depicted in Fig. 1.22, Guatemala has a rather narrow Caribbean coast to the east, but a fairly extensive Pacific Ocean coast to the south. While lagoons and sand bars extend the length of the gently curving Pacific coast, just inland are fertile coastal lowlands for about 25 miles. The coastal Pacific lowlands then give way to the highlands of the southern and central region, while the north is occupied by the plains of Petén.

Approximately two-thirds of the country is occupied by highlands with the main mountain range being a southeast extension of Mexico's Sierra Madre, paralleling the coast only about 40 miles inland. With many high volcanic peaks, some active, the inland highlands extend from 3500 – 8000 feet in elevation. Very near the western border and at 13,845 feet, the Tajumulco Volcano is the *highest* peak in Central America. But between volcanic peaks lie volcanic rich basins.

Guatemala's longest river, the Motagua, lies just north of the main mountain range and flows eastward to the Gulf of Honduras and the Caribbean Sea. From another valley, not far to the north, the Polochic River runs parallel to the Motagua, flowing into Guatemala's largest lake, Izabal, before reaching Amatique Bay in the Gulf of Honduras. While the sparsely populated limestone plains of Petén comprise most of northern Guatemala, the relatively low Maya Mountains extend into southern Belize. A narrow, fertile coastal plain exists along the short Caribbean coast (The Diagram Group, 1985).

Climate

General The cooling effects of both coasts and highlands provide a variety of climates within Guatemala. The coasts are hot and humid, about 80°F (27°C) throughout the year. Inland highlands are cooler; for example, at Guatemala City, at nearly 5000 feet above sea level, the average annual temperature is 64.4°F (18°C). The months of December and January are coolest.

The rainy season lasts from May to November—October, if you use Guatemala City rainfall, (not shown). While the Caribbean-facing slopes get rain almost all year, the Pacific coast receives heavy summer rain, but stays dry during the winter. Annual rainfall varies from 80 inches in the highlands to about half that amount in parts of eastern Guatemala (The Diagram Group, 1985).



Rainy Season: May – October. The rainy season is characterized by mostly cloudy skies²⁰, with warm to hot temperatures, and frequent rain showers and thunderstorms. At night, the temperatures below about 3000 feet and at coastal locations fall to the mid to upper 70's (°F), then rises to the upper 80's or lower 90's during the afternoon. However, the upper plateau which includes Guatemala City, is cooler with lows near 55–60°F and highs 70–80°F. Rainfall, which is moderate on the interior plateau, increases to very heavy on seaward-facing mountain slopes and lower elevations. While most rain falls as brief showers, the "temporal" can bring low ceilings and visibilities, as well as continuous rain, for periods from 12 hours to 6 days.

Thunderstorm days occur in the lowlands at a frequency of 8–14 per month, with a considerably higher frequency on exposed mountain slopes. While the interior plateau has only 2–8 thunderstorm days per month (see monthly totals below), both the lowlands and interior plateau have a thunderstorm maximum in the midafternoon, with a secondary thunderstorm maximum found at coastal stations between midnight and sunrise. The thunderstorms may be accompanied by strong gusty winds and severe lightning. See Section 5 and Appendix C for tracks of tropical cyclones affecting Guatemala.

Flying weather: Poor to fair flying weather may be expected during the rainy season due to heavy cloud cover, rain and thunderstorms. Cloud-enshrouded mountain slopes naturally present a hazard to aircraft operations. See Appendix B for specific statistics at Huehuetenango and Puerto Barrios.

Terminal weather: Guatemala City/La Aurora Airport. While the terminal weather is fair to good, early morning fog may frequently restrict flying activity. Ceiling less than 300 feet and/or visibility less than 1 mile²¹ occurs only 1–3 percent of the time, and thunderstorms are most frequent from mid-afternoon to early evening. Crosswinds greater than 15 knots and occur less than 1 percent of the time (USAFETAC, 1985).

Monthly temperature, precipitation, thunderstorms & twilight (USAFETAC, 1985):

GUATEMALA CITY	MAY	JUN	JUL	AUG	SEP	OCT
TEMPERATURE (°F)						
Absolute maximum	90	89	83	88	88	84
Mean maximum	80	76	76	77	76	74
Mean minimum	60	60	59	59	59	58
Absolute minimum	49	54	50	53	52	46
MEAN PRECIPITATION (INCHES)	9.2	10.1	8.0	7.4	10.4	6.0
MEAN NUMBER OF DAYS						
Precipitation	11	21	16	20	22	10
Thunderstorms	4	7	5	8	8	2
CIVIL TWILIGHT (15th of month)						
First light (local standard time)	0512	0509	0517	0526	0529	0532
Last light (local standard time)	1845	1856	1858	1847	1825	1804

²⁰Clear = 0/10 sky cover, partly cloudy = 1/10–5/10, cloudy = 6/10–9/10 and overcast = 10/10.

²¹Henceforth, ceiling/visibility, e.g., 300/1 indicates "ceiling of 300 feet and/or visibility of 1 mile".

Dry Season: November – April. Contrasted to the rainy season, the dry season is characterized by only *partly* cloudy skies, and warm to hot temperatures. Precipitation is infrequent except in the northern lowlands and on the Caribbean slopes of mountains. While these two locations record minimum precipitation amounts during this season, they do not experience the very dry conditions that occur in the interior and on the Pacific mountain slopes. Morning fog occurs frequently in the interior highlands and valleys. While temperatures in the lowlands range from 65–75°F in the morning to 80–90°F in the afternoon, the interior highlands warm from morning lows of 35–40°F to highs of 65–70°F. Above 7000 feet elevation, subfreezing temperatures are not uncommon. Precipitation occurs only 0–3 days per month on the Pacific mountain slopes and in the interior highlands. Snowfall is infrequent, confined to the highest mountain peaks; and thunderstorms are uncommon in the dry season. However, on the Caribbean mountain slopes and northern lowlands, rainfall occurs 3–20 days per month, with the greatest amount of rainfall occurring on the mountain slopes; nonetheless, thunderstorms are still infrequent. Not only may mid-latitude cold fronts penetrate as far south as Guatemala (if not further) with their associated strong, gusty northerly winds and one or two days of cloudy skies and rain, but tropical cyclones are still a possibility on the Caribbean coast during November.

Flying weather: Generally good except in the Caribbean lowlands and on mountain slopes. The weather begins to deteriorate along the North Pacific coast in February, and by April the ceiling/visibility is less than 5000/6 as often as 90 percent of the time; however, elsewhere less than 5000/6 occurs only 20–40 percent of the time. On the plateau due to fog near sunrise, 1500/3 occurs as often as 60 percent of the time, while 500/1 occurs as often as 15 percent (see Appendix B for Huehuetanango and Puerto Barrios data).

Terminal weather: Guatemala City/La Aurora Airport. Generally good, except that ceiling/visibility less than 300/1 occurs as often as 12 percent of the the time, likely around sunrise (early morning fog). Thunderstorms are infrequent, and as in the rainy season, occurrence of crosswinds greater than 15 knots is less than 1 percent (USAFETAC, 1985).

Monthly temperature, precipitation, thunderstorms & twilight (USAFETAC, 1985):

GUATEMALA CITY	NOV	DEC	JAN	FEB	MAR	APR
TEMPERATURE (°F)						
Absolute maximum	86	84	86	89	92	91
Mean maximum	73	74	75	77	80	82
Mean minimum	55	54	53	53	56	58
Absolute minimum	45	41	42	41	45	47
MEAN PRECIPITATION (INCHES)	0.8	0.4	0.1	*	0.3	0.7
MEAN NUMBER OF DAYS						
Precipitation	3	2	1	1	4	3
Thunderstorms	1	*	*	*	1	2
CIVIL TWILIGHT (15th of month)						
First light (local standard time)	0540	0556	0608	0604	0549	0527
Last light (local standard time)	1753	1759	1815	1828	1834	1838

(NOTE: * = less than 0.05 inch or 0.5 day, as appropriate)

1.3.2 Belize

Land

Belize, lying in the southeastern portion of the Yucatan Peninsula, has Mexico on its northern border, Guatemala on its western border as well as on its very narrow southern border, while it has the Caribbean Sea (actually the Gulf of Honduras) along its entire eastern boundary. While its neighbor Guatemala is the *most* populated, Belize has the smallest population of the seven Central American nations. However, it is the second *smallest* nation—only El Salvador is smaller—having an area just smaller than the state of New Hampshire.

As depicted in Fig. 1.23, Belize has a much larger north-south dimension (174 miles) than east-west dimension (68 miles at its widest). It can be divided into three regions: the northern lowlands, southern uplands and the coast. Most of the northern lowlands are swampy, lying less than 200 feet above sea level. In the southern uplands are found the hills and valleys of both the Maya Mountains, and its northeast extension, the Cockscomb Mountains. Considerably lower than Guatemala's Tajumulco, Belize's highest mountain is Victoria Peak at 3681 feet. The rivers, all running eastward and draining into the Caribbean Sea are: Hondo (forming the northern border with Mexico), New, Belize, Monkey, Sarstoon (forming most of Belize's southern border, with Guatemala) and others. Inland from its low and swampy coast, lie numerous lagoons. In addition to many small, low islands (cays), the world's second-largest barrier reef lies 10–40 miles offshore (The Diagram Group, 1985).

Climate

General Belize's climate is subtropical, with onshore trade winds. While the *mean* temperature at Belize City on the coast ranges from 74° in December to 85° in July, inland days are hotter and nights are cooler. Annual rainfall ranges from 50 inches in the flatter northern lowlands to 170 inches in the more mountainous south. While hurricanes can sweep westward over Belize from the Caribbean Sea, droughts are possible (The Diagram Group, 1985).

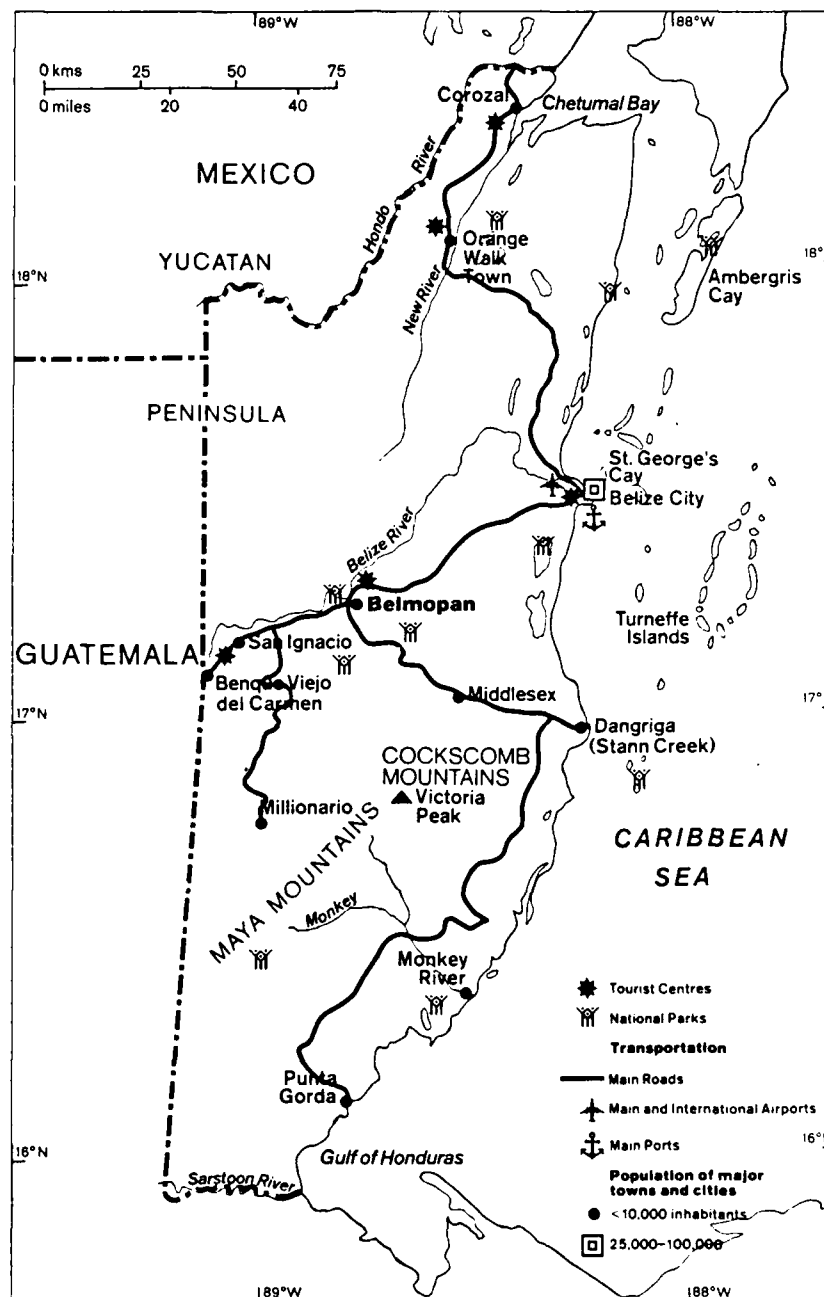


Figure 1.23: Belize (The Diagram Group, 1985)

The climate of Belize will *not* be divided into a rainy season and a dry season as is done with the other countries. However, while the climate is treated as an *annual* one which is hot, humid and cloudy, rainfall is generally moderate to heavy from May through January (with the monthly maximum in October at Belize City; see next page), with a reduction of cloudiness and rainfall during February and March.

More specifically, rainfall is extremely heavy from only June through September in the southern one-quarter of the country. While mean cloudiness is 55-70 percent from April through January, it is slightly less than 50 percent in February and March.

As noted below, for Belize City, mean maximum temperatures are in the upper 80's (°F) during the summer and lower 80's during the winter, while mean minimum temperatures are in the 70's from March through October and in the 60's from November through February.

Again, as noted below, the thunderstorm frequency is greatest from June through September. While thunderstorms are quite uncommon in northern Belize, their frequency increases southward. Additionally, they occur during the morning along the coast, but during the afternoon inland. Mean surface winds are northeast to east, 8-15 kt. Being the country farthest north, Belize frequently experiences a day or two of rain and strong northerly winds ushered in by mid-latitude cold fronts, from November through March.

Affected by tropical storms and hurricanes from May through November, the monthly probability of having at least one tropical storm and/or hurricane strike Belize ranges from 5 to 20 percent with the greatest probability in September (see Section 5).

Flying weather: Fair to good, although flying weather may be restricted by early morning fog, heavy rainfall or thunderstorms. The percentage frequency of ceiling/visibility less than 5000/6 ranges from 25-50 percent, while 1500/3 ranges from 10-20 percent (see Appendix B for specific ceiling/visibility statistics for Belize City).

Terminal weather: Belize City. Hot and humid, with moderate to heavy rainfall. Mean relative humidities lie between 75 and 90 percent. While rainfall is expected 4-18 days per month, the heaviest rainfall accumulation is from June through January. Ceiling/visibility is less than 300/1 about 1 percent of the time, mostly during early morning hours. Visibility is restricted primarily by rain, haze/smoke and early morning fog. Runway crosswinds are greater than 15 kt during 1-3 percent of the time (USAFETAC, 1985)

Monthly temperature, precipitation, thunderstorms & twilight (USAFETAC, 1985):

BELIZE CITY	JAN	FEB	MAR	APR	MAY	JUN
TEMPERATURE (°F)						
Absolute maximum	90	93	98	99	97	97
Mean maximum	82	83	85	87	88	88
Mean minimum	68	69	72	74	75	76
Absolute minimum	50	49	50	55	57	62
MEAN PRECIPITATION (INCHES)	5.7	2.7	1.6	2.4	5.0	9.1
MEAN NUMBER OF DAYS						
Precipitation	12	6	4	4	7	14
Thunderstorms	0	*	0	0	1	4
CIVIL TWILIGHT (15th of month)						
First light (local standard time)	0604	0558	0540	0515	0458	0454
Last light (local standard time)	1802	1817	1825	1832	1841	1853
	JUL	AUG	SEP	OCT	NOV	DEC
TEMPERATURE (°F)						
Absolute maximum	95	96	97	95	95	93
Mean maximum	88	88	89	86	84	82
Mean minimum	76	76	75	73	69	68
Absolute minimum	63	61	60	58	52	46
MEAN PRECIPITATION (INCHES)	7.6	7.3	9.5	12.4	9.8	7.2
MEAN NUMBER OF DAYS						
Precipitation	18	16	18	15	13	14
Thunderstorms	2	4	5	1	*	0
CIVIL TWILIGHT (15th of month)						
First light (local standard time)	0503	0513	0519	0524	0535	0552
Last light (local standard time)	1855	1842	1817	1753	1740	1745

(NOTE: * = less than 0.5 day)

1.3.3 Honduras

Land

Honduras occupies the *upper* portion of the "knee" of Central America. As Central America's second-largest nation (only Nicaragua is larger), Honduras is a little larger than the state of Tennessee. While Guatemala and El Salvador form its western border, and Nicaragua its long southeastern boundary, Honduras has a short stretch of Pacific coast line in the south, compared with a long northern Caribbean coast. Its small Pacific coast borders the Gulf of Fonseca, while the extensive Caribbean coast includes the Gulf of Honduras in the west (see Fig. 1.24).

With its wedge shape, Honduras is about 400 miles from west to east, but only about 180 miles from south to north. Honduras, although nearly two-thirds occupied by uplands and mountains, has no *active* volcanoes as do its neighbors, but its highest peak is Cerro de las Minas (9,347 feet) in the west. Mountain ranges approach the northern coast at an angle, with one range continuing submerged out to sea and reappearing as the Islas de la Bahía (Bay Islands) chain. While much of the northern coast is rimmed by a lowland of rich clay and loam soils, the Caratasca Lagoon, a swampy lowlands, occupies the northeast corner, along the Mosquito Coast²². Rivers flowing north, including the Ulúa in the northwest, form fertile valleys. To the south, the Gulf of Fonseca, which contains an archipelago of nearly 300 tiny islands, is surrounded by a narrow lowland (The Diagram Group, 1985).

Climate

General While the coastal lowlands are hot and humid, the upland interior is cooler and much drier. Although average temperatures in the highlands at 7000 feet are only in the high 50's (°F), they reach the mid 80's on the coast. Tegucigalpa, the capital, has an annual temperature range of only 11°F. While the northeast is the wettest region of the country, where onshore winds are associated with up to 110 inches of rain per year, some inland valleys receive only 40 inches (The Diagram Group, 1985).

²²A strip along the Caribbean Sea (including both northeastern Honduras and the entire east coast of Nicaragua) named for its Miskito Indians.

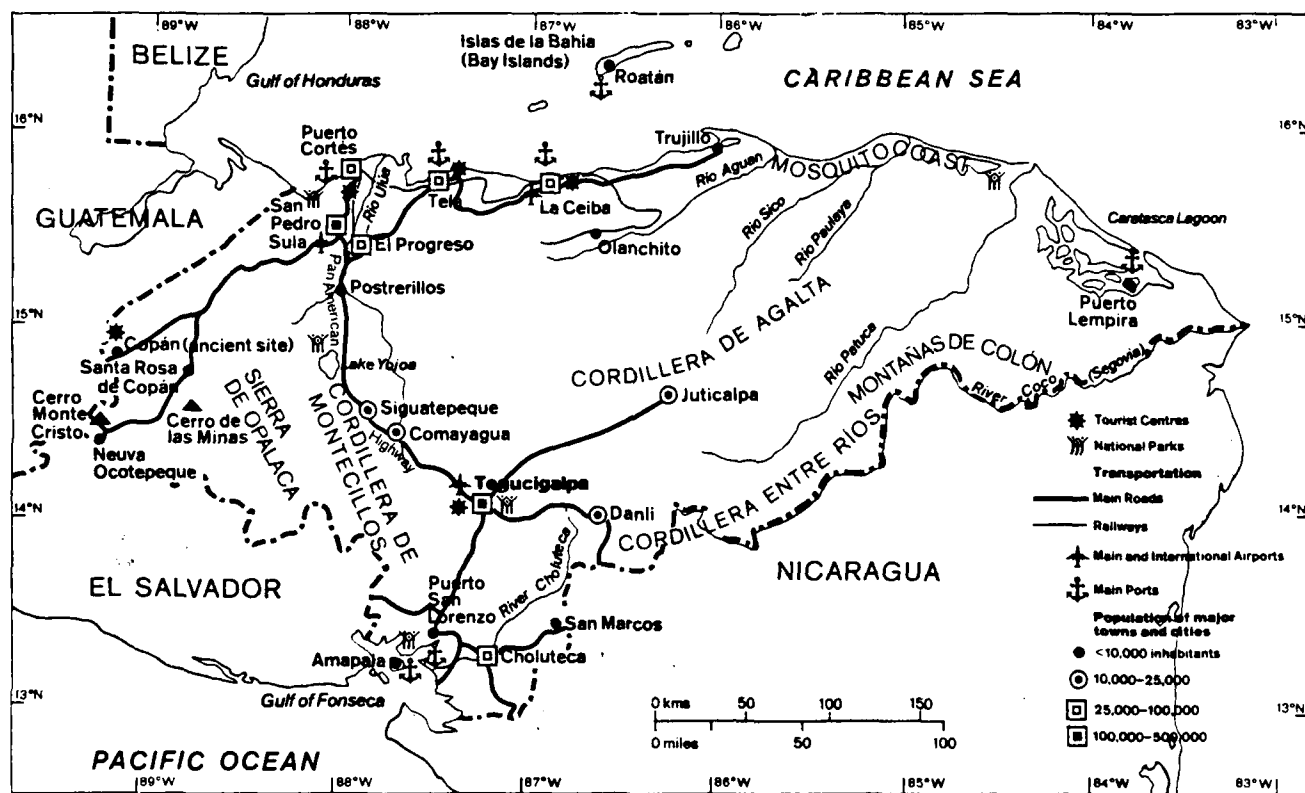


Figure 1.24: Honduras (The Diagram Group, 1985)

Rainy Season: May - October. During this season, the weather is characterized by mostly cloudy skies and hot temperatures, with frequent rain showers and thunderstorms. Surprisingly, however, along the north coast on the Gulf of Honduras some stations record the minimal precipitation at this time of year. While precipitation amounts on the Caribbean coast are often very heavy, only moderate amounts are expected in the interior. Mean monthly cloudiness varies between 50 and 85 percent. Depending upon elevation, mean minimum temperatures vary between the 60's and the upper 70's (°F). Note that the data given below are for Tegucigalpa (3,304 feet). Maximum monthly temperatures range from the upper 80's to the lower 90's, with particularly hot low lying Pacific coast stations. Thunderstorms occur with greater frequency at coastal stations. Surface winds are normally northerly or northeasterly at 6-10 kt. See Section 5 for details concerning tropical storms or hurricanes that primarily affect the Caribbean coastal areas.

Flying weather: Usually good, except in the vicinity of thunderstorms. Ceiling/visibility less than 5000/6 occurs 25-45 percent of the time, while less than 1500/3 occurs 5-10 percent, and less than 500/1 occurs 1-6 percent. Icing and turbulence are not expected except near rain showers and thunderstorms; however, early morning fog can be a problem at mountain stations (see Appendix B for ceiling/visibility statistics at several coastal and inland cities).

Terminal weather: Tegucigalpa. Generally good. Ceiling/visibility less than 300/1 rarely occurs; yet fog forms on 14-22 mornings per month, but rarely restricts visibility below 3 miles. As indicated below, thunderstorms occur on 6-12 days per month, normally during early evening. Occurrence of crosswinds greater than 15 kt is 1-3 percent, normally during late afternoon and early evening (USAFETAC, 1985).

Monthly temperature, precipitation, thunderstorms & twilight (USAFETAC, 1985):

TEGUCIGALPA	MAY	JUN	JUL	AUG	SEP	OCT
TEMPERATURE (°F)						
Absolute maximum	94	90	89	91	90	88
Mean maximum	85	82	81	83	83	80
Mean minimum	64	65	64	63	63	63
Absolute minimum	49	56	55	54	55	52
MEAN PRECIPITATION (INCHES)	5.7	6.3	3.5	3.9	7.2	5.4
MEAN NUMBER OF DAYS						
Precipitation	11	17	15	14	19	16
Thunderstorms	9	12	7	7	11	6
CIVIL TWILIGHT (15th of month)						
First light (local standard time)	0459	0457	0505	0513	0516	0518
Last light (local standard time)	1831	1841	1844	1833	1812	1751

Dry Season: November – April. The weather during this season is characterized by *partly* cloudy skies and infrequent rainfall, yet warm to hot temperatures. **However**, in the eastern part of the country near the Caribbean Sea the rainy season does not end until December, and **moreover**, the north coast, on the Gulf of Honduras, receives its maximum rainfall at this time. Rain occurs 5–20 days per month along the northern coast, but generally less than 5 days per month in the interior (see Tegucigalpa data below) and on the Pacific coast. Mean monthly cloudiness in the interior is about 55–75 percent, and 30–50 percent on the Pacific coast, where offshore winds dominate. While minimum temperatures range from 55 to 75 (°F), maximum temperatures range from 70 to 85 (°F). Along the narrow Pacific coast, extremely high temperatures (over 100°F) occur daily. Thunderstorms occur 2–6 days per month in November and December (less in Tegucigalpa, see below), but less frequently in later months. Mean surface winds are north to northeast at 8–15 kt (i.e., stronger than in the rainy season). Extratropical cold fronts occasionally reach the north coast causing one to two days of rain and strong northerly winds.

Flying weather: Usually good. Ceiling/visibility less than 5000 feet and/or 6 miles occurs 15–45 percent, while less than 1500/3 occurs 1–5 percent, and less than 500/1 rarely occurs. Along the north coast, aircraft icing can occur above the freezing level in stratified cloudiness (see Appendix B for ceiling/visibility statistics at several cities).

Terminal weather: Tegucigalpa. Good. Ceiling/visibility less than 300/1 seldom occurs; morning fog is common, but it seldom restricts visibility significantly. While precipitation occurs 2–9 days per month, thunderstorms are rare except in April (see below). Occurrence of crosswinds greater than 15 kt is 2–5 percent (USAFETAC, 1985).

Monthly temperature, precipitation, thunderstorms & twilight (USAFETAC, 1985):

TEGUCIGALPA	NOV	DEC	JAN	FEB	MAR	APR
TEMPERATURE (F)						
Absolute maximum	91	88	89	91	93	96
Mean maximum	78	77	77	80	84	86
Mean minimum	60	58	57	57	58	62
Absolute minimum	48	47	39	43	46	48
MEAN PRECIPITATION (INCHES)	1.7	0.5	0.5	0.2	0.4	1.1
MEAN NUMBER OF DAYS						
Precipitation	9	6	4	2	2	4
Thunderstorms	1	0	*	0	1	3
CIVIL TWILIGHT (15th of month)						
First light (local standard time)	0527	0542	0554	0551	0535	0514
Last light (local standard time)	1740	1746	1803	1816	1821	1824

(NOTE: * = less than 0.5 day)

1.3.4 El Salvador

Land

While El Salvador is the most *densely* populated, it is the smallest nation in Central America—about the size of the state of Massachusetts.

As indicated in Fig. 1.25, El Salvador, unlike the other six Central American nations, has no Caribbean coast. With Guatemala to the west and Honduras to the north and east, El Salvador has the Pacific Ocean coast as its entire southern border. Note, however, that only the Gulf of Fonseca separates its southeastern corner from the western tip of Nicaragua.

The shape of El Salvador is roughly rectangular, 160 miles from west to east, and 60 miles from north to south. Although not immediately evident, El Salvador can be divided into four regions, running *roughly* the length of the country. The four regions are, from south to north, the Pacific lowlands, the southern mountains, the plateau and the northern mountains.

While only 12 percent of El Salvador consists of coastal lowlands and hills, lagoons form part of the southeast coastline. Another third of the nation is formed by the southern mountain chain, at the western end of which is Santa Ana, with a peak at 7,812 feet. Even the nation's largest lake, Llopango, lies in an extinct volcanic crater. While some of its more than 20 volcanoes are active, with the commensurate expectation of earthquakes, volcanic ash and lava provide the nation's richest soils. The plateau, at an elevation averaging 2000 feet and comprising more than two-thirds of the country, is drained by the deep valleys of the Rivers Lempa and San Miguel in the eastern half of El Salvador. Finally, the northern mountains cover about 15 percent of the nation; here El Salvador's highest peak, Cerro El Pital (8,956 feet), is located (The Diagram Group, 1985).

Climate

General The nation's temperature varies with altitude. While the coast is hot and humid, the high inland regions are cooler. The capital San Salvador, at 2,290 feet, has an annual average temperature of only 73°F, with a small range of 5.4°F. While the hottest months are April and May, the coolest months are December through February. The country's annual rainfall is 72 inches; however, the higher mountains receive more and the valleys less than this average (The Diagram Group, 1985).

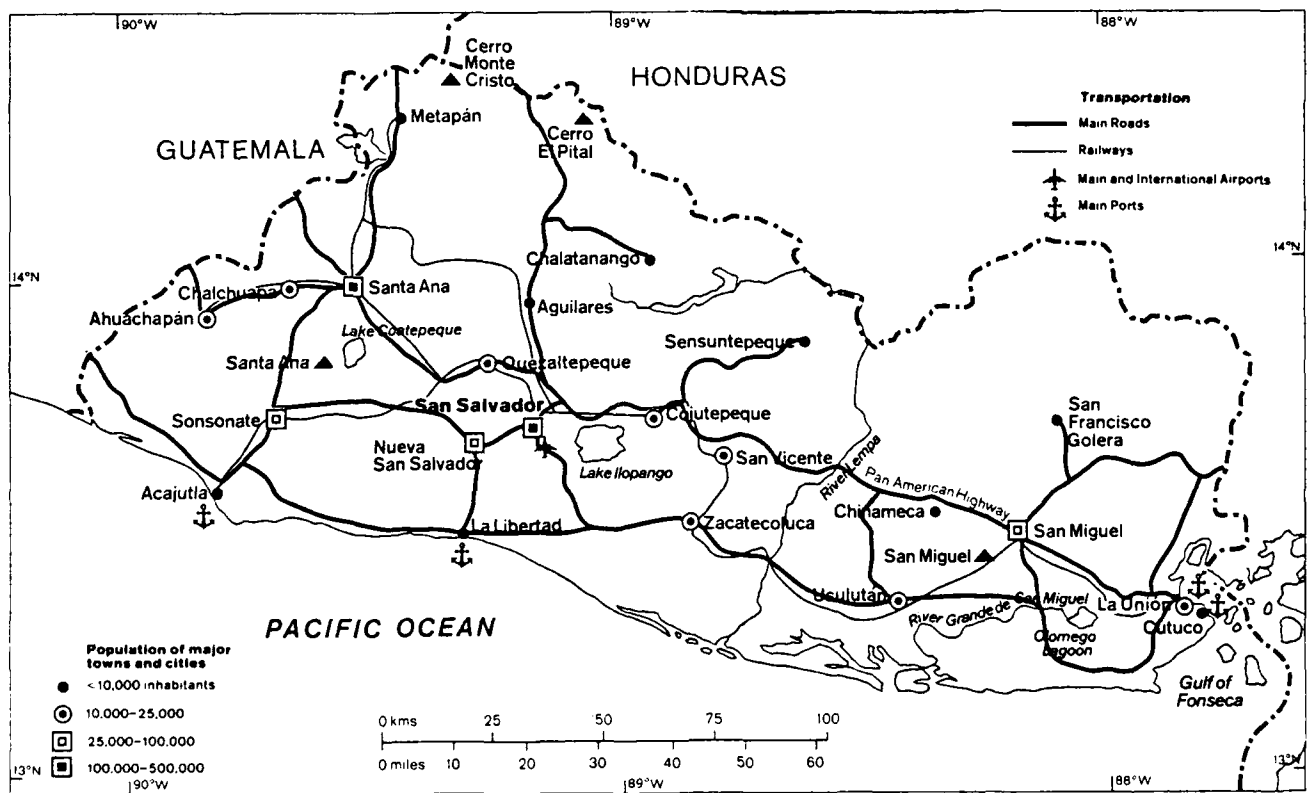


Figure 1.25: El Salvador (The Diagram Group, 1985)

Rainy season: May - October. Heavy rainfall is expected in warm and cloudy weather, with an occasional tropical storm or hurricane. Cloudy skies dominate with: clear skies, 1-3 percent; partly cloudy, 15-35 percent; cloudy, 50-70 percent; and overcast, 10-20 percent of the time. Rain is expected 10-25 days per month, usually associated with thunderstorms. However, gusty surface winds in excess of 16 kt are expected less than 1 percent of the time, with gale force winds (33 kt) rare. The monthly probability of tropical cyclones and/or hurricanes affecting El Salvador increases from 15 percent in May through July to 30 percent in August through October (see Section 5).

Flying weather: Fair to Poor. The percentage frequencies of ceiling/visibility are : less than 5000 feet and/or 6 miles, 10-25 percent; less than 1500/3, 5-10 percent; and less than 500/1, 1-2 percent. Not only are thunderstorms and rain very heavy at times, but heavy rain showers and early morning fog can restrict flying conditions. (See Appendix B for ceiling/visibility statistics at Acajutla and San Salvador.)

Terminal weather: San Salvador. The weather is warm and cloudy, with numerous thunderstorms and heavy rain showers, leading to ceiling/visibility less than 300/1 for 1-2 percent of the time. Runway crosswinds in excess of 15 kt are expected only about 1 percent of the time. Gusty surface winds in excess of 16 kt are expected less than 1 percent, with gale force winds a rarity. Visibility is obstructed 5-10 percent due primarily to haze/smoke and early morning fog; however, during May visibility is obstructed 30 percent of the time due to haze/smoke, dust and early morning fog (USAFETAC, 1985).

Monthly temperature, precipitation, thunderstorms & twilight (USAFETAC, 1985):

SAN SALVADOR	MAY	JUN	JUL	AUG	SEP	OCT
TEMPERATURE (°F)						
Absolute maximum	103	98	98	98	99	101
Mean maximum	91	87	89	89	87	87
Mean minimum	67	66	65	66	66	65
Absolute minimum	58	56	58	60	53	54
MEAN PRECIPITATION (INCHES)	7.4	12.7	12.5	11.7	12.5	9.0
MEAN NUMBER OF DAYS						
Precipitation	13	20	22	21	21	16
Thunderstorms	13	17	18	18	18	10
CIVIL TWILIGHT (15th of month)						
First light (local standard time)	0507	0505	0513	0521	0524	0526
Last light (local standard time)	1838	1848	1851	1840	1819	1759

Dry season: November – April. The weather is hot and dry (see data below), with clear to partly cloudy skies. Partly cloudy skies dominate with: clear skies, 10–35 percent; partly cloudy, 45–50 percent; cloudy 20–40 percent; and overcast, 1–5 percent of the time. Rain occurs only 1–5 days per month, and is usually associated with a thunderstorm. Visibility is obstructed 5–15 percent of the time during November through March, but this percentage increases to 40 percent in April, with the primary restrictions to visibility being haze/smoke and dust. While gusty surface winds in excess of 16 kt are expected 5 percent of the time, gale force winds are rare. Tropical cyclones and/or hurricanes are rare during this period (see Section 5).

Flying weather: Generally good. The percentage frequencies of ceiling/visibility are: less than 5000 feet and/or 6 miles, 5–10 percent, November through March and 25 percent in April; less than 1500/3 miles, 1–2 percent; and less than 500/1, rare. However, early morning fog can restrict flying activities in the highlands (see Appendix B for ceiling/visibility statistics at Acajutla and San Salvador).

Terminal weather: San Salvador, El Salvador. The weather is hot and dry with ceiling/visibility less than 300/1 a rarity. Precipitation is expected 1–5 days per month (see data below), usually associated with a thunderstorm. Primary restrictions to visibility are haze/smoke and dust, leading to obstruction to visibility 5–10 percent from November through February, 15 percent in March, and increasing to 40 percent in April; however, visibility rarely goes below 3 miles. While gusty runway crosswinds in excess of 15 kt are expected about 1–2 percent of the time, gusty surface winds in excess of 16 kt are expected 5 percent of the time, but gale force winds are rare (USAFETAC, 1985).

Monthly temperature, precipitation, thunderstorms & twilight (USAFETAC, 1985):

SAN SALVADOR	NOV	DEC	JAN	FEB	MAR	APR
TEMPERATURE (°F)						
Absolute maximum	102	101	101	103	105	104
Mean maximum	87	89	90	92	94	93
Mean minimum	63	61	60	60	62	65
Absolute minimum	49	47	45	49	45	54
MEAN PRECIPITATION (INCHES)	1.6	0.4	0.2	0.2	0.4	2.1
MEAN NUMBER OF DAYS						
Precipitation	5	1	1	1	1	5
Thunderstorms	5	1	1	1	5	5
CIVIL TWILIGHT (15th of month)						
First light (local standard time)	0534	0549	0601	0558	0543	0522
Last light (local standard time)	1748	1755	1811	1823	1828	1831

1.3.5 Nicaragua

Land

Nicaragua is the largest nation of Central America—a little larger than the state of New York. With the Caribbean Sea to its east and the Pacific Ocean to its west, Nicaragua occupies a “mid” position within Central America (see Fig. 1.26). Only two countries have borders with Nicaragua, Honduras along the long boundary to the north, and Costa Rica to the south.

The shape of Nicaragua somewhat resembles a triangle formed by the Honduran border, the Caribbean coast, and finally a line produced by the Pacific coast and the Costa Rican border. The country's highest mountain Pico Mogotón (6,913 feet) lies in the northwest near the Honduran border. From the Honduran border southward there are three separate mountain chains (“cordilleras”) in the center of the country: Cordillera Isabella running nearly parallel to the Honduran border, next Cordillera De Darien running east-west, and finally Sierra De Amerique (also known as Cordillera Chontaleña) lying to the northeast of Lake Nicaragua. There are many rivers, with River Coco forming much of Nicaragua's border with Honduras, while the San Juan, likewise, forms much of the southern border with Costa Rica.

To the east of these central mountain chains lies Nicaragua's Mosquito coast, one of the broadest Caribbean lowlands in Central America. This coast extends approximately 336 miles, including deltas, sandbars and lagoons, with offshore reefs²³ and islands (“cayos”).

Lake Nicaragua, Central America's largest lake, lies southwest of the mountain chains. This lake and smaller Lake Managua, lie parallel to the Pacific coast but inland of about 40 volcanoes (some active) which also form a line parallel to the Pacific coastline. The Pacific coast of Nicaragua extends from the Gulf of Fonseca to the Salinas Bay. Volcanic ash here, as well as in the central valleys, has produced fertile soil (The Diagram Group, 1985).

Climate

General The lowlands are hot and humid. On the Pacific coast, average annual temperature is 81°F, on the Caribbean coast, 79°F; however, mountains, in the northern portion of the country, have lower temperatures, i.e., about 64°F.

With 150 inches of rainfall per year, the Caribbean side of Nicaragua has one of the highest rainfalls in Central America. However, with the prevailing winds (primarily *katabatic*) blowing from the northeast, the Pacific side of Nicaragua receives only about half that amount with a more marked dry season from January through April (The Diagram Group, 1985).

²³For further oceanographic details, see Section 4.

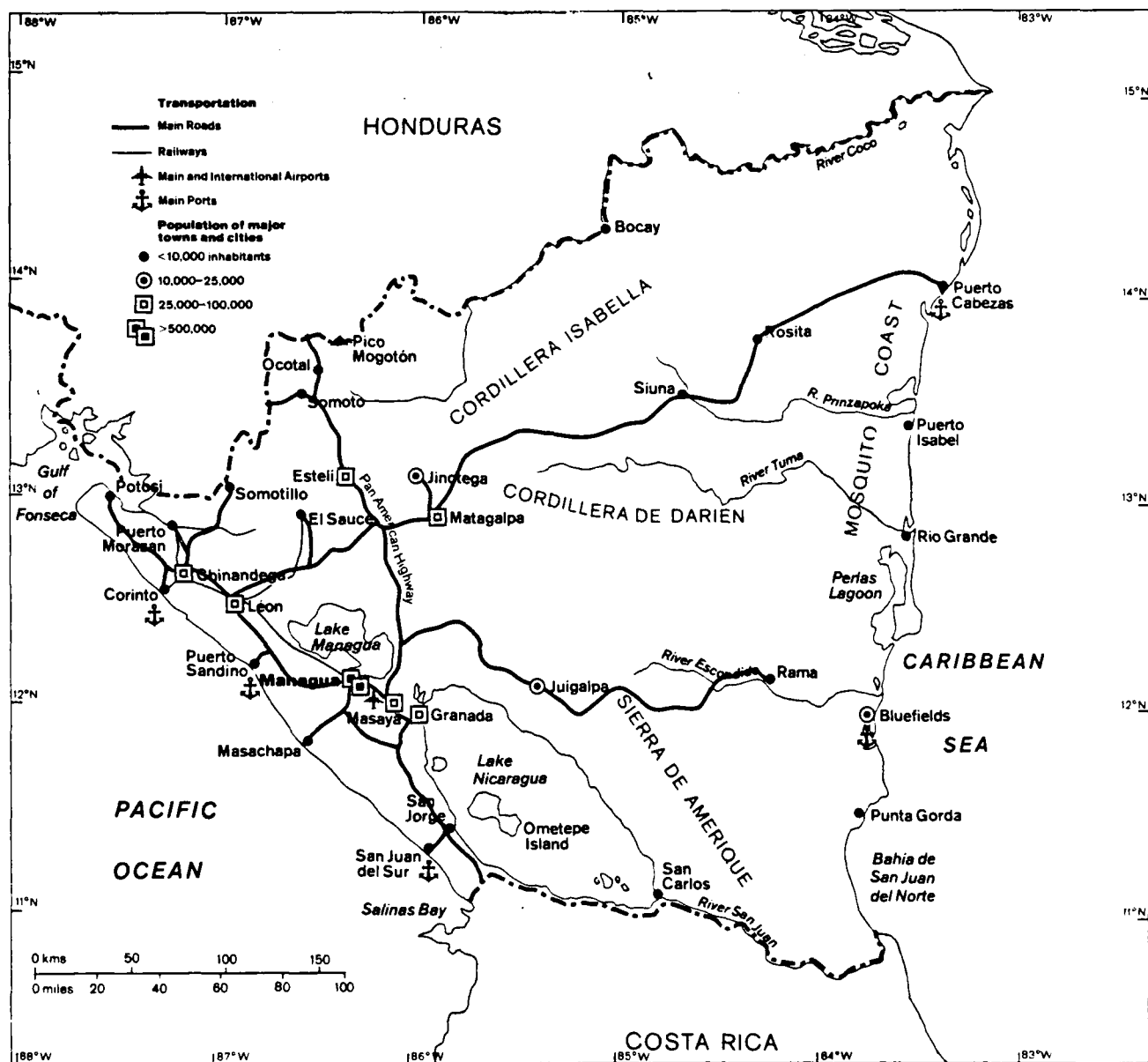


Figure 1.26: Nicaragua (The Diagram Group, 1985)

Rainy season: June - October

These months are characterized by frequent precipitation and heavy cloudiness. Night-time temperatures are quite warm, then climb from the low 70's (°F) in the early morning to the 80's or low 90's by afternoon. Mean sky cover, primarily in the form of low clouds, ranges from 70 to 80 percent. Precipitation, which is smaller in the interior, is most frequent along the Caribbean lowlands where the monthly average is 10-26 inches. Precipitation can be expected 17-30 days per month, and thunderstorms are frequently accompanied by strong, gusty winds and violent lightning. Visibilities are generally good, except along the coast. Fog, heavy rain showers, haze and/or smoke restrict coastal region visibilities to less than 6 miles, 10-20 days per month. Winds, averaging less than 15 kt, are usually calm during the night and then increase during the day, with 55 kt possible during severe thunderstorms. The average monthly probability of a tropical storm and/or hurricane affecting Nicaragua ranges from 15 to 25 percent (see Section 5).

Monthly temperature, precipitation, thunderstorms & twilight (USAFETAC, 1985):

MANAGUA	JUN	JUL	AUG	SEP	OCT
<hr/>					
TEMPERATURE (°F)					
Absolute maximum	95	92	93	94	94
Mean maximum	88	88	89	89	88
Mean minimum	73	73	73	73	72
Absolute minimum	69	70	70	69	66
MEAN PRECIPITATION (INCHES)	8.2	3.6	5.1	6.8	6.3
MEAN NUMBER OF DAYS					
Precipitation	13	11	10	11	10
Thunderstorms	13	13	10	14	7
CIVIL TWILIGHT (15th of month)					
First light (local standard time)	0457	0504	0511	0513	0513
Last light (local standard time)	1833	1837	1827	1807	1748
BLUEFIELDS					
<hr/>					
TEMPERATURE (°F)					
Absolute maximum	94	93	92	94	94
Mean maximum	87	85	87	89	88
Mean minimum	73	73	73	72	71
Absolute minimum	66	67	62	66	64
MEAN PRECIPITATION (INCHES)	19.8	26.2	21.5	12.3	13.6
MEAN NUMBER OF DAYS					
Precipitation	N/A	N/A	N/A	19	20
Thunderstorms	*	*	*	*	*

(* = less than 0.5 day)

(N/A = data not available)

Flying weather: Fair to good. The heavy rainfall along the Caribbean coast, such as at Bluefields (see totals on previous page), produces ceiling/visibility less than 5000 feet and/or 6 miles for 1-15 percent of the time, with less than 1500/3, 1-3 percent. While heavy rain showers and thunderstorms are frequent throughout the country, they are especially prevalent along the coast. Tops of thunderstorms often reach 60,000 feet, some being reported as high as 80,000 feet. Severe turbulence is expected with these storms, plus mountain-wave turbulence presents a hazard to flying west of the mountain ridges, i.e., "downwind" of the ridges (see Appendix B for ceiling/visibility statistics for Bluefields, Chinadega, Managua and Puerto Cabezas).

Terminal weather: Good. At Managua, the percentage frequency of ceiling/visibility less than 300/1 is 0-1 percent; at Bluefields it is 1-2 percent. While mean winds are less than 10 kt during the evening, winds are 15 kt in the afternoon, with even stronger winds associated with thunderstorms, tropical storms and/or hurricanes. Heavy rain showers, fog, smoke and/or haze provide the primary restrictions to visibility (USAFETAC, 1985).

Transitional months: November - December

November and December are the transitional months between the rainy and dry seasons. The hot temperatures and cloudy skies continue; however, there is a general decline in precipitation (particularly notice Managua's rainfall on the following page). While morning temperatures (high 60's (°F)) are slightly cooler than the rainy season, the afternoons still warm to the low 90's. Mean sky cover (20-40 percent) is lower in the inland portion of Nicaragua, but the coastal regions remain near 70 percent. Likewise, the mean precipitation is much less inland than on the coast (compare Managua and Bluefields), with the mean monthly rainfall ranging from 2-20 inches over the country. Thunderstorm days reduce to only 4-6 per month. Fog, smoke and/or haze reduce visibilities to less than 2.5 miles approximately 1 day per month. Usually occurring in the afternoon, winds greater than 16 kt are expected 1-2 days per month. While the probability of at least one tropical storm and/or hurricane affecting Nicaragua is 10 percent in November, tropical cyclones in December are rare (see Section 5).

Flying weather: Fair to good. Despite the larger rainfall at Bluefields, the percentage frequency that ceiling/visibility is less than 5000 feet and/or 6 miles is approximately 5 percent, but at Managua, ceiling/visibility less than 5000/6 is about 15 percent. Expectation of ceiling/visibility less than 1500/3 is 1 percent at both stations. Turbulence is anticipated in thunderstorms; additionally, low-level clear air turbulence is sometimes present on hot, sunny days (see Appendix B for ceiling/visibility statistics for several cities).

Terminal weather:

Managua (Las Mercedes), Nicaragua. Warm and cloudy conditions prevail, with light rain storms and occasionally gusty surface winds. Skies are clear only 5 percent of the time; partly cloudy to cloudy skies dominate 70-80 percent, with overcast, 10-25 percent. Visibility is generally good, as early morning fog occurs less than one day per month. Rain is expected seven days in November, but its frequency decreases to only two days in December (see data below). While gusty winds are expected 2-5 percent of the time, gale force winds are rare and ceiling/visibility less than 300/1 has not been observed.

Bluefields, Nicaragua. Cloudy and rainy, with clear skies a rarity. Skies are partly cloudy to cloudy 75-80 percent; overcast, 20-25 percent. Although rainfall is expected 22 days per month (see data below), the ceiling/visibility rarely goes below 300/1. While gusty surface winds are expected 2-5 percent of the time, gale force winds are a rarity (USAFETAC, 1985).

Monthly temperature, precipitation, thunderstorms & twilight (USAFETAC, 1985):

MANAGUA	NOV	DEC
<hr/>		
TEMPERATURE (°F)		
Absolute maximum	92	91
Mean maximum	88	87
Mean minimum	71	70
Absolute minimum	64	59
MEAN PRECIPITATION (INCHES)	1.2	0.3
MEAN NUMBER OF DAYS		
Precipitation	7	2
Thunderstorms	1	*
<hr/>		
BLUEFIELDS		
TEMPERATURE (°F)		
Absolute maximum	93	93
Mean maximum	86	85
Mean minimum	70	69
Absolute minimum	62	62
MEAN PRECIPITATION (INCHES)	15.3	15.7
MEAN NUMBER OF DAYS		
Precipitation	22	22
Thunderstorms	1	*
CIVIL TWILIGHT (15th of month)		
MANAGUA (LAS MERCEDES)		
First light (local standard time)	0520	0534
Last light (local standard time)	1839	1745

(* = less than 0.5 day)

Dry season: January - April

Distinguished by a marked decline in rainfall (especially note the small precipitation for Managua, below), this season is characterized by hot days, cooler nights and partly cloudy skies. Of course, the Caribbean coast remains an exception where cloudiness and rain persist throughout the year (see the precipitation totals for Bluefields, below). Temperatures range from near 70°F at night to the low 90's during the afternoon, although the afternoon temperatures at Bluefields are not quite so high. Mean sky cover is lower on the Pacific coast and inland (40-50 percent), but, it is near 70 percent along the Caribbean coast. Whereas much of the country experiences only 0.5 inch to 2.0 inches of rainfall, totals reach a maximum near 10 inches along the Caribbean coast, with rain occurring as often as 23 days of the month. Visibility is generally good, decreasing to 2.5 miles only one-three days per month, although visibility is restricted by haze/smoke near industrial centers. While wind speeds average 10-12 kt, gusty surface winds generally occur as often as six days per month. (See Section 5 for hurricane data.)

Monthly temperature, precipitation, thunderstorms & twilight (USAFETAC, 1985):

MANAGUA	JAN	FEB	MAR	APR
<hr/>				
TEMPERATURE (°F)				
Absolute maximum	92	93	94	98
Mean maximum	88	89	91	94
Mean minimum	69	70	72	73
Absolute minimum	62	63	67	68
MEAN PRECIPITATION (INCHES)	*	*	*	*
MEAN NUMBER OF DAYS				
Precipitation	2	2	1	2
Thunderstorms	0	0	0	0
CIVIL TWILIGHT (15th of month)				
First light (local standard time)	0547	0545	0531	0511
Last light (local standard time)	1802	1813	1817	1818
BLUEFIELDS				
<hr/>				
TEMPERATURE (°F)				
Absolute maximum	90	90	91	93
Mean maximum	85	85	87	88
Mean minimum	69	69	71	72
Absolute minimum	60	61	62	62
MEAN PRECIPITATION (INCHES)	10.5	5.1	3.2	2.9
MEAN NUMBER OF DAYS				
Precipitation	22	15	12	11
Thunderstorms	0	0	0	0

(* = less than 0.05 inch)

Flying weather: Fair to good. Bluefields on the Caribbean coast experiences ceiling/visibility less than 5000 feet and/or 6 miles, 1-3 percent of the time; and less than 1500/3, less than 1 percent of the time. In the west, Managua experiences ceiling/visibility less than 5000/6, 10-15 percent; and less than 2000/2.5, approximately 1 percent of the time (see Appendix B for ceiling/visibility statistics at several cities).

Terminal weather:

Managua (Las Mercedes), Nicaragua. Warm and cloudy with gusty surface winds and *little* precipitation. Skies are clear 10-15 percent of the time, with rain expected only 1-2 days per month (see data on preceding page). The visibility is restricted by haze and/or smoke 45-50 percent, but rarely goes below 6 miles. While gusty surface winds generally exist 5-10 percent of the time, gale force winds are experienced less than 1 percent of the time. Ceiling/visibility less than 300/1 is a rarity.

Bluefields, Nicaragua. Cloudy and **rainy**. Partly cloudy to cloudy skies (85-90 percent) dominate, with overcast skies 10-15 percent of the time and clear skies a rarity. Mean monthly rainfall, totally 10.5 inches (22 rainfall days) in January, decreases to 2.9 inches (11 rainfall days) in April (see data on preceding the page). Gusty surface winds are expected 2-5 percent of the time; however, gale force winds are rare. Visibility is restricted by haze/smoke 25-30 percent of the time, but it rarely goes below 6 miles. While, early morning fog forms occasionally, it dissipates rapidly after sunrise (USAFETAC, 1985).

Transitional month: May

May is the transition month between the dry and rainy seasons. Rainfall and cloudiness both increase in all parts of Nicaragua. Cloudy skies dominate with: clear 1-5 percent, partly cloudy 20-25 percent, cloudy 40-60 percent and overcast 15-35 percent of the time. While rain occurs on 10-17 days, thunderstorms occur only 2-4 days, depending on location. As expected, skies are cloudiest and rainfall heaviest on the Caribbean side of mountains. While winds in excess of 16 kt are expected approximately 5 percent of the time, gale force winds are rare. The monthly probability of a tropical storm and/or hurricane affecting Nicaragua, being near zero during the dry season, increases to 5 percent (see Section 5).

Flying weather: Fair to good. At Managua, ceiling/visibility is less than 5000 feet and/or 6 miles, 30 percent of the time; less than 1500/3, approximately 1 percent; and less than 500/1, near zero. Heavy rainfall and cloudiness may restrict flying, particularly on the eastern side of the mountains. Additionally, mountain-wave turbulence is possible over and near mountains (see Appendix B for ceiling/visibility statistics for several cities).

Terminal weather: Generally good. While ceiling/visibility is less than 300/1, approximately 1-2 percent of the time; rain is, nonetheless, frequent and heavy at times. Fog is expected only 1 percent of the time, primarily during the early morning hours. At Managua, the visibility is restricted 60 percent of the time by haze and/or smoke. While gusty winds greater than 16 kt are expected 5 percent of the time, gale force winds are a rarity (USAFETAC, 1985).

Monthly temperature, precipitation, thunderstorms & twilight (USAFETAC, 1985):

MANAGUA (LAS MERCEDES) MAY

TEMPERATURE (°F)

Absolute maximum	98
Mean maximum	93
Mean minimum	74
Absolute minimum	65

MEAN PRECIPITATION (INCHES) 3.1

MEAN NUMBER OF DAYS

Precipitation	10
Thunderstorms	2

BLUEFIELDS

TEMPERATURE (°F)

Absolute maximum	94
Mean maximum	87
Mean minimum	74
Absolute minimum	67

MEAN PRECIPITATION (INCHES) 13.6

MEAN NUMBER OF DAYS

Precipitation	17
Thunderstorms	0

CIVIL TWILIGHT (15th of month)

MANAGUA (LAS MERCEDES)

First light (local standard time)	0458
Last light (local standard time)	1824

1.3.6 Costa Rica

Land

Costa Rica, Central America's fifth-largest nation, is slightly larger than Vermont and New Hampshire combined. Long and narrow, it has a mountainous spine running from Nicaragua in the north to Panama in the southeast (see Fig. 1.27). Its long irregular Pacific coastline measures 631 miles compared with a much shorter and more straight Caribbean shore of only 132 miles.

While the swampy Caribbean coastal plain forms 30 percent of Costa Rica, the mountainous spine consists of three mountain ranges (cordilleras), from the northwest to the southeast: Guanacaste, Central and Talamanca. It's highest mountain peak Chirripó (12,529 feet) is found in the southeastern portion of the country in the Talamanca range. Within these ranges, the mountains are flanked by fertile tablelands. The soil has been made rich by volcanic ash, such as that which fell from the eruption of Irazú (in central Costa Rica, see Fig. 1.27) in 1963-1964.

On the irregular, low Pacific coast are found both the hilly Nicoya and Osa peninsulas. While the River El Coco (also known as the Rio Grande) flows from central Costa Rica westward into the Gulf of Nicoya, the country's largest river is the navigable San Juan, shared in part by Nicaragua, which flows into the Caribbean Sea (The Diagram Group, 1985).

Climate

General Typical of Central America, Costa Rica has hot, humid coasts, but cooler uplands. Average temperatures range from above 80°F near the coast, 69°F in the capital San José, at 3,800 feet, to only 59°F near 7,500 feet. The "temperate" or "cold" zones start at about 1,000 feet, but are lower on the Pacific than on Caribbean slopes.

Not only on the Caribbean coast, but also on the southern Pacific coast, rainfall totals over 126 inches per year. In particular, on the Caribbean side, northeast winds can provide 300 days with rain—the orographically produced cloudiness on the east side of the mountain ranges is frequently evident on satellite imagery (The Diagram Group, 1985).

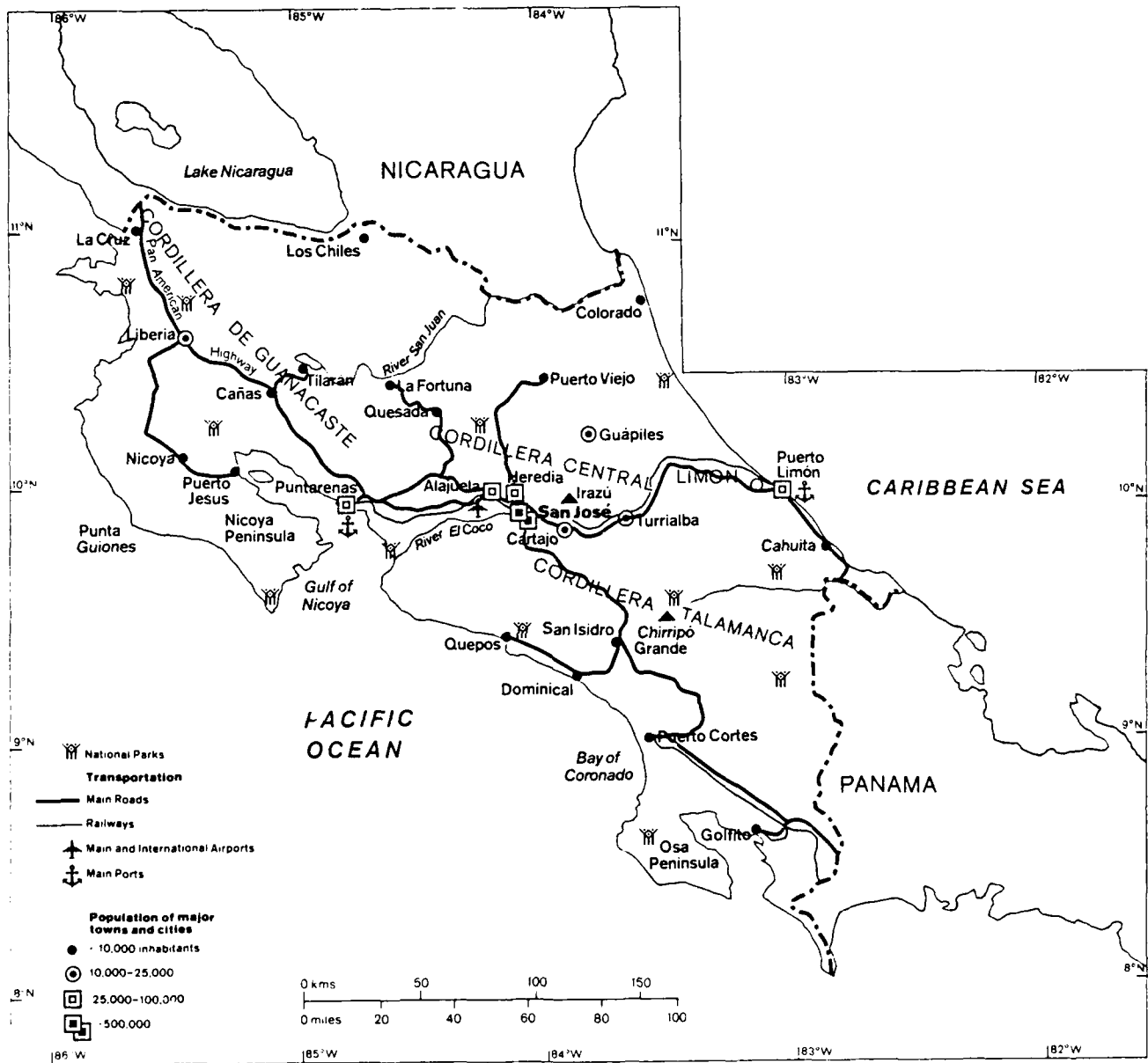


Figure 1.27: Costa Rica (The Diagram Group, 1985)

Rainy season: May – November. This is the rainy season with moderate to heavy rain, cloudy skies and warm temperatures. Mean rainfall averages 10 to even 26 inches per month at some locations. While thunderstorms are expected on 5–10 days per month; skies are clear less than 5 percent of the time; partly cloudy to cloudy, 40–55 percent; and overcast, 50–60 percent. Weather generally improves in November, as the dry season approaches (see Section 5 for the rather unlikely possibility of tropical storm or hurricane threat).

Flying weather: Poor to fair due to rainfall and cloudiness. Ceiling/visibility is less than 5000 feet and/or 6 miles between 10 to 25 percent of the time; less than 1500/3, 5 to 10 percent of the time. Thunderstorms are numerous, as noted below (see Appendix B for ceiling/visibility statistics for Liberia, Puerto Limón, Puntarenas and San José).

Terminal weather: San José/El Coco International, Costa Rica. The weather is warm, cloudy, windy and rainy. While the skies are: clear, less than 5 percent of the time; partly cloudy, 10–20 percent; cloudy, 25–30 percent; and overcast, 40–60 percent, the frequency that the ceiling/visibility is less than 300/1 is only 2 percent. Whereas winds greater than 16 kt are present 5–25 percent of the time, their maximum frequency is realized in July, with their minimum in September–October. Nevertheless, gale force winds are expected less than 1 percent of the time (USAFETAC, 1985).

Monthly temperature, precipitation, thunderstorms & twilight (USAFETAC, 1985):

SAN JOSÉ/EL COCO	MAY	JUN	JUL	AUG	SEP	OCT	NOV
TEMPERATURE (°F)							
Absolute maximum	88	92	84	85	86	85	84
Mean maximum	80	79	77	78	79	77	77
Mean minimum	62	62	62	61	61	60	60
Absolute minimum	54	56	54	56	56	55	52
MEAN PRECIPITATION (INCHES)	9.3	9.6	7.6	7.4	12.4	14.0	4.8
MEAN NUMBER OF DAYS							
Precipitation	18	21	23	23	26	26	15
Thunderstorms	7	5	5	5	8	6	1
CIVIL TWILIGHT (15th of month)							
First light (local standard time)	0453	0453	0500	0506	0505	0504	0509
Last light (local standard time)	1812	1821	1824	1816	1758	1741	1733

Dry season: December - April. The weather, dry and windy in the mountains and western Costa Rica in accordance with the season's name, is, nonetheless, cloudy with **moderate to heavy rainfall** on the Caribbean or eastern side of the mountains. Although rainfall averages 1 inch or less in the mountains and Pacific coast regions, it remains high on the eastern side, 5-22 inches. Thunderstorm occurrence varies from 1-3 days per month (see data below). While occasional outbreaks of cold air from North America provide below-normal temperatures and fresh breezes, normal temperatures average in the mid 60's to low 70's (°F) during the morning hours and then reach the mid 80's to low 90's in the afternoon. High winds can be expected in mountainous regions during all months; moreover, isolated mountain locations may be slightly cooler than mentioned earlier.

Flying weather: Generally good. Although the mountains and western Costa Rica generally have clear to partly cloudy skies, flying may be restricted in eastern Costa Rica in clouds and moderate to heavy rain showers. At San José/El Coco International, ceiling/visibility is less than 5000 feet and/or 6 miles approximately 5 percent of the time, while ceiling/visibility less than 1500/3 is approximately 1 percent of the time (see Appendix B for ceiling/visibility statistics at several cities).

Terminal weather: San José/El Coco International, Costa Rica. While warm and windy conditions exist with clear to partly cloudy skies 45-75 percent of the time, cloudiness increases in April with the approach of the rainy season. Rainfall is expected only 1-2 days per month during the driest months, January through March (see data below). Fog is rare, but visibility is occasionally restricted by haze and/or smoke. The ceiling/visibility is less than 300/1 less than 1 percent of the time. Note that winds greater than 16 kt occur 50-65 percent of the time; gale force winds, 5-10 percent of the time. Runway crosswinds greater than 15 kt occur 15-20 percent of the time (USAFETAC, 1985).

Monthly temperature, precipitation, thunderstorms & twilight (USAFETAC, 1985):

SAN JOSÉ/EL COCO	DEC	JAN	FEB	MAR	APR
TEMPERATURE (°F)					
Absolute maximum	87	87	88	91	89
Mean maximum	75	75	76	79	79
Mean minimum	58	58	58	59	62
Absolute minimum	49	49	51	50	53
MEAN PRECIPITATION (INCHES)	1.3	0.2	0.6	0.6	1.7
MEAN NUMBER OF DAYS					
Precipitation	7	1	2	2	6
Thunderstorms	0	*	*	1	3
CIVIL TWILIGHT (15th of month)					
First light (local standard time)	0522	0535	0535	0523	0505
Last light (local standard time)	1741	1757	1807	1808	1808

(* = less than 0.5 day)

1.3.7 Panama

Land

Panama is the fourth largest and southernmost of the nations of Central America. It is bordered on the west by Costa Rica and on the east by Colombia, with the Caribbean Sea and North Pacific Ocean forming its northern and southern shores, respectively. While Panama is the most narrow country of Central America, its coastline is the longest of any of the seven nations. At its most narrow width Panama is only 31 miles across (see Fig. 1.28); however, its Pacific coastline extends for 760 miles, and its Caribbean coastline is 470 miles long.

Low mountain ranges run the length of the country, reaching the greater heights in the west, including the country's highest peak, the volcano Chiriquí, with an elevation of 11,411 feet. The mountain range shown as Serranía de Tabasara (see Fig. 1.28) is also known as Cordillera Central. While three-fifths of Panama is mountainous, between parallel mountain ranges lie fertile valleys and plains, in addition to the low-lying, sometimes swampy, coastal strips. Located in the eastern half of the country are the chief rivers: the Chagres, near the canal; the Chepo; and the Tuira, with its source in Colombia. Its only large lake, Gatún, is man-made.

Obvious from Fig. 1.28, its Pacific coast is much indented, with the Azuero Peninsula forming the western side of the Gulf of Panama. While the country's southeastern coast is on the Gulf of Panama in the Pacific Ocean, much of the northwestern coastline is on the Mosquito Gulf in the Caribbean Sea. The eastern side of the Gulf of Panama contains the Pearl Island archipelago, while its largest island, Coiba, lies in the Pacific Ocean to the west of the Azuero Peninsula.

The Panama Canal cuts across²⁴ the center of Panama, from northwest to southeast (The Diagram Group, 1985).

²⁴Geography students are often surprised to learn that the Pacific entrance to the Panama Canal is *east* of the Caribbean (or Atlantic) entrance to the canal.

Climate

General The climate of Panama is generally tropical and rainy. While lowland temperatures average over 80°F, uplands are cooler at 66°F or less. Along the Caribbean coast and in the high mountains, more than 120 inches of rain falls per year; however, parts of the Pacific coast around the Gulf of Panama have less than 60 inches per year. Panama is considered to be outside the "hurricane belt" (The Diagram Group, 1985).

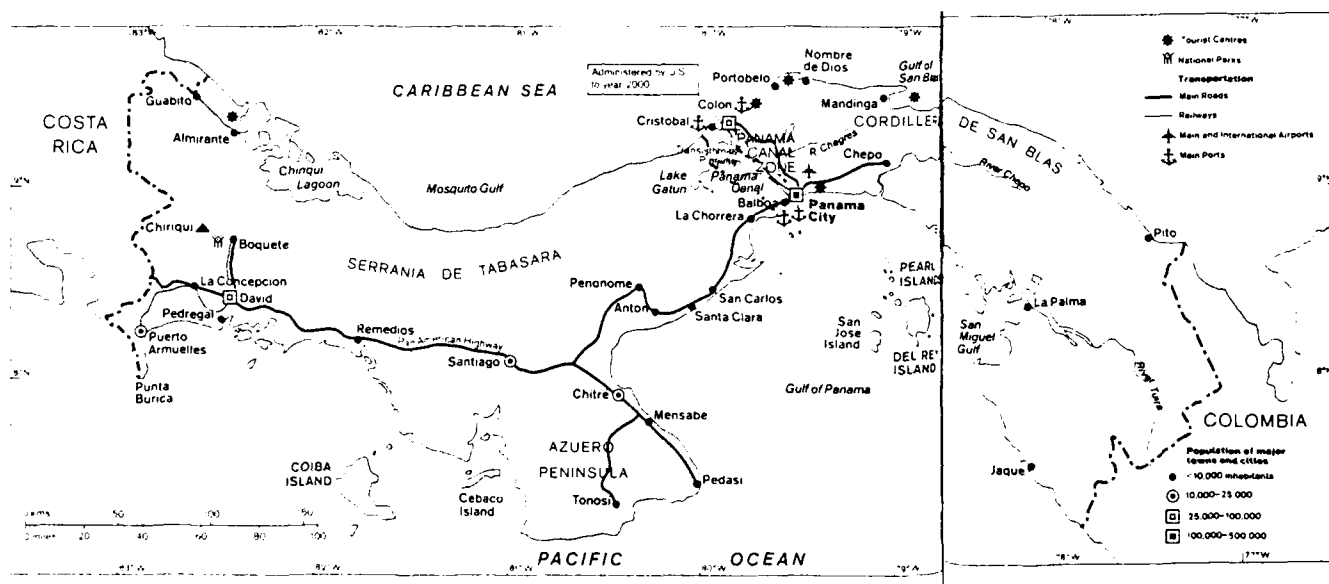


Figure 1.28: Panama (The Diagram Group, 1985)

Summer: June - August. During this season²⁵, the Intertropical Convergence Zone (ITCZ) passes to the north of Panama. The passage of the ITCZ is marked by an increase in precipitation, but there is a decrease as the ITCZ moves farther north. The typical weather in Panama consists of cloudy skies, high humidity, very warm temperatures and frequent afternoon showers and thunderstorms. Maximum temperatures are near 90°F along the coasts and 70°F-80°F in the mountains; whereas, minima are generally in the low 70's near the coast and mid 50's in the mountains. Mean cloudiness is a relative large 70-95 percent, and the average relative humidity is near 85 percent. Precipitation is likely 15-25 days per month, with thunderstorms 10-15 days per month. Gale force winds are a rarity.

Flying weather: While ceiling/visibility less than 5000 feet and/or 6 miles occurs *only* 10-30 percent of the time along the southern coast, ceiling/visibility less than 5000/6 occurs 40-65 percent of the time along the northern coast and over the mountain ranges. Similarly, ceiling/visibility less than 1500/3 occurs 2-12 percent of the time along the southern coast, but 15-35 percent along the northern coast or mountain ranges. Finally, ceiling/visibility less than 500/1 occurs 1-2 percent along the southern coast, yet 2-10 percent along the northern coast and mountain ranges. Expect late afternoon thunderstorms to affect any late afternoon flying operations; however, conditions normally improve at night. (See Appendix B for ceiling/visibility statistics for Fort Sherman, Howard Air Force Base and Rio Hato.)

Terminal weather:

Panama City/Torrijos International. While ceiling/visibility less than 300/1 occurs only 1-5 percent of the time, the most likely time is in the afternoon. Thunderstorms (about 17 or 18 days per month, see data on following page) provide the greatest problem (US-AFETAC, 1985).

²⁵Unlike the other six countries of Central America, with their rainy season and dry season, the proximity and effects of the Intertropical Convergence Zone (ITCZ) dictate the use of the more classical four seasons for Panama.

Monthly temperature, precipitation, thunderstorms & twilight (USAFETAC, 1985):

PANAMA CITY/TORRIJOS INTERNATIONAL JUN JUL AUG

TEMPERATURE (°F)

Absolute maximum	95	95	97
Mean maximum	87	88	86
Mean minimum	75	74	74
Absolute minimum	69	69	68

MEAN PRECIPITATION (INCHES)

7.9 7.6 7.5

MEAN NUMBER OF DAYS

Precipitation	21	21	22
Thunderstorms	17	17	18

CIVIL TWILIGHT (15th of month)

First light (local standard time)	0537	0544	0549
Last light (local standard time)	1901	1905	1905

CHANGUINOLA INTERNATIONAL *

TEMPERATURE (°F)

Absolute maximum	93	93	93
Mean maximum	89	88	88
Mean minimum	73	73	73
Absolute minimum	69	68	69

MEAN PRECIPITATION (INCHES)

7.9 11.3 9.3

MEAN NUMBER OF DAYS

Precipitation	18	21	18
Thunderstorms	13	17	17

(*Changuinola is near the northwest Caribbean coast, just east of Guabito.)

Autumn: September – November. The autumn marks the return southward of the ITCZ. The table on the next page indicates a secondary precipitation maximum in October for Panama City, but in November for Changuinola. This season generally has the most precipitation, highest mean relative humidity and lowest wind speed. Maximum temperatures are in the mid to high 80's (°F) along the coast, but only in the 70°F–80°F range in the mountains. Both relative humidity averages (87 percent) and mean cloud cover (70 to 95 percent) are high. While precipitation occurs on 22–27 days per month, thunderstorms can be expected 10–20 days per month. Gale force winds remain extremely rare.

Flying weather: Ceiling/visibility below 5000 feet and/or 6 miles occurs 5–25 percent of the time along the Pacific coast, but 15–40 percent along the Caribbean coast and on the continental divide. Less than 1500/3 occurs 3–10 percent of the time along the Pacific coast, however, 1–25 percent along the Caribbean coast and on the continental divide. While ceiling/visibility less than 500/1 occurs less than 1 percent along the southern coast, 500/1 occurs about 3 percent along the northern coast and on the continental divide. Afternoon showers and thunderstorms produce low ceilings that may restrict flight operations. (See Appendix B for ceiling/visibility statistics for several stations.)

Terminal weather:

Panama City/Torrijos International. While ceiling/visibility less than 300/1 occurs only 1–4 percent of the time, thunderstorms are numerous during this season occurring an average of 18 days in October (see data on the following page) (USAFETAC, 1985).

Monthly temperature, precipitation, thunderstorms & twilight (USAFETAC, 1985):
PANAMA CITY/TORRIJOS INTERNATIONAL SEP OCT NOV

<u>TEMPERATURE (°F)</u>			
Absolute maximum	95	95	94
Mean maximum	85	85	85
Mean minimum	75	74	74
Absolute minimum	69	69	66
MEAN PRECIPITATION (INCHES)	7.5	11.6	10.2
MEAN NUMBER OF DAYS			
Precipitation	23	24	22
Thunderstorms	15	18	10
CIVIL TWILIGHT (15th of month)			
First light (local standard time)	0547	0545	0549
Last light (local standard time)	1839	1823	1817

CHANGUINOLA INTERNATIONAL *

<u>TEMPERATURE (°F)</u>			
Absolute maximum	94	94	93
Mean maximum	89	89	89
Mean minimum	73	72	71
Absolute minimum	58	59	58
MEAN PRECIPITATION (INCHES)	5.1	5.5	10.1
MEAN NUMBER OF DAYS			
Precipitation	14	16	18
Thunderstorms	15	13	9

(*Changuinola is near the northwest
Caribbean coast, just east of Guabito.)

Winter: December – February. Winter (although such a seasonal title does not seem appropriate to mid-latitude dwellers) in Panama is the start of the dry season—more evident at Panama City than at Changuinola (see precipitation totals, on the following page). During this season, skies are partly cloudy, and temperatures remain high with windy conditions. The ITCZ moves far to the south of Panama, permitting the northeast winds to dominate (see Fig. 1.4). Maximum temperatures are in the high 80's (°F) along the coasts, and near 70°F in the central mountains. Minimum temperatures lie in the low 70's (°F) along the coast, but in the range 46°F to 59°F in the central mountains. While mean cloudiness is 50–70 percent, higher values are found along the northern coast (note the greater rainfall at Changuinola, on the following page) and in the mountains. Relative humidity values range from 50–90 percent, also highest in December and along the northern coast. Precipitation occurs mainly from afternoon and evening showers and thunderstorms: 5–15 days per month along the southern coast; and 10–25 days per month in the mountains and along the northern coast. However, thunderstorms are at a minimum averaging 0–5 days per month. While winds 17 kt or greater occur 5–20 percent of the time in January and February, gale force winds are rare, occurring only 2 percent of the time.

Flying weather: Fair to good. Ceiling/visibility below 5000 feet and/or 6 miles occurs 2–12 percent of the time on the southern coast, but 10–30 percent over the continental divide and the northern coast. Similarly, ceiling/visibility less 1500/3 occurs about 1 percent of the time over the southern coast, yet 5–15 percent over the mountains and northern coast. Ceiling/visibility less than 500/1 rarely occurs. The least favorable flying weather occurs in the late afternoon due to shower activity (see Appendix B for ceiling/visibility statistics at several stations).

Terminal weather:

Panama City/Torrijos International. Good. Ceiling/visibility less than 500/1 occurs less than 1 percent of the time, with the worst flying conditions in late afternoon. Thunderstorm frequency, highest in December, is much smaller in January and February (USAFETAC, 1985).

Monthly temperature, precipitation, thunderstorms & twilight (USAFETAC, 1985):
PANAMA CITY/TORRIJOS INTERNATIONAL DEC JAN FEB

<u>TEMPERATURE (°F)</u>			
Absolute maximum	94	94	95
Mean maximum	87	88	89
Mean minimum	73	72	73
Absolute minimum	64	64	64
MEAN PRECIPITATION (INCHES)	5.6	1.5	0.9
MEAN NUMBER OF DAYS			
Precipitation	15	8	5
Thunderstorms	4	1	0
CIVIL TWILIGHT (15th of month)			
First light (local standard time)	0603	0616	0616
Last light (local standard time)	1825	1840	1849

CHANGUINOLA INTERNATIONAL #

<u>TEMPERATURE (°F)</u>			
Absolute maximum	92	96	91
Mean maximum	87	87	87
Mean minimum	71	70	71
Absolute minimum	66	65	65
MEAN PRECIPITATION (INCHES)	13.4	9.3	6.2
MEAN NUMBER OF DAYS			
Precipitation	21	17	14
Thunderstorms	2	*	0

(#Changuinola is near the northwest
 Caribbean coast, just east of Guabito.)
 (* = less than 0.5 day)

Spring: March - May. As the ITCZ begins its return northward, spring marks the end of Panama's dry season. However, rainfall doesn't increase dramatically until May, especially in Panama City (see data on next page). Additionally, most locations have their minimum rainfall during the month of March (which in this particular seasonal grouping comes a month *after* the "dry" season). Compared with the winter values, mean cloudiness increases to 45-90 percent, with higher values in the mountains. While daily maximum temperatures are in the mid to high 80's (°F) along the coast, the maximum temperature averages in the 70°F - 79°F range in the mountains. Average minimum temperatures along the coast are in the mid 70's (°F), with 46°F - 60°F in the mountains. Average relative humidity is 75-80 percent. Precipitation gradually increases, especially noticeable at Panama City where the average of four precipitation days per month during March increases to 22 in May (see data on the following page). Thunderstorms also increase at Panama City, from one per month in March to 15 in May. Gale force winds, although slightly more frequent on the southwest coast, have an average frequency of only 1 percent.

Flying weather: Fair to good. Ceiling/visibility less than 5000 feet and/or 6 miles occurs 5-15 percent of the time along the southern coast, yet 15-40 percent along the northern coast and in the mountains. Similarly, ceiling/visibility less than 1500/3 occurs only 1-5 percent along the southern coast, compared to 10-20 percent along the northern coast and continental divide. Although ceiling/visibility less than 500/1 averages less than 1 percent, diurnal showers and thunderstorms lead to deteriorating conditions in the late afternoon and evening (see Appendix B for ceiling/visibility statistics for several stations).

Terminal weather:

Panama City/Torrijos International. Good. While ceiling/visibility less than 300/1 occurs only 1-2 percent of the time, the worst conditions occur in the morning near inland lakes and bays, and in the afternoon in the mountains. Thunderstorm frequency triples in May compared with March and April (USAFETAC. 1985).

Monthly temperature, precipitation, thunderstorms & twilight (USAFETAC, 1985):
PANAMA CITY/TORRIJOS INTERNATIONAL MAR APR MAY

TEMPERATURE (°F)			
Absolute maximum	97	94	96
Mean maximum	90	90	88
Mean minimum	74	74	75
Absolute minimum	63	64	69
MEAN PRECIPITATION (INCHES)	0.3	2.7	8.8
MEAN NUMBER OF DAYS			
Precipitation	4	9	22
Thunderstorms	1	4	15
CIVIL TWILIGHT (15th of month)			
First light (local standard time)	0604	0548	0537
Last light (local standard time)	1850	1849	1901

CHANGUINOLA INTERNATIONAL #

TEMPERATURE (°F)			
Absolute maximum	92	93	94
Mean maximum	88	88	89
Mean minimum	71	72	73
Absolute minimum	66	68	64
MEAN PRECIPITATION (INCHES)	5.7	7.2	8.4
MEAN NUMBER OF DAYS			
Precipitation	10	12	12
Thunderstorms	*	2	10

(#Changuinola is near the northwest
 Caribbean coast, just east of Guabito.)
 (* = less than 0.5 day)

THIS PAGE
INTENTIONALLY BLANK

1. TROPICAL METEOROLOGY OF CENTRAL AMERICA

1.1 General Introduction

This Handbook describes the analysis and forecasting of both atmospheric and oceanic conditions important to air/sea operations over Central America and adjacent waters.

Central America, as addressed in this handbook, includes the following seven nations, commencing with the nation located farthest west: Guatemala, Belize, El Salvador, Honduras, Nicaragua, Costa Rica and Panama (Figs. 1.1, 1.2).

Central America, lying between 7°N and 19°N, has its weather primarily influenced by features carried by the low-level “easterlies”¹ for most of the year, yet it is susceptible to the penetration of cold fronts (shear lines or “Atemporalados”²) during the Northern Hemisphere winter. While the time of the “rainy season” cannot be generalized for all of Central America, Portig (1976) depicts the rainy season for the North Pacific portion of Central America from about May through October, while it is a month later for the North Atlantic portion, i.e., from about June through November—despite appreciable rain in December.

While the threat of tropical storms or hurricanes is small, it cannot be dismissed, since all of the countries³ have experienced tropical cyclones, especially northeastern Honduras and Nicaragua, and Belize.

¹Meteorological convention dictates that wind direction is the direction **from** which the wind is blowing i.e., easterly winds blow **from** the east (toward the west).

²See Subsubsection 3.2.3.

³Panama and Costa Rica, minimally.

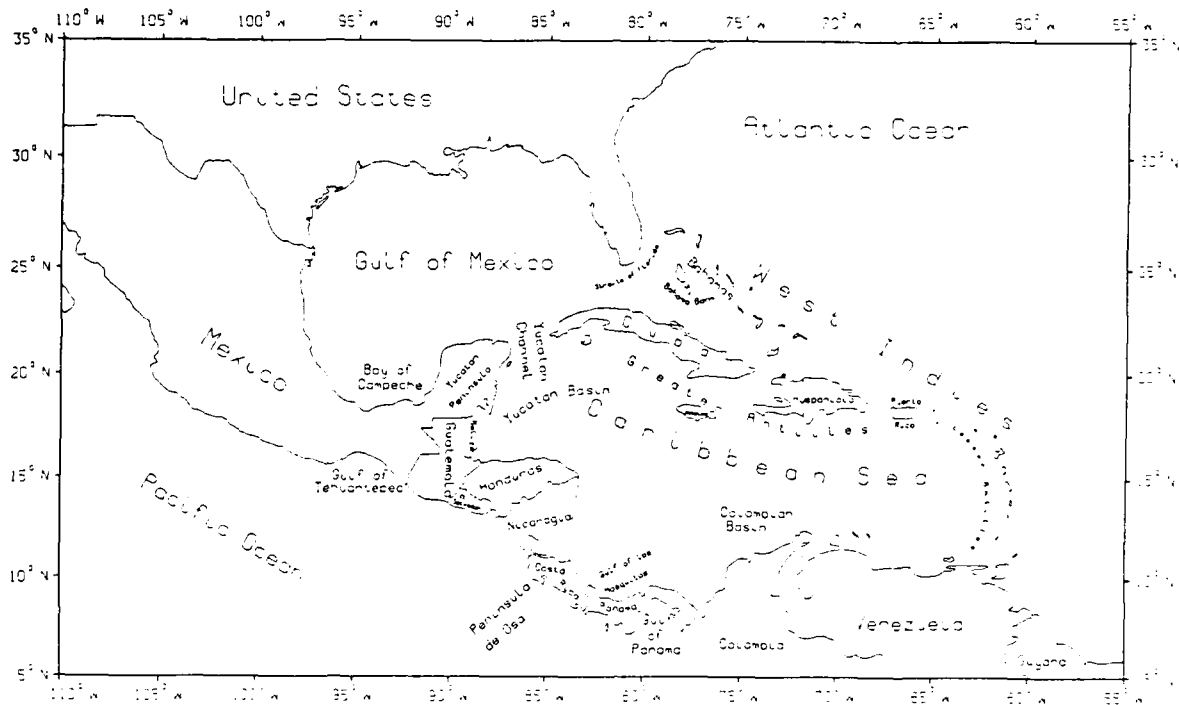


Figure 1.1: Central America and Surrounding Region (NOCD, Asheville, 1985)

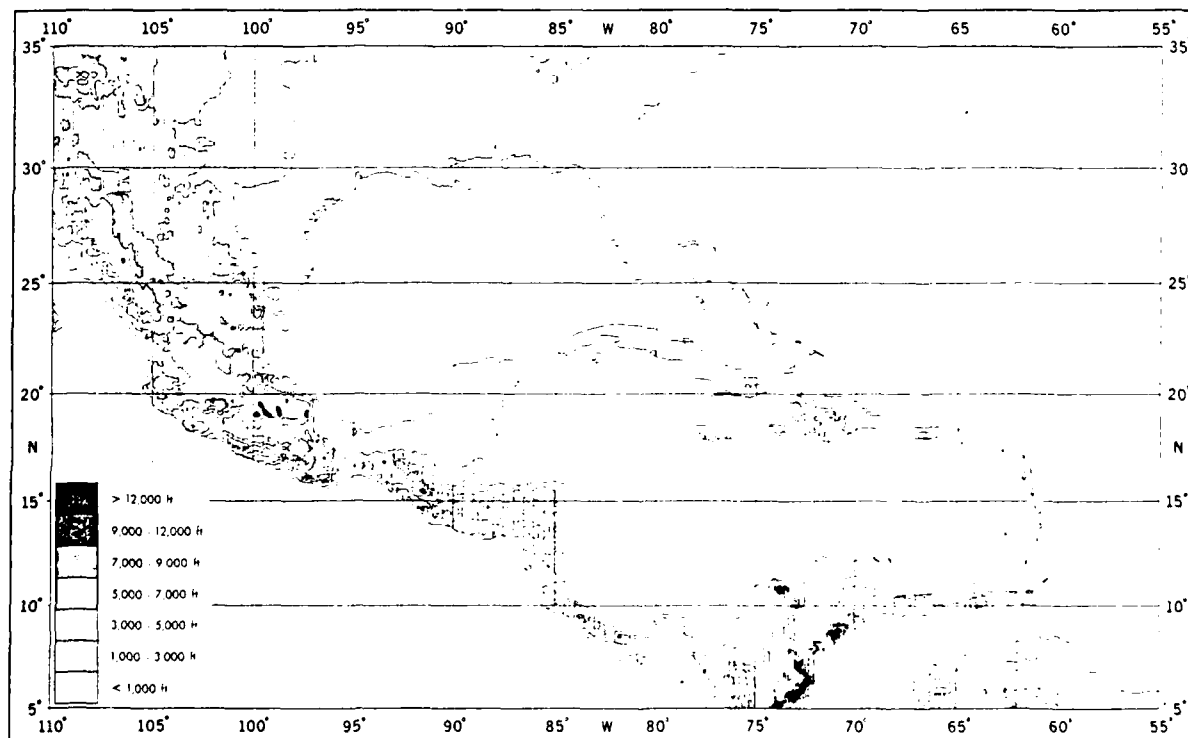


Figure 1.2: Topography (NOCD, Asheville, 1985)

1.2 Regional Climatologies

1.2.1 Rainy Season and Dry Season Charts

While the appendices have extensive excerpts from more complete climatological references, the following sets of charts portray the features of the "rainy season" (August)⁴ and the "dry season" (February).

Figures 1.3 and 1.4, from Sadler et al. (1987)⁵, depict the resultant surface wind direction and speed, for August and February, respectively. The migration of surface convergence over the North Pacific Ocean, from near 10°N in August southward to near 5°N in February, is obvious.

Figures 1.5 and 1.6, from Sadler and Wann (1984), depict the mean 200 mb (upper tropospheric) flow⁶ for August and February, respectively. In August, the mean position of the Tropical Upper Tropospheric Trough (TUTT) extends eastward from just north of Belize separating the subtropical ridge (in the northern Gulf of Mexico) and the subequatorial ridge (extending from southern Guatemala through Nicaragua, eastward). The greater geopotential heights found in the subequatorial ridge correlate well with the enhanced convection associated with the more northerly August position of surface convergence (called, by some, the Intertropical Convergence Zone (ITCZ)). However, the mean 200 mb flow in February is southwesterly, increasing from an average 10 kt south of Panama to 40 kt just north of Belize.

Figures 1.7 and 1.8 from Sadler et al. (1987) depict averaged sea-level pressure for August and February, despite the preference of streamline/isotach analysis over pressure (or contour) analysis in the tropics (see Appendix A). It is immediately obvious that the lowest average sea-level pressure (for this large (synoptic) scale) is found over Panama and Costa Rica in both the rainy and dry seasons.

⁴These representative months have been rather arbitrarily selected. See Subsection 1.2.2 for further explanation. While Portig (1976) divides Central America into 14 rainfall regimes, USAFETAC (1985) supports the selection of these months, but includes "transitional" months between the rainy and dry seasons for Nicaragua, as well as a secondary rainfall maximum for Panama in October.

⁵Only the last 80 years, 1900 - 1979, have been used from the Comprehensive Ocean-Atmosphere Data Set (COADS). COADS is a continuing cooperative effort to compile global ship observations (initially for the period 1850 - 1979) between the National Oceanic and Atmospheric Administration (NOAA)—its Environmental Research Laboratories, National Climatic Data Center (NCDC) and Cooperative Institute for Research in Environmental Sciences (CIRES)—and the National Science Foundation's National Center for Atmospheric Research (NCAR). Details of how the ship observations were collected, evaluated and compiled are contained in Woodruff et al. (1987).

⁶The period of record is 1960 - 1973, consisting of 175,000 PIREP and RAWIN observations per month.

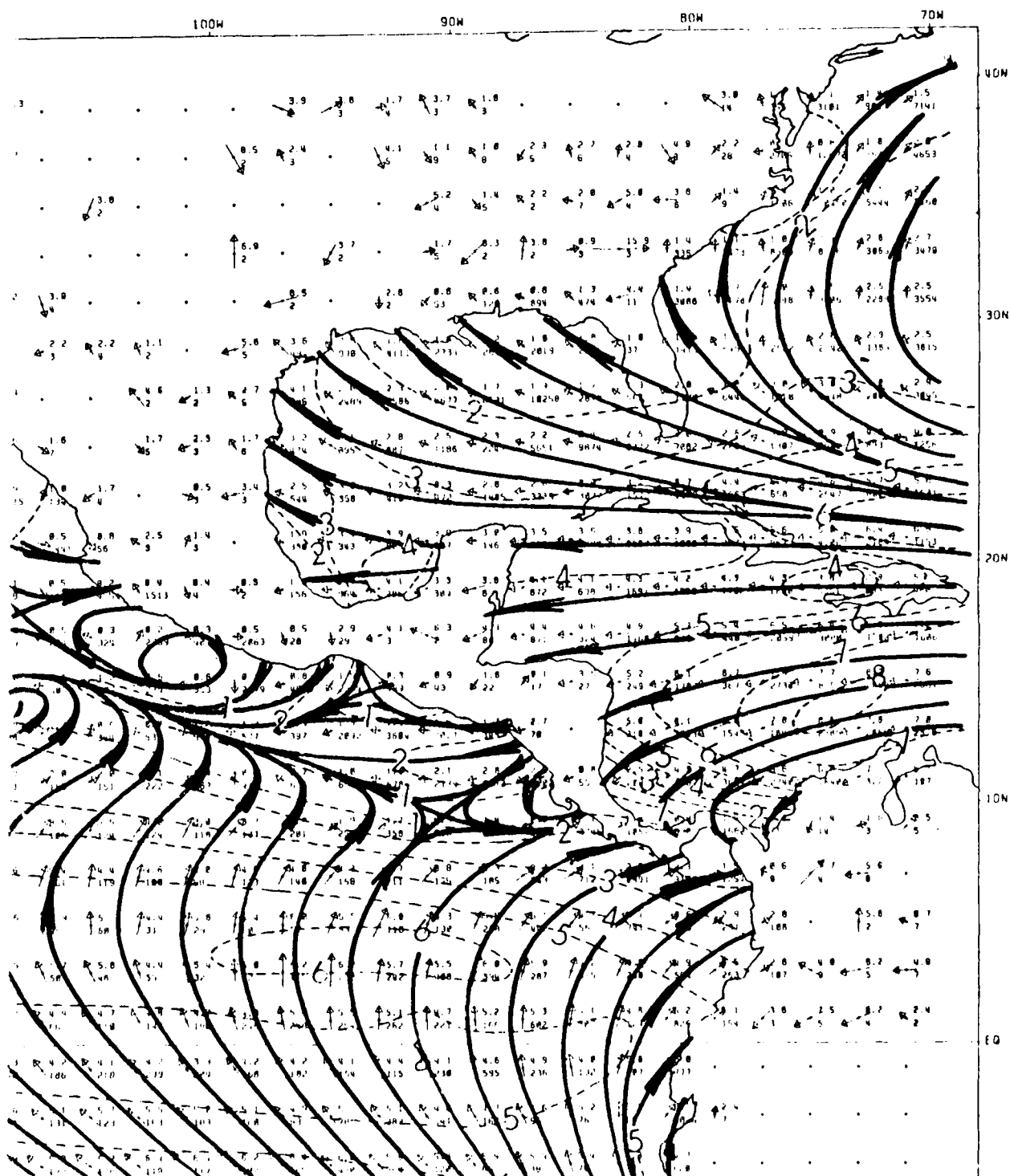


Figure 1.3: Surface Wind Direction / Speed (2° by 2°) Grid, August (Sadler et al., 1987)
 The resultant direction is depicted by streamlines and the resultant speed in m/sec by dashed lines. (Data plots contain (1) upper number: monthly average wind speed and (2) lower number: number of observations within each 2° square arrow shaft length is proportional to wind speed.)

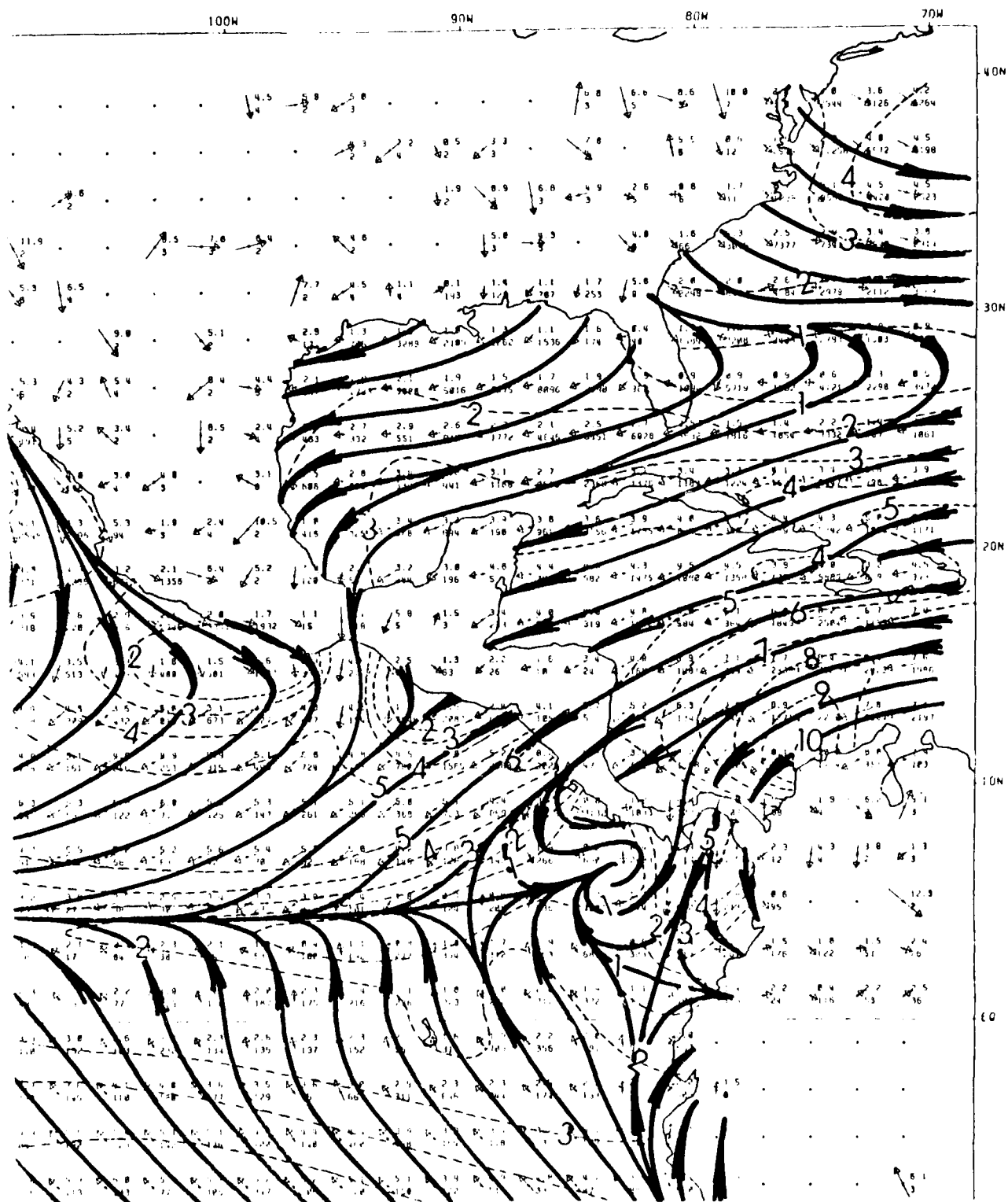


Figure 1.4: Surface Wind Direction / Speed (2° by 2°) Grid, February (Sadler et al., 1987)
 The resultant direction is depicted by streamlines and the resultant speed in m/sec by dashed lines. (Data plots contain (1) upper number: monthly average wind speed and (2) lower number: number of observations within each 2° square arrow shaft length is proportional to wind speed.)

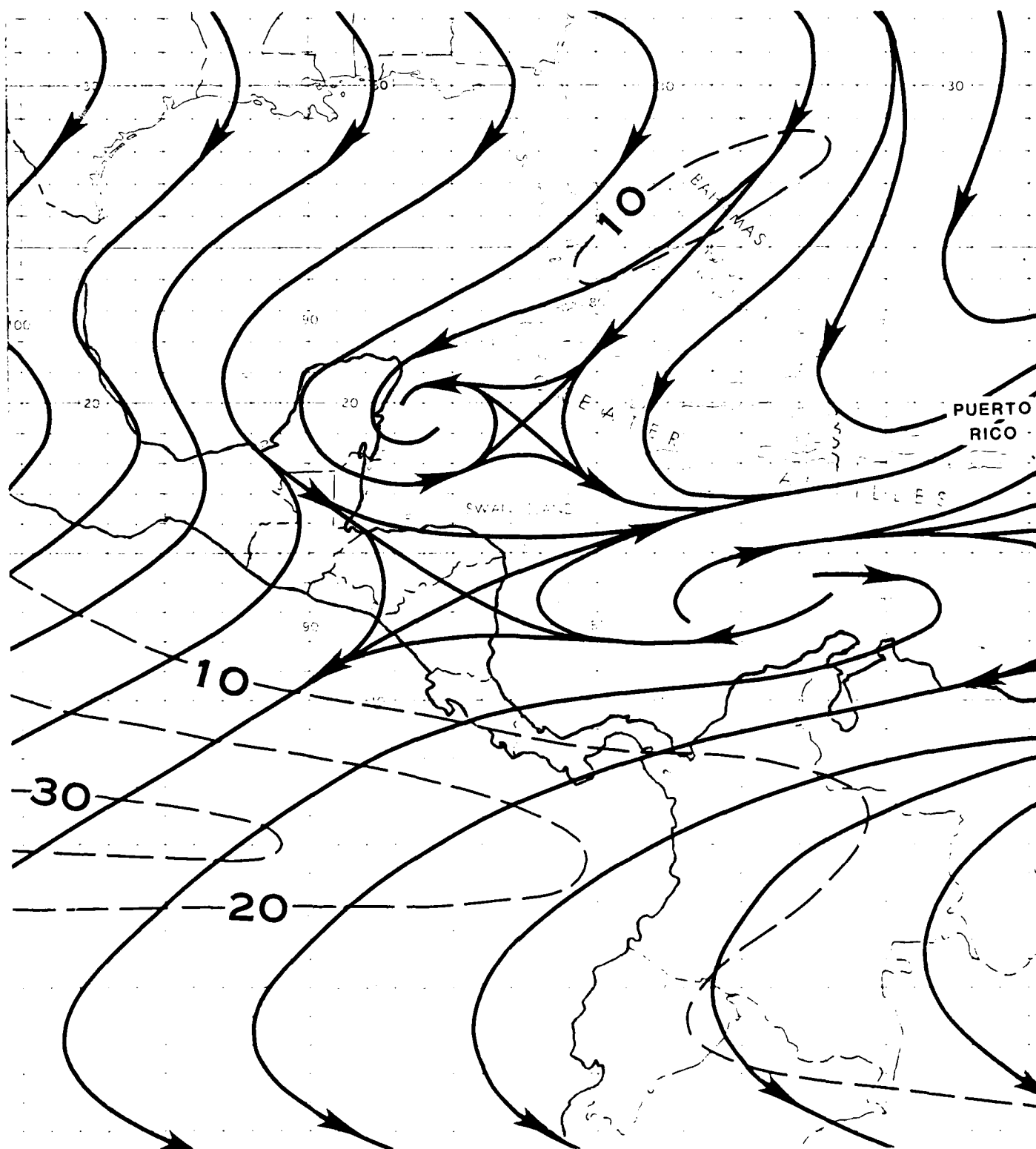


Figure 1.5: Mean 200 mb Flow, August (Sadler and Wann, 1984)
Streamlines (solid, with arrows indicating direction of flow) and isotachs (dashed) in knots

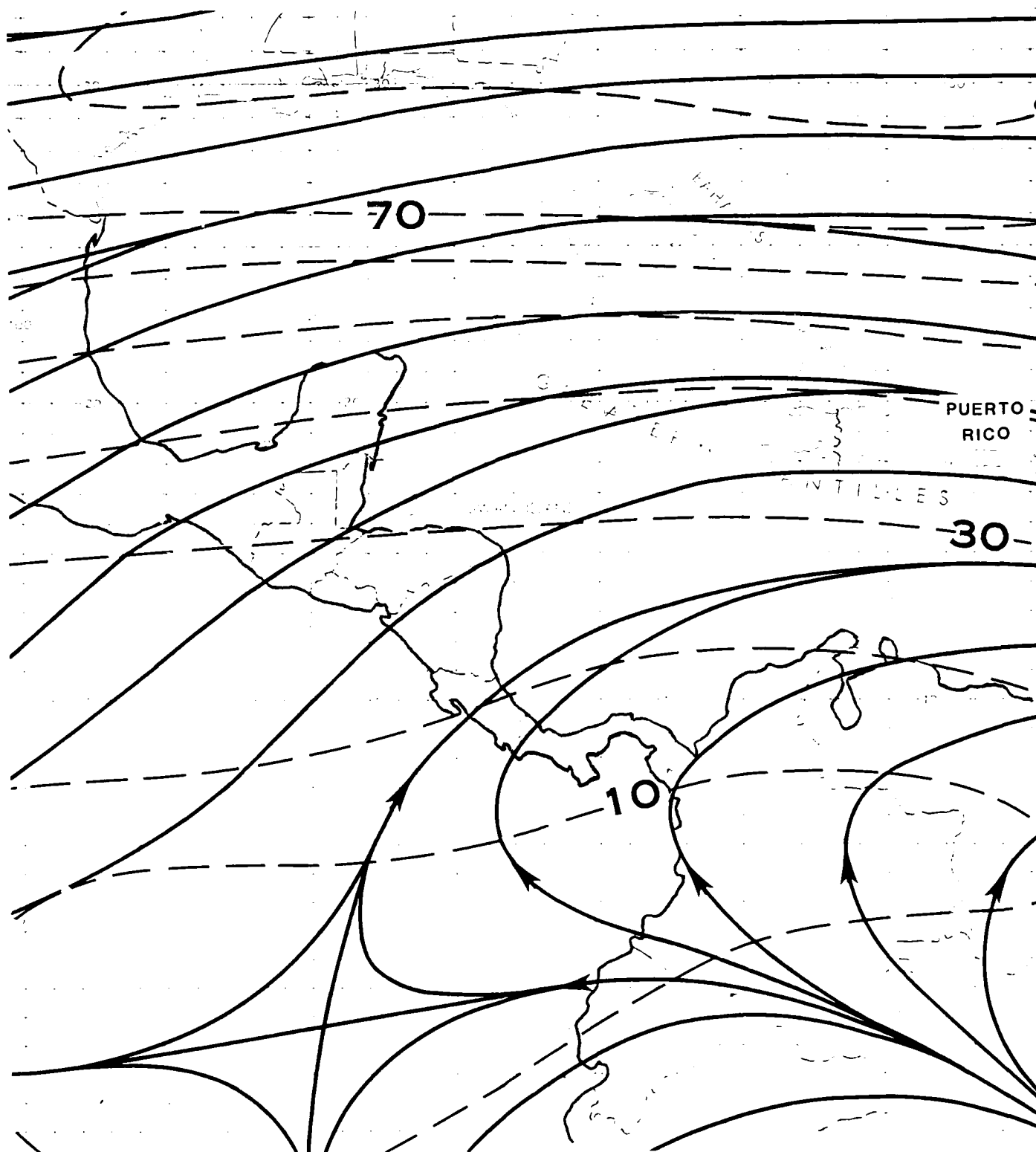


Figure 1.6: Mean 200 mb Flow, February (Sadler and Wann, 1984)
Streamlines (solid, with arrows indicating direction of flow) and isotachs (dashed) in knots

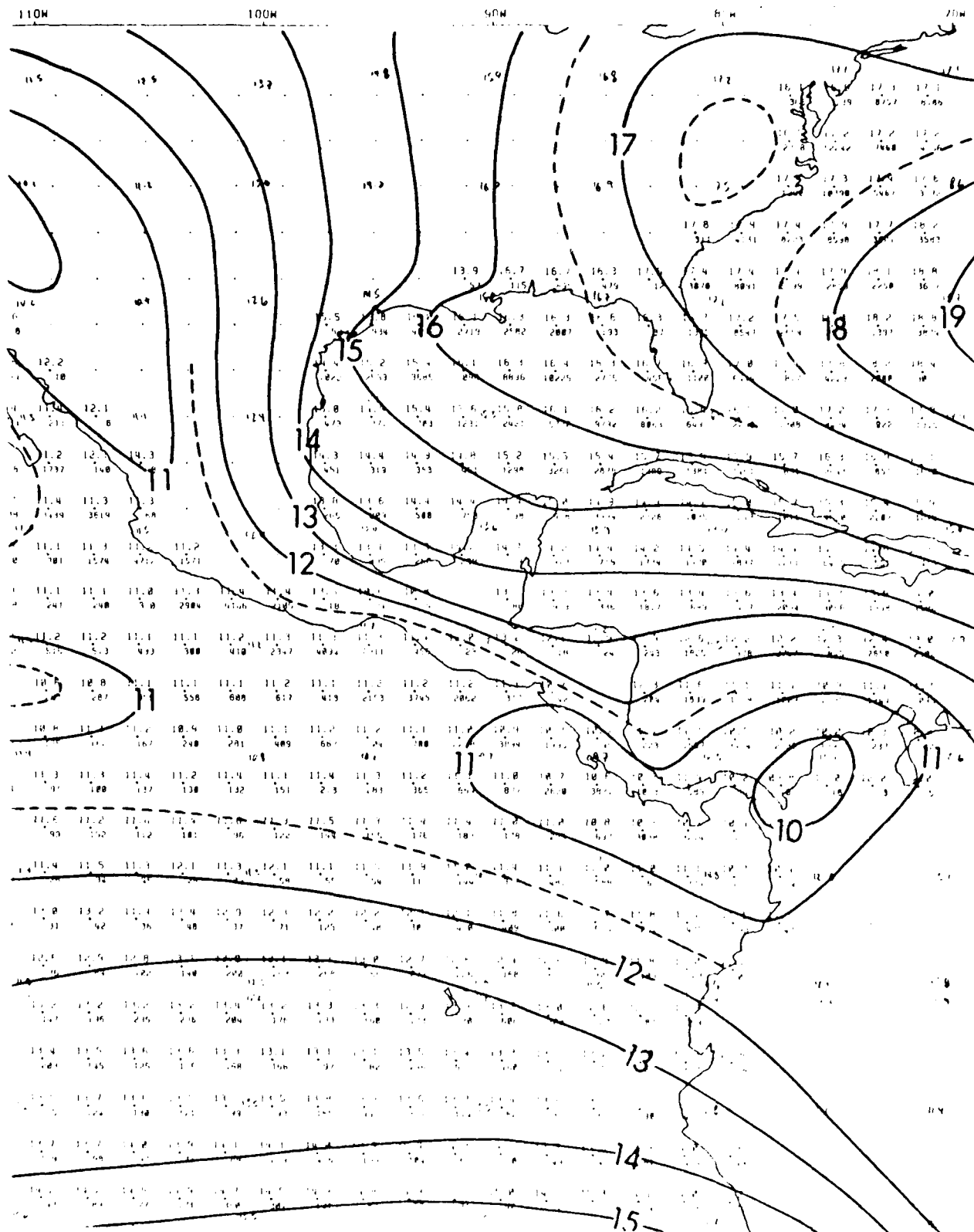


Figure 1.7: Mean sea-level Pressure, August (Sadler et al., 1987)
 The isobars are labeled in millibars (or hectopascals (hPa)) with the leading 10 omitted.
 Selected one-half millibar intervals are shown as dashed lines.

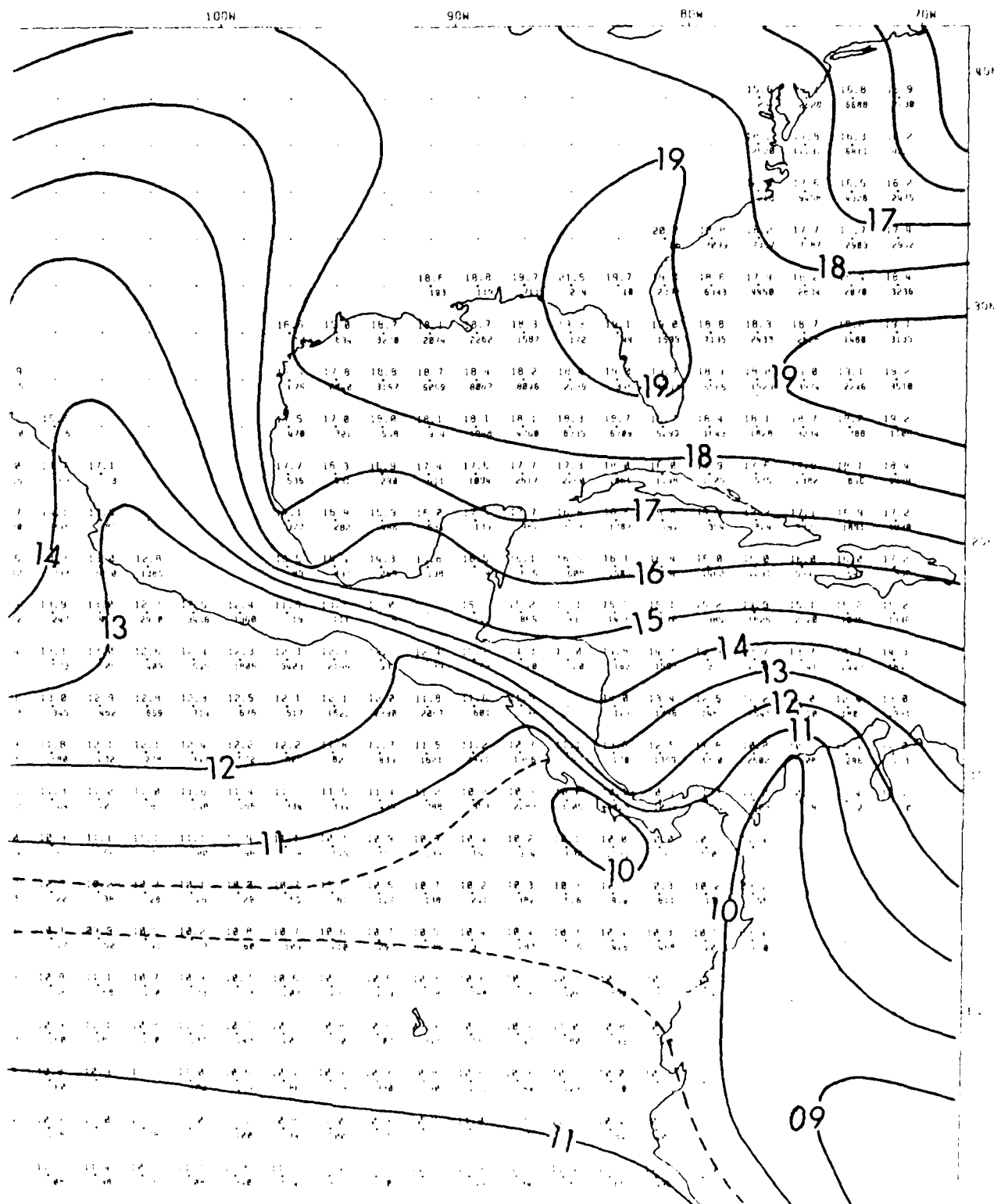


Figure 1.8: Mean sea-level Pressure, February (Sadler et al., 1987)
 The isobars are labeled in millibars (or hectopascals (hPa)) with the leading 10 omitted.
 Selected one-half millibar intervals are shown as dashed lines.

Figures 1.9 and 1.10 (NOCD, Asheville, 1985) depict the mean scalar wind speed for August and February. Note that the sea-level pressure figures, (1.7 and 1.8), and these figures of mean surface wind speed are from *different* references. The strength of the wind is greatest off the Caribbean coast of Columbia—a region known by oceanographers as the “Columbian Basin”. Recalling, again, that these are *average* winds, note the strength of the trade winds in February, reaching into the North Pacific Ocean after crossing the relatively flat southern Nicaragua, as contrasted to the very light winds southwest of the mountainous Costa Rica.

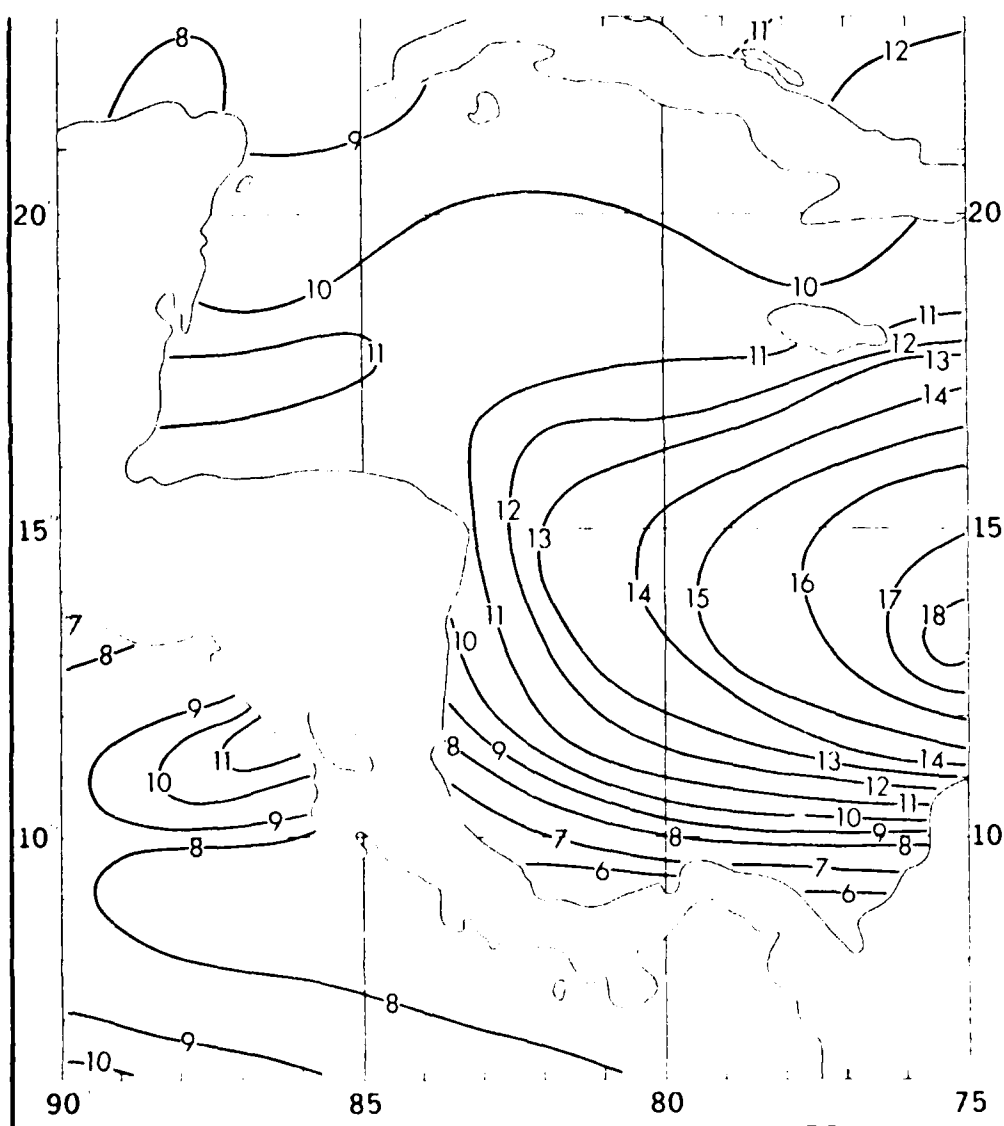


Figure 1.9: Mean Scalar Surface Wind Speed (kt), August (NOCD, Asheville, 1985)

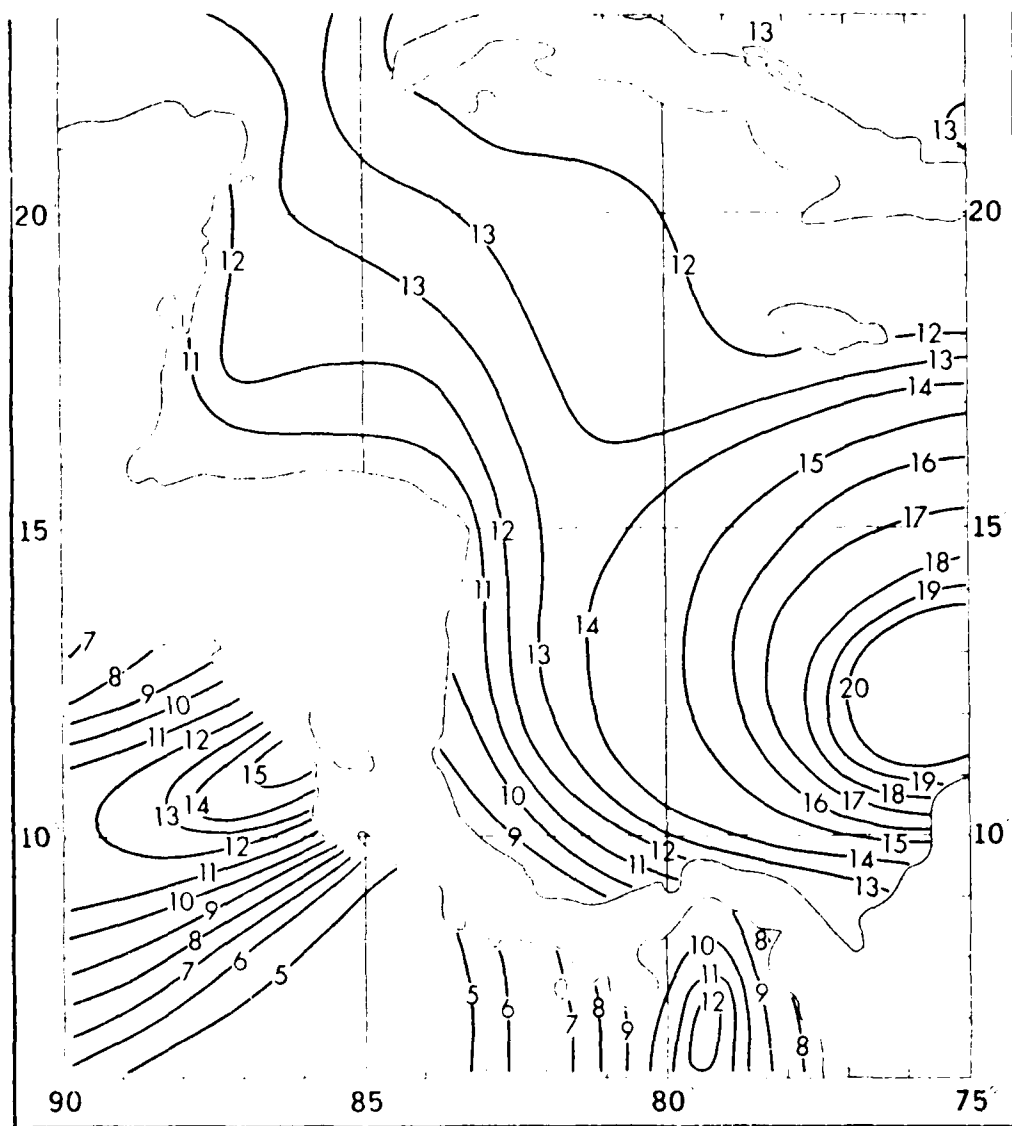


Figure 1.10: Mean Scalar Surface Wind Speed (kt), February (NOCD, Asheville, 1985)

Figures 1.11 and 1.12 (NOCD, Asheville, 1985) depict isopleths showing the percentage frequencies of wave heights ≥ 3 feet (solid lines) and ≥ 8 feet (dashed lines) for August and February. In agreement with the wind speed depicted in Figs. 1.9 and 1.10, large wave heights are more often found over the Columbian Basin, regardless of season. While wave heights surrounding Central America are generally high more often on the Caribbean side (the windward side) in February, note that wave heights on the North Pacific Ocean side are smaller in the lee of mountainous Costa Rica, but much larger west of Nicaragua.

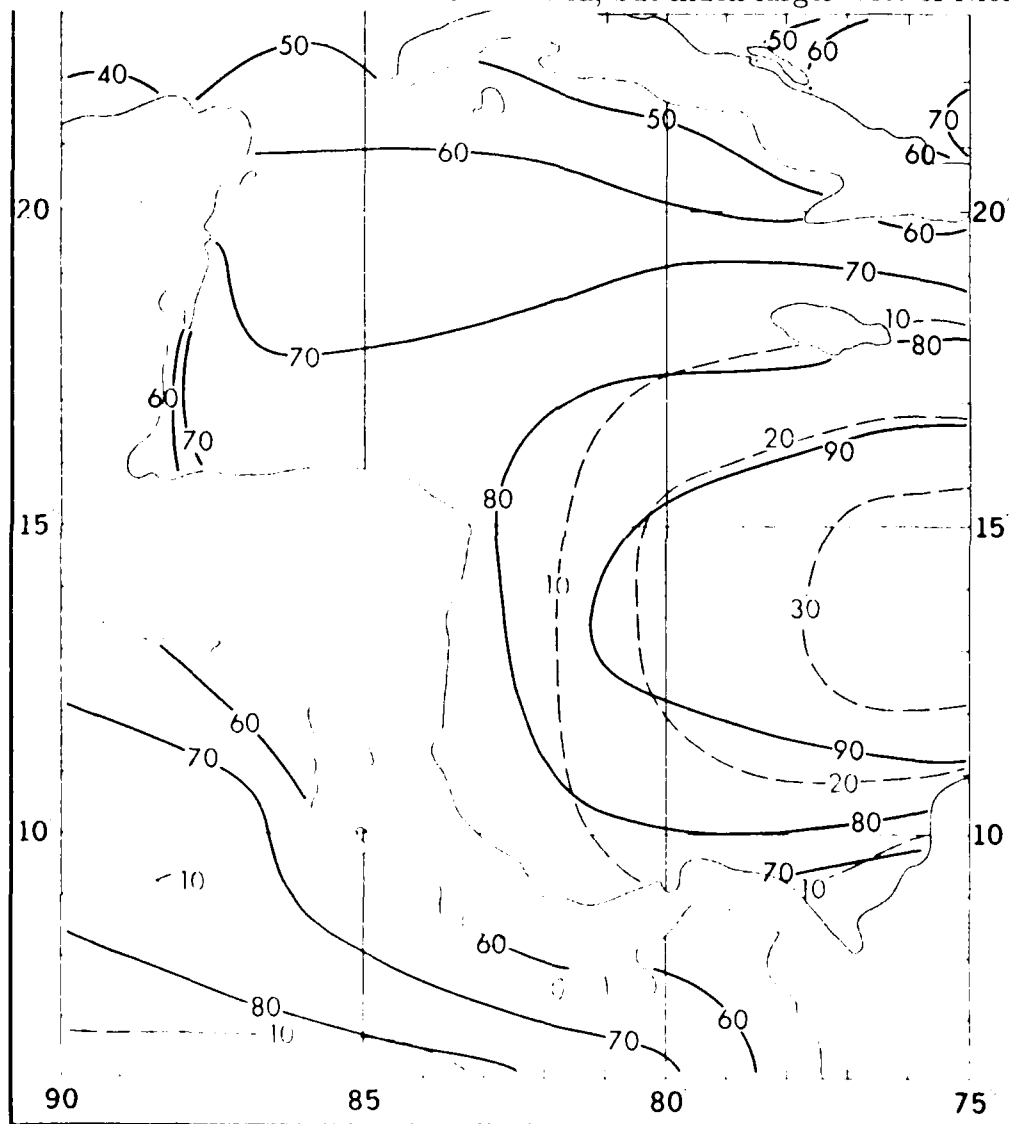


Figure 1.11: Wave-height Isopleths (Percent Frequency) August (NOCD, Asheville, 1985)
Solid line - Wave height ≥ 3 feet; Dashed line - Wave height ≥ 8 feet.
The wave height is the higher of sea or swell for observations containing both wave trains.
Sea is defined as waves generated by local winds.

Figures 1.13 and 1.14 (Sadler and Wann, 1984) depict the mean monthly cloudiness over Central America and the adjacent waters during the period 1965–1973. The analysis was derived from operational nephanalyses⁷ with isopleths labeled in “octas”⁸ (eighths) of total cloud cover. There is no satisfactory “ground truth” monthly average cloud analyses to which this analysis can be compared. However, the patterns of cloudiness and the positions of the maximum and minimum areas of cloudiness are essentially identical to other *satellite* derived analyses—although there is an average difference of about 1 octa between different satellite analyses.

It is readily apparent that average monthly cloudiness over much of Central America decreases from $\sim 5/8$ in August (the rainy season, Fig. 1.13) to $\sim 3/8$ in February (the dry season, Fig. 1.14).

Figures 1.15 and 1.16 (Sadler et al., 1987), depict the mean sea-surface temperature (SST) during the months of August and February. During August, monthly SST in the waters surrounding Central America is generally between 28°C and 29°C. Again, note that the higher winds blowing from land toward the North Pacific Ocean, west of Nicaragua in February, lead to mixing of the upper layer of the ocean and to cooler temperatures ($\sim 26^\circ\text{C}$) than found in the North Pacific Ocean west of Costa Rica ($\sim 28^\circ\text{C}$) where winds are weaker.

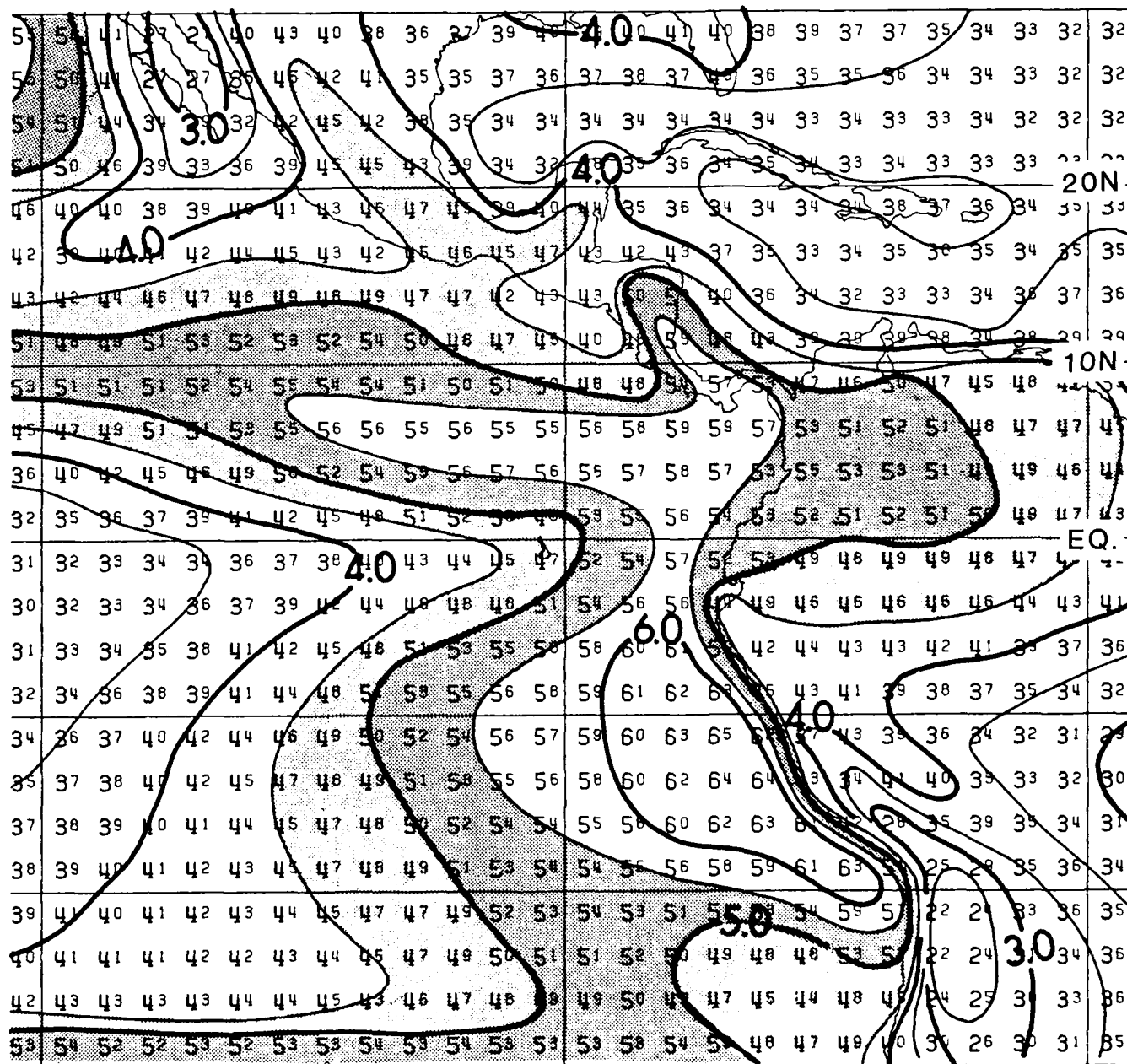
⁷Nephanalysis is a mapped analysis of the cloud distribution or “the analysis of a synoptic chart in terms of the types and amount of clouds and precipitation” (Huschke, 1959).

⁸Sadler emphasized the spelling of these labels so as to differentiate them from the fraction of cloud cover in “oktas” used by the World Meteorological Organization for *ground* based estimates.

120W

90W

60W



120W

90W

60W

Figure 1.13: Mean Monthly Cloudiness in Octas, August (Sadler and Wann, 1984)
The average cloud cover is plotted for each 2.5° latitude-longitude square.

120W

90W

60W

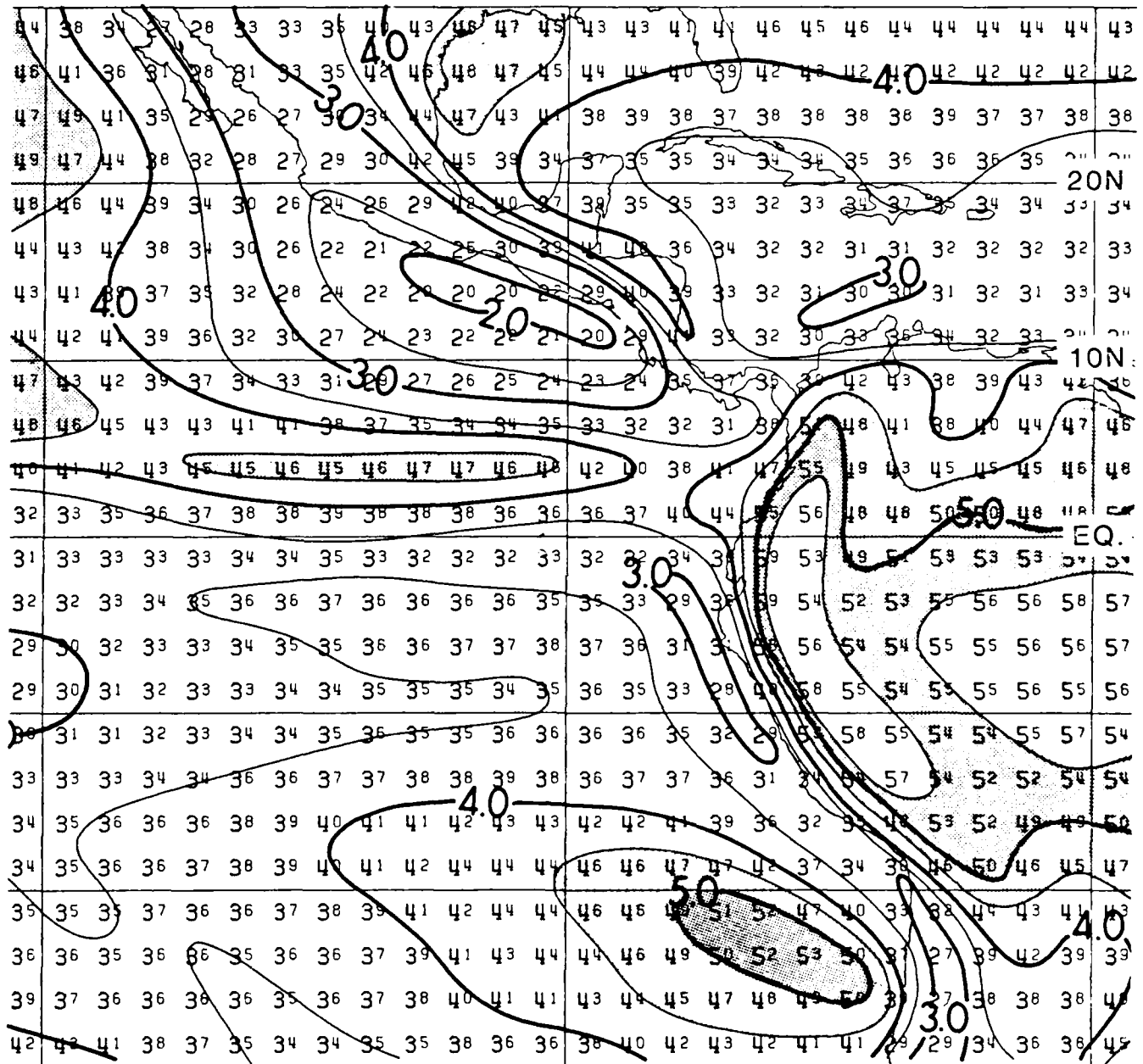


Figure 1.14: Mean Monthly Cloudiness in Octas, February (Sadler and Wam, 1984)
The average cloud cover is plotted for each 2.5° latitude-longitude square.

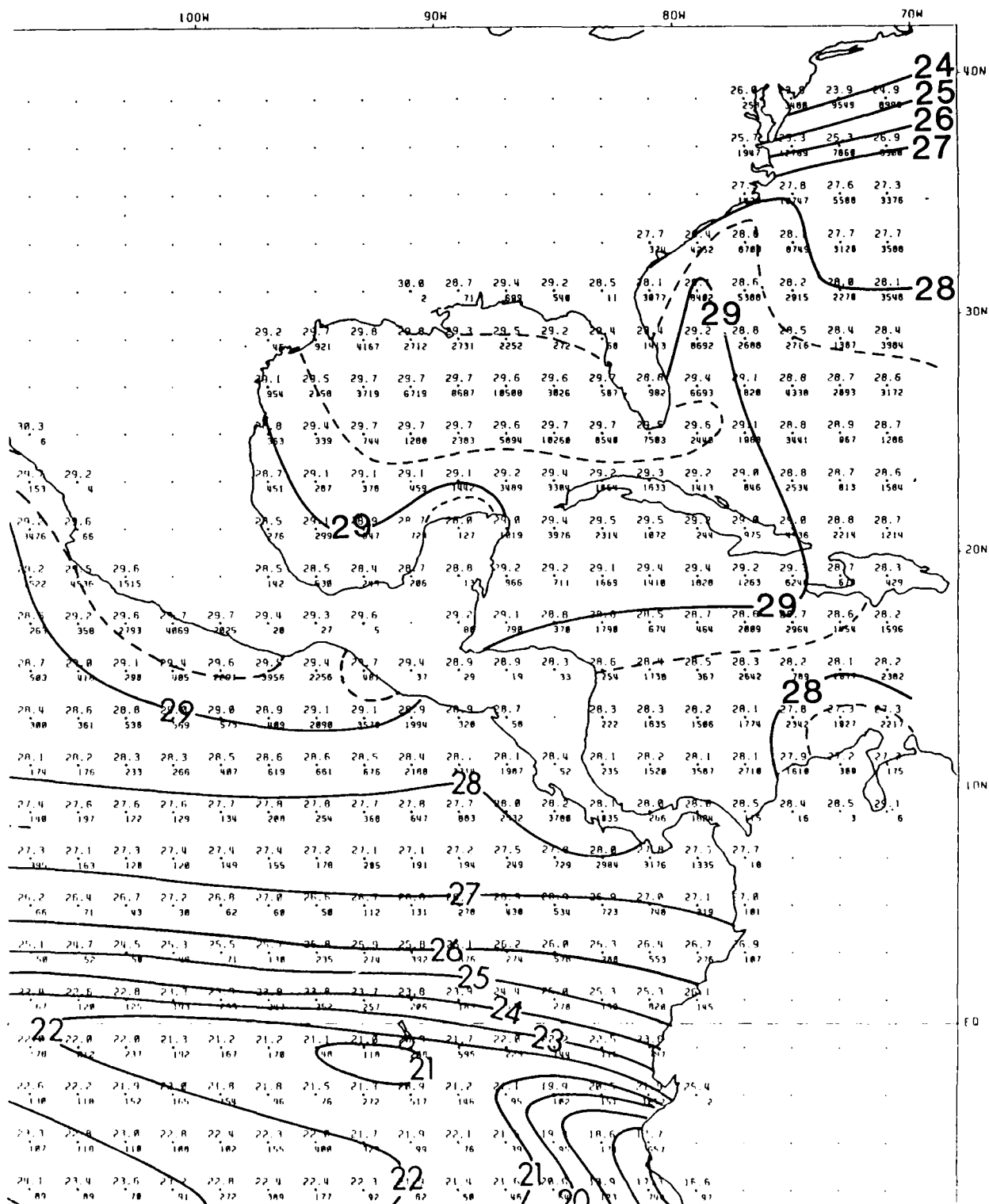


Figure 1.15: Mean Sea-Surface Temperature, August (Sadler et al., 1987)
 The isotherms are labeled in degrees Celsius. Where needed, one-half degree intervals are shown as dashed lines.

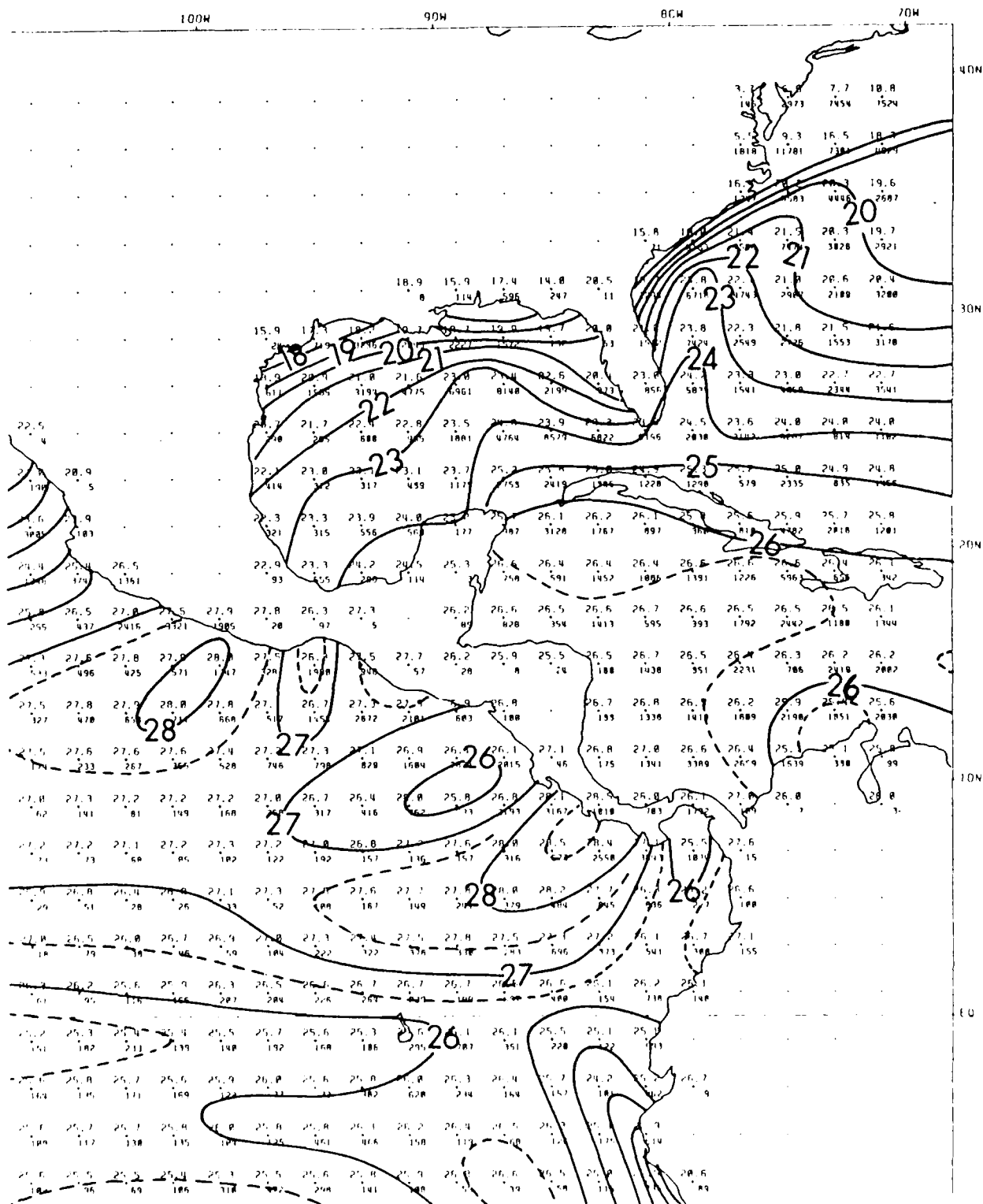


Figure 1.16: Mean Sea-Surface Temperature, February (Sadler et al., 1987)
 The isotherms are labeled in degrees Celsius. Where needed, one-half degree intervals are shown as dashed lines.

Finally, to assist mid-latitude meteorologists to adapt to the tropical setting of Central America, a *mean* sounding will be presented. While the International Civil Aviation Organization (ICAO) sounding⁹ with sea-level temperature of 15°C, as well as 500 mb height of 5574 m and temperature of -21.2°C, is so commonly used in extratropical applications, the mean atmosphere of Central America is obviously much warmer (and much more moist) with typically higher heights for constant pressure surfaces.

Jordan (1958) prepared a mean sounding from ten years of data from three stations: Miami, Florida; San Juan, Puerto Rico; and Swan Island¹⁰. The *annual* sounding is considered less useful and will not be presented since it provides a rather nonexistent sounding between the rainy and dry seasons.

Table 1.1 depicts the mean pressure, height, temperature and specific humidity of the four months¹¹, July through October, typical of the rainy season. To avoid the effects of daytime radiation, Jordan averaged only night time soundings—0300 GMT, as obtained operationally during the 1946–1955 period. Figure 1.17 presents a plot of this mean tropical sounding for the four summer months. Unlike the so familiar ICAO (or “U. S. Standard Atmosphere”) *extratropical* mean sounding, there is a dewpoint temperature sounding, available from the specific humidity data provided in Table 1.1.

⁹Identical with the U. S. Standard Atmosphere up to a height of 32 km.

¹⁰Swan Island is located at 17°N, 84°W in the western Caribbean Sea, ~100 miles north of eastern Honduras (see Fig. 1.21).

¹¹Defined by Jordan to be the “hurricane season”.

Table 1.1: Mean Tropical Atmosphere (West Indies) during Rainy Season (Jordan, 1958)

Pressure (mb)	Height (m)	Temperature (°C)	Specific Humidity (g/kg)
80	17883	-69.8	
100	16568	-73.5	
125	15260	-72.2	
150	14177	-67.6	
175	13236	-61.5	
200	12396	-55.2	
250	10935	-43.3	
300	9682	-33.2	
350	8581	-24.8	
400	7595	-17.7	
450	6703	-11.9	1.4
500	5888	-6.9	2.1
550	5138	-2.5	3.2
600	4442	1.4	3.6
650	3792	5.1	4.6
700	3182	8.6	5.8
750	2609	11.8	7.1
800	2063	14.6	8.4
850	1547	17.3	11.0
900	1054	19.8	13.0
950	583	23.0	15.3
1000	132	26.0	17.6

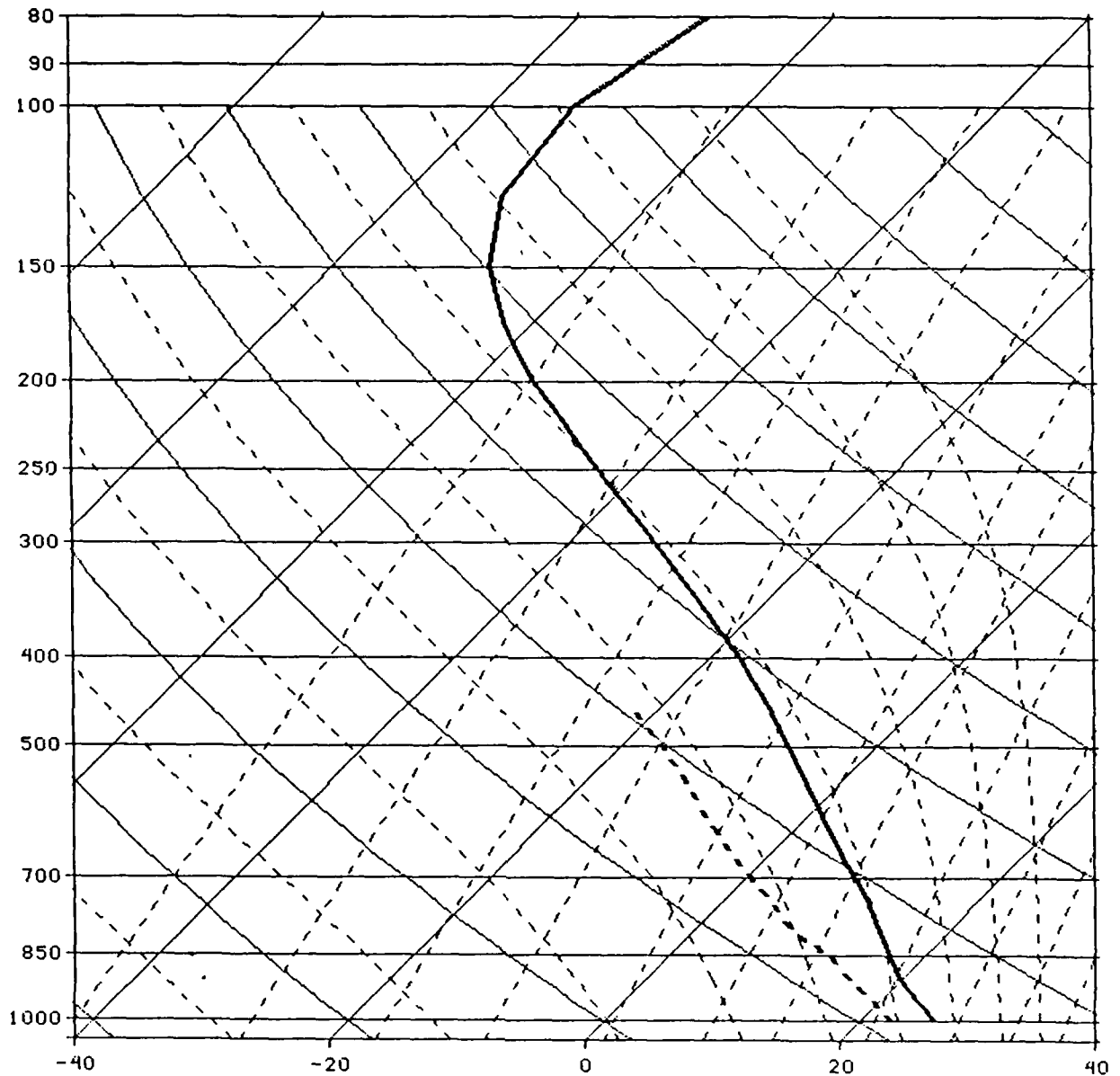


Figure 1.17: Mean Tropical Atmosphere (West Indies) during Rainy Season (Jordan, 1958) The temperature (heavy solid line) and dewpoint temperature (heavy dashed line) are plotted on a "Skew T, Log P" thermodynamic diagram, with isobars (thin solid horizontal lines), "skewed" isotherms (thin solid lines) sloping from lower left to upper right, dry adiabats (thin solid lines) sloping from lower right to upper left, pseudoadiabats (thin dashed lines) sloping from lower right to upper left, and mixing ratio lines (thin dashed lines) sloping from lower left to upper right.

1.2.2 General Climatology (Portig, 1976)

The following outline contains summary statements gleaned from Portig (1976) concerning the various climatological elements for Central America. (The reader is cautioned that these summaries do not refer to the figures (from other sources) presented in the previous subsection.)

Wind

Because wind is among the climatological elements most affected by local influences in the near Equatorial portion of Central America, one cannot use the geostrophic or gradient approximation for the wind. Using earlier data based primarily on ship observations (yet, not so complete as COADS), Portig (1976) states that mean streamlines from September (rainy season) and December (dry season) have the greatest month-to-month mutual deviations (see Fig. 1.18 below)¹². While the more northerly direction of the December winds is obvious, he notes that "in no month is there any (average) *southerly* component of the wind over the open Caribbean Sea".

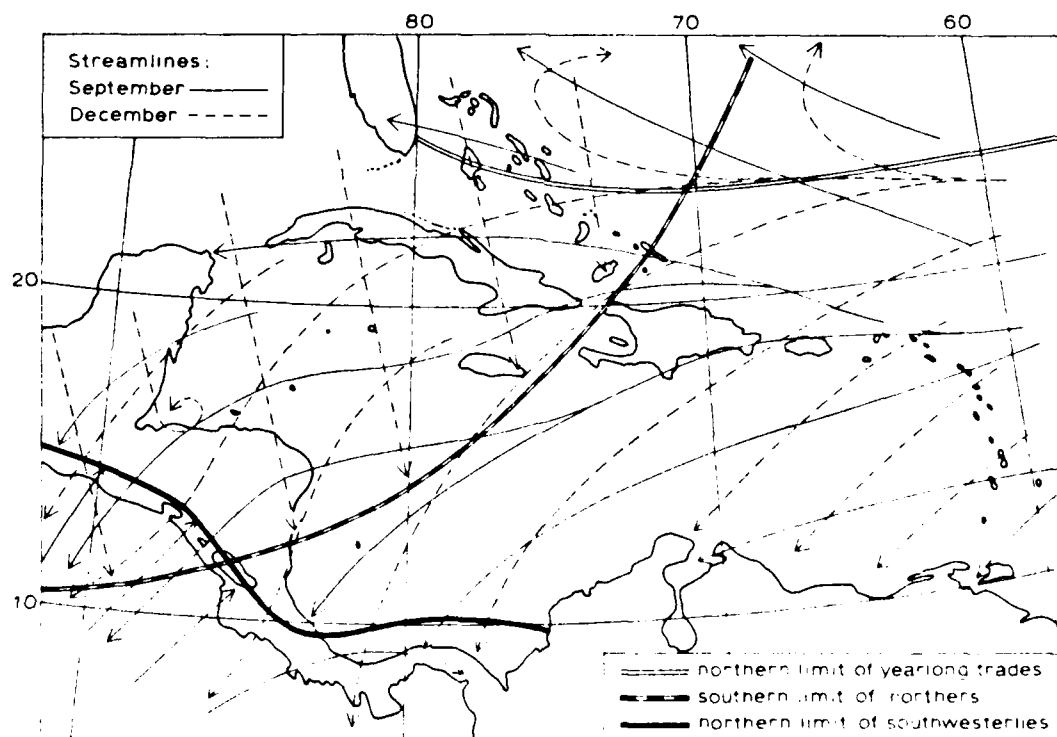


Figure 1.18: Mean Streamlines. Over the North Pacific coast of Central America two wind regimes alternate in September (Portig, 1976)

¹²The dashed lines from the north-northwest over the western Caribbean Sea indicate the presence of "northers", **intermittently** present with the north-northeasterly tradewinds during December. Northers are defined as "...strong, cold winds...associated with the southward movement of a cold anticyclone." (Huschke, 1959). However, other sources document northers reaching **Panama**.

Although hurricanes do occur in the region, they affect individual stations so seldom that their presence is not evident in wind statistics compiled over many years.

Not only do *inland* stations have a high percentage of calms, but there are periods (of hours) during which the wind speed is zero. Balloon records have revealed layers, several thousand meters thick, having no horizontal motion.

Stations have distinct diurnal variations, with the expected higher wind speeds in the afternoon and early evening. Stations with extensive land mass behind them, such as along the North Pacific coast, experience "sea breeze fronts". However, local orographic effects, "northers" and trade winds have their particular months (as well as time of day) of dominance.

Barometric Pressure

Relative maxima in mean pressure are found in December (or January) and in July. More importantly, the atmospheric pressure displays the familiar **double** wave every day, with minima near 0400L¹³ and 1600L, and maxima near 1000L and 2200L. At San Salvador, the magnitude of this twice daily pressure variation is as large as 4.2 mb in March.

Cloudiness

Central America is often under a canopy of cirrus (often tenuous), and even well-experienced observers often have difficulty in locating the edges of thin cirrus. However, tropical clouds show a high correlation with geographic features, such that not only mountain ranges but also coastlines are often identified in satellite imagery. The largest annual range of cloudiness over ocean areas (i.e., clearer in February/March, cloudier in September) is observed in the North Pacific Ocean, off the coast of Central America. Maximum cloud cover is also found along the east coast of Central America, from Belize to Panama.

Sunshine

Mean monthly sunshine, in percentage of the possible, shows a tendency for stations to have their sunshine extremes out of phase and a month or so earlier than rainfall extremes. That is, minimum sunshine occurs one month before the rainfall maximum, and maximum sunshine occurs one month before the rainfall minimum.

Temperature

Since Central America is tropical and primarily maritime, temperature changes are small. Portig (1976) found that the *hourly* temperature variations from observations in a well ventilated shelter depend mostly on cloud cover.

¹³L = Local Time

In most of Central America (except for the Caribbean coasts of Honduras and northern Nicaragua), the monsoon temperature variation dominates with the highest temperatures just before the onset of the summer rains. On land, the average temperature of the *warmest* month (at sea level) is less than 29°C, except at some island locations on the Pacific side of Central America where the mean April temperature rises to 31°C (e.g., in Amapala, a Honduran island in the Gulf of Fonseca¹⁴). Conversely, at sea level the average temperature of the *coldest* month is 19°C. The annual temperature range for most of Honduras is more than 4°C, dropping to less than 4°C at the coast, and to about 1.5°C at the Panama Canal. (The temperature range of stations at higher elevations is generally of the same magnitude as for nearby lowlands.)

Cold winter air invasions from North America affect the absolute temperature minima. While lowland temperatures almost never drop below 15°C southeast of a line running from Puerto Rico to Costa Rica, the lowland temperatures in Central America northwest of this line reach an absolute minima of approximately 7°C. Such low temperatures usually occur due to the combined effects of cold air intrusion and nocturnal cooling. The highest mountains of Guatemala and Costa Rica have experienced *below freezing* air temperatures.

The diurnal temperature range exceeds the annual temperature range, although the diurnal range is reduced by the nearness to sea. Also, the dry season has a larger daily temperature variation than the rainy season, in general.

Moisture

Most Central American climatological summaries do not include dewpoint temperatures; however, Appendix B contains average **monthly** relative humidity, vapor pressure and dewpoint temperature for selected stations. Although the strong influence of nearby oceans and warm temperatures dictates relatively high moisture for Central America, it is noted that moisture *can* drop to sufficiently low values where hygrometers become inaccurate.

Rainfall

Portig (1976) states that "the most important meteorological element in the tropics is the rainfall". Although Central America is practically always under the influence of maritime air masses, seasonal variation of precipitation are surprisingly high (see Fig. 1.19). While much of the variation can be attributed to orographic effects, significant differences in the timing of the rainfall seasons exists over short distances.

Areas of *lesser* rainfall (less than 100 cm (~40 in) include regions of elevated plains of central Guatemala, Honduras and northwestern Nicaragua, plus very small parts of the North Pacific coast west of the Gulf of Fonseca and southwest of Panama City.

¹⁴See Subsection 1.3 for geographical locations within respective countries.

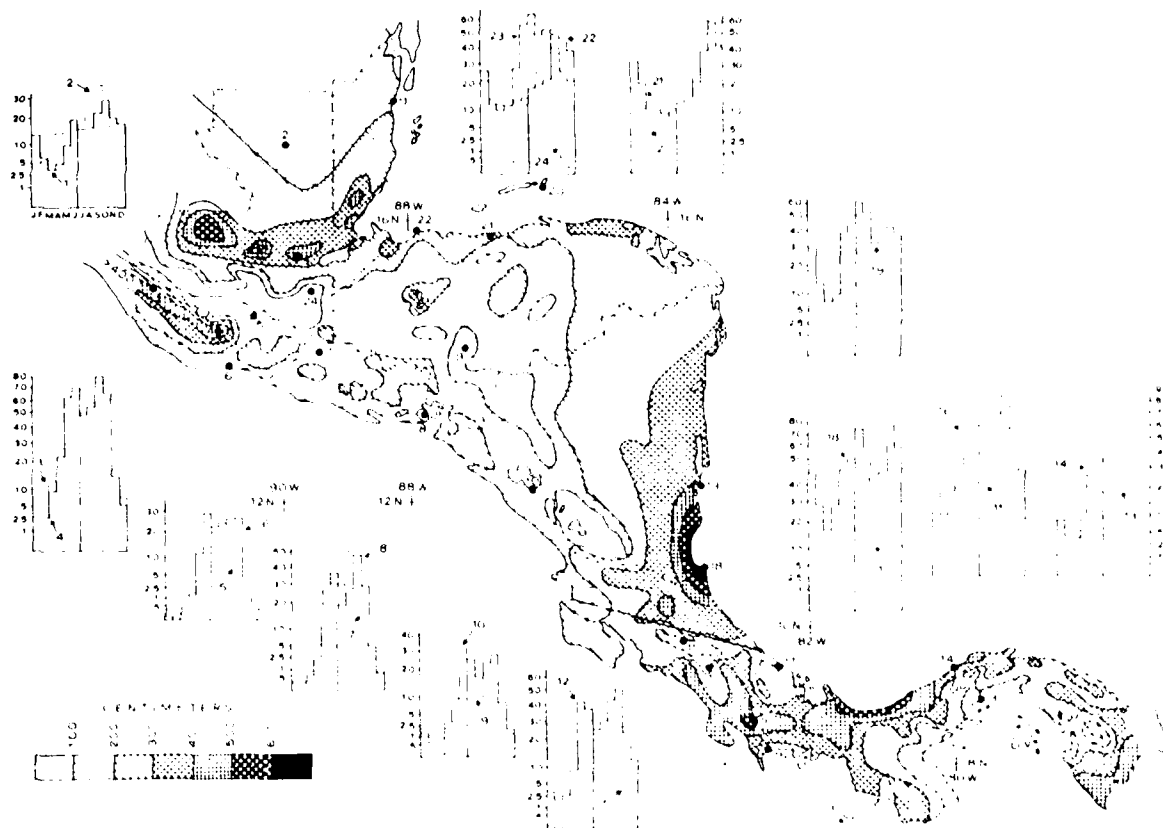


Figure 1.19: Mean annual rainfall (cm) in Central America (Portig, 1976). Numbers (1 through 24) locate the following stations: 1-Belize City, 2-Flores, 3-Santa Teresa, 4-San Andrés Osuna, 5-Guatemala City, 6-San José, G., 7-Taxis Junction, 8-Cutuco, 9-Tegucigalpa, 10-Managua, 11-San José, C. R., 12-Villa Mills, 13-Panama City, 14-Colón, 15-Puerto Armuelles, 16-Caracol, 17-Guabito, 18-San Juan del Norte, 19-Bluefields, 20-Guanaja, 21-La Ceiba, 22-Puerto Cortés, 23-Sepacuite, 24-Zacapa.

In contrast, areas of excessive rainfall are found in the mountains of Guatemala and the mountains connecting Costa Rica and Panama. The tops of lesser mountains and the slopes of the higher mountains receive large rainfall totals, while crests above 2,500 m receive less than half that falling on the slopes.

The other areas receiving excessive rains include the Caribbean coast near southern Belize to Puerto Barrios, Guatemala, the Caribbean coast of Nicaragua at and south of Bluefields, the Caribbean coast of Panama near the Gulf of Los Mosquitos, the southeast corner of Panama, and the *southern* coast of Costa Rica.

While most of the rain-bearing disturbances come from the Caribbean, leading to larger rainfall on the Caribbean side, the reader must keep in mind that diurnal sea breezes provide their rainfall production ashore on the North Pacific Ocean side as well, with winds from the south or west. Drier areas, such as west of the Gulf of Fonseca, are believed to be partly caused by katabatic winds¹⁵. Also, the drier eastern side of the Peninsula of Azuero, Panama may be shielded from disturbances of North Pacific origin by the mountain range on the western half of the peninsula.

¹⁵Winds blowing down an incline, the opposite of anabatic wind (Huschke, 1959).

With only a couple of exceptions, all of Central America has two rainfall maxima, with generally higher totals on the Caribbean Sea side. The main dry season occurs in winter or early spring and is much more intense (drier) on the North Pacific Ocean side of Central America.

With the drier winter and spring, the North Pacific Ocean side has appreciable accumulation from June through October, yet with a relative minimum during the two summer months of July and August. This relative minimum is locally labeled the "varanillo" (little summer). While **all** months have a diurnal rainfall maximum between sunset and midnight, June and September have an additional rainfall accumulation¹⁶ in the early afternoon (1200L-1600L). Thus the North Pacific side maxima are in June and September.

Again, while the Caribbean side has a not-so-dry late winter (as does the North Pacific Ocean side), the general pattern of its maxima consists of a summer maximum near June or July and another relative maximum in December.

Thunderstorms

While thunderstorms are a common occurrence in Central America, the two regions of maximum thunderstorm activity are (1) the Gulf of Fonseca (116 storm days¹⁷ per year on Amapala) and (2) the center of the Canal Zone (196 storm days at Madden Dam). The minima are 37 at Chimax, in central Guatemala and a questionable **three** at Belize City.

Visibility

Portig (1976) reports that fog practically never occurs at sea and at coastal stations, but that inland stations occasionally have shallow fog in the morning that is rapidly dissipated by the sun. (However, one of the authors observed **heavy** coastal morning fog during a winter (dry season) approach to the Caribbean side of the Panama Canal in February 1963.)

The dry season has many days with haze, providing a real hazard for aircraft. However, **above** the haze, the trade wind inversion provides unlimited visibility. Furthermore, the Pacific side of Central America has the "best" and the "worst" visibilities, i.e., the Pacific side has a larger variation in visibility, than the Caribbean side.

Overall Weather

In winter and spring, i.e., the dry season, the steadily blowing trades produce generally fine weather. Of course, the incursions of cold air from North America (or the Gulf of Mexico) interrupt this fine weather, with less effect equatorward of Nicaragua. (GOES imagery, examined during 1988, verified these statements.)

¹⁶From Portig(1976) data which is predominantly from San Salvador.

¹⁷While Portig (1976) does not define *storm day*, Huschke (1959) defines a *thunderstorm day* as "...an **observational day** during which thunder is heard at the station. Precipitation need not occur".

Most of the winter rain for northern Honduras comes from the long-lasting rain and drizzle accompanying cold fronts reaching the mountains. Again these cold fronts tend to be dry on the Pacific Ocean side because of the foehn¹⁸ effect. The cold north wind is called norte, norther, or tehuntepeco. While it can become destructively strong, it is often welcomed during the monotonous dry season. As mentioned earlier, the lowest temperatures occur when the wind subsides and cooling by nocturnal radiation follows.

While the first norther of the seasons tends to bring a distinct weather change, subsequent incursions become less potent. Accordingly, Portig (1976) states that it is difficult to determine the exact number of northers per season. Estimates run from 30-40 per year or less.

Chapel (1927), who has defined northers by wind rather than through weather patterns, studied the average conditions of six northers reaching Colon, Panama, noting that the wind nearly doubled in strength on the day of arrival, with a pressure rise **only** on the day of arrival, but with increased rainfall amounts for three days after arrival. While no rain may fall when a cold front passes, heavy downpours can occur where the front finally stalls. Such heavy rainfalls can be found on the Caribbean coastal area of southeastern Nicaragua.

However, the rainy season has more synoptically driven events than does the dry season. In the rainy season, they are manifest as hurricanes, tropical depressions, waves in the easterlies or even displaced fragments of the Intertropical Convergence Zone (ITCZ). Rainfall from hurricanes is considered beneficial in many areas, but hurricanes are **not** responsible for the rainfall maximum in the fall. Portig (1976) reports that "tropical lows or depressions occur at varying intensities all over region, and occasionally in the dry season"; moreover, personal communication¹⁹ in 1986 revealed that development of a tropical depression near the Canal in December 1985 required immediate measures to control the water level of the Canal, before the depression moved slowly toward the northwest.

Local developments

Portig (1976) defines the "temporal" as a longlasting rain, with no, or little, electrical activity. While categorizing them as "local" is debatable, they are typical of two areas: the north coast of Honduras (caused by invasions of cold air from the north during the winter (dry season) and the Pacific Ocean coast of all of Central America. While continued research is needed, the temporals along the Pacific Ocean coast may often be tropical depressions moving slowly westward. Portig (1976) suggests that they may transform from "temporal"-lows into hurricanes, and vice versa. While the Pacific temporal may have hurricane-like spiral bands, its winds are generally light and moderate, without lightning and thunder, but its rainfall, covering a relatively large area, can cause water damage.

¹⁸Foehn—A warm, dry wind on the lee side of a mountain range, the warmth and dryness of the air being due to adiabatic compression upon descending the mountain slopes (Huschke, 1959).

¹⁹Conversation between Joe Corelli, Hydrologist of the Panama Canal Commission and one of the authors.

Portig (1976) further reports that "it is not possible to clearly distinguish between the temporals and temporal-like situations ('tiempo atemporalado' as the man on the street says), but a fair estimate calls for one or two temporals a year for each location on the North Pacific coast of Central America". The greatest probability is in September or October, with a secondary maximum in June.

As a local phenomena, the sea breeze may be strong enough at times to overcome the large-scale wind regime, blowing from the west in a typical trade wind area. For example, in western Panama, it can reach 30 km inland.

Squalls are frequent, and over water thunderstorms frequently generate waterspouts. Tornadoes are less frequent than waterspouts, and hail is rare, even in locations experiencing many thunderstorms. Hail has fallen on the Pacific Ocean side of Guatemala and in Panama, and snow falls on elevations above 3400 m in Guatemala (Portig, 1976).

1.3 National Climatologies

Following closer examination of Central America and its topography, this section will discuss the climate and terrain of each country. On the following two pages, Fig. 1.20 (The Diagram Group, 1985) with its shading, and Spanish names for mountain ranges and volcanoes, provides a better perspective of terrain elevation, while Fig. 1.21 (The Diagram Group, 1985) with its *larger* scale (compared to Fig. 1.1) displays the national boundaries of the seven countries more clearly.

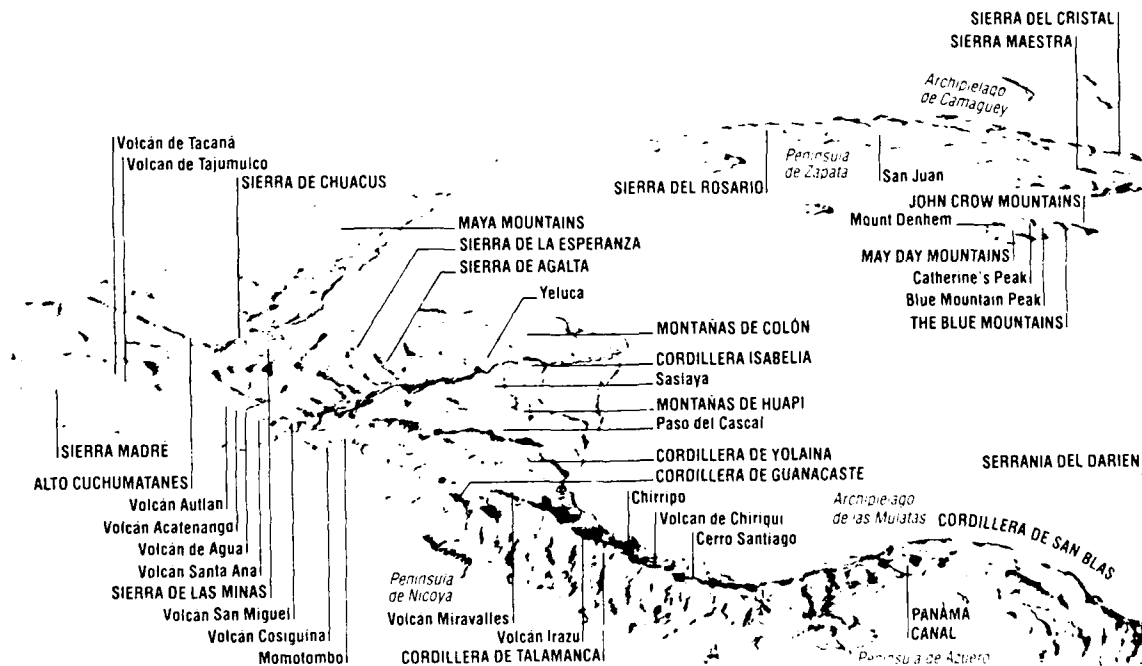


Figure 1.20: Topography of Central America (The Diagram Group, 1985)



Figure 1.21: Seven Countries of Central America (The Diagram Group, 1985)

1.3.1 Guatemala

Land

While having the most people of any nation in Central America, Guatemala is the third largest nation, equivalent to the size of Tennessee. In addition to bordering Mexico on the north and west, its Pacific coastline is located to the southwest. On its eastern border (starting from the north) is Belize, followed by a short Caribbean coastline, and then finally Honduras and El Salvador.

As depicted in Fig. 1.22, Guatemala has a rather narrow Caribbean coast to the east, but a fairly extensive Pacific Ocean coast to the south. While lagoons and sand bars extend the length of the gently curving Pacific coast, just inland are fertile coastal lowlands for about 25 miles. The coastal Pacific lowlands then give way to the highlands of the southern and central region, while the north is occupied by the plains of Petén.

Approximately two-thirds of the country is occupied by highlands with the main mountain range being a southeast extension of Mexico's Sierra Madre, paralleling the coast only about 40 miles inland. With many high volcanic peaks, some active, the inland highlands extend from 3500 – 8000 feet in elevation. Very near the western border and at 13,845 feet, the Tajumulco Volcano is the *highest* peak in Central America. But between volcanic peaks lie volcanic rich basins.

Guatemala's longest river, the Motagua, lies just north of the main mountain range and flows eastward to the Gulf of Honduras and the Caribbean Sea. From another valley, not far to the north, the Polochic River runs parallel to the Motagua, flowing into Guatemala's largest lake, Izabal, before reaching Amatique Bay in the Gulf of Honduras. While the sparsely populated limestone plains of Petén comprise most of northern Guatemala, the relatively low Maya Mountains extend into southern Belize. A narrow, fertile coastal plain exists along the short Caribbean coast (The Diagram Group, 1985).

Climate

General The cooling effects of both coasts and highlands provide a variety of climates within Guatemala. The coasts are hot and humid, about 80°F (27°C) throughout the year. Inland highlands are cooler; for example, at Guatemala City, at nearly 5000 feet above sea level, the average annual temperature is 64.4°F (18°C). The months of December and January are coolest.

The rainy season lasts from May to November—October, if you use Guatemala City rainfall, (not shown). While the Caribbean-facing slopes get rain almost all year, the Pacific coast receives heavy summer rain, but stays dry during the winter. Annual rainfall varies from 80 inches in the highlands to about half that amount in parts of eastern Guatemala (The Diagram Group, 1985).



Figure 1.22: Guatemala (The Diagram Group, 1985)

Rainy Season: May - October. The rainy season is characterized by mostly cloudy skies²⁰, with warm to hot temperatures, and frequent rain showers and thunderstorms. At night, the temperatures below about 3000 feet and at coastal locations fall to the mid to upper 70's (°F), then rises to the upper 80's or lower 90's during the afternoon. However, the upper plateau which includes Guatemala City, is cooler with lows near 55-60°F and highs 70-80°F. Rainfall, which is moderate on the interior plateau, increases to very heavy on seaward-facing mountain slopes and lower elevations. While most rain falls as brief showers, the "temporal" can bring low ceilings and visibilities, as well as continuous rain, for periods from 12 hours to 6 days.

Thunderstorm days occur in the lowlands at a frequency of 8-14 per month, with a considerably higher frequency on exposed mountain slopes. While the interior plateau has only 2-8 thunderstorm days per month (see monthly totals below), both the lowlands and interior plateau have a thunderstorm maximum in the midafternoon, with a secondary thunderstorm maximum found at coastal stations between midnight and sunrise. The thunderstorms may be accompanied by strong gusty winds and severe lightning. See Section 5 and Appendix C for tracks of tropical cyclones affecting Guatemala.

Flying weather: Poor to fair flying weather may be expected during the rainy season due to heavy cloud cover, rain and thunderstorms. Cloud-enshrouded mountain slopes naturally present a hazard to aircraft operations. See Appendix B for specific statistics at Huehuetenango and Puerto Barrios.

Terminal weather: Guatemala City/La Aurora Airport. While the terminal weather is fair to good, early morning fog may frequently restrict flying activity. Ceiling less than 300 feet and/or visibility less than 1 mile²¹ occurs only 1-3 percent of the time, and thunderstorms are most frequent from mid-afternoon to early evening. Crosswinds greater than 15 knots and occur less than 1 percent of the time (USAFETAC, 1985).

Monthly temperature, precipitation, thunderstorms & twilight (USAFETAC, 1985):

GUATEMALA CITY	MAY	JUN	JUL	AUG	SEP	OCT
TEMPERATURE (°F)						
Absolute maximum	90	89	83	88	88	84
Mean maximum	80	76	76	77	76	74
Mean minimum	60	60	59	59	59	58
Absolute minimum	49	54	50	53	52	46
MEAN PRECIPITATION (INCHES)	9.2	10.1	8.0	7.4	10.4	6.0
MEAN NUMBER OF DAYS						
Precipitation	11	21	16	20	22	10
Thunderstorms	4	7	5	8	8	2
CIVIL TWILIGHT (15th of month)						
First light (local standard time)	0512	0509	0517	0526	0529	0532
Last light (local standard time)	1845	1856	1858	1847	1825	1804

²⁰Clear = 0/10 sky cover, partly cloudy = 1/10-5/10, cloudy = 6/10-9/10 and overcast = 10/10.

²¹Henceforth, ceiling/visibility, e.g., 300/1 indicates "ceiling of 300 feet and/or visibility of 1 mile".

Dry Season: November - April. Contrasted to the rainy season, the dry season is characterized by only *partly* cloudy skies, and warm to hot temperatures. Precipitation is infrequent except in the northern lowlands and on the Caribbean slopes of mountains. While these two locations record minimum precipitation amounts during this season, they do not experience the very dry conditions that occur in the interior and on the Pacific mountain slopes. Morning fog occurs frequently in the interior highlands and valleys. While temperatures in the lowlands range from 65-75°F in the morning to 80-90°F in the afternoon, the interior highlands warm from morning lows of 35-40°F to highs of 65-70°F. Above 7000 feet elevation, subfreezing temperatures are not uncommon. Precipitation occurs only 0-3 days per month on the Pacific mountain slopes and in the interior highlands. Snowfall is infrequent, confined to the highest mountain peaks; and thunderstorms are uncommon in the dry season. However, on the Caribbean mountain slopes and northern lowlands, rainfall occurs 3-20 days per month, with the greatest amount of rainfall occurring on the mountain slopes; nonetheless, thunderstorms are still infrequent. Not only may mid-latitude cold fronts penetrate as far south as Guatemala (if not further) with their associated strong, gusty northerly winds and one or two days of cloudy skies and rain, but tropical cyclones are still a possibility on the Caribbean coast during November.

Flying weather: Generally good except in the Caribbean lowlands and on mountain slopes. The weather begins to deteriorate along the North Pacific coast in February, and by April the ceiling/visibility is less than 5000/6 as often as 90 percent of the time; however, elsewhere less than 5000/6 occurs only 20-40 percent of the time. On the plateau due to fog near sunrise, 1500/3 occurs as often as 60 percent of the time, while 500/1 occurs as often as 15 percent (see Appendix B for Huehuetanango and Puerto Barrios data).

Terminal weather: Guatemala City/La Aurora Airport. Generally good, except that ceiling/visibility less than 300/1 occurs as often as 12 percent of the the time, likely around sunrise (early morning fog). Thunderstorms are infrequent, and as in the rainy season, occurrence of crosswinds greater than 15 knots is less than 1 percent (USAFETAC, 1985).

Monthly temperature, precipitation, thunderstorms & twilight (USAFETAC, 1985):

GUATEMALA CITY	NOV	DEC	JAN	FEB	MAR	APR
TEMPERATURE (°F)						
Absolute maximum	86	84	86	89	92	91
Mean maximum	73	74	75	77	80	82
Mean minimum	55	54	53	53	56	58
Absolute minimum	45	41	42	41	45	47
MEAN PRECIPITATION (INCHES)	0.8	0.4	0.1	*	0.3	0.7
MEAN NUMBER OF DAYS						
Precipitation	3	2	1	1	4	3
Thunderstorms	1	*	*	*	1	2
CIVIL TWILIGHT (15th of month)						
First light (local standard time)	0540	0556	0608	0604	0549	0527
Last light (local standard time)	1753	1759	1815	1828	1834	1838

(NOTE: * = less than 0.05 inch or 0.5 day, as appropriate)

1.3.2 Belize

Land

Belize, lying in the southeastern portion of the Yucatan Peninsula, has Mexico on its northern border, Guatemala on its western border as well as on its very narrow southern border, while it has the Caribbean Sea (actually the Gulf of Honduras) along its entire eastern boundary. While its neighbor Guatemala is the *most* populated, Belize has the smallest population of the seven Central American nations. However, it is the second *smallest* nation—only El Salvador is smaller—having an area just smaller than the state of New Hampshire.

As depicted in Fig. 1.23, Belize has a much larger north-south dimension (174 miles) than east-west dimension (68 miles at its widest). It can be divided into three regions: the northern lowlands, southern uplands and the coast. Most of the northern lowlands are swampy, lying less than 200 feet above sea level. In the southern uplands are found the hills and valleys of both the Maya Mountains, and its northeast extension, the Cockscomb Mountains. Considerably lower than Guatemala's Tajumulco, Belize's highest mountain is Victoria Peak at 3681 feet. The rivers, all running eastward and draining into the Caribbean Sea are: Hondo (forming the northern border with Mexico), New, Belize, Monkey, Sarstoon (forming most of Belize's southern border, with Guatemala) and others. Inland from its low and swampy coast, lie numerous lagoons. In addition to many small, low islands (cays), the world's second-largest barrier reef lies 10–40 miles offshore (The Diagram Group, 1985).

Climate

General Belize's climate is subtropical, with onshore trade winds. While the *mean* temperature at Belize City on the coast ranges from 74° in December to 85° in July, inland days are hotter and nights are cooler. Annual rainfall ranges from 50 inches in the flatter northern lowlands to 170 inches in the more mountainous south. While hurricanes can sweep westward over Belize from the Caribbean Sea, droughts are possible (The Diagram Group, 1985).

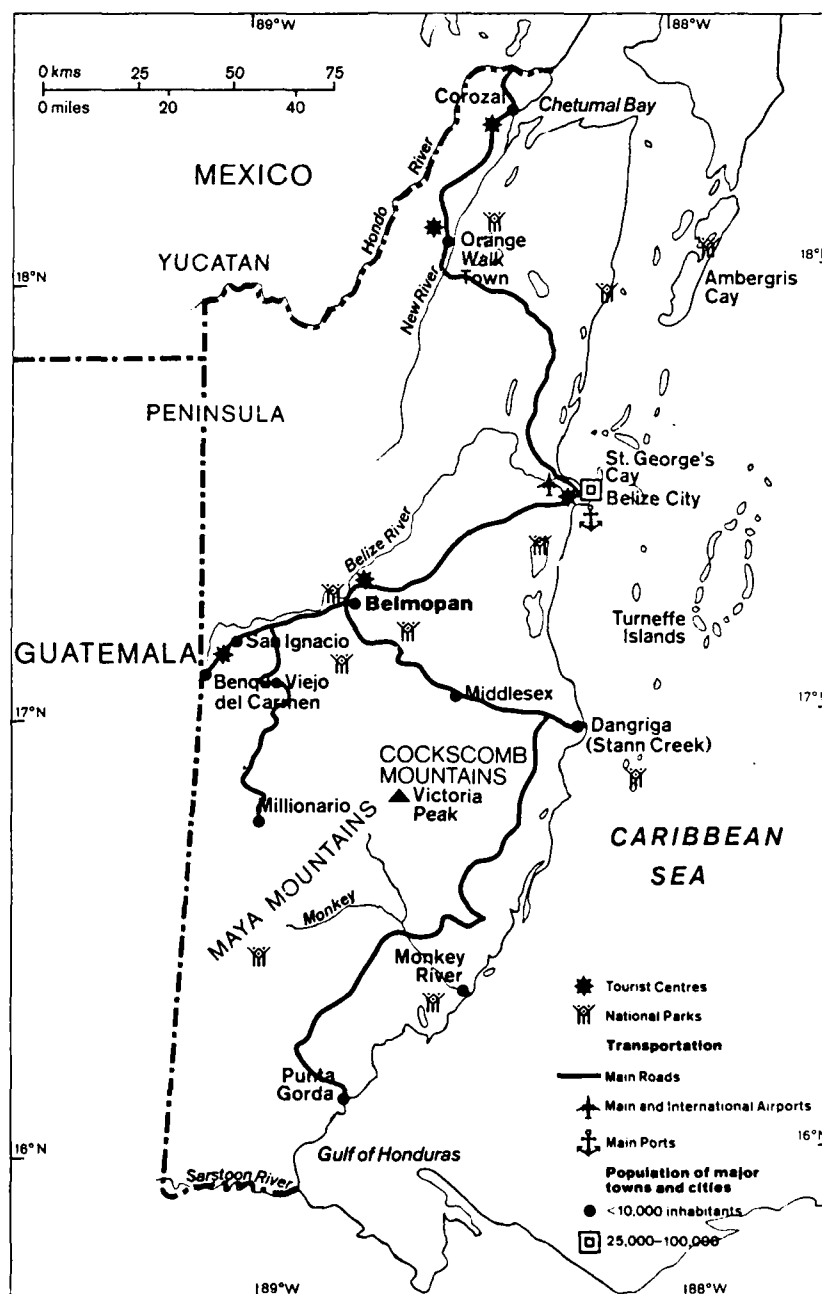


Figure 1.23: Belize (The Diagram Group, 1985)

The climate of Belize will *not* be divided into a rainy season and a dry season as is done with the other countries. However, while the climate is treated as an *annual* one which is hot, humid and cloudy, rainfall is generally moderate to heavy from May through January (with the monthly maximum in October at Belize City; see next page), with a reduction of cloudiness and rainfall during February and March.

More specifically, rainfall is extremely heavy from only June through September in the southern one-quarter of the country. While mean cloudiness is 55-70 percent from April through January, it is slightly less than 50 percent in February and March.

As noted below, for Belize City, mean maximum temperatures are in the upper 80's (°F) during the summer and lower 80's during the winter, while mean minimum temperatures are in the 70's from March through October and in the 60's from November through February.

Again, as noted below, the thunderstorm frequency is greatest from June through September. While thunderstorms are quite uncommon in northern Belize, their frequency increases southward. Additionally, they occur during the morning along the coast, but during the afternoon inland. Mean surface winds are northeast to east, 8-15 kt. Being the country farthest north, Belize frequently experiences a day or two of rain and strong northerly winds ushered in by mid-latitude cold fronts, from November through March.

Affected by tropical storms and hurricanes from May through November, the monthly probability of having at least one tropical storm and/or hurricane strike Belize ranges from 5 to 20 percent with the greatest probability in September (see Section 5).

Flying weather: Fair to good, although flying weather may be restricted by early morning fog, heavy rainfall or thunderstorms. The percentage frequency of ceiling/visibility less than 5000/6 ranges from 25-50 percent, while 1500/3 ranges from 10-20 percent (see Appendix B for specific ceiling/visibility statistics for Belize City).

Terminal weather: Belize City. Hot and humid, with moderate to heavy rainfall. Mean relative humidities lie between 75 and 90 percent. While rainfall is expected 4-18 days per month, the heaviest rainfall accumulation is from June through January. Ceiling/visibility is less than 300/1 about 1 percent of the time, mostly during early morning hours. Visibility is restricted primarily by rain, haze/smoke and early morning fog. Runway crosswinds are greater than 15 kt during 1-3 percent of the time (USAFETAC, 1985)

Monthly temperature, precipitation, thunderstorms & twilight (USAFETAC, 1985):

BELIZE CITY	JAN	FEB	MAR	APR	MAY	JUN
TEMPERATURE (°F)						
Absolute maximum	90	93	98	99	97	97
Mean maximum	82	83	85	87	88	88
Mean minimum	68	69	72	74	75	76
Absolute minimum	50	49	50	55	57	62
MEAN PRECIPITATION (INCHES)	5.7	2.7	1.6	2.4	5.0	9.1
MEAN NUMBER OF DAYS						
Precipitation	12	6	4	4	7	14
Thunderstorms	0	*	0	0	1	4
CIVIL TWILIGHT (15th of month)						
First light (local standard time)	0604	0558	0540	0515	0458	0454
Last light (local standard time)	1802	1817	1825	1832	1841	1853
	JUL	AUG	SEP	OCT	NOV	DEC
TEMPERATURE (°F)						
Absolute maximum	95	96	97	95	95	93
Mean maximum	88	88	89	86	84	82
Mean minimum	76	76	75	73	69	68
Absolute minimum	63	61	60	58	52	46
MEAN PRECIPITATION (INCHES)	7.6	7.3	9.5	12.4	9.8	7.2
MEAN NUMBER OF DAYS						
Precipitation	18	16	18	15	13	14
Thunderstorms	2	4	5	1	*	0
CIVIL TWILIGHT (15th of month)						
First light (local standard time)	0503	0513	0519	0524	0535	0552
Last light (local standard time)	1855	1842	1817	1753	1740	1745

(NOTE: * = less than 0.5 day)

1.3.3 Honduras

Land

Honduras occupies the *upper* portion of the "knee" of Central America. As Central America's second-largest nation (only Nicaragua is larger), Honduras is a little larger than the state of Tennessee. While Guatemala and El Salvador form its western border, and Nicaragua its long southeastern boundary, Honduras has a short stretch of Pacific coastline in the south, compared with a long northern Caribbean coast. Its small Pacific coast borders the Gulf of Fonseca, while the extensive Caribbean coast includes the Gulf of Honduras in the west (see Fig. 1.24).

With its wedge shape, Honduras is about 400 miles from west to east, but only about 180 miles from south to north. Honduras, although nearly two-thirds occupied by uplands and mountains, has no *active* volcanoes as do its neighbors, but its highest peak is Cerro de las Minas (9,347 feet) in the west. Mountain ranges approach the northern coast at an angle, with one range continuing submerged out to sea and reappearing as the Islas de la Bahía (Bay Islands) chain. While much of the northern coast is rimmed by a lowland of rich clay and loam soils, the Caratasca Lagoon, a swampy lowlands, occupies the northeast corner, along the Mosquito Coast²². Rivers flowing north, including the Ulúa in the northwest, form fertile valleys. To the south, the Gulf of Fonseca, which contains an archipelago of nearly 300 tiny islands, is surrounded by a narrow lowland (The Diagram Group, 1985).

Climate

General While the coastal lowlands are hot and humid, the upland interior is cooler and much drier. Although average temperatures in the highlands at 7000 feet are only in the high 50's (°F), they reach the mid 80's on the coast. Tegucigalpa, the capital, has an annual temperature range of only 11°F. While the northeast is the wettest region of the country, where onshore winds are associated with up to 110 inches of rain per year, some inland valleys receive only 40 inches (The Diagram Group, 1985).

²²A strip along the Caribbean Sea (including both northeastern Honduras and the entire east coast of Nicaragua) named for its Miskito Indians.

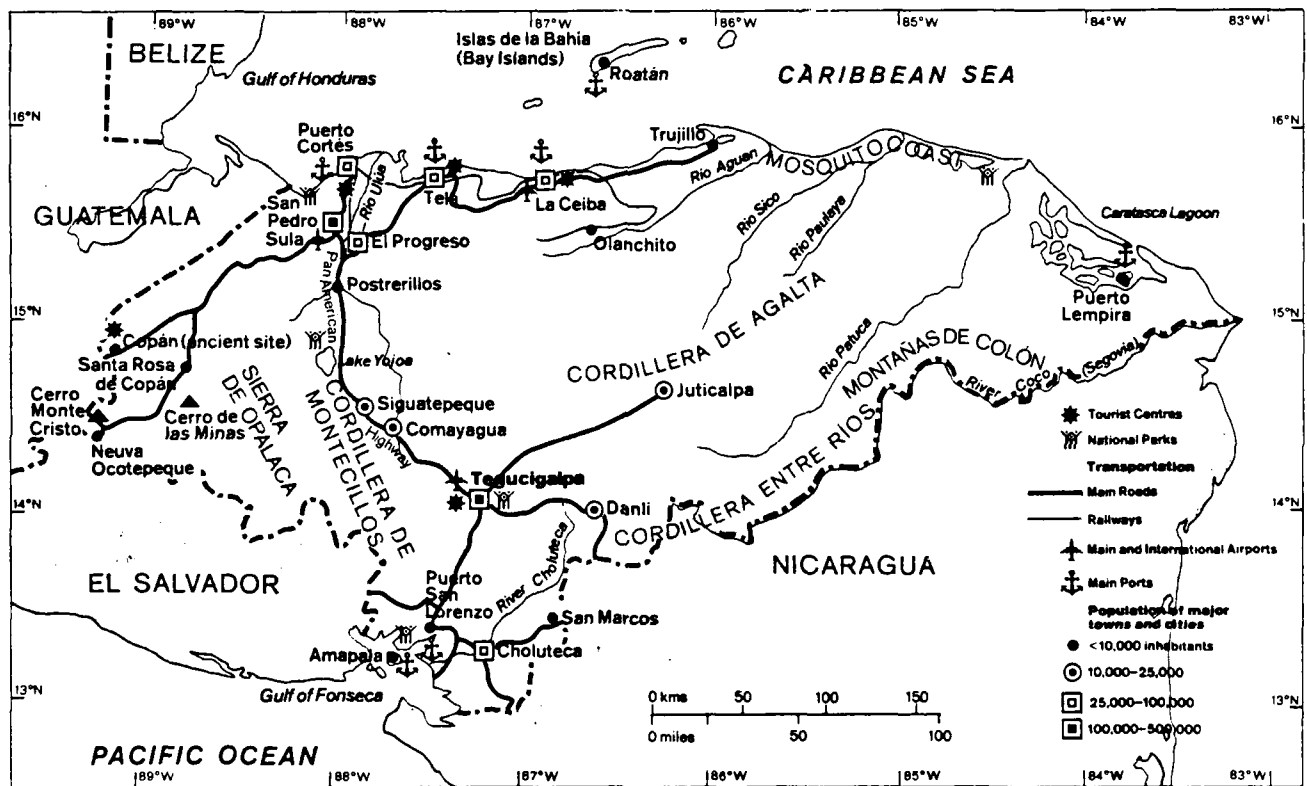


Figure 1.24: Honduras (The Diagram Group, 1985)

Rainy Season: May - October. During this season, the weather is characterized by mostly cloudy skies and hot temperatures, with frequent rain showers and thunderstorms. Surprisingly, however, along the north coast on the Gulf of Honduras some stations record the minimal precipitation at this time of year. While precipitation amounts on the Caribbean coast are often very heavy, only moderate amounts are expected in the interior. Mean monthly cloudiness varies between 50 and 85 percent. Depending upon elevation, mean minimum temperatures vary between the 60's and the upper 70's (°F). Note that the data given below are for Tegucigalpa (3,304 feet). Maximum monthly temperatures range from the upper 80's to the lower 90's, with particularly hot low lying Pacific coast stations. Thunderstorms occur with greater frequency at coastal stations. Surface winds are normally northerly or northeasterly at 6-10 kt. See Section 5 for details concerning tropical storms or hurricanes that primarily affect the Caribbean coastal areas.

Flying weather: Usually good, except in the vicinity of thunderstorms. Ceiling/visibility less than 5000/6 occurs 25-45 percent of the time, while less than 1500/3 occurs 5-10 percent, and less than 500/1 occurs 1-6 percent. Icing and turbulence are not expected except near rain showers and thunderstorms; however, early morning fog can be a problem at mountain stations (see Appendix B for ceiling/visibility statistics at several coastal and inland cities).

Terminal weather: Tegucigalpa. Generally good. Ceiling/visibility less than 300/1 rarely occurs; yet fog forms on 14-22 mornings per month, but rarely restricts visibility below 3 miles. As indicated below, thunderstorms occur on 6-12 days per month, normally during early evening. Occurrence of crosswinds greater than 15 kt is 1-3 percent, normally during late afternoon and early evening (USAFETAC, 1985).

Monthly temperature, precipitation, thunderstorms & twilight (USAFETAC, 1985):

TEGUCIGALPA	MAY	JUN	JUL	AUG	SEP	OCT
TEMPERATURE (°F)						
Absolute maximum	94	90	89	91	90	88
Mean maximum	85	82	81	83	83	80
Mean minimum	64	65	64	63	63	63
Absolute minimum	49	56	55	54	55	52
MEAN PRECIPITATION (INCHES)	5.7	6.3	3.5	3.9	7.2	5.4
MEAN NUMBER OF DAYS						
Precipitation	11	17	15	14	19	16
Thunderstorms	9	12	7	7	11	6
CIVIL TWILIGHT (15th of month)						
First light (local standard time)	0459	0457	0505	0513	0516	0518
Last light (local standard time)	1831	1841	1844	1833	1812	1751

Dry Season: November - April. The weather during this season is characterized by *partly* cloudy skies and infrequent rainfall, yet warm to hot temperatures. **However**, in the eastern part of the country near the Caribbean Sea the rainy season does not end until December, and **moreover**, the north coast, on the Gulf of Honduras, receives its maximum rainfall at this time. Rain occurs 5-20 days per month along the northern coast, but generally less than 5 days per month in the interior (see Tegucigalpa data below) and on the Pacific coast. Mean monthly cloudiness in the interior is about 55-75 percent, and 30-50 percent on the Pacific coast, where offshore winds dominate. While minimum temperatures range from 55 to 75 (°F), maximum temperatures range from 70 to 85 (°F). Along the narrow Pacific coast, extremely high temperatures (over 100°F) occur daily. Thunderstorms occur 2-6 days per month in November and December (less in Tegucigalpa, see below), but less frequently in later months. Mean surface winds are north to northeast at 8-15 kt (i.e., stronger than in the rainy season). Extratropical cold fronts occasionally reach the north coast causing one to two days of rain and strong northerly winds.

Flying weather: Usually good. Ceiling/visibility less than 5000 feet and/or 6 miles occurs 15-45 percent, while less than 1500/3 occurs 1-5 percent, and less than 500/1 rarely occurs. Along the north coast, aircraft icing can occur above the freezing level in stratified cloudiness (see Appendix B for ceiling/visibility statistics at several cities).

Terminal weather: Tegucigalpa. Good. Ceiling/visibility less than 300/1 seldom occurs; morning fog is common, but it seldom restricts visibility significantly. While precipitation occurs 2-9 days per month, thunderstorms are rare except in April (see below). Occurrence of crosswinds greater than 15 kt is 2-5 percent (USAFETAC, 1985).

Monthly temperature, precipitation, thunderstorms & twilight (USAFETAC, 1985):

TEGUCIGALPA	NOV	DEC	JAN	FEB	MAR	APR
TEMPERATURE (F)						
Absolute maximum	91	88	89	91	93	96
Mean maximum	78	77	77	80	84	86
Mean minimum	60	58	57	57	58	62
Absolute minimum	48	47	39	43	46	48
MEAN PRECIPITATION (INCHES)	1.7	0.5	0.5	0.2	0.4	1.1
MEAN NUMBER OF DAYS						
Precipitation	9	6	4	2	2	4
Thunderstorms	1	0	*	0	1	3
CIVIL TWILIGHT (15th of month)						
First light (local standard time)	0527	0542	0554	0551	0535	0514
Last light (local standard time)	1740	1746	1803	1816	1821	1824

(NOTE: * = less than 0.5 day)

1.3.4 El Salvador

Land

While El Salvador is the most *densely* populated, it is the smallest nation in Central America—about the size of the state of Massachusetts.

As indicated in Fig. 1.25, El Salvador, unlike the other six Central American nations, has no Caribbean coast. With Guatemala to the west and Honduras to the north and east, El Salvador has the Pacific Ocean coast as its entire southern border. Note, however, that only the Gulf of Fonseca separates its southeastern corner from the western tip of Nicaragua.

The shape of El Salvador is roughly rectangular, 160 miles from west to east, and 60 miles from north to south. Although not immediately evident, El Salvador can be divided into four regions, running *roughly* the length of the country. The four regions are, from south to north, the Pacific lowlands, the southern mountains, the plateau and the northern mountains.

While only 12 percent of El Salvador consists of coastal lowlands and hills, lagoons form part of the southeast coastline. Another third of the nation is formed by the southern mountain chain, at the western end of which is Santa Ana, with a peak at 7,812 feet. Even the nation's largest lake, Llopango, lies in an extinct volcanic crater. While some of its more than 20 volcanoes are active, with the commensurate expectation of earthquakes, volcanic ash and lava provide the nation's richest soils. The plateau, at an elevation averaging 2000 feet and comprising more than two-thirds of the country, is drained by the deep valleys of the Rivers Lempa and San Miguel in the eastern half of El Salvador. Finally, the northern mountains cover about 15 percent of the nation; here El Salvador's highest peak, Cerro El Pital (8,956 feet), is located (The Diagram Group, 1985).

Climate

General The nation's temperature varies with altitude. While the coast is hot and humid, the high inland regions are cooler. The capital San Salvador, at 2,290 feet, has an annual average temperature of only 73°F, with a small range of 5.4°F. While the hottest months are April and May, the coolest months are December through February. The country's annual rainfall is 72 inches; however, the higher mountains receive more and the valleys less than this average (The Diagram Group, 1985).

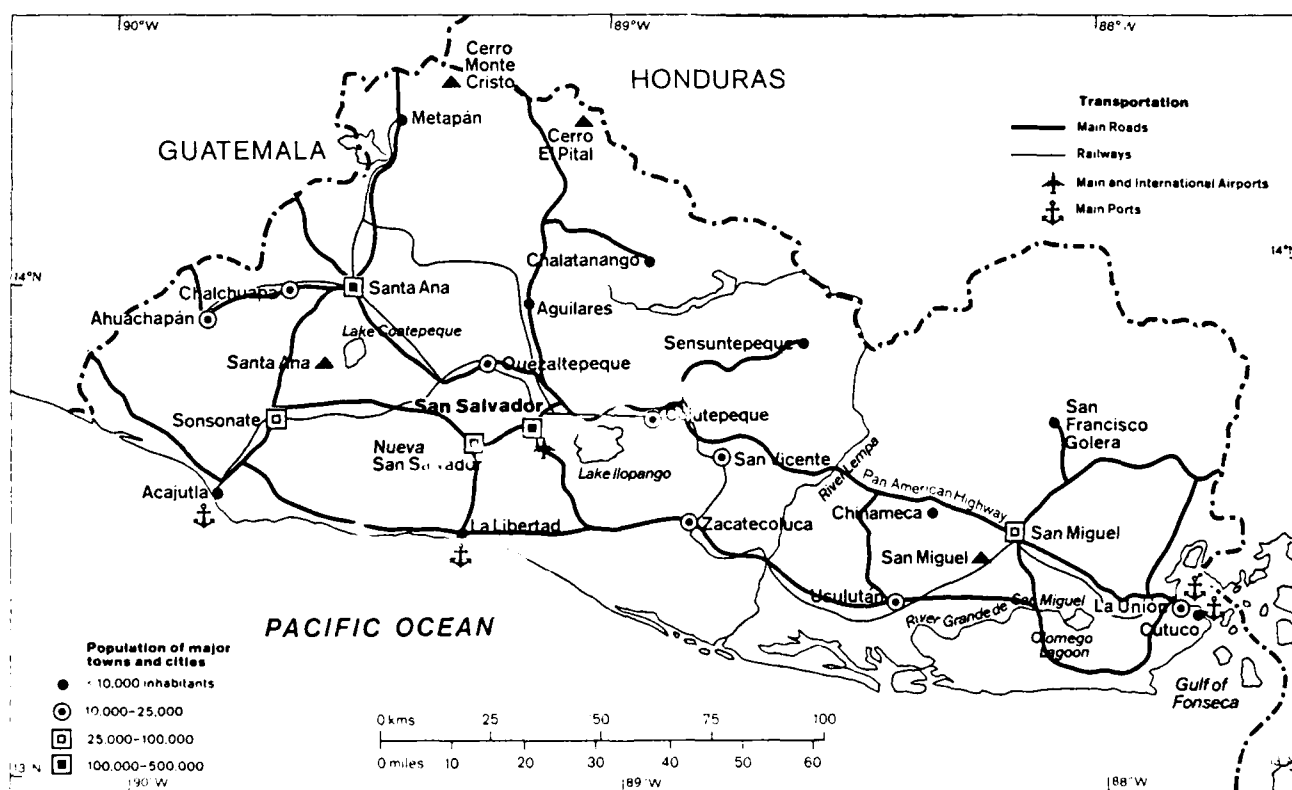


Figure 1.25: El Salvador (The Diagram Group, 1985)

Rainy season: May – October. Heavy rainfall is expected in warm and cloudy weather, with an occasional tropical storm or hurricane. Cloudy skies dominate with: clear skies, 1–3 percent; partly cloudy, 15–35 percent; cloudy, 50–70 percent; and overcast, 10–20 percent of the time. Rain is expected 10–25 days per month, usually associated with thunderstorms. However, gusty surface winds in excess of 16 kt are expected less than 1 percent of the time, with gale force winds (33 kt) rare. The monthly probability of tropical cyclones and/or hurricanes affecting El Salvador increases from 15 percent in May through July to 30 percent in August through October (see Section 5).

Flying weather: Fair to Poor. The percentage frequencies of ceiling/visibility are : less than 5000 feet and/or 6 miles, 10–25 percent; less than 1500/3, 5–10 percent; and less than 500/1, 1–2 percent. Not only are thunderstorms and rain very heavy at times, but heavy rain showers and early morning fog can restrict flying conditions. (See Appendix B for ceiling/visibility statistics at Acajutla and San Salvador.)

Terminal weather: San Salvador. The weather is warm and cloudy, with numerous thunderstorms and heavy rain showers, leading to ceiling/visibility less than 300/1 for 1–2 percent of the time. Runway crosswinds in excess of 15 kt are expected only about 1 percent of the time. Gusty surface winds in excess of 16 kt are expected less than 1 percent, with gale force winds a rarity. Visibility is obstructed 5–10 percent due primarily to haze/smoke and early morning fog; however, during May visibility is obstructed 30 percent of the time due to haze/smoke, dust and early morning fog (USAFETAC, 1985).

Monthly temperature, precipitation, thunderstorms & twilight (USAFETAC, 1985):

SAN SALVADOR	MAY	JUN	JUL	AUG	SEP	OCT
TEMPERATURE (°F)						
Absolute maximum	103	98	98	98	99	101
Mean maximum	91	87	89	89	87	87
Mean minimum	67	66	65	66	66	65
Absolute minimum	58	56	58	60	53	54
MEAN PRECIPITATION (INCHES)	7.4	12.7	12.5	11.7	12.5	9.0
MEAN NUMBER OF DAYS						
Precipitation	13	20	22	21	21	16
Thunderstorms	13	17	18	18	18	10
CIVIL TWILIGHT (15th of month)						
First light (local standard time)	0507	0505	0513	0521	0524	0526
Last light (local standard time)	1838	1848	1851	1840	1819	1759

Dry season: November – April. The weather is hot and dry (see data below), with clear to partly cloudy skies. Partly cloudy skies dominate with: clear skies, 10–35 percent; partly cloudy, 45–50 percent; cloudy 20–40 percent; and overcast, 1–5 percent of the time. Rain occurs only 1–5 days per month, and is usually associated with a thunderstorm. Visibility is obstructed 5–15 percent of the time during November through March, but this percentage increases to 40 percent in April, with the primary restrictions to visibility being haze/smoke and dust. While gusty surface winds in excess of 16 kt are expected 5 percent of the time, gale force winds are rare. Tropical cyclones and/or hurricanes are rare during this period (see Section 5).

Flying weather: Generally good. The percentage frequencies of ceiling/visibility are: less than 5000 feet and/or 6 miles, 5–10 percent, November through March and 25 percent in April; less than 1500/3 miles, 1–2 percent; and less than 500/1, rare. However, early morning fog can restrict flying activities in the highlands (see Appendix B for ceiling/visibility statistics at Acajutla and San Salvador).

Terminal weather: San Salvador, El Salvador. The weather is hot and dry with ceiling/visibility less than 300/1 a rarity. Precipitation is expected 5 days per month (see data below), usually associated with a thunderstorm. Primary restrictions to visibility are haze/smoke and dust, leading to obstruction to visibility 5–10 percent from November through February, 15 percent in March, and increasing to 40 percent in April; however, visibility rarely goes below 3 miles. While gusty runway crosswinds in excess of 15 kt are expected about 1–2 percent of the time, gusty surface winds in excess of 16 kt are expected 5 percent of the time, but gale force winds are rare (USAFETAC, 1985).

Monthly temperature, precipitation, thunderstorms & twilight (USAFETAC, 1985):

SAN SALVADOR	NOV	DEC	JAN	FEB	MAR	APR
TEMPERATURE (°F)						
Absolute maximum	102	101	101	103	105	104
Mean maximum	87	89	90	92	94	93
Mean minimum	63	61	60	60	62	65
Absolute minimum	49	47	45	49	45	54
MEAN PRECIPITATION (INCHES)	1.6	0.4	0.2	0.2	0.4	2.1
MEAN NUMBER OF DAYS						
Precipitation	5	1	1	1	1	5
Thunderstorms	5	1	1	1	5	5
CIVIL TWILIGHT (15th of month)						
First light (local standard time)	0534	0549	0601	0558	0543	0522
Last light (local standard time)	1748	1755	1811	1823	1828	1831

1.3.5 Nicaragua

Land

Nicaragua is the largest nation of Central America—a little larger than the state of New York. With the Caribbean Sea to its east and the Pacific Ocean to its west, Nicaragua occupies a “mid” position within Central America (see Fig. 1.26). Only two countries have borders with Nicaragua, Honduras along the long boundary to the north, and Costa Rica to the south.

The shape of Nicaragua somewhat resembles a triangle formed by the Honduran border, the Caribbean coast, and finally a line produced by the Pacific coast and the Costa Rican border. The country's highest mountain Pico Mogotón (6,913 feet) lies in the northwest near the Honduran border. From the Honduran border southward there are three separate mountain chains (“cordilleras”) in the center of the country: Cordillera Isabella running nearly parallel to the Honduran border, next Cordillera De Darien running east-west, and finally Sierra De Amerique (also known as Cordillera Chontaleña) lying to the northeast of Lake Nicaragua. There are many rivers, with River Coco forming much of Nicaragua's border with Honduras, while the San Juan, likewise, forms much of the southern border with Costa Rica.

To the east of these central mountain chains lies Nicaragua's Mosquito coast, one of the broadest Caribbean lowlands in Central America. This coast extends approximately 336 miles, including deltas, sandbars and lagoons, with offshore reefs²³ and islands (“cayos”).

Lake Nicaragua, Central America's largest lake, lies southwest of the mountain chains. This lake and smaller Lake Managua, lie parallel to the Pacific coast but inland of about 40 volcanoes (some active) which also form a line parallel to the Pacific coastline. The Pacific coast of Nicaragua extends from the Gulf of Fonseca to the Salinas Bay. Volcanic ash here, as well as in the central valleys, has produced fertile soil (The Diagram Group, 1985).

Climate

General The lowlands are hot and humid. On the Pacific coast, average annual temperature is 81°F, on the Caribbean coast, 79°F; however, mountains, in the northern portion of the country, have lower temperatures, i.e., about 64°F.

With 150 inches of rainfall per year, the Caribbean side of Nicaragua has one of the highest rainfalls in Central America. However, with the prevailing winds (primarily *katabatic*) blowing from the northeast, the Pacific side of Nicaragua receives only about half that amount with a more marked dry season from January through April (The Diagram Group, 1985).

²³For further oceanographic details, see Section 4.

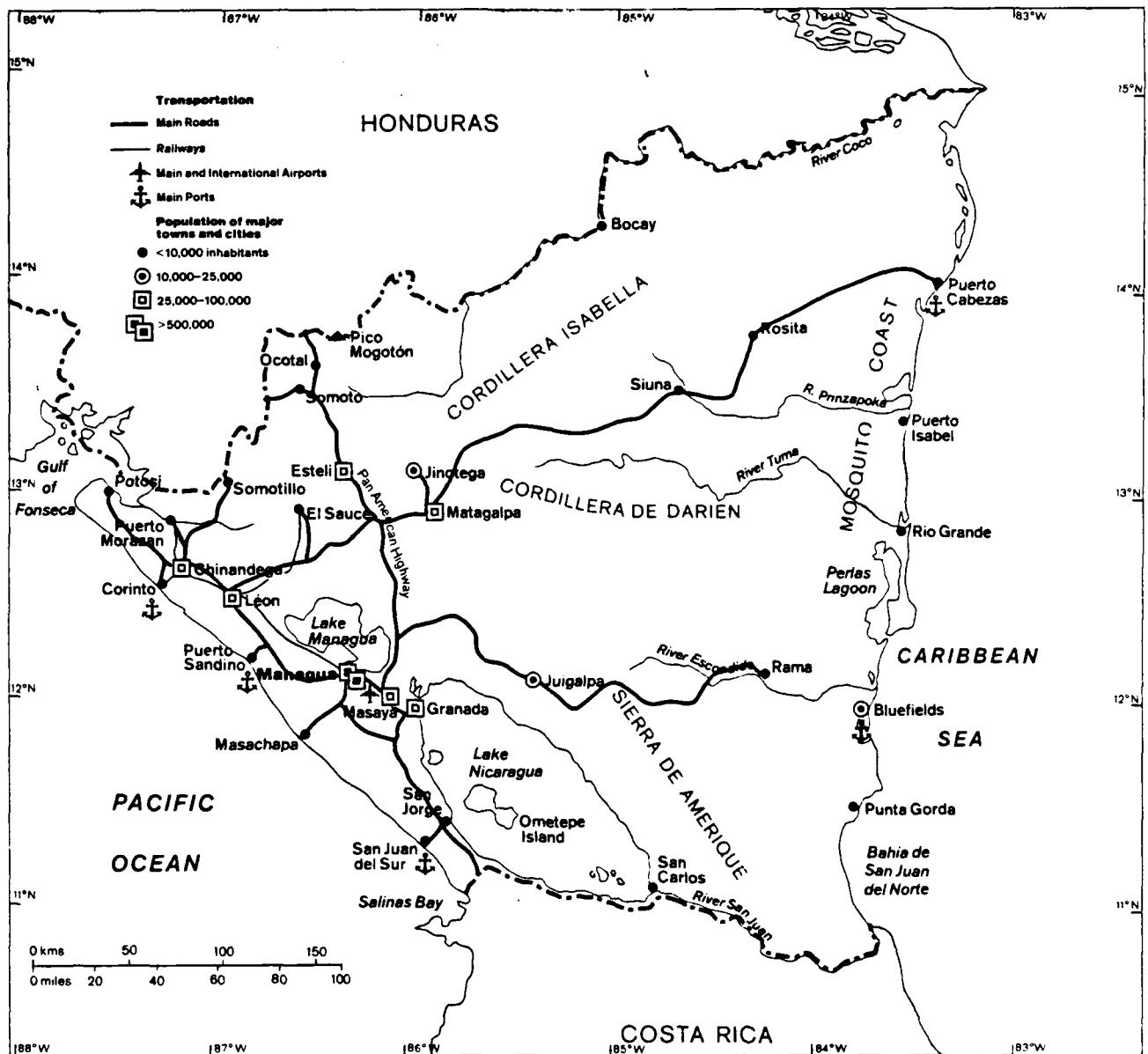


Figure 1.26: Nicaragua (The Diagram Group, 1985)

Rainy season: June - October

These months are characterized by frequent precipitation and heavy cloudiness. Night-time temperatures are quite warm, then climb from the low 70's (°F) in the early morning to the 80's or low 90's by afternoon. Mean sky cover, primarily in the form of low clouds, ranges from 70 to 80 percent. Precipitation, which is smaller in the interior, is most frequent along the Caribbean lowlands where the monthly average is 10-26 inches. Precipitation can be expected 17-30 days per month, and thunderstorms are frequently accompanied by strong, gusty winds and violent lightning. Visibilities are generally good, except along the coast. Fog, heavy rain showers, haze and/or smoke restrict coastal region visibilities to less than 6 miles, 10-20 days per month. Winds, averaging less than 15 kt, are usually calm during the night and then increase during the day, with 55 kt possible during severe thunderstorms. The average monthly probability of a tropical storm and/or hurricane affecting Nicaragua ranges from 15 to 25 percent (see Section 5).

Monthly temperature, precipitation, thunderstorms & twilight (USAFETAC, 1985):

MANAGUA	JUN	JUL	AUG	SEP	OCT
<hr/>					
TEMPERATURE (°F)					
Absolute maximum	95	92	93	94	94
Mean maximum	88	88	89	89	88
Mean minimum	73	73	73	73	72
Absolute minimum	69	70	70	69	66
MEAN PRECIPITATION (INCHES)	8.2	3.6	5.1	6.8	6.3
MEAN NUMBER OF DAYS					
Precipitation	13	11	10	11	10
Thunderstorms	13	13	10	14	7
CIVIL TWILIGHT (15th of month)					
First light (local standard time)	0457	0504	0511	0513	0513
Last light (local standard time)	1833	1837	1827	1807	1748
BLUEFIELDS					
<hr/>					
TEMPERATURE (°F)					
Absolute maximum	94	93	92	94	94
Mean maximum	87	85	87	89	88
Mean minimum	73	73	73	72	71
Absolute minimum	66	67	62	66	64
MEAN PRECIPITATION (INCHES)	19.8	26.2	21.5	12.3	13.6
MEAN NUMBER OF DAYS					
Precipitation	N/A	N/A	N/A	19	20
Thunderstorms	*	*	*	*	*

(* = less than 0.5 day)

(N/A = data not available)

Flying weather: Fair to good. The heavy rainfall along the Caribbean coast, such as at Bluefields (see totals on previous page), produces ceiling/visibility less than 5000 feet and/or 6 miles for 1-15 percent of the time, with less than 1500/3, 1-3 percent. While heavy rain showers and thunderstorms are frequent throughout the country, they are especially prevalent along the coast. Tops of thunderstorms often reach 60,000 feet, some being reported as high as 80,000 feet. Severe turbulence is expected with these storms, plus mountain-wave turbulence presents a hazard to flying west of the mountain ridges, i.e., "downwind" of the ridges (see Appendix B for ceiling/visibility statistics for Bluefields, Chinadega, Managua and Puerto Cabezas).

Terminal weather: Good. At Managua, the percentage frequency of ceiling/visibility less than 300/1 is 0-1 percent; at Bluefields it is 1-2 percent. While mean winds are less than 10 kt during the evening, winds are 15 kt in the afternoon, with even stronger winds associated with thunderstorms, tropical storms and/or hurricanes. Heavy rain showers, fog, smoke and/or haze provide the primary restrictions to visibility (USAFETAC, 1985).

Transitional months: November - December

November and December are the transitional months between the rainy and dry seasons. The hot temperatures and cloudy skies continue; however, there is a general decline in precipitation (particularly notice Managua's rainfall on the following page). While morning temperatures (high 60's (°F)) are slightly cooler than the rainy season, the afternoons still warm to the low 90's. Mean sky cover (20-40 percent) is lower in the inland portion of Nicaragua, but the coastal regions remain near 70 percent. Likewise, the mean precipitation is much less inland than on the coast (compare Managua and Bluefields), with the mean monthly rainfall ranging from 2-20 inches over the country. Thunderstorm days reduce to only 4-6 per month. Fog, smoke and/or haze reduce visibilities to less than 2.5 miles approximately 1 day per month. Usually occurring in the afternoon, winds greater than 16 kt are expected 1-2 days per month. While the probability of at least one tropical storm and/or hurricane affecting Nicaragua is 10 percent in November, tropical cyclones in December are rare (see Section 5).

Flying weather: Fair to good. Despite the larger rainfall at Bluefields, the percentage frequency that ceiling/visibility is less than 5000 feet and/or 6 miles is approximately 5 percent, but at Managua, ceiling/visibility less than 5000/6 is about 15 percent. Expectation of ceiling/visibility less than 1500/3 is 1 percent at both stations. Turbulence is anticipated in thunderstorms; additionally, low-level clear air turbulence is sometimes present on hot, sunny days (see Appendix B for ceiling/visibility statistics for several cities).

Terminal weather:

Managua (Las Mercedes), Nicaragua. Warm and cloudy conditions prevail, with light rain storms and occasionally gusty surface winds. Skies are clear only 5 percent of the time; partly cloudy to cloudy skies dominate 70-80 percent, with overcast, 10-25 percent. Visibility is generally good, as early morning fog occurs less than one day per month. Rain is expected seven days in November, but its frequency decreases to only two days in December (see data below). While gusty winds are expected 2-5 percent of the time, gale force winds are rare and ceiling/visibility less than 300/1 has not been observed.

Bluefields, Nicaragua. Cloudy and rainy, with clear skies a rarity. Skies are partly cloudy to cloudy 75-80 percent; overcast, 20-25 percent. Although rainfall is expected 22 days per month (see data below), the ceiling/visibility rarely goes below 300/1. While gusty surface winds are expected 2-5 percent of the time, gale force winds are a rarity (USAFETAC, 1985).

Monthly temperature, precipitation, thunderstorms & twilight (USAFETAC, 1985):

MANAGUA	NOV	DEC
<hr/>		
TEMPERATURE (°F)		
Absolute maximum	92	91
Mean maximum	88	87
Mean minimum	71	70
Absolute minimum	64	59
MEAN PRECIPITATION (INCHES)	1.2	0.3
MEAN NUMBER OF DAYS		
Precipitation	7	2
Thunderstorms	1	*
<hr/>		
BLUEFIELDS		
TEMPERATURE (°F)		
Absolute maximum	93	93
Mean maximum	86	85
Mean minimum	70	69
Absolute minimum	62	62
MEAN PRECIPITATION (INCHES)	15.3	15.7
MEAN NUMBER OF DAYS		
Precipitation	22	22
Thunderstorms	1	*
CIVIL TWILIGHT (15th of month)		
MANAGUA (LAS MERCEDES)		
First light (local standard time)	0520	0534
Last light (local standard time)	1839	1745

(* = less than 0.5 day)

Dry season: January - April

Distinguished by a marked decline in rainfall (especially note the small precipitation for Managua, below), this season is characterized by hot days, cooler nights and partly cloudy skies. Of course, the Caribbean coast remains an exception where cloudiness and rain persist throughout the year (see the precipitation totals for Bluefields, below). Temperatures range from near 70°F at night to the low 90's during the afternoon, although the afternoon temperatures at Bluefields are not quite so high. Mean sky cover is lower on the Pacific coast and inland (40-50 percent), but, it is near 70 percent along the Caribbean coast. Whereas much of the country experiences only 0.5 inch to 2.0 inches of rainfall, totals reach a maximum near 10 inches along the Caribbean coast, with rain occurring as often as 23 days of the month. Visibility is generally good, decreasing to 2.5 miles only one-three days per month, although visibility is restricted by haze/smoke near industrial centers. While wind speeds average 10-12 kt, gusty surface winds generally occur as often as six days per month. (See Section 5 for hurricane data.)

Monthly temperature, precipitation, thunderstorms & twilight (USAFETAC, 1985):

MANAGUA	JAN	FEB	MAR	APR
<hr/>				
TEMPERATURE (°F)				
Absolute maximum	92	93	94	98
Mean maximum	88	89	91	94
Mean minimum	69	70	72	73
Absolute minimum	62	63	67	68
MEAN PRECIPITATION (INCHES)	*	*	*	*
MEAN NUMBER OF DAYS				
Precipitation	2	2	1	2
Thunderstorms	0	0	0	0
CIVIL TWILIGHT (15th of month)				
First light (local standard time)	0547	0545	0531	0511
Last light (local standard time)	1802	1813	1817	1818
BLUEFIELDS				
<hr/>				
TEMPERATURE (°F)				
Absolute maximum	90	90	91	93
Mean maximum	85	85	87	88
Mean minimum	69	69	71	72
Absolute minimum	60	61	62	62
MEAN PRECIPITATION (INCHES)	10.5	5.1	3.2	2.9
MEAN NUMBER OF DAYS				
Precipitation	22	15	12	11
Thunderstorms	0	0	0	0

(* = less than 0.05 inch)

Flying weather: Fair to good. Bluefields on the Caribbean coast experiences ceiling/visibility less than 5000 feet and/or 6 miles, 1-3 percent of the time; and less than 1500/3, less than 1 percent of the time. In the west, Managua experiences ceiling/visibility less than 5000/6, 10-15 percent; and less than 2000/2.5, approximately 1 percent of the time (see Appendix B for ceiling/visibility statistics at several cities).

Terminal weather:

Managua (Las Mercedes), Nicaragua. Warm and cloudy with gusty surface winds and *little* precipitation. Skies are clear 10-15 percent of the time, with rain expected only 1-2 days per month (see data on preceding page). The visibility is restricted by haze and/or smoke 45-50 percent, but rarely goes below 6 miles. While gusty surface winds generally exist 5-10 percent of the time, gale force winds are experienced less than 1 percent of the time. Ceiling/visibility less than 300/1 is a rarity.

Bluefields, Nicaragua. Cloudy and **rainy**. Partly cloudy to cloudy skies (85-90 percent) dominate, with overcast skies 10-15 percent of the time and clear skies a rarity. Mean monthly rainfall, totally 10.5 inches (22 rainfall days) in January, decreases to 2.9 inches (11 rainfall days) in April (see data on preceding the page). Gusty surface winds are expected 2-5 percent of the time; however, gale force winds are rare. Visibility is restricted by haze/smoke 25-30 percent of the time, but it rarely goes below 6 miles. While, early morning fog forms occasionally, it dissipates rapidly after sunrise (USAFETAC, 1985).

Transitional month: May

May is the transition month between the dry and rainy seasons. Rainfall and cloudiness both increase in all parts of Nicaragua. Cloudy skies dominate with: clear 1-5 percent, partly cloudy 20-25 percent, cloudy 40-60 percent and overcast 15-35 percent of the time. While rain occurs on 10-17 days, thunderstorms occur only 2-4 days, depending on location. As expected, skies are cloudiest and rainfall heaviest on the Caribbean side of mountains. While winds in excess of 16 kt are expected approximately 5 percent of the time, gale force winds are rare. The monthly probability of a tropical storm and/or hurricane affecting Nicaragua, being near zero during the dry season, increases to 5 percent (see Section 5).

Flying weather: Fair to good. At Managua, ceiling/visibility is less than 5000 feet and/or 6 miles, 30 percent of the time; less than 1500/3, approximately 1 percent; and less than 500/1, near zero. Heavy rainfall and cloudiness may restrict flying, particularly on the eastern side of the mountains. Additionally, mountain-wave turbulence is possible over and near mountains (see Appendix B for ceiling/visibility statistics for several cities).

Terminal weather: Generally good. While ceiling/visibility is less than 300/1, approximately 1-2 percent of the time; rain is, nonetheless, frequent and heavy at times. Fog is expected only 1 percent of the time, primarily during the early morning hours. At Managua, the visibility is restricted 60 percent of the time by haze and/or smoke. While gusty winds greater than 16 kt are expected 5 percent of the time, gale force winds are a rarity (USAFETAC, 1985).

Monthly temperature, precipitation, thunderstorms & twilight (USAFETAC, 1985):

MANAGUA (LAS MERCEDES) MAY

TEMPERATURE (°F)

Absolute maximum	98
Mean maximum	93
Mean minimum	74
Absolute minimum	65

MEAN PRECIPITATION (INCHES) 3.1

MEAN NUMBER OF DAYS

Precipitation	10
Thunderstorms	2

BLUEFIELDS

TEMPERATURE (°F)

Absolute maximum	94
Mean maximum	87
Mean minimum	74
Absolute minimum	67

MEAN PRECIPITATION (INCHES) 13.6

MEAN NUMBER OF DAYS

Precipitation	17
Thunderstorms	0

CIVIL TWILIGHT (15th of month)

MANAGUA (LAS MERCEDES)

First light (local standard time)	0458
Last light (local standard time)	1824

1.3.6 Costa Rica

Land

Costa Rica, Central America's fifth-largest nation, is slightly larger than Vermont and New Hampshire combined. Long and narrow, it has a mountainous spine running from Nicaragua in the north to Panama in the southeast (see Fig. 1.27). Its long irregular Pacific coastline measures 631 miles compared with a much shorter and more straight Caribbean shore of only 132 miles.

While the swampy Caribbean coastal plain forms 30 percent of Costa Rica, the mountainous spine consists of three mountain ranges (cordilleras), from the northwest to the southeast: Guanacaste, Central and Talamanca. It's highest mountain peak Chirripó (12,529 feet) is found in the southeastern portion of the country in the Talamanca range. Within these ranges, the mountains are flanked by fertile tablelands. The soil has been made rich by volcanic ash, such as that which fell from the eruption of Irazú (in central Costa Rica, see Fig. 1.27) in 1963-1964.

On the irregular, low Pacific coast are found both the hilly Nicoya and Osa peninsulas. While the River El Coco (also known as the Rio Grande) flows from central Costa Rica westward into the Gulf of Nicoya, the country's largest river is the navigable San Juan, shared in part by Nicaragua, which flows into the Caribbean Sea (The Diagram Group, 1985).

Climate

General Typical of Central America, Costa Rica has hot, humid coasts, but cooler uplands. Average temperatures range from above 80°F near the coast, 69°F in the capital San José, at 3,800 feet, to only 59°F near 7,500 feet. The "temperate" or "cold" zones start at about 1,000 feet, but are lower on the Pacific than on Caribbean slopes.

Not only on the Caribbean coast, but also on the southern Pacific coast, rainfall totals over 126 inches per year. In particular, on the Caribbean side, northeast winds can provide 300 days with rain—the orographically produced cloudiness on the east side of the mountain ranges is frequently evident on satellite imagery (The Diagram Group, 1985).

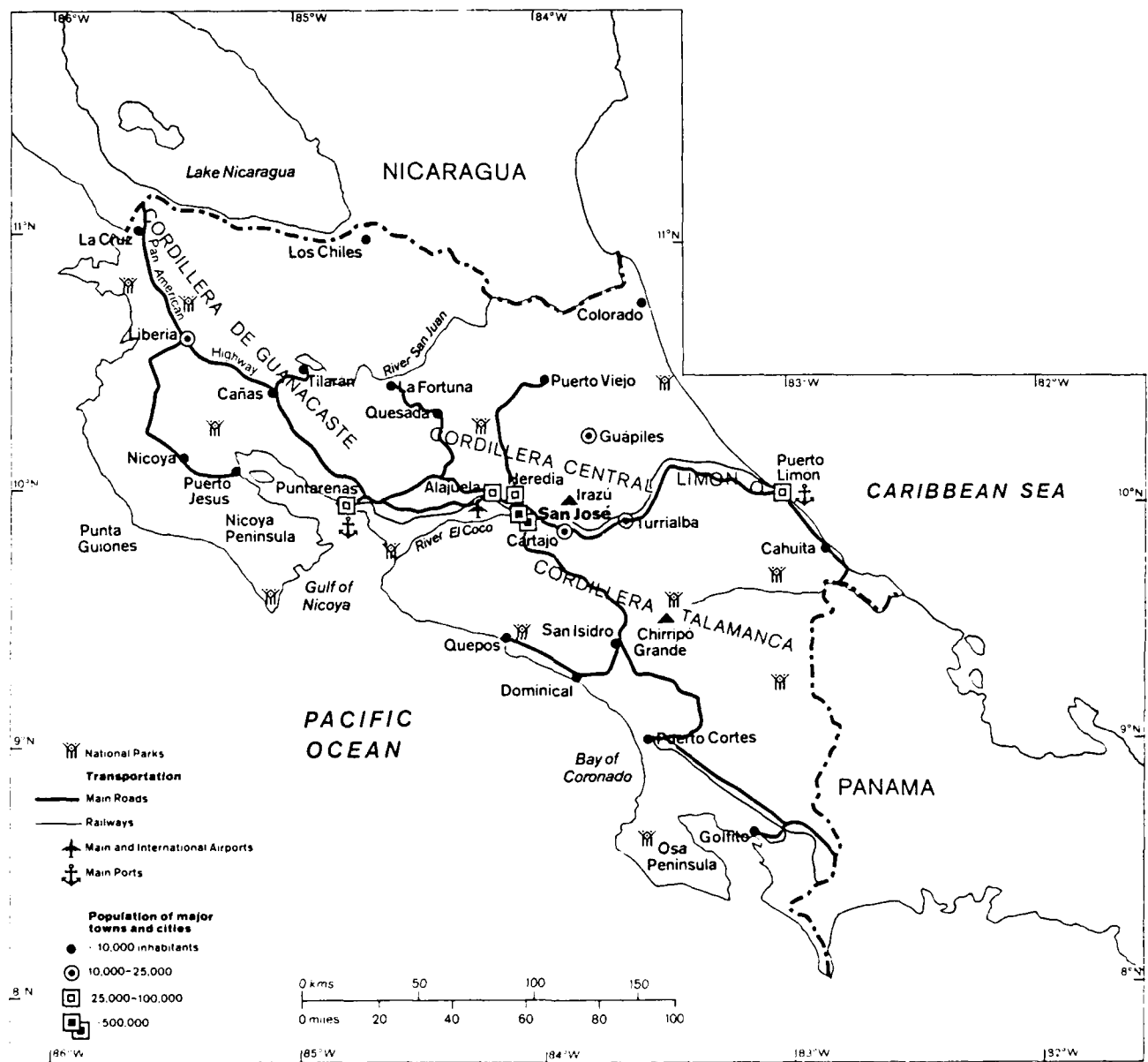


Figure 1.27: Costa Rica (The Diagram Group, 1985)

Rainy season: May – November. This is the rainy season with moderate to heavy rain, cloudy skies and warm temperatures. Mean rainfall averages 10 to even 26 inches per month at some locations. While thunderstorms are expected on 5–10 days per month; skies are clear less than 5 percent of the time; partly cloudy to cloudy, 40–55 percent; and overcast, 50–60 percent. Weather generally improves in November, as the dry season approaches (see Section 5 for the rather unlikely possibility of tropical storm or hurricane threat).

Flying weather: Poor to fair due to rainfall and cloudiness. Ceiling/visibility is less than 5000 feet and/or 6 miles between 10 to 25 percent of the time; less than 1500/3, 5 to 10 percent of the time. Thunderstorms are numerous, as noted below (see Appendix B for ceiling/visibility statistics for Liberia, Puerto Limón, Puntarenas and San José).

Terminal weather: San José/El Coco International, Costa Rica. The weather is warm, cloudy, windy and rainy. While the skies are: clear, less than 5 percent of the time; partly cloudy, 10–20 percent; cloudy, 25–30 percent; and overcast, 40–60 percent, the frequency that the ceiling/visibility is less than 300/1 is only 2 percent. Whereas winds greater than 16 kt are present 5–25 percent of the time, their maximum frequency is realized in July, with their minimum in September–October. Nevertheless, gale force winds are expected less than 1 percent of the time (USAFETAC, 1985).

Monthly temperature, precipitation, thunderstorms & twilight (USAFETAC, 1985):

SAN JOSÉ/EL COCO	MAY	JUN	JUL	AUG	SEP	OCT	NOV
TEMPERATURE (°F)							
Absolute maximum	88	92	84	85	86	85	84
Mean maximum	80	79	77	78	79	77	77
Mean minimum	62	62	62	61	61	60	60
Absolute minimum	54	56	54	56	56	55	52
MEAN PRECIPITATION (INCHES)	9.3	9.6	7.6	7.4	12.4	14.0	4.8
MEAN NUMBER OF DAYS							
Precipitation	18	21	23	23	26	26	15
Thunderstorms	7	5	5	5	8	6	1
CIVIL TWILIGHT (15th of month)							
First light (local standard time)	0453	0453	0500	0506	0505	0504	0509
Last light (local standard time)	1812	1821	1824	1816	1758	1741	1733

Dry season: December – April. The weather, dry and windy in the mountains and western Costa Rica in accordance with the season's name, is, nonetheless, cloudy with **moderate to heavy rainfall** on the Caribbean or eastern side of the mountains. Although rainfall averages 1 inch or less in the mountains and Pacific coast regions, it remains high on the eastern side, 5–22 inches. Thunderstorm occurrence varies from 1–3 days per month (see data below). While occasional outbreaks of cold air from North America provide below-normal temperatures and fresh breezes, normal temperatures average in the mid 60's to low 70's (°F) during the morning hours and then reach the mid 80's to low 90's in the afternoon. High winds can be expected in mountainous regions during all months; moreover, isolated mountain locations may be slightly cooler than mentioned earlier.

Flying weather: Generally good. Although the mountains and western Costa Rica generally have clear to partly cloudy skies, flying may be restricted in eastern Costa Rica in clouds and moderate to heavy rain showers. At San José/El Coco International, ceiling/visibility is less than 5000 feet and/or 6 miles approximately 5 percent of the time, while ceiling/visibility less than 1500/3 is approximately 1 percent of the time (see Appendix B for ceiling/visibility statistics at several cities).

Terminal weather: San José/El Coco International, Costa Rica. While warm and windy conditions exist with clear to partly cloudy skies 45–75 percent of the time, cloudiness increases in April with the approach of the rainy season. Rainfall is expected only 1–2 days per month during the driest months, January through March (see data below). Fog is rare, but visibility is occasionally restricted by haze and/or smoke. The ceiling/visibility is less than 300/1 less than 1 percent of the time. Note that winds greater than 16 kt occur 50–65 percent of the time; gale force winds, 5–10 percent of the time. Runway crosswinds greater than 15 kt occur 15–20 percent of the time (USAFETAC, 1985).

Monthly temperature, precipitation, thunderstorms & twilight (USAFETAC, 1985):

SAN JOSÉ/EL COCO	DEC	JAN	FEB	MAR	APR
TEMPERATURE (°F)					
Absolute maximum	87	87	88	91	89
Mean maximum	75	75	76	79	79
Mean minimum	58	58	58	59	62
Absolute minimum	49	49	51	50	53
MEAN PRECIPITATION (INCHES)	1.3	0.2	0.6	0.6	1.7
MEAN NUMBER OF DAYS					
Precipitation	7	1	2	2	6
Thunderstorms	0	*	*	1	3
CIVIL TWILIGHT (15th of month)					
First light (local standard time)	0522	0535	0535	0523	0505
Last light (local standard time)	1741	1757	1807	1808	1808

(* = less than 0.5 day)

1.3.7 Panama

Land

Panama is the fourth largest and southernmost of the nations of Central America. It is bordered on the west by Costa Rica and on the east by Colombia, with the Caribbean Sea and North Pacific Ocean forming its northern and southern shores, respectively. While Panama is the most narrow country of Central America, its coastline is the longest of any of the seven nations. At its most narrow width Panama is only 31 miles across (see Fig. 1.28); however, its Pacific coastline extends for 760 miles, and its Caribbean coastline is 470 miles long.

Low mountain ranges run the length of the country, reaching the greater heights in the west, including the country's highest peak, the volcano Chiriquí, with an elevation of 11,411 feet. The mountain range shown as Serranía de Tabasara (see Fig. 1.28) is also known as Cordillera Central. While three-fifths of Panama is mountainous, between parallel mountain ranges lie fertile valleys and plains, in addition to the low-lying, sometimes swampy, coastal strips. Located in the eastern half of the country are the chief rivers: the Chagres, near the canal; the Chepo; and the Tuira, with its source in Colombia. Its only large lake, Gatún, is man-made.

Obvious from Fig. 1.28, its Pacific coast is much indented, with the Azuero Peninsula forming the western side of the Gulf of Panama. While the country's southeastern coast is on the Gulf of Panama in the Pacific Ocean, much of the northwestern coastline is on the Mosquito Gulf in the Caribbean Sea. The eastern side of the Gulf of Panama contains the Pearl Island archipelago, while its largest island, Coiba, lies in the Pacific Ocean to the west of the Azuero Peninsula.

The Panama Canal cuts across²⁴ the center of Panama, from northwest to southeast (The Diagram Group, 1985).

²⁴Geography students are often surprised to learn that the Pacific entrance to the Panama Canal is *east* of the Caribbean (or Atlantic) entrance to the canal.

Climate

General The climate of Panama is generally tropical and rainy. While lowland temperatures average over 80°F, uplands are cooler at 66°F or less. Along the Caribbean coast and in the high mountains, more than 120 inches of rain falls per year; however, parts of the Pacific coast around the Gulf of Panama have less than 60 inches per year. Panama is considered to be outside the "hurricane belt" (The Diagram Group, 1985).

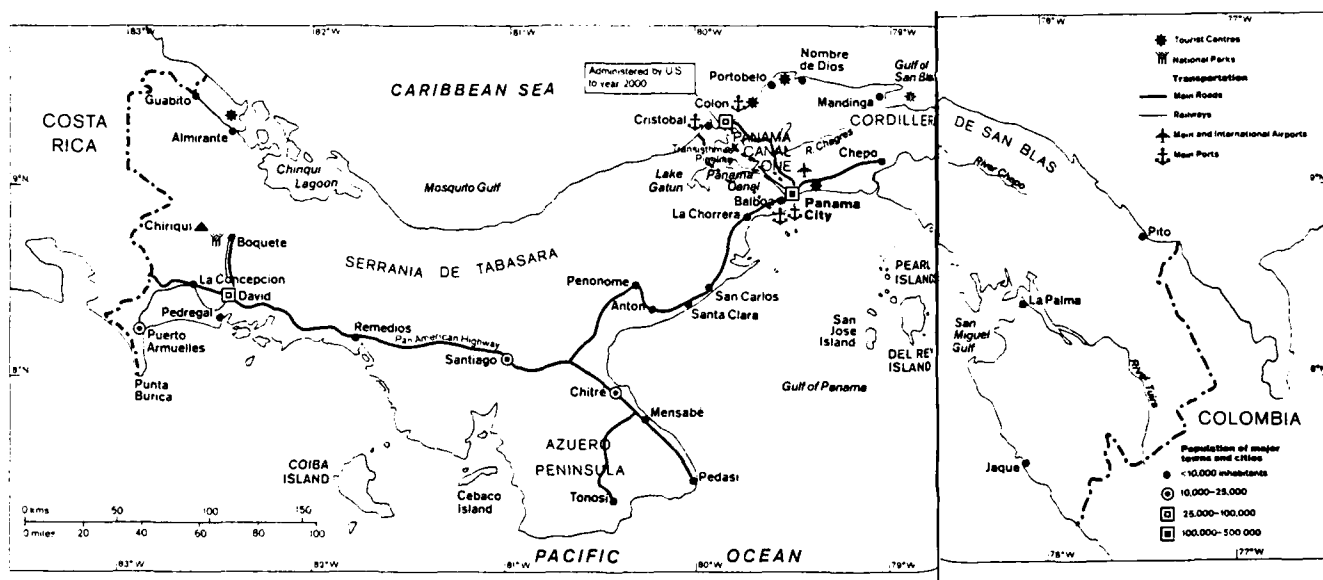


Figure 1.28: Panama (The Diagram Group, 1985)

Summer: June - August. During this season²⁵, the Intertropical Convergence Zone (ITCZ) passes to the north of Panama. The passage of the ITCZ is marked by an increase in precipitation, but there is a decrease as the ITCZ moves farther north. The typical weather in Panama consists of cloudy skies, high humidity, very warm temperatures and frequent afternoon showers and thunderstorms. Maximum temperatures are near 90°F along the coasts and 70°F-80°F in the mountains; whereas, minima are generally in the low 70's near the coast and mid 50's in the mountains. Mean cloudiness is a relative large 70-95 percent, and the average relative humidity is near 85 percent. Precipitation is likely 15-25 days per month, with thunderstorms 10-15 days per month. Gale force winds are a rarity.

Flying weather: While ceiling/visibility less than 5000 feet and/or 6 miles occurs *only* 10-30 percent of the time along the southern coast, ceiling/visibility less than 5000/6 occurs 40-65 percent of the time along the northern coast and over the mountain ranges. Similarly, ceiling/visibility less than 1500/3 occurs 2-12 percent of the time along the southern coast, but 15-35 percent along the northern coast or mountain ranges. Finally, ceiling/visibility less than 500/1 occurs 1-2 percent along the southern coast, yet 2-10 percent along the northern coast and mountain ranges. Expect late afternoon thunderstorms to affect any late afternoon flying operations; however, conditions normally improve at night. (See Appendix B for ceiling/visibility statistics for Fort Sherman, Howard Air Force Base and Rio Hato.)

Terminal weather:

Panama City/Torrijos International. While ceiling/visibility less than 300/1 occurs only 1-5 percent of the time, the most likely time is in the afternoon. Thunderstorms (about 17 or 18 days per month, see data on following page) provide the greatest problem (US-AFETAC, 1985).

²⁵Unlike the other six countries of Central America, with their rainy season and dry season, the proximity and effects of the Intertropical Convergence Zone (ITCZ) dictate the use of the more classical four seasons for Panama.

Monthly temperature, precipitation, thunderstorms & twilight (USAFETAC, 1985):

PANAMA CITY/TORRIJOS INTERNATIONAL JUN JUL AUG

TEMPERATURE (°F)

Absolute maximum	95	95	97
Mean maximum	87	88	86
Mean minimum	75	74	74
Absolute minimum	69	69	68

MEAN PRECIPITATION (INCHES) 7.9 7.6 7.5

MEAN NUMBER OF DAYS

Precipitation	21	21	22
Thunderstorms	17	17	18

CIVIL TWILIGHT (15th of month)

First light (local standard time)	0537	0544	0549
Last light (local standard time)	1901	1905	1905

CHANGUINOLA INTERNATIONAL *

TEMPERATURE (°F)

Absolute maximum	93	93	93
Mean maximum	89	88	88
Mean minimum	73	73	73
Absolute minimum	69	68	69

MEAN PRECIPITATION (INCHES) 7.9 11.3 9.3

MEAN NUMBER OF DAYS

Precipitation	18	21	18
Thunderstorms	13	17	17

(*Changuinola is near the northwest Caribbean coast, just east of Guabito.)

Autumn: September – November. The autumn marks the return southward of the ITCZ. The table on the next page indicates a secondary precipitation maximum in October for Panama City, but in November for Changuinola. This season generally has the most precipitation, highest mean relative humidity and lowest wind speed. Maximum temperatures are in the mid to high 80's (°F) along the coast, but only in the 70°F–80°F range in the mountains. Both relative humidity averages (87 percent) and mean cloud cover (70 to 95 percent) are high. While precipitation occurs on 22–27 days per month, thunderstorms can be expected 10–20 days per month. Gale force winds remain extremely rare.

Flying weather: Ceiling/visibility below 5000 feet and/or 6 miles occurs 5–25 percent of the time along the Pacific coast, but 15–40 percent along the Caribbean coast and on the continental divide. Less than 1500/3 occurs 3–10 percent of the time along the Pacific coast, however, 1–25 percent along the Caribbean coast and on the continental divide. While ceiling/visibility less than 500/1 occurs less than 1 percent along the southern coast, 500/1 occurs about 3 percent along the northern coast and on the continental divide. Afternoon showers and thunderstorms produce low ceilings that may restrict flight operations. (See Appendix B for ceiling/visibility statistics for several stations.)

Terminal weather:

Panama City/Torrijos International. While ceiling/visibility less than 300/1 occurs only 1–4 percent of the time, thunderstorms are numerous during this season occurring an average of 18 days in October (see data on the following page) (USAFETAC, 1985).

Monthly temperature, precipitation, thunderstorms & twilight (USAFETAC, 1985):

PANAMA CITY/TORRIJOS INTERNATIONAL SEP OCT NOV

TEMPERATURE (°F)

Absolute maximum	95	95	94
Mean maximum	85	85	85
Mean minimum	75	74	74
Absolute minimum	69	69	66

MEAN PRECIPITATION (INCHES) 7.5 11.6 10.2

MEAN NUMBER OF DAYS

Precipitation	23	24	22
Thunderstorms	15	18	10

CIVIL TWILIGHT (15th of month)

First light (local standard time)	0547	0545	0549
Last light (local standard time)	1839	1823	1817

CHANGUINOLA INTERNATIONAL *

TEMPERATURE (°F)

Absolute maximum	94	94	93
Mean maximum	89	89	89
Mean minimum	73	72	71
Absolute minimum	58	59	58

MEAN PRECIPITATION (INCHES) 5.1 5.5 10.1

MEAN NUMBER OF DAYS

Precipitation	14	16	18
Thunderstorms	15	13	9

(*Changuinola is near the northwest
Caribbean coast, just east of Guabito.)

Winter: December – February. Winter (although such a seasonal title does not seem appropriate to mid-latitude dwellers) in Panama is the start of the dry season—more evident at Panama City than at Changuinola (see precipitation totals, on the following page). During this season, skies are partly cloudy, and temperatures remain high with windy conditions. The ITCZ moves far to the south of Panama, permitting the northeast winds to dominate (see Fig. 1.4). Maximum temperatures are in the high 80's (°F) along the coasts, and near 70°F in the central mountains. Minimum temperatures lie in the low 70's (°F) along the coast, but in the range 46°F to 59°F in the central mountains. While mean cloudiness is 50–70 percent, higher values are found along the northern coast (note the greater rainfall at Changuinola, on the following page) and in the mountains. Relative humidity values range from 50–90 percent, also highest in December and along the northern coast. Precipitation occurs mainly from afternoon and evening showers and thunderstorms: 5–15 days per month along the southern coast; and 10–25 days per month in the mountains and along the northern coast. However, thunderstorms are at a minimum averaging 0–5 days per month. While winds 17 kt or greater occur 5–20 percent of the time in January and February, gale force winds are rare, occurring only 2 percent of the time.

Flying weather: Fair to good. Ceiling/visibility below 5000 feet and/or 6 miles occurs 2–12 percent of the time on the southern coast, but 10–30 percent over the continental divide and the northern coast. Similarly, ceiling/visibility less 1500/3 occurs about 1 percent of the time over the southern coast, yet 5–15 percent over the mountains and northern coast. Ceiling/visibility less than 500/1 rarely occurs. The least favorable flying weather occurs in the late afternoon due to shower activity (see Appendix B for ceiling/visibility statistics at several stations).

Terminal weather:

Panama City/Torrijos International. Good. Ceiling/visibility less than 500/1 occurs less than 1 percent of the time, with the worst flying conditions in late afternoon. Thunderstorm frequency, highest in December, is much smaller in January and February (USAFETAC, 1985).

Monthly temperature, precipitation, thunderstorms & twilight (USAFETAC, 1985):			
PANAMA CITY/TORRIJOS INTERNATIONAL	DEC	JAN	FEB
<hr/> TEMPERATURE (°F)			
Absolute maximum	94	94	95
Mean maximum	87	88	89
Mean minimum	73	72	73
Absolute minimum	64	64	64
MEAN PRECIPITATION (INCHES)	5.6	1.5	0.9
MEAN NUMBER OF DAYS			
Precipitation	15	8	5
Thunderstorms	4	1	0
CIVIL TWILIGHT (15th of month)			
First light (local standard time)	0603	0616	0616
Last light (local standard time)	1825	1840	1849

CHANGUINOLA INTERNATIONAL #			
<hr/> TEMPERATURE (°F)			
Absolute maximum	92	96	91
Mean maximum	87	87	87
Mean minimum	71	70	71
Absolute minimum	66	65	65
MEAN PRECIPITATION (INCHES)	13.4	9.3	6.2
MEAN NUMBER OF DAYS			
Precipitation	21	17	14
Thunderstorms	2	*	0

(#Changuinola is near the northwest
Caribbean coast, just east of Guabito.)
(* = less than 0.5 day)

Spring: March - May. As the ITCZ begins its return northward, spring marks the end of Panama's dry season. However, rainfall doesn't increase dramatically until May, especially in Panama City (see data on next page). Additionally, most locations have their minimum rainfall during the month of March (which in this particular seasonal grouping comes a month *after* the "dry" season). Compared with the winter values, mean cloudiness increases to 45-90 percent, with higher values in the mountains. While daily maximum temperatures are in the mid to high 80's (°F) along the coast, the maximum temperature averages in the 70°F - 79°F range in the mountains. Average minimum temperatures along the coast are in the mid 70's (°F), with 46°F - 60°F in the mountains. Average relative humidity is 75-80 percent. Precipitation gradually increases, especially noticeable at Panama City where the average of four precipitation days per month during March increases to 22 in May (see data on the following page). Thunderstorms also increase at Panama City, from one per month in March to 15 in May. Gale force winds, although slightly more frequent on the southwest coast, have an average frequency of only 1 percent.

Flying weather: Fair to good. Ceiling/visibility less than 5000 feet and/or 6 miles occurs 5-15 percent of the time along the southern coast, yet 15-40 percent along the northern coast and in the mountains. Similarly, ceiling/visibility less than 1500/3 occurs only 1-5 percent along the southern coast, compared to 10-20 percent along the northern coast and continental divide. Although ceiling/visibility less than 500/1 averages less than 1 percent, diurnal showers and thunderstorms lead to deteriorating conditions in the late afternoon and evening (see Appendix B for ceiling/visibility statistics for several stations).

Terminal weather:

Panama City/Torrijos International. Good. While ceiling/visibility less than 300/1 occurs only 1-2 percent of the time, the worst conditions occur in the morning near inland lakes and bays, and in the afternoon in the mountains. Thunderstorm frequency triples in May compared with March and April (USAFETAC, 1985).

Monthly temperature, precipitation, thunderstorms & twilight (USAFETAC, 1985):

PANAMA CITY/TORRIJOS INTERNATIONAL MAR APR MAY

TEMPERATURE (°F)

Absolute maximum	97	94	96
Mean maximum	90	90	88
Mean minimum	74	74	75
Absolute minimum	63	64	69

MEAN PRECIPITATION (INCHES)

0.3 2.7 8.8

MEAN NUMBER OF DAYS

Precipitation	4	9	22
Thunderstorms	1	4	15

CIVIL TWILIGHT (15th of month)

First light (local standard time)	0604	0548	0537
Last light (local standard time)	1850	1849	1901

CHANGUINOLA INTERNATIONAL #

TEMPERATURE (°F)

Absolute maximum	92	93	94
Mean maximum	88	88	89
Mean minimum	71	72	73
Absolute minimum	66	68	64

MEAN PRECIPITATION (INCHES)

5.7 7.2 8.4

MEAN NUMBER OF DAYS

Precipitation	10	12	12
Thunderstorms	*	2	10

(#Changuinola is near the northwest
Caribbean coast, just east of Guabito.)

(* = less than 0.5 day)

THIS PAGE
INTENTIONALLY BLANK

2. THE RAINY SEASON

2.1 General

This section will examine analyses (and a few prognoses), with appropriate discussion of weather conditions, for the "rainy season" (MAY through OCTOBER) of Central America. While no selection of the months of the "rainy season" appears to be satisfactory for *all* seven republics (see Subsection 1.3) or for *all* climatological regions of Central America, the above months appear to best satisfy the existing diverse pattern of seasons. Nevertheless, in the two most southern republics (Costa Rica and Panama), the rainy season reasonably could be extended through November due to the enhanced rainfall as the Monsoon Trough passes during its equatorward migration. Additionally, several stations on the Caribbean Sea such as La Ceiba, Honduras; Bluefields, Nicaragua and Changuinola, Panama receive relatively large rainfall during November, December and January due to the strong onshore tradewind flow. Admittedly, there is a relative minimum in rainfall experienced at some stations during July or August, often attributed to a temporary westward extension of a high pressure ridge.

During the rainy season, heavy precipitation returns to Central America in the form of tropical waves (inverted troughs), sea breeze convection, diurnal showers and thunderstorms (due to instability from daytime heating over land surfaces) and, to a lesser extent, tropical storms or hurricanes.

2.2 Tropical Waves (Riehl, 1979)

As reported by Riehl, 75% of the total precipitation received in most tropical areas come from the "synoptic" scale troughs moving from east to west across the Caribbean Sea, before striking Central America. Riehl further states that two or three such rain episodes can easily account for half of the rain during the season. While these phenomena were originally labeled "Easterly Waves" by Riehl, they will be referred to as "Tropical Waves" in this document, following the current practice of the National Hurricane Center.

On the average, a tropical wave can be expected to move across Central America once every five days, tracking westward approximately 5° longitude per day (i.e., ~ 15 kt), with a wavelength of approximately 1600 n mi. Observations indicate deviations from these average values are common, i.e., the cloudy areas that serve to identify these tropical waves (troughs) often move much faster, yet sometimes much slower, and the wave length is often shorter (frequently near 1200 n mi) or longer than the average given.

Within the Caribbean Sea region, **large** fluctuations of high-tropospheric (200 mb) wind direction are found above **small** wind direction changes in the low-level easterlies as the westward moving troughs pass, (see Fig. 2.1). Thus, while the passage of a tropical wave (or trough) **can** be accompanied by surface wind direction shifts (i.e., northeasterly becoming southeasterly), it is much more common to see the westward moving troughs within the Caribbean Sea identified by changes of low-level wind **speed**, hence vorticity changes due almost exclusively to wind shear.

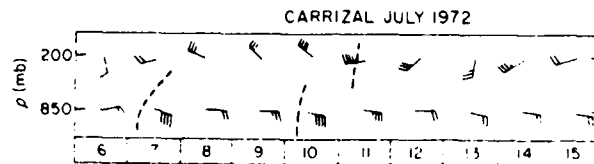


Figure 2.1:
Winds at 850 mb and 200 mb at Carrizal, Venezuela (9.5°N , 67°W)
6–15 July 1972. Wind speed in knots. Dashed lines: passage of axes
of synoptic systems (Riehl, 1979).

The just described vertical configuration is much different from that typically found in the *eastern* North Atlantic Ocean, near Africa. Note that in Fig. 2.2, 200 mb winds near 24°W remain easterly (oscillating in magnitude), while the low-level (900 mb) winds exhibit considerable fluctuation, often becoming westerly.

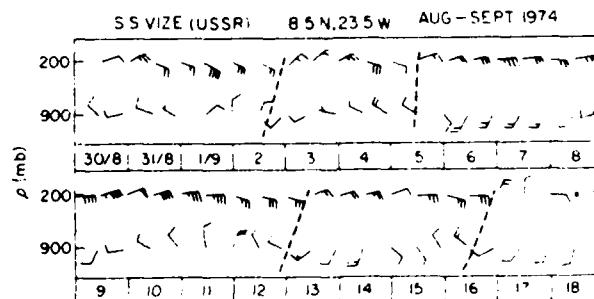


Figure 2.2: Winds at 900 mb and 200 mb at the USSR ship *VISE*
(8.5°N , 23.5°W), 30 August-18 September, 1974. Other notations as
in Fig. 2.1 (Riehl, 1979).

Riehl (1979) states that an individual station can expect to receive only one strong shower—in the majority of cases—during the passage of a disturbance (i.e., a tropical wave). While about 1 inch of rain falls (in two hours) from an identified (*moving*) cloud mass, the rainfall total at individual stations varies widely.

A vertical view of “Riehl’s” disturbance is shown in Fig. 2.3 where the disturbance (or precipitation event, as labeled by Riehl) slopes slightly eastward with height. A completely rainless day (21 June) preceded its arrival, which was marked by large cyclonic vorticity (note the sharp wind shift) at low levels. Figure 2.3 further identifies the passage of the tropical wave with above average rainfall during 22 June. Low-level **cooling** (near and behind the tropical wave) can be inferred by extending (extrapolating) the dashed line to the surface, i.e, negative values of 24-hour pressure-height change indicate a decrease in layer thickness—thus a cooler layer. However, the +40 m center of pressure-height change (near 200 mb) identifies the presence of **warming** temperatures aloft²⁶. This is further supported by high-tropospheric outflow.

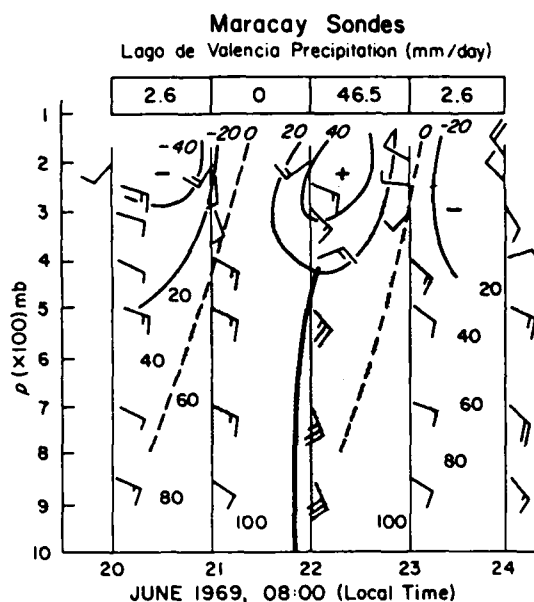


Figure 2.3: Time Section for Upper Winds (kt), Relative Humidity (per cent, shaded) and 24-hour Height Changes (m) at Maracay, Venezuela (10.2°N, 67.4°W) for the Heavy Precipitation Event. Daily rainfall at the top. Heavy solid line: axis of weather system (Riehl, 1979).

Despite the preceding discussion depicting a case where increased cloudiness and convection exist to the east of a tropical wave, cloudiness and convection often are **observed** both **ahead** and **behind** the westward moving wave.

²⁶See Appendix A for discussion of the existence of a “direct” cell, providing the conversion of potential energy into kinetic energy, despite the presence of *cold* air near the surface.

Figure 2.4 is an example of the *operational* low-level streamline (ATOLL-Analysis of Tropical Oceanic Lower Layer) chart developed by the National Hurricane Center (NHC) and computer produced by the National Meteorological Center (NMC). Initiated by the *shear* present in the equatorward extension of a mid-latitude cold front, tropical storm Florence had formed in the southern portion of the Gulf of Mexico. In addition to the circulation of tropical storm Florence depicted near the northwestern tip of the Mexican Yucatan Peninsula, Fig. 2.4 identifies a tropical wave near 53°W (just east of the Windward Islands) and another tropical wave in the eastern Caribbean near 69°W (extending from the Dominican Republic (eastern side of Hispaniola) southward to Venezuela). Note that while the *cyclonic* curvature of the streamlines of the tropical wave south of Hispaniola is barely perceptible (as anticipated from Fig. 2.1), it is more obvious when viewed in relation to the flanking ridges, identified by the strong anticyclonic curvature near 82°W and 61°W.

While the use of streamline analyses is preferred in the tropics, Fig. 2.5 presents the 1000 mb analysis²⁷ corresponding to the streamline analysis of Fig. 2.4. Again the tropical wave near Hispaniola is barely evident, but the surface observations permit a comparison of the "present weather" and "cloud cover" observations of Fig. 2.5 with the infrared satellite imagery of Fig. 2.7. In particular, note the continuous drizzle at Merida, Mexico (station 76644) on the northwest coast of the Yucatan Peninsula (on the periphery of the tropical storm), the thunderstorm at Choluteca, Honduras, station 78724, (unassociated with any tropical wave), the multi-layered overcast over Howard Air Force Base, station 78806, in Panama, as well as the clear sky over Barahona, Dominican Republic, station 78482 (*ahead* of the approaching tropical wave).

Figure 2.6 is an example of the *operational* 200 mb streamline chart developed by NHC and computer produced by NMC. Note that the anticyclonic vortex²⁸ depicted above the position of the tropical wave south of Hispaniola (near 69°W) is in good agreement with the convective cloudiness (over the eastern Caribbean Sea between Puerto Rico and Columbia) shown in the GOES (Geostationary Operational Environmental Satellite) East satellite image in Fig. 2.7.

²⁷All 1000 mb analyses presented in the handbook will contain *unlabeled stream function* contours. For operational applications, a **stream function on a constant pressure (1000 mb) surface is comparable to an isobar on a constant level (sea-level) surface**. From Huschke (1959): "stream function—A parameter of two-dimensional, nondivergent flow, the value of which is constant along each streamline...In meteorology the most common application of the stream function is in the assumption of **geostrophic equilibrium**. If variations in the **coriolis parameter f** are ignored, the stream function in a constant-pressure surface is proportional to the **geopotential gz** ...", and stream function contours are height contours of the constant pressure surface.

²⁸Anticyclonic vortices are *also* depicted above tropical storm Florence and the tropical wave at 53°W.

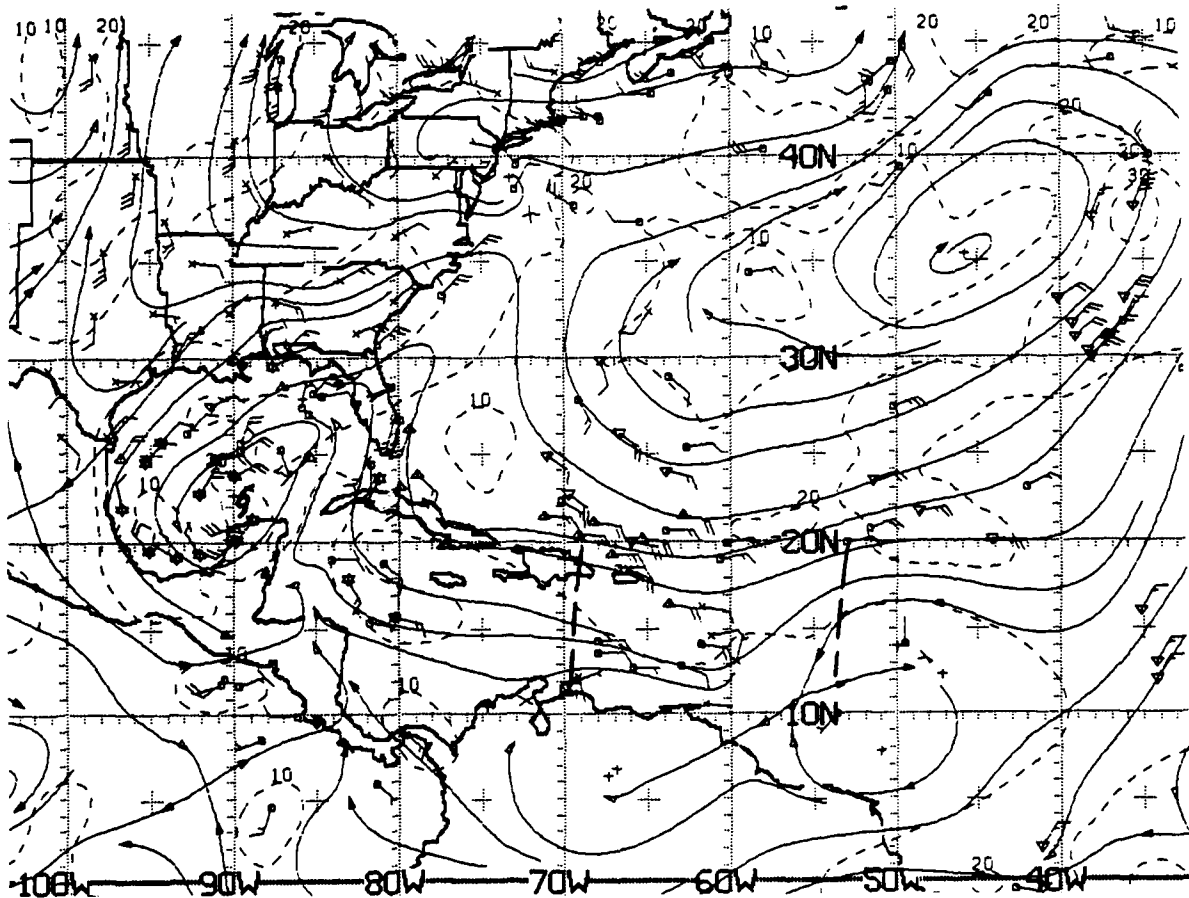


Figure 2.4: NMC ATOLL Operational Streamline Chart 0000 UTC 8 SEP 1988. Reports include: × (RAWIN/PIBAL-2000 ft), □ (AIREP), Δ (low-level wind vector derived from satellite cloud movement vectors provided by NHC Miami), ▽ (satellite vectors provided by National Environmental Satellite and Data Information System (NESDIS) WASH DC) and "octagons" (BOGUS wind entries). The wind flow pattern is depicted by solid streamlines, and isotachs are drawn as dashed lines at 10-kt intervals; the two tropical waves (**heavy dashed lines**) and the tropical storm position are from the manual NHC sea-level pressure analysis.

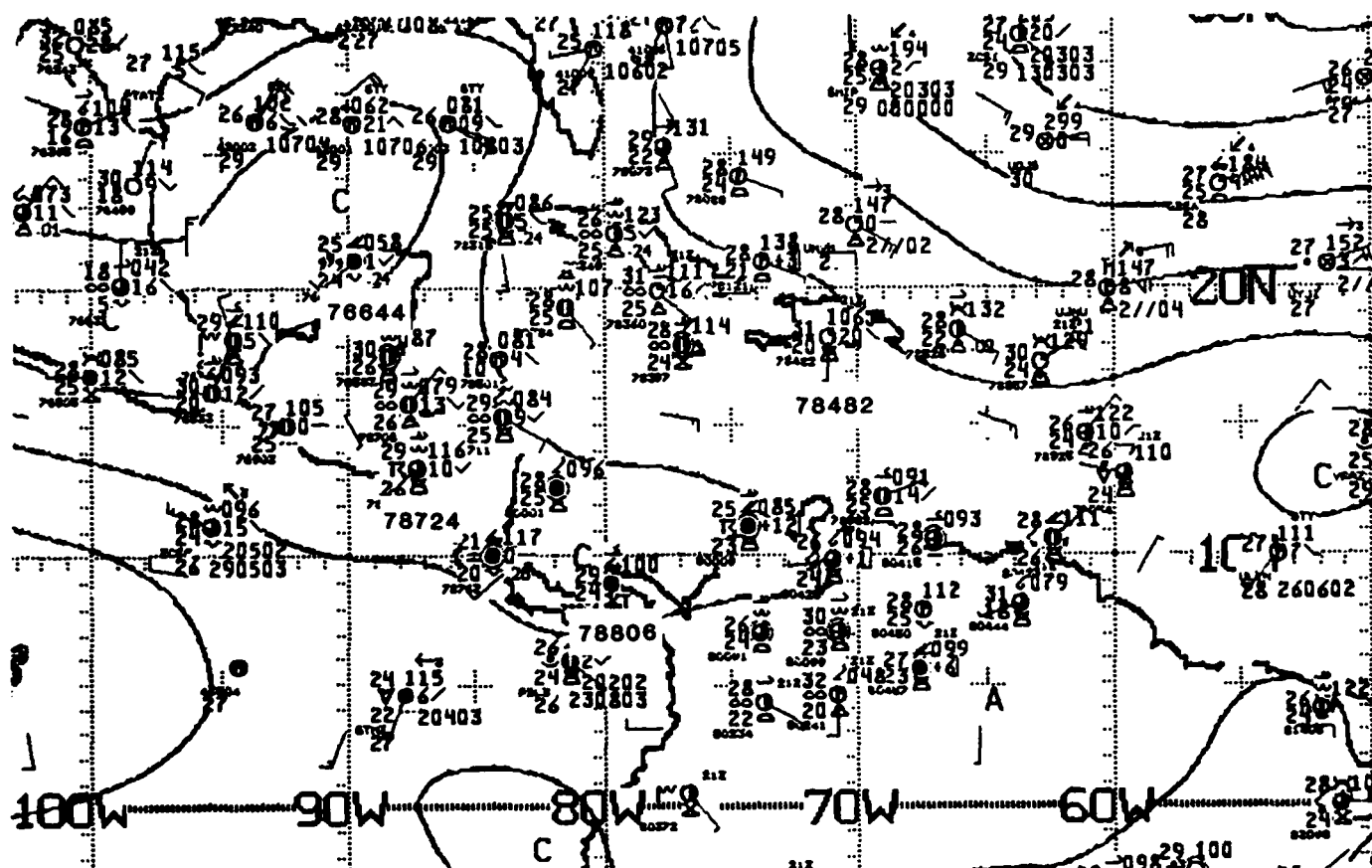


Figure 2.5: NMC 1000 mb Analysis 0000 UTC 8 SEP 1988.

Contours are unlabeled stream functions from optimum interpolation analysis, with C identifying cyclonic centers and A identifying anticyclonic centers.

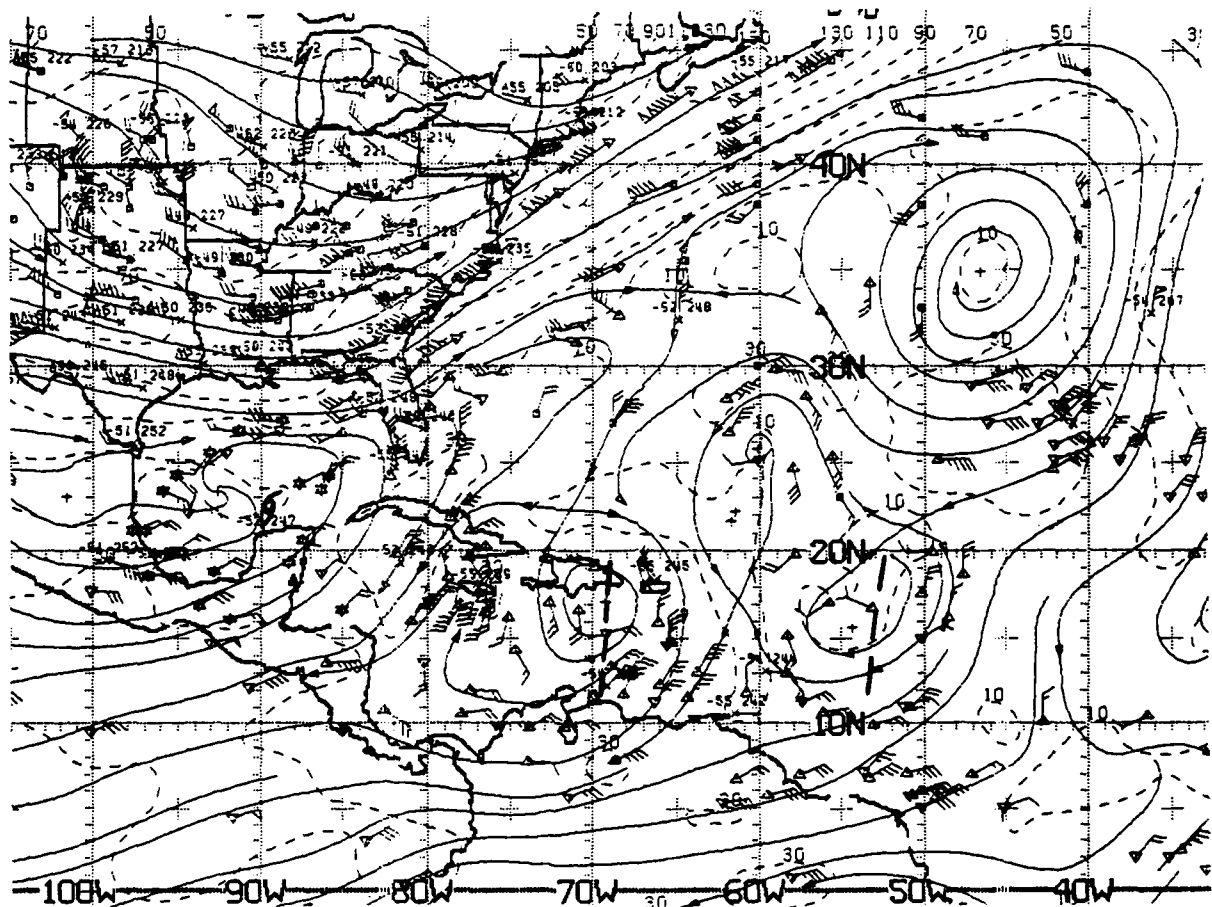


Figure 2.6: NMC 200-mb Operational Streamline Chart 0000 UTC 8 SEP 1988. Reports include: × (RAWIN/PIBAL), □ (AIREP), Δ (high-level wind vector derived from satellite cloud movement vectors provided by NHC Miami), ▽ (satellite vectors provided by NESDIS WASH DC) and "octagons" (BOGUS wind entries). The wind flow pattern is depicted by solid streamlines, and isotachs are drawn as dashed lines at 20-kt intervals, starting at 10 kt. The two tropical waves (**heavy dashed lines**) and the tropical storm position are from the manual NHC sea-level pressure analysis.



Figure 2.7: GOES East Infrared Satellite Imagery 0001 UTC 8 SEP 1988, 4 km resolution

While some practicing tropical meteorologists are very sceptical as to the usefulness of "tropical wave" theory in the Caribbean Sea and Central American regions, a study of westward propagating cloud lines (Chang, 1970) demonstrated that cloud clusters do propagate across the North Pacific Ocean at approximately 18 kt. Figure 2.8 depicts a rather orderly progression of the cloud clusters in the 10–15°N latitude band starting²⁹ from **Central America** (near 80°W) on the right. During this *particular* period, weaker wave activity was found west of 150°W within this particular latitude band, however in the 5–10° latitude band (just to the south of the band depicted in Fig. 2.8, but *not* shown) the diagonals depicting the propagating cloud patterns were distinctly connected across the *entire* North Pacific Ocean. Note, *however*, the **persistent** cloudiness (i.e., the vertical band of clouds) near Central America on the right hand side of the figure, indicating that additional convection occurs, no doubt enhanced by the daily warming of the land mass plus low-level convergence patterns, etc. Thus, while the cloudiness may be enhanced every four or five days (by the propagating pattern), an observer in Central America, during the rainy season, will experience cloudiness even during the days *between* the arrivals of the propagating wave-associated cloud patterns.

Despite the availability of high-resolution satellite imagery, the problem still remains in the Caribbean Sea (i.e., *upwind* of Central America) of identifying and tracking small-amplitude tropical disturbances. The associated cloud patterns assume a variety of shapes and changes in intensity from day to day (Chang, 1970).

Although no case study will be offered, the "Temporal" is an atmospheric perturbation (without significant electrical activity) occurring over Central America, having persistent rainfall for an average duration of **2 to 3 days** during the *rainy* season—sometimes accompanied by gale force winds. As described by Lessman (1963) in his study of El Salvador and the North Pacific coast, the Temporal is a warm-core low-level cyclone, often with its origin linked to the ITCZ or to a resonance depression promoted by a hurricane crossing the western Caribbean Sea. It often travels slowly along the North Pacific coast of Central America toward the northwest, yet others are quasi-stationary or move differently.

²⁹It is assumed that such westward propagation is continuous, i.e., it is present to the *east* of Fig. 2.8 (that is, to the east of Central America across the Caribbean Sea and the Atlantic Ocean).



Figure 2.8: Time-Longitude Section of Satellite Photographs of the period 1 July-10 August 1967 for the 10-15°N latitude band over the North Pacific Ocean. The following data are missing: 4 July (150°E-155°W), 8 July (150°E-160°W), 17 July (150°E-150°W, 130°W-100°W), 29 July (130°W-100°W) (Chang, 1970).

2.3 Case Studies during the Rainy Season

It is the purpose of this subsection to present the weather and satellite imagery associated with the "low-level" ³⁰ (925 mb) and "upper-level" (200 mb) streamline analyses and prognoses of the Navy Operational Global Analysis Prediction System (NOGAPS) produced by Fleet Numerical Oceanography Center (FNOC). Both the sparsity of reporting stations and the resolution³¹ ($\sim 2.5^\circ$ latitude) of the streamline or wind barb analysis provides minimal detection of tropical waves ("inverted troughs") progressing westward across the Caribbean Sea toward Central America. However, satellite imagery³² assists in the identification of areas of convection associated with tropical waves.

While the analysis of any *single* operational weather center can **not** be accepted as unimpeachable "truth", the NOGAPS streamline analyses will be compared with the operational ATOLL and 200 mb streamline analyses produced by the U. S. National Meteorological Center (NMC). The many satellite winds (plotted over the western North Atlantic Ocean, the Caribbean Sea, the eastern North Pacific Ocean and the Gulf of Mexico) on the NMC ATOLL and 200 mb streamline analyses give great credibility to these analyses of NMC.

³⁰The NOGAPS low-level streamlines are at 925 mb (having an elevation of ~ 1000 m), while comparison streamlines are from the National Meteorological Center (NMC) Atlantic Tropical Operational Low Level (ATOLL) model which includes RAWIN/PIBAL (2000 ft), AIREP, satellite cloud wind vectors (NHC Miami and National Environmental Satellite, Data and Information Service (NESDIS) WASH DC), as well as BOGUS wind reports.

³¹The NOGAPS 3.0 model, the U. S. Navy's first spectral forecast model, which became operational in January 1988, has a resolution of $\sim 2.5^\circ$ latitude. NOGAPS 3.1, expected to become operational in early 1989, will have a new radiational package which should improve tropical prognosis. Improved moisture parameters and better resolution are expected later in 1989.

³²Unless otherwise specified, satellite imagery has 4 km resolution.

THIS PAGE
INTENTIONALLY BLANK

2.3.1 Case I - Tropical Waves (3 – 7 October 1988)

3 October 1988

This first case study will follow the trek of a tropical wave from the eastern Caribbean Sea until its arrival over Central America. At 0000 UTC on 3 October 1988, the tropical wave is over the eastern Caribbean Sea (Dominican Republic to northern Venezuela) near 69°W (see Fig. 2.9). The present wave (identified by the NHC sea-level analyses, not shown) had approached the Windward Islands from the North Atlantic Ocean as Tropical Storm Isaac, but had been “downgraded” on 1 October, possibly due to strong westerly shear in the upper air. Unlike many Caribbean Sea tropical waves, this one displays considerable cyclonic curvature in the lower troposphere. Figure 2.9 also displays the *upstream* and *downstream* tropical waves (from the NHC sea-level pressure analysis). The *flanking* tropical waves at $\sim 86^{\circ}\text{W}$ and $\sim 53^{\circ}\text{W}$ identify an average wavelength, between the troughs, of only ~ 900 n mi. Figure 2.10 shows the anticyclonic streamlines (centered over northern Venezuela) at 200 mb over the eastern Caribbean Sea. Thus the upper-level anticyclone (associated with the tropical wave) is trailing the surface position of the tropical wave, as depicted in Fig. 2.3 from Riehl (1979). At this time, the infrared satellite imagery indicates that most of the convection, associated with the tropical wave in the eastern Caribbean Sea (near 69°W), is to the *east* of the tropical wave axis (Fig. 2.11). It is probable that compensating *sinking* motion is keeping the western side of Hispaniola relatively clear, as the eastern side experiences the convection of the approaching tropical wave. Although there is no “trailing” convection associated with the NHC-identified wave approaching the Yucatan Peninsula, Fig. 2.11 identifies early evening convective activity over the land masses of the Yucatan Peninsula, Cuba, Costa Rica, Panama, etc.

Figure 2.12 displays the Navy 925 mb (~ 1000 m) wind barbs provided by FNOG for 0000 UTC 3 October 1988 (i.e., corresponding to the NMC ATOLL analysis (Fig. 2.9). There is general agreement between the two products; in particular, note the cyclonic curvature implied by the 925 mb wind barbs south of Hispaniola as well as the anticyclonic curvature over the western Caribbean Sea east of Honduras.

The Navy 200 mb streamlines of Fig. 2.13 similarly can be compared with those of NMC in Fig. 2.10. Agreement is found in the two anticyclonic vortices (centered over Guatemala and northern Venezuela) separated by a trough at 200 mb over the western Caribbean Sea.

Finally, Fig. 2.14 displays the visible satellite imagery in early afternoon, and Fig. 2.15 the corresponding infrared (IR) imagery, about 4 hours **before** the “synoptic time” observations just reviewed. Especially note the convection just commencing over western Honduras, the northern Yucatan Peninsula and Cuba—compare with the imagery four hours later in Fig. 2.11, when the convection was more developed. However, even at 1931 UTC, the convection was well developed over Costa Rica and Panama.

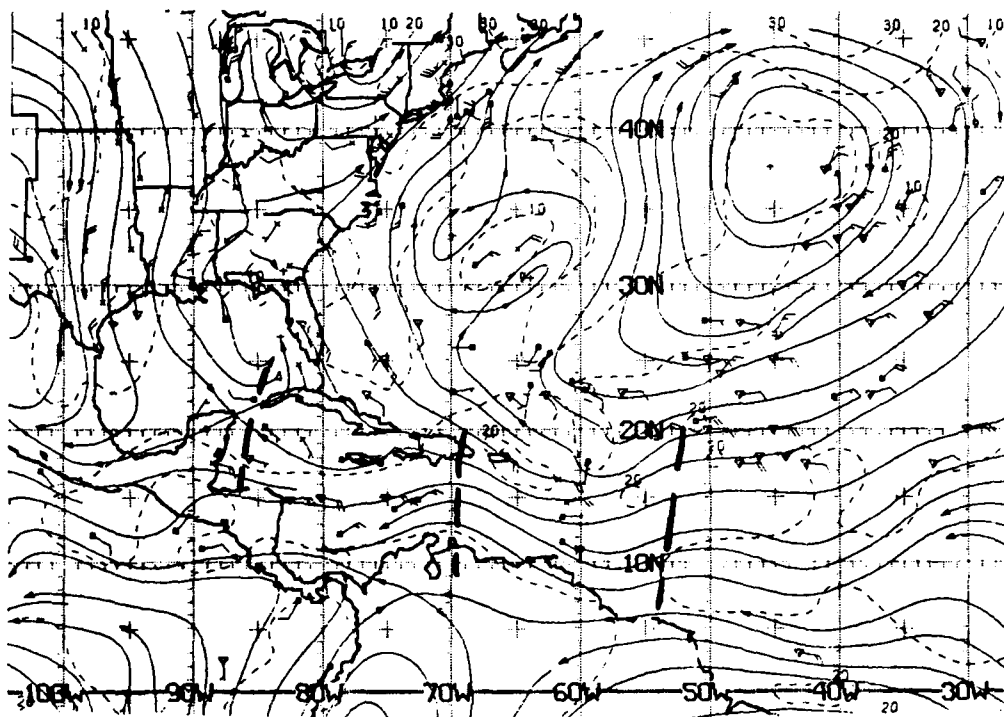


Figure 2.9: NMC ATOLL Operational Streamline Chart, 0000 UTC 3 OCT 1988
As in Fig. 2.4.

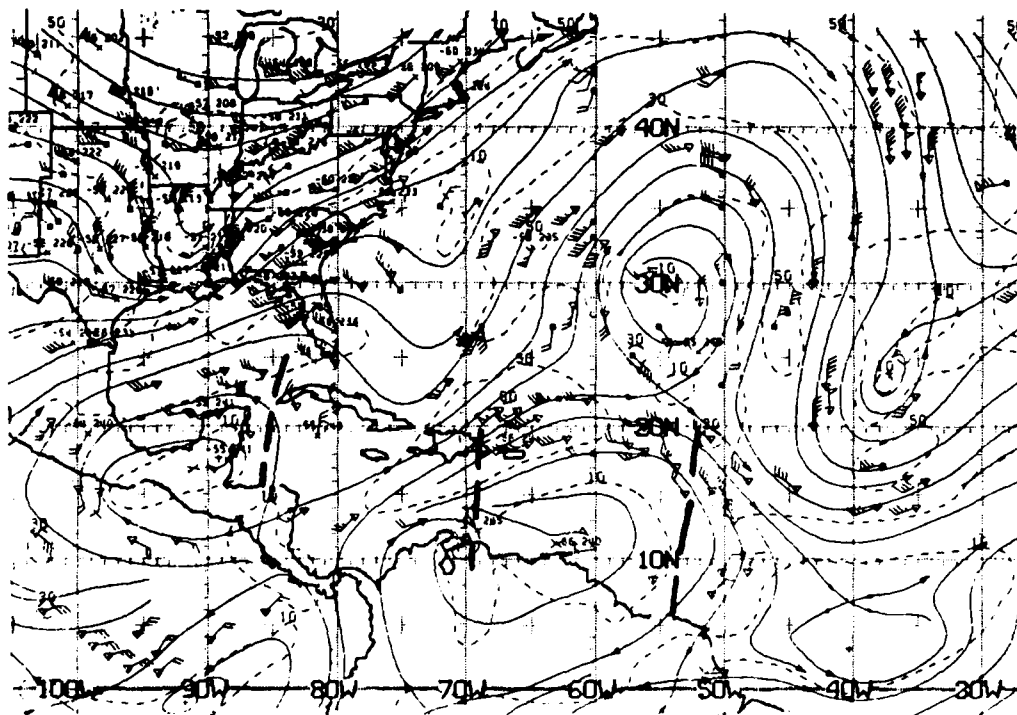


Figure 2.10: NMC 200 mb Operational Streamline Chart, 0000 UTC 3 OCT 1988
As in Fig. 2.6.

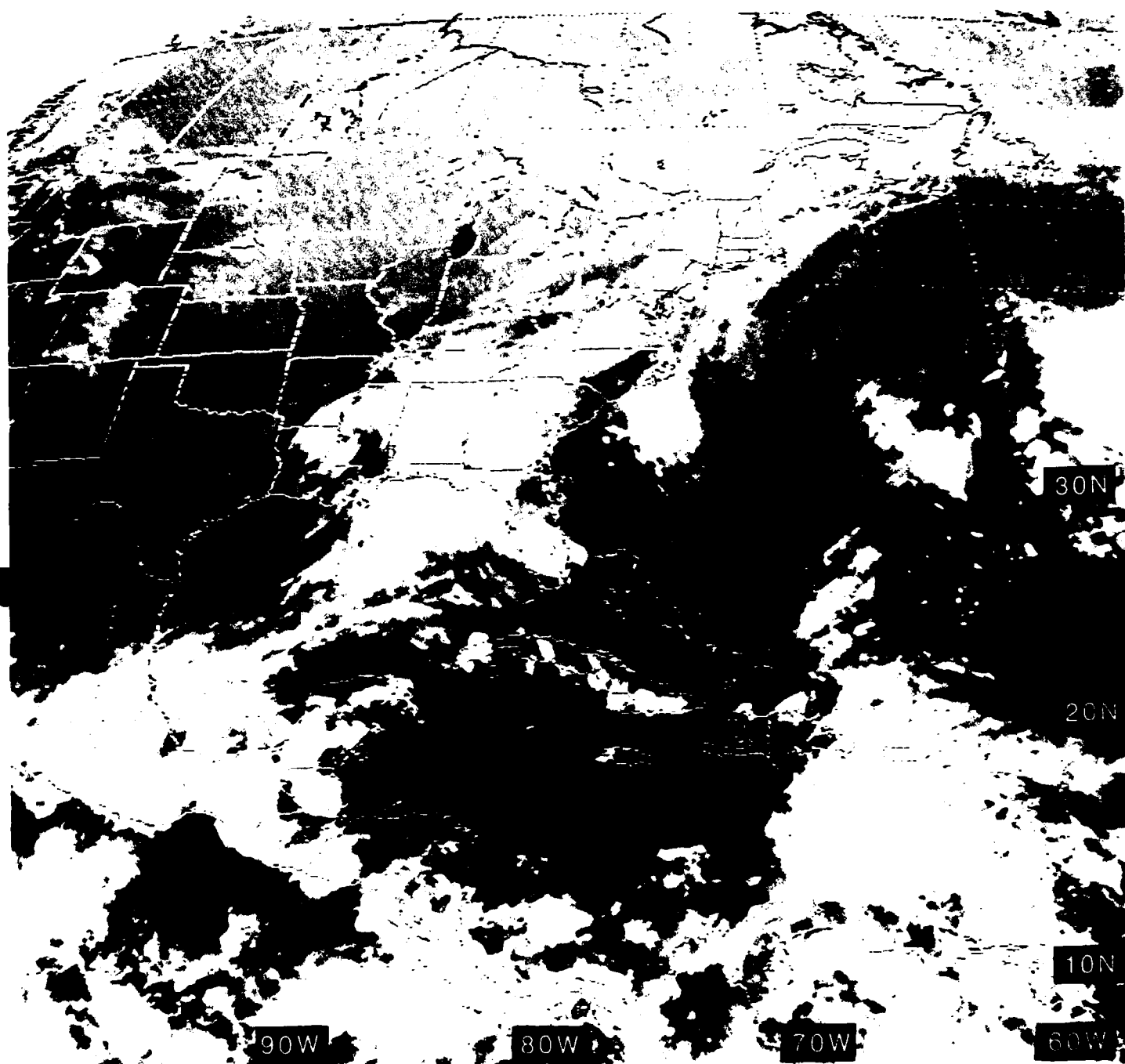


Figure 2.11: GOES East Infrared Satellite Imagery, 0001 UTC 3 OCT 1988

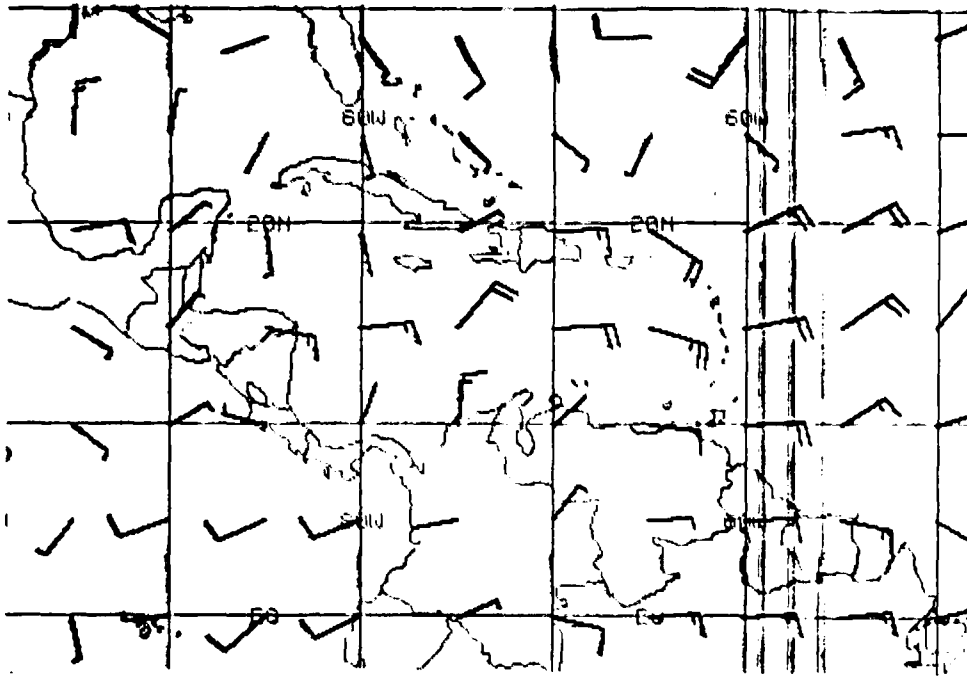


Figure 2.12: FNOc 925 mb Winds, 0000 UTC 3 OCT 1988.
Each barb represents 10 kt. (Ignore vertical printer lines near 60°W.)

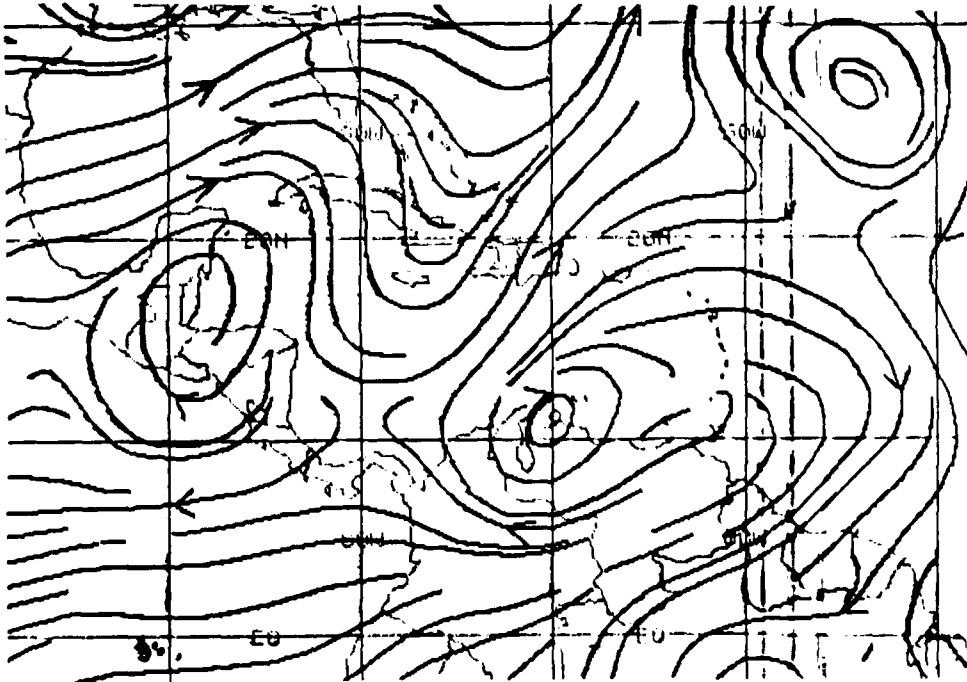


Figure 2.13: FNOc 200 mb Streamline Analysis, 0000 UTC 3 OCT 1988.
(Ignore vertical printer lines near 60°W)

1931 020088 39A-4 00902 15701 EC1

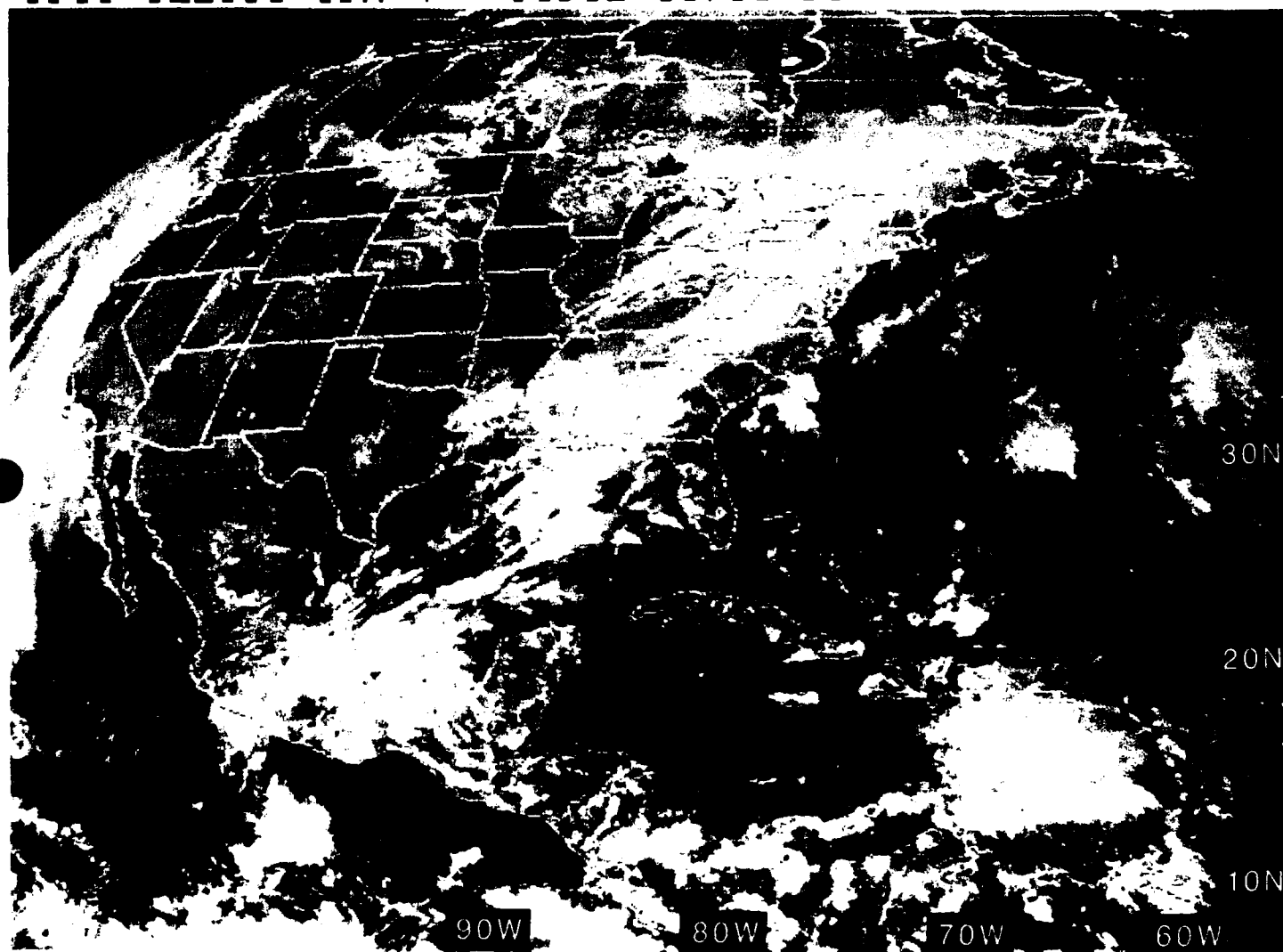


Figure 2.14: GOES East Visible Satellite Imagery, 1931 UTC 2 OCT 1988

2001 020C88 39E-4ZA 00901 15701 EC1

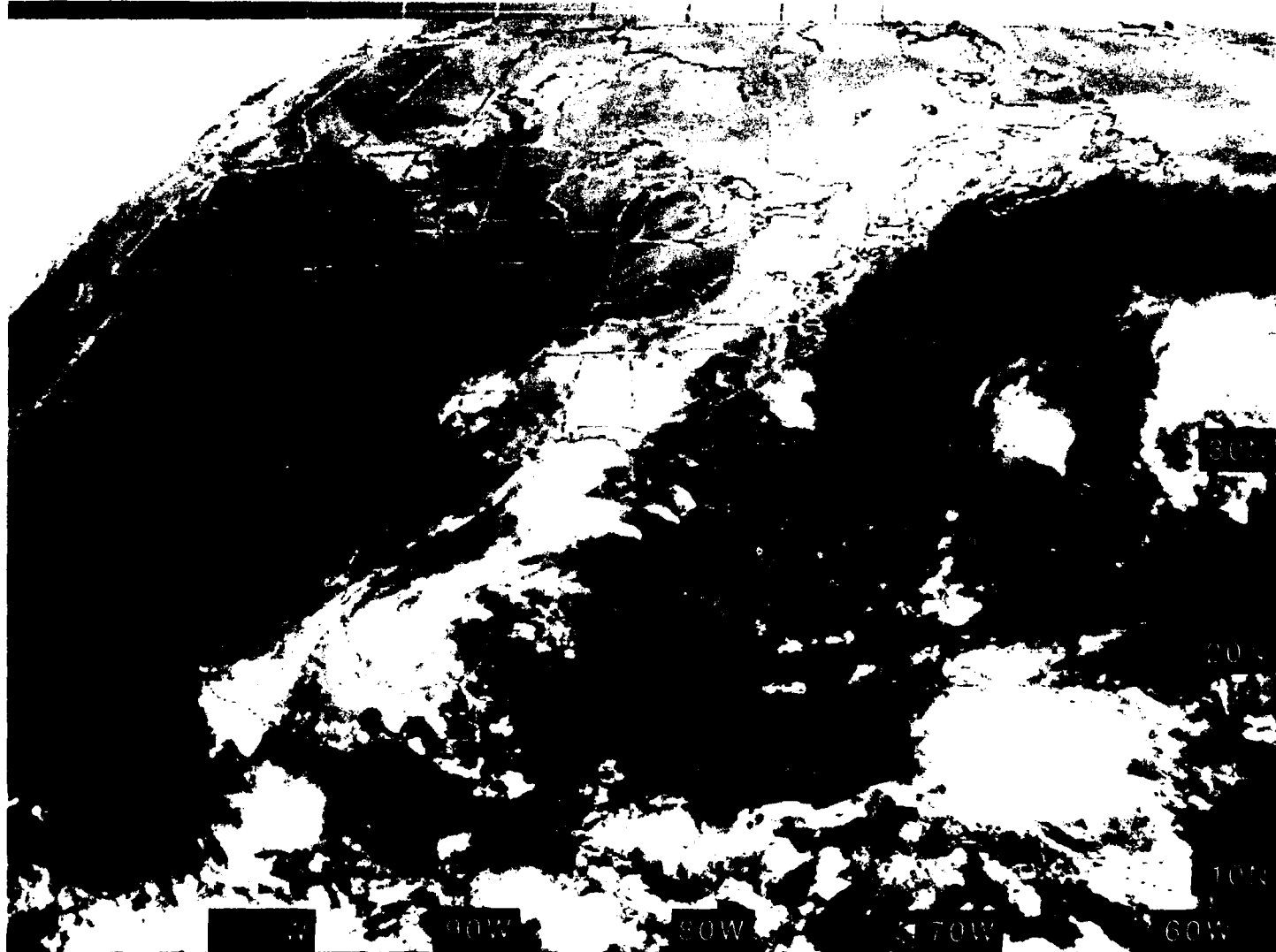


Figure 2.15: GOES East Infrared Satellite Imagery, 2001 UTC 2 OCT 1988

4 October 1988

By 0000 UTC on 4 October 1988, the tropical wave in the center of the Caribbean Sea is located at $\sim 74^\circ\text{W}$ by NHC. Having moved at a speed of ~ 12.5 kt, the axis of the tropical wave is depicted on Fig. 2.16 between Haiti and Columbia amidst cyclonically curved streamlines in the lower troposphere. The 200 mb streamline analysis (Fig. 2.17) does depict anticyclonic curvature (aloft) to the east of the tropical wave axis, i.e., south of the Dominican Republic centered near 70°W coincident with the convective cloudiness of the GOES East infrared imagery of Fig. 2.18. However, there is a *very small* cyclonic vortex at 200 mb, near the surface axis position of the tropical wave. This 200-mb cyclonic vortex, just south of Jamaica on Fig. 2.17, is located within an upper-level mid-latitude trough³³, extending from near 30°N , 65°W toward Jamaica. The slow movement of the tropical wave *westward* may be attributed to the presence of this upper-level trough with its embedded vortex.

The tropical wave approaching the Windward Islands is located at $\sim 61^\circ\text{W}$ by NHC, having moved at ~ 18 kt. However, while NHC positioned this second tropical wave within cyclonic curved **isobars** (not shown), it is located mostly within straight or *anticyclonically* curved streamlines on the ATOLL³⁴ analysis, i.e., near 61°W in Fig. 2.16.

Figures 2.19 and 2.20, the coincident low-level and upper-level wind barb analyses provided by FNOC appear to be in general agreement with those provided by NMC. Figure 2.19 depicts the low-level cyclonic flow pattern associated with the tropical wave south of Haiti, and Fig. 2.20 depicts an anticyclonic upper-level flow southeast of the Dominican Republic as seen also in Fig 2.17. (Of course, the coarse resolution provided by the 5° wind barb analyses of FNOC will not show the finer detail available on the NMC analyses.)

Figure 2.21 is the 1000 mb analysis at 0000 UTC 4 October 1988, with the surface station observations. Comparison of the station observations with the IR imagery of Fig. 2.18 reveals: showers (from San Juan, Puerto Rico (station 78526) to Curaçao, Netherlands Antilles (station 78988 off northern Venezuela)) under the IR-revealed cloudiness to the east of the tropical wave axis; rain at San José, Costa Rica (station 78762) and drizzle at Tapachula, Mexico (station 76903, just west of the Guatemalan Pacific coast) under IR-revealed convective towers; a thunderstorm at Saqua La Grande, Cuba (station 78338) under an IR-revealed tower; and partly cloudy skies over Kingston, Jamaica (station 78397) in the clearer (warmer/darker) portion of the IR image.

³³Note that this upper-level trough, which also existed on the previous day (2 October) in Figs. 2.10 and 2.13 (extending from near 30°N , 65°W toward Jamaica), is *not* an example of the Tropical Upper Tropospheric Trough (TUTT). The TUTT is a climatological feature of the summer season over the tropical North Atlantic Ocean (as well as the tropical North Pacific Ocean) extending from the northeast toward the southwest. Research (Sadler, 1976) in the tropical North Pacific Ocean identified upper-level diffluence, to the *east* of the TUTT, leading to enhanced upward motion and convection. The TUTT which is normally weaker by October (Sadler and Wann, 1984) appears farther to the east—yet with significant magnitude—on this date in Fig. 2.17, extending from $\sim 30^\circ\text{N}$, 30°W southwestward.

³⁴Anticyclonic flow is also depicted on the Navy's 925 mb wind barb analysis in Fig. 2.19.

Figures 2.22 and 2.23 are visible and IR images, respectively, of Central America and the western Caribbean Sea, about four hours **before** the synoptic analyses and observations, just reviewed. Even at coarse resolution (4 km), the meteorological conditions are remarkably revealed. There is isolated shower activity over the Yucatan Peninsula and north of the Canal Zone over Panama, while extensive convective cloudiness exists over Costa Rica and western Panama (no doubt enhanced by the mountainous terrain).

Note the thin line of cirrus (faintly visible in Fig. 2.22, but well identified on the white "cold" imagery of the IR in Fig. 2.23) extending from the Gulf of Fonseca, across northern Nicaragua, into the western Caribbean. Neither the FNOC (Fig. 2.20) nor the NMC (Fig. 2.17) upper-level analyses depict a westerly flow pattern associated with this cirrus streak. However, the NESDIS WASH DC satellite wind "triangles" (just east of Nicaragua) on the NMC 200-mb chart (Fig. 2.17) depict westerly winds coincident with the cirrus streak.

While there is considerable convective³⁵ cloudiness over the southern Mosquito Banks (i.e., near the southeastern coast of Nicaragua) in Fig. 2.22, the cloudiness associated with the approaching tropical wave can be seen south of Jamaica. Note that even at this early afternoon hour, practically all of the cloudiness seen in the visible imagery (Fig. 2.22) extends to great heights (Fig. 2.23) in this warm, moist tropical air mass.

³⁵Four hours later San Andrés Island (station 80001) is reporting cumulus of considerable development (see Fig. 2.21).

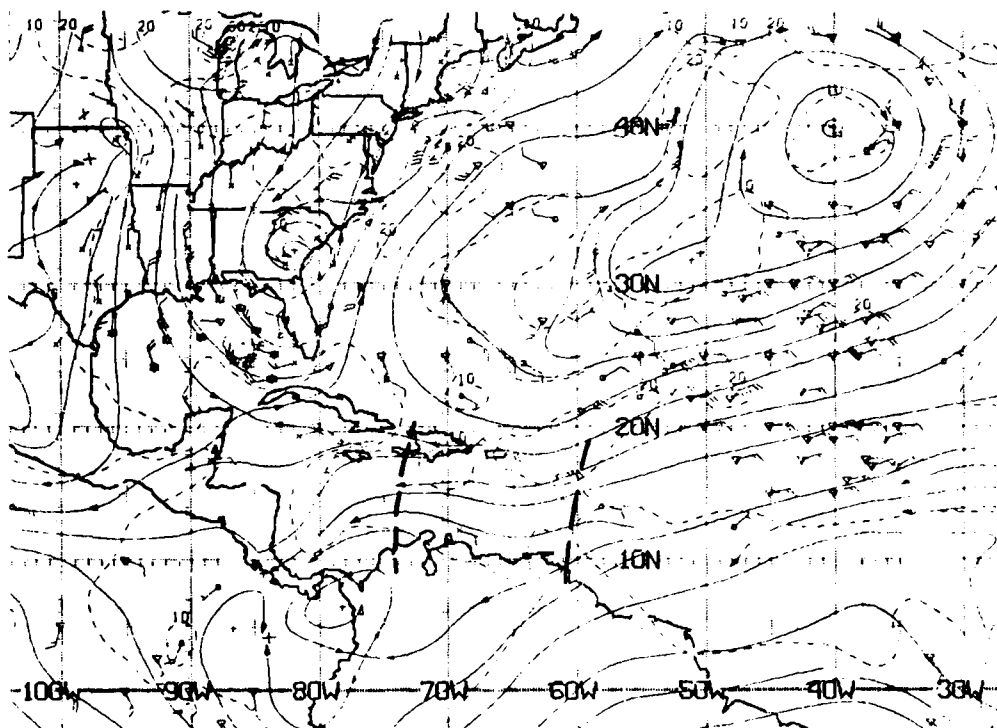


Figure 2.16: NMC ATOLL Operational Streamline Chart, 0000 UTC 4 OCT 1988
As in Fig. 2.4.

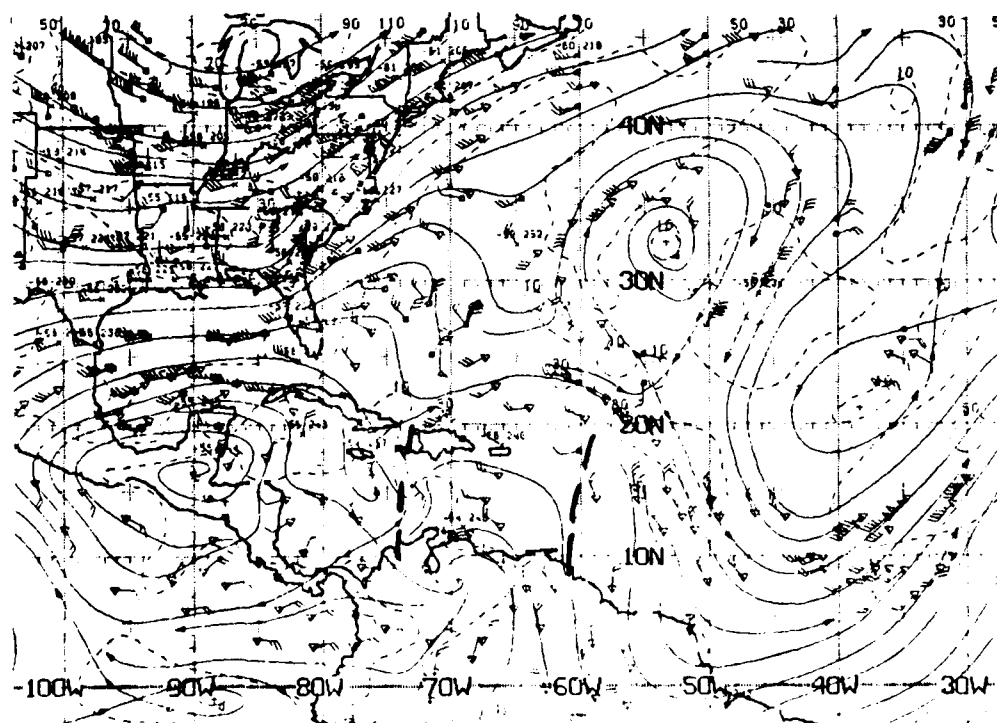


Figure 2.17: NMC 200 mb Operational Streamline Chart, 0000 UTC 4 OCT 1988
As in Fig. 2.6.

0001 040088 39E-42A 00921 15711 EC1

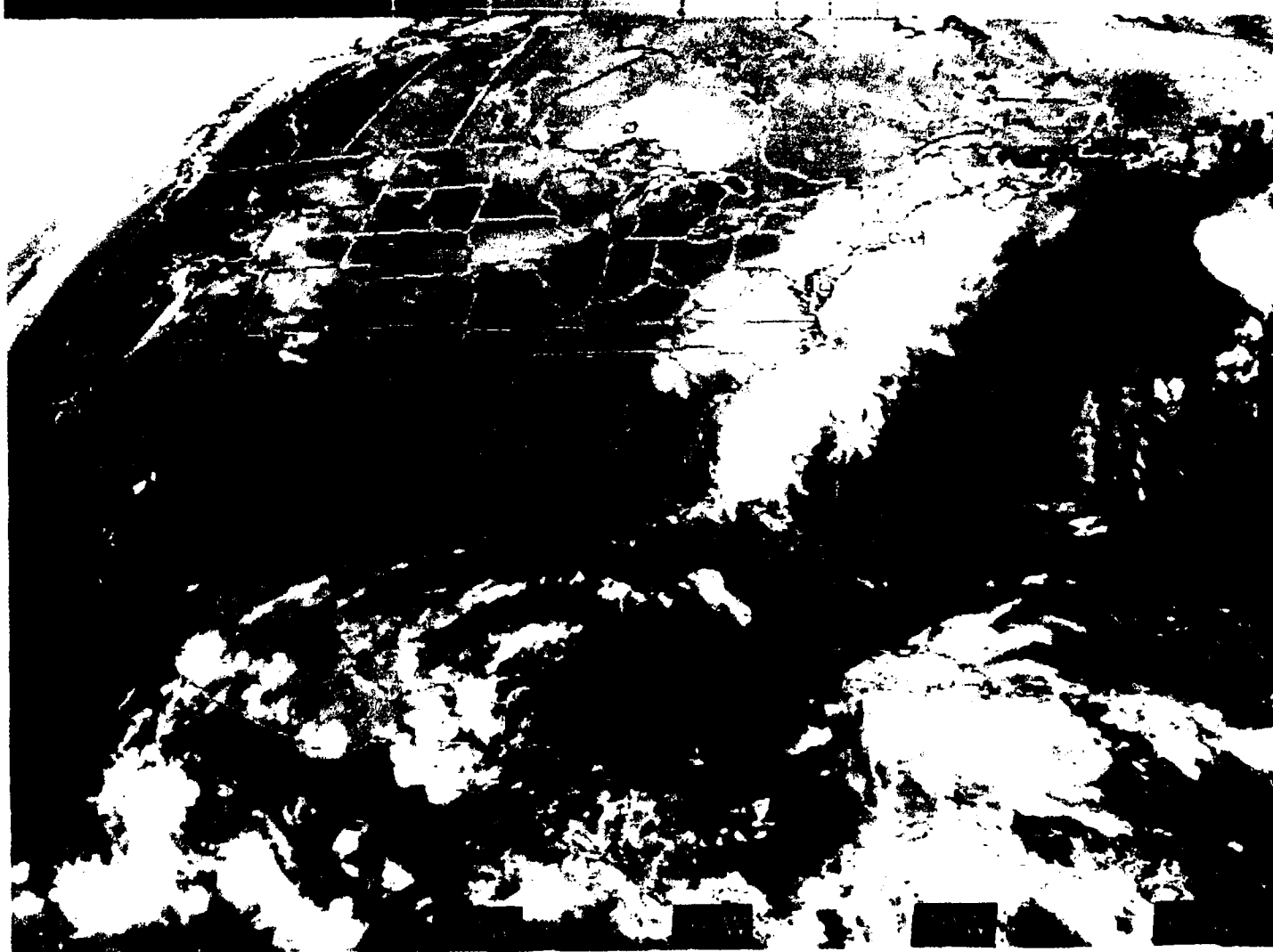


Figure 2.18: GOES East Infrared Satellite Imagery, 0001 UTC 4 OCT 1988

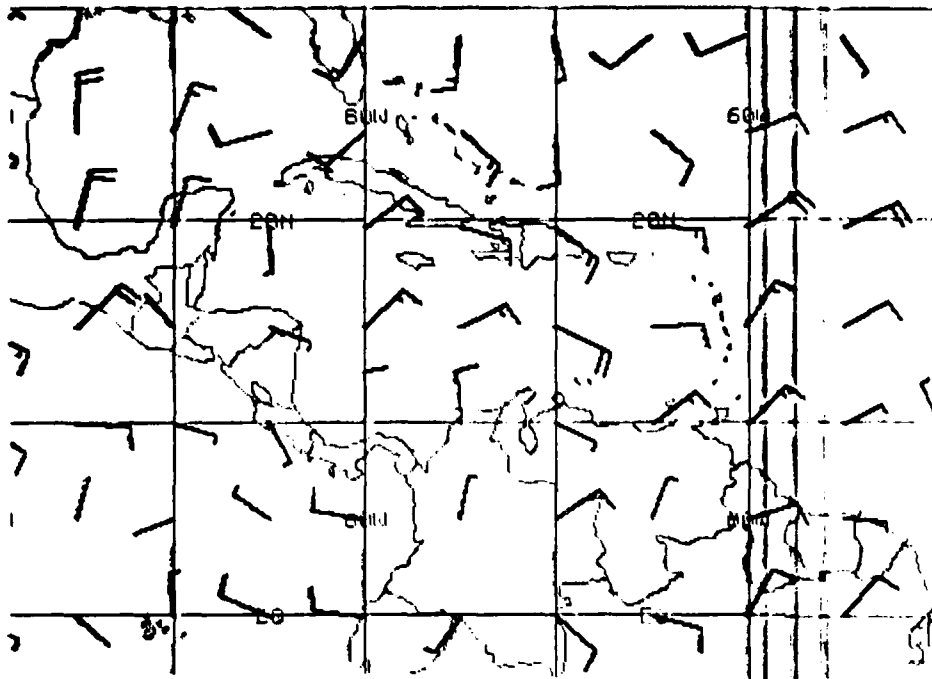


Figure 2.19: FNOG 925 mb Winds, 0000 UTC 4 OCT 1988.
Each barb represents 10 kt. (Ignore vertical printer lines near 60°W.)

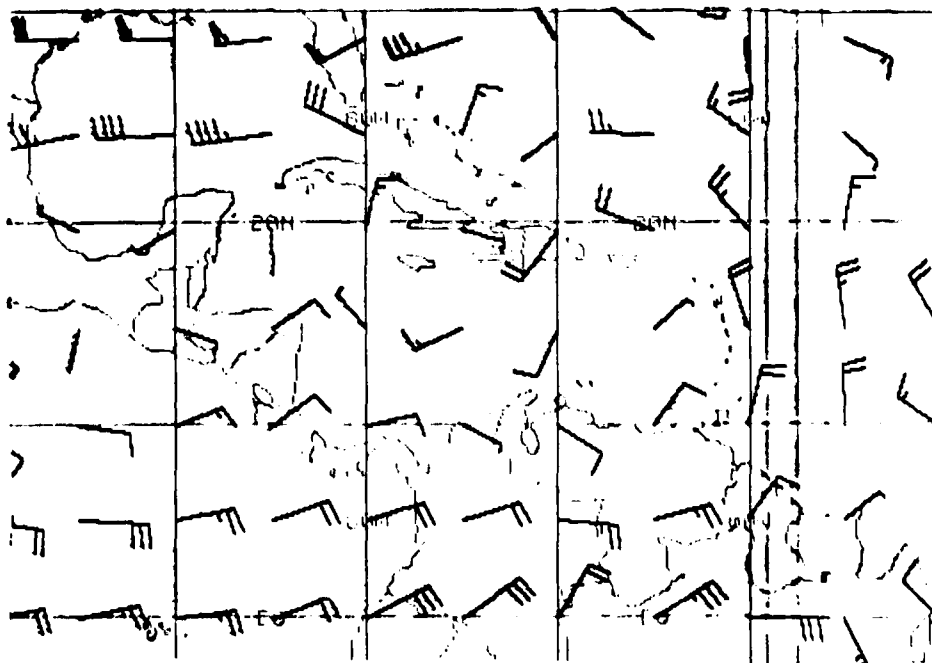


Figure 2.20: FNOG 200 mb Winds, 0000 UTC 4 OCT 1988.
Each barb represents 10 kt, each pennant 50 kt. (Ignore vertical printer lines near 60°W.)

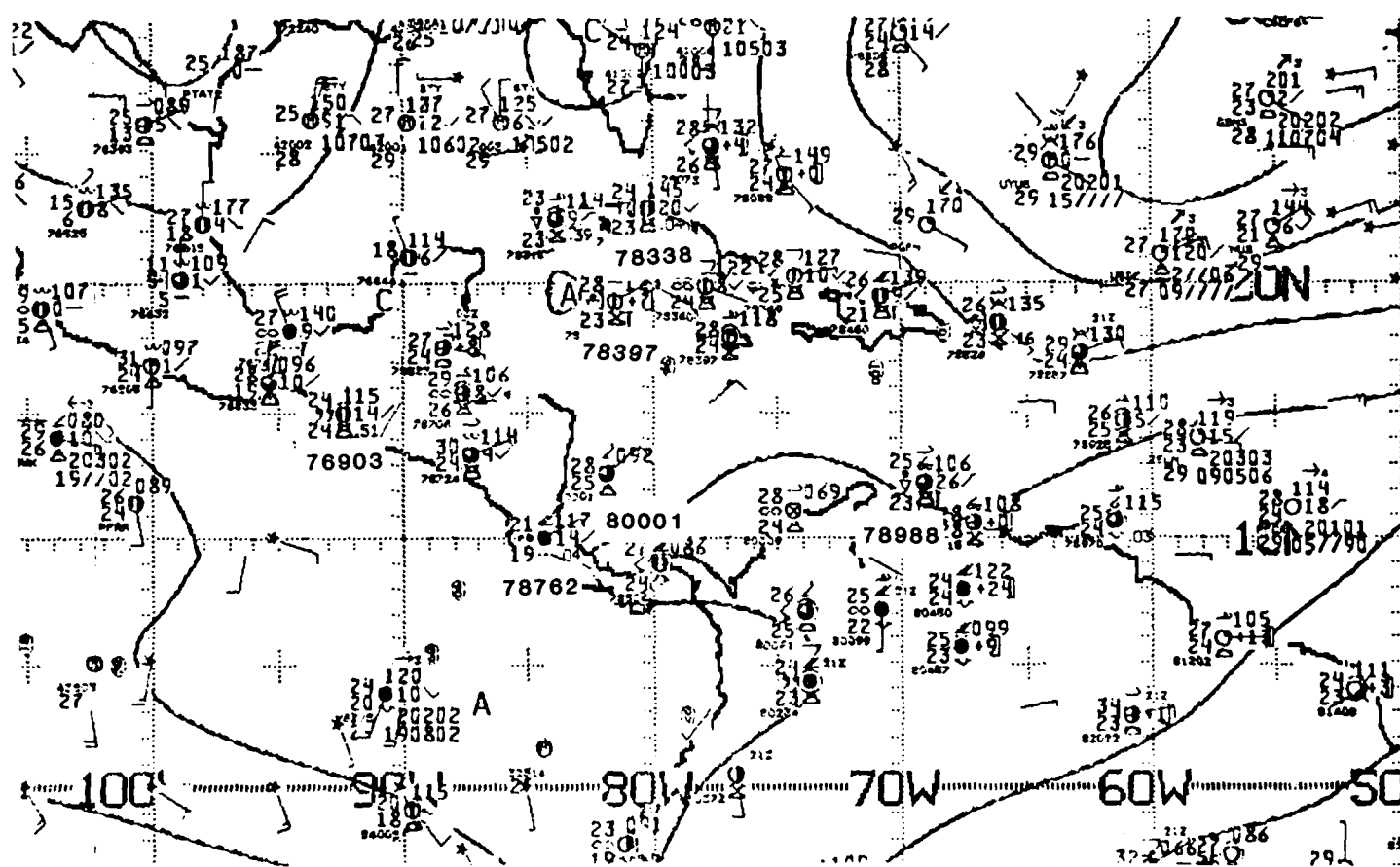


Figure 2.21: NMC 1000 mb Analysis, 0000 UTC 4 OCT 1988.

Contours are unlabeled stream functions from optimum interpolation analysis, with C identifying cyclonic centers and A identifying anticyclonic centers.

1931 030088 39A-4 00911 15711 EC1

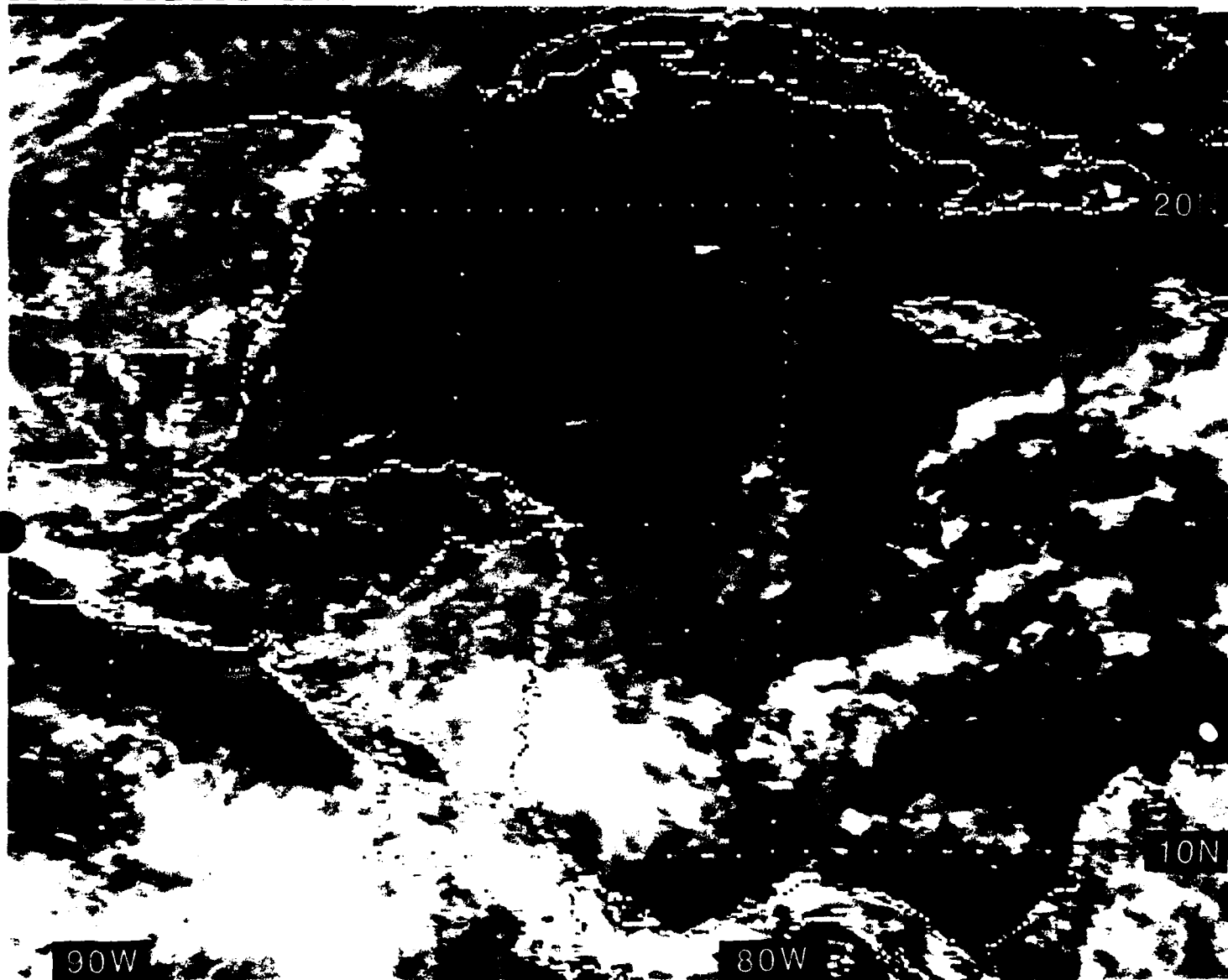


Figure 2.22: GOES East Visible Satellite Imagery, 1931 UTC 3 OCT 1988

2001 030088 39E-42A 00901 15711 EC1

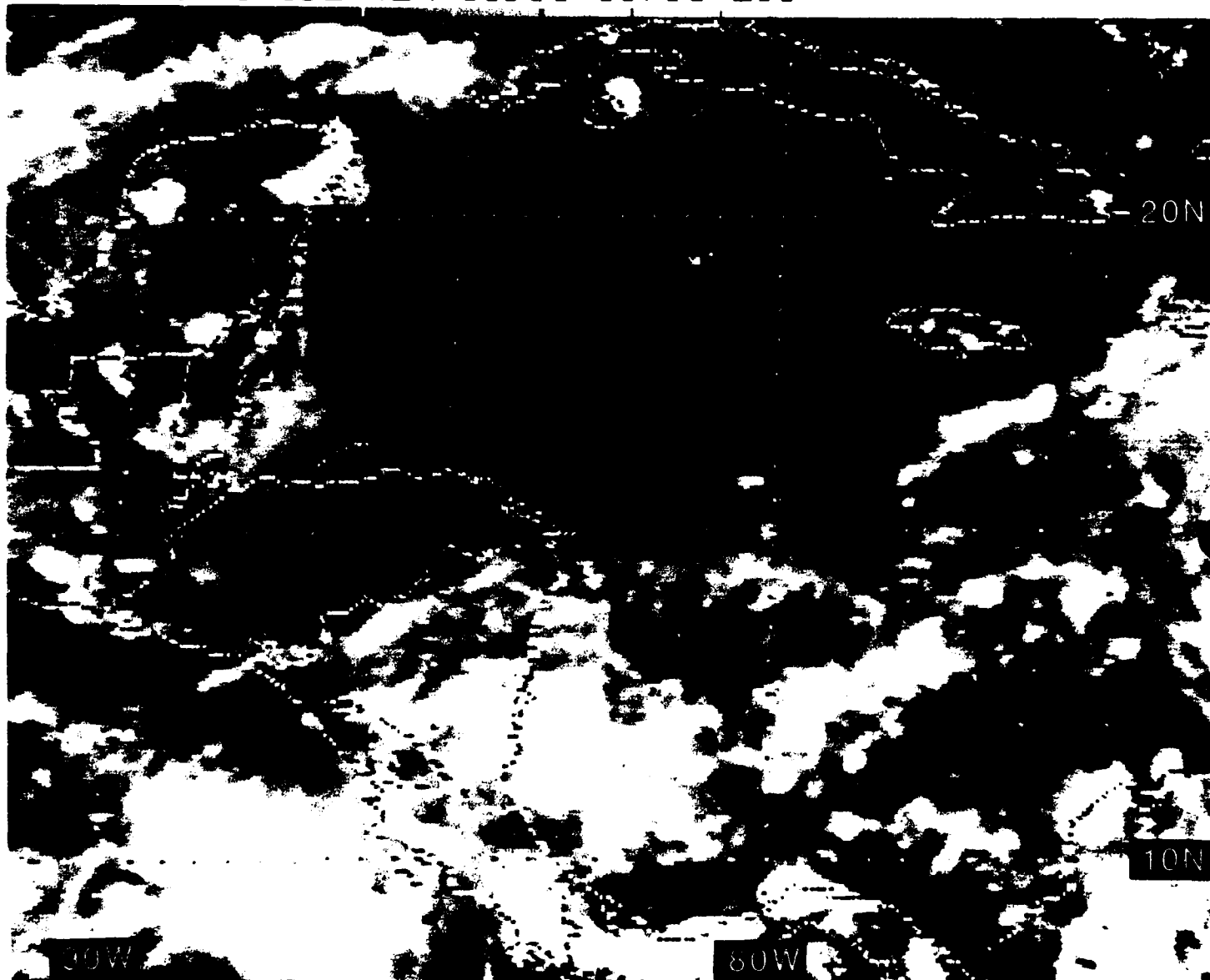


Figure 2.23: GOES East Infrared Satellite Imagery, 2001 UTC 3 OCT 1988

5 October 1988

At 0000 UTC on 5 October, NHC analyzes the tropical wave at $\sim 78^\circ\text{W}$ between central Cuba and a low pressure center³⁶ just north of the Canal Zone, Panama (see Fig. 2.24). Weak cyclonic curvature is present (at least in the southern part of the Caribbean Sea) on the NMC analysis (see Fig. 2.24—cyclonic curvature can also be inferred from the Navy's 925 mb analysis (Fig. 2.28)). The concurrent IR imagery of Fig. 2.26 depicts supporting heavy convection just east of the tropical wave axis (between $12\text{--}15^\circ\text{N}$), as well as late afternoon convection over the northern Yucatan Peninsula, Nicaragua, Panama, central Cuba and Haiti. The surface observations depicted on the 1000 mb analysis Fig. 2.27 confirm the above references to expected precipitation, i.e., drizzle within the past hour at Merida, Mexico (station 76644), continuous rain at Howard Air Force Base, Panama (station 78806), lightning at both Sancti Spiritus, Cuba (station 78349) and Santiago, Dominican Republic (station 78460), as well as moderate or heavy rain with a thunderstorm within the past hour at a ship at 14°N , 74°W (under the convection east of the tropical wave axis in Fig. 2.26).

The lack of organized convection over the eastern Caribbean Sea, as well as the anticyclonically curved low-level streamlines present there (see Figs. 2.26 and 2.24) probably led to the discontinuance of the tropical wave which had been identified on the previous day (4 October 1988) near the Windward Islands. At 200 mb (Fig. 2.25) the expected anticyclonic vortex over the convection to the east of the tropical wave axis is weakly, if at all, depicted. There is a weak mid-latitude trough, penetrating southwestward between Cuba and Hispaniola, separating the two anticyclonic centers associated with the convection over the northern Yucatan Peninsula and Puerto Rico—there is **no** anticyclonic curvature over the convection *just* to the east of the tropical wave axis (see Fig. 2.25).

While the Navy's low- and high-level wind barb charts (Figs. 2.28 and 2.29) are in general agreement³⁷ with their NMC counterparts (Figs. 2.24 and 2.25), the very weak **northwesterly** upper-level flow southeast of Jamaica on Fig. 2.25 disagrees with the **southwesterly** 5 kt wind barb on Fig. 2.29.

Finally, Figs. 2.30 and 2.31 show the convection present later on 5 October 1988. Figure 2.30, the infrared imagery at *synoptic* time (1200 UTC), depicts the often observed convection over the warm, shallow waters of the Miskito Banks (just east of Nicaragua)³⁸ and over the Gulf of the Mosquitos (north of western Panama). By this time, the convection east of the tropical wave axis has advanced slowly westward and is very prominent south of Jamaica in Fig. 2.30. Fig. 2.31 is the first *visible* imagery available from GOES East (1431 UTC), i.e., two and a half hours after Fig. 2.30.)

³⁶The low center north of Panama is identified by "C" on the NMC 1000 mb analysis in Fig. 2.27.

³⁷Disagreement between NMC and FNOC low-level analyses was often noted south of the Gulf of Panama; however on this date the northwesterly wind barb present at 5°N , 80°W (Fig. 2.28) may be reconciled with a streamline exiting from the neutral point at the southwestern tip of Panama on Fig. 2.24.

³⁸The very large rainfall totals at coastal stations (e.g., 159.7 inches of rain per year at Bluefields on the southeastern coast of Nicaragua, see Appendix B) attest to the persistence of this convection.

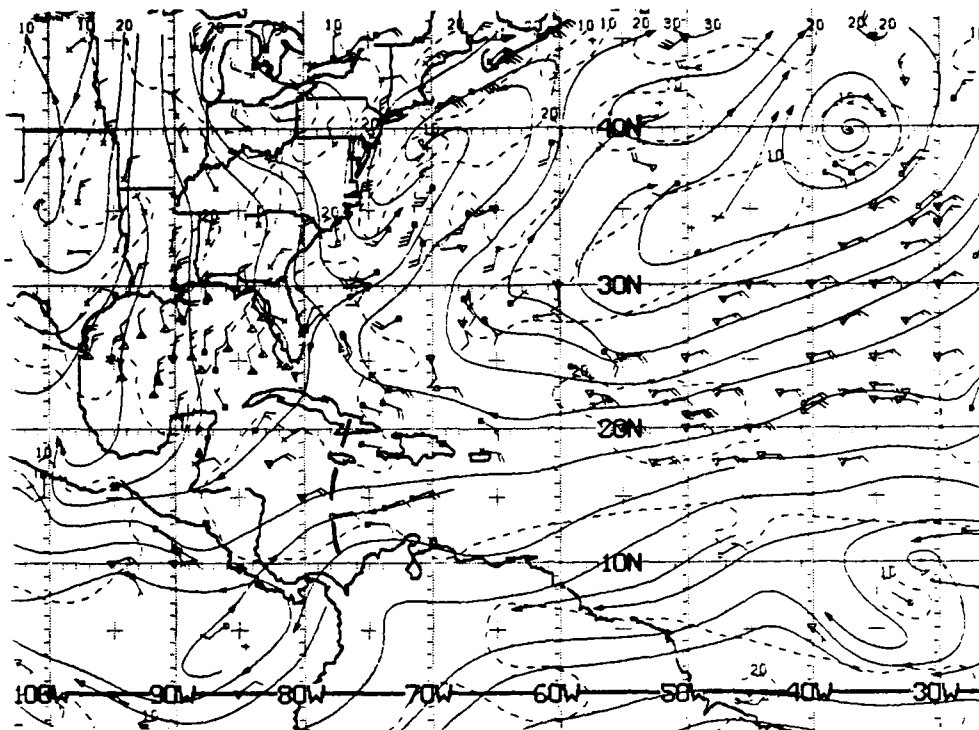


Figure 2.24: NMC ATOLL Operational Streamline Chart, 0000 UTC 5 OCT 1988
As in Fig. 2.4.

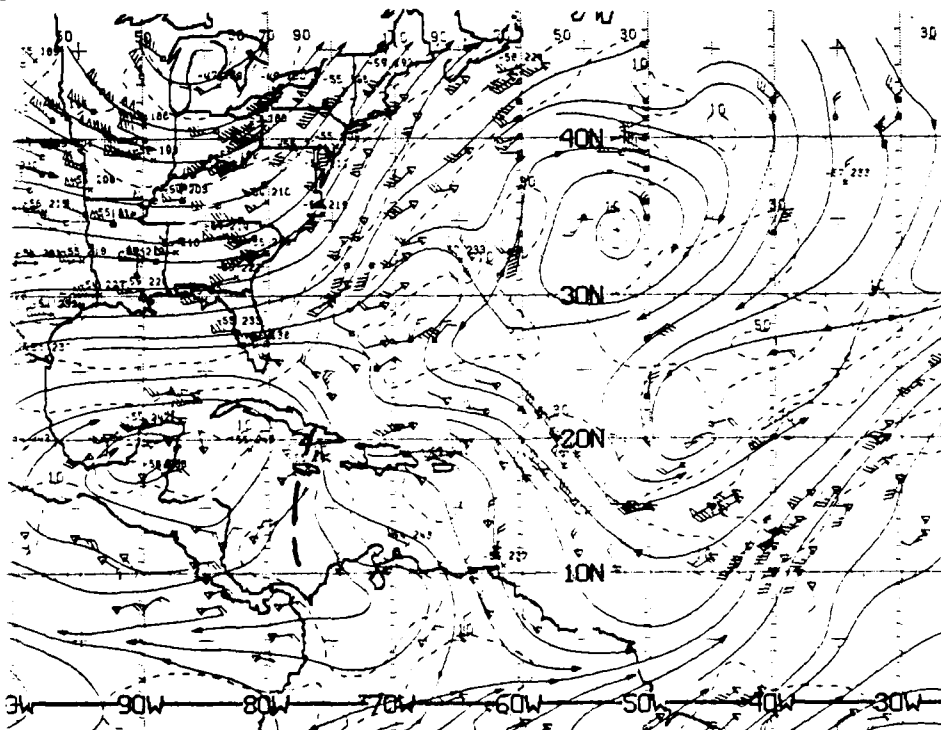


Figure 2.25: NMC 200 mb Operational Streamline Chart, 0000 UTC 5 OCT 1988
As in Fig. 2.6.

0001 050088 39E-42A 00911 15721 EC1

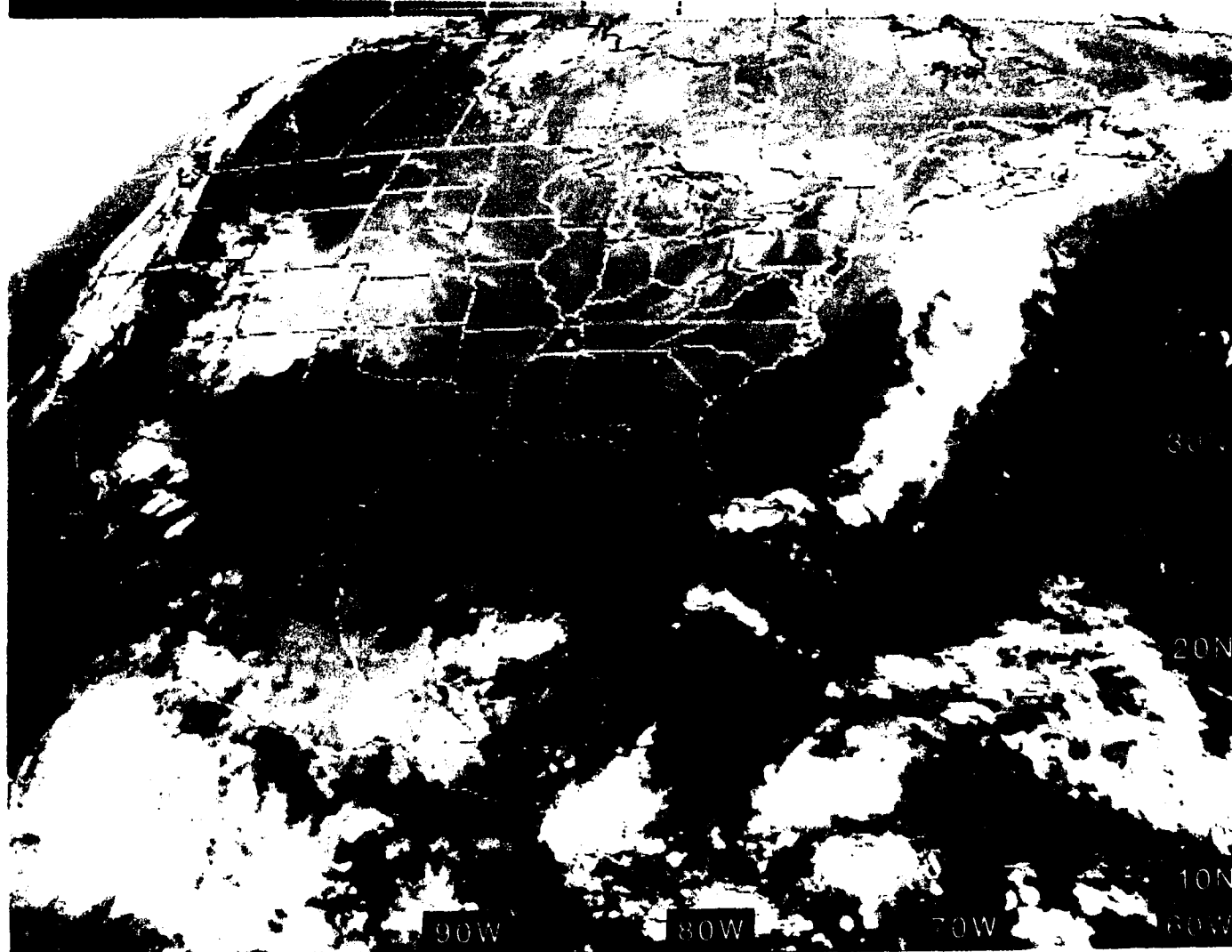


Figure 2.26: GOES East Infrared Satellite Imagery, 0001 UTC 5 OCT 1988

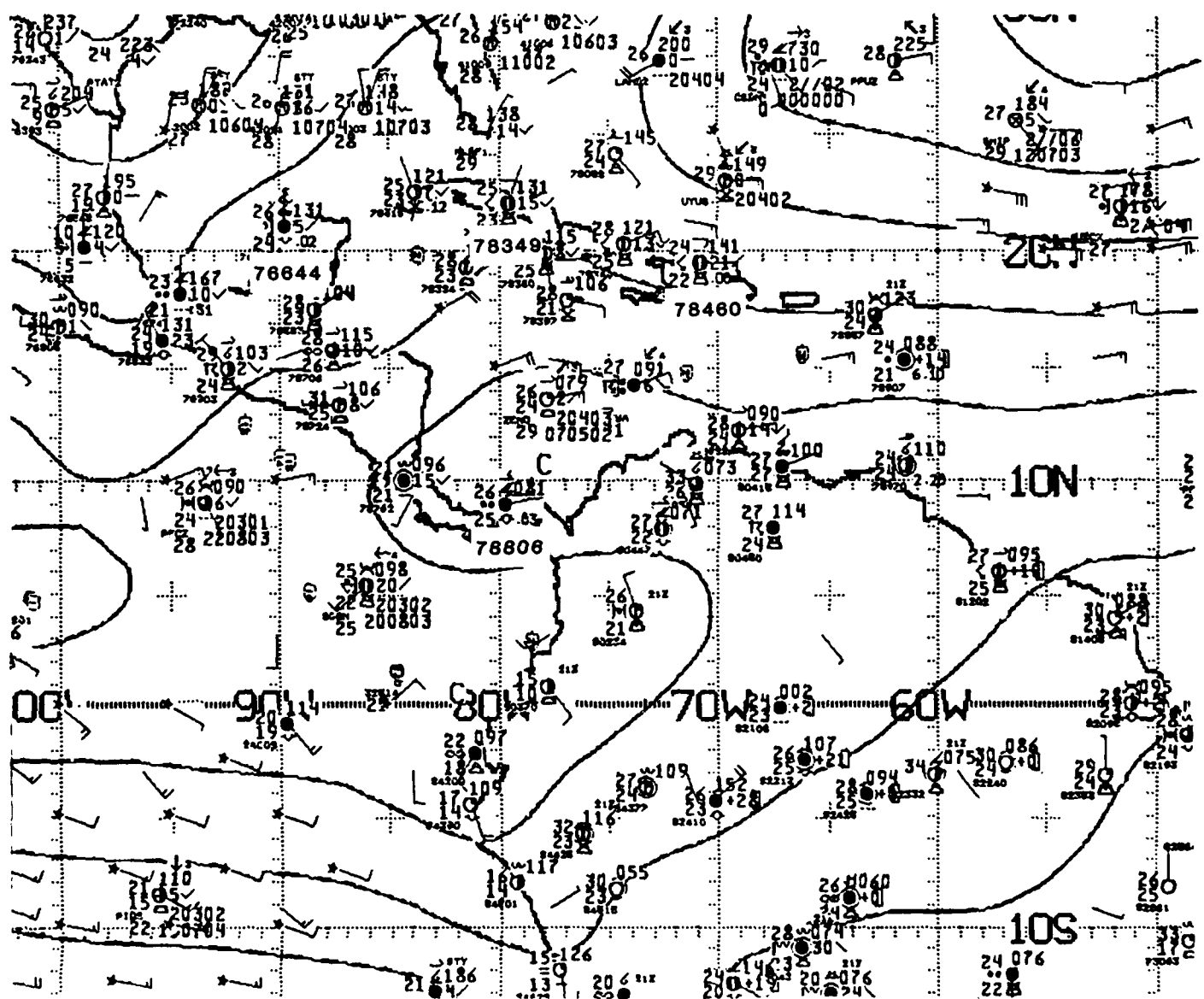


Figure 2.27: NMC 1000 mb Analysis, 0000 UTC 5 OCT 1988. As in Fig. 2.21.

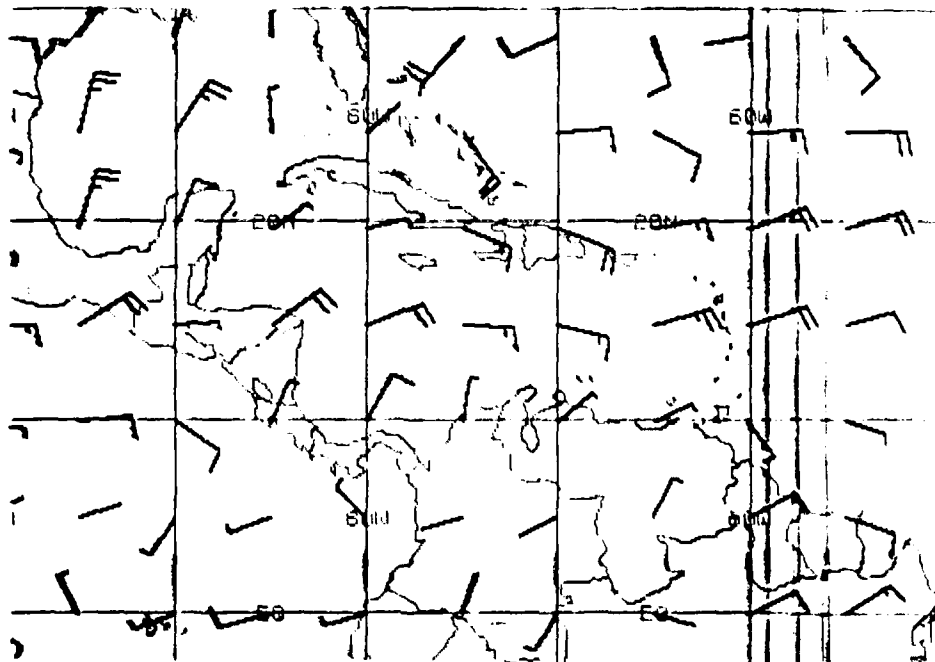


Figure 2.28: FNOc 925 mb Winds, 0000 UTC 5 OCT 1988. As in Fig. 2.19.

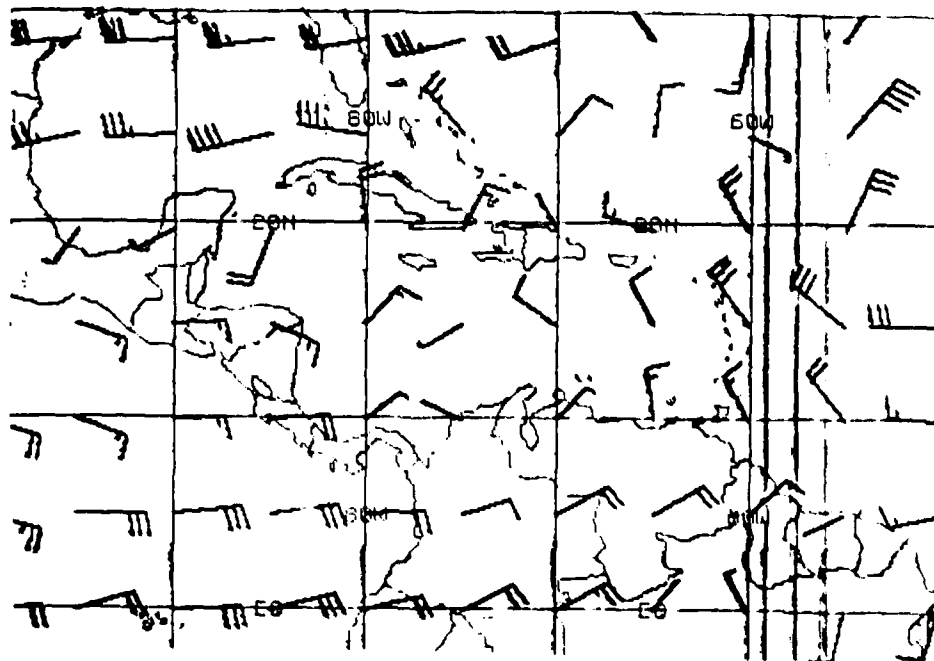


Figure 2.29: FNOc 200 mb Winds, 0000 UTC 5 OCT 1988. As in Fig. 2.20.

1201 050088 39E-42A 00921 15781 EC1

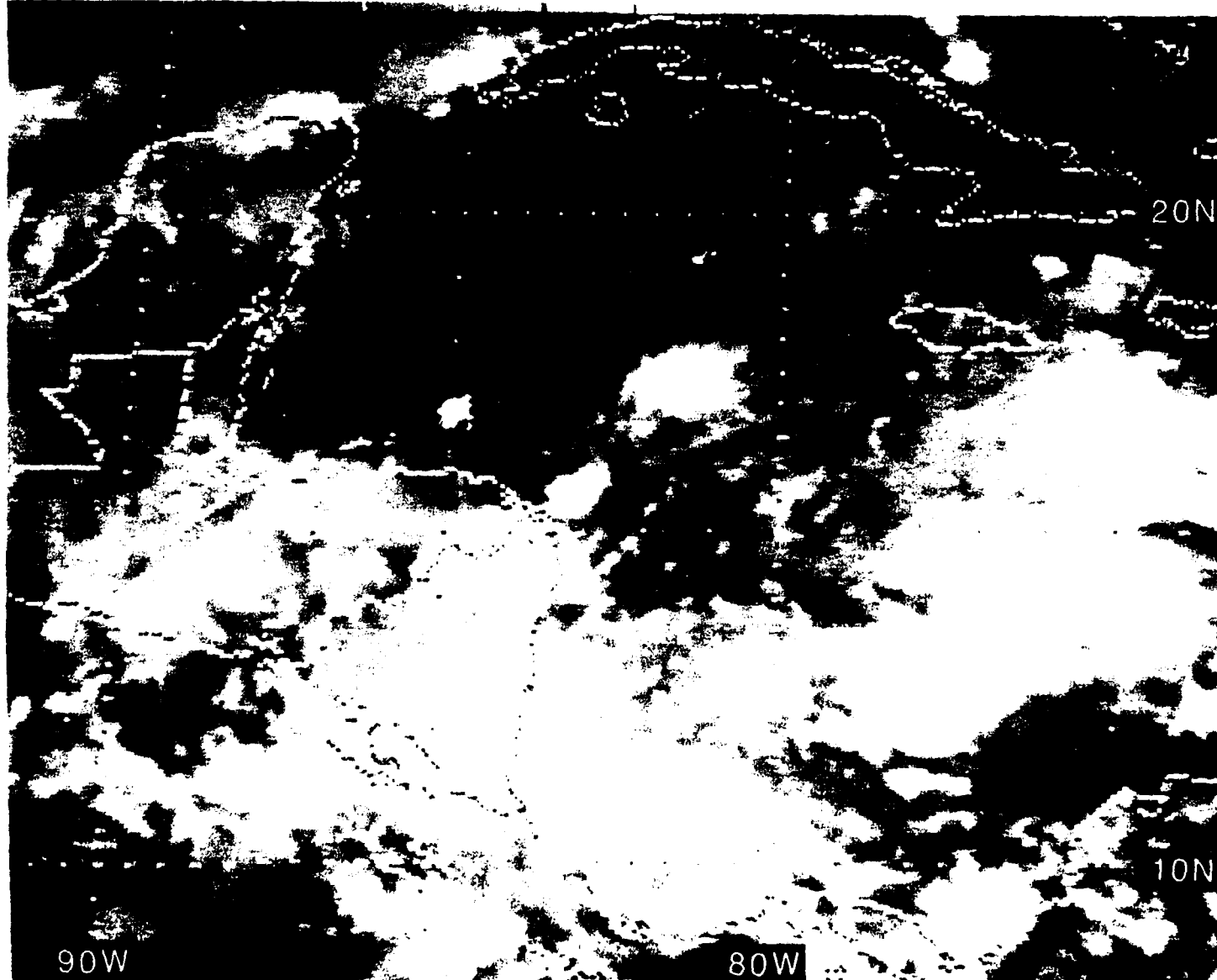


Figure 2.30: GOES East Infrared Satellite Imagery, 1201 UTC 5 OCT 1988

1431 050088 39A-4 00901 15771 EC1

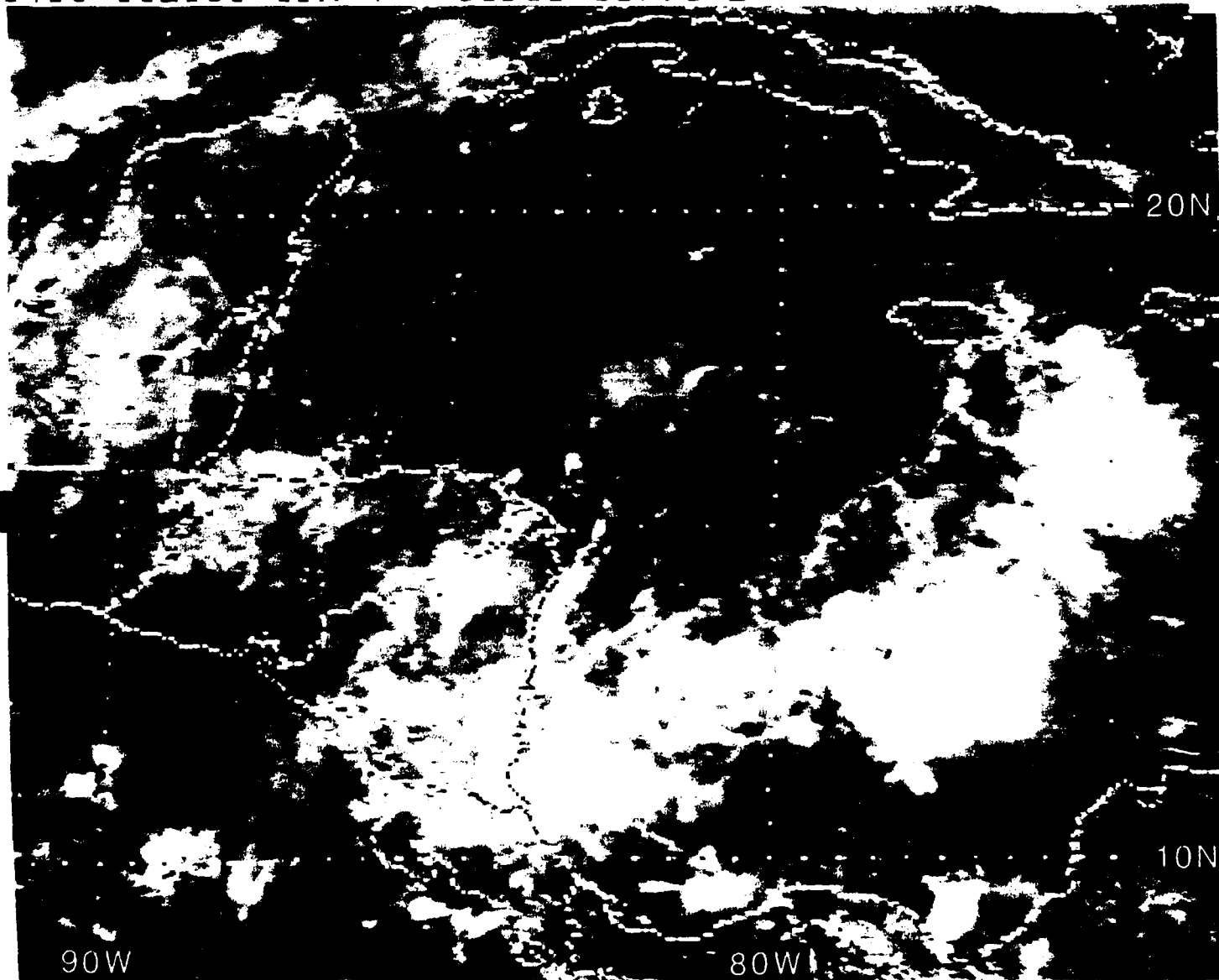


Figure 2.31: GOES East Visible Satellite Imagery, 1431 UTC 5 OCT 1988

6 October 1988

On the following day at 0000 UTC 6 October 1988 (Fig. 2.32), the National Hurricane Center (NHC) locates the tropical wave near 82°W—having moved at ~12.5 kt during the past 24 hours. The IR imagery (Fig. 2.34) at this time reveals that the convective cloudiness *behind* the propagating tropical wave has appeared to join the cloudiness³⁹ over the Mosquito Banks. (While the Riehl tropical wave model for the Caribbean supports cloudiness and precipitation *trailing* the wave axis, it does **not** prohibit the possibility of convection also preceding the wave.) Note, also, that the streamlines of Fig. 2.32 show cyclonic curvature south of Puerto Rico, in the eastern Caribbean Sea. Moreover, there is strong cyclonic shear vorticity approaching the Windward Islands (i.e., note the 30 kt PIBAL/RAWIN report at 14.5°N, 61°W on Fig. 2.32). The possibility of another tropical wave located at the cyclonically curved streamlines, extending southward from Puerto Rico⁴⁰ to Venezuela, is supported by the intense convection depicted on the IR imagery east of 66°W. Figure 2.34 also depicts the convection associated with a cold front (not shown) extending southwestward from the western North Atlantic Ocean to western Cuba.

The NMC 200 mb streamline analysis (Fig. 2.33) depicts strong divergence above the convection of the tropical wave near 82°W. (Note that the high resolution of the diffluence above the wave in Fig. 2.33 is provided by satellite wind vectors from NESDIS WASH DC.) However, rather than supportive upper-level anticyclonic streamlines over the convection east of the possible wave near 66°W, there are cyclonic streamlines—i.e., the warming aloft, from the release of latent heat, is small.

Figure 2.35 with its surface observations correlates well with the IR imagery (Fig. 2.34) for the same time. Note, for example: overcast and drizzle at San Andrés Island (station 80001) just east the Miskito Banks under heavy cloudiness; a thunderstorm at Torrijos International Air Port (IAP) (station 78792) at Panama City, Panama under convective cloudiness; overcast at San José, Costa Rica (station 78762) under IR-revealed cloudiness; 50% cloud cover with multilayer cloudiness and sea breeze from the east at Belize City, Belize (station 78583); while a thunderstorm exists just west of Guatemala at Tapachula on the North Pacific coast of Mexico (station 76903) and a multilayered overcast is present at Campeche, Mexico (station 76695) on the western Yucatan Peninsula.

³⁹Described in the text for 5 October.

⁴⁰However, informal communication with NHC indicated that the tropical wave in the eastern Caribbean Sea was nearer 63°W at 0000 UTC on 6 October 1988.

The Navy's 925 mb wind barb chart (Fig. 2.36) depicts the tropical wave near 82°W with weak cyclonic vorticity; however, little, if any, indication of the possible wave south of Puerto Rico is evident. Northeasterly flow over the western Caribbean and the Gulf of Mexico as well as westerly flow south of the Gulf of Panama are depicted by both NMC (Fig. 2.32) and FNOC (Fig. 2.36); however, south of the Gulf of Tehuantepec, NMC has *reasonable* northerly flow at 30 kt while FNOC has easterly flow at 50 kt—the wind symbol on Fig. 2.36 is a pennant. While there is general agreement elsewhere at 200 mb, NMC (Fig. 2.33), with its *mesoscale* analysis of satellite derived winds over the convection near 82°W and its satellite supported *easterly* flow over Guatemala, Honduras, El Salvador, Nicaragua and Costa Rica, appears superior to the FNOC 200 mb wind barbs (Fig. 2.37).

Figures 2.38 and 2.39 show the comparison between visible and IR imagery near the time of the last visible imagery, about four hours before the *synoptic* time of the analyses just reviewed. Note that while El Salvador was free of convection at 2001 UTC (Fig. 2.38), four hours later Fig. 2.34 depicts heavy convection, although the nearest observation is east of the Gulf of Fonseca (Choluteca, Honduras (station 78724) in Fig. 2.35) where cumulus of considerable development and $\geq 90\%$ cloud cover are reported. This is an example of the instability which can develop when relatively *clear* air is heated at lower levels by the warm land surface—of course, low-level convergence of air blowing from the cooler *surrounding* regions (covered earlier by cloudiness) adds to the ultimate instability. Figures 2.38 and 2.39 also show the initial stages of a squall line which later grew to a length of ~ 250 mi extending from the northeast coast of Honduras by 0000 UTC (see Fig. 2.34).

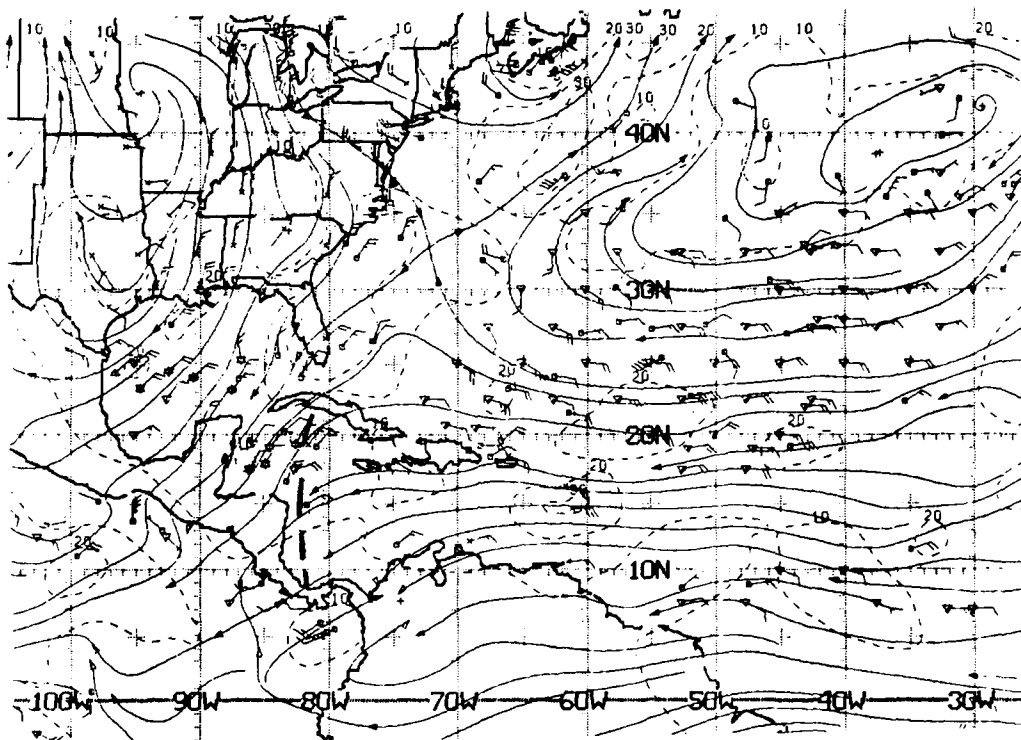


Figure 2.32: NMC ATOLL Operational Streamline Chart, 0000 UTC 6 OCT 1988
As in Fig. 2.4.

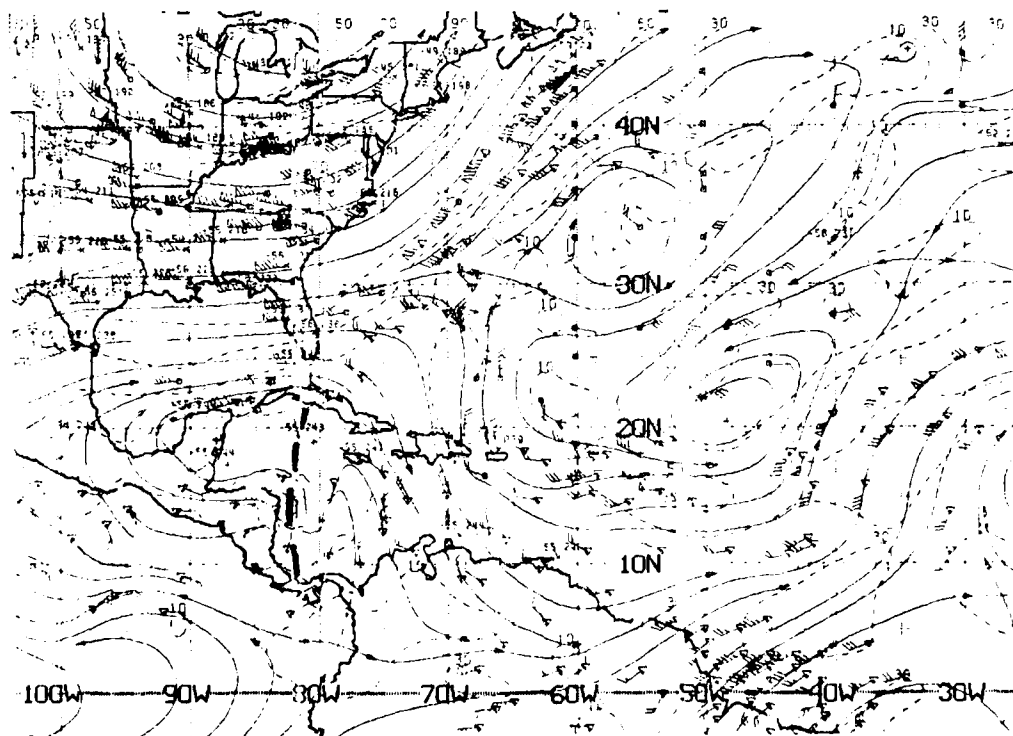


Figure 2.33: NMC 200 mb Operational Streamline Chart, 0000 UTC 6 OCT 1988
As in Fig. 2.6.

0001 060C88 39E-42A 00911 15731 EC1

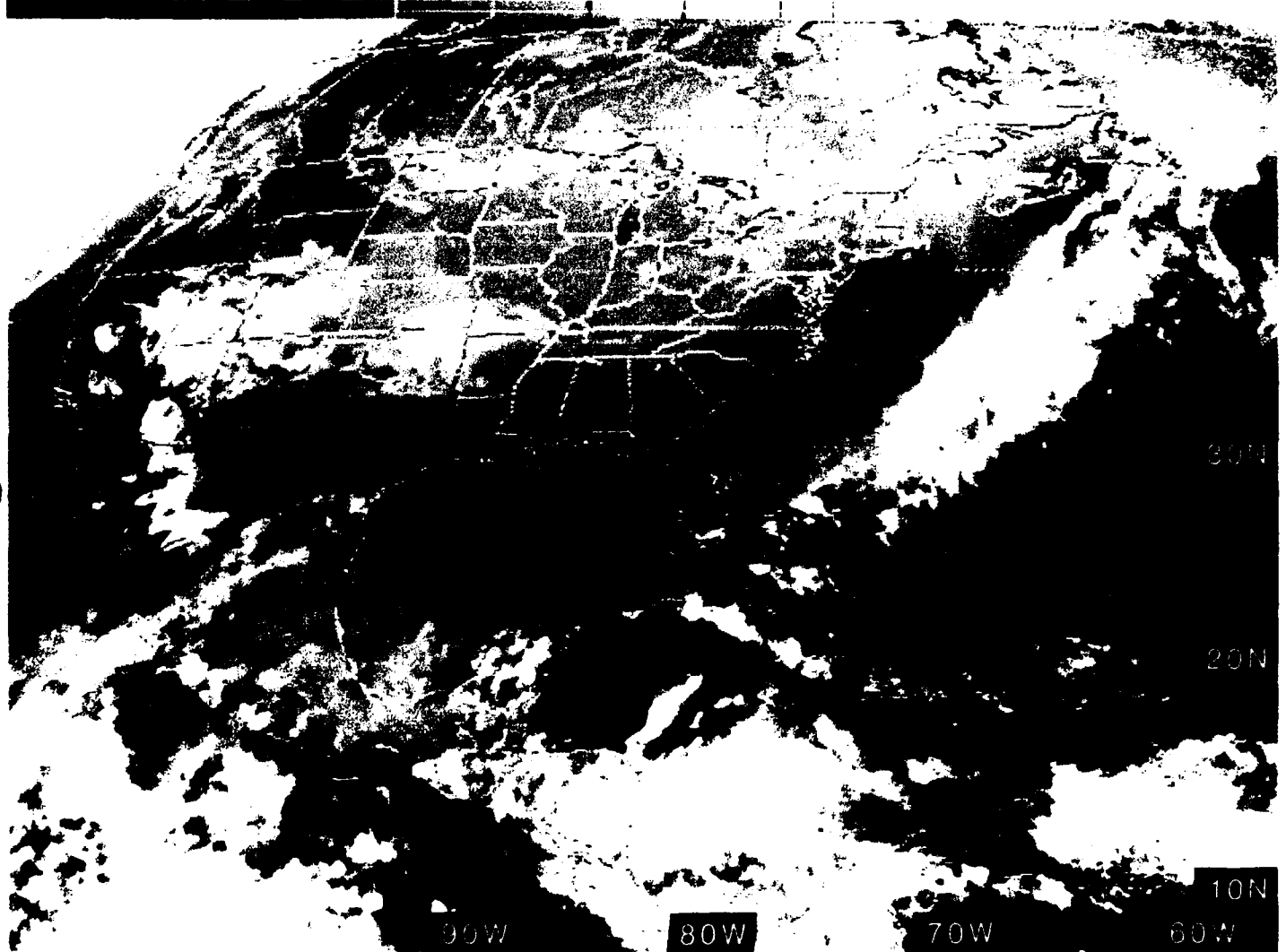


Figure 2.34: GOES East Infrared Satellite Imagery, 0001 UTC 6 OCT 1988

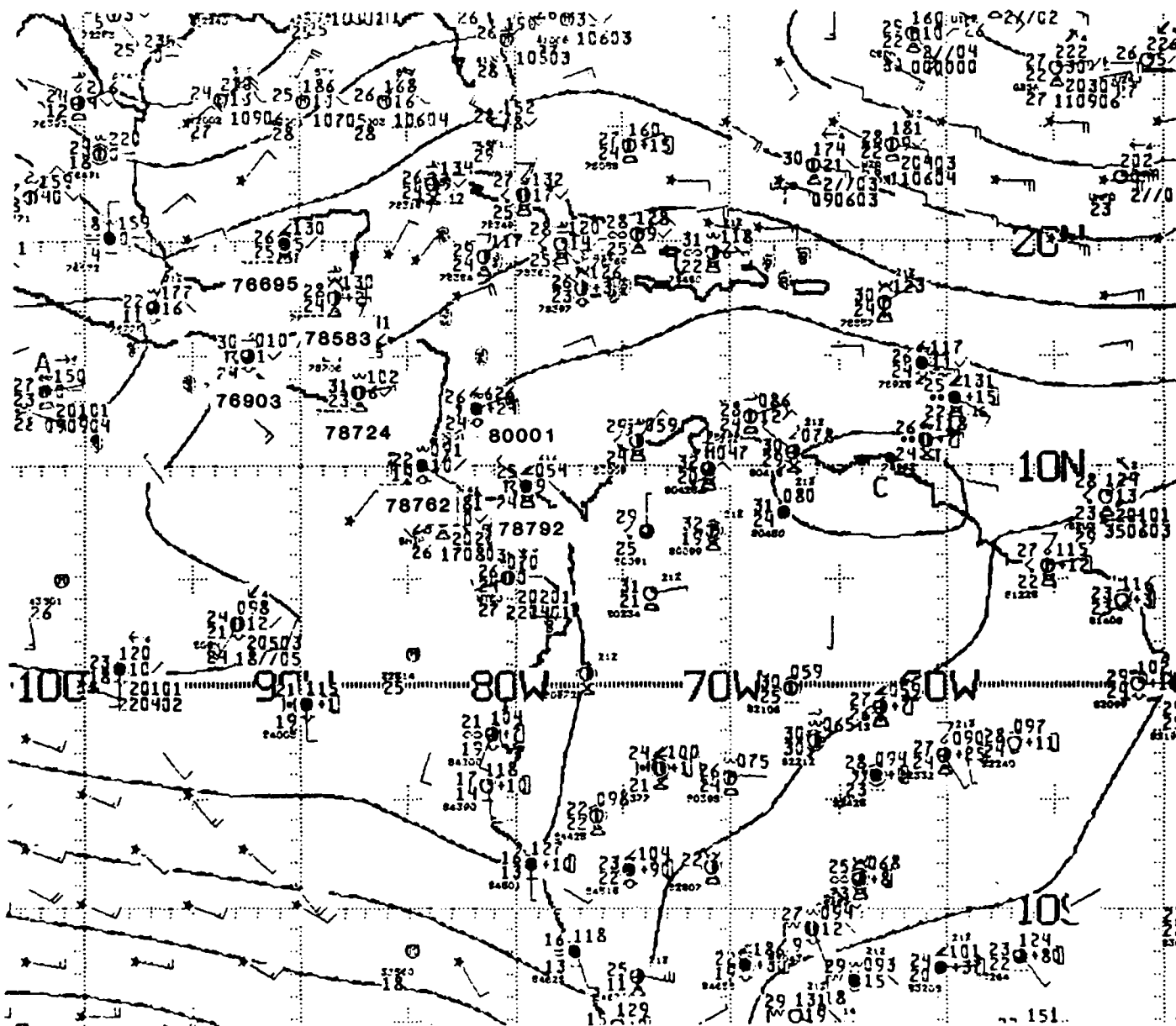


Figure 2.35: NMC 1000 mb Analysis, 0000 UTC 6 OCT 1988. As in Fig. 2.21.

2001 050088 39E-42A 00901 15731 EC1

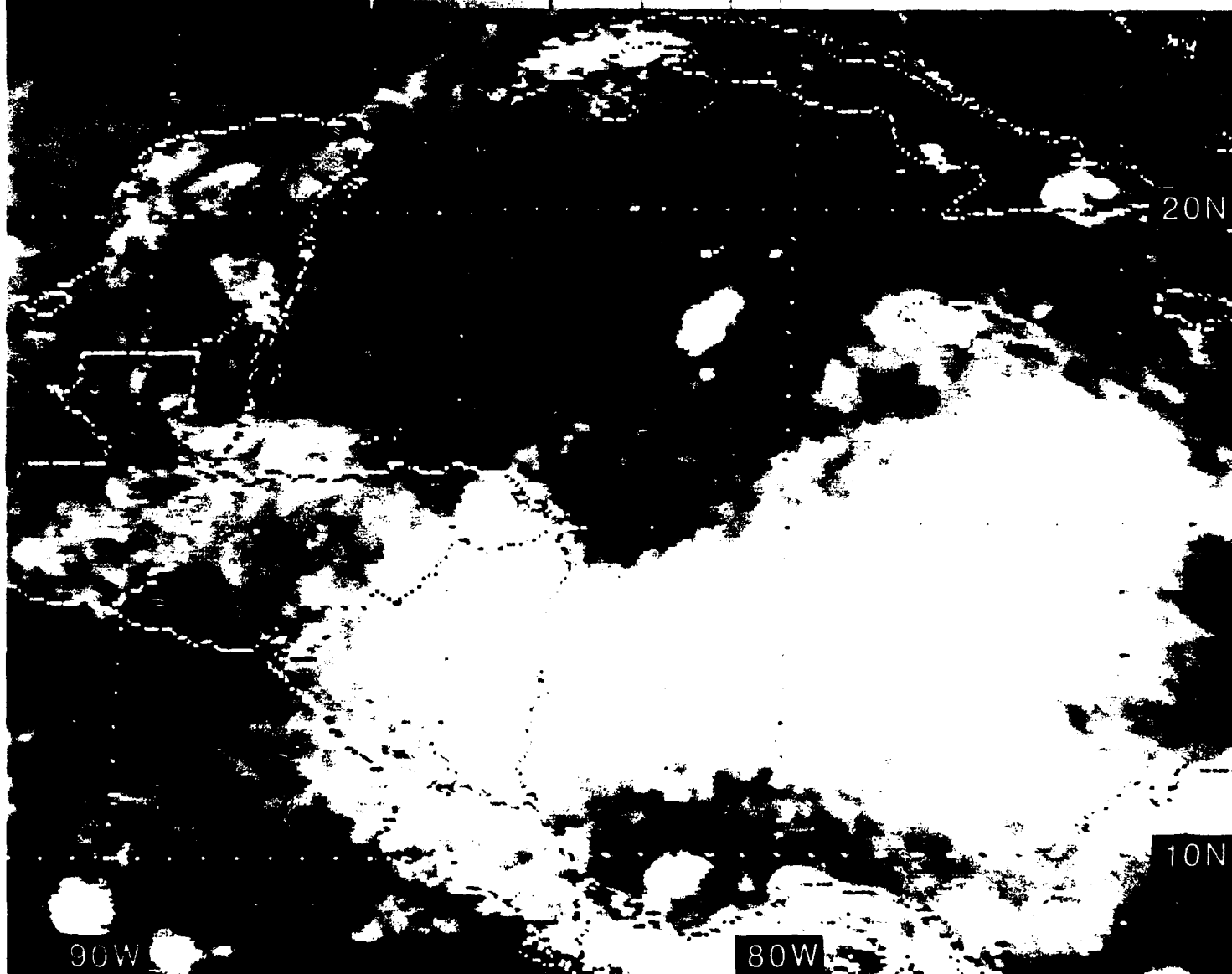


Figure 2.38: GOES East Infrared Satellite Imagery, 2001 UTC 5 OCT 1988

2031 050C88 39A-4 00902 15731 EC1

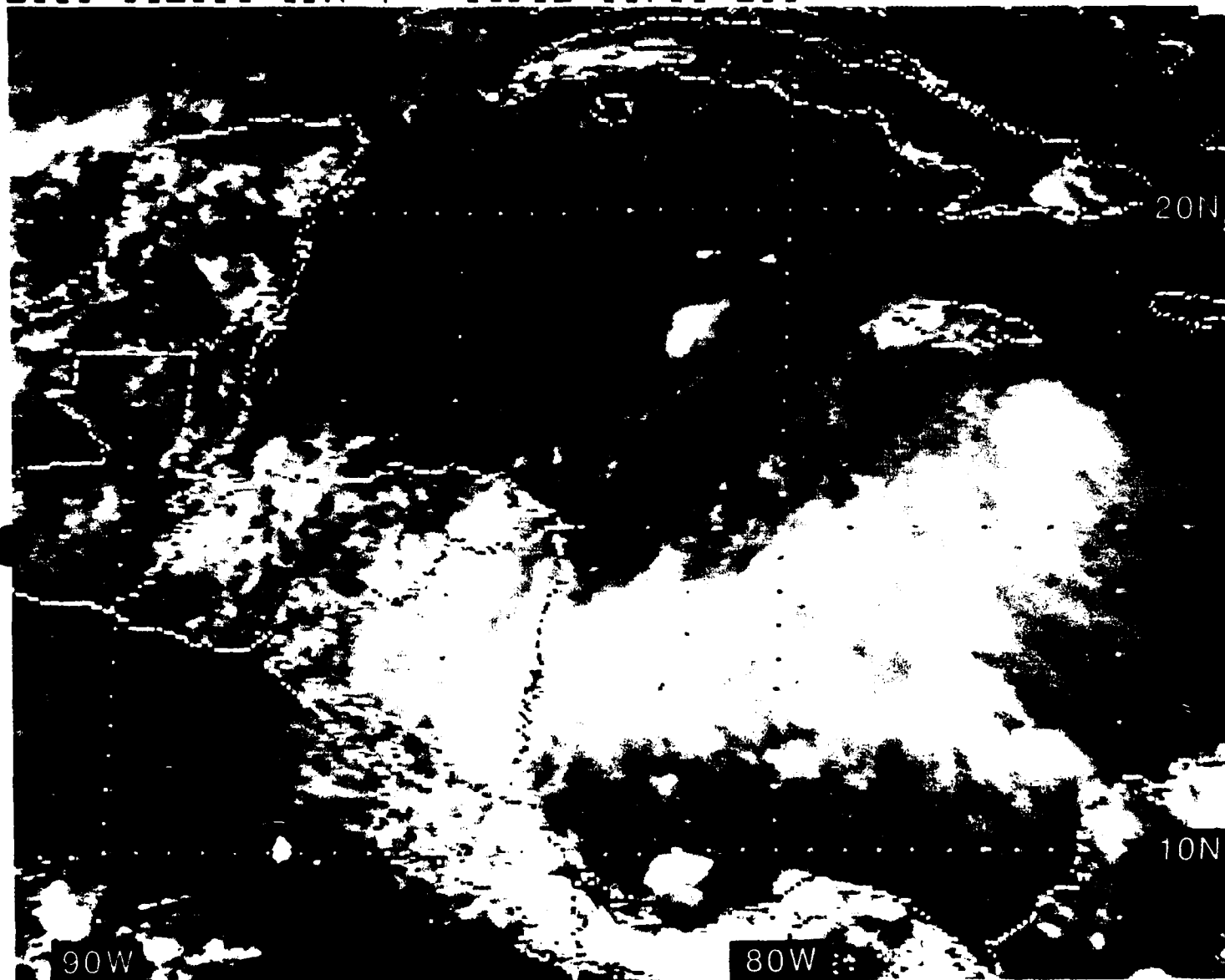


Figure 2.39: GOES East Visible Satellite Imagery, 2031 UTC 5 OCT 1988

7 October 1988

By 0000 UTC on 7 October, the tropical wave is positioned by NHC near 87°W extending from the northeastern tip of the Yucatan Peninsula to the northern coast of Honduras (see Fig. 2.40). The possibility of another tropical wave in the eastern Caribbean Sea, as discussed for the previous day (6 October), is supported by the large group of ESE wind observations ≥ 20 kt (southeast of Hispaniola between 70°W and 60°W (Fig. 2.40)) identifying shear cyclonic vorticity just east of 70°W; however, the streamlines depict anticyclonic curvature. The convective cloudiness depicted on Fig. 2.42 in the eastern Caribbean Sea has **not** progressed from its position the previous day on Fig. 2.34. No doubt, the upper-level trough (*now* possibly the TUTT) at 200 mb, extending NE-SW to a position just south of Puerto Rico (see Fig. 2.41), has prevented the westward progression of the convective region. Moreover, the *upper-level* diffluence so apparent east of the trough (commencing near $\sim 60^\circ\text{W}$ in Fig. 2.41) favors development (convective cloudiness) as shown in Fig. 2.42⁴¹.

The clear and cloudy conditions displayed on Fig. 2.42 are well correlated with the surface reports of Fig. 2.43. For example: the intermittent moderate rain at Tela, Honduras (station 78706), the drizzle within the past hour at Choluteca, Honduras (station 78724) and the continuous slight rain at San José, Costa Rica (station 78762), all within the cloud shield to the east of the tropical wave depicted in Fig. 2.40; the relatively clear observations in the central Caribbean Sea at Curaçao, Netherlands Antilles (station 78988) and at Santiago de Cuba, Cuba (station 78264) despite the report of local cumulus of considerable development; and finally the reports of continuous light rain at Piarco, Trinidad (station 78970) and thunderstorms at two stations in the Windward Islands under the convective cloudiness.

While the Navy's NOGAPS 925 mb wind barb chart (Fig. 2.44) displays excellent agreement with the NMC ATOLL analysis (Fig. 2.40), the Navy's 200 mb wind barb chart (Fig. 2.45) differs considerably over and east of Honduras and Nicaragua. The Navy analysis does depict the anticyclonic vortex over the convective cloudiness of the tropical wave; however, it does not contain the "mesoscale" features depicted by the NESDIS WASH DC satellite-derived winds plotted on the NMC 200 mb analysis (Fig. 2.41).

⁴¹While NHC *still* did not identify a tropical wave in the eastern Caribbean on the following day (8 October), by 12 October a disturbance that eventually developed into Hurricane Joan was located near 50°W approaching the Caribbean Sea (see case study in Section 5).

Figures 2.46 and 2.47 are examples of currently available NOGAPS low- and high-level 24-hour **prognoses**. While the rather persistent easterly flow over much of the Caribbean sea is fairly well depicted by the 925 mb wind barb prognosis (Fig. 2.46), the "prog" missed the strong northerly flow (30 kt) south of the Gulf of Tehuantepec and the weak southerly wind on the western coast of Costa Rica⁴² (see Fig. 2.44). However, no defense will be attempted for the NOGAPS 200 mb tropical prognosis (Fig. 2.47). While depiction of the strong **extratropical** westerlies, from the Gulf of Mexico *northward*, is commendable, the NOGAPS 200 mb (Fig. 2.47) prognosis over Central America and the western Caribbean Sea is much too weak and often near 180° in disagreement with the *analyzed* wind direction. (While this upper-level *tropical* prognosis is poor, the new NOGAPS model 3.1, which became operational on March 15, 1989, should provide a better prognosis.)

Figure 2.48 shows the IR imagery at 1201 UTC on the following morning, while Fig. 2.49 is the first available visible imagery, i.e., two and one-half hours later. Much of the white (cold) imagery on the IR (Fig. 2.48) is seen to be cirrus, when the visible imagery of Fig. 2.49 is examined. Isolated convection still remains over Belize, the northeastern portion of Honduras and Nicaragua, the northern and southern Miskito Banks, the Columbia Basin (northeast of Panama), etc. Over the North Pacific Ocean, convection is evident both far offshore and just west of Costa Rica, where an early morning "land breeze", enhanced by the "downslope wind" from mountainous Costa Rica, has formed a line of thunderstorms in the offshore convergent air streams.

⁴²Despite, the agreement of this southerly flow depicted by both the ATOLL and FNOC **analyses**, it is possible that a northeasterly wind might be present over southern Costa Rica as an "outflow" from the convective precipitation over much of mountainous Costa Rica (see Fig. 2.42).

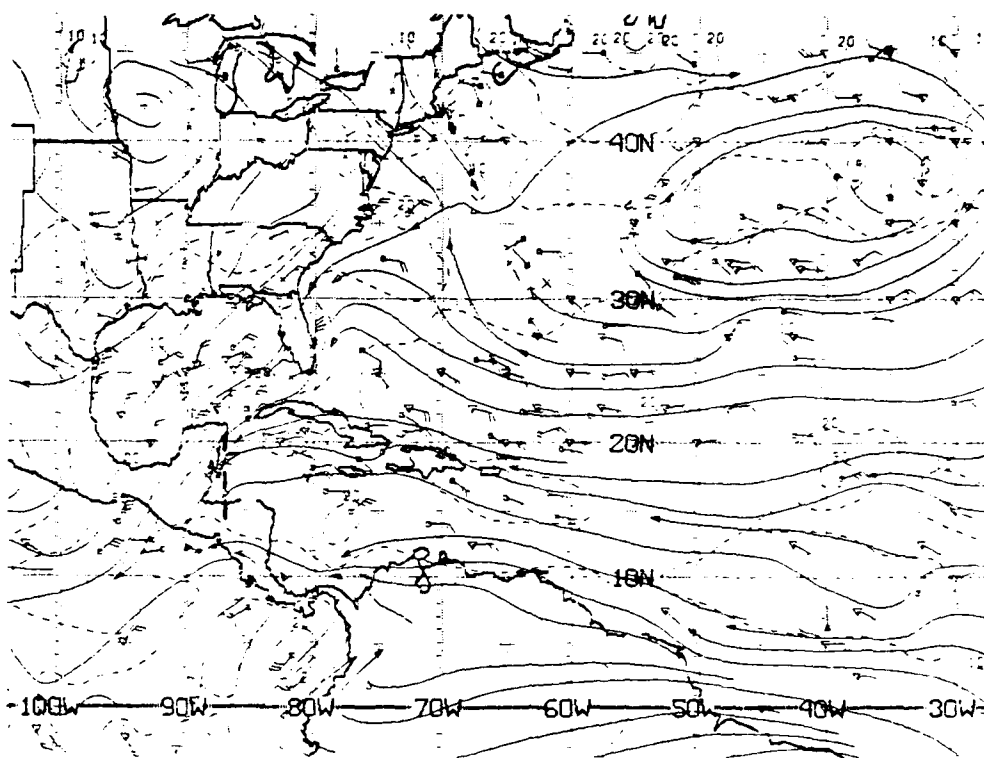


Figure 2.40: NMC ATOLL Operational Streamline Chart, 0000 UTC 7 OCT 1988
As in Fig. 2.4.

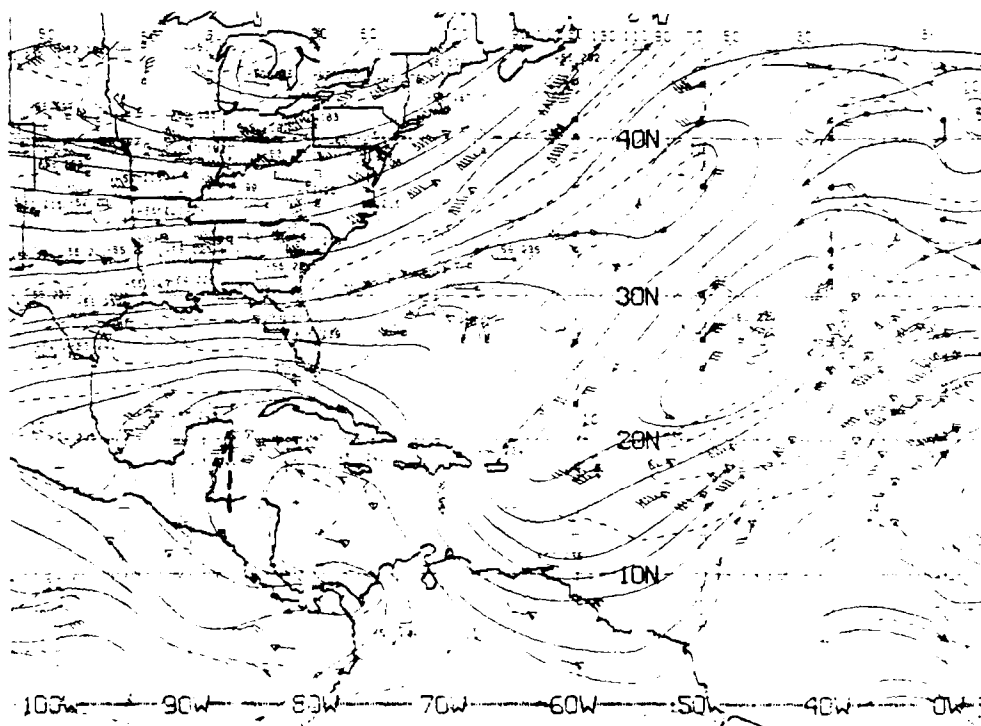


Figure 2.41: NMC 200 mb Operational Streamline Chart, 0000 UTC 7 OCT 1988
As in Fig. 2.6.

0001 070088 39E-42A 00911 15741 EC1

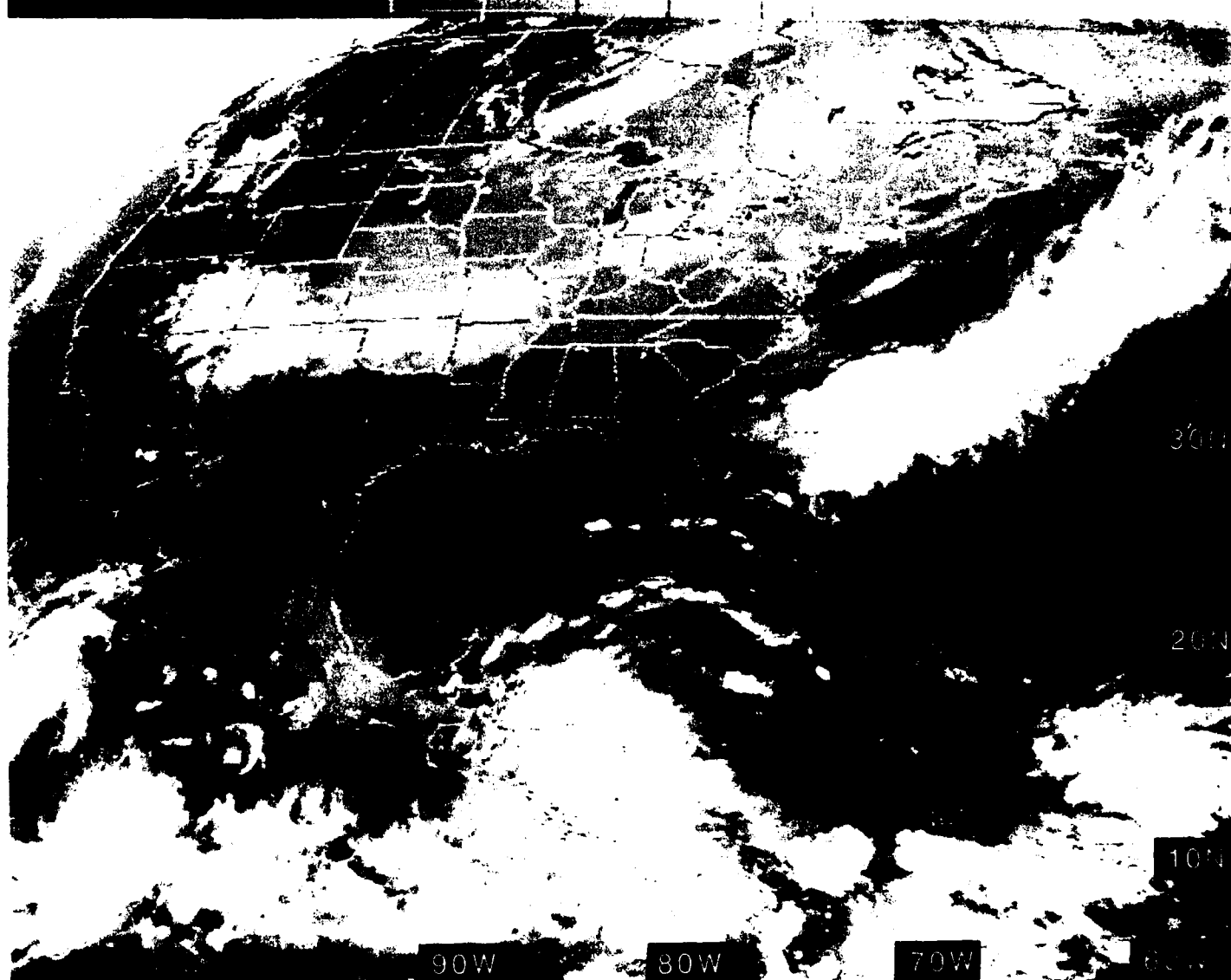


Figure 2.42: GOES East Infrared Satellite Imagery, 0001 UTC 7 OCT 1988

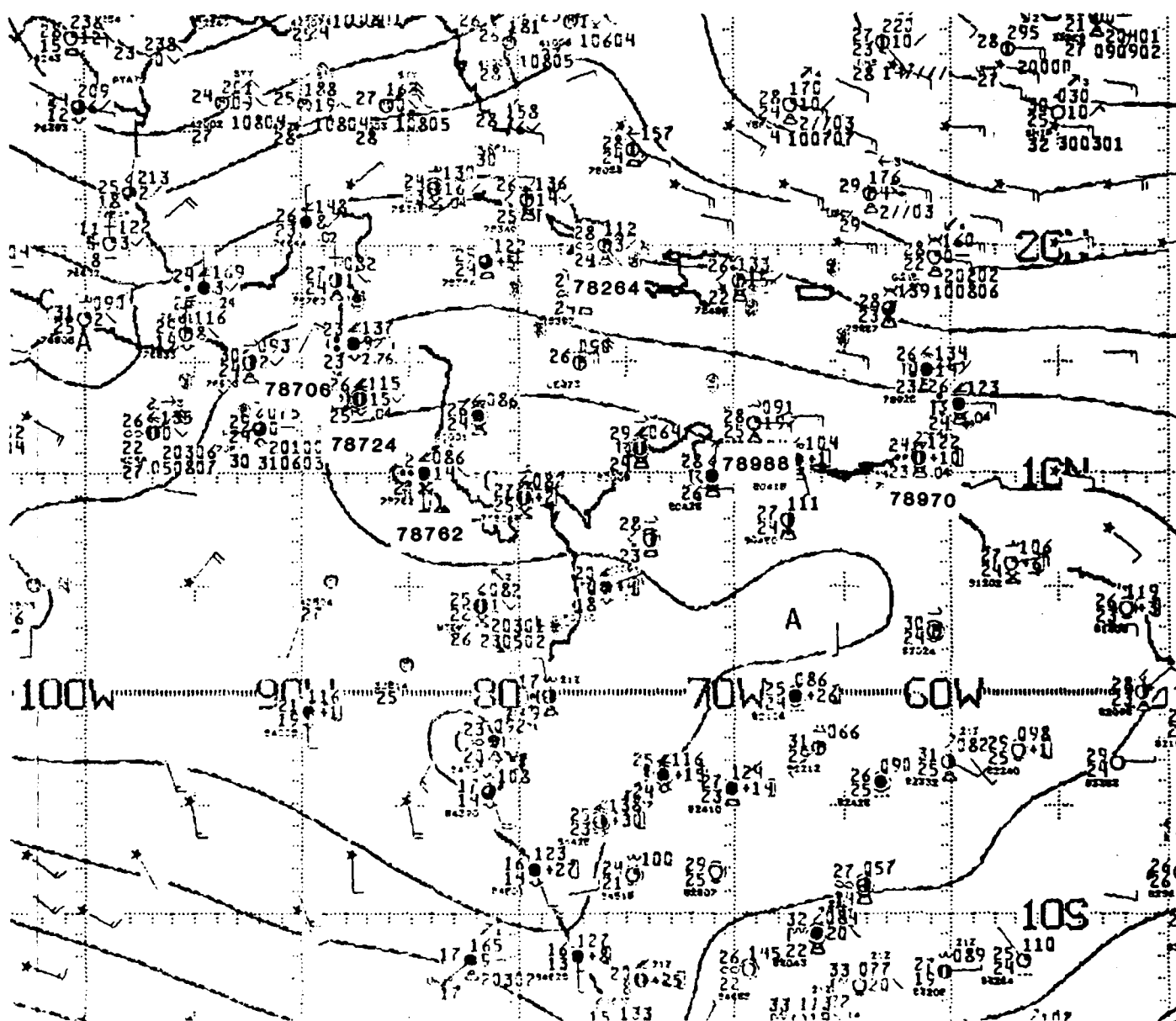


Figure 2.43: NMC 1000 mb Analysis, 0000 UTC 7 OCT 1988. As in Fig. 2.21.

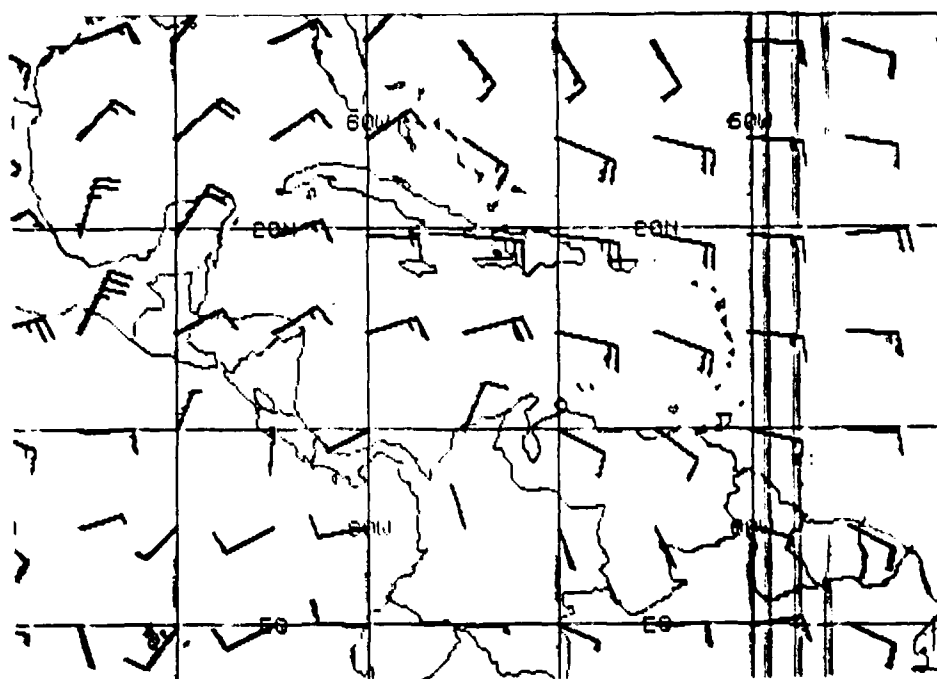


Figure 2.44: FNOc 925 mb Winds, 0000 UTC 7 OCT 1988. As in Fig. 2.19.

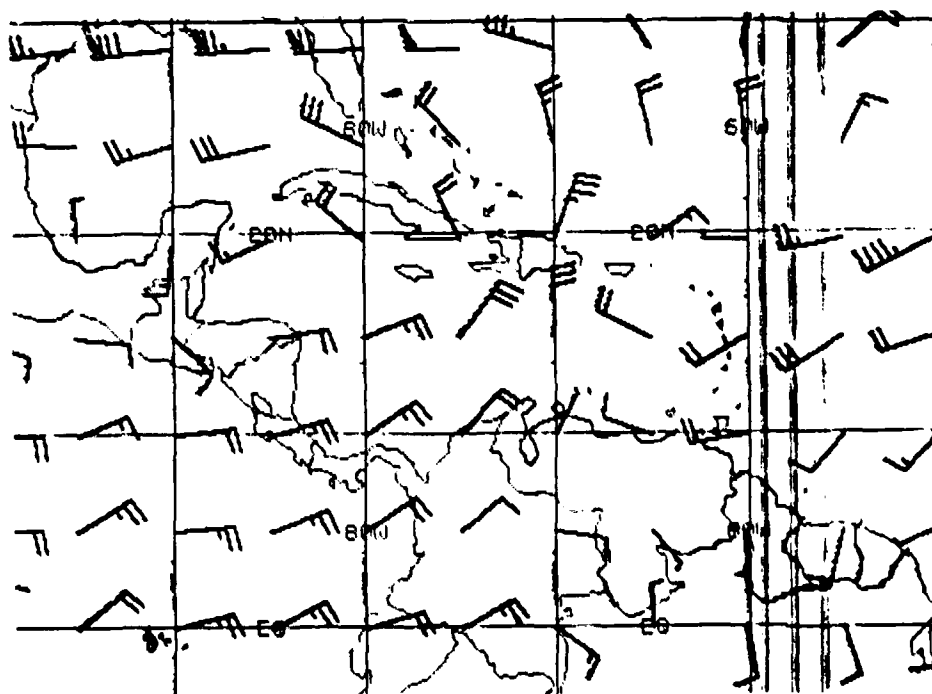


Figure 2.45: FNOc 200 mb Winds, 0000 UTC 7 OCT 1988. As in Fig. 2.20.

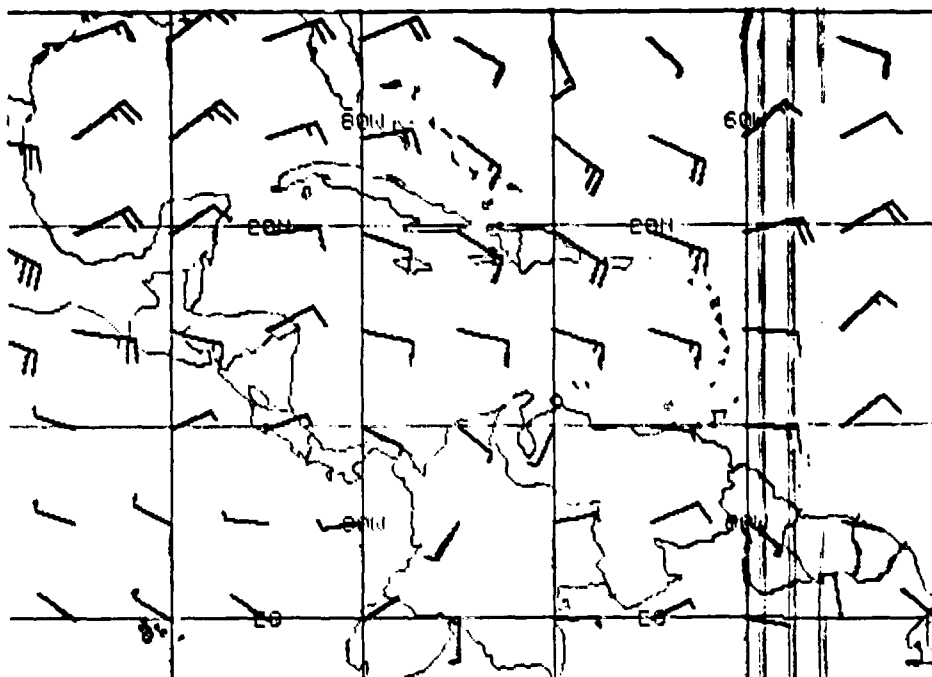


Figure 2.46: FNOC 925 mb Winds 24 HR PROG VT 0000 UTC 7 OCT 1988.
As in Fig. 2.19.

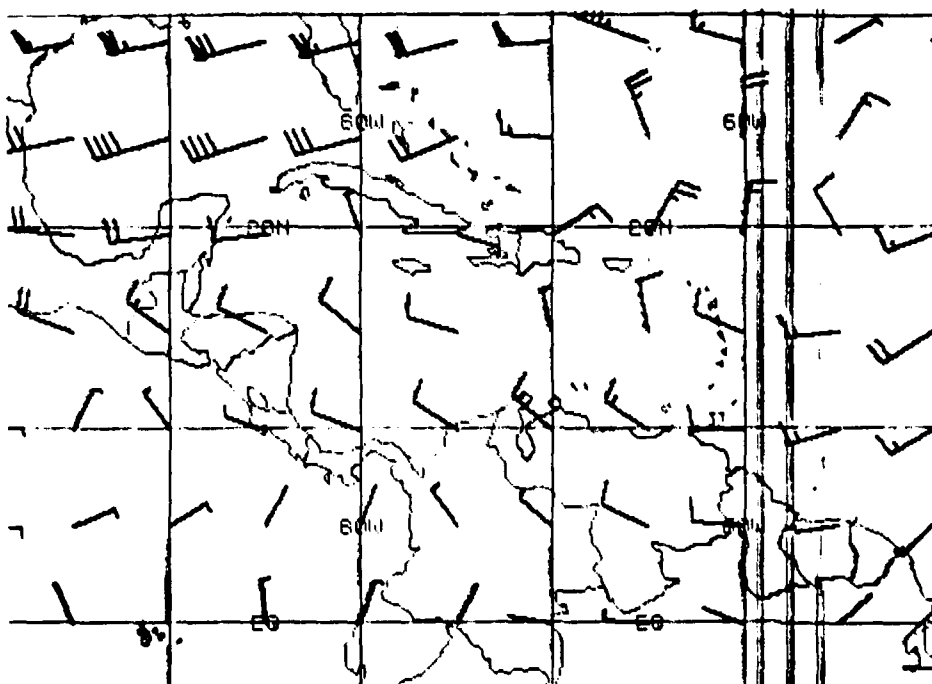


Figure 2.47: FNOC 200 mb Winds 24 HR PROG VT 0000 UTC 7 OCT 1988.
As in Fig. 2.20.

1201 070088 39E-42A 00912 15801 EC1

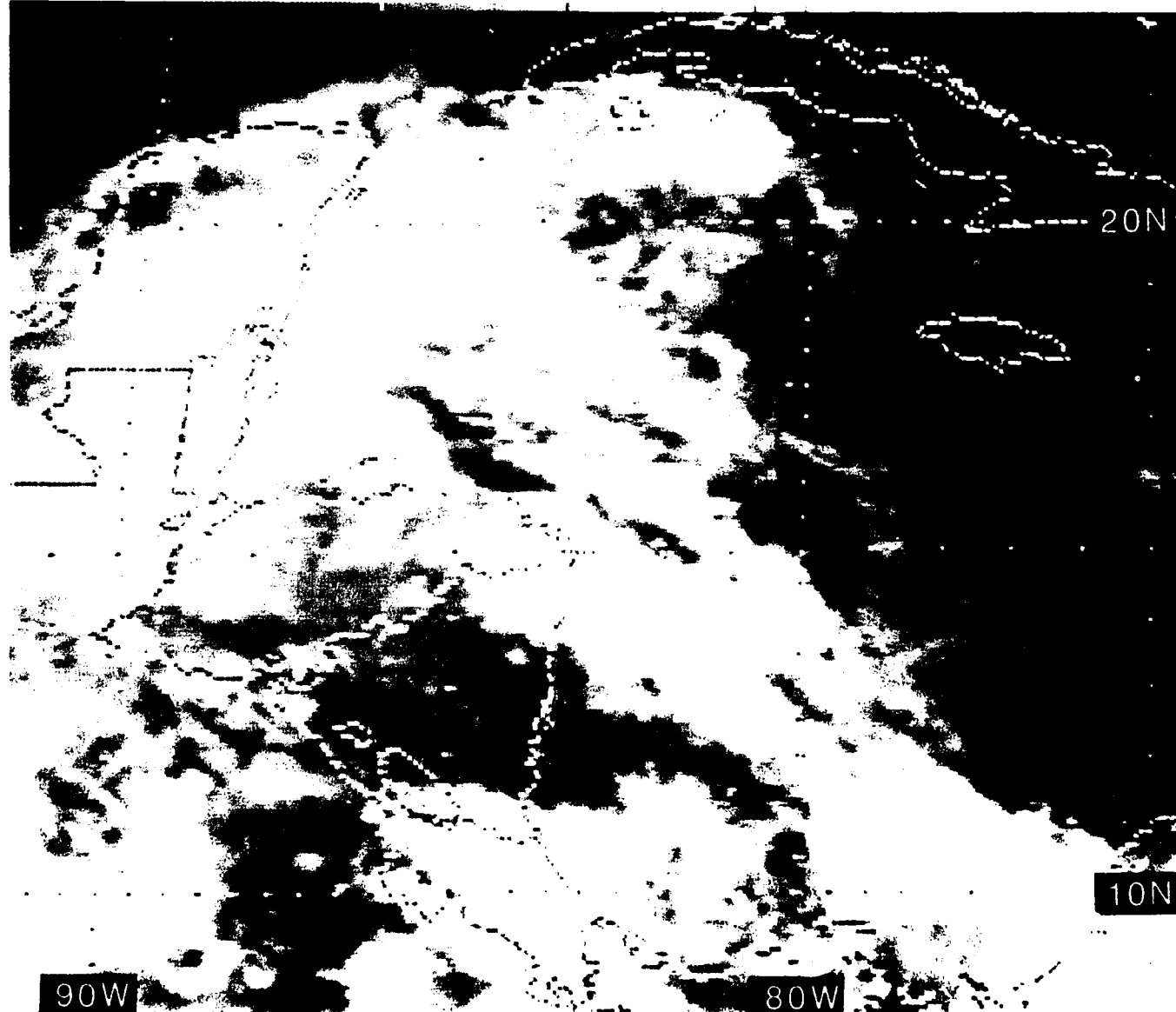


Figure 2.48: GOES East Infrared Satellite Imagery, 1201 UTC 7 OCT 1988

1431 070C88 39A-4 00902 15791 EC1

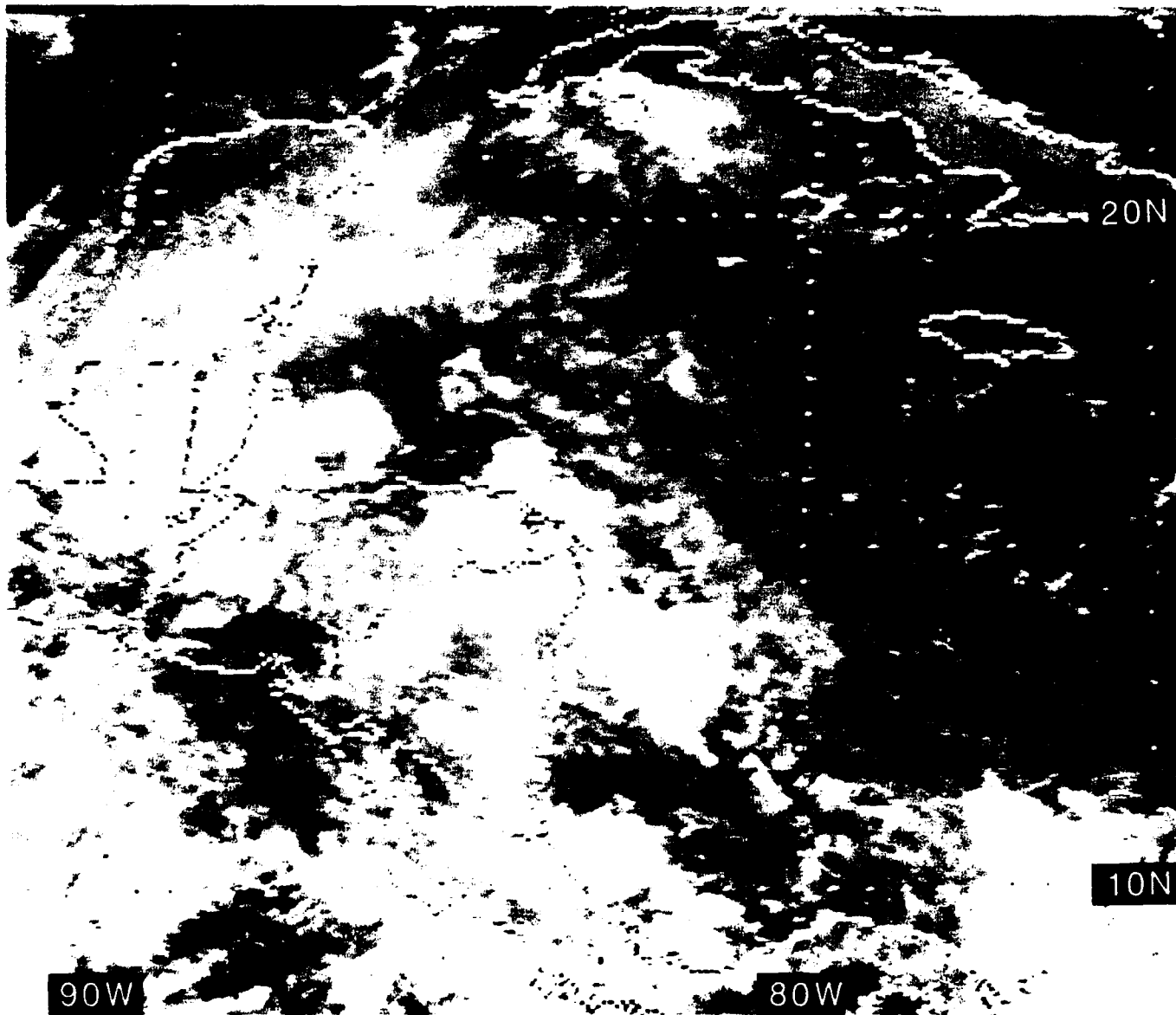


Figure 2.49: GOES East Visible Satellite Imagery, 1431 UTC 7 OCT 1988

2.3.2 Case II - Tropical Waves (1 – 6 August 1988)

1 August 1988

At 0000 UTC on 1 August 1988, the National Hurricane Center (NHC) surface analysis identifies a tropical wave extending from the Gulf of Honduras (near 16°N, 88°W) through western Cuba to Key West, Florida. The wave is located near the center of the cloudiness extending from the northwestern Caribbean Sea to southern Florida (see the imagery of Fig. 2.50). NHC analyzes another tropical wave in the eastern Caribbean Sea extending from northern Venezuela (10°N, 65°W) northeastward through 16°N, 60°W. This wave is associated with the cloudiness near the Windward Islands (see Fig. 2.50), where the majority of cloudiness is located to the *east* of the tropical wave axis—more typical of the *classic* tropical wave.

Tegucigalpa, Honduras had issued a Caribbean Area Forecast⁴³ predicting a tropical wave in the vicinity of the northern portion of Honduras/Nicaragua for 0000 UTC on 1 August. The Navy's FNOG 925 mb wind analysis (Fig. 2.51) weakly depicts the cyclonic curvature east of Belize and the Yucatan Peninsula associated with the western tropical wave identified by NHC, but does *not* locate the wave that NHC identifies near the Windward Islands.

Figures 2.52 and 2.53 present, respectively, the station observations and infrared imagery **12 hours later**. The "scattered" nature of the cloudiness over the northwestern Caribbean Sea and eastern Gulf of Mexico indicates the *current* weakness of the western tropical wave. (Much of the convective cloudiness near the northwestern Caribbean Sea in Fig. 2.50, attributed to diurnal heating, has dissipated by the time of Fig. 2.53, i.e., early morning in Central America (0601 LST)). Note the correlation of the station reports (Fig. 2.52) with the IR imagery of Fig. 2.53, i.e., showers during the past hour at Belize City, Belize (station 78583), a thunderstorm at Le Fé, Cuba (station 78321), no reports over Dominican Republic and only 1/4 sky cover at San Juan, Puerto Rico (station 78526) in the relatively clear region between the two tropical waves, but considerable cloudiness in the Windward Islands, including a rain shower at Crown Point Airport, Tobago (station 78962). Again, note that the poor resolution of this satellite imagery, 4 kilometers, does *not* depict the towering cumulus clouds reported in the scattered cloudiness at San Juan, Puerto Rico.

2 August 1988

Figure 2.54 presents the visible imagery, just 3 1/2 hours before 0000 UTC. Note the enhanced convection over the Yucatan Peninsula, western Cuba and the eastern Gulf of Mexico—near to (or to the east of) the most western tropical wave—while eastern Cuba and Hispaniola remain relatively clear. Nevertheless, the operational forecaster cannot ignore the heavy convection depicted over central Nicaragua and eastern Honduras resulting from the combined effects of the sea breeze, elevated terrain to the west and diurnal

⁴³Available via the MANOP message heading "FACA MHTG".

heating. Present also in Fig. 2.54 is the convection over the warm shallow water over the Mosquito Banks, as well as a line of thunderstorms in western Panama along the ridges of the Serranía de Tabasará mountains (see Fig. 1.21).

The GOES EAST IR imagery at 0001 UTC on 2 August (Fig. 2.55) depicts upper-level cloudiness in the Caribbean Sea south of Hispaniola, but the more intense convective cells are identified just east of the Windward Islands—this will be identified as a “new” tropical wave on 3 August by NHC—, as well as the diurnal thunderstorms over land mass areas (northern Venezuela, the Panama Canal, the Yucatan Peninsula, Honduras and Nicaragua). At this time, the NHC surface analysis identifies three tropical waves (see Fig. 2.56): (1) near the center of the Gulf of Mexico extending southward to *just* west of the Yucatan Peninsula (having moved at ~ 16 kt, since 0000 UTC on 1 August), (2) near the center of Hispaniola extending southward to $\sim 73^\circ\text{W}$ just off the coast of Venezuela (having moved at ~ 20 kt, since 0000 UTC on 1 August) and (3) far to the east in the North Atlantic Ocean near 38°W . Thus, while the NHC tropical waves (1) and (2) are supported by the satellite imagery, NHC had not *yet* identified the intense convection *just* east of the Windward Islands, near 60°W . The NMC automated streamlines do not support the position of the most western NHC tropical wave—i.e., the streamlines have anticyclonic curvature at the tropical wave position near 81°W in Fig. 2.56; however, the FNOC wind analyses (Fig. 2.58) does infer cyclonic curvature just west of the Yucatan Peninsula. The NMC and FNOC low-level analyses indicate slightly stronger winds “trailing” the tropical wave located just south of Hispaniola by NHC. The ATOLL analysis identifies a cyclonic vortex near 10°N , 33°W in the vicinity of the NHC tropical wave identified in the eastern Atlantic Ocean; however, there is disagreement between NHC and FNOC on low-level flow in the Gulf of Panama.

The NMC 200 mb (Fig. 2.57) streamlines show a positive point (high center) near western Cuba, supporting the convective cloudiness (and associated increased thickness in the upper troposphere). However, both the NMC (Fig. 2.57) and the FNOC (Fig. 2.59) 200 mb analyses depict a **mid-latitude trough**⁴⁴ near 65°W extending across Puerto Rico southward into the eastern Caribbean Sea. The existence of this (upper-level) **cyclonic flow** at the location where a typical tropical wave would have strong **anticyclonic flow** may explain the lack of intense convection noted in the satellite imagery south of Hispaniola (see Fig. 2.54). (Note that the west-northwest wind near 20°N , 85°W on the FNOC 200 mb analysis is in disagreement with the NMC 200 mb streamlines which have the support of numerous satellite-derived winds.)

The 0000 UTC station reports of 2 August (Fig. 2.60) continue to show good agreement with the simultaneous satellite imagery (Fig. 2.55), i.e., a thunderstorm at Howard Air Force Base, Panama (station 78806), rain with 3/4 sky cover and towering cumulus clouds near the Gulf of Fonseca at Choluteca, Honduras (station 78724), heavy (“four-dot”) rain at Tapachula, Mexico (station 76903) adjacent to the southwest tip of Guatemala, while

⁴⁴This trough is **not** the Tropical Tropospheric Upper Trough (TUTT) which extends from the eastern Atlantic Ocean southwestward through northern Hispaniola and then westward to the Yucatan Peninsula during August (see Fig. 1.5).

only 3/8 cloud cover exists at Belize City, Belize (station 78583) and at Kingston, Jamaica (station 78397).

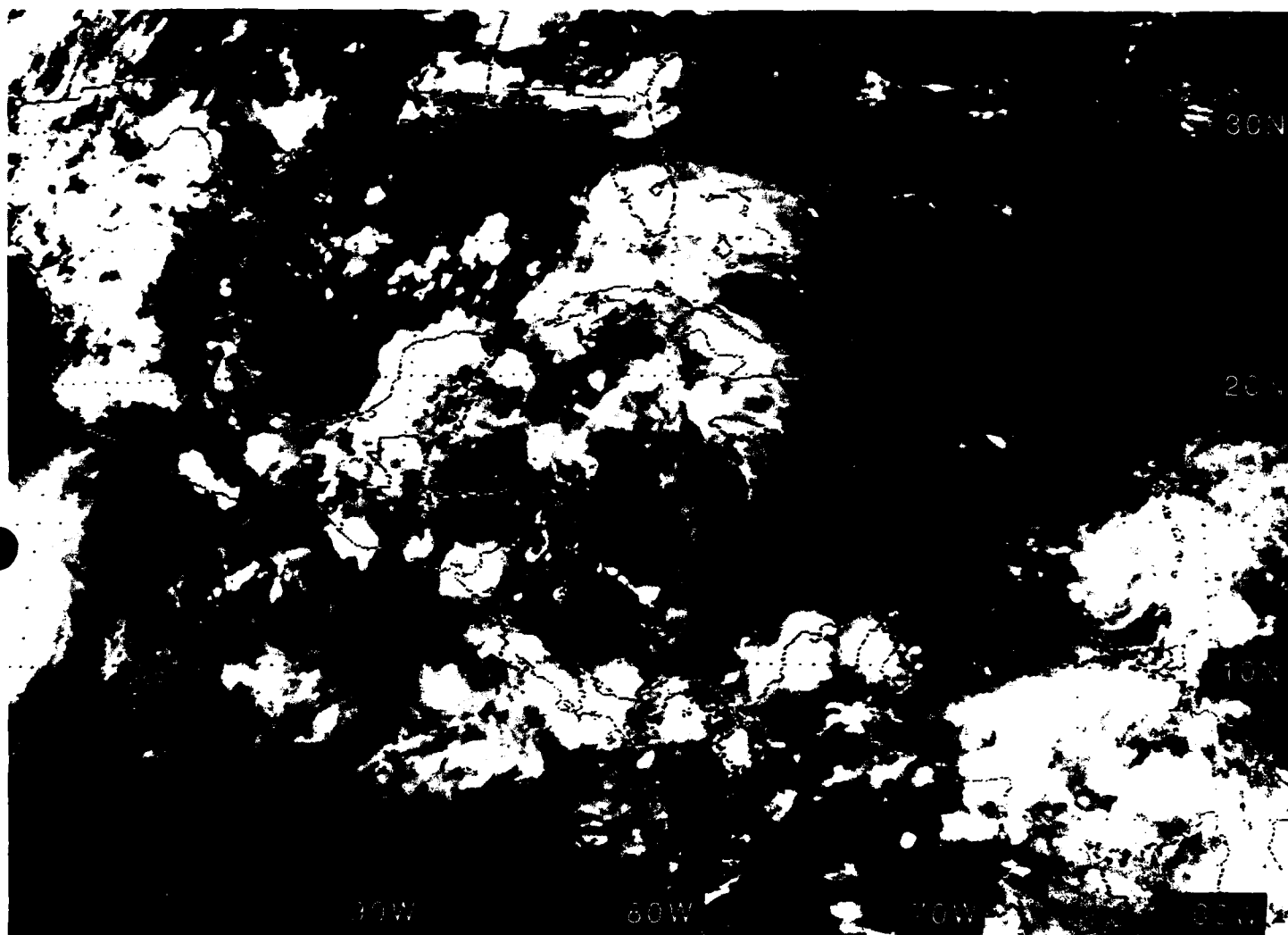


Figure 2.50: GOES East Infrared Satellite Imagery, 0001 UTC 1 AUG 1988

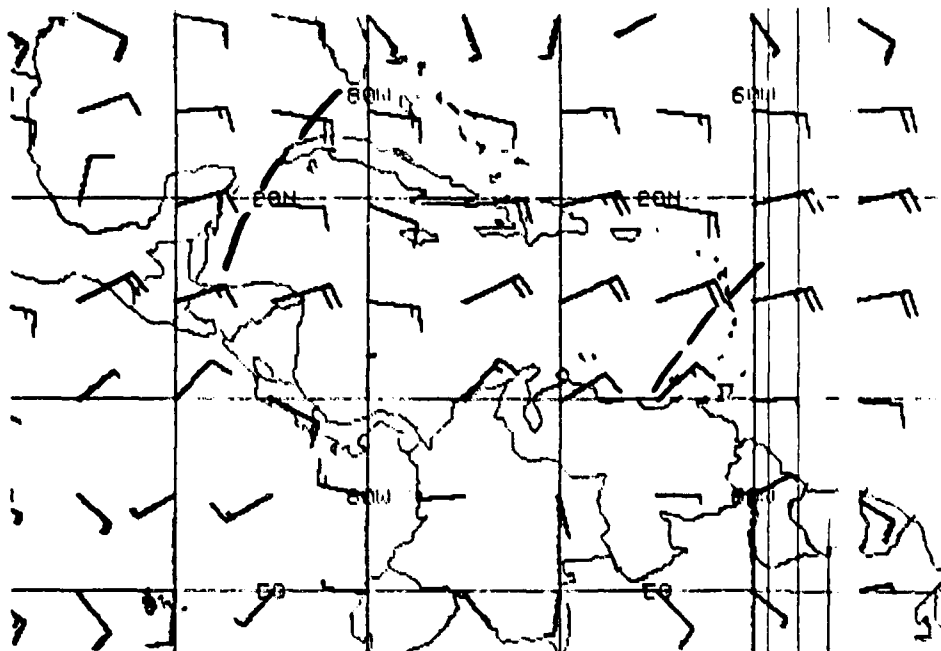


Figure 2.51: FNOG 925 mb Winds, 0000 UTC 1 AUG 1988.
Each barb represents 10 kt. Dashed lines indicate NHC tropical waves.

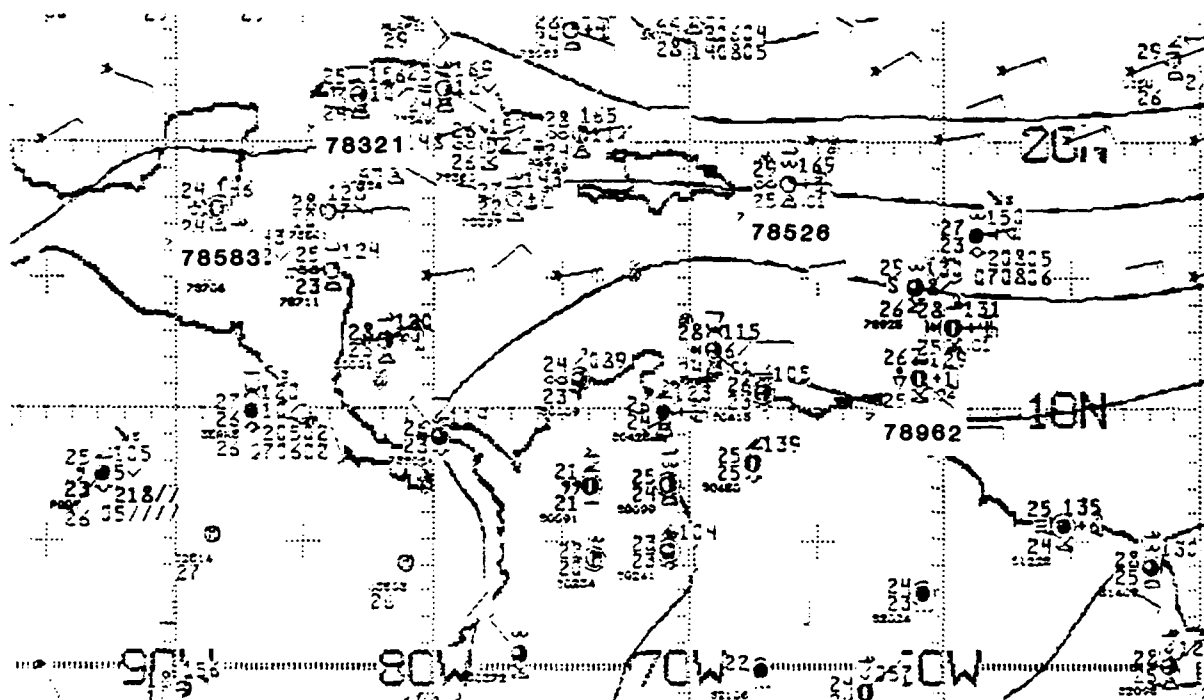


Figure 2.52: NMC 1000 mb Analysis, 1200 UTC 1 AUG 1988.
Contours are unlabeled stream functions from optimum interpolation analysis,
with C identifying cyclonic centers and A identifying anticyclonic centers.

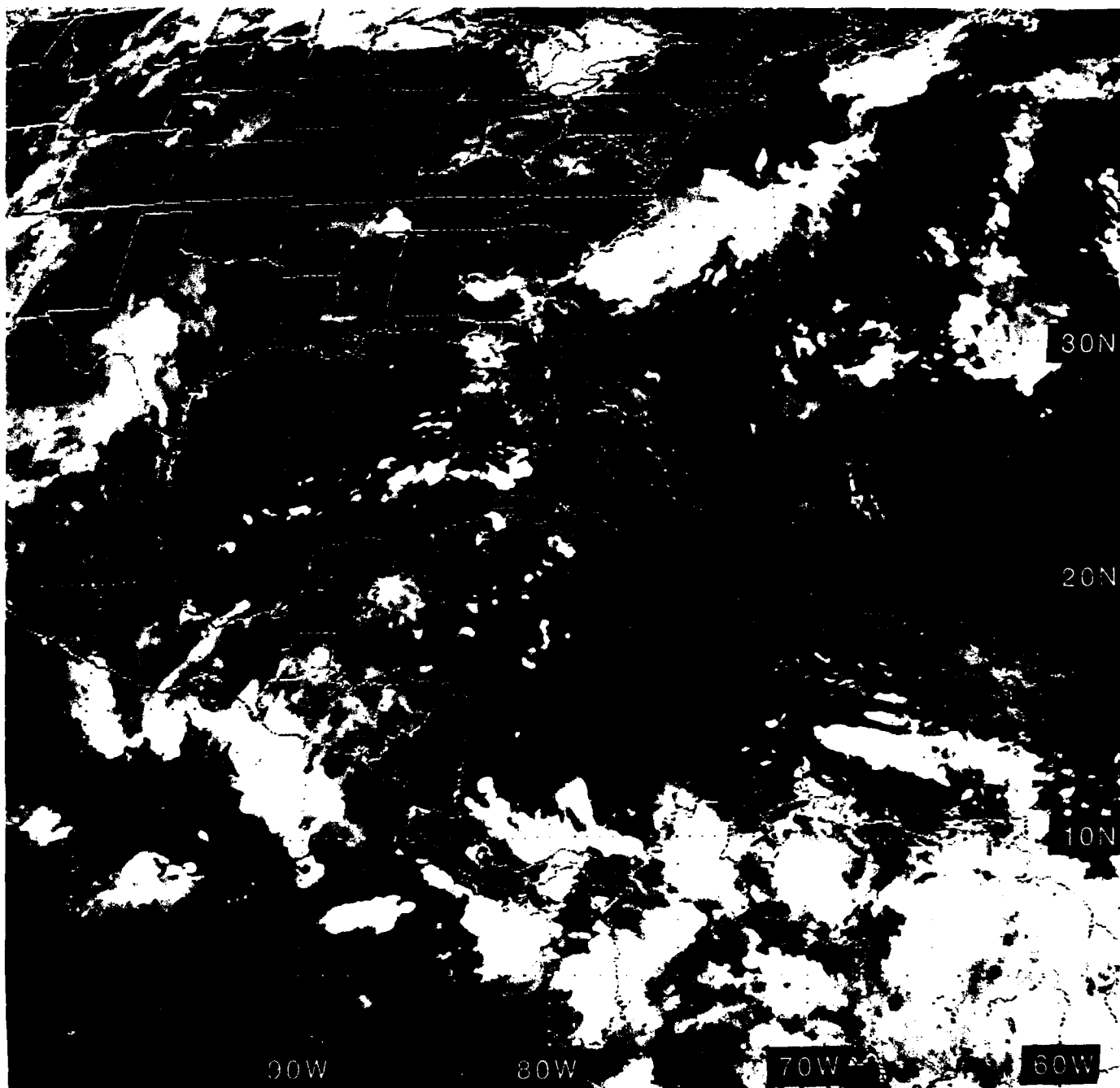


Figure 2.53: GOES East Infrared Satellite Imagery, 1201 UTC 1 AUG 1988

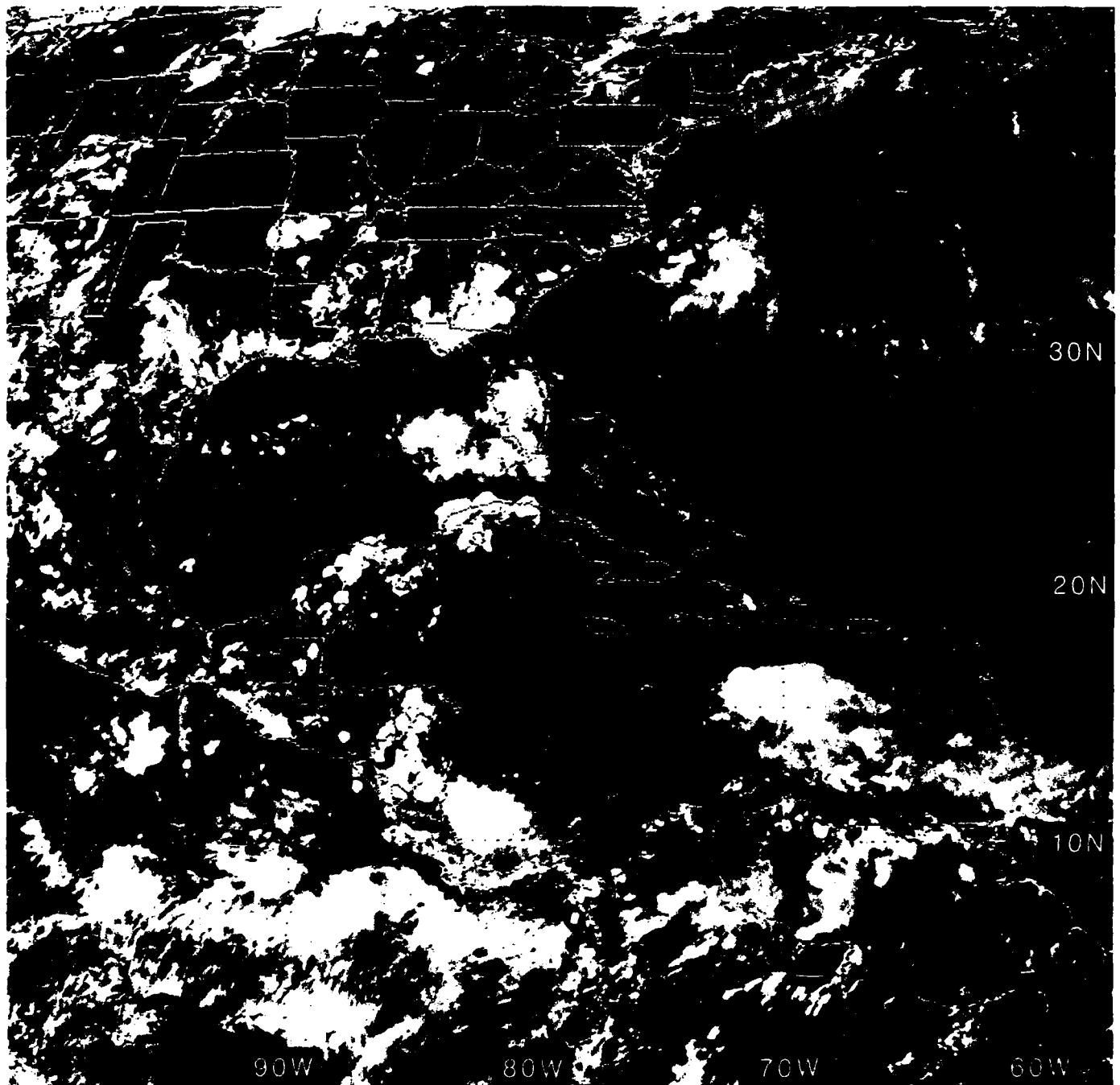


Figure 2.54: GOES East Visible Satellite Imagery, 2031 UTC 1 AUG 1988

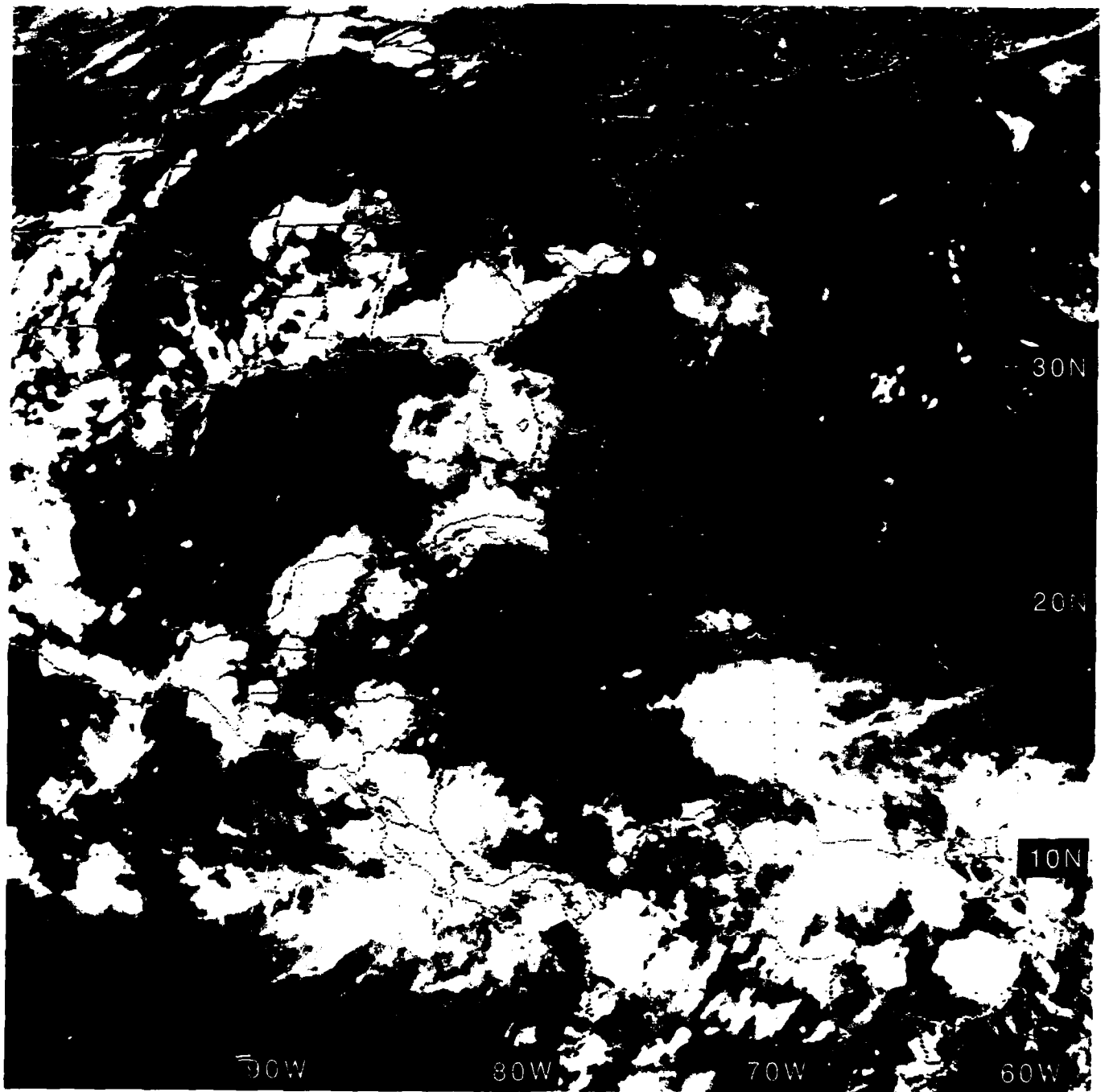


Figure 2.55: GOES East Infrared Satellite Imagery, 0001 UTC 2 AUG 1988

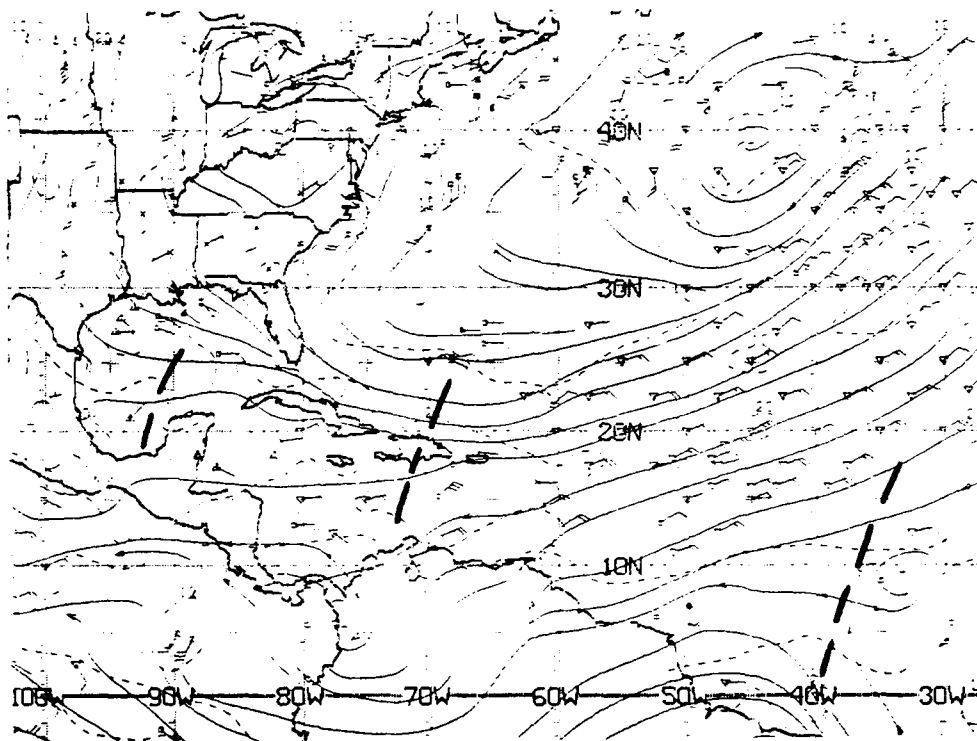


Figure 2.56: NMC ATOLL Operational Streamline Chart, 0000 UTC 2 AUG 1988
As in Fig. 2.4.

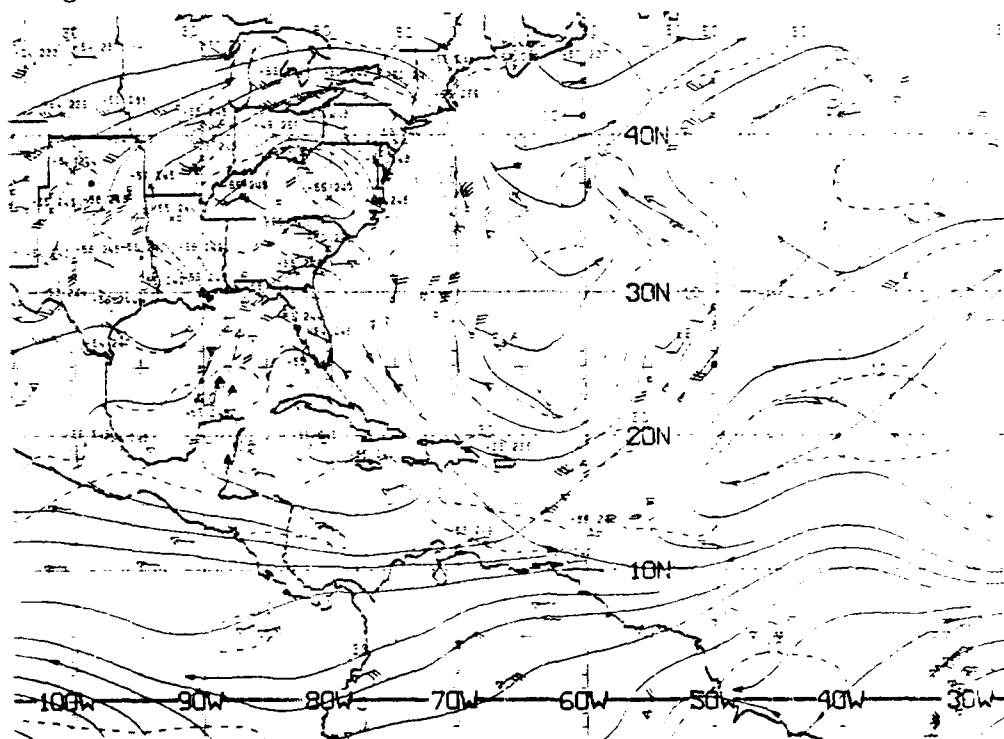


Figure 2.57: NMC 200 mb Operational Streamline Chart, 0000 UTC 2 AUG 1988
As in Fig. 2.6.

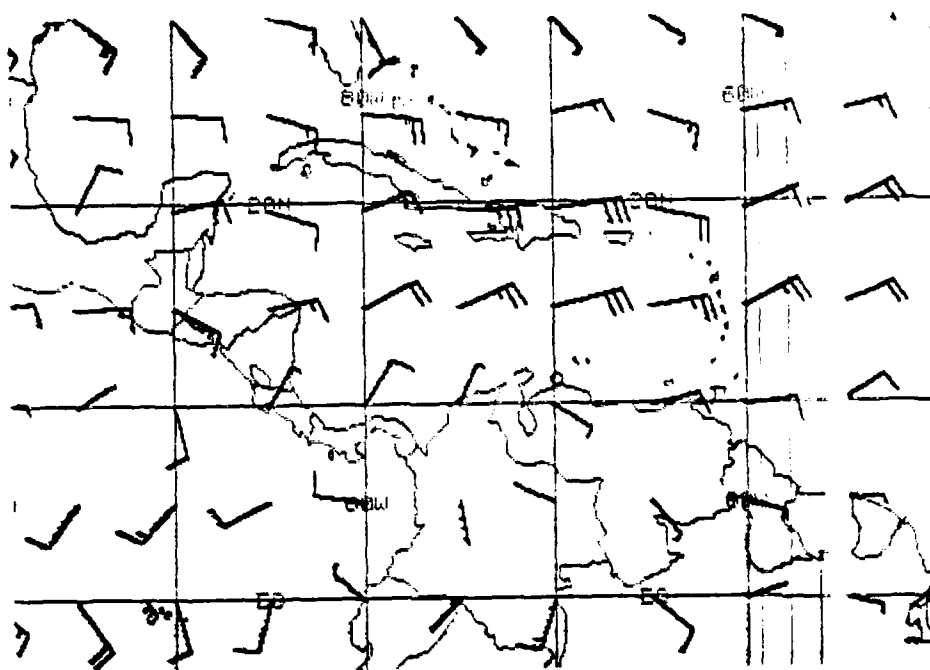


Figure 2.58: FNO 925 mb Winds, 0000 UTC 2 AUG 1988.

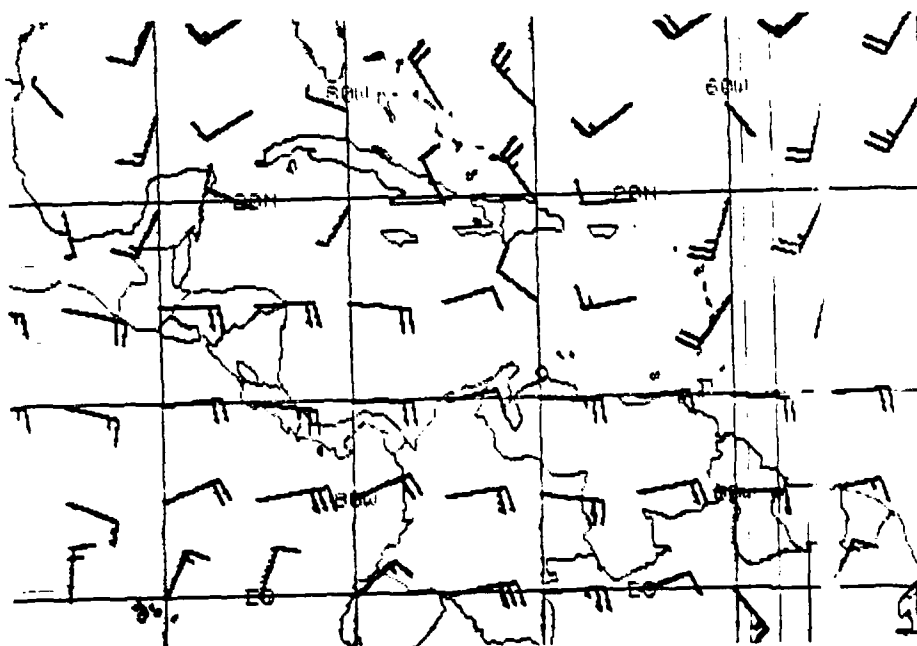


Figure 2.59: FNO 200 mb Winds, 0000 UTC 2 AUG 1988.

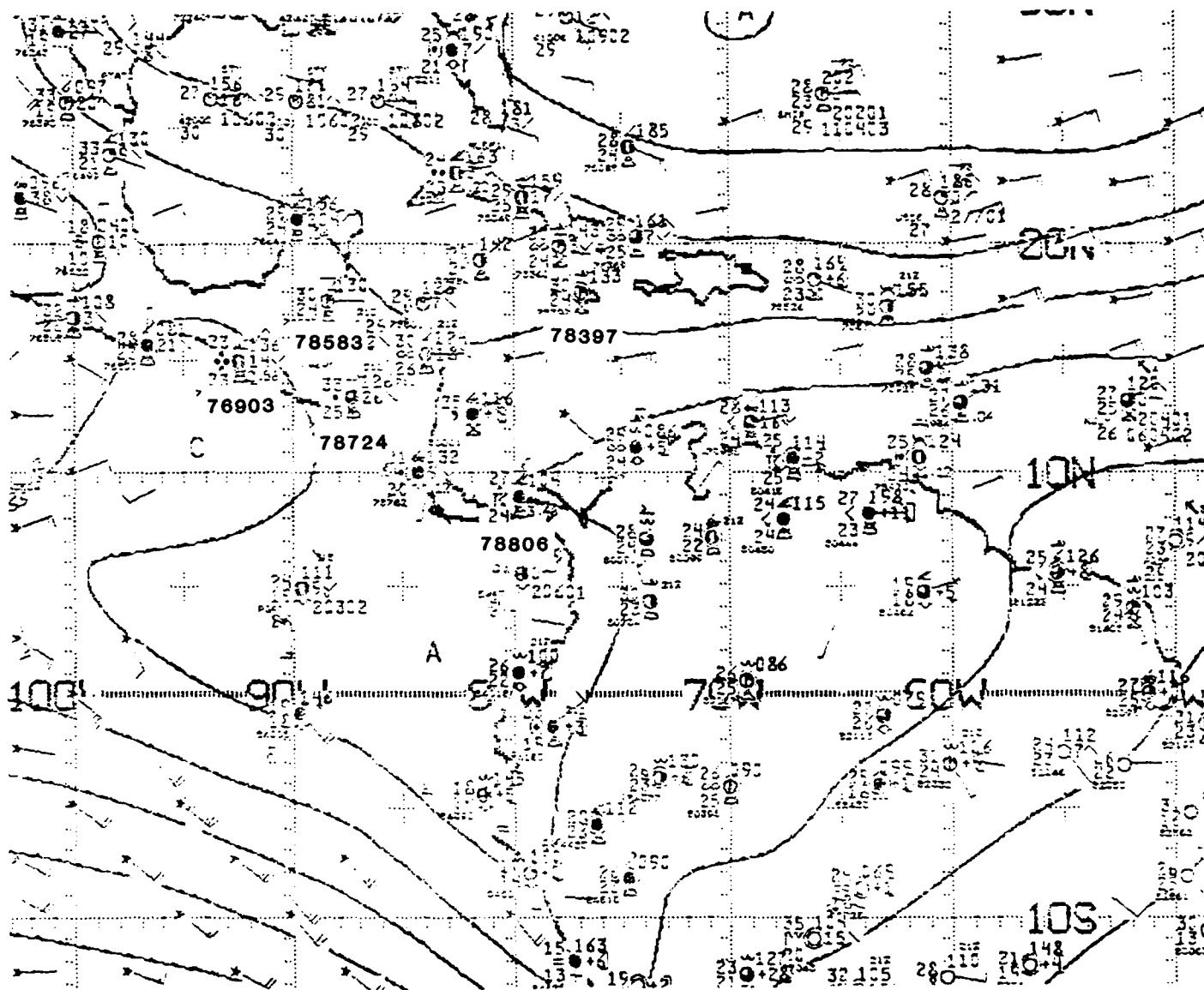


Figure 2.60: NMC 1000 mb Analysis, 0000 UTC 2 AUG 1988.

Contours are unlabeled stream functions from optimum interpolation analysis, with C identifying cyclonic centers and A identifying anticyclonic centers.

3 August 1988

The NHC surface analysis now depicts two tropical waves in the Caribbean Sea (see Fig. 2.61), i.e., one near 81°W (having moved rapidly⁴⁵ at ~20 kt from its position near Hispaniola on 2 August), a **new** one near 62°W—recall the intense convection depicted on the IR imagery on 2 August just *east* of the Windward Islands on Fig. 2.55—, plus another tropical wave far to the east in the Atlantic Ocean, now near 40°W (having moved slowly at 10 kt).

The GOES EAST IR satellite imagery (Fig. 2.64) at 0001 UTC on 3 August shows extensive convection extending from the northeastern tip of Nicaragua to Jamaica supporting the western tropical wave, i.e., the cloudiness associated with this tropical wave is **both** ahead and behind the wave axis. Additionally, Fig. 2.64 depicts convection in the northern Windward Islands, in support of the wave near 62°W. As usual, the forecaster must anticipate the diurnal afternoon and evening convection over land mass regions of northern South America, as well as the Panama Canal, central Nicaragua, eastern Honduras, northern Guatemala and the Yucatan Peninsula—all this convection is generally independent of tropical waves. (Figure 2.63 provides the visible imagery, 3 1/2 hours before the IR imagery, permitting an appreciation of the evolution from the initial cells (*mid afternoon*) to the larger cirrus (or cumulonimbus “blow-off”) canopies (*early evening*) depicted on the IR imagery by 0001 UTC in Fig. 2.64.)

From about 20°N southward, the NMC ATOLL analysis (Fig. 2.61) and the FNOC 925 mb wind analysis (Fig. 2.65), show cyclonic flow near 81°W in support of the NHC wave position. While neither of the low-level flow analyses depicts the cyclonic flow of the “new” tropical wave near 63°W, east of 60°W the ATOLL analysis shows slightly stronger winds near 20°N than at 15°N indicating **cyclonic** shear vorticity to the *east* of the tropical wave axis.

The NMC 200 mb analysis (Fig. 2.62) strongly supports the convection near (and to the east of both tropical wave axes) with streamline positive points (high centers) located near 14°N, 79°W and 17°N, 53°W. Additionally the NMC upper-level streamlines (Fig. 2.62) particularly depicts diffuence to the south of Jamaica. While the FNOC wind analysis (Fig. 2.66) depicts anticyclonic gyres in the same general positions, they appear smaller and are more difficult to visualize.

An examination of the station observations (Fig. 2.67) indicates the diurnal land mass convection: rain at Merida, Mexico (station 76644), a recent shower at Belize City, Belize (station 78583), a thunderstorm at Tela, Honduras (station 78706), “two-dot” rain at San José, Costa Rica (station 78762) and lightning at Howard AFB, Panama (station 78806). Convection associated with the tropical wave near the Windward Islands is verified by a shower reported at Lamentin, Martinique (station 78925) and 3/4 sky cover at Bridgetown, Barbados (station 78954), while the convection associated with the wave in the western

⁴⁵This study examines only the 0000 UTC positions of NHC tropical waves. Since NHC performs a surface pressure analysis every 6 hours, it is possible that the previous (6-hourly) positions of tropical waves are adjusted (or “relocated”, following the inclusion of additional or later data) making the estimated speeds of advance of the tropical waves in these case studies *first-iteration* estimates.

Caribbean Sea (between eastern Honduras and Jamaica) is mostly over water and ship reports are missing.

4 August 1988

24 hours later at 0000 UTC on 4 August 1988, Fig. 2.68 shows the positions of three NHC-analyzed tropical waves. One over the Yucatan Peninsula (moving at ~ 20 kt), one in the central part of the Caribbean Sea near 70°W (moving at ~ 20 kt) and another wave over the North Atlantic Ocean near 45°W (moving at ~ 15 kt). The Tegucigalpa "area forecast" calls for a tropical wave in the western portion of Honduras at 0000 UTC on 4 August, and the 2201 UTC 3 August IR imagery (Fig. 2.70) (two hours before 0000 UTC 4 August) shows intense convection in southwestern Honduras. While the analyses give questionable support for locating the western tropical wave, both NMC (Fig. 2.68) and FNOC (Fig. 2.71) analyses show cyclonic low-level flow in the vicinity of the tropical wave near Hispaniola.

Aloft at 200 mb, both the NMC (Fig. 2.69) and the FNOC (Fig. 2.72) analyses show supportive anticyclonic flow over the convection east of the two tropical waves affecting the Caribbean, i.e., centered near 18°N , 88°W and east of Puerto Rico. Again, as on 2 August, the upper-level mid-latitude trough lying over Jamaica (see Fig. 2.69) can be associated with the relative clearness in the middle of the Caribbean Sea, especially to the west of the mid-latitude trough (see Fig. 2.70). (However, about 14 hours later, Fig. 2.74 depicts convection south of Jamaica, which has been enhanced by the diffluence to the east of the upper-level trough—starting at the apex of the cloudiness near 14°N , 78°W , the widening wedge (toward the northeast) outlines the upper-level diffluent flow.)

Again, to emphasize the cloudiness associated with the tropical waves (as well as with the Central American land mass), a few of the reporting stations will be cited. Figure 2.73 (*just* two hours after the imagery of Fig. 2.70) displays the following station observations: drizzle at Merida Mexico (station 76644), a thunderstorm near the Gulf of Fonseca at Choluteca, Honduras (station 78724) and precipitation within sight at San José, Costa Rica (station 78762). To the east, San Juan, Puerto Rico (station 78526) is reporting a shower within the past hour; however, Lamentin, Martinique (station 78925), which had reported a shower under 7/8 sky cover 24 hours earlier, is now reporting only 3/8 sky cover.

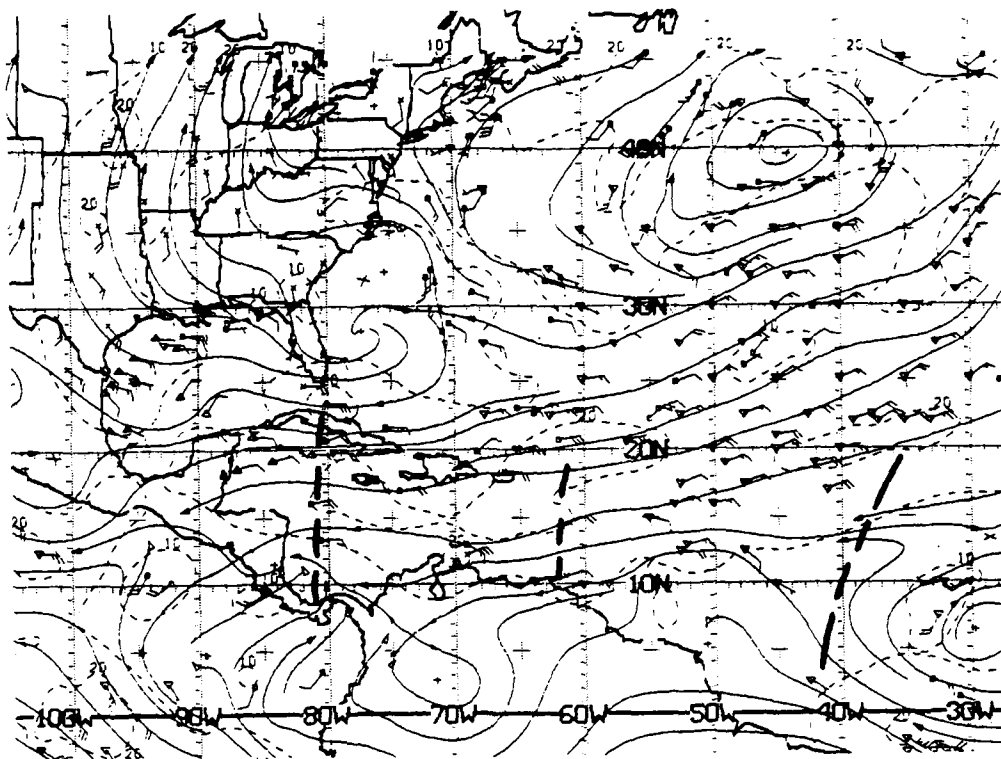


Figure 2.61: NMC ATOLL Operational Streamline Chart, 0000 UTC 3 AUG 1988
As in Fig. 2.4.

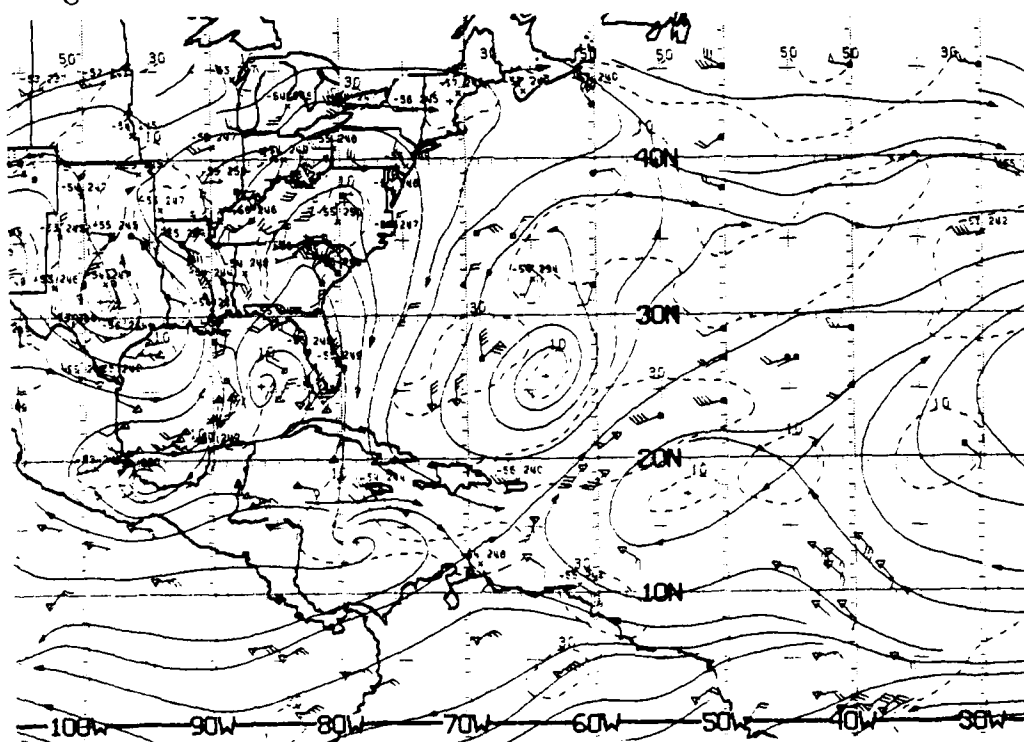


Figure 2.62: NMC 200 mb Operational Streamline Chart, 0000 UTC 3 AUG 1988
As in Fig. 2.6.

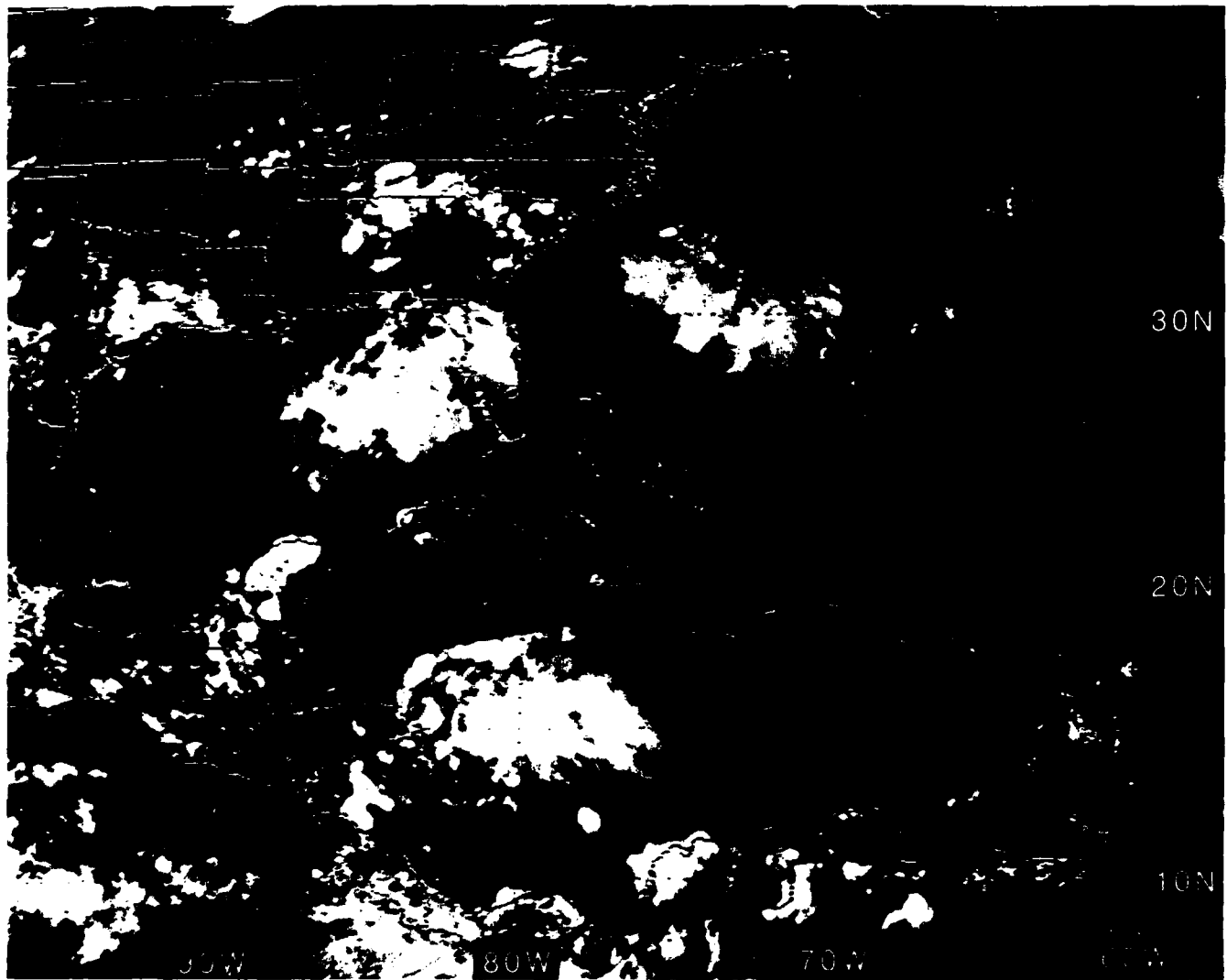


Figure 2.63: GOES East Visible Satellite Imagery, 2031 UTC 2 AUG 1988

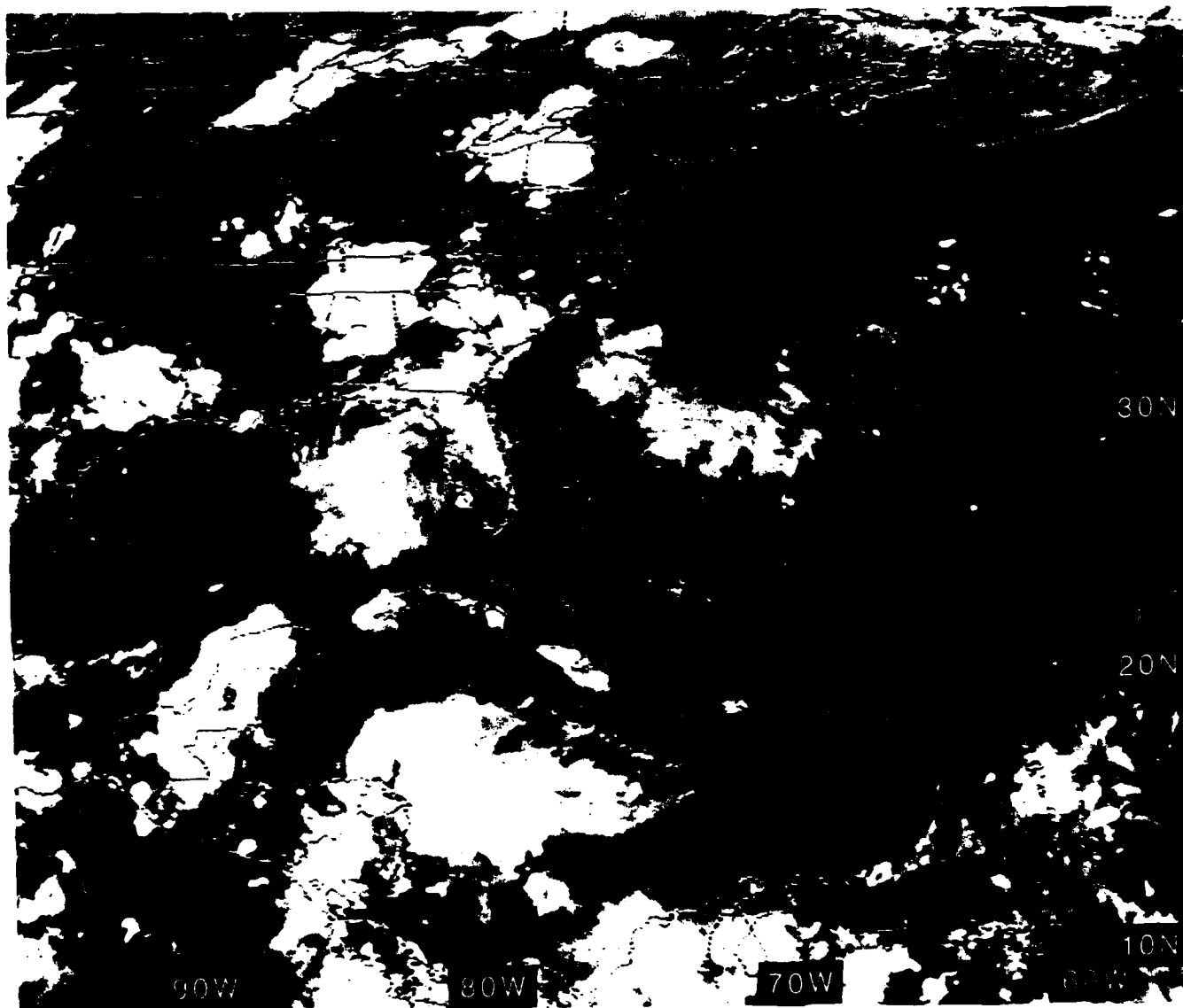


Figure 2.64: GOES East Infrared Satellite Imagery, 0001 UTC 3 AUG 1988

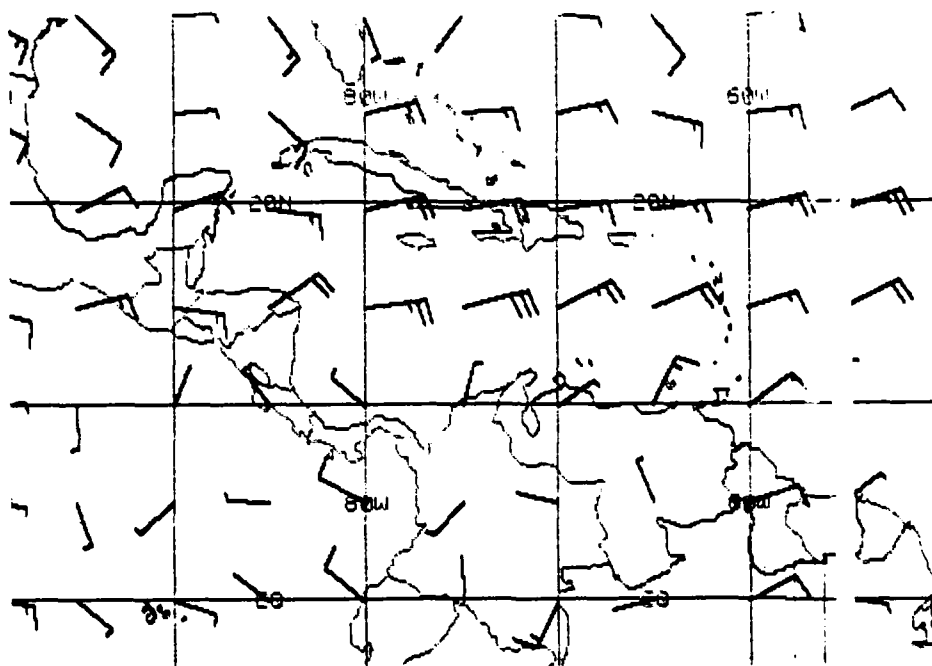


Figure 2.65: FNOc 925 mb Winds, 0000 UTC 3 AUG 1988.

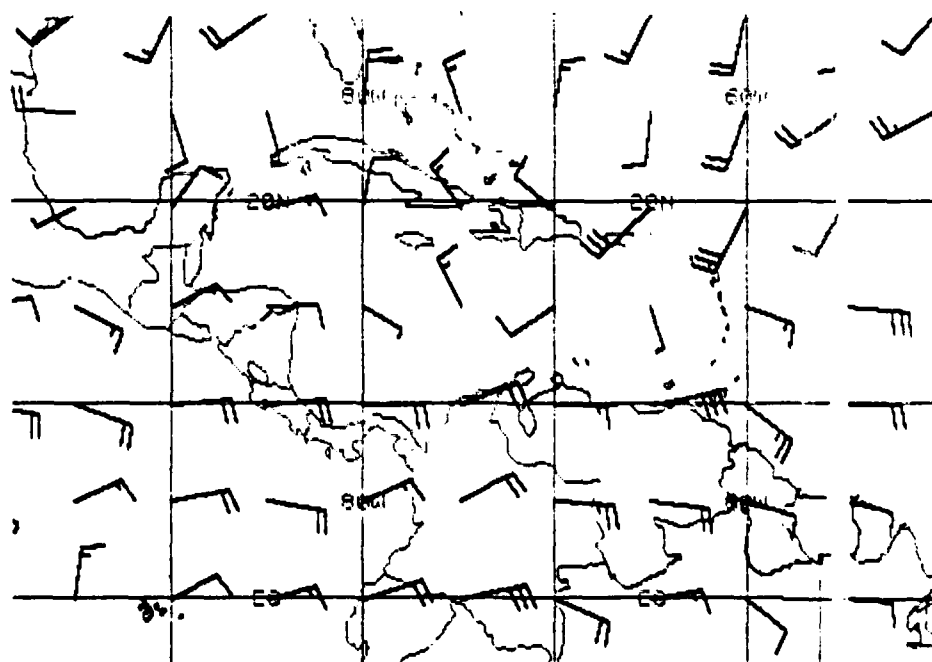
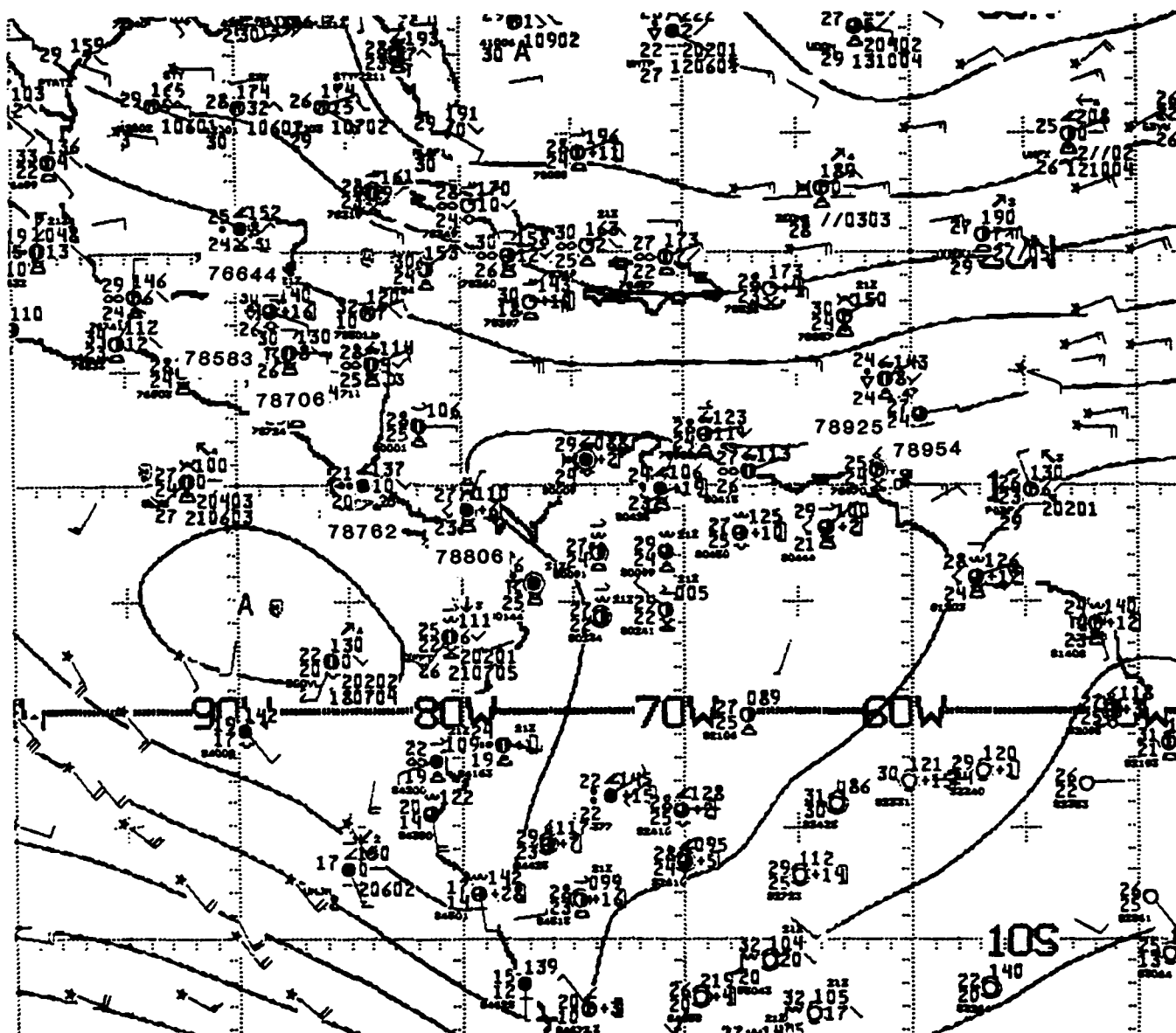


Figure 2.66: FNOc 200 mb Winds, 0000 UTC 3 AUG 1988.



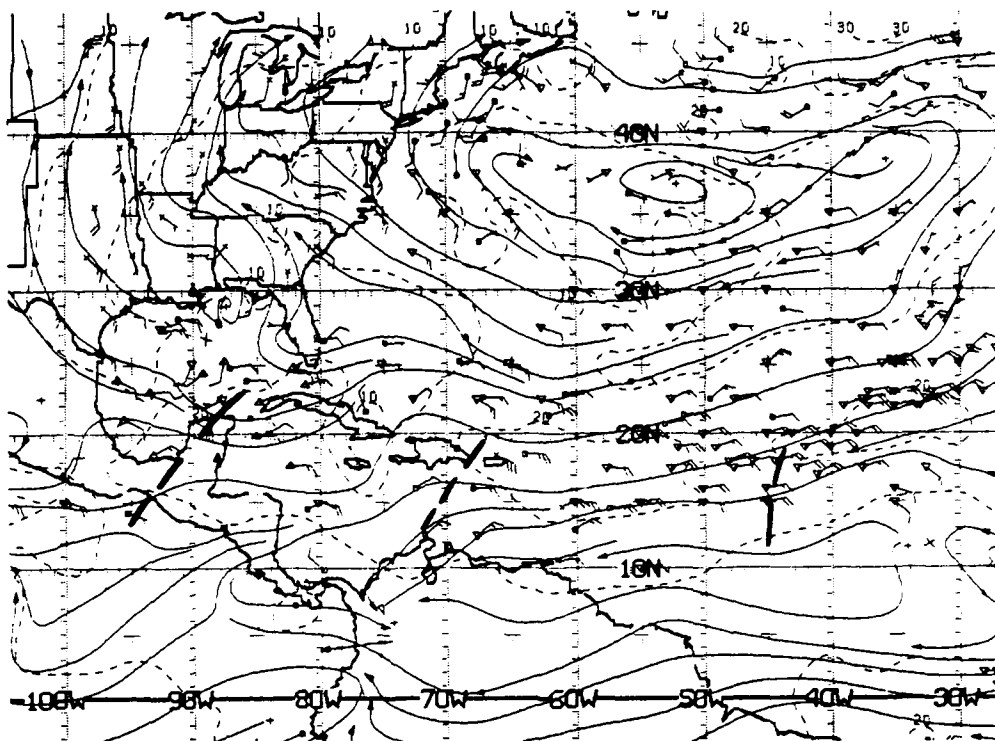


Figure 2.68: NMC ATOLL Operational Streamline Chart, 0000 UTC 4 AUG 1988
As in Fig. 2.4.

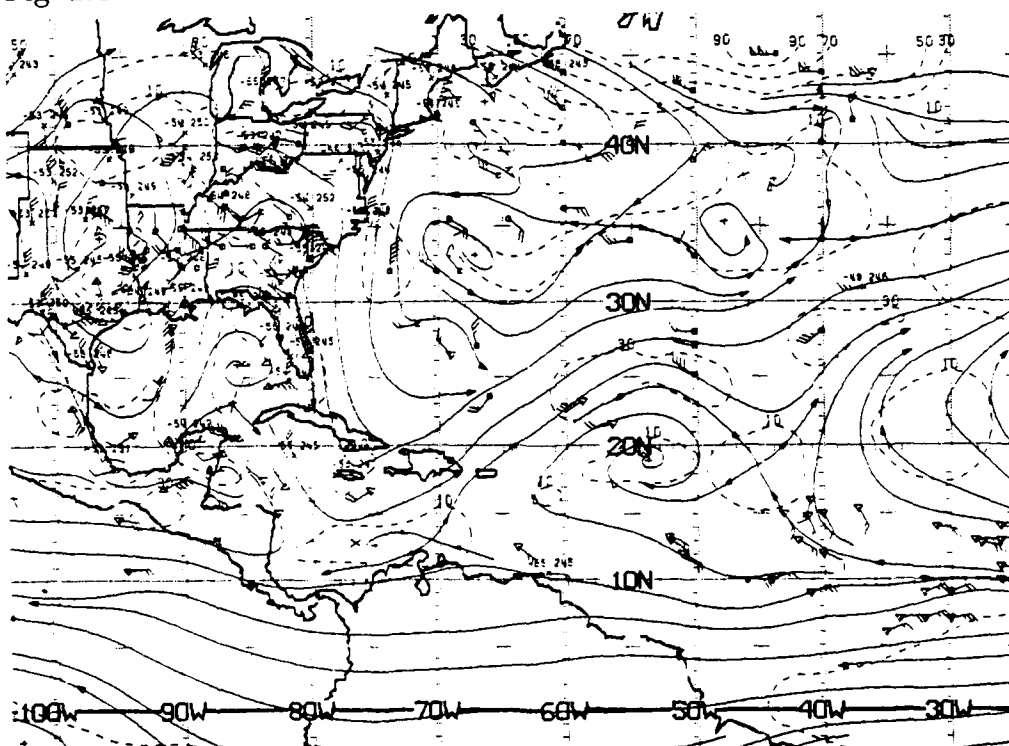


Figure 2.69: NMC 200 mb Operational Streamline Chart, 0000 UTC 4 AUG 1988
As in Fig. 2.6.

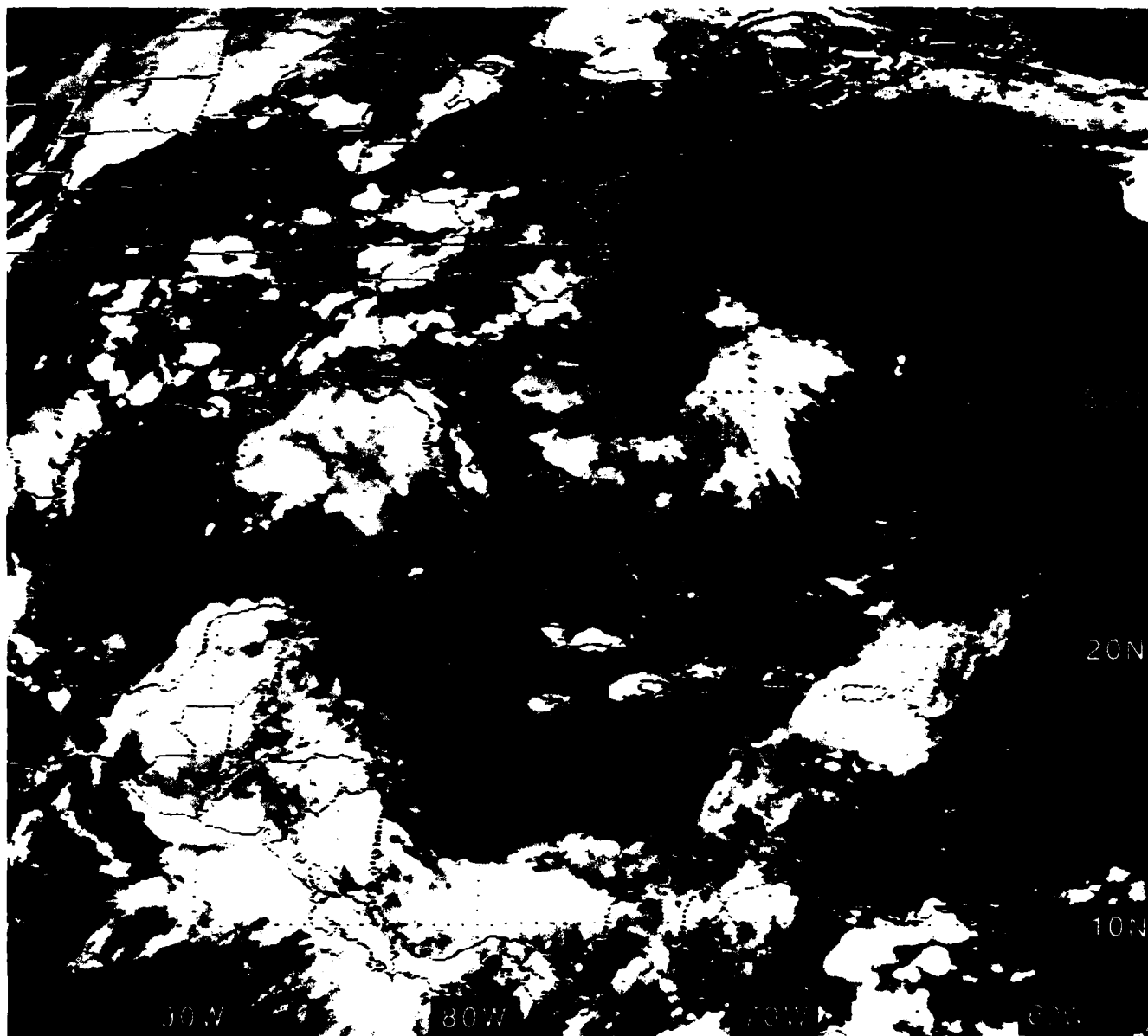


Figure 2.70: GOES East Infrared Satellite Imagery, 2201 UTC 3 AUG 1988

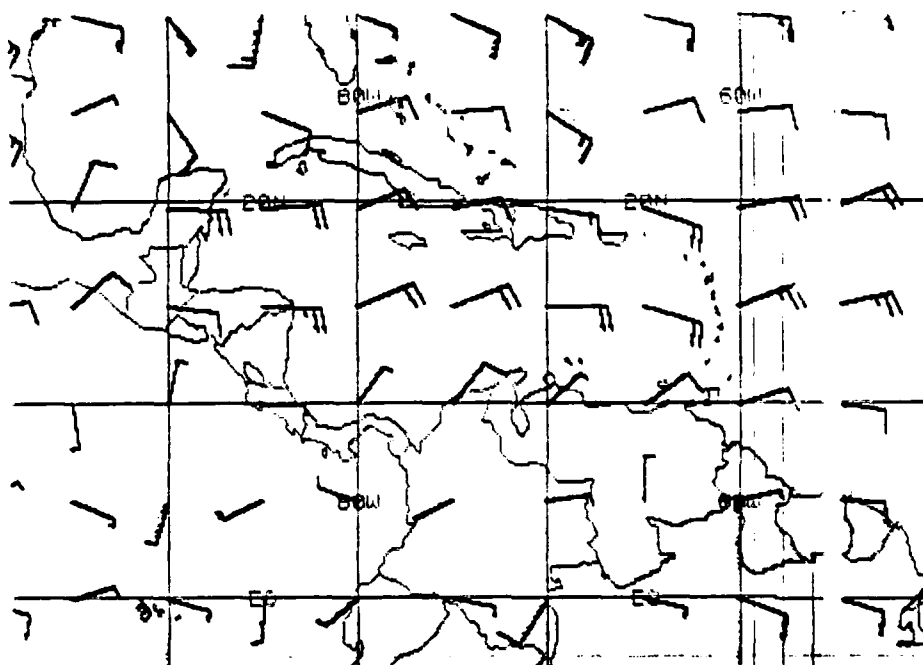


Figure 2.71: FNOC 925 mb Winds, 0000 UTC 4 AUG 1988.

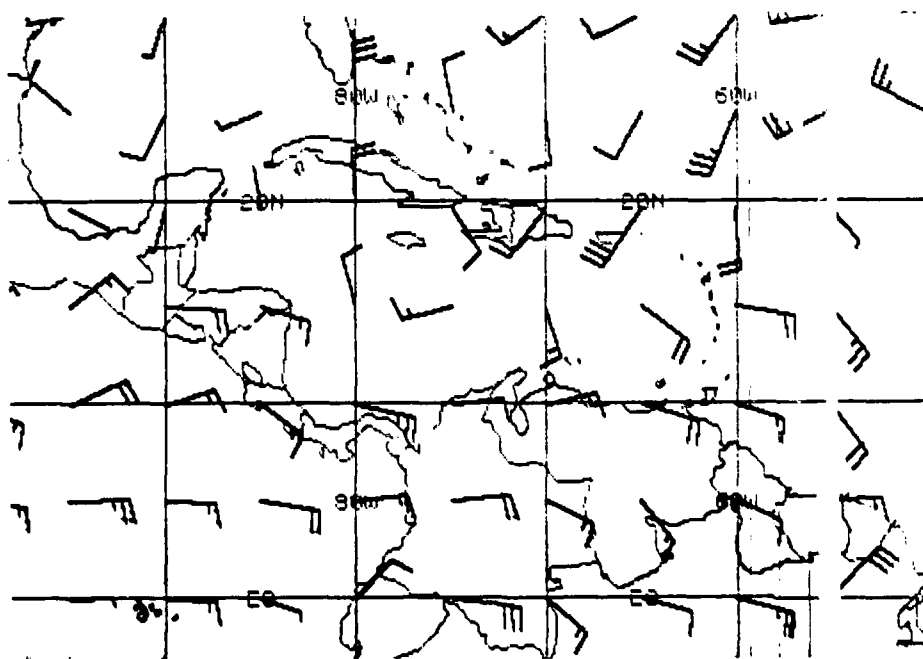


Figure 2.72: FNOC 200 mb Winds, 0000 UTC 4 AUG 1988.

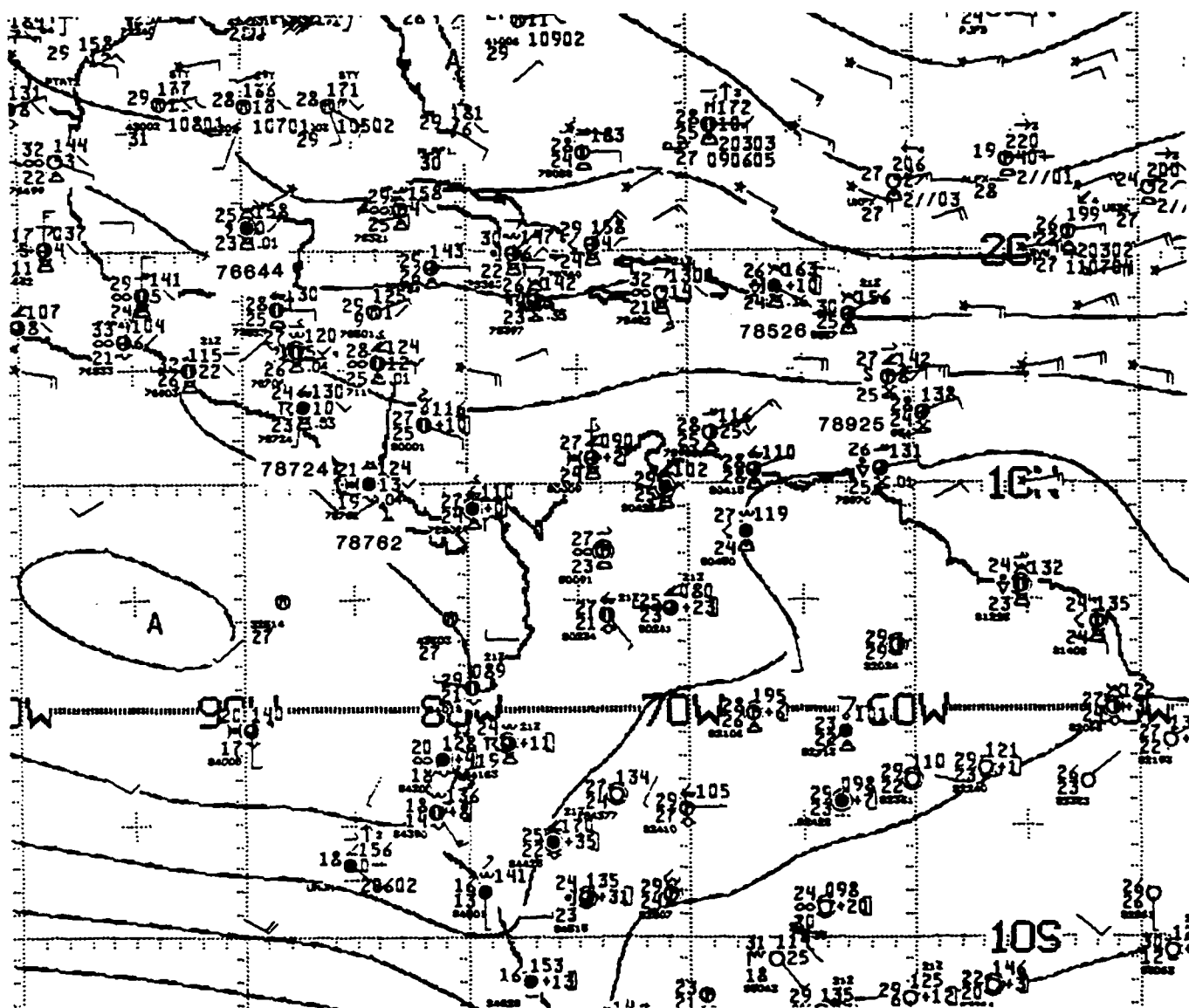


Figure 2.73: NMC 1000 mb Analysis, 0000 UTC 4 AUG 1988.

Contours are unlabeled stream functions from optimum interpolation analysis, with C identifying cyclonic centers and A identifying anticyclonic centers.

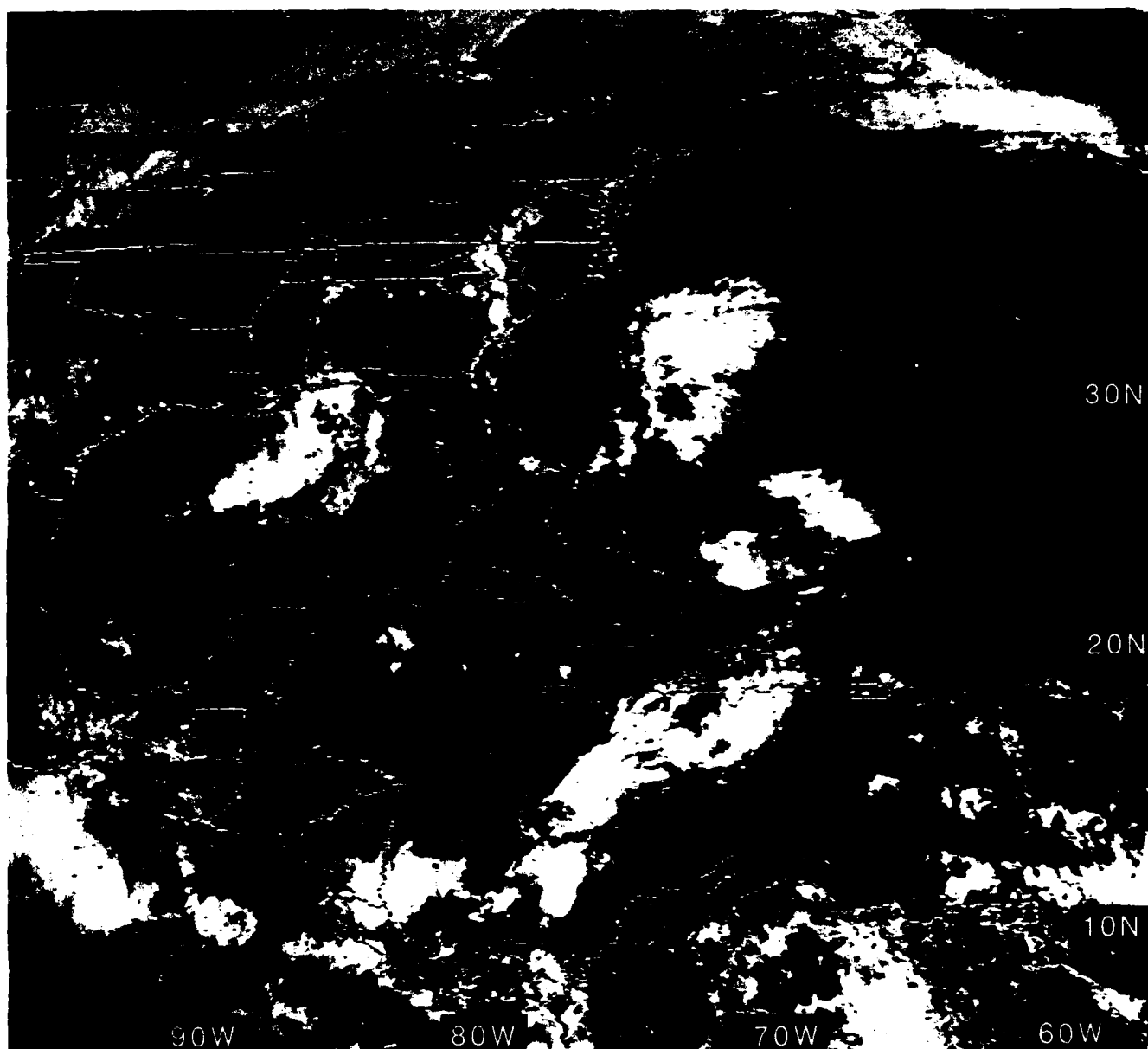


Figure 2.74: GOES East Visible Satellite Imagery, 1431 UTC 4 AUG 1988

5 August 1988

By 0000 UTC on 5 August, NHC now locates one tropical wave extending across Jamaica south-southwestward toward the Panama Canal (see Fig. 2.75), having moved at ~ 18 kt. Another tropical wave, also moving at ~ 18 kt, is approaching the Windward Islands and is centered near 15°N , 53°W . While Fig. 2.77 provides an overview showing the wave in the center of the Caribbean Sea with relatively clear skies over the western and eastern Caribbean Sea, Figs. 2.78 and 2.79 provide “zoomed”⁴⁶ visible and infrared imagery (separated by only $1\frac{1}{2}$ h) showing the cloudiness associated with the tropical wave beginning to merge with the convection which had existed over the warm shallow water of the Mosquito Banks (east of Bluefields, Nicaragua) for over six hours (see Fig. 2.74). The scattered thunderstorms in the relatively clear region *directly* west of Jamaica in Fig. 2.78 have their anvil towers advected slowly southward (at 15 – 20 kt) in Fig. 2.79 and confirm the upper-level *northerly* flow depicted by both the NMC 200 mb (Fig. 2.76) and the FNOC 200 mb analysis (at 20°N , 85°W in Fig. 2.81).

These satellite images depict the convection along (and to the east) of the tropical wave extending from Jamaica south-southwestward. Both the NMC (Fig. 2.75) and FNOC (Fig. 2.80) low-level analyses depict cyclonic flow near the wave axis, as well as slightly stronger winds to the east of the axis of the tropical wave. Additionally, the ATOLL streamline analysis (Fig. 2.75) shows significant low-level cyclonic curvature near 56°W , i.e., **not** far from the axis of the NHC-analyzed tropical wave in the vicinity of 53°W .

At 0001 UTC on 5 August, Fig. 2.82 presents the IR imagery corresponding to the station observations of Fig. 2.83: a thunderstorm at Kingston, Jamaica (station 78397) (on the axis of the tropical wave) and continuous drizzle at San Andrés Island (station 80001), contrasted to only $3/8$ sky cover reported both far to the *east* of the tropical wave (reported by a ship at 15°N , 71°W) and far to the *west* of the tropical wave at Puerto Lempira, Honduras (station 78711).

The area forecast issued by Tegucigalpa, Honduras predicts a tropical wave in the vicinity of the eastern tip of Honduras/Nicaragua for the period 0000–2400 UTC 5 August.

Figure 2.84 presents early morning infrared imagery at 1201 UTC, 12 hours after Fig. 2.82. The cloudiness associated with the central Caribbean tropical wave has moved northwestward at ~ 15 kt, with the “leading edge” of the cloudiness now extending from central Cuba southwestward to the northeastern coast of Honduras—Puerto Lempira (station 78711) sky cover (not shown) increased from $3/8$ to $3/4$ during the past 12 hours. Figure 2.85 presents the visible imagery only $1\frac{1}{2}$ h after the IR imagery of Fig. 2.84.

6 August 1988

Finally, on the last day of this case study, the infrared imagery at 0001 UTC on 6 August (Fig. 2.86) depicts areas of convective cloudiness at both the western and eastern ends

⁴⁶While the imagery has been *expanded*, the resolution remains at only 4 km. The user will experience the sensation of “putting on” corrective glasses when viewing 1 km resolution imagery!

of the Caribbean Sea, both associated with tropical waves—while another tropical wave exists far to the east in the North Atlantic Ocean near 31°W.

While the operational staff at NHC has placed tropical wave positions near 82°W and 62°W (see Fig. 2.87), an analyst, using *only* the cyclonic curvature of NMC streamlines of the ATOLL chart (Fig. 2.87), might likely place both tropical waves farther west—at ~87°W (cyclonic curvature in streamlines north of the Yucatan Peninsula) and at ~66°W (cyclonic curvature in streamlines south of Puerto Rico)—, placing the convective cloudiness to the east of the wave axis, in agreement with classic tropical wave configuration. However, such placements would move the tropical waves at speeds of ≥ 25 kt, if their NHC positions at 0000 UTC on 5 August are used.

While the FNOC 925 mb (Fig. 2.89) shows only weak cyclonic curvature in the vicinity of the western tropical wave, it does depict significant cyclonic curvature (although with *weak* circulation, 5–10 kt winds) at Trinidad near the eastern tropical wave. Thus the FNOC low-level wind analysis supports the NHC position of the eastern tropical wave.

To permit the reader to compare the flow at 850 mb with that at 925 mb, the FNOC 850 mb winds (Fig. 2.91) for the same time are presented. In preparing the case studies, the 850 mb analyses were continuously compared with the 925 mb analyses; however, no advantage of using the 850 mb analysis was discovered. (Using the European Centre for Medium Range Weather Forecasts (ECMWF) 850 mb analyses, Reed et al. (1988) followed waves and vortices crossing the North Atlantic Ocean, the Caribbean Sea and the Gulf of Mexico. In data sparse areas, even the use of the ECMWF *high-resolution* 850 mb analyses did not prevent instances of positioning a vortex *far* from the *preferred* satellite-derived location.)

Both upper-level analyses (NMC Fig. 2.88 and FNOC Fig. 2.90) show supportive anticyclonic flow above the convective cloudiness to the northeast of Honduras; however, both analyses have *only* weak anticyclonic flow over the cloudiness associated with the tropical wave entering the Caribbean Sea.

At this time, Tegucigalpa, Honduras was continuing to issue an area forecast calling for a tropical wave in the vicinity of eastern Honduras and Nicaragua for the period 0000–2400 6 August 1988.

While some tropical meteorologists claim that tropical wave theory provides little assistance for operational forecasting, the enhancement of daily cloudiness and convection afforded by these westward-moving waves (identified by trough positions) is well documented in case studies I and II. However, the user must be aware that the NMC or FNOC low- and upper-level analyses are automated “tools”. The demonstrated difference between automated NMC streamline trough positions and the more-subjective placement of *tropical-wave* trough positions—using satellite interpretation and other information—by the operational staff at NHC, indicates the continued need for “man/woman-machine” mix. While analysts may disagree as to the precise positions of individual waves, the *recognition* of their presence provides an excellent base from which mesoscale forecasting can proceed.

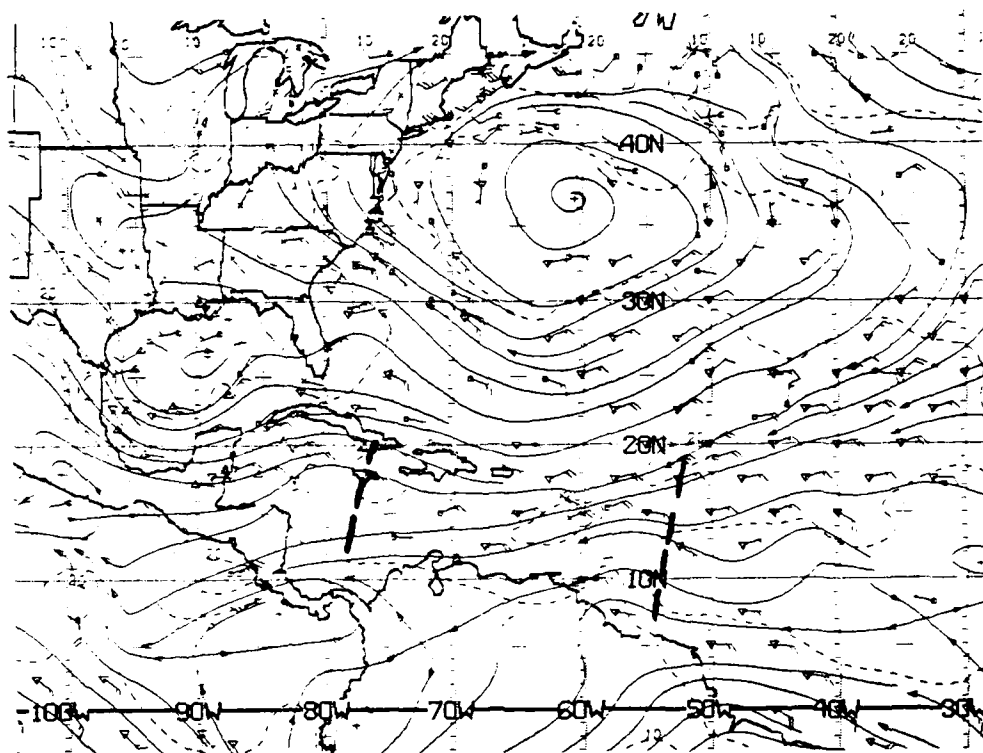


Figure 2.75: NMC ATOLL Operational Streamline Chart, 0000 UTC 5 AUG 1988
As in Fig. 2.4.

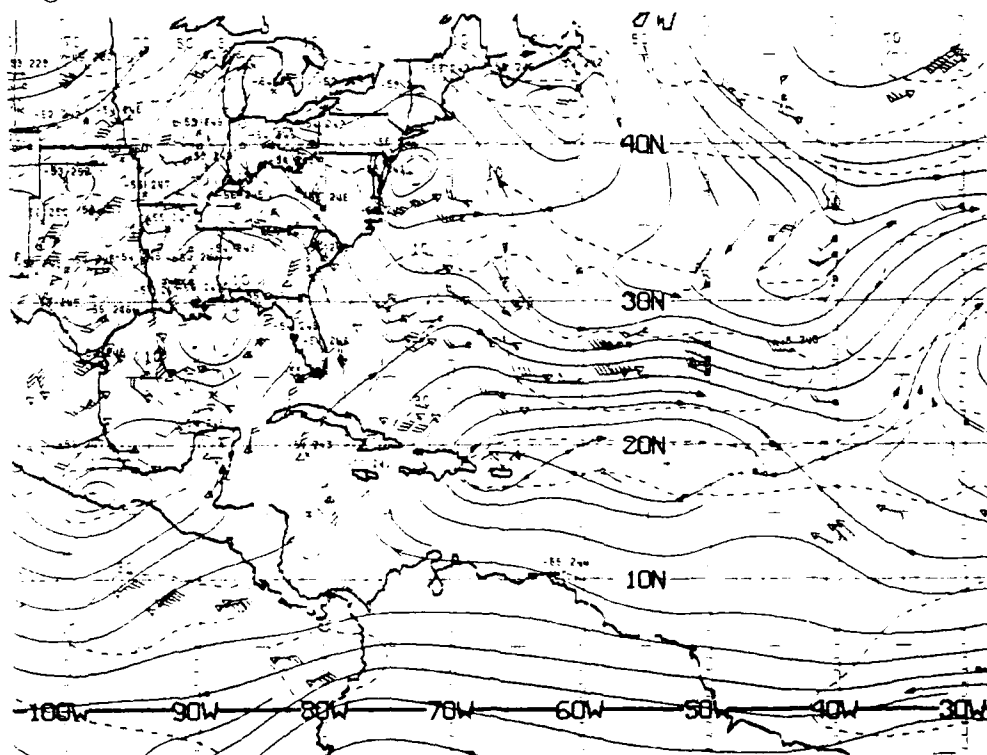


Figure 2.76: NMC 200 mb Operational Streamline Chart, 0000 UTC 5 AUG 1988
As in Fig. 2.6.



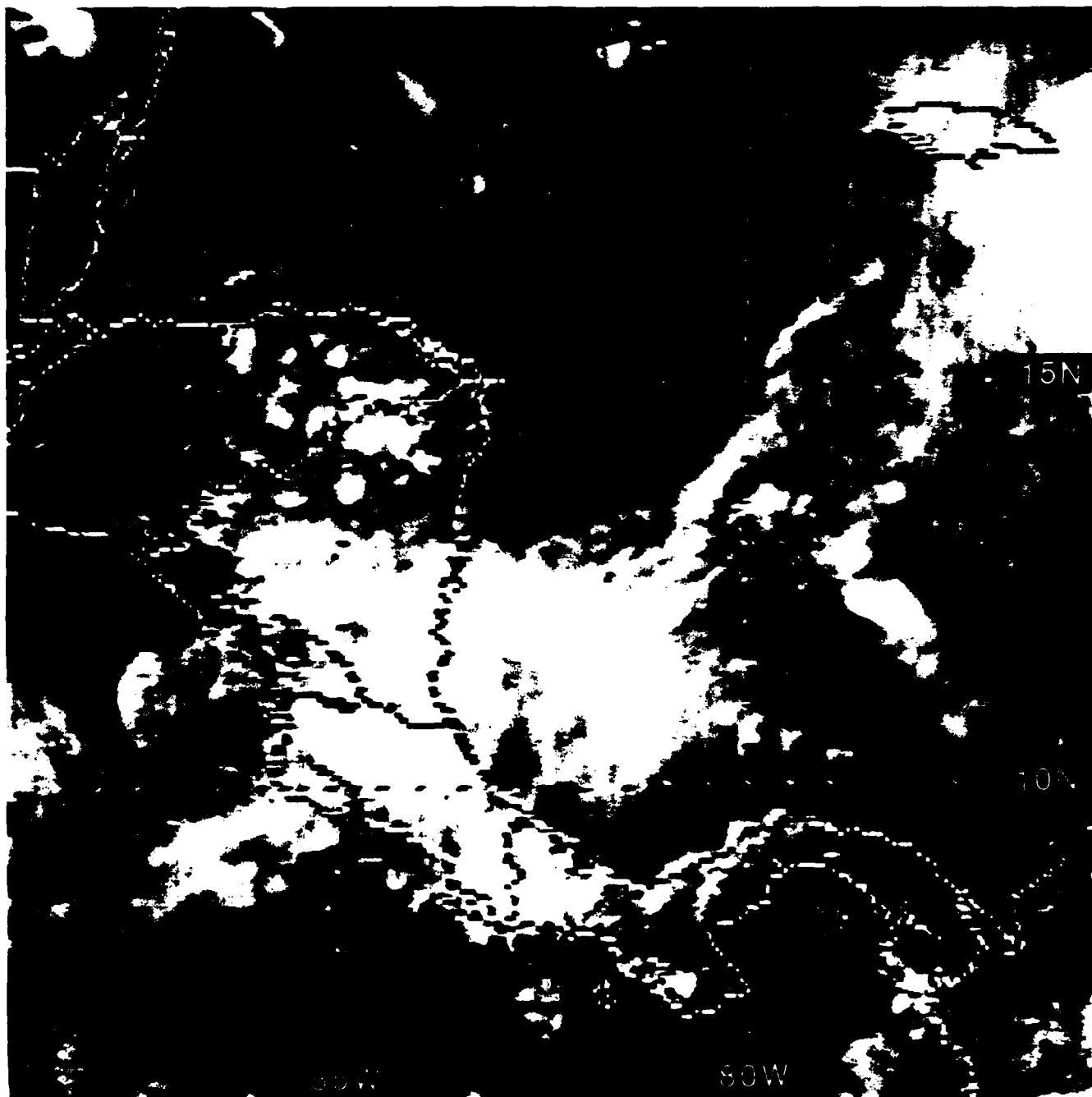


Figure 2.78: GOES East Vis. Imagery ("Zoomed"), 2031 UTC 4 AUG 1988

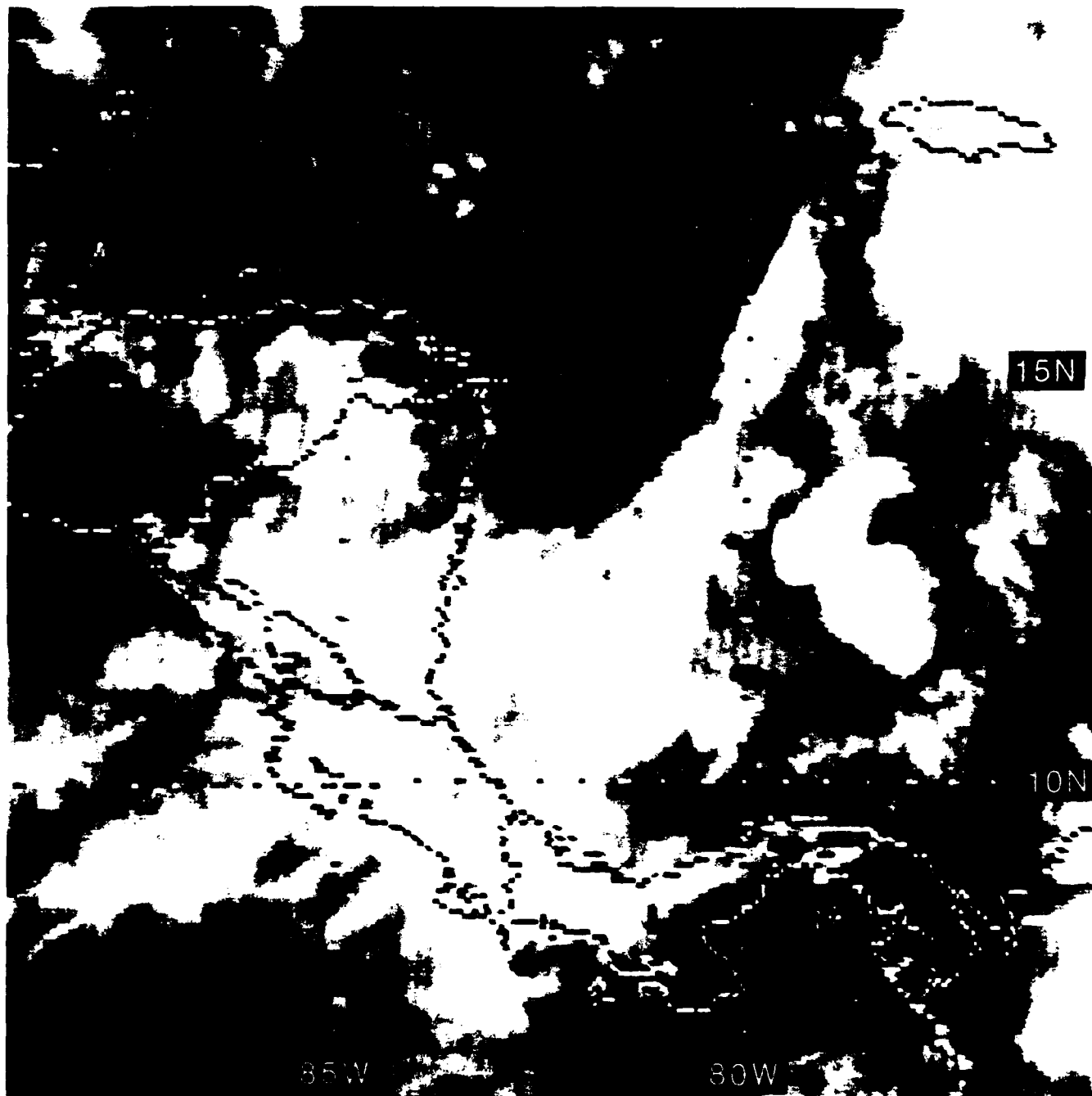


Figure 2.79: GOES East IR Imagery ("Zoomed"), 2201 UTC 4 AUG 1988

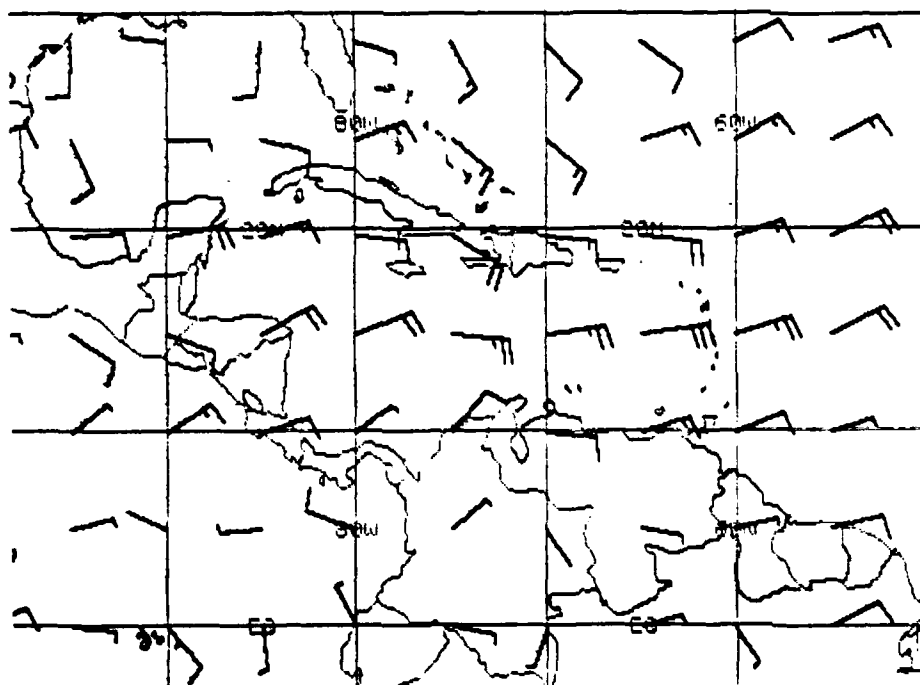


Figure 2.80: FNOC 925 mb Winds, 0000 UTC 5 AUG 1988.

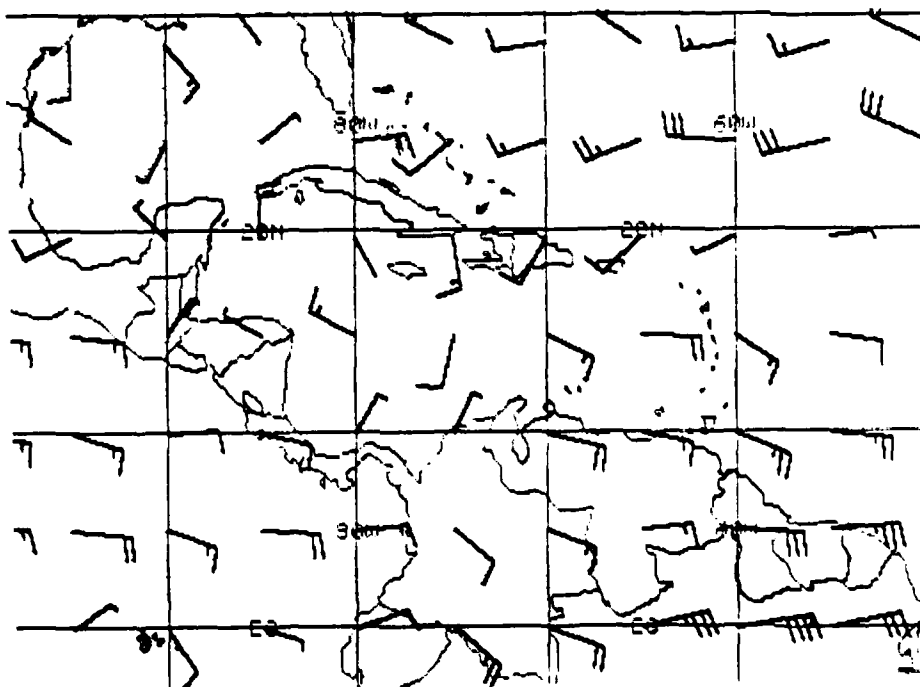


Figure 2.81: FNOC 200 mb Winds, 0000 UTC 5 AUG 1988.

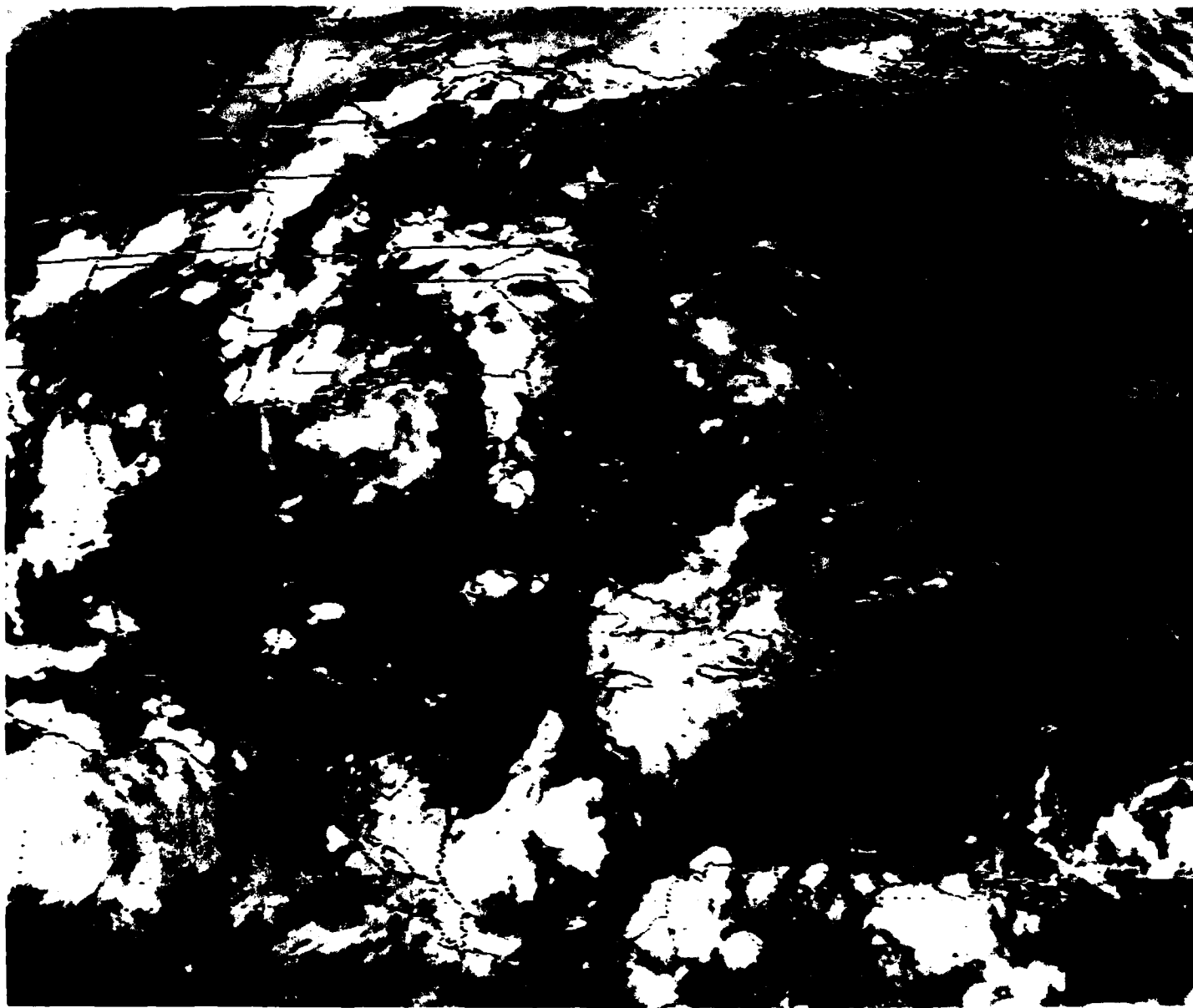


Figure 2.82: GOES East Infrared Satellite Imagery, 0001 UTC 5 AUG 1988

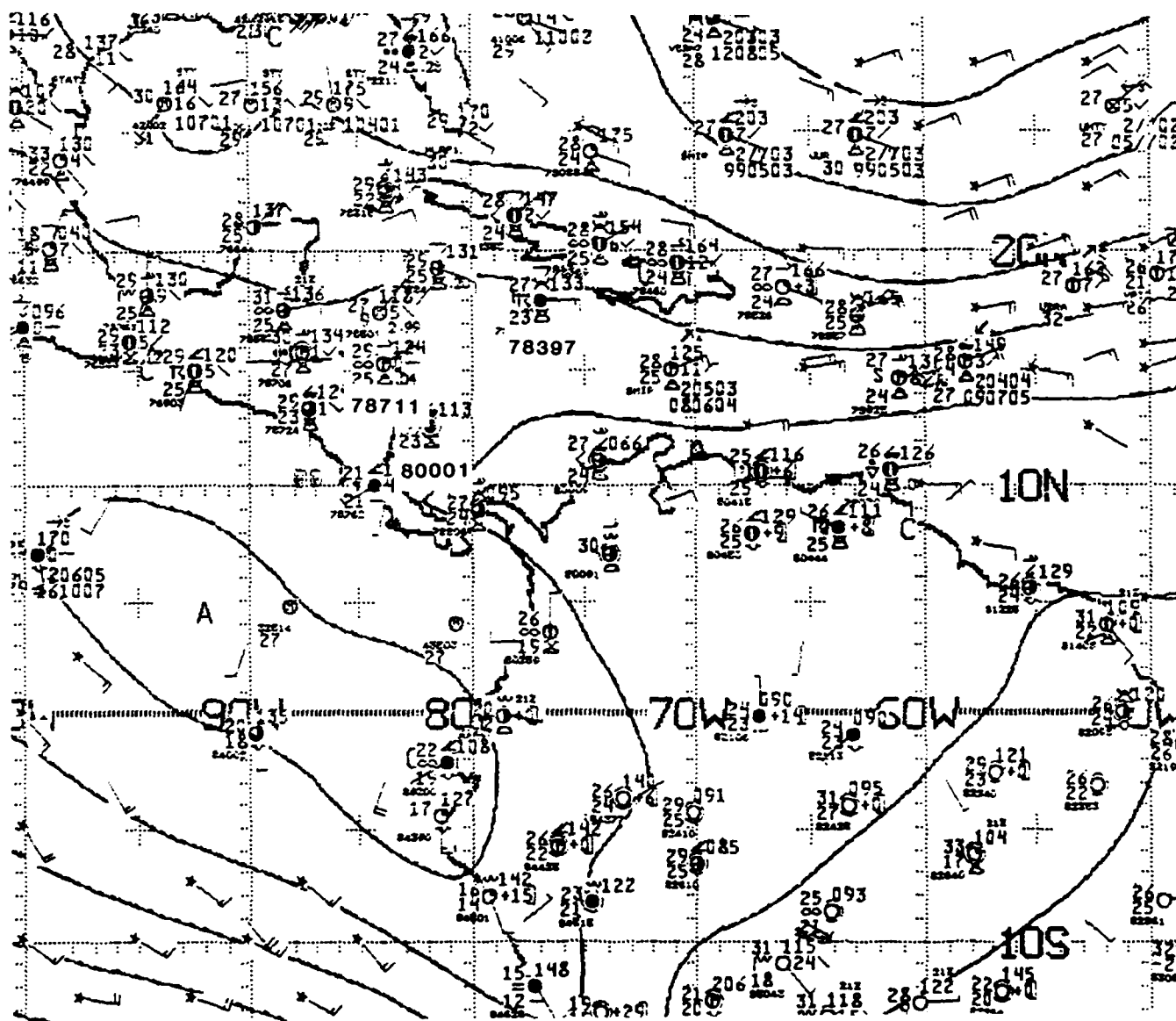


Figure 2.83: NMC 1000 mb Analysis, 0000 UTC 5 AUG 1988.
Contours are unlabeled stream functions from optimum interpolation analysis,
with C identifying cyclonic centers and A identifying anticyclonic centers.

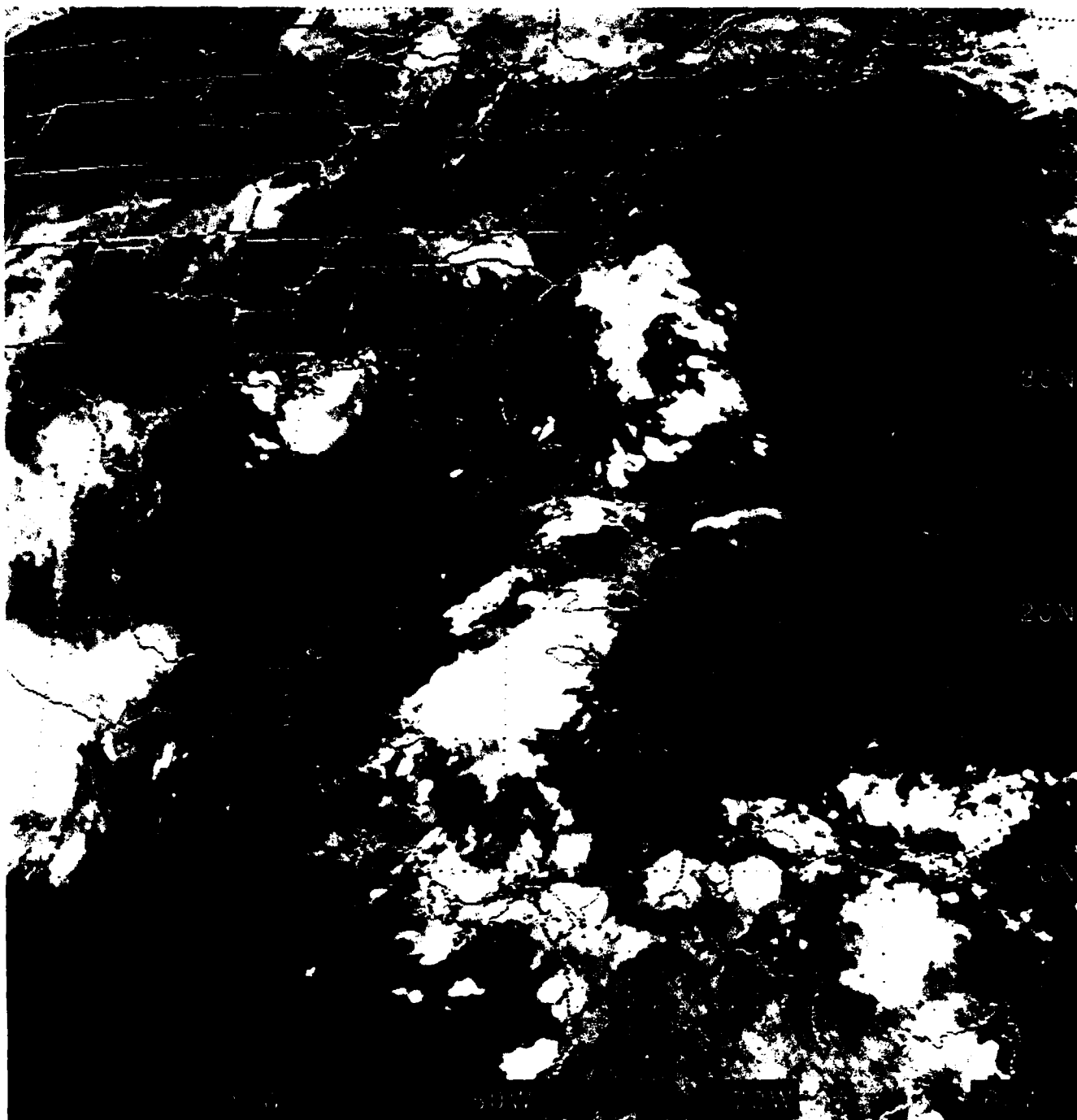


Figure 2.84: GOES East Infrared Satellite Imagery, 1201 UTC 5 AUG 1988

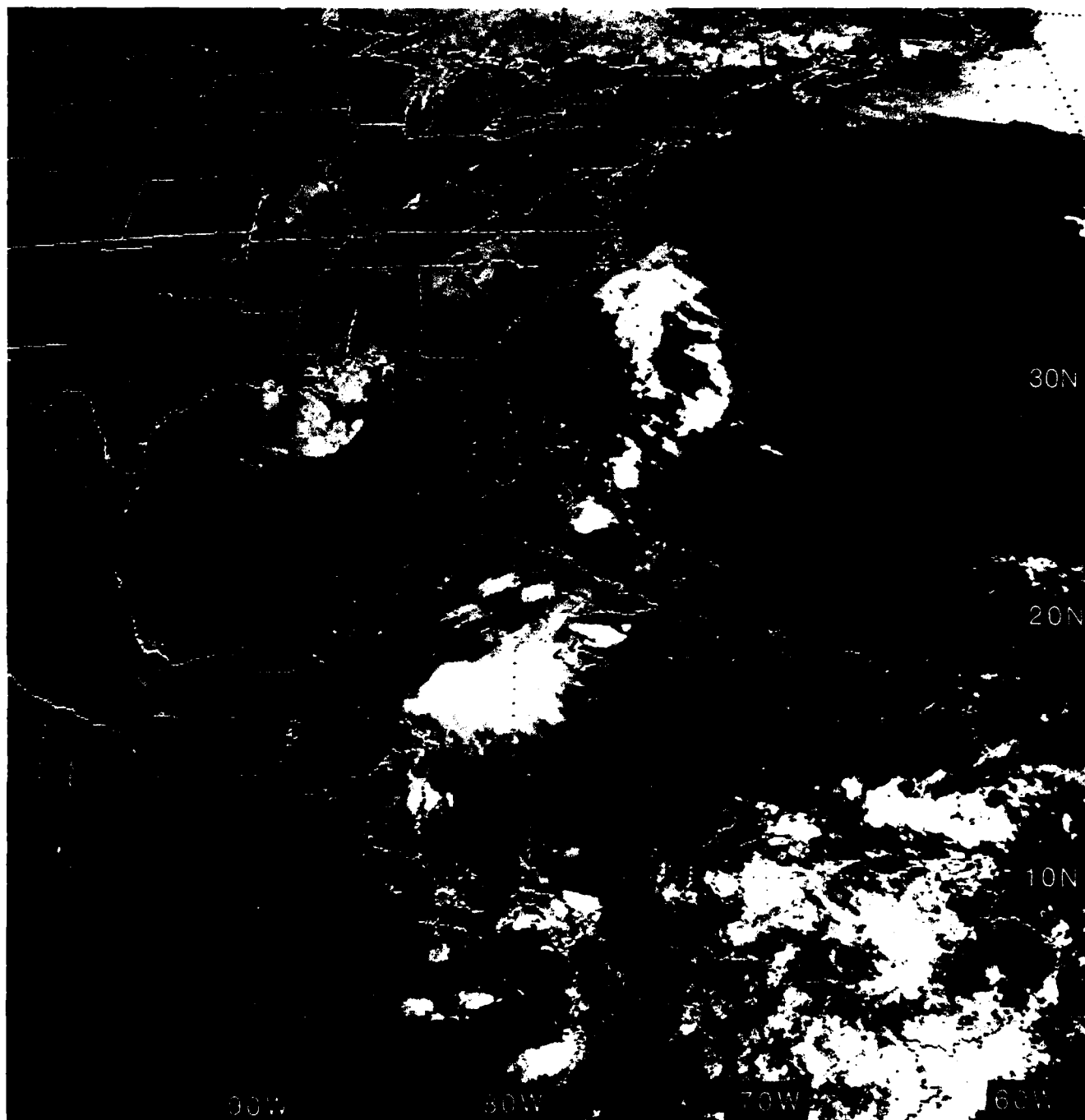


Figure 2.85: GOES East Visible Satellite Imagery, 1331 UTC 5 AUG 1988

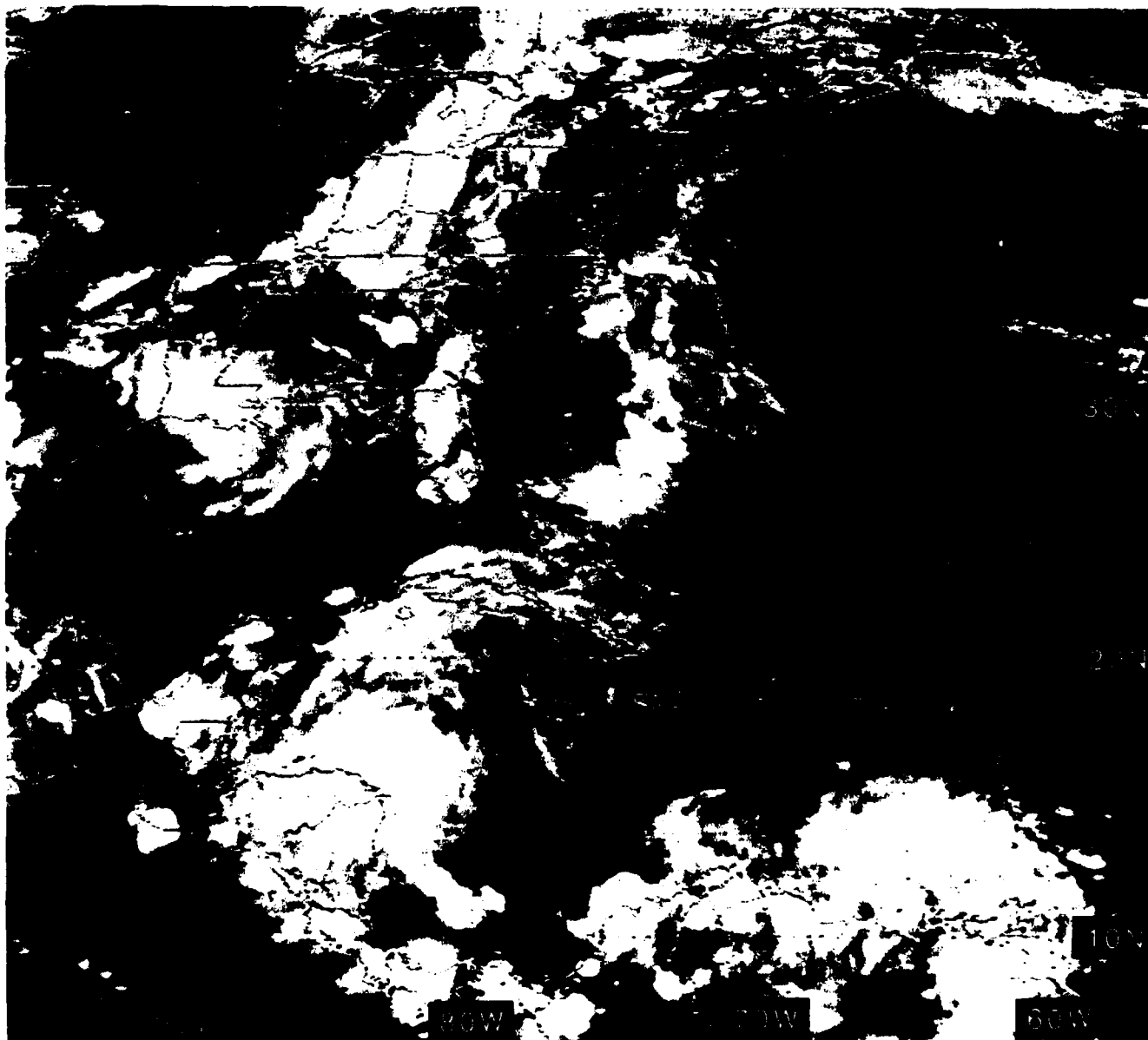


Figure 2.86: GOES East Infrared Satellite Imagery, 0001 UTC 6 AUG 1988
Ignore the "light" horizontal line between Key West and Brownsville.

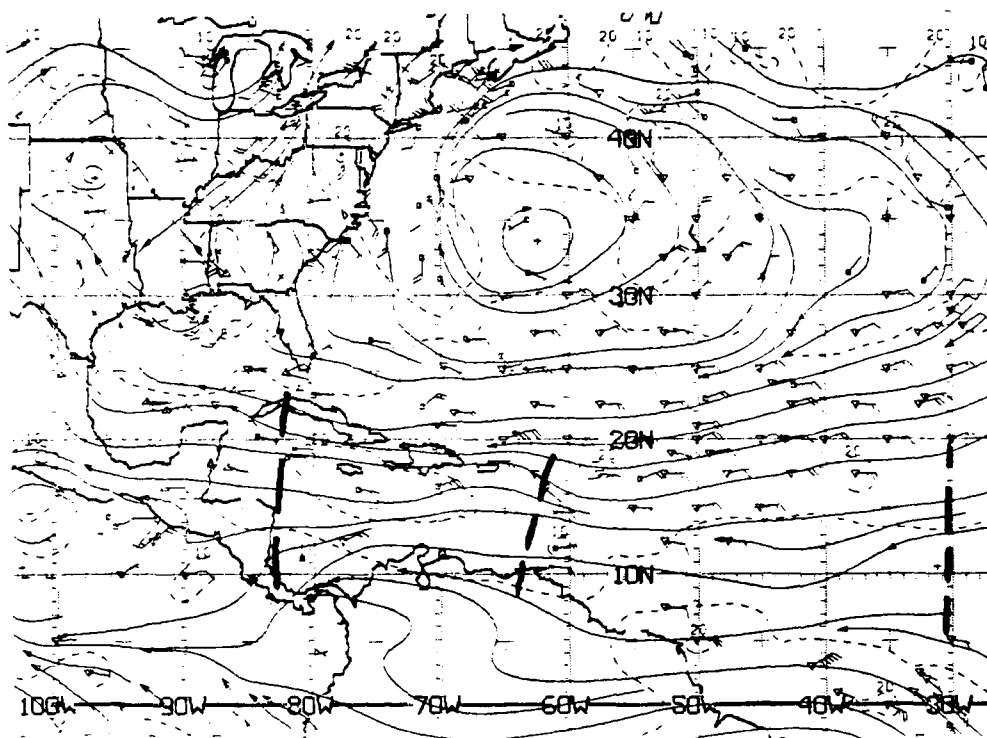


Figure 2.87: NMC ATOLL Operational Streamline Chart, 0000 UTC 6 AUG 1988
As in Fig. 2.4.

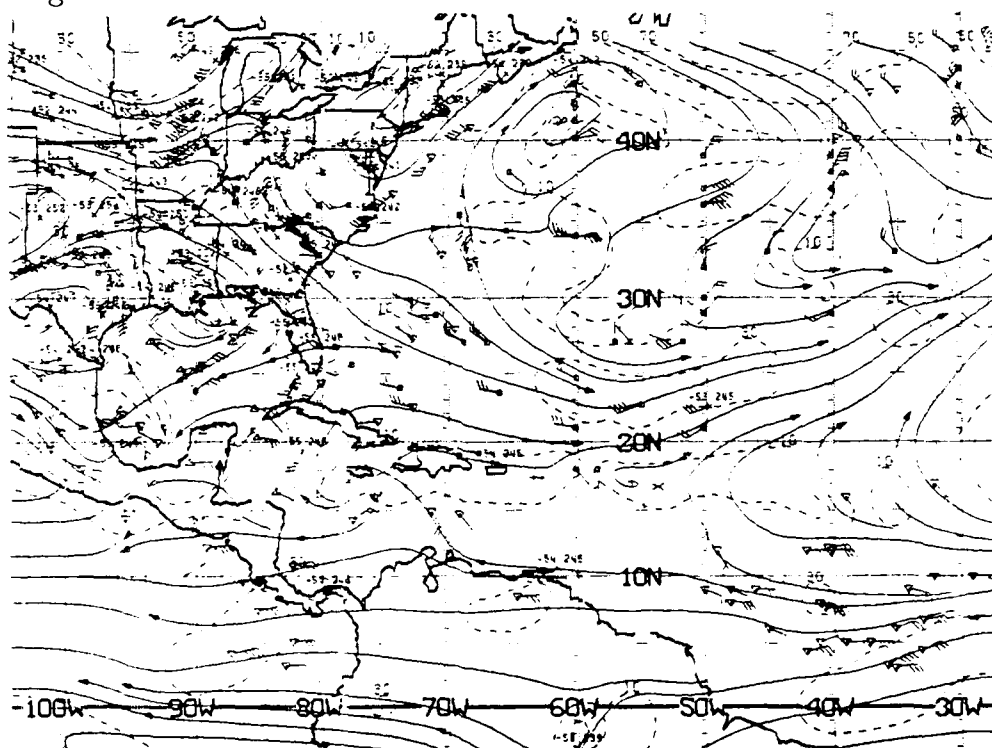


Figure 2.88: NMC 200 mb Operational Streamline Chart, 0000 UTC 6 AUG 1988
As in Fig. 2.6.

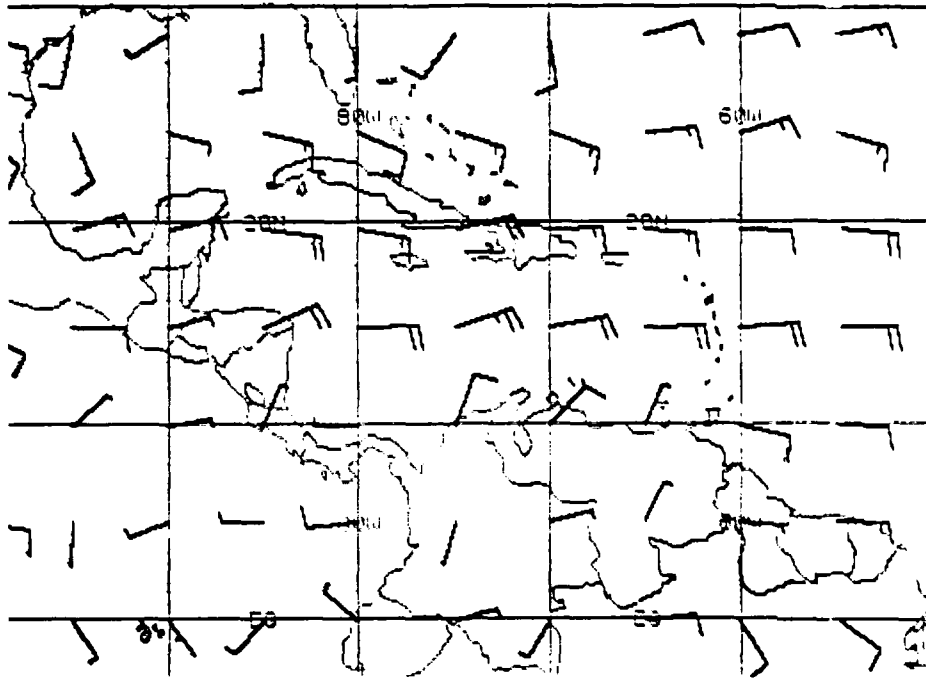


Figure 2.89: FNOc 925 mb Winds, 0000 UTC 6 AUG 1988.

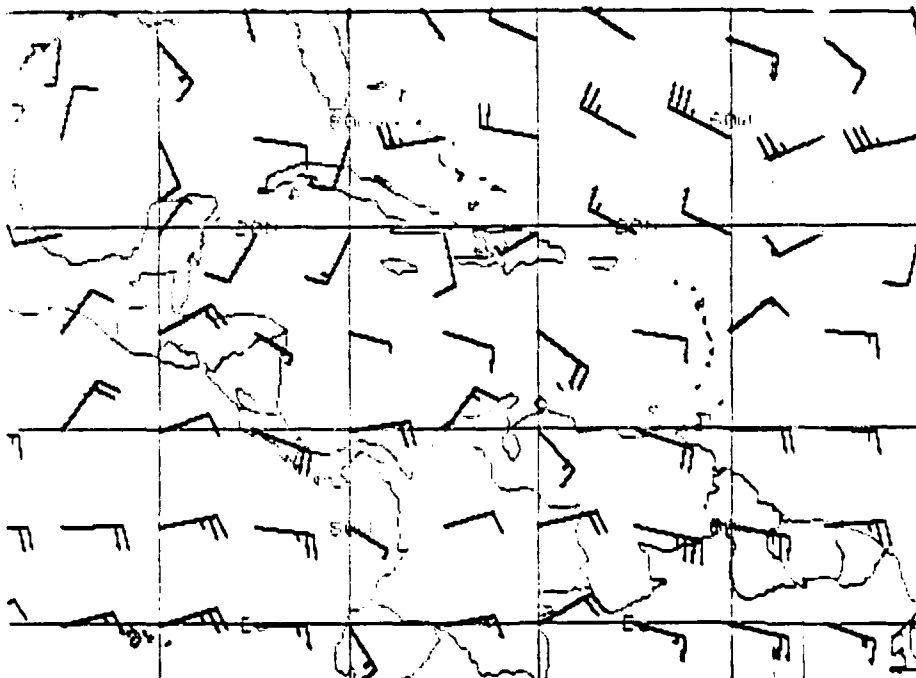


Figure 2.90: FNOc 200 mb Winds, 0000 UTC 6 AUG 1988.



Figure 2.91: FNOC 850 mb Winds, 0000 UTC 6 AUG 1988.

2.3.3 Arc Cloud (2 October 1988)

On the day preceding the first day of Case Study I, an arc cloud was observed which expanded westward rapidly from the west side (or *leading edge*) of the cloudiness associated with an advancing tropical wave.

Figures 2.92 and 2.93 show the NMC low-level and upper-level streamlines at 0000 UTC 2 October 1988. Similarly, Figs. 2.94 and 2.95 display the FNOC (Navy) wind analyses. A tropical wave had entered the eastern Caribbean Sea, and its associated cloudiness (from south of Puerto Rico, *eastward*) is shown in Fig. 2.96. Examination of the low-level ATOLL streamlines (Fig. 2.92) alone places the tropical wave axis near 63°W at 0000 UTC. Also, note the anticyclonic curvature in the upper-level streamlines over the southern Windward Islands (near 12°N, 62°W, see Fig. 2.93) coincident with the more intense convection shown on Fig. 2.96.

12 hours later, the IR imagery of Fig. 2.97 shows that the western edge of the cloudiness has advanced westward, at ~15 kt, and is near 71°W, south of the island of Hispaniola. Note that, at this time, the imagery depicts very cold tops—no doubt in association with intense convection, including thunderstorms—between 70°W and 68°W.

Figures 2.98a, 2.98b, 2.99a and 2.99b are the “zoomed”⁴⁷ visible images depicting the movement of the **arc cloud** (in one-hour time steps) from the western periphery of the tropical wave cloudiness. The arc cloud, representing the outer radius of the low-level “outflow” from the thunderstorms (near 72°W, or just to the east of the western boundary of the tropical wave cloudiness), expands outward at a speed of ~30 kt. The southern portion of the arc cloud has advanced to near 73.5°W by 1731 UTC.

The visible imagery of Fig. 2.100 shows the arc cloud on a smaller scale (larger area) at the same time (1731 UTC) as Fig. 2.99b. Figure 2.101 shows the IR imagery *just* 31 minutes *earlier*. The arc cloud is hardly (if at all) discernible⁴⁸ in the IR imagery, indicating that the tops of the convection of the arc cloud are **relatively low**—certainly low compared to the high level (cold tops) indicated by the extremely white imagery near 69°W in Fig. 2.101. In fact, the colder (whiter) tops in the IR imagery of Fig. 2.101, east of 70°W, correspond with the more *solid* cloud cells in the visible imagery of Fig. 2.100.

Finally, by 1931 UTC, the visible imagery of Fig. 2.102 shows that the arc cloud has completely dissipated.

⁴⁷Note that the resolution remains at 4 km.

⁴⁸On the original “hard copy” of IR imagery of Fig. 2.101, it is possible to see the very narrow, dark grey line—representing the arc cloud.

While no ship reports were available to confirm the extent of the convection associated with the arc cloud, it is likely that it was accompanied by at least light rain showers; furthermore, while it propagated at ~ 30 kt, ships and stations near the arc cloud would likely experience wind speeds ≥ 30 kt. However, its life span was only about 5 hours, with its demise probably resulting from large scale **downward** motion. It appears that downward vertical motion, in the relatively clear region—through which the arc cloud propagated—ahead, and to the **west**, of the advancing tropical wave, compensates for the strong **upward** motion in the intense convection to the **east** of the tropical wave position. 4 1/2 hours later (see Fig. 2.11 of Case Study I), the *leading* cloudiness of the tropical wave still has not advanced much past 71°W longitude—indicating that the rapid passage of *this* arc cloud did not appreciably alter the air mass immediately ahead of the tropical wave.

During the rainy season of 1988, one of the authors observed another arc cloud in the *western* Caribbean Sea with a similar short life span. However, arc clouds are closely watched in the mid-latitudes⁴⁹ and a prudent *tropical* or *subtropical* forecaster should continue to monitor the IR imagery—as well as interactions with other synoptic indicators—in order to be alert to any continuation of (or enhancement of) convection.

⁴⁹Intense convective activity results when separate arc clouds intersect as they progress outward from different parent thunderstorms.

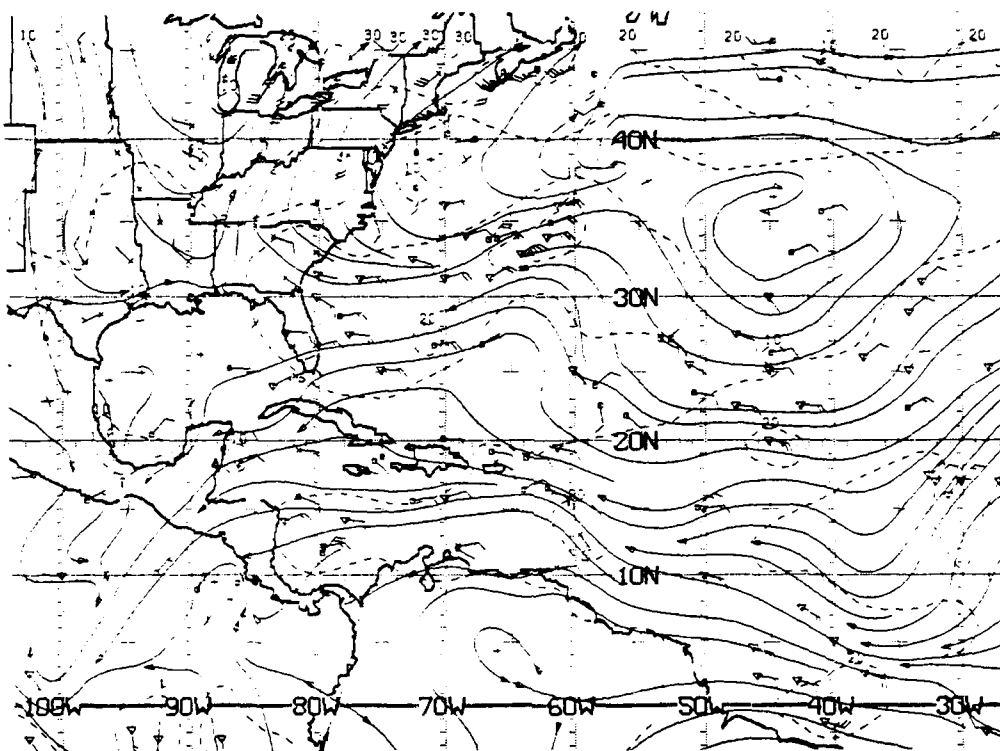


Figure 2.92: NMC ATOLL Operational Streamline Chart, 0000 UTC 2 OCT 1988
As in Fig. 2.4.

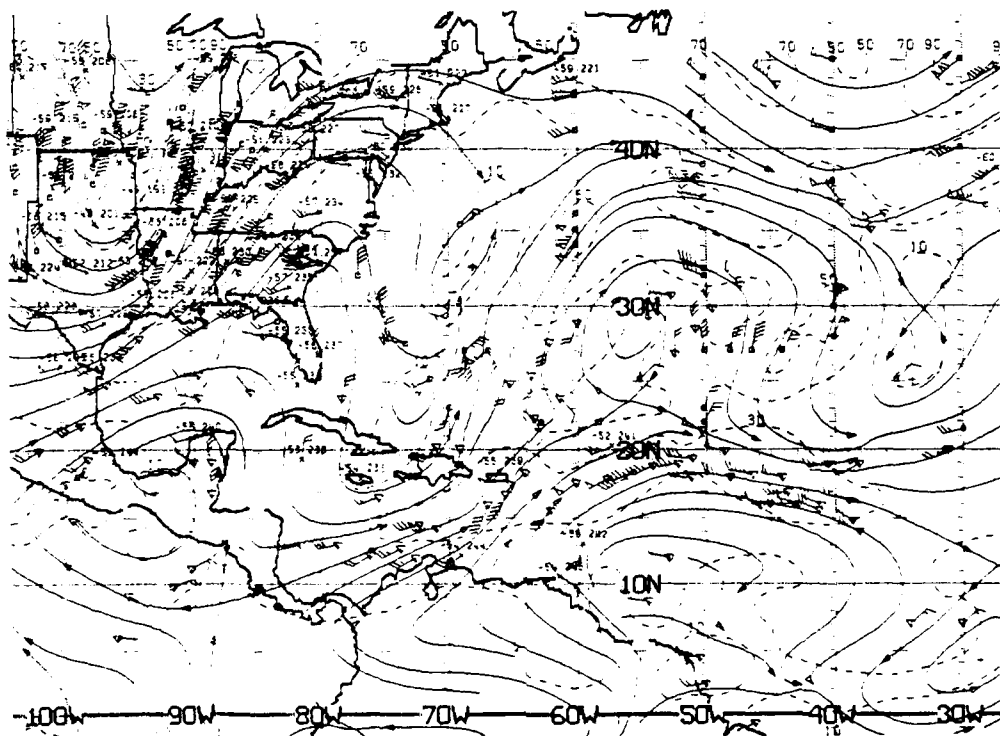


Figure 2.93: NMC 200 mb Operational Streamline Chart, 0000 UTC 2 OCT 1988
As in Fig. 2.6.

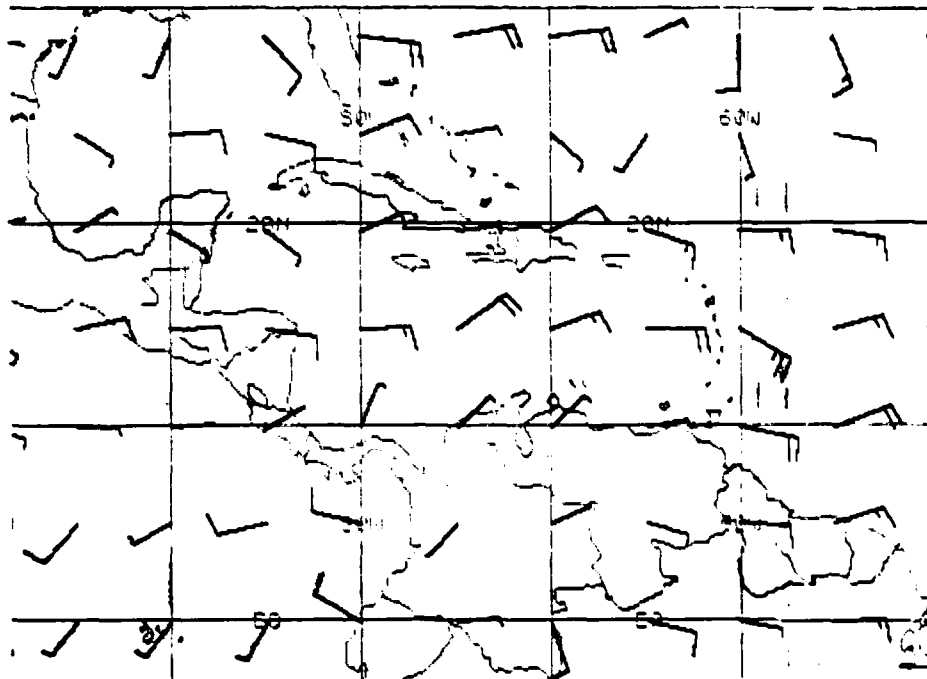


Figure 2.94: FNO 925 mb Winds, 0000 UTC 2 OCT 1988.

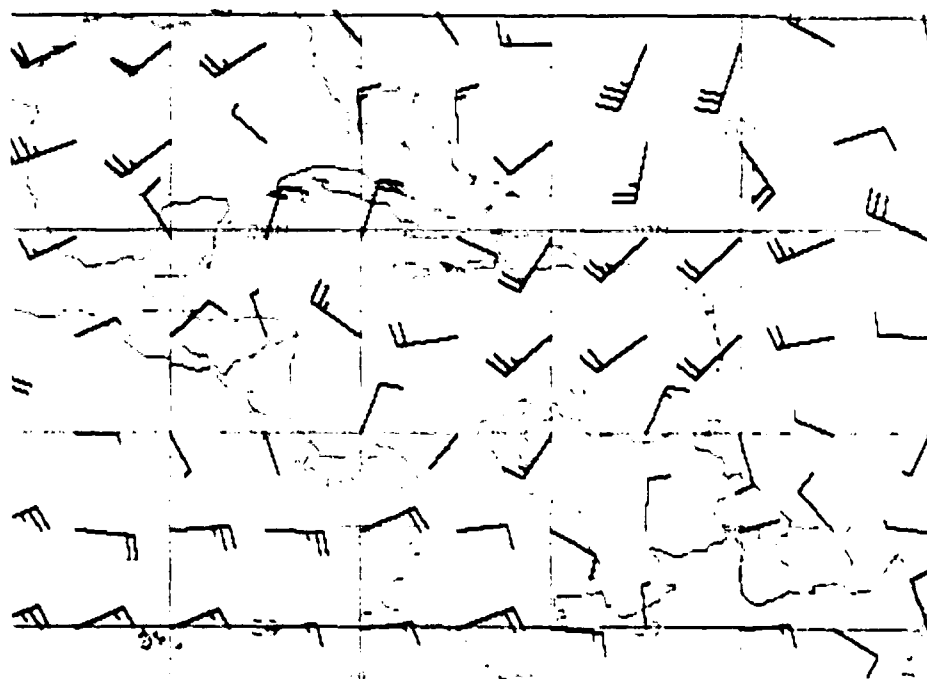


Figure 2.95: FNO 200 mb Winds, 0000 UTC 2 OCT 1988.

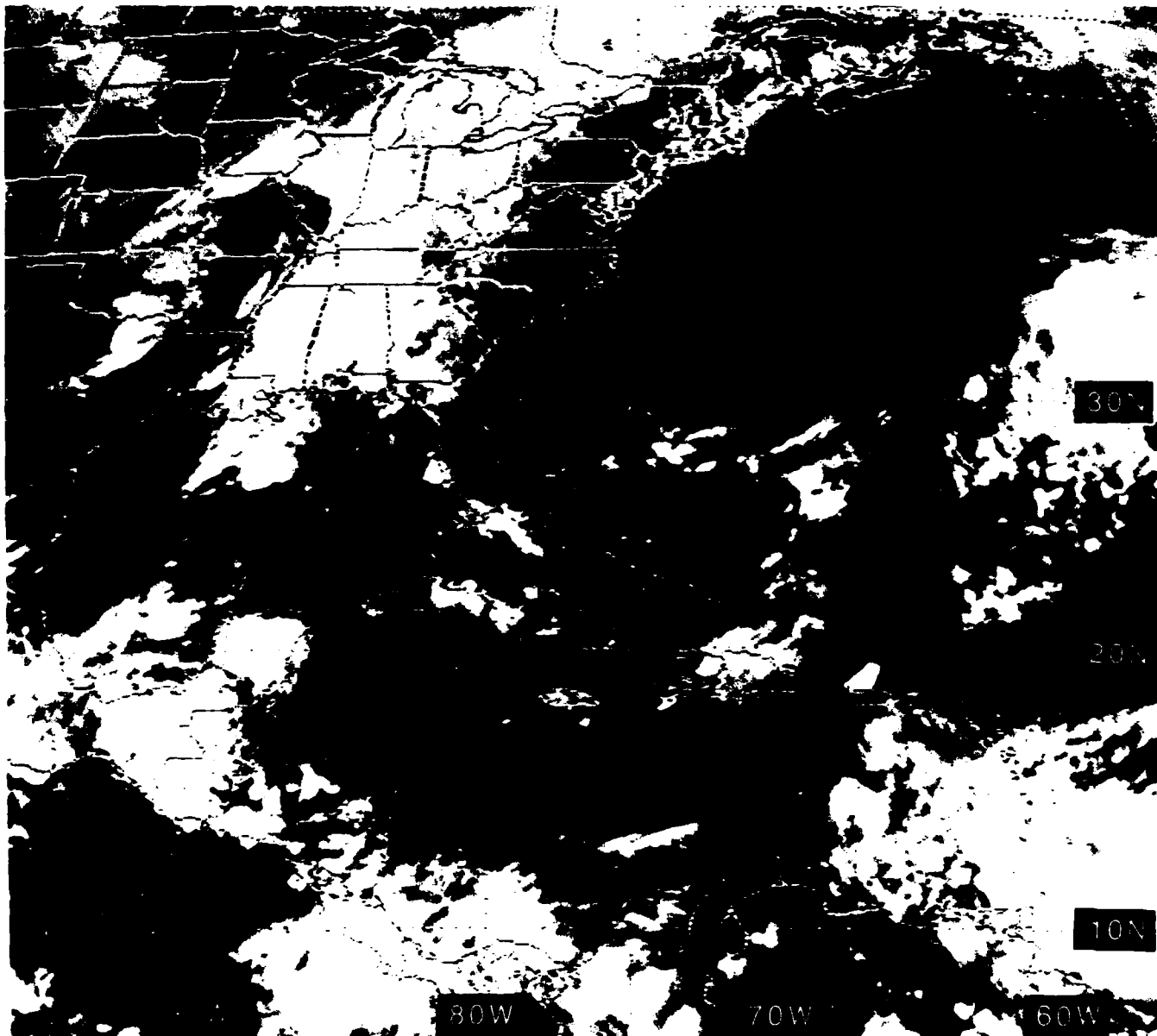


Figure 2.96: GOES East Infrared Satellite Imagery, 0001 UTC 2 OCT 1988

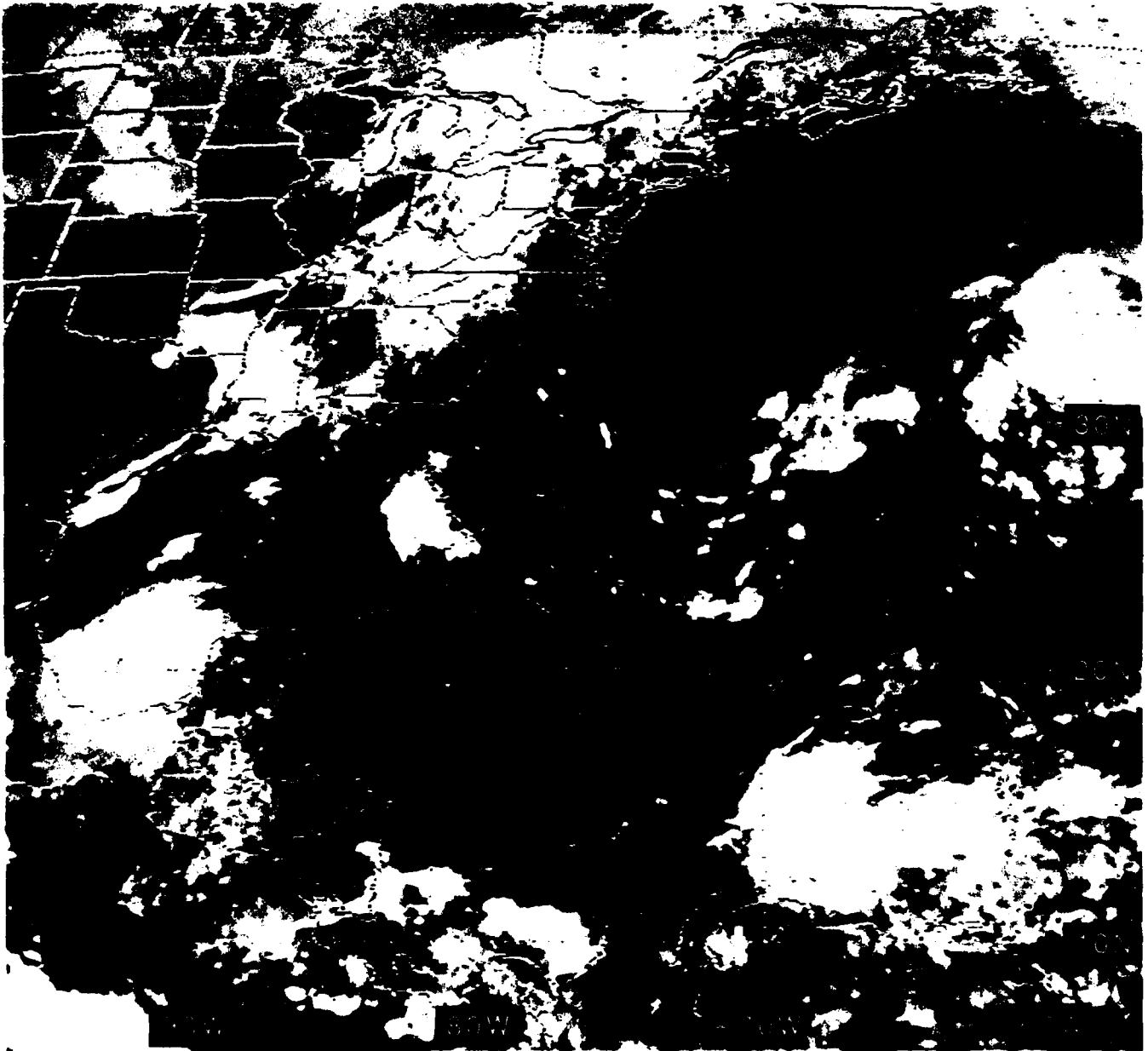
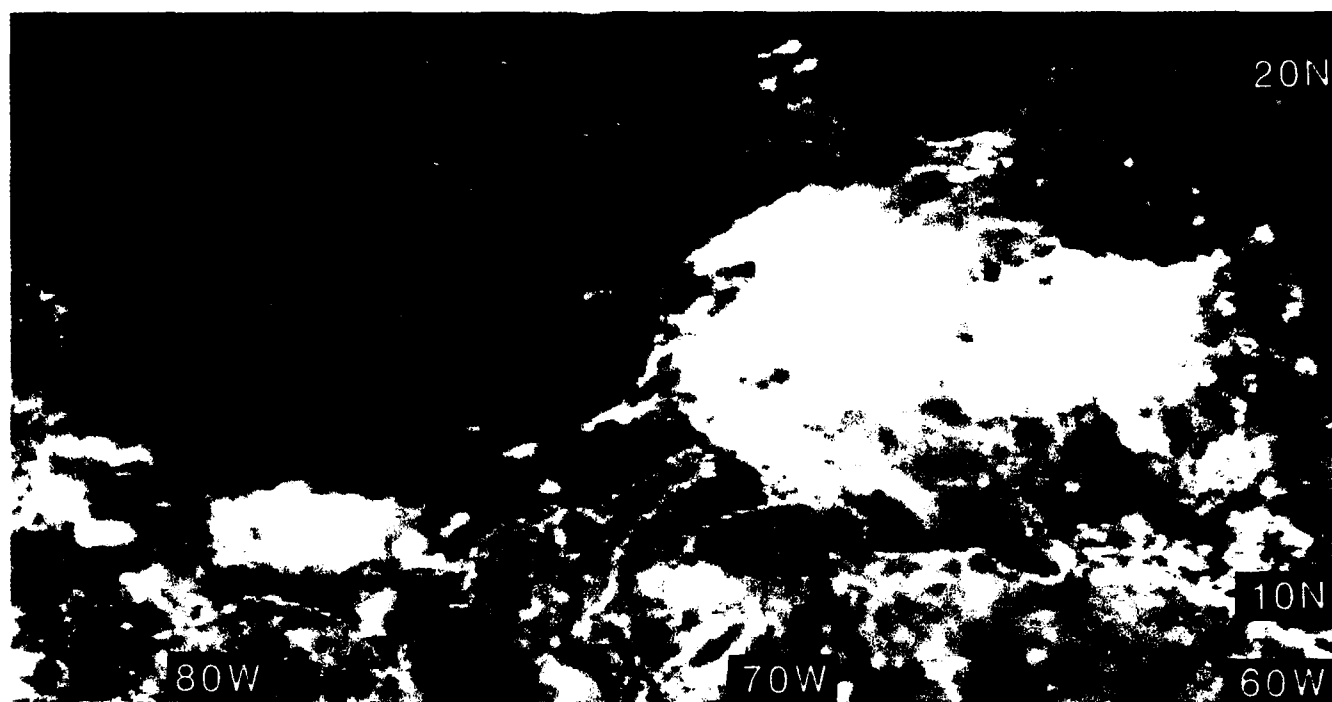
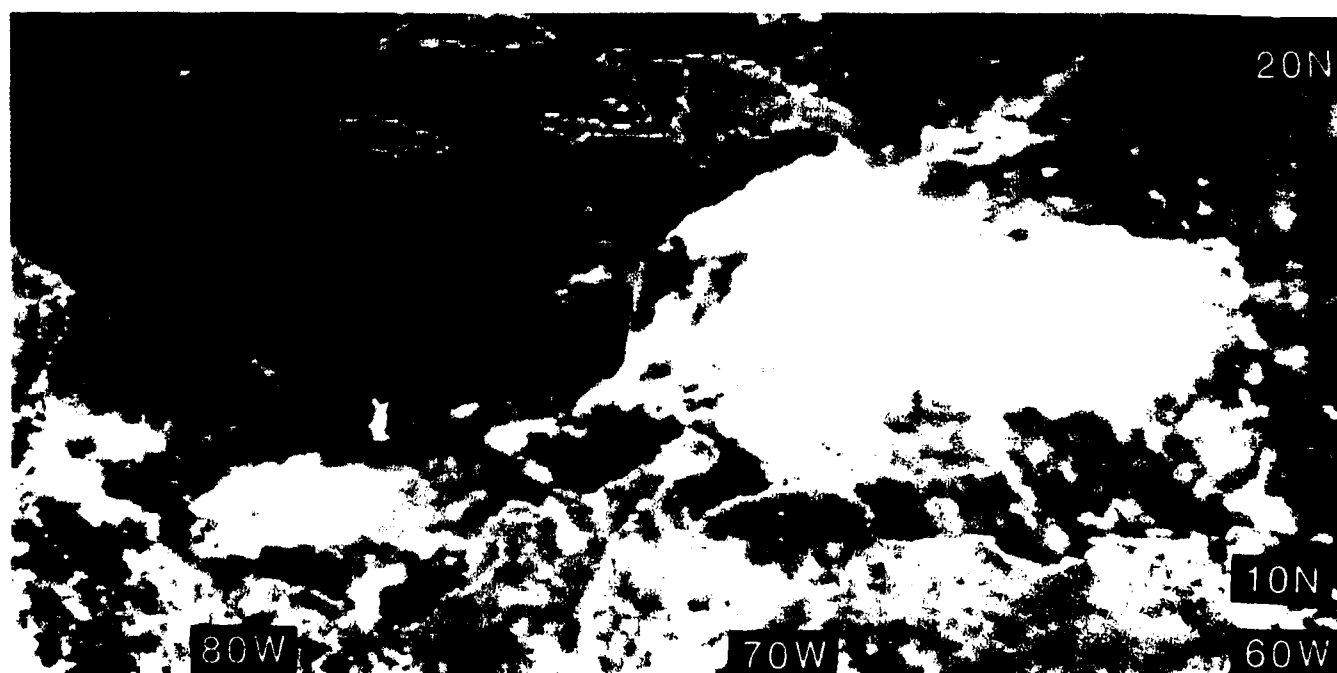


Figure 2.97: GOES East Infrared Satellite Imagery, 1201 UTC 2 OCT 1988

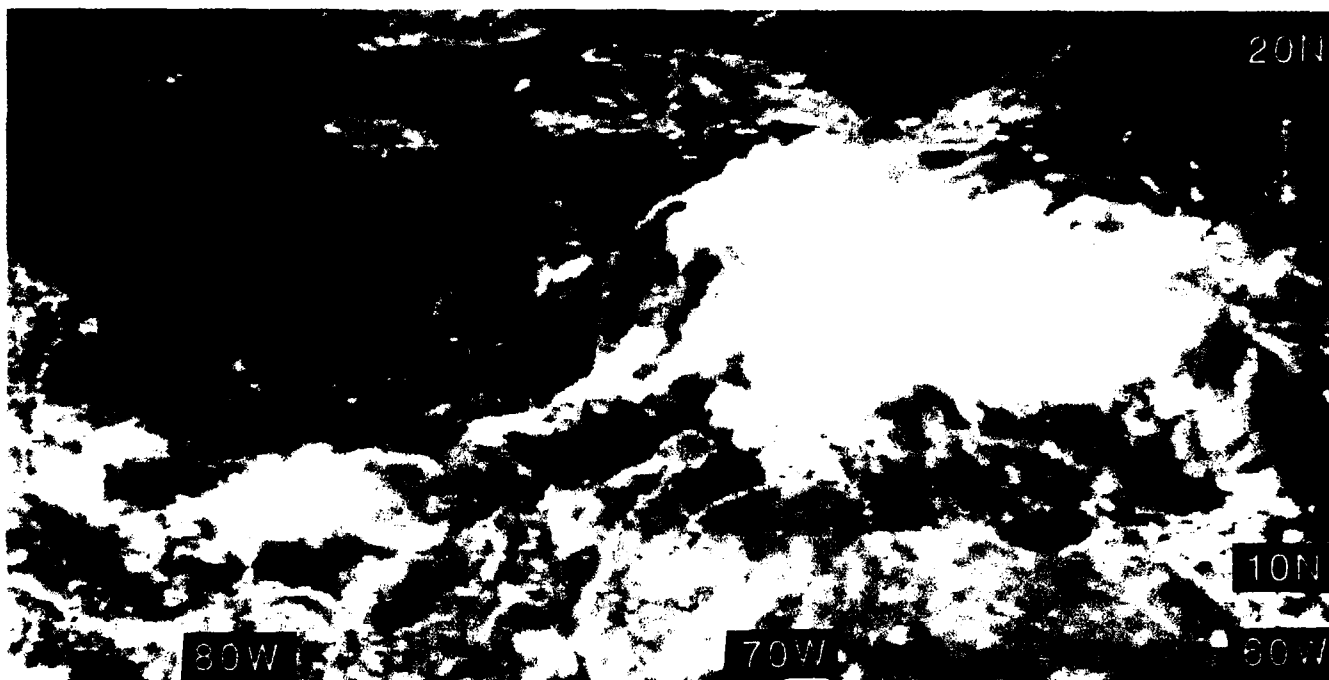


(a)

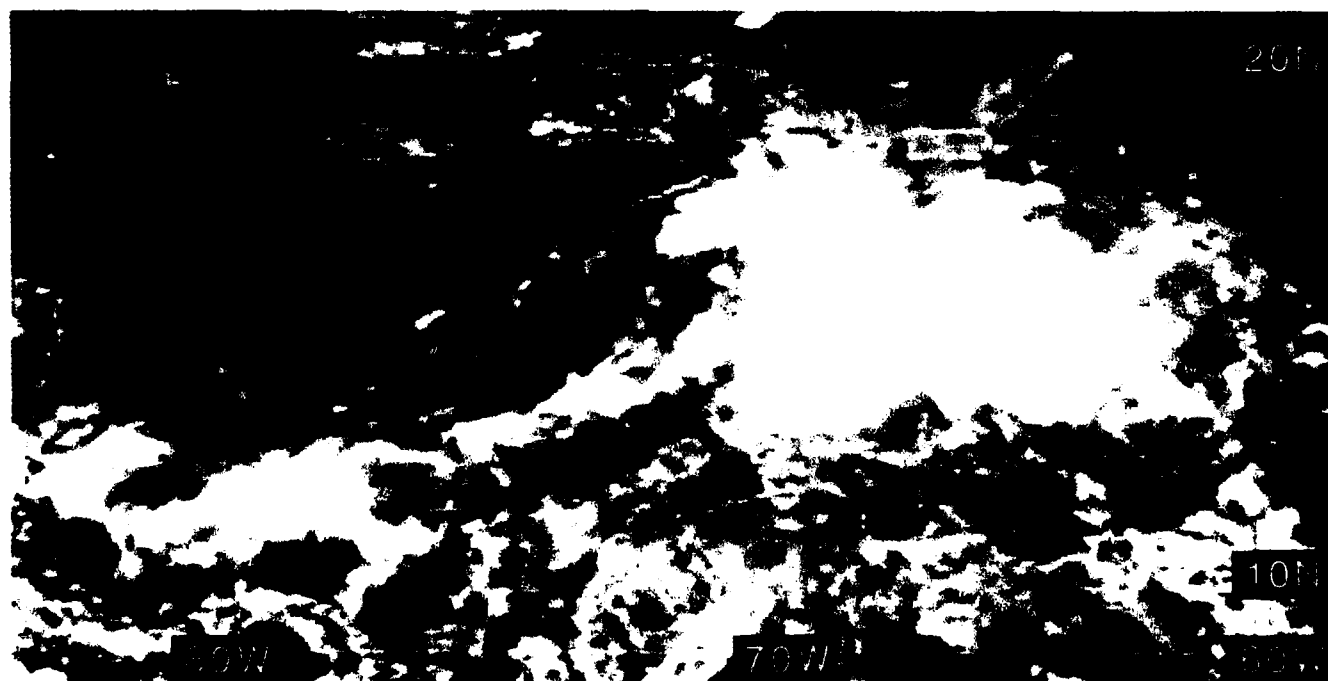


(b)

Figure 2.98: GOES E. Vis. Imag. ("Zoomed"), (a) 1431 / (b) 1531 UTC 2 OCT 1988



(a)



(b)

Figure 2.99: GOES E. Vis. Imag. ("Zoomed"), (a) 1631 / (b) 1731 UTC 2 OCT 1988

1731 020C88 39A-4 00901 15721 EC1

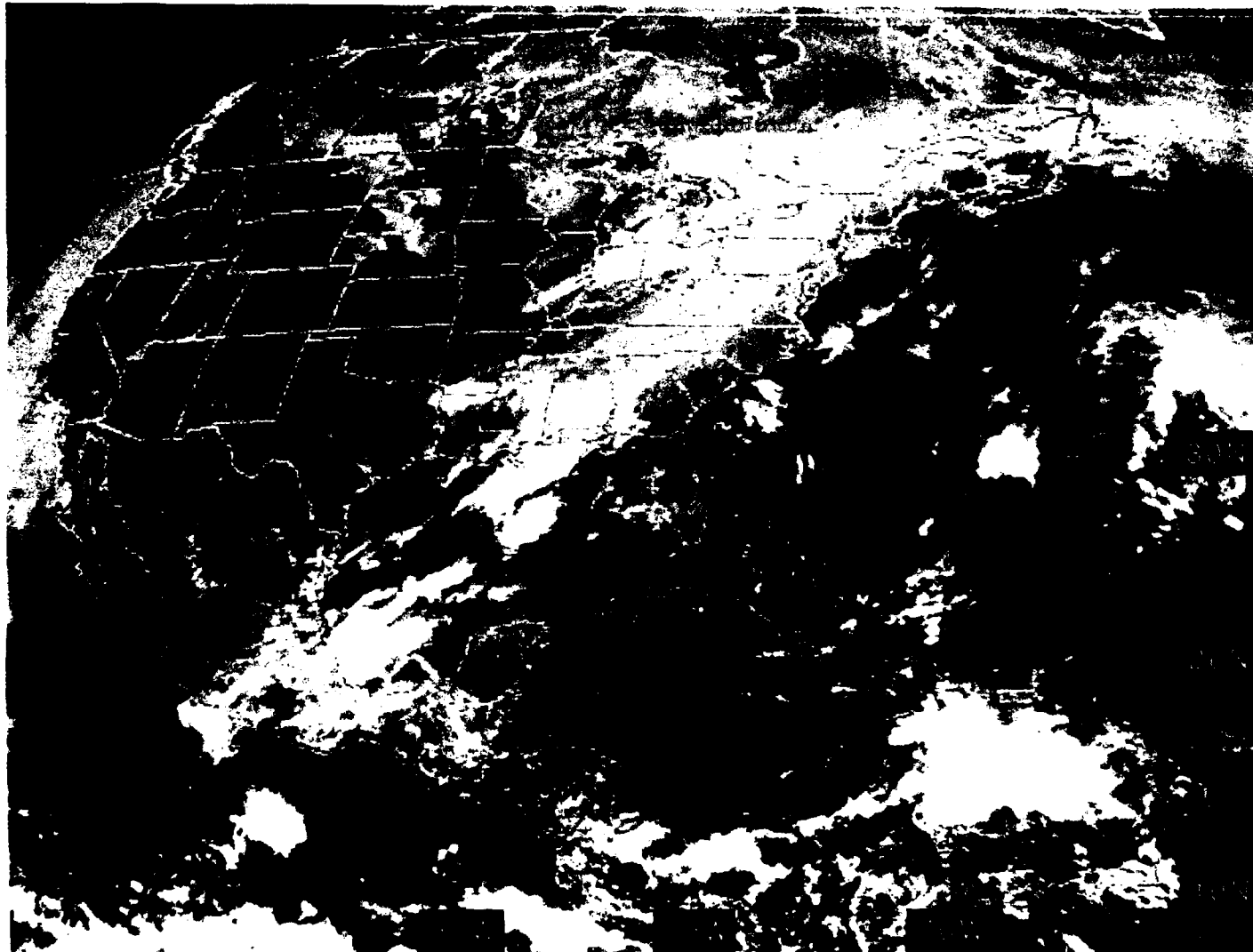


Figure 2.100: GOES East Visible Satellite Imagery, 1731 UTC 2 OCT 1988



Figure 2.101: GOES East Infrared Satellite Imagery, 1701 UTC 2 OCT 1988

1931 020088 39A-4 00902 15701 EC1

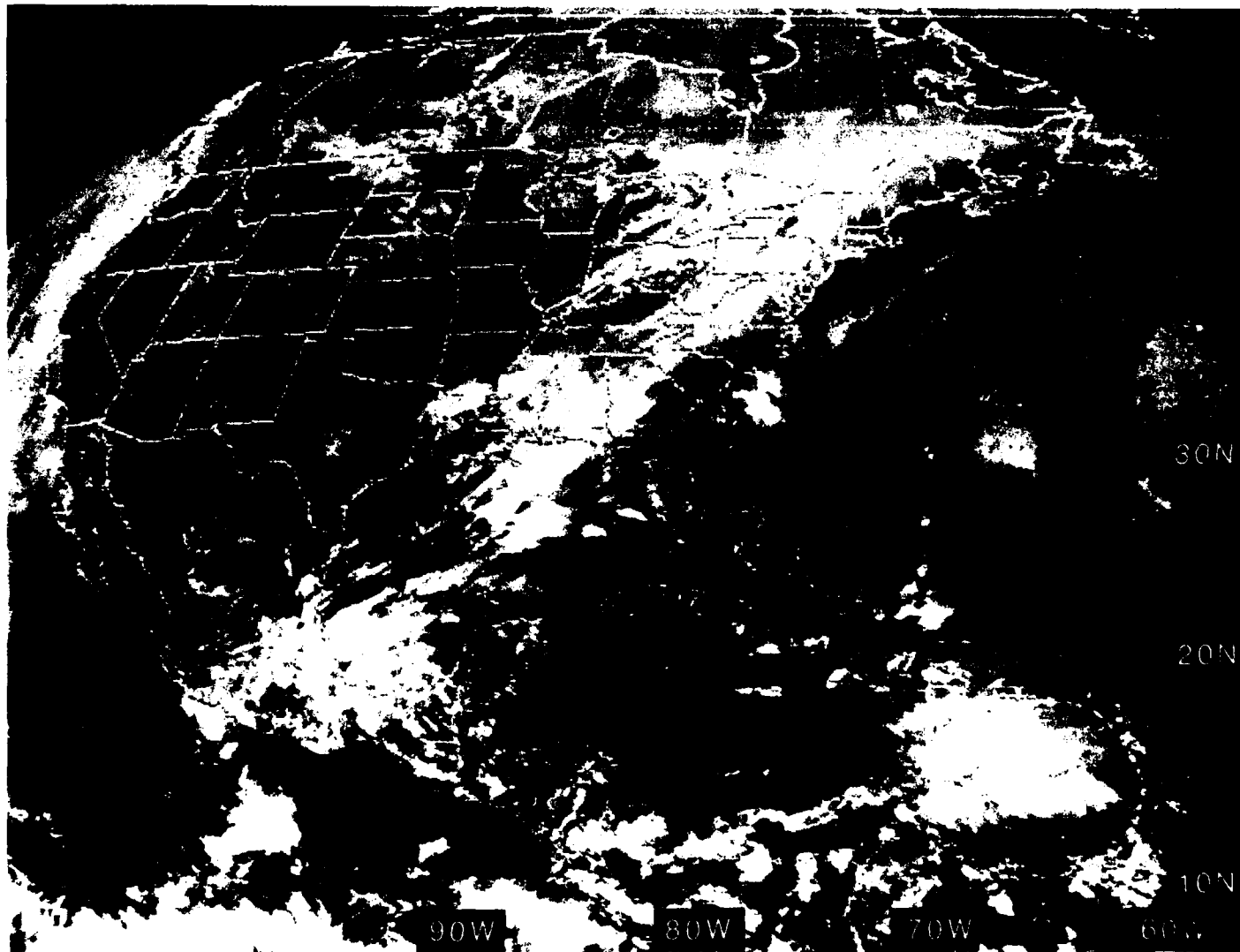


Figure 2.102: GOES East Visible Satellite Imagery, 1931 UTC 2 OCT 1988

2.4 Analysis & Forecasting “Thumb Rules” for the Rainy Season

- Real-time high resolution satellite imagery is currently⁵⁰ the best mesoscale analysis/forecasting tool.
- The NMC ATOLL “low-level” and the NMC 200 mb “upper-level” analyses are excellent tools from which to *start* the analysis/forecasting cycle. (If real-time satellite or conventional data are available, perform local station streamline/isotach analysis, to locate the upper-level divergence and/or low-level convergence. Time cross-sections of available *upstream* radiosonde soundings may also prove helpful in tracking approaching tropical waves.)
- Streamlines sometimes fail to display low-level cyclonic *curvature* at the tropical wave (trough) axis, i.e., the cyclonic vorticity present near the tropical wave axis may be due to *shear* vorticity. While the more classic tropical wave has convective cloudiness trailing (*east* of) the axis, there are instances when instability and convective cloudiness exist both ahead (*west* of) and behind (*east* of) the tropical wave. (Informal communication with the staff of NHC indicates that the 700 mb surface is currently used to track tropical disturbances crossing the North Atlantic Ocean.)
- During the rainy season, in general, some portion of the countries of Central America receive rain every day—even when a tropical wave is distant.
- Anticipate enhanced convection and rainfall at stations when a tropical wave axis arrives at a station. (Their wave lengths and speeds are quite variable and should be calculated by noting their positions for several days *prior* to their arrival at the station or ship.)
- Tropical waves tend to slow their westward propagation when they approach an upper-level trough having strong divergence/diffuence to the east of the trough. (This divergence will enhance convection to the east of the upper-level trough.)
- Enhanced convection⁵¹ (the sea breeze front) often develops during the late morning/early afternoon—due to the cumulative effect of the *easterly* sea breeze and the *easterly* component of the Tradewind—along a north-south axis as the terrain rises about 50 mi inland from the Nicaraguan Caribbean coastline. Its westward progress may slow over mountainous central Nicaragua, but it normally continues to western Honduras and El Salvador during the evening and early morning—assuming the

⁵⁰However, in the near future doppler radar and vertical profilers promise greatly improved analysis.

⁵¹Pearson et al. (1987), in a detailed high-resolution satellite case study, find this occurrence more likely in the late rainy season (August to October). On the North Pacific coast (e.g., El Salvador) where the sea breeze opposes the prevailing easterlies, the convection normally develops later and dissipates in late afternoon.

700 mb wind flow is between 10 and 20 kt and the 200 mb flow pattern displays sufficient ridging/diffuence to support thunderstorm activity (Pearson et al., 1987).

- In the absence of tropical waves and temporals, etc., diffuent sea breezes normally provide clearing in the late morning in the vicinity of the Gulf of Fonseca; however, land breeze confluence enhances convection during the evening and early morning in the same vicinity.
- In addition to the enhanced rainfall attributed to the arrival of tropical waves, "Temporals" cause lengthy and heavy rainfall episodes, mostly near the North Pacific coast of Central America. They last an average of 2 to 3 days with embedded very strong convective activity sometimes accompanied by gale force winds, but without significant electrical activity. Although not discussed in detail in this handbook, the Temporal is expected to move slowly along the North Pacific coast toward the northwest—yet some Temporals are quasi-stationary or may move in another direction. Expect an average occurrence of one Temporal⁵² per year in both September and October, but only one *every two years* in June (Lessman, 1963).
- While the monsoon trough—a line of low-level confluence, frequently with embedded low centers—is normally located on the North Pacific Ocean side of Central America, it occasionally relocates to the western Caribbean Sea producing heavy convection off the east coasts of Honduras, Nicaragua and Costa Rica for several days. With the monsoon trough on the Caribbean side of Central America, *southerly* flow will lead to convection and cloudiness on the southwest-facing slopes and clearing on the northeast-facing slopes of Central America (Pearson et al., 1987).
- Enhanced convection⁵³ can be expected periodically over the warm, shallow Mosquito Banks (east of Nicaragua), as well as in the Gulf of Mosquitos (north of western Panama). Mostly cloudy skies with heavy convection is prevalent over the Caribbean-facing slopes of the Corallera de Talamanca mountains of Costa Rica and western Panama.
- If only NOGAPS analyses are available, synoptic features may be depicted; however, mesoscale features likely will be missing due to the coarse resolution. Improved Navy models are expected in 1989.

⁵²Lessman (1963) reports that rainfall records measured continuous rainfall of up to 426 mm (~17 inches) during ~23 hours which was only part of the whole Temporal during 6 to 8 September 1961. Lessman, in his study of El Salvador and the North Pacific coast, further describes the Temporal as a warm-core low level cyclone, often with its origin linked to the ITCZ or to a resonance depression promoted by a hurricane crossing the western Caribbean Sea.

⁵³See Appendix B for coastal stations bordering the Mosquito Banks, such as Bluefields, Nicaragua, exhibiting inordinately high rainfall totals during the rainy season.

3. THE DRY SEASON

3.1 General

In a manner similar to the previous section on the rainy season, this section will examine analyses for the "dry season" (November through April⁵⁴). The selection of these months—relatively dry over the majority of Central America—does not negate the relatively large rainfall at several Caribbean coastal stations (e.g., La Ceiba, Honduras; Bluefields, Nicaragua and Changuinola, Panama) due to the strong onshore tradewind flow during November, December and January. A quick examination of rainfall totals at representative stations in subsection 1.3 will support the identification of these months as the dry season—especially in Guatemala, El Salvador and Honduras. While transition months have been identified for Nicaragua, satellite observations verify the relative minimum of convection over Central America, as a whole, from November through April.

3.2 Fronts or "Shear Lines"

Since air mass thunderstorms are relatively infrequent during the dry season in Central America, fronts (and dissipating fronts) penetrating from North America and the Gulf of Mexico are important sources of precipitation in the tropics—especially from northern Nicaragua poleward. Since the across-the-front surface temperature and dewpoint contrast normally becomes very small or obliterated by the time the front reaches Central America, only a shear line⁵⁵ (or "shear zone") may be present (Atkinson, 1971). However, its passage may be associated with a squall line, gale force winds, torrential rains and *occasionally* extreme temperature fluctuations.

DiMego et al. (1976), in a study of the period 1965–1972, found that the number of fronts penetrating equatorward to Belize and northern Guatemala increases from one per month in October to a maximum of four per month in January (see Fig. 3.1). In January, on the average, three extratropical fronts penetrate as far equatorward as southern Belize and central Guatemala, two into Honduras and one to southern Nicaragua. Between June and September less than one front per month reaches as far south as Belize; however, this

⁵⁴See subsection 2.1 for the discussion concerning selection of months for the dry season.

⁵⁵A line or narrow zone across which there is an abrupt change in the horizontal wind component parallel to this line...(Huschke, 1959).

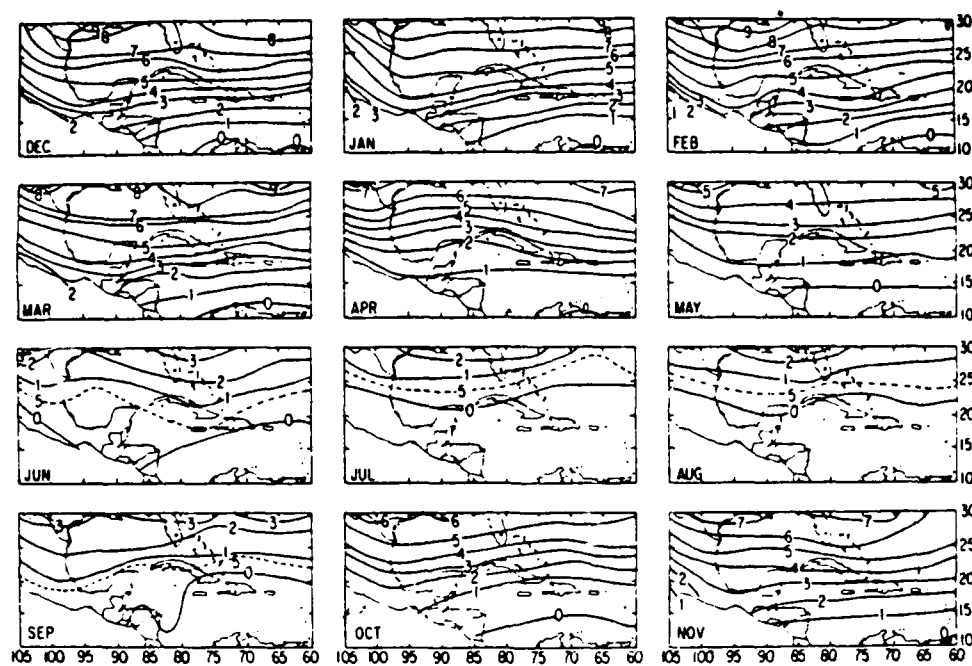


Figure 3.1: Mean-Monthly Frequency of Frontal Systems for the 1965–1972 Period, Expressed as the Number of Frontal Passages per Month (from DiMego et al., 1976).

study was based on NMC hemispheric analyses which often terminate the existence of fronts which are *still* carried on regional⁵⁶ analyses (Henry, 1980). The study also found that during the months of July and August, no front penetrated Central America during the 1965–1972 period—coinciding with the retreat of the temperate westerlies to Canada, along with the cyclones and upper-level waves required to initiate and sustain cold front penetrations. However, a northern hemisphere winter having mid-latitude westerlies which reach abnormally far southward will produce frontal passages reaching deeper into Central America than during winters when the polar front jet is not so far south. DiMego et al. (1976) found a strong correlation between periods of frequent frontal penetrations and periods⁵⁷ during which the mid-latitude westerlies are situated over southern latitudes—that is, periods with a low-latitude zonal jet stream implying that cyclones and their accompanying frontal systems are already in close proximity to the tropics. In a separate study, Henry (1979) found that from 1967–1977, during the period of greatest activity (November–February), that more than 60% of the fronts entering the Gulf of Mexico (from the north or west) continue equatorward and enter the Caribbean Sea. Also, while dry season “winter” fronts normally have a NE to SW orientation, the “summer” season fronts are almost east to west and generally reach no further than *just south of* Cuba or the northern Yucatan Peninsula.

⁵⁶Analyses performed within one of the Central American countries.

⁵⁷Or periods during which westerly streamlines are highly amplified, i.e., strong meridional currents are present.

DiMego et al. (1976) also noted that a large frontal *duration*⁵⁸ coincided with an unusual anomaly in rainfall along the northern coast of Honduras. This feature was attributed to the presence of both the coastline and an inland mountain range oriented from east to west where heavy rainfall is present in the late "fall" and early "winter". This relationship is found also, to varying degrees, for the northern slopes of other east-west mountain ranges in Central America. The study further describes frontal passages, near Central America, which have characteristics different from those of mid-latitude regimes. Radiosonde data were used to construct time-sections. Fig. 3.2 displays time cross sections for the following *three* groups of stations (number of cases in parentheses): Group 1, Merida, Mexico (27) and Havana, Cuba (19); Group 2, Guantanamo, Cuba (11), Sabana de la Mar, Dominican Republic (12) and Kingston, Jamaica (9); and Group 3, Grand Cayman (11), Swan Island (14) and San Andrés (6). Note that while Groups 1 and 2 are to the north or northeast of Central America, Group 3 contains island stations very near Central America—Swan Island is ~90 n mi from northeastern Honduras and San Andrés Island is ~90 n mi from the central Caribbean coast of Nicaragua. Thus, the time-sections of Group 3 are *more* applicable to frontal passages over Central America. In Fig. 3.2, time 5 represents the first radiosonde sounding *after* the actual passage of the cold front, bracketed by four reporting times *before* and four reporting times *after* the frontal passage (at 12-h intervals). Averaging pressure, temperature and dew points for all fronts for each of the three groups of stations yielded *mean* data in centered time-section form.

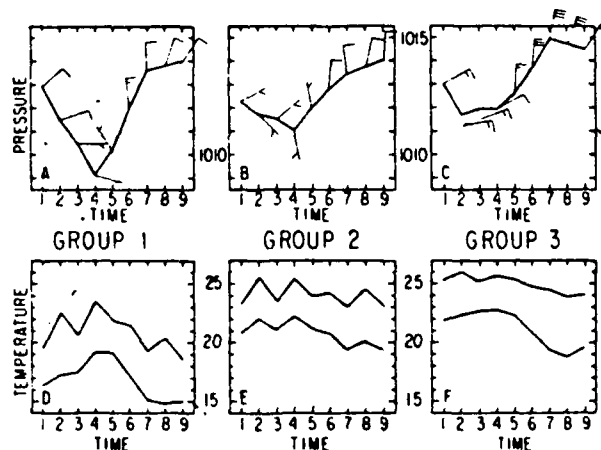


Figure 3.2: Centered Time-Sections of Surface Parameters (during Frontal Passages) for Group 1 (A & D), Group 2 (B & E) and Group 3 (C & F). Surface pressure (mb) is plotted in the upper graphs (A-C) with surface winds plotted at the data points (full barb equals $5 \text{ m}\cdot\text{s}^{-1}$). Temperature and dew point ($^{\circ}\text{C}$) are plotted in the lower graphs (D-F) (from DiMego et al., 1976).

⁵⁸The average number of six-hour periods that each front remained within a $2.5^{\circ}\text{lat} \times 2.5^{\circ}\text{long}$ grid box.

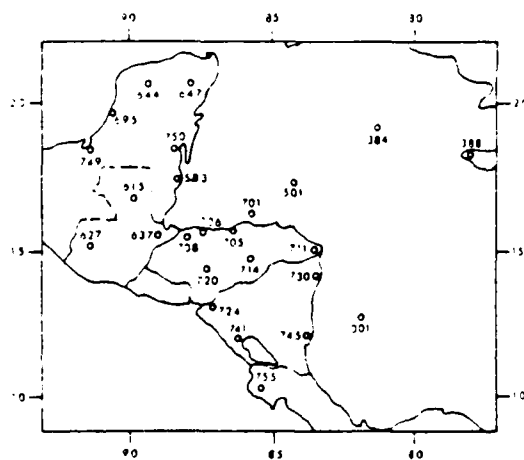
Note that the surface pressure for Groups 1 and 2 falls steadily while the frontal trough approaches, then rises rapidly after the frontal passage—much like that expected of extratropical fronts. However, for Group 3, the pressure reaches a minimum at time 2 (>24 hours before arrival of the front), holds steady until the front passes, rises sharply to time 7 and begins to fall again.

DiMego et al. (1976) also examined isentropic surfaces during a composite case of frontal passages (not shown). Their study concluded—despite the presence of such a trough in other studies—that the tendency for a trough to run ahead of the front in the western Caribbean is *not* clearly evident. Rather, it appears to coincide with (or is overshadowed by) development of an *inverted* trough. Note that the pressure oscillation is greatest for Group 1, with a weakening of the pressure gradient across fronts as they progress farther east and south in the area of Groups 2 and 3. Surface winds for all three groups *back* with time and *increase* in speed in the post-frontal period. In particular, note that *all* groups record an abrupt wind shift to north or northwest with the passage of the front.

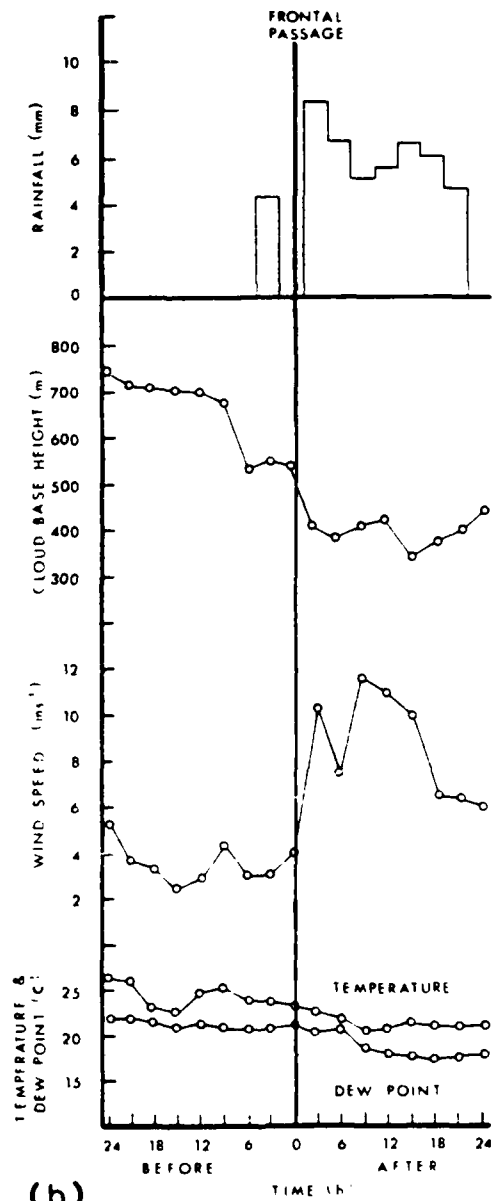
Aside from diurnal variations, surface temperatures increase at Group 1, but remain relatively steady for Groups 2 and 3 prior to arrival of the front (see Fig. 3.2). The cooling is nearly linear after frontal passage for Group 3 (western Caribbean Sea). Also note the decrease in the temperature gradient across fronts in Groups 2 and 3 as compared with fronts farther north and west in Group 1, i.e., the frontal temperature discontinuity *decreases* as the fronts progress southward and eastward. Cloudiness leads to much of the cooling at Groups 2 and 3. The dew-point temperature, which generally rose during the pre-frontal period, falls for ~24 h following passage of the front. The dew point then recovers after time 7 or 8—indicating the effect of warm underlying waters in the Caribbean Sea on the cool dry air mass. The study also indicates that the trade-wind inversion may actually disappear during the pre-frontal period (near time 2 or 3) and then reintensify by time 7 or 8, i.e., about 36 hours after passage of the front as more stable conditions return (DiMego et al., 1976).

3.2.1 Frontal Passage over Coastal Honduras

In a study by Ladd and Henry (1980), the fluctuations in various meteorological parameters during *five* frontal passages along the northern coast of Honduras were examined. While the air-mass modification often masks the characteristics of the approaching air mass, a composite analysis based on mean values of the parameters from the five frontal episodes for *four* stations was prepared. The four stations are Guanaja, Honduras (station 78701)—actually an island station ~25 n mi offshore—; La Ceiba, Honduras (station 78705); Tela, Honduras (station 78706) and San Pedro Sula, Honduras (station 78708) (see Fig. 3.3a).



(a)



(b)

Figure 3.3: a. Distribution of Surface Stations in Honduras and Vicinity.
b. Composite Analysis of Mean Changes in the Various Parameters at four stations (701, 705, 706 and 708) in Honduras in November 1975 (from Ladd and Henry, 1980).

Figure 3.3b represents a model of variations⁵⁹ in the parameters accompanying frontal passage for coastal Honduras. Note that rainfall proves to be one of the best indicators of frontal passage, i.e., almost all of the rainfall associated with these frontal systems occurs in the "cold" air behind the surface frontal boundary. Low cloud base heights show marked decreases before and after frontal passage. Additionally, this lowering of cloud base heights is accompanied by a change of cloud type from cumuliform to stratiform clouds. Unlike the study by DiMego et al. (1976), the wind direction in this study shows little or no systematic variation during the frontal episode; however, changes in wind *speed* are very noticeable. Note in Fig. 3.3b, that wind speed increases very rapidly after frontal passage and maintains high values for approximately 12 hours—wind speeds as high as $15 \text{ m}\cdot\text{s}^{-1}$ ($\sim 30 \text{ kt}$) were observed in a few of the frontal passages. Although there is slight, but continual, decrease in the temperature and dew point, these two parameters are not as useful as the previous three (Ladd and Henry, 1980).

To provide an appreciation for a frontal episode, Fig. 3.4 is presented. This figure shows the frontal passage on 14 November 1975 which was deemed representative of the five cases studied (Ladd and Henry, 1980).

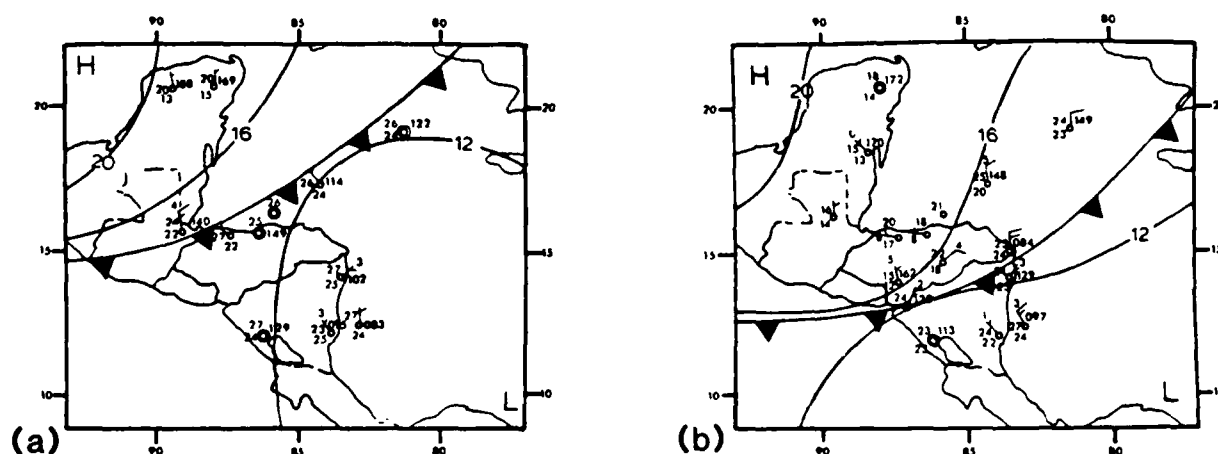


Figure 3.4: Frontal positions for (a) 0000 UTC on 14 November 1975 and (b) 1200 UTC on 14 November 1975 (from Ladd and Henry, 1980)

⁵⁹As a result of the smoothing process used, the first and last points of the profiles were eliminated (Ladd and Henry, 1980).

3.2.2 Frontal Passage over Belize

In a study by Horvath and Henry (1980), meteorological parameters were sought which

1. would indicate a frontal passage over Belize and
2. are precursors of fronts.

As expected, the standard criteria associated with mid-latitude frontal passages are not found in Belize—yet significant local weather changes were observed.

The study examined 3- and 12-hour surface observations from the Belize International Airport (station 78583 (station 583 in Fig. 3.3a), International Civil Aviation Organization Identification: MZBZ). The station has relatively flat terrain to the north and west, i.e., the directions from which the fronts approach. The data used were from the years 1969 to 1978 for the months of November through March.

Table 3.1 shows the frontal criteria using 12-h interval data, Table 3.2 shows the frontal criteria using 3-h interval data for 8 cases during the years 1975–1978 when the observations were recorded in a more continuous manner, while Fig. 3.5 shows the composite graph for a 48-hour period, centered on frontal passage time and using data points for every 3 hours. In this study, Horvath and Henry (1980) found that *only* 1 cold front per month, *on the average*, passed Belize International Airport during the months of November through March. Note that this is fewer than found by the study of DiMego et al. (1976), discussed earlier in Subsection 3.2.

While all the data were summed and averaged, it should be noted that of the eight cases that were examined, six occurred approximately at sunrise so that much of the cooling prior to the front is nocturnal. While both temperature and dew-point temperature decreases after the front passes, equivalent temperature⁶⁰ (T_e) decreases in a more distinct manner, *especially* at the time of frontal passage. A specific pattern for low cloud base height could not be determined as for nearby coastal Honduras in Subsubsection 3.2.1. Generally the cloud bases at ~900 m lower somewhat (0–300 m) during the 6-hour period following frontal passage. Also note in Fig. 3.5 that the pressure rises steadily from a weak minimum 21 hours before frontal passage. Rainfall starts *just* before the arrival of the front; however, its maximum value occurs just after the front passed. The wind shift is very obvious, changing from calm (where 1 kt winds were considered calm) to a speed of 5–10 kt from a northerly direction.

After examining all frontal passages in the 9-year period of study, the items in Tables 3.1 and 3.2 are listed in order of importance. The decreases of the equivalent temperature (T_e) of the magnitude listed in Table 3.1 are expected with about 60% of the fronts.

⁶⁰Equivalent temperature—"The temperature that an air parcel would have if all water vapor were condensed out..." (Huschke, 1959)

Table 3.1: Time Changes of Weather Elements with Frontal Passage at Belize using 12 h data (Horvath and Henry, 1980)

1. Wind shifts to a northerly direction and increases speed
2. Pressure rises 4 mb in 12 h
3. T_e decreases 5 K in 12 h T_e decreases 10 K in 24 h T_e decreases 10 K in 36 h

Table 3.2: Time Changes of Weather Elements Occurring with Frontal Passage at Belize using 3 h data (Horvath and Henry, 1980)

1. Wind shifts to a northerly direction and increases speed					
Time changes for other parameters:					
		3 h before to 3 h after	6 h before to 6 h after	9 h before to 9 h after	12 h before to 12 h after
2. Pressure rise (mb)		2	4	5	6
3. T_e drop (K)		10	10	12	12
4. Precipitation	before after	none prob. rain	prob. drizzle prob. rain	prob. drizzle none	none none
5. T_d drop ($^{\circ}\text{C}$)		2	4	4	4
6. Sky cover amount	before after	scattered broken	broken broken	broken broken	scattered broken

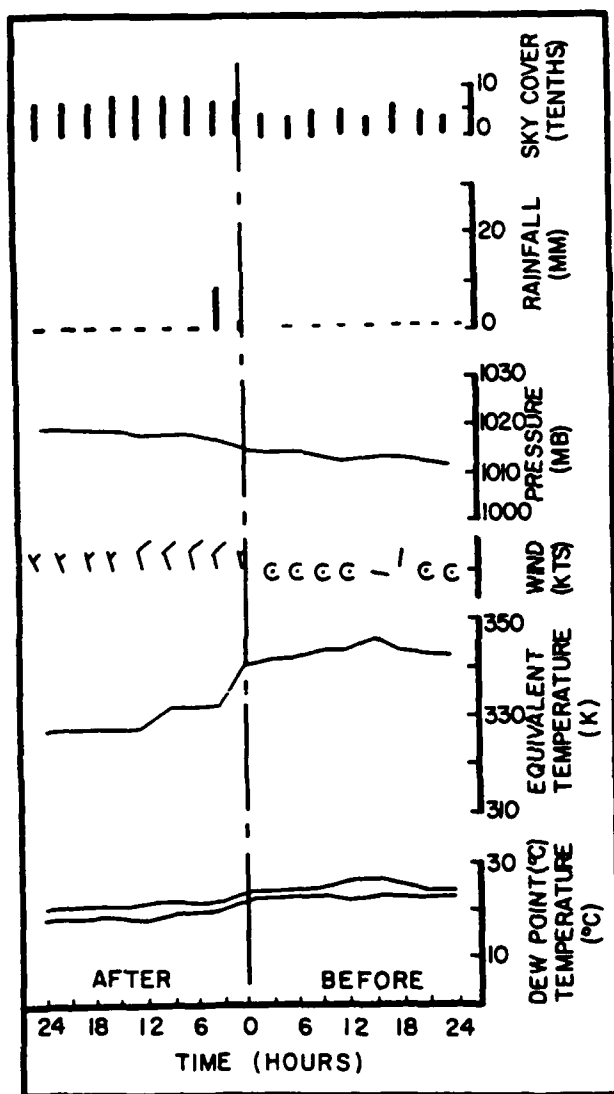


Figure 3.5: The Graph of Mean Parameters, before and after a Frontal Passage in Belize (- means zero value). (from Horvath and Henry, 1980)

Finally, the study provided a *very* limited forecasting rule. An initial surface pressure drop was followed by a *rising* trend which starts 6–18 hours before the front passage—plus, fog, drizzle, haze, rain or rain showers *often* occur in the period 3–15 hours before frontal passage. The study also found that on the average, NMC misses about 50% of the fronts that move through Belize—NMC appears to have considered some of the rain producing events as simply “rainbands” (Horvath and Henry, 1980).

Currently, the forecaster will certainly use visible and infrared satellite imagery to locate fronts approaching Central America, and then extrapolate their future movement, as applicable.

3.2.3 Atemporalado—with a Forecasting Index

Although the preceding subsections have associated the rainy episodes in Honduras and Belize⁶¹, during the dry season, with the arrival of mid-latitude cold fronts or “northers”, both operational forecasters and researcher often refer to these episodes as “Atemporalados”⁶². Ladd and Henry (1980) define the Atemporalado as “...a term used in Central America to describe a rain event occurring during the early winter. A light rain falls from stratus clouds and may have a duration of 12–15 hours. The activity is caused by a cold front”.

Using data from the dry seasons of 1983–84 and 1984–85, Brooks (1985) has produced a simple index to aid forecasters in predicting the rate of movement of cold fronts (or Atemporalados) into Central America. Not only may restricted ceilings and low visibilities affect aviation operations in Honduras for periods greater than 24 h during an Atemporalado, but destructive winds have been observed at elevated stations in Central America during Atemporalado episodes. The use of the index can assist the forecaster in timing the arrival of the front or shear zone, as well as indicate whether or not it is expected to continue southward, even past Nicaragua, to Costa Rica and Panama.

While Subsubsection 3.2.1 has discussed the effects on precipitation, cloud base height and wind speed of cold fronts arriving in Honduras from the north, it was also noted that these phenomena are often labeled shear lines (or shear zones) since the thermal characteristics of the cold air are often modified during overwater trajectory.

Modifying a shear line model from a study over the central North Pacific by Palmer et al. (1955), Brooks (1985) provided a streamline and isotach configuration applicable to Central America (see Fig. 3.6). This model depicts the shear line defined by the convergent asymptote *west* and equatorward of the neutral point in the streamlines, while the front is depicted by the convergent asymptote *east* and poleward of the neutral point. The colder air is deflected (or funneled) toward the south by the Sierra Madras mountains of Mexico and then “backed” by surface friction to produce *northwesterly* winds rather than the *northeasterly* winds depicted by the streamlines northwest of the Yucatan Peninsula in Fig. 3.6. Note the increase in wind speed depicted by the isotachs “behind” the shear line. (Brooks defines the shear line as the *leading* edge of the shear zone.) Relatively weak, convergent flow and *cumuliform* clouds are found on the equatorward side of the

⁶¹The northward facing slopes of the central Guatemalan highlands also receive the cloudiness and precipitation of approaching cold fronts during the dry season; however, no study will be presented for Guatemala as was done for Honduras and Belize in the previous two subsubsections.

⁶²It should be noted that the term “Atemporalado” is used by the Central American countries referring to its relation to the more *intense* “Temporal”. The Temporal is described as a *rainy* season phenomenon having persistent rainfall for several days (see page 78).

shear line, with stronger convergent flow (capped by an inversion) and stratiform clouds on the poleward side. Occurring between November and March, an average of 6 shear line occurrences per season may be expected during relatively warm *Northern Hemisphere* winters, contrasted to as many as 18 in an unusually cold winter (Brooks, 1985).

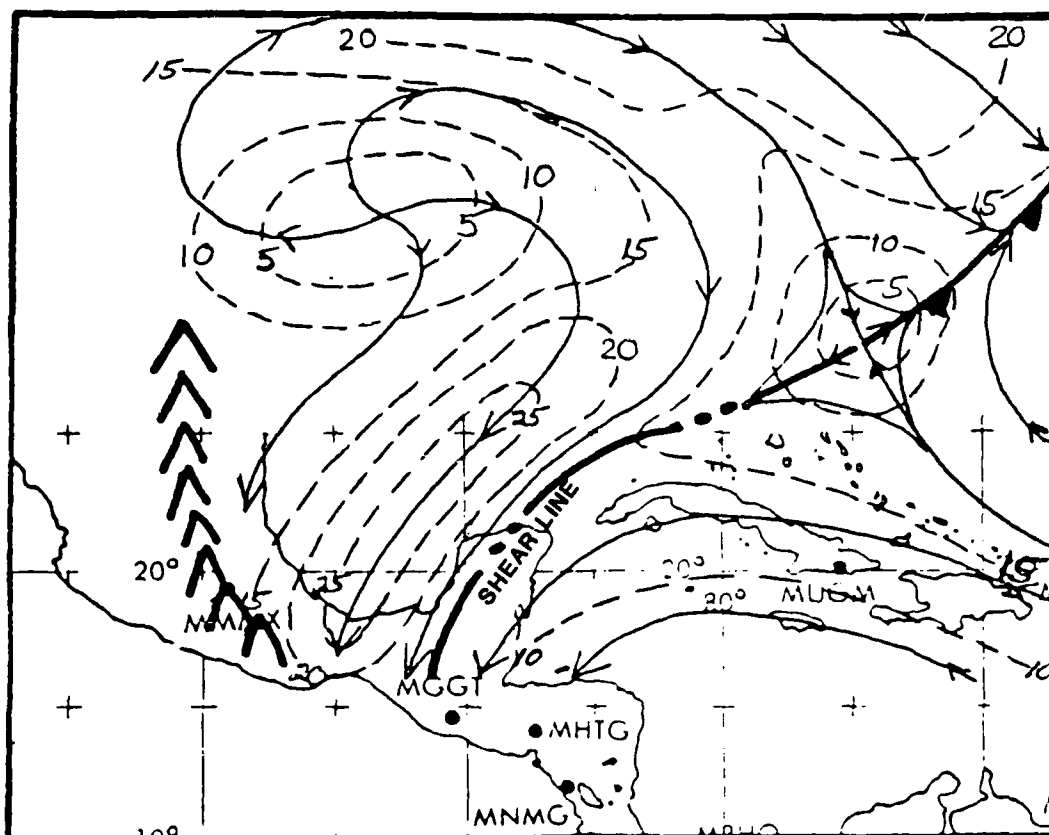


Figure 3.6: Palmer Model Adapted to the Cold Surge over the Gulf of Mexico or Caribbean Sea, Depicting the Associated Surface Streamline/Isotach Pattern. Streamlines—solid (arrows). Isotachs—dashed (kt) (from Brooks, 1985).

The prediction method of Brooks (1985) was adapted from a forecast technique developed by Riehl (1968) for predicting cold surges during the northeast monsoon over the South China Sea (and westward into the mountains of Vietnam). The cold surges which produce low ceilings over the northern South China Sea and poor weather enhanced by the upslope conditions over coastal Vietnam are similar to the effects of shear lines (or shear zones) moving from the Gulf of Mexico toward the mountains of Honduras. Similarly the “downslope” drying conditions over the interior of Southeast Asia are similar to those found for shear lines reaching El Salvador or the North Pacific coastline.

Following Riehl’s method of using a surface pressure differential between Hong Kong (22°N, 115°E) and a poleward point at 30°N, 115°E, Brooks (1985) chose Merida, Mexico (station 76644) at 20.9°N, 89.5°W for his equatorward point. However, since the configura-

tion of the surface high pressure dome entering the Gulf of Mexico is distorted equatorward by the channeling effect of the Sierra Madre mountain barrier of Mexico, Brooks's method selects the poleward pressure from the following western Gulf of Mexico station (i.e., to the northwest of Merida) producing the *largest* sea-level pressure difference with Merida, Mexico:

1. Houston, TX (station 72243) at 30°N, 95.5°W or,
2. Brownsville, TX (station 72250) at 26°N, 97.5°W or
3. Tampico, Mexico (station 76548) at 22.3°N, 97.8°W.

For example: A cold air mass with high sea-level pressure (e.g., 1025 mb) over Houston, TX with a lower sea-level pressure at Merida Mexico (e.g., 1010 mb) would provide a +15 mb pressure differential—i.e., the **INDEX = +15 mb**. During the period of study, pressure differential values ranged from -15 to +25 mb. Significant pressure gradients (>10 mb) between Merida, Mexico and Texas (or the adjacent Mexican coastline) developed earlier (sooner) than between Merida and New Orleans (30°N, 90°W), which is directly north of Merida (Brooks, 1985).

FORECASTING ASSOCIATIONS USING THE INDEX

Examining the index (i.e., the pressure differential) values when a shear line is progressing across the Gulf of Mexico provides an indication of the weather conditions expected **24 h later** in Honduras. The following associations were derived (verbatim from Brooks, 1985):

1. **NO SURGE - INDEX LESS THAN 12 mb:** Shear zone becomes quasi-stationary northwest of Central America, either in the Gulf of Mexico or across the Yucatan Peninsula.
2. **MARGINAL SURGE - INDEX 12–14 mb:** Shear zone at the northern coastal areas of Honduras approximately 24 h later but advances no farther. Associated weather *less* intense than with a nominal case described in 3. below.
3. **NOMINAL SURGE - INDEX 15–19 mb:** Shear zone moves into central Honduras ~24 h later. Weather conditions expected during the onset:
 - (a) Moderate to strong north-northwest surface winds gusting from 20 to 30 kt (10 to $18\text{ m}\cdot\text{s}^{-1}$) across most of Honduras with the strongest low level winds on the north coast for a period of 12–24 hours after the passage of the leading edge of the shear zone;
 - (b) Low stratiform ceiling ranging from 300–500 feet (90–150 m) on the northern coast of Honduras to 1500–2000 feet (450–600 m) over the interior valleys;
 - (c) Continuous light rain (occasionally moderate or heavy)

- (d) Very strong winds gusts of up to 80 kt ($40 \text{ m}\cdot\text{s}^{-1}$) with cloudy conditions expected at higher elevations well into the interior of central and even southern Honduras;
- (e) A foehn or drying effect on the leeward slopes of the continental divide, with clearing conditions over most of El Salvador and the west coast of Central America.

(After the shear zone arrives, expect it to progress through Honduras and then become quasi-stationary on the northeast Honduras-Nicaragua border. Dissipation will follow in 48-72 hours.)

4. **STRONG SURGE - INDEX 20 mb OR GREATER:** Shear zone moves into central Honduras ~24 h later. These strong shear zones will continue to move through Central America rather than becoming quasi-stationary at the northeast border of Honduras and Nicaragua, as described in the nominal case. These strong cases will advect enough cold air to the south to cause cold air stratiform clouds to pile up against the mountains on the east coast of Costa Rica and the north coast of Panama 48-72 h after the index reaches 20 mb or more. The shear zone will then become quasi-stationary and dissipate in eastern Panama.

The index is not meant as a hard and fast rule, but rather as a guideline or tool for operational forecasters. Diurnal and topographic effects must also be considered for specific locations (Brooks, 1985).

Additionally, it was noted, by one of the authors, during the dry season of 1987-88 that the FNOC-produced Navy Operational Global Atmospheric Prediction (NOGAPS, model 3.0) **24-h prognosis** of winds and streamlines at 925 mb (~1000 m) accurately predicted shifting of the wind direction and strengthening of winds following the passage of shear lines over Honduras and Nicaragua. Continued improvements⁶³ in both the FNOC tropical analysis and prognosis is expected with the improved radiation package of NOGAPS 3.1 and the improved resolution of NOGAPS 3.2.

Although the area is west of Central America, forecasters must be alert to phenomena occurring in the Gulf of Tehuantepec (~15°N, 95°W). Following the passage of cold fronts into Central America, northerly or northeasterly winds accelerate as they pass through the Mexican Isthmus of Tehuantepec and descend over the North Pacific Ocean. Winds (40 kt and higher), haze, increased sea heights and squall lines often result (see Naval Western Oceanography Center (1989) and Fett et al. (1977)). During the winter of 1989, on at least one occasion, the NOGAPS low-level wind 24-h prognosis accurately predicted such an event. Following an analysis of light winds (~10 kt) over the Gulf of Tehuantepec, a prognosis of northerly winds (~50 kt) verified.

⁶³NOGAPS 3.1 became operational on 15 March 1989 and NOGAPS 3.2 is expected to become operational later in 1989.

3.3 Case Studies during the Dry Season

3.3.1 Case III - Cold Front Passage (12 – 15 December 1988)

This case study ⁶⁴ examines the progress of a cold front or shear line over the Yucatan Peninsula moving toward Guatemala, Belize and Honduras. With only a 10 mb pressure difference between Tampico, Mexico (station 76548—1028.1 mb) on the western coast of the Gulf of Mexico and Merida, Mexico (station 76644—1018.5 mb) at 0000 UTC 13 December 1988 (see Fig. 3.15), the Brooks Index labels this event as **below** the “Marginal Surge” (see Subsubsection 3.2.3) which requires a 12–14 mb pressure difference.

12 December 1988

Figures 3.7 and 3.8 depict low-level analyses as received from Fleet Numerical Oceanography Center (FNOC) at 0000 UTC on 12 December 1988 which was during the early portion of the dry season. While the expected northeasterly flow is present over Honduras and Nicaragua—so typical of the dry season—, note the *north-northwesterly* flow over the western Gulf of Mexico. Also, compare the streamline pattern near the Yucatan Peninsula in the discontinuous streamlines⁶⁵ produced by FNOC (Fig. 3.8) with the streamlines and “shear line” configuration of Fig. 3.6 (Subsubsection 3.2.3). While Fig. 3.6 is more typical of a “stronger” surge and has its neutral point north of Cuba, Fig. 3.8 has similar asymptotes, with its neutral point over the Yucatan Peninsula. Although not shown, the FNOC 200 mb wind barbs show strong southwesterly flow from Guatemala, over the Yucatan Peninsula, to Cuba, with a high center located over the southern Caribbean Sea just north of Venezuela. (With the onset of the dry season—when the strong baroclinic zone of the Northern Hemisphere winter often pushes south to Mexico—, strong southwesterly flow exists aloft over Central America almost every day.)

13 December 1988

Figure 3.9 shows the visible image 3 1/2 hours before the synoptic-time IR imagery of Fig. 3.10 at 0000 UTC on 13 December. Figure 3.9 depicts the low-level cloudiness which has filled the Bay of Campeche (west of the Yucatan Peninsula)—a quick reference to Fig. 1.2 will confirm the containment of this *low* cloudiness by the Mexican terrain. Both figures indicate the presence of the shear line (or cold front) from the northeastern Yucatan Peninsula southwestward to near the Gulf of Tehuantepec on the Mexican Pacific coast, i.e., the associated cloudiness is on the poleward side of the shear line. The NMC low-level ATOLL streamlines of Fig. 3.11 appear to place the shear line farther south (near the northern border of Belize), while the upper-level streamlines of Fig. 3.12 agree well with the alignment of the streaks of cirrus (light grey imagery) in Fig. 3.10. The NHC sea-level pressure analysis (not shown) locates the cold front (with several waves near

⁶⁴See Subsection 2.3 for descriptions of the analyses and imagery used in the case studies.

⁶⁵The streamlines produced by FNOC do not include “neutral points”, but they can be visualized by the experienced analyst.

Florida) lying through the northeastern tip of the Yucatan Peninsula to the northwestern corner of Guatemala to the Gulf of Tehuantepec. (Since this event is classified *below* the marginal surge, the upper-level mid-latitude trough is of small magnitude extending from the southeastern United States southwestward to *only* the center of the Gulf of Mexico in Fig. 3.12).

The FNOC low-level analyses of Figs 3.13 and 3.14 agree well with the NMC Fig. 3.11 for the same time, i.e., placing the shear line from central Cuba to Belize. The station reports at 0000 UTC on 13 December in Fig. 3.15 confirm the arrival of the low cloudiness and cooler temperatures behind the shear line, i.e., note the 21°C and overcast conditions⁶⁶ reported at Merida (station 76644) on the northwest tip of the Yucatan Peninsula. Warmer temperatures are found *ahead* of the approaching shear line, with 28°C, 5/10 cloud cover and a rain shower reported by Belize City (station 78583).

14 hours later, the visible imagery of Fig. 3.16 shows the leading edge of the low-cloudiness (behind the shear line) having advanced to the center of the northern Honduran coastline, while its southern progress is slowed by the mountains of southern Guatemala and Honduras. Figure 3.17 provides an excellent example of the use of IR imagery in identifying the portions of the cloudiness which are cirrus clouds (*ahead* of, and unassociated with, the approaching shear line), i.e., extending from eastern Honduras to southern Cuba. (Although the imagery of Fig. 3.17 is 12 hours after the 200 mb streamline analysis of Fig. 3.12, the cirrus streaks in the satellite imagery follow the general configuration of the 200 mb streamlines in Fig. 3.12.)

Figure 3.18 shows the 1200 UTC 13 December radiosonde sounding (T and T_d) from Belize City (**solid lines**). Note that the *morning* temperature is ~21°C, with a **northerly** surface wind (plotted second from right on the figure), and that the lower tropospheric cloudiness, (identified by the dewpoint temperature trace (on the left)) consists of two layers of clouds, a lower layer with its top near 925 mb and a thicker layer between ~825 mb and ~725 mb, during the passage of the shear line. The faint white imagery near Belize City on Fig. 3.17 correlates well with the increased moisture near 430 mb on Fig. 3.18, i.e., the existence of a very thin cirrus cloud is supported.

For comparison, a dry season sounding, made when a shear line is **not** present, is plotted. The **dashed lines** on Fig. 3.18 show the *early morning* Belize City sounding (1200 UTC 1 March 1989 during relatively **clear skies**)—this sounding was made one week *after* the passage of a strong shear line. Note that this “dry season” sounding (**dashed lines**) is much warmer at the surface, than the “shear line” sounding (**solid lines**), and it is **dry** above ~925 mb, with a **calm** surface wind and a **SE 15 kt** wind at 850 mb (plotted at far right). In the “dry season” sounding, note that the top of the low-level moisture is **much lower**, ~925 mb, and that the sounding is **very stable** to about 850 mb (1509 m) on this *particular* day (1 March 1989). Walters et al. (1988) state that the most dominant feature of this northern region of Central America *during the dry season* is the

⁶⁶Note that Merida is reporting nimbostratus (or altostratus) clouds in Fig. 3.15, while Coatzacoalcas, Mexico (station 76741) on the Mexican coast to the southwest (under the same cloud mass) is reporting the same cloud symbol, but with intermittent slight drizzle.

tradewind inversion which limits diurnal convection. In accordance with Walters et al. (1988), the inversion base is *typically* encountered at about 6,000 feet (1,830 m), and its mean thickness is 900 feet (275 m), i.e., the dry season sounding (dashed lines) shown in Fig. 3.18 on 1 March 1989 has an inversion base much lower than the average.

Despite the fact that this case study is during the early "dry season", the existence of thunderstorm clusters just east of Bluefields, Nicaragua—more typical of the rainy season—is confirmed in the imagery of Figs. 3.16 and 3.17. (It is possible that the shallow water over the Mosquito Banks is still relatively warm, enhancing the instability—note its average October value of 28.8°C on Fig. 4.12). This convection certainly cannot be associated with the approaching shear line (cold front).

Finally Fig. 3.19, at 1931 UTC, graphically depicts the strong northerly flow in the central Gulf of Mexico where the cloud streets widen as cooler air continues to move southward.

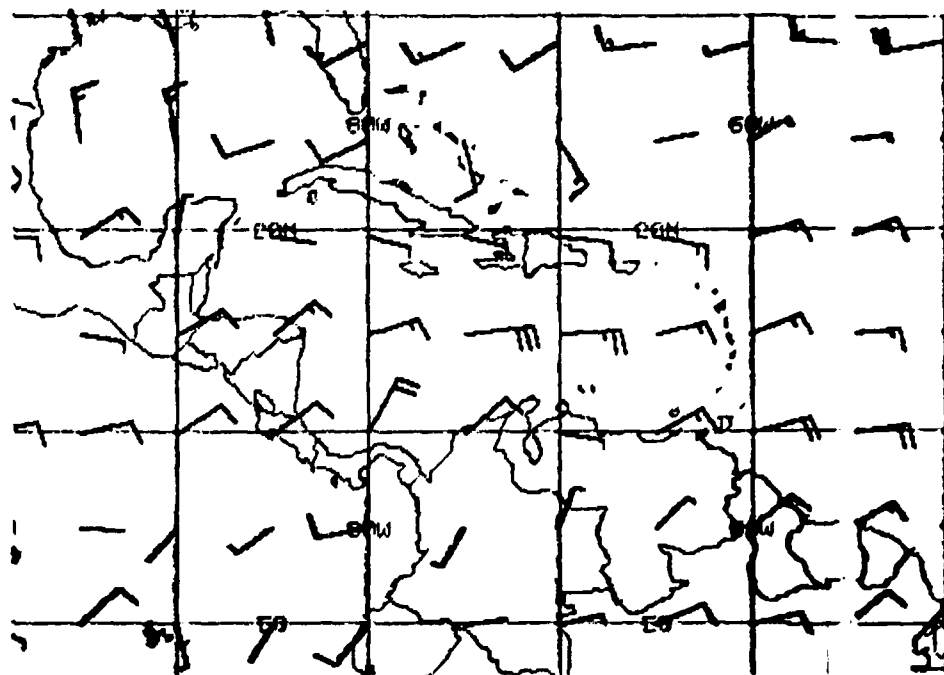


Figure 3.7: FNOG 925 Winds, 0000 UTC 12 DEC 1988. Each barb represents 10 kt.

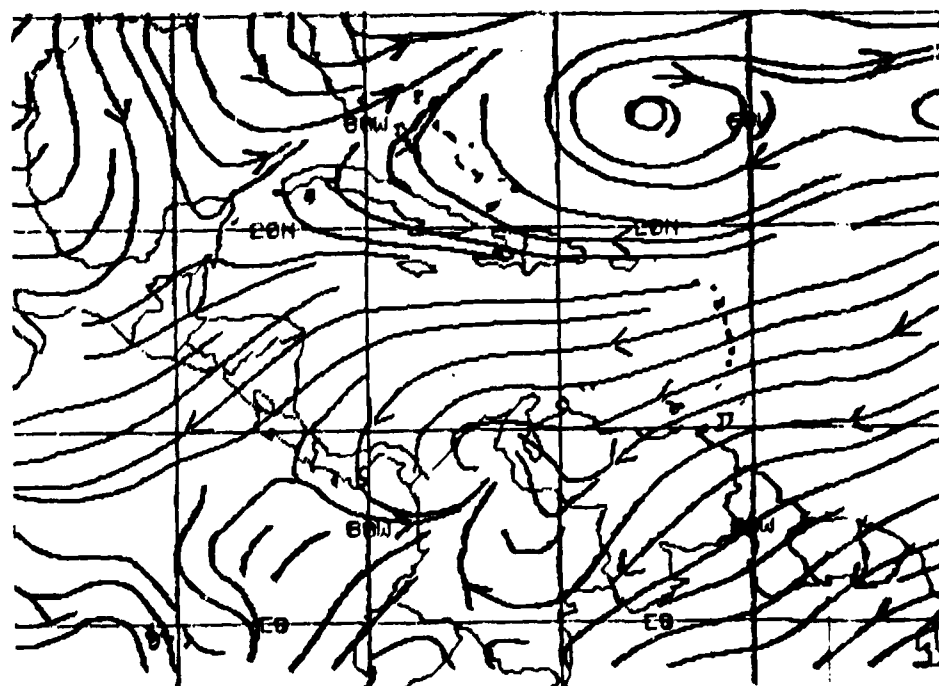


Figure 3.8: FNOG 925 Streamline Analysis, 0000 UTC 12 DEC 1988.

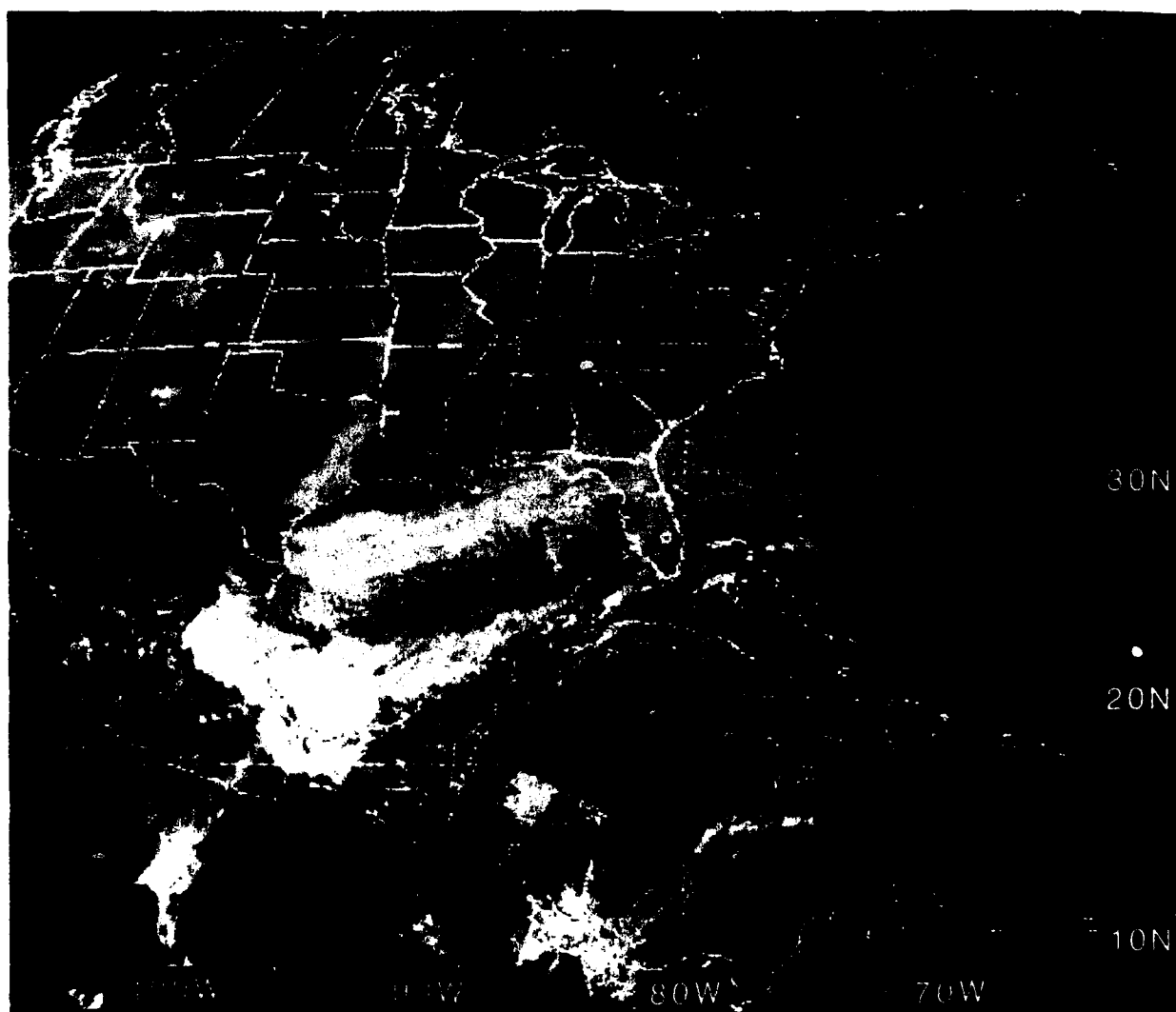


Figure 3.9: GOES East Visible Satellite Imagery, 2031 UTC 12 DEC 1988

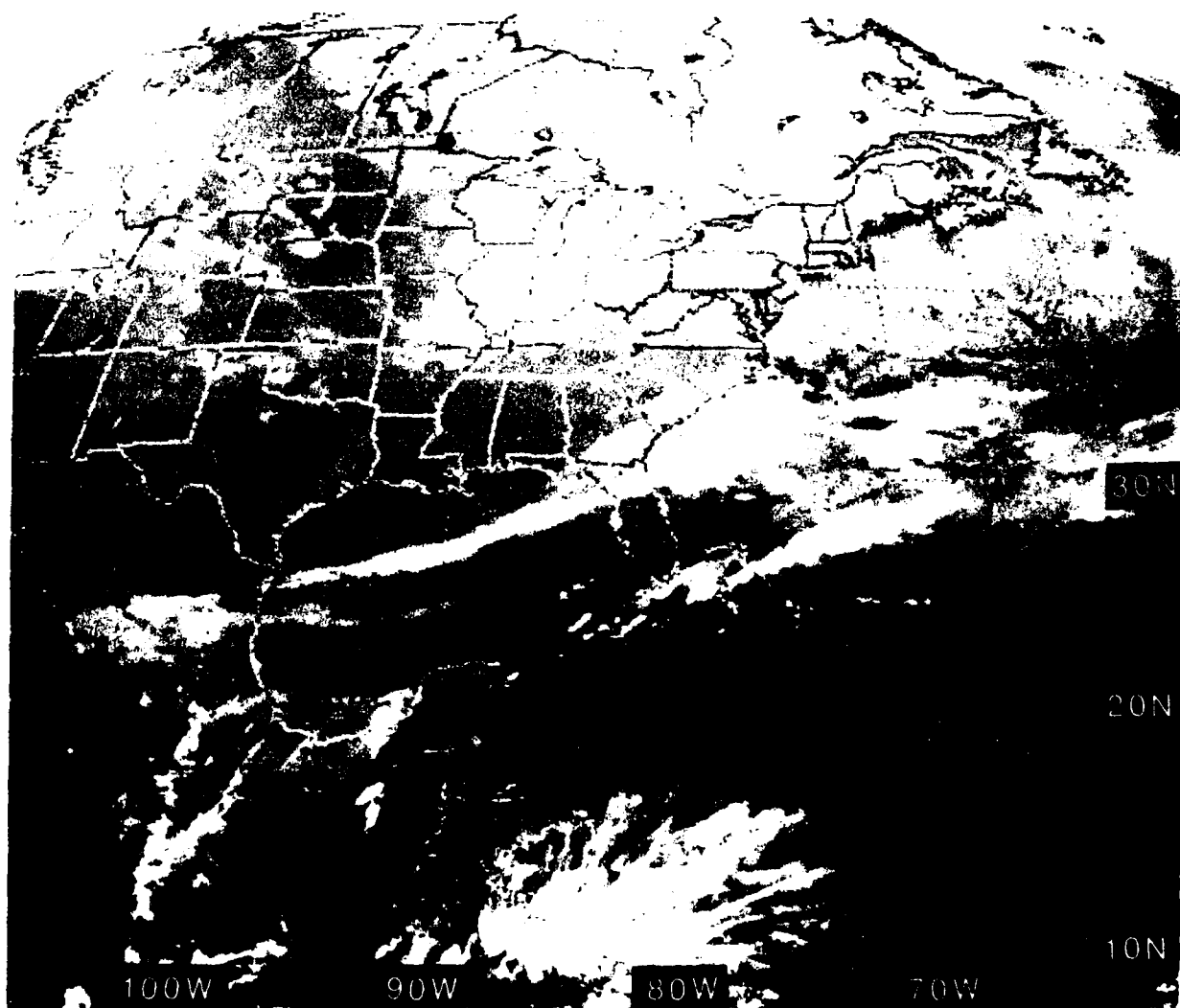


Figure 3.10: GOES East Infrared Satellite Imagery, 0001 UTC 13 DEC 1988

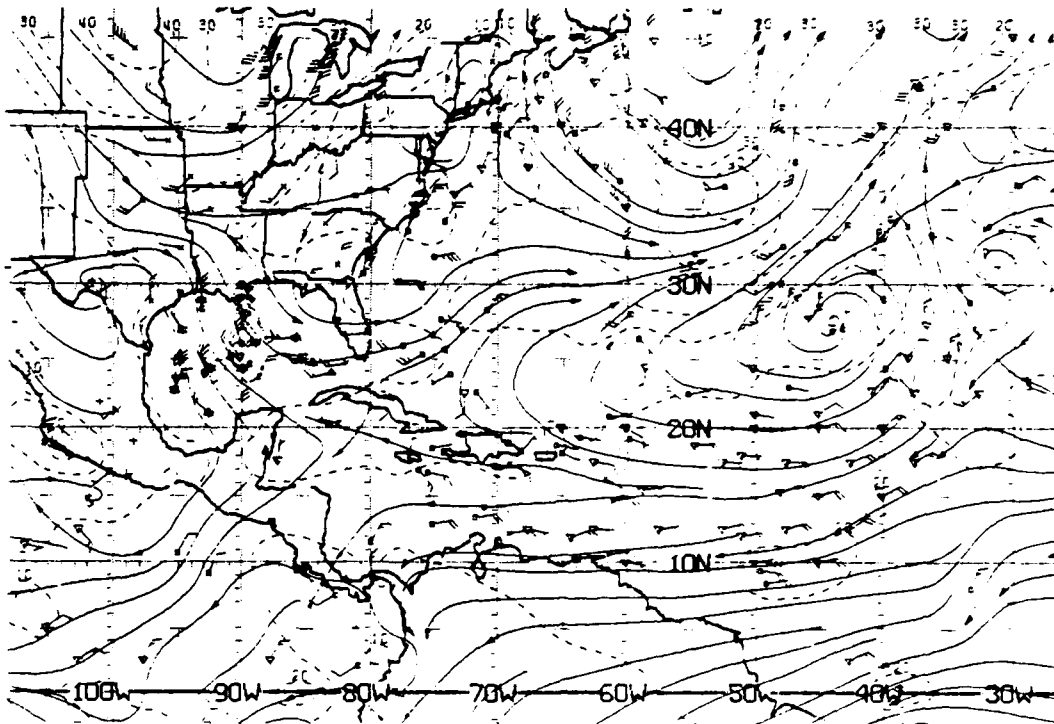


Figure 3.11: NMC ATOLL Operational Streamline Chart, 0000 UTC 13 DEC 1988
As in Fig. 2.4.

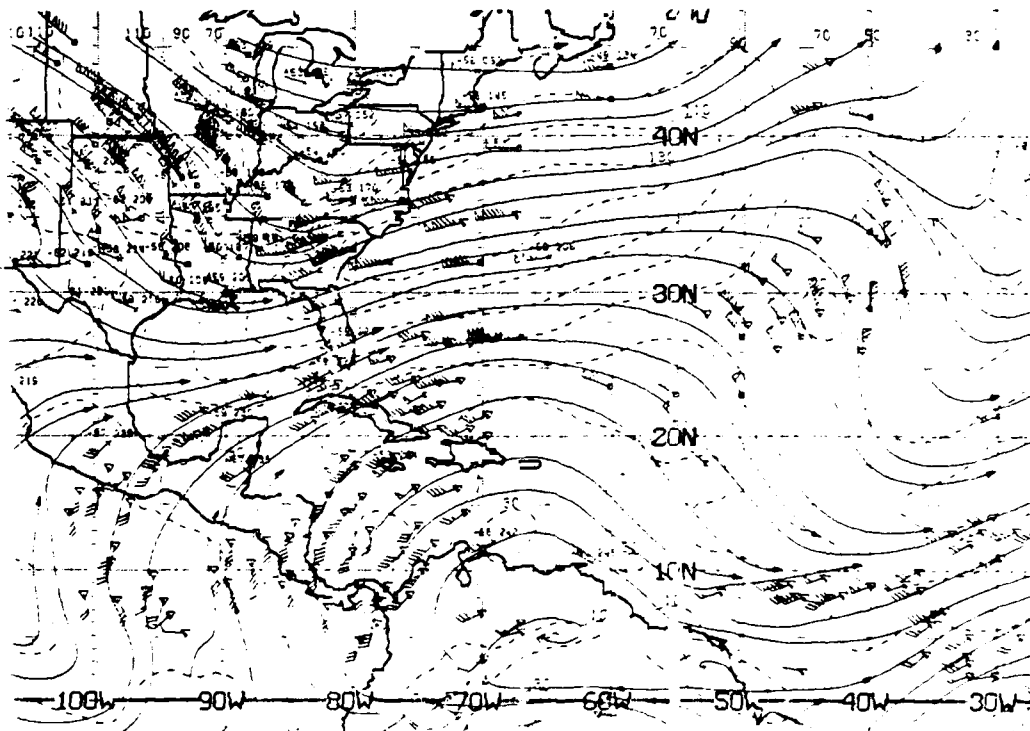


Figure 3.12: NMC 200-mb Operational Streamline Chart, 0000 13 UTC DEC 1988
As in Fig. 2.6.

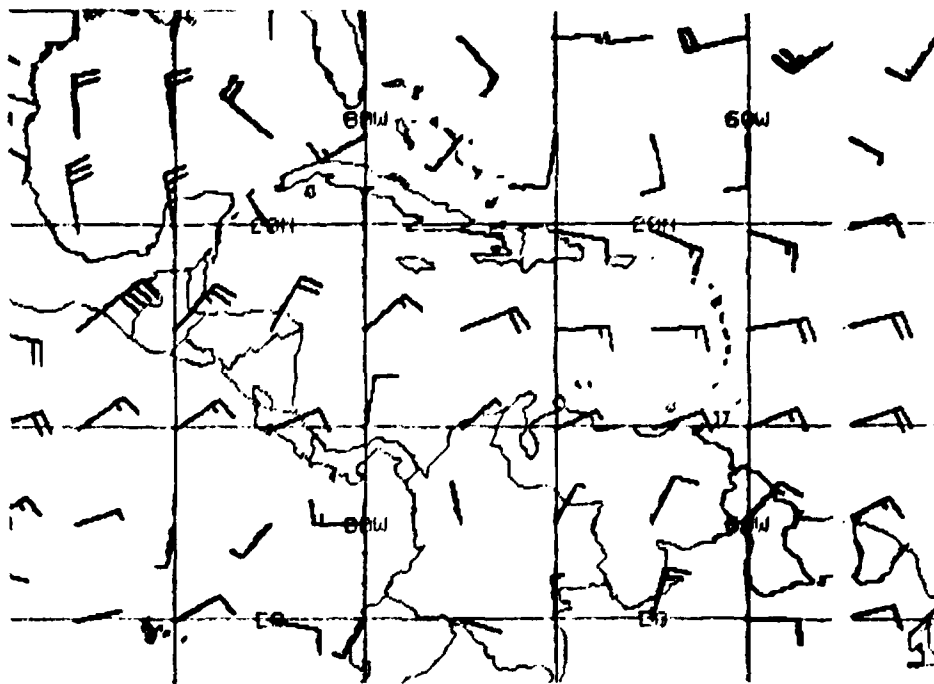


Figure 3.13: FNOc 925 Winds, 0000 UTC 13 DEC 1988. Each barb represents 10 kt.

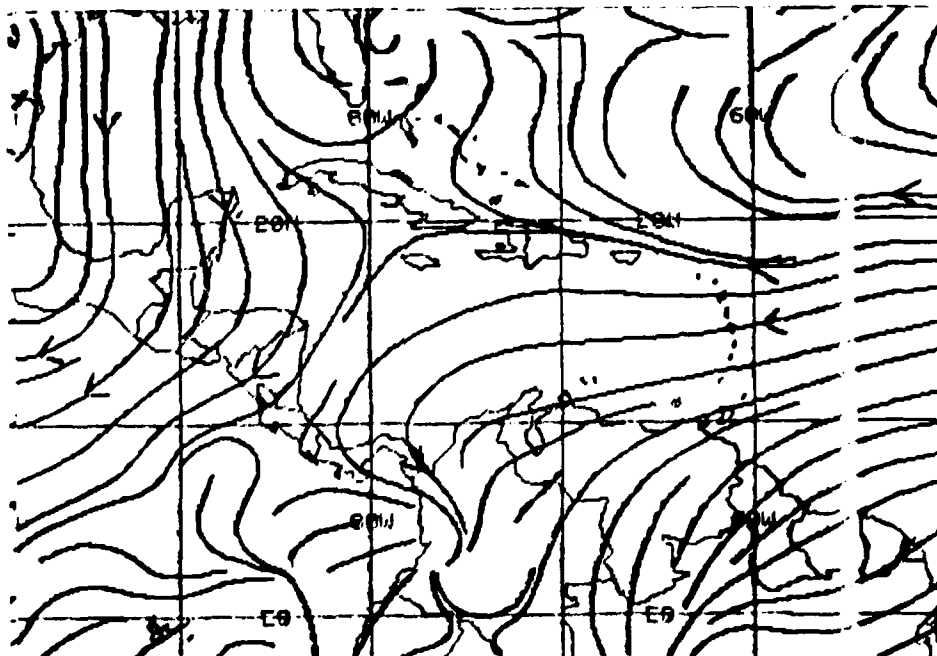


Figure 3.14: FNOc 925 Streamline Analysis, 0000 UTC 13 DEC 1988.

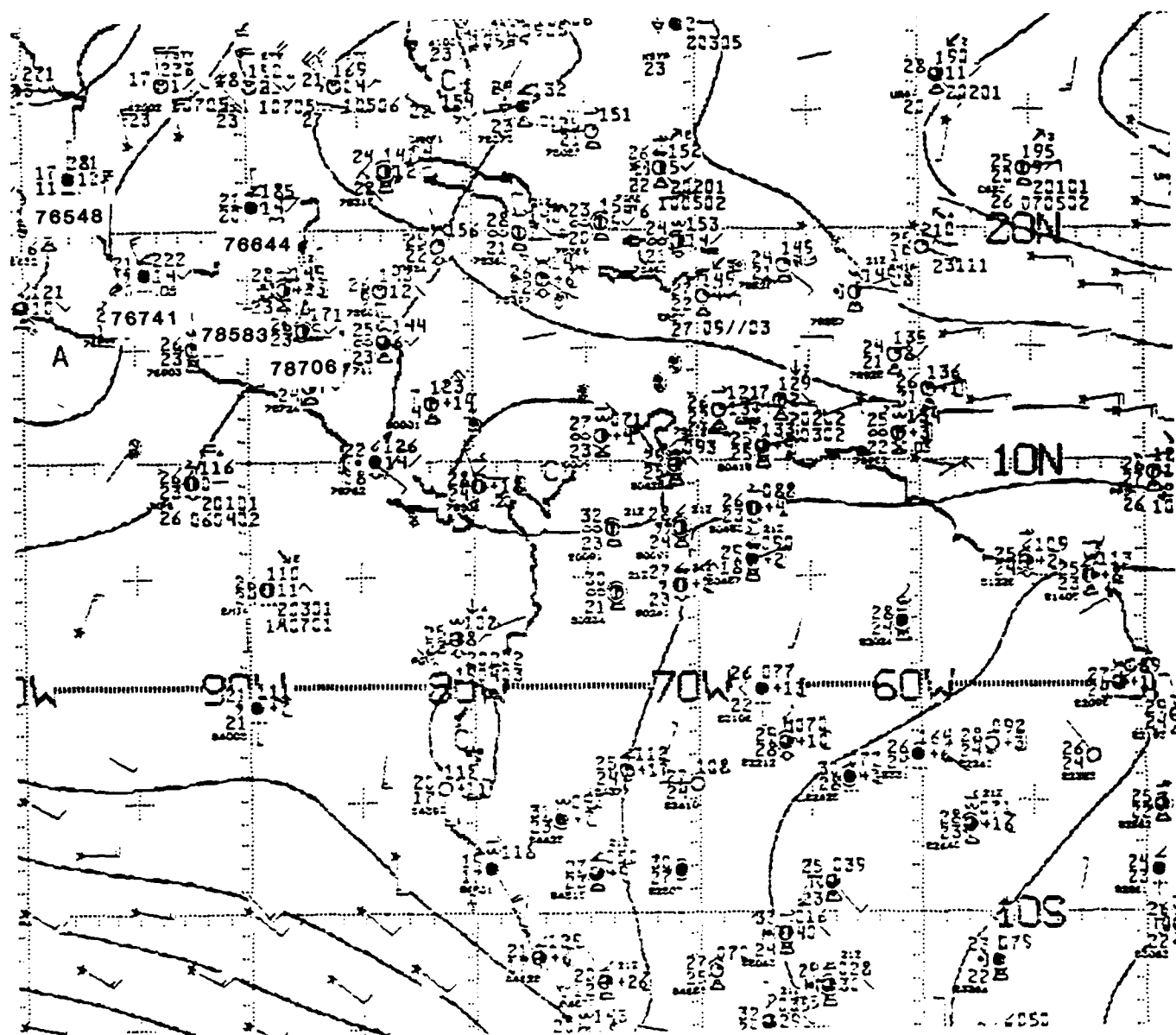


Figure 3.15: NMC 1000 mb Analysis, 0000 UTC 13 DEC 1988.

Contours are unlabeled stream functions from optimum interpolation analysis, with C identifying cyclonic centers and A identifying anticyclonic centers.

1431 13DE88 19A-4 00891 17301 EC1

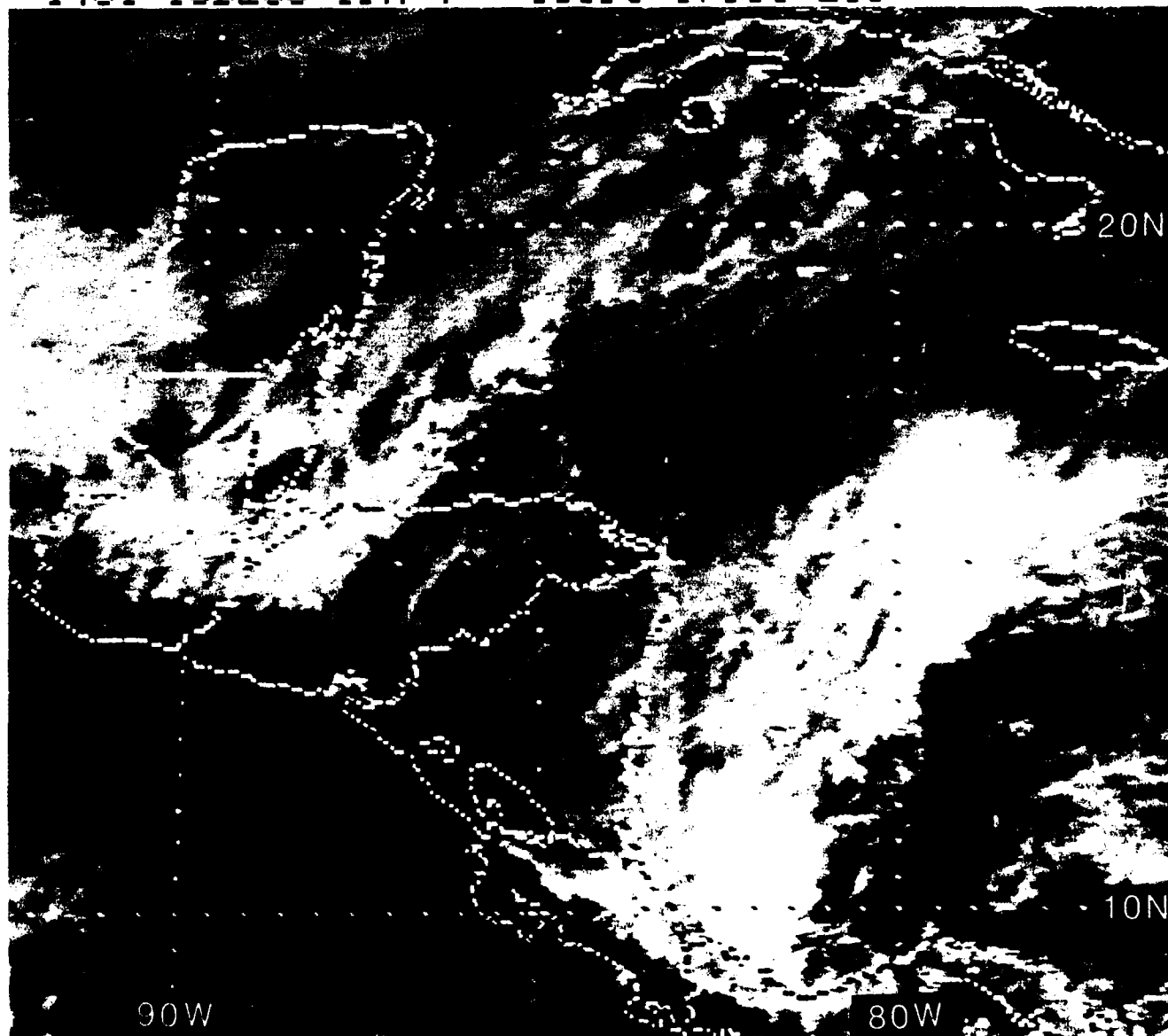


Figure 3.16: GOES East Visible Satellite Imagery, 1431 UTC 13 DEC 1988

1201 13DE88 19E-42A 00892 17311 EC1

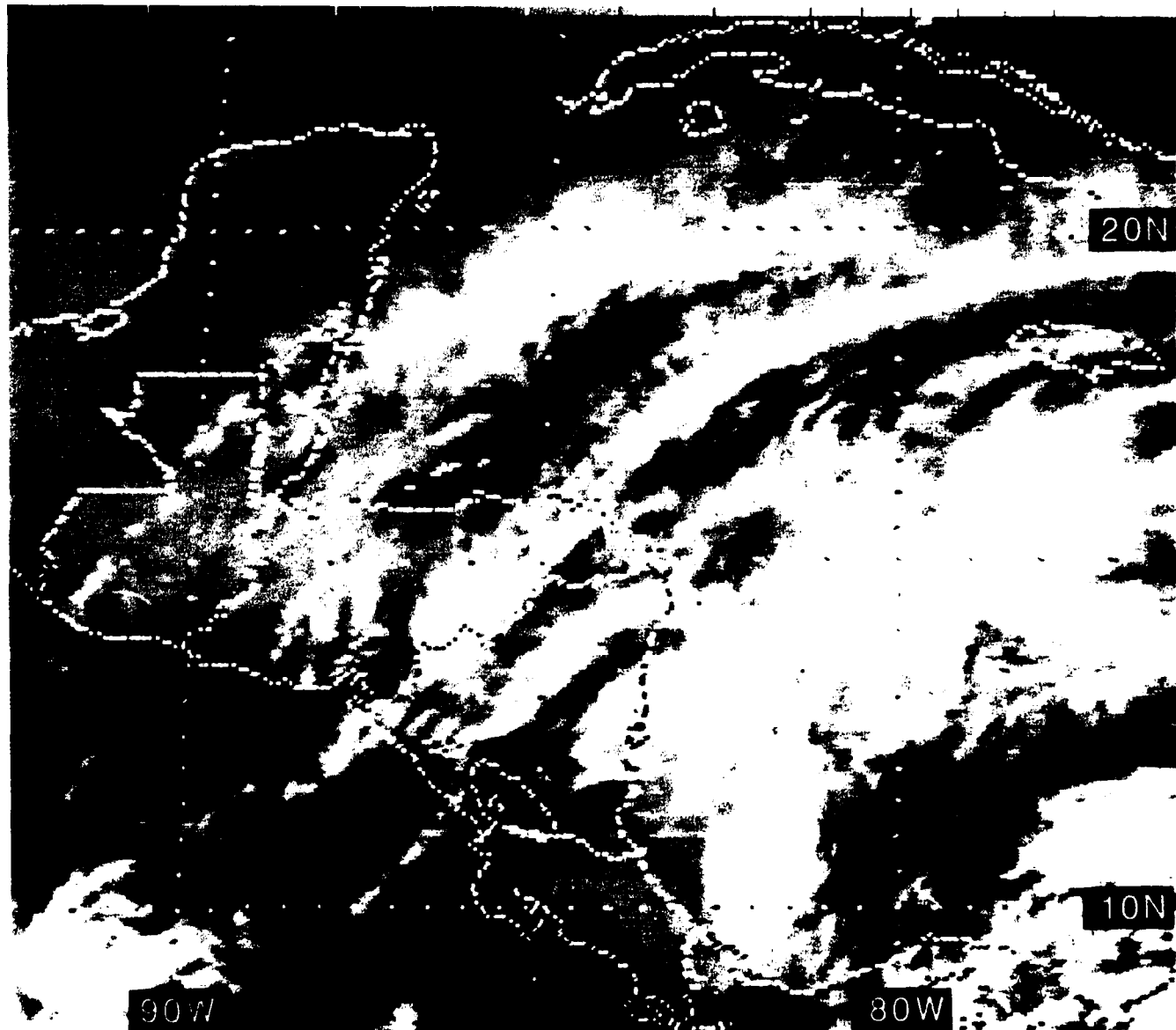


Figure 3.17: GOES East Infrared Satellite Imagery, 1201 UTC 13 DEC 1988

13 DEC 1 MAR

88

89

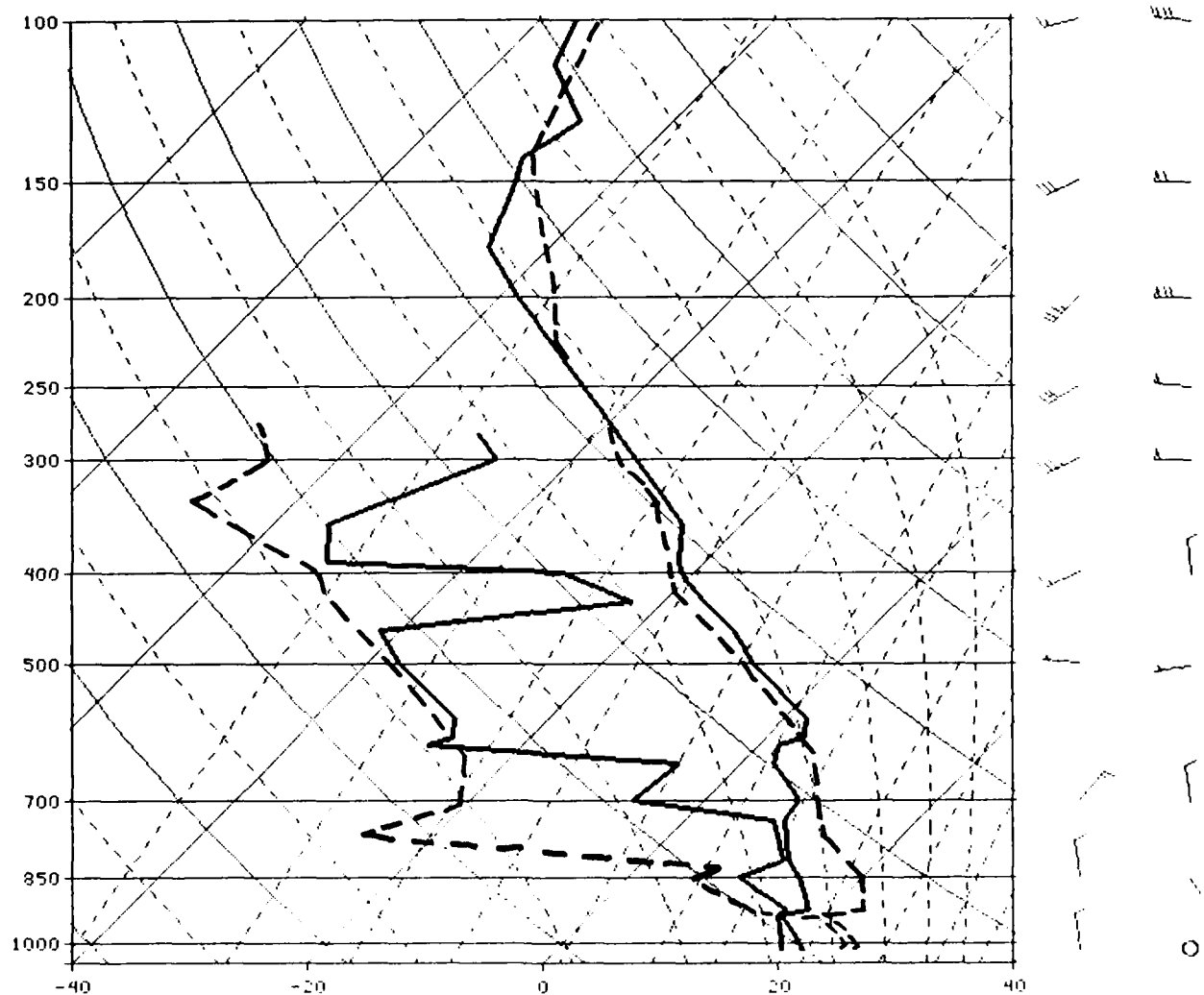


Figure 3.18: Belize City, Belize Sounding (solid lines) 1200 UTC 13 DEC 1988, Belize City sounding during clear skies (dashed lines) 1200 UTC 1 March 1989. The data for these soundings were received operationally.

1931 13DE88 19A-4 00901 17291 EC1

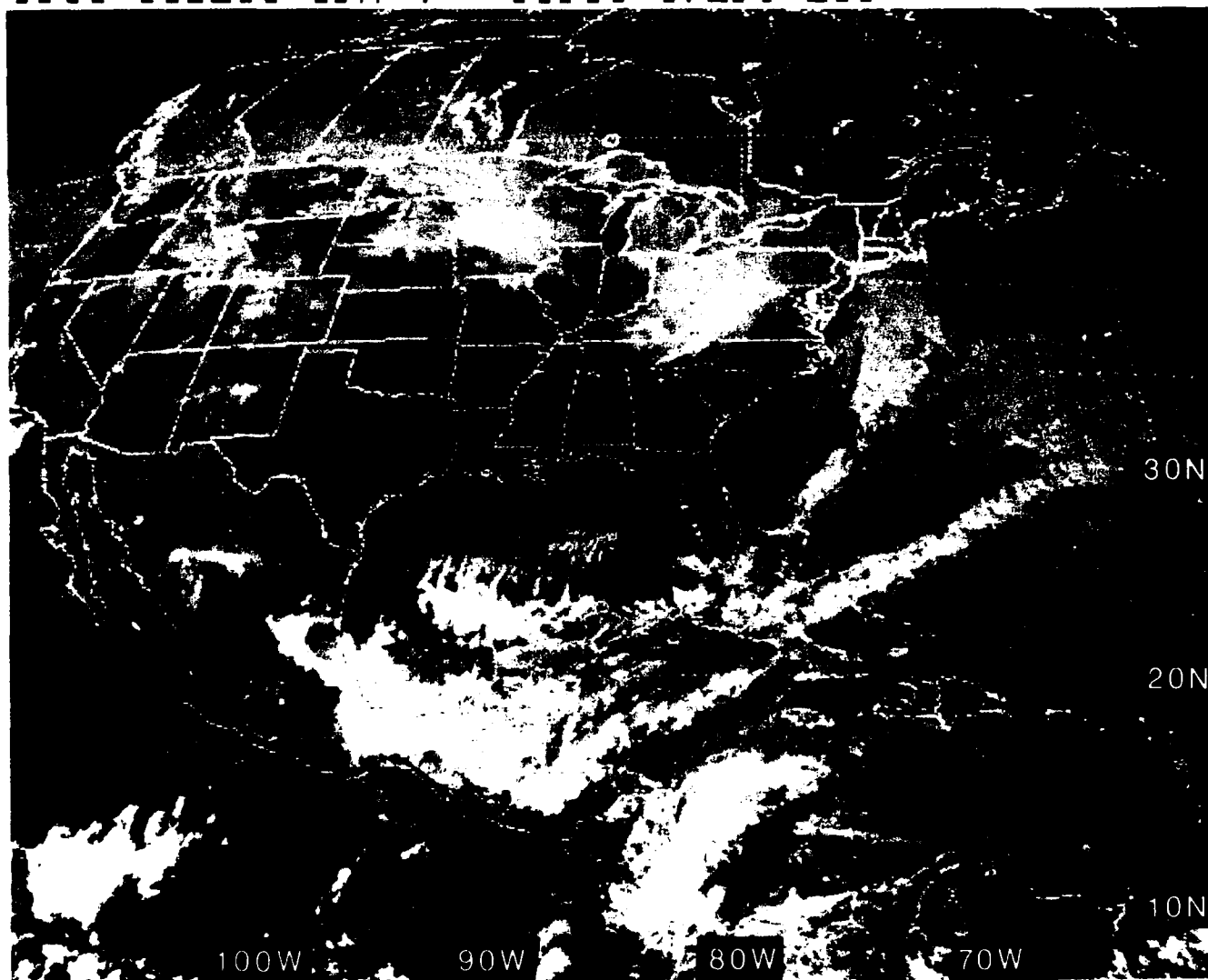


Figure 3.19: GOES East Visible Satellite Imagery, 1931 UTC 13 DEC 1988

14 December 1988

By 0000 UTC 14 December 1988, the National Hurricane Center *manual* surface analysis (not shown) placed the cold front extending from the western North Atlantic Ocean through eastern Cuba (20°N, 77°W) southwestward to (but terminating at) the northeast corner of Honduras (16°N, 84°W). This position appears to be identified by the “wavy” band of discontinuous upper-level clouds on the 0001 UTC IR imagery (Fig. 3.20)—although the brighter clusters of convection now over Costa Rica and east of Nicaragua (in the low-level northeasterly flow and unassociated with the cold front or shear line) are more dominate on this imagery.

The NMC streamline analyses, Figs. 3.21 and 3.22 (with their numerous satellite-derived *lower-level* and *upper-level* winds), depict the position of the shear line at the northeastern corner of Honduras, as well as the *continuing* upper-level southwesterly flow. (Figure 3.21 has the *incomplete* neutral point near western Hispaniola; however, its streamline configuration near the northeastern corner of Honduras is quite unorthodox—yet, it does graphically depict the horizontal shear between the north-northwesterly flow just north of Honduras and the northeasterly flow east of Nicaragua.) The FNOC wind analyses (Figs. 3.23 and 3.24) agree in general with the NMC products. Keeping in mind that the 925 mb winds are quite a distance from the surface (~1000 m), the Navy NOGAPS, Fig. 3.23, analysis depicts a northeast 30-kt wind in eastern Honduras indicating the expected stronger flow *behind* the shear line, yet in Fig. 3.21, the NMC low-level analysis depicts only ~15 kt. At 200 mb, the *west* 45 kt wind in the Yucatan Channel (near 20°N, 85°W) on the FNOC wind analysis (Fig. 3.24) is questionable—the southwesterly flow at that location in the smoother NMC 200 mb streamline analysis of Fig. 3.22 is preferred.

With drizzle (during the past hour), overcast and a northwest wind, Tela, Honduras (station 78706) on the northwest coast of Honduras now reports much colder temperature (23°C) (see Fig. 3.25) than 24 h earlier (26°C) under 5/10 cloud cover (see Fig. 3.15). However, as on the 13th, convection still exists in this particular study, *even* in the northeasterly flow, equatorward of (and unassociated with) the shear line, i.e., note the overcast and drizzle⁶⁷ at both San José, Costa Rica (station 78762) and at San Andrés Island (station 80001), underneath the high (white) cloudiness of Fig. 3.20.

⁶⁷The linking of “convective cloudiness” with station observations of “drizzle” is discomforting to most meteorologists since drizzle is associated with stratiform cloudiness having limited vertical thickness. Among other explanations, the authors offer the following: (1) some portions of the IR-revealed high cloudiness may consist of a thin cloud layer (possibly cirrostratus) with a low cloud deck underneath producing the drizzle or (2) with the large areal extent of the convective cloudiness, the reporting station may be on the periphery of the convective cells.

By ~12 h later, the imagery of Figs. 3.26 and 3.27 show the "line" of cloudiness associated with the shear line (or cold front) extending no further (toward the southeast) than a line connecting the western tip of the island of Jamaica to Cabo Gracias a Dios, on the extreme northeast tip of Nicaragua. Still later (6 h) at 2031 UTC, Fig. 3.28 shows that the line of cloudiness west of Jamaica has started to disperse and **to retreat**.

15 December 1988

Finally at 0000 UTC on 15 December, Figs. 3.29 and 3.30 depict the concurrence of both NMC and FNOC that low-level easterly flow has returned to the western Caribbean Sea between the Yucatan Peninsula and Jamaica. Additionally, note that with the passage east of the surface high pressure center (to near Florida), the original air mass which *had* "surged" equatorward, has now begun to return northward in the *southerly* flow of the western Gulf of Mexico.

While Fig. 3.31 depicts the return of the 1000 mb surface to a "prefrontal condition", the IR imagery of Fig. 3.32 indicates that low-level moisture still remains, especially over the Gulf of Honduras and most of Honduras.

Although this surge did **not** have the prerequisites of a marginal surge, it did subsequently reach Honduras. Stronger surges would be expected to proceed equatorward into Nicaragua or farther. This case study agrees with the conclusion of Pearson et al. (1987) that when the high moves too far east, only the "tail" of the shear line will touch Honduras. Fronts (or shear lines) with a more north-south alignment (having strong trailing high centers near the southern Texas coast) often effect a penetration farther equatorward.

0001 14DE88 19E-4ZA 00911 17321 EC1

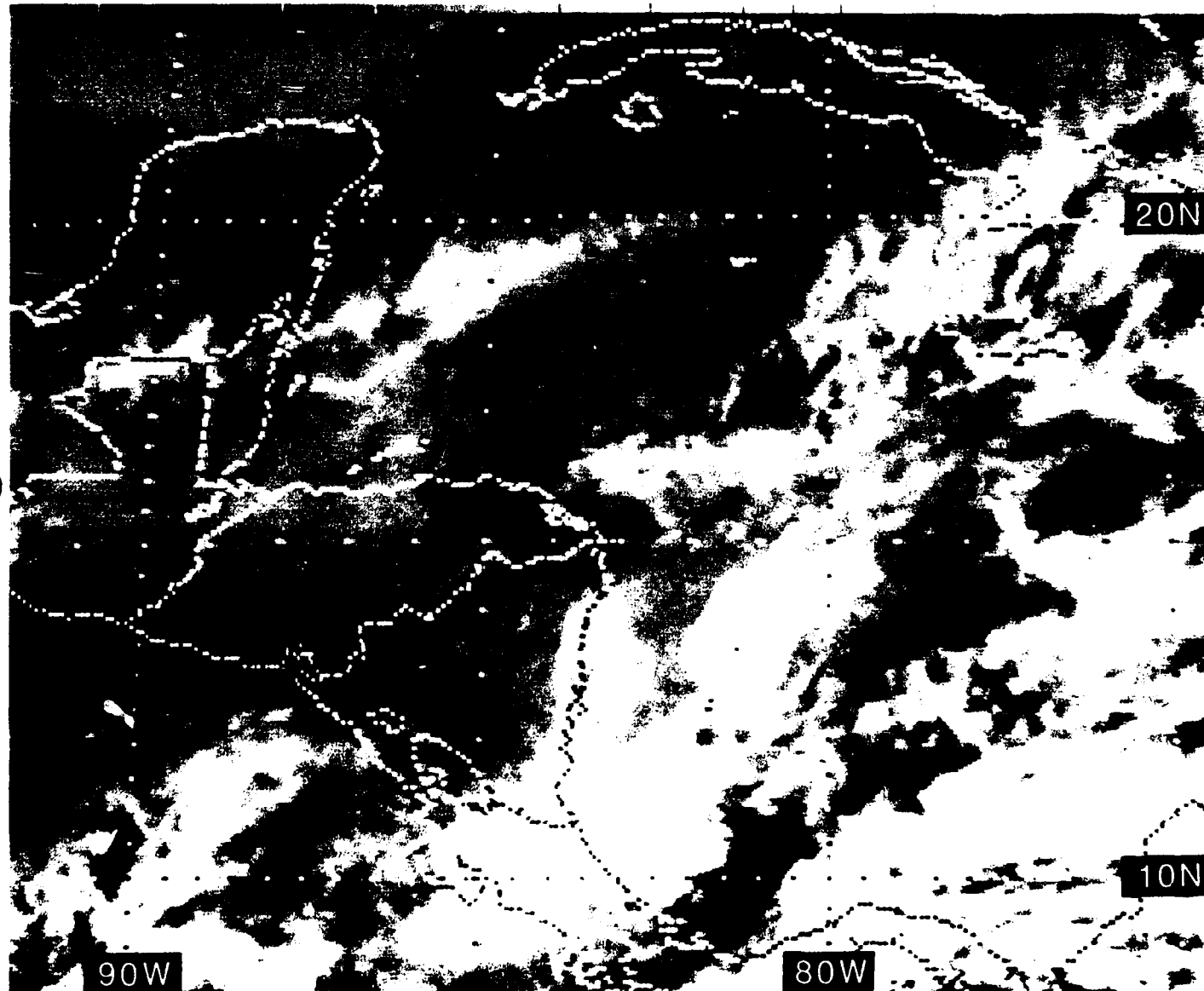


Figure 3.20: GOES East Infrared Satellite Imagery, 0001 UTC 14 DEC 1988

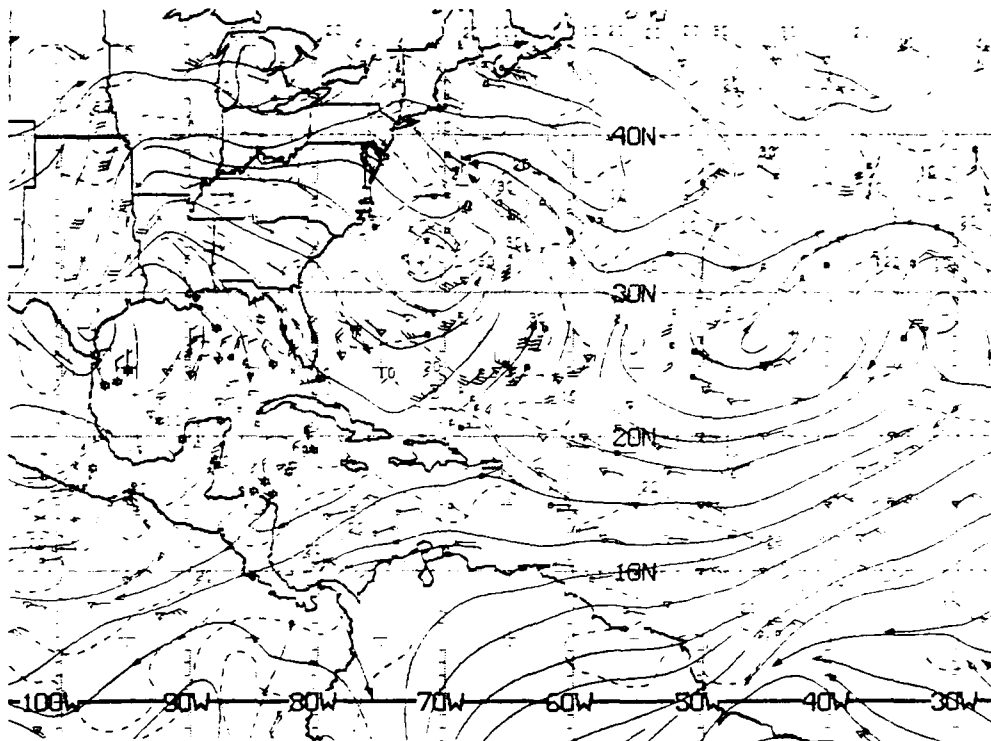


Figure 3.21: NMC ATOLL Operational Streamline Chart, 0000 UTC 14 DEC 1988
As in Fig. 2.4.

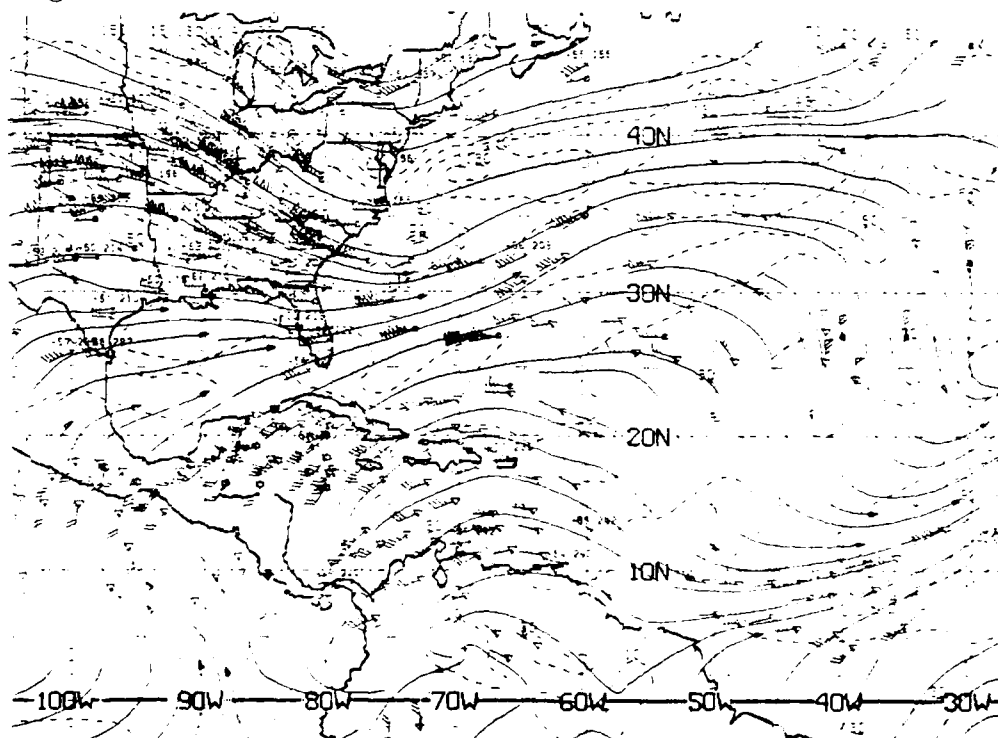


Figure 3.22: NMC 200-mb Operational Streamline Chart, 0000 14 UTC DEC 1988
As in Fig. 2.6.

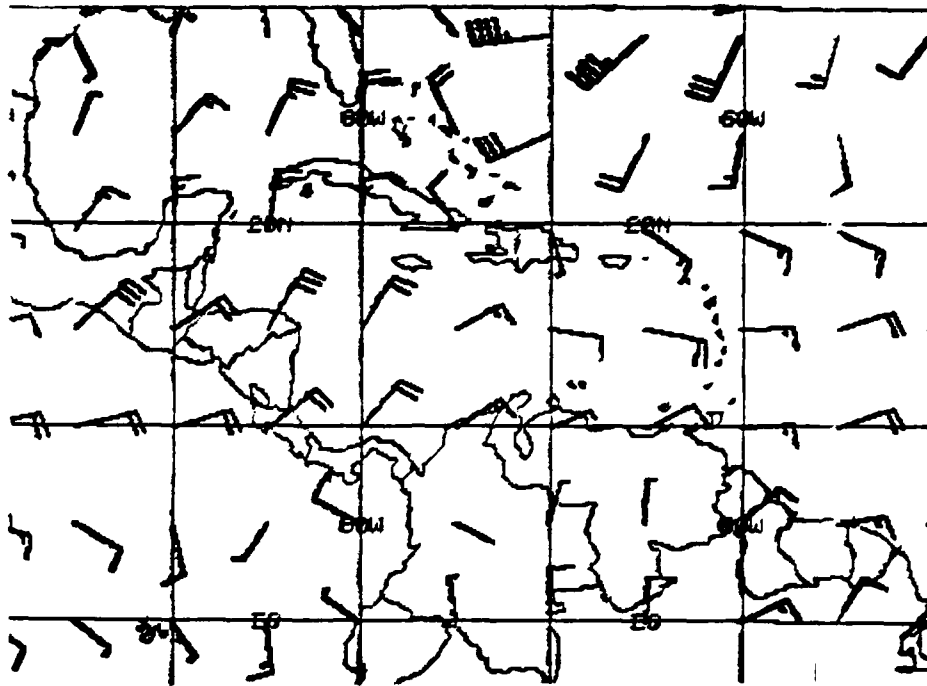


Figure 3.23: FNOc 925 mb Winds, 0000 UTC 14 DEC 1988.
Each barb represents 10 kt.

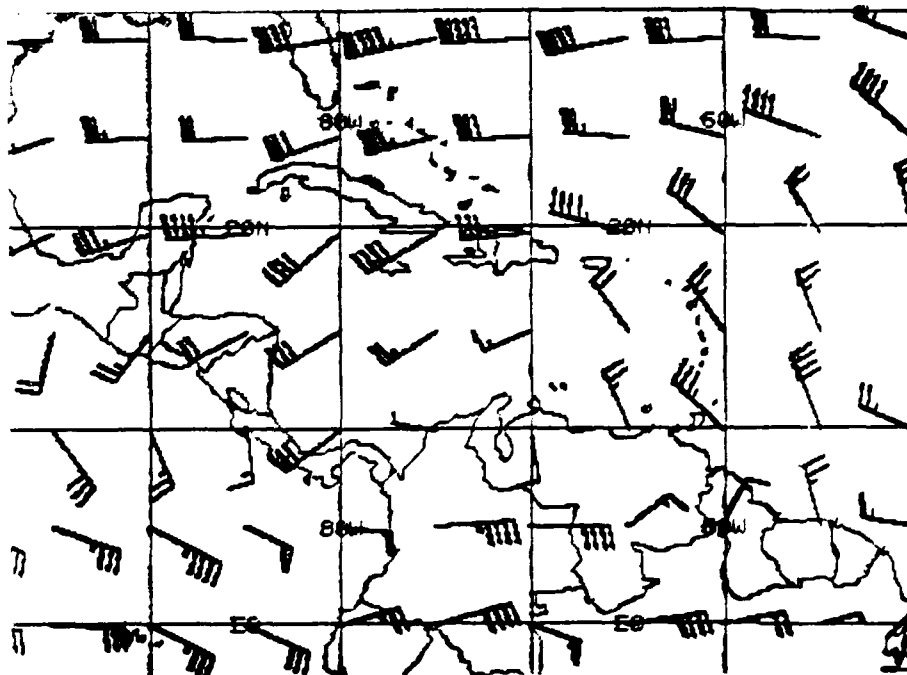


Figure 3.24: FNOc 200 mb Wind Analysis, 0000 UTC 14 DEC 1988.
(Each barb = 10 kt; each pennant = 50 kt.)

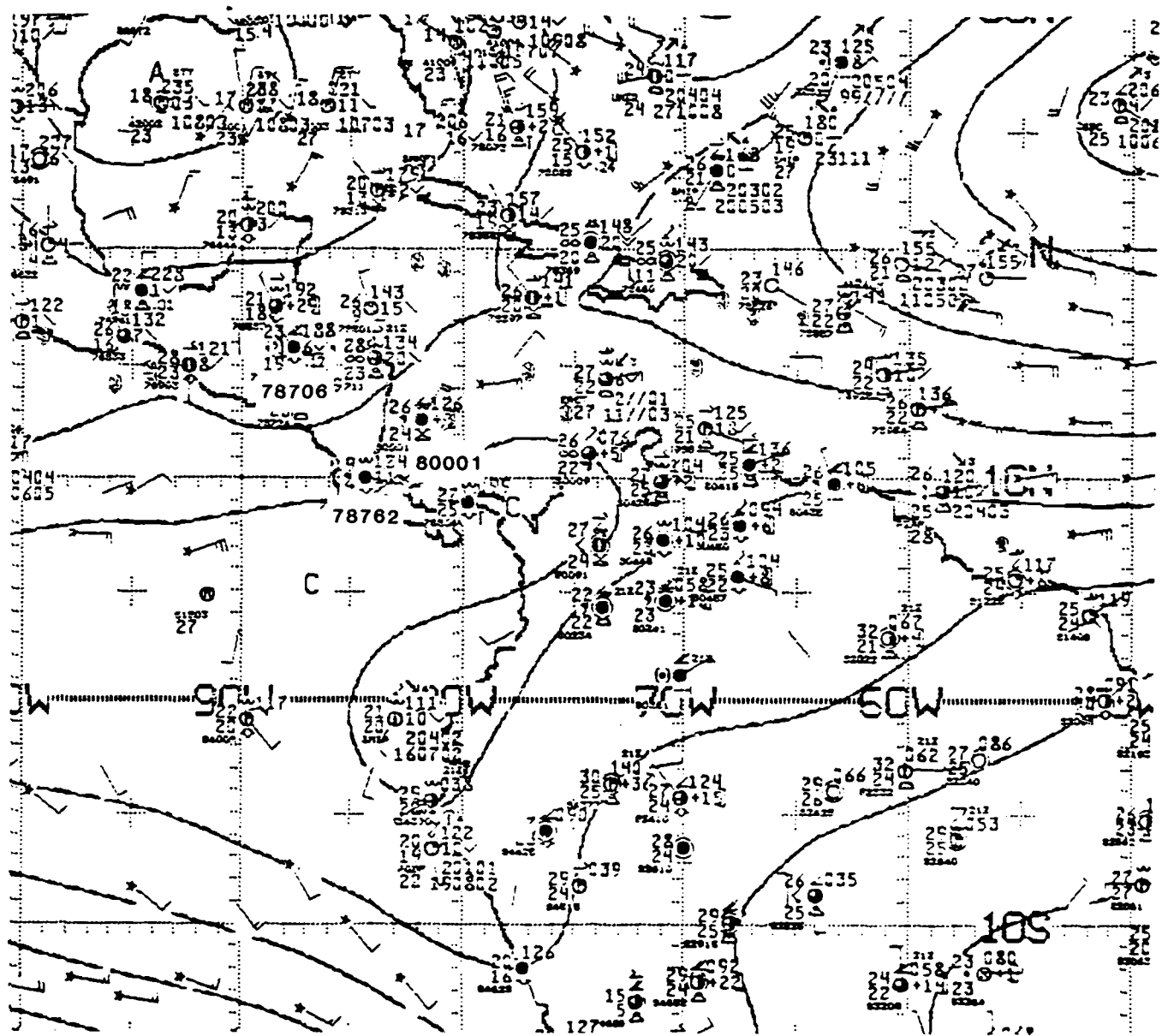
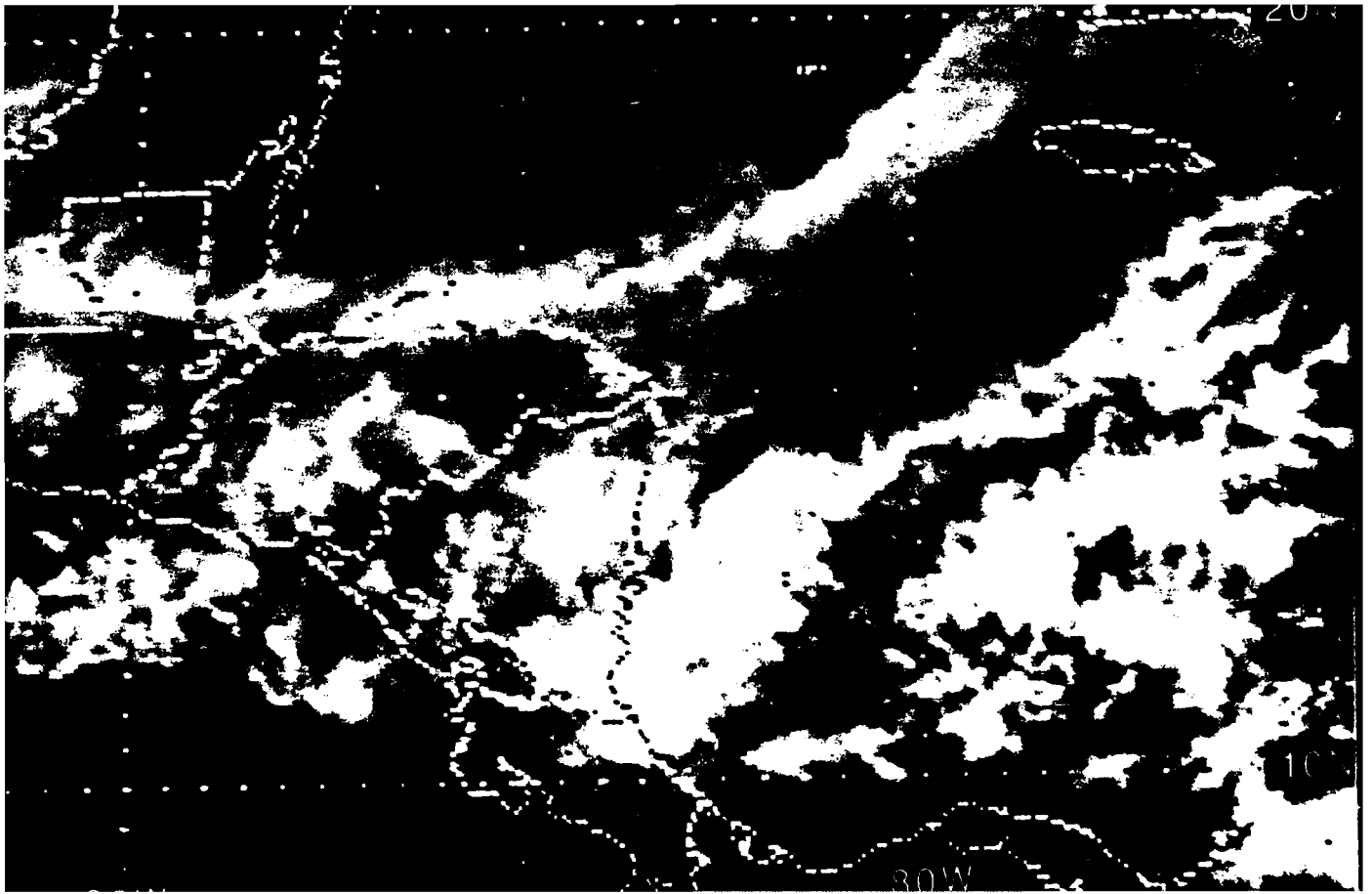


Figure 3.25: NMC 1000 mb Analysis, 0000 UTC 14 DEC 1988.

Contours are unlabeled stream functions from optimum interpolation analysis, with C identifying cyclonic centers and A identifying anticyclonic centers.



1431 14DE88 19A-4 00892 17331 EC1

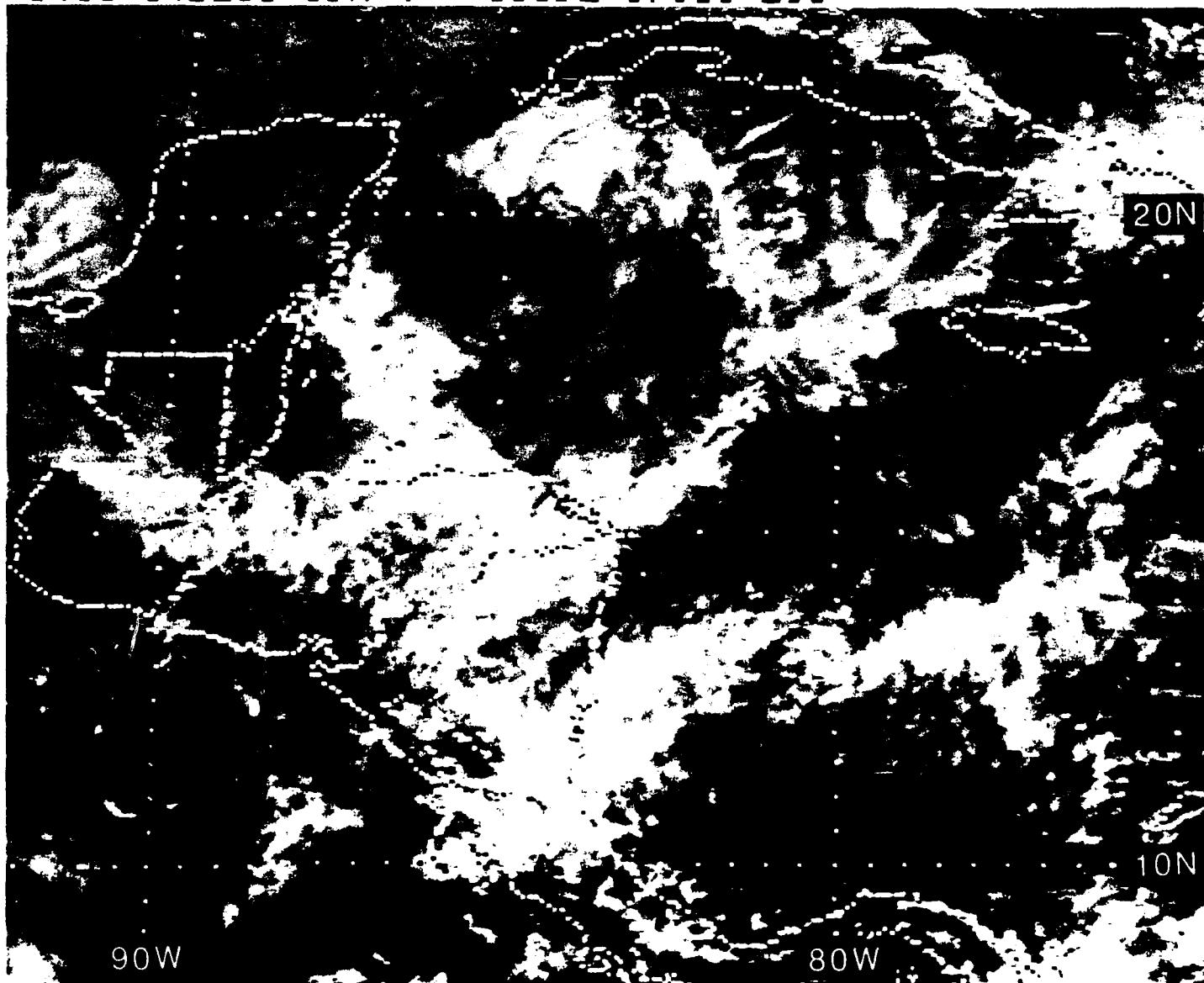


Figure 3.27: GOES East Visible Satellite Imagery, 1431 UTC 14 DEC 1988

2031 14DE88 19A-4 00911 17331 EC1

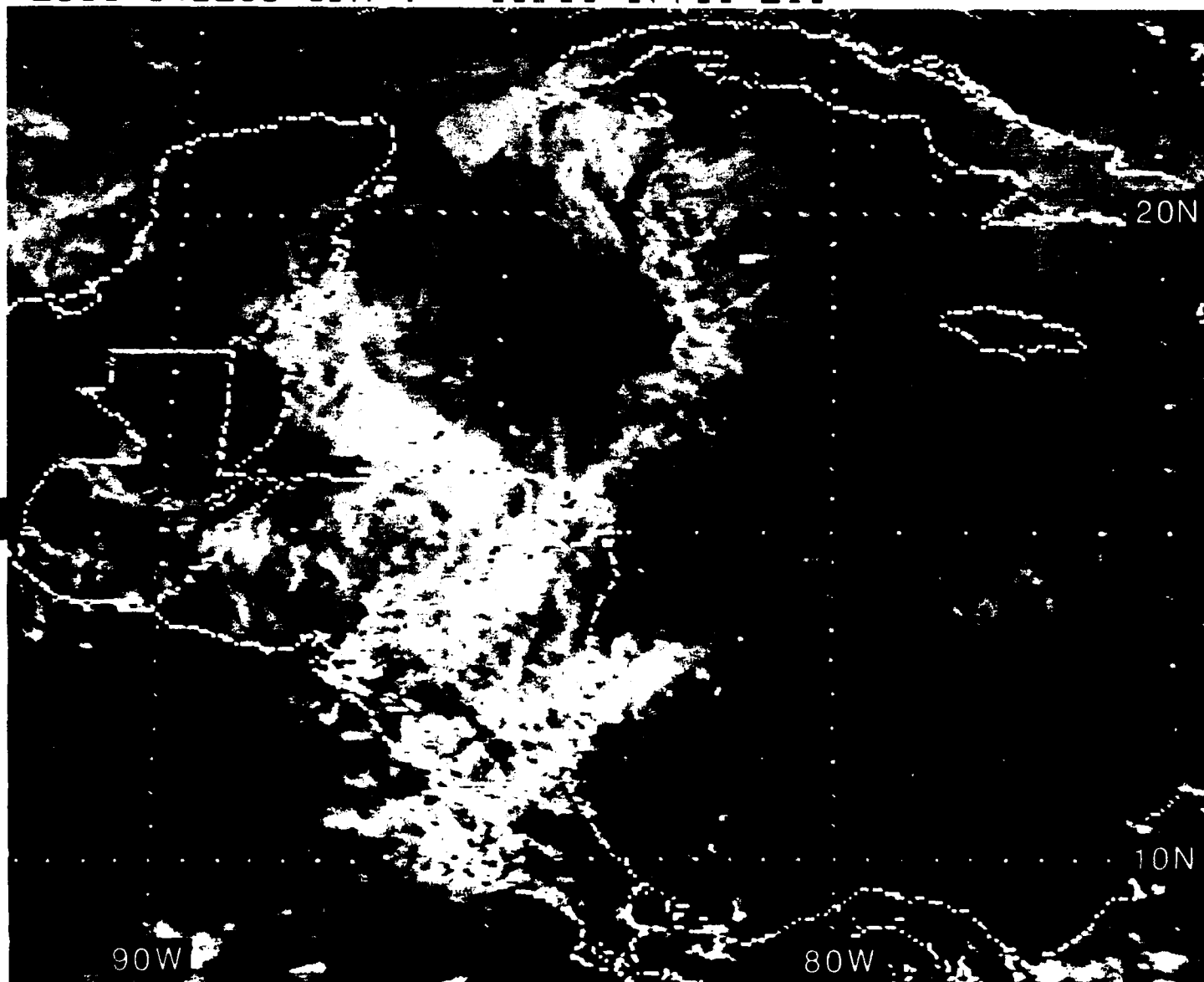


Figure 3.28: GOES East Visible Satellite Imagery, 2031 UTC 14 DEC 1988

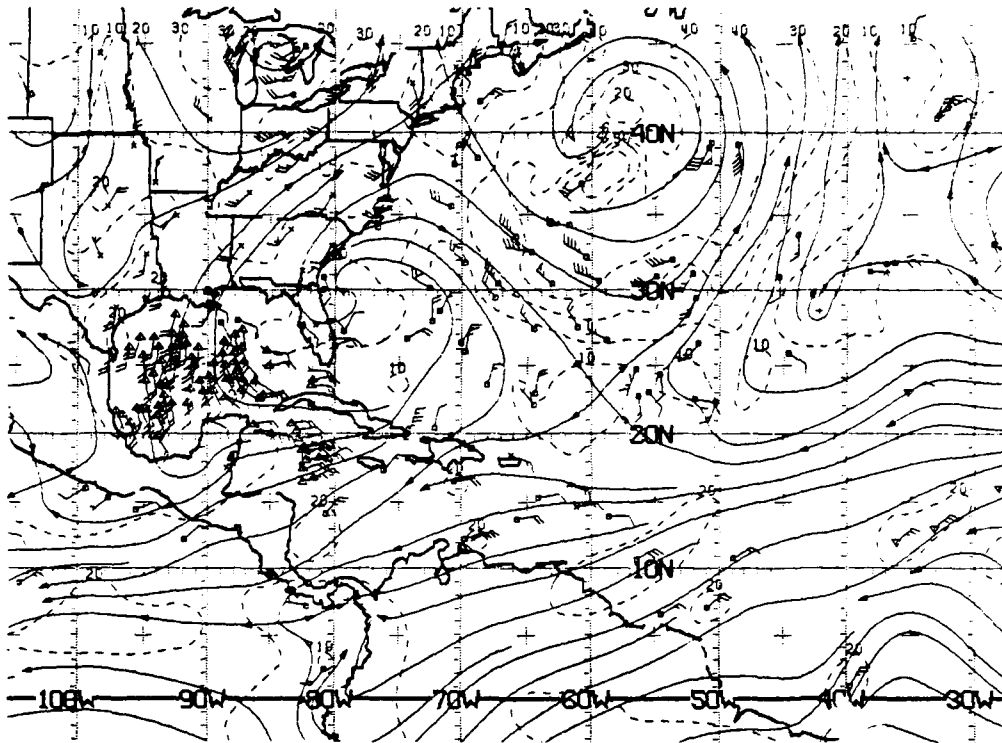


Figure 3.29: NMC ATOLL Operational Streamline Chart, 0000 UTC 15 DEC 1988
As in Fig. 2.4.

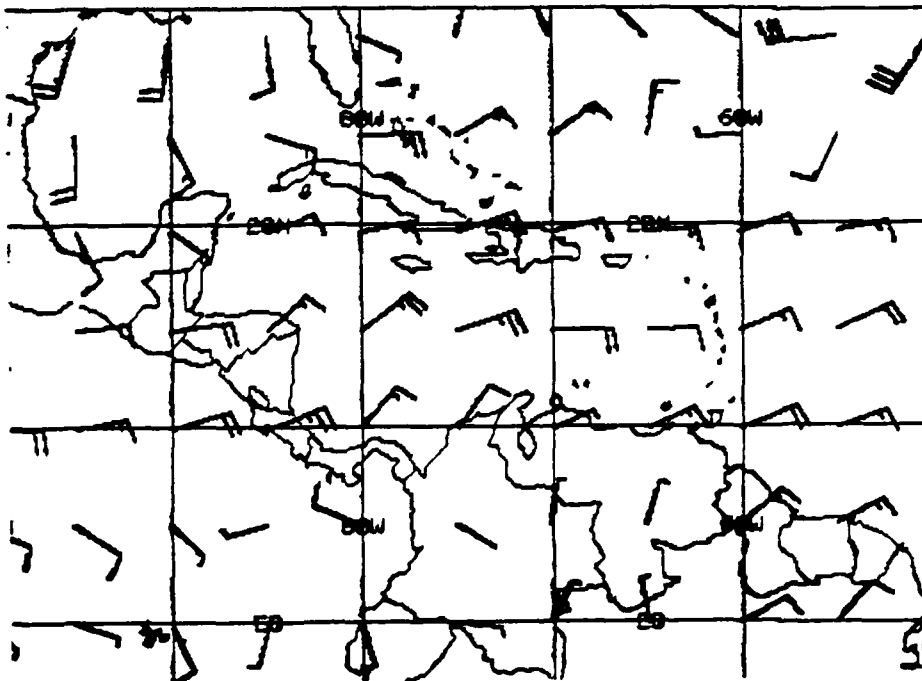


Figure 3.30: FNOF 925 mb Winds, 0000 UTC 15 DEC 1988. Each barb represents 10 kt.

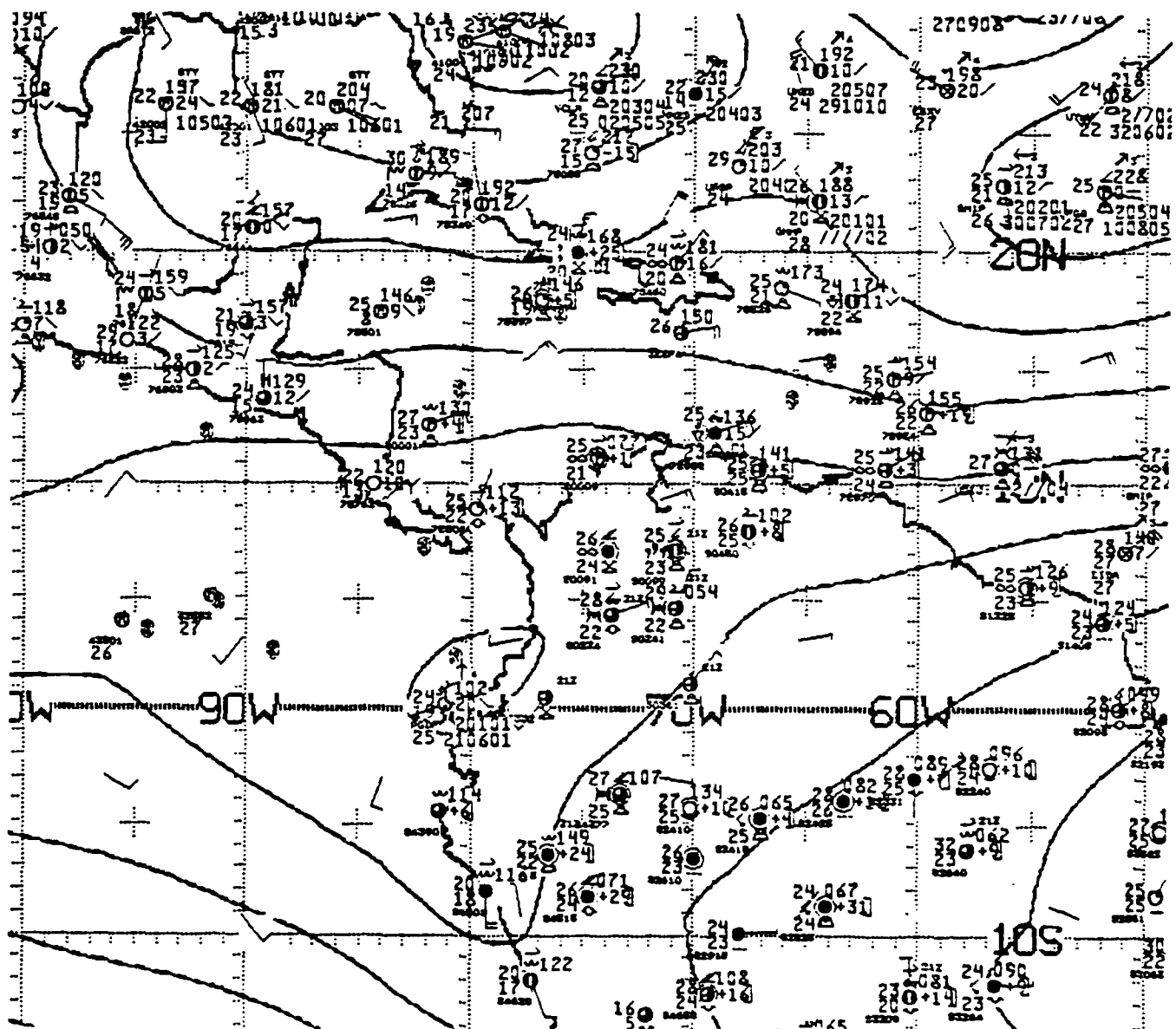


Figure 3.31: NMC 1000 mb Analysis, 0000 UTC 15 DEC 1988.
Contours are unlabeled stream functions from optimum interpolation analysis,
with C identifying cyclonic centers and A identifying anticyclonic centers.

0001 15DE88 19E-42A 00912 17351 EC1

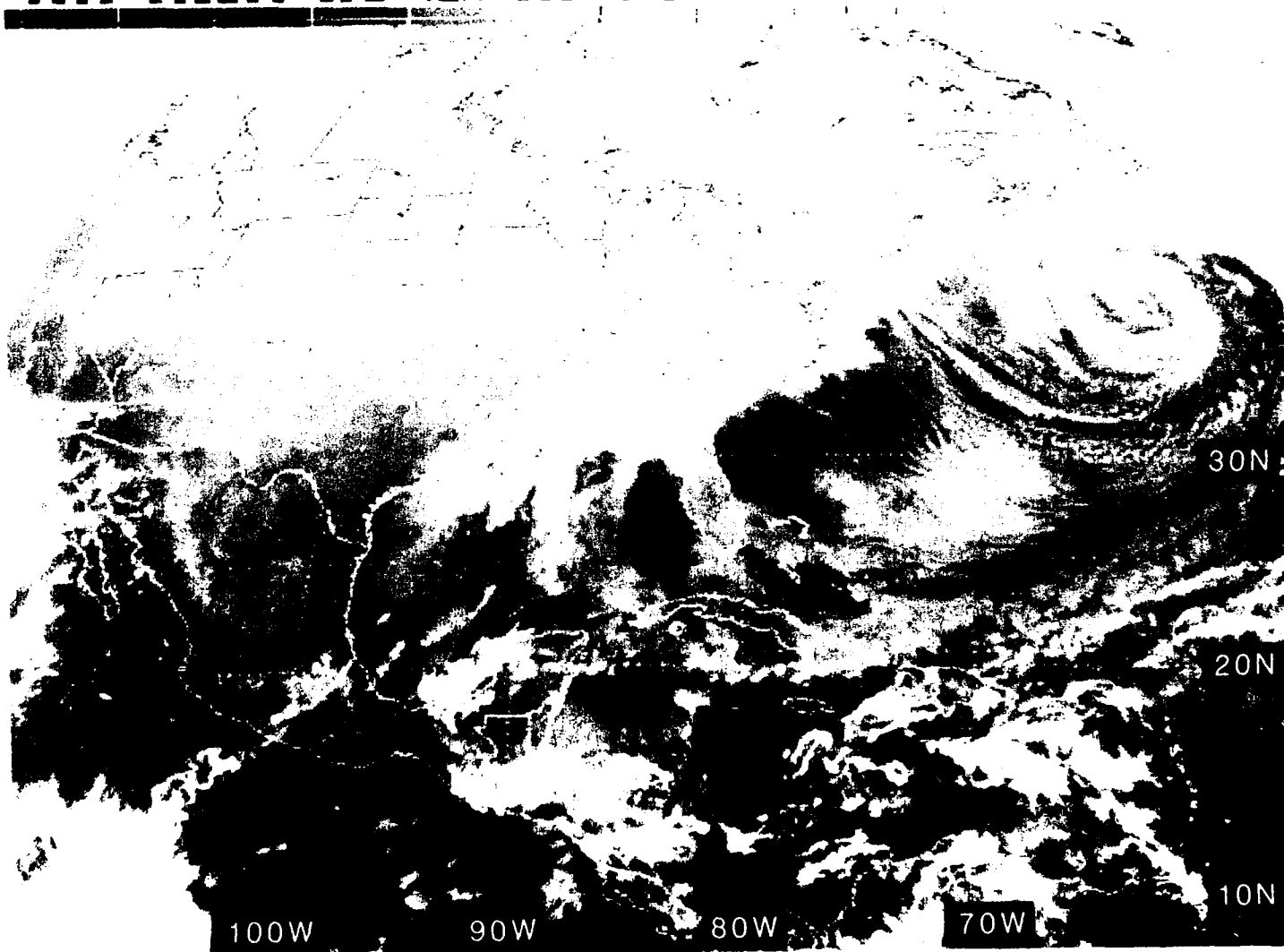


Figure 3.32: GOES East Infrared Satellite Imagery, 0001 UTC 15 DEC 1988

3.3.2 Case IV - Cold Front Passage (14 - 17 March 1988)

As in Case Study III, this study will examine the movement of a cold front, during the dry season, as it moves from the Gulf of Mexico into Central America and the western Caribbean Sea. Additionally, this study will demonstrate the accuracy of the NOGAPS 24-h low-level wind prognosis promulgated by FNOC. While fronts penetrating into Central America during the *early* dry season are normally more intense, this *late* dry season cold front (or "Atemporalado") meets the criteria for a Nominal Surge (Brooks, 1985).

14 March 1988

The wind barbs of the FNOC 925 mb analysis at 0000 UTC 14 March (Fig. 3.33) depict the more northerly flow in the western Gulf of Mexico in contrast with the more southerly flow over the Yucatan Peninsula. (This analysis will be used later to measure the skill of the FNOC 24-h 925 mb wind prognosis.) The IR imagery for 0001 UTC 14 March (Fig. 3.34) depicts low cloudiness in the western Gulf of Mexico. However, 12 hours later, the grey line on the IR imagery of Fig. 3.35 (extending from central Florida west-southwestward to ~100 n mi south of Brownsville, Texas) closely approximates the position of the NMC cold front (not shown).

Figure 3.36 shows the station surface observations at 1200 UTC on 14 March. Note the 8°C temperature reported at buoy⁶⁸ PTAT2 on the Texas coast (contrasted with 21°C reported at Merida, Mexico (station 76644) on the Yucatan Peninsula), as well as the strong northerly wind (25 kt reported by buoy 42002) in the northwestern Gulf. Moreover, the sea-level pressure at Merida is **1010.8 mb**, while buoy PTAT2 is reporting a sea-level pressure of **1025.9 mb**. Thus, the Brooks index is **15.1 mb** (i.e., 1025.9 - 1010.8), a **Nominal Surge**, predicting that the cold front will penetrate as far south as Nicaragua (see Subsubsection 3.2.3).

Further examination of the station reports (Fig. 3.36) alerts the forecaster to the fact that the--barely discernible--very faint, *dark* grey imagery⁶⁹ over Nicaragua on Fig. 3.35, during this early morning hour, indicates **fog**. The satellite imagery Fig. 3.35 clearly depicts the high (and multilayered) cloudiness over San José, Costa Rica (station 78762), but provides little indication of the *scattered* multilayer cloudiness over Howard AFB, Panama (station 78806). Note also that the presence of a low, yet rather continuous, cloud layer, *near* the Gulf of Tehuantepec, is associated with **3-dot rain** at Salina Cruz, Mexico (station 76833).

5 1/2 hours later, the visible imagery of Fig. 3.37 depicts the cold front, which now extends from the southern tip of Florida to *just* north of the Yucatan Peninsula. The extensive low cloudiness, extending from northern and central Guatemala westward to the Bay of Campeche and nearly reaching the North Pacific Ocean across the isthmus of Tehuantepec (i.e., **ahead** of the approaching front), is attributed to a cold front which passed, three days *earlier* on 11 March.

⁶⁸PTAT2 is the Port Aransas coastal buoy located between Houston and Brownsville, Texas.

⁶⁹The minimal information available from the 4 km resolution IR imagery of Fig. 3.35 is greatly improved by imagery having 1 km resolution.

15 March 1988

Figures 3.38 and 3.39 show the NMC low-level and upper-level streamline analyses at 0000 UTC on 15 March 1988. As in the other case studies, these analyses benefit from numerous satellite-derived winds. Note the neutral point, near the northeast corner of the Yucatan Peninsula on Fig. 3.38, approximating the axis of the low-level "shear line" (see Fig. 3.6). In the upper-level flow (Fig. 3.39), the high center (located just north of Panama) produces 200 mb anticyclonic flow over Central America so typical⁷⁰ of the dry season.

Figures 3.40 and 3.41 show *both* the FNOC 24-h 925 mb wind **prognosis** and the *verifying* FNOC 925 mb wind **analysis** at 0000 UTC 15 March. It is important to note that the analysis, from which the Navy NOGAPS prognosis was made, is 0000 UTC on 14 March (see Fig. 3.33). Note that at 0000 UTC on 14 March, the analyzed low-level wind over the Yucatan Peninsula (near 20°N, 90°W in Fig. 3.33) was south-southwest at 5 kt; whereas, the wind "progged" at that grid point in Fig. 3.40 is 30 kt from the north-northeast. The verifying analysis, Fig. 3.41 shows that the 30 kt wind **verified**; additionally, the "progged" NW 30 kt wind to the west, in the Bay of Campeche, quite accurately predicts the verifying 25 kt wind, analyzed there. (Although it is *not* shown, the FNOC NOGAPS 200 mb analyses also had the anticyclonic gyre (or high center) centered in the western Caribbean Sea.)

The IR imagery of Fig. 3.42 clearly depicts the position of the cold front extending from the North Atlantic Ocean southwestward across western Cuba to the northern Yucatan Peninsula at 0001 UTC on 15 March. At this time, the NMC Final Analysis (not shown) locates the cold front extending *southwestward* through the northern border of Belize and terminating at a position just east of the Gulf of Tehuantepec. Figure 3.43 is a "zoomed" image of *just* Central America.

The 0000 UTC station observations of Fig. 3.44 show that the calm wind, at Merida Mexico (station 76644) just 12 hours earlier (see Fig. 3.36), has been replaced by a 10-kt northerly wind, and the pressure has begun to rise at Chetumal, Mexico (station 76750) just north of Belize—the net pressure tendency is +0.5 mb, which includes a decrease earlier in the past three-hour period. Note, that since it is now late afternoon (local time 1800)—and that the front has *just* arrived—the temperature at Chetumal is a warm 32°C. The position of the front (at 0000 UTC) is further confirmed by a 5 kt west-northwest wind, a rising barometer, with overcast skies and a rain shower, at Sagua La Grande, Cuba (station 78338) on Fig. 3.44. However, the high cloudiness (white imagery in Fig. 3.43) over western Honduras as well as Panama and Costa Rica (2-dot rain at San José (station 78762) in Fig. 3.44) is obviously not associated with the front.

The IR imagery 12 hours later (Fig. 3.45) shows that the front has reached the Gulf of Honduras, moving at a speed of <10 kt. The line of low clouds (with some high cloudiness near the Gulf of Honduras) in the imagery clearly shows the front extending from the

⁷⁰Nevertheless, perturbations to this typical pattern do exist. In early February 1989, a 200 mb "TUTT-like" trough extended from the North Atlantic Ocean westward into Belize for over a week.

western North Atlantic Ocean, across central Cuba and into the Gulf of Honduras. While the station observations at 1200 UTC (Fig. 3.46) show that the temperature at Chetumal, Mexico (station 76750) has cooled to 22°C (a 10°C decrease in 12 hours), **most** of the decrease is diurnal—i.e., its temperature was only 23°C, 24 hours ago (see Fig. 3.36). Figure 3.46 shows a rain shower during the past hour, with NNE 15 kt wind, at Roberts Field, Grand Cayman (station 78384 at 19°N, 81.5°W), coinciding **with** the passage of the cold front (see Fig. 3.45). The satellite imagery of Fig. 3.45 indicates that the front has not quite reached Tela, Honduras (station 78905 on the northwest coast of Honduras); nevertheless, 3-dot rain is reported at 1200 UTC.

Finally, ~3 hours later at 1531 UTC, the visible imagery of Fig. 3.47 vividly depicts the advancing cold front (with an associated “rope” cloud) extending from the Bahamas, across eastern Cuba and entering Central America along the *central* northern coast of Honduras. Figure 3.48 (just 30 minutes earlier) provides nearly simultaneous IR imagery for comparison with the visible imagery of Fig. 3.47.

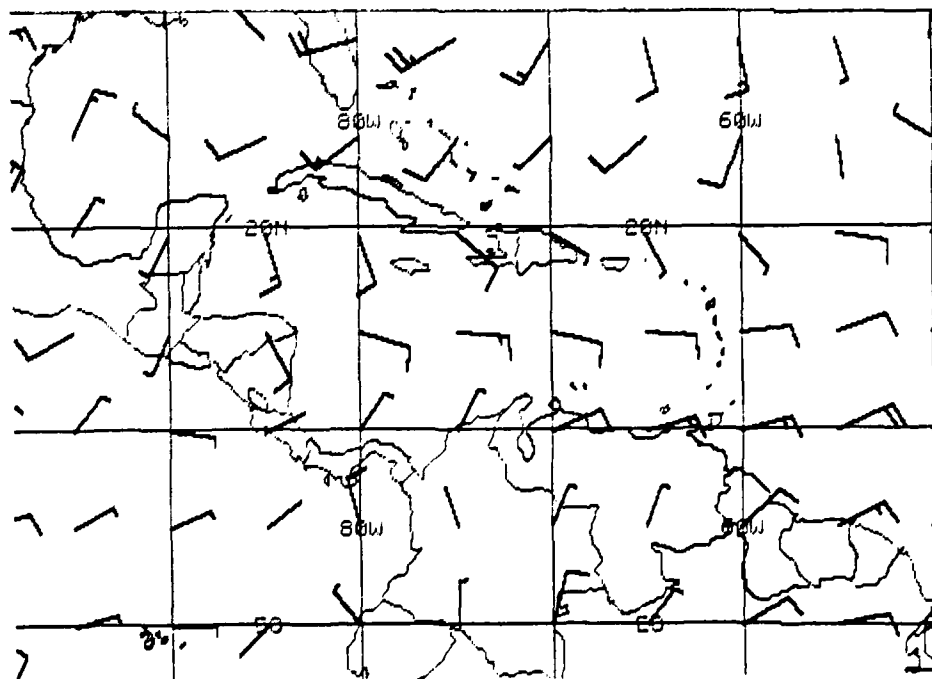


Figure 3.33: FNOG 925 mb Winds, 0000 UTC 14 MAR 1988. Each barb represents 10 kt.

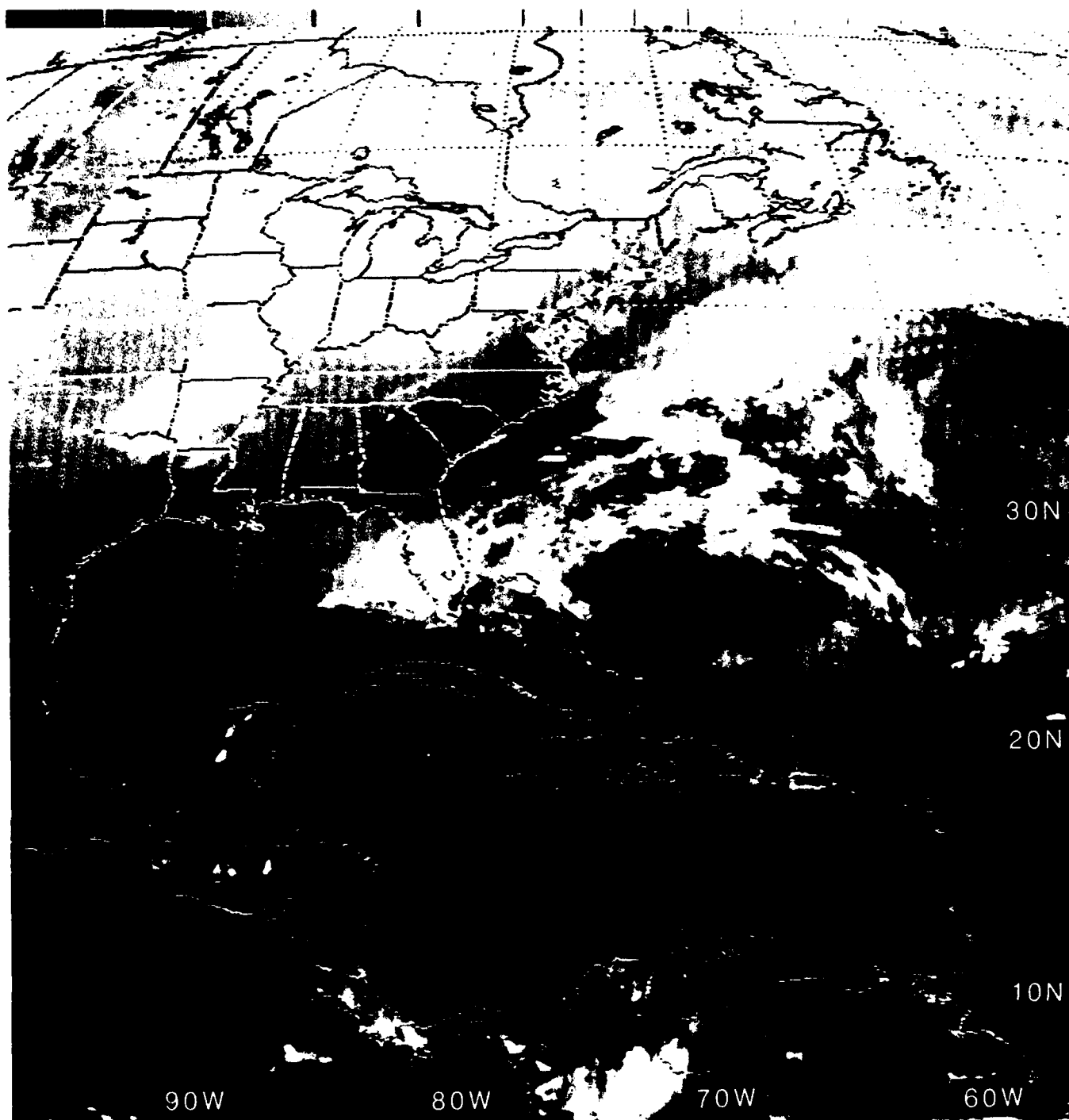


Figure 3.34: GOES East Infrared Satellite Imagery, 0001 UTC 14 MAR 1988

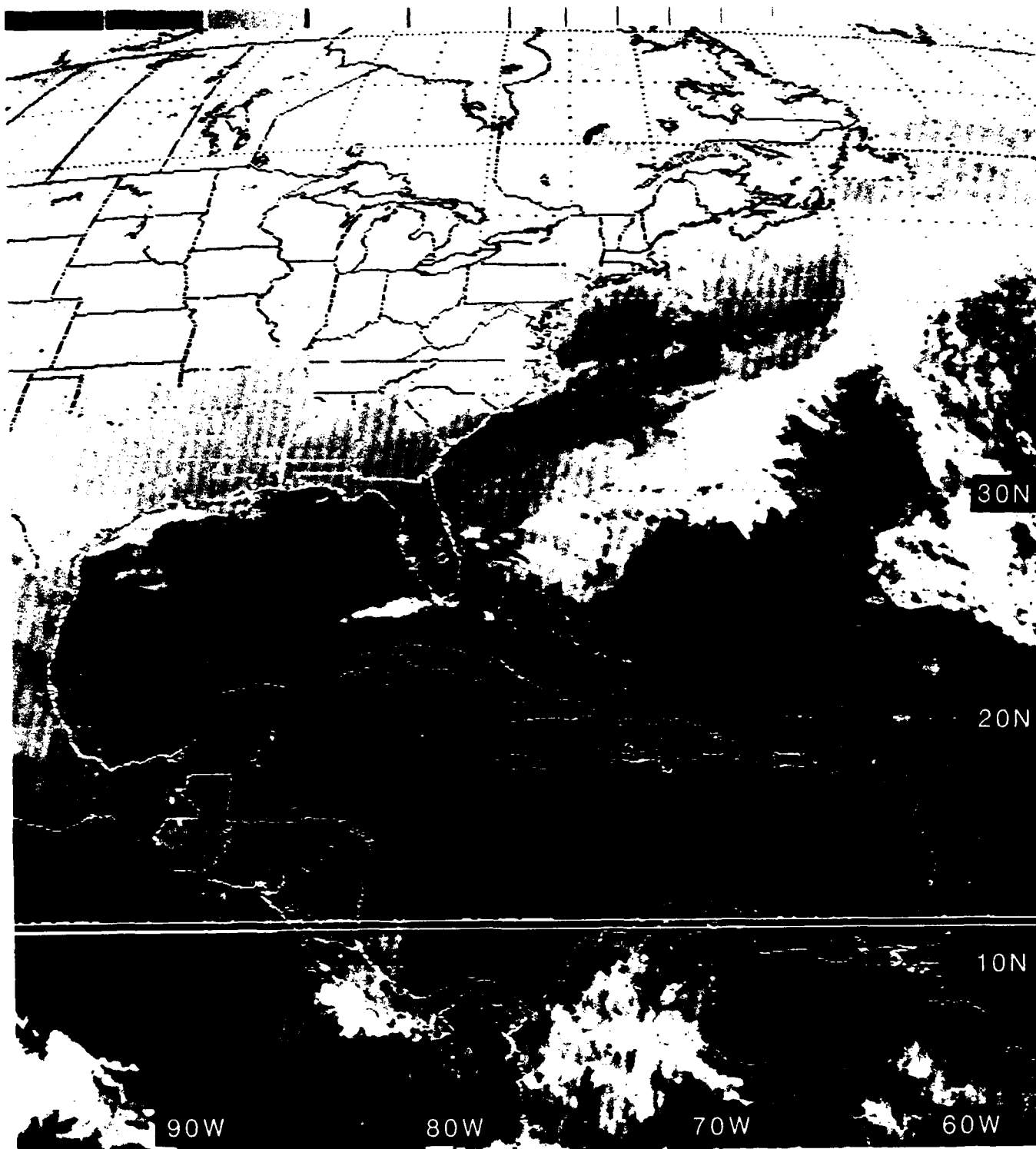


Figure 3.35: GOES East Infrared Satellite Imagery, 1201 UTC 14 MAR 1988
(Ignore the two horizontal lines crossing Nicaragua.)

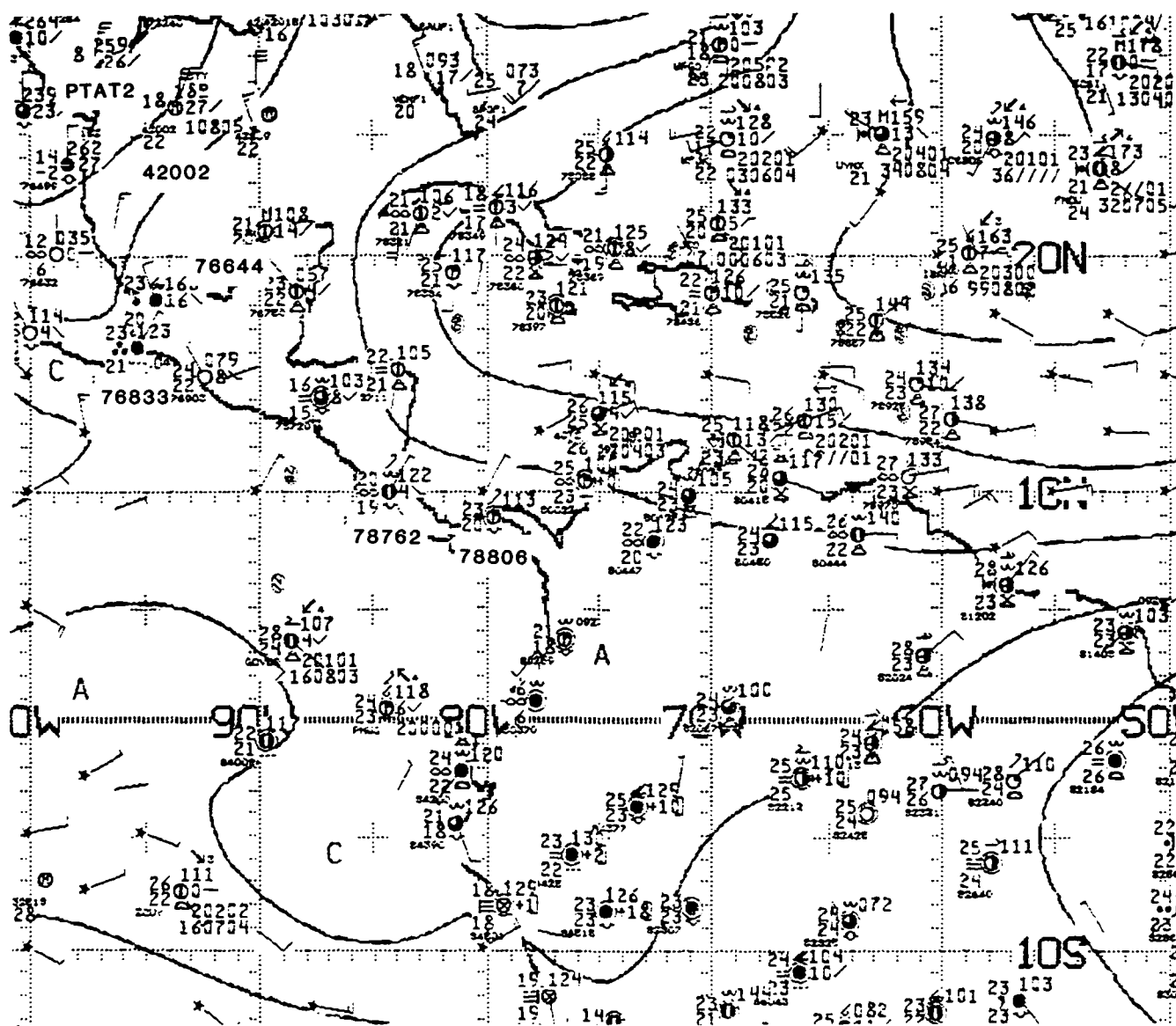


Figure 3.36: NMC 1000 mb Analysis, 1200 UTC 14 MAR 1988.
 Contours are unlabeled stream functions from optimum interpolation analysis,
 with C identifying cyclonic centers and A identifying anticyclonic centers.

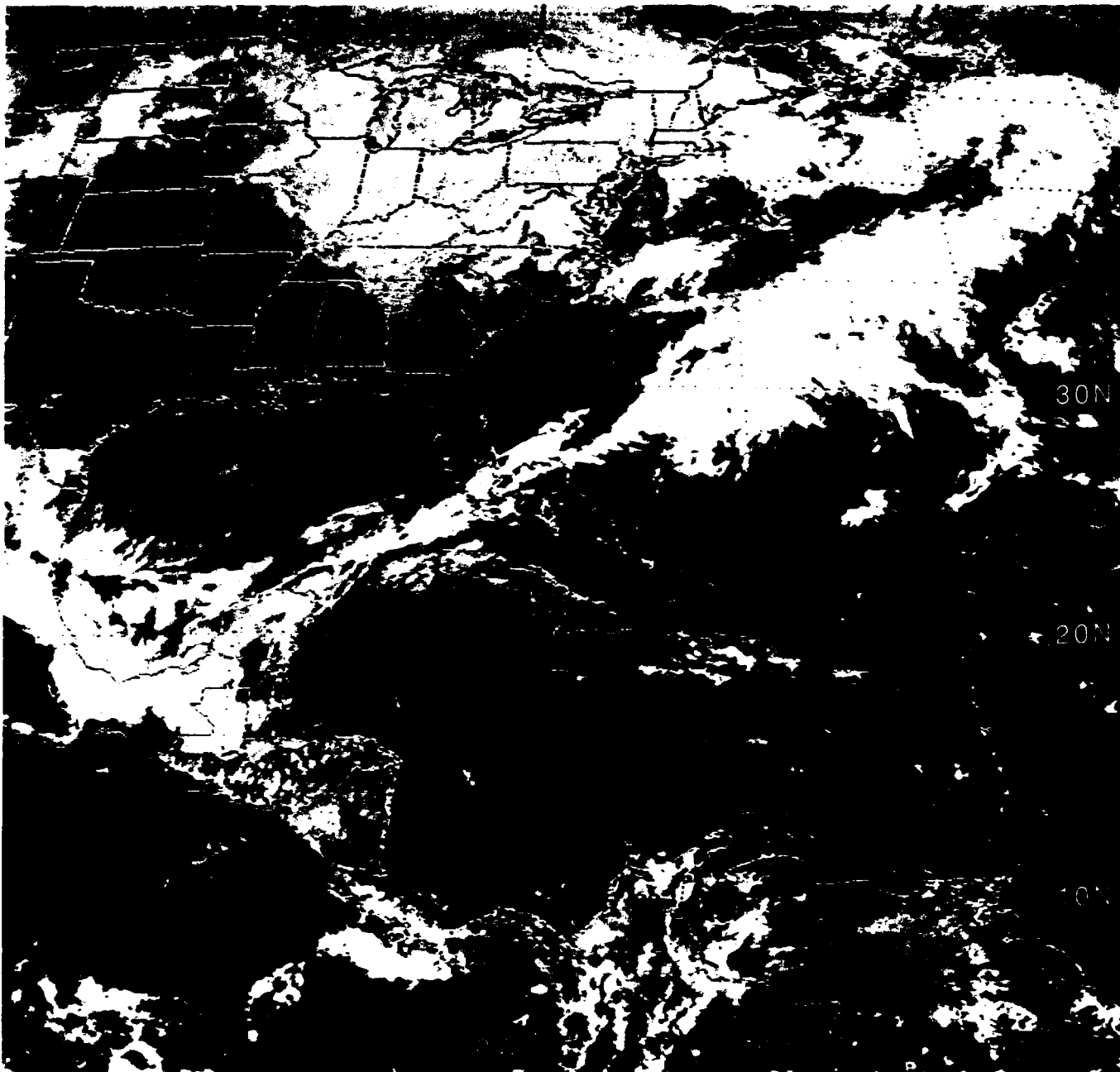


Figure 3.37: GOES East Visible Satellite Imagery, 1731 UTC 14 MAR 1988

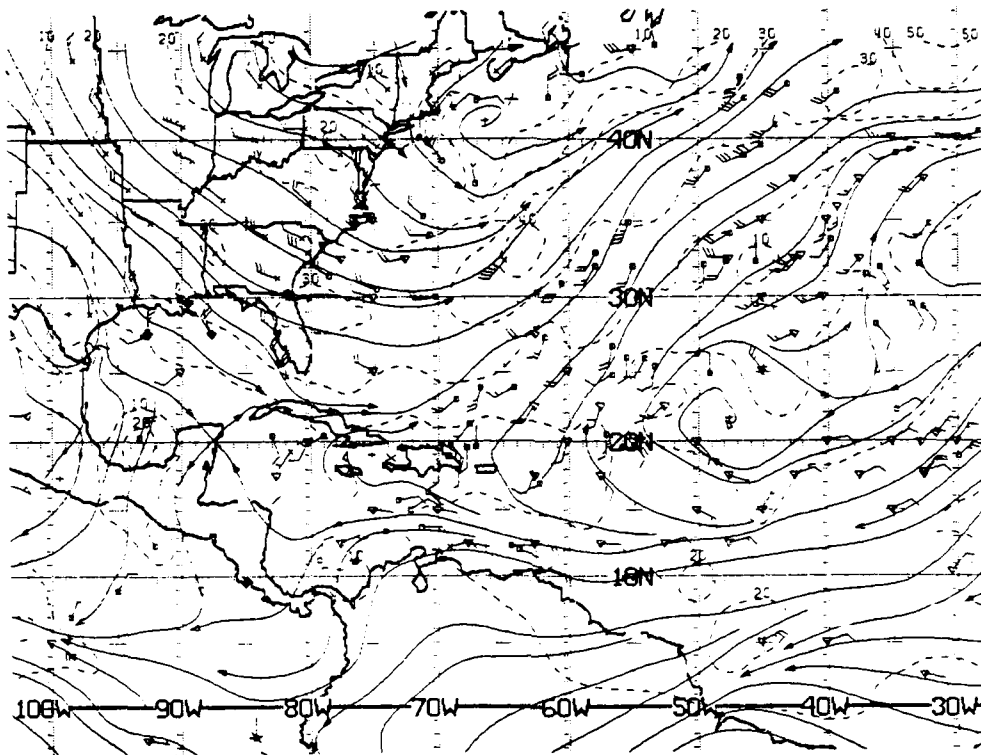


Figure 3.38: NMC ATOLL Operational Streamline Chart, 0000 UTC 15 MAR 1988
As in Fig. 2.4.

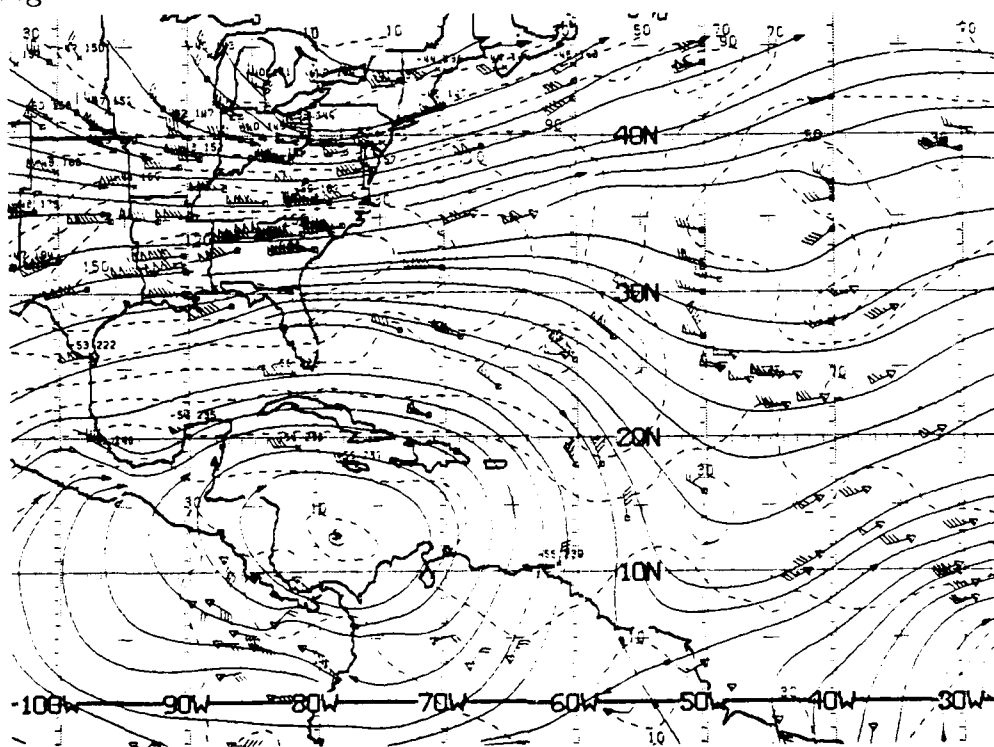


Figure 3.39: NMC 200 mb Operational Streamline Chart, 0000 15 UTC MAR 1988
As in Fig. 2.6.

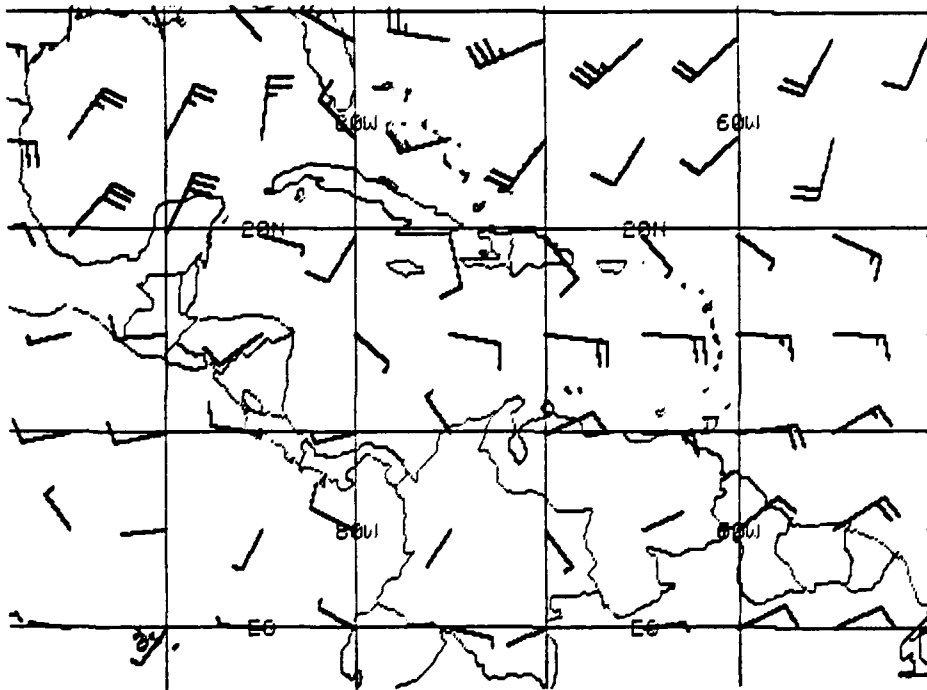


Figure 3.40: FNOC 925 mb Winds 24-H PROG VT 0000 UTC 15 MAR 1988.
Each barb represents 10 kt.

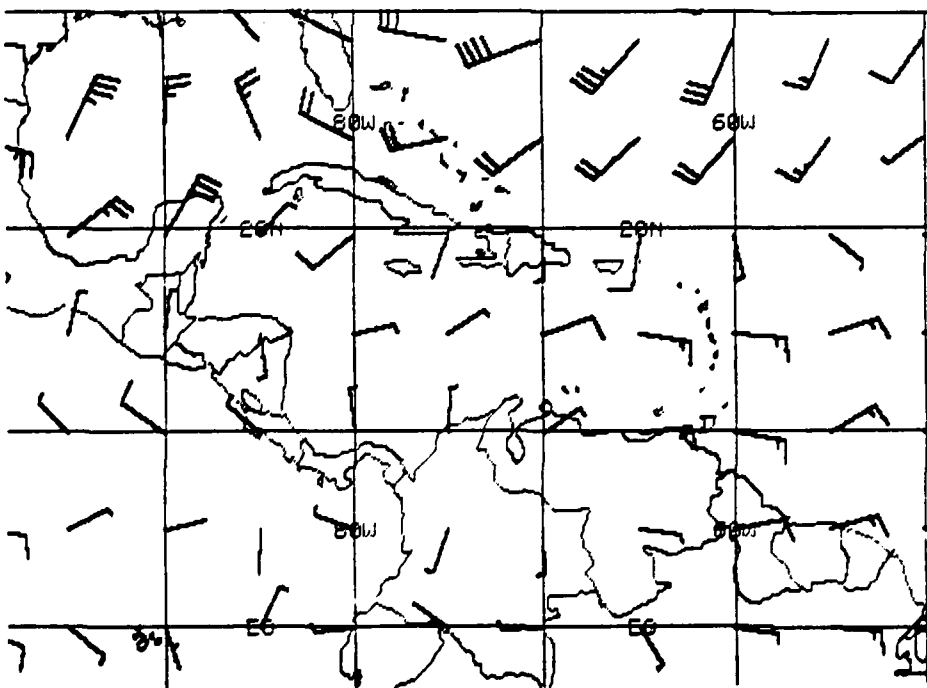


Figure 3.41: FNOC 925 mb Winds. 0000 UTC 15 MAR 1988. Each barb represents 10 kt.

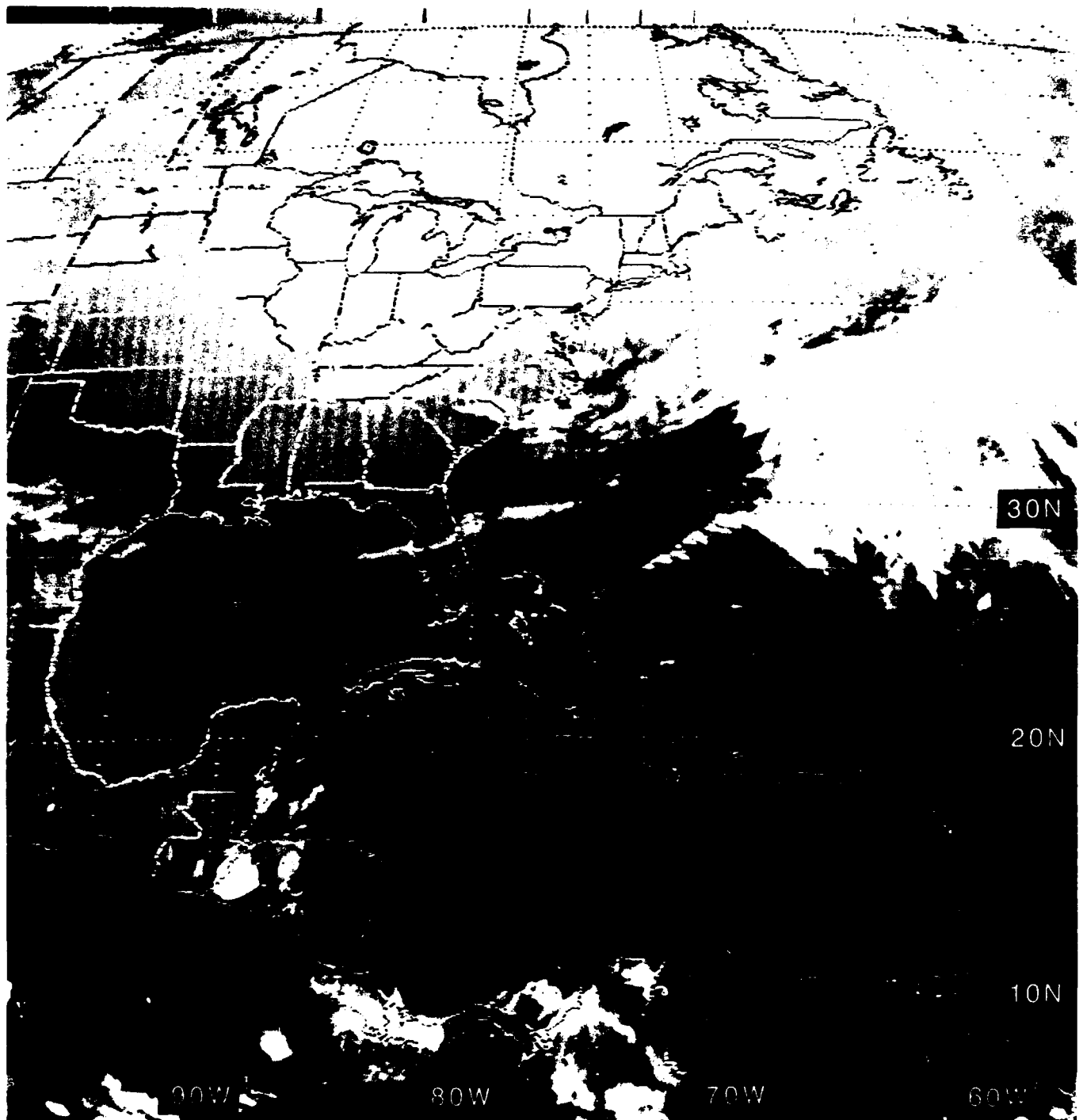


Figure 3.42: GOES East Infrared Satellite Imagery, 0001 UTC 15 MAR 1988

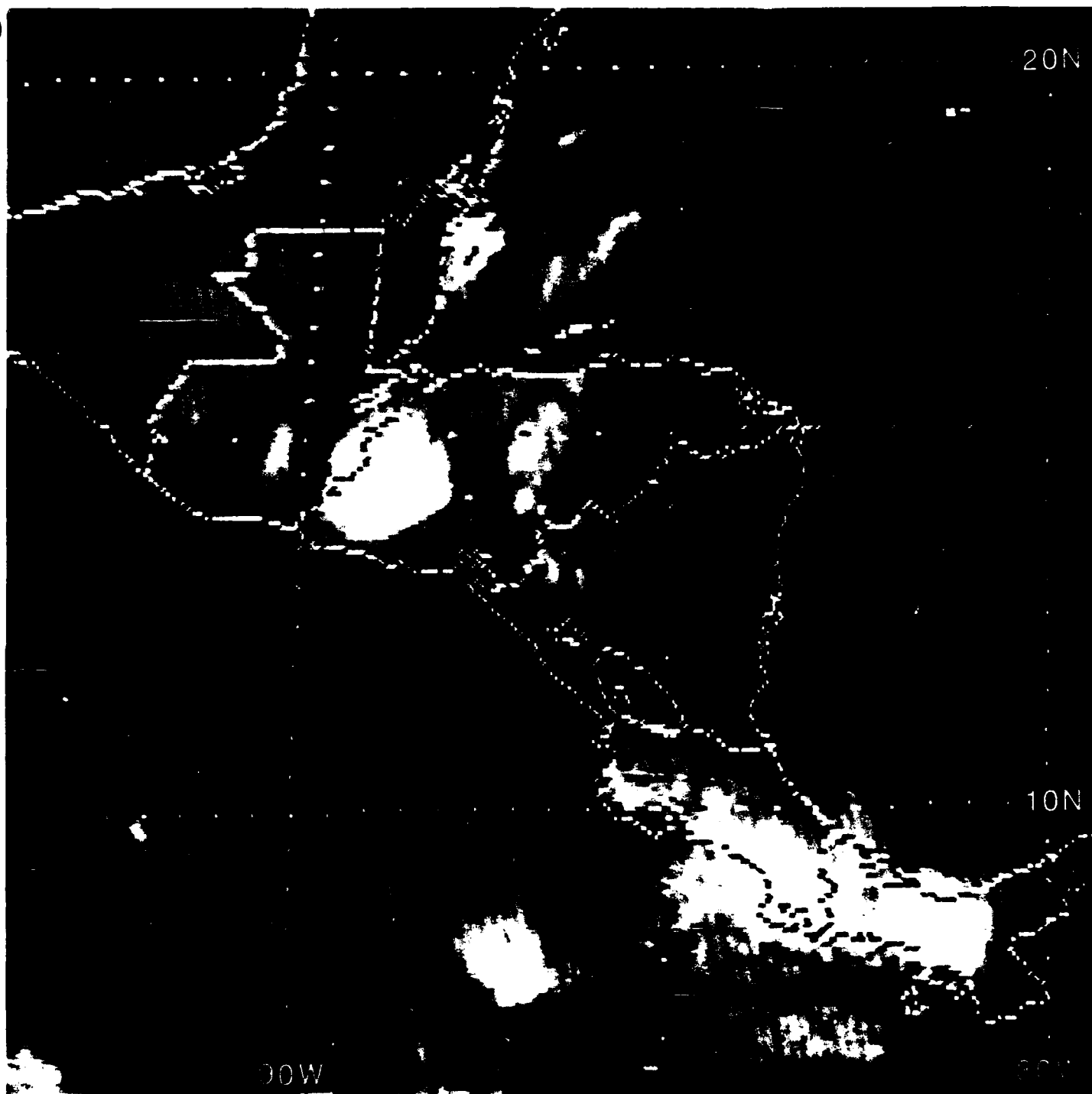


Figure 3.43: GOES E. IR Imag. ("Zoomed"), 0001 UTC 15 MAR 1988

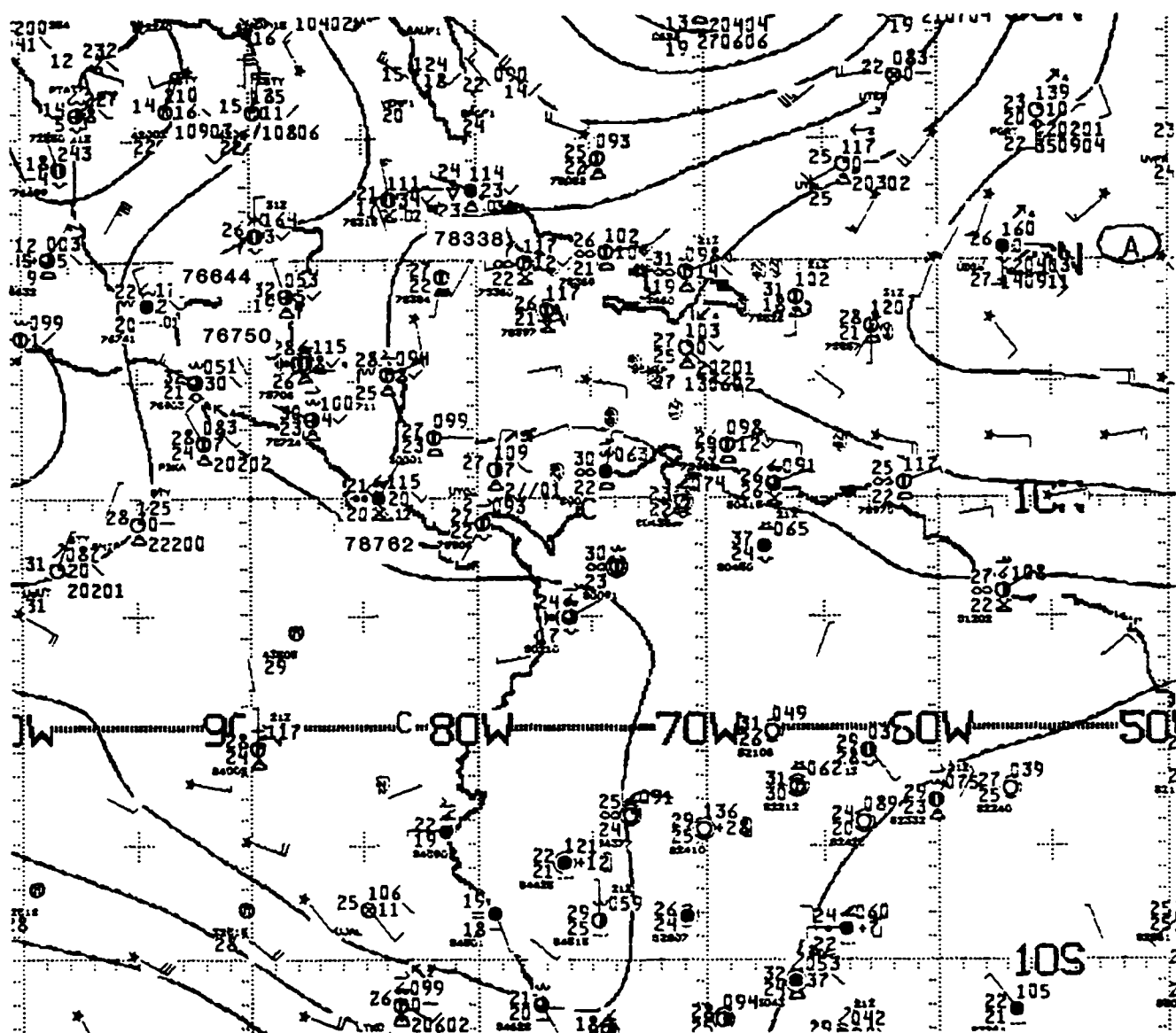


Figure 3.44: NMC 1000 mb Analysis, 0000 UTC 15 MAR 1988.

Contours are unlabeled stream functions from optimum interpolation analysis, with C identifying cyclonic centers and A identifying anticyclonic centers.

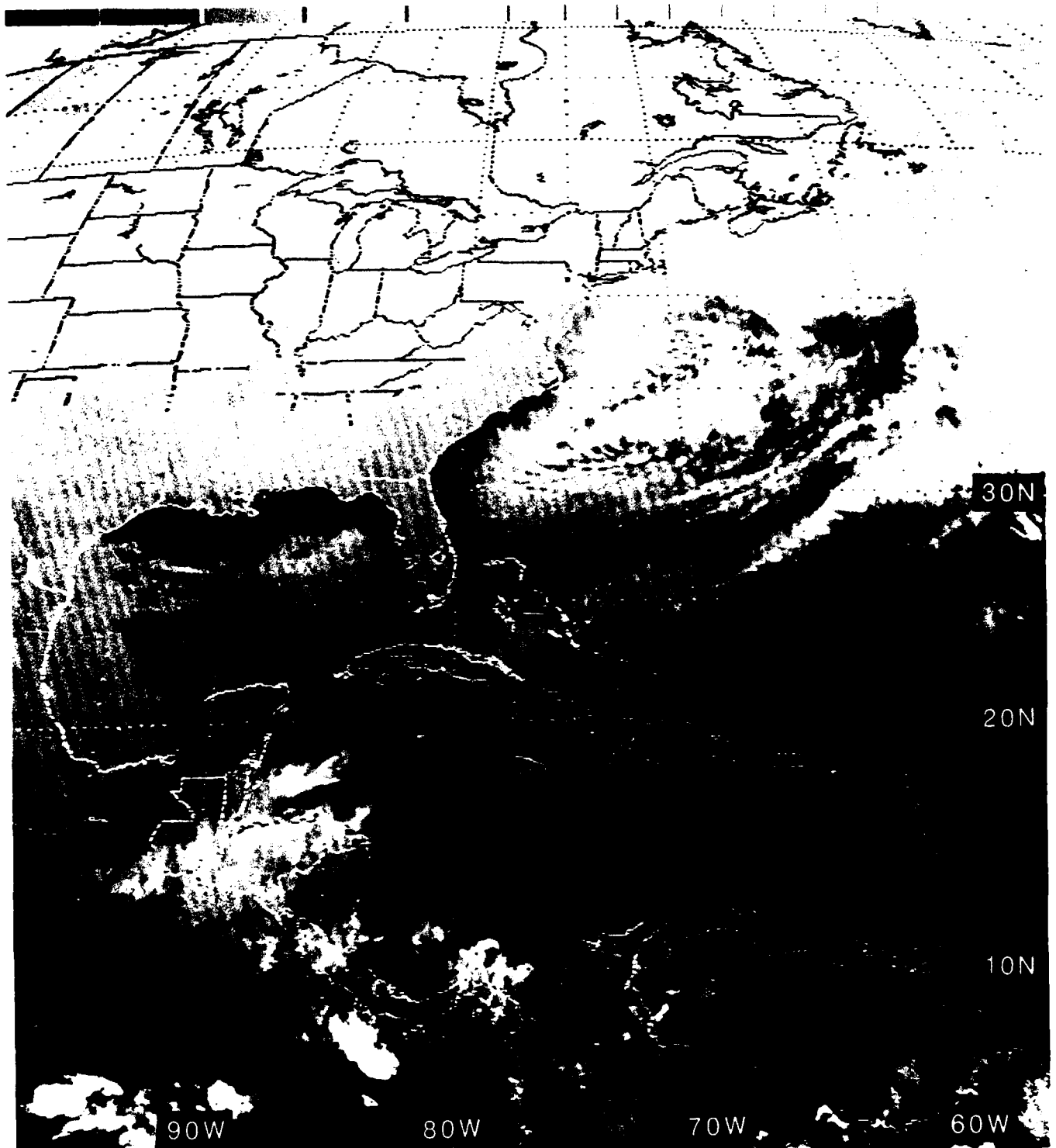


Figure 3.45: GOES East Infrared Satellite Imagery, 1201 UTC 15 MAR 1988

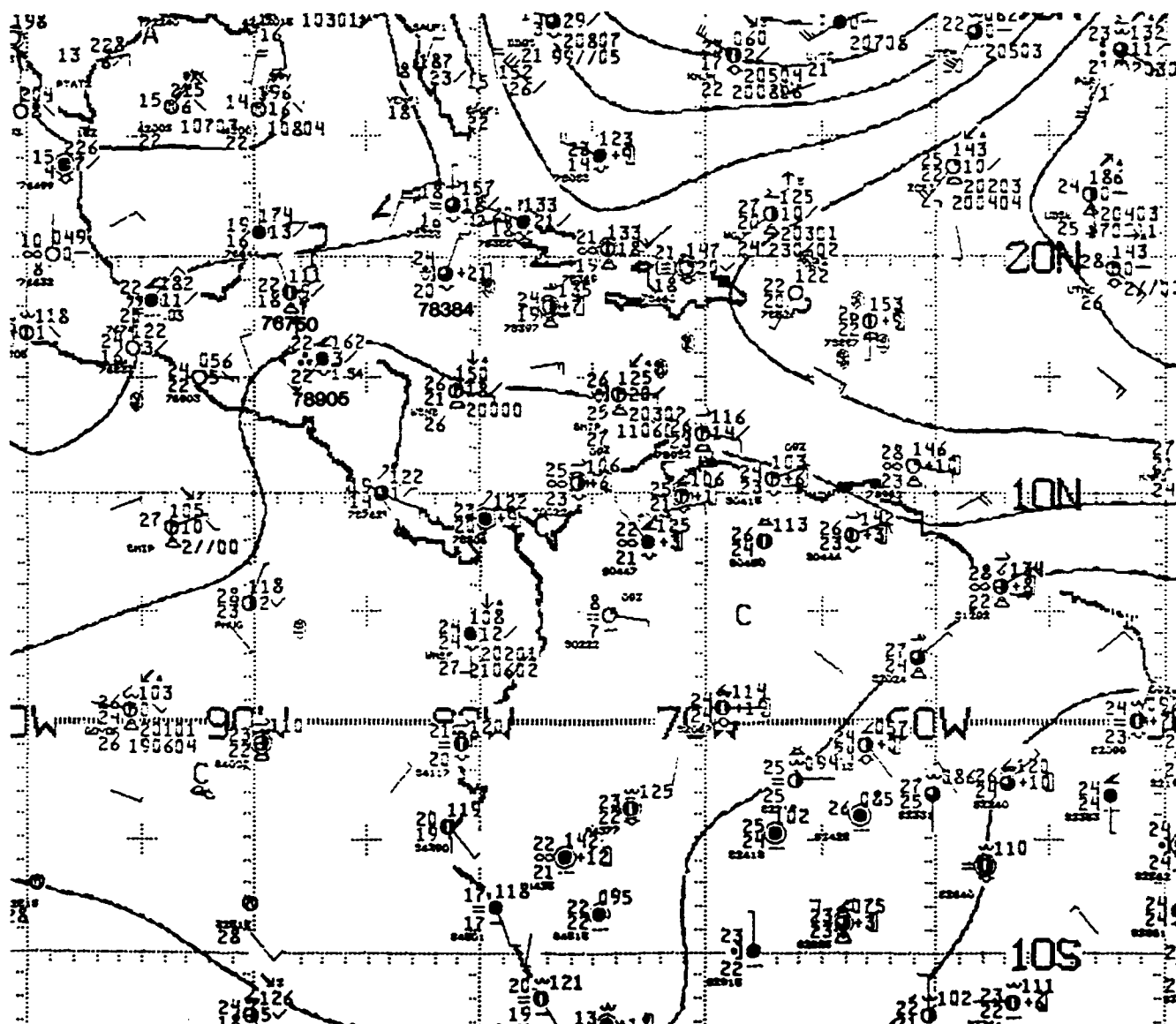


Figure 3.46: NMC 1000 mb Analysis, 1200 UTC 15 MAR 1988.

Contours are unlabeled stream functions from optimum interpolation analysis, with C identifying cyclonic centers and A identifying anticyclonic centers.

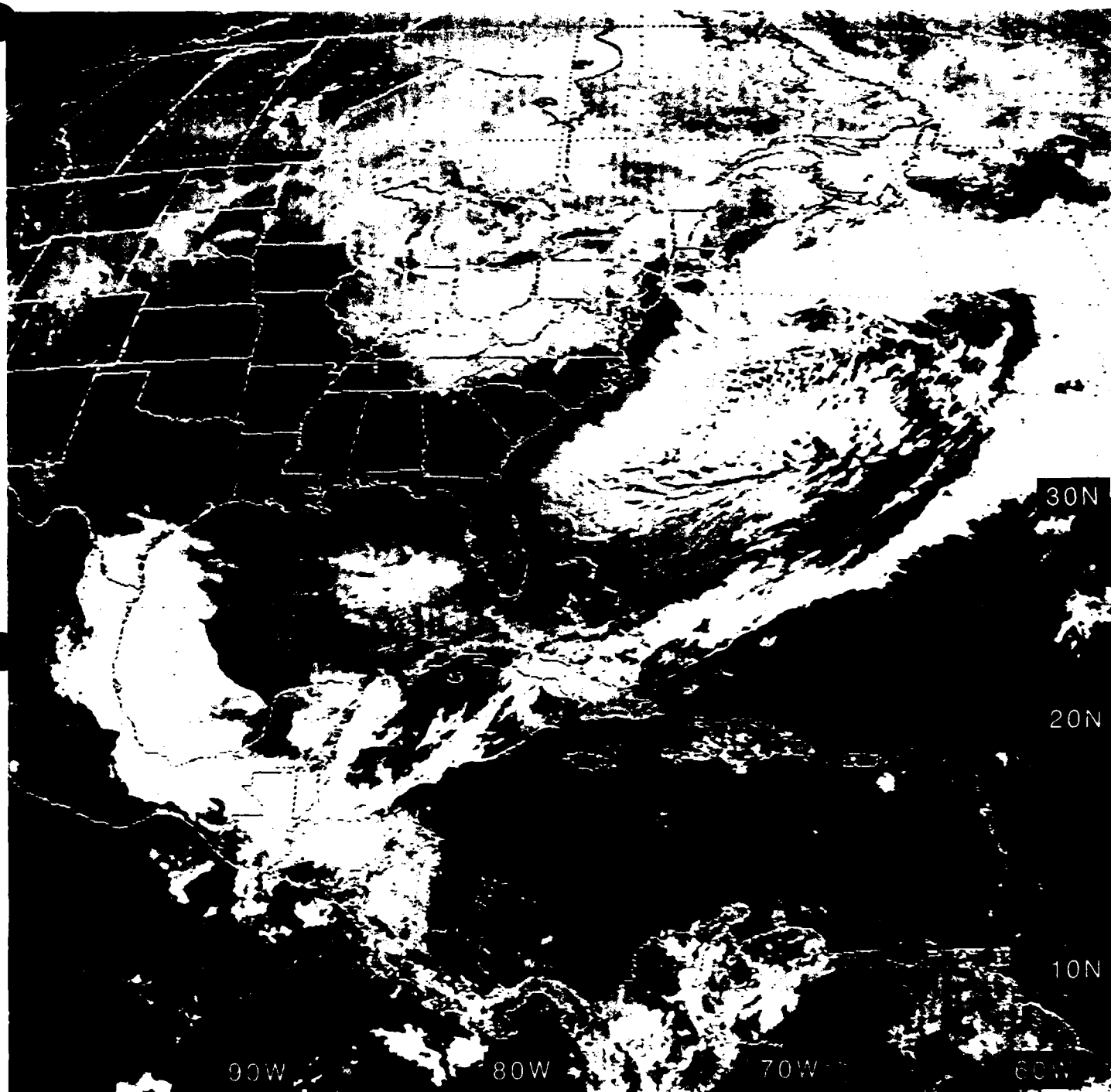


Figure 3.47: GOES East Visible Satellite Imagery, 1531 UTC 15 MAR 1988

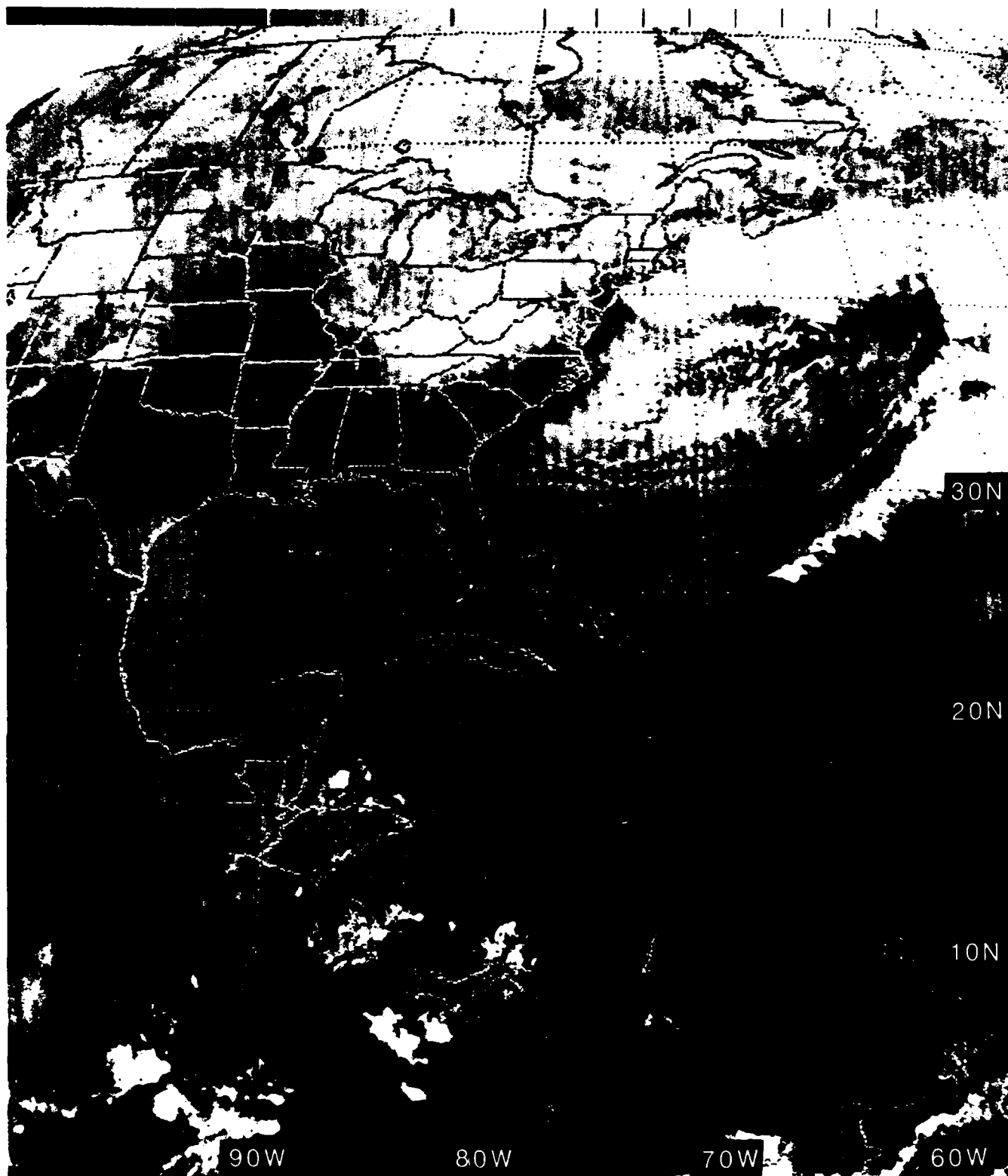


Figure 3.48: GOES East Infrared Satellite Imagery, 1501 UTC 15 MAR 1988

16 March 1988

Figures 3.49 and 3.50 are “zoomed” (4 km resolution) visible and IR images of Central America about 3 hours before the 0000 UTC 16 March analyses to follow. In particular, note that the clouds,—including the “rope” cloud—associated with the cold front, now extending through southern Cuba to the north central coast of Honduras, are primarily low clouds, i.e., dark grey on the IR imagery of Fig. 3.50. The cirroform clouds, *over* southern Nicaragua and *north* of Panama (the “blurred” imagery on the visible imagery of Fig. 3.49), are identified by their white (cold) appearance on the IR imagery of Fig. 3.50.

By 0000 UTC on 16 March, The NHC surface analysis (not shown) locates the cold front extending southwestward through 24°N, 65°W in the North Atlantic Ocean, through the Windward Passage (between Cuba and Hispaniola), across Jamaica and the northeast coast of Honduras (near 16°N, 85°W), across the western border of Honduras, before terminating in southern Guatemala (see Fig. 3.51). Tracking the front’s movement toward the southeast from Grand Cayman to Jamaica in 12 hours, its speed is ~10 kt. At this time, the NMC ATOLL streamline analysis (Fig. 3.52) gives little assistance in locating the front; although there is a 10-kt isotach extending from western Cuba into northeastern Honduras. The NMC 200 mb streamline analysis (Fig. 3.53) maintains the strong anticyclone aloft, while moving it slightly westward to a position over the Mosquito Banks.

Noting that the low-level flow over northeastern Honduras had a **southerly** component 24-h earlier at 0000 UTC on 15 March—see both the FNOC 925 mb winds in Fig. 3.41 and the NMC ATOLL streamlines in Fig. 3.38—, the skill of the FNOC NOGAPS 24-h 925 mb prognosis again will be examined. That is, the FNOC 24-h 925 mb “prog” (Fig. 3.54) forecasts a **ENE** 15 kt wind in northeast Honduras at 0000 UTC on 16 March, and it **verifies** in Fig. 3.55. Additionally, the FNOC 24-h 925 mb wind prognosis calls for a trough near the Hispaniola—i.e., near the verifying position of the front. However, the 925 mb wind prognosis (Fig. 3.54) over the Dominican Republic is northwesterly, while on the analysis (Fig. 3.55) a southwesterly wind verifies at 925 mb⁷¹. That is, the front has passed at the surface, but has not passed at 925 mb—hence, the FNOC 925 mb wind prognosis is very good.

Figure 3.56 (with its absence of station observations at 0000 UTC over Guatemala, Honduras, Nicaragua) confirms the overcast conditions (of low cloudiness) over the Bay of Campeche, the Yucatan Peninsula and at Roberts Field, Grand Cayman (station 78384)—near, but behind, the front—(see Fig. 3.51). Elsewhere only scattered cloudiness exists over San Andrés Island (station 80001) and Howard AFB, Panama (station 78806), although precipitation is within sight at San José, Costa Rica (station 78762).

⁷¹Note, however, that the 0000 UTC 16 March 1988 **surface** wind at Santiago, Dominican Republic (station 78460) is northwest in Fig. 3.56 (contrasted to its northeast wind 24 h earlier in Fig. 3.44)—indicating the possibility of the front having already passed at the surface.

At 1200 UTC, comparison of the IR imagery of Fig. 3.57 with the more plentiful station reports of Fig. 3.58, reveals cooler temperatures and overcast skies poleward from the 23°C, with continuous drizzle, at Tela, Honduras (station 78706). Relatively clear skies are found from Nicaragua to Panama, although the grey IR imagery of Fig. 3.57 on the northeast slopes of the mountain chains of Costa Rica (the Cordillera Central and Cordillera Talamanca (see Fig. 1.27)) indicates orographic cloudiness (and possibly some precipitation) in the northeasterly flow. Multilayered clouds reported at Puerto Plata (station 78457) on the northern coast of the Dominican Republic, with 7/8 sky cover, rain during the past hour and a rising barometer (2.3 mb during the past 3 hours), correlates well with the recent passage of the front (see Fig. 3.57).

By 1531 UTC, the visible imagery of Fig. 3.59 clearly places the front extending through the eastern Dominican Republic—then past a *faint* cloud line about 75 n mi south of Jamaica—into Central America *just* north of the Honduras-Nicaragua border.

17 March 1988

By 0000 UTC on 17 March, the NMC Final Analysis (not shown) locates the front (which is now designated a stationary front by NMC west of 29°N, 48°W. Fig. 3.60 depicts the frontal cloudiness from 24°N, 55°W through the southern coast of Hispaniola, terminating on the east coast of Nicaragua at 12°N. While the IR imagery at the same time (Fig. 3.60) gives little support for moving the front so far south, the IR imagery of Fig. 3.61 at 1205 UTC (i.e., 12 hours later) shows the low (and possibly middle) cloudiness extending about 150 n mi **south** of Jamaica. The NMC Final Analysis at 1800 UTC on 17 March (not shown) terminates the front (now receding slowly northward) near 13°N, 83°W; and the visible imagery at 1631 UTC (Fig. 3.63) (1 1/2 h earlier) does show a *faint* band of clouds entering the east coast of Nicaragua between 13°N and 15°N. In support of the 1200 UTC NMC position of the front—or, by now, more properly called a **shear line**—, the station surface reports of Fig. 3.62 indicate *weak* confluence between east-northeasterly flow at Puerto Lempiro, Honduras (station 78711) and an east-southeasterly 20 kt wind at an *inserted* ship report near San Andrés Island (station 80001).

Although no data will be presented for 18 March, by 0000 UTC on that date NMC extends the front **no farther west** than a point 120 n mi south of Jamaica.

While this “Atemporalado” minimally meets the criteria for a Nominal Surge, the Brooks index scheme accurately predicts its movement through Honduras, becoming “quasi-stationary on (or near) the Honduras-Nicaragua border” (see Subsubsection 3.2.3). While neither of the two dry season case studies shows a Strong Surge—leading to cloudiness and precipitation as far south as the Caribbean facing slopes of mountain ranges in Costa Rica and Panama, they **do** exist—see the following Subsubsection 3.3.3.

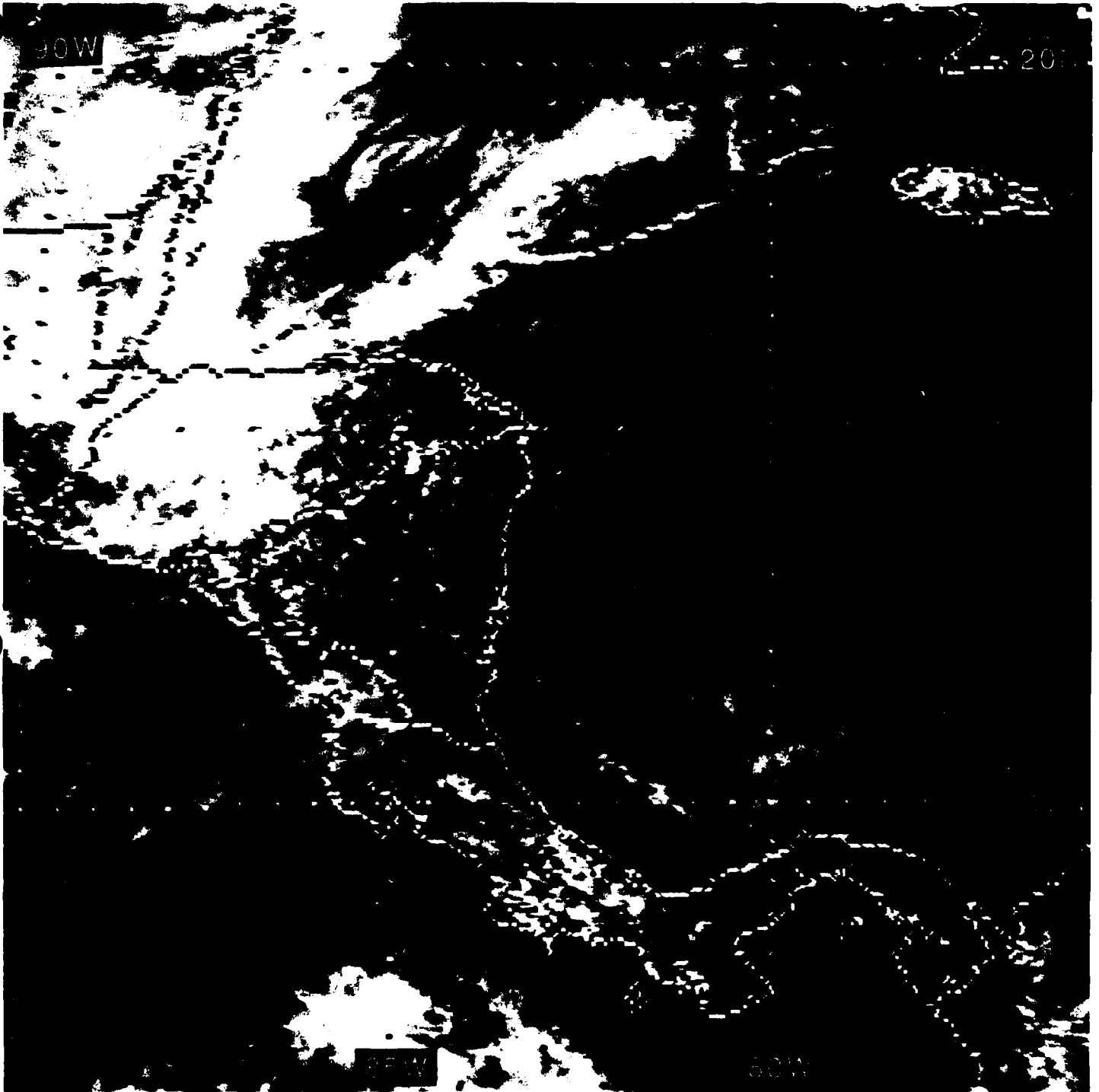


Figure 3.49: GOES E. Visible Imag. ("Zoomed"), 2031 UTC 15 MAR 1988

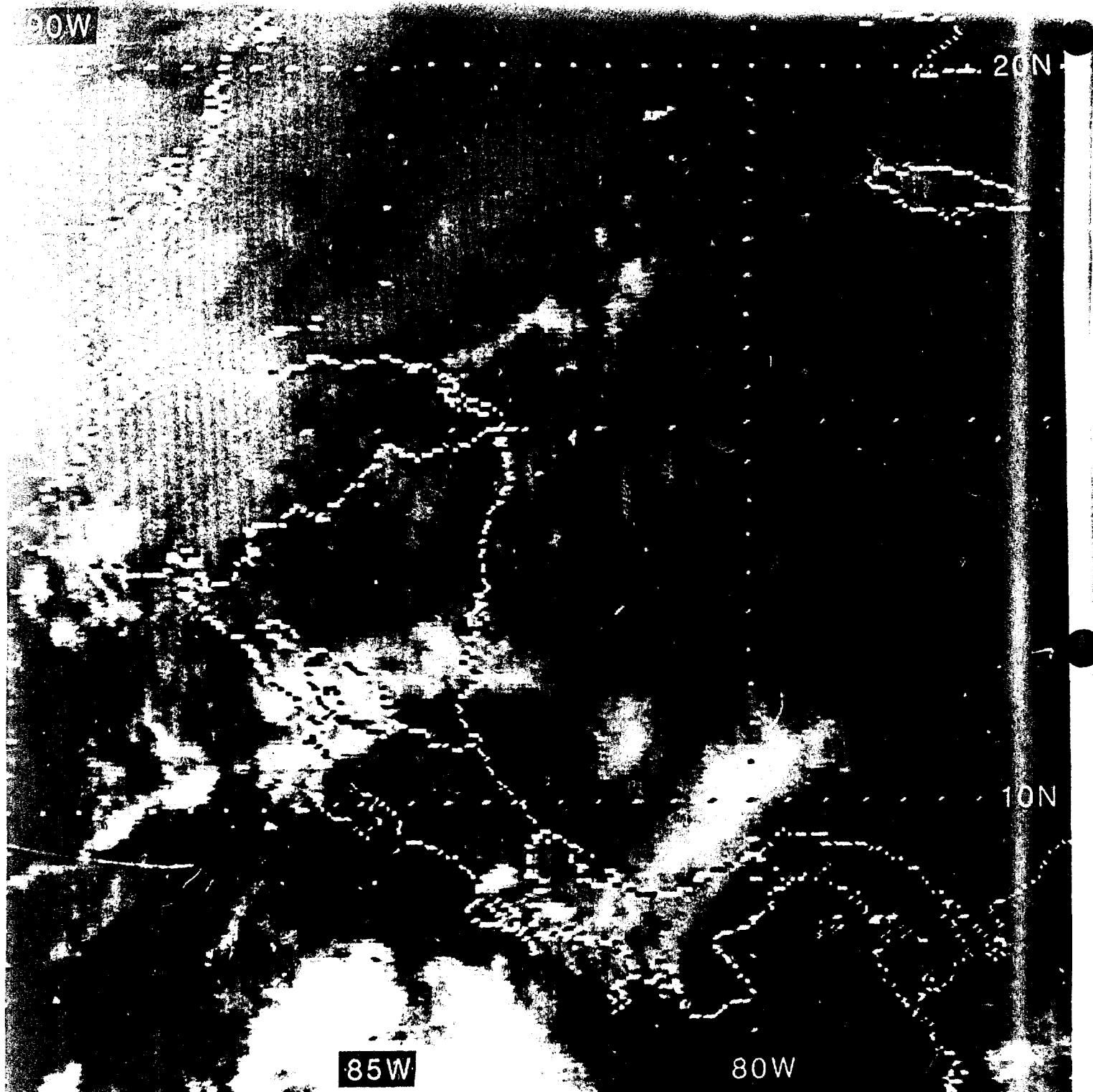


Figure 3.50: GOES E. IR Imag. ("Zoomed"), 2101 UTC 15 MAR 1988

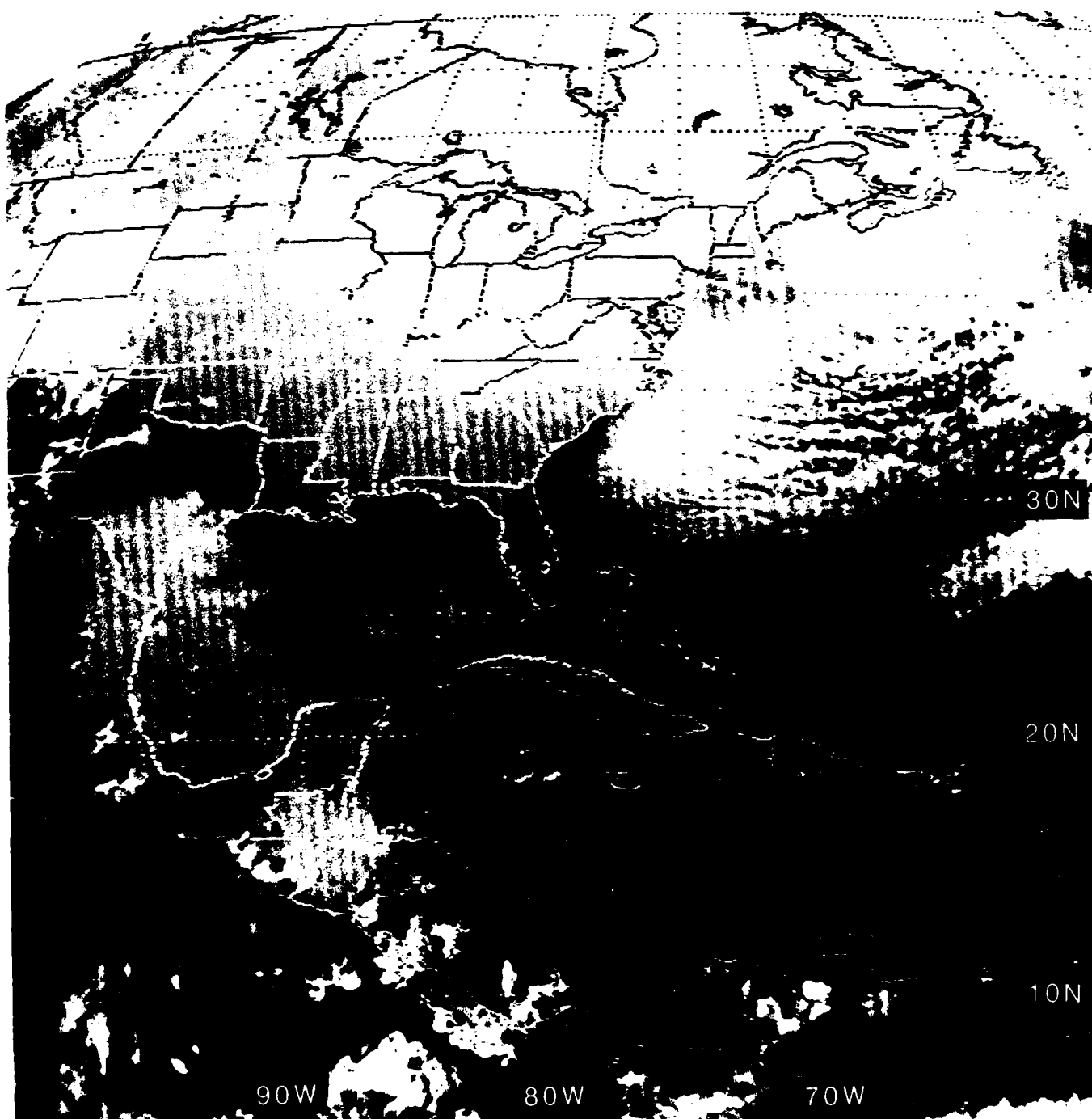


Figure 3.51: GOES East Infrared Satellite Imagery, 0001 UTC 16 MAR 1988

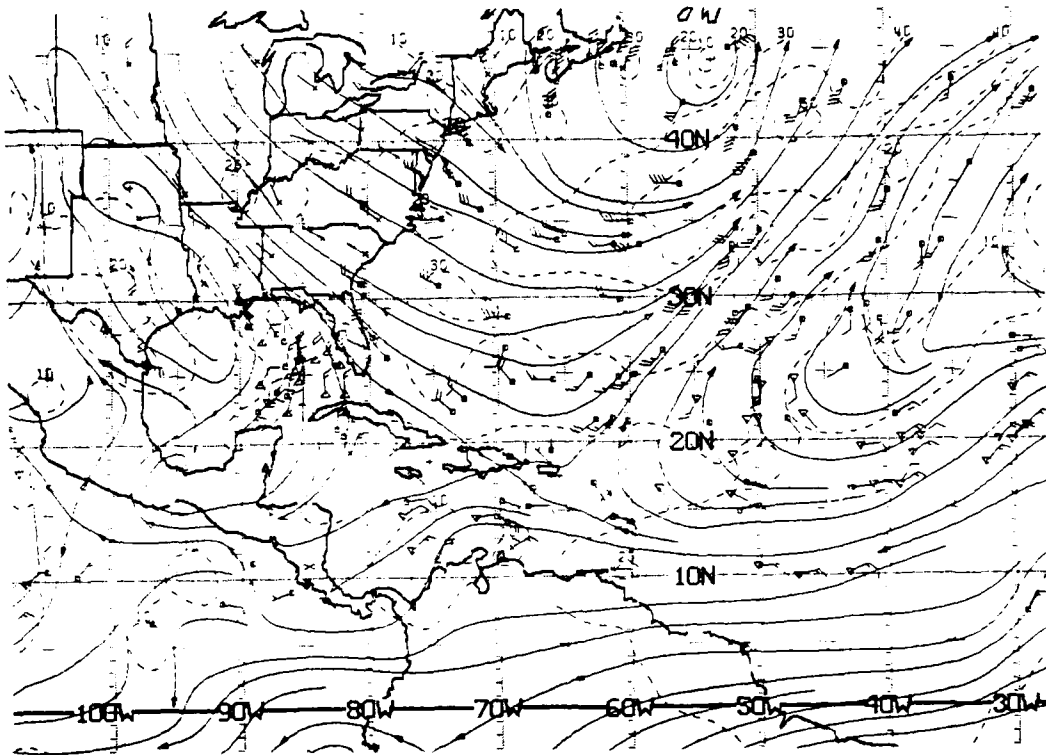


Figure 3.52: NMC ATOLL Operational Streamline Chart, 0000 UTC 16 MAR 1988
As in Fig. 2.4.

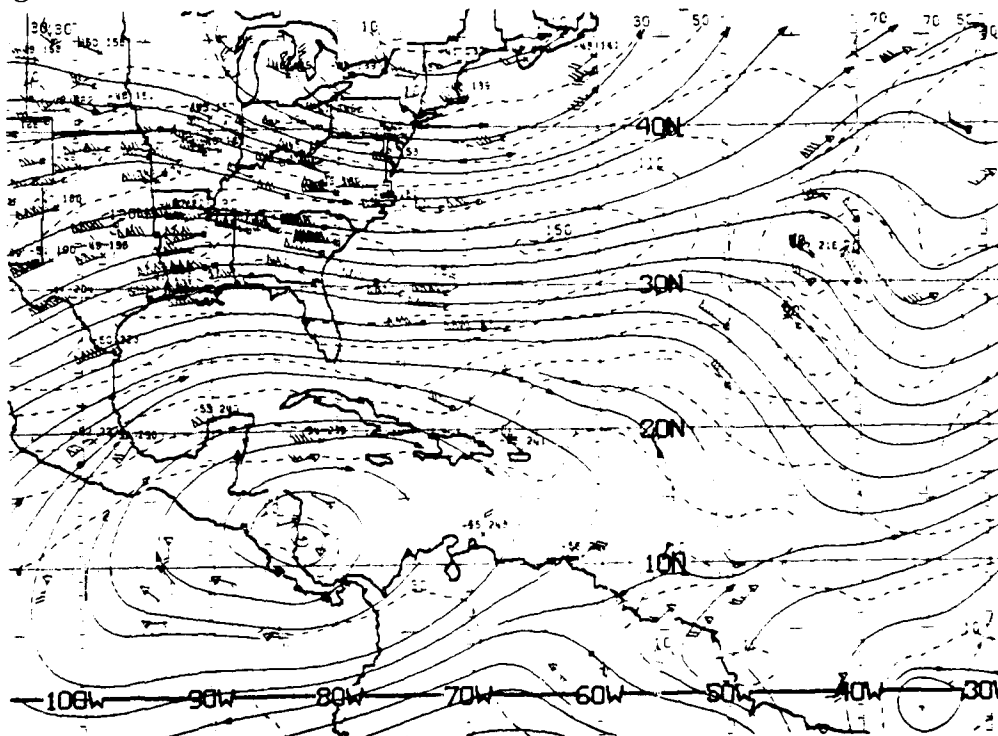


Figure 3.53: NMC 200 mb Operational Streamline Chart, 0000 16 UTC MAR 1988
As in Fig. 2.6.

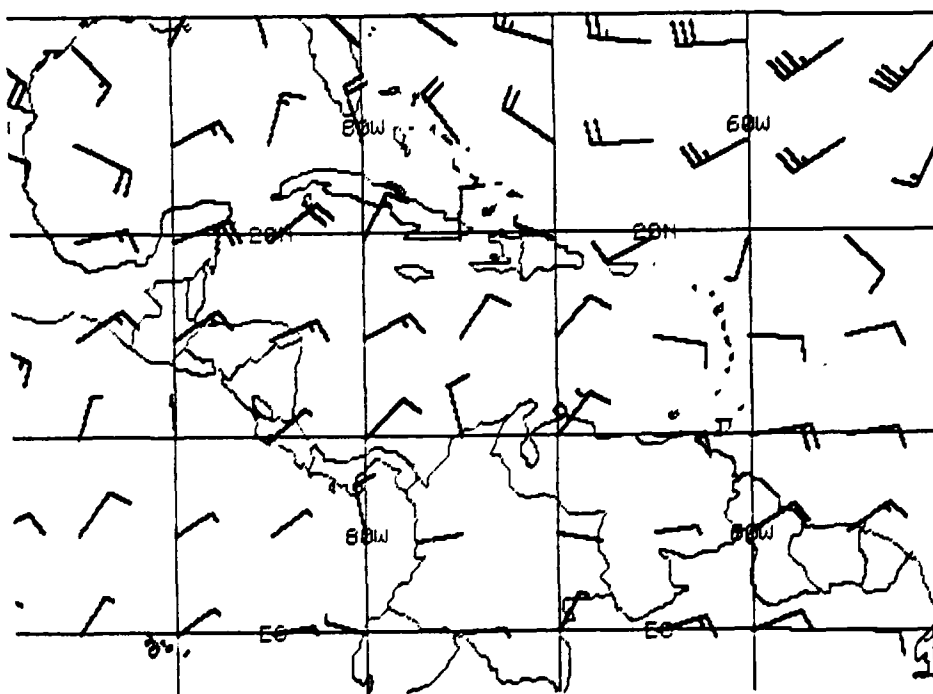


Figure 3.54: FNOC 925 mb Winds 24-h PROG VT 0000 UTC 16 MAR 1988.
Each barb represents 10 kt.

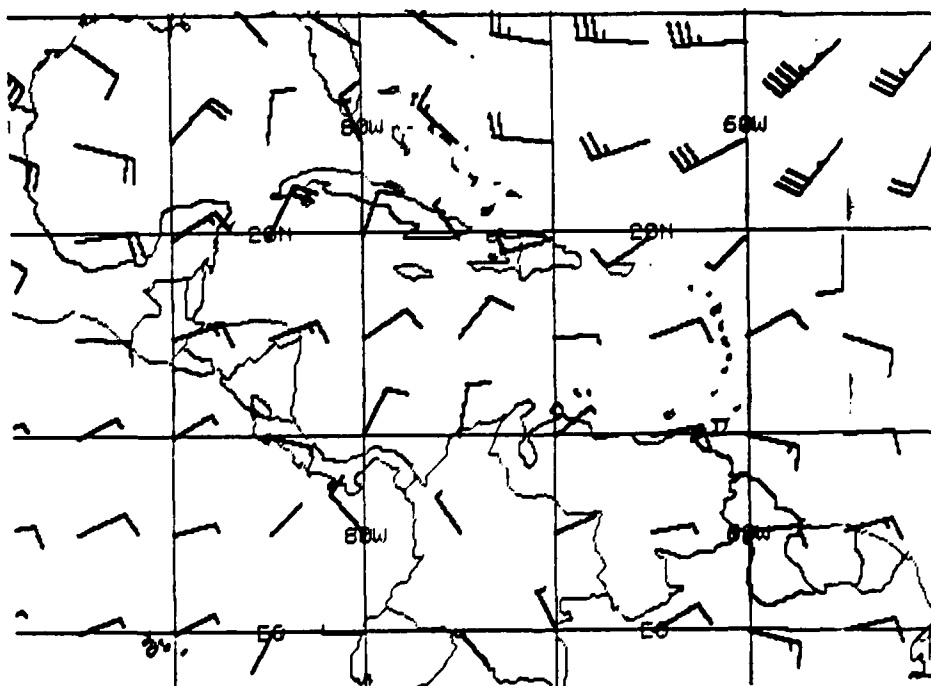
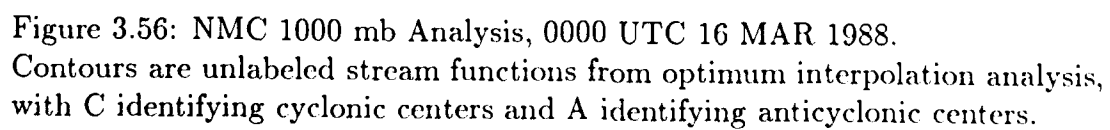


Figure 3.55: FNOC 925 mb Winds, 0000 UTC 16 MAR 1988. Each barb represents 10 kt.



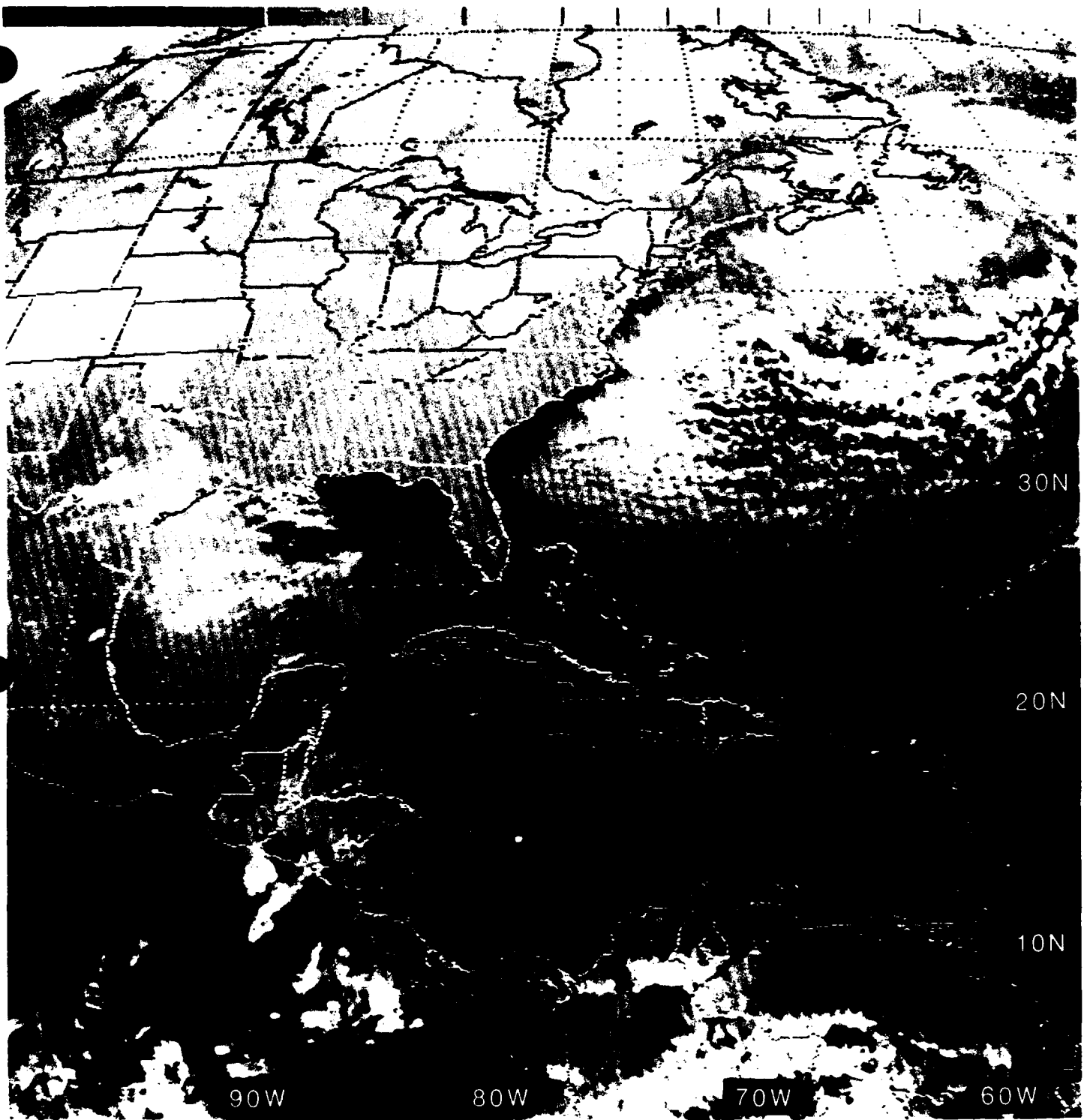


Figure 3.57: GOES East Infrared Satellite Imagery, 1201 UTC 16 MAR 1988

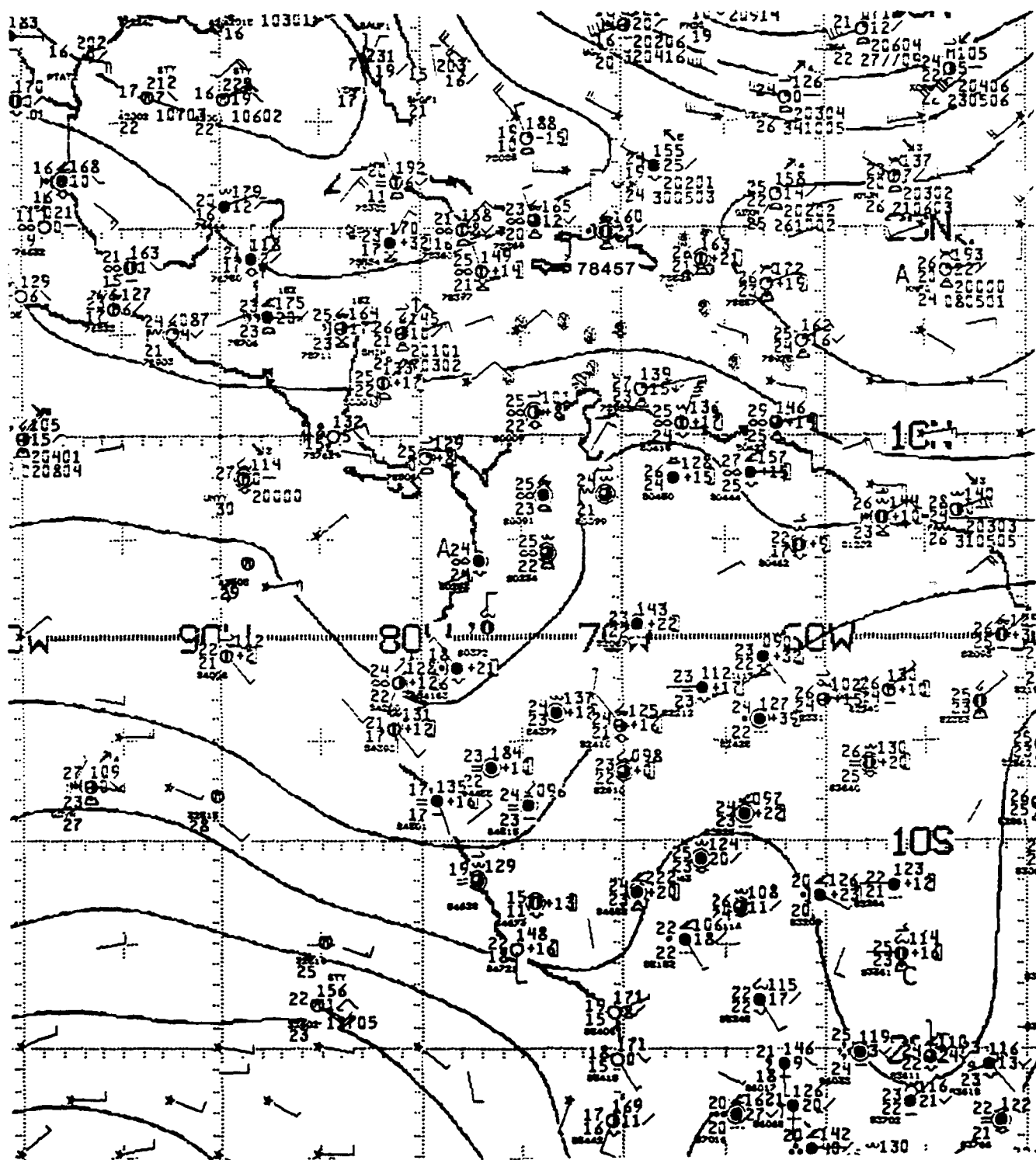


Figure 3.58: NMC 1000 mb Analysis, 1200 UTC 16 MAR 1988.

Contours are unlabeled stream functions from optimum interpolation analysis, with C identifying cyclonic centers and A identifying anticyclonic centers.

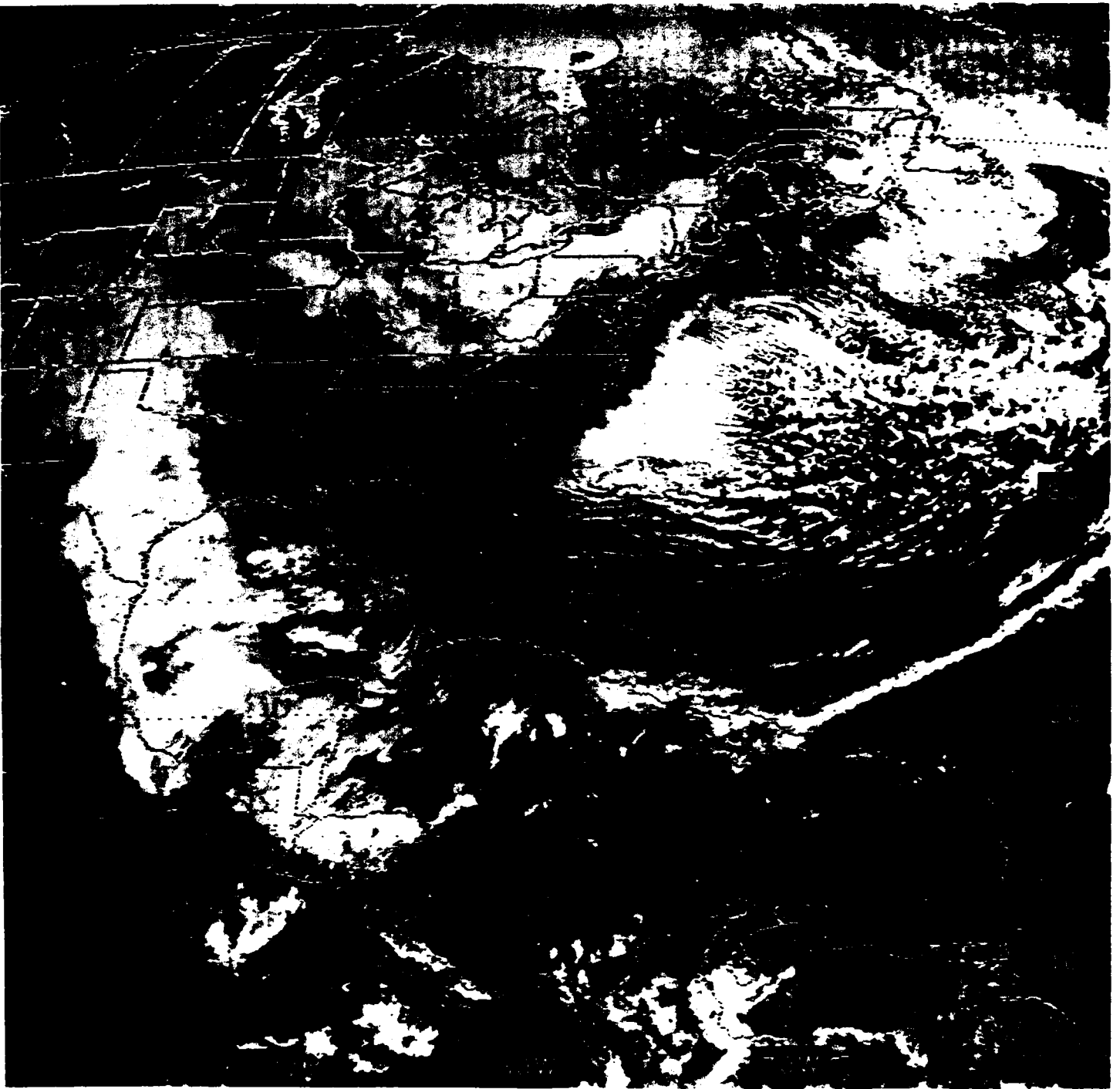


Figure 3.59: GOES East Visible Satellite Imagery, 1531 UTC 16 MAR 1988

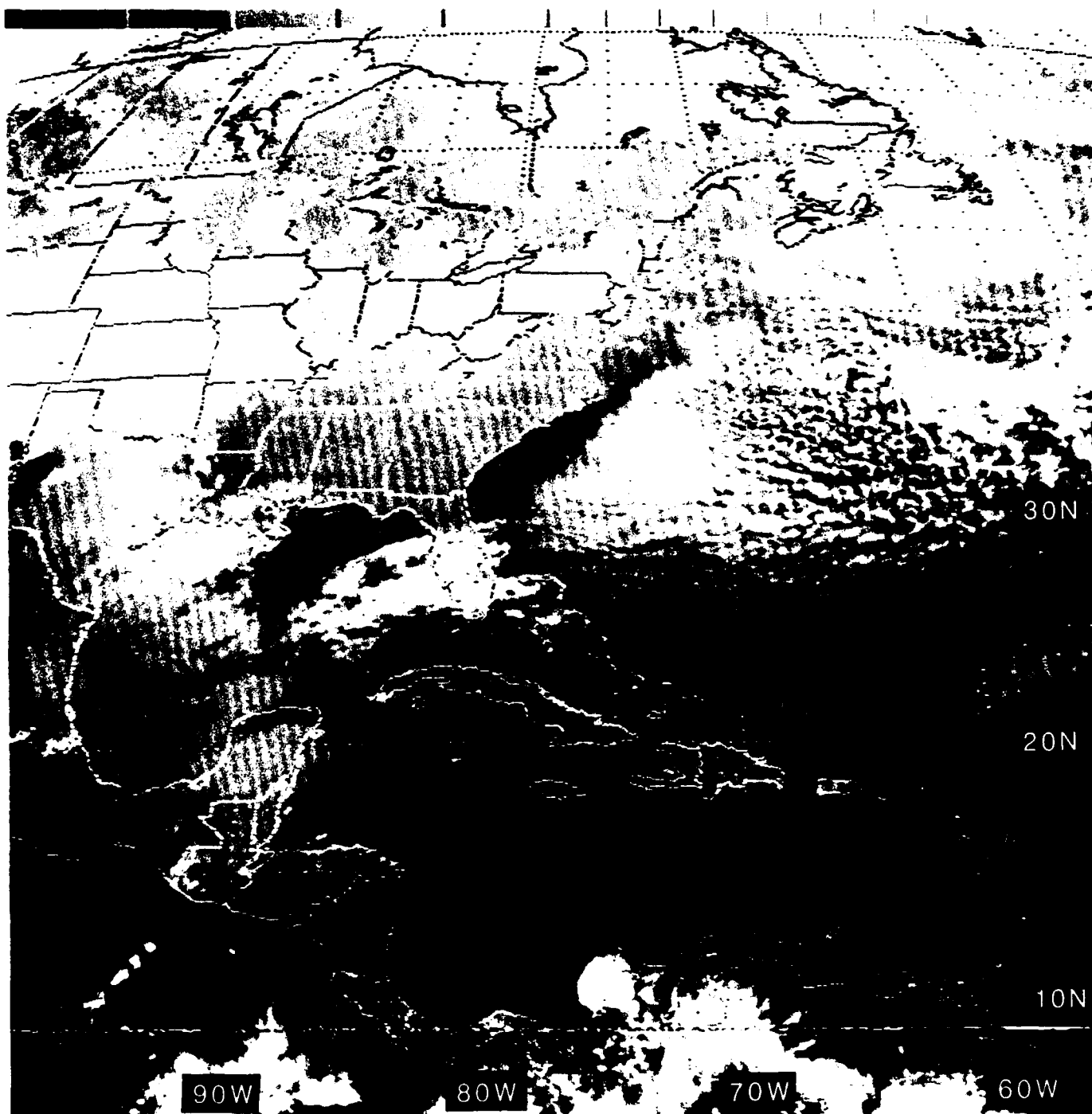


Figure 3.60: GOES East Infrared Satellite Imagery, 0001 UTC 17 MAR 1988

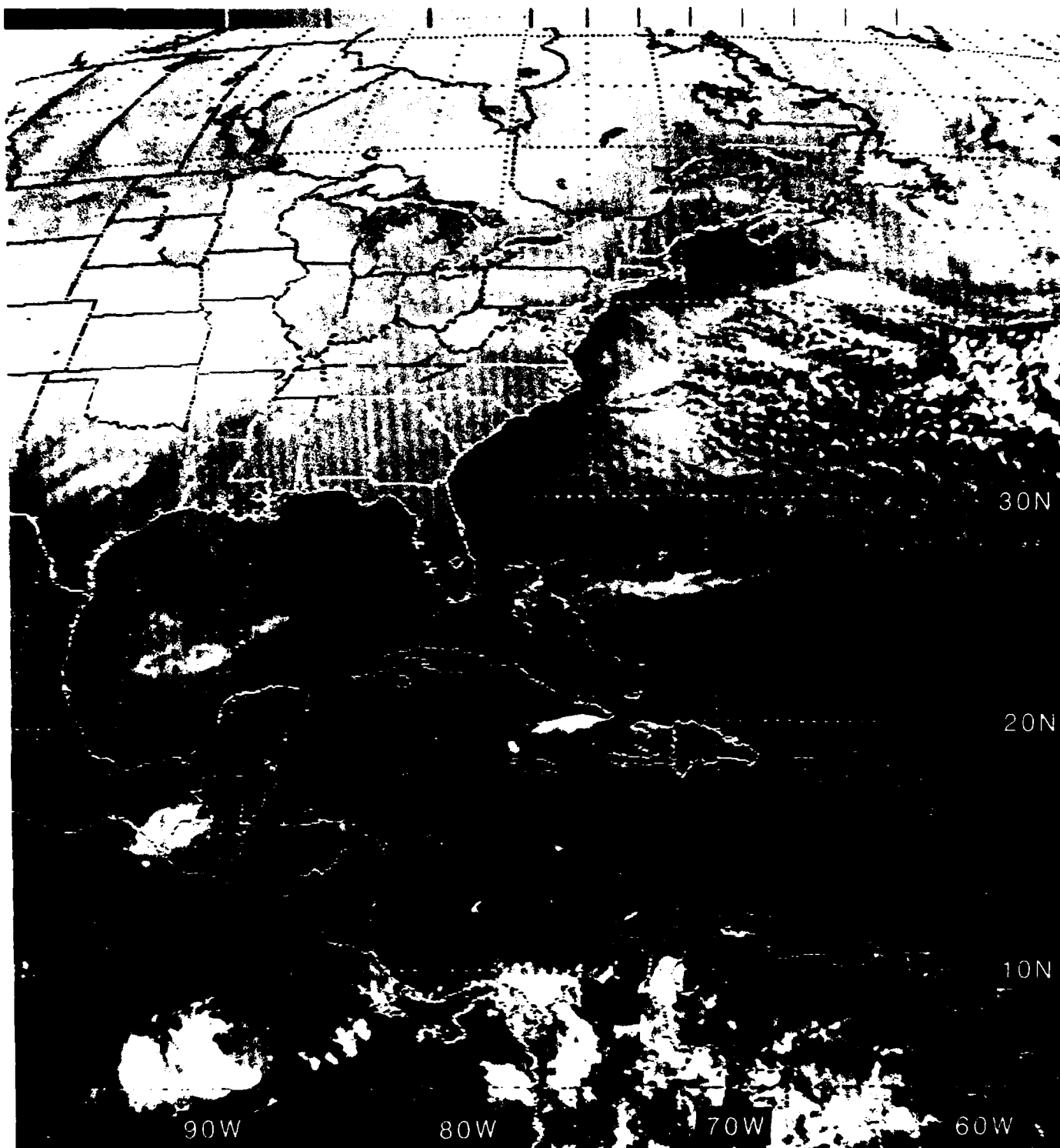


Figure 3.61: GOES East Infrared Satellite Imagery, 1205 UTC 17 MAR 1988

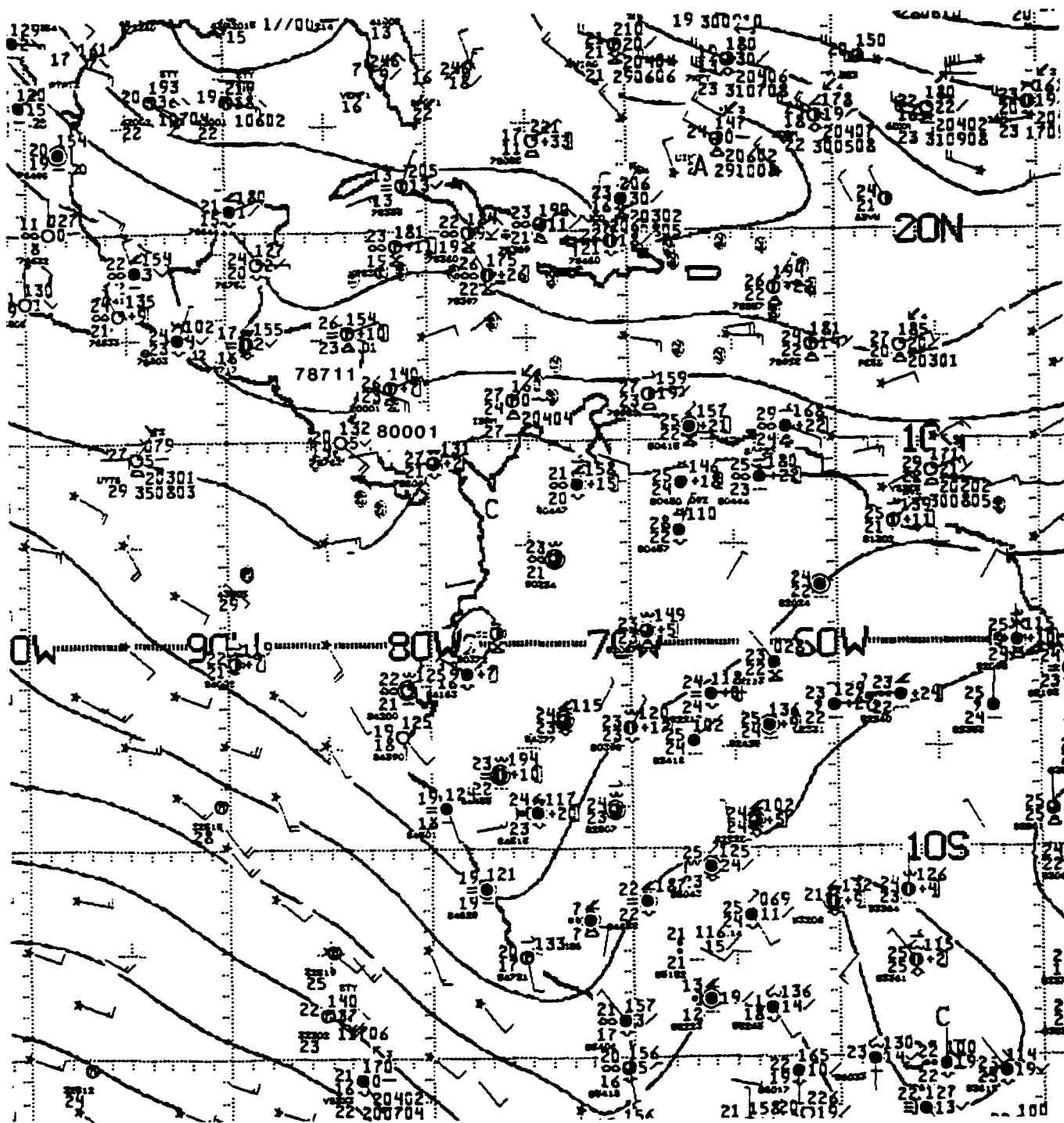


Figure 3.62: NMC 1000 mb Analysis, 1200 UTC 17 MAR 1988.

Contours are unlabeled streamfunctions from optimum interpolation analysis, with C identifying cyclonic centers and A identifying anticyclonic centers.

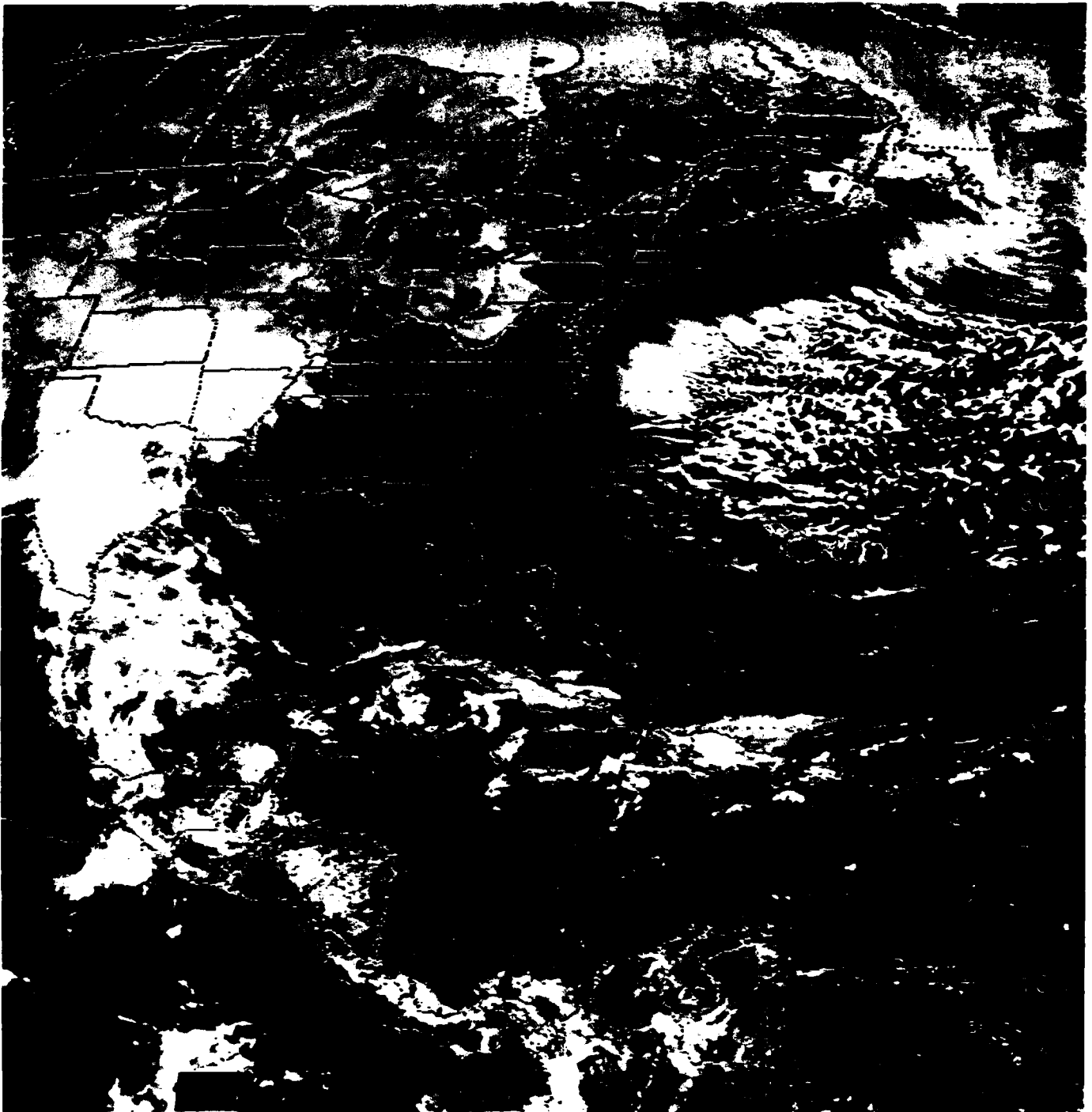


Figure 3.63: GOES East Visible Satellite Imagery, 1631 UTC 17 MAR 1988

3.3.3 Strong Surge during the Dry Season

As mentioned in Case Study III, shear lines (or cold fronts) having a more north-south alignment—as opposed to an east-west alignment—are more likely to penetrate farther into Central America⁷².

The visible imagery⁷³ of Fig. 3.64 at 1803 UTC on 21 February 1989 depicts the cloudiness associated with a cold front (or shear line) crossing the Gulf of Mexico, as it approaches the Yucatan Peninsula. The IR imagery of Figs. 3.65 and 3.66 show the convection in the cold air, just 30 minutes before the station observations at 0000 UTC on 22 February 1989 of Fig. 3.67. The ≥ 20 kt northerly winds reported from the two buoys in the northwestern Gulf of Mexico and the clear sky conditions at Merida, Mexico (station 76644 on the Yucatan Peninsula) in Fig. 3.67 depict the expected conditions across the shear line.

12 hours later at 1200 UTC, the FNOC NOGAPS 925 mb analysis shows a strong 30 kt low-level wind over the Yucatan Peninsula, with a contrasting SSW 15 kt wind just to the east at 20°N, 85°W (Fig. 3.68). Aloft at 200 mb, the mid-latitude trough is approaching the western Gulf of Mexico (Fig. 3.69)—note that the upper-level winds, at this time, are only 20–40 kt over the Yucatan Channel and the Yucatan Peninsula. The IR imagery at 1131 UTC of Fig. 3.70 depicts the NNE-SSW orientation of the cold front with strong convection at the leading edge of the cloudiness over the Yucatan Channel. Figure 3.71, with its surface observations at 1200 UTC (0600 LST), confirms the southerly flow over western Cuba, as well as the strong northerly⁷⁴ flow over the western Gulf of Mexico, with a 10 kt northerly wind at Merida.

Figures 3.72 and 3.73, the visible and IR imagery (6 and 9 1/2 h later), respectively, confirm the movement of the cold front into western Cuba and northwestern Honduras. Tracking the movement of the leading edge of the visible clouds, the front has moved toward the southeast at ~ 25 kt during the past 24 hours. As in the two preceding case studies, note that the mountainous terrain of Mexico, Guatemala and Honduras has led to the containment of low-level cloudiness on their windward (northern) slopes.

At 0000 UTC on 23 February, the FNOC low-level and upper-level winds (Figs. 3.74 and 3.75, respectively) show that northerly low-level flow (*behind* the shear line), has reached Honduras—however, a low-level southerly wind is still depicted *ahead* of the shear line south of central Cuba at 20°N, 80°W. Also, note that strong polar jet stream winds (70–80 kt) have reached the Gulf of Mexico, and a 50 kt wind is analyzed over the Yucatan Peninsula (Fig. 3.75).

However, by 1200 UTC, IR imagery of Fig. 3.76 shows that the low cloudiness has moved passed 20°N, 80°W (just south of central Cuba)—confirmed by the NNW 15 kt wind, analyzed on the FNOC 1200 UTC 925 mb wind analysis at 20°N, 80°W (Fig. 3.77).

⁷²This subsection is not entitled a *case study* since a full set of comparative analyses is not presented, i.e., there are no NMC streamline analyses. As the handbook was about to be published, a strong surge occurred over Central America. Since the two dry season “surges”, already prepared, discussed relatively weak surges, this presentation briefly discusses the features of a strong surge.

⁷³In early 1989, the GOES WEST satellite failed and GOES EAST was moved *west* to 108°W.

⁷⁴The “star” reports in the NW Gulf are low-level satellite-derived winds.

Moreover, both the IR imagery (Fig. 3.76) and the FNOC 925 mb wind analysis (Fig. 3.77) show the low-level cloudiness having moved southward, past Bluefields, Nicaragua and into Costa Rica. Meanwhile, the 200 mb flow is westerly from the Yucatan Peninsula to Costa Rica, with a sharp mid-latitude trough over the northwestern Gulf of Mexico (Fig. 3.78). The visible imagery of Fig. 3.79 vividly depicts the shear line 3 hours later.

At 0001 UTC on 24 February, the IR imagery of Fig. 3.80 shows the low level cloudiness, *trailing* the shear line, now extending through the Windward Passage (between Cuba and Hispaniola) south-southwestward to the northwest coast of Panama, near the Gulf of Mosquitos. The USAF Weather Detachment 25, 5th Weather Wing, Howard Air Force Base, Panama issued a Caribbean Area Forecast⁷⁵ at 2230 UTC 23 February forecasting a shear line between 75°W–80°W from 0000 UTC to 2400 UTC on 24 February.

Figures 3.81 and 3.82 are the Navy's FNOC NOGAPS 48-h and 24-h 925 mb wind prognoses, both verifying at 0000 UTC on 24 February. Note that initial conditions 48 hours **earlier**, from which the 48-h prognosis was made, included: a **calm** wind at Merida, a **weak** and **easterly** wind over San Andrés Island (station 80001), and a **weak** and **southerly** wind over David, Panama (station 78793) (see Fig. 3.67). The FNOC 48-h 925 mb winds (verifying at 0000 UTC on 24 February (Fig. 3.81)) are **northerly 25–30 kt** from central Cuba and Jamaica to Costa Rica. The 24-h prognosis, verifying at the same time is similar, but continues with a **NE 20 kt wind** at 10°N, 80°W, just north of eastern Panama (Fig. 3.82).

The 925 mb wind analysis⁷⁶ at 0000 UTC on 24 February (Fig. 3.83) shows that the FNOC forecasts verifies extremely well, with easterly winds in the Caribbean (east of Jamaica)—although, admittedly, the analyzed wind over eastern Honduras (see Fig. 3.83) is stronger (45 kt) than the prognosis (35 kt). In Fig. 3.84, note that the upper-level winds over the northern portion of Central America have strengthened, appreciably, since 22 February, i.e., the wind over the Yucatan Peninsula at 200 mb is now 65 kt—with the jet stream strength reaching 105 kt over Cape Hatteras⁷⁷, North Carolina (not shown).

The station observations at 0000 UTC on 24 February (Fig. 3.85) correlate very well with the FNOC low-level winds (Fig. 3.83), as well as the 0001 UTC 24 February IR imagery (Fig. 3.80): rain and overcast over eastern Cuba, strong northerly surface winds over Puerto Lempira, Honduras (station 78711), NE 25 kt wind reports from ships west of Costa Rica, overcast at David, Panama (station 78793) and a N 10 kt wind at Howard AFB, Panama (station 78806). The visible imagery at 1501 UTC on 24 February (Fig. 3.86) shows the western half of the Caribbean Sea covered with cloudiness.

While all intermediate surface analyses were **not** examined, it appears that this strong

⁷⁵Available via the MANOP message heading "FACA MPHIO".

⁷⁶Note that the 925 mb winds may be northerly **ahead** of the shear line, but the arrival of the shear line ("surge") is manifested by **stronger winds**. That is, the northerly winds along 80°W (between Cuba and Panama) at 1200 UTC 23 February in Fig. 3.77 are replaced by stronger northerly winds (30 kt) at 0000 UTC 24 February in Fig. 3.83.

⁷⁷As an aside, this very cold trough (now existing southward to the Bay of Campeche) brought record snows and blizzard conditions to the East Coast of the United States—snow fell as far south as the North Atlantic coast of South Carolina on 24 February.

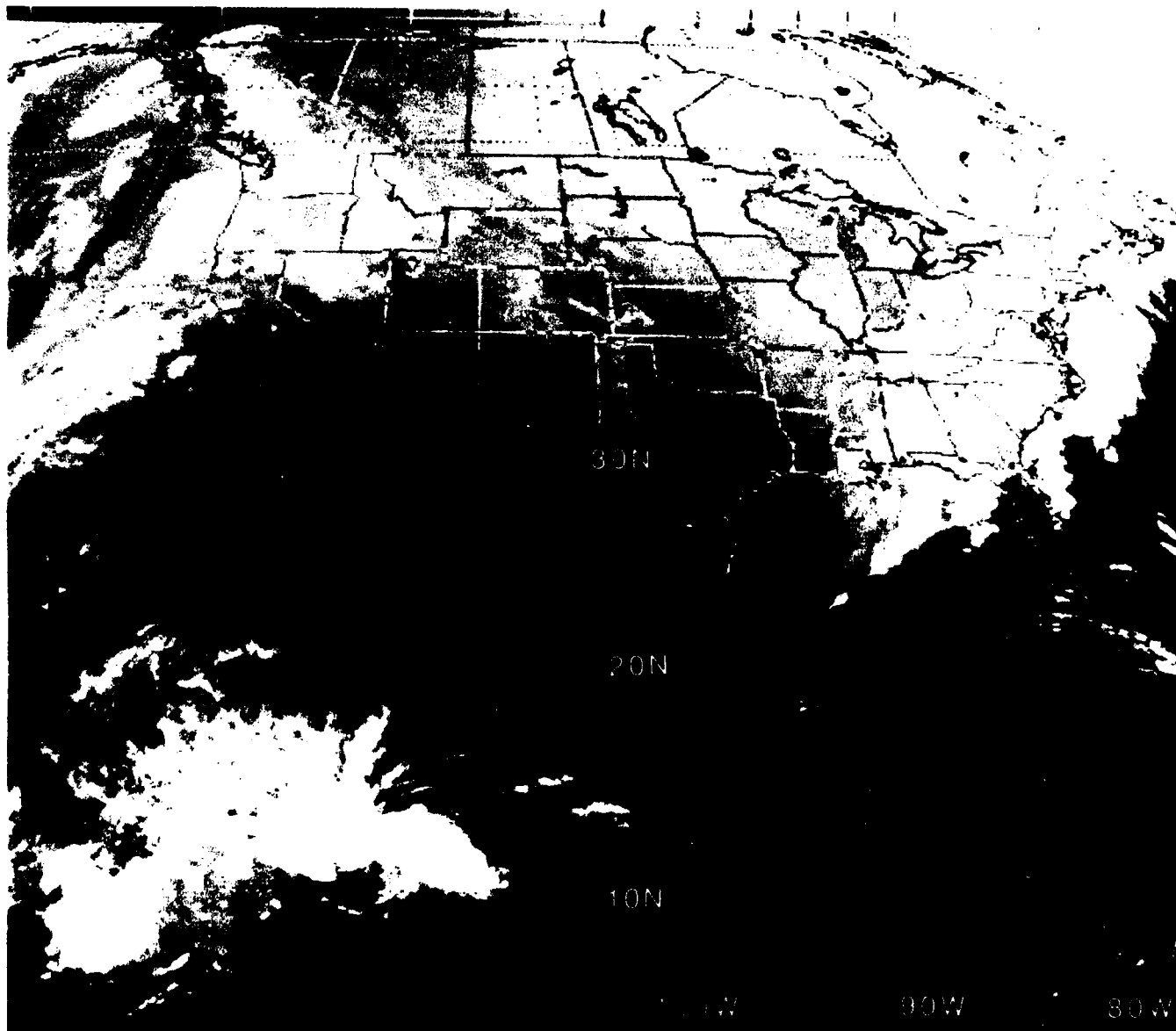


Figure 3.65: GOES Infrared Satellite Imagery, 2331 UTC 21 FEB 1989

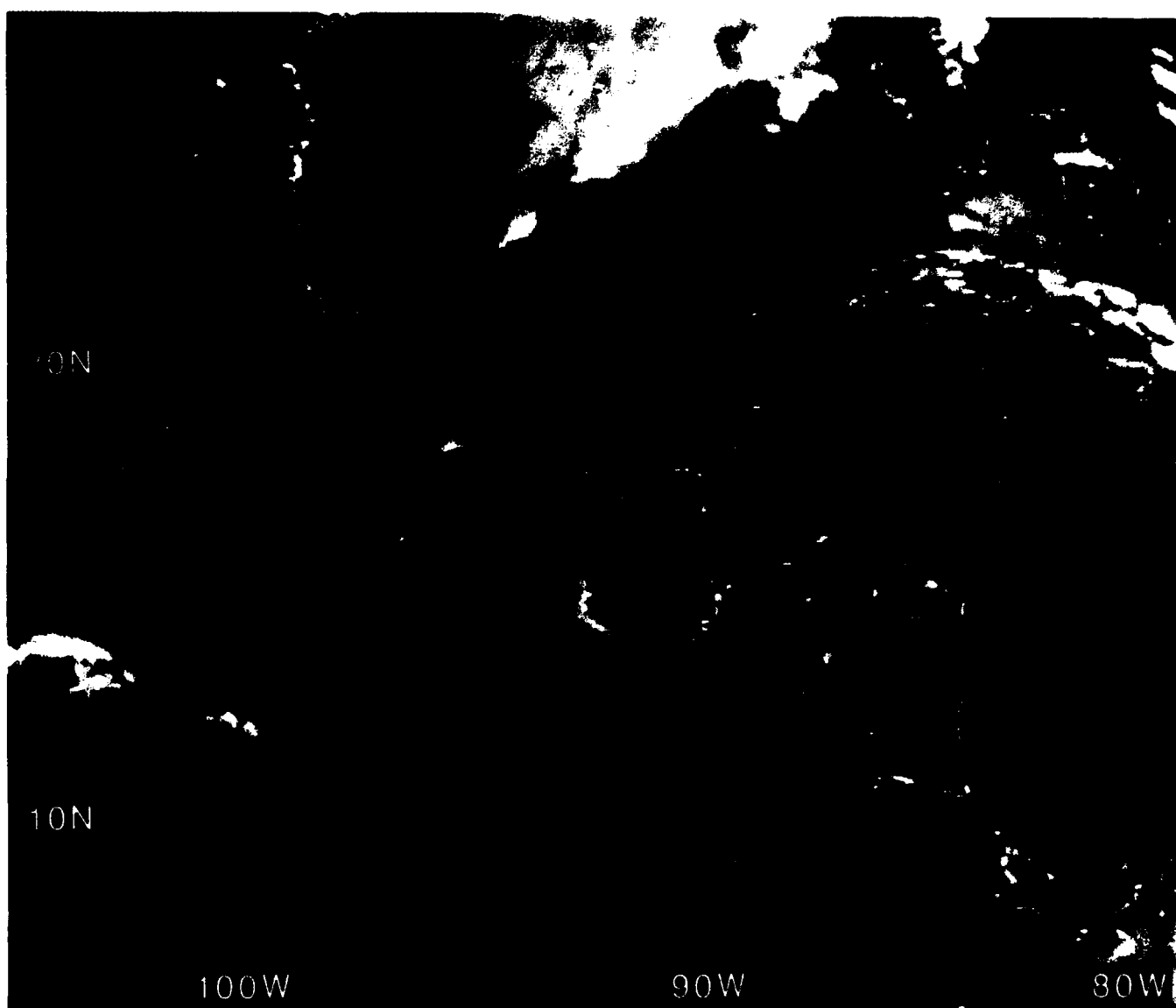


Figure 3.66: GOES IR Imagery ("Zoomed"), 2331 UTC 21 FEB 1989

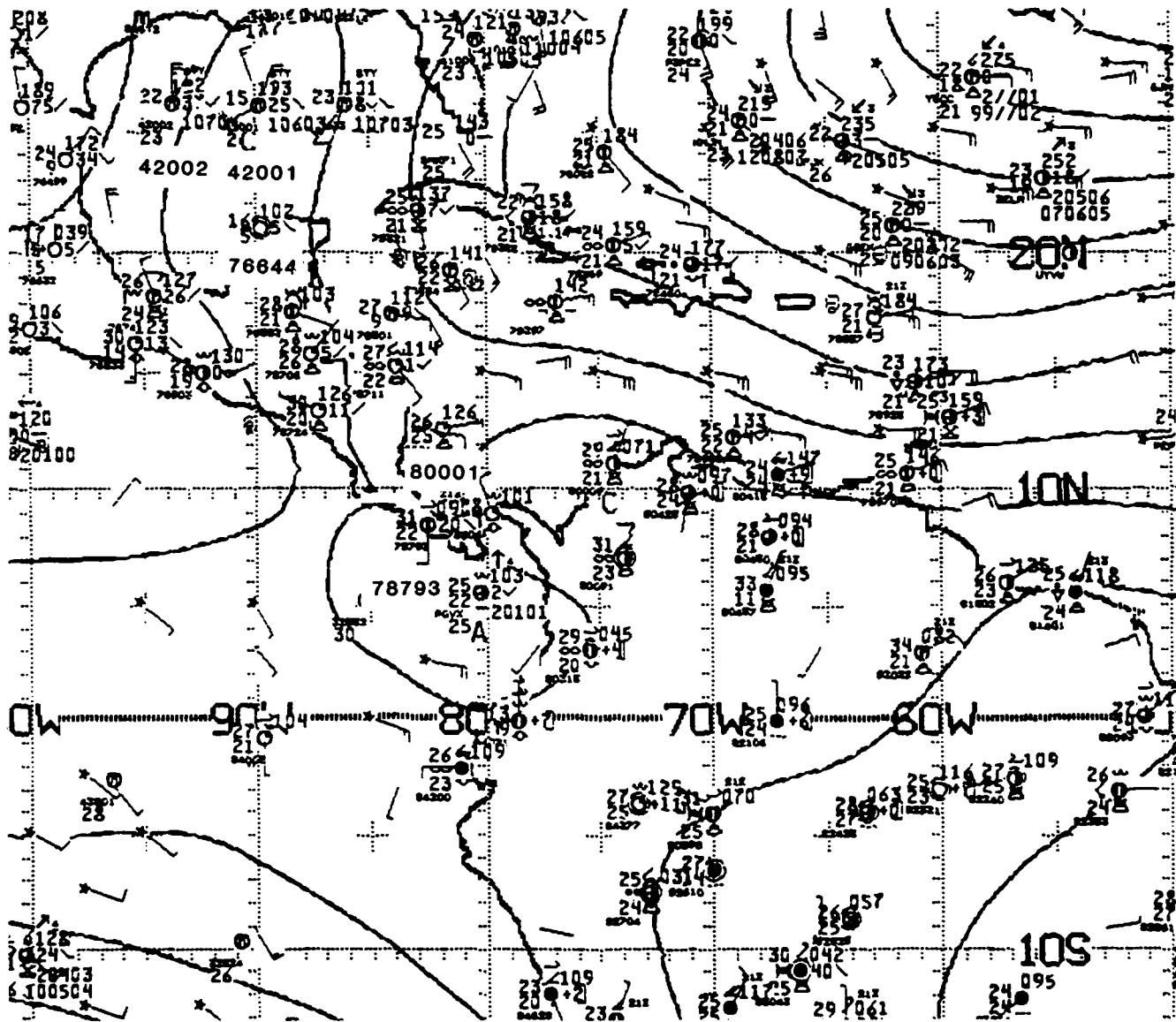


Figure 3.67: NMC 1000 mb Analysis, 0000 UTC 22 FEB 1989.

Contours are unlabeled stream functions from optimum interpolation analysis, with C identifying cyclonic centers and A identifying anticyclonic centers.

surge existed with a maximum Brooks index of only ~ 10 mb. As Brooks (1985) states: "This index is not meant as a hard and fast rule, but rather as a guideline or tool...". The existence of greater north-south orientation of a shear line may be the better precursor of a strong surge.

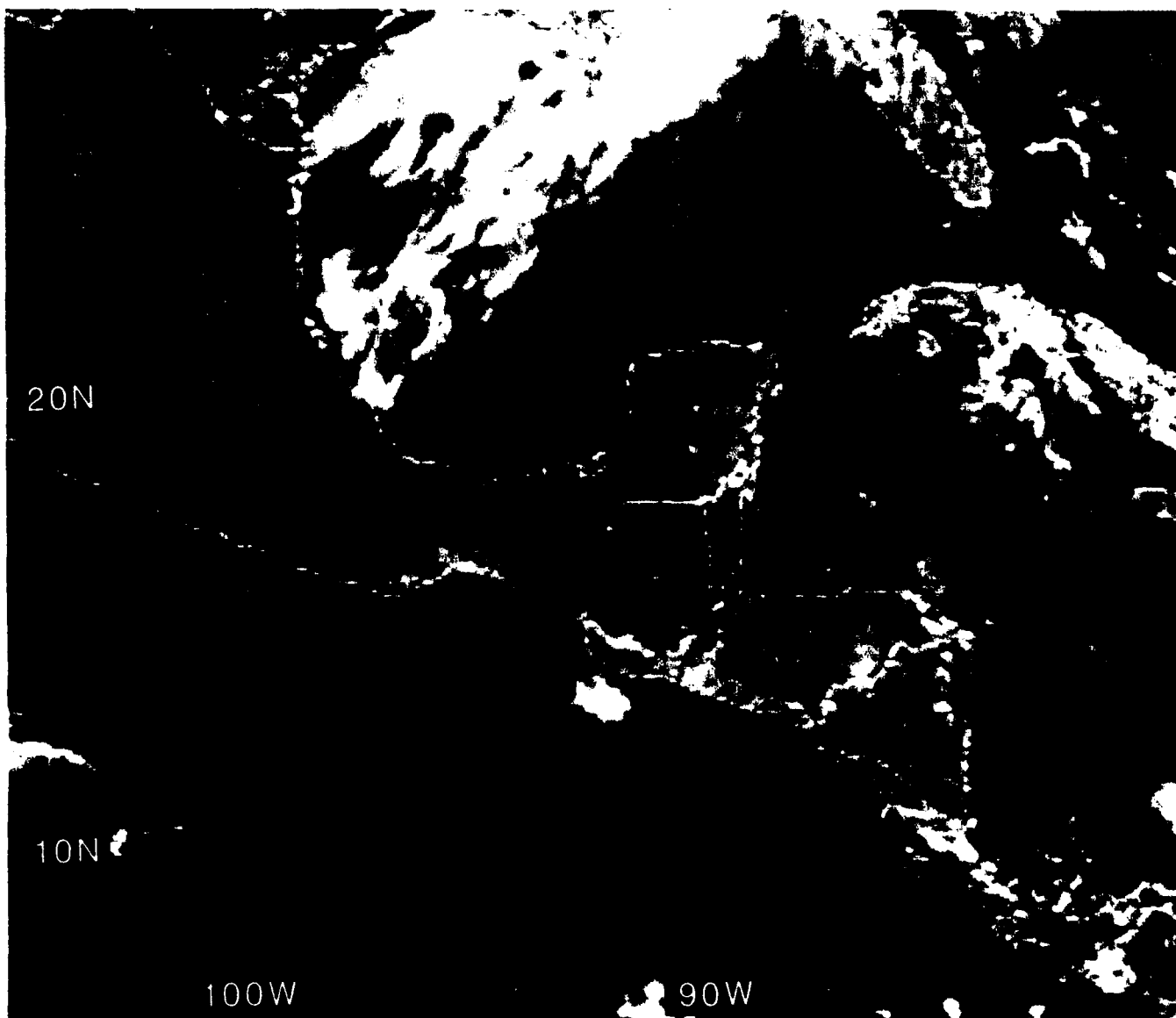


Figure 3.64: GOES Visible Imagery ("Zoomed"), 1803 UTC 21 FEB 1989

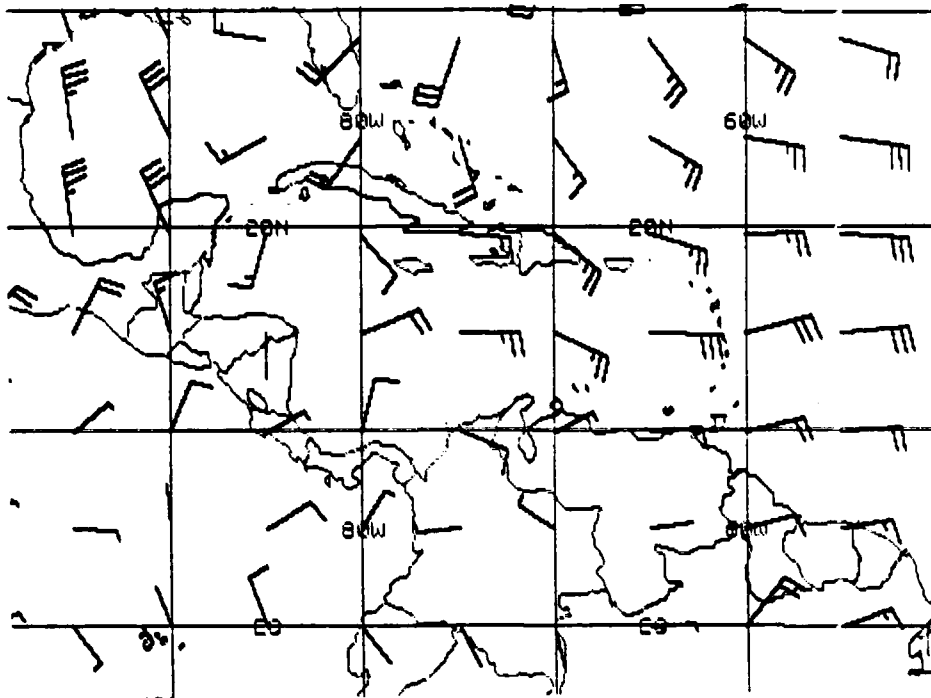


Figure 3.68: FNOC 925 mb Winds, 1200 UTC 22 FEB 1989.As in Fig. 2.19.

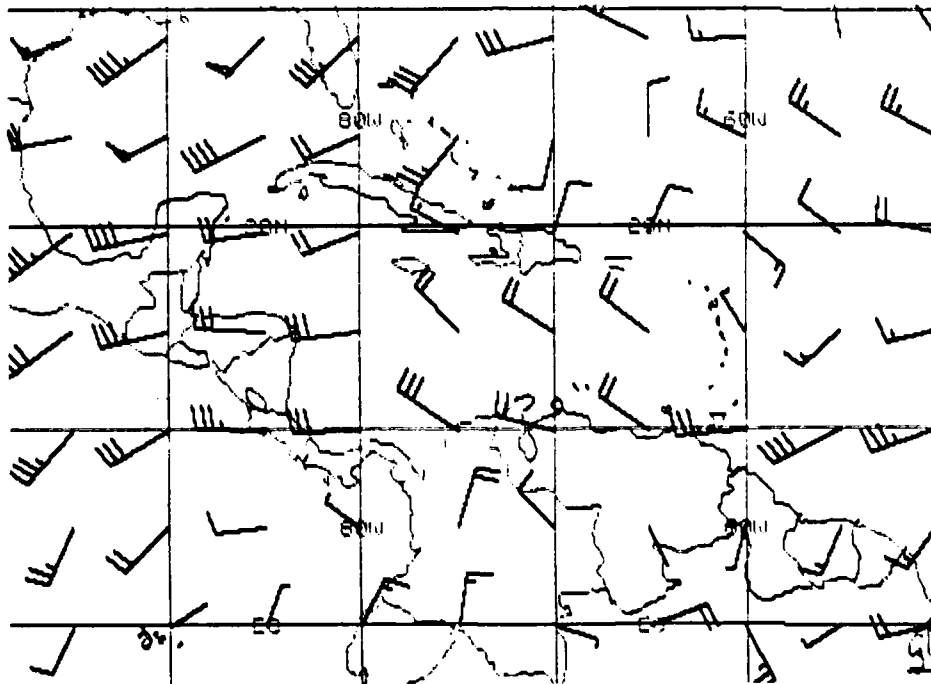


Figure 3.69: FNOC 200 mb Winds, 1200 UTC 22 FEB 1989.As in Fig. 2.20.

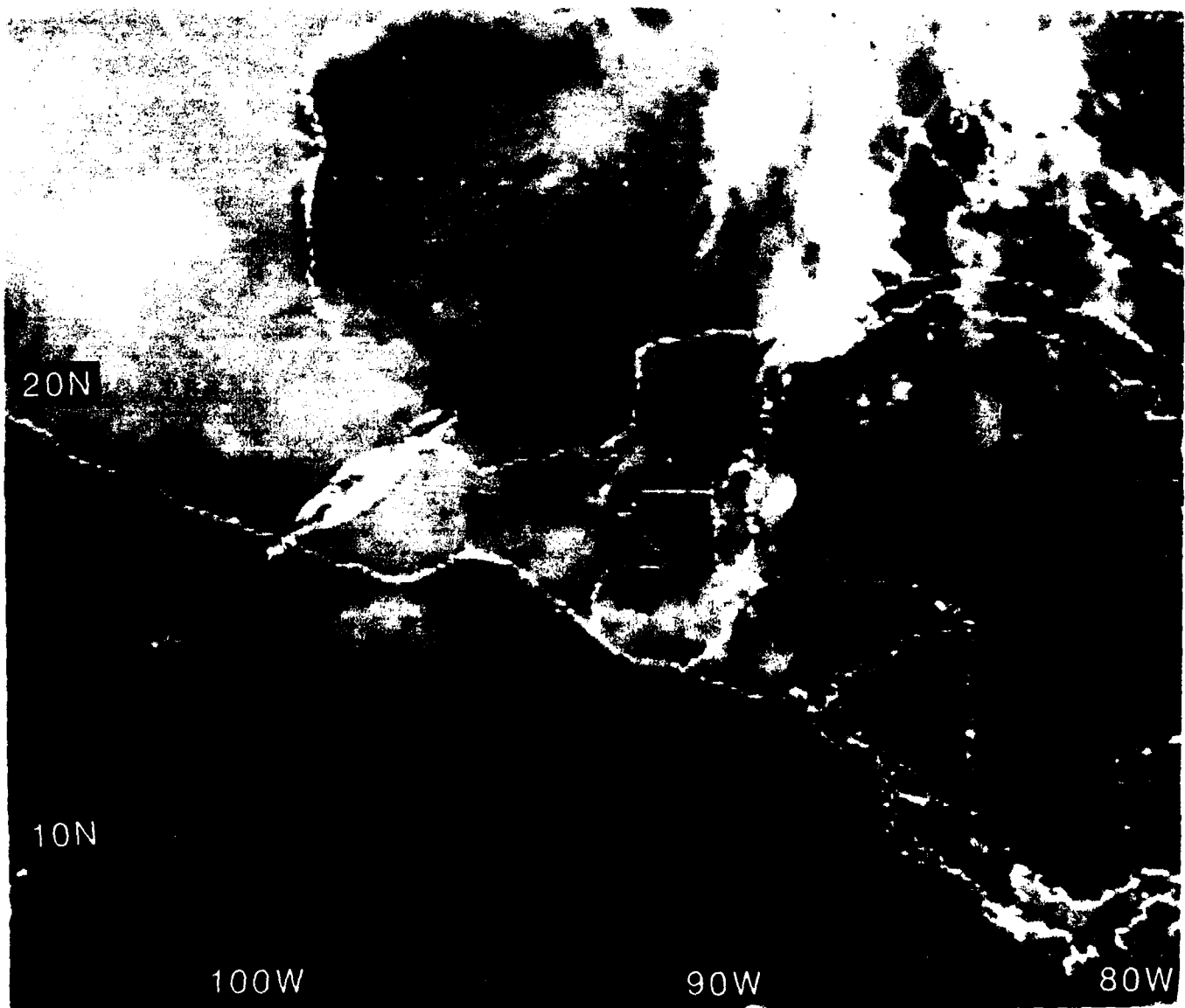


Figure 3.70: GOES IR Imagery ("Zoomed"), 1131 UTC 22 FEB 1989

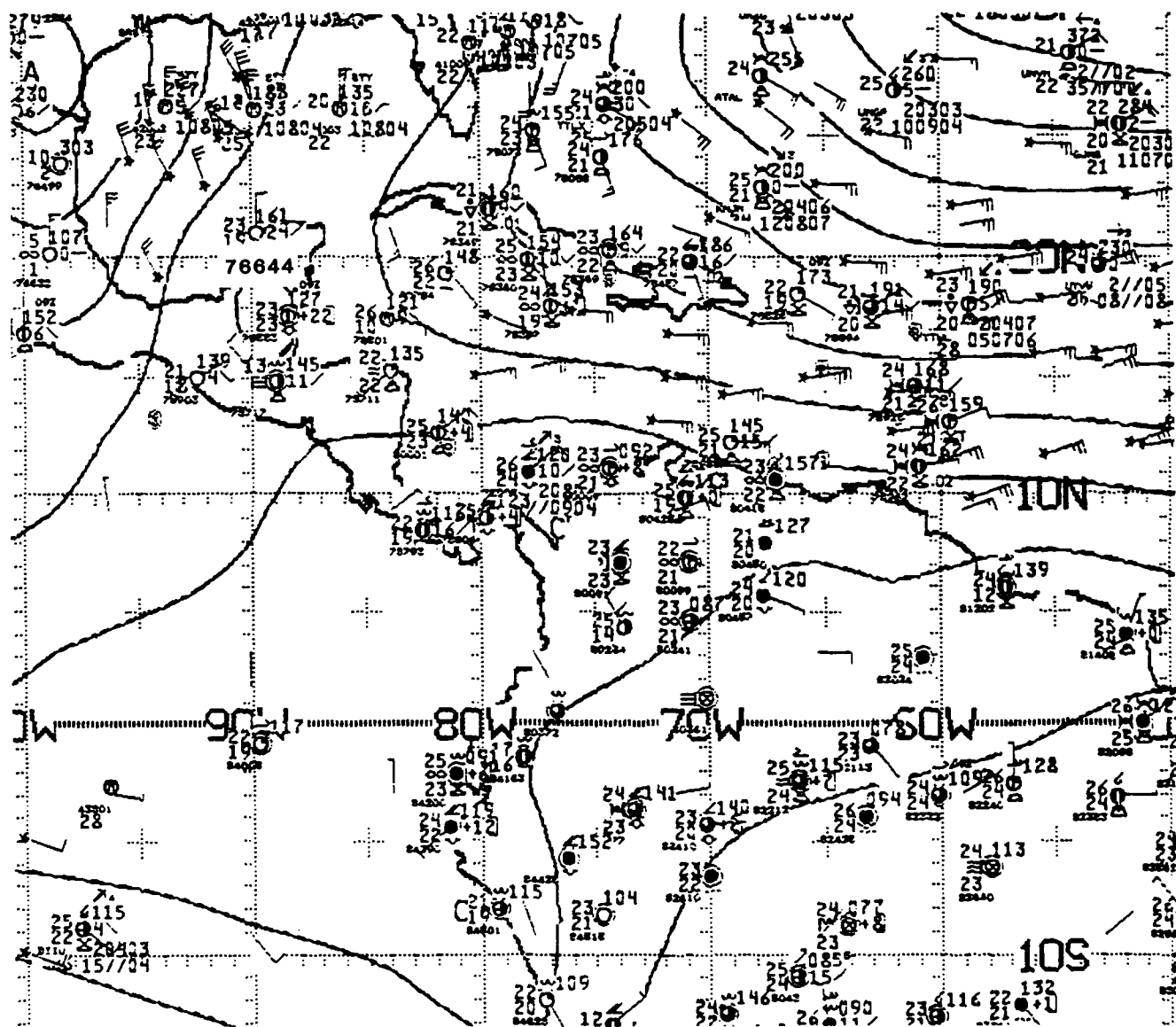


Figure 3.71: NMC 1000 mb Analysis, 1200 UTC 22 FEB 1989.

Contours are unlabeled stream functions from optimum interpolation analysis, with C identifying cyclonic centers and A identifying anticyclonic centers.

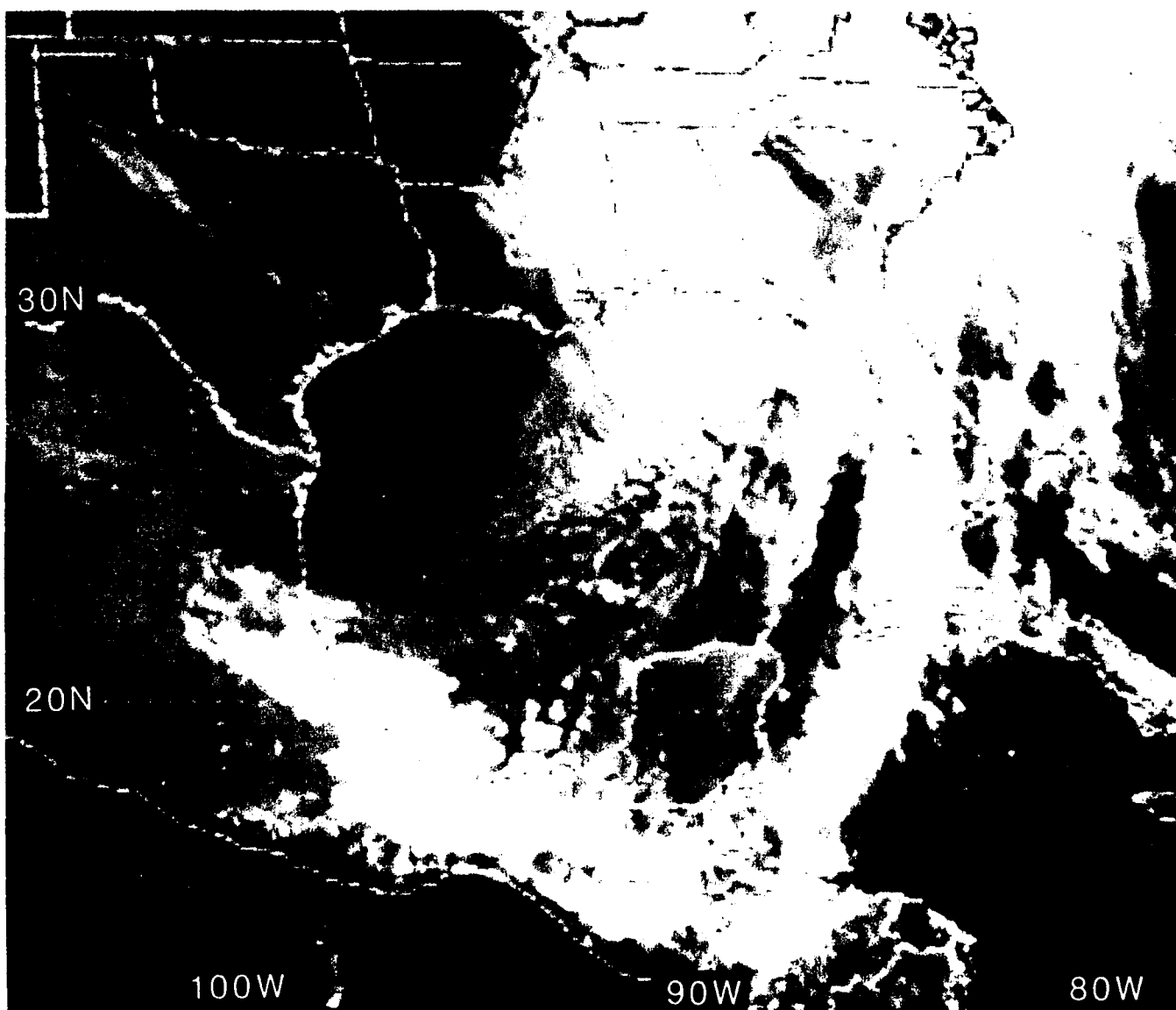


Figure 3.72: GOES Visible ("Zoomed"), 1801 UTC 22 FEB 1989

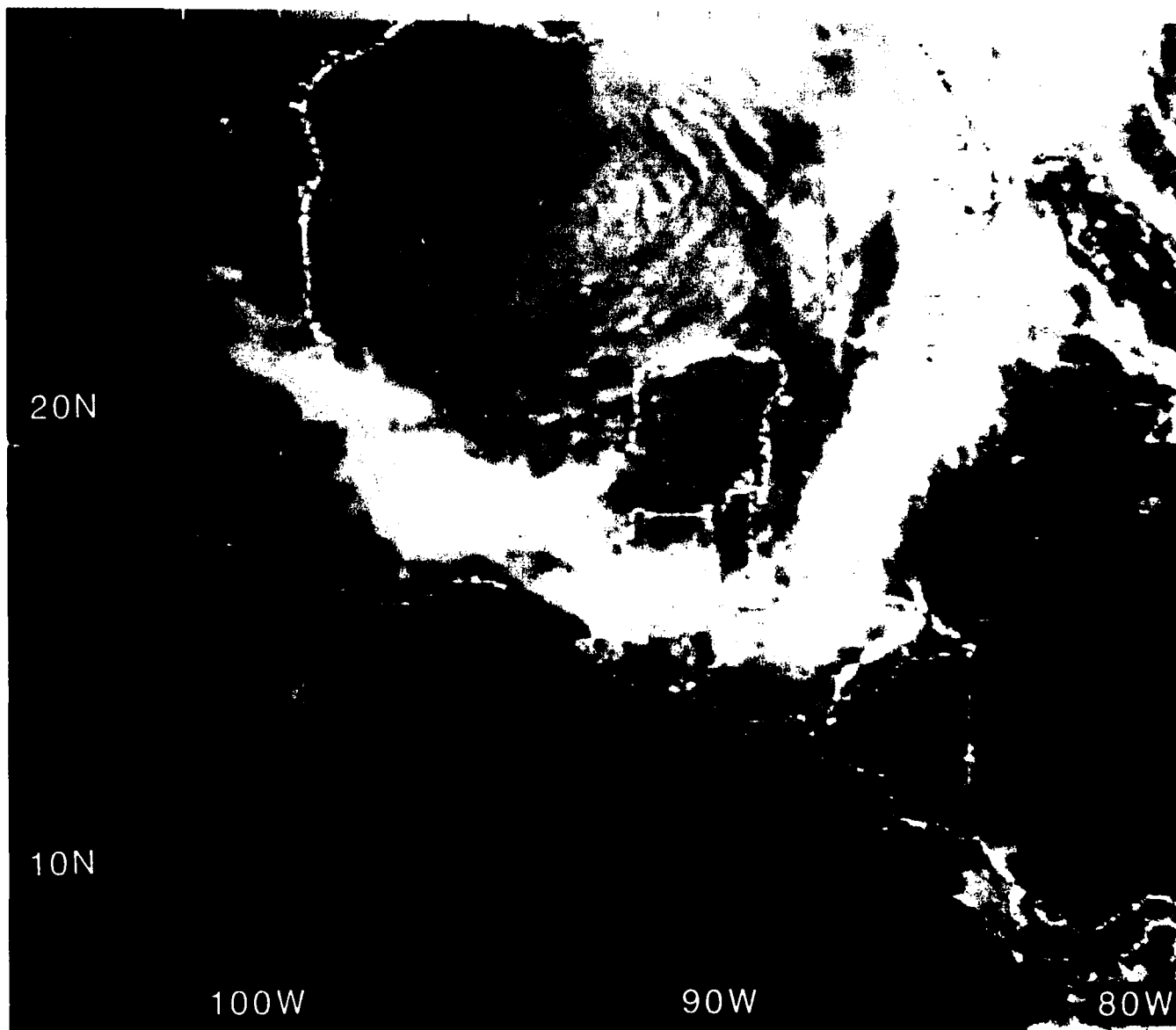


Figure 3.73: GOES IR Imagery ("Zoomed"), 2131 UTC 22 FEB 1989

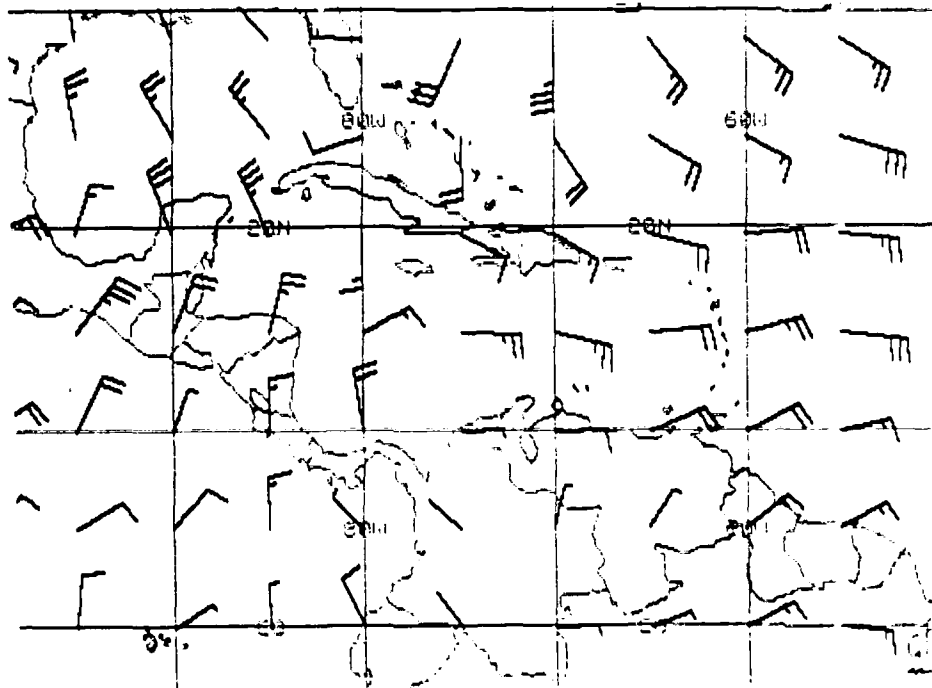


Figure 3.74: FNOc 925 mb Winds, 0000 UTC 23 FEB 1989. As in Fig. 2.19.

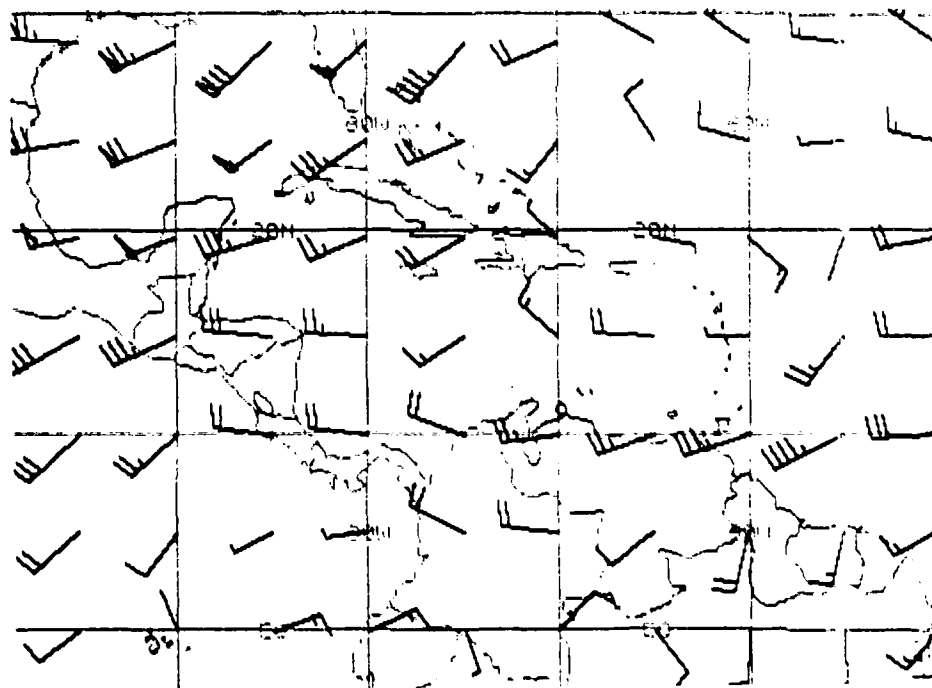


Figure 3.75: FNOc 200 mb Winds, 0000 UTC 23 FEB 1989. As in Fig. 2.20. Each barb represents 10 kt. Each pennant represents 50 kt.

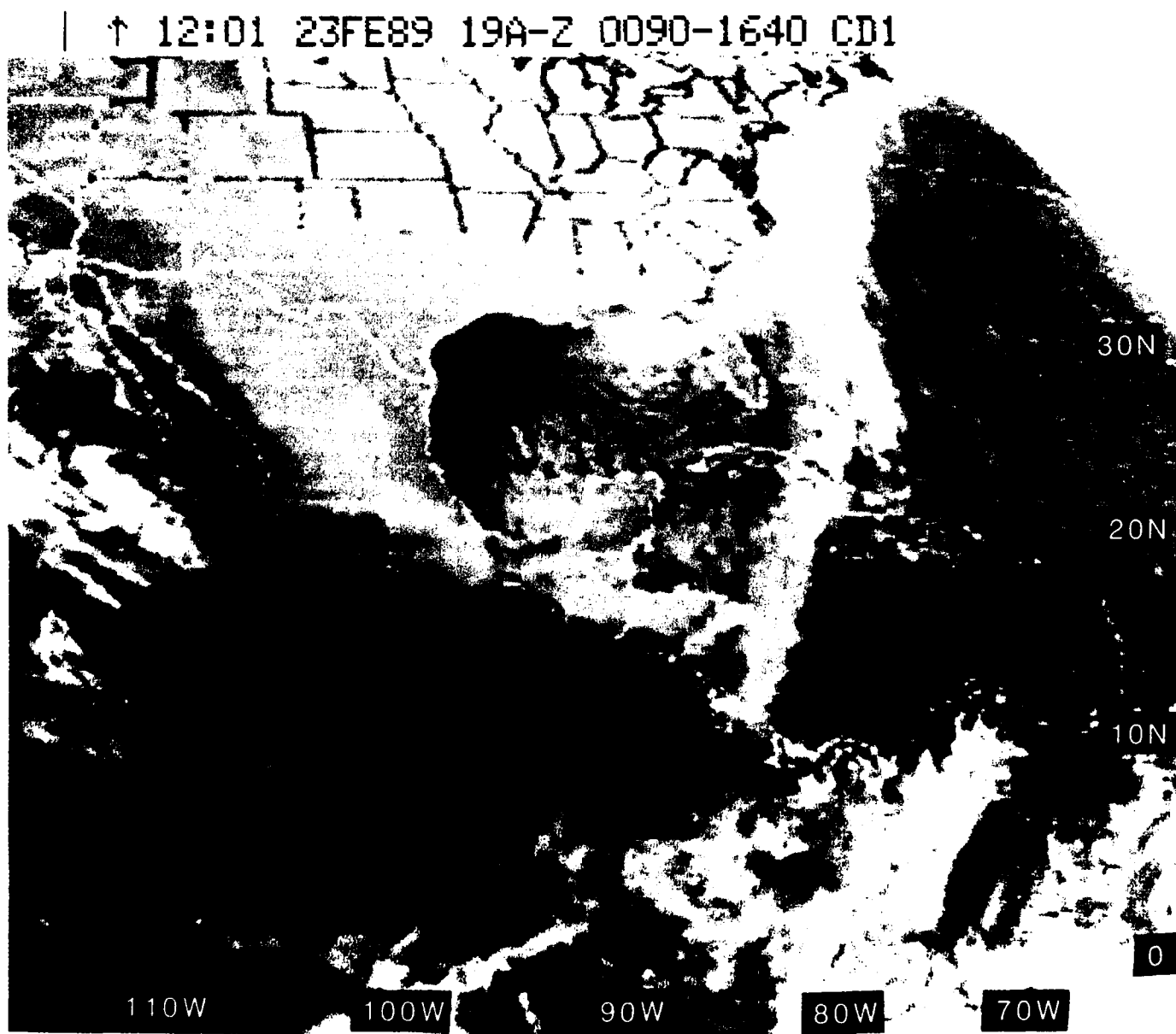


Figure 3.76: GOES Infrared Satellite Imagery, 1201 UTC 23 FEB 1989

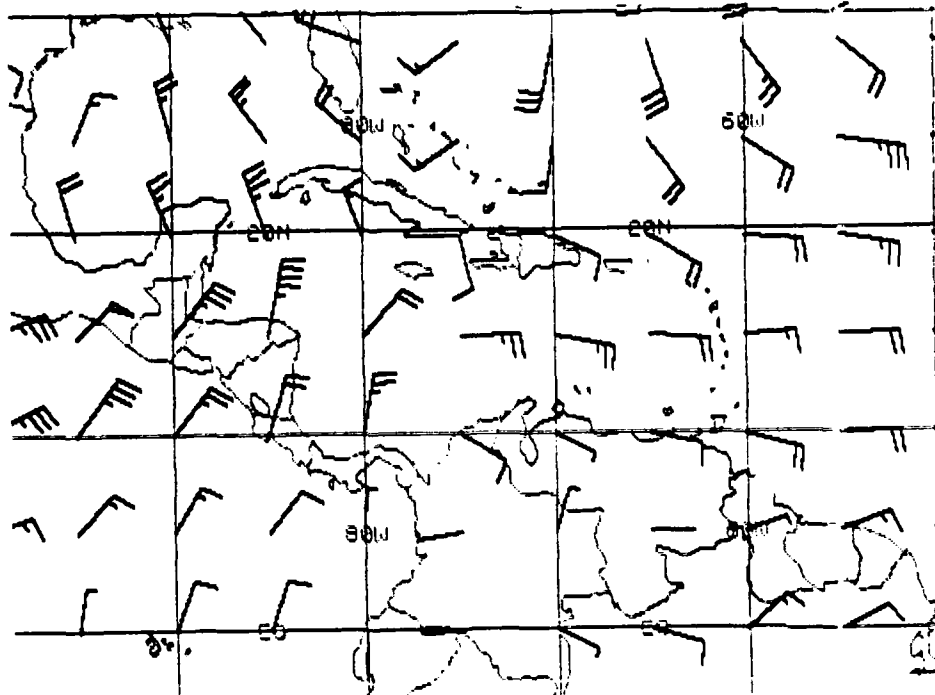


Figure 3.77: FNOc 925 mb Winds, 1200 UTC 23 FEB 1989.As in Fig. 2.19.

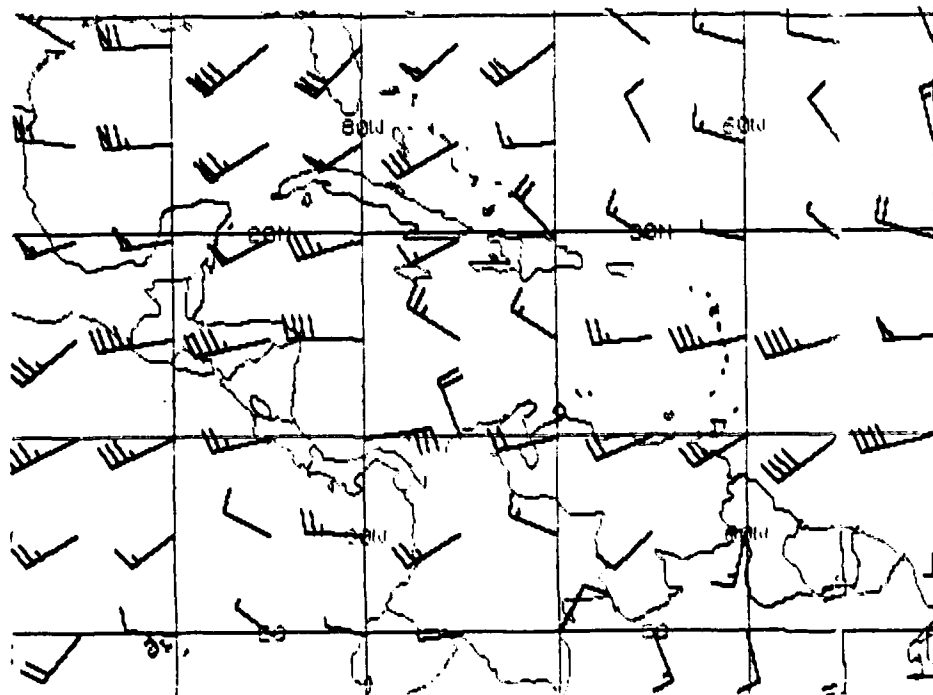


Figure 3.78: FNOc 200 mb Winds, 1200 UTC 23 FEB 1989.As in Fig. 2.20.

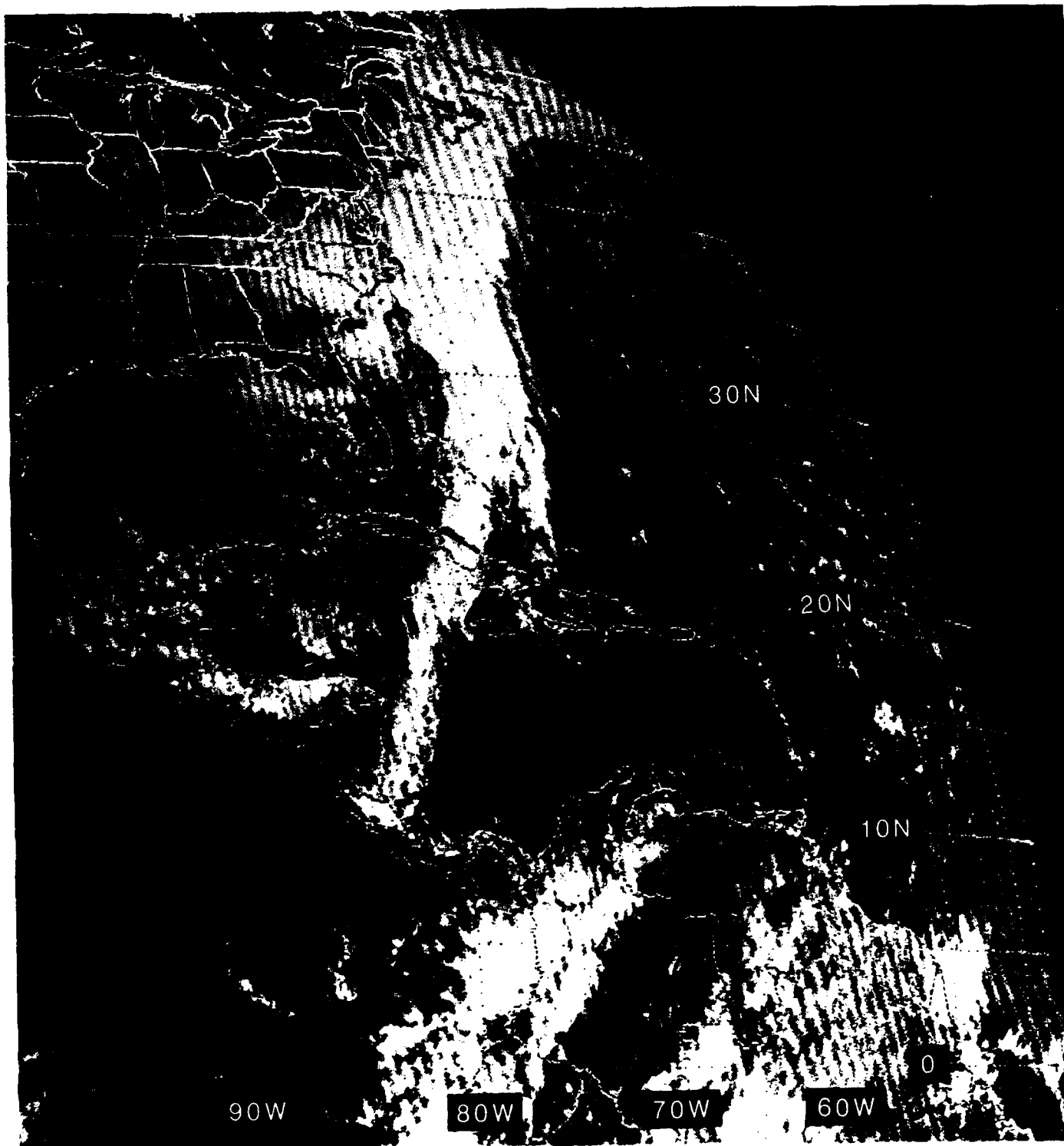


Figure 3.79: GOES Visible Satellite Imagery, 1501 UTC 23 FEB 1989

00:01 24FE89 29A-Z 0090-0950 CD1

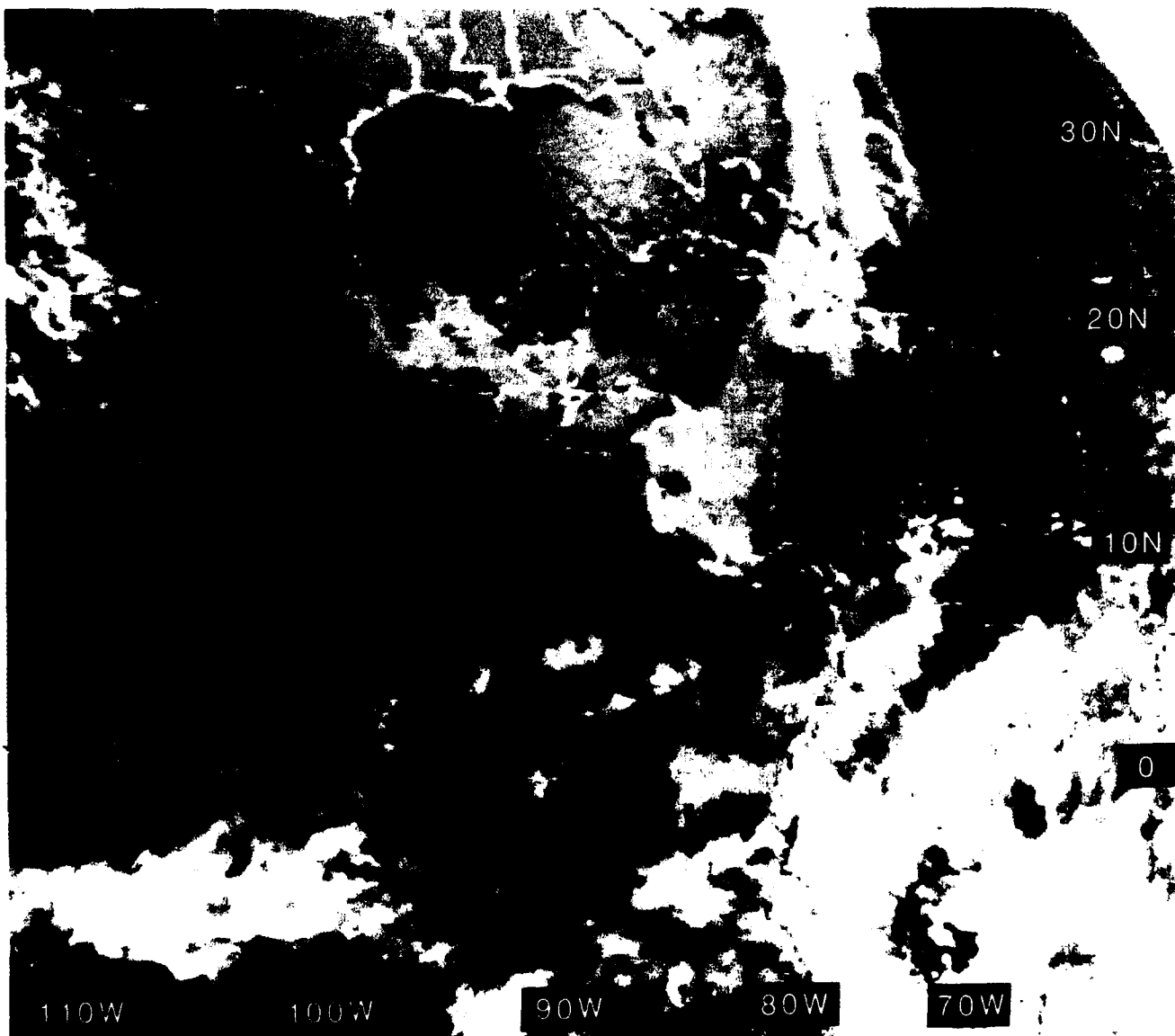


Figure 3.80: GOES Infrared Satellite Imagery, 0001 UTC 24 FEB 1989

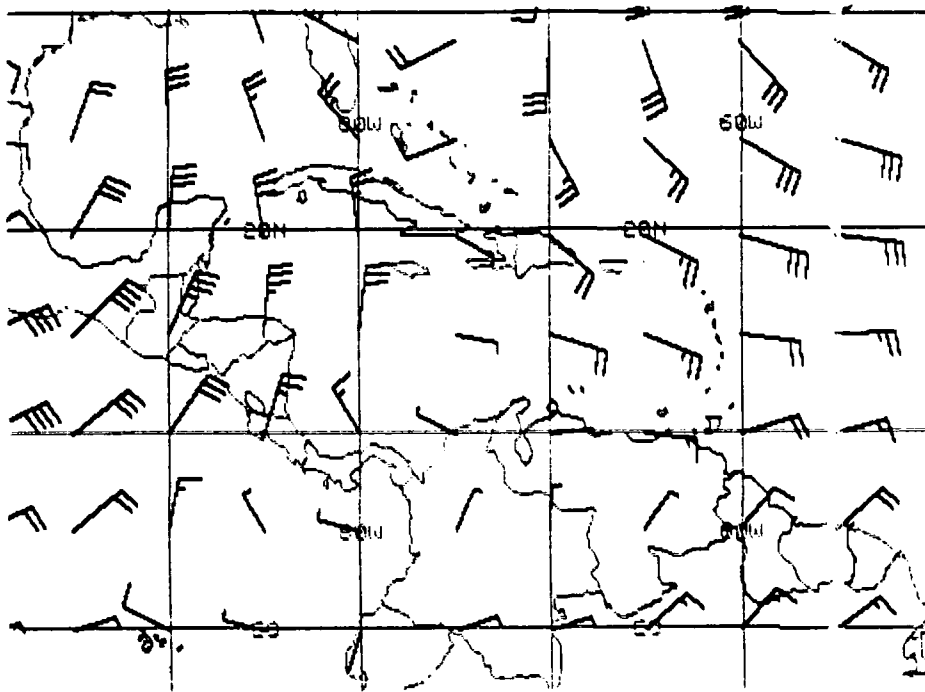


Figure 3.81: FNOC 925 mb Winds 48-h PROG VT 0000 UTC 24 FEB 1988.
Each barb represents 10 kt.

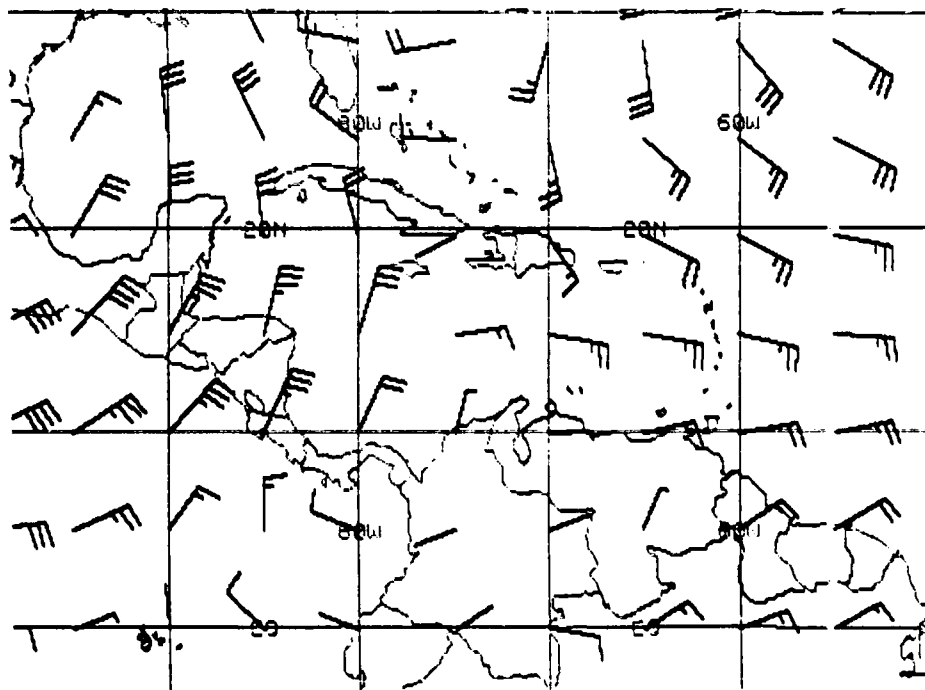


Figure 3.82: FNOC 925 mb Winds 24-h PROG VT 0000 UTC 24 FEB 1988.
Each barb represents 10 kt.

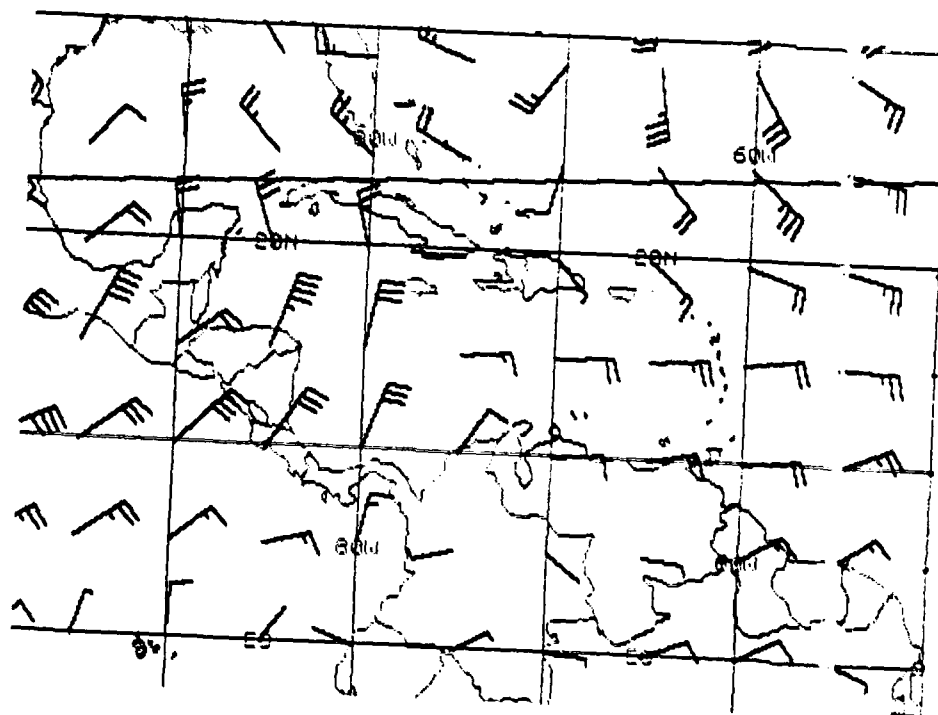


Figure 3.83: FNOC 925 mb Winds, 0000 UTC 24 FEB 1989. As in Fig. 2.19.

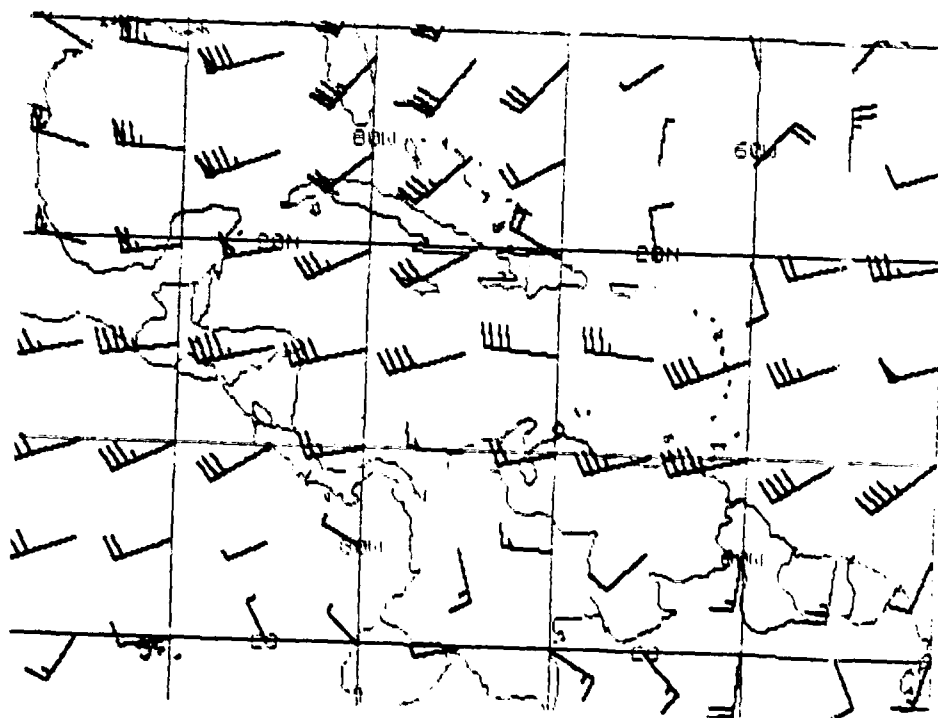


Figure 3.84: FNOC 200 mb Winds, 0000 UTC 24 FEB 1989. As in Fig. 2.20.

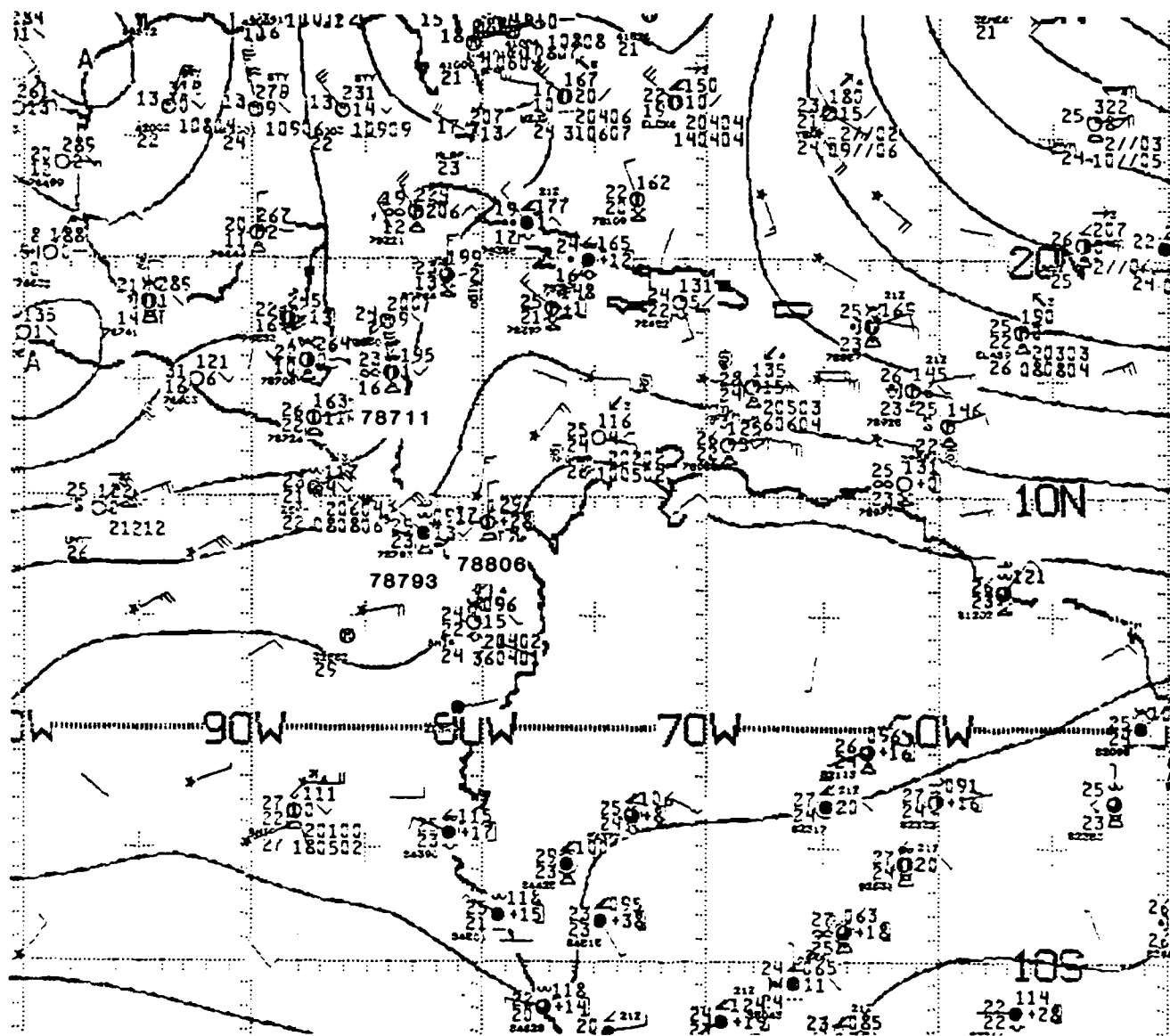


Figure 3.85: NMC 1000 mb Analysis, 0000 UTC 24 FEB 1989.
 Contours are unlabeled stream functions from optimum interpolation analysis,
 with C identifying cyclonic centers and A identifying anticyclonic centers.



Figure 3.86: GOES Visible Satellite Imagery, 1501 UTC 24 FEB 1989

3.4 Analysis & Forecasting “Thumb Rules” for the Dry Season

- Real-time high resolution satellite imagery is currently⁷⁸ the best mesoscale analysis/forecasting tool.
- During the dry season, in the absence of a front, Central America is dominated by northeast tradewinds. Mostly scattered clouds prevail north of the Continental Divide with a slight increase in clouds during the afternoon due to surface heating. South of the divide, downslope adiabatic drying keeps skies clear—often evident over El Salvador and southern Guatemala. Over coastal areas and areas exposed to onshore flow, clouds remain scattered to broken with very occasional and brief rain showers during the afternoon (Pearson et al., 1987).
- Cloud cover greatly depends on the strength of the tradewinds. With strong wind flow, cloud formation is enhanced on the windward side of mountains and inhibited on the lee side—if strong enough, it may prevent sea breeze formation on the North Pacific coasts of Costa Rica and Panama. Under light wind flow, increased afternoon clouds may develop in all areas. (Occasionally—for only a few days—the northeasterly flow may be replaced by *southerly* winds which provide clouds to the *south* and clearing to the *north* of Continental Divide. In particular this will lead to the appearance of “sea breeze” fronts in southwest Guatemala, El Salvador, the west coast of Nicaragua and Panama’s Azuero Peninsula—areas normally clear at this time. In contrast, **northern** Guatemala and Honduras will be *unusually* clear.) (Pearson et al., 1987)
- In the late dry season, haze and smoke produced by annual agricultural burning becomes trapped under the tradewind inversion, significantly reducing low-level visibility (Pearson et al. 1987). This is particularly noticeable to the southwest of the Continental Divide, e.g., over El Salvador.
- Cold fronts frequently discontinued by NMC due to the lack of thermal gradient still strike Belize and Honduras as shear lines with attendant wind speed increase, lowering ceilings and rainfall. (There *may* be a surface pressure minimum several hours before the front (or shear line) reaches the ship or station.)
- Using only 12 hour data, fronts passing Belize are accompanied by wind shifts to a northerly direction and wind speed increases, pressure rises of 4 mb, and equivalent temperature (T_e) decreases of about 5 K. (Using 3 hour data, the surface pressure 6 hours after frontal passage is 4 mb **higher** than 6 hours before frontal passage.)

⁷⁸However, in the near future doppler radar and vertical profilers promise greatly improved analysis.

- Mid-latitude cold fronts, northers, shear lines or Atemporalados—i.e., different names that may be given to the same phenomena—strike Central America from September through June, with a maximum of 4 per month striking Belize during January. Although temperature and dew point are not always affected, cold fronts reaching Honduras are followed by significant rainfall, lowering of low cloud base heights, formation of stratiform cloud types, and often either a northerly wind component or an increase in wind speed. (Henry (1979) found a rather high average number of fronts (~18) entering the Caribbean Sea from the Gulf of Mexico during the dry season. This number will be smaller during mild Northern Hemisphere winters and larger during severe winters.)
- As cold fronts approach the Yucatan Peninsula, the magnitude of the *trailing* high pressure over the western Gulf of Mexico or Texas can be used to indicate the expected penetration of the front into Central America. A NOMINAL SURGE exists when the sea-level pressure difference (INDEX) is between 15–19 mb between Houston, Texas; Brownsville, Texas or Tampico, Texas and Merida, Mexico. The NOMINAL SURGE indicates that the shear zone will move into central Honduras ~24 h later, with NNW 20–30 kt winds (stronger winds at higher elevations inland), low stratiform clouds (300–500 feet) on the coast, and continuous rain (although clearing on the leeward slopes), and then dissipating near the Honduras-Nicaragua border in 48–72 hours. Pressure differences smaller than 14 mb indicate a lesser penetration into Central America, while pressure differences ≥ 20 mb indicate the likelihood that the shear zone will penetrate to Costa Rica and Panama (Brooks, 1985). (The index is a tool to be used *with* diurnal, topographic and other considerations.)
- The existence of greater north-south—as opposed to east-west—alignment of a shear line normally indicates that the shear line will penetrate further into Central America.
- The Navy NOGAPS 24-h wind prognoses often accurately predict the changing of direction and the strengthening of winds over Honduras, Nicaragua, the western Caribbean Sea and the Gulf of Tehuantepec, following shear line passages.
- Even in the dry season, the northeasterly flow typically brings cloudy skies and convection to the Caribbean-facing slopes of the Corallera de Talamanca mountains of Costa Rica and western Panama.
- Near the end of the dry season, the return poleward of the ITCZ (or monsoon trough) will bring increased cloudiness and convection *first* to Panama and Costa Rica.
- If only NOGAPS analyses are available, synoptic features may be depicted; however, mesoscale features will likely be missing due to the coarse resolution. While the NOGAPS low-level wind prognoses during shear line penetration were very good, the NOGAPS upper-level tropical prognoses were especially weak; however, new models, expected to become operational in 1989, promise improved resolution and performance.

THIS PAGE
INTENTIONALLY BLANK

4. COASTAL OCEANOGRAPHIC INFLUENCES

4.1 Geological Structure of Central America and the Adjacent Ocean Basins

The mountains in Central America developed when the crustal plates surrounding the Caribbean Plate (which contains the Caribbean Sea and most of the islands surrounding it) either slid over it, or dived beneath the Caribbean Plate; see Figs. 4.1 and 4.2. The mountains are either old rocks forced upward, or later volcanic intrusions. More than 250 volcanoes stand in a row bordering the Pacific edge of Central America; see Fig. 4.3. This mountain-building history results in a wide variety of landforms and landscapes in Central America. One result from this history is the Middle America Trench that lies offshore, adjacent to the Pacific coastline northwestward from Costa Rica. A similar trench occurs in the northwestern Caribbean Sea, offshore from the Cayman Islands. These trenches have resulted from the collision between crustal plates in the earth's surface, when one plate was forced beneath another plate in the trench regions. Figure 4.4 illustrates the location of the Middle America Trench; it also shows the Cayman Rift to the west of Jamaica in the Caribbean Sea.

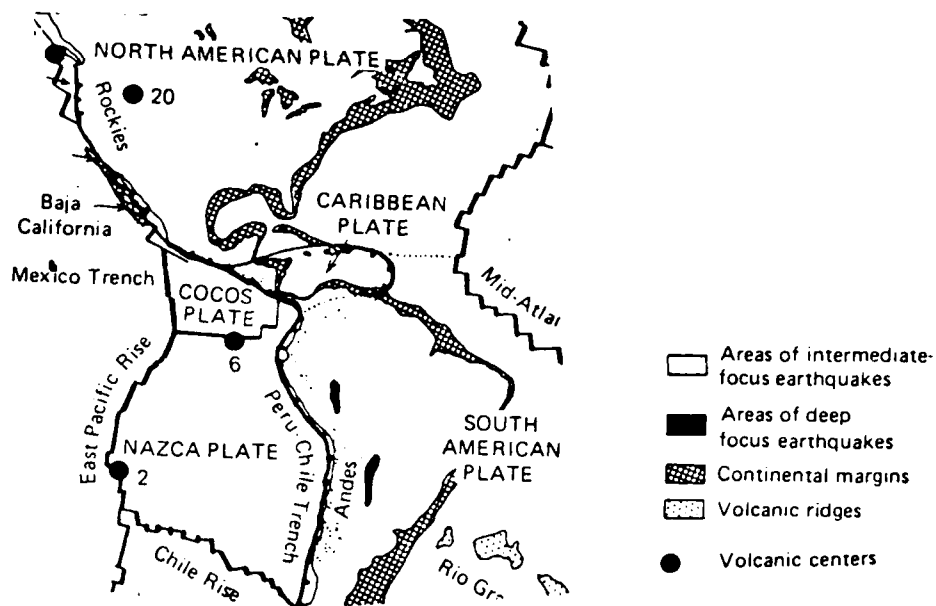


Figure 4.1: The Crustal Plates that affect the Central American region: North American; Caribbean; Cocos; Nazca and South American. (Adapted from Gross (1982).)



Figure 4.2: Motion of Crustal Plates, and regions of intensive earthquake activity as indicated by dots. Each plate moves the distance equivalent to the length of the arrow in 20 million years. (Adapted from Leet, Judson and Kauffman (1978).)

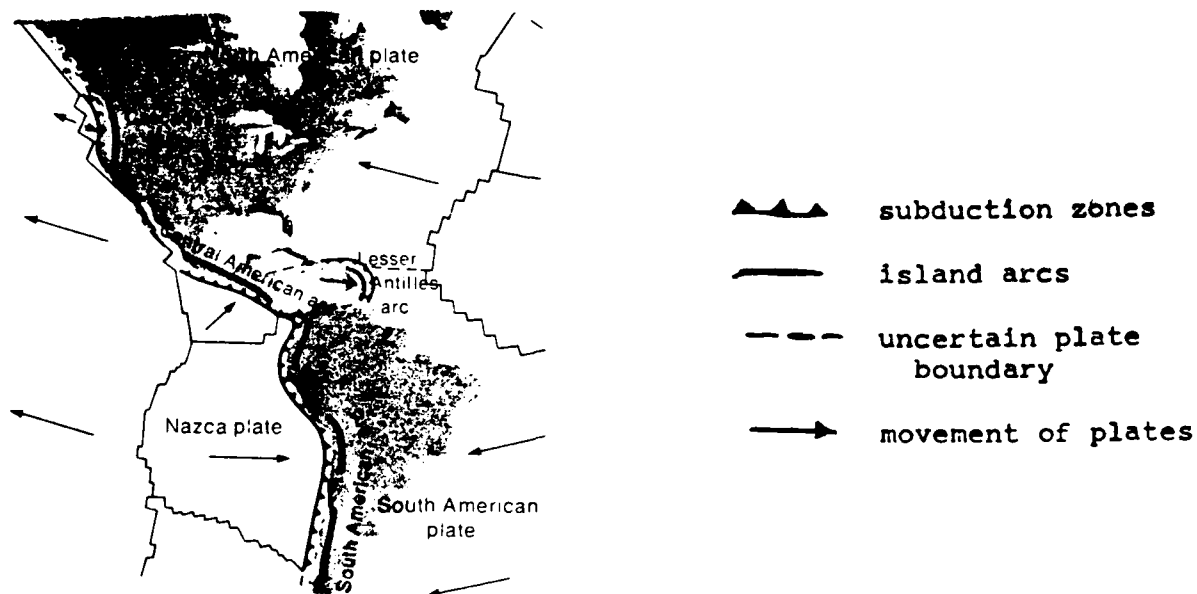


Figure 4.3: Volcanic Fronts and Island Arcs develop parallel to the trenches or deeps marked by subduction zones, where plates are consumed into the inner earth; plates form originally at the mid-ocean ridges. (Adapted from Skinner (1980).)

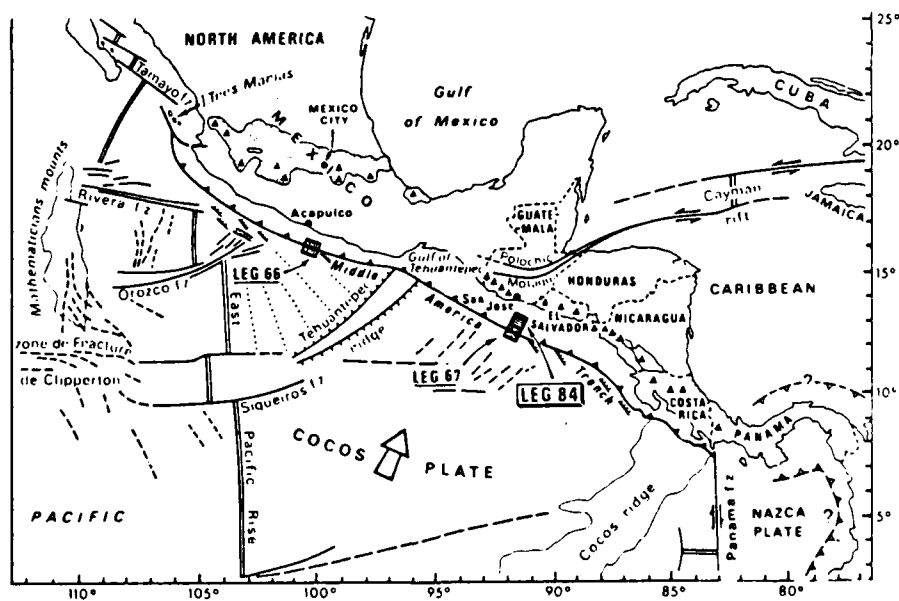


Figure 4.4: Location of the Middle America Trench is shown adjacent to the Pacific coast-line northwestward from Costa Rica, where the Cocos Plate is forced underneath the Caribbean and North American Plates in the earth's crust; the location of the Cayman Rift is also shown in the northwestern Caribbean Sea, along the boundary of the Caribbean Plate. (Adapted from Aubouin et al. (1982).)

Seismicity. The Pacific coast of Central America is very active seismically, while only scattered epicenters appear on the shelf off the Caribbean coast. Thus, while the Caribbean coast and the land area of Central America should be considered relatively stable, the shelf has shown continual signs of seismic activity, as indicated by Collins et al. (1970). Figure 4.5 illustrates the epicenter density of the region; note that recorded loci are usually shallow.

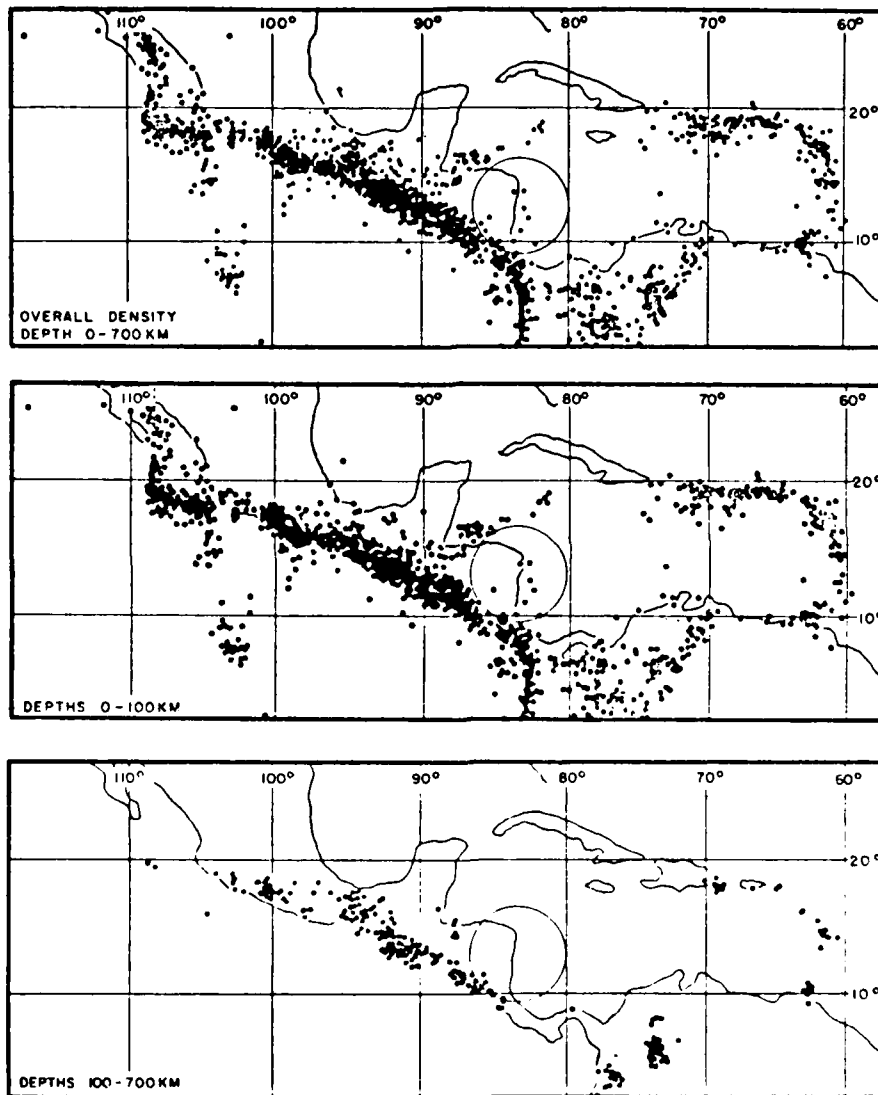


Figure 4.5: Epicenter Density in Regions Adjacent to Central America, (1961-1967). Ignore the large circle (from original work) near Nicaragua (Collins et al., 1970).

Ocean Currents. Long-term mean ocean current charts adjacent to the coastlines of North, Central and South America have been produced by Meehl (1982). He made use of a seasonal ocean current data set from long-term mean currents derived from ship-drift shown on pilot charts; these data have been digitized on a 5° grid (see Fig. 4.6). These data agree favorably with ocean currents measured by buoys and current meters. Variability of surface current direction is summarized in Fig. 4.7, which indicates no seasonal current direction reversal occurs in the Caribbean Sea, but pronounced seasonal change (April to October) occurs in the eastern tropical North and South Pacific Oceans. This is described in detail in the Pacific Ocean discussion.

In the western Caribbean Sea, the ocean current flows in a relatively constant direction, toward the northwest, throughout the year. In October, a counterflow appears along the coast of Nicaragua, Costa Rica and Panama directed toward the southeast, as part of an eddy which forms to the west of the main ocean current flow.

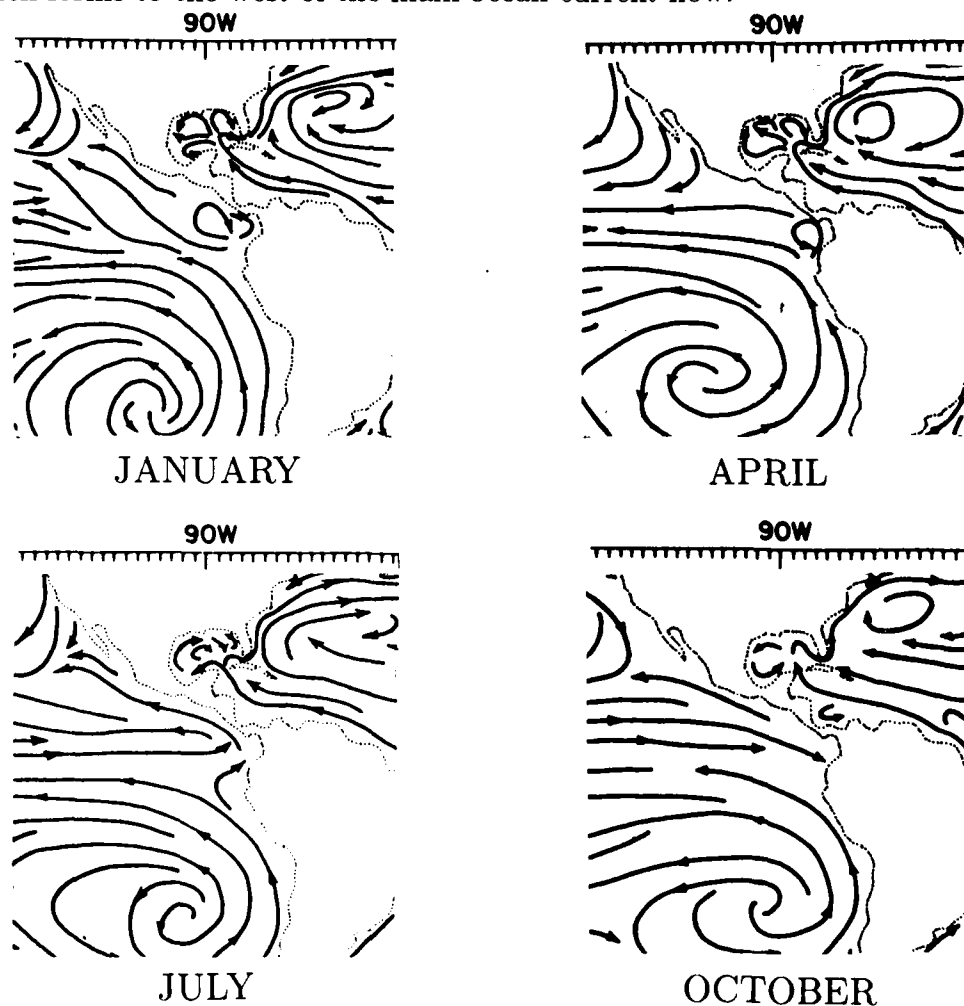


Figure 4.6: Observed Ocean Surface Currents; seasonal long-term currents based on ship-drift data from pilot charts (adapted from Meehl, 1982).

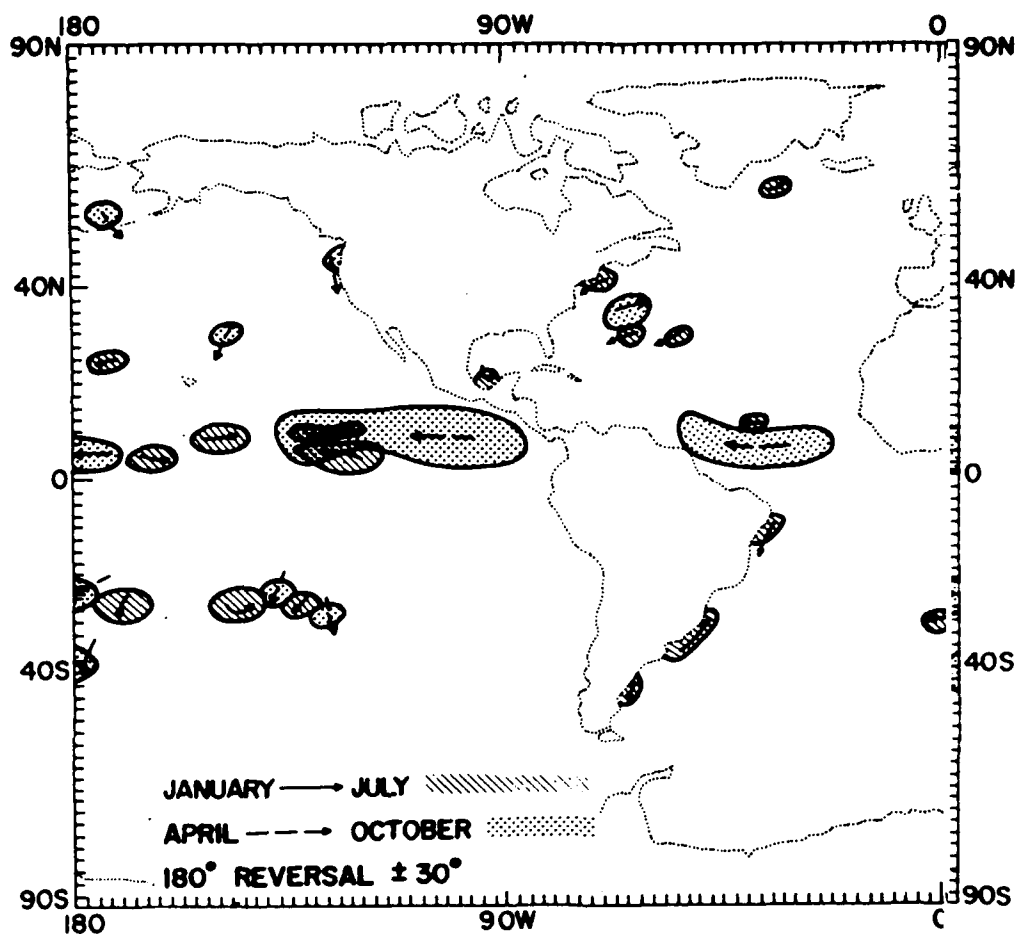


Figure 4.7: Surface Current Variability. Reversal change in direction ($180^\circ \pm 30^\circ$) between two seasons: January reversing in July—solid arrows; April reversing in October—dashed arrows. (Adapted from Meehl, 1982.)

Tides along the Central American Coast. Figure 4.8 from Gross (1982) shows that the tides along the coasts of Central American are mixed tides, and the tidal range for spring tides is shown at three stations. The tidal range is about 10 times greater along the Pacific coastline than it is along the Caribbean coast. Collins et al. (1970) note the tides along the Nicaraguan coast are mixed tides in the Caribbean (semi-diurnal plus diurnal, that yield two unequal tidal cycles per day); and that the tides progress there from south to north, usually with a range of less than two feet. Three stations (locations are shown in Fig. 4.25) are listed in Table 4.1, with high tide at Puerto Cabezas arriving 49 minutes after high tide at the Bluefields Lagoon entrance; and high tide occurs at Cabo Gracias a Dios with a delay of 3 hours, 31 minutes after it arrives at Bluefields. This Table summarizes tidal range and levels for these stations. Murray et al. (1982) note the tidal range on Miskito Bank off Nicaragua is about 20 cm.

Table 4.1: Summary of Tides at Coastal Stations along Caribbean Coast of Nicaragua (Collins et al., 1970)

Station	Mean Tide Range	Diurnal Tide Range	Spring Tide Range	Mean Tide Level
Cabo Gracias a Dios	1.2 feet	1.6 feet	1.9 feet	0.8 feet
Puerto Cabezas	1.4 feet	1.9 feet	2.1 feet	0.7 feet
Bluefields (Lagoon Entrance)	0.7 feet	1.0 feet	1.0 feet	0.3 feet

Tidal currents occur with greatest speeds at high and low tides, except near Cabo Gracias a Dios, where the strongest currents occur at mid-tide. The currents are small, usually less than 0.25 kt, according to Collins et al. (1970). On Miskito Bank, the maximum current speed is 7 cm/sec from calculations by Murray et al. (1982). They note maximum observed tidal currents at four shelf locations were 4–8 cm/sec; these tidal currents appear to be a major component of the total currents in the central Miskito Bank region; however, these tidal current values are nearly an order of magnitude smaller than the higher current speeds of the Coastal Boundary Layer nearshore (see later discussion).

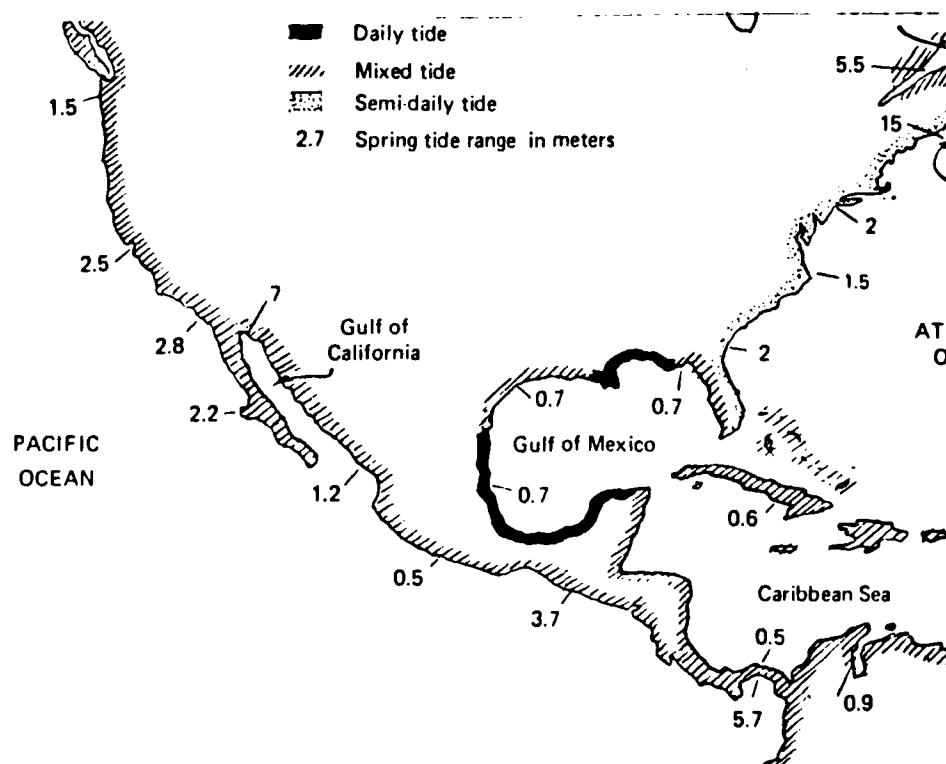


Figure 4.8: Types of Tides and Spring Tide Ranges (in meters) along indicated coastlines (adapted from Gross, 1982)

Sea-Surface Temperatures Adjacent to Central America. Since Central America is in tropical latitudes, between 8°N and 19°N, temperatures of the sea surface adjacent to this landmass are relatively warm. However, there are influences which act to provide small seasonal fluctuations in these temperatures. Some of these seasonal effects are in response to influences well outside the immediate coastal region of Central America .

On the other hand, the local wind field also affects these temperatures as the winds respond to seasonal influences that change their direction and speed. These seasonal effects from winds produce localized upwelling, with associated cooler temperatures, seaward from the Pacific coastline. This occurs when strong Northeast Tradewinds are able to penetrate through mountain passes or low-lying regions in Central America, and reach beyond the Pacific coastline during northern hemisphere winter and spring. During these seasons, also, less intense upwelling is observed in the southern Caribbean, along the northwestern coast of Venezuela.

Advection of cooler water in response to wind occurs in the Gulf of Panama in winter and spring, as well as along the equator, as water is carried northward and westward from the upwelling region off South America.

Local heating and cooling of the water surface also is affected by seasonal changes in cloud cover which occurs as the ITCZ⁷⁹ moves and changes in its progression through this region.

Charts showing wind flow direction and wind speed, and the associated sea-surface temperature charts have been adapted from Sadler et al. (1987) for the months of January, April, July and October. These are shown as Figs. 4.9 through 4.12. The following brief summary depends on these Figures.

Western Caribbean Sea Coastline of Central America: in January, temperatures are 26°C or slightly higher; by April, these have increased to 27°C or slightly higher; in July, temperatures are near 28°C; in October, a maximum temperature center has developed near Belize with temperatures of 28 to 29°C. Temperature gradients are weak throughout the year as coastal temperatures undergo their small annual variation.

Eastern North Pacific Ocean Coastline along Central America: this region lies between the upwelling centers observed at higher latitudes along the North American and South American western coasts; and only a small area in the Gulf of Panama is affected by advection from the South American upwelling during January–April, with temperatures of 26 to 27°C there. Local upwelling along the Pacific coastline in January produces two small upwelling centers with cool temperatures (less than 26°C) off the Guatemala–Mexican border, and off Nicaragua; these alternate with warm centers along the coastline; temperatures are 27°C plus off Honduras–Guatemala and 28°C plus off Costa Rica. In April, an upwelling center off Nicaragua drives temperatures below 28°C; this separates two warmer centers—one off Guatemala and one off Costa Rica, each with temperatures above 29°C. Temperature gradients along the coastline are much more pronounced than along the Caribbean coastline. This changes by July, when there is a very weak temperature

⁷⁹To provide continuity with the meteorological sections, the acronym ITCZ (for Inter-tropical Convergence Zone) will be used vice ITC.

gradient along the Pacific coastline in the absence of pronounced upwelling. Temperatures range from a few tenths degree C above and below 28°C. In October, the temperature maximum (above 29°C) off Guatemala contributes to the moderate temperature gradient along the Guatemala-El Salvador coastline; the gradient becomes very weak from Nicaragua southeastward, with temperatures there just below 28°C.

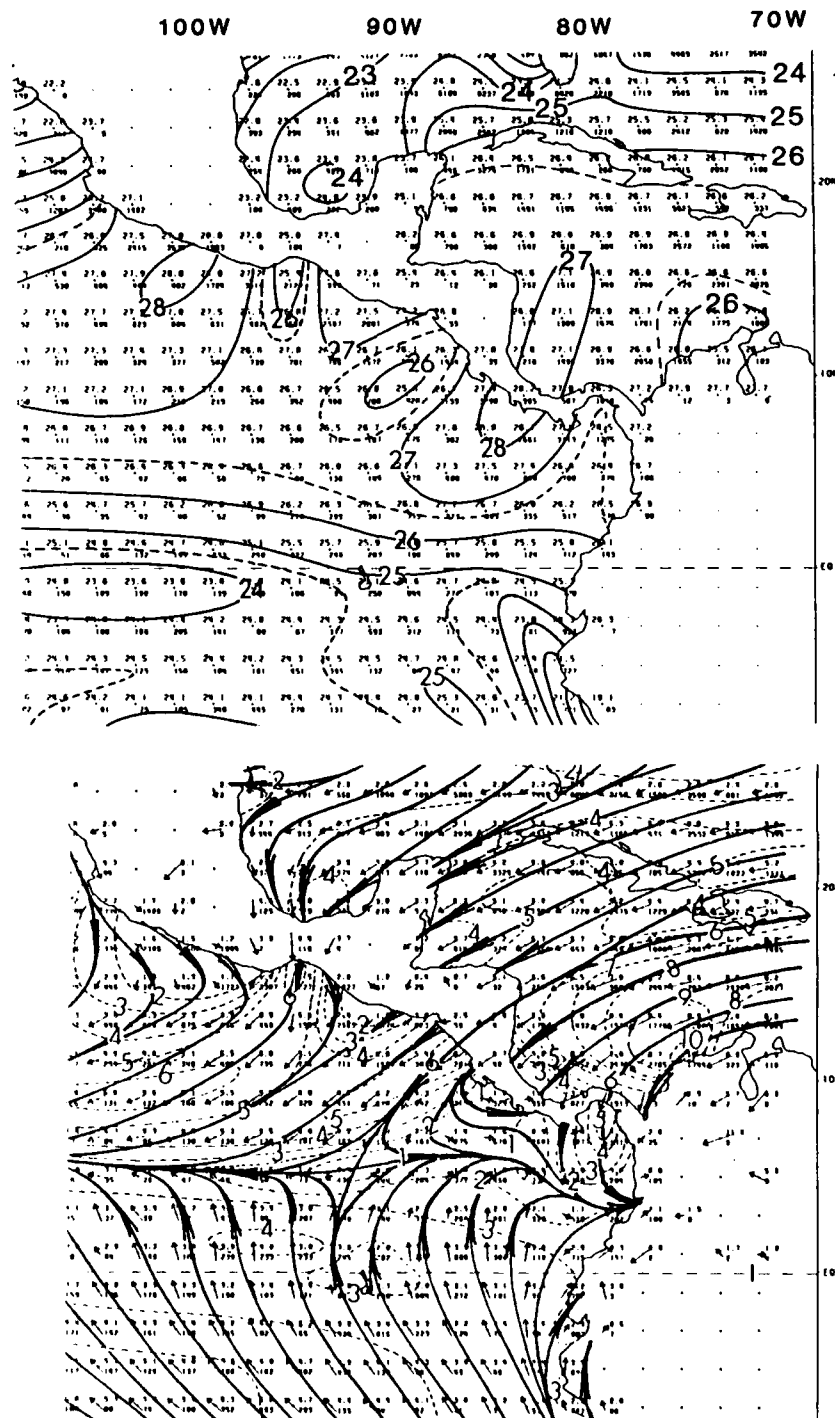


Figure 4.9: Sea-Surface Temperature (SST) and Wind Pattern for January. SST in °C; streamlines (solid lines), wind speed (in m sec^{-1} (dashed lines)) (adapted from Sadler et al., 1987)

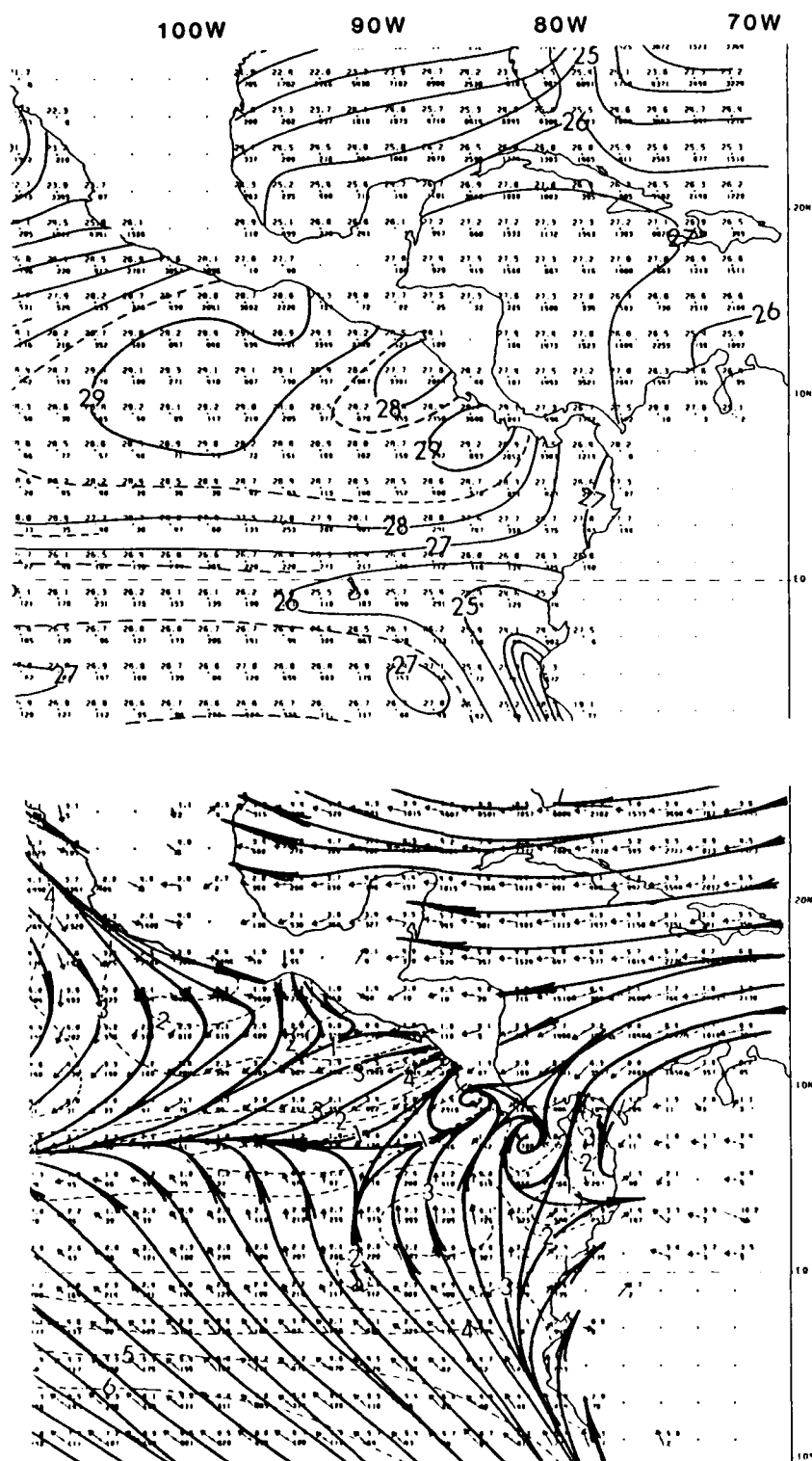


Figure 4.10: As in Fig. 4.9 for April (adapted from Sadler et al., 1987)

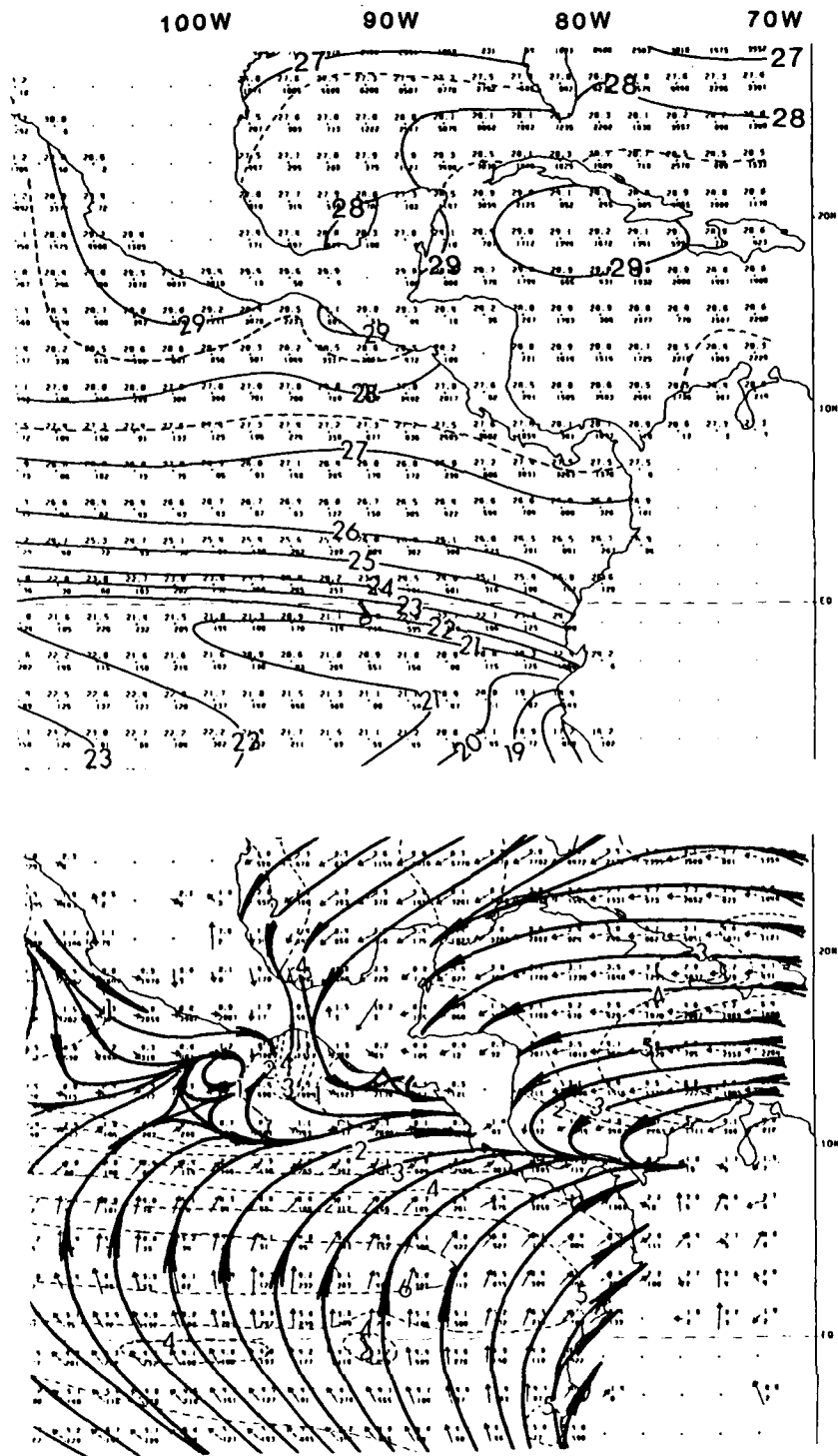


Figure 4.12: As in Fig. 4.9 for October (adapted from Sadler et al., 1987)

4.2 The Pacific Coast of Central America

Introduction. Several influences affect the distribution of the ocean temperatures, both at the surface and below; salinity distribution is affected, too, as well as ocean current distribution along the Pacific coastline of Central America. The wind patterns, as they undergo their seasonal migrations, are included among these influences; the ocean currents, arriving from distant parts of the lower latitudes and equatorial regions, are influential. The peculiar configuration of the coastline of Central American relative to the winds and ocean currents also has its effect. In discussing these influences, it seems appropriate to consider the effects of the geography of the Central American region first.

Physical Geography of Central America. The irregular land bridge between the broad landmass of North America as it narrows along its thrust equatorward through Mexico, and the bulky continent of South America which straddles the equator at its broadest extent, makes up Central America. Central America joins South America in the Isthmus of Panama which represents the most southerly and eastern extension of this land bridge, as well as its most narrow point where the Panama Canal has been built.

The peculiar land configuration results from complex geological patterns in earth's crustal behavior underlying this region. No less than four of earth's crustal plates affect the area—Caribbean, South American, Nazca and Cocos Plates. The nature of the mountain chain in the region and the continental shelves are determined by these plates, as well as the offshore bathymetry, plus sediment covering and materials of the sea floor.

A chain of volcanic mountains forms the irregular backbone of Central America and is the extension southward from the volcanic mountain chains of Mexico, as well as the northward extension from the volcanic Andes Mountains of South America. These volcanoes accompany the trench configuration just offshore from the Pacific Ocean coastline, along with the very narrow (or non-existent) continental shelf extending under the nearshore waters from the narrow land bridge. The complex bathymetry offshore from Panama is illustrated in the relatively broad view of Fig. 4.13 taken from Lonsdale (1980), which shows the near-shore trenches that direct substantial deep-water flow across deep ridges into the various basins. The Cocos Ridge marks the boundary of the Cocos Plate, which moves, ever-so-slowly, in a different direction from the Nazca Plate on which the Panama Basin occurs; the boundary between these plates is marked by a series of smaller ridges and trenches within the Panama Fracture Zone, illustrated in Fig. 4.14 from Lowrie et al. (1979).

The mountain chain of Central America is not continuous, but saddles or gaps occur along the chain (especially through Nicaragua, Costa Rica and Panama). Protrusions of the wind systems, that arrive from further east over the Caribbean Sea, can penetrate through these gaps. These penetrating winds can provide ocean effects along the Pacific coast of Central America. Otherwise, these volcanic mountains generally provide barriers to the circulation patterns of the lower atmosphere.

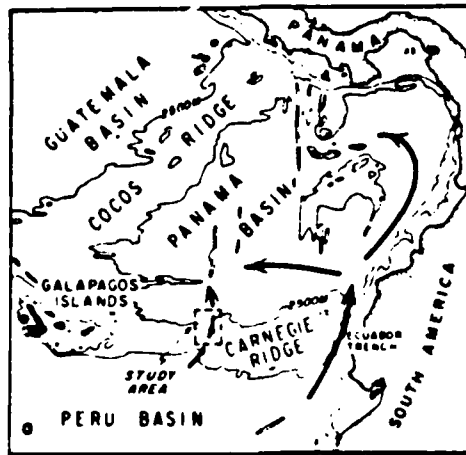


Figure 4.13: Bottom Topography showing complex nearshore ridge and basins off the Pacific coastline of Panama (adapted from Lonsdale, 1980)

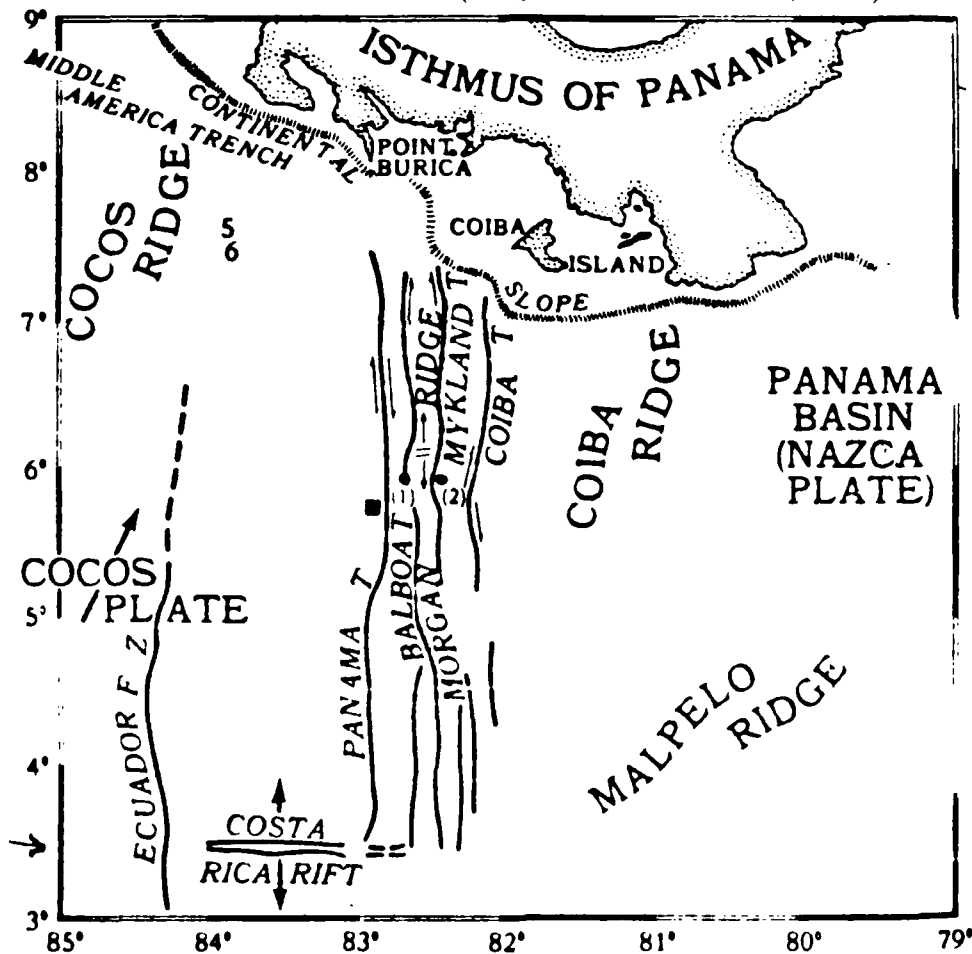


Figure 4.14: Ridges and Troughs within the Panama Fracture Zone. Large arrow in southwest corner denotes motion of Cocos Plate relative to Nazca Plate. Heavy double lines mark active spreading ridges, light double lines mark inactive spreading ridges, and arrows mark spreading directions (Lowrie et al., 1979).

Wind Patterns: Doldrums and Inter-tropical Convergence (ITCZ).

According to Stroup (1969), the Pacific Ocean area adjacent to Central America remains subject to the influence of the Northeast and Southeast Tradewinds, as they alternate in pushing over this tropical region during various times of the year. Because the Pacific coastline of Central America extends sharply toward the northwest, the Northeast Tradewinds must extend themselves much further west (at least 30 degrees of longitude) before they begin to exert a marked influence on the Pacific Ocean, compared to the Southeast Tradewinds; those Southeast Tradewinds originate in the southern hemisphere and extend northward across the equator into this region during portions of the annual cycle in wind patterns observed here. Thus, the Northeast Tradewinds of the Pacific Ocean play a less important role in this easternmost part of the tropical North Pacific than do the Northeast Tradewinds of the Caribbean; those Caribbean Northeast Tradewinds cross the narrow Central American land bridge on a regular basis during the seasonal shifts of wind patterns within this area.

Surface Current Patterns in the eastern tropical Pacific Ocean. There are two current gyres between the middle latitudes and equatorial regions of the Pacific Ocean. In the northern hemisphere, the gyre consists of a clockwise flow that includes the broad, slow California Current that flows equatorward along the Pacific coastline of North and Central America; it turns westward before it reaches the region dominated by the ITCZ, and becomes the westward-flowing North Equatorial Current which extends across the width of the Pacific Ocean.

The gyre within the southern hemisphere is a mirror image, generally, of the northern hemisphere gyre just described; the broad westward flow of the South Equatorial Current of the southern hemisphere usually extends to the equator; it represents the outflow from the Peru Current, whose speed and volume is greater than the California Current, its northern hemisphere counterpart. There is little penetration from this southern hemisphere gyre into the easternmost tropical Pacific Ocean that is adjacent to Central America, because of the configuration of the South American Pacific coastline relative to central America and because of the Galapagos Islands.

Instead, that region is dominated by the outflow from the North Equatorial Countercurrent which is narrow and strong; it is directed toward the east, flowing between the North and South Equatorial Currents which flow toward the west. This North Equatorial Countercurrent occupies the latitude belt between 5°N and 10°N; the extent and pattern of this Countercurrent outflow as it penetrates into this tropical region of the eastern Pacific Ocean varies with season and accompanying wind pattern.

Stroup describes two periods of the year when the currents here are quasi-stationary, separated by periods of transition. The quasi-stationary periods correspond to the extreme positions of the ITCZ in its seasonal migration; the transition periods for the ocean currents correspond to the periods when the ITCZ changes latitude rapidly from one extreme position to the other.

The August-December Current Pattern (one stable period) occurs when the Southeast Tradewinds are strong, with the ITCZ in its northernmost position. The North Equatorial Countercurrent has extended eastward to the vicinity of the Central American coastline between 5–10°N, having speeds of 0.75 kt; most of its flow turns northwestward along the coast and supplies the Costa Rica Current which then is strongly developed and extends to 20°N in August. Later, as the ITCZ moves southward, this northwesterly flow of the Costa Rica Current separates from the coast, replaced by a band of water that flows toward the southeast and gradually increases in area along the coast. By December, the northwesterly⁸⁰ flow appears along the coastline only in the region from 15–16°N, with speeds in the Costa Rica Current diminished to 0.5 kt.

After the Costa Rica Current reaches its northern extreme, it turns toward the west and becomes that part of the North Equatorial Current which is south of 20°N. North of 20°N, the North Equatorial Current is supplied by the California Current flowing from the north; the California Current is weak during this season, with speeds of 0.1 kt along Baja California that increase well offshore only to 0.3 kt. The North Equatorial Current matches that speed of 0.3 kt.

On the south side of the North Equatorial Countercurrent, the South Equatorial Current that flows westward is strongly developed; speeds over 1 kt prevail between 5°N and the equator. The speed diminishes southward from the equator during this period. Water for the South Equatorial Current comes from the Peru Current which has speeds of 0.2–0.3 kt near the coast and slightly higher speeds offshore. The coastal Peru Current weakens after August, when the Southeast Tradewinds weaken. The Peru Current leaves the Peru coastline at about 5°S, turns westward and increases in speed. Between the coast of Peru and the Galapagos Islands (at about 4°S), a distinct front develops between the colder, saltier water of the Peru Current and the warmer, fresher water to the north (which is present along the equatorial eastern Pacific coastline of Central America).

During the January Transition Period, the North Equatorial Countercurrent weakens, breaks up, and vanishes as a coherent flow east of about 120°W. At the same time, the California Current strengthens and the southeasterly flow that results penetrates increasingly into the eastern tropical North Pacific area. The South Equatorial Current weakens as the ITCZ shifts southward rapidly.

The February-April Current Pattern (the second stable period) is marked by the disappearance of the North Equatorial Countercurrent east of 120°W; it is replaced by flow toward the west and northwest at 5–10°N. Two eddies occur in the nearshore region: one is clockwise in circulation, centered at 5°N, 88°W; the second eddy has counter-clockwise circulation and is centered at 5°N, 89°W. Between the two eddies is a small zone of persistent easterly flow. The shallow vertical temperature gradient (thermocline) in the upper ocean region of this second eddy forms the "Costa Rica Dome", a well-documented ocean feature of the area. The northwestward coastal flow associated with this second eddy makes up the limited Costa Rica Current during this season; it turns westward from the coastline at about 11–12°N.

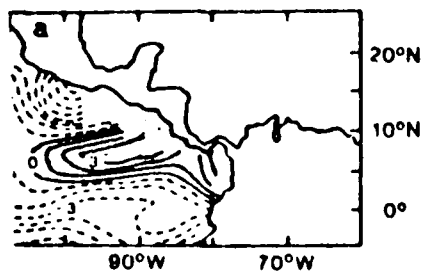
⁸⁰Note—"northwesterly" refers to **toward the northwest**, as opposed to its meteorological interpretation.

The California Current supplies most of the water for the Northern Equatorial Current as it turns westward, after penetrating far southeastward into our region of interest. The California Current has been relatively strong at 0.2 kt to 0.3 kt near the Baja California coastline in this season. Offshore, the California Current speed and that of the North Equatorial Current are almost constant throughout the year.

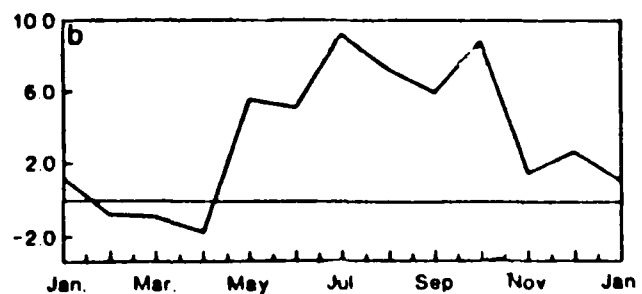
In March and April, the South Equatorial Current, usually present along the equator between 120°W and 100°W, is replaced frequently by an easterly flow there, with speeds under 1 kt.

In the May-July Transition Period, the North Equatorial Countercurrent reforms east of 120°W, adding to the Costa Rica Current flowing along the coast as it again penetrates northwestward to 20°N. The California Current moves offshore and weakens. The South Equatorial Current is so weak in May that flow along the equator is toward the east from 100°W to 120°W, even though Southeast Tradewinds are present there. In June, however, the South Equatorial Current along the equator strengthens and develops speeds of over 1 kt toward the west. The ITCZ is now shifted well to the north of the equator.

Hoffman et al. (1981) have suggested that the northward migration of the ITCZ during the summer is accompanied by the intensification of cyclonic wind stress curl over the "Costa Rica Dome" region centered near 8°N, 90°W, and which is about 200 km–400 km in diameter (see Fig. 4.15a).



(a)



(b)

Figure 4.15: (a) Mean Annual Wind Stress Curl (10^{-9} dyne·cm⁻³). Dashed lines are negative values. (b) Time series of the mean monthly wind stress curl at 10°N, 91°W. These maps are derived from a ten-year record of wind observations (Hoffman et al., 1981).

Noticeable upwelling occurs in the upper ocean here, with the thermocline displaced upward 20 m-30 m from its earlier position (upwelling velocities are about 10^{-4} cm·sec⁻¹). In the autumn, as the ITCZ moves southward again, the cyclonic wind stress curl weakens over this region so that the upwelling is no longer balanced; a low-frequency internal wave occurs as the uplifted thermocline leaves the region and moves toward the northeast. This is in response to overriding advective influences from the North Equatorial Countercurrent flowing toward the east (which strengthens to 40 cm·sec⁻¹) and from the northward flowing Costa Rica (coastal) Current. (Similar "domes" are found in the Atlantic and Indian Oceans at the eastern extremities of equatorial countercurrents there; this suggests that cyclonic wind stress curl is a key reason for this upwelling to occur, and that ocean current configurations and fluctuations are not a sufficient explanation). The Costa Rica Dome is not a stationary feature, but fluctuates seasonally with the variation in local cyclonic wind stress curl (see Fig. 4.15b).

Sub-surface Current Patterns in the eastern tropical Pacific Ocean. In the upper 500-600 meters of the ocean, currents generally are parallel to the overlying surface currents, with speeds that decrease with depth below the surface. One notable exception to this occurs within the region, however. The Equatorial Undercurrent (Cromwell Current) is a shallow, narrow current just below the ocean surface that has a strong and persistent flow toward the east which opposes the flow of the South Equatorial Current at the ocean surface above. The core of highest current speed (2 to 3 kt) lies at a depth of 50 to 100 meters below the surface in the eastern equatorial Pacific Ocean. This thin current is only a few hundred meters in vertical extent, and about three hundred kilometers wide, running along the equator.

When the Southeast Tradewinds are light or absent, this current appears to reach the sea surface. The volume is the same magnitude as flow in the North or South Equatorial Currents; however, the water characteristics in the Undercurrent flow differ greatly from those in the surface currents. The eastward flow in this current is blocked at 92°W by the Galapagos Islands.

Surface Temperature. Most earlier surface temperature studies in this general region have been concerned with the limited upwelling that occurs in the Gulf of Tehuantepec, the Gulf of Panama and the Costa Rica Dome. There are two stable periods in the annual variation of surface temperatures in the region, and the gross features of these periods have been described well by Wyrtki (1964).

(1) September: A band of highest surface temperatures extends west-east and is centered about 11°N , near the location of the northern edge of the North Equatorial Countercurrent in the ocean, and at the mean location of the ITCZ in the atmosphere. The temperature is over 29°C near the coast, and high temperature extends northward along the coastline into the Gulf of California. West of the Galapagos, along the equator, there is a band of lower temperatures (about $19\text{-}20^{\circ}\text{C}$) extending east-west and associated with the equatorial upwelling that is driven by the strong Southeast Tradewinds. The advection of cold water northward from the coastal upwelling region off Peru also contributes to this low temperature band. A front often forms at the northern boundary of this band, from the coast out to, and at times beyond, the Galapagos Islands. Coastal upwelling is usually not present off Baja California, with relatively high temperatures ($27\text{-}28^{\circ}\text{C}$) observed there.

(2) March: The North Equatorial Countercurrent is absent now, and the ITCZ has shifted southward; the band of highest ocean surface temperature follows the ITCZ and is centered at about 5°N . Temperatures in this band are about $28\text{-}29^{\circ}\text{C}$, about one degree C cooler than in September. Winds which cross Central America from the Caribbean cause offshore flow and consequent upwelling and lower temperatures in the Gulfs of Tehuantepec, Fonseca and Panama; this is responsible for complex surface temperatures along the Pacific coastline. High temperature no longer extends northward along the coastline toward the Gulf of California, since coastal ocean currents are directed southward now. Along the equator, evidence of upwelling and the advection of cold water is much reduced compared with September. There, temperatures have increased to $26\text{-}27^{\circ}\text{C}$ (compared to $20\text{-}21^{\circ}\text{C}$ in September) so there is an annual temperature range of over 5°C along the equator in this region. No equatorial temperature minimum is observed east of 110°W in March. The lower temperature off Baja California is a consequence of the increased strength of the Northeast Tradewinds, which also cause increased intensity of the California Current and its southeastward penetration further along the coastline of Central America.

There is evidence of quasi-circular eddies that occur along the Pacific Ocean coastal area off Central America. The eddies have associated circulations and temperature differences from surrounding water. Figure 4.16 (Brown, 1987) shows such an eddy off the Gulf of Fonseca in an infrared satellite image; the superimposed velocity vectors were measured by a ship transiting the eddy, indicating a clockwise circulation.

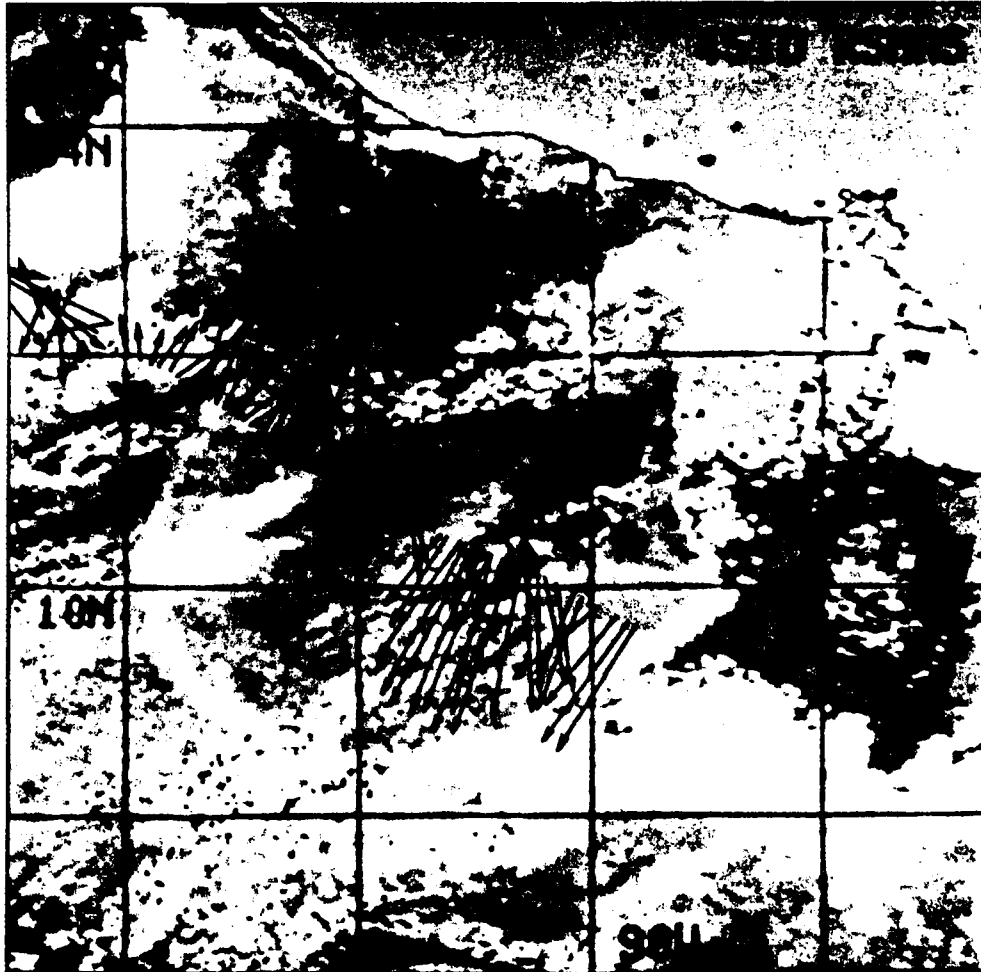


Figure 4.16: The Warm Surface Water of an Eddy shows up as a circular patch in this heat-sensitive satellite image in the Gulf of Fonseca off the Pacific Coast of El Salvador/Nicaragua. Superimposed lines show direction and relative speed of actual current measurements made by EXXON JAMESTOWN. Change in current direction as the ship crossed the approximate center of the eddy indicates a water mass in clockwise rotation (Brown, 1987).

Vertical Temperature Structure. In the upper ocean layers between about 20°N and 20°S, a permanent thermocline occurs in the basic temperature-depth structure (see Fig. 4.17); this thermocline occurs in a series of troughs and ridges as its spatial distribution is traced from south to north. These features of the thermocline extend generally east-west and are associated with the major equatorial surface currents. Superimposed on its general distribution is a usual increase in the depth of the thermocline as one moves toward the west. However, this general pattern of thermocline distribution is strongly modified near the Pacific coastline of Central America.

Along this eastern boundary of the Pacific Ocean, the thermocline generally becomes shallower toward the coast within the equatorward flow of the California Current. In the Costa Rica Current that flows northward, the thermocline deepens between the shallow Costa Rica Dome and the coastline. Above the Costa Rica Dome, the thermocline is very shallow; and in the region near the equator just west of the Galapagos Islands, the thermocline extends upward to less than 20 m below the ocean surface; occasionally in this region the thermocline reaches the surface.

Within the thermocline, the temperature gradient may be intense; along the northern edge of the North Equatorial Countercurrent this vertical gradient may reach more than $0.5\text{ }^{\circ}\text{C}\cdot\text{m}^{-1}$, especially in the shallow thermocline of the Costa Rica Dome. Just to the west of the Galapagos Islands, where the thermocline is very shallow immediately to the north and south of the equator, there are zones of relatively large temperature gradient within the thermocline. Along the equator itself the vertical temperature gradient in the thermocline is smaller. This appears as a spreading of the thermocline in vertical extent in a north-south vertical cross-section across the equator; the upper isotherms form a ridge extending east-west, while the lower isotherms of the thermocline appear as a trough according to Wooster and Cromwell, quoted by Stroup (1969).

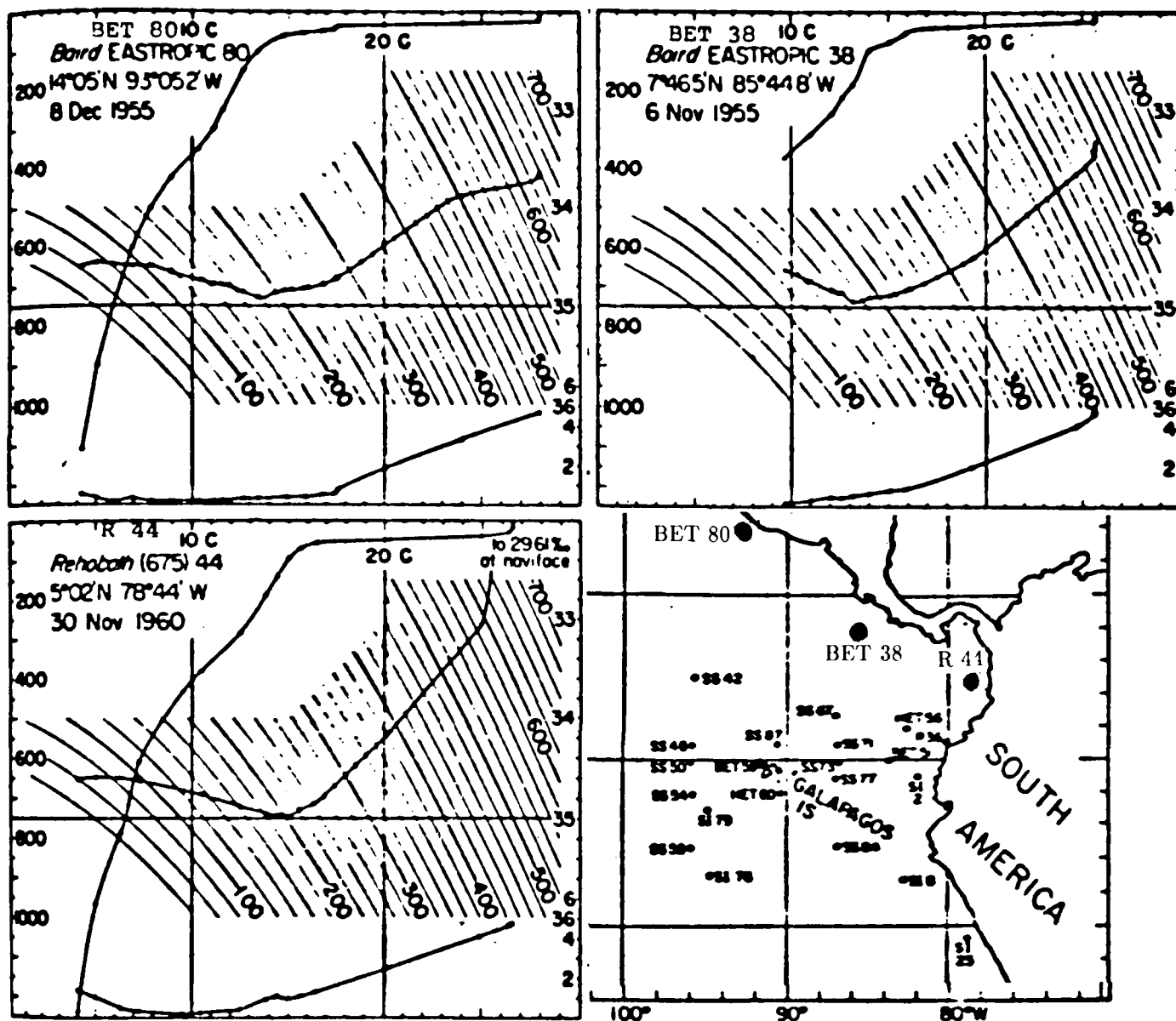


Figure 4.17: Soundings of Temperature-Depth, Temperature-Salinity and Temperature-Oxygen; for stations BET 80, BET 38, and R 44 along Pacific Coast of Central America. Scales are for temperature in $^{\circ}\text{C}$; depth is in meters, along left side; scales on the right side are for salinity in ‰ ; and oxygen in ml/l . Inset chart shows station locations with large dots (adapted from Stroup, 1969).

Surface Salinity. Bennett (1966) has published monthly charts of surface salinity which are for the area 30°N to 30°S, and from 140°W to the Central American coastline. North of the equator, Bennett shows high offshore salinities only in the northwest corner of this eastern intertropical area, near 30°N, 140°W. Seasonal variations in this northwest corner are small. A high-salinity area occurs in the Gulf of California, with values above 35‰.

Low surface salinity values extend as an east-west band centered near 10°N, excepting in the easternmost region; there, low-salinity water extends southward to the front that marks the northern boundary of the colder water of higher salinity in the Peru Current; the front reaches from 5°S at the coastline to the equator near the Galapagos Islands. The salinity change across this front is substantial throughout the year. The temperature change within the front varies with the seasonal changes of the Peru Current.

Seasonal Changes of Salinity occur in our region of interest.

In September the low-salinity band of this region is well-developed; this occurs when the ITCZ is in its northernmost position and the North Equatorial Countercurrent is strong. Salinity is less than 30‰ in the Gulf of Panama; and the water is less than 33.5‰ that extends along the coast to about 15°N, and then westward to beyond 130°W. The coastal waters have salinities less than 34‰ to about 20°N; off the Gulf of California, water with salinity above 34.5‰ extends seaward only a few hundred kilometers.

In March the band of minimum surface salinity is not well-developed; the ITCZ is far to the south, and the North Equatorial Countercurrent is not present in this region. The surface salinity has increased to over 34.5‰ in the Gulf of Panama, then experiencing upwelling. The lowest salinity (near 31‰) occurs offshore at about 5°N, northeast of the Galapagos Islands. Water with salinity less than 35.5‰ touches the coastline near the equator, extending northward only to about 10°N, and westward to 95-100°W. The California Current has strengthened and extended southeastward; salinity above 34.5‰ is at 15°N, and 34.0‰ values have reached to about 10°N along the coastline—some 2000 km southeast of the location with these values in September.

Year-to-Year Changes of Salinity Distribution accompany the dramatic temperature changes of this region in the El Nino occurrences with their global effects on ocean and weather circulation patterns. The El Nino is a warm ocean current setting south along the coast of Ecuador, so called because it generally develops just after Christmas (Huschke, 1959). Donguy and Henin (1980) have developed charts of surface salinity for the eastern tropical Pacific Ocean based on observational studies within the region just before, during and after El Nino occurrences of 1972 and 1976; also, they prepared graphs of surface salinity by month along a track from Tahiti to Panama City, Panama, based on observations taken by ships of opportunity during 1974-1978. (These ships also observed surface temperatures, but those results are less unique and are not shown here). The Tahiti-Panama track crosses the equator at 100°W; our interest centers on the northern hemisphere observations, from the equator crossing to the Gulf of Panama.

The geographical variation in surface salinity is illustrated for this region first by Figs. 4.18, 4.19, and 4.20 (Donguy and Henin, 1980). In each figure, the upper chart is associated with the El Nino event of 1972 (the stronger event of the two), while the

lower chart is for the 1976 event. The heavy solid arrows depict wind flow over the ocean surface; the heavy dashed line represents the position of the ITCZ; and light solid lines represent the salinity value contours; the dots represent data points.

Conditions just preceding the El Nino events are indicated in Fig. 4.18. The ITCZ is at 5°N (five degrees further south than its usual late autumn position). Waters north of the equator, from 95°W to the coastline, have salinities below 34‰.

Figure 4.19 shows salinity patterns in February–March 1972 and 1976, during the El Nino events. Winds east of 95°W were from the northwest along the equator and equatorial upwelling was not present. The low salinity water spread southward across the equator, with 33.00‰ observed at almost 8°S (not shown in the figure) in 1972 and at about 5°S in 1976.

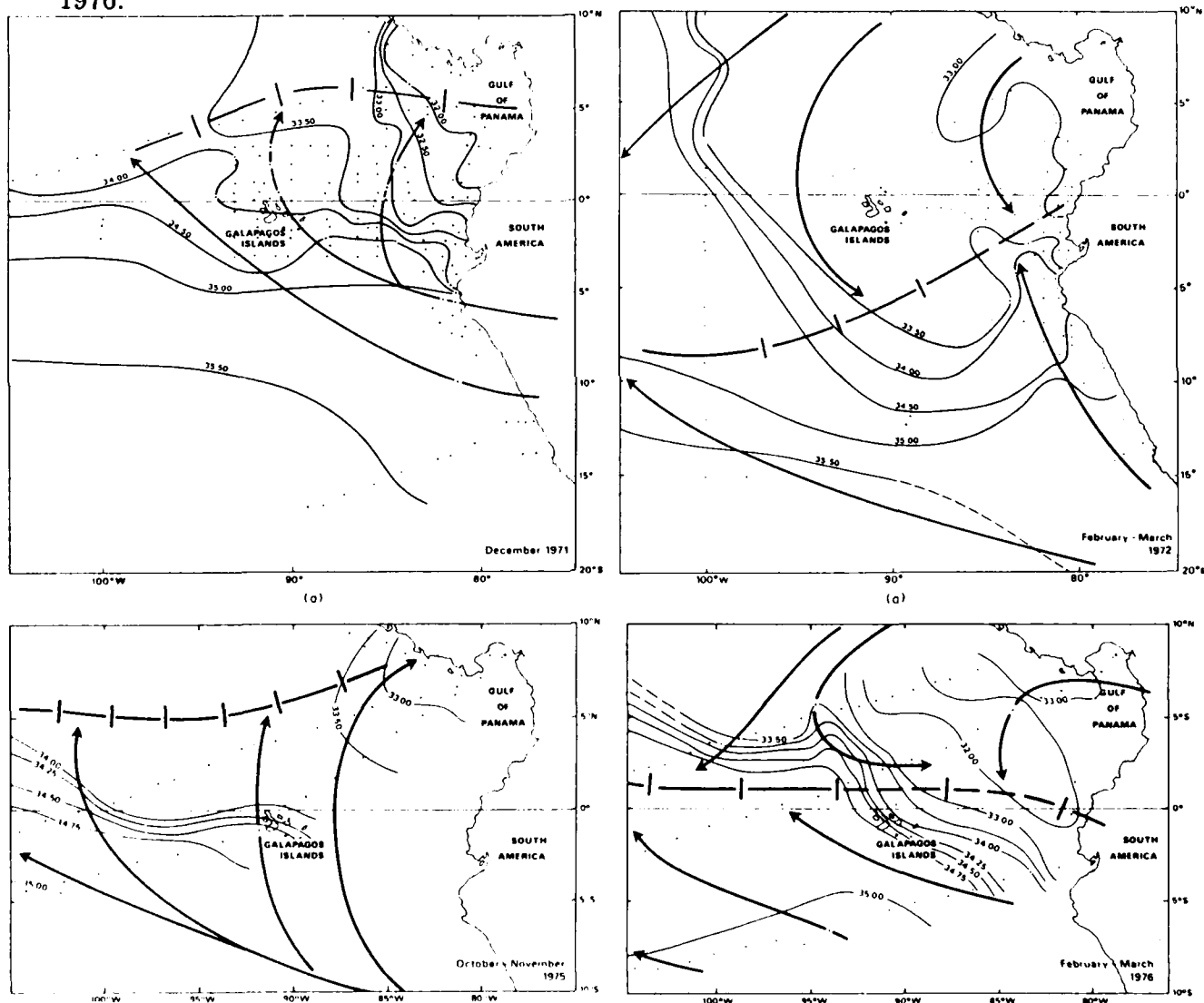
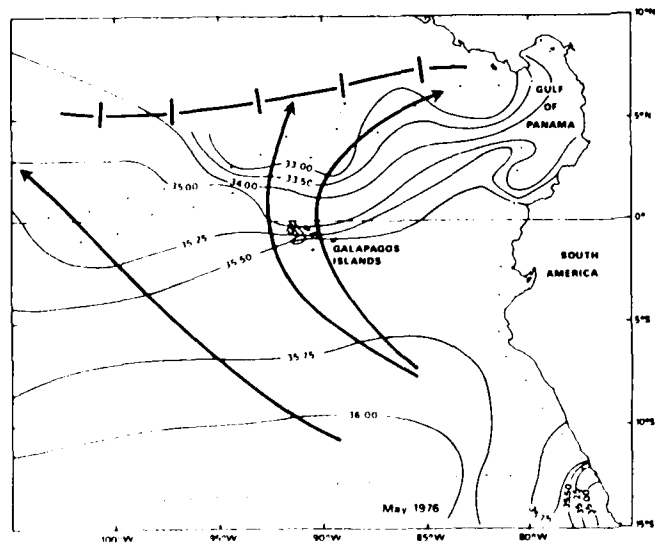
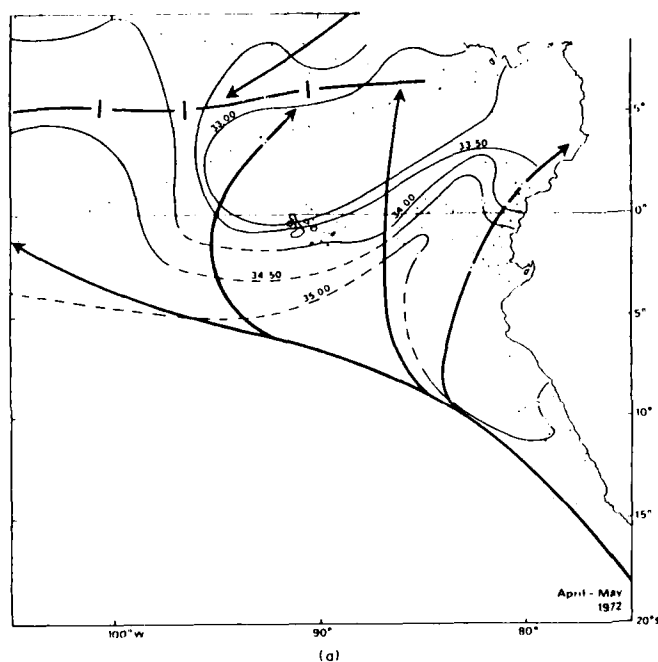


Figure 4.18: Surface Salinity in ‰ in December 1971 and in October-November 1975, prior to El Nino events (Donguy and Henin, 1980)

Figure 4.19: Surface Salinity in ‰ in February-March 1972 and in February-March 1976, during El Nino events (Donguy and Henin, 1980)

Figure 4.20 illustrates the salinity distribution at the surface after the El Nino events. In both years the ITCZ is at 7°N to the east of 95°W and north of the equator; the Southeast Tradewinds are deflected and blow from the southwest. The Southeast Tradewinds again produce coastal upwelling along the coastline of South America south of the equator, which brings high salinities to the sea surface there. This high salinity water is carried northward across the equator near 80°W, and extends as a tongue into the southwestern Gulf of Panama during April–May. Water having salinity less than 33.5‰ occurs generally to the north and seaward from this tongue of higher salinity that reaches the Gulf of Panama.



To summarize, the low-salinity water along Central America spreads into the southern hemisphere during an El Nino event. The position of the ITCZ appears to govern this spreading as the El Nino develops; this is true also during the El Nino withdrawal later as the El Nino event weakens and disappears.

During El Nino, the ITCZ moves southward from its usual position, bringing northwest winds to the equator, along with an interruption of equatorial upwelling. Low salinity water then is pushed across the equator into the southern hemisphere by the northwest winds. The ITCZ also has high precipitation amounts associated with it, which acts to lower surface salinity when the ITCZ crosses into the southern hemisphere during an El Nino event.

Figure 4.20: Similar to previous Figures, after El Nino events, in April–May 1972 and May 1976 (Donguy and Henin, 1980)

Figure 4.21 shows the variation of salinity by month and latitude along the Tahiti-Panama ship track; there have been three voyages per month to produce the data for this picture, for the 1974-1978 time frame. On this track, the 1976 El Nino event does not stand out strikingly from the adjacent years; the main El Nino effects are observed to the east of this ship track, between the Galapagos Islands at 90°W, and the South American coastline. North of the equator the salinity is generally below 35‰ and reaches 34‰ beyond 3°N. The salinity values reflect the seasonal variation in equatorial upwelling. In January-June, salinity values are lower when no equatorial upwelling occurs; and in July-December, salinity values are higher as equatorial upwelling brings higher salinity water from below the surface. A salinity front is present on the north side of the equatorial upwelling area, nearly always north of the equator. The year-to-year variation is small along this track. Figure 4.22 shows the 4-year averaged salinities by month and latitude along this track.

Subsurface Salinity. In the equatorial region, the salinity within the thermocline increases toward the west from the coastline to about 160°W. In the immediate vicinity of the equator the strong Equatorial Undercurrent flows toward the east and carries higher salinity water along with it. A high-salinity core is a common and permanent feature within the Undercurrent just to the south of the equator. To the east of the Galapagos Islands, some of the equatorial subsurface water turns northward near the coast and then spreads in a broad flow back toward the west. This flow is marked as a salinity maximum layer (since the surface salinity is low in this region) that extends to 19°N in the coastal area. The relatively small variations in salinity that occur in this salinity maximum layer appear to be associated with flow pattern variations at these depths.

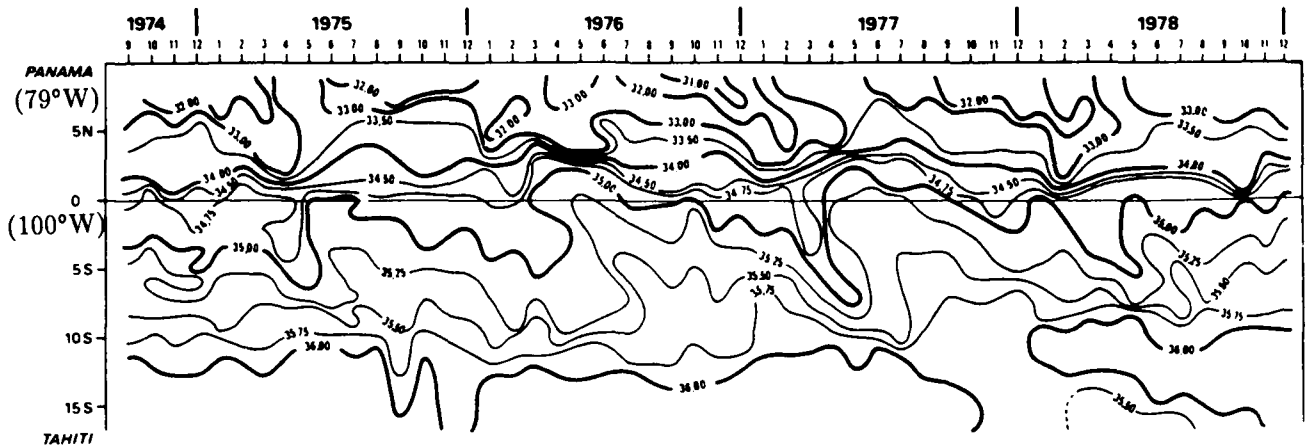


Figure 4.21: Surface Salinity (‰) along the Track between Tahiti and Panama, 1974-1978 (Donguy and Henin, 1980)

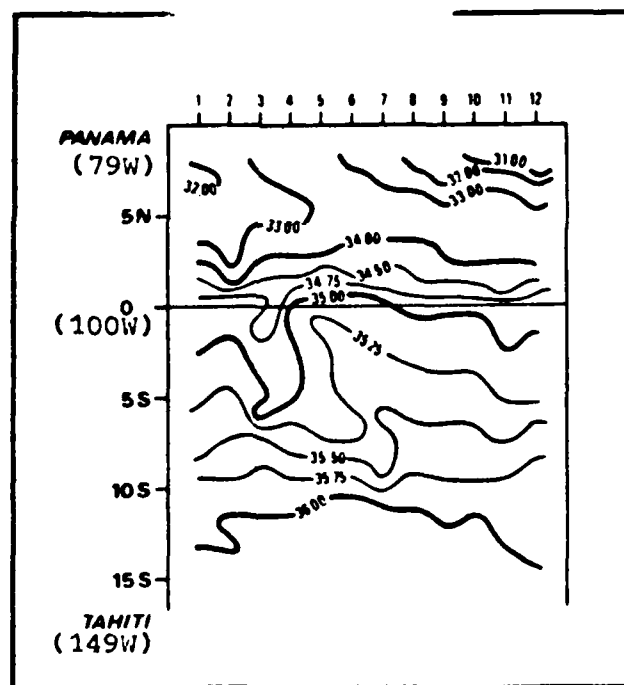


Figure 4.22: Mean Surface Salinity (‰) along the Track between Tahiti and Panama (Donguy and Henin, 1980)

4.3 The Caribbean Coast of Central America

Caribbean Circulation Limited by Bathymetry. According to Fairbridge (1966), great depths in the western Caribbean Sea occur in the Yucatan and Cayman Basins (>5000 m), and the Colombian Basin (>4000 m); the latter is separated from the former basins by the broad and shallow Jamaica Ridge. The greatest depth occurs in the Cayman Trench (24,720 ft or 7,535 m) which lies just east of Grand Cayman Island—the island is located at 19°N, 81°W, about 180 miles west-northwest of Jamaica (see Fig. 1.21). This trench occurs on the boundary between the Caribbean and North American Plates in the earth's crust. The Cayman Islands are on the Cayman Ridge, the narrow and relatively deep separation between the Yucatan and Cayman Basins. Water exchange occurs freely across the Cayman Ridge.

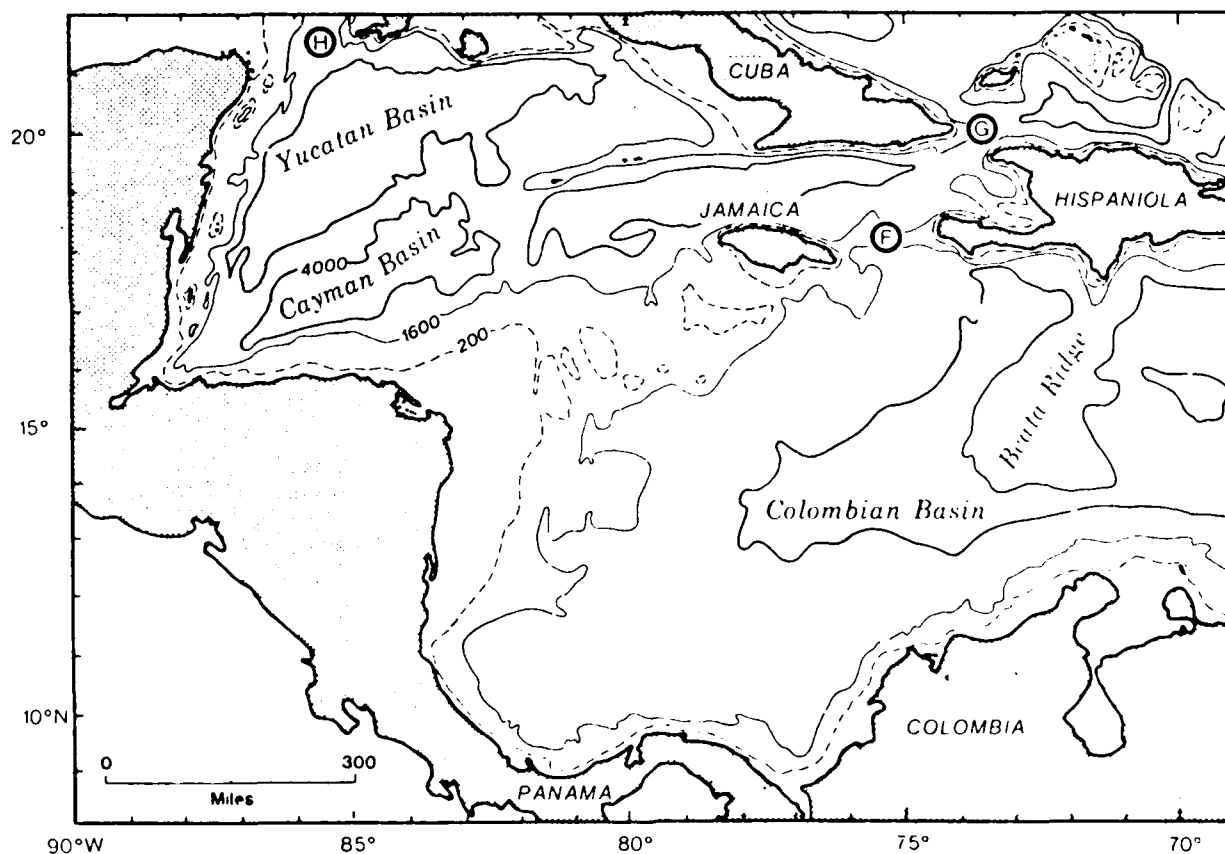


Figure 4.23: Bathymetric chart of the Western Caribbean Sea (after Uchupi, 1971). Passages identified for reference are: (F) between Jamaica and Hispaniola, (G) Windward Passage, and (H) Yucatan Channel. Depths are in meters. (Adapted from Morrison and Nowlin, 1982).

On the other hand, water exchange is limited by the extensive and shallow ridge containing Jamaica as it extends eastward from Honduras/Nicaragua toward Hispaniola; the greatest depth on this ridge (~ 1500 m) occurs between Jamaica and Hispaniola, indicated by (F) in Fig. 4.23; free water circulation occurs only above this restrictive depth along the Jamaica Rise (Ridge), and thus circulation is limited between the Columbian Basin (off Panama and Costa Rica) and the western Caribbean (Yucatan and Cayman Basins). Deeper water exchange for the western basins is similarly limited to that which can occur above about 1600 meters (~ 800 fa) through the Windward Passage ((G) in Fig. 4.23) which separates Hispaniola from Cuba. Thus the deeper waters of the Cayman and Yucatan Basins are affected more by the exchange with the Atlantic Ocean through the Windward Passage than by deep water exchange with the Columbian Basin of the Caribbean. In fact, such exchange of waters deeper than 1600 meters between the different basins occurs very slowly, if at all. Figure 4.24 shows greater detail for these bathymetric features, with depth contours shown in fathoms.

Considerable detail has been described for the Miskito Bank off the Caribbean coastline of Nicaragua by Collins et al. (1970) and Murray et al. (1982). This submerged feature of the Jamaica Ridge is only about 30 meters deep and extends to more than 200 kilometers offshore; the edge of the bank drops abruptly to great depths (shown by the inset on Fig. 4.25, from Murray et al., 1982). This abrupt depth change contrasts greatly with the continental slope usually found adjacent to continental shelves; this contrast is illustrated in Fig. 4.25 (inset) by comparison with the small continental slope profile off the west Florida shelf in the Gulf of Mexico.

Collins et al. (1970) note these additional features: large coral formations and scattered patches of coral cover from $1/3$ to $1/2$ of the Miskito Bank area, with definite influence on both its topography and sediments; also, several inner basins occur on the Bank which lie several meters below the surrounding depths. Fig. 4.26 (adapted from Collins et al., 1970) indicates the bank topography in great detail with extensive depth soundings (in fathoms). Two locations are marked, at 14.5°N and 13°N , along the shelf edge at which wave hindcast studies (reported later) were made. A submarine canyon system appears to originate between Quita Sueno bank (near the 14.5°N wave hindcast point) and the edge of the Miskito Bank. Note the position of Isla San Andres (off Miskito Bank at about 12.5°N , east-northeast of Bluefields) on Fig. 4.25 and 4.26; this is a reference location in the description of coastal currents which follows later.

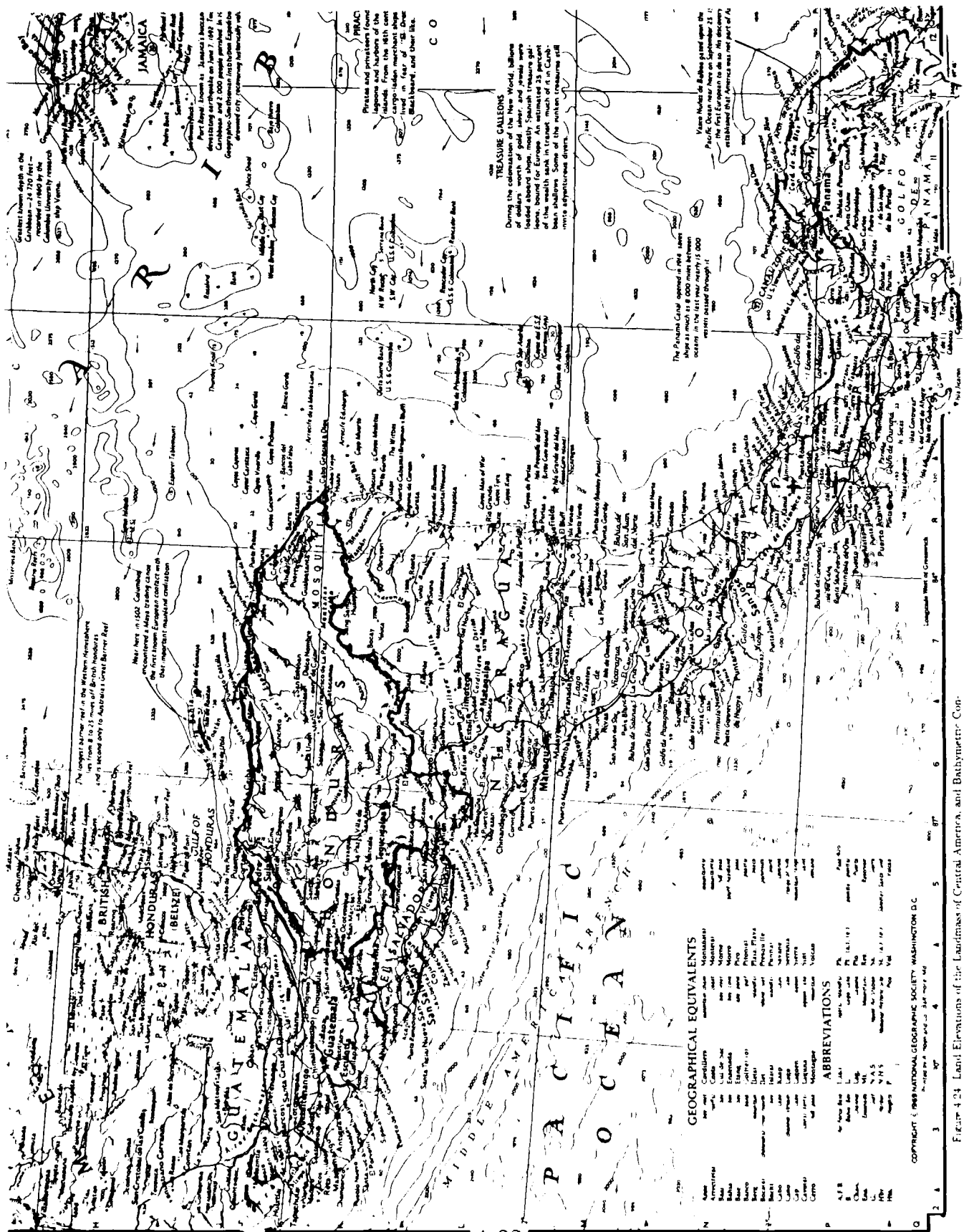


FIGURE 4-24 Land Elevations of the Landmass of Central America, and Bathymetric Contours in Fathoms of North Pacific Ocean and Caribbean Sea Adjacent to Central America, adapted from Chart of West Indies and Central America, Supplement to National Geographic, Vol. 137, No. 1, January 1970.

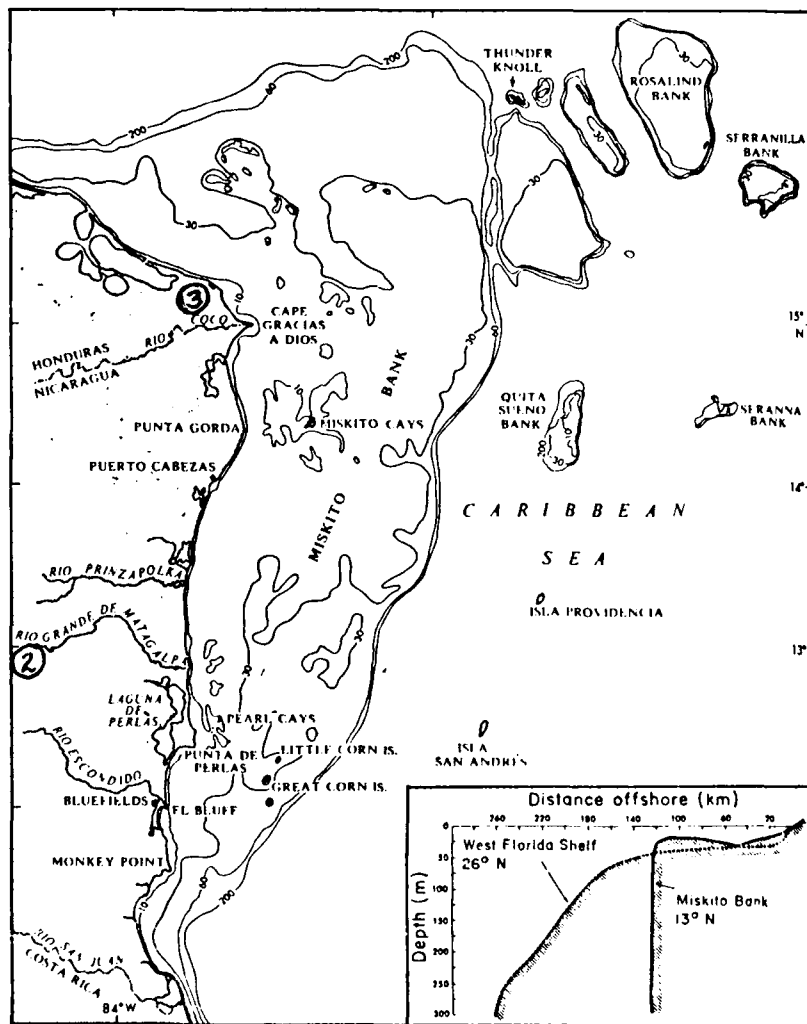
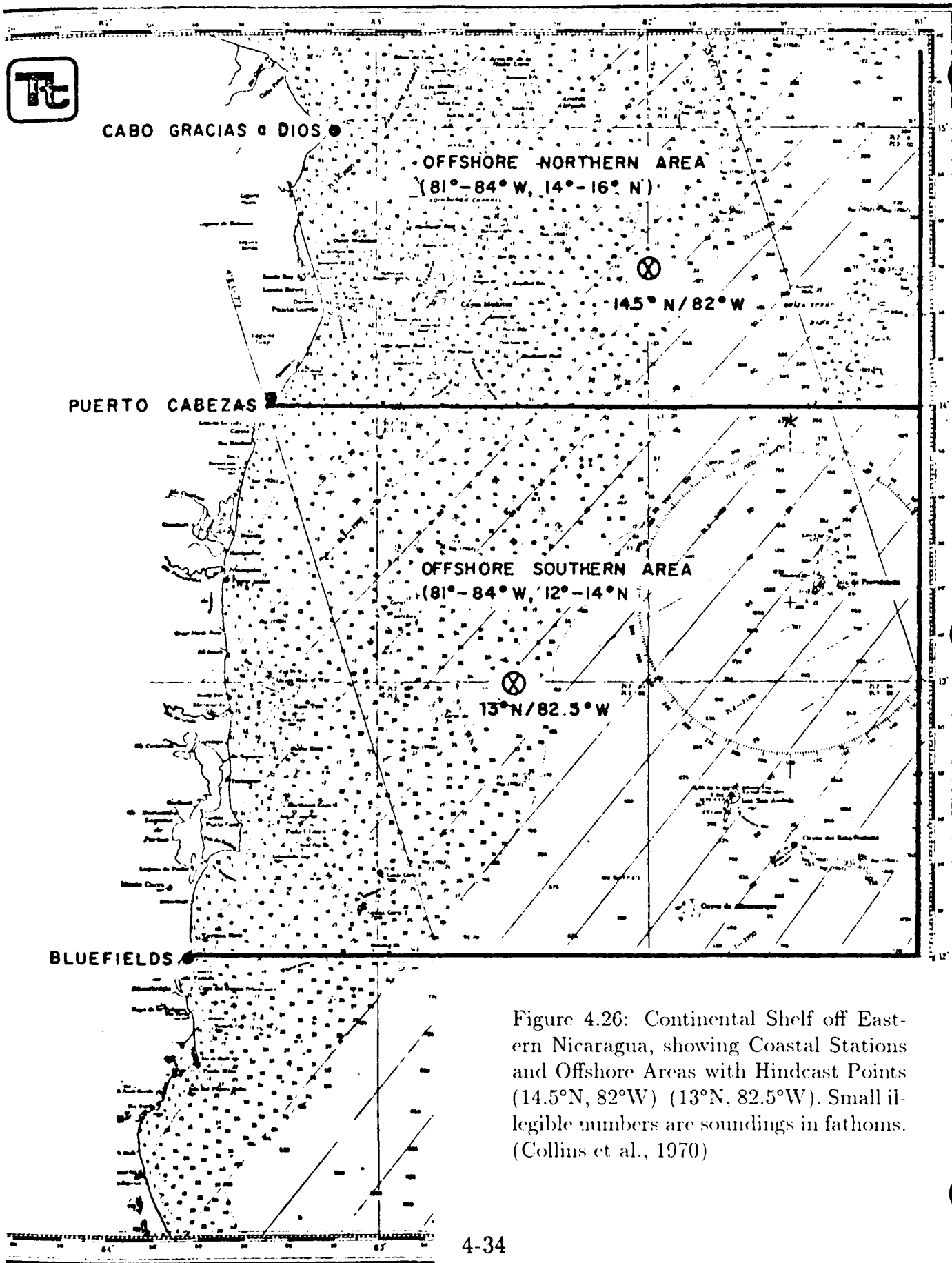


Figure 4.25: Location Map of Miskito Bank of the East Coast of Nicaragua. Inset: Comparative Bathymetric Cross-Sections across the Miskito Bank and the West Florida Shelf (Murray et al., 1982).



Caribbean Current. This upper flow through the western Caribbean Sea originates partly from the North Equatorial Current driven westward by the Northeast Tradewinds in the North Atlantic Ocean, and partly from the Guiana Current which originates in the southern hemisphere Atlantic Ocean and has been diverted northward by the land configuration of Brazil. These currents are driven through the Lesser Antilles island chain at the eastern boundary of the Caribbean, and become mixed as they move west. The main stream, according to Fairbridge (1966), flows 200 to 300 kilometers north of the Venezuela coast and crosses the Jamaica Ridge to the southwest of Jamaica, turns westward through the Cayman basin, and then northward to enter the Yucatan Strait ((H) in Fig. 4.23); the core of the flow generally follows the line of greatest depths. The flow is strong near the surface and decreases with depth; mean flow speeds are 0.7 to 0.8 kt, with maximum values up to almost 3 kt; at depths of about 1500 meters the flow diminishes to about 0.1 kt over deep basins. The transport amount is about 30 Sverdrups ($10^6 \text{ m}^3 \text{ sec}^{-1}$), or about 1/3 the amount of the Gulf Stream transport off North Carolina. Only about 1/4 of this total originates through the Windward Passage ((G) in Fig. 4.23) while the remaining 3/4 has originated in the eastern Caribbean via the Lesser Antilles. There is a small seasonal variation, with higher values in late winter, and again in early summer; this depends on seasonal strength variations in the Tradewinds.

Since free circulation in the Caribbean is restricted by the shallow Jamaica Ridge, water flow deeper than about 1500 meters is very slow and variable in direction.

Effects of the Jamaica Ridge and Miskito Bank on the surface current pattern along the Caribbean coastline of Nicaragua, Costa Rica and Panama are illustrated by the tracks of drifting buoys described in a study by Kinder (1983). Table 4.2 notes characteristics of four drifting buoys released near St. Vincent Passage in the Lesser Antilles in November 1977; these buoys were tracked by satellite for periods of four to nine months, as they were carried westward by currents through the Caribbean, Gulf of Mexico and past Florida. Figure 4.27 shows the drifter tracks; two of the drifters were caught in nearshore eddy circulations and grounded along the coasts of Panama (Drifter 1600) and Venezuela (Drifter 667). Both of these nearshore eddies showed counterclockwise circulations. Kinder indicates that such an eddy often exists in the Golfo de los Moskitos, but is not a permanent gyre.

Table 4.2: Basic Drifter Statistics (Kinder, 1983)

Buoy Identifier	667	1312	1371	1600
Launch Date	15 Nov 1977	15 Nov 1977	15 Nov 1977	12 Nov 1977
Ran Aground Date	26 Mar 1978	19 Jun 1978	15 May 1978	30 Apr 1978
Position	11°42'N,70°14'W	30°24'N,80°48'W	24°27'N,82°16'W	9°08'N,80°24'W
Last Position	29 Mar 1978	7 Jul 1978	22 Jul 1978	9 Aug 1978
Track Length Days	134	234	249	270
Kilometers	2,100	9,400	7,900	5,700

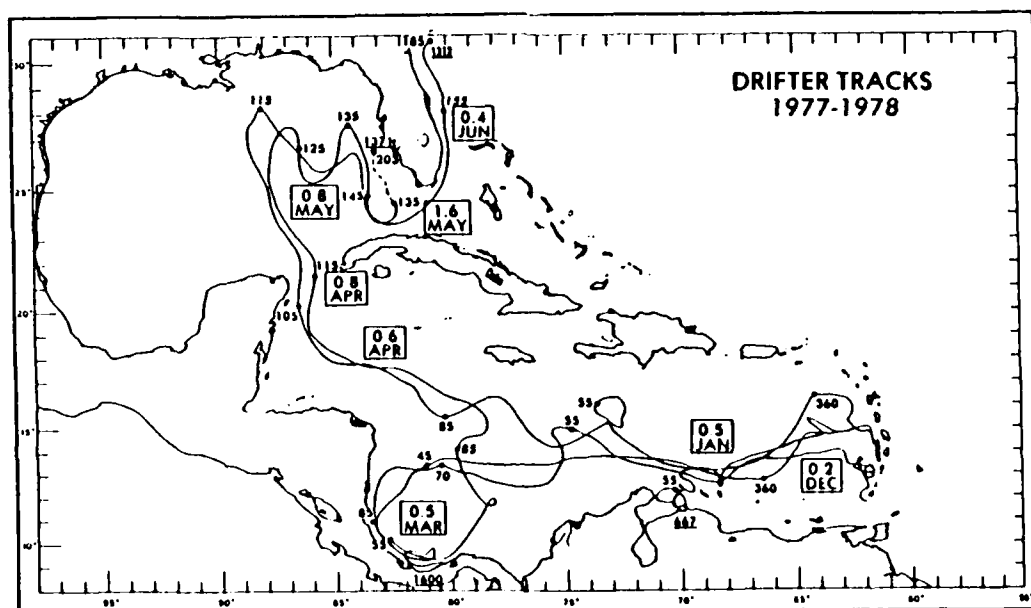


Figure 4.27: Composite of all Drifter Tracks, which show Meanders and Ed-
dies not present in Average Current Flow Charts. Boxes adjacent to drifter
tracks show typical speeds (m/sec) and time of year. Buoys are identified by
numbers near end of tracks; numbers at dots on track are Julian day 1977
or 1978 (Kinder, 1983)

Different scales of variability occur in the western Caribbean (200-500 km) compared to the east (~100 km); Kinder suggests this scale also applies to variation in direction of current flow, kinetic energy for mixing near islands, and depth of the upper mixed layer. He notes that the drifter measurements indicate there is a strong variability in space and time in the Caribbean currents. Table 4.3 indicates velocity statistics from this drifter study.

Table 4.3: Statistics from Drifter Study (Kinder, 1983)

Region	Number of Drifters	Duration (days)	Scalar Speed (m/sec)	Vector Speed (m/sec)	Direction (°True)
Columbia Basin (to 75°W)	4	21-34	0.21 to 0.64	0.20 to 0.52	246 to 276
Golfo de los Moskitos eddy	2	18-44	0.49 to 0.54	- - -	- - -
Cayman & Yucatan Basins (80-85°W)	2	11-13	0.65	0.54 to 0.59	286 to 295

The current variability is also indicated by current roses for the area 80-85°W, 10-15°N for summer and winter. See Figs. 4.28 and 4.29 from Collins et al. (1970). Nearshore off the Miskito Bank, surface current vectors are shown in Fig. 4.30 from Murray et al. (1982); they especially note the divergence zone in the vicinity of San Andres Island (Isla San Andres of Fig. 4.25), and indicate this zone probably moves north and south along this coast, seasonally. From the divergence region northward to Cape Gracias a Dios ((3) on Fig. 4.25), northward-flowing currents dominate the Bank; from the divergence zone southward to Rio Grande de Matagalpa ((2) on Fig. 4.25), currents are directed southward. Note the scale of the vectors in Fig. 4.30 is km/day.

In a study of volume flux of the coastal boundary layer (CBL) along the Nicaragua coast off Bluefields and El Bluff, Fig. 4.31 indicates the manner in which coastal flow occurs, reported by Murray et al. (1982). Such a study is of particular interest for nearshore amphibious maneuvers.

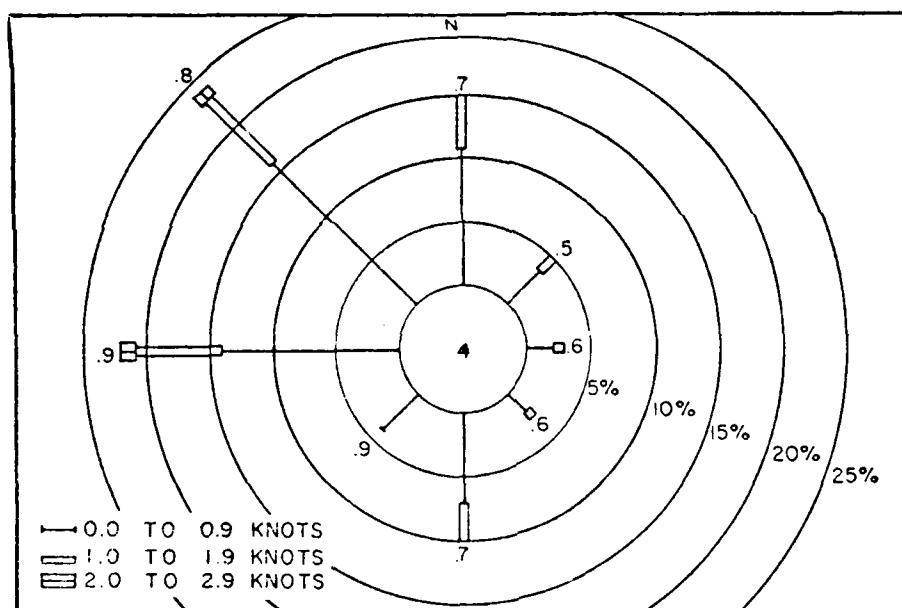


Figure 4.28: Current Rose for the Area 80-85°W, 10-15°N (Summer). These data are enlarged from original summaries given in H. O. 700 (Collins et al., 1970).

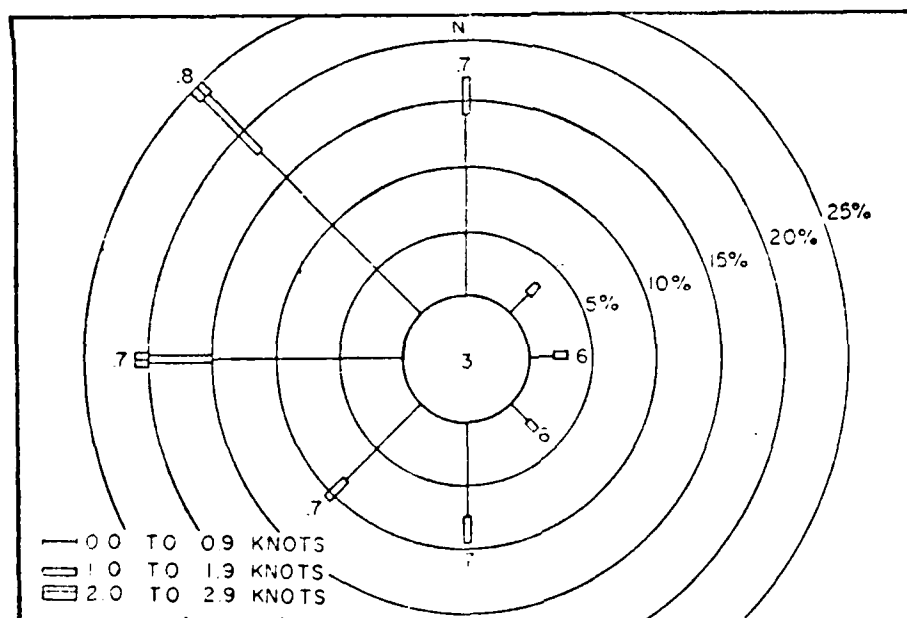


Figure 4.29: Current Rose for the Area 80-85°W, 10-15°N (Winter) (Collins et al., 1970)

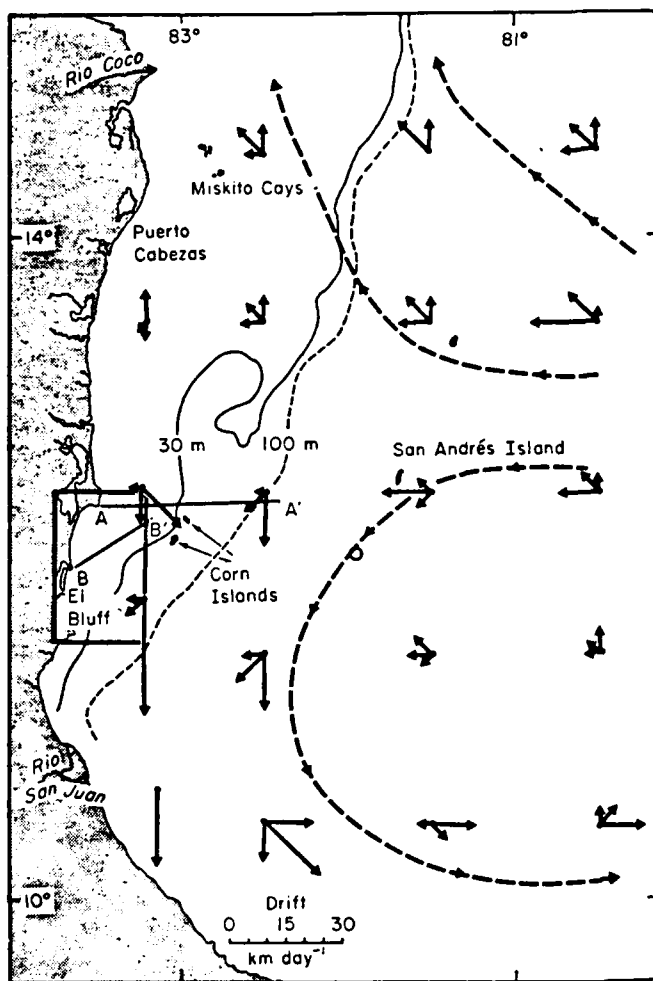


Figure 4.30: Surface Current Vectors along Miskito Bank, plotted by 1° squares from National Oceanographic Data Center data. The rectangle outlined shows the site of a detailed study whose results are shown in adjacent Fig. 4.31. (Also see Figs. 4.35 and 4.41.) (Murray et al., 1982)

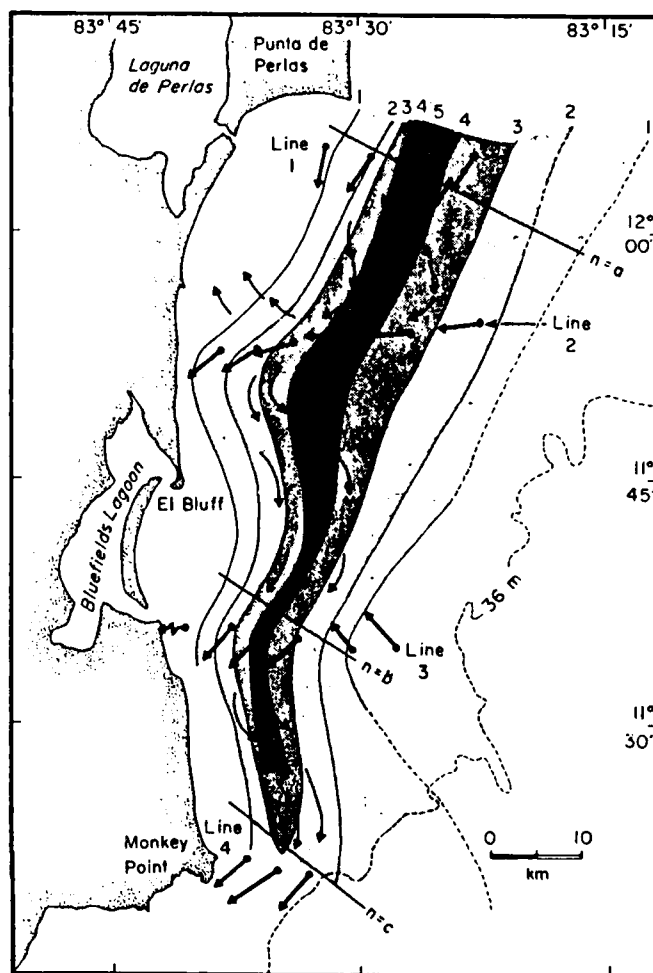


Figure 4.31: Volume Flux Magnitude in the Coastal Boundary Layer in $(\text{m}^3\text{sec}^{-1})\text{m}^{-1}$. Heavy vectors show direction of flux at each observed station; light arrows interpolate flux direction between stations. Dashed contours are estimated from earlier observations (Murray et al., 1982).

Temperature Variation in the Vertical Direction in the Caribbean Sea. Gordon (1966) describes this vertical temperature distribution as tropical, with warm surface temperatures (as were illustrated in the earlier discussion on page 4-9) extending through the mixed layer to the top of a well-developed thermocline (100–200 meters depth) that hinders vertical mixing, and confines surface heating to the upper water layers near the surface. This is illustrated by the vertical temperature cross-section in the Colombian Basin (see Fig. 4.32), which shows a pronounced temperature gradient in the thermocline between the depths of 100 and 1000 meters. Below 1000 meters the gradient weakens greatly, and below 1500 meters the temperature of the Basin water is about 4°C, varying little from one basin to another in the Caribbean. While very little seasonal variation occurs near the surface, no seasonal variation at all occurs below 150 meters.

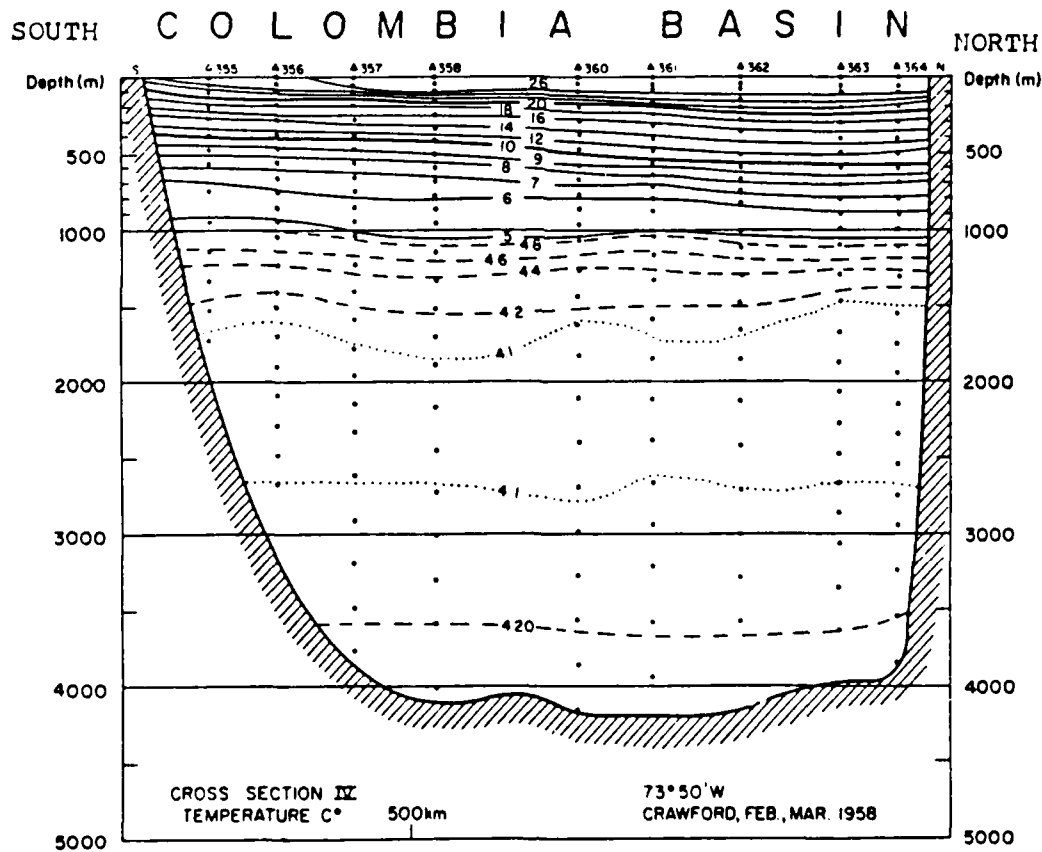


Figure 4.32: Temperature Distribution in the Colombian Basin of the Caribbean Sea (Gordon, 1966)

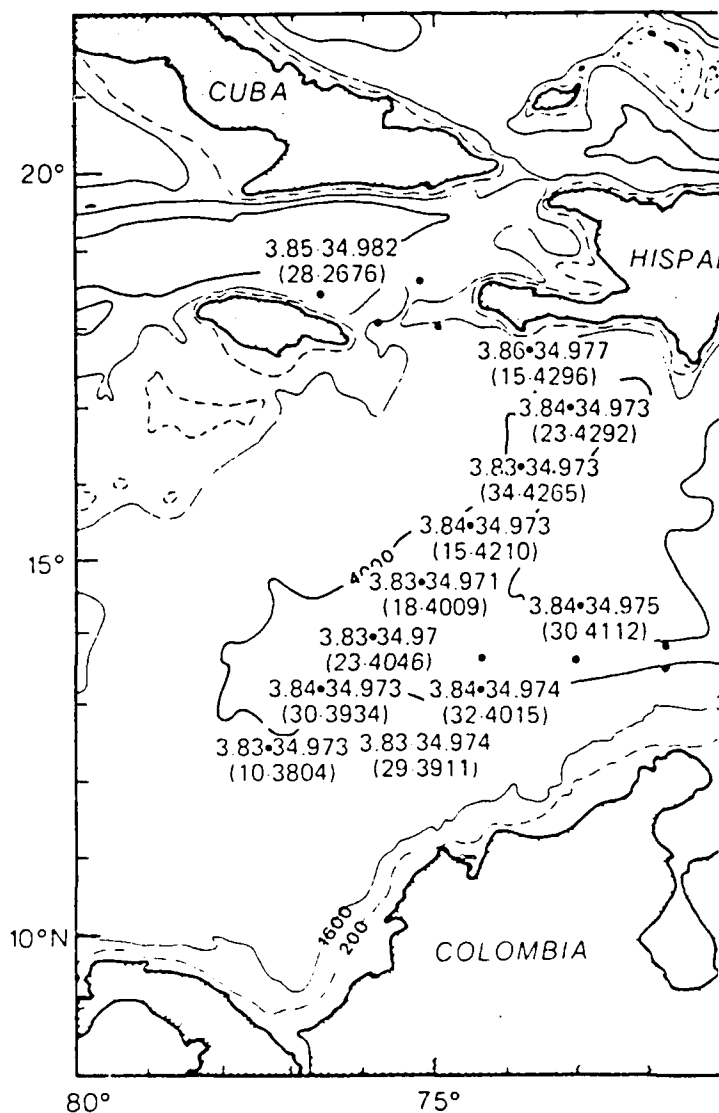


Figure 4.33: Bottom Potential Temperature ($^{\circ}\text{C}$) and Salinity (‰) in Colombian Basin; data from cruise CARO-I, during the fall of 1973 (adapted from Morrison and Nowlin, 1982)

Bottom water potential temperatures (i.e., the temperature the water would have at the sea surface, with pressure effects, due to the great depths, removed) and salinities for the Colombian Basin are shown in Fig. 4.33, adapted from Morrison and Nowlin (1982). In very deep ocean basins, potential temperature usually replaces temperature in oceanographic observational studies. The depth of the bottom, and the distance above that depth for the observation (displayed in reverse order, in meters) are shown, where the measurements were made.

In Fig. 4.34 Murray et al. (1982) show the temperature and salinity variations which may occur between the deep basins and coastline, over the shallow shelf of Miskito Bank; this cross-section location is along the line A-A' in the northern part of the inset of Fig 4.30, north of Corn Islands. Temperatures are contoured for each 0.1°C and show the strongest gradient (about 1°C change) at the outer edge of the Bank.

Salinity variations occur very close to the coastline, with fresher water salinities being replaced with oceanic values (35‰ and above) where the flatter shelf "floor" begins. Pools of higher and lower salinities (varying by 0.5‰) occur on the shelf, and this occurrence probably is variable with time. Salinity values of 36.0‰ and above are present at the shelf edge and at greater depths.

The strong gradient in both temperature and salinity about 12 kilometers offshore marks the seaward edge of the Coastal Boundary Layer, flowing southward, shown earlier in Fig. 4.31.

Salinity in the Caribbean Sea Adjacent to Central America. Gordon (1966) notes the surface salinity is affected by evaporation, precipitation, runoff from land and advection by currents. Upwelling also brings higher salinity values to the surface from deeper, saltier layers in certain regions along the coast. In the northern half of the Caribbean, values decrease to less than 35.5‰. Salinity values are highest in the western basins of the Caribbean, however, just south of Cuba (>36.0‰), decreasing toward the southwest and reaching <35.5‰ at the coast of Honduras.

Higher precipitation values and land runoff in the summer can cause lower surface salinities; values in the north diminish by 1‰ then, and are about 0.5‰ lower in the southern Caribbean. Values are not well observed in the far western Caribbean, requiring extrapolation of the values observed further east into this region.

The vertical distribution of salinity varies substantially between the surface and 1000 meters depth; this is illustrated in Fig. 4.35, which shows the vertical distribution of salinity in the western Colombian Basin and in the Yucatan Basin. In Fig. 4.35 (adapted from Gordon, 1966) a water layer with a salinity maximum is associated with the bottom of the upper mixed layer, the dominant feature of the Subtropical Underwater. The horizontal distribution of the maximum salinity values in this layer is shown in Fig. 4.36, with particular seasonal values for Fall 1973 and Winter 1972 shown in Figs. 4.37 and 4.38, adapted from Morrison and Nowlin (1982). Salinity values are lower in the Colombian Basin and westward; higher salinity values associated with the flow through the Lesser Antilles from the Atlantic Ocean into the Caribbean, become diluted somewhat as the upper flow proceeds westward. Higher values are carried closer to the coastline along the Colombian Basin, compared to those observed off the Cayman and Yucatan Basin coastlines further northwest (see Fig. 4.36). Figures 4.37 and 4.38 for Winter 1972 and Fall 1973 illustrate that some variation occurs over the central Colombian Basin and the eastern Jamaica Ridge regions (the western extent of data).

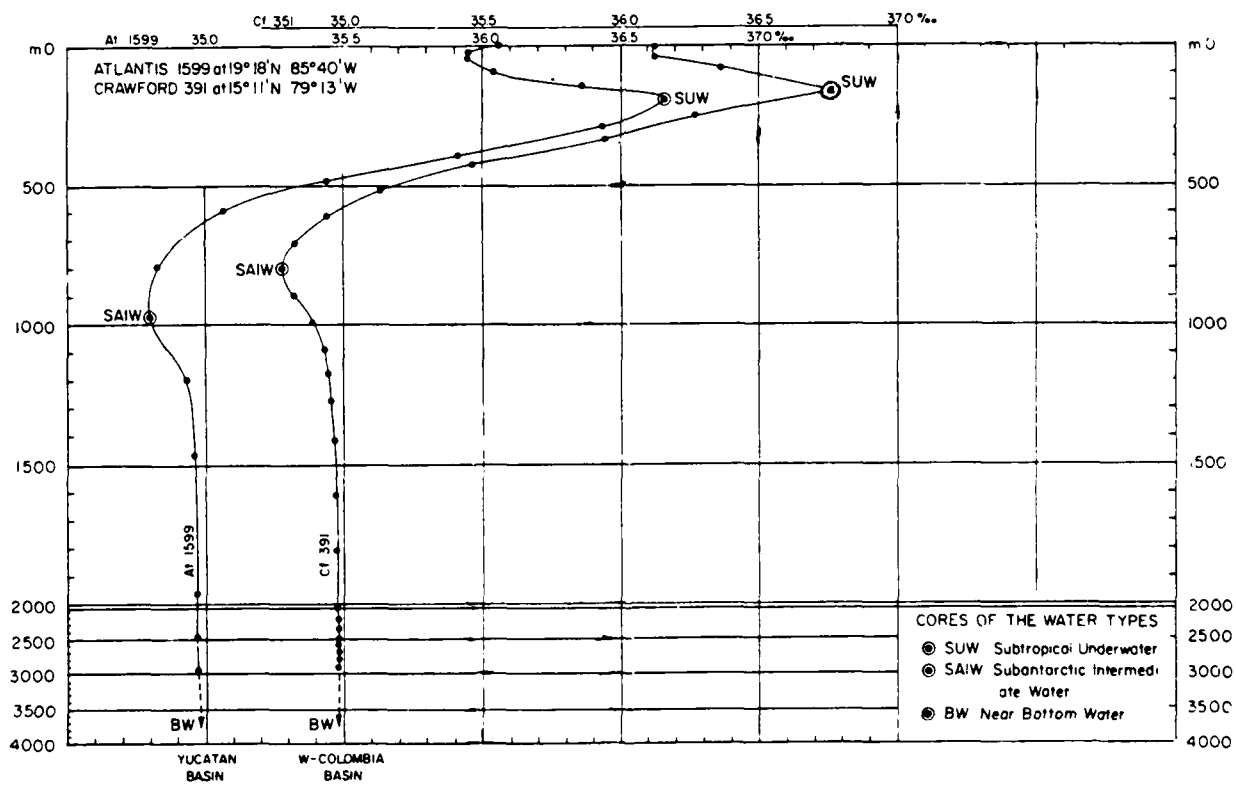


Figure 4.35: Vertical Distribution of Salinity in the Western Colombian Basin and Yucatan Basin, with Water Types indicated (adapted from Gordon, 1966)

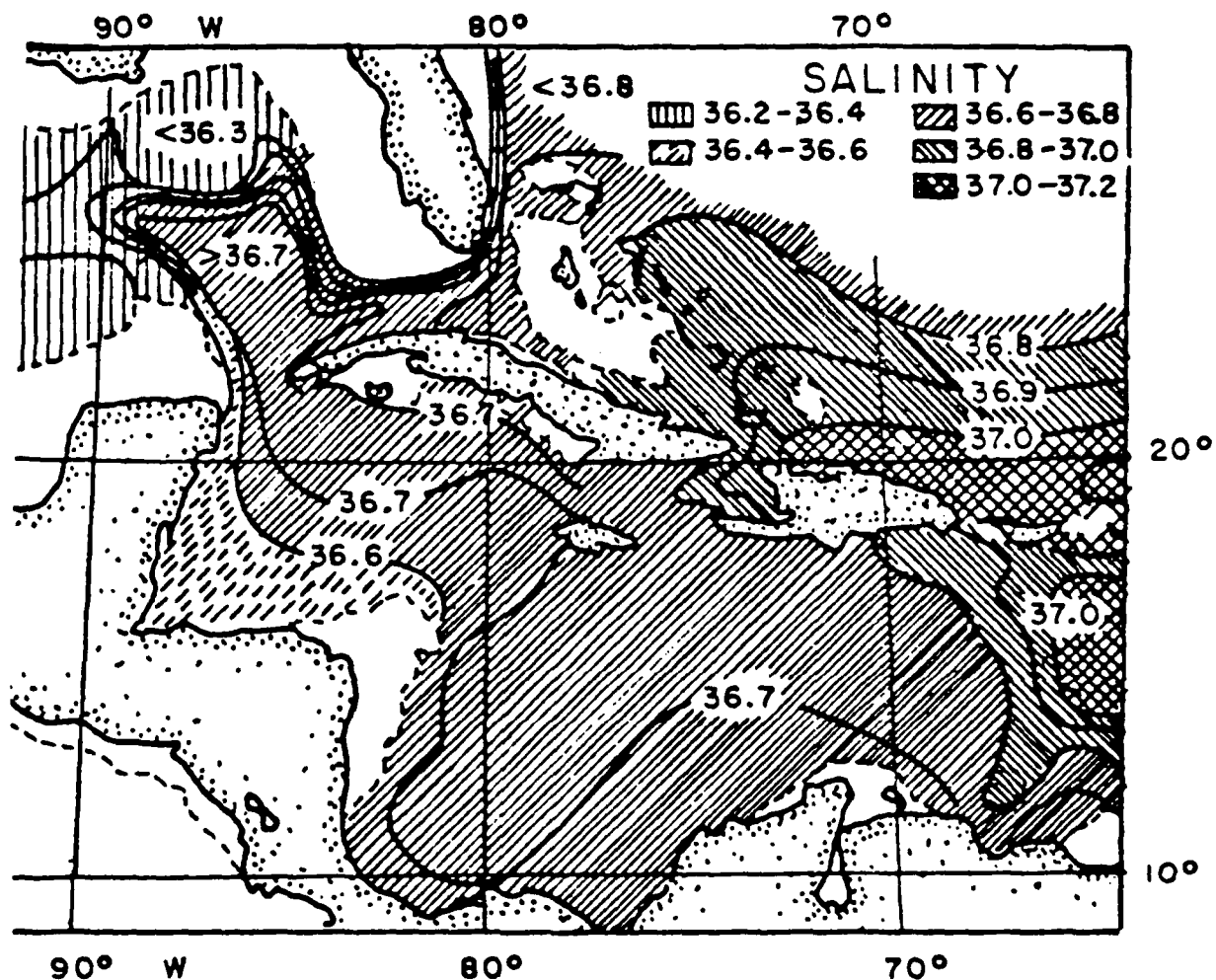


Figure 4.36: Salinity Distribution in the Core of the Subtropical Underwater Layer (according to Dietrich; after Defant, 1961 (adapted from Harding and Nowlin, 1966))

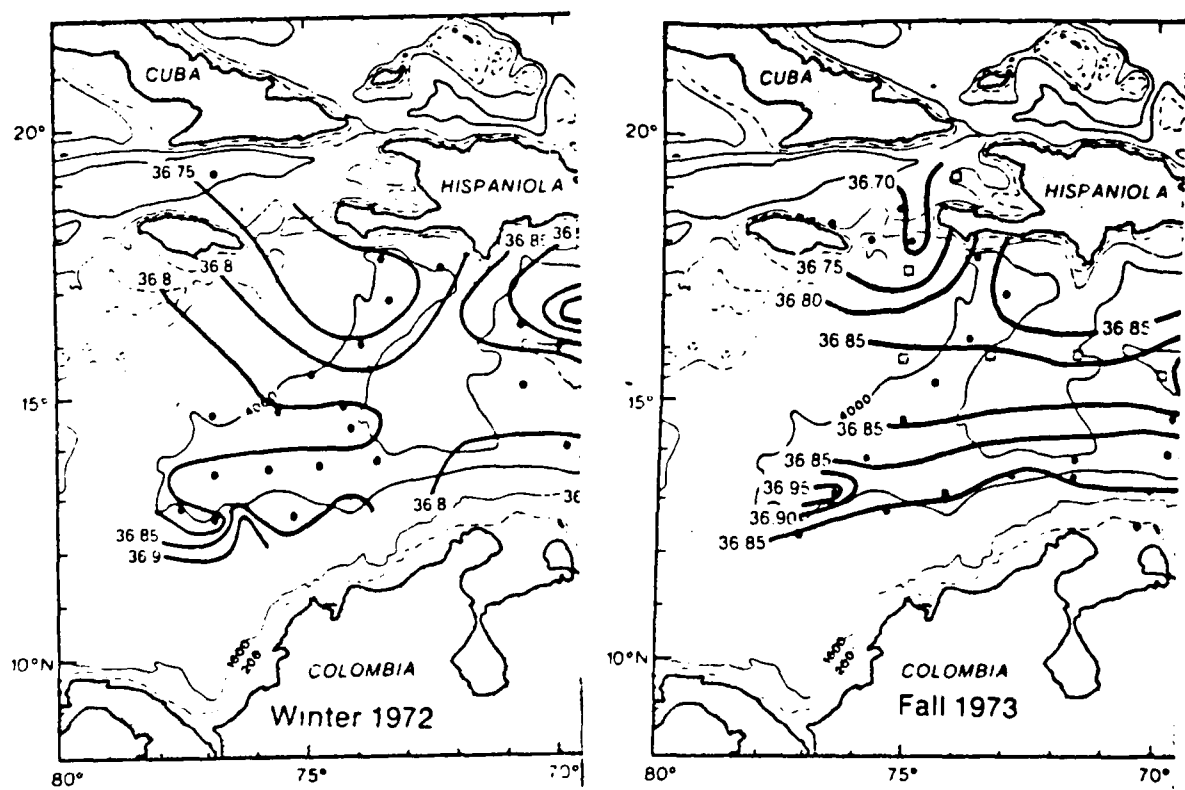


Figure 4.37: Salinity Values (‰) at Depth of 150-250 Meters in Subtropical Underwater over Colombian Basin and Eastern Jamaica Ridge for Winter 1972 (data from Kane 8287) and Fall 1973 (data from CARO-I, dots; Atlantis II-078, squares); (adapted from Morrison and Nowlin, 1982).

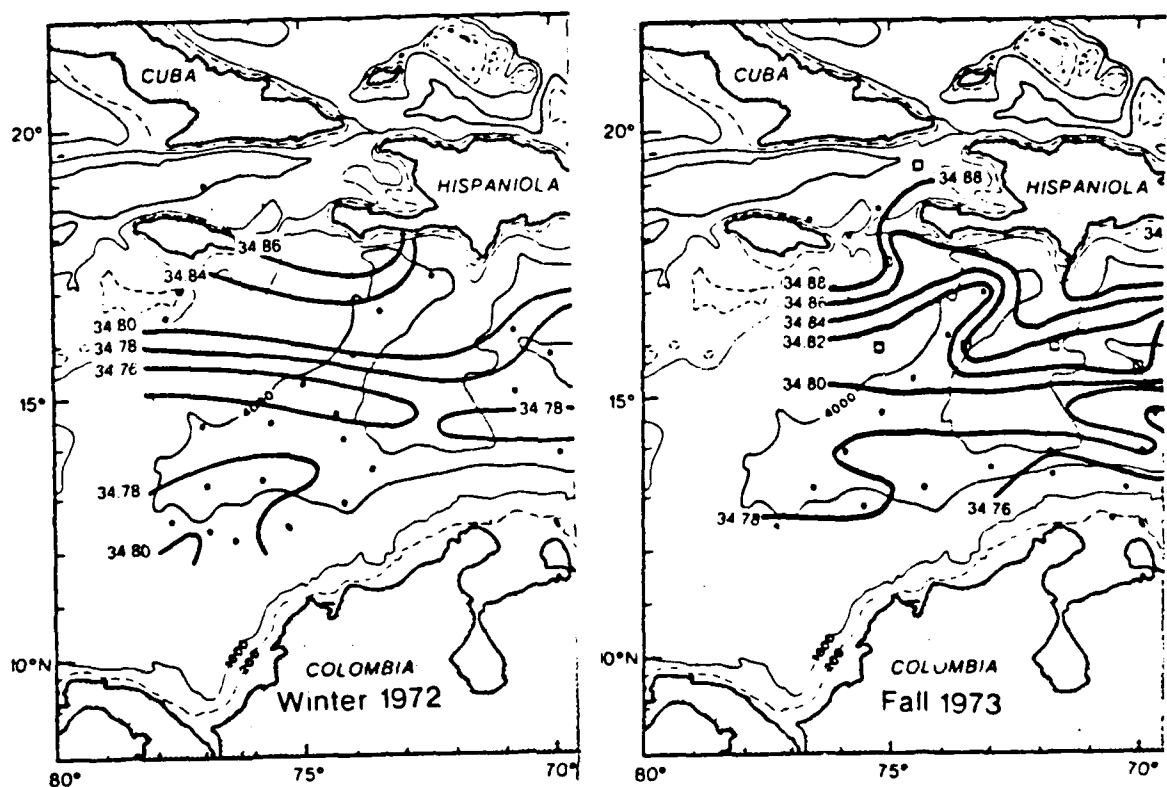
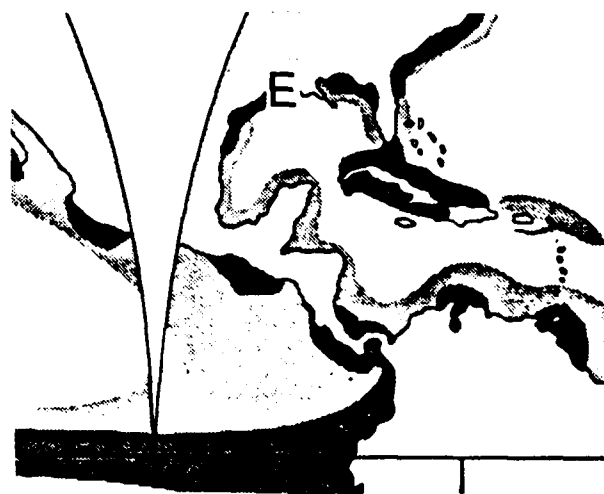


Figure 4.38: Salinity Values (‰) at Depth of 600-900 Meters in Antarctic Intermediate Water over Colombian Basin and Eastern Jamaica Ridge for Winter 1972 (data from Kane 8287) and Fall 1973 (observations: dots, CARO-I; squares, Atlantis II-078);(adapted from Morrison and Nowlin, 1982).

Corredor (1979) notes that the upwelling observed off the northwest coast of South America brings the high salinity Subtropical Underwater to the surface from its usual depth of 50–150 meters. The Subtropical Underwater originates in the surface layer of the North Atlantic Ocean, where inorganic nutrient content is low; the upwelling observed in the southern Caribbean also shows nutrient levels that are low. These nutrients do stimulate growth of phytoplankton in the upwelled water, but the growth rates are much less (about 1/5) than those in the upwelling areas along the Pacific coasts of California or Peru. This limited amount of inorganic nutrients is shown to play a major role in the dynamics of phytoplankton growth here, which contrasts with conditions in other upwelling regions of the world. Underwater visibility is limited, especially in regions of high marine life productivity; also sonar propagation may be affected adversely there.

Upwelling regions in the Caribbean and those in the Pacific coastal areas near Central America are shown in Fig. 4.39, from Issacs (1969). Light grey areas indicate upwelling with moderate marine life productivity; dark grey shading shows high productivity. Note the dark grey areas occur, in addition to the northwestern South American area, off the Costa Rica and Panama coasts of the Caribbean and of the Pacific; and also along the coast of Cuba in the Caribbean, and the Guatemalan coast in the Pacific Ocean.

Figure 4.39: Upwelling Areas of the Caribbean Sea and the eastern North Pacific Ocean; light grey shading and dark grey shading indicate regions of moderate and high marine productivity, respectively (adapted from Issacs, 1969). (Ignore the white "wedge", which refers to the original text of Issacs, 1969.)



The Subantarctic Intermediate Water is identified primarily on the basis of its salinity minimum, occurring in the layer 600–900 meters below the sea surface. This layer is shown in Fig. 4.40 (a South-North cross-section across the Columbian Basin) as the deeper hatched region with salinity values less than 34.8‰. (The upper hatched region indicates the location there of the Subtropical Underwater, with salinity values greater than 36.5‰ in that near-surface layer.) In Fig. 4.38 Morrison and Nowlin (1982) illustrate seasonal differences which can occur in the salinity values of the Antarctic Intermediate Water layer; horizontal distribution of values for the Columbian Basin and eastern Jamaica Ridge are shown for Winter 1972 and Fall 1973. Those authors indicate this water flows into the western Caribbean from the Atlantic Ocean primarily through the Windward Passage, similar to the flow described later for the deeper water in those Basins.

Below 1000 meters, the salinity values increase slightly through the local deep water to values that remain below 35.0‰ at greatest depths (see the bottom water salinity values in Fig. 4.40). Morrison and Nowlin indicate waters in the Columbian, Yucatan and Cayman Basins deeper than 1500 meters originated primarily in the Atlantic Ocean near Cuba and Hispaniola, and flow into the eastern Cayman Basin through the Windward Passage between those islands. From there, they spread southward into the Columbian Basin across the deeper openings in the Jamaica Ridge between Jamaica and Hispaniola; they also spread into the western Cayman Basin and then northward into the Yucatan Basin.

A second section crossing the Miskito Bank is shown along line B-B' of the inset region of Fig. 4.30, in a northeast direction from El Bluff; the salinity gradients of this section are shown in Fig. 4.41. The strong Coastal Boundary Layer is directed southward in the upper, near-coast region. Calculations of Murray et al. (1982) indicate this Coastal Boundary Layer is a mixture of 22% freshwater and 78% shelf water; the shelf water, in turn, is composed of 95% offshore water, and only 5% Coastal Boundary Layer water. Despite such a small contribution to the shelf water, this Coastal Boundary Layer is very high in energy and in turbidity. It is confined to within 20 kilometers of the coast; it is strongly associated with the zone of strong salinity gradients; and the 35.5‰ salinity contour appears to distinguish the region of fast-moving (toward the southwest) Coastal Boundary Layer water from the slowly-moving (northward) shelf water.

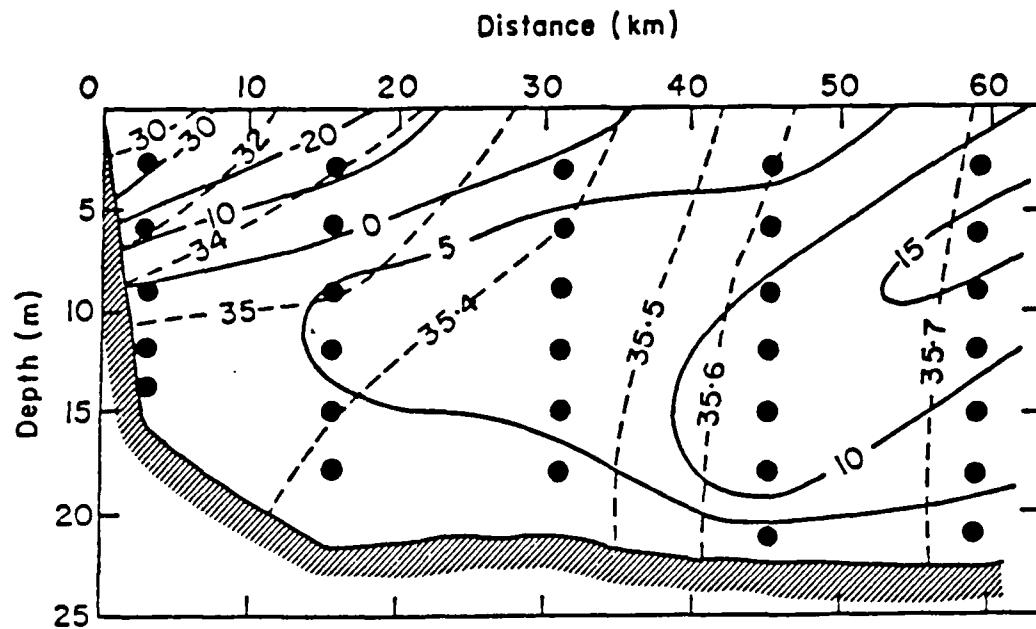


Figure 4.41: Salinity and Current Speed Cross-Section on Miskito Bank off the Nicaraguan Coastline, along Line B-B' as shown in the Inset of Fig. 4.30, extending northeast from El Bluff (Murray et al., 1982). Salinity (‰), dashed lines; Speed (cm/sec), solid contours.

Table 4.4: Water Masses of the Caribbean Sea, with Identifying Properties (Morrison and Nowlin, 1982)

Water Mass	Primary Identifying Feature	Approximate Depth Range (m)
Subtropical Underwater	Salinity Maximum	150-250
18°C Sargasso Sea Water	Oxygen Maximum (~18°C Temperature)	200-400
Tropical Atlantic Central Water	Oxygen Minimum	400-700
Antarctic Intermediate Water	Salinity Minimum	600-900
Upper North Atlantic Deep Water	Salinity Maximum	1100-1600
Lower North Atlantic Deep Water	Oxygen Maximum	2000

Water Masses in the Caribbean Sea. The use of salinity extremes within a vertical sounding has identified several of the water masses found in the Caribbean Sea, the discussion on salinity includes the Subtropical Underwater and Antarctic Intermediate Water, each marked by an extreme salinity value.

Oxygen values as they vary in the vertical direction are used to identify three additional water mass layers of the Caribbean: the 18°C Sargasso Sea Water; the Tropical Atlantic Central Water; and the Lower North Atlantic Deep Water (see Table 4.4). Distribution of oxygen values in the horizontal direction is used to indicate the flow pattern of deeper, slow-moving water mass layers. Horizontal distribution charts for two of these water masses are shown for the Columbian Basin during the Fall of 1973 (from Morrison and Nowlin, 1982). Oxygen values for the 18°C Sargasso Sea Water represent maximum values in the vertical water column that occur at depths of 200–400 meters, shown in Fig. 4.42; these values range from 3.6 to 4.2 milliliters/liter (ml/l). A similar distribution chart shows the low oxygen values of the Tropical Atlantic Central Water, at depths of 400–700 meters; these values range from 2.9 to 3.0 ml/l, shown in Fig. 4.43. The distribution of oxygen values for the Lower Deep North Atlantic Water, at about 2000 meters depth, shows that this water probably enters the Caribbean Sea through the Windward Passage; see Fig. 4.44, from Gordon (1966). Values exceed 6.0 ml/l in the Cayman and Yucatan Basins, diminishing to 4.7 ml/l in the southern Columbian Basin off Panama. This Deep Water flow appears to enter the Columbian Basin over the sill in the Jamaica Ridge between Jamaica and Hispaniola.

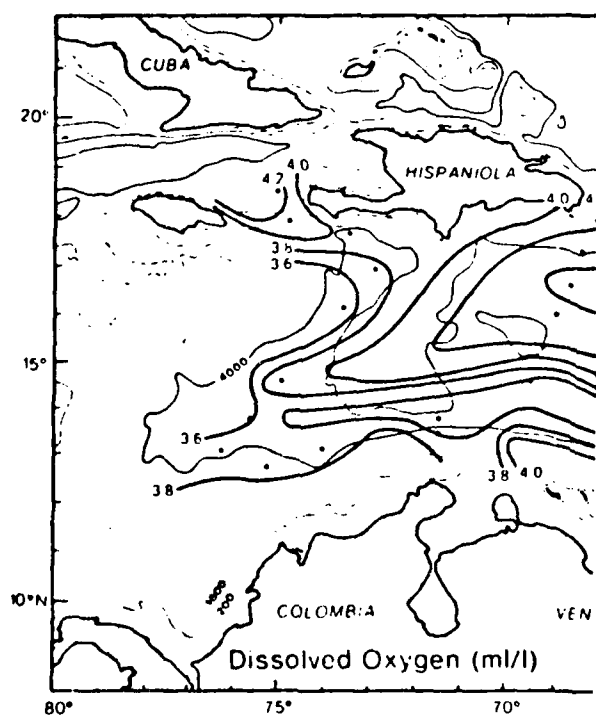


Figure 4.42: Distribution of Dissolved Oxygen in 18° Sargasso Sea Water at Depths of 200-400 m; data are from CARO-I during Fall 1973 (adapted from Morrison and Nowlin, 1982).

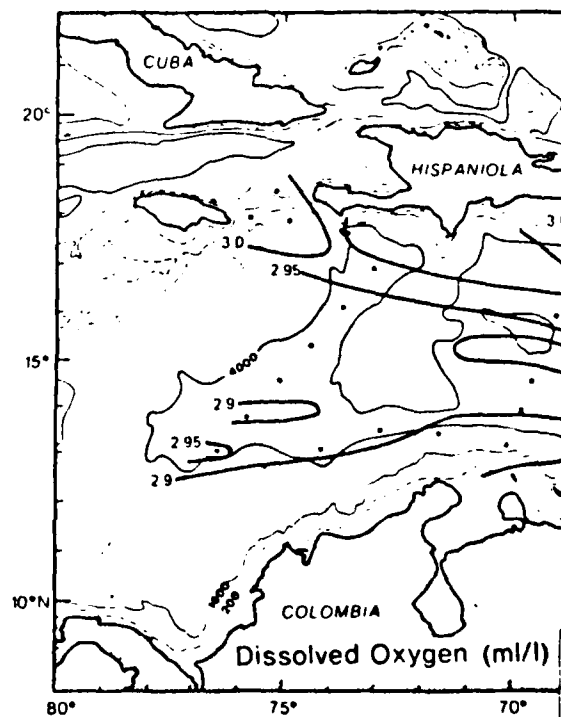


Figure 4.43: Distribution of Dissolved Oxygen in Tropical North Atlantic Central Water at Depths of 400-700 m; data are from CARO-I, Fall 1973 (adapted from Morrison and Nowlin, 1982).

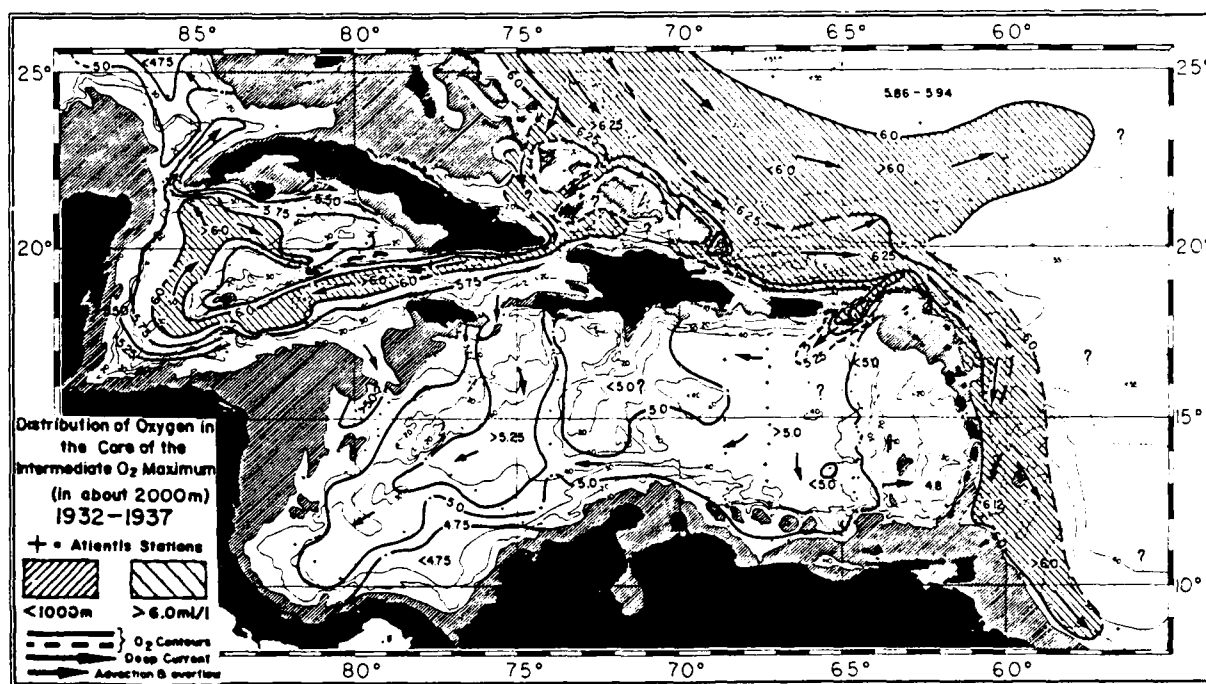


Figure 4.44: Distribution of Dissolved Oxygen (ml/l) in the Lower Deep North Atlantic Water at about 2000 meters depth for the Caribbean Sea (Gordon, 1966)

Waves Near the Caribbean Coastline of Central America. Collins et al. (1970) have summarized wave data made available from the National Climatic Data Center for the region 10-15°N, 80-85°W in the west Columbian Basin. Fig 4.45 is a brief summary of wave heights observed throughout the year; statistics presented are the percentage of time the observed wave heights lie below the stated values, averaged for months in the year. This summary is based on wave and wind data obtained from ship reports; since ships usually avoid storms if possible, these data are biased toward low values of wave heights and wind speeds. Thus percentages greater than 95% should be viewed with caution (and percentages greater than 99% are not shown). For more extreme values, wave heights based on storm data, as presented in a later section, should be used.

Tables showing wave height by direction, and wave height for wave period, are given for the months of January, April, July and October in Tables 4.5 through 4.6. Values in these Tables show the percentage of time wave observations occur in the various wave height/direction or wave height/period categories during normal (non-storm) conditions.

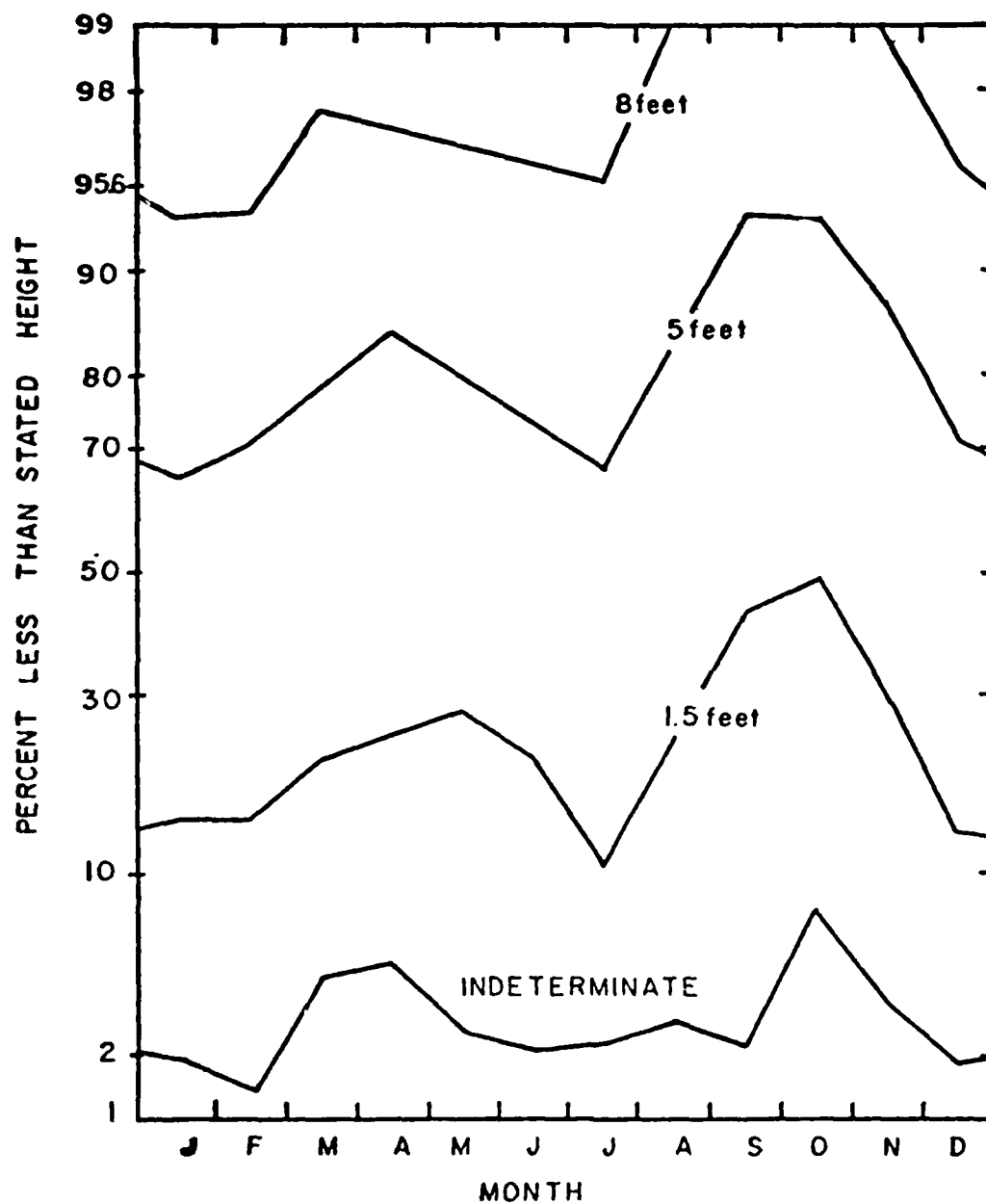


Figure 4.45: Wave Height Summary for Region 10-15°N, 80-85°W (Collins et al., 1970)

Table 4.5: Wave Height versus Direction during normal (non-storm) conditions for region 10-15°N, 80-85°W for indicated months (Collins et al., 1970)

Height	<1.5	1.5-5.0	5-8	8-11	11-14	>14	Ind.	Total
Direction								
N	2.2	8.6	2.8	0.9	0.1	0	0.1	14.7
NE	4.5	22.4	12.9	2.8	0.6	0	0.2	43.4
E	3.9	18.6	12.3	2.1	0.2	0	0.6	37.7
SE	0.6	0.7						1.3
S	0.5	0.3						0.8
SW								
W	0.1	0.1						0.2
NW	0.5	0.2	0.1	0.1				0.9
Calm	0.6							0.6
Indeterm.	0.2		0.1				0.1	0.4
Total	13.1	50.9	28.2	5.9	0.9	0	1.0	100.0

JANUARY

Height	<1.5	1.5-5.0	5-8	8-11	11-14	>14	Ind.	Total
Direction								
N	2.5	6.0	1.3	0.4	0	0.1	0.3	10.6
NE	5.3	24.3	6.1	0.7	0	0	0.9	37.3
E	10.3	25.9	4.8	1.1	0.1	0	0.5	42.7
SE	2.2	2.9	0.7					5.8
S	0.4	0.8				0.1		1.3
SW	0.1	0.1				0.1		0.3
W						0.1		0.1
NW	0.1	0.1						0.2
Calm	1.2						0.1	1.3
Indeterm.		0.3					0.1	0.4
Total	22.1	60.4	12.9	2.2	0.1	0.4	1.9	100.0

APRIL

Height	<1.5	1.5-5.0	5-8	8-11	11-14	>14	Ind.	Total
Direction								
N	0.6	1.4	0.7				0.2	2.9
NE	2.5	16.6	7.6	0.7		0.1	0.4	27.9
E	4.2	36.8	19.0	3.6	0.3		0.3	64.2
SE	0.2	1.7	0.4	0.2				2.5
S		0.2				0.1		0.3
SW	0.1							0.1
W	0.2							0.2
NW	0.1	0.5	0.3			0.1		1.0
Calm	0.8							0.8
Indeterm.					0.1			0.1
Total	8.7	57.2	28.0	4.5	0.4	0.3	0.9	100.0

JULY

Height	<1.5	1.5-5.0	5-8	8-11	11-14	>14	Ind.	Total
Direction								
N	4.5	3.6	0.7		0.1		0.7	9.6
NE	11.7	12.7	1.5	0.1			0.5	26.5
E	13.4	17.9	2.6	0.1			0.4	34.4
SE	2.6	3.1	0.3				0.1	6.1
S	2.5	2.1	0.1				0.2	4.9
SW	1.4	1.3	0.1				0.1	2.9
W	2.1	2.7	0.4		0.1		0.1	5.4
NW	2.1	2.1	0.4				0.1	4.7
Calm	4.2						0.1	4.3
Indeterm.	0.5	0.2	0.1				0.4	1.2
Total	45.0	45.7	6.2	0.2	0.2		2.7	100.0

OCTOBER

Table 4.6: Wave Height versus Wave Period during normal (non-storm) conditions for region 10-15°N, 80-85°W for indicated months (Collins, et al., 1970)

Period	<5	5-7	7-9	9-11	11-13	13-15	>15	Ind	Total
Height									
<1.5	8.7	1.1	0.3		0.2	0.2	0.9	1.4	12.8
1.5-5	19.0	24.0	6.0	0.9	0.1		0.5	0.6	51.1
5-8	3.1	13.4	8.3	2.7	0.2	0.2		0.4	28.3
8-11	1.3	2.0	0.9	1.2	0.1			0.1	5.6
11-14	0.1	0.2	0.4	0.2					0.9
>14									
Indeterm.	0.1		0.1					1.1	1.3
Total	32.3	40.7	16.0	5.0	0.6	0.4	1.4	3.6	100.0

JANUARY

Period	<5	5-7	7-9	9-11	11-13	13-15	>15	Ind	Total
Height									
<1.5	16.7	1.5	0.4	0.1			2.2	1.1	22.0
1.5-5	28.6	23.6	3.6	1.7	0.1		0.1	2.1	59.8
5-8	0.5	6.4	4.7	0.8	0.5				12.9
8-11	0.3	0.5	0.6	0.4	0.3				2.1
11-14				0.1					0.1
>14	0.2	0.2							0.4
Indeterm.		0.4	0.1				0.4	1.8	2.7
Total	46.3	32.6	9.4	3.1	0.9		2.7	5.0	100.0

APRIL

Period	<5	5-7	7-9	9-11	11-13	13-15	>15	Ind	Total
Height									
<1.5	6.0	0.8	0.2				0.6	1.1	8.7
1.5-5	19.9	29.2	5.2	1.9		0.4	0.2	0.4	57.2
5-8	2.4	12.9	8.9	2.8	0.7	0.1		0.3	28.1
8-11	0.5	1.2	1.2	1.0	0.5				4.4
11-14					0.1	0.2			0.3
>14		0.1		0.1			0.1		0.3
Indeterm.		0.1				0.1		0.8	1.0
Total	28.8	44.3	15.5	5.8	1.3	0.8	0.9	2.6	100.0

JULY

Period	<5	5-7	7-9	9-11	11-13	13-15	>15	Ind	Total
Height									
<1.5	30.1	4.7	0.4	0.5	0.1		2.5	6.0	44.3
1.5-5	21.1	19.2	3.5	0.7	0.1		0.2	0.9	45.7
5-8	1.0	1.7	1.1	1.8	0.5				6.1
8-11		0.1		0.1					0.2
11-14			0.2						0.2
>14									
Indeterm.	0.5		0.1					2.9	3.5
Total	52.7	25.7	5.3	3.1	0.7		2.7	9.8	100.0

OCTOBER

Wave Heights and Frequency of Occurrence for Storm Conditions. In the western Caribbean Sea two types of storm conditions may generate waves with heights substantially greater than normal: 1) the intrusion of middle-latitude storm conditions into the region during winter as "northers"; and 2) the occasional intrusion of tropical storms and hurricanes during the North Atlantic hurricane season from June through November.

During northers, the occurrence of high winds is less frequent than with hurricanes; however, the fetches over which they blow are larger, and substantial wave heights can be generated, even though the wave development is generally fetch-limited. Occasionally the fetch does not reach the shoreline, so waves arrive as swell; however, this is usually not the case. Fig 4.46 from Collins et al. (1970) shows significant wave height versus return period (maximum value expected in that number of years) for northers that affect the east coast of Nicaragua. The sea conditions should last for several hours in a typical norther. Maximum wave height expected is the significant wave height multiplied by a factor of 1.86.

Hurricanes and tropical storms may either pass near the coastline (usually to the north, or offshore to the east), or they may be traveling from east to west and cross the coastline. Major occurrences in both categories during this century were used by Collins et al. (1970) along with standard hindcast models for wind fields to generate wave fields; results were then interpolated for the two hindcast points (14.5°N, 82°W; and 13°N, 82.5°W) shown on Fig. 4.26 of the continental shelf of Nicaragua. Results are shown in Fig. 4.46; the significant wave height versus return period is shown for the ten significant hurricanes and tropical storms at each hindcast point. Data are summarized for all storms (including northers) at one location and compared with values for northers alone; only slight differences occur, for all storm conditions, at the second hindcast point (not shown). Table 4.7 from Collins et al. (1970) shows the greatest values for significant wave height (H_s) and wave period (T_s) that occur with hurricane wind speed (V) for the two hindcast points in 20 years and 100 years (return periods).

Table 4.7: Significant Waves for 20-Year and 100-Year Return Period (Collins et al., 1970)

Return Period years	14.5°N, 82.0°W			13.0°N, 82.5°W		
	H_s , ft	T_s , sec	V , kt	H_s , ft	T_s , sec	V , kt
20	30.0	12.0	100	26.4	11.0	90
100	50.0	14.5	120	46.0	14.2	120

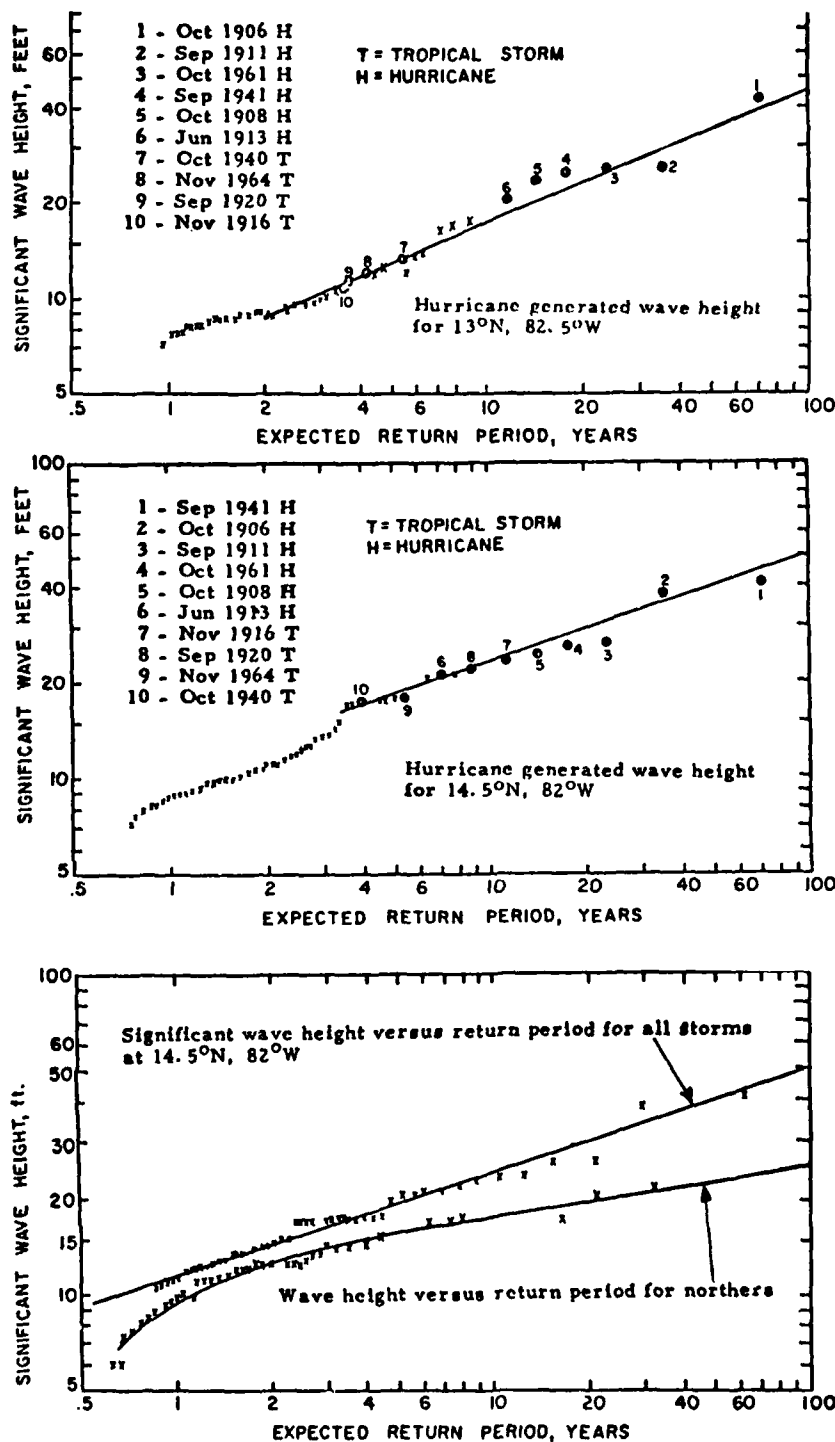


Figure 4.46: Significant Wave Height versus Return Period generated by hurricanes and tropical storms for the locations 13°N, 82.5°W and 14.5°N, 82°W; and for all storms compared to the result for northers only at 14.5°N, 82°W (Collins et al., 1970)

Table 4.8 summarizes conditions based on these results; H_M is the most probable maximum wave height in a group of N waves; T is the wave period and H_s is the significant wave height. It has been assumed that the forward speed for hurricane movement in this area, V_F , is 9 kt. Collins et al. state that considerable confidence can be placed in these extreme wave predictions for these shelf edge locations.

Table 4.8: Ratio of Most Probable Maximum Wave Height, H_M , to Significant Wave Height, H_s , for N Waves; Hurricane Forward Speed is 9 kt (Collins et al., 1970)

T (sec)	10	12	15
N	600	500	400
H_M/H_s	1.79	1.77	1.73

Nearer shore, significant wave heights will be reduced by bottom friction on the shallow bank; Figure 4.47 from Collins et al. (1970) indicates the decay curves, applying to the waves for the return period of 100 years at one hindcast point, as they travel toward shore from the Bank edge. These authors note wave heights could be reduced further by local topographic effects from offshore islands and cays. Otherwise, refraction effects may be assumed as negligible, except very close to the shoreline; there, they may act either to reduce or to increase wave heights.

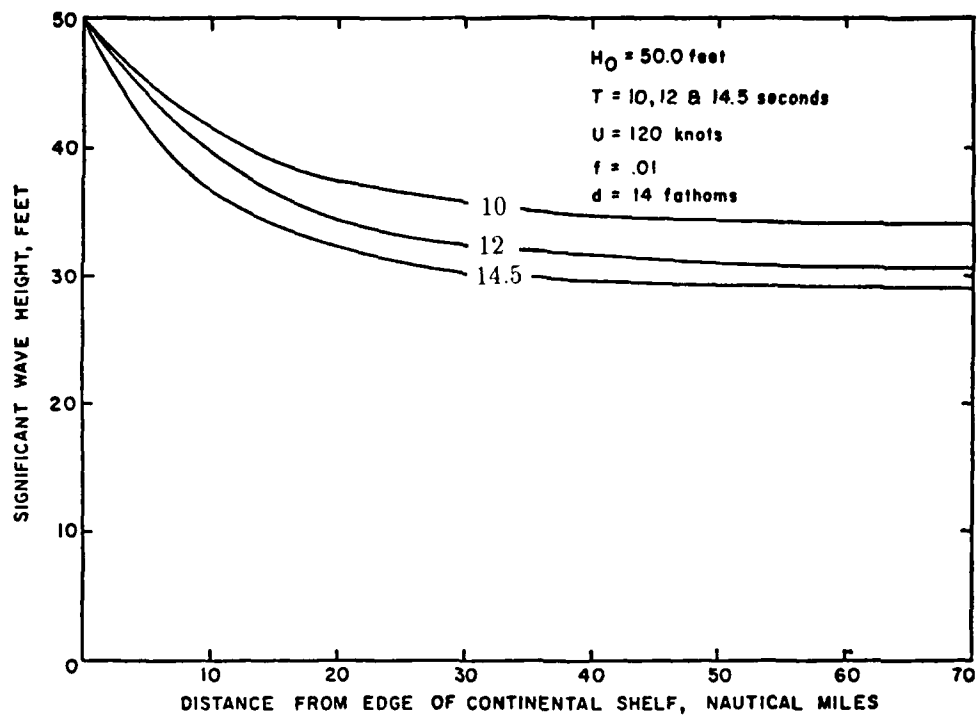


Figure 4.47: Decay of 50-foot Wave at indicated periods (T) as it travels shoreward over the continental shelf along Caribbean Coast of Nicaragua (Collins et al., 1970)

Storm Surges (Tides) and Currents along the western Caribbean coastline of Nicaragua have been calculated by Collins et al. (1970). Winds during northers are parallel to the shore; these cause southward-directed currents along the Miskito Bank off Nicaragua. These authors used model equations for calculating currents and storm surge for the two cases that apply to Miskito Bank, where the shelf either has a gentle slope (m), or where the shelf is flat. Results are shown in Table 4.9; D_o is water depth at the edge of the shelf; V is storm current speed; S is the storm surge height at the shoreline, and it decreases linearly to zero at the shelf edge. These values are calculated for a norther with a 50-knot wind speed. The currents are strong; and (not shown) they vary linearly with wind speed; the surge values are low, and higher values may occur locally over reefs and cays (not shown).

Table 4.9: Summary of Longshore Currents and Storm Surge, S , during a 50-kt Norther (Collins et al., 1970)

Latitude	12.0°	12.5°	13.0°	13.5°	14.0°	14.5°	15.0°
m	.00064	0	0	0	0	0	0
D_o , ft	210	120	90	80	60	80	70
V , kt	2.1	1.9	1.8	1.8	1.7	1.8	1.7
S at shore, ft	0.60	0.95	1.15	1.55	1.50	1.65	1.75

Hurricane surges are more complex than those for northers. An estimate by Collins et al. (1970) was made from hurricane data for this region since 1899. Hurricane wind fields were calculated from a model using hurricane size, forward speed, position, central pressure, maximum wind speed and radius to the maximum winds. The model yielded wind field components for successive hurricane positions along any selected offshore traverse. These computed wind field components then were used as input to the bathystrophic storm tide equations to give longshore mass flux (Q) and storm surge (S). Calculations were made for the six hurricanes which have crossed the coastline during the 70-year period; computer outputs for several critical traverses for all storms were scanned for maximum values of Q and WL (total surge). Envelopes for maximum values for current speed (from Q) and storm surge are shown in Figs. 4.48 and 4.49. More precise values should be calculated for points very close to shore or near reefs and cays.

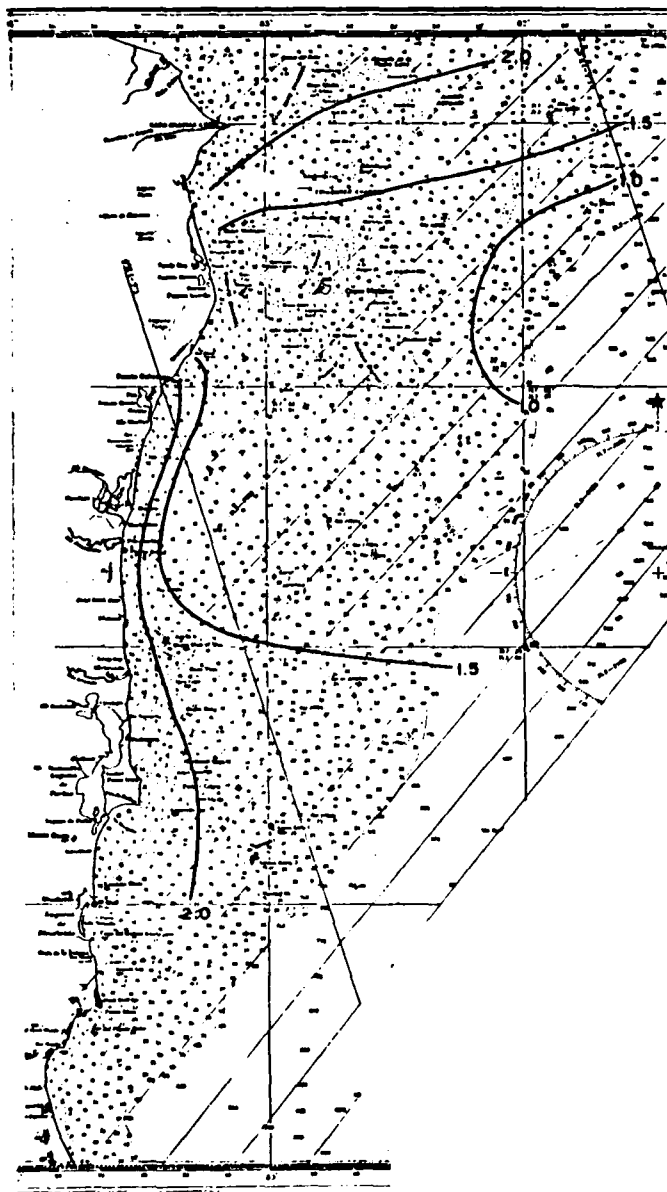


Figure 4.48: Maximum Current Values (kt). Small illegible numbers are soundings in fathoms. (Collins et al., 1970)

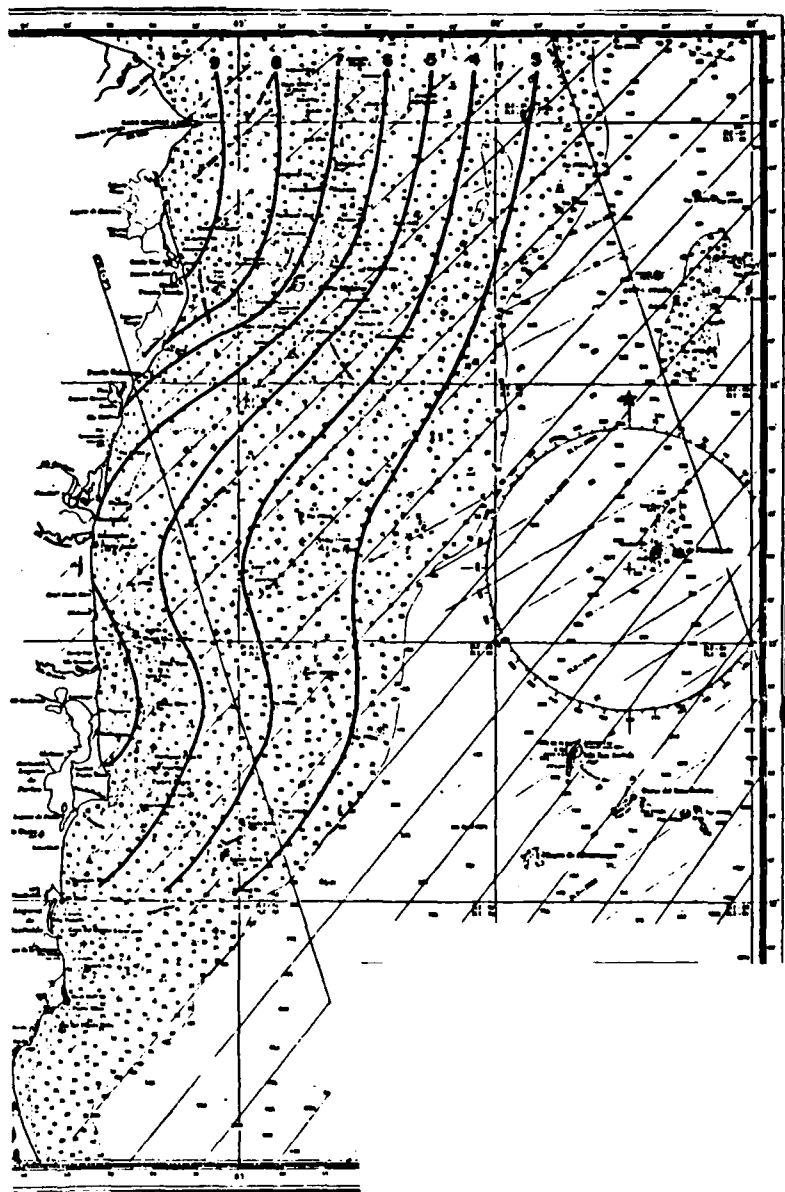


Figure 4.49: Maximum Storm Surge (feet). Small illegible numbers are soundings in fathoms. (Collins et al., 1970)

Bottom Sediments and Character of the Earth's Crust underneath the Western Caribbean Sea. Ewing and Edgar (1966) describe results of data interpretation from direct sampling methods (coring and dredging) and from indirect geophysical methods (refraction, reflection and gravity). Characteristics of the crust reported here have been determined only by the indirect methods. Figure 4.50 indicates major geological features of the western Caribbean, and the line drawn northwestward from Columbia to the Yucatan Basin indicates the track of the refraction cross-section (shown as Fig. 4.52 later).

Sediments. Recent sediments in the Caribbean are largely carbonates, in the form of tan to brown muds with added coarse organic and inorganic fragments of varying percentages. Foraminifera and pteropods commonly are dominant organic fragments. Turbidity currents are believed to dominate the mechanisms for deposition of most Caribbean sediments. This can account for the very flat topography in the Yucatan and Columbian Basins.

Total sediment thickness in some Caribbean regions is determined only by refraction measurements. Underneath the North Venezuelan Trough there is sediment and sedimentary rock up to 12 kilometers thick—the thickest measured in the Caribbean. Average seismic sections in the Yucatan and Columbian Basins are compared with similar sections for continents and the Atlantic Ocean Basins; the upper shaded region for each seismic section indicates sedimentary rocks. Note these are much thicker in the Caribbean Basins than in the North Atlantic Basins, shown in Fig. 4.51. The refraction cross-section along the track indicated above in Fig 4.50, is shown as Fig 4.52, from Ewing and Edgar (1966). Lower speeds in the upper part of the section, near the basin floors, are associated with sediments.

Profile reflection tracing (not shown here) indicates that two strong sub-bottom reflectors may be present underneath the thick turbidity deposits in the Columbian and Yucatan Basins, which nearly mask the reflectors. In cores on Beata Ridge, hard consolidated carbonate mud, light grey in color, has been recovered from about the depth of the first strong sub-bottom reflector.

Crust. Refraction speeds for the crustal layer in the Caribbean vary from 5.8 to 7.8 km/sec, increasing with depth as the rock densities increase. The average thickness of the crust in the Caribbean Basins is greater than in the Atlantic Ocean Basins, but is very small compared to the continents (see Fig. 4.51). The refraction section in Fig. 4.52 shows the crust is thick below high bottom topography; the crust underneath the Columbian Basin is thicker than that beneath the Yucatan Basin, and the water depth is about 1 kilometer less. The crust is somewhat thicker under the Beata Ridge, and it so thick underneath the Jamaica Ridge (called the Nicaraguan Rise in Fig. 4.50) and Cayman Ridge, that the depth to the mantle has not been recorded by seismic refraction profiles; it may be comparable to continental crust thickness there. It thins to about 4 kilometers in the Cayman Trough, and the mantle is at 11 kilometers below sea level there. This is the shallowest mantle depth in the Caribbean.

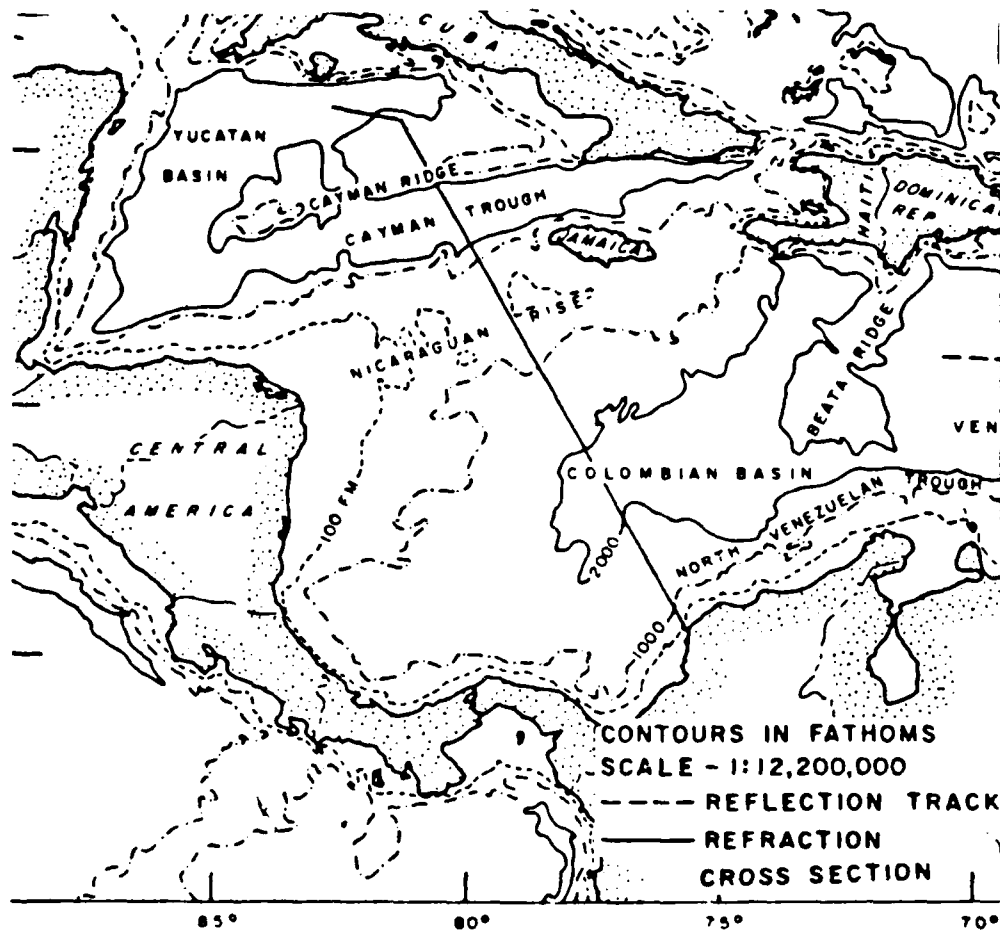


Figure 4.50: Bathymetry of the Western Caribbean Sea indicating Major Topographic Features. Track for the refraction cross-section shown in Fig. 4.52 is the solid line across the central area (adapted from Ewing and Edgar, 1966).

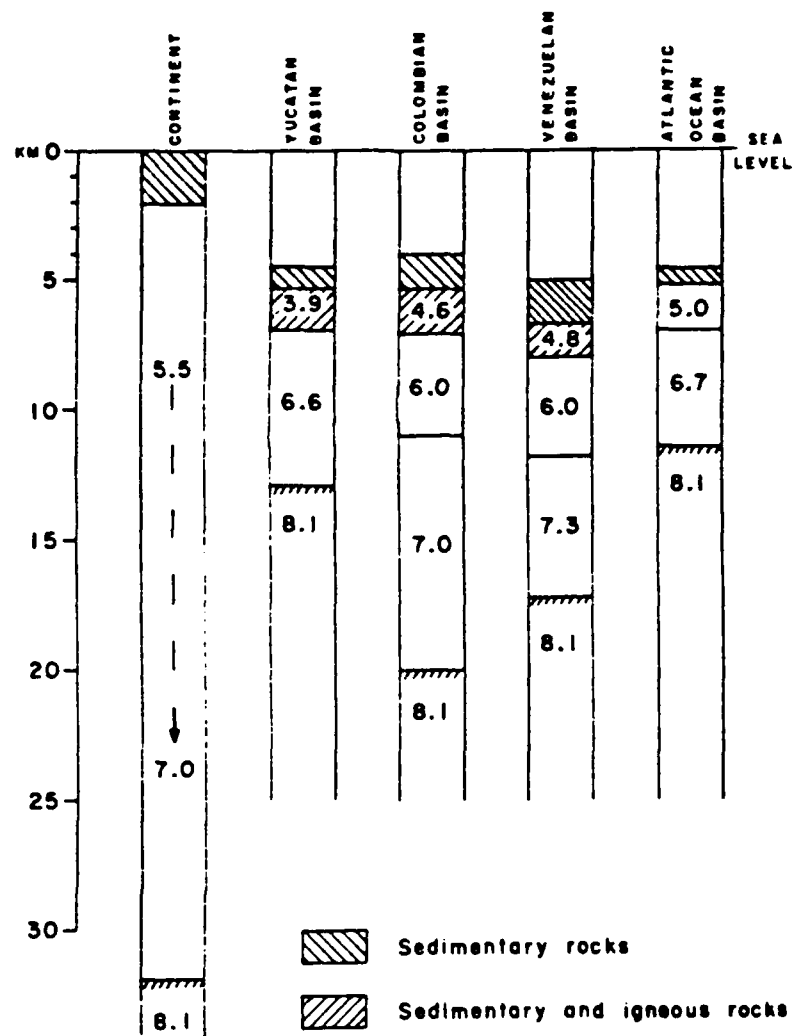


Figure 4.51: Average Seismic Sections for the Continents, North Atlantic Ocean and Caribbean Sea Basins (Ewing and Edgar, 1966)

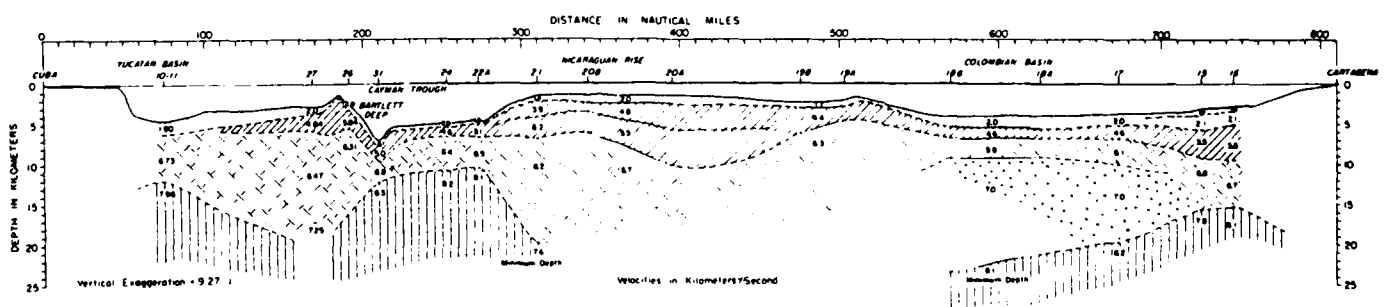


Figure 4.52: Structure Section across the Colombian and Yucatan Basins (Ewing and Edgar, 1966)

Shelf and Shoreline Characteristics of Miskito Bank on the Caribbean Coastline of Nicaragua. Murray et al. (1982) made an extensive study of Miskito Bank and their excellent study results are summarized in the following section.

Shelf Sediments have characteristics determined largely by the strong currents of the Coastal Boundary Layer and by the unusual shelf topography. The shelf may be divided into four zones, which are located by underlined "Z" designations on Fig. 4.53(b), and are described by echo-sounder profiles in Fig. 4.53(a). The zones are: (Z_1), a smooth ramp of deposited land sediment near the coast; (Z_2), flat-lying areas of carbonate deposits on mid-shelf; (Z_3), the shelf margin with rough bottom coral reefs; and (Z_4), platforms and smaller regions of higher topography on mid-shelf, with rough bottom contours.

Zone Z_1 sediment size and mineral properties depend on neighboring river mouths, the offshore distance, variations in the Coastal Boundary Layer drift, and in sediment sources. Coarse volcanic sands are common near river mouths. Clays and silty-clays are in coastal recesses and seaward from coastal bar systems. Maximum speeds in the Coastal Boundary Layer occur near the sea surface, and usually they do not reach the bottom. Coastal headlands, such as Monkey Point (located in Fig. 4.31), cause currents to increase in this zone, and migratory bars are observed.

In Zone Z_2 , carbonates are dominant beyond about 20 kilometers from shore, the seaward edge of the Coastal Boundary Layer. In Fig. 4.53(c) the carbonate fraction is shown in sediments, taken along the dotted station line (5), (10), (15) on Fig. 4.53(b) from the coastline to the shelf edge; carbonate is dominant beyond station (6). Sediments in Z_2 are at depths of 20-30 meters and lie below the depth reached by typical Tradewind surface waves; thus, only small-scale features occur in this mid-shelf zone. Calcareous green algae occur in productive communities and form sediments for Z_2 , which are large particle sizes deposited in aragonitic mud (from disintegrating products of the calcareous green algae).

Open ocean water at the shelf edge moves actively and contributes toward the growth of shelf-margin reefs in Zone Z_3 . These attain a relief of 10 meters or more, growing in regions free from land sediments. Coarse particles are abundant in sediments here, products of both biological and mechanical breaking up of the corals.

Zone Z_4 is formed by the coral platforms or reefs on mid-shelf, with characteristics of Z_3 : irregular floor relief which diminishes effects of ocean waves reaching the region; sites of active coral growth; a vast carbonate plain dominated by calcareous green algae. Collins et al. (1970) note this region has excellent underwater visibility to support diving or television operations.

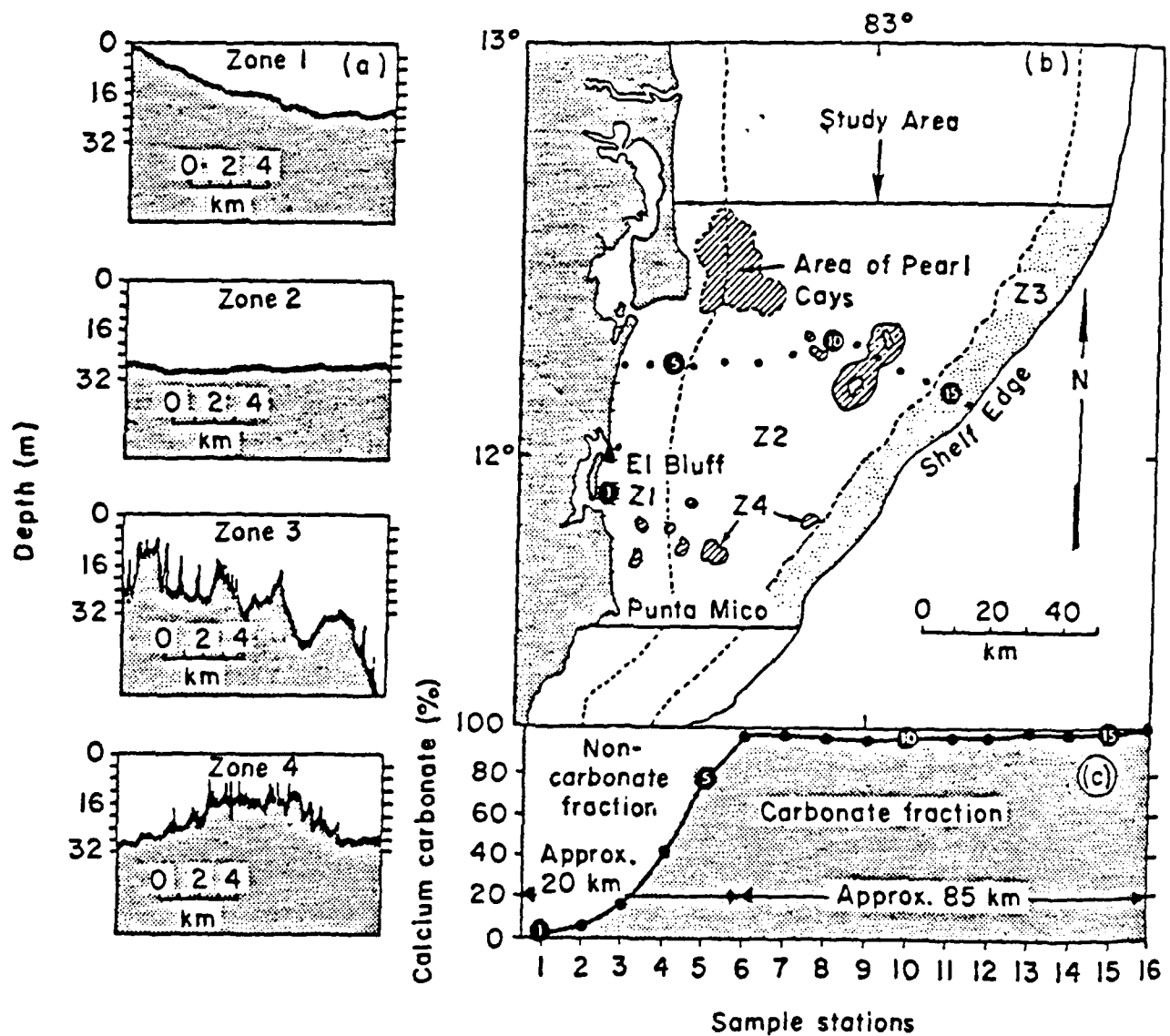


Figure 4.53: Zones in Study Area based on nature of echo-sounder profiles. Four Zones: Z_1 , Z_2 , Z_3 , and Z_4 are defined in (a); (b) shows regions where each Zone occurs on Miskito Bank; (c) shows carbonate fraction observed in samples along dotted line south of Pearl Cays (Murray et al., 1982).

Coastal Morphology. Local ocean currents generally determine the environmental character of much of Miskito Bank, with surface wave action being definitely secondary, excepting in the immediate vicinity of the coastline. There, littoral currents driven by shoaling and breaking waves reach speeds of 75-150 cm/sec in a narrow zone (100-200 yards wide) between the shoreline and the inner edge of the Coastal Boundary Layer.

These littoral currents have caused such large-scale features as deltas and cusped forelands, as well as small-scale beach bars. There is systematic change that occurs in these features from north to south along this coast, which reflects steadily-increasing wave energy toward the south. This has arisen because the shallow shelf is very broad to the north, which acts to attenuate deepwater waves greatly as they move across the shelf of 200-km width there. In contrast, the shelf is narrow at the southern end (about 20 km) where it borders Costa Rica. Murray et al. (1982) note this permits about three times more wave energy to reach the coast near Rio San Juan (in the south) compared to that near Rio Coco (in the north). The development of coastline features reflects this change in incident wave energy along the coast, in addition to sheltering effects by offshore islands or shoals.

River Deltas are prime examples of such effects. Rio Coco, at the Honduras/Nicaragua border to the north where the shelf is wide, has a protruding delta due to the reduced marine influences; a single river channel has developed, with active sediment deposits along its margins allowed by a diverging longshore current system. Spits and beaches attached to the shoreline develop from the sands composed of beach and beach ridge deposits.

Rio San Juan, which has about the same river discharge and sediment load as Rio Coco, shows a greatly different delta formation at the southern end of the Miskito Bank shelf. The narrow shelf there experiences the higher wave energy levels that produce an associated north-to-south longshore current drift. To the south along Costa Rica, the bend in the coastline there gives rise to a northward drift current that converges with the former drift. The combined effects of the longshore drift convergence and the high wave energy produce a delta spread along the coast with only little extension seaward. Figure 4.54 shows the contrasting delta forms, as well as the littoral current drift directions along the shorelines.

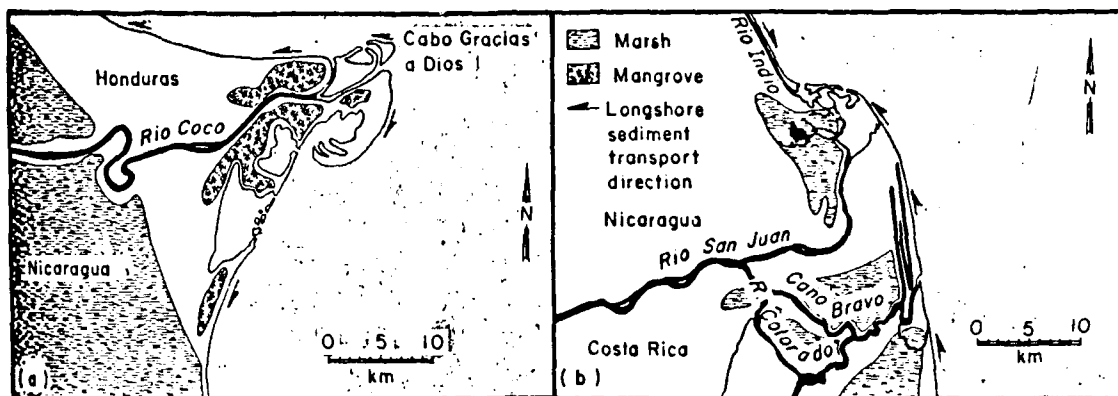


Figure 4.54: Generalized Morphology of (a) the Coco and (b) the San Juan-Colorado Deltas. The small arrows give the direction of the littoral drift driven by wave shoaling and breaking (Murray et al., 1982).

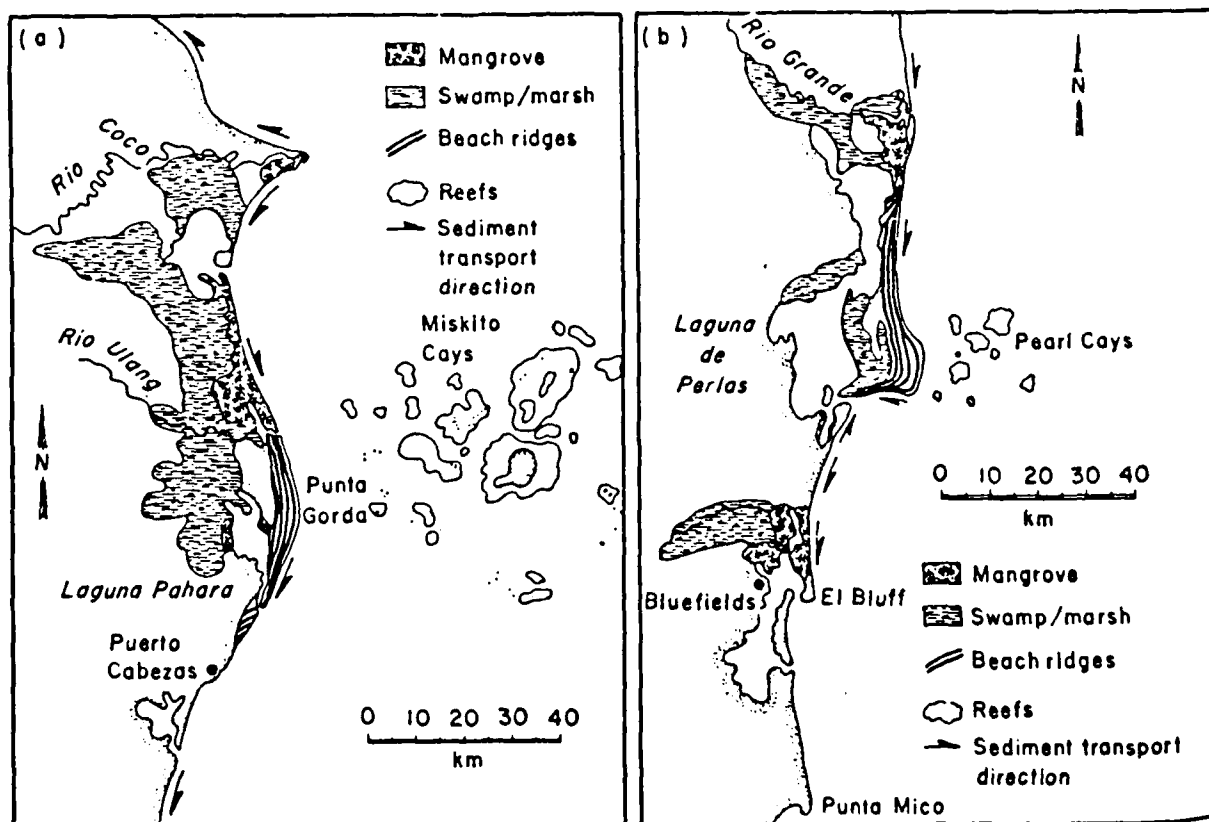


Figure 4.55: Effects of Wave Shadowing from Offshore Shoals shown for (a) Punta Gorda and (b) Punta Perlas (Murray et al., 1982)



Figure 4.56: Straight Shoreline with a Single Linear Bar to the North of Prinzapolka (12 April 1977)(Murray et al., 1982)



Figure 4.57: Well-defined Rhythmic Topography at Cano el Pescado, about 25 kilometers north of the San Juan-Colorado Delta (12 April 1977)(Murray et al., 1982)

The summary is **quoted** below from the detailed study by Murray et al. (1982) regarding the character of Miskito Bank, which is subjected to high weathering rates and intense rainfall on the adjacent coastal watersheds as these act to provide large quantities of sediment-laden water to the coastal region:

1. This sediment-charged water forms a tightly organized Coastal Boundary Layer (CBL), heavily influenced by the persistent Northeast Tradewinds. The southward-flowing jet has maximum speeds of 50-75 cm/sec; it is closely confined to the coastline, with little evidence of horizontal (seaward) mixing.
2. Seaward of the turbid CBL, clear, high-salinity shelf water moves slowly across the outer Bank, providing ideal conditions for the carbonate production typical of (these) tropical latitudes.
3. Sediment characteristics and bathymetry relief across the Bank are closely coupled with the current regimes acting on it. Coarse volcanic sands are found in the beach-bar systems affected by wave-driven littoral currents. This narrow zone merges seaward into a smooth depositional ramp composed of clays and silty clays which directly underlies the turbid, fast-moving water of the CBL. Further seaward these sediments are replaced by carbonates. The interior expanse of the Bank is a flat plane covered with the disintegration products of calcareous green algae. This surface is interrupted occasionally by rough-bottomed mid-shelf platforms topped with actively growing coral-algal reefs. A high-relief coral reef grows along the steep dropoff at the Bank edge, its growth enhanced by the observed upwelling of cooler, higher salinity waters.
4. Modification by wave action along the shoreline is affected by the great width of the shallow bank. Decreasing shelf width and decreasing frictional effects from north to south cause a threefold increase in wave-energy levels along the southern shoreline.
5. The variation in nearshore and shoreline wave-energy levels results in (a) a river-dominated deltaic environment at the mouth of the Rio Coco in the north; (b) a marine-(wave)-dominated deltaic environment at the mouth of the Rio San Juan in the south; and (c) a systematic change from straight linear bars and beaches in the north to rhythmic topography in the south.
6. Wave shadow zones behind two major submerged plateaus, dotted with mangrove island cays and numerous submerged reefs and shoals, have led to development of large cusped forelands composed of prograding beach ridge components on the coastline.

5. HURRICANES AND TROPICAL STORMS

5.1 General (including Track "Thumb Rules")

While Belize and the northeastern coasts of Nicaragua and Honduras are *most likely* to experience the wrath of hurricanes or tropical storms, the document would be incomplete without this section. During the preparation of this handbook, Hurricane Joan caused extensive damage and deaths in Nicaragua in October 1988, entering the country on the Caribbean coast at Bluefields and finally exiting west of the capital, Managua. Moreover, while there was minimal impact to the seven countries of Central America, Hurricane Gilbert brought devastation and loss of lives to Jamaica, the Cayman Islands, the Yucatan Peninsula, and coastal Mexico (just south of Brownsville, Texas) as well in September 1988. Hurricane Gilbert was the most powerful hurricane (category 5, i.e., having winds >135 kt⁸¹) to strike the western hemisphere in recorded history. Winds and rainfall from the outer perimeter of Hurricane Gilbert reached northern Guatemala, Belize and northern Honduras.

Extensive *yearly* track histories and statistics of North Atlantic hurricanes and tropical storms are contained in Neumann et al. (1987). The following excerpts concern their effects on Central America. While the "official" North Atlantic hurricane season extends from 1 June through 30 November, hurricanes occasionally occur both *earlier* and *later*. Tropical cyclones in the early season are confined almost entirely to the **western Caribbean Sea** and the Gulf of Mexico—note particularly in Appendix C that during the first ten days of the "official" season (1 June–10 June), there have been only 12 tropical cyclones during the period of record (1886–1986). By later June and early July, the area of formation gradually shifts eastward. However, in late July and early August the frequency **increases**, as the area of formation continues its march eastward (see Appendix C). By mid-September, the frequency begins to decline, and the formative area starts to return **westward**. In early October, the formative area is *generally* confined west of 50°W and the area of maximum occurrence is again found in the **western Caribbean Sea** (Neumann et al., 1987). Mean tropical cyclone tracks for the eastern North Pacific Ocean are shown in Appendix D.

⁸¹Tropical depression (<34 kt), tropical storm (34–63 kt) and hurricane (≥ 64 kt). Saffir-Simpson Scale (Category): No.1 (64–82 kt), No.2 (83–95 kt), No.3 (96–113 kt), No.4 (114–135 kt) and No.5 (>135 kt)

A cursory examination of the *yearly* tracks⁸² of North Atlantic tropical cyclones reveals the following:

1. Only once, in more modern records, have tropical cyclones⁸³ failed to move *over* any part of Central America for a period as long as six consecutive years: (1981–1986).
2. However during the 16-year period⁸⁴, 1871–1886, no tracks crossed Central America, although during two of the years (1874 and 1879) tropical cyclones passed over the Yucatan Peninsula just north of Belize, and in 1882 a tropical cyclone formed just off the northeast coast of Nicaragua before moving northward.
3. In December of following year, 1887, the *only* recorded tropical cyclone (a tropical storm) to move over Costa Rica approached from the east, having moved from the Windward Islands via the northern coast of Columbia—much like Hurricane Joan which struck just north of Costa Rica (Bluefields, Nicaragua) in 1988.
4. Still in the earlier portion of the record, no tropical cyclone struck Central America for the four-year period 1894–1897. Three-year absences were recorded three times, in 1903–1905, 1928–1930 and 1957–1959, while there have been several two-year absences: 1914–1915, 1947–1948, 1962–1963 and 1975–1976.
5. The only record of a tropical cyclone moving over Panama was Hurricane Martha, late November 1969, which formed about 120 miles north of the Gulf of Mosquitos, moved slowly southward and came ashore about two days later at a point 75 miles west of the Panama Canal.
6. There have been about 20 tropical cyclones to form within 120 miles north of Panama, but, except for Hurricane Martha in 1969, they tracked northward, i.e., away from Panama.
7. **The majority of tropical cyclones⁸⁵ affecting Central America are those whose tracks take them over the northeastern portions of Honduras and Nicaragua on westward tracks which then pass over Belize.**
8. Of the numerous tracks passing over Belize, about 20 have continued over Guatemala, although over one-third of them arrive in the dissipation stage.

⁸²Period of record: 1871–1986 (Neumann et al., 1987), not presented here.

⁸³The term tropical cyclone implies hurricane, tropical storm or tropical depression.

⁸⁴Obviously before more modern communications or the availability of satellite imagery (1960).

⁸⁵The 10-day period track histories of Appendix C provides limited guidance as to the relative frequency and expected area of tropical cyclone occurrence.

9. Several tropical cyclones moving over Guatemala did *not* come from the east. In 1949, a hurricane, after forming in the North Pacific Ocean south of El Salvador in late September, moved northward through Guatemala, eventually entering the Gulf of Mexico in the eastern Bay of Campeche. There was a similar northward moving tropical storm in June 1965. In August of 1973, Hurricane Brenda formed near southeastern Cuba, crossed the Yucatan Peninsula, then curved cyclonically (toward the south) and dissipated over northwestern Guatemala.
10. In October 1923, a tropical storm (while not directly affecting Central America) moved from the North Pacific Ocean northward, just west of Tehuantepec, becoming a hurricane in the western Gulf of Mexico, and then moved ashore into Louisiana. There was a similar track in October of 1902, although just to the *east* of Tehuantepec.
11. Few tropical cyclone tracks have moved over El Salvador directly, although their peripheral effects are often experienced. In September 1911, a tropical storm moved across north-central Nicaragua, then crossed southeastern El Salvador on a westward course. While 1933 was an especially "busy" tropical cyclone year, with more than 20 tracks over the Caribbean Sea and the Gulf of Mexico (tracks of both the "straight" and "recurving" varieties), in June of 1934 a tropical storm formed over the Gulf of Honduras, then proceeded to "loop" over Belize, central Guatemala, northern El Salvador, western Honduras, and then returned to the Gulf of Honduras before moving northward. After crossing the Yucatan Peninsula, it made another (although smaller) cyclonic loop just north of the Bay of Campeche before continuing on to strike the U. S. mainland at Louisiana.
12. Tracks which have been similar to the track of Hurricane Joan (see case study, Sub-subsection 5.2.1), which moved westward across central Nicaragua in October 1988, are:
 - (a) Hurricane Irene in September 1971, which was renamed Tropical Storm Olivia in the North Pacific Ocean.
 - (b) A tropical storm in November 1933, which dissipated in central Nicaragua.
 - (c) A hurricane in September of 1911, which continued west to strike Costa Rica.
 - (d) A hurricane in October 1906, which dissipated in central Nicaragua.
13. While tropical cyclones forming on the Pacific Ocean side of Central America have struck Guatemala, generally only their cloudiness and *weaker* peripheral winds and rain affect the west coast of Central America as they move westward into the eastern North Pacific Ocean.

5.2 Case Studies during Hurricanes

5.2.1 Case V - Hurricane Joan (14 - 25 October 1988)

By 14 October, just one week after the end of Case Study I (see section 2), a disturbance, then "Tropical Storm" Joan, was approaching the Windward Islands while the equatorward extension of an early fall cold front was dissipating over the Gulf of Honduras with its attendant convective cloudiness (see Fig. 5.1).

The NMC ATOLL low-level streamline analysis on 14 October depicts a *closed* cyclonic circulation near 11°N, 59°W; at 200 mb, the NMC streamline analysis depicts an anticyclonic gyre although it was *centered* some distance *ahead* of the surface vortex position, near 13°N, 66°W, with northerly flow (supported by satellite derived winds) *over* the surface position of the tropical storm. However, the FNOC low-level 925 mb wind analysis⁸⁶, in this data sparse region, did *not* locate the tropical vortex, but did depict cyclonic curvature in the vicinity of 58°W; the Navy's 200 mb wind analysis did show an anticyclonic circulation above the eastern Caribbean Sea, similar to the NMC 200 mb streamline analysis. (In the interest of brevity, none of the above analyses at this *early* stage of Hurricane Joan's development is shown.)

18 October 1988

Four days later at 0000 UTC on 18 October, the tropical cyclone, now Hurricane Joan, had skirted the northern coasts of Venezuela and Columbia at an average speed of ~9 kt causing considerable damage while moving westward. The hurricane was now located *officially* at 11.9°N, 74.0°W (see Fig. 5.2). The NMC ATOLL low-level streamline analysis depicts the cyclonic circulation, while the NMC 200 mb streamline analysis depicts anticyclonic outflow aloft, although the upper circulation is centered on an elongated high⁸⁷ center extending from Curaçao to the Windward Islands (see Figs. 5.3 and 5.4).

With the *coarse* five-degree resolution available in the NOGAPS wind analysis, the Navy's analysis cannot depict the *finer* scales of the flow surrounding the hurricane. While the 925 mb (low-level) winds provided by FNOC *do* depict the cyclonic circulation around Joan (see Fig. 5.5), the strong NMC 30 kt *southwesterly* winds spiralling out at 200 mb appears more correct than the weak (5 kt) *easterly* winds at both 15°N, 75°W and 15°N, 80°W on the Navy's 200 mb winds of Fig. 5.6.

⁸⁶The FNOC 850 mb wind plot was no better in locating the tropical storm.

⁸⁷The extensive upper-air "outflow area" appears logical in the presence of the heavy convection depicted in Fig. 5.2 extending eastward to Trinidad. In fact, from such extensive cloudiness and convection, a short-lived tropical depression is later identified at 13.0°N, 72.7°W (i.e., rather close to and in the wake of Hurricane Joan) two days later at 0000 UTC 20 October.

While the NMC 1000 mb chart (Fig. 5.7) also does *not* have the resolution permitting it to depict the hurricane's vortex, note that the station observations correlate well with the IR imagery of Fig. 5.2. For example: the moderate rain at Santa Marta (station 80009), located on the northern Colombian coast on the southern periphery of the hurricane's IR signature; the thunderstorm reports at both San Andrés Island⁸⁸ (station 80001) and Caracas, Venezuela (station 80415) under deep IR convection; the reports of rain at Howard Air Force Base, Panama (station 78806) and at Port of Spain, Trinidad (station 78970); and while most of the Caribbean stations are reporting cloudy conditions, San Juan, Puerto Rico (station 78526) is reporting only 1/10 sky cover despite the presence of low cumulus and high cirrus.

Figure 5.8 is the Navy's transmission of the NHC Hurricane Joan forecast track, starting with its warning position at 1200 UTC (black circle farthest east) on 18 October 1988 and the subsequent 12-, 24-, 48- and 72-hour forecast positions. The forecasted position of "landfall" over the northeastern coast of Costa Rica was excellent—it actually went ashore in southeastern Nicaragua at Bluefields—; however, while the hurricane was moving at a speed of 10 kt at the time of the forecasted warning, it became quasi-stationary near 81°W and did not make landfall until about 0800 UTC 22 October⁸⁹ vice 1200 UTC 20 October as forecasted in Fig. 5.8. Figure 5.9 is the FNOC significant wave height chart, showing sea heights >27 feet at 1200 UTC 18 October (the time of the hurricane position in Fig. 5.8).

Next, it is desired to demonstrate the ability of the Navy's model to *forecast* significant sea heights. Fig. 5.10 shows the sea height analysis at 1200 UTC 17 October 1988, the initial analysis from which the 24-hr significant sea height forecast was made verifying at 1200 UTC 18 October 1988 (Fig. 5.11). Note that while the maximum wave heights on the periphery of the hurricane were only >15 feet on the 17th of October (Fig. 5.10), the **forecast** of maximum seas >24 feet, predicted *ahead* of the hurricane on the 18th (Fig. 5.11), verifies quite well on the **analysis** of significant sea heights (Fig. 5.9), where the analyzed maximum seas were >27 feet.

⁸⁸Which is subsequently hit with the full force of Hurricane Joan.

⁸⁹The nearly two-day delay of landfall permitted better hurricane preparation by Nicaragua.

0001 140C88 39E-42A 00902 15841 EC1

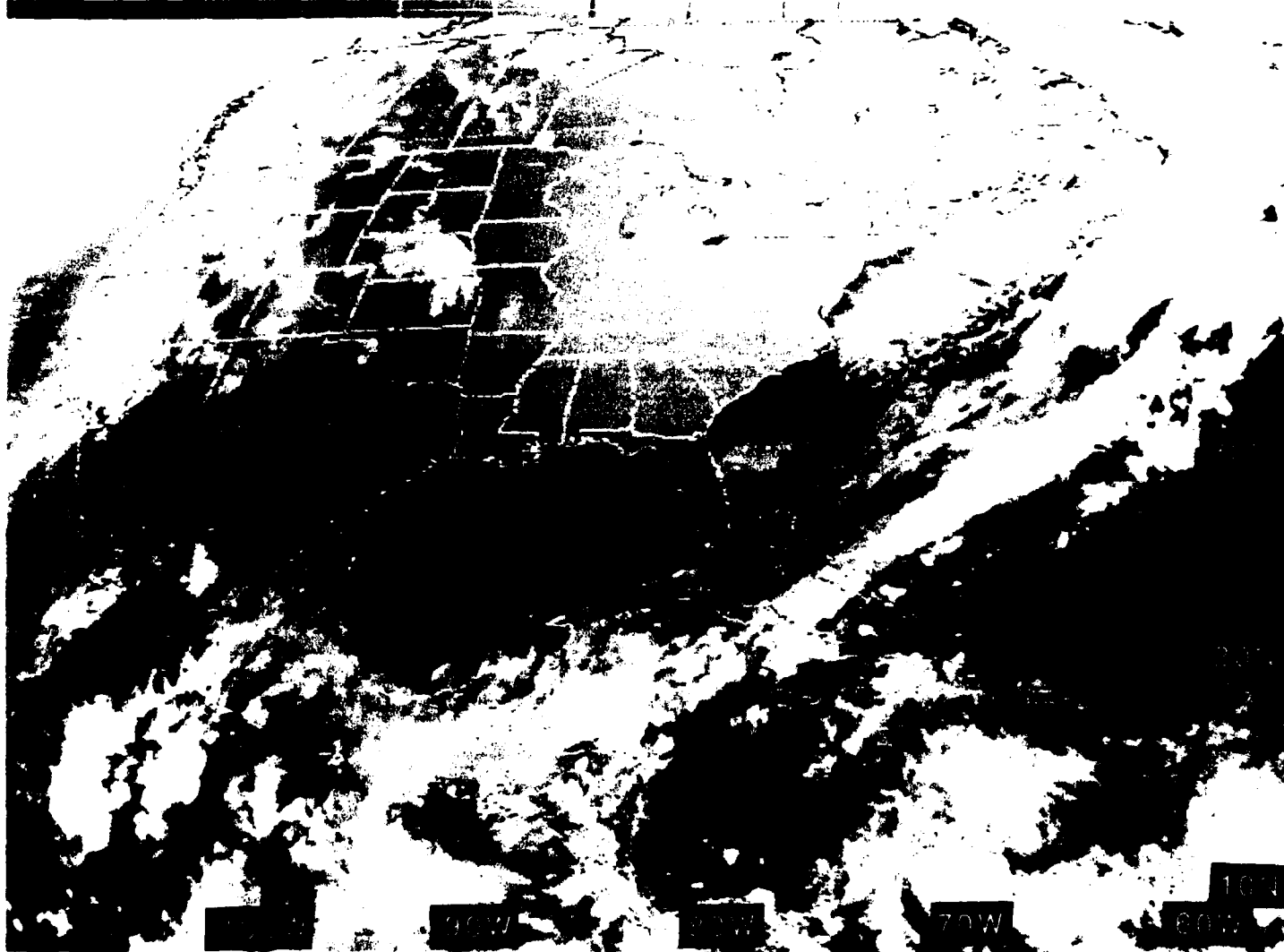


Figure 5.1: GOES East Infrared Satellite Imagery, 0001 UTC 14 OCT 1988

0001 180088 39E-42A 00911 15901 EC1

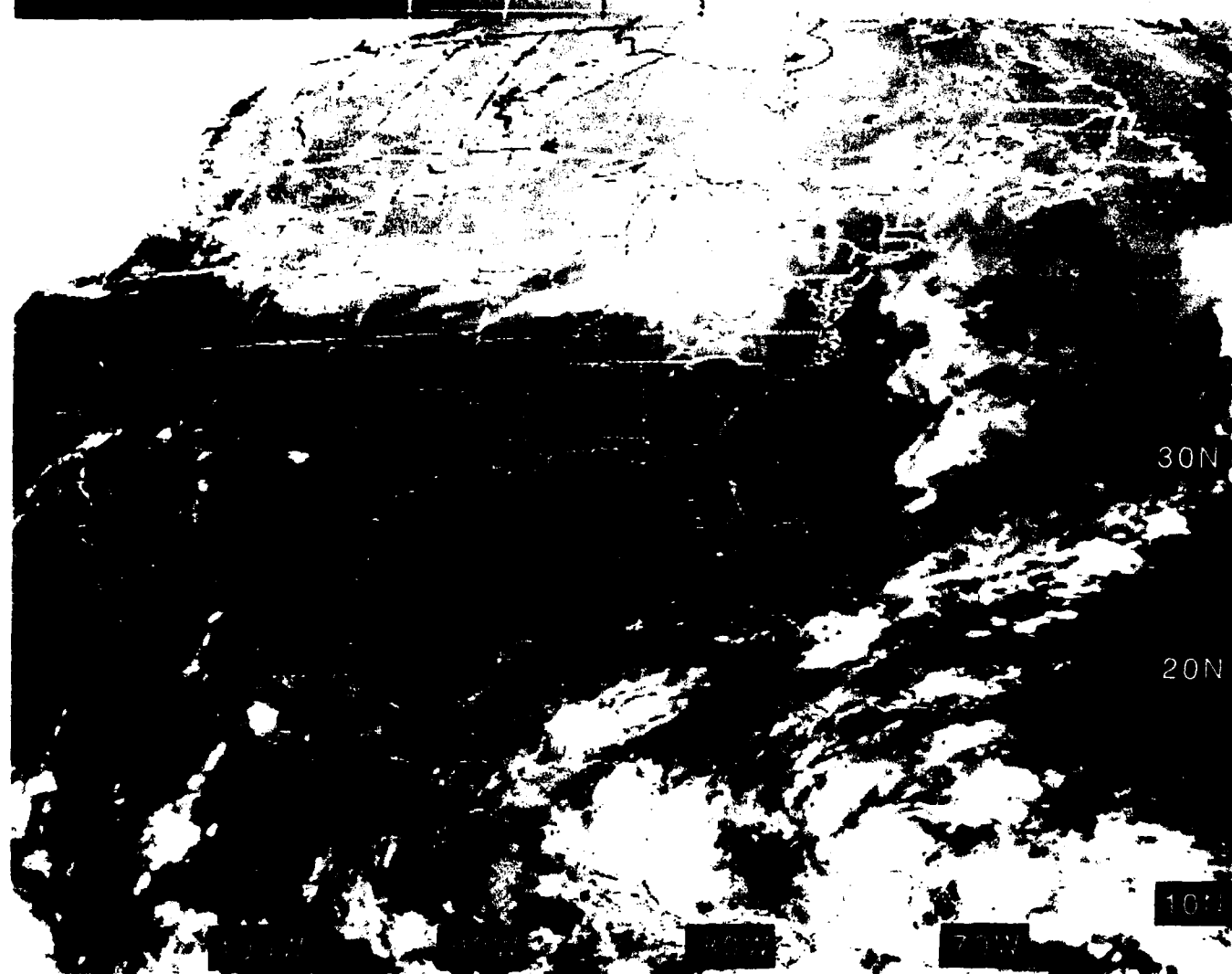


Figure 5.2: GOES East Infrared Satellite Imagery, 0001 UTC 18 OCT 1988

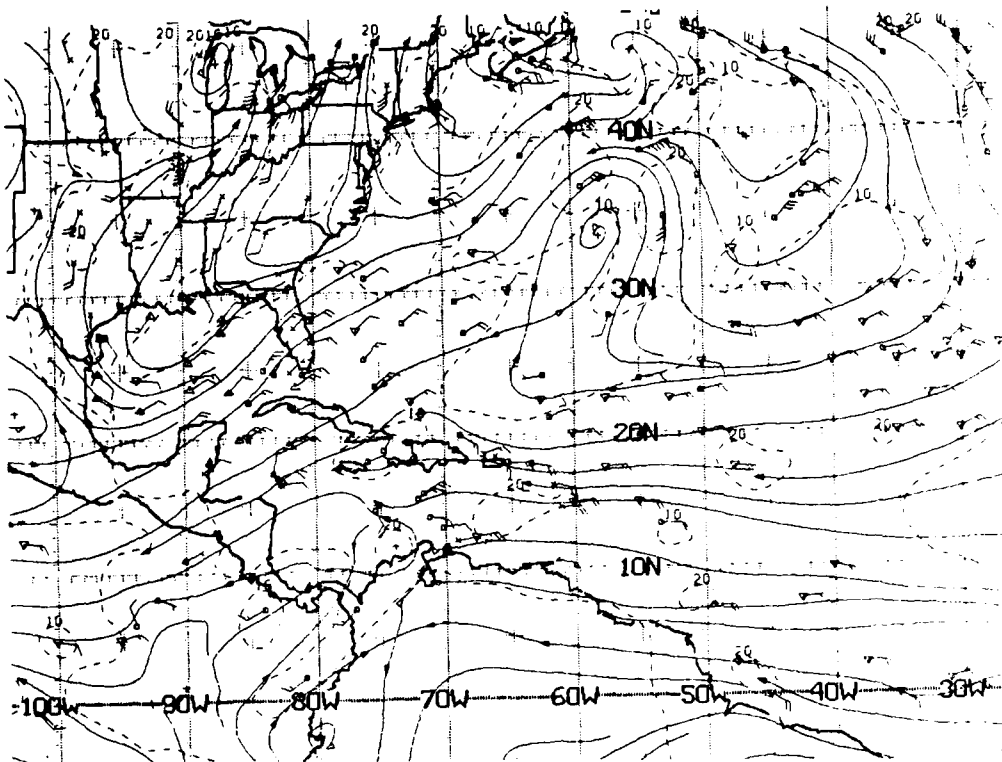


Figure 5.3: NMC ATOLL Operational Streamline Chart, 0000 UTC 18 OCT 1988
As in Fig. 2.4.

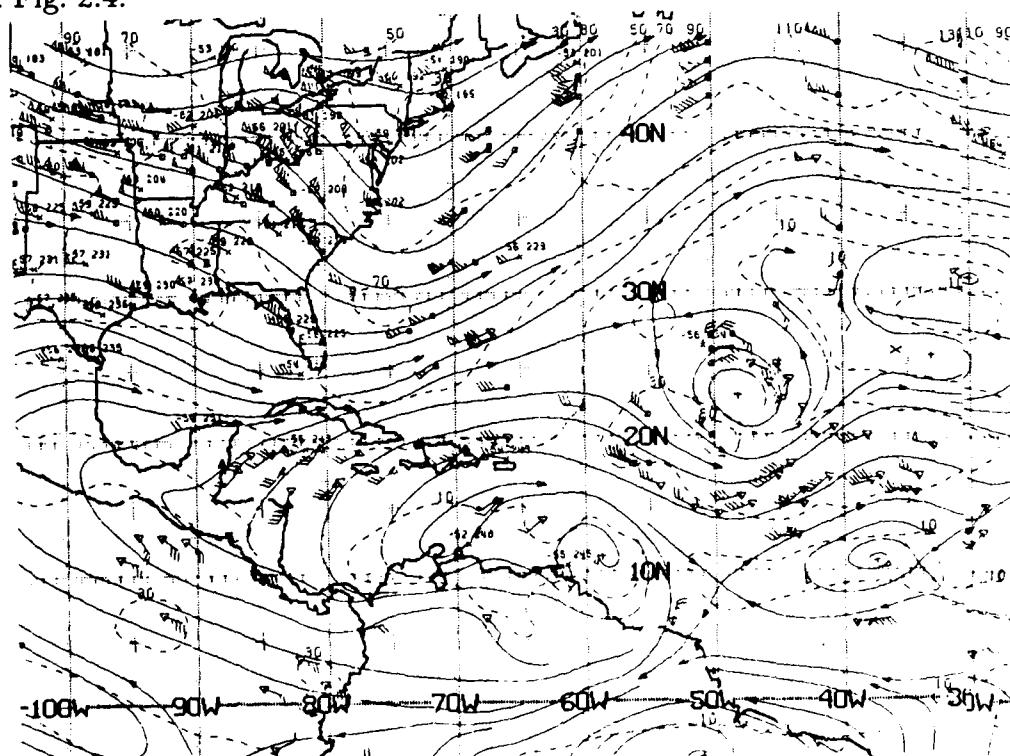


Figure 5.4: NMC 200-mb Operational Streamline Chart, 0000 UTC 18 OCT 1988
As in Fig. 2.6.

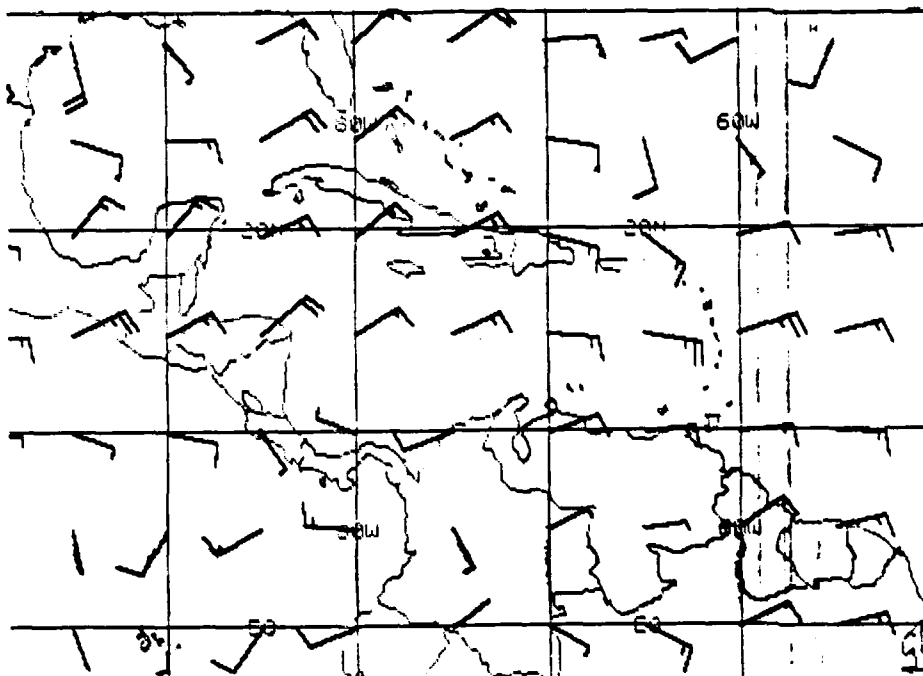


Figure 5.5: FNOc 925 mb Winds, 0000 UTC 18 OCT 1988. As in Fig. 2.19.

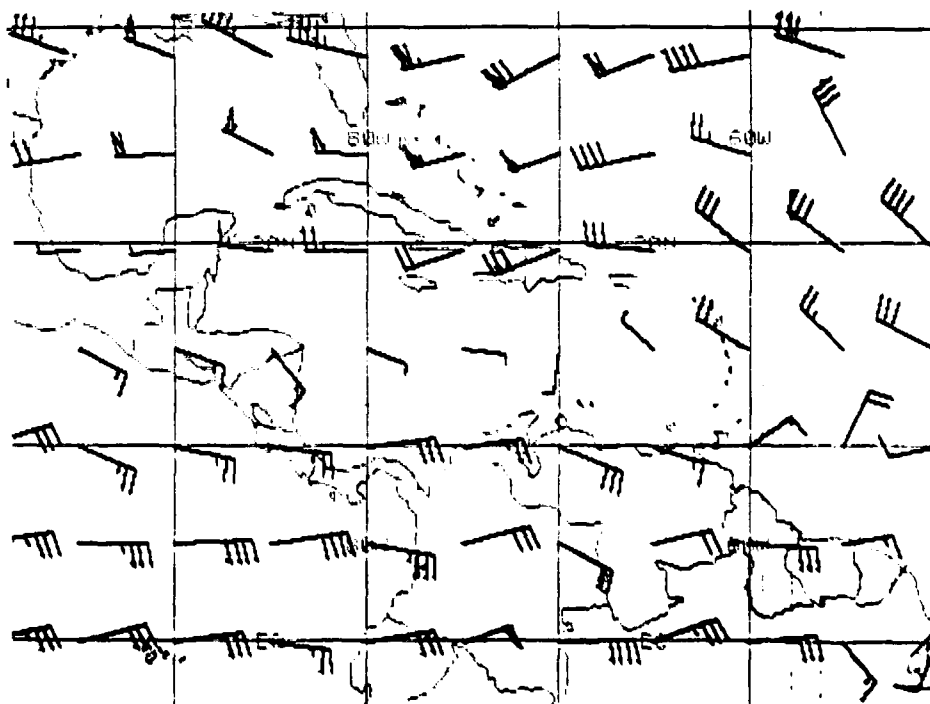


Figure 5.6: FNOc 200 mb Winds, 0000 UTC 18 OCT 1988. As in Fig. 2.20.

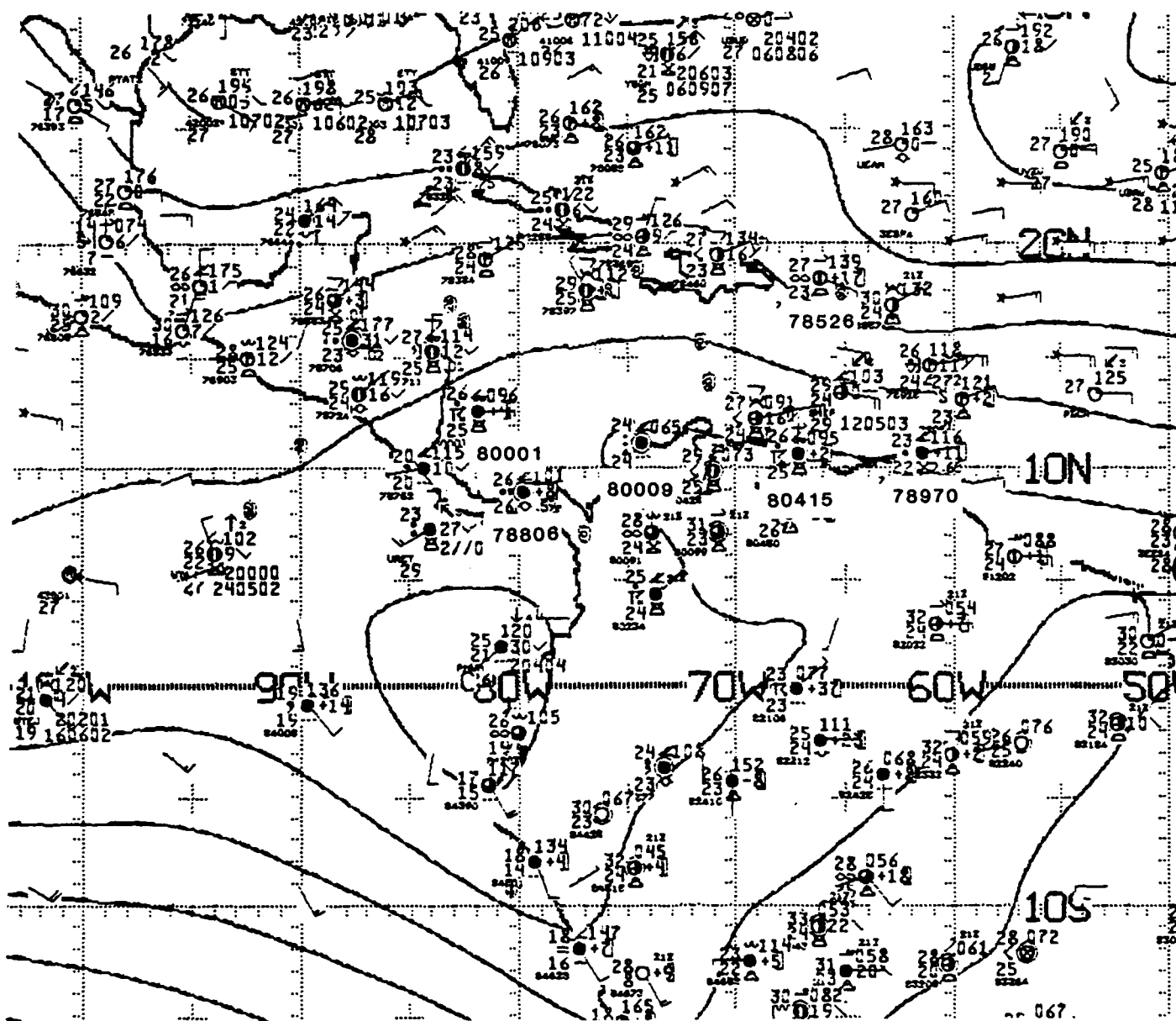


Figure 5.7: NMC 1000 mb Analysis, 0000 UTC 18 OCT 1988. As in Fig. 2.21.

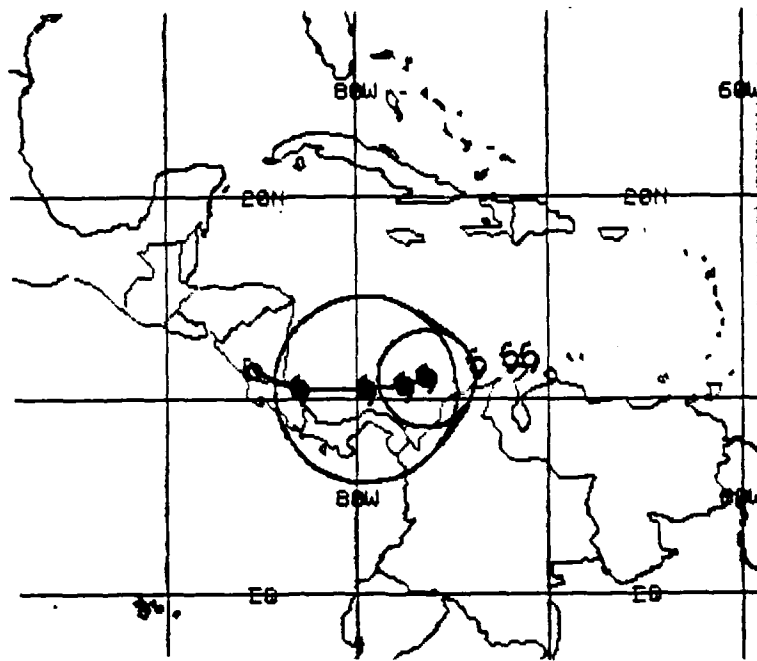


Figure 5.8: Tropical Cyclone FORECAST Track from 1200 UTC 18 OCT 1988.

Current position of hurricane is rightmost *black* symbol enclosed by the circle depicting the outer radius of gale force winds. Next toward the left is the 12-hr forecast position, followed by the 24-hr forecast position enclosed by the circle depicting the outer radius of probable gale force winds at 24 hours—the inclusion of the expected 24-hr position error produces such a **large** radius. The 48-hr forecast position is on the coast of Costa Rica, with the weakened storm over Lake Nicaragua in 72-hours.

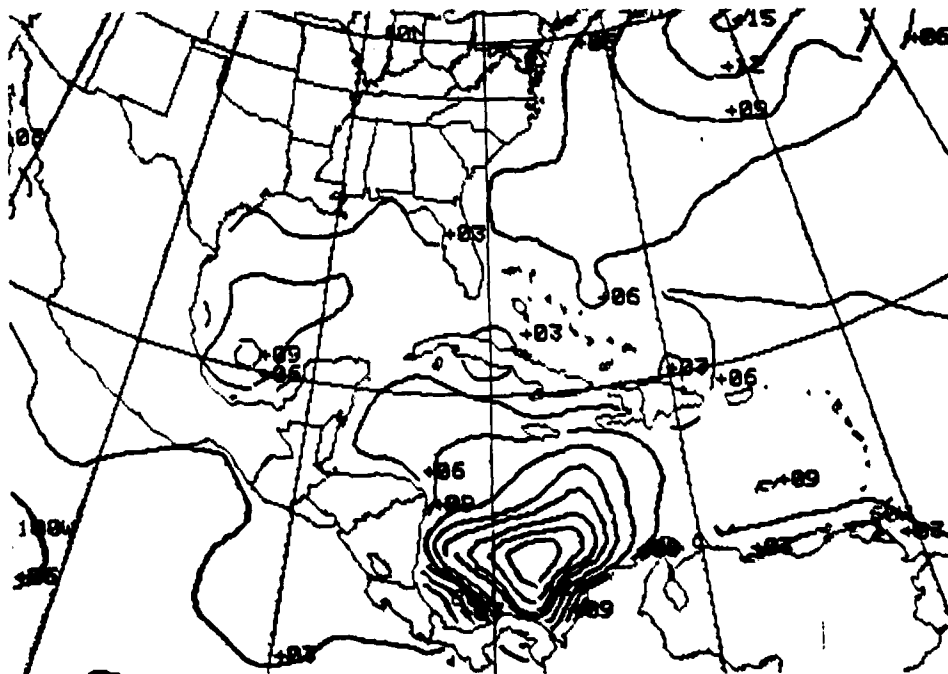


Figure 5.9: FNOG Significant Wave Heights, 1200 UTC 18 OCT 1988.
Isopleths are at 3-foot intervals.

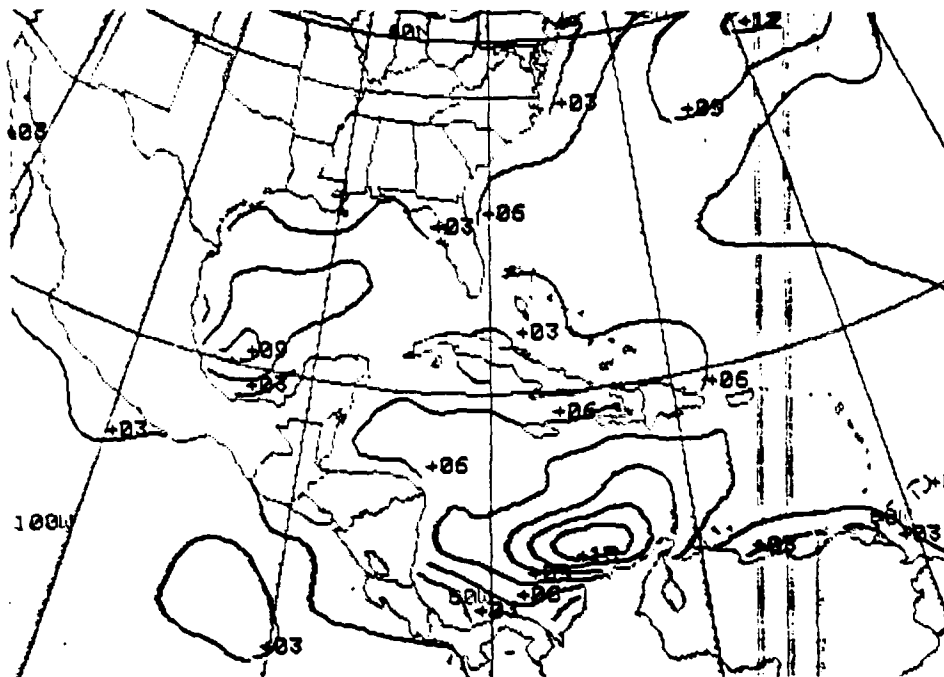


Figure 5.10: FNOG Significant Wave Heights, 1200 UTC 17 OCT 1988. Isopleths are at 3-foot intervals.

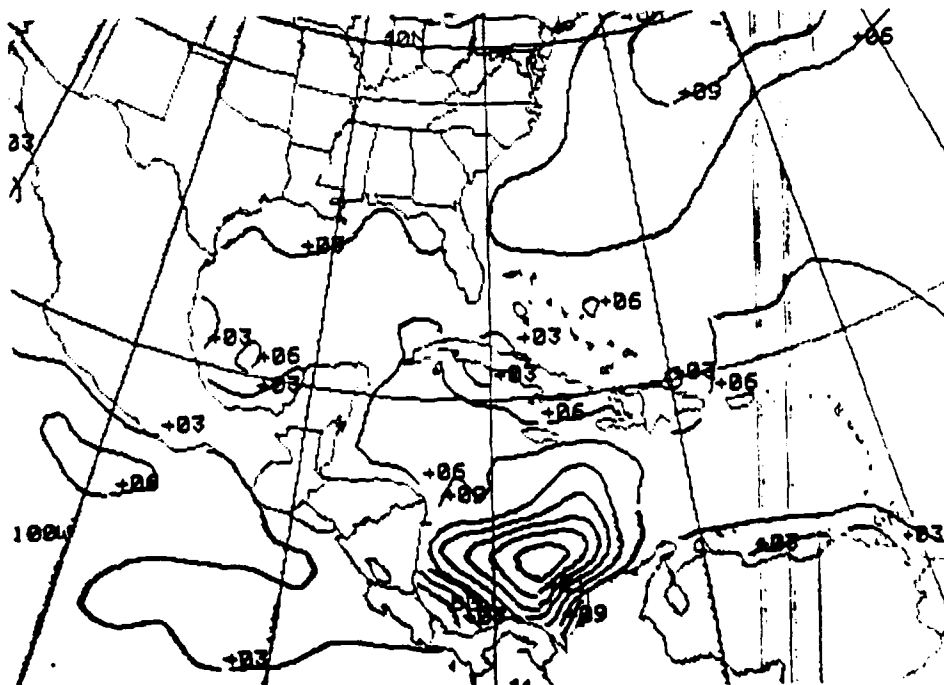


Figure 5.11: FNOG Sig. Wave Ht. Prog., VT 1200 UTC 18 OCT 1988. Isopleths are at 3-foot intervals.

19 October 1988

Two and one-half hours before 0000 UTC 19 October, the last visible imagery of the day, Fig. 5.12 (with its corresponding IR imagery, Fig. 5.13), permits a view of the eye of Hurricane Joan. The hurricane is increasing in intensity as it moves slowly westward and leaves the friction of the Columbian coast behind; at 2200 UTC 18 October, the National Hurricane Center official warning placed the hurricane at 11.3°N, 76.9°W (based on satellite imagery), moving toward the west (270°) at 7 kt and having maximum sustained winds of 80 kt, with gusts to 95 kt. The imagery of Fig. 5.12 is at 1631 local standard time, and it depicts well both the eye and the rain bands (or "banding features") encircling the eye. Most of Central America has become cloud covered, with only the Yucatan Channel and its Caribbean entrance relatively cloud free.

By 0001 UTC on 19 October, Fig. 5.14 shows the IR imagery corresponding to the streamline analysis by NMC (Fig. 5.15). At this time the NHC official position of Hurricane Joan was 11.3°N, 77.2°W which is well depicted by the whitest circular pattern, just northeast of Panama on Fig. 5.14. While the low-level streamlines of the simultaneous NMC ATOLL chart (Fig. 5.15) locate the hurricane position, the upper-level NMC 200 mb chart (Fig. 5.16) disappointingly places a "neutral point" within 120 n mi of the hurricane center. Nonetheless, the 200 mb "outflow" streamlines of Fig. 5.16 fit the inferred diffuence aloft on Fig. 5.14, i.e., the south-southwesterly flow from the Miskito Banks region toward Jamaica and Hispaniola. The Navy's NOGAPS low-level wind directions (Fig. 5.17) conform rather well to the hurricane cyclonic circulation, assuming that the *northwest* wind on the Caribbean coast of Columbia is in error. While the NOGAPS 200 mb winds (Fig. 5.18) provide a coarse depiction of anticyclonic flow over the hurricane, weak winds along 15°N (just south of Jamaica) do *not* follow the direction implied by the IR imagery of Fig. 5.14 as well as do the NMC streamlines of Fig. 5.16.

12 hours later, Fig. 5.19 shows the IR imagery as Hurricane Joan, still moving slowly toward the west (6 kt), continues to increase in intensity (the NHC 1600 UTC warning indicated that Joan's maximum sustained winds had increased to 100 kt, with gusts to 120 kt). Figure 5.20 is the first visible GOES imagery after the IR imagery of Fig. 5.19. On the visible imagery, the faint eye of the hurricane appears at 11.4°N, 78.6°W, at least to the accuracy of the satellite image.

Figure 5.21 presents the NMC 1000 mb analysis along with the station observations at the *same* time as Fig. 5.19. Note the correspondence of surface observations with satellite imagery: a rain shower reported from a ship 150 n mi northeast of the hurricane center, plus reports of rain from Howard Air Force Base, Panama (station 78806) and San José, Costa Rica (station 78762). While the visible imagery of Fig. 5.20 might, at first, lead to expectation of *only* cirriform cloudiness in the hurricane band from the northeast corner of Nicaragua toward Jamaica, the observation at Kingston Jamaica (station 78397) includes both low clouds (stratocumulus) and middle clouds (altocumulus) and the observation at the Guantanamo Bay Naval Air Station, Cuba (station 78367) is overcast with multilayered cloudiness. The station in central Cuba, believed to be Camagüey (station 78255), *does* report only two- to three-tenths cloud cover which is in agreement with the apparent lack of cloudiness on the IR imagery of Fig. 5.19; however, that station is reporting both cumulus of considerable development and cirrus—obviously imagery having only 4 km resolution **fails** to show scattered cloudiness!

Figure. 5.22 is the Navy's transmission of the NHC Hurricane Joan forecast track, starting with its warning position (black circle farthest east) at 1200 UTC on 19 October. While the forecast landfall near Bluefields, Nicaragua is near perfect, the forecast time of landfall (1200 UTC 21 October) is still *too early*, as the hurricane is about to become quasi-stationary. Finally, Fig. 5.23 shows the FNOC significant wave height analysis at 1200 UTC 19 October, indicating that wave heights have continued to increase and are now >30 feet just ahead of the hurricane.

2131 180088 39A-4 00911 15921 501

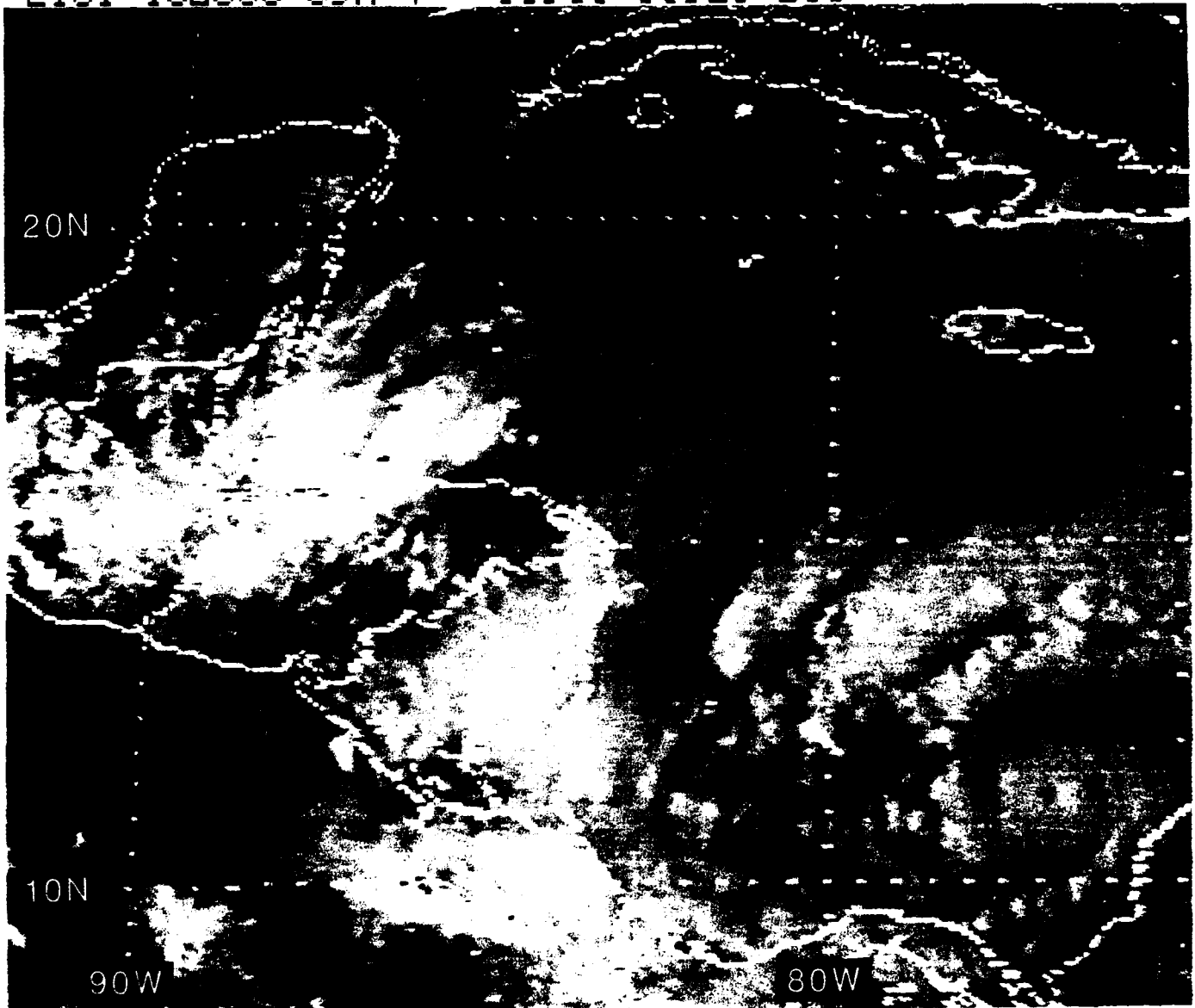


Figure 5.12: GOES East Visible Satellite Imagery, 2131 UTC 18 OCT 1988

2101 180C88 39E-42A 00901 15921 EC1

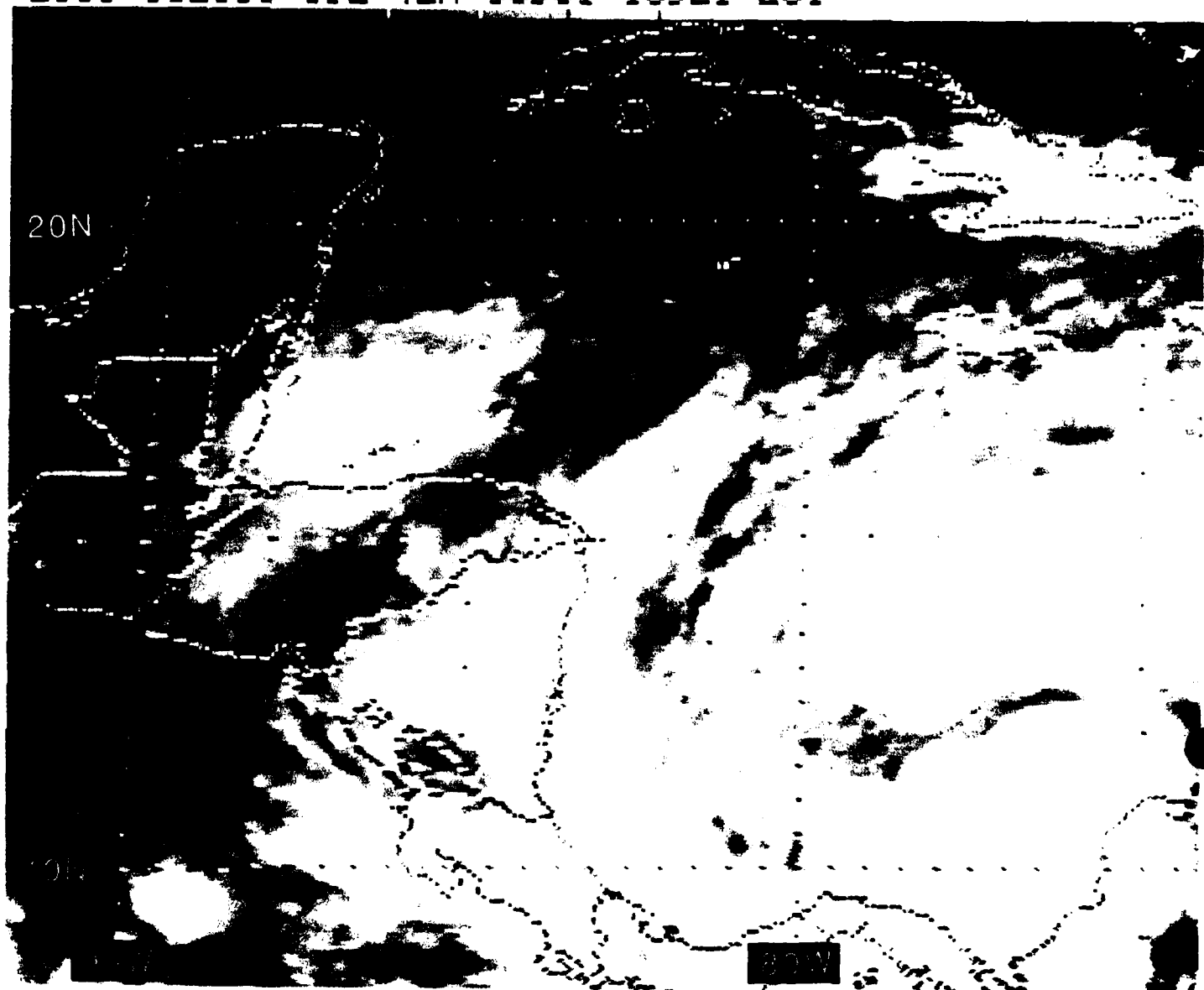


Figure 5.13: GOES East Infrared Satellite Imagery, 2101 UTC 18 OCT 1988

0001 190028 39E-42A 00911 15921 EC1

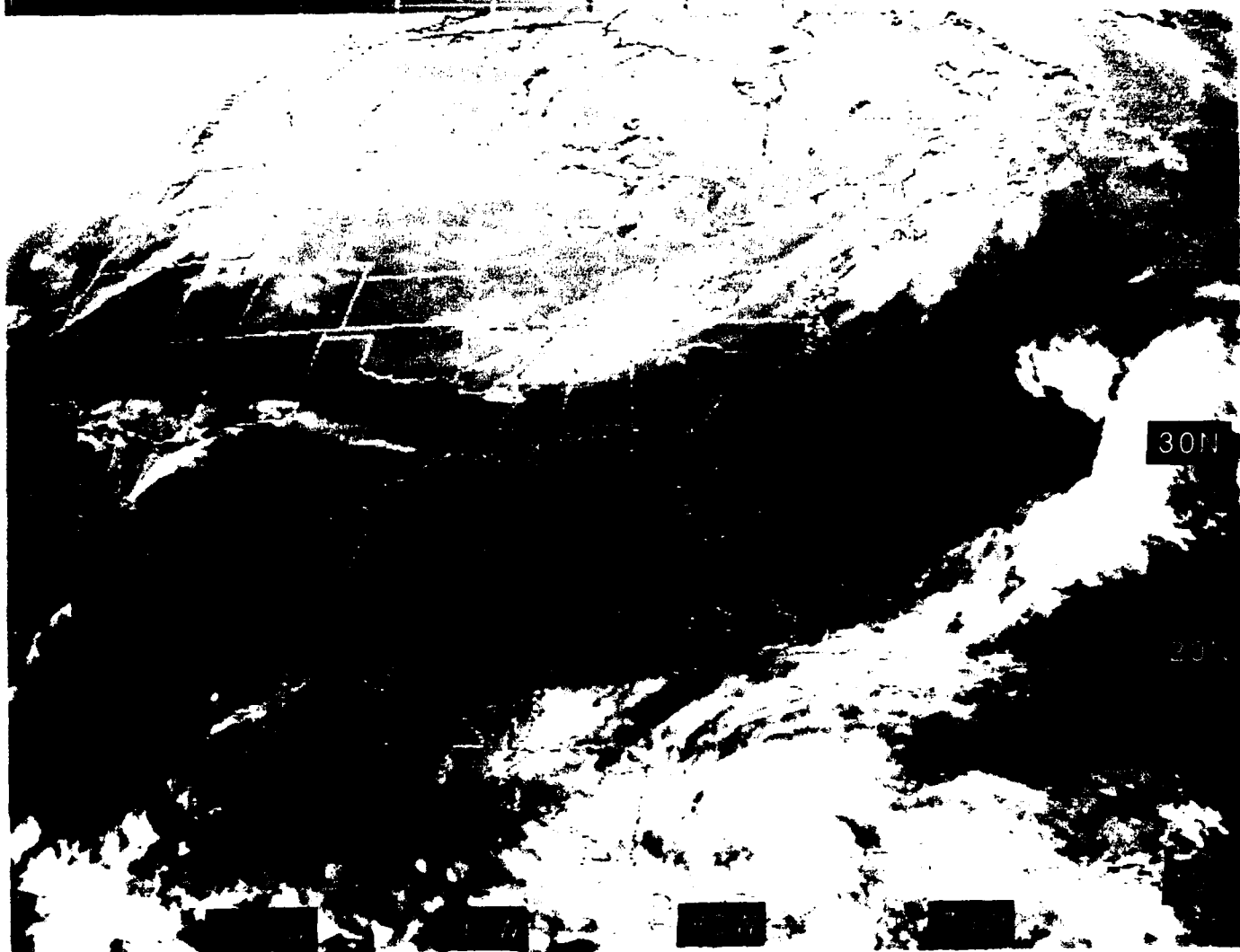


Figure 5.14: GOES East Infrared Satellite Imagery, 0001 UTC 19 OCT 1988

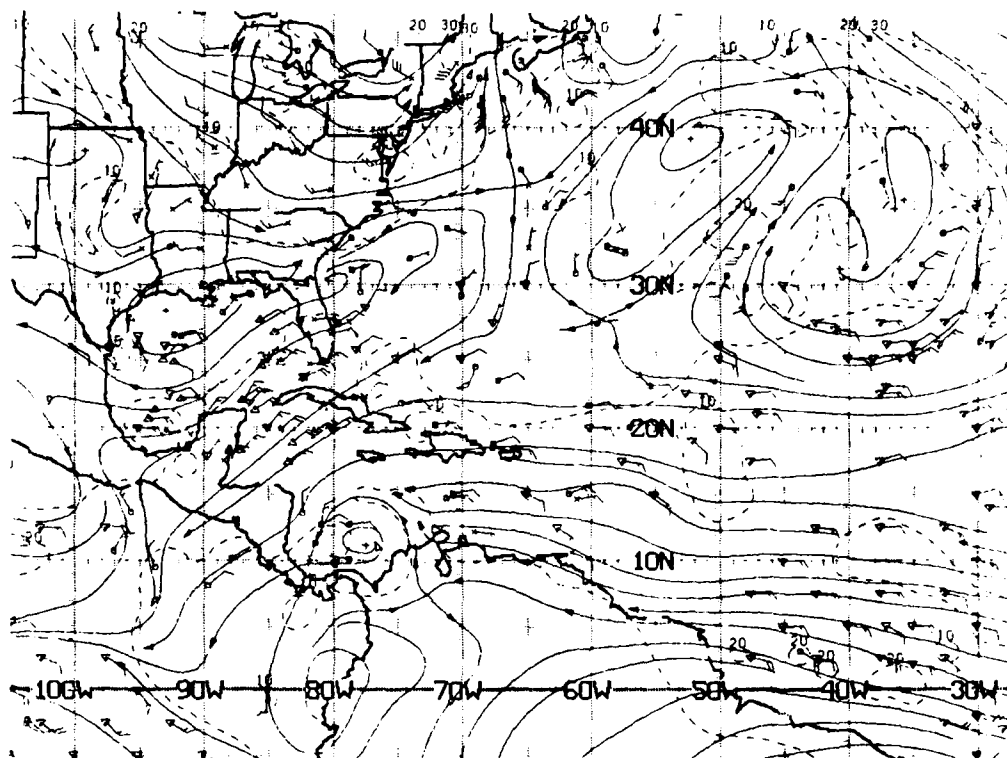


Figure 5.15: NMC ATOLL Operational Streamline Chart, 0000 UTC 19 OCT 1988
As in Fig. 2.4.

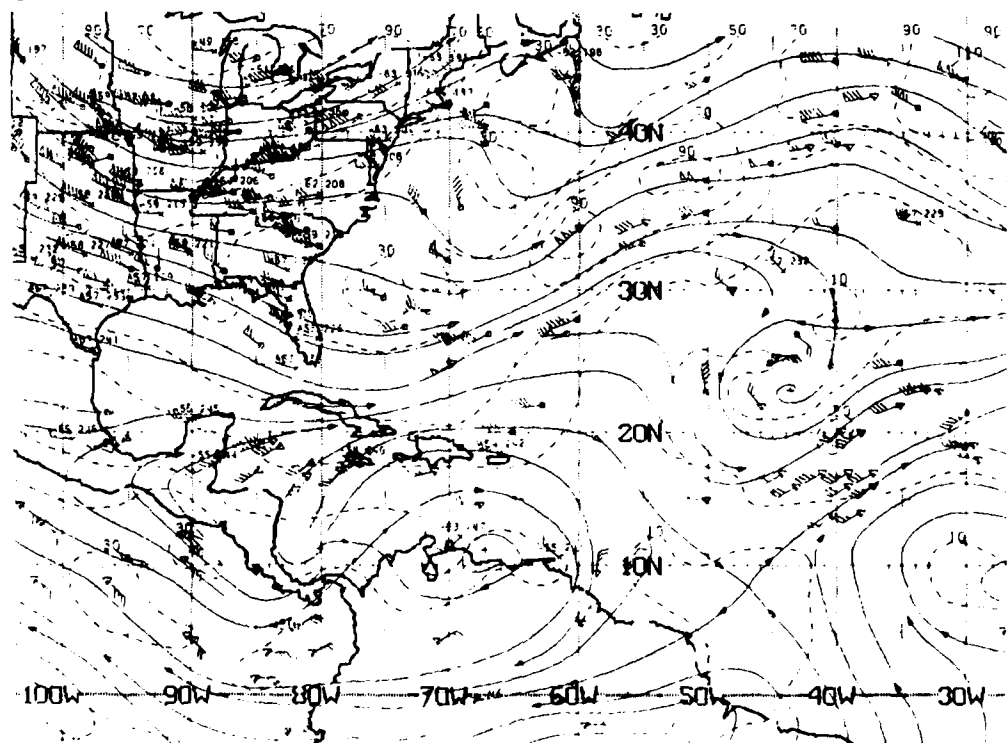


Figure 5.16: NMC 200 mb Operational Streamline Chart, 0000 UTC 19 OCT 1988
As in Fig. 2.6.

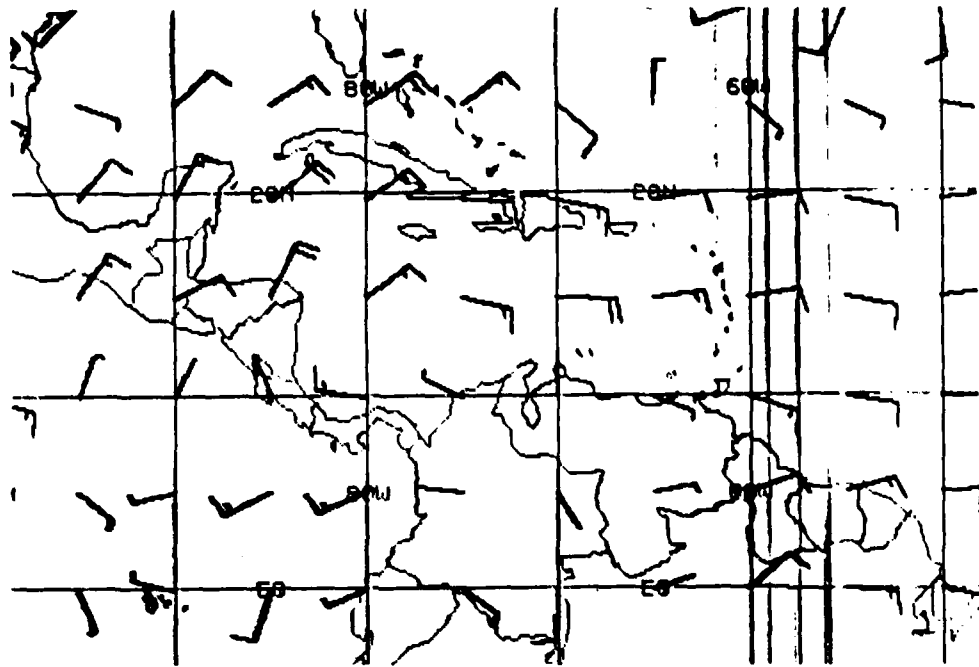


Figure 5.17: FNOG 925 mb Winds, 0000 UTC 19 OCT 1988. As in Fig. 2.19.

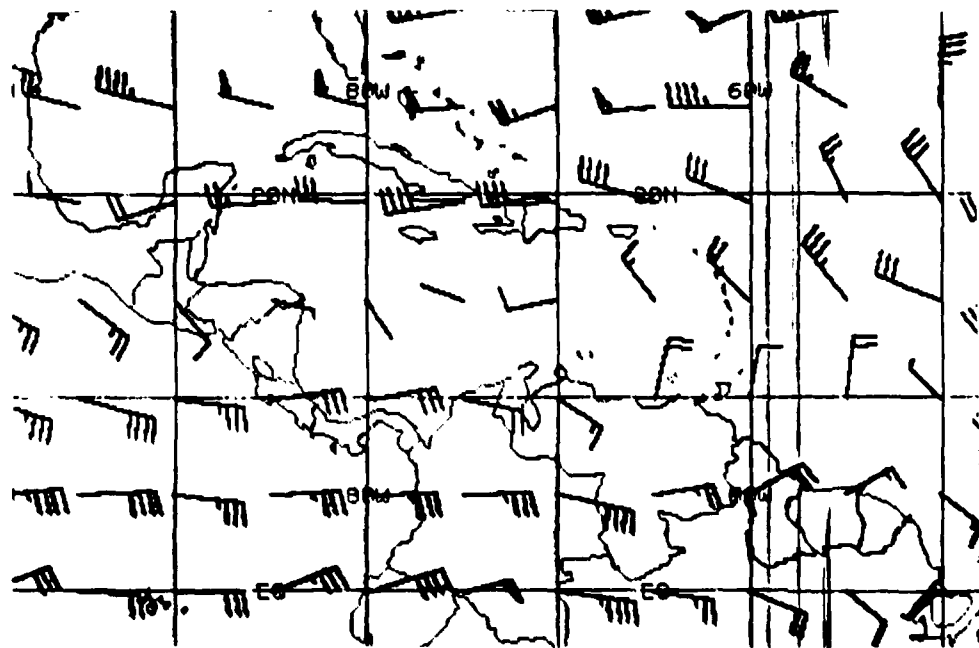


Figure 5.18: FNOG 200 mb Winds, 0000 UTC 19 OCT 1988. As in Fig. 2.20.

1201 190C88 39E-42A 00921 15971 EC1

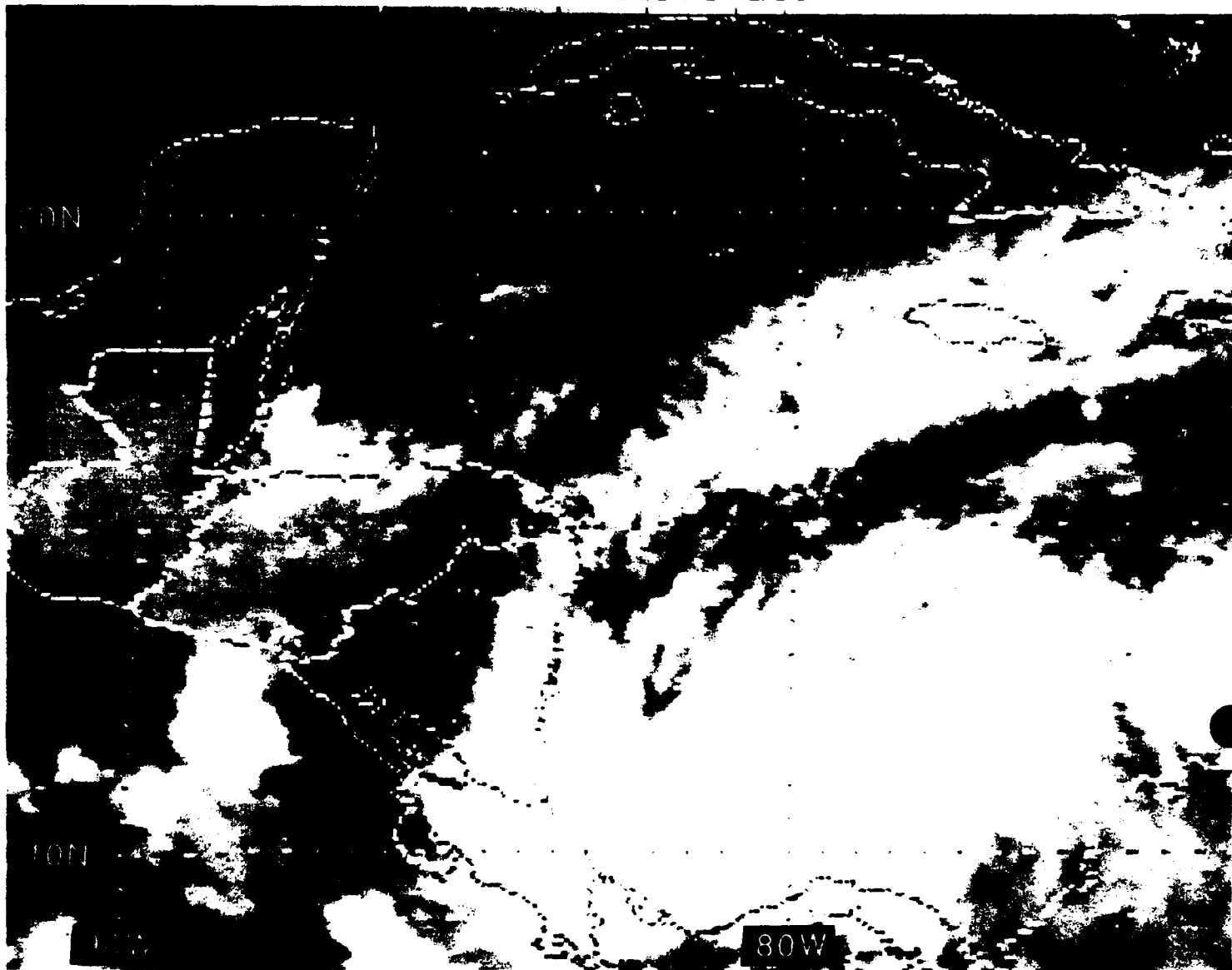


Figure 5.19: GOES East Infrared Satellite Imagery, 1201 UTC 19 OCT 1988

1431 190C88 39A-4 00911 15961 EC1

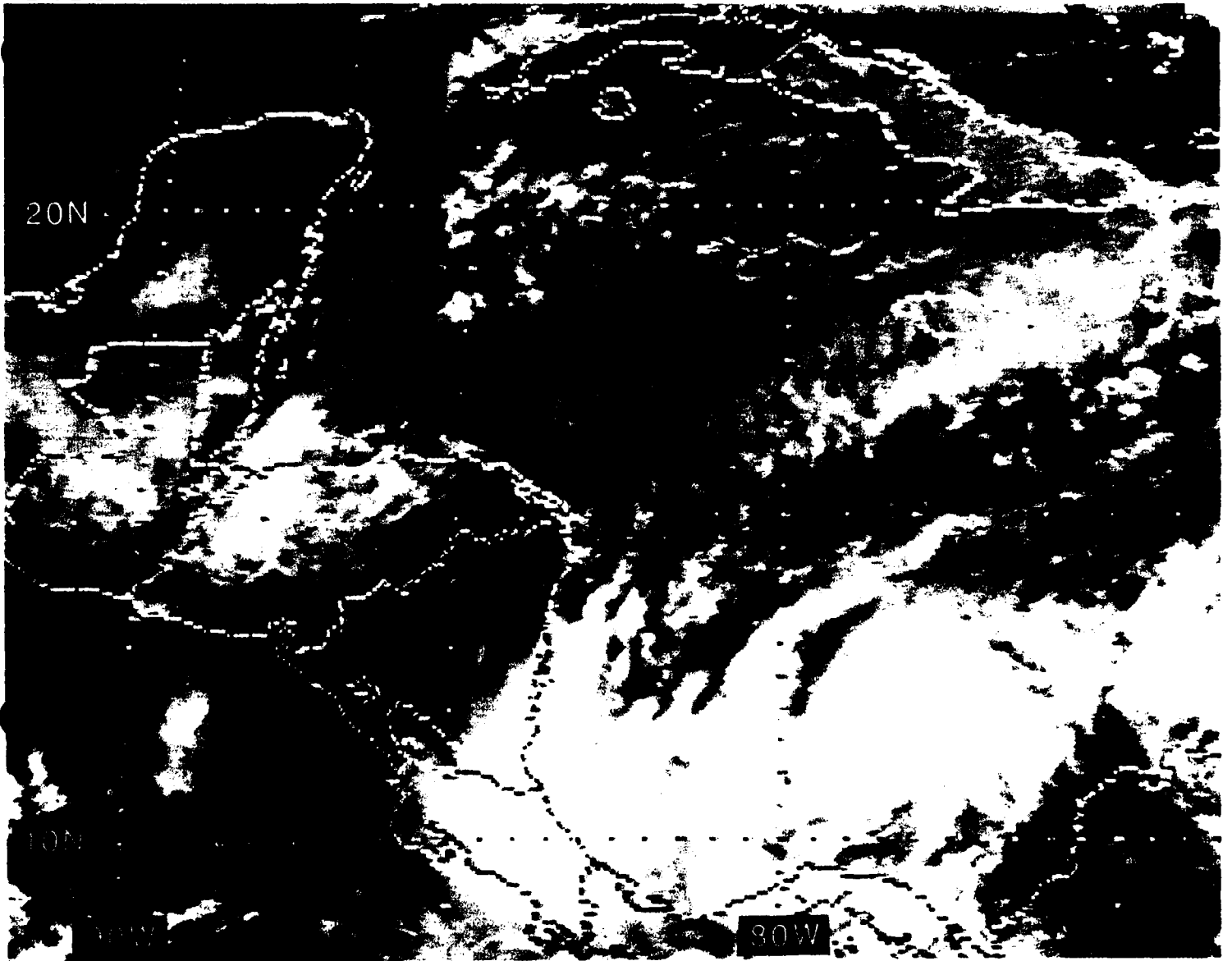


Figure 5.20: GOES East Visible Satellite Imagery, 1431 UTC 19 OCT 1988

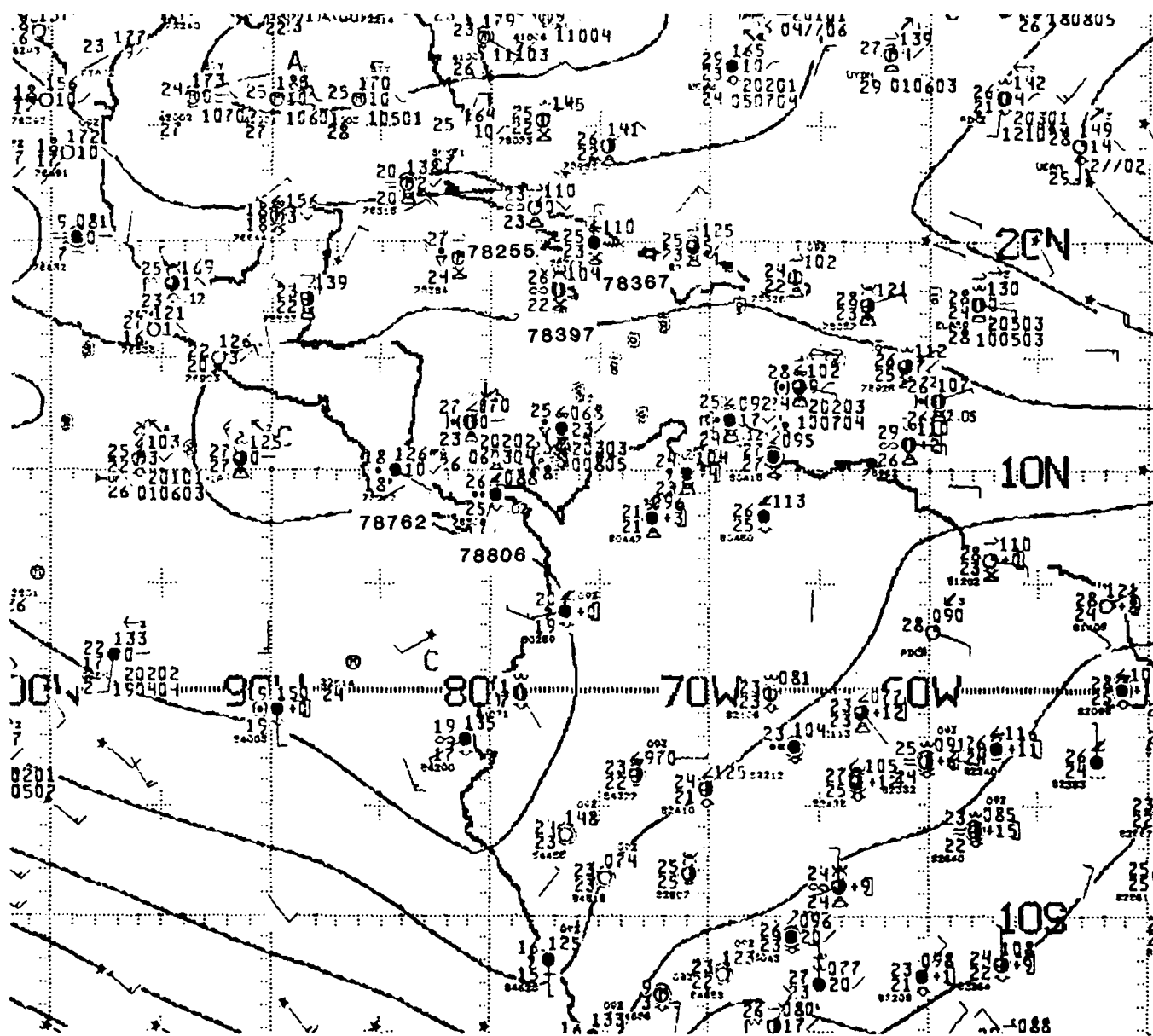


Figure 5.21: NMC 1000 mb Analysis, 1200 UTC 19 OCT 1988. As in Fig. 2.21.

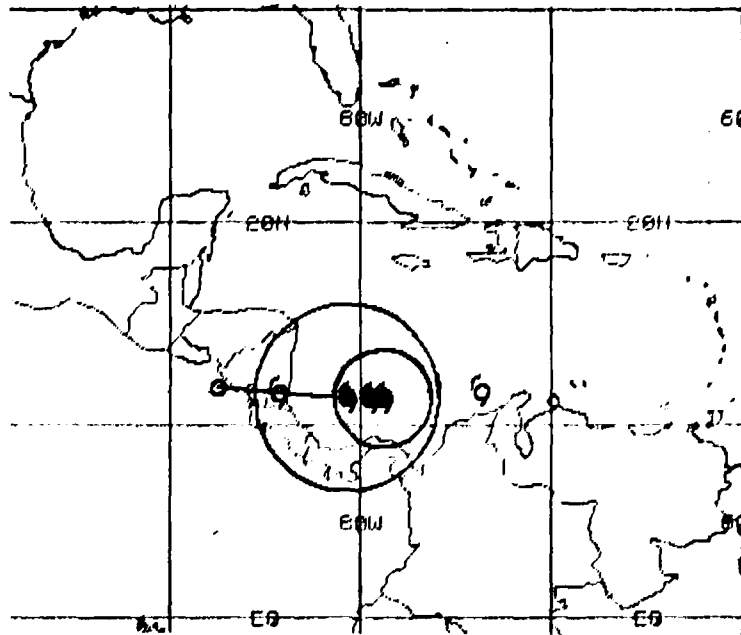


Figure 5.22: Tropical Cyclone FORECAST Track from 1200 UTC 19 OCT 1988.

Current position of hurricane is rightmost *black* symbol *enclosed* by the circle depicting the outer radius of gale force winds. Next, toward the left is the 12-h forecast position, followed by the 24-h forecast position *enclosed* by the circle depicting the outer radius of probable gale force winds—the inclusion of the expected 24-h position *error* produces such a **large** radius. The 48-h forecast position is a *downgraded* tropical storm on the southeastern coast of Nicaragua; finally, the 72-h forecast position is in the North Pacific Ocean.

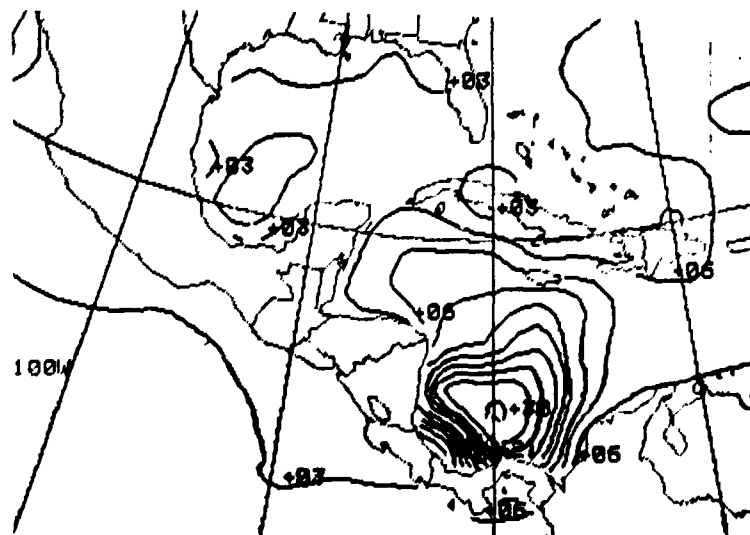


Figure 5.23: FNO Significant Wave Heights, 1200 UTC 19 OCT 1988. Isopleths are at 3-foot intervals.

20 October 1988

While this is a relatively uninteresting day as Hurricane Joan became *temporarily* stationary, it is unusual in that a tropical depression formed *only* ~400 n mi in the wake of Hurricane Joan. Figure 5.24, the IR imagery at 0001 UTC 20 October, shows both the position of the hurricane (11.3°N, 79.4°W) and the much smaller area of convection associated with Tropical Depression #18 placed at 13.0°N, 72.7°W⁹⁰ north of the Columbian coast by the National Hurricane Center.

The NMC low-level and high-level streamlines (Figs. 5.25 and 5.26), with their satellite and reconnaissance winds, depict both the hurricane's cyclonic inflow near the surface and the diffuent anticyclonic outflow aloft. The FNOC 925 mb winds (Fig. 5.27) depicts the low-level flow well; however, the FNOC 200 mb winds (Fig. 5.28) over both Honduras and Columbia do not possess the "outflow" components expected from such a strong hurricane, and confirmed in the satellite imagery and on the NMC 200 mb streamline analysis.

Comparing the 0000 UTC surface observations of Fig. 5.29 with the concurrent IR imagery of Fig. 5.24, note: a thunderstorm at Choluteca, Honduras (station 78724), continuous rain at David, Panama (station 78793), rain at Howard Air Force Base, Panama (station 78806), drizzle within the past hour at San Andrés Island (station 80001)—all under the high (cold) clouds in the IR imagery. However, Puerto Lempira, Honduras (station 78711) is under only 6/10 cloud cover; Merida, Mexico (station 76644 on the Yucatan peninsula) has only 1/4 cloud cover; plus western and central Cuban stations are reporting relatively clear conditions in agreement with the IR imagery of Fig. 5.24.

Figure 5.30 shows the FNOC significant wave heights. The maximum significant wave heights are surprisingly only >21 feet *now* compared to >30 feet just 12 hours earlier (see Fig. 5.23), despite the hurricane's having maintained its 100 kt winds.

In Fig. 5.31, the Navy's transmission of the NHC forecast track, the *four* 6-hourly positions of the hurricane preceding its warning position at 0600 UTC depicts its deceleration. The 48-h forecast places the hurricane's landfall correctly on the southeastern coast of Nicaragua at 0600 UTC 22 October, which was within two hours of the time of actual landfall.

While Fig. 5.32 depicts the 1201 UTC infrared imagery, the visible imagery in Fig. 5.33 shows that the eye of Hurricane Joan has **not** yet reached the 80th meridian by 1431 UTC 20 October.

⁹⁰The center of the depression is on the *western* periphery of the small convective area depicted on the IR imagery of Fig. 5.24.

0001 200C88 39E-42A 00911 15941 EC1

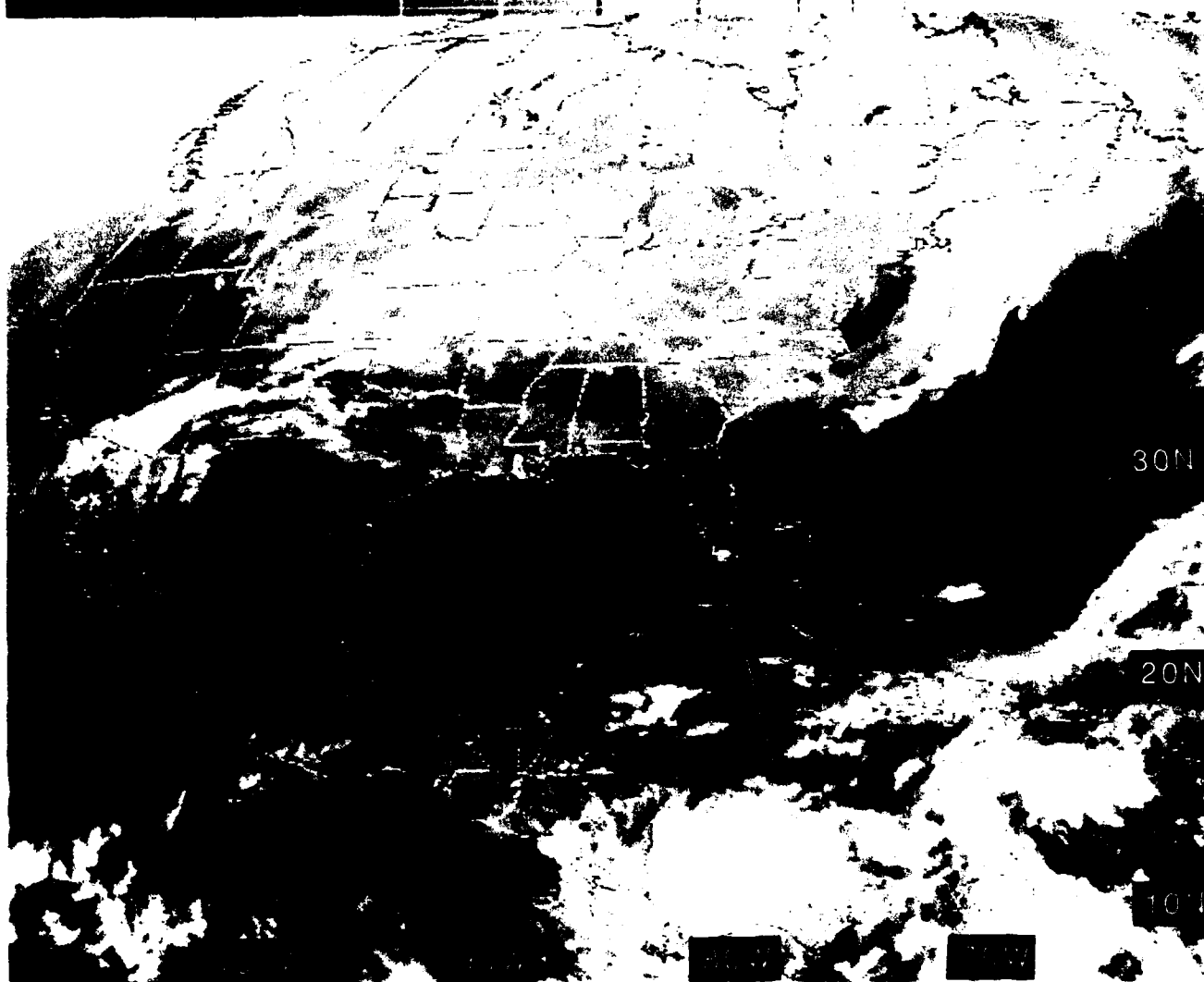


Figure 5.24: GOES East Infrared Satellite Imagery, 0001 UTC 20 OCT 1988

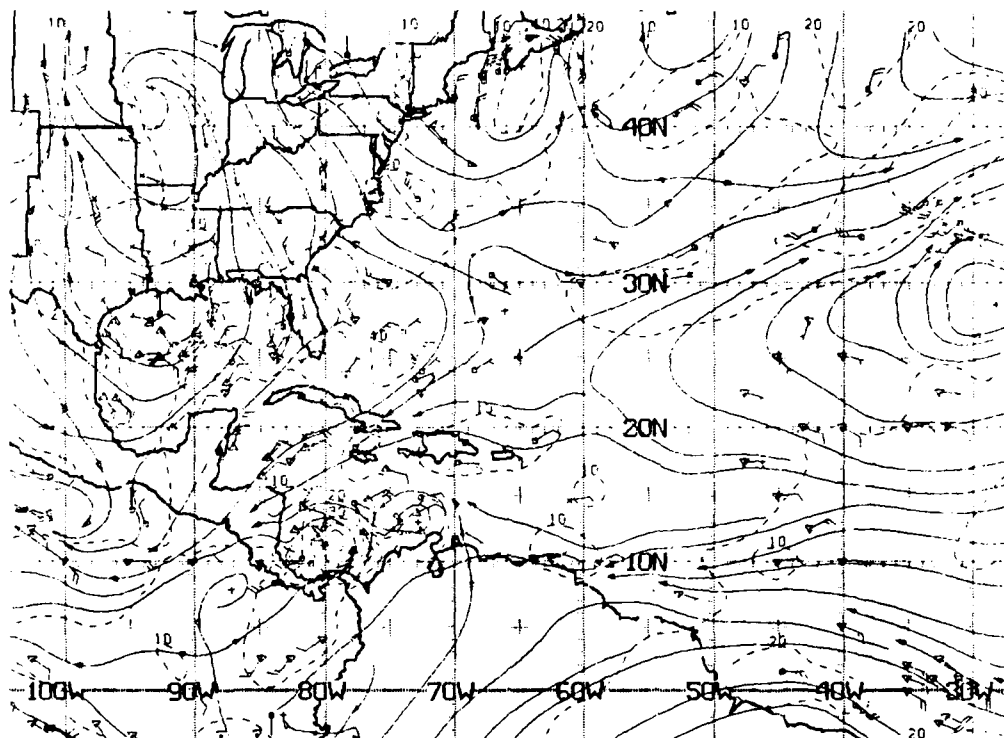


Figure 5.25: NMC ATOLL Operational Streamline Chart, 0000 UTC 20 OCT 1988
As in Fig. 2.4.

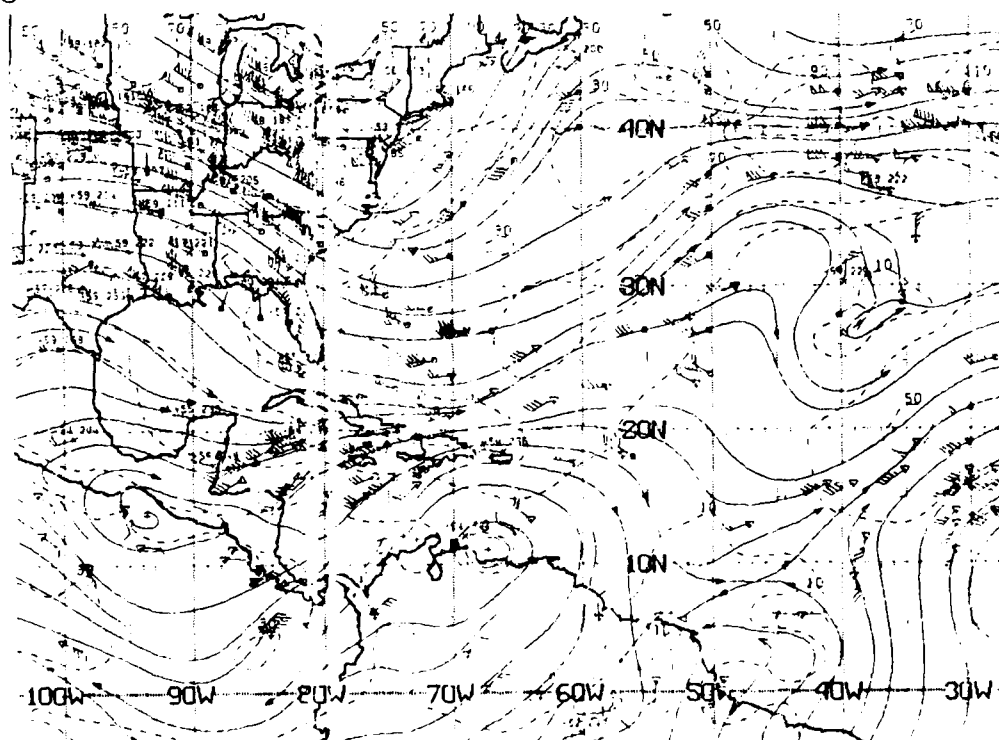


Figure 5.26: NMC 200 mb Operational Streamline Chart, 0000 UTC 20 OCT 1988
As in Fig. 2.6.

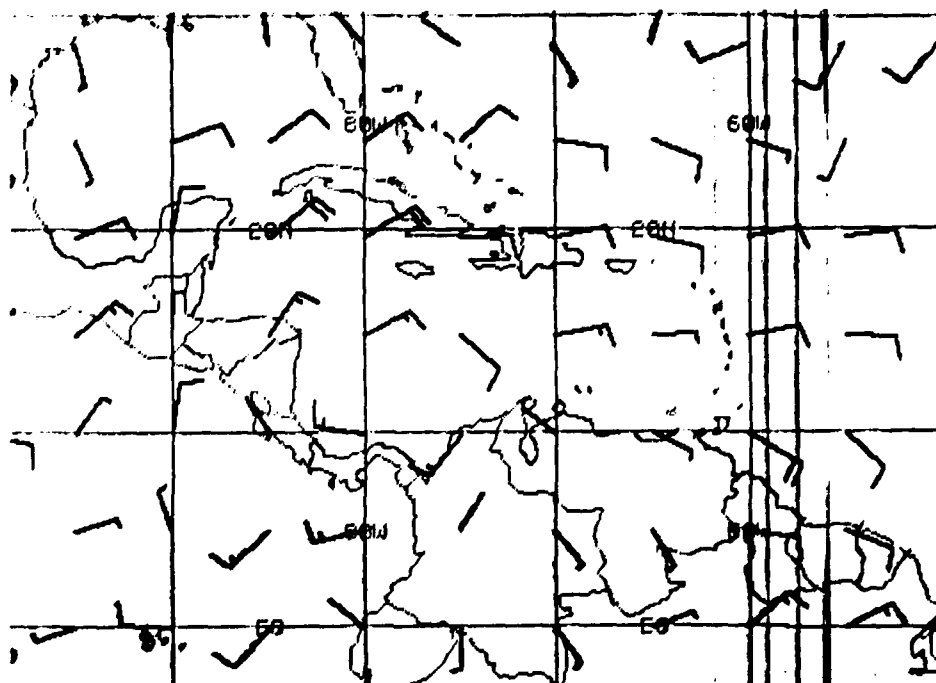


Figure 5.27: FNOC 925 mb Winds, 0000 UTC 20 OCT 1988. As in Fig. 2.19.

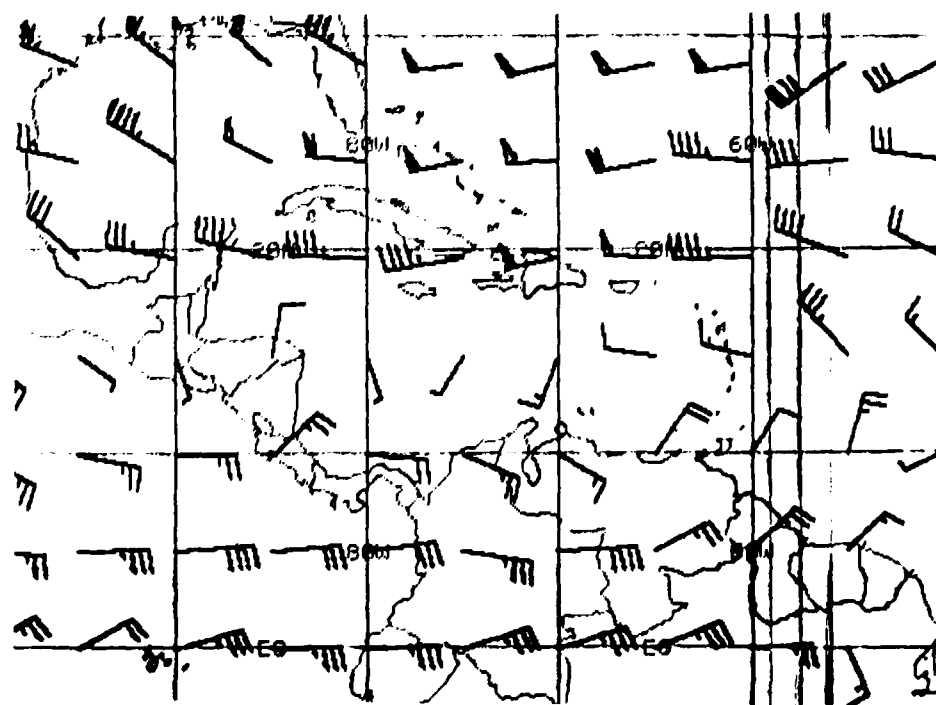


Figure 5.28: FNOC 200 mb Winds, 0000 UTC 20 OCT 1988. As in Fig. 2.20.

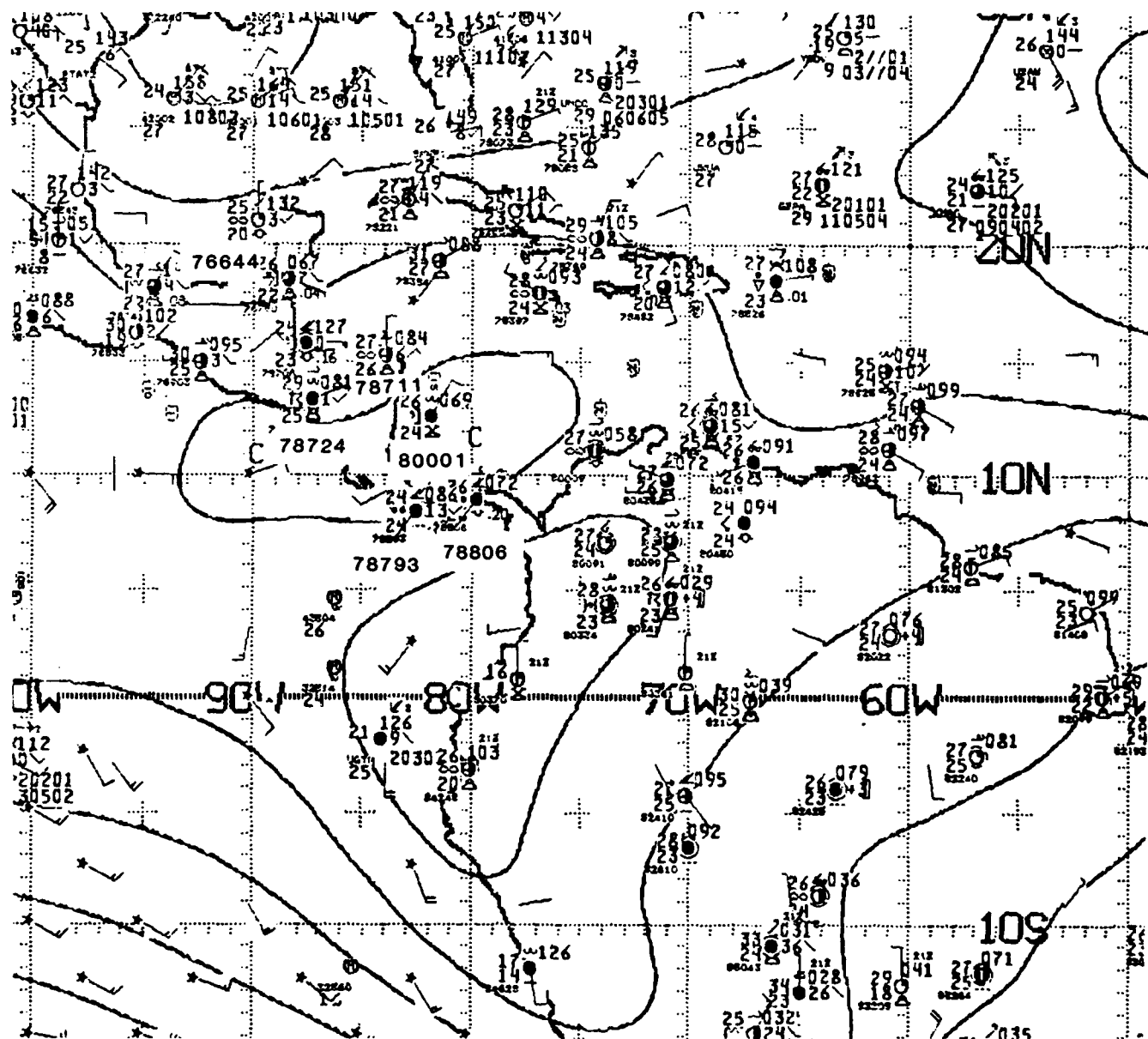


Figure 5.29: NMC 1000 mb Analysis, 0000 UTC 20 OCT 1988. As in Fig. 2.21.

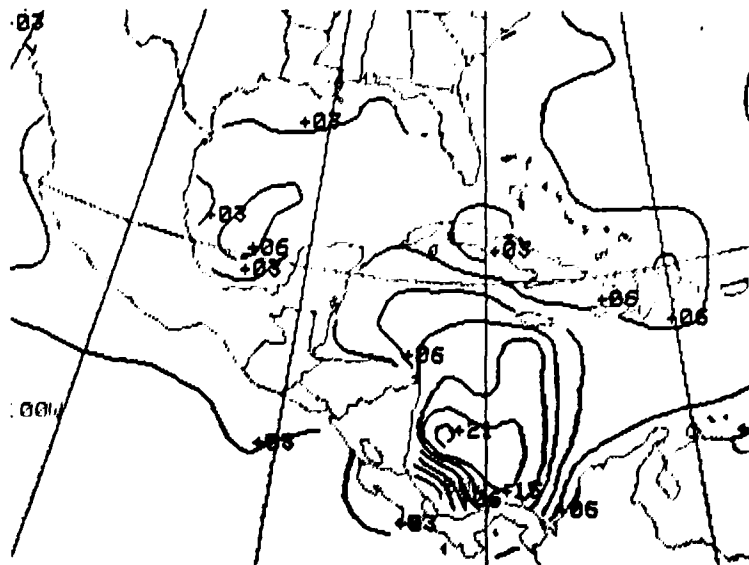


Figure 5.30: FNOC Significant Wave Heights, 0000 UTC 20 OCT 1988. Isopleths are at 3-foot intervals.

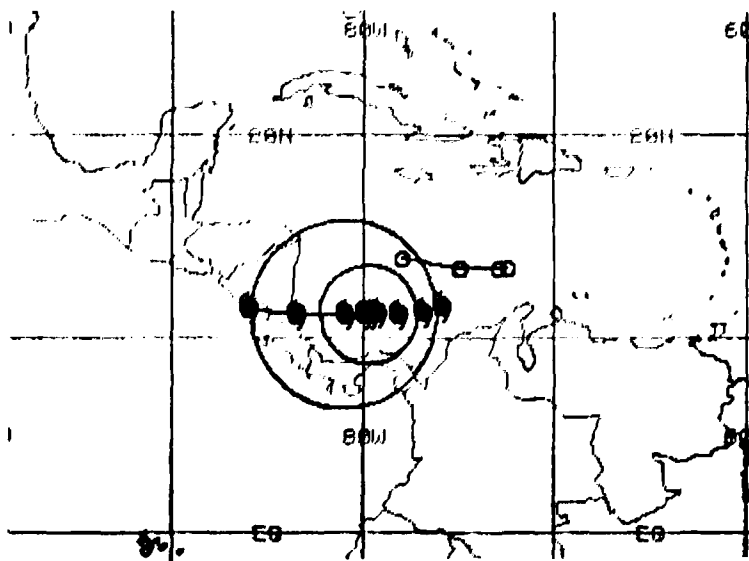


Figure 5.31: Tropical Cyclone FORECAST Track from 0600 UTC 20 OCT 1988. Current position of hurricane is fifth hurricane symbol (from the right) *enclosed* by the smaller circle depicting the outer radius of gale force winds. The larger circle depicts the outer radius of gale winds centered on the 24-h forecast position—expanded outward to include the expected 24-h forecast position error. The 48-h and 72-h forecast positions are, respectively, on the Caribbean and Pacific coasts Nicaragua. The warning and forecast positions of *short-lived* Tropical Depression #18 are plotted on the starboard quarter of Hurricane Joan's track.

1201 20DC88 39E-4ZA 00912 15991 EC1

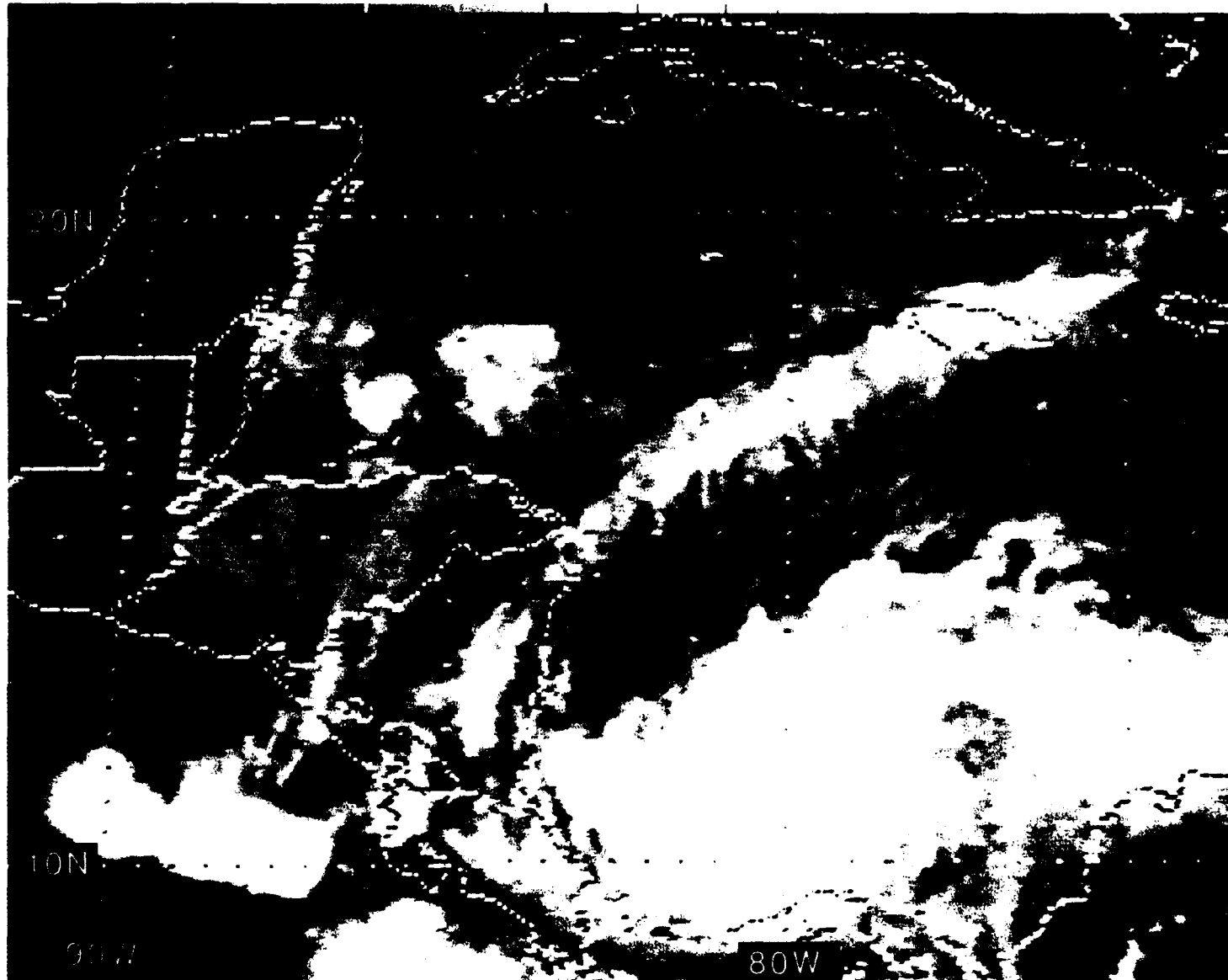


Figure 5.32: GOES East Infrared Satellite Imagery, 1201 UTC 20 OCT 1988

1431 200088 39A-4 00901 15981 EC1

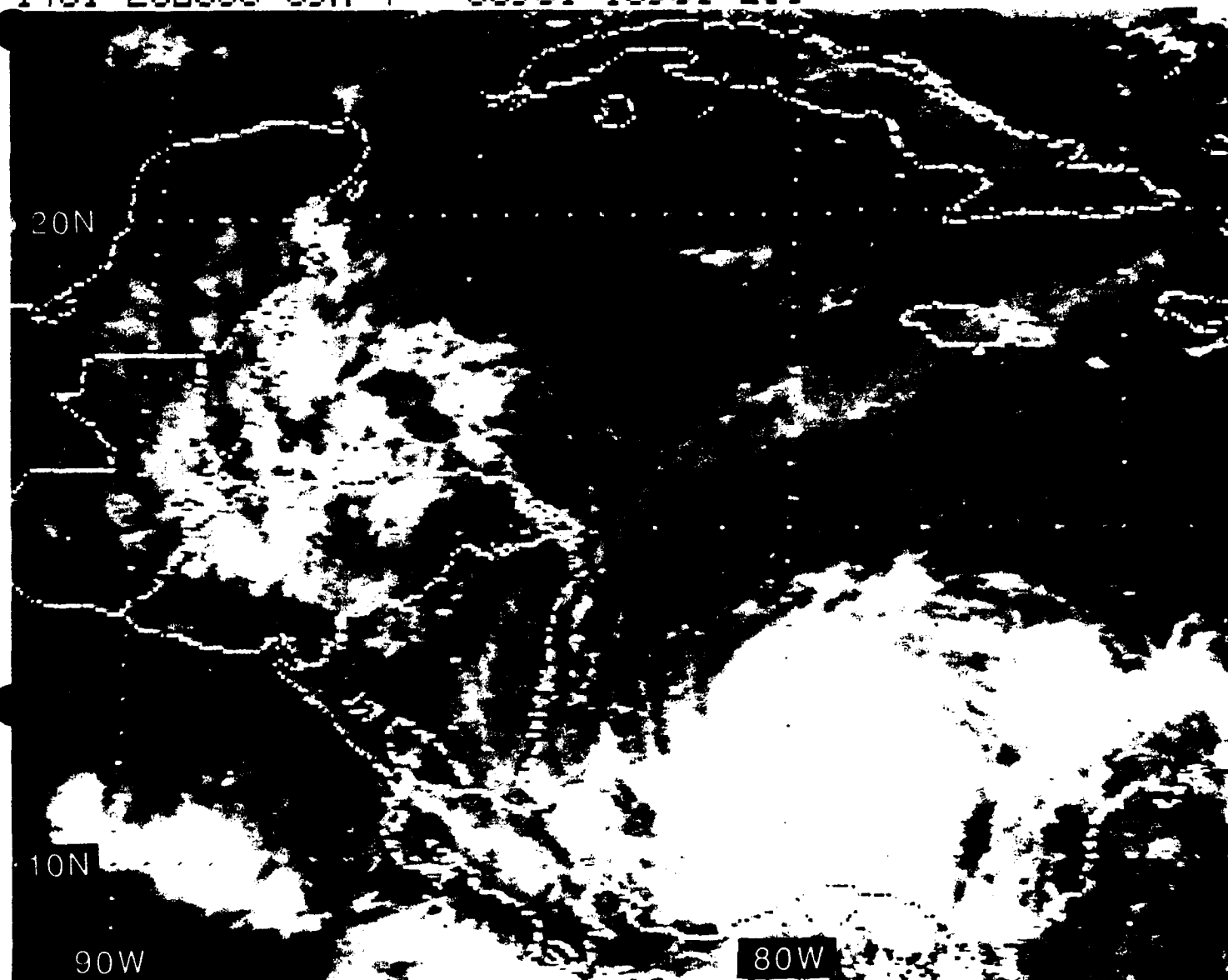


Figure 5.33: GOES East Visible Satellite Imagery, 1431 UTC 20 OCT 1988

21 October 1988

The infrared imagery of Fig. 5.34 shows that Hurricane Joan has finally moved past 80°W and is located by NHC at 11.5°N, 80.2°W at 0000 UTC 21 October. While Tropical Depression #18 is identified near 14°N, 71°W and stationary, it dissipated before 2200 UTC on 21 October. Figure 5.35, the NMC ATOLL chart, depicts very well the low-level cyclonic flow around Hurricane Joan, while the neutral point on the southwest coast of Costa Rica is easily visualized. However, Tropical Depression #18 is not identifiable. Figure 5.36, the NMC 200 mb chart, with its many satellite winds depicts the strong divergence aloft over the hurricane. In particular, one of the upper-level *outflow* channels, with its southwesterly winds, extending beyond Jamaica and Hispaniola, is located over the opposing *inflow* near the surface (Fig. 5.35).

The FNOC winds at 0000 UTC (Figs. 5.37 and 5.38) are in good agreement with the NMC streamlines. However, the FNOC 200 mb winds south of Jamaica (Fig. 5.38) should be more southwesterly as seen in the streamlines of Fig. 5.36.

The station observations in Fig. 5.39, correspond to the time of the IR imagery of Fig. 5.40, which is a "blown-up" portion of Fig. 5.34. Note the rain at Howard Air Force Base, Panama (station 78806), but only drizzle within the past hour at San Andrés Island (station 80001—located near the double dots on Fig. 5.40 at the western side of the upper-level cloud shield of Hurricane Joan). San Andrés Island will shortly receive the full force of the hurricane. Isolated precipitation depicted by the small areas of white on the IR imagery of Fig. 5.40 are confirmed by continuous drizzle over Tela, Honduras (station 78706) and lightning with towering cumulus at Kingston, Jamaica (station 78397) as reported on Fig. 5.39. The dark gray imagery on Fig. 5.40 over the Yucatan peninsula identifies a *low* overcast with no precipitation at Merida, Mexico (station 76644) on Fig. 5.39.

Figures 5.41 and 5.42 show the respective IR and visible imagery about 12 hours later, with the eye of the hurricane ~100 n mi southeast of San Andrés Island. Just two hours earlier, the NHC located Hurricane Joan based on Air Force reconnaissance and satellite imagery at 11.6°N, 81.1°W, moving west at 5 kt, having maximum sustained winds of 90 kt, with gusts to 105 kt.

At 1200 UTC, Fig. 5.43 shows the FNOC significant wave heights >27 feet in the vicinity of San Andrés Island, while the latest hurricane forecast chart, (Fig. 5.44), predicts landfall for Hurricane Joan shortly after 1200 UTC on 22 October.

0001 21DC88 39E-4ZA 00911 15951 EC1

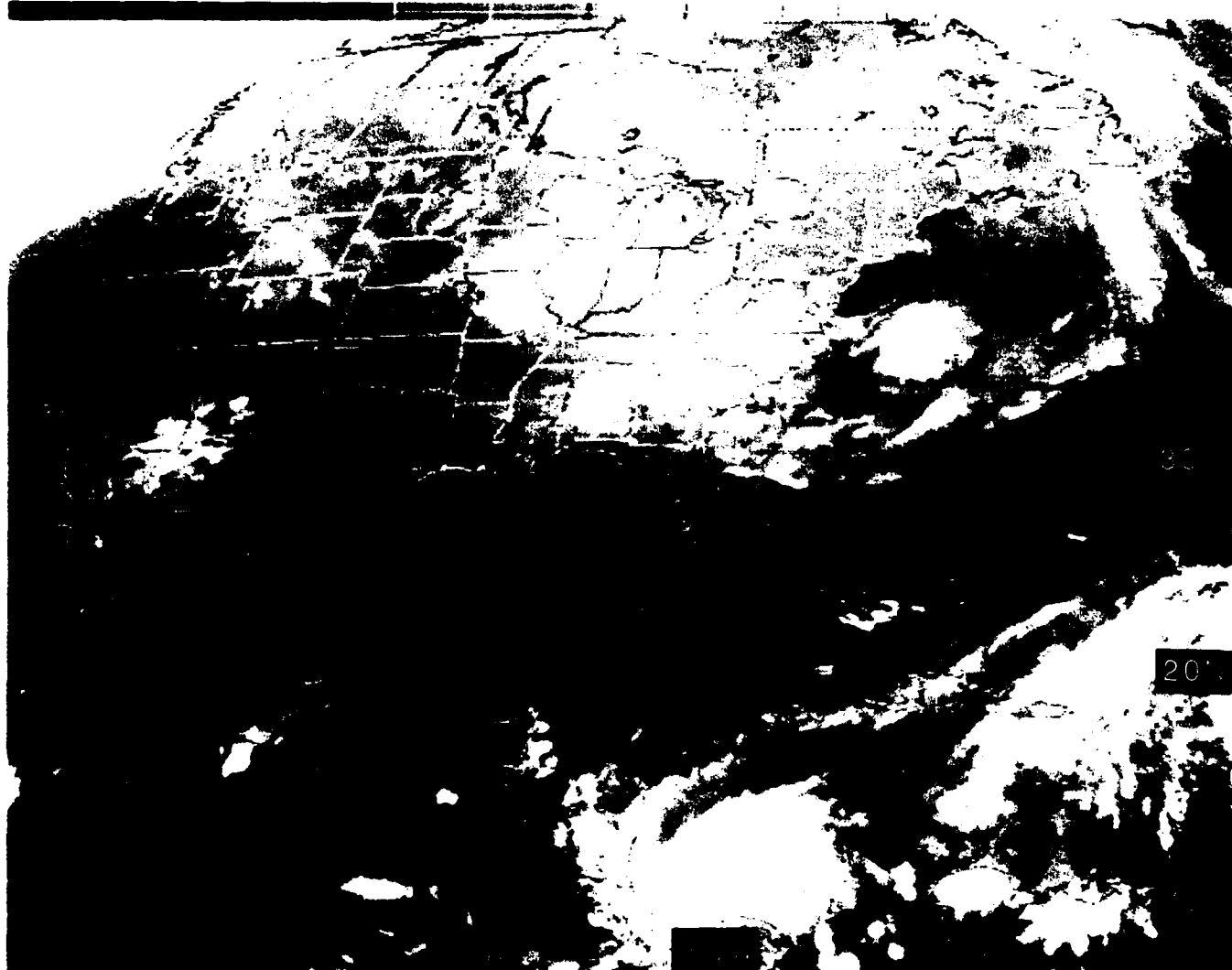


Figure 5.34: GOES East Infrared Satellite Imagery, 0001 UTC 21 OCT 1988

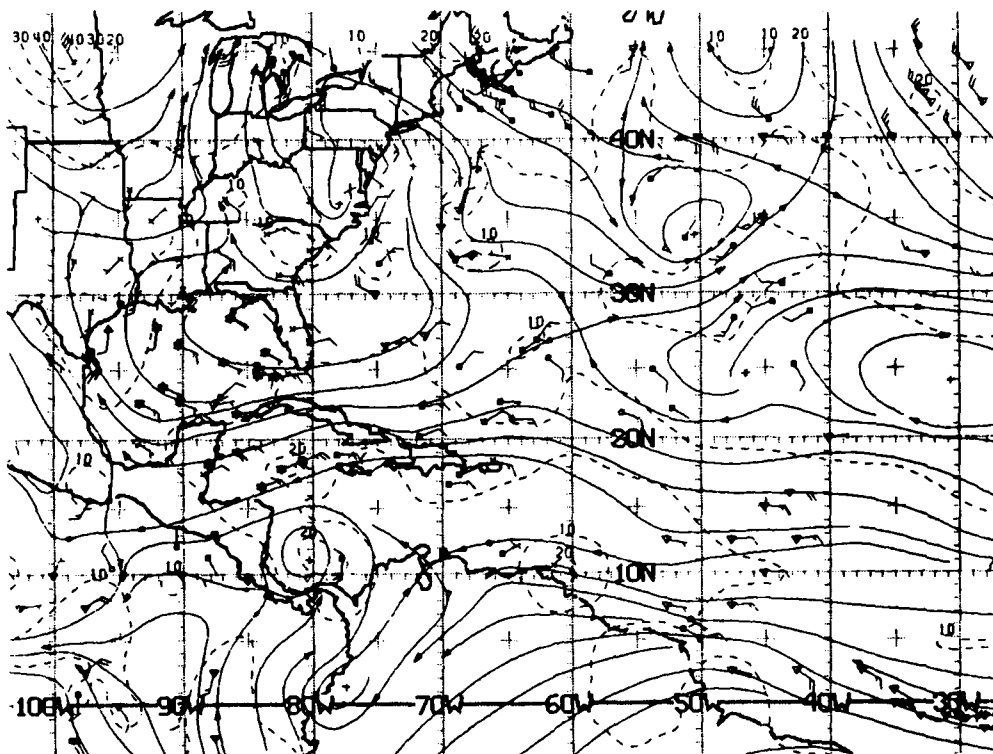


Figure 5.35: NMC ATOLL Operational Streamline Chart, 0000 UTC 21 OCT 1988
As in Fig. 2.4.

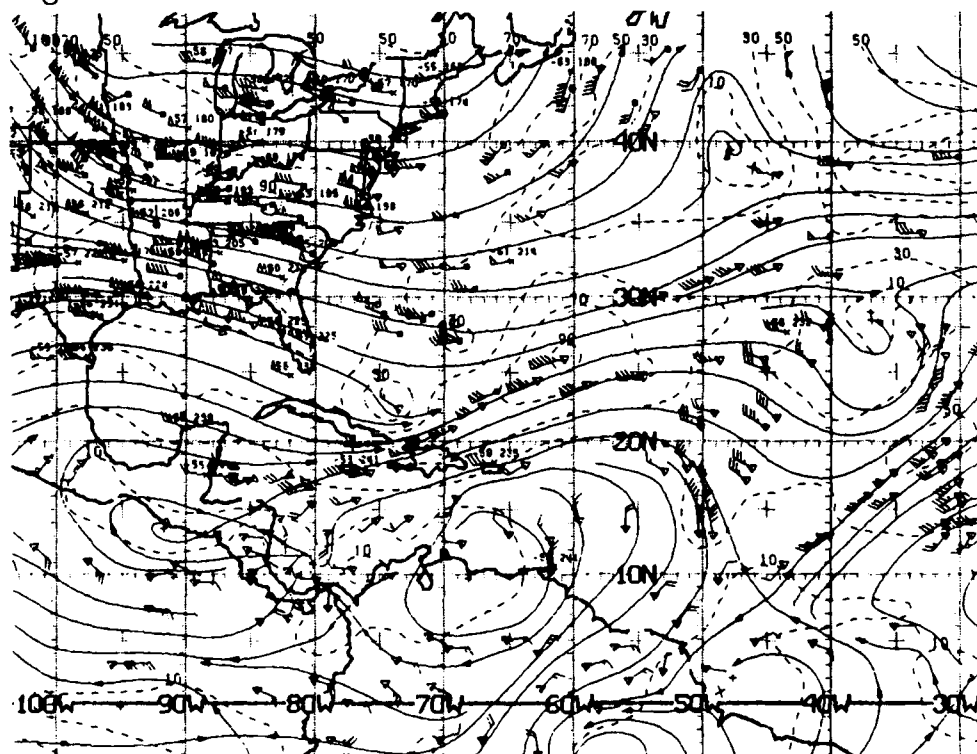


Figure 5.36: NMC 200 mb Operational Streamline Chart, 0000 UTC 21 OCT 1988
As in Fig. 2.6.

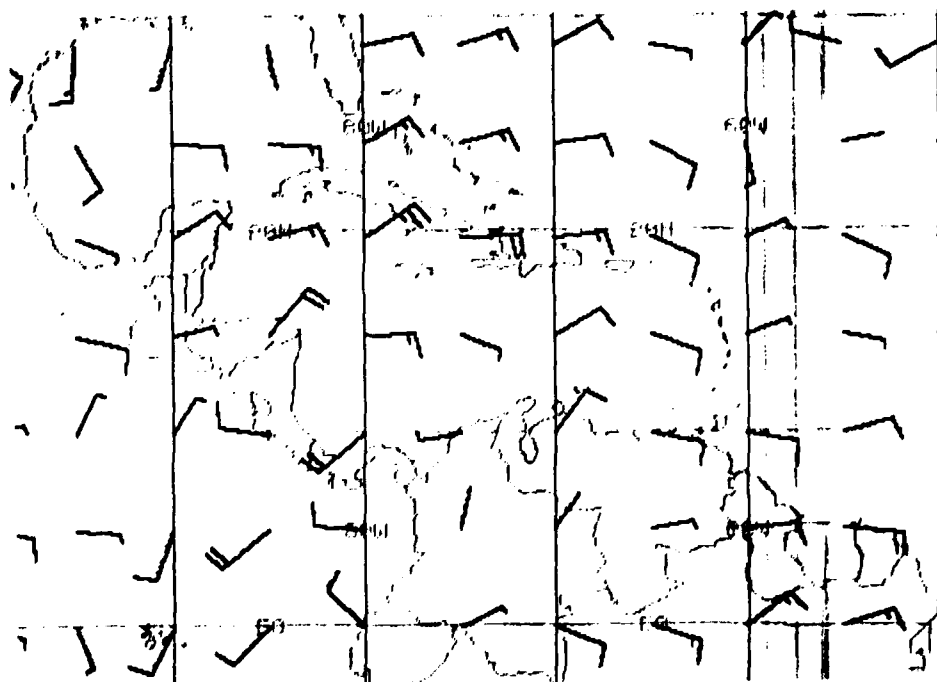


Figure 5.37: FNOG 925 mb Winds, 0000 UTC 21 OCT 1988. As in Fig. 2.19.

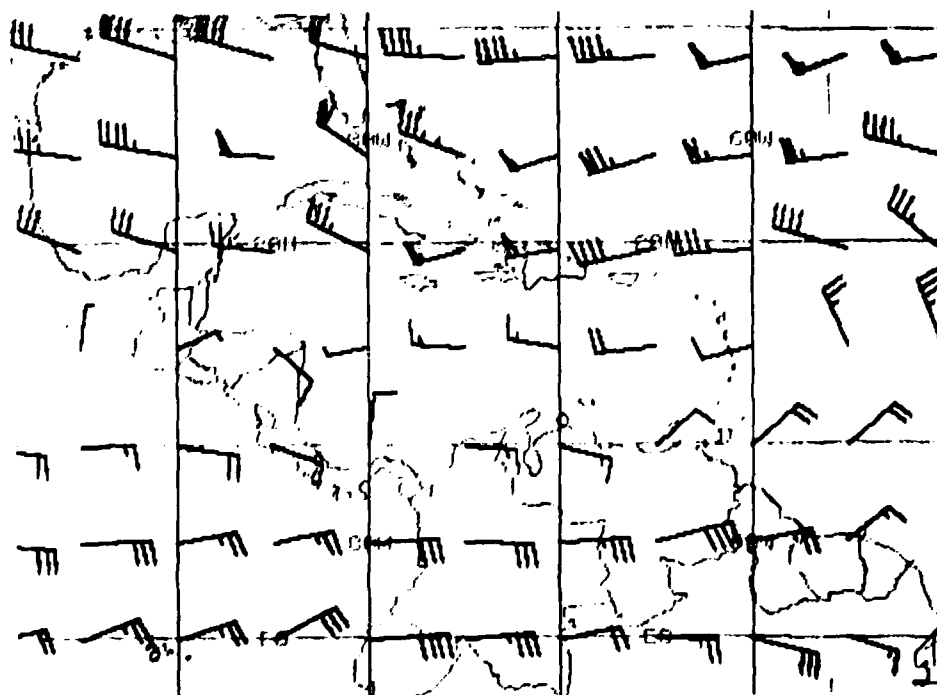


Figure 5.38: FNOG 200 mb Winds, 0000 UTC 21 OCT 1988. As in Fig. 2.20.

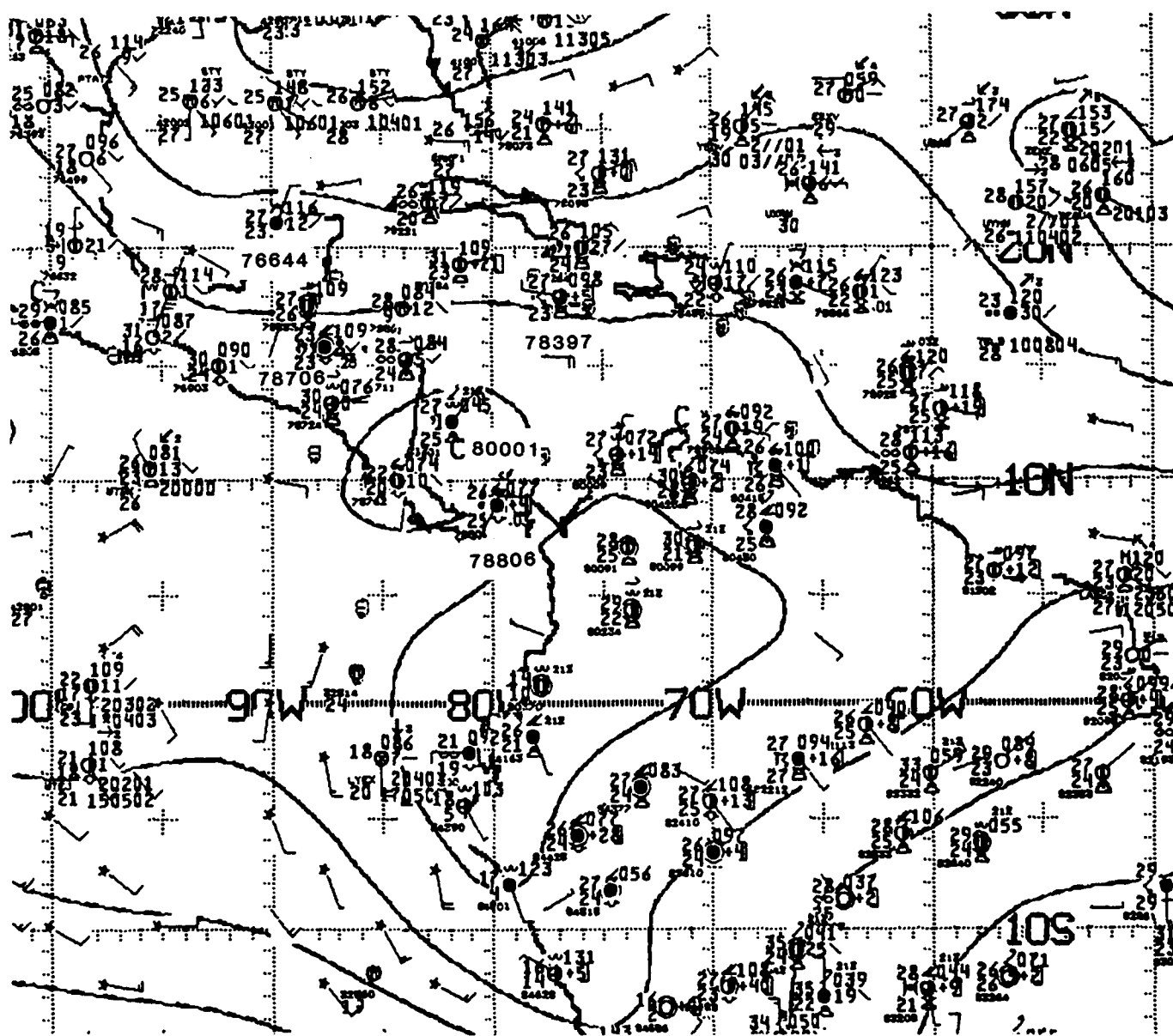


Figure 5.39: NMC 1000 mb Analysis, 0000 UTC 21 OCT 1988. As in Fig. 2.21.

0001 210C88 39E-42A 00911 15951 EC1

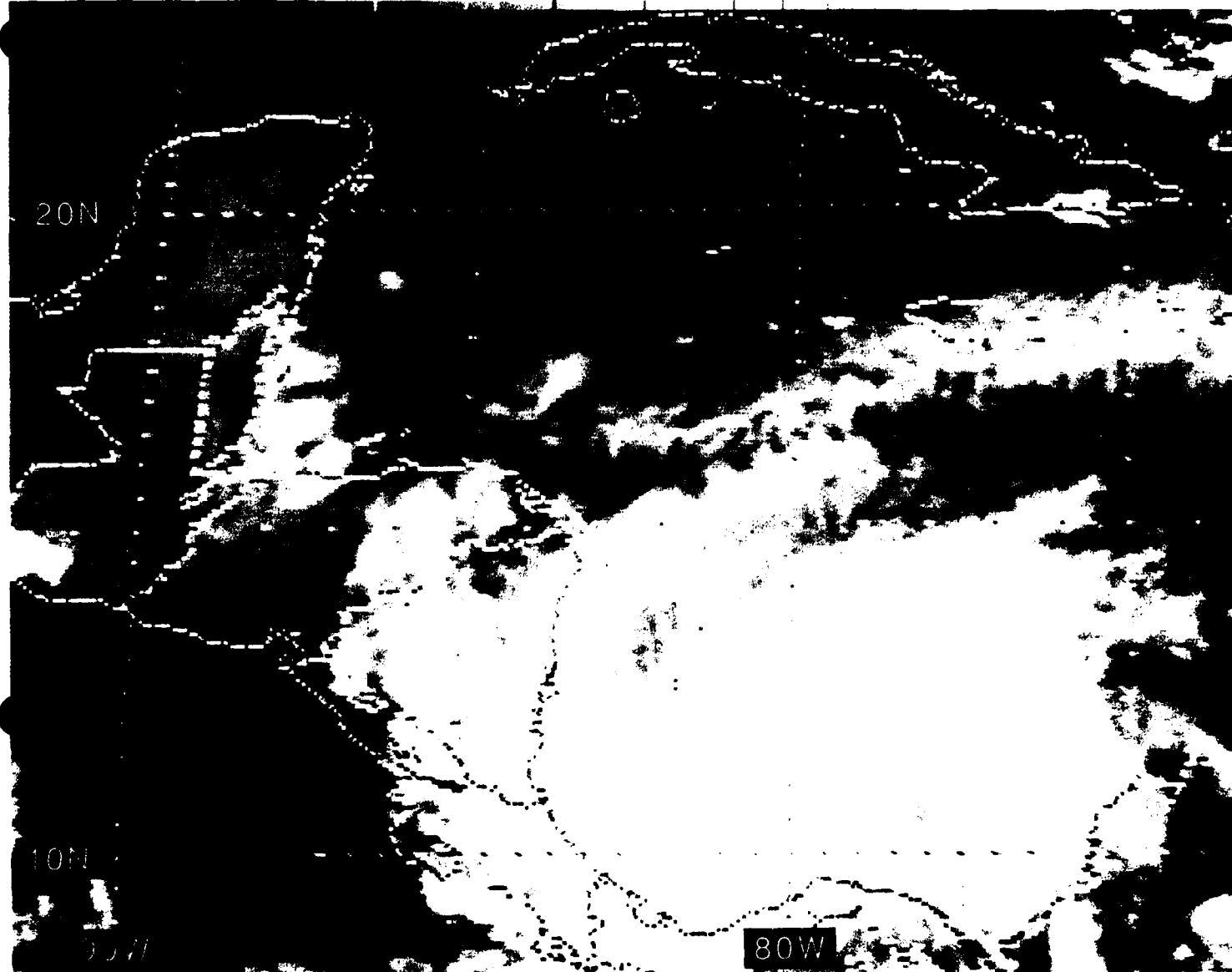


Figure 5.40: GOES East Infrared Satellite Imagery, 0001 UTC 21 OCT 1988

1201 21DC88 39E-4ZA 00921 16011 EC1

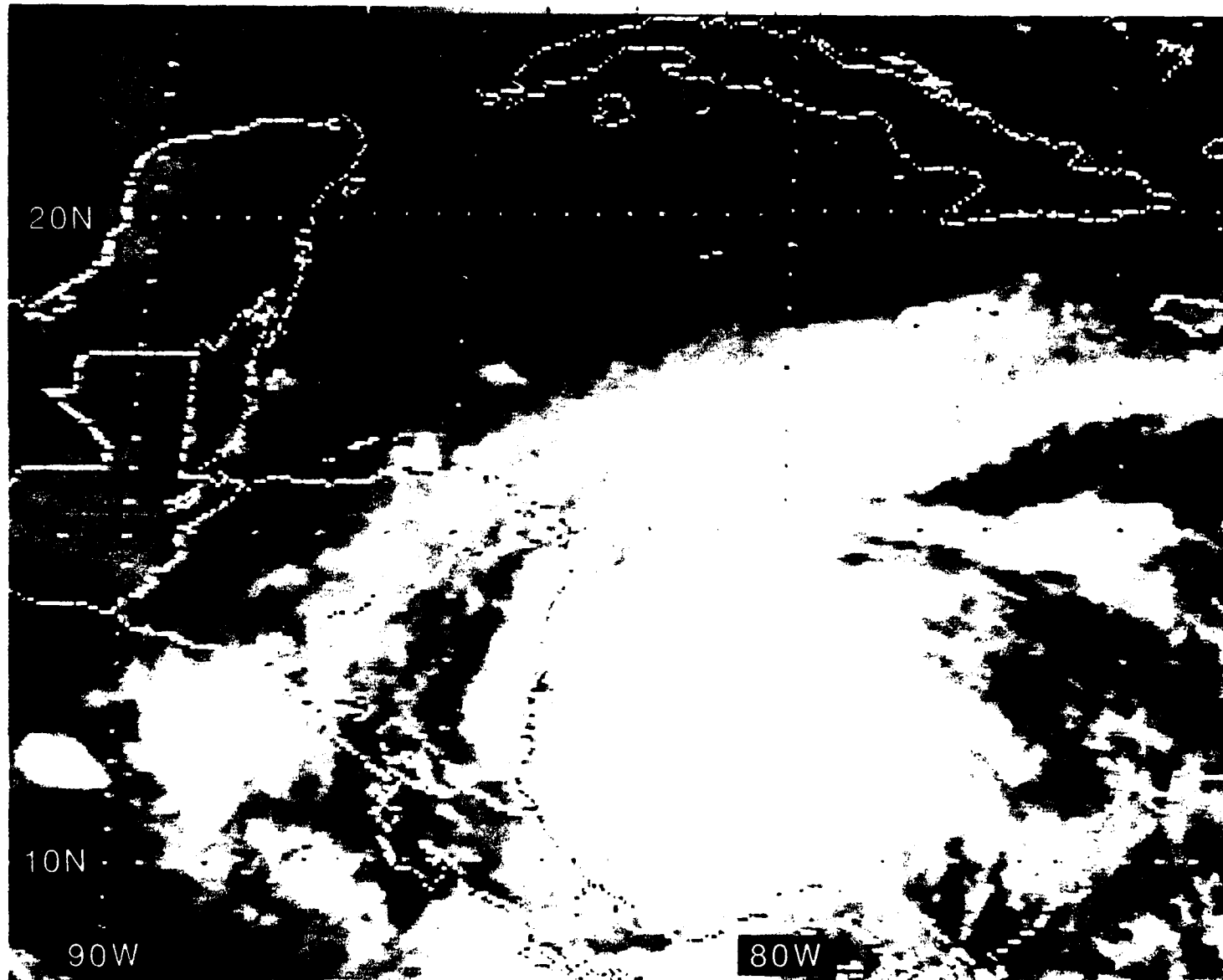


Figure 5.41: GOES East Infrared Satellite Imagery, 1201 UTC 21 OCT 1988

1431 21OCT88 39A-4 00911 16001 EC1

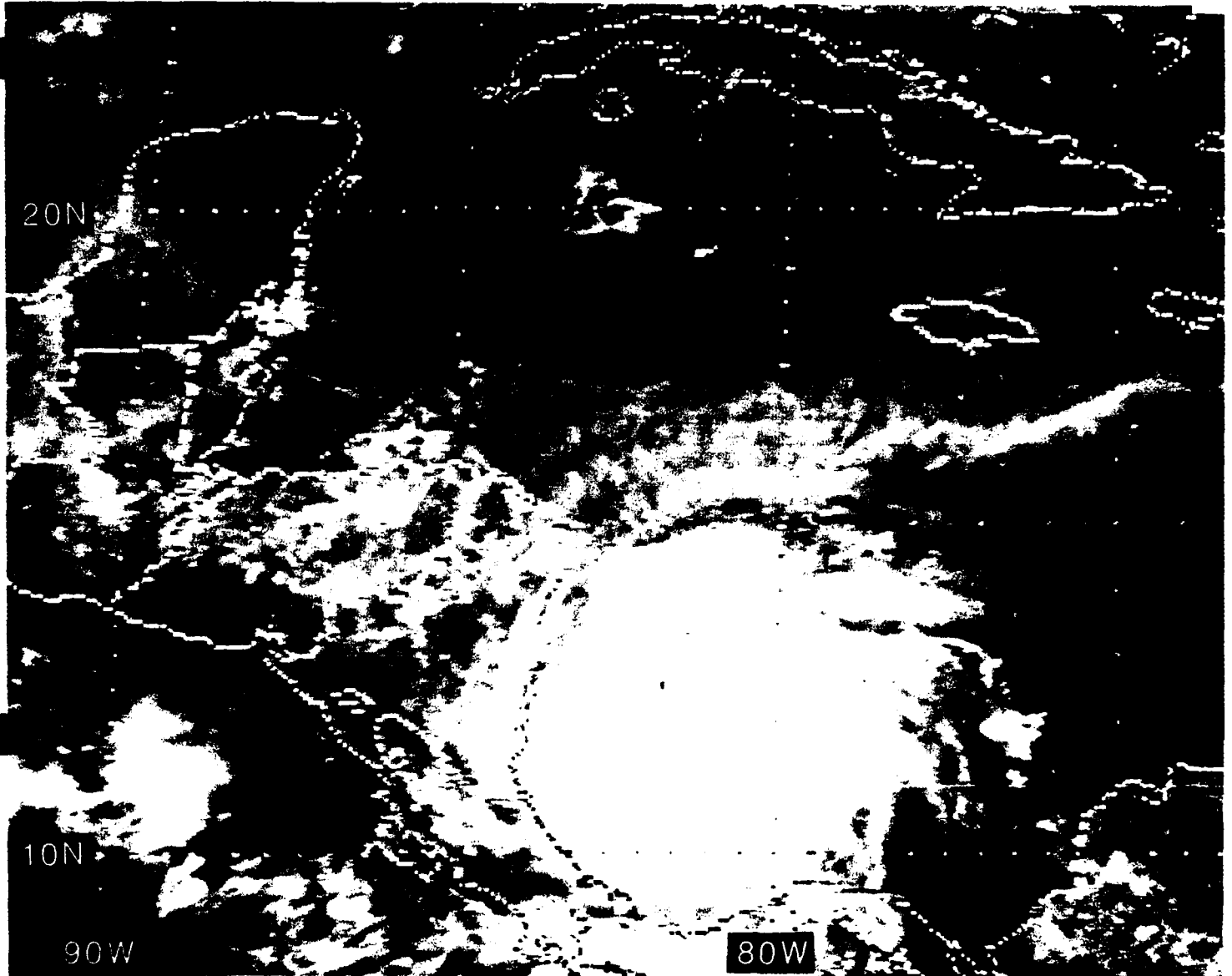


Figure 5.42: GOES East Visible Satellite Imagery, 1431 UTC 21 OCT 1988

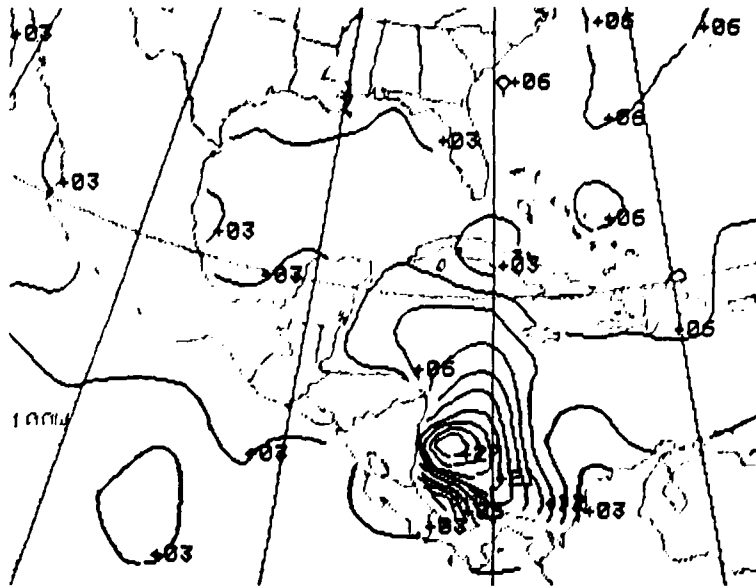


Figure 5.43: FNOG Significant Wave Heights, 1200 UTC 21 OCT 1988. Isopleths are at 3-foot intervals.

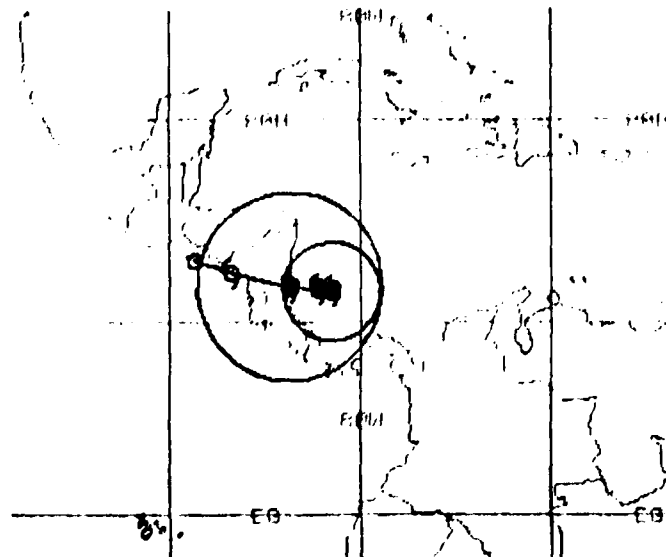


Figure 5.44: Tropical Cyclone FORECAST Track from 1200 UTC 21 OCT 1988. Current position of hurricane is the rightmost hurricane symbol *enclosed* by the smaller circle depicting the outer radius of gale force winds. The larger circle depicts the outer radius of gale winds—expanded outward to include the expected 24-h forecast position error—centered on the 24-h forecast position, just off the southeastern Nicaraguan coast. The 48-h position, downgraded to a tropical storm, is on the North Pacific coast of Nicaragua, while the 72-h forecast position (weakened below tropical storm strength) is just south of El Salvador.

22 October 1988

Figure 5.45 shows the visible imagery depicting Hurricane Joan 3 1/2 hours before the analyses to be examined on 22 October—the eye of the hurricane appears to have passed about 50 n mi south of San Andrés Island. Only 1 1/2 hours later at 2200 UTC on 21 October, the National Hurricane Center, Miami, located the hurricane at 11.8°N, 82.1°W based on NOAA reconnaissance aircraft and satellite imagery, moving toward 270° at 5 kt, having maximum sustained winds of 105 kt with gusts to 125 kt. Hurricane force winds extended 40 n mi to the north and 25 n mi to the south of the eye, while gale force winds reached out 125 n mi to the north and 75 n mi to the south.

By 0001 UTC 22 October, Fig. 5.46 depicts the hurricane moving slowly westward with the eye only ~75 n mi from landfall on the southeastern Nicaraguan coast. Figure 5.46 shows the more intense convection from northwestern Panama, over all of Costa Rica, and over the eastern half of Nicaragua to about 300 n mi seaward.

Figures 5.47 and 5.48 provide, with their satellite-derived winds and reconnaissance observations, an excellent depiction of both the low-level and upper-level streamline analyses around Hurricane Joan. While the low-level inflow is evident from the ATOLL chart, Fig. 5.47, the upper-level divergence over the hurricane is obvious, with a primary channel of exhaust toward the northeast moving over Hispaniola (see Fig. 5.48). The NOGAPS wind analyses, Figures 5.49 and 5.50 are in fair agreement with the NMC streamline analyses.

Again, examination of the station surface observations at 0000 UTC (Fig. 5.51) shows good correspondence with the satellite imagery of Fig. 5.45. That is: overcast, with light fog, and very light west-southwest winds at San José, Costa Rica (station 78762), about 150 n mi southwest of the eye of the hurricane; 7/8 cloud cover with cumulonimbus and multi-layered clouds and a northeast wind at Puerto Lempira, Honduras (station 78711), about 200 n mi northwest of the eye; dense cirrus, from the upper-level outflow (along with cumulus and stratocumulus) at Kingston, Jamaica (station 78397); and no report from San Andrés Island, —which is no surprise, since the island was still experiencing near-hurricane force winds! Figure 5.52 shows the FNOC analysis of > 21 foot significant wave heights in the vicinity of San Andrés Island, just north of the storm track.

Satellite imagery indicates that the eye of the hurricane first struck the Nicaraguan coastline at about 0800 UTC 22 October, having increased its speed of advance to 8 kt before making landfall. By 1100 UTC, the continued westward progression of Hurricane Joan proceeding inland was evident in IR satellite imagery (not shown). Figure 5.53 shows the tropical cyclone warning at 1200 UTC 22 October. The cyclone has now been downgraded to a tropical storm, and is forecast to reach the North Pacific coast of Nicaragua by 1200 UTC 23 October and then proceed along the North Pacific coast of El Salvador and Guatemala.

Finally, the IR imagery of Fig. 5.54 depicts the expansive cirrus shield as the cyclone center has now moved inland. Figure 5.55 shows the first visible imagery available, 2 1/2 hours later—the faint circulation center can be discerned about 25 miles inland. The NHC warning at 1600 UTC (1 1/2 hours later) placed Tropical Storm Joan at 11.9°N, 84.5°W, 30 n mi southwest of Bluefields, Nicaragua.

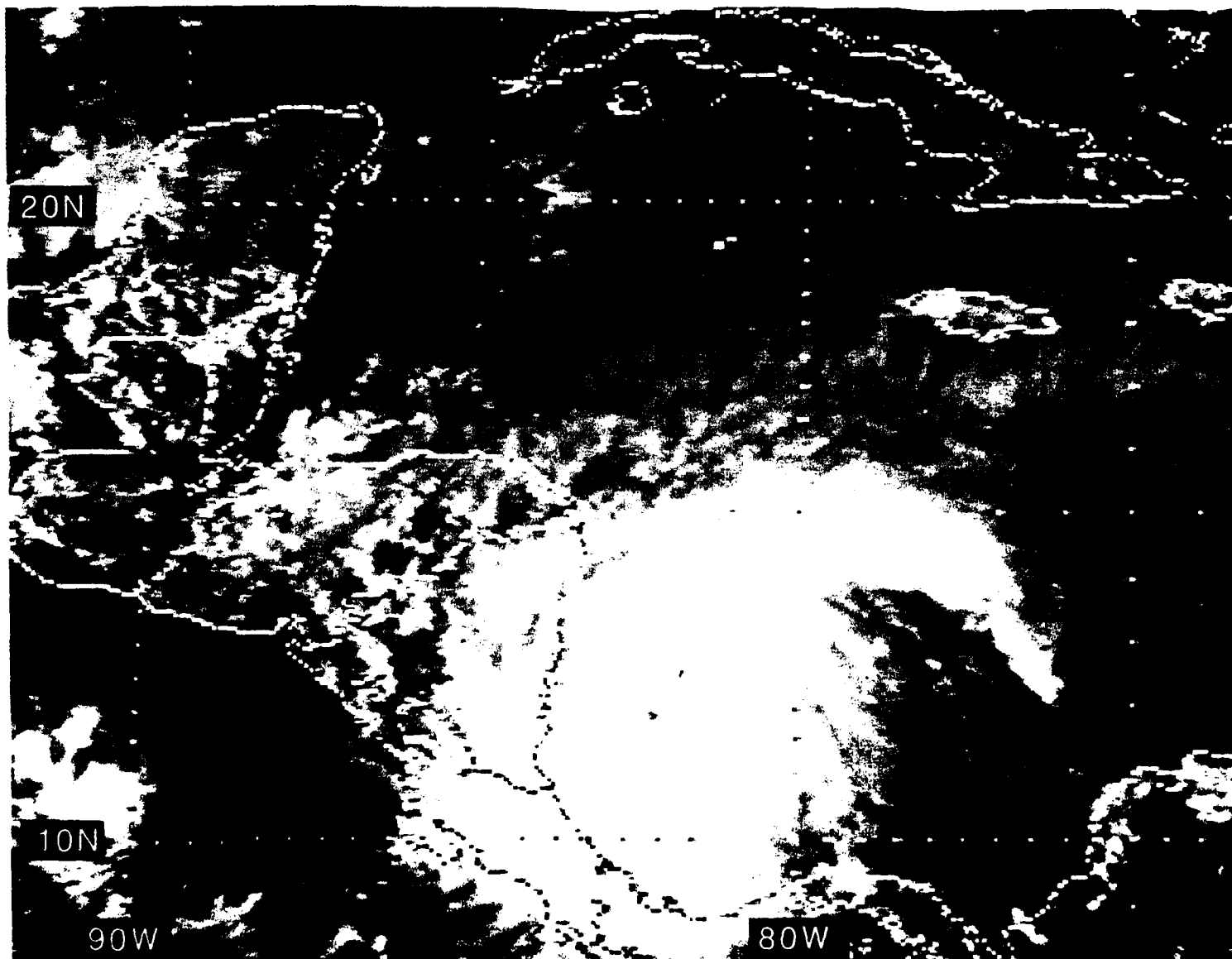


Figure 5.45: GOES East Visible Satellite Imagery, 2031 UTC 21 OCT 1988

0001 220C88 39E-42A 00911 15971 EC1

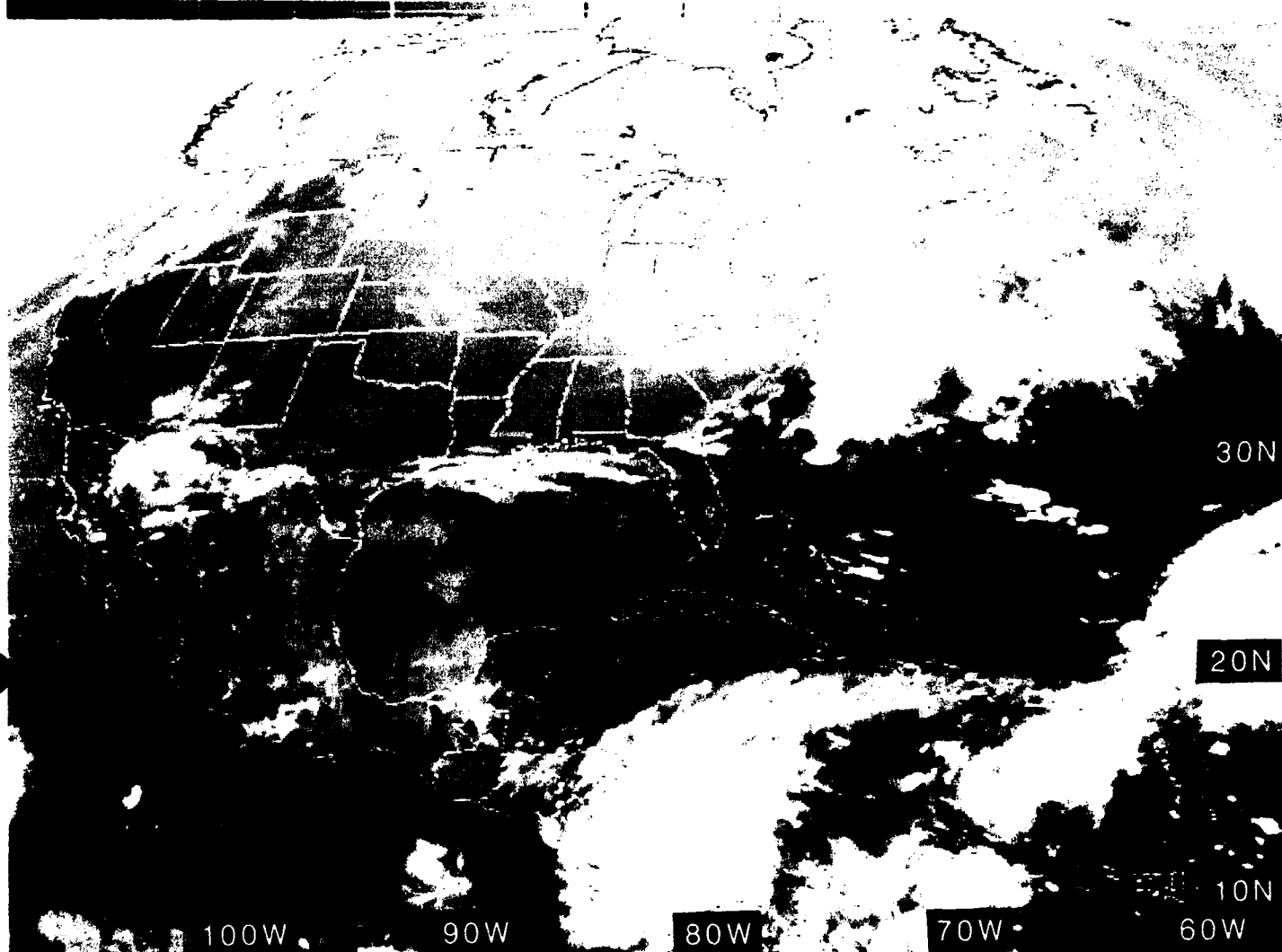


Figure 5.46: GOES East Infrared Satellite Imagery, 0001 UTC 22 OCT 1988

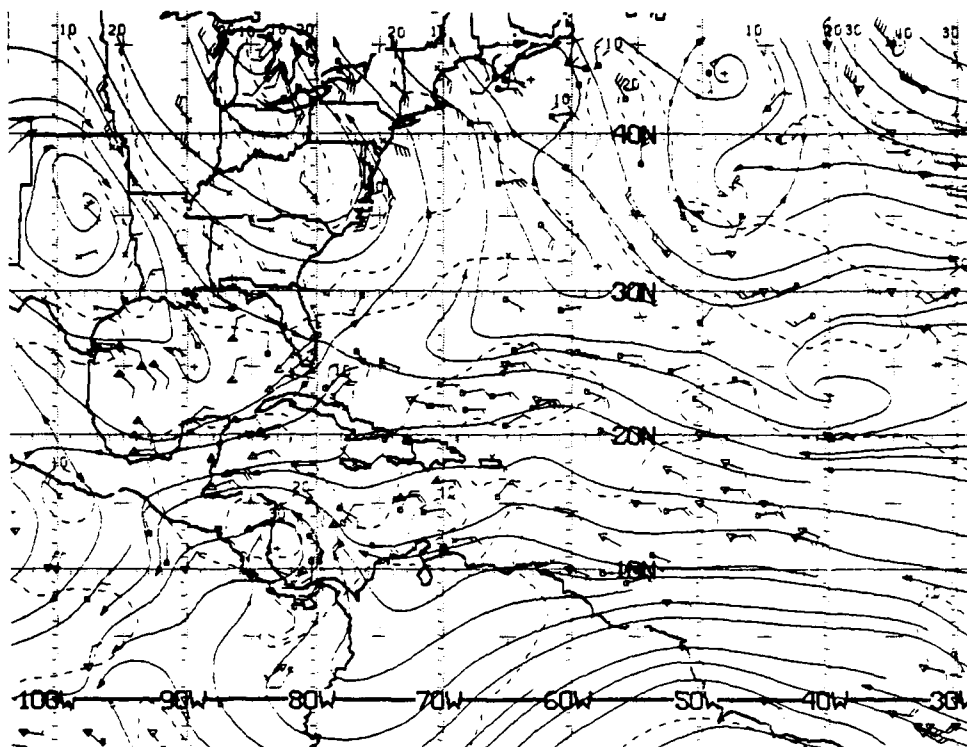


Figure 5.47: NMC ATOLL Operational Streamline Chart, 0000 UTC 22 OCT 1988
As in Fig. 2.4.

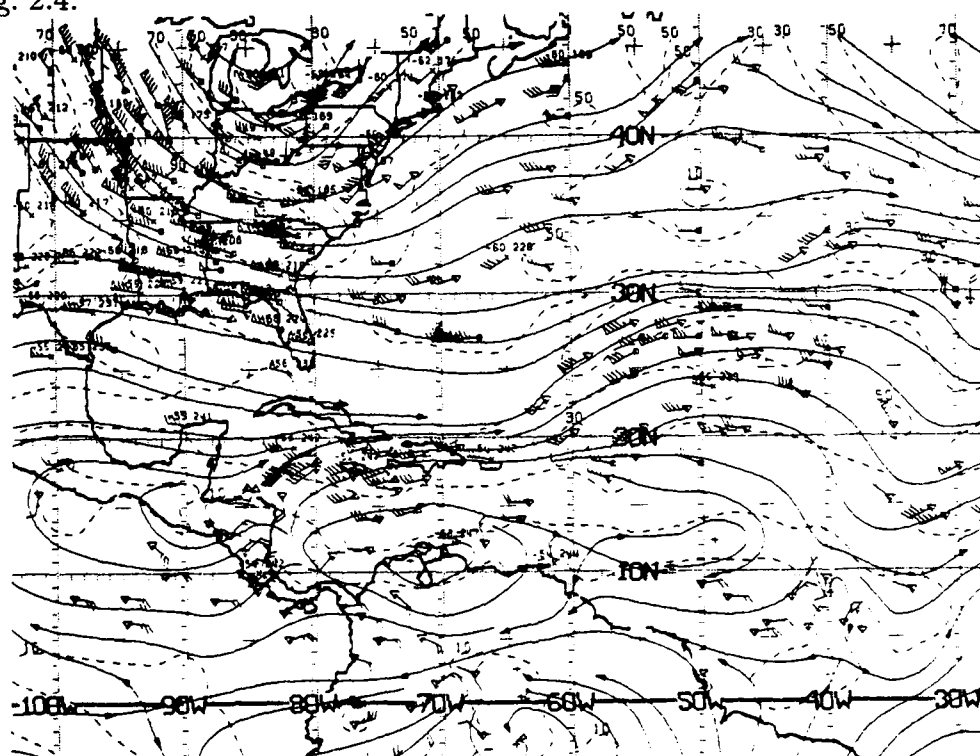


Figure 5.48: NMC 200 mb Operational Streamline Chart, 0000 UTC 22 OCT 1988
As in Fig. 2.6.

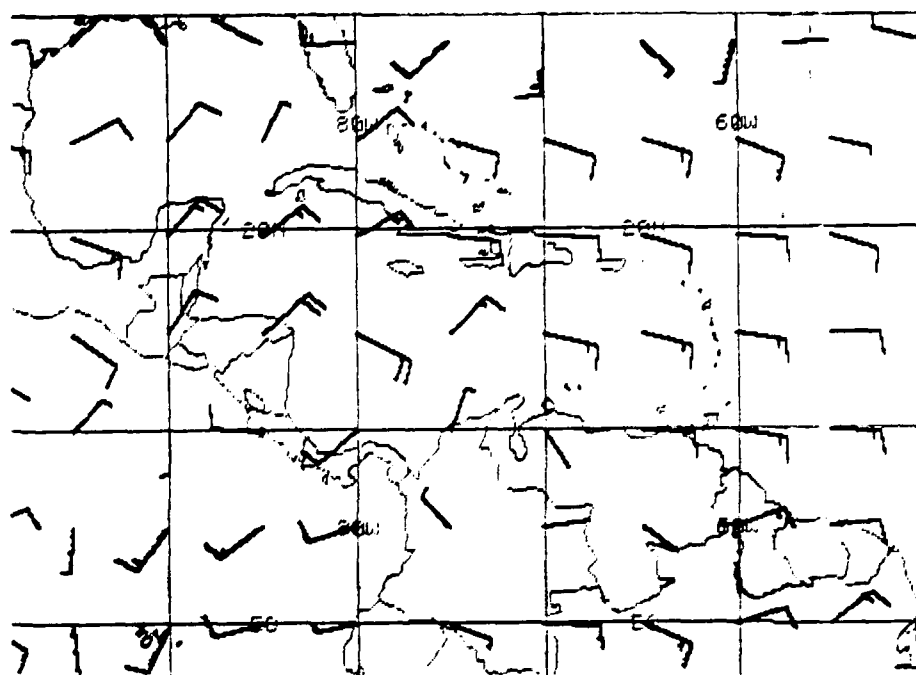


Figure 5.49: FNOC 925 mb Winds, 0000 UTC 22 OCT 1988. As in Fig. 2.19.

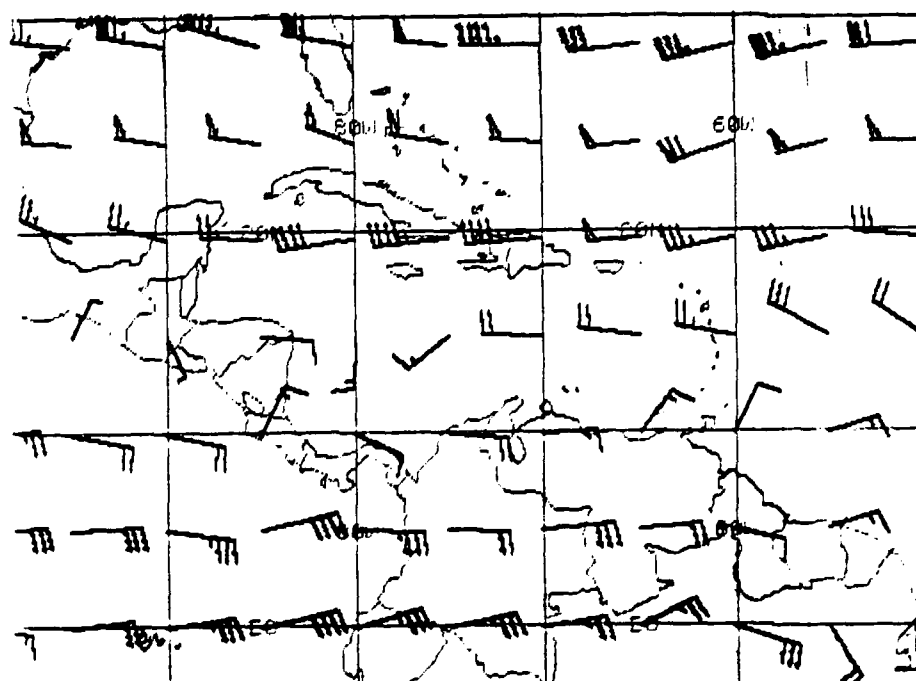


Figure 5.50: FNOC 200 mb Winds, 0000 UTC 22 OCT 1988. As in Fig. 2.20.

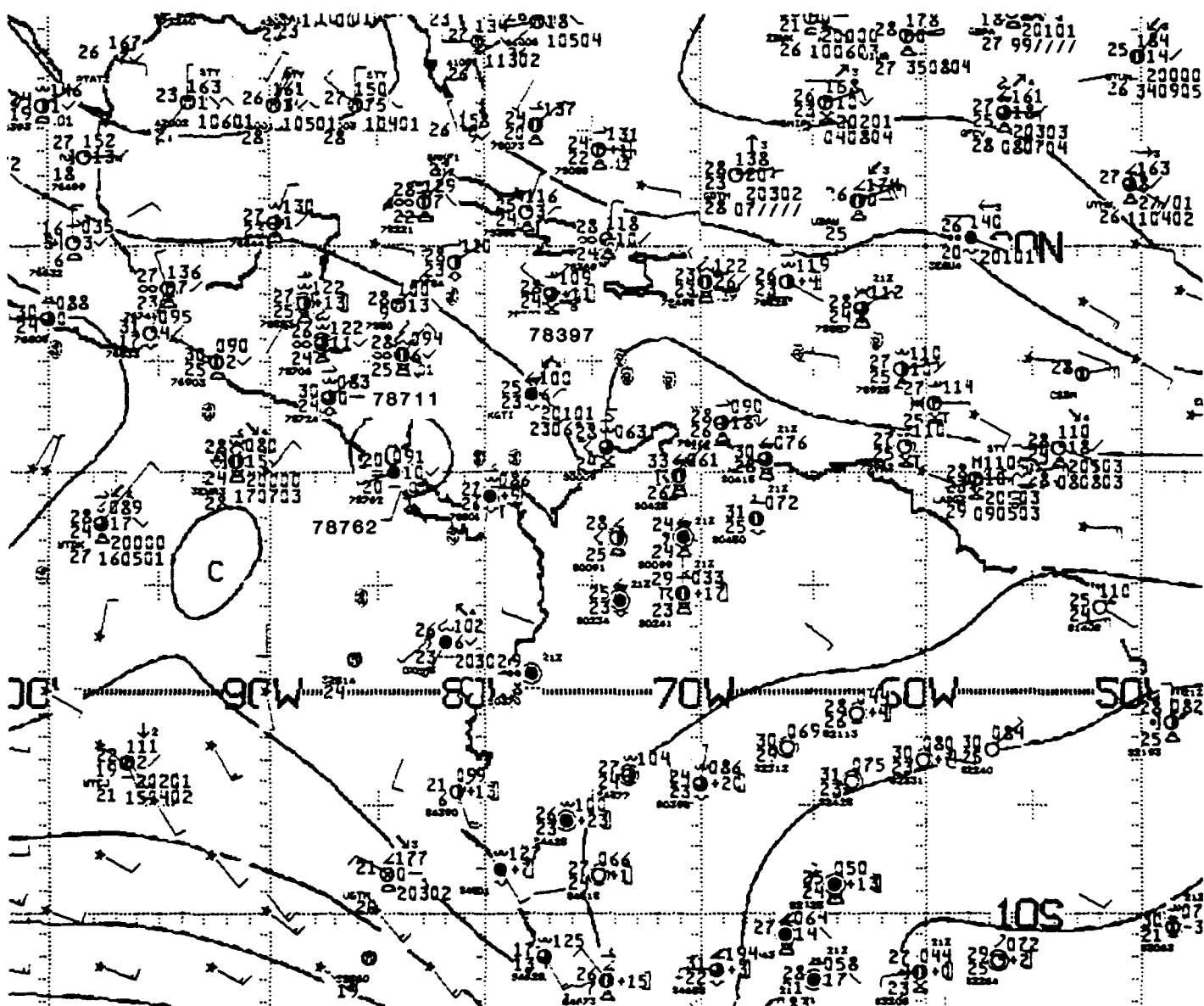


Figure 5.51: NMC 1000 mb Analysis, 0000 UTC 22 OCT 1988. As in Fig. 2.21.

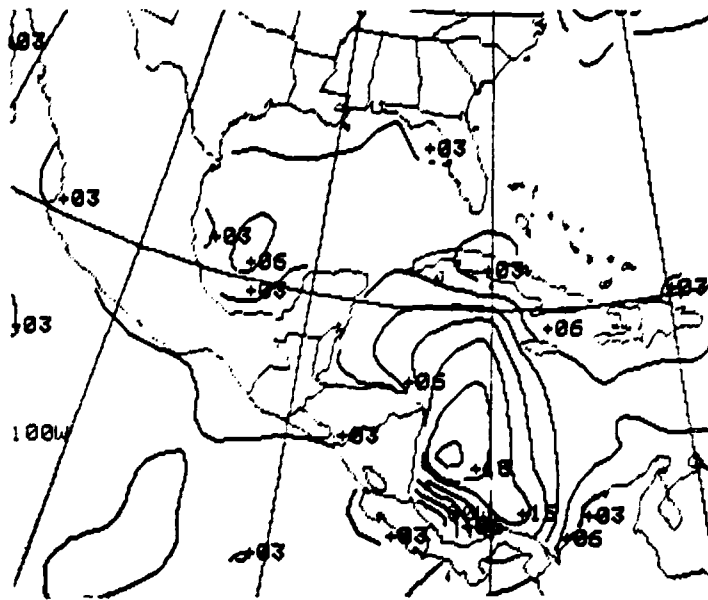


Figure 5.52: FNOG Significant Wave Heights, 0000 UTC 22 OCT 1988. Isopleths are at 3-foot intervals.

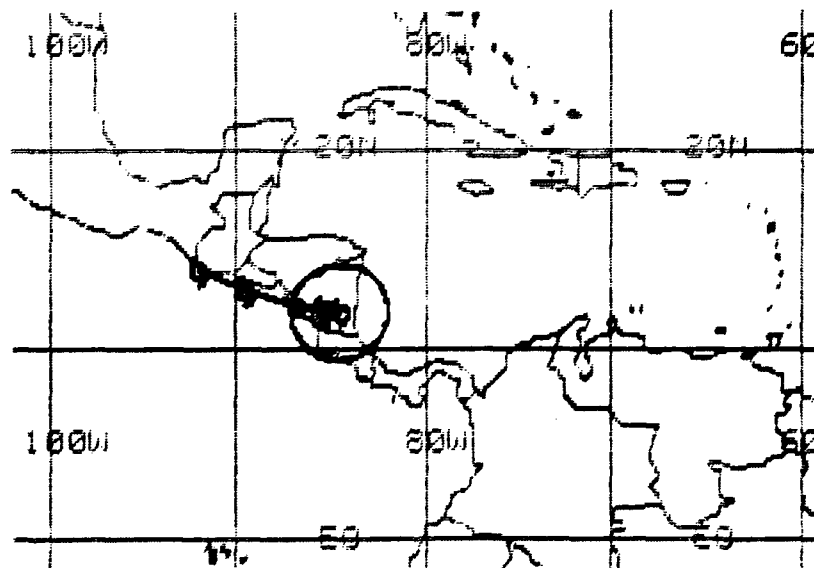


Figure 5.53: Tropical Cyclone FORECAST Track from 1200 UTC 22 OCT 1988. Current position of Joan is the rightmost tropical storm symbol *enclosed* by the circle depicting the outer radius of gale force winds. The 12-, 24-, 48- and 72-h forecast positions follow toward the west-northwest, with the 72-h position located at the southwest corner of Guatemala.

1201 220C88 39E-4ZA 00921 16031 EC1

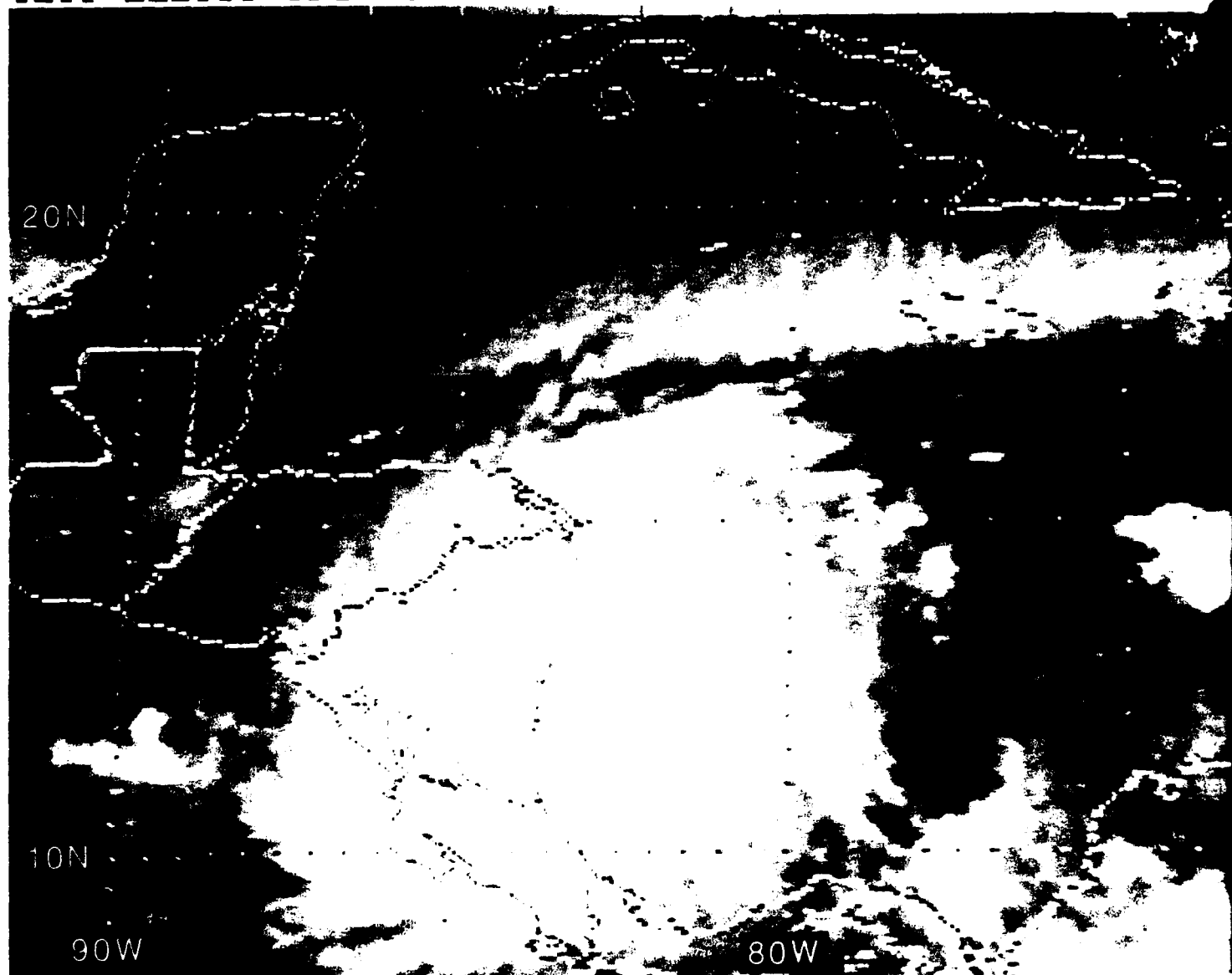


Figure 5.54: GOES East Infrared Satellite Imagery, 1201 UTC 22 OCT 1988

1431 220C88 39A-4 00902 16021 EC1

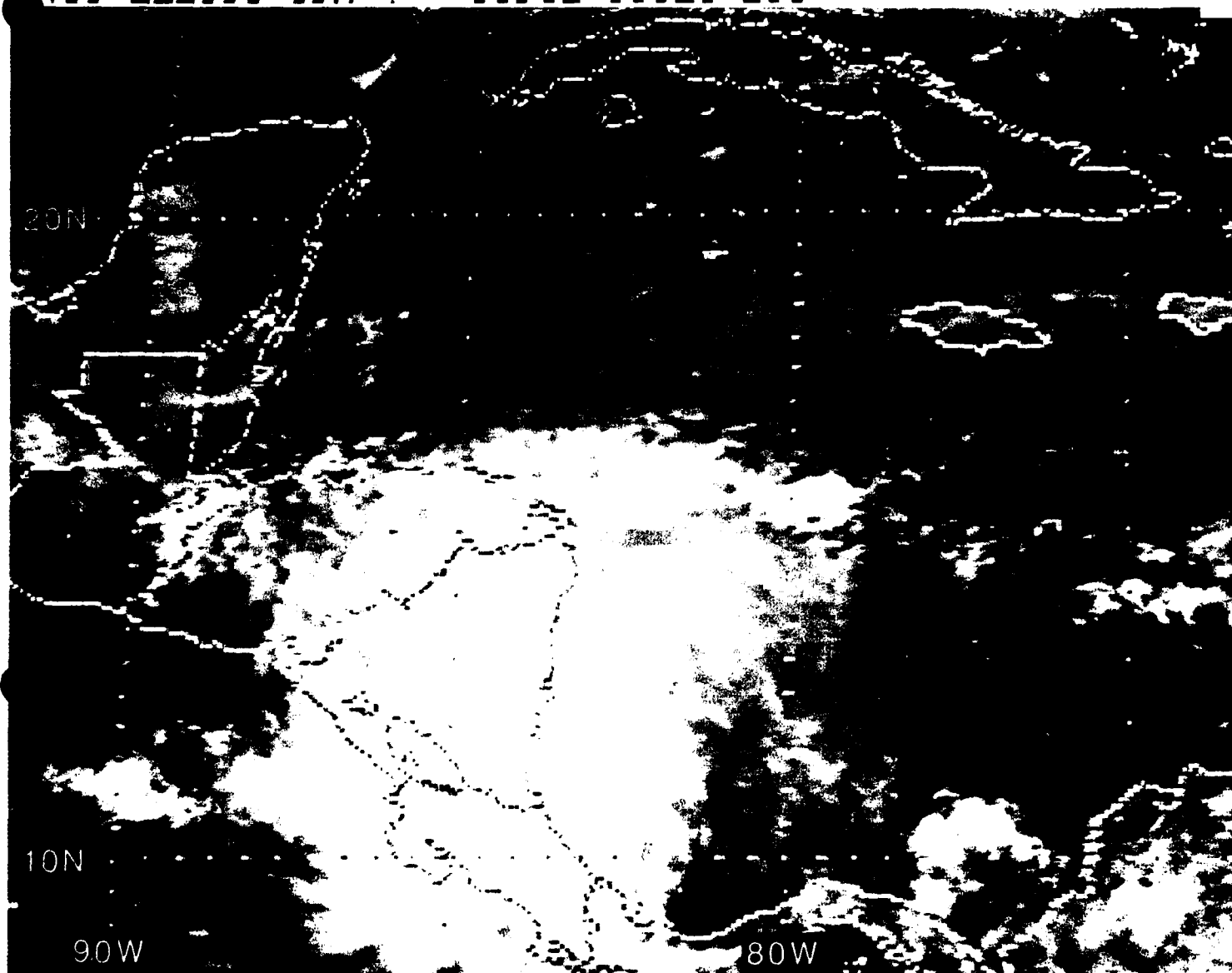


Figure 5.55: GOES East Visible Satellite Imagery, 1431 UTC 22 OCT 1988

23 October 1988

While Tropical Storm Joan is now overland at 0000 UTC 23 October, near the center of Nicaragua, there is much damage and flooding occurring. The city of Bluefields had 6000 homes destroyed, and roofs were blown from most of its remaining buildings. Bluefields, with a population of 38,000, suffered the loss of 21 lives—Joan claimed 111 lives from Venezuela to Costa Rica. In the capital of Nicaragua, Managua, the storm toppled electrical towers and tore down telephone lines and trees. Figure 5.56 provides the IR satellite imagery corresponding to the low- and upper-level NMC streamlines of Figs. 5.57 and 5.58 at 0000 UTC 23 October. The last two figures exemplify the low-level convergence and upper-level divergence so typical of tropical cyclones. Figure 5.59, depicting the FNOG significant wave height analysis at 0000 UTC, shows that the waves have quickly decreased to >12 feet along the Caribbean coast only about 16 hours after the storm had moved over land. Figure 5.61 indicates that, as might be expected, the station surface observations from Nicaragua and Costa Rica are unavailable. On the periphery of the storm, Choluteca, Honduras (station 78724) just inland from the Gulf of Fonseca has 7/8 cloud cover, multi-layered clouds with a weak northeasterly wind; Puerto Lempira, Honduras (station 78711), under the IR canopy of high clouds shown in Fig. 5.56, is overcast with slight drizzle and northeasterly wind; while Belize City, Belize (station 78583) ~350 n mi northwest of the storm center has only 3/4 multi-layered cloud cover and east-northeasterly wind. Figure 5.62 shows the 0000 UTC sounding profile at Belize City, just *outside* the heavy cloudiness and moisture associated with Tropical Storm Joan.

At 0400 UTC, the National Hurricane Center located the tropical storm at 12.0°N, 86.0°W, near the northwestern edge of Lake Nicaragua, based on satellite data. Its movement was still 270° at 8 kt, but its maximum winds had decreased to 35 kt with gusts to 50 kt. Two hours later at 0600 UTC, Fig. 5.60 shows the warning position of the storm on the North Pacific coast of Nicaragua, with the 12-, 24-, 48- and 72-hour forecast storm positions. The actual track of the storm after it reached the North Pacific Ocean was more northwesterly⁹¹—closely paralleling the west coast of Central America as it proceeded toward the North Pacific coast of Guatemala.

By 1200 UTC, the IR imagery of Fig. 5.63 shows the center of Tropical Storm Joan near the northwest tip of Nicaragua, while the first visible imagery available 2 1/2 hours later (Fig. 5.64) locates the storm center about 20 n mi offshore, south of the Gulf of Fonseca.

At 1600 UTC 23 October 1988, Tropical Storm Joan was designated an Eastern North Pacific Ocean tropical cyclone. Subsequent warnings called the vortex—originally associated with “Joan”—Tropical Storm “Miriam”.

⁹¹More in agreement with the NHC warning of 1800 UTC on 22 October (not shown).

0001 230088 39E-42A 00902 15991 EC1

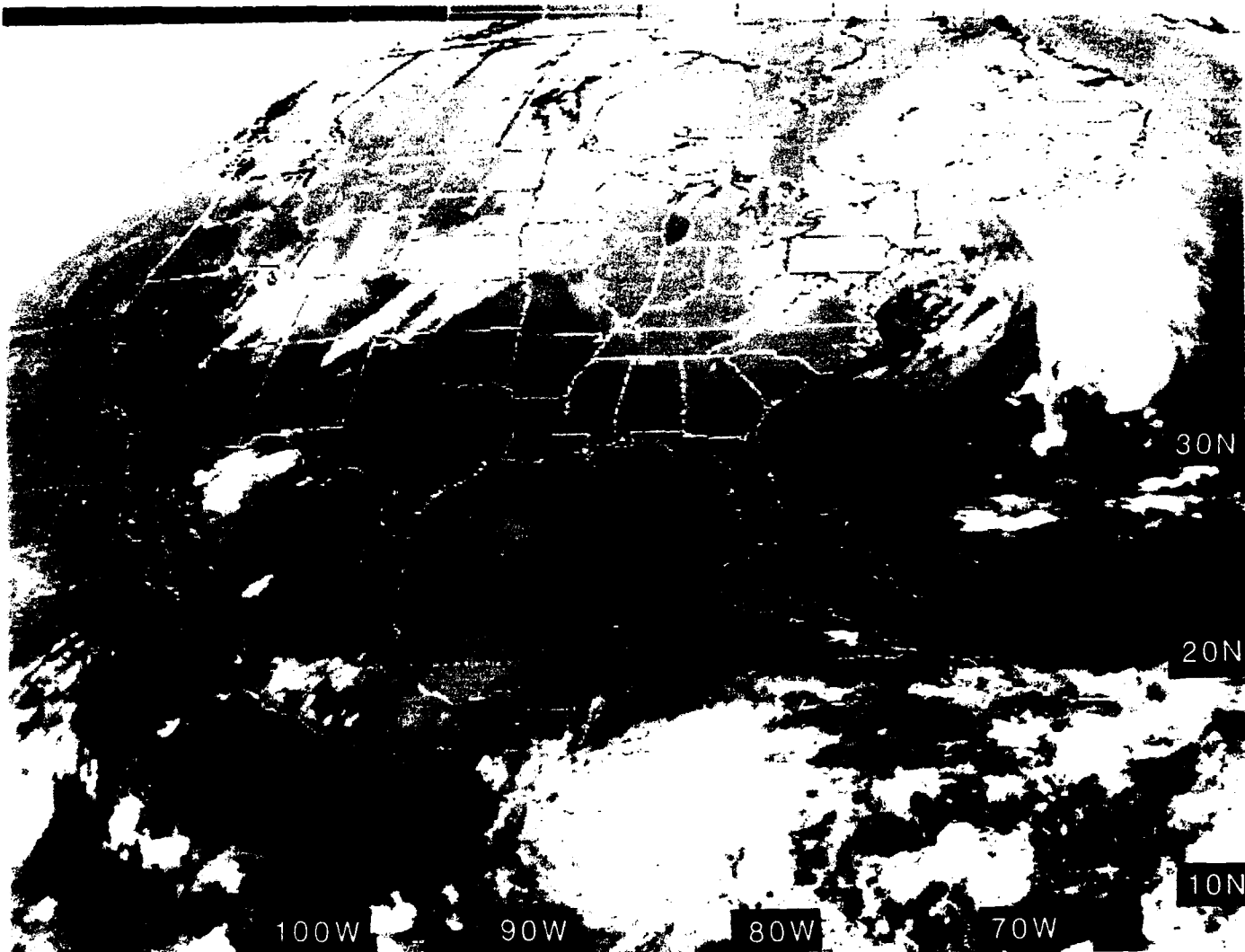


Figure 5.56: GOES East Infrared Satellite Imagery, 0001 UTC 23 OCT 1988

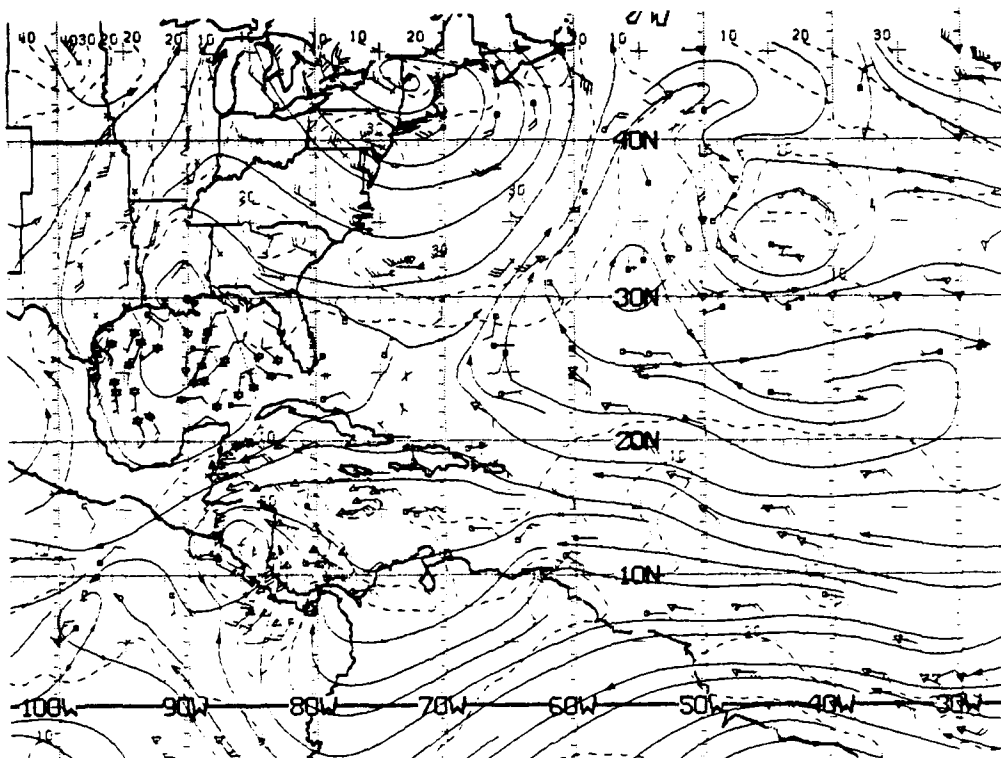


Figure 5.57: NMC ATOLL Operational Streamline Chart, 0000 UTC 23 OCT 1988
As in Fig. 2.4.

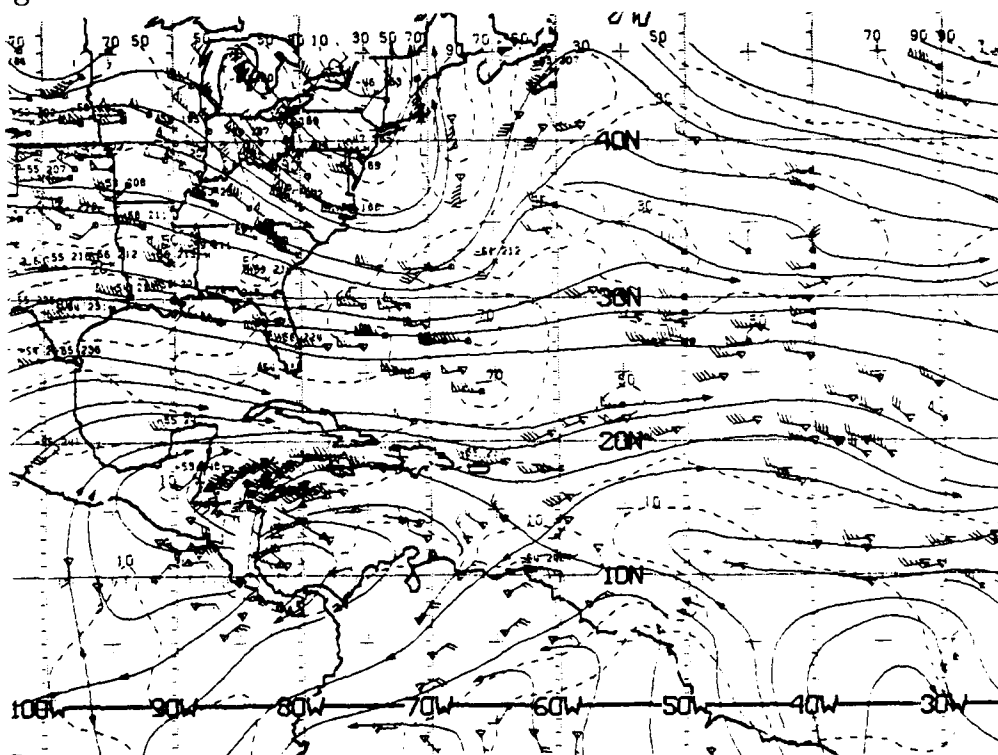


Figure 5.58: NMC 200 mb Operational Streamline Chart, 0000 UTC 23 OCT 1988
As in Fig. 2.6.

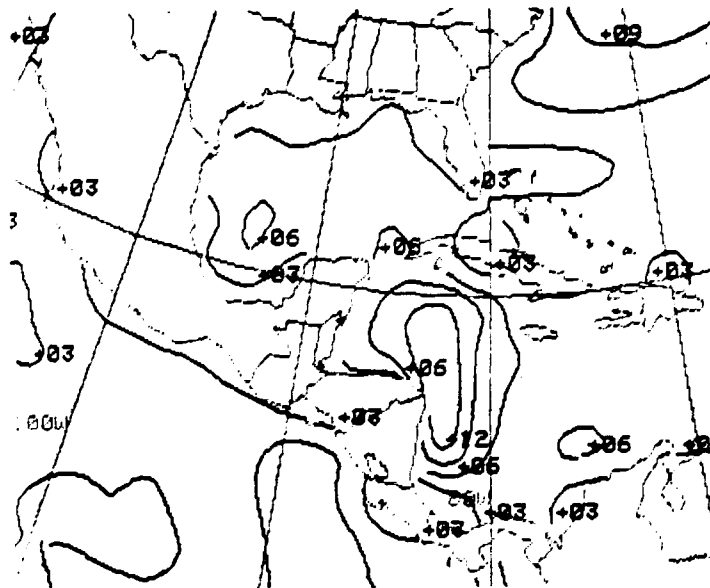


Figure 5.59: FNOG Significant Wave Heights, 0000 UTC 23 OCT 1988. Isopleths are at 3-foot intervals.

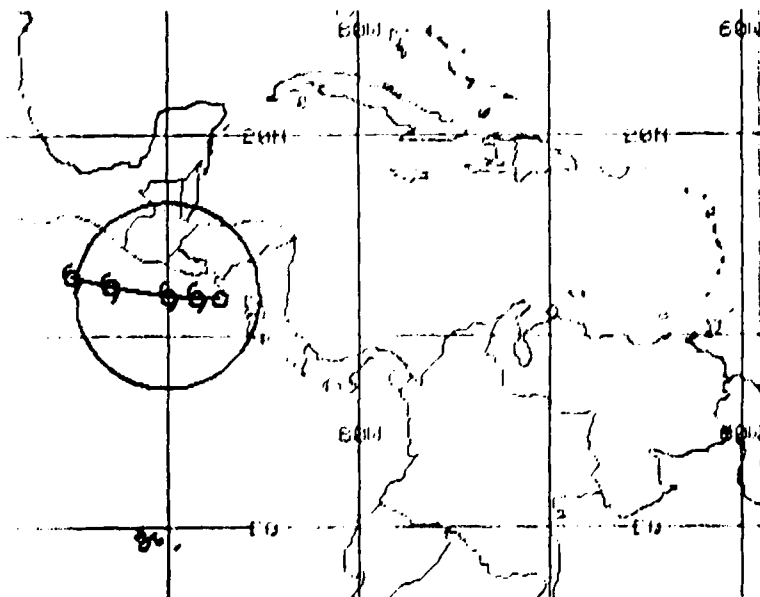


Figure 5.60: Tropical Cyclone FORECAST Track from 0600 UTC 23 OCT 1988. Current position of the cyclone is the small circle near the west coast of Nicaragua. The 12-, 24-, 48- and 72-h forecast positions follow toward the west-northwest, with the 24-h position enclosed by a circle depicting the probable radius of gale force winds.

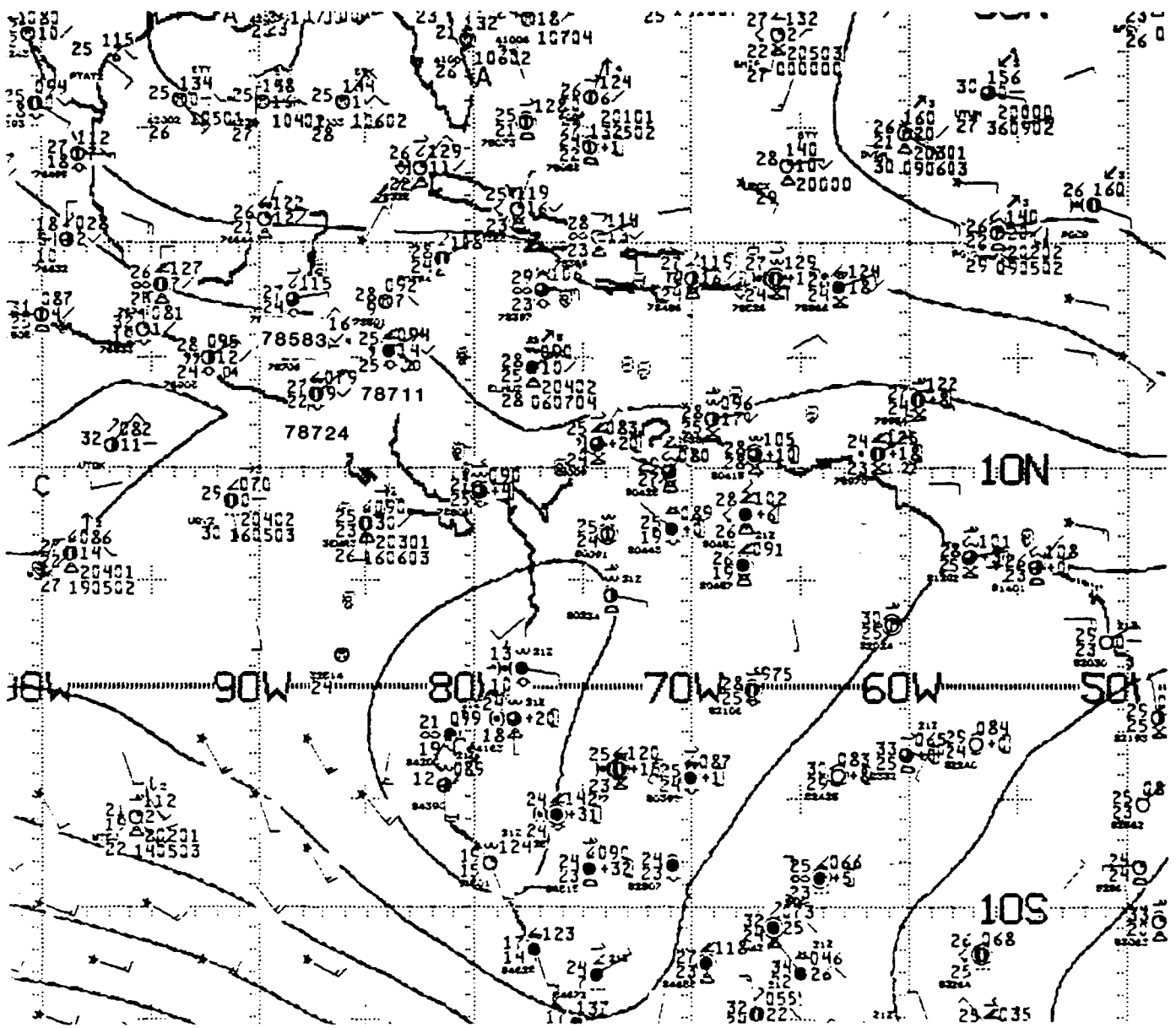


Figure 5.61: NMC 1000 mb Analysis, 0000 UTC 23 OCT 1988. As in Fig. 2.21.

881023/0000 78583 MZBZ LIFT TOTL KINX SWET
-2 39 13 193

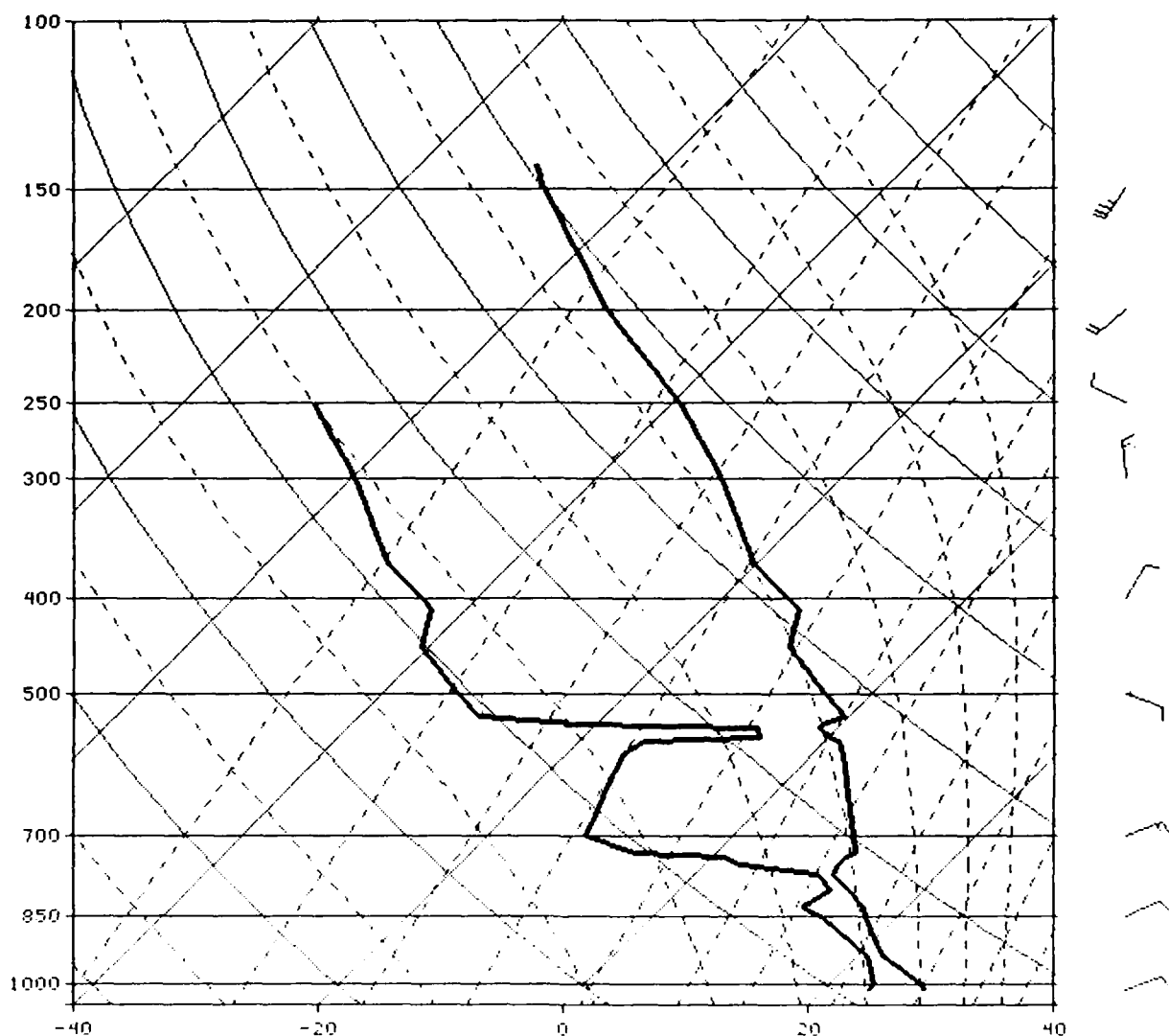


Figure 5.62: Belize City, Belize Radiosonde Sounding 0000 UTC 23 OCT 1988
Station 78583 MZBZ (Lifting Index = -2, K Index = +13)

1201 230C88 39E-42A 00912 16051 EC1

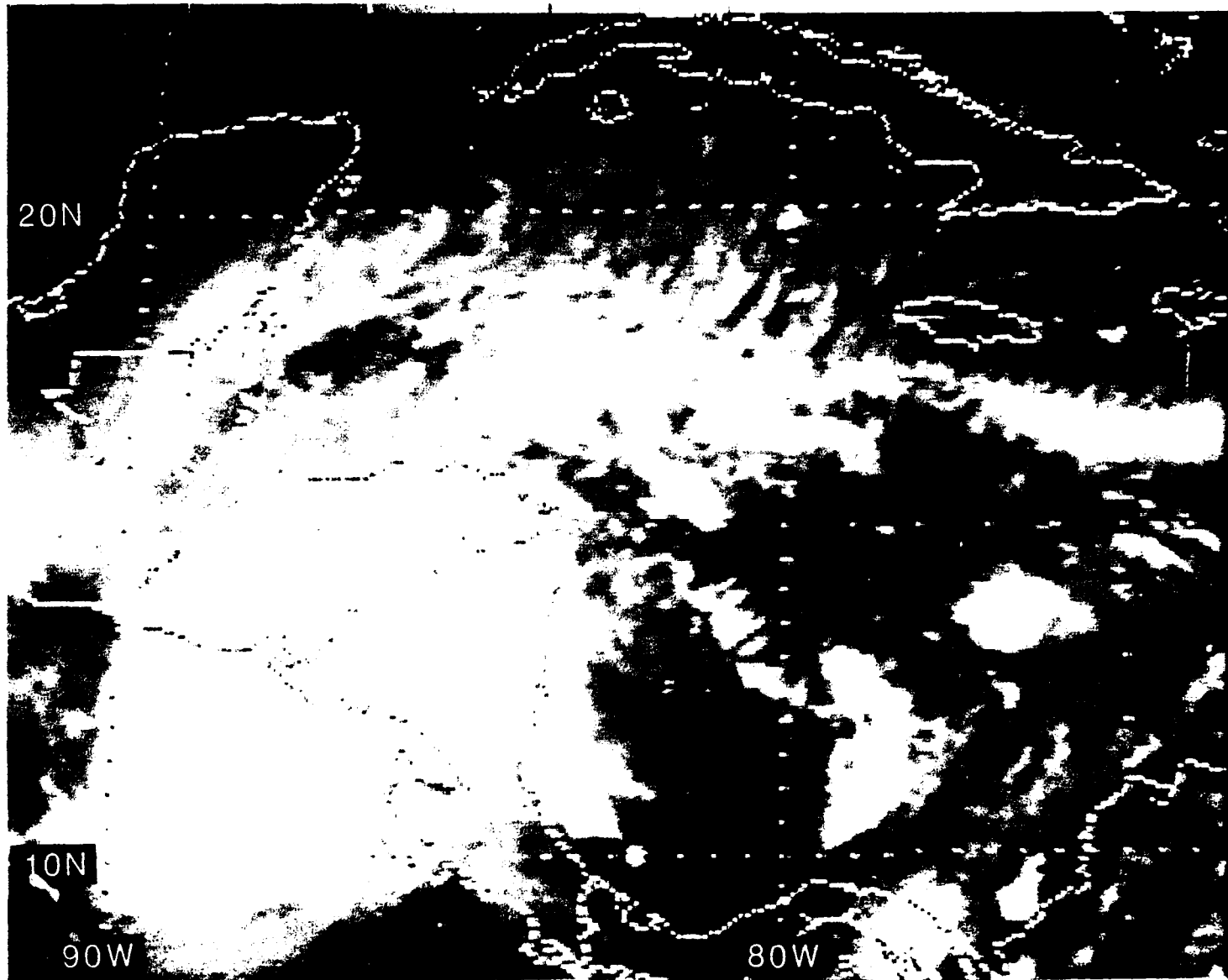


Figure 5.63: GOES East Infrared Satellite Imagery, 1201 UTC 23 OCT 1988

1431 230C88 39A-4 00902 16041 EC1

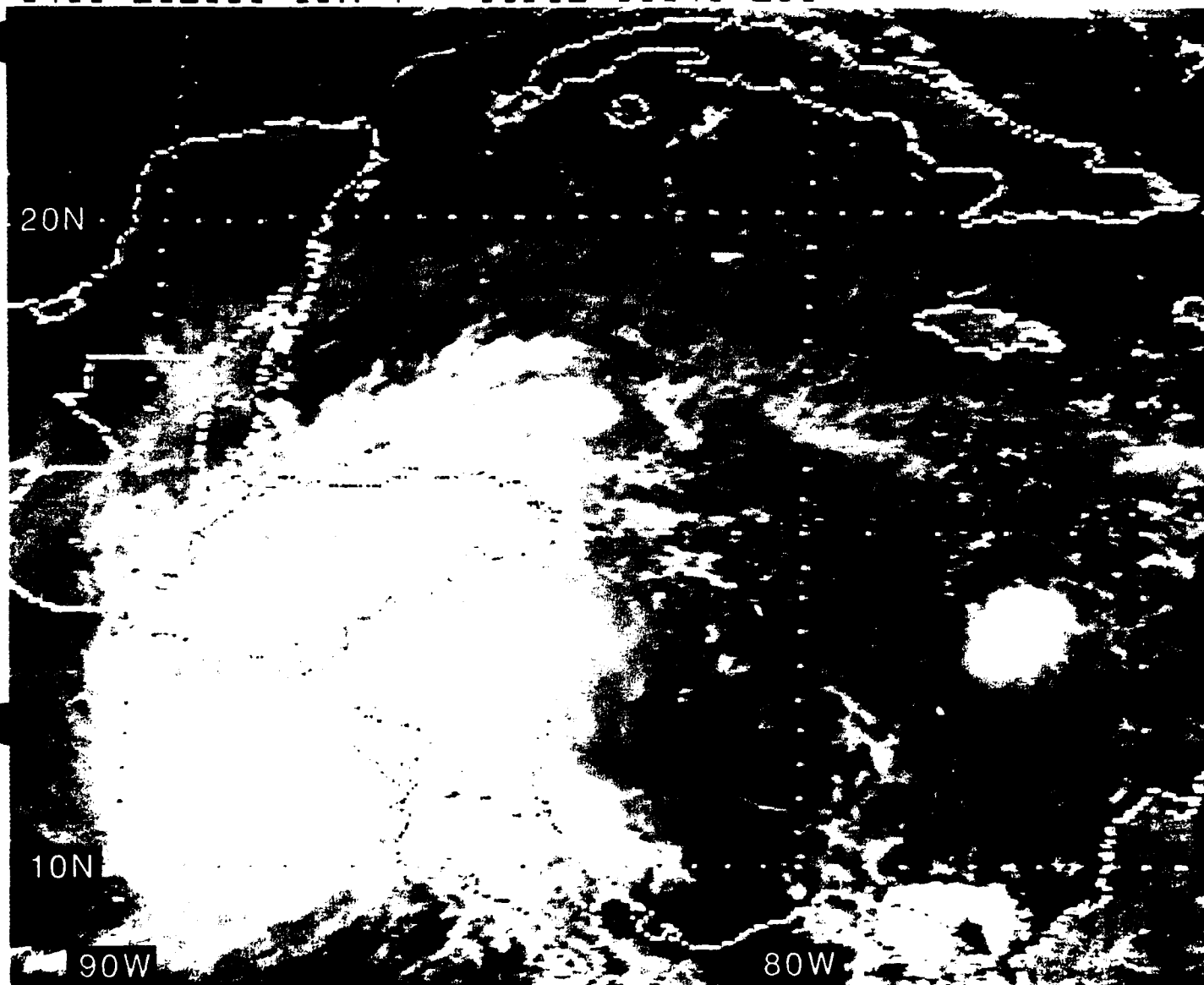


Figure 5.64: GOES East Visible Satellite Imagery, 1431 UTC 23 OCT 1988

24 & 25 October 1988

Figures 5.65 and 5.66 show the IR and visible imagery locating Tropical Storm Miriam (previously "Joan" before entering the North Pacific Ocean), about 3 hours before the 0000 UTC charts to be discussed.

The 0001 UTC IR imagery (Fig. 5.67) appears to depict the eye of the storm very near the coast of El Salvador and at 0400 UTC the official warning position of Tropical Storm Miriam was 13.1°N, 89.5°W moving toward 285° at 9 kt and having maximum winds of 50 kt with gusts to 65 kt—accurate to within 30 n mi based on satellite imagery.

The NMC analyses (Figs. 5.68 and 5.69) again well depict the low-level and upper-level streamlines in the vicinity of the tropical storm, with Fig. 5.69 having a wealth of satellite derived winds. In fact, the upper-level diffluence is manifested by the large area of convection east of the Yucatan Peninsula and north of Honduras (see Fig. 5.67). The Navy wind analyses (Figs. 5.70 and 5.71) *generally* indicate the low-level convergence and upper-level divergence in the right places.

The station observations of Fig. 5.72 correlate well with the IR imagery of Fig. 5.67, i.e., 7/8 cloud cover with towering and multilayer cloudiness at both Tapachula, Mexico (station 76903) and Choluteca, Honduras (station 78724); overcast with continuous drizzle at Tela, Honduras (station 78706); a thunderstorm at Puerto Lempira (station 78711); and only 4/10 cloud cover at Merida, Mexico (station 76644) on the northwest tip of the Yucatan peninsula.

The satellite imagery of Figs. 5.73 and 5.74 depict the west-northwestward progression of the Tropical Storm Miriam and indicate that the storm was still well organized at 1200 UTC on 24 October. The official position of the storm at 1000 UTC is 13.5°N, 90.2°W, moving toward 295° at 9 kt, having maximum winds of 50 kt, with gusts to 65 kt.

The tropical storm was officially located at 14.2°N, 92.5°W at 2200 UTC on 24 October and its strength had diminished to 45 kt with gusts to 55 kt, however the accuracy of its position was only to within 90 miles. The IR image (Fig. 5.75) depicts its general location at 0001 UTC on 25 October; 16 hours later it was downgraded to a tropical depression having only 30 kt winds with gusts to 40 kt.

However, even as the storm was drifting slowly westward and weakening, the southerly flow, in its eastern quadrant, appears to have greatly enhanced the upslope flow, inland, along the southern coasts of Guatemala, El Salvador, Honduras, and even western Nicaragua. Note the convection commencing at 1901 UTC about 100-120 n mi inland from the North Pacific Ocean along the El Salvador/Honduras border⁹² and about 100 n mi inland from the North Pacific Ocean over Nicaragua (see Fig. 5.76). Two hours later, the IR imagery (Fig. 5.77) shows the very heavy convection which has subsequently developed. Both Guatemala City and Tegucigalpa were reporting extensive towering cumulus and cumulonimbus clouds at 2200 UTC.

Tropical Storm Miriam drifted slowly westward, reaching 11.8°N, 97.7°W at 1000 UTC on 27 October, before turning northwestward and finally dissipating over water near

⁹²The national boundary between El Salvador and Honduras is not shown in the satellite imagery.

18.1°N, and 117.5°W on 2 November.

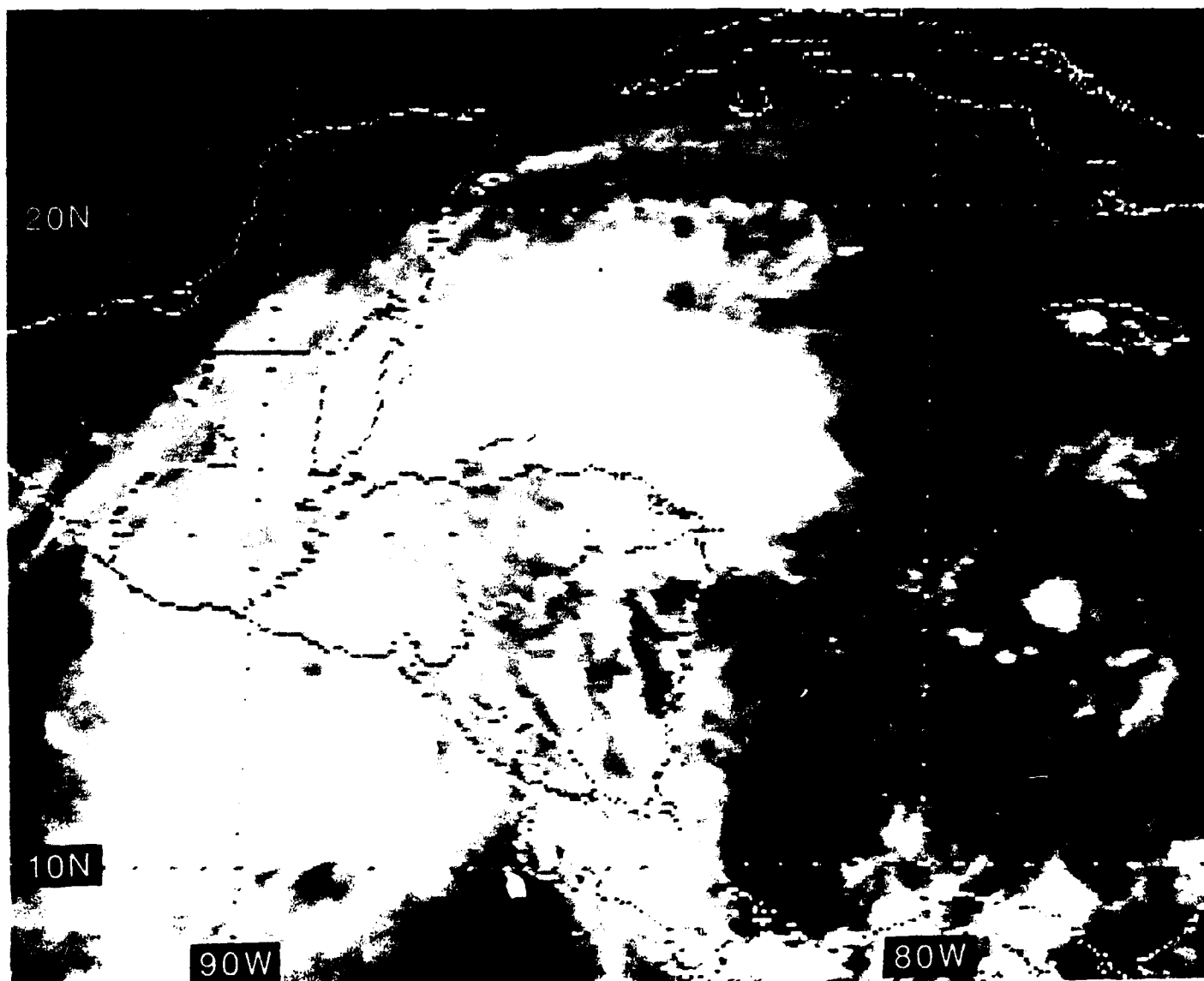


Figure 5.65: GOES East Infrared Satellite Imagery, 2101 UTC 23 OCT 1988

2131 230088 39A-4 00912 16011 EC1

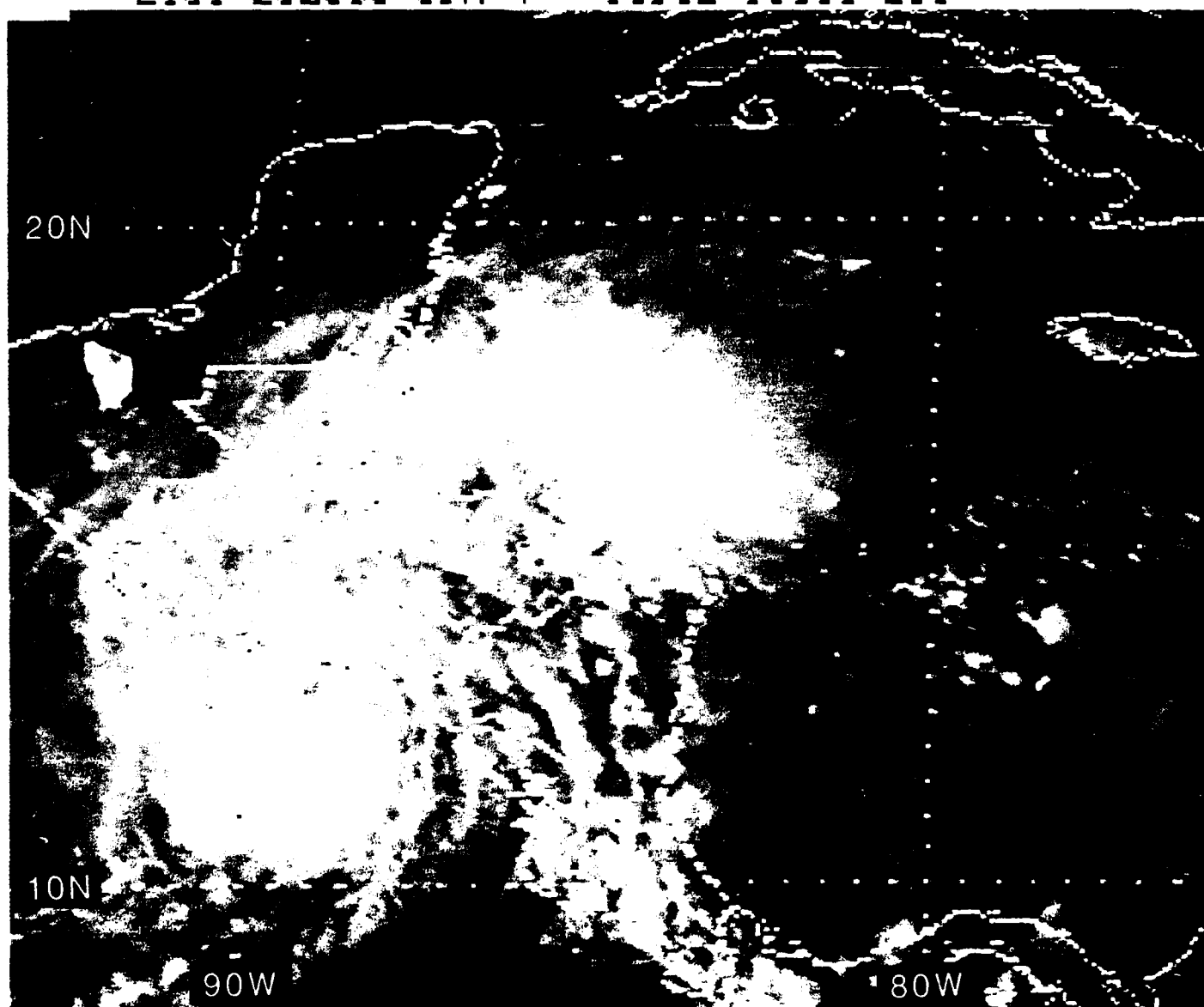


Figure 5.66: GOES East Visible Satellite Imagery, 2131 UTC 23 OCT 1988

0001 240C88 39E-4ZA 00912 16011 EC1

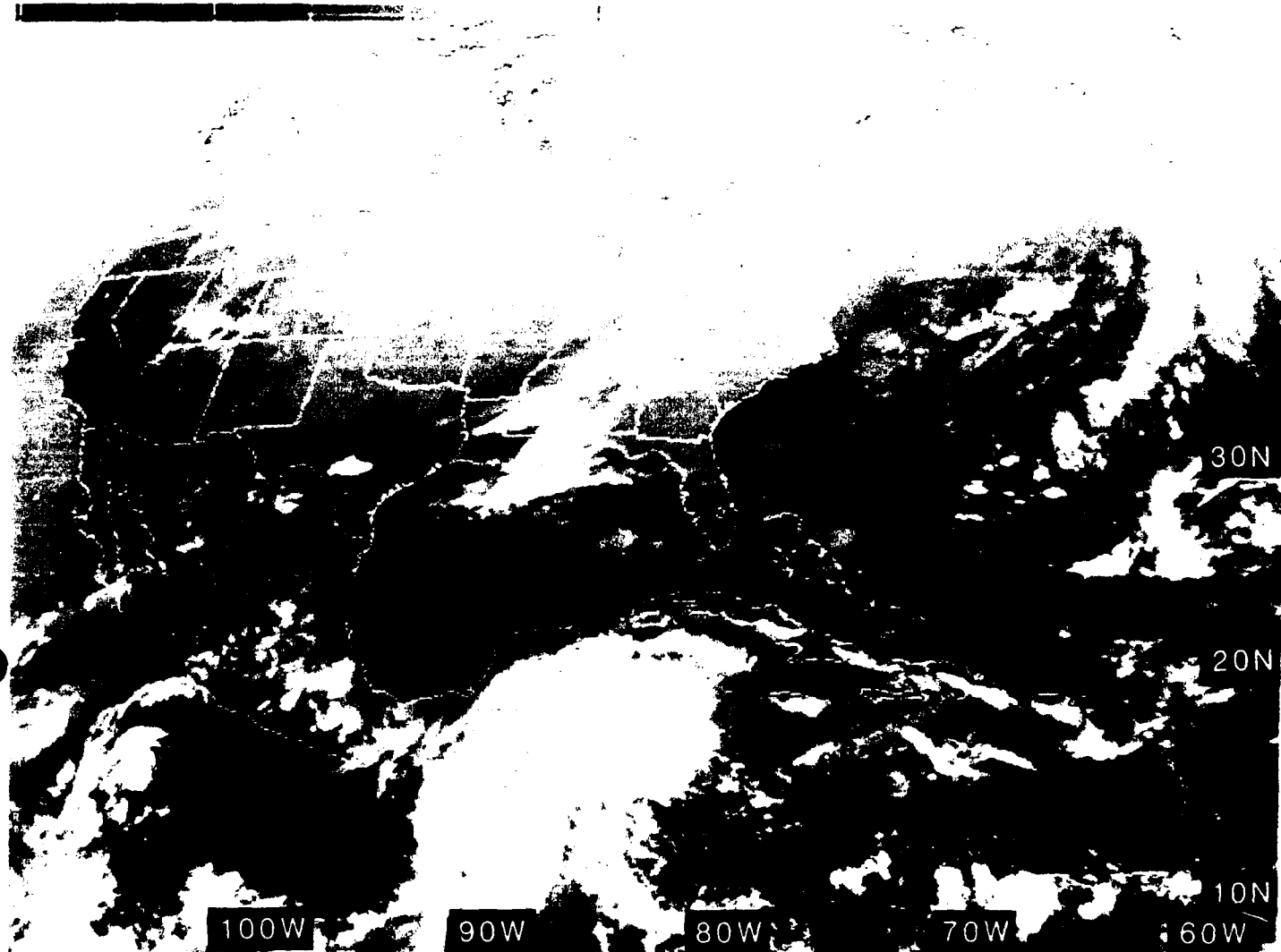


Figure 5.67: GOES East Infrared Satellite Imagery, 0001 UTC 24 OCT 1988

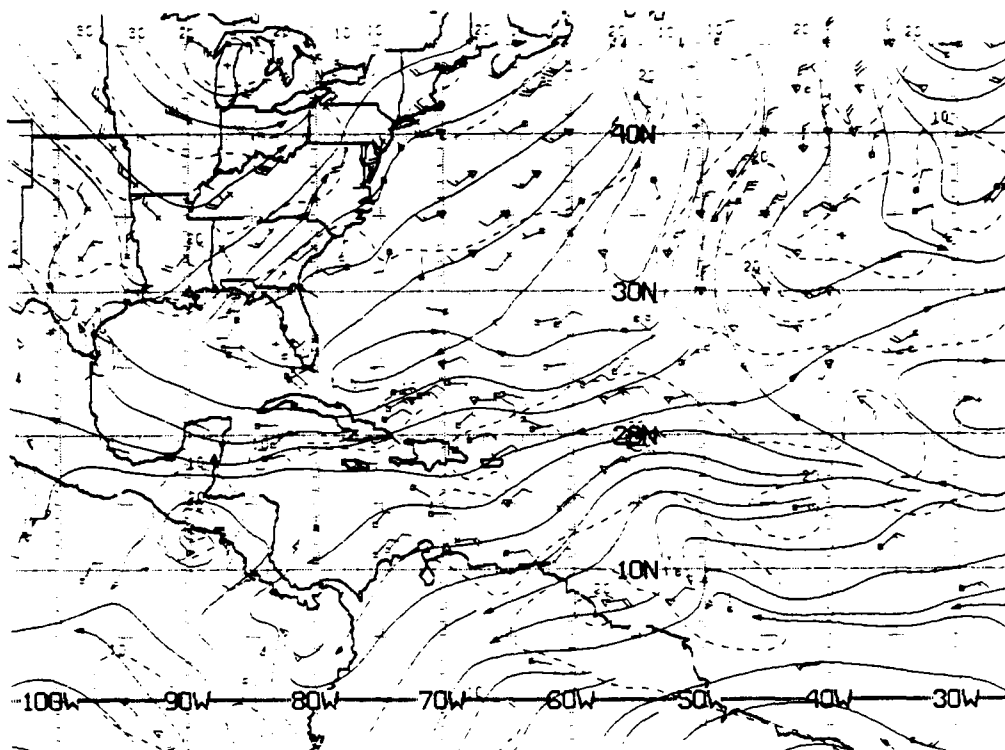


Figure 5.68: NMC ATOLL Operational Streamline Chart, 0000 UTC 24 OCT 1988
As in Fig. 2.4.

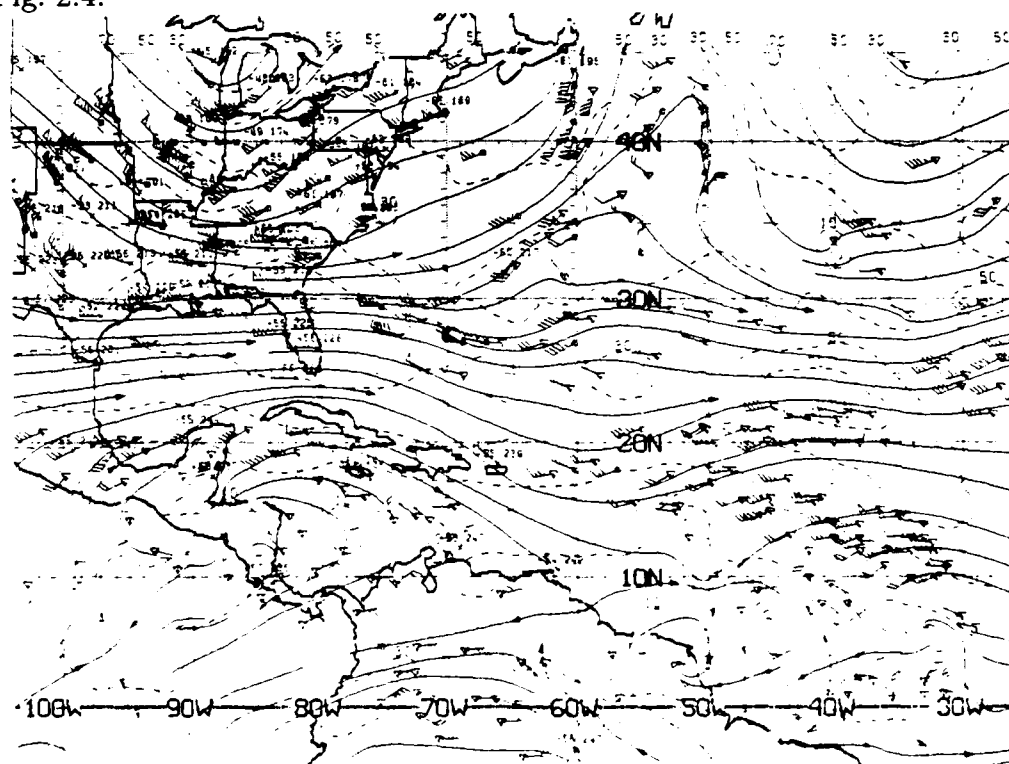


Figure 5.69: NMC 200 mb Operational Streamline Chart, 0000 UTC 24 OCT 1988
As in Fig. 2.6.

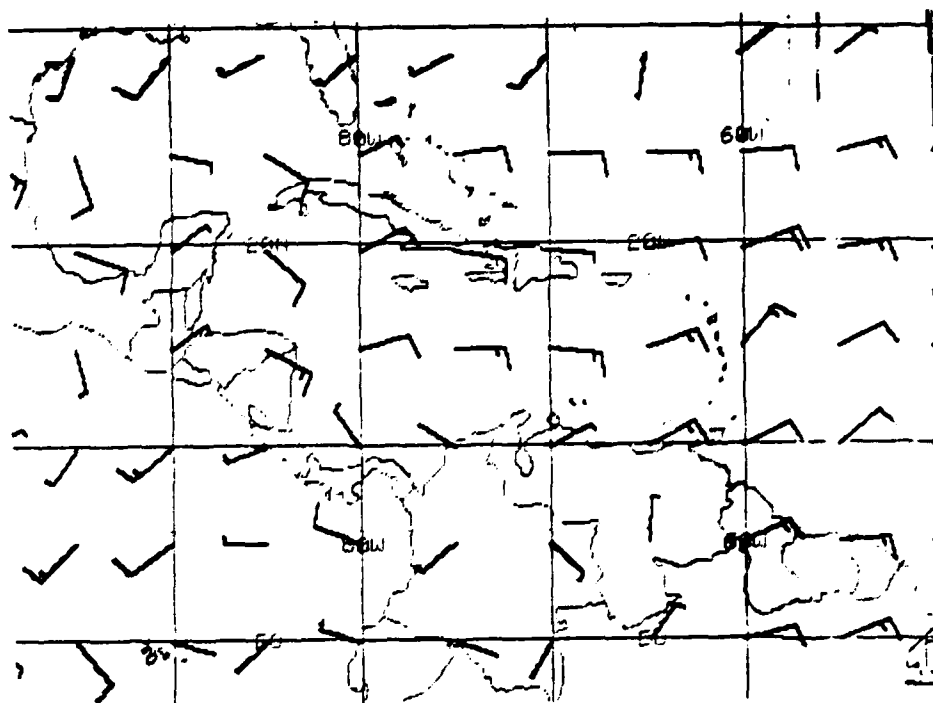


Figure 5.70: FNOc 925 mb Winds, 0000 UTC 24 OCT 1988. As in Fig. 2.19.

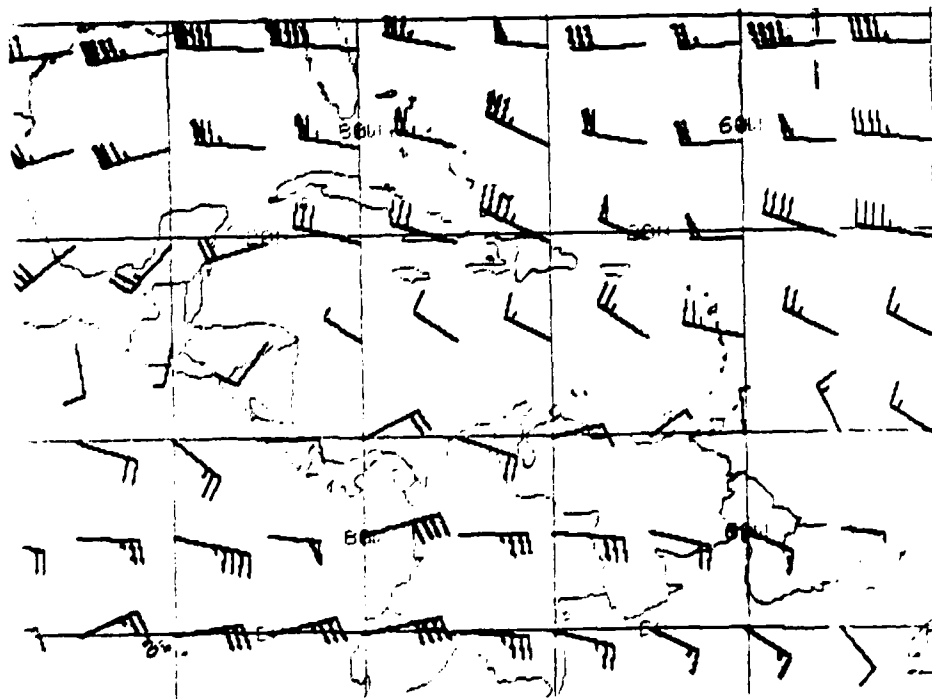


Figure 5.71: FNOc 200 mb Winds, 0000 UTC 24 OCT 1988. As in Fig. 2.20.

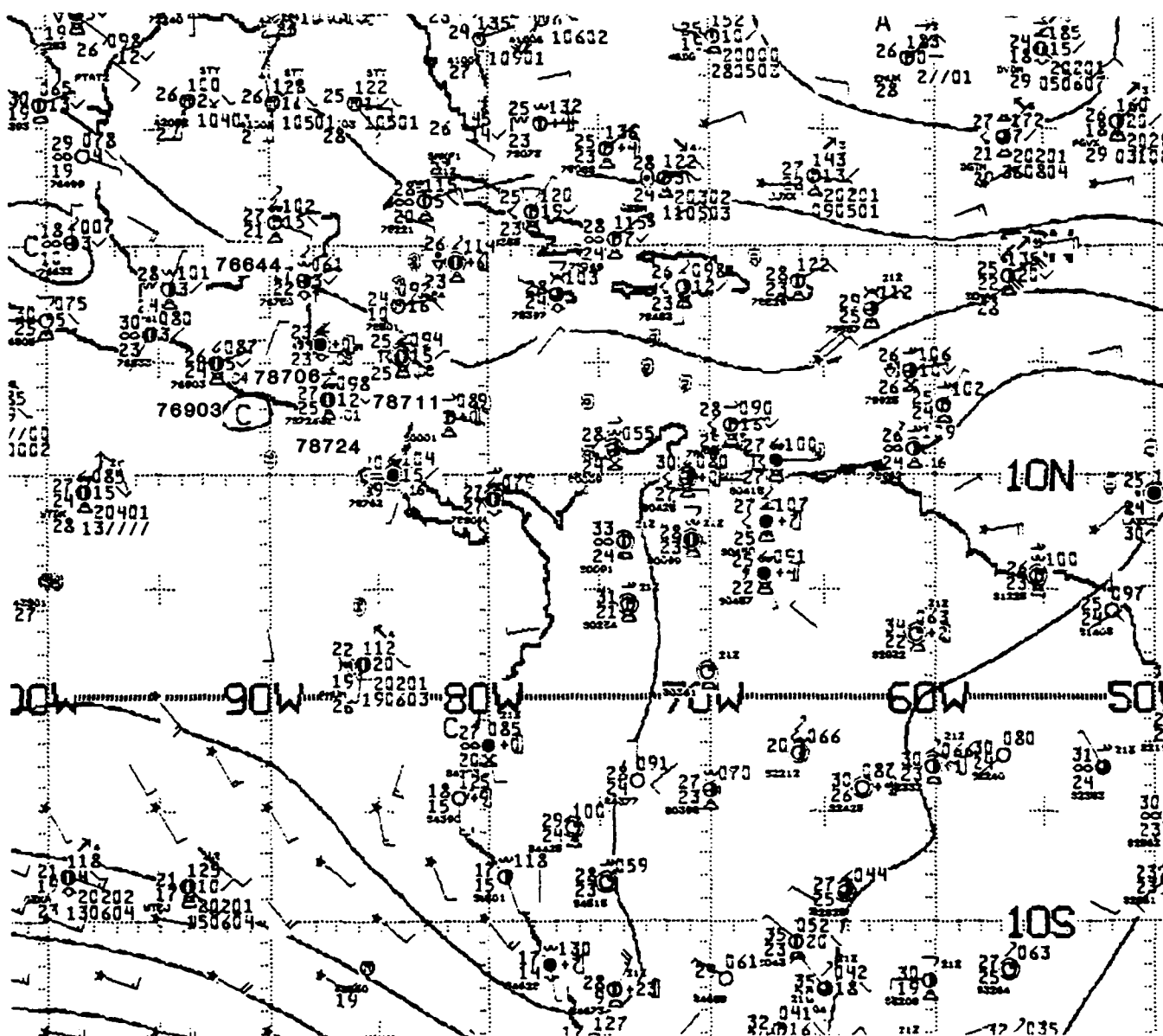


Figure 5.72: NMC 1000 mb Analysis, 0000 UTC 24 OCT 1988. As in Fig. 2.21.

1201 240C88 39E-42A 00912 16071 EC1

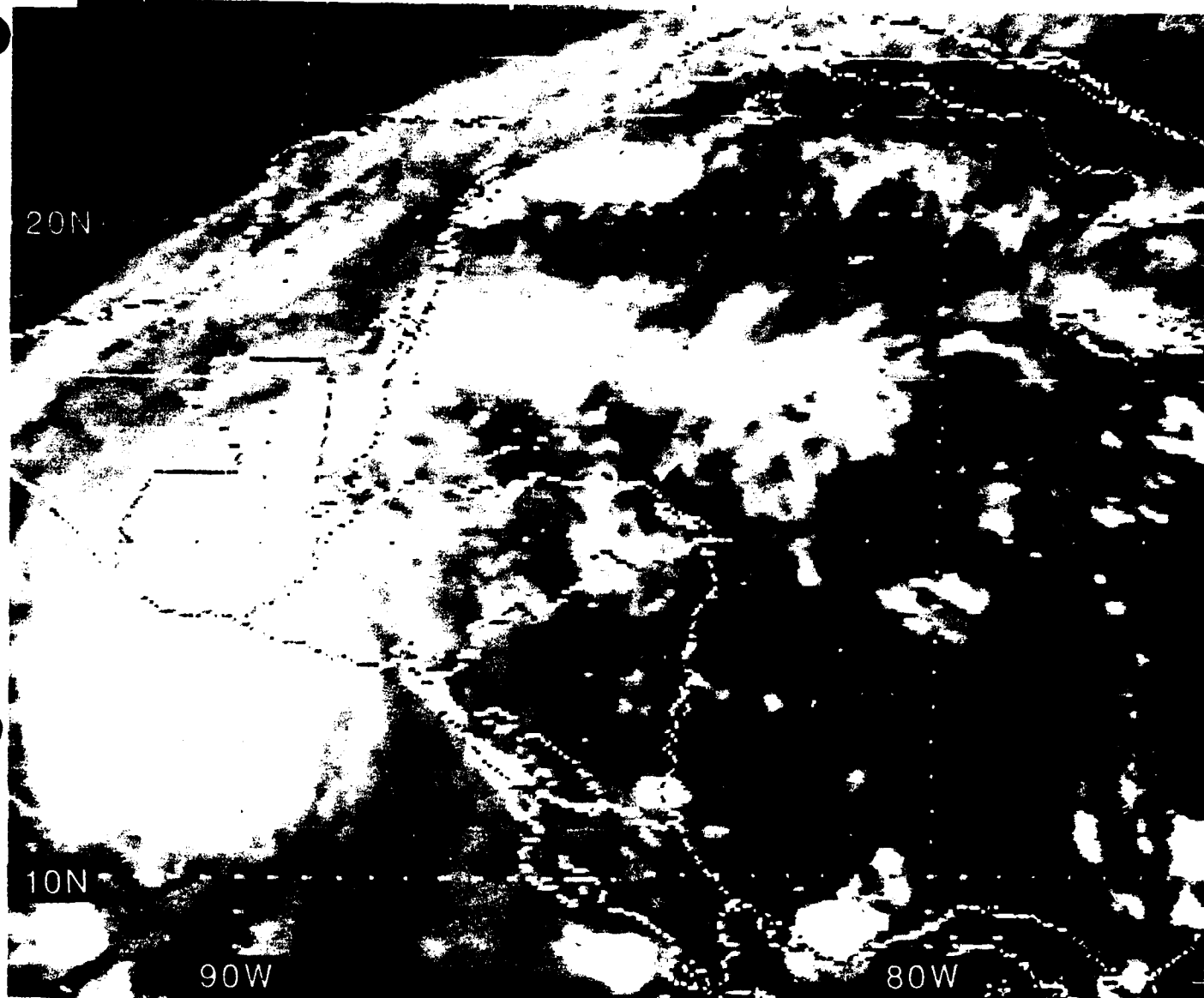


Figure 5.73: GOES East Infrared Satellite Imagery, 1201 UTC 24 OCT 1988

1431 240C88 39A-4 00901 16061 EC1

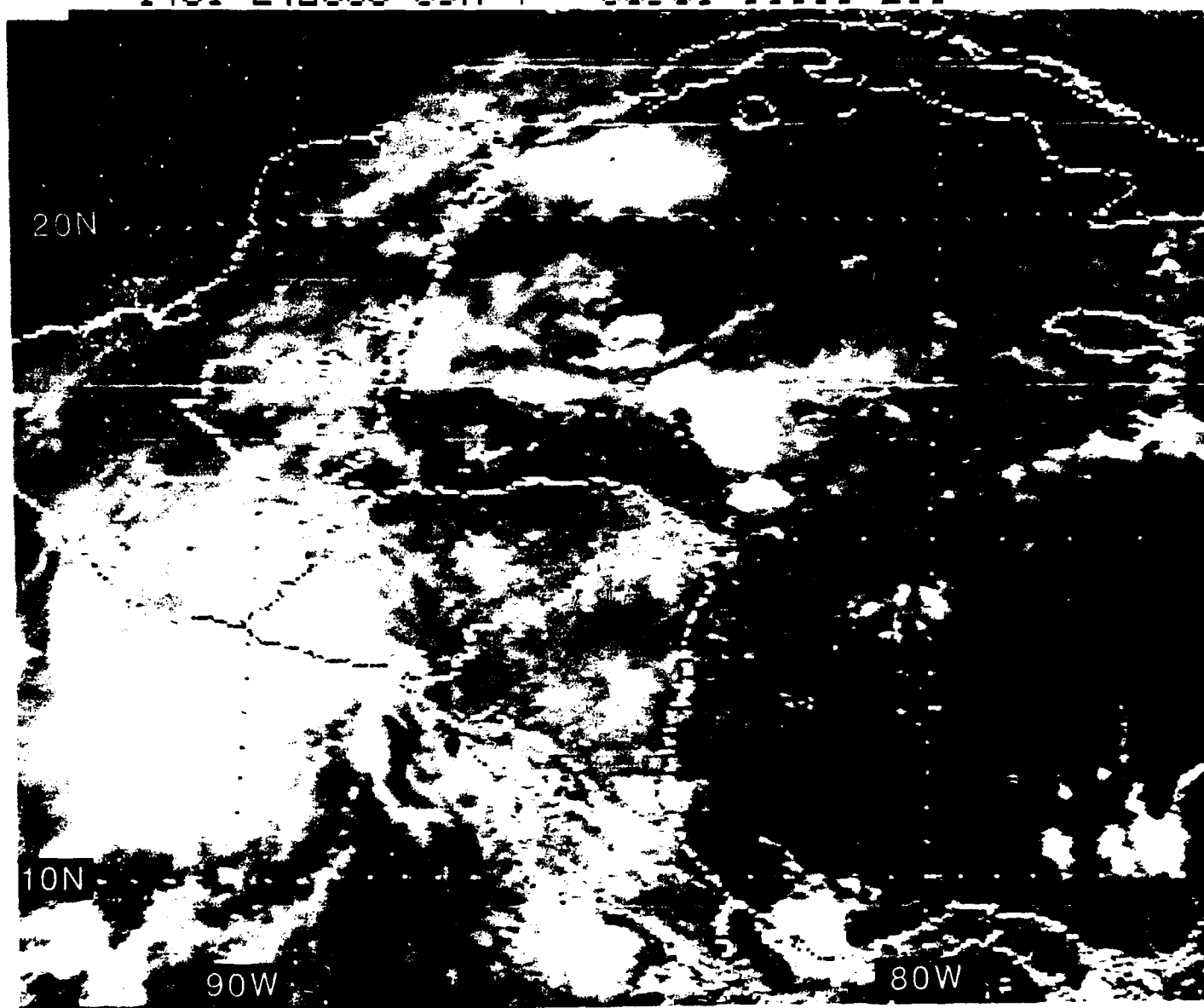


Figure 5.74: GOES East Visible Satellite Imagery, 1431 UTC 24 OCT 1988

0001 250C88 39E-4ZA 00911 16031 EC1

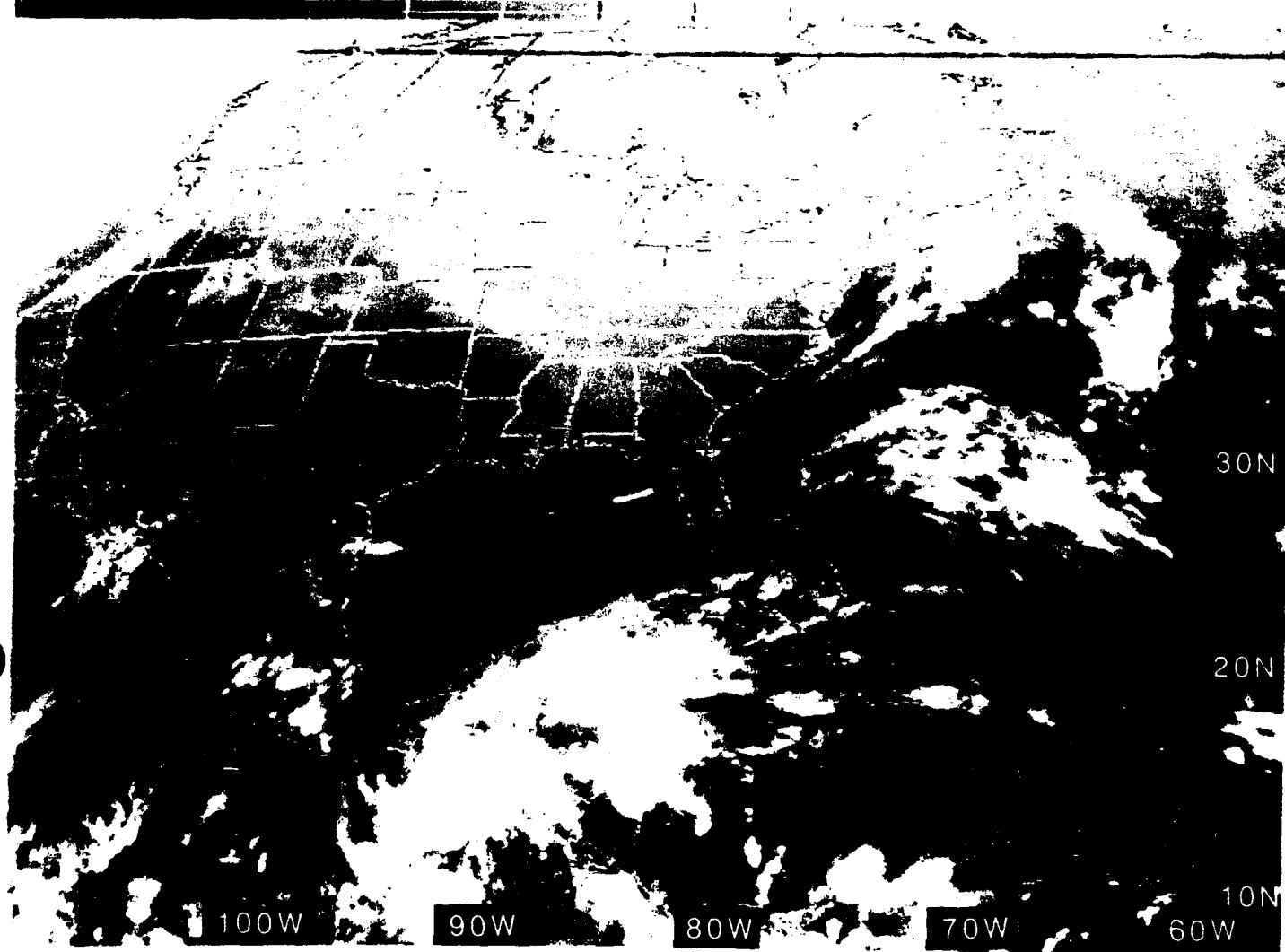


Figure 5.75: GOES East Infrared Satellite Imagery, 0001 UTC 25 OCT 1988

1901 250088 39E-42A 00911 16061 EC1

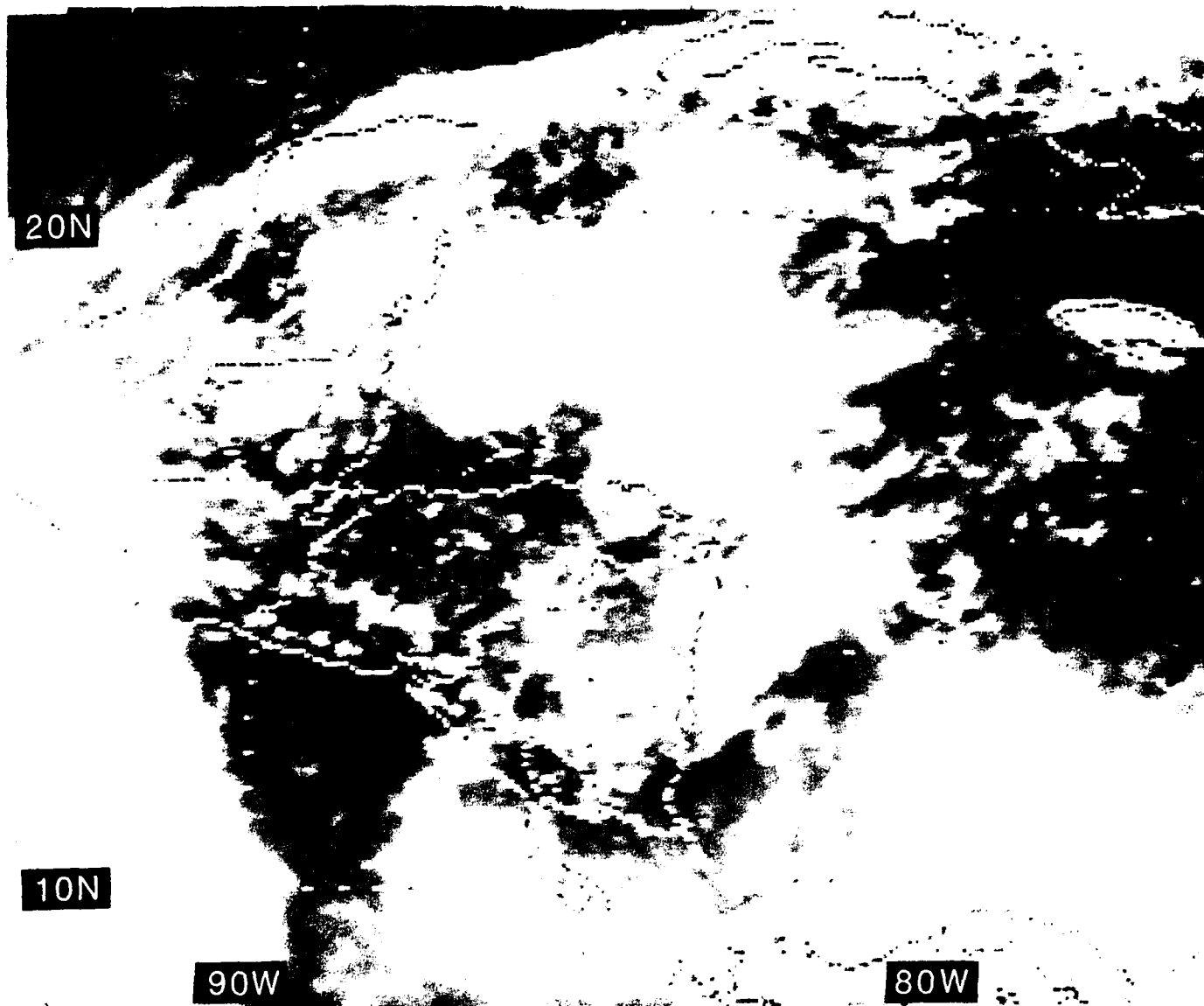


Figure 5.76: GOES East Infrared Satellite Imagery, 1901 UTC 25 OCT 1988

2101 250088 39E-4ZA 00302 16051 EC1

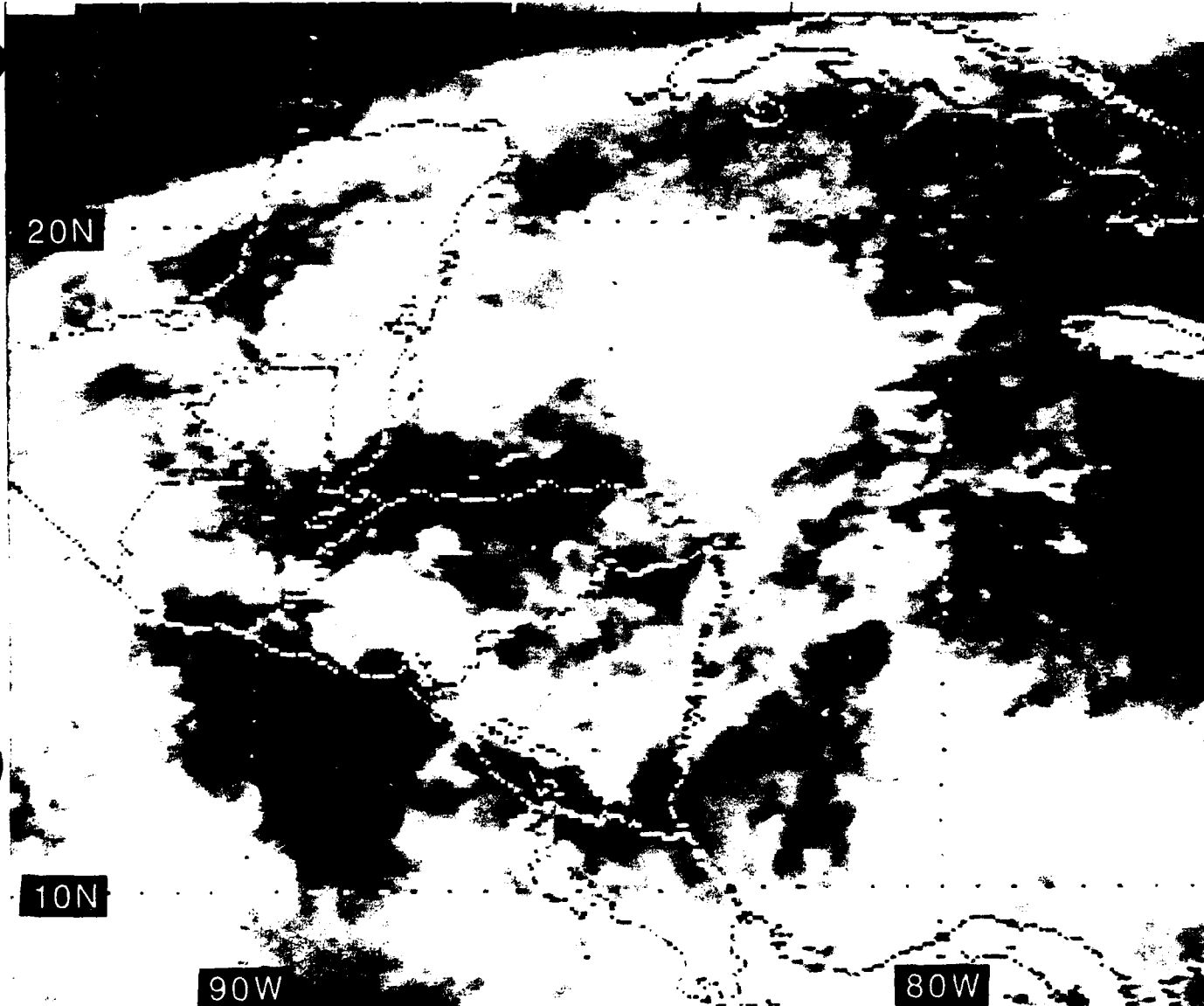


Figure 5.77: GOES East Infrared Satellite Imagery, 2101 UTC 25 OCT 1988

5.2.2 Case VI - Hurricane Gilbert (9 – 14 September 1988)

While its center passed far north of Belize, Hurricane Gilbert's size, strength, minimum pressure, maximum wind, storm surge and damage to life⁹³ and property dictate its inclusion as a case study. When Hurricane Gilbert made landfall on the northeastern Yucatan Peninsula, it was the first category 5 hurricane (>135 mph) to make landfall in the western hemisphere since Hurricane Camille in 1969.

The tropical wave that was to become Hurricane Gilbert emerged from the northwest African coast on 3 September. The *preliminary* best track of Hurricane Gilbert by the National Hurricane Center (NHC, 1988) is presented in Fig. 5.78. (Unless stated otherwise, the following data concerning Hurricane Gilbert⁹⁴ are from the Diagnostic Report of the National Hurricane Center-August and September 1988 (NHC, 1988)).

9 September 1988

The 1000 mb analysis of Fig. 5.79 shows station observations at 1200 UTC on 9 September as Tropical Depression #12 approaches the Windward Islands. Note the correlation of the following station observations with the visible imagery of Fig. 5.80 (although 3 1/2 hours later at 1531 UTC): overcast with a rain shower at Le Lamentin, Martinique (station 78925), with a thunderstorm reported at the station to the southeast (Barbados); overcast with continuous rain at San Juan, Puerto Rico (station 78526); lightning with towering cumulus clouds at Kingston, Jamaica (station 78397); *yet* only 1/4 sky cover at the station reporting from eastern Cuba and 1/8 sky cover at Playa Giron, Cuba (station 78333). Hurricane Florence is seen moving inland across the Louisiana coastline in Fig. 5.80.

Moving on a west northwest course at ~ 15 kt, Tropical Depression #12 is classified as Tropical Storm Gilbert at 1800 UTC on 9 September.

10 September 1988

The IR imagery of Fig. 5.81 shows the intense convection associated with Tropical Storm Gilbert at 0001 UTC on 10 September 1988. At this time the tropical storm is located at 14.8°N , 61.5°W , with a minimum sea-level pressure of 1002 mb and sustained surface winds of 40 kt. Figures 5.82 and 5.83 are the Navy's FNOG low-level and upper-level wind analyses at 0000 UTC on 10 September. Even this coarse 5-degree grid wind analysis depicts the cyclonic rotation of the tropical storm at the 925 mb pressure surface in the eastern Caribbean Sea. The 200 mb wind analysis shows strong anticyclonic flow above the convection, associated with the tropical storm and its release of latent heat.

The visible imagery of Fig. 5.84 at 1731 UTC on 10 September shows the increase in the storm's circulation. 30 minutes later at 1800 UTC, the storm is located by NHC at 15.7°N , 65.4°W , with a sea-level pressure of 992 mb and 55 kt winds.

⁹³As of 26 October 1988, in addition to large losses of life in Mexico (202) and Jamaica (45), the following Central American countries attributed storm related deaths to Hurricane Gilbert: Guatemala 12, Honduras 12, Nicaragua 2 and Costa Rica 2.

⁹⁴This is in contrast to the data presented in the preceding case study of Hurricane Joan in which operational warning positions, etc. were presented.

11 September 1988

At 0000 UTC on 11 September, the tropical cyclone was upgraded to a hurricane. The NMC ATOLL and 200 mb streamline analyses (Figs. 5.85 and 5.86) depict the low-level and upper-level flow at this time. The hurricane is located at 15.9°N, 66.8°W (~ 120 n mi south of Puerto Rico), with a sea-level pressure of 989 mb and 65 kt winds.

The station observations at 1200 UTC (Fig. 5.87) may be compared to the visible satellite imagery (Fig. 5.88, 1 1/2 hours later): overcast with a rain shower and ESE winds at San Juan, Puerto Rico (station 78526); overcast with towering cumulus and SW winds at Curaçao, Netherlands Antilles (station 78988); yet, only calm winds with 1/8 sky cover at Kingston, Jamaica (station 78397) and 1/8 sky cover at Camaguey, Cuba (station 78283).

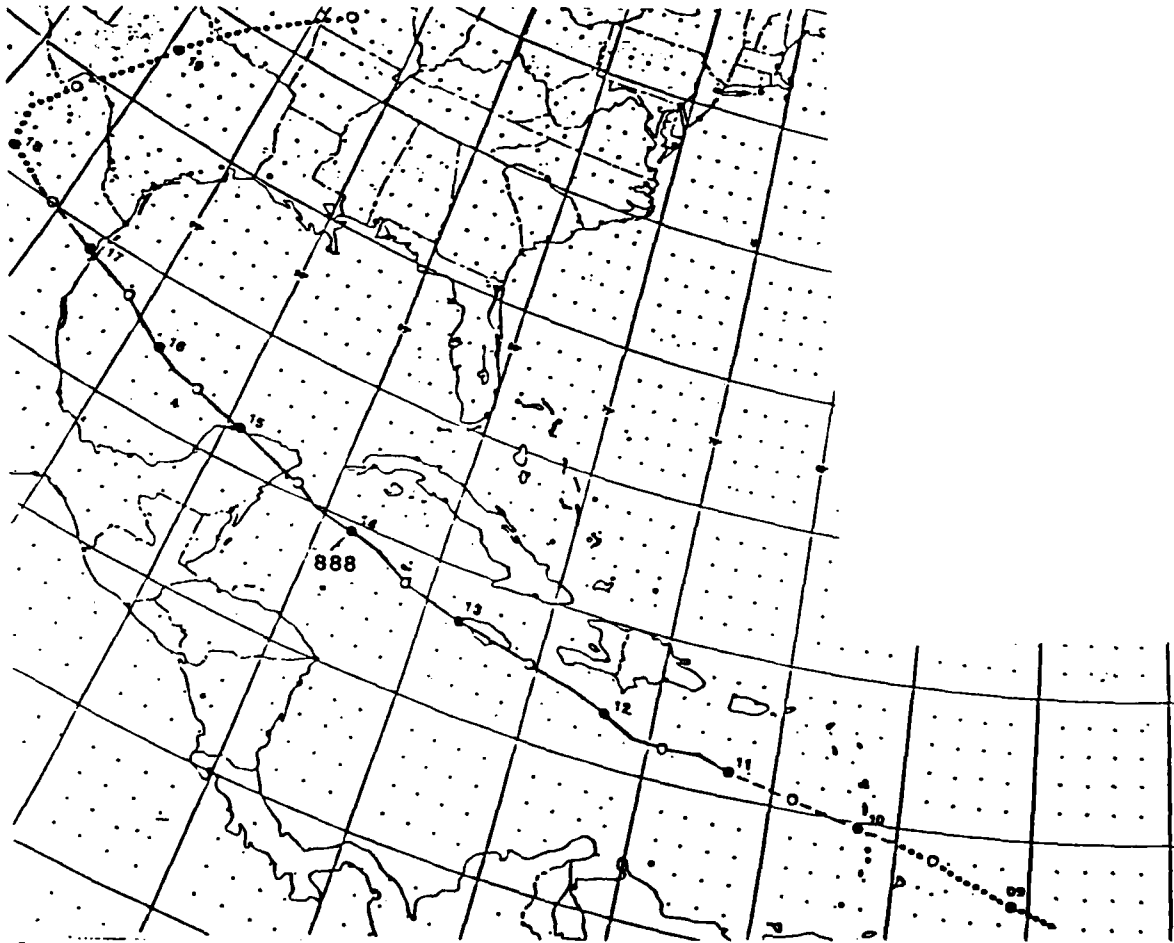


Figure 5.78: Best Track Positions for Hurricane Gilbert, 8-19 September 1988
(From NHC, 1988)

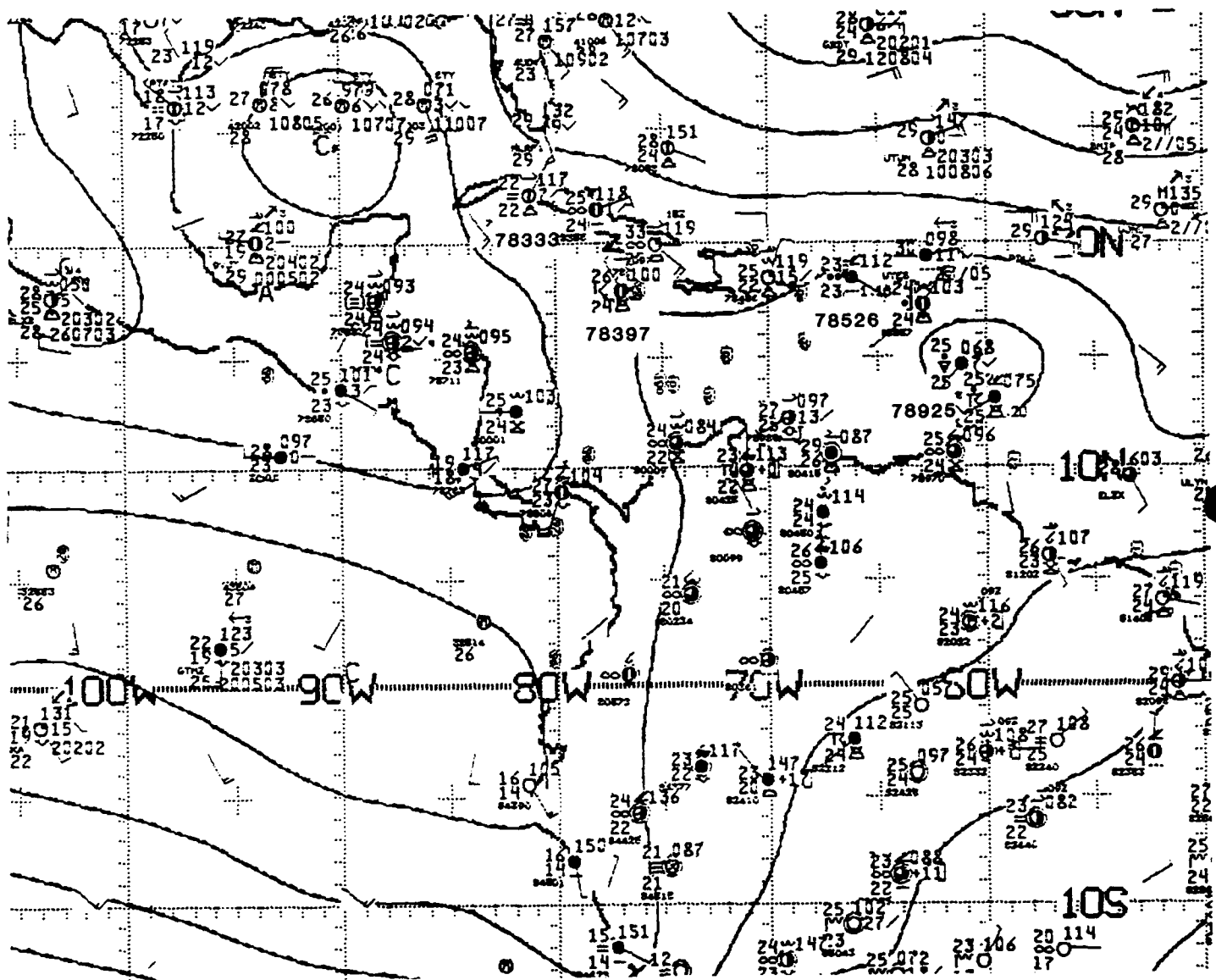


Figure 5.79: NMC 1000 mb Analysis, 1200 UTC 9 SEP 1988. As in Fig. 2.21.

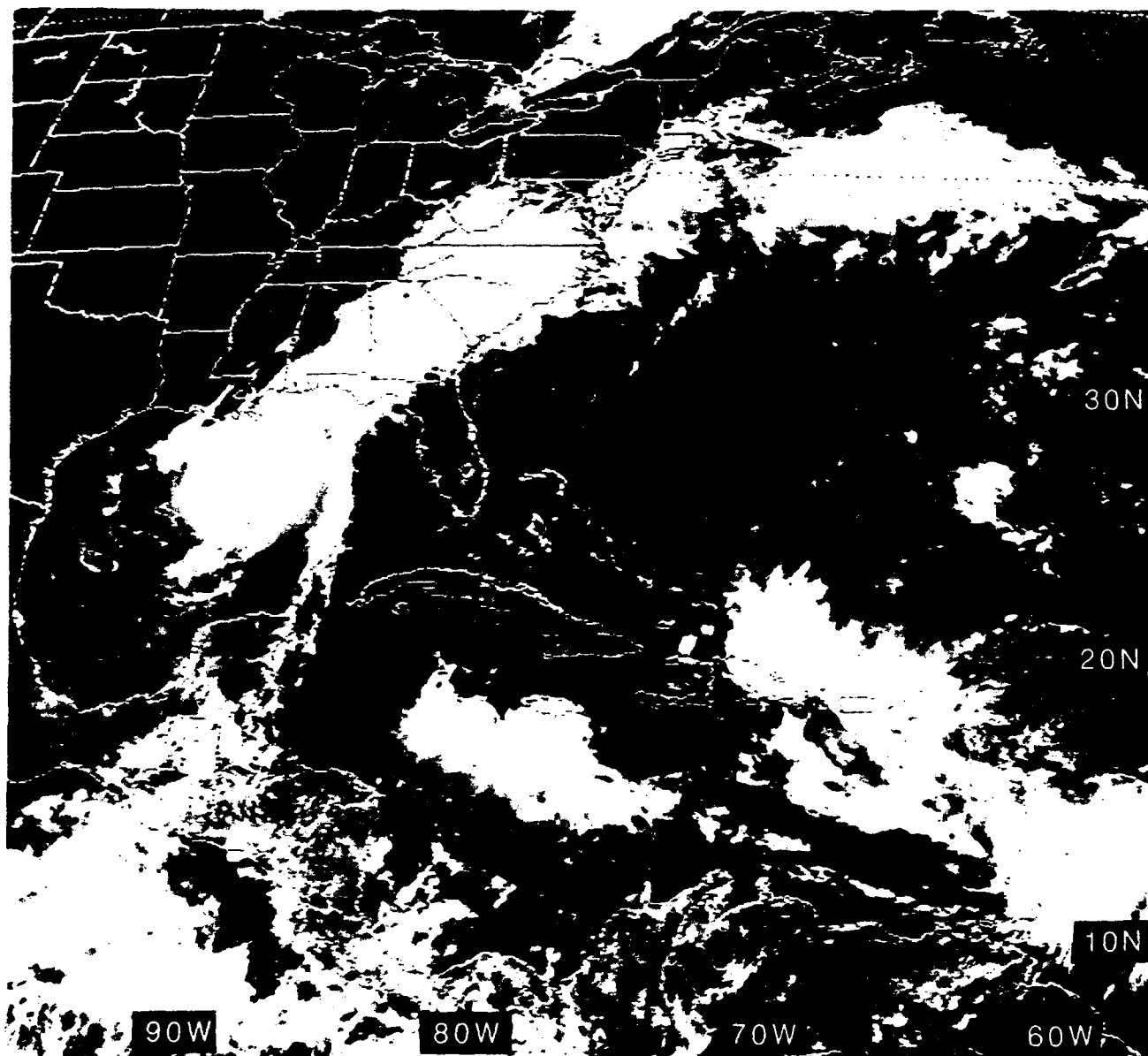


Figure 5.80: GOES East Visible Satellite Imagery, 1531 UTC 9 SEP 1988

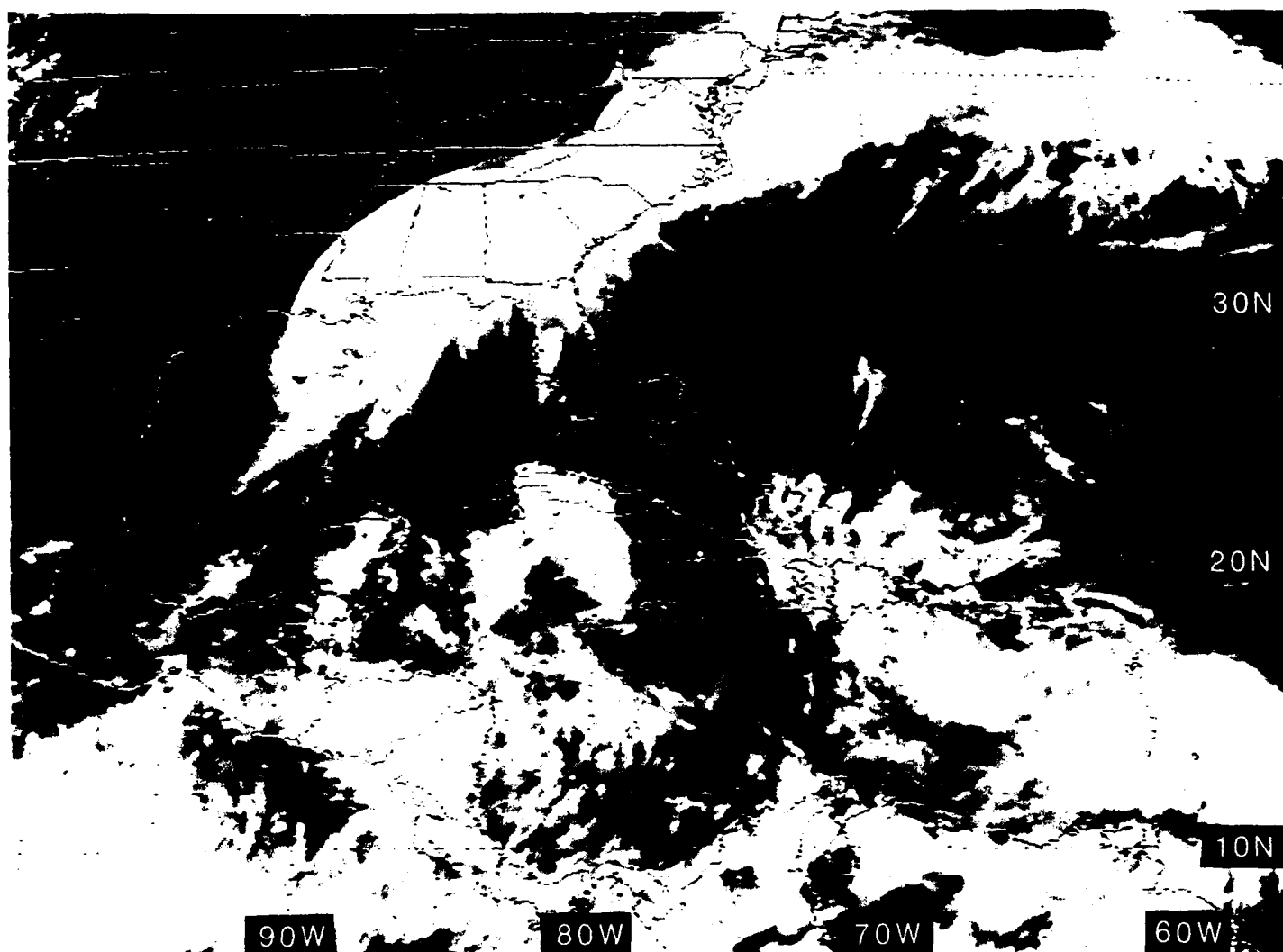


Figure 5.81: GOES East Infrared Satellite Imagery, 0001 UTC 10 SEP 1988

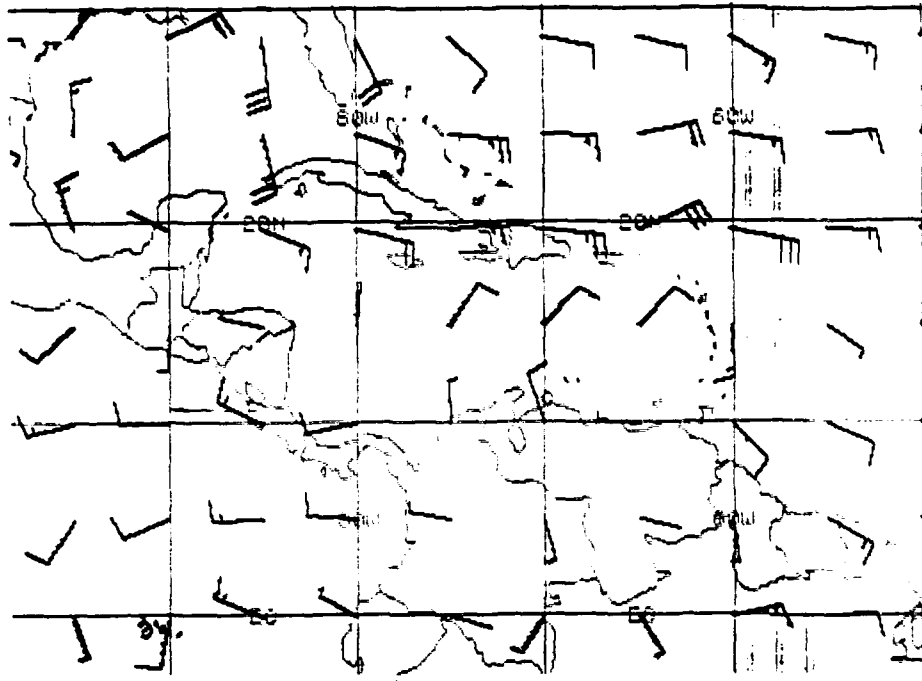


Figure 5.82: FNO 925 mb Winds, 0000 UTC 10 SEP 1988. As in Fig. 2.19.

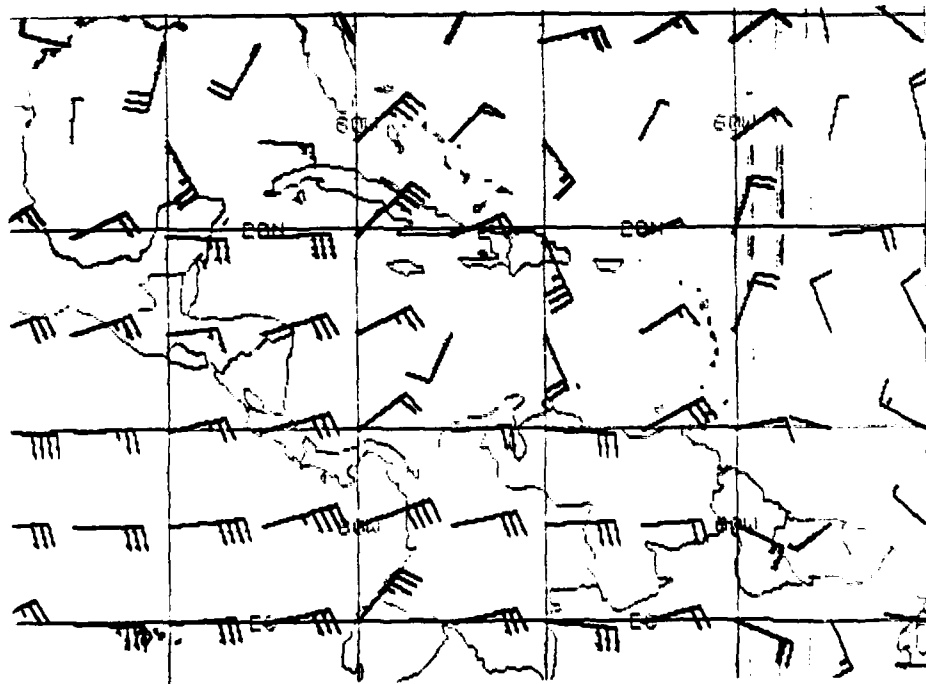


Figure 5.83: FNO 200 mb Winds, 0000 UTC 10 SEP 1988. As in Fig. 2.20.

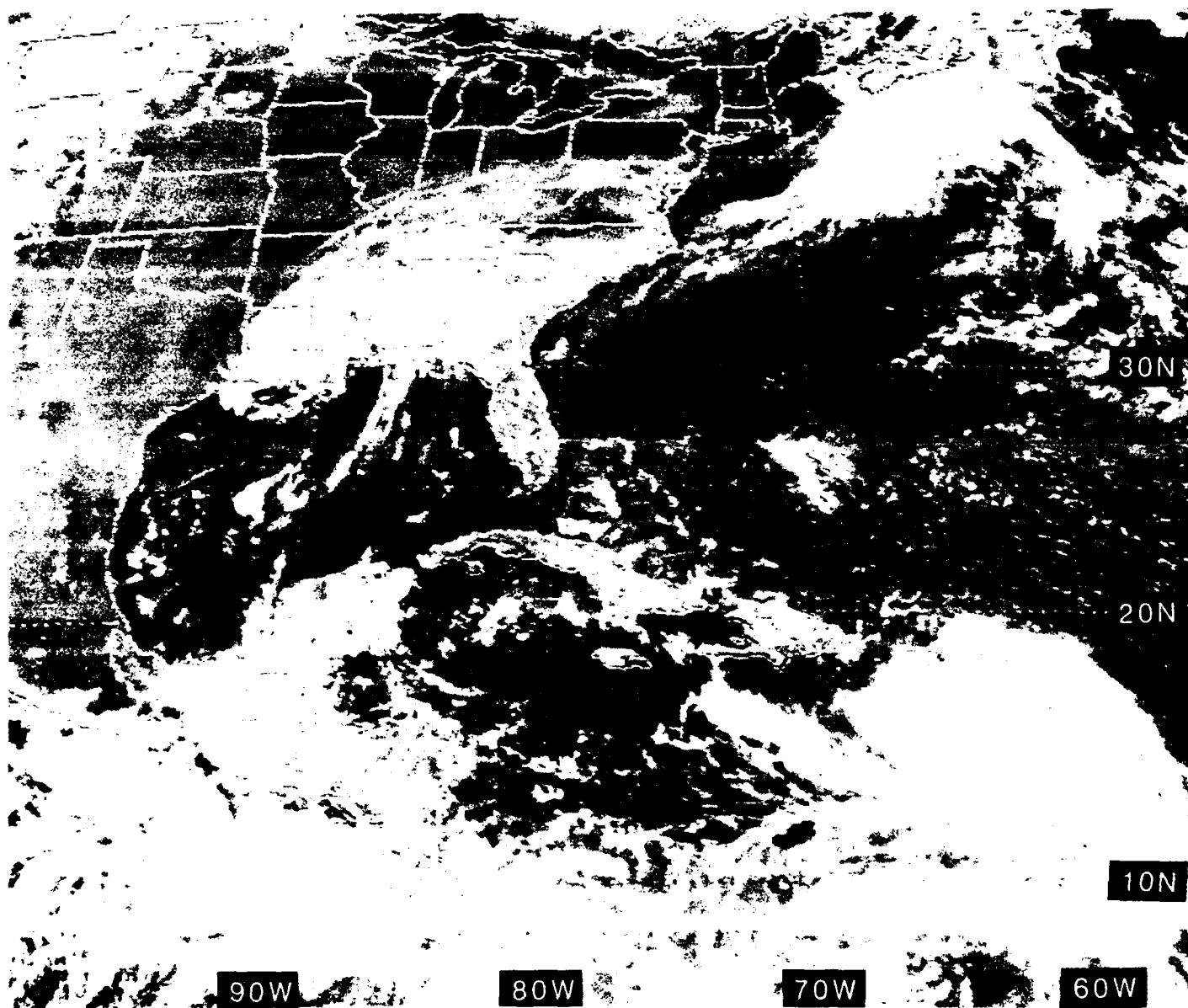


Figure 5.84: GOES East Visible Satellite Imagery, 1731 UTC 10 SEP 1988

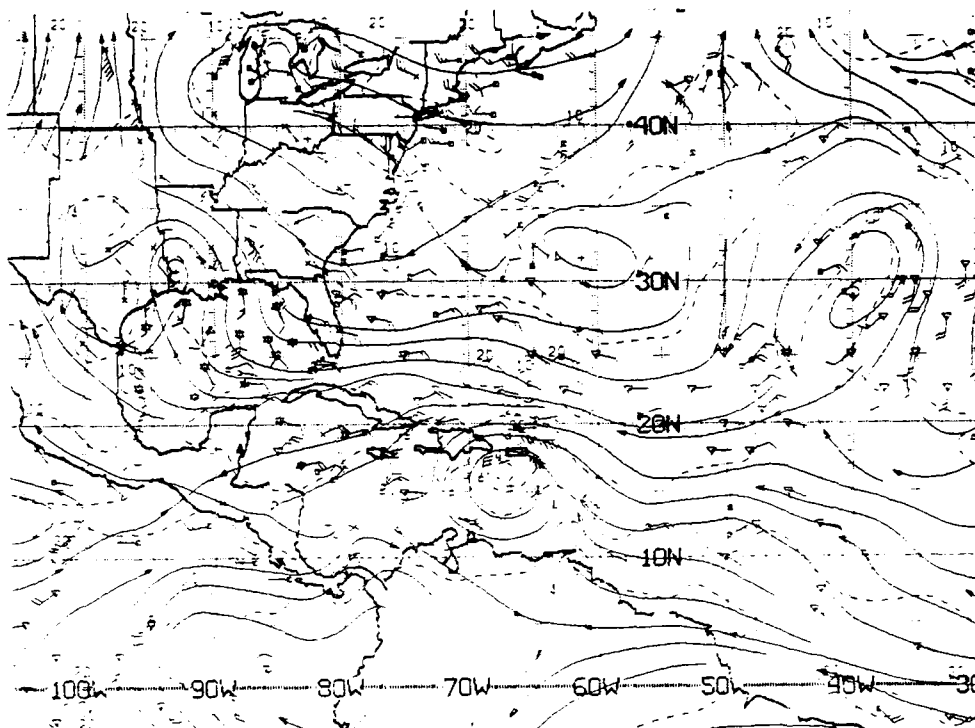


Figure 5.85: NMC ATOLL Operational Streamline Chart, 0000 UTC 11 SEP 1988
As in Fig. 2.4.

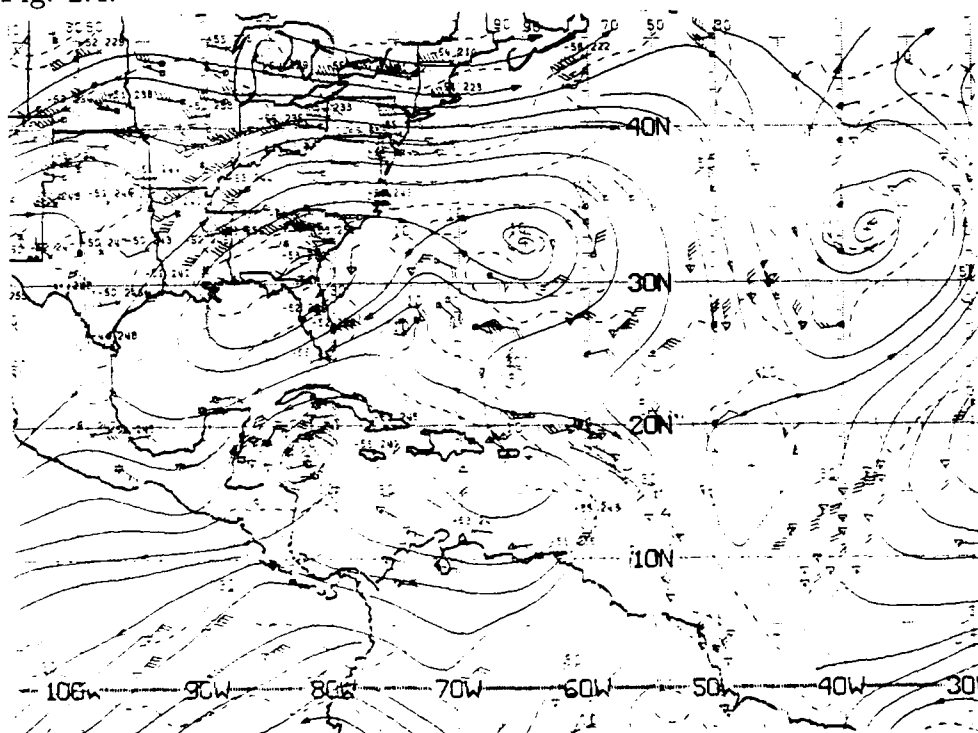


Figure 5.86: NMC 200 mb Operational Streamline Chart, 0000 UTC 11 SEP 1988
As in Fig. 2.7.

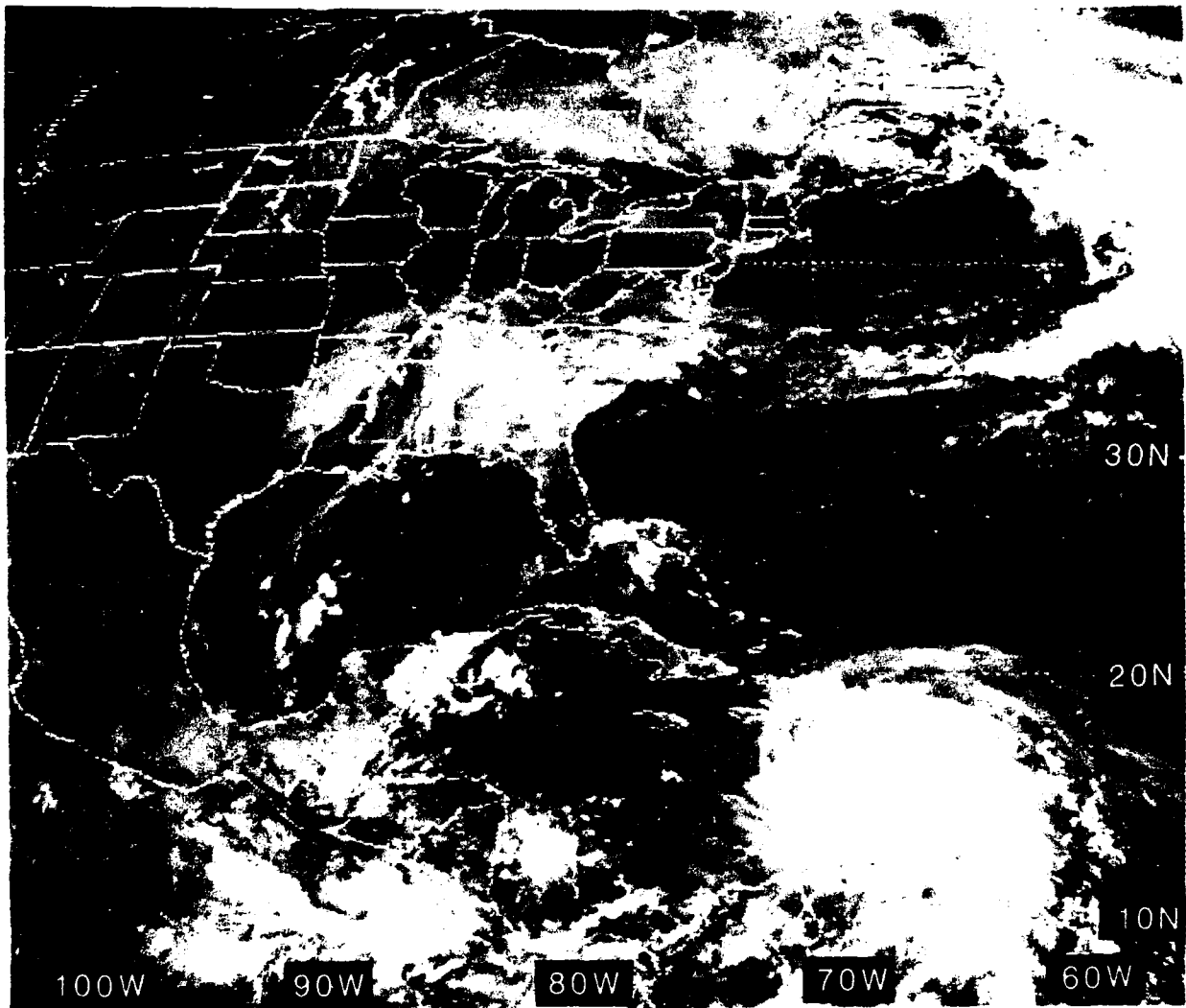


Figure 5.88: GOES East Visible Satellite Imagery, 1331 UTC 11 SEP 1988

12 September 1988

The low-level and upper-level streamlines associated with Hurricane Gilbert at 0000 UTC on 12 September are depicted by the NMC charts (Figs. 5.89 and 5.90). The Navy wind analyses (Figs. 5.91 and 5.92) are included for comparison. At this time the hurricane is located at 16.8°N, 72.0°W (see the IR imagery at 0001 UTC in Fig. 5.93), with a sea-level central pressure of 964 mb and sustained winds of 105 kt.

The Navy NOGAPS 24-hour 925 mb wind prognosis verifying at 0000 UTC 12 September (Fig. 5.94) provides a good forecast of Hurricane Gilbert's peripheral winds—recall that at the time this prognosis was prepared, Hurricane Gilbert was located at 15.9°N, 66.8°W, i.e., south of Puerto Rico.

Six hours later (0600 UTC 12 September), Fig. 5.95 shows the official forecast of the expected path of Hurricane Gilbert for the next 72 hours. Despite the erroneous "recurvature" forecast, which places the hurricane track to the right of its landfall on the northeast coast of the Yucatan Peninsula coast, the 48-h error is relatively small—compare with the preliminary best track in Fig 5.78.

Figure 5.96 gives the surface observations at 1200 UTC, while the visible imagery of Figs. 5.97 and 5.98 show the eye of the hurricane approaching the eastern tip of Jamaica. At 1730 UTC, Kingston, Jamaica reported its maximum wind of 101 kt with gusts to 122 kt. Then at 1815 UTC, Kingston, Jamaica reported its lowest pressure (964.8 mb). The northeast coast of Jamaica reported tides 9 feet above normal (NHC, 1988).

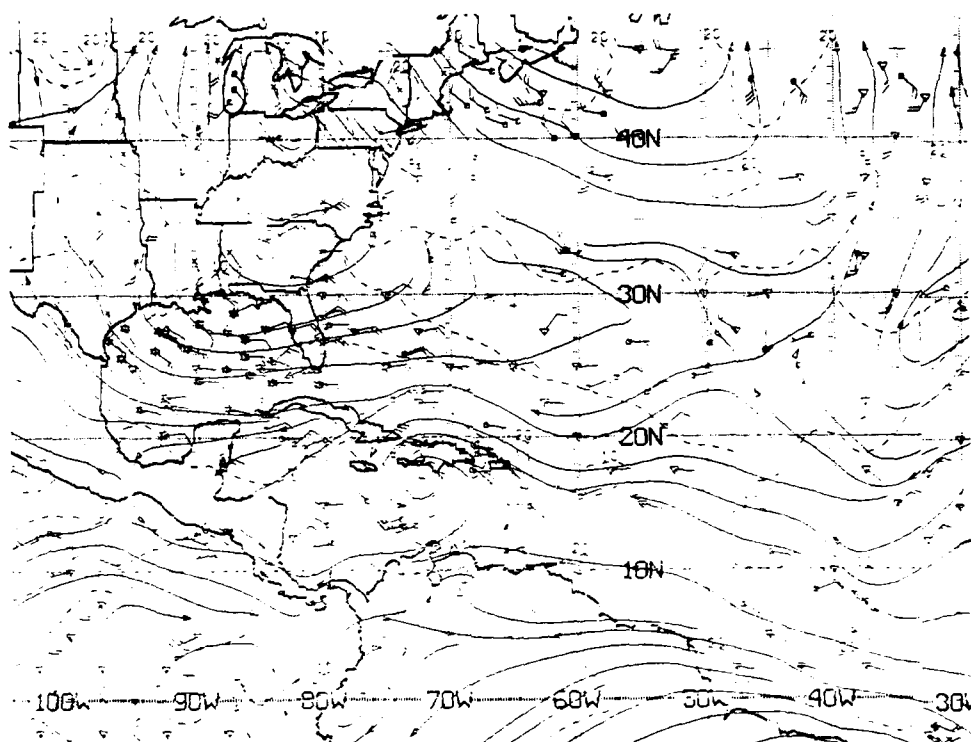


Figure 5.89: NMC ATOLL Operational Streamline Chart, 0000 UTC 12 SEP 1988
As in Fig. 2.4.

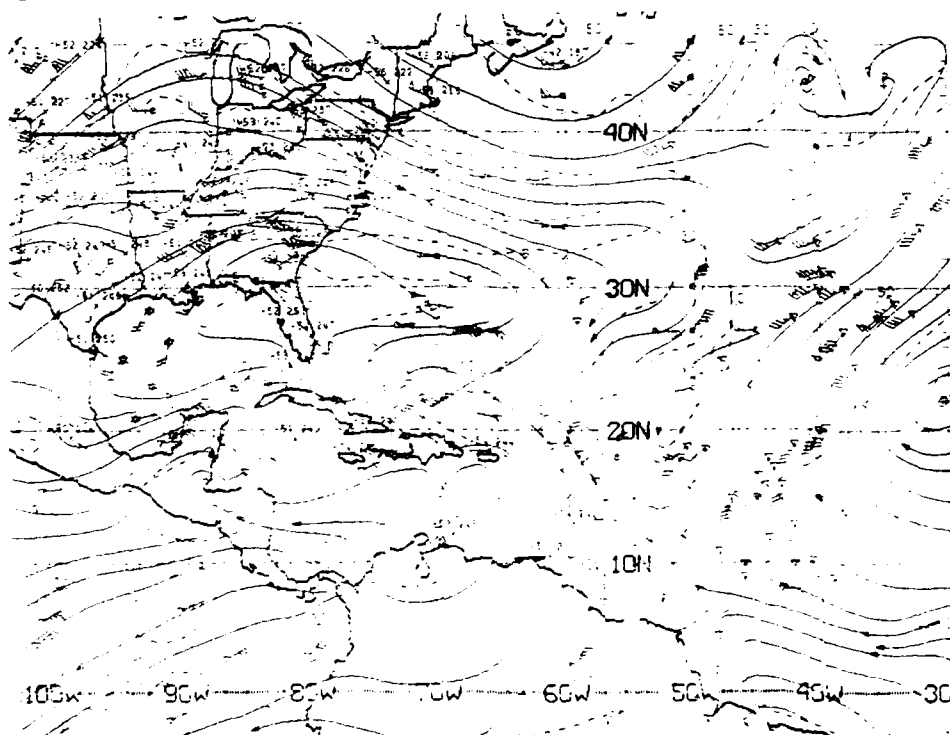


Figure 5.90: NMC 200 mb Operational Streamline Chart, 0000 UTC 12 SEP 1988
As in Fig. 2.7.

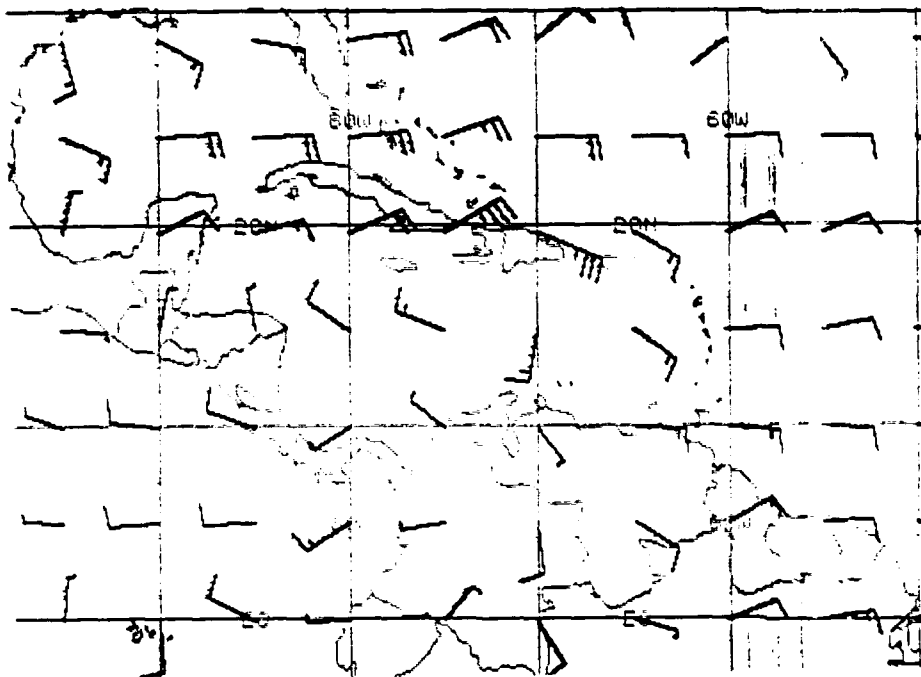


Figure 5.91: FNOc 925 mb Winds, 0000 UTC 12 SEP 1988. As in Fig. 2.19.

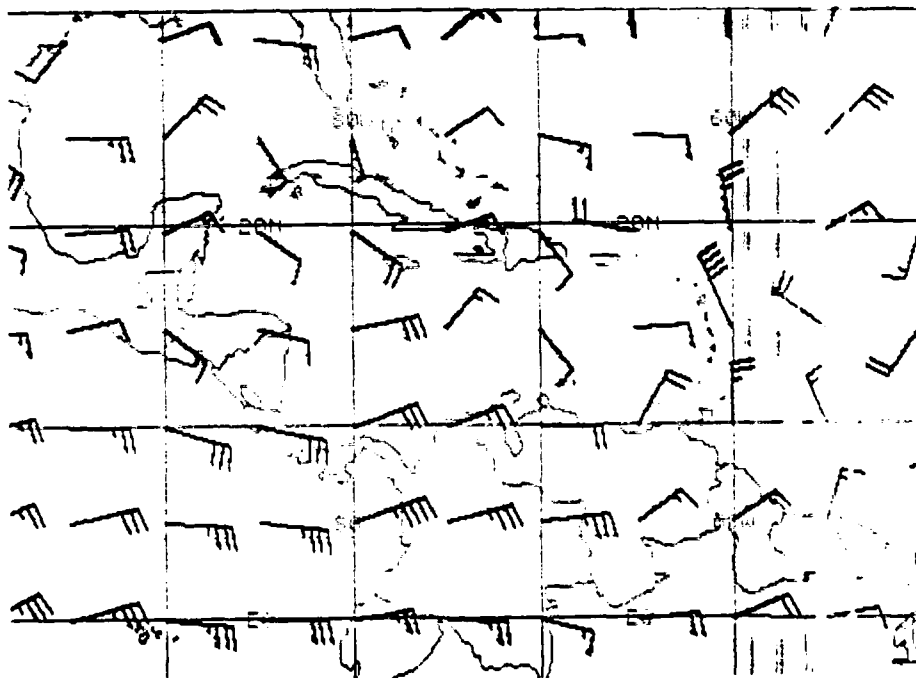


Figure 5.92: FNOc 200 mb Winds, 0000 UTC 12 SEP 1988. As in Fig. 2.20.

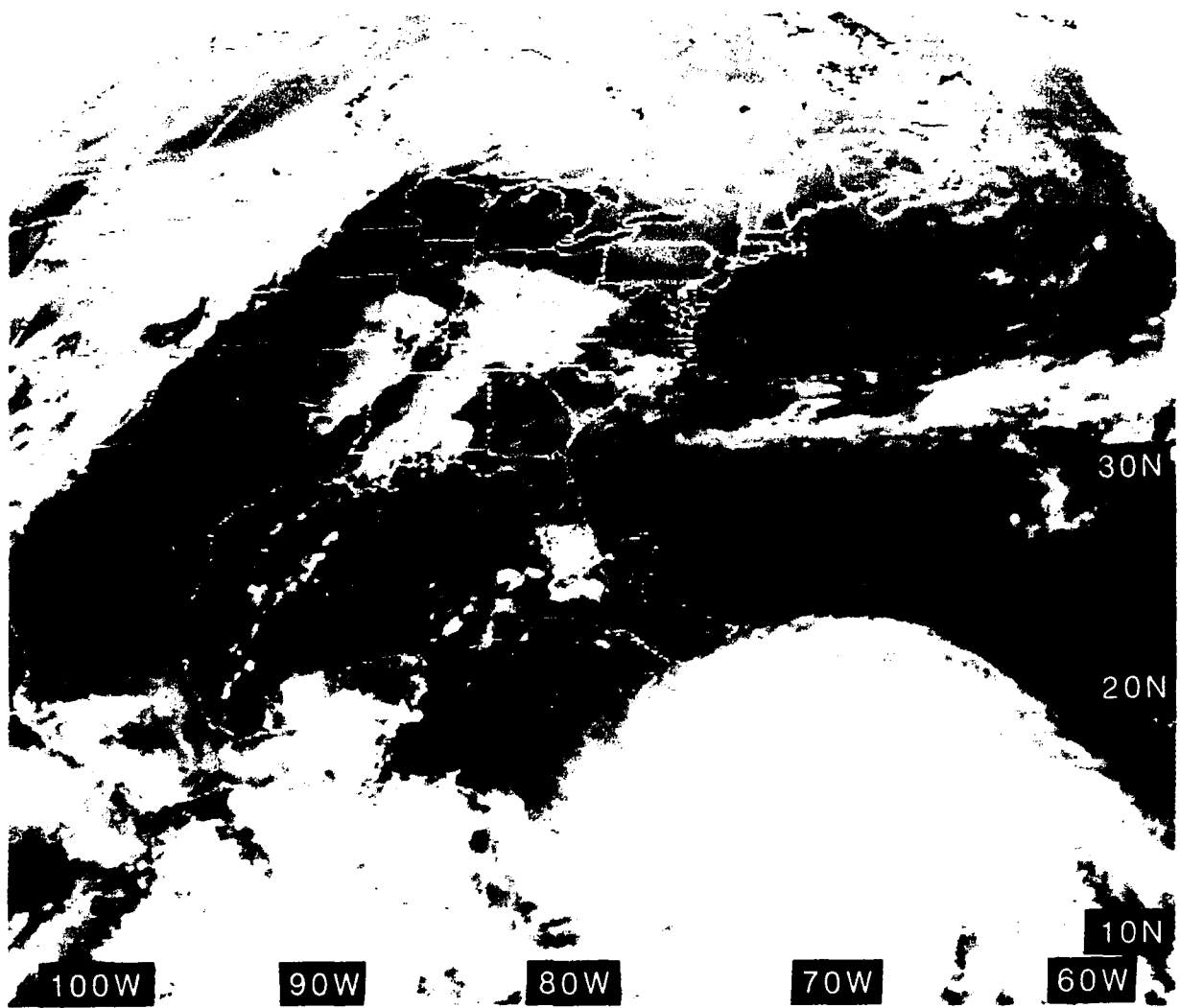


Figure 5.93: GOES East Infrared Satellite Imagery, 0001 UTC 12 SEP 1988

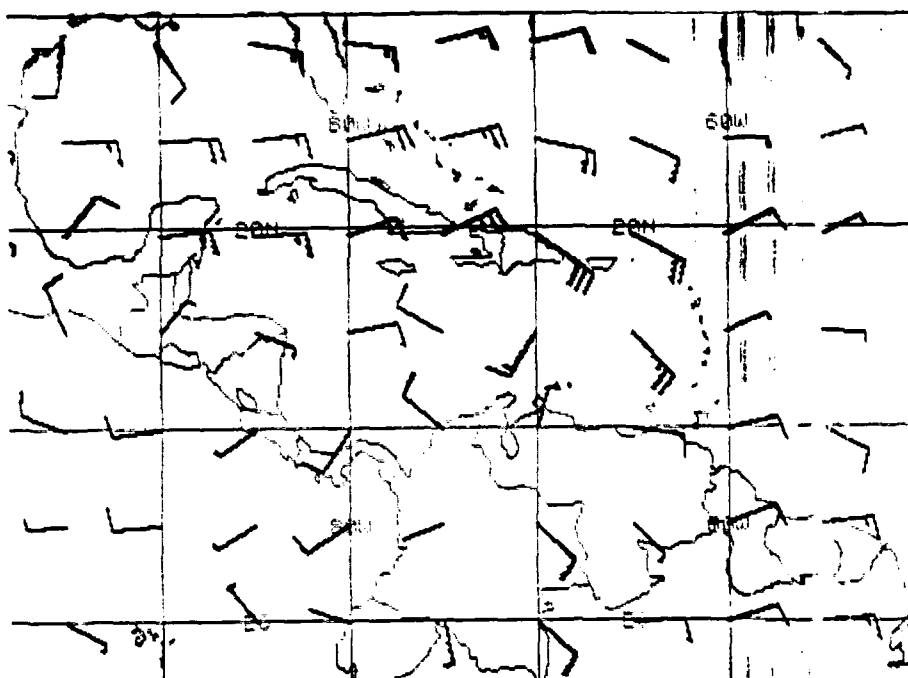


Figure 5.94: FNOc 925 mb Winds 24-h PROG VT 0000 UTC 12 SEP 1988.
As in Fig. 2.19.

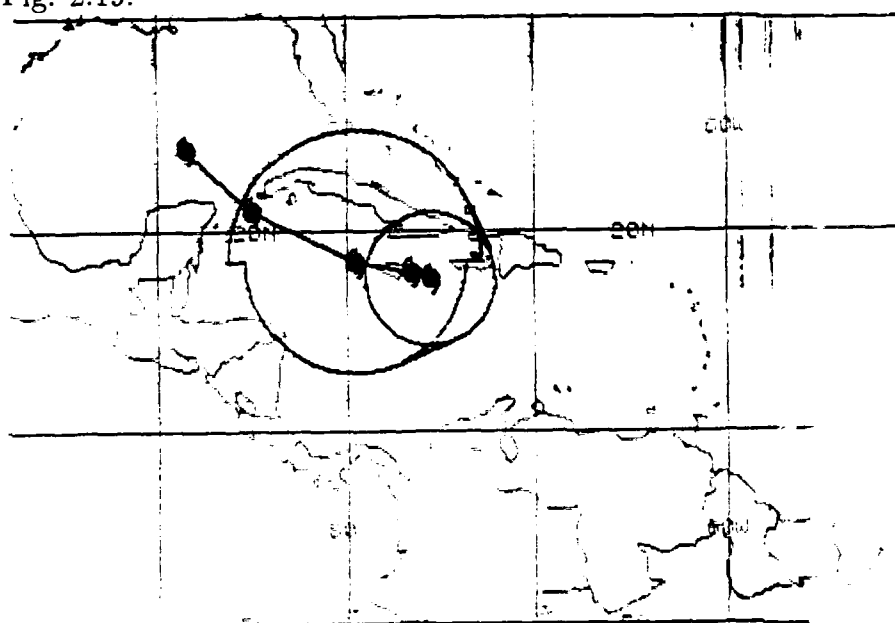


Figure 5.95: Tropical Cyclone FORECAST Track from 0600 UTC 12 SEP 1988.
Current position of Gilbert is the rightmost hurricane symbol *enclosed* by the circle depicting the radius of gale force winds. The 12-, 24-, 48- and 72-h forecast positions follow toward the northwest, with the larger semicircles indicating the probable radii of gale force winds in 24 hours.

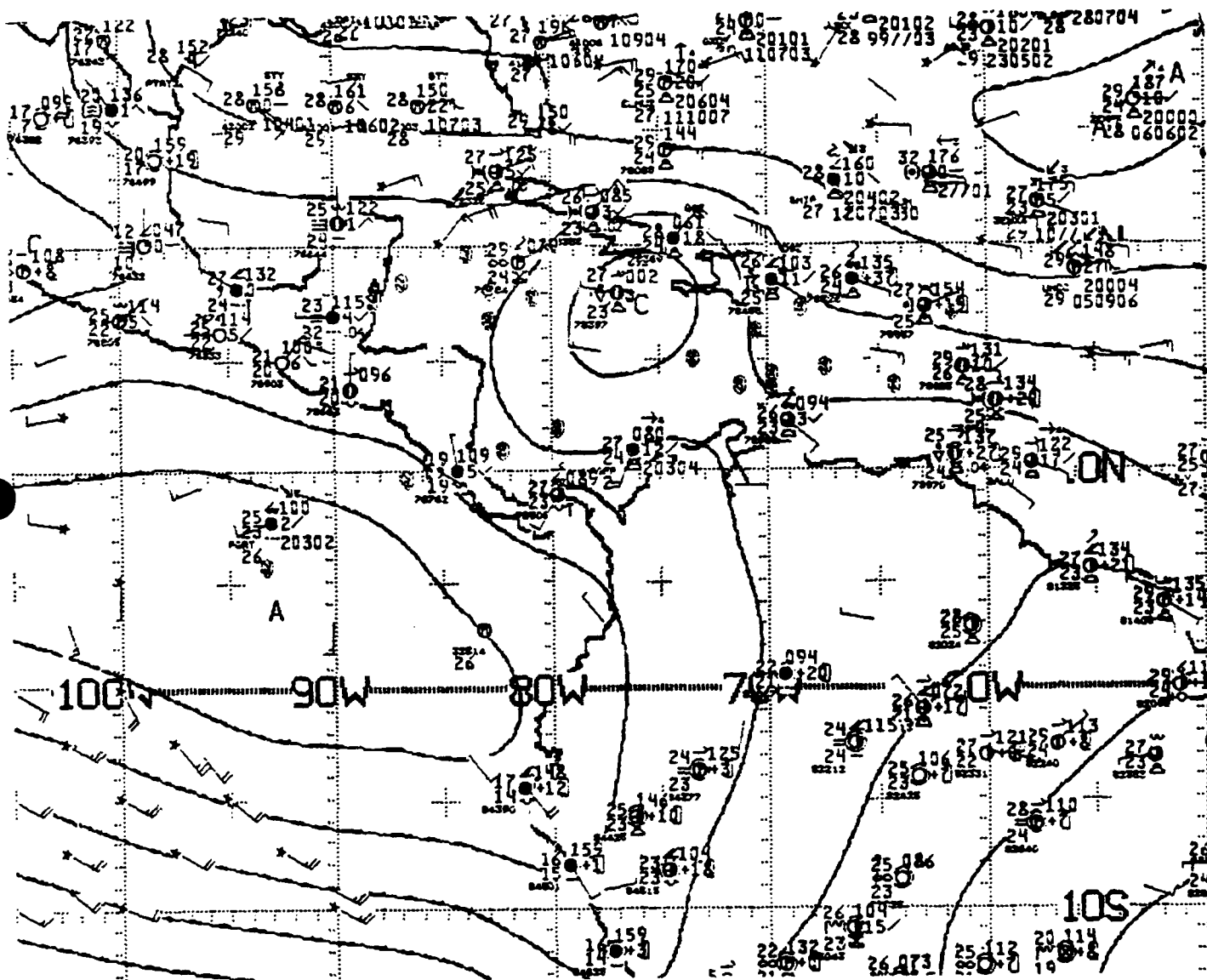


Figure 5.96: NMC 1000 mb Analysis, 1200 UTC 12 SEP 1988. As in Fig.2.21.

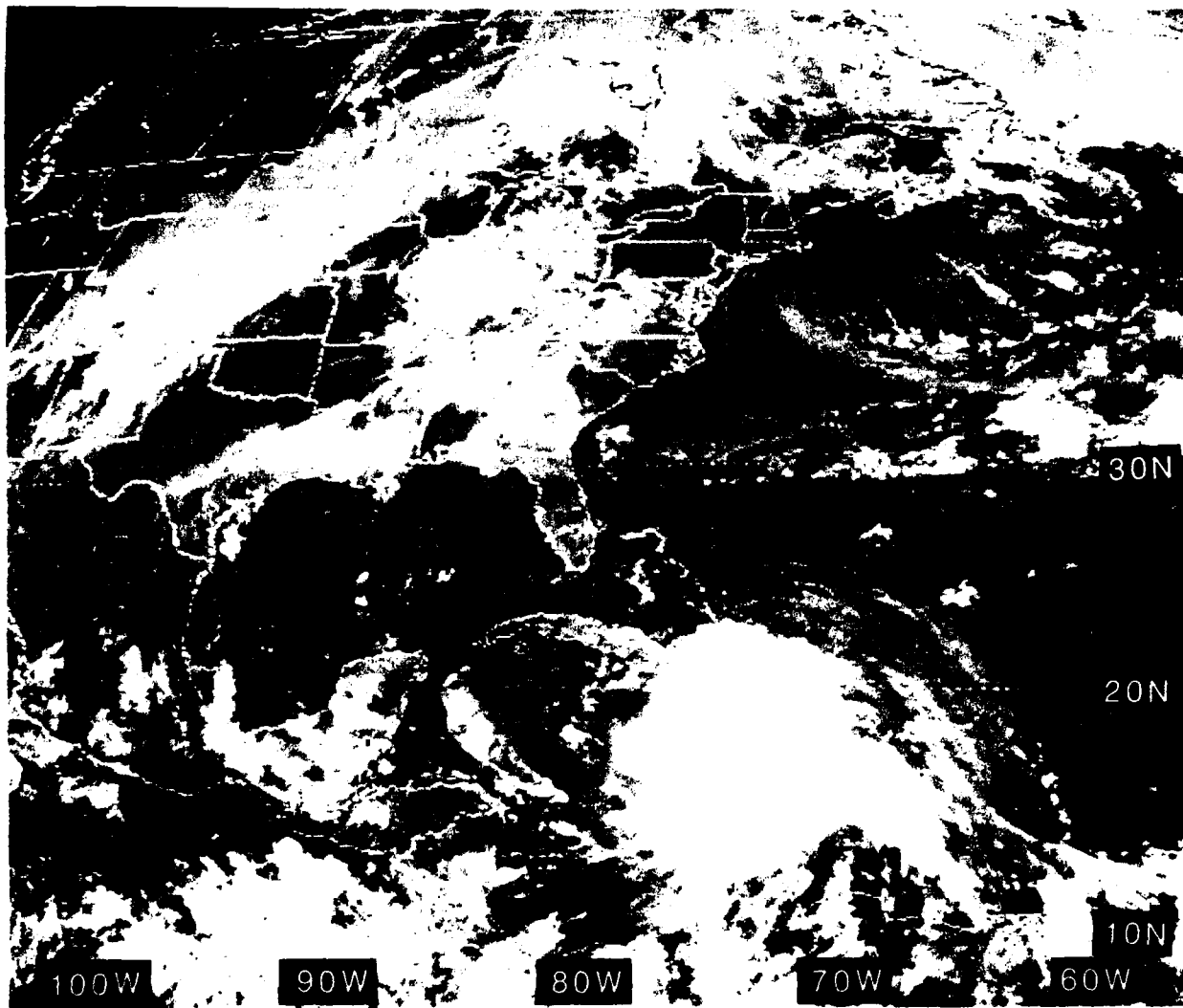


Figure 5.97: GOES East Visible Satellite Imagery, 1431 UTC 12 SEP 1988

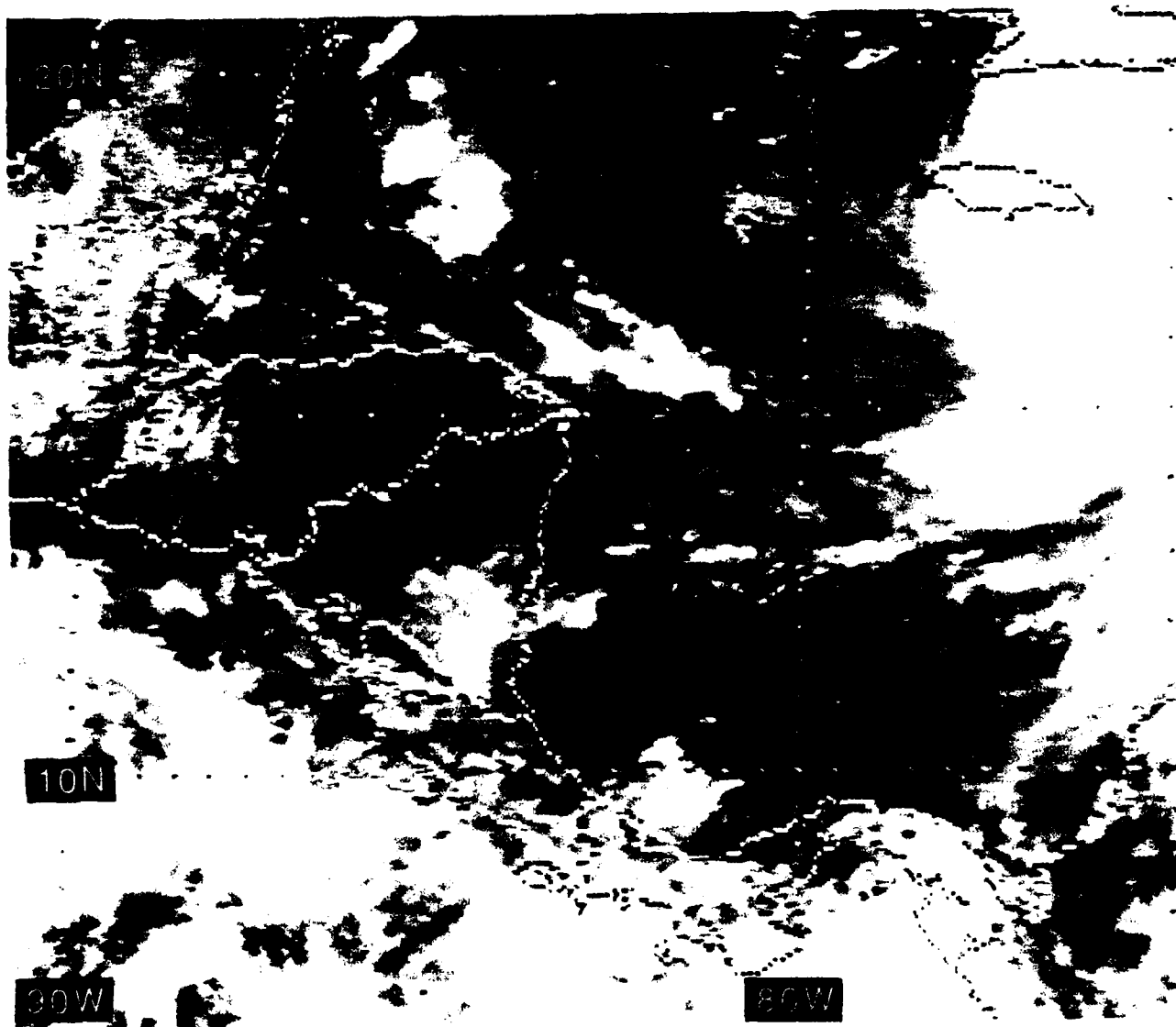


Figure 5.98: GOES E. Visible Imag. ("Zoomed"), 1531 UTC 12 SEP 1988

13 September 1988

After the eye of Hurricane Gilbert moved west of Jamaica at ~0000 UTC, (see Fig. 5.99 and station reports⁹⁵ on Fig. 5.100), the hurricane experienced a "remarkable intensification period", with the pressure falling from 960 mb (28.35 inches) to 888 mb (26.22 inches) in 24 hours (NHC, 1988). As on the 12th, the 0000 UTC NMC streamlines (Figs. 5.101 and 5.102) and the FNOC NOGAPS winds (Figs. 5.103 and 5.104) are presented for comparison—note the strong low-level confluence and upper-level diffluence, even before the central pressure of the hurricane commences its plunge. (However, as identified in previous case studies the 200 mb satellite winds plotted on the NMC analysis are much preferred, e.g., the 35-kt southerly wind between Cuba and Florida on Fig. 5.102 is accepted and the SE 20-kt wind on Fig. 5.104 rejected.)

Figure 5.108 is an example of the discontinuous streamline analysis available from FNOC. Compare to Fig. 5.103 (FNOC) and Fig. 5.101 (NMC).

By 1200 UTC, Hurricane Gilbert is passing just south of the Grand Cayman Island (see the early morning visible imagery of Fig. 5.105 and the IR imagery of Fig. 5.106). The surface station reports for 1200 UTC are shown in Fig. 5.107. The satellite images depict that the hurricane circulation is producing convection over the Gulf of Honduras, southward to Nicaragua and Costa Rica.

Figure 5.109 shows the official forecast of the expected path of the hurricane commencing at 1800 UTC. While the hurricane is now forecast to strike the Yucatan Peninsula, its subsequent forecast track *north northwestward* toward the northern Texas coastline was in error—compare with the preliminary best track in Fig 5.78.

As the hurricane is reaching its minimum central pressure (888 mb) and maximum sustained winds (~160 kt), Figs. 5.110 and 5.111 show its eye position about 100 n mi west of the Grand Cayman Island. At 1900 UTC, as the pressure in the eye of the hurricane is approaching its lowest value and despite the fact that it is moving away from the island, Grand Cayman Island records its maximum sustained wind of 119 kt with gusts to 136 kt (NHC, 1988).

Figures 5.112 and 5.113 present the best track minimum central pressure curve and maximum wind speed curve, respectively, for Hurricane Gilbert from the various sources and analysis centers (NHC, 1988).

⁹⁵The SSE 70 kt surface wind at Belize City (station 78583) on Fig.5.100 must be rejected.

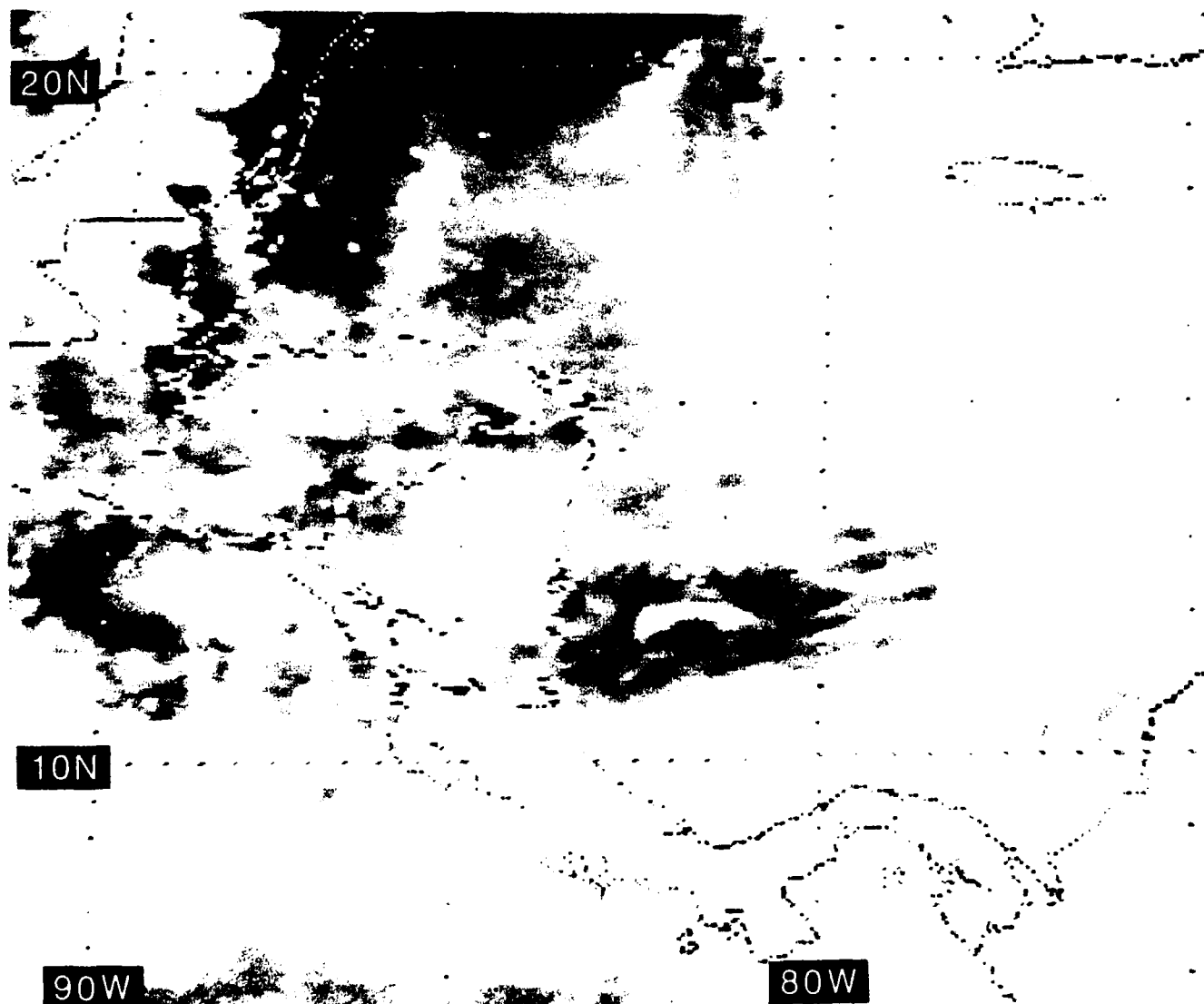


Figure 5.99: GOES E. IR Imagery ("Zoomed"), 0001 UTC 13 SEP 1988

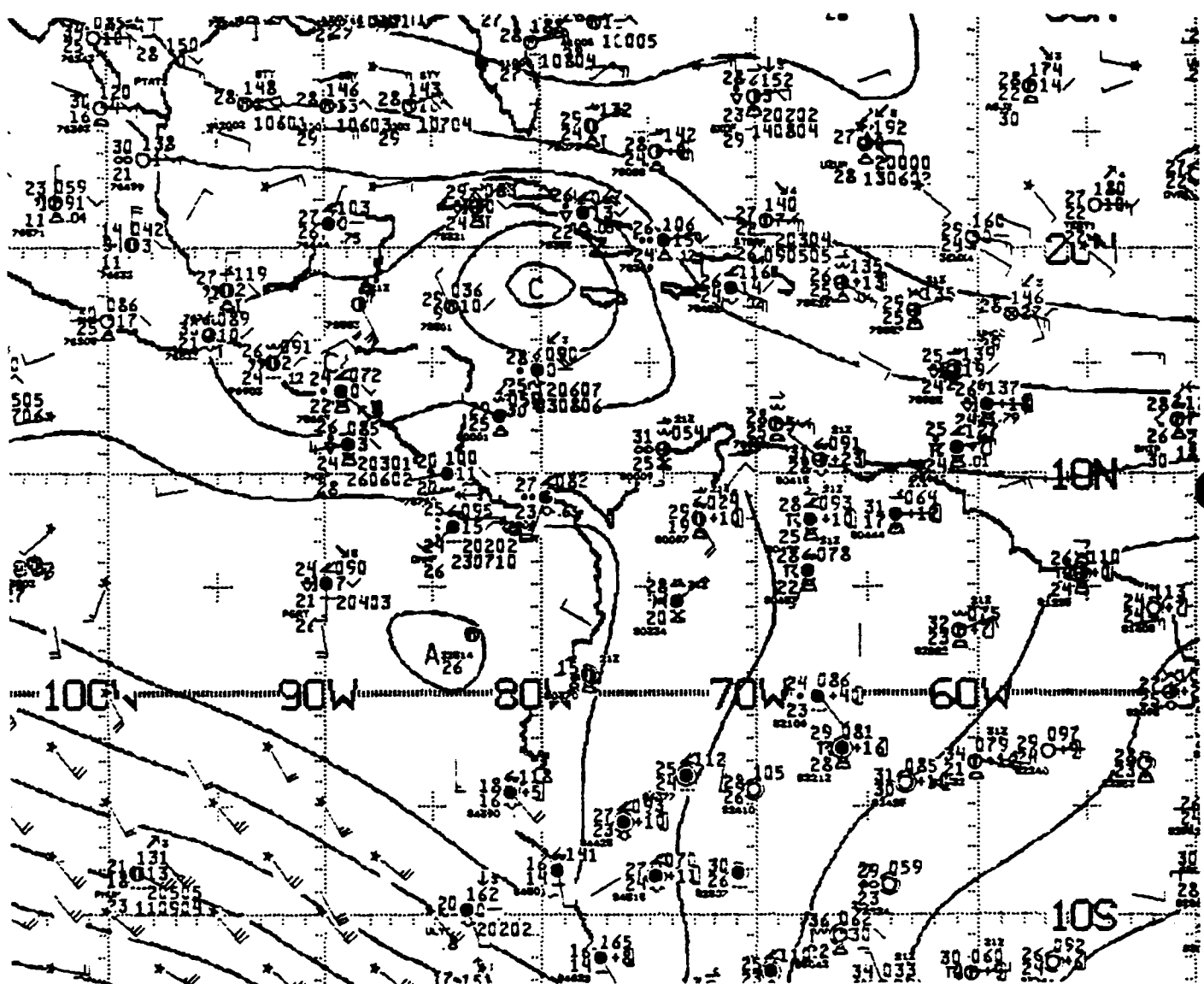


Figure 5.100: NMC 1000 mb Analysis, 0000 UTC 13 SEP 1988. As in Fig.2.21.

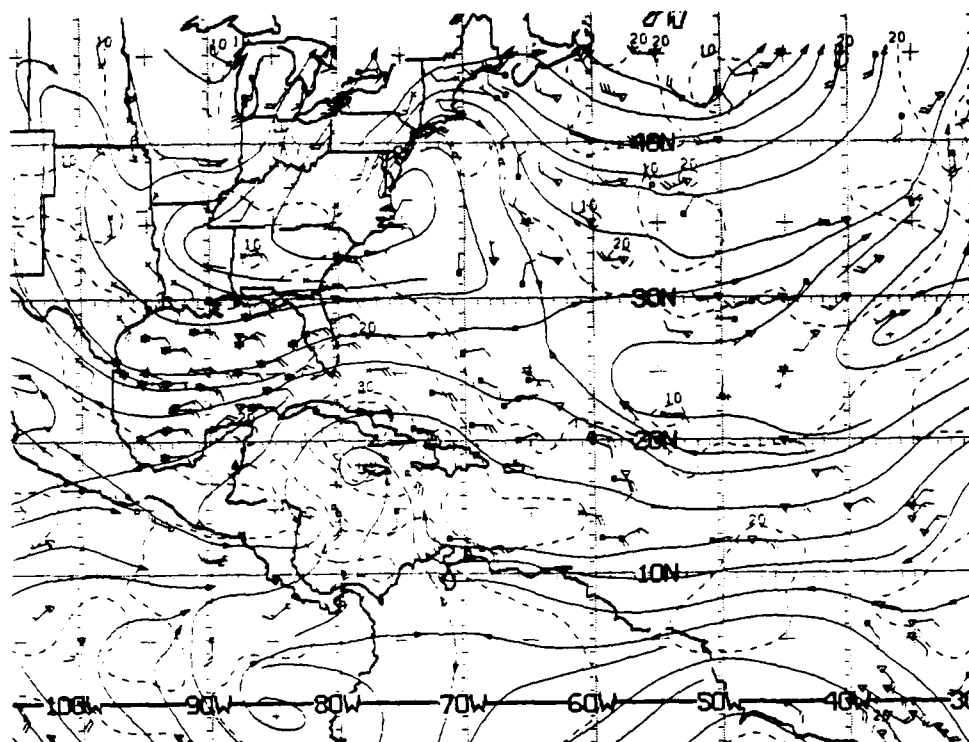


Figure 5.101: NMC ATOLL Operational Streamline Chart, 0000 UTC 13 SEP 1988
As in Fig. 2.4.

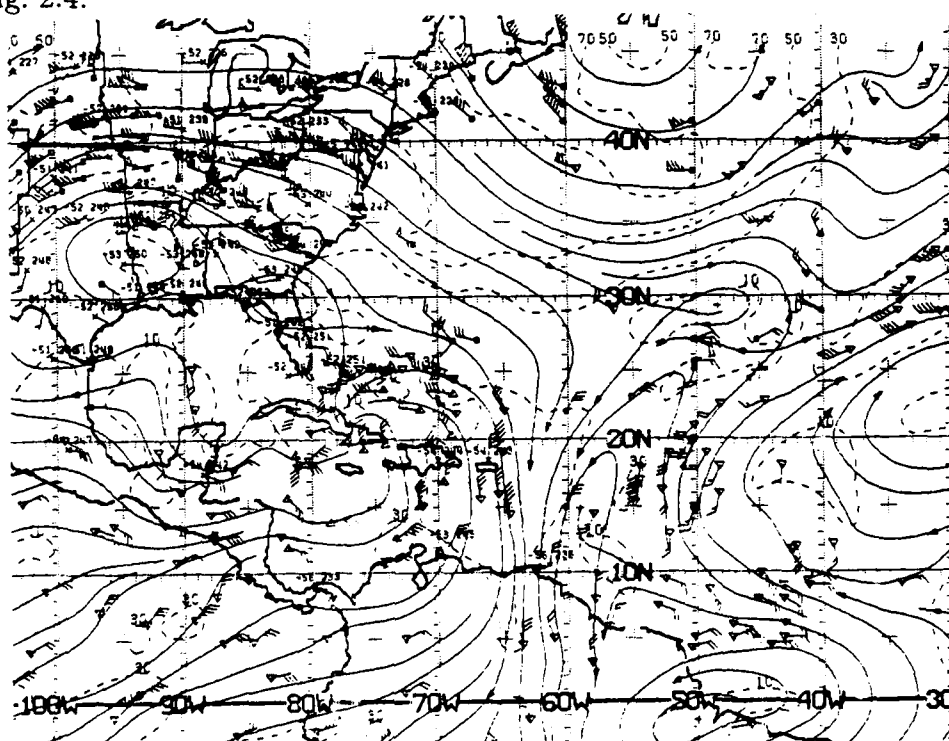


Figure 5.102: NMC 200 mb Operational Streamline Chart, 0000 UTC 13 SEP 1988
As in Fig. 2.7.

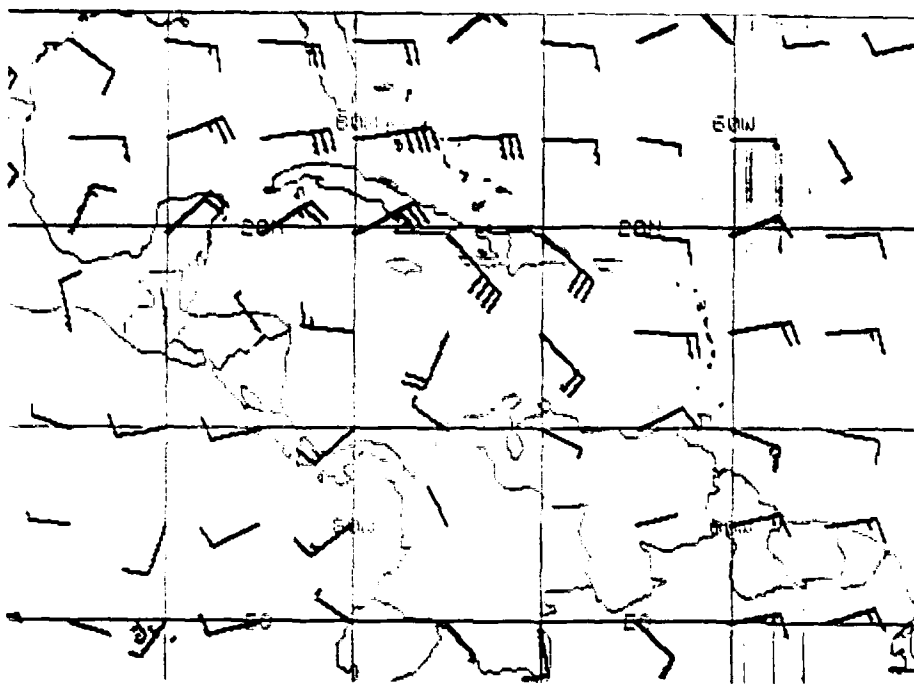


Figure 5.103: FNO 925 mb Winds, 0000 UTC 13 SEP 1988. As in Fig. 2.19.

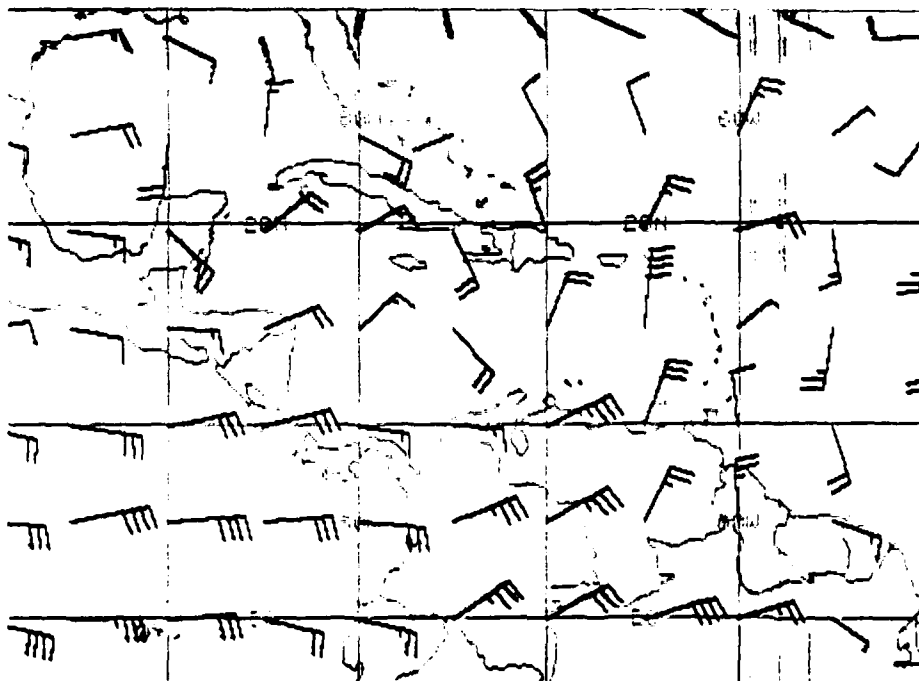


Figure 5.104: FNO 200 mb Winds, 0000 UTC 13 SEP 1988. As in Fig. 2.20.

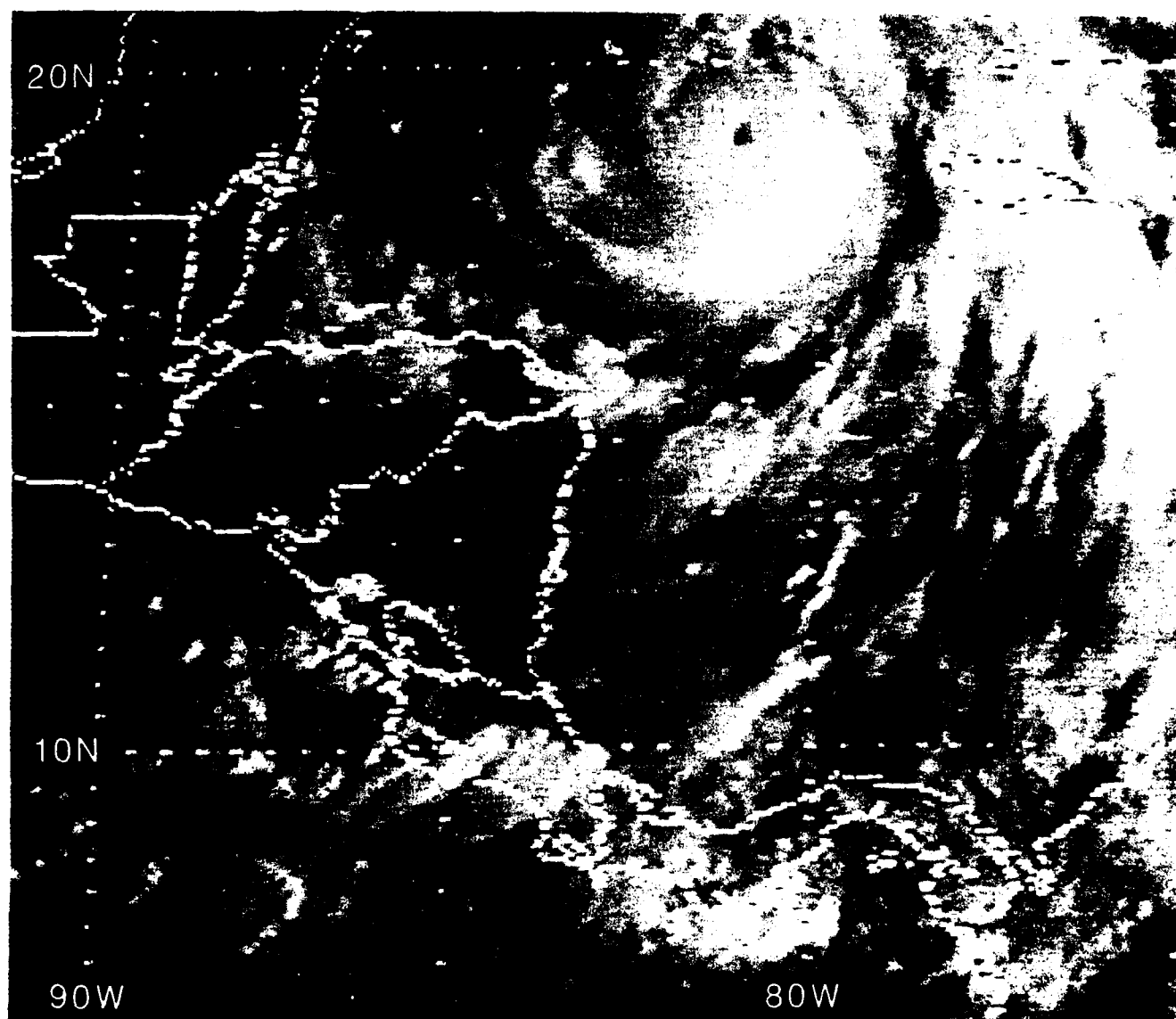


Figure 5.105: GOES E. Visible Imag. ("Zoomed"), 1231 UTC 13 SEP 1988
Grand Cayman Island is the "white" plot just north of the hurricane eye.

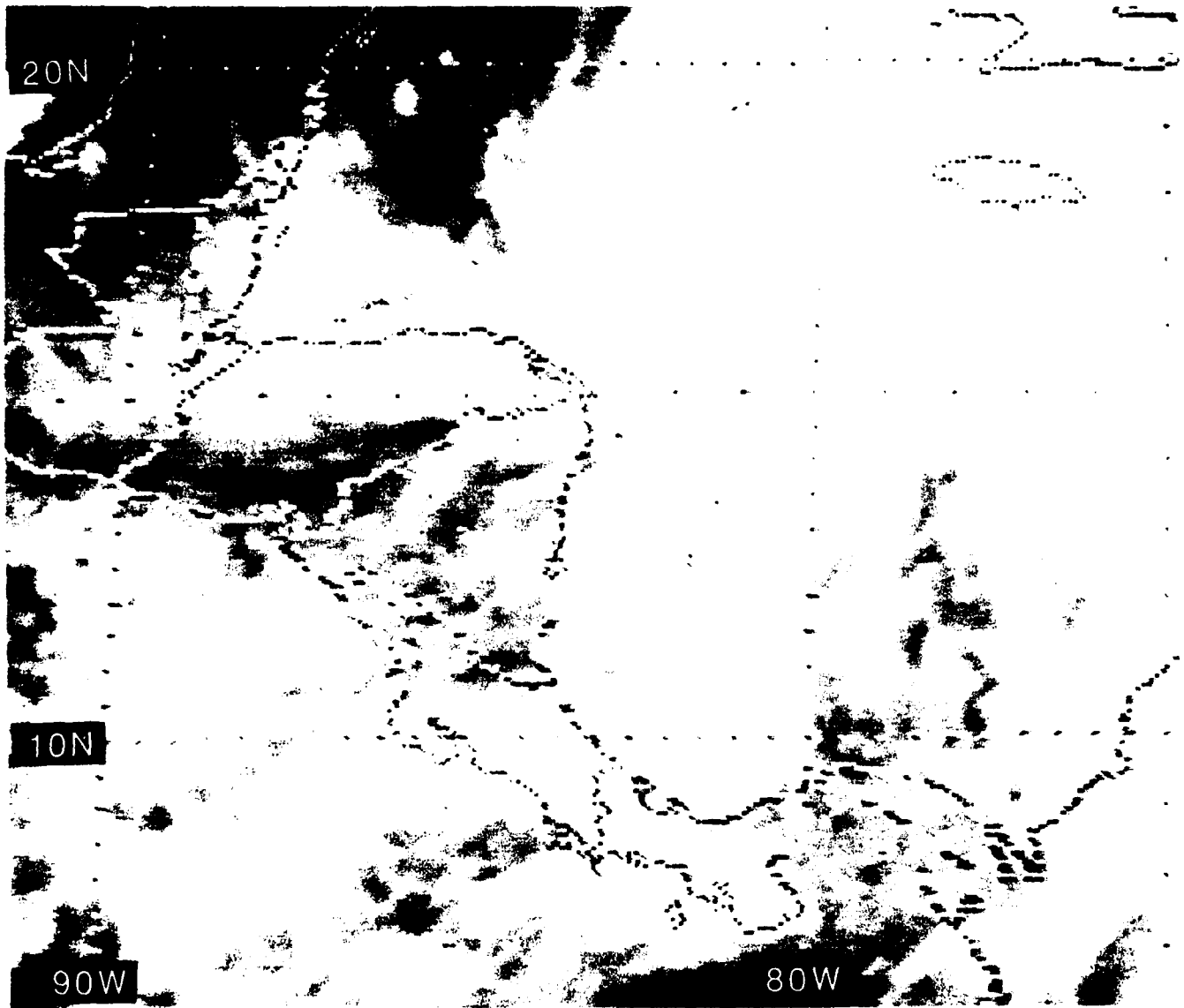


Figure 5.106: GOES E. IR Imagery ("Zoomed"), 1201 UTC 13 SEP 1988

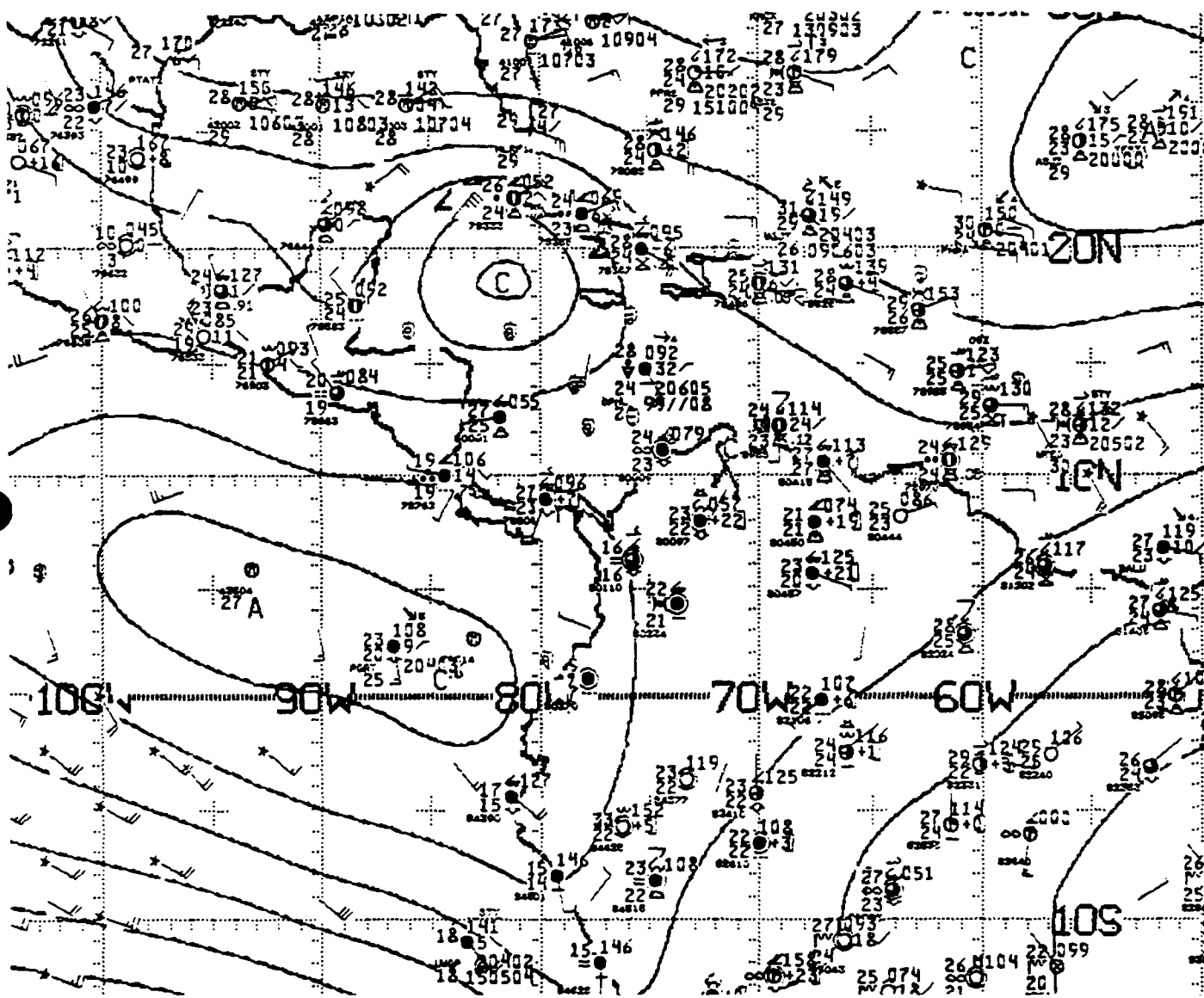


Figure 5.107: NMC 1000 mb Analysis, 1200 UTC 13 SEP 1988. As in Fig. 2.21.



Figure 5.108: FNOc 925 mb Streamlines, 0000 UTC 13 SEP 1988.

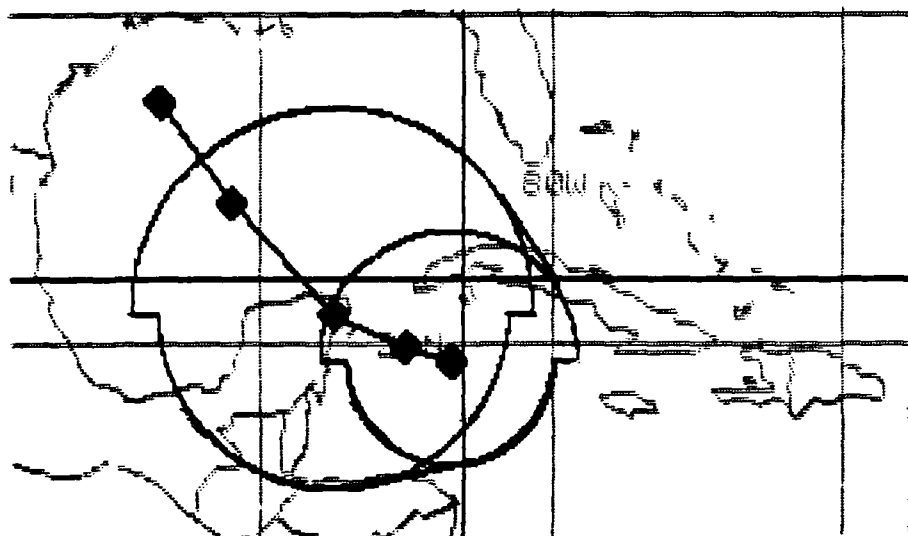


Figure 5.109: Tropical Cyclone FORECAST Track from 1800 UTC 13 SEP 1988. Current position of Gilbert is the rightmost black diamond symbol. The 12-, 24-, 48- and 72-h forecast positions follow toward the northwest. The smaller semicircles define the outer radii of gale force winds at the current position, while the larger semicircles define the probable outer radii of gale force winds in 24 hours. (The diamond symbol was erroneously plotted vice the hurricane symbol.)

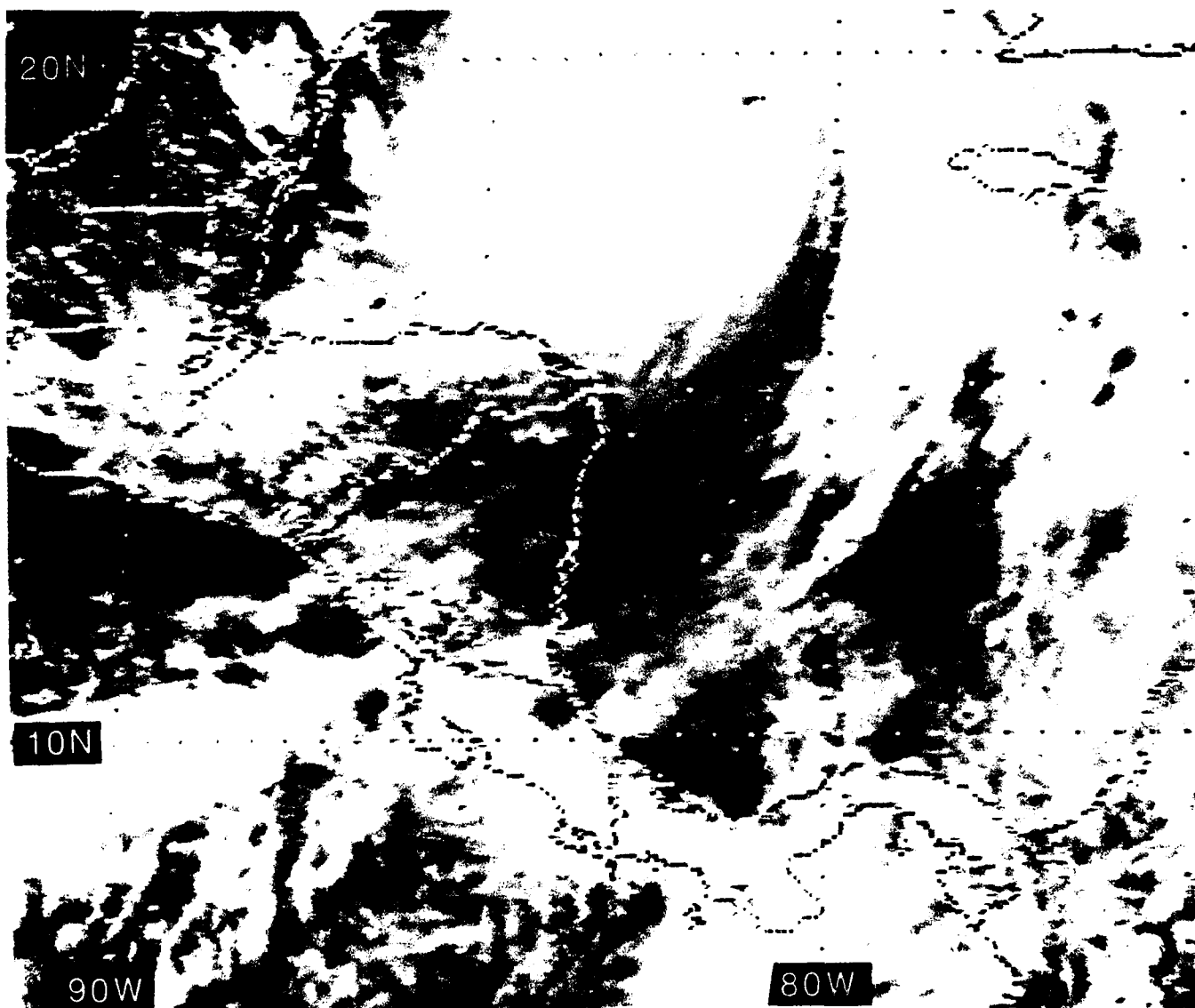


Figure 5.110: GOES E. Visible Imag. ("Zoomed"), 1831 UTC 13 SEP 1988
Grand Cayman Island is the "white" plot just north of the hurricane eye.

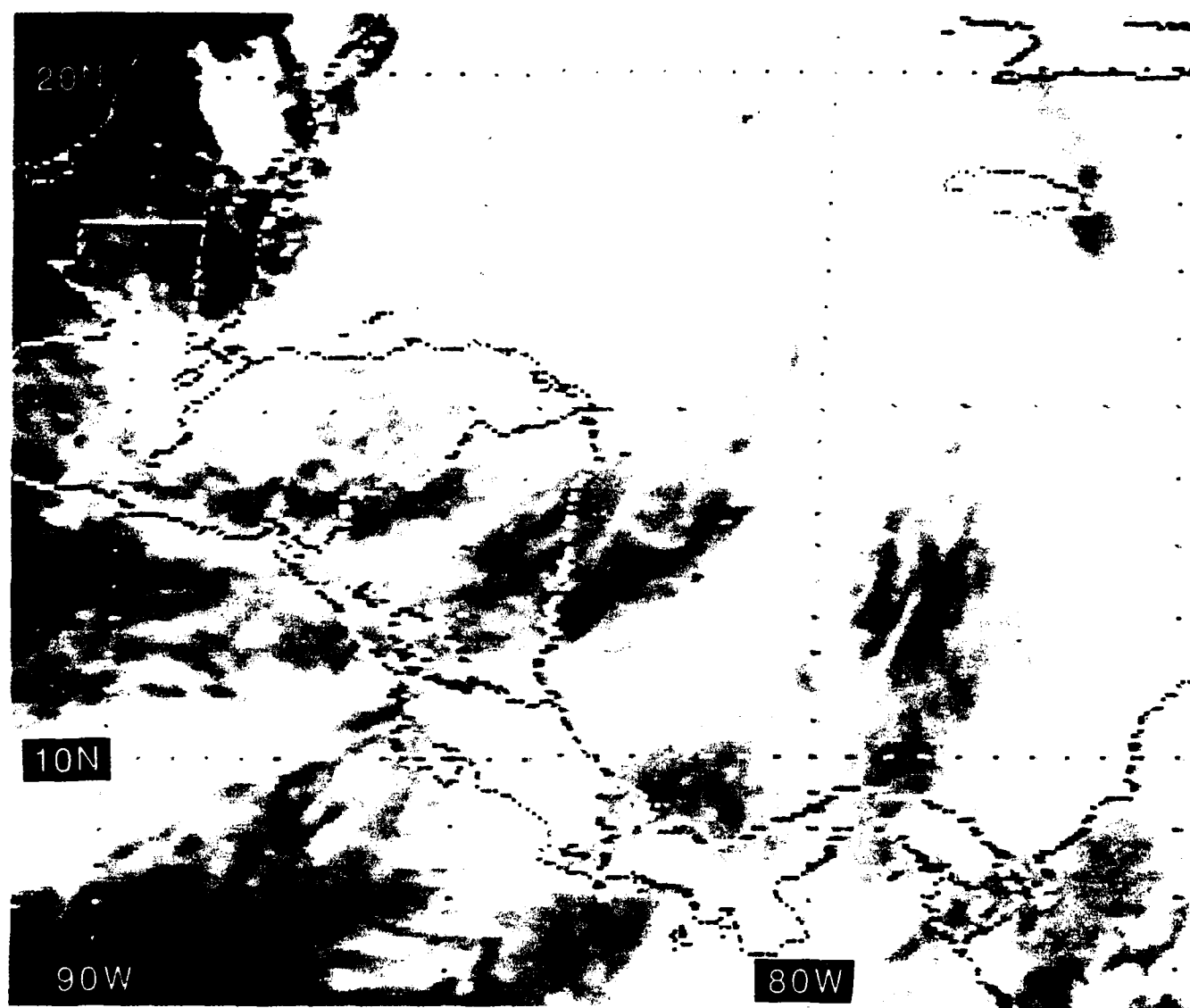


Figure 5.111: GOES E. IR Imagery ("Zoomed"), 1901 UTC 13 SEP 1988

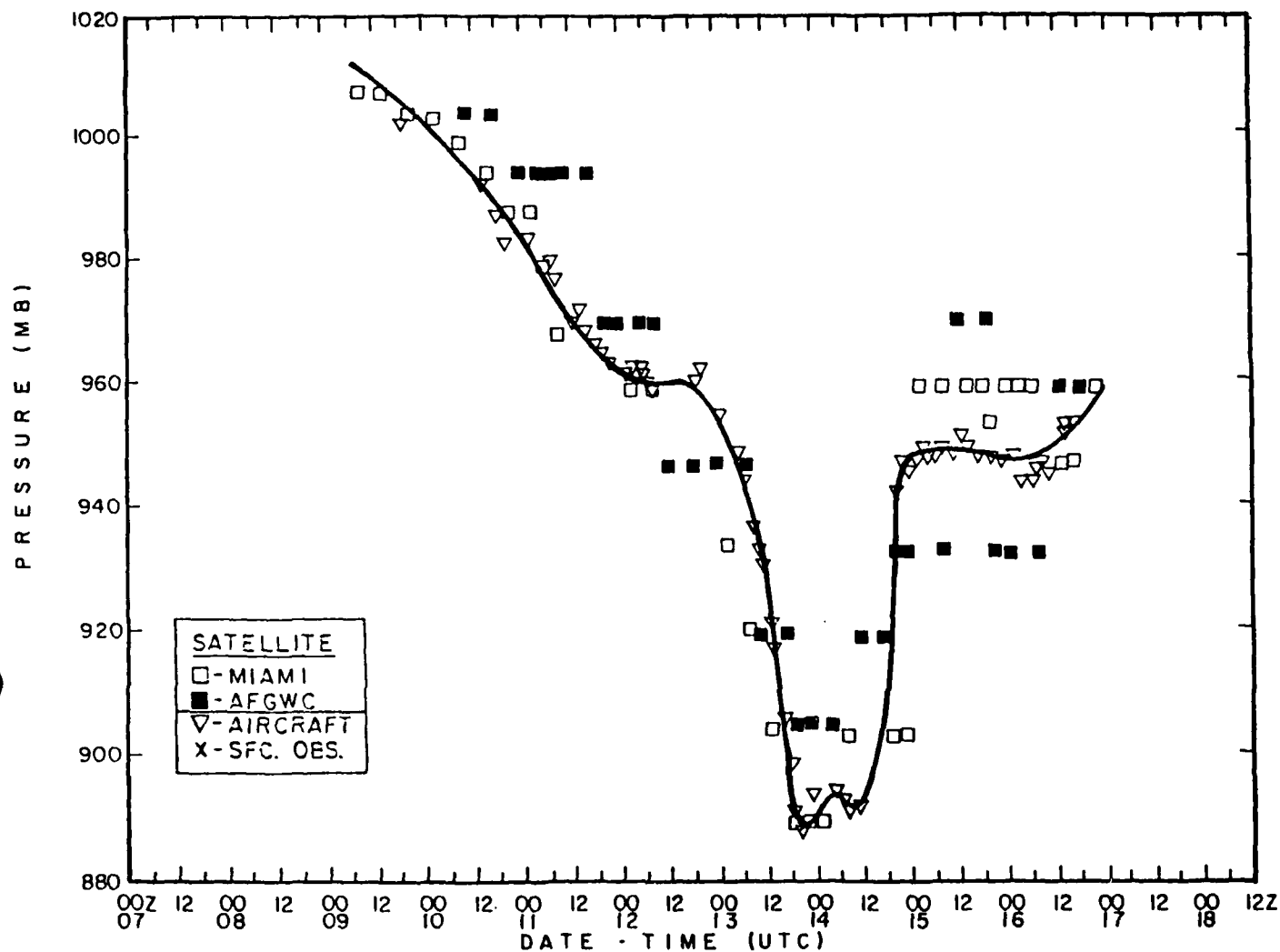


Figure 5.112: Best Track Minimum Pressure Curve for Hurricane Gilbert, 8-19 SEP 1988
(From NHC, 1988)

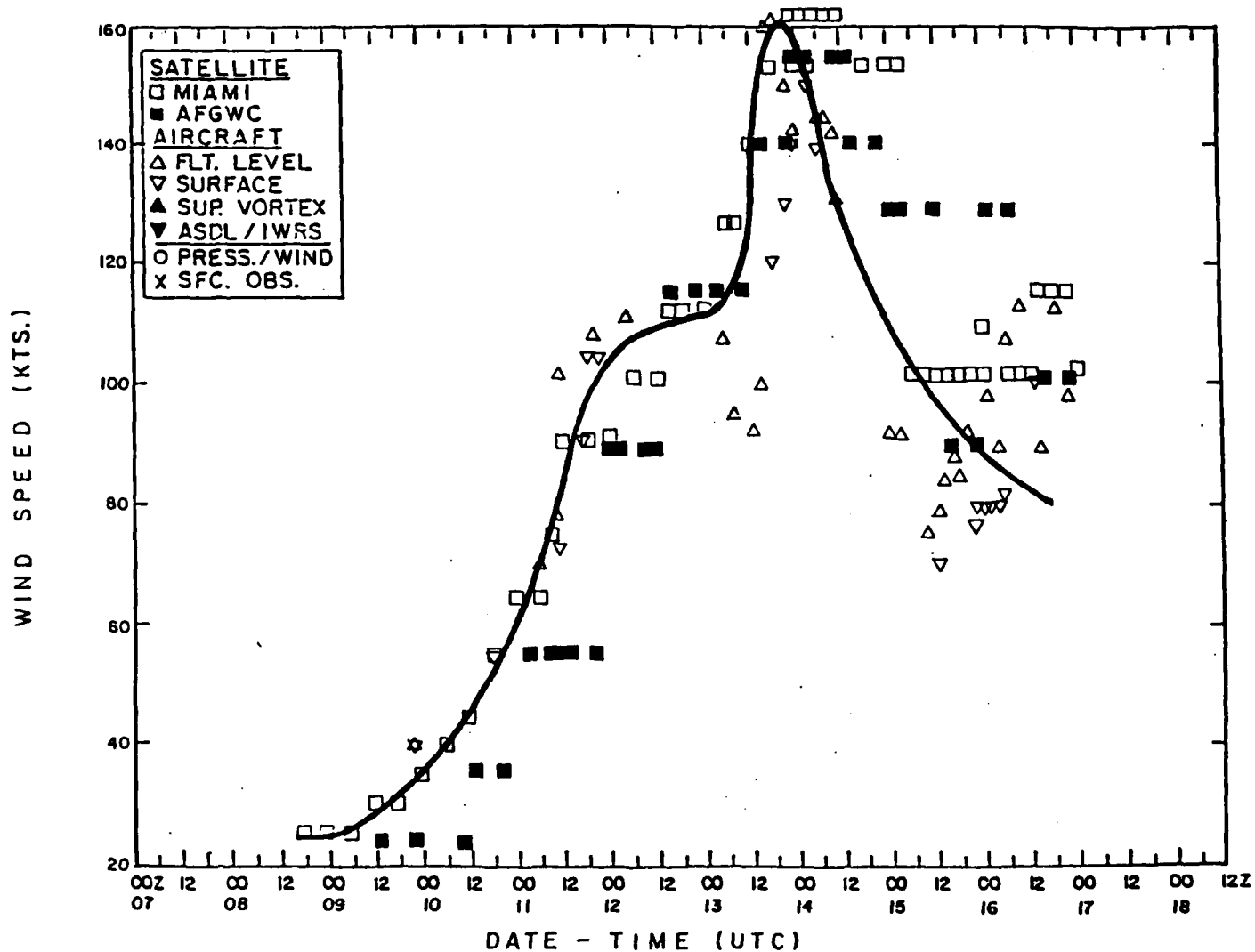


Figure 5.113: Best Track Maximum Sustained Wind Speed Curve for Hurricane Gilbert, 8-19 SEP 1988 (From NHC, 1988)

14 September 1988

The station observations and 1000 mb analysis of Fig. 5.114 and the IR imagery of Fig. 5.115 (2301 UTC on 13 September) clearly indicate that the circulation of Hurricane Gilbert is bringing convection to all the Central American countries at 0000 UTC on 14 September. At this time the hurricane is located at 19.7°N , 83.8°W , with a central pressure of 888 mb (the lowest recorded in the western hemisphere) and sustained winds of 160 kt. Figures 5.116 and 5.117 show the NMC low-level and upper-level streamlines, while Figs. 5.118 and 5.119 provide the Navy's wind analyses for comparison. (Again, as on the 13th, the NOGAPS 200 mb wind between Cuba and Florida is suspect.) Continuing on a north northwest course at 15 kt, Hurricane Gilbert moves over the northeast portion of the Yucatan Peninsula shortly after 1200 UTC (NHC, 1988).

The National Hurricane Center (1988) reports that a 15–20 foot storm surge (rise of the level of the sea) likely occurred along the immediate coast just to the north of where the hurricane center moved inland over the northeast Yucatan Peninsula, with a 8–13 foot surge farther north of the landfall. Although the northern Central American nations (Guatemala, Belize and Honduras) were no closer than ~ 200 n mi to the track of the hurricane, they experienced heavy precipitation from the peripheral circulation of this Western Hemisphere record hurricane.

The visible imagery of Fig. 5.120 shows the center of Hurricane Gilbert over the Yucatan Peninsula at 1831 UTC. At 1800 UTC (30 minutes earlier), the hurricane was at 20.9°N , 87.8°W , and its central pressure (925 mb) had commenced to rise with a maximum sustained wind of 130 kt. Figure 5.121 contains the radiosonde sounding taken at Belize City, Belize (station 78583) at 1800 UTC. Although the center of the Hurricane was 200 n mi north, the entire sounding is very moist (with a saturated layer between ~ 650 mb and ~ 475 mb) and Belize City is experiencing 50 kt winds at 850 mb.

By end of 14 September, the central pressure has increased to near 950 mb and the surface winds of Hurricane Gilbert have decreased to < 100 kt, mostly due to the land friction. Moving over water, the hurricane's winds increase to 115 kt before striking Mexico south of Brownsville, Texas, about 48 hours later (see Fig. 5.78). This portion of the history of the hurricane will not be discussed since the hurricane is neither over the Caribbean Sea nor over Central America. Interested readers may refer to National Hurricane Center (1988) for a discussion of the final days in the life of Hurricane Gilbert.

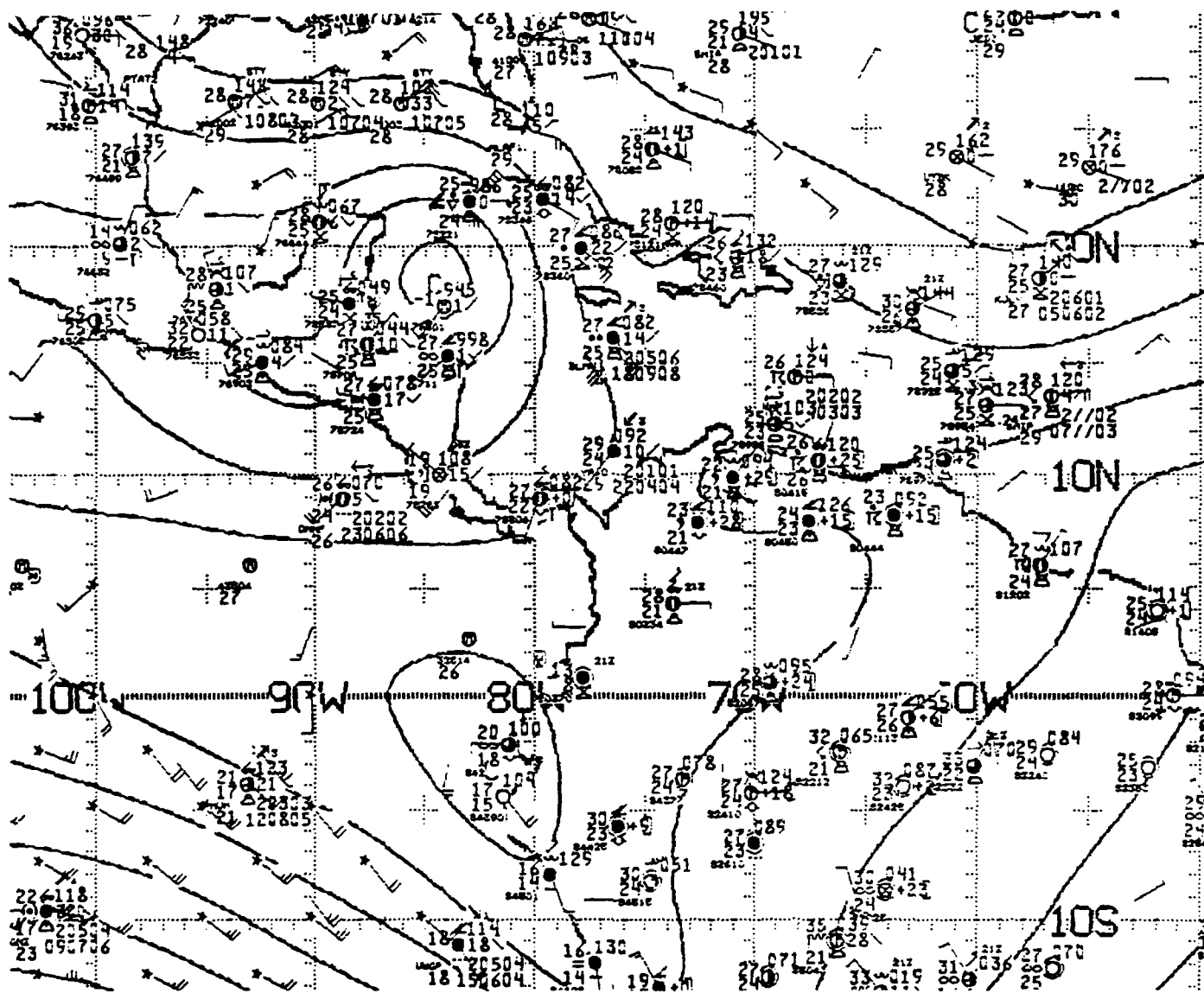


Figure 5.114: NMC 1000 mb Analysis, 0000 UTC 14 SEP 1988. As in Fig.2.21.

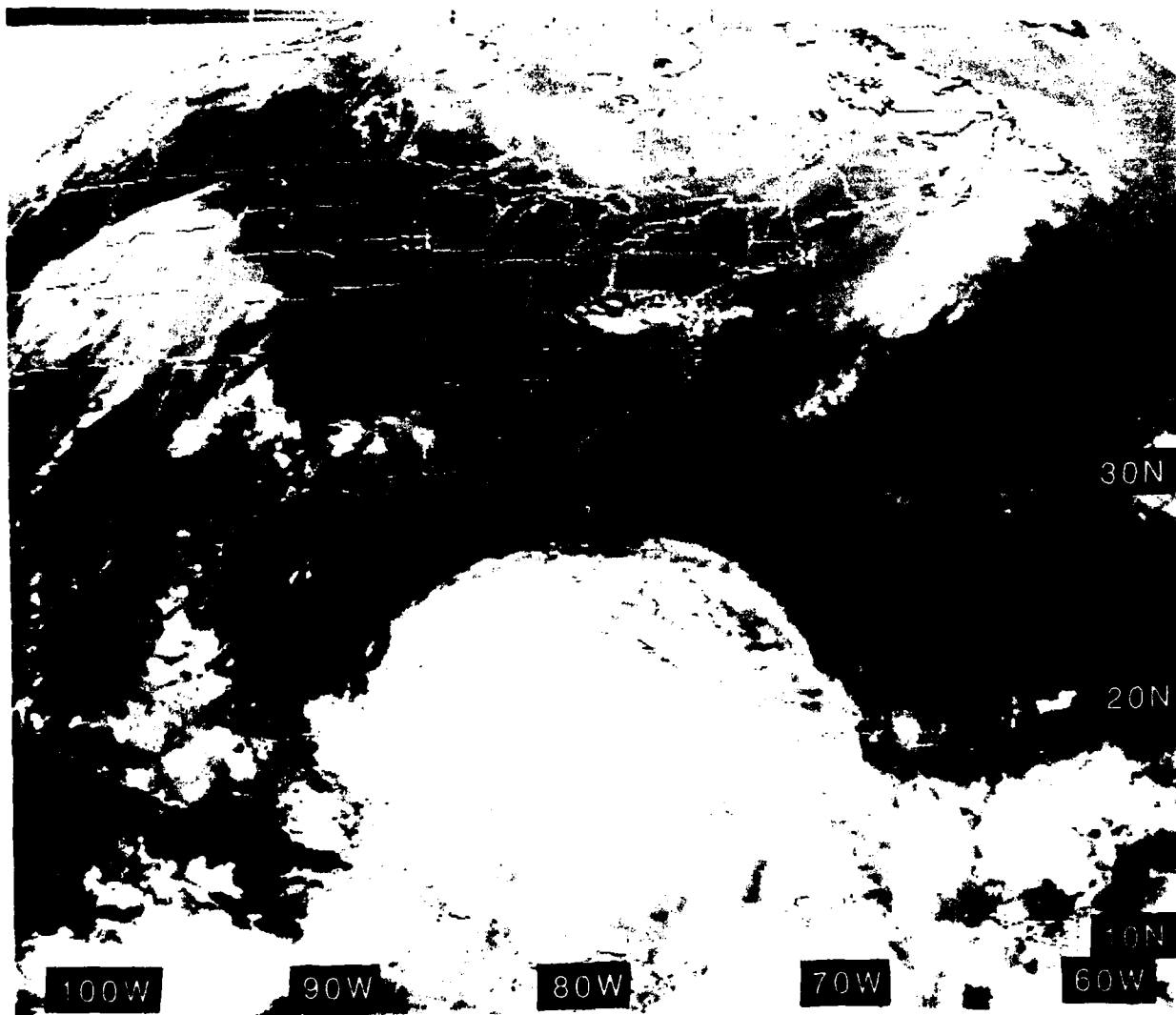


Figure 5.115: GOES East IR Imagery, 2301 UTC 13 SEP 1988

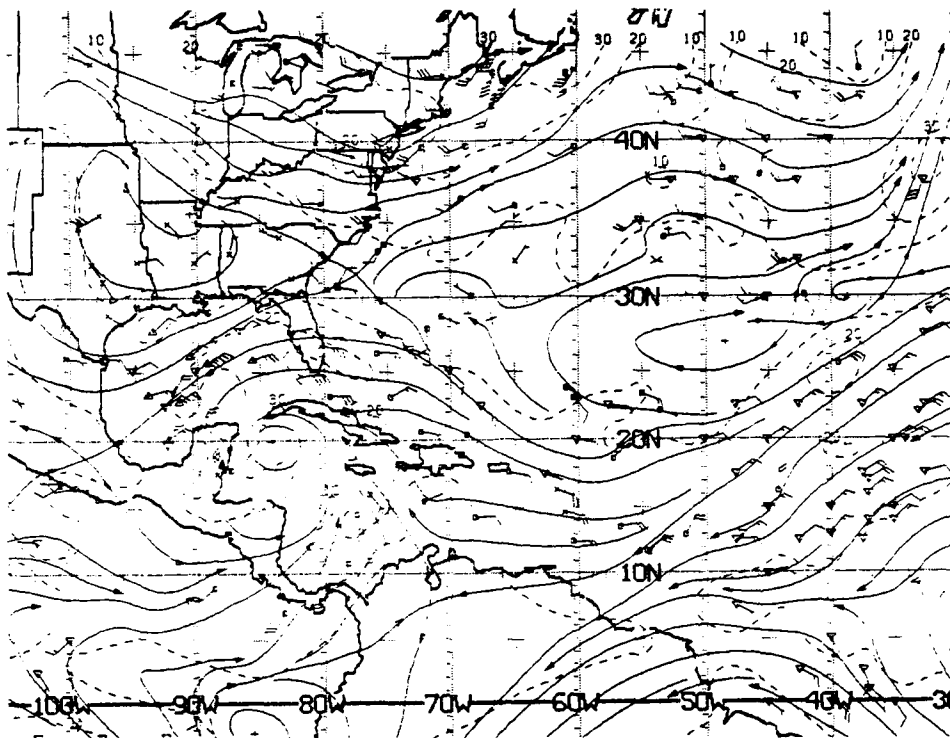


Figure 5.116: NMC ATOI Operational Streamline Chart, 0000 UTC 14 SEP 1988
As in Fig. 2.4.

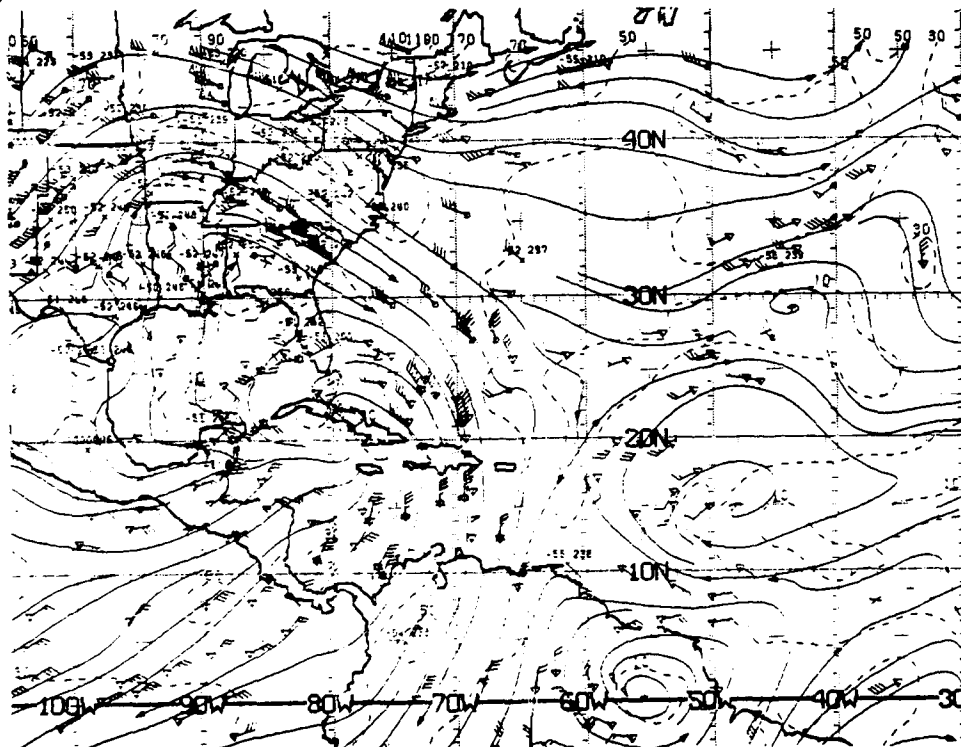


Figure 5.117: NMC 200 mb Operational Streamline Chart, 0000 UTC 14 SEP 1988
As in Fig. 2.7.

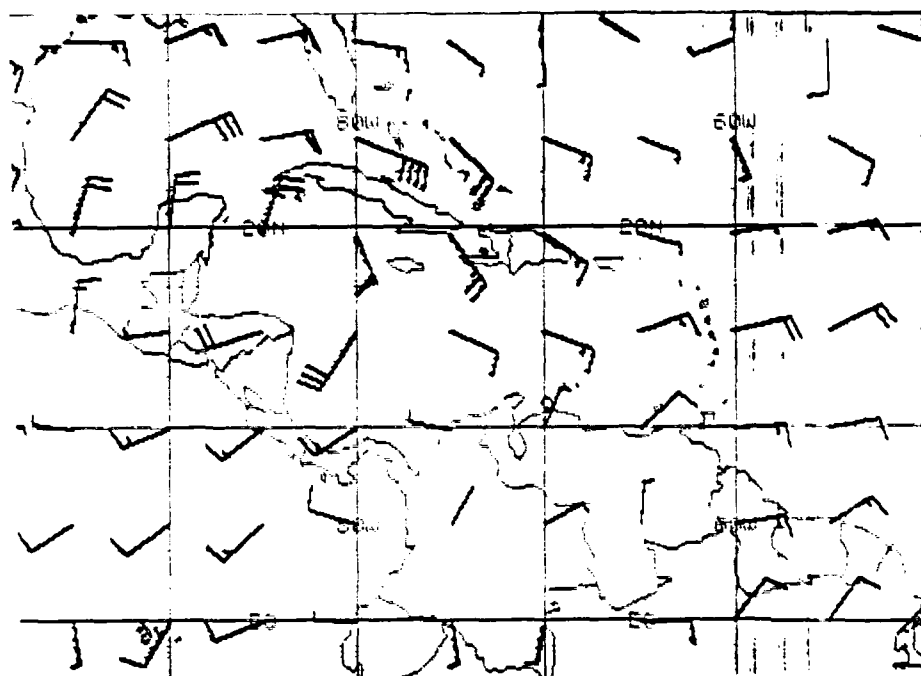


Figure 5.118: FNOc 925 mb Winds, 0000 UTC 14 SEP 1988. As in Fig. 2.19.

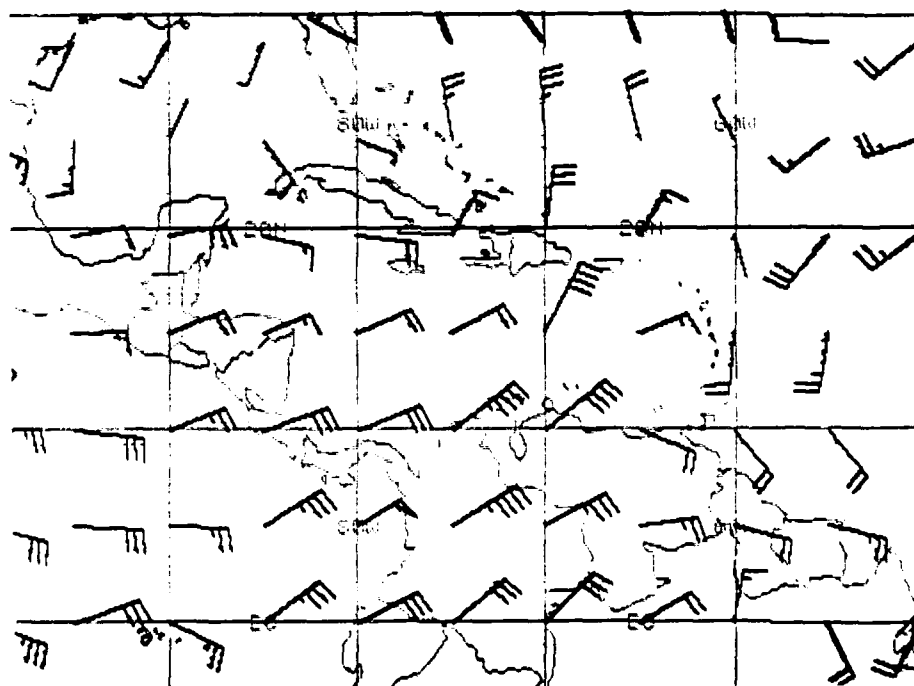


Figure 5.119: FNOc 200 mb Winds, 0000 UTC 14 SEP 1988. As in Fig. 2.20.

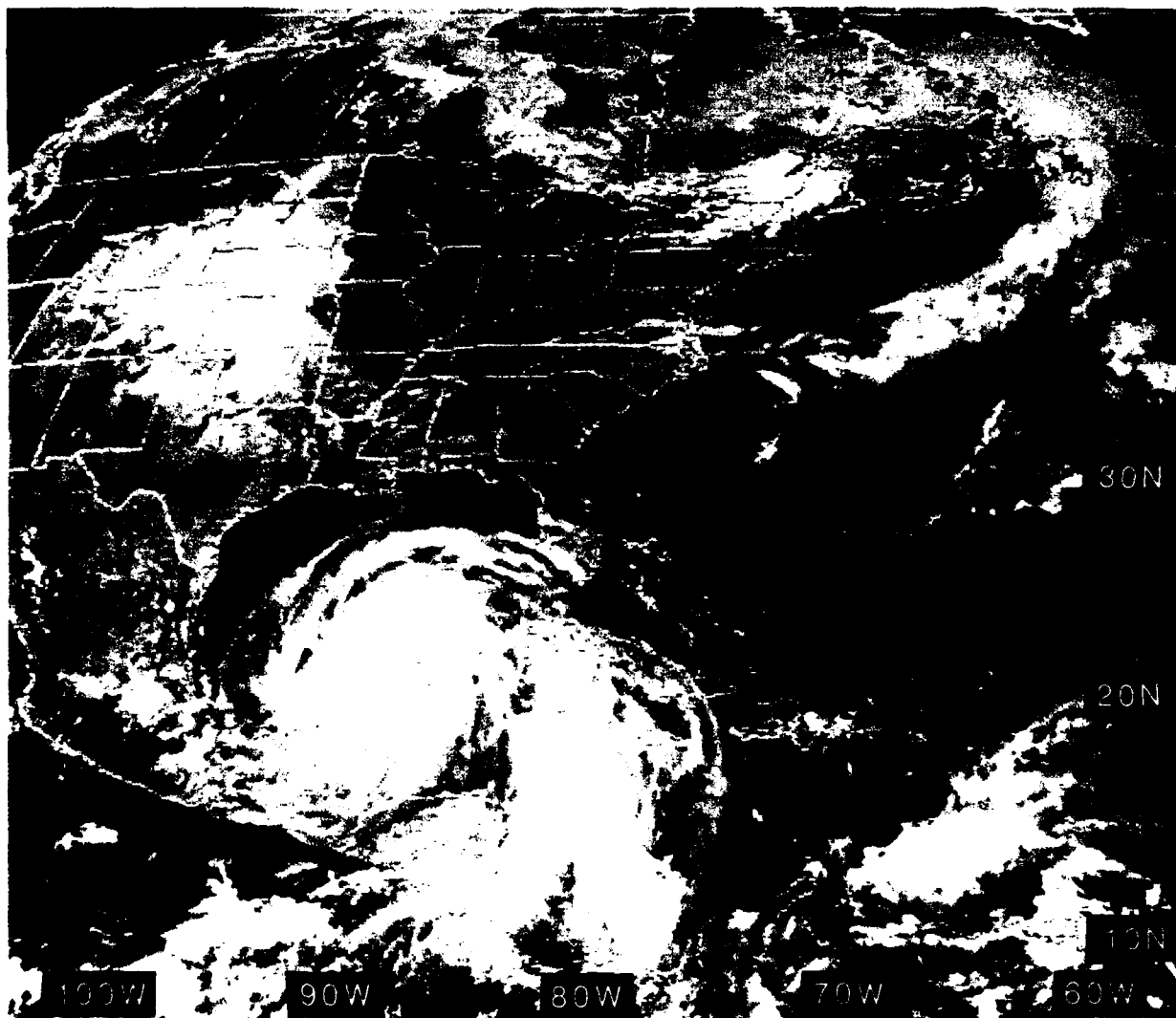


Figure 5.120: GOES East IR Imagery, 1831 UTC 14 SEP 1988

980914/1800 78583 MZBZ LIFT TOTL KINX SWET
-2 42 34 311

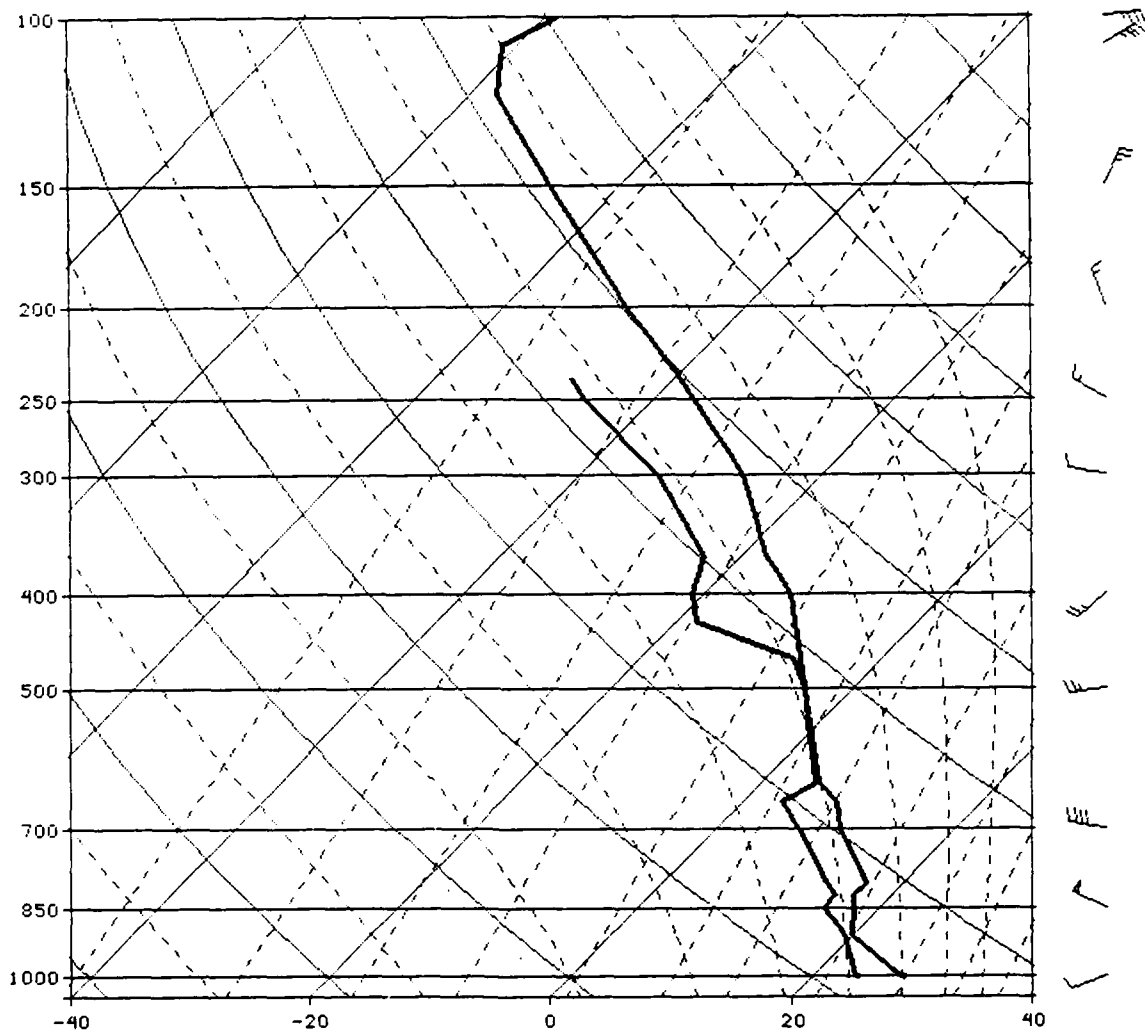


Figure 5.121: Belize City, Belize Sounding (solid lines) 1800 UTC 14 SEP 1988. The data for this sounding were received operationally.

References

- Atkinson, G. D., 1971: Forecaster's guide to tropical meteorology. AWS Technical Report 240, Air Weather Service (MAC) USAF, 360 pp.
- Aubouin, J., R. Von Huene, M. Baltuck, R. Arnott, J. Bourjois, M. Filewicz, K. Kvenvolden, B. Leinert, T. McDonald, K. McDougall, Y. Ogawa, E. Taylor and B. Winsborough, 1982: Leg 84 of the Deep Sea Drilling Project; Subduction without accretion: Middle America Trench off Guatemala. *Nature*, **297** (5866), 458-460.
- Bennett, E. B., 1966: Monthly Charts of Surface Salinity in the Eastern Tropical Pacific Ocean. *Bull. Inter.-Amer. Trop. Tuna Comm*, **11**(1), 1-44.
- Brooks, B. H., 1985: Forecasting the "Atemporalado" in Honduras. Unpublished forecast study. Air Force Global Weather Central, Offutt AFB, NE, 14 pp.
- Brown, S., 1987: Watch Out for Nelson Eddy. *Mariners Weather Log.*, **31**(3), 2-6.
- Chang, C. -P., 1970: Westward propagating cloud patterns in the tropical Pacific as seen from time-composite satellite photographs. *J. Atmos. Sci.*, **27**, 133-138.
- Chang, C. -P., 1987: Unpublished Tropical Meteorology Lecture Notes. Naval Postgraduate School, Monterey, CA.
- Chapel, L. T., 1927: Winds and storms on the isthmus of Panama. *Mon. Wea. Rev.*, **55**, 519-530.
- Collins, J. I., A. Rossfelder and M. Smith, 1970: Offshore Environmental Survey, Continental Shelf, East Coast of Nicaragua. Final Report, Contract TC-184, Tetra Tech, Inc., Pasadena, CA., 115 pp.
- Corredor, J. E., 1979: Phytoplankton response to low level nutrient enrichment through upwelling in the Columbian Caribbean Basin. *Deep-Sea Res.*, **26**(7A), 731-741.
- DiMego, G. J., L. F. Bosart and G. W. Endersen, 1976: An examination of the frequency of mean conditions surrounding frontal incursions into the Gulf of Mexico and Caribbean Sea. *Mon. Wea. Rev.*, **104**, 709-718.
- Donguy, J. R. and C. Henin, 1980: Surface conditions in the eastern equatorial Pacific related to the intertropical convergence zone of the winds. *Deep-Sea Res.*, **27A** (9), 693-714.
- Elsberry, R. L., W. M. Frank, G. J. Holland, J. D. Jarrell and R. L. Southern, 1987: *A Global View of Tropical Cyclones*. Marine Meteorology Program, Office of Naval Research, Washington, DC, 185 pp.
- Ewing, J. and T. Edgar, 1966: Caribbean Sea—Sediments and Crust. *Encyclopedia of Oceanography*, R. W. Fairbridge, Ed., Reinhold Publishing Corp., NY., 181-184.

- Fairbridge, R. W., 1966: Caribbean Current. *Encyclopedia of Oceanography*, R. W. Fairbridge, Ed., Reinhold Publishing Corp., NY., p. 175.
- Fett, R. W., P. E. La Violette, M. Nestor, J. W. Nickerson and K. Rabe, 1977: *Navy Tactical Applications Guide. Volume 2: Environmental Phenomena and Effects*. TR 77-04, Naval Environmental Prediction Research Facility, Monterey, CA 93924, 2E-8 to 2E-11.
- Gordon, A., 1966: Caribbean Sea—Oceanography. *Encyclopedia of Oceanography*, R. W. Fairbridge, Ed., Reinhold Publishing Corp., NY., 175–181.
- Graham, N. E. and T. P. Barnett, 1987: Sea Surface Temperature and Convection over Tropical Oceans. *Research in Air-Sea Interaction and Short-Term Climate Variability at the University of California 1987*, (C. R. Mechoso and J. O. Roads, eds.), 24–35.
- Gross, M. G., 1982: *Oceanography, A View of the Earth.*, 3rd Ed. Prentice-Hall, NJ., pp. 68, 241.
- Guard, C. P., 1986: Local and Regional Influences on the Meteorology of Central America. Air Weather Service Forecaster Memo (AWS/FM-86/006), Headquarters, Air Weather Service, Scott AFB, IL, 23 pp.
- Harding, J. L. and W. D. Nowlin, Jr., 1966: Gulf of Mexico (4) Regional Oceanography (a) The Water Masses. *Encyclopedia of Oceanography*, R. W. Fairbridge, Ed., Reinhold Publishing Corp., NY., p. 328.
- Henry, W. K., 1979: Some aspects of the fate of cold fronts in the Gulf of Mexico. *Mon. Wea. Rev.*, **107**, 1078–1082.
- Henry, W. K., 1980: Three late spring fronts in the Caribbean. *National Weather Digest*, **5** (1), 18–24.
- Hoffmann, E. E., A. J. Busalacchi and J. J. O'Brien, 1981: Wind generation of the Costa Rica Dome. *Science*, **214** (4520), 552–554.
- Horvath, N. C. and W. K. Henry, 1980: Some Aspects of Cold Fronts in Belize. *National Weather Digest*, **5** (4), 25–32.
- Huschke, R. E., ed., 1959: *Glossary of Meteorology*. American Meteorological Society, Boston, MA, reprinted 1980, 638 pp.
- Isaacs, J., 1969: The Nature of Oceanic Life. *Scientific American*, Offprint No. 884. W. H. Freeman and Company, San Francisco, CA.
- Jordan, C. L., 1958: Mean soundings for the West Indies area. *J. Meteor.*, **15**, 91–97.
- Kinder, T. H., 1983: Shallow currents in the Caribbean Sea and Gulf of Mexico as observed with satellite-tracked drifters. *Bull. Mar. Sci.*, **33**(2), 239–246.
- Ladd, J. W. and W. K. Henry, 1980: An examination of some indicators of Frontal Passage in Coastal Honduras. *National Weather Digest*, **5** (3), 2–7.

- Leet, L. D., S. Judson and M. E. Kauffman, 1978: *Physical Geology*, 5th Ed. Prentice-Hall, NJ, pp. 230, 234.
- LePichon, X., J. Franchetau and J. Bonnin, 1973: Plate Tectonics. *Develop. in Geotectonics*, 6, Elsevier Sci. Pub. Co., NY., pp. 81, 83, 85.
- Lessman, H., 1963: Synoptic and climatological views on rainfall in Central America (especially in El Salvador). *Preprints Symposium on Tropical Meteorology, Rotorua, New Zealand*, World Meteorological Organization, 295-305.
- Lonsdale, P., 1980: Manganese-nodule bedforms and thermohaline density flows in a deep-sea valley on Carnegie Ridge, Panama Basin. *J. Sed. Petrology*, 50(4), 1033-1048.
- Lowrie, A., T. Aitkin, P. Grim and L. McRaney, 1979: Fossil spreading center and faults within the Panama Fracture Zone. *Mar. Geophys. Res.*, 4(2), 153-166.
- Mantyla, A. W. and J. L. Reid, 1983: Abyssal Characteristics of the world ocean waters. *Deep-Sea Res.*, 30(8A), 805-834.
- Meehl, G. A., 1982: Characteristics of surface current flow inferred from a global ocean current data set. *J. Phys. Oceanogr.*, 12(6), 540-542, 548.
- Miller, R. J., T. L. Tsui and A. J. Schrader, 1988: *Climatology of North Pacific Tropical Cyclone Tracks*. Technical Report TR 88-10, Naval Environmental Prediction Research Facility, Monterey CA, 511 pp.
- Morrison, J. M. and W. D. Nowlin, Jr., 1982: General distribution of water masses within the eastern Caribbean Sea during the winter of 1972 and fall of 1973. *J. Geophys. Res.*, 87(C6), 4207-4229.
- Murray, S. P., S. A. Hsu, H. H. Roberts, E. H. Owens and R. L. Crout, 1982: Physical processes and sedimentation on a broad, shallow bank. *Estuar. Coast. Shelf Sci.*, 14 (2), 135-157.
- National Geographic Society, 1970: Chart of West Indies and Central America. Supplement to National Geographic 137 (1).
- National Hurricane Center, 1988: Diagnostic Report of the National Hurricane Center. August and September 1988, 1 (2), 155 pp.
- Naval Oceanography Command Detachment (NOCD), Asheville, N.C., 1985: *U. S. Navy Climatic Study of the Caribbean and Gulf of Mexico*, Vol. 1, Western Caribbean Sea and Central American Waters. NAVAIR 50-1C-543, 198 pp.
- Naval Oceanography Command Detachment (NOCD), Asheville, N.C., 1986: *U. S. Navy Climatic Study of the Caribbean and Gulf of Mexico*, Vol. 4, Gulf of Mexico and Gulf of Tehuantepec. NAVAIR 50-1C-546, 198 pp.
- Naval Western Oceanography Center, 1989: *Area of Responsibility (AOR) Forecaster's Handbook*. Naval Western Oceanography Center, Pearl Harbor, Hawaii. Prepared for Commander Naval Oceanography Command, III-5 to III-14.

- Neumann, C. J., B. R. Jarvinen, A. C. Pike, and J. D. Elms, 1987: *Tropical Cyclones of the North Atlantic Ocean 1871-1986*. Historical Climatology Series 6-2, prepared by the National Climatic Data Center, Asheville, NC 28801, in cooperation with the National Hurricane Center, Coral Gables, FL, 186 pp.
- Palmer, C. E., C. W. Wise, L. W. Stempson and G. H. Duncan, 1955: The practical aspect of tropical meteorology. AWS Manual 105-48, Vol I (redesignated in 1970 as Vol I of *AWS Tech Report 241*), 195 pp.
- Pearson, D. C., M. Michel-Howell, C. S. Strager and C. H. Larcomb, 1987: Seasons in Review: GOES Satellite Photos over Central America. 5th Weather Wing Forecaster Memo (5WW/FM-87/006), Headquarters 5th Weather Wing (MAC), Langley Air Force Base, VA 23665-6345, 78 pp.
- Portig, W. H., 1976: The Climate of Central America. *World Survey of Climatology* (W. Schwerdtfeger, Ed.), Vol. XII, Elsevier Scientific Publishing Company, Amsterdam, The Netherlands, 405-478.
- Reed, R. J., A. Hollingsworth, W. A. Heckley and F. Delsol, 1988: An Evaluation of the Performance of the ECMWF Operational System in Analyzing and Forecasting Easterly Wave Disturbances over Africa and the Tropical Atlantic. *Mon. Wea. Rev.*, **116**, 824-865.
- Riehl, H., 1968: Surface winds over the South China Sea during the northeast monsoon season. NAVWEARSCHFAC Tech Paper No. 22-68. (Available from the Naval Environmental Prediction Research Facility, Monterey, CA 93943), 24 pp.
- Riehl, H., 1979: *Climate and Weather in the Tropics*. Academic Press Inc., 111 Fifth Avenue, New York, NY 611 pp.
- Sadler, J. C., 1976: *Tropical Cyclone Initiation By The Tropical Upper Tropospheric Trough*. University of Hawaii, NAVENVPREDRSCHFAC Technical Paper No. 2-76, 104 pp.
- Sadler, J. C. and T. C. Wann, 1984: *Mean Upper Tropospheric Flow over the Global Tropics, Volume II*. AWS/TR-83/002 Air Weather Service (MAC), Scott AFB, Illinois 62225, 48 pp.
- Sadler, J. C., B. Kilonsky, L. Oda and A. Hori, 1984: *Mean Cloudiness over the Global Tropics from Satellite Observations*. University of Hawaii, NAVENVPREDRSCHFAC Contract Report 84-09, 73 pp.
- Sadler, J. C., M. A. Lander, M. A. Hori and L. K. Oda, 1987: *Tropical Marine Climatic Atlas. Vol. II (Pacific Ocean)*. Dept. Met., U. of Hawaii. Tropical oceans global atmosphere (TOGA) and Equatorial Pacific ocean climatic studies (EPOCS). UHMET Report 87-02, 27 pp.
- Skinner, B. J. (Ed.), 1980: *Earth's History, Structure and Materials. Readings from American Scientist*. William Kauffman, Inc., Los Altos, CA., pp. 69, 81, 100.

- Stroup, E. D., 1969: The Thermostat of the 13-C Water in the Equatorial Ocean. Doctor of Philosophy Dissertation, Johns Hopkins University, Baltimore, MD., 205 pp.
- The Diagram Group, 1985: *Atlas of Central America and the Caribbean*. Macmillan Publishing Company, New York, 144 pp.
- United States Air Force Environmental Technical Applications Center (USAFETAC), 1985: Situation Climatic Briefs. USAFETAC/DS-85/030. Scott Air Force Base, Illinois, 62225-5438, Latin America: pp. F-5 – F-6, F-21 – F-23, F-31 – F-35, F-41 – F-43, F-51 – 5-56-3.
- United States Air Force Environmental Technical Applications Center (USAFETAC), 1987: Station Climatic Summaries – Latin America. USAFETAC/DS-87/032. Scott Air Force Base, Illinois, 62225-5438, 394 pp.
- Walters, K., M. Vojtesak and A. Korik, 1988: *Caribbean Basin—Climatology Study*, USAFETAC (in press, available from the Naval Environmental Prediction Research Facility, Monterey, CA 93943 by late 1989).
- Woodruff, S. D., R. J. Slutz, R. L. Jenne and P. M. Steurer, 1987: A Comprehensive Ocean-Atmosphere Data Set. *Bull. Amer. Meteor. Soc.*, **68**, 1239–1250.
- Wyrtki, K., 1964: The thermal structure of the eastern tropical Pacific Ocean. *Deutsch hydrographische Zeitschrift, Ergänzungsheft Reihe A*, Nr. 6, 84 pp.

Appendix A

Tropical Analysis

The understanding of tropical meteorology is less complete than that of extratropical meteorology—especially so in prognosis of weather patterns. Additionally, the definition of the “geostrophic” wind from the pressure pattern is less useful in the tropics (becoming undefined as the equator is approached), and thermal structures of tropical systems are different from the thermal structures of mid-latitude systems. While the introduction of meteorological satellites in the 1960s *has* enhanced our surveillance of the tropics, conventional data (observations) are still scarce. Research continues on data obtained from World Meteorological Organization (WMO) sponsored experiments, and other investigations, to enhance the understanding of tropical atmospheric and oceanic processes. See Chapter 1 of *A Global View of Tropical Cyclones* (Elsberry et al., 1987) for the status of tropical analysis at international tropical cyclone centers.

Streamline and Isotach Analysis Preferred for Tropics

Scale analysis shows that while mid-latitude geopotential height fluctuations (on the synoptic scale) are of the order of 100 meters; in the tropics, synoptic height fluctuations are of the order of *only* 10 meters. In the absence of tropical cyclones, the horizontal temperature gradient in the tropics is *small*. Thus, thickness perturbations are *small*, resulting in *small* height perturbations. Height gradients, so evident on mid-latitude constant-pressure charts, are normally less prominent on tropical charts, in the absence of tropical cyclones. Accordingly, streamline and isotach analyses are much preferred (over geopotential height analyses) in tropical meteorology.

A Tropical “Direct Cell”, despite a Cold Surface Tropical Wave (Trough)

Assuming no long-term change in the mean temperature and small horizontal temperature advection in the tropical troposphere and lower stratosphere, the First Law of Thermodynamics reveals that in **clear** areas the mean large-scale vertical motions average $-0.3 \text{ cm} \cdot \text{s}^{-1}$, i.e., small magnitude **sinking** providing adiabatic warming to balance the cooling caused by *outgoing* long wave radiation. Conversely, in **cloudy** areas, the large magnitude of warming, provided by the release of latent heat as water vapor condenses to liquid cloud droplets, must be *opposed* by the adiabatic cooling of **ascent**. While the initial solution is $+1.5 \text{ cm} \cdot \text{s}^{-1}$ averaged in the vertical, it is nearer $+3.0 \text{ cm} \cdot \text{s}^{-1}$ in the middle of the deep tropical troposphere, since the vertical motion is assumed to be zero at both the earth’s surface and in the stratosphere.

While developing tropical cyclones have warm cores, most incipient tropical waves (or troughs) have been identified as having cold cores. Studies (as early as the 1940’s) of Waves in the Easterlies in the Caribbean Sea by Riehl (1979) identified waves having a period of 3-4 days, wavelength of 2000 km, westward propagation, an axis tilted toward the east with height, disturbed weather *closely* trailing its surface position and a *lower tropospheric* cold core.

Convection (upward motion with associated cloudiness) located near the cold trough was at first troublesome, since cold air rising, i.e., $\overline{w'T'} < 0$, converts kinetic energy to potential energy and contributes to the demise of the wave. (When cold air rises, the center of gravity of the air column is lifted (z is increased), increasing the potential energy gz and consequently decreasing the kinetic energy $\frac{1}{2}mv^2$, if the total energy is assumed constant.) However, noting the tilt of the axis with height, at mid troposphere the wave is one-half wavelength toward the west, placing **warm** air over the surface wave position. Thus, at the geographic position of the Wave in the Easterlies, a warm perturbation is found in mid troposphere, where, as noted (previously) in cloudy areas, a large **upward** vertical motion perturbation is present, $w \doteq +3.0 \text{ cm}\cdot\text{s}^{-1}$. Therefore, noting that w is near zero at the top and bottom of the troposphere (where the $T' < 0$), but w is large and positive where $T' > 0$, the vertical integrated product of w' and T' is positive, i.e., $\overline{w'T'} > 0$. Therefore, potential energy is converted into kinetic energy, i.e., overall there is a "direct cell" with **rising warm air**, allowing for the possibility of continued development of the wave into a tropical cyclone of increased intensity (Chang, 1987). (Obviously all Waves in the Easterlies do **not** develop into tropical storms or hurricanes, but the identification of a direct cell at least provides a necessary, though not sufficient, condition.)

Appendix B

Operational Climatic Data Summaries (USAFETAC, 1987)

PAGE	STATION
B-2	BELIZE CITY, BELIZE
B-3	HUEHUETENANGO, GUATEMALA
B-4	PUERTO BARRIOS, GUATEMALA
B-5	CATACAMAS, HONDURAS
B-6	CHOLUTECA, HONDURAS
B-7	LA CEIBA, HONDURAS
B-8	PALMEROLA, HONDURAS
B-9	SAN PEDRO SULA, HONDURAS
B-10	SANTA ROSA DE COPAN, HONDURAS
B-11	SWAN ISLAND, HONDURAS
B-12	TEGUCIGALPA, HONDURAS
B-13	ACAJUTLA, EL SALVADOR
B-14	SAN SALVADOR, EL SALVADOR
B-15	BLUEFIELDS, NICARAGUA
B-16	CHINADEGA, NICARAGUA
B-17	MANAGUA, NICARAGUA
B-18	PUERTO CABEZAS, NICARAGUA
B-19	LIBERIA, COSTA RICA
B-20	LIMON INTL, COSTA RICA
B-21	PUNTARENAS, COSTA RICA
B-22	SAN JOSE, COSTA RICA
B-23	FORT SHERMAN, PANAMA
B-24	PANAMA CITY, PANAMA
B-25	RIO HATO, PANAMA
B-26	SAN ANDRES ISLAND, COLUMBIA

STATION: BELIZE CITY, BELIZE

STATION #: 785830

ICAO ID: MZBZ (USAFETAC, 1987)

LOCATION: 17° 32'N, 088° 18'W

ELEVATION (FEET): 16 LST = GMT: -6

PREPARED BY: USAFETAC/ECR, SEP 1986

PERIOD: VARIED (except items 6 & 7: JAN 73 - DEC 85)

SOURCE NO.	JAN	FEB	MAR	APR	MAY	JUN	JUL	AUG	SEP	OCT	NOV	DEC	ANN
1. TEMPERATURE (°F)													
EXTREME MAX	2	90	93	98	99	97	97	95	96	97	95	95	99
MEAN DLY MAX	2	82	83	85	87	88	88	88	88	89	86	84	86
MEAN	2	75	76	79	81	82	82	82	82	82	80	77	79
MEAN DLY MIN	2	68	69	72	74	75	76	76	76	75	73	69	73
EXTREME MIN	2	50	49	50	55	57	62	63	61	60	58	52	46
# DAYS ≥ 90	2	#	#	3	8	12	11	9	14	12	6	1	#
# DAYS < 32	3	0	0	0	0	0	0	0	0	0	0	0	0
# DAYS ≤ 0	3	0	0	0	0	0	0	0	0	0	0	0	0
2. PRECIPITATION (INCHES)													
MAXIMUM	2	9.0	7.9	4.2	8.5	10.7	22.3	26.3	15.5	21.3	26.9	25.7	109.9
MEAN	2	5.7	2.7	1.6	2.4	5.0	9.1	7.6	7.3	9.5	2.4	9.8	80.3
MINIMUM	2	0.8	0.0	0.0	0.0	0.1	2.3	1.9	2.2	4.1	1.7	1.9	40.8
MAX 24 HR	2	4.2	2.9	2.8	7.8	6.6	16.6	10.6	6.2	8.2	7.7	9.8	16.6
# DAYS ≥ 0.01	2	12	6	4	4	7	14	18	16	18	15	13	14
# DAYS ≥ 0.5	2	*	*	*	*	*	*	*	*	*	*	*	*
3. MEAN RELATIVE HUMIDITY (%) / VAPOR PRESSURE (IN Hg) / DEWPOINT (°F)													
RH (06 LST)	1	95	95	92	90	90	91	92	93	95	95	95	93
RH (12 LST)	1	71	72	69	67	66	74	72	72	75	74	70	72
VAPOR PRESS.	1	.72	.76	.79	.84	.89	.92	.91	.92	.92	.88	.79	.76
DEWPOINT	1	69	70	71	73	75	76	76	76	76	75	71	73
4. SURFACE WINDS (16 PT/KNOTS) / 99.95% HIGHEST PRESSURE ALTITUDE (FEET)													
PVLG DRCTN	1	\$E	E	E	E	E	E	E	E	\$E	\$E	\$E	E
MEAN SPEED													
(PVLG DRCTN)	1	7	8	8	9	9	9	9	8	7	7	7	8
MEAN SPEED													
(ALL OBS)	1	5	6	7	7	7	7	7	6	5	5	5	6
MAX (PK GST)		*	*	*	*	*	*	*	*	*	*	*	*
PRESSURE ALT	1	150	200	250	200	200	200	150	200	150	150	100	250
5. MEAN CLOUD COVER (EIGHTHS) / THUNDERSTORMS / FOG / BLOWING SAND (BNBD)													
CLD COVER	1	4	4	4	4	5	6	5	5	6	5	5	5
DAYS TSTMS	1	1	#	1	1	4	8	8	8	10	5	2	50
DAYS FOG < 7	1	4	2	1	1	1	1	1	2	1	3	3	23
DAYS BNBD < 7	1	0	0	#	0	#	#	#	0	0	0	0	#
6. PERCENTAGE FREQUENCY OF OCCURRENCE (% FREQ) OF THUNDERSTORMS:													
	JAN	FEB	MAR	APR	MAY	JUN	JUL	AUG	SEP	OCT	NOV	DEC	ANN
00-02 LST	0	0	1	0	7	2	6	5	12	3	0	3	3
03-05 LST	0	0	0	0	1	7	7	4	11	3	0	1	3
06-08 LST	#	0	0	0	1	5	4	4	7	2	1	1	2
09-11 LST	0	#	0	1	1	2	4	4	4	3	1	#	2
12-14 LST	#	0	#	1	1	4	3	3	4	2	1	#	2
15-17 LST	#	#	0	1	#	2	1	2	3	1	#	#	1
18-20 LST	1	0	0	1	1	2	3	3	1	1	1	0	1
21-23 LST	0	0	0	1	1	4	2	3	4	1	0	0	1
ALL HOURS	#	#	#	1	2	4	4	4	6	2	1	1	2
7. % FREQ OF RAIN AND/OR DRIZZLE:													
00-02 LST	9	4	10	1	4	16	10	9	25	11	11	13	10
03-05 LST	11	7	6	3	5	20	11	7	21	14	5	11	9
06-08 LST	7	5	3	3	5	13	8	7	15	16	7	9	9
09-11 LST	6	8	4	3	4	12	9	7	7	9	8	8	7
12-14 LST	7	5	6	2	3	13	7	8	7	9	7	9	7
15-17 LST	7	6	3	2	1	9	7	3	4	8	5	4	5
18-20 LST	3	4	6	2	3	13	8	3	3	8	3	10	6
21-23 LST	8	2	7	2	5	10	7	8	10	9	6	9	7
ALL HOURS	7	5	6	2	4	3	8	7	12	11	7	9	8
8. PERCENTAGE FREQUENCY OF OCCURRENCE (% FREQ) OF CEILING AND/OR VISIBILITY													
(CIG/VIS) < 1500/3 STATUTE MILES (MI) (SOURCE NO. 1):													
00-02 LST	7	5	4	7	4	7	7	4	10	12	8	13	7
03-05 LST	19	7	1	3	6	14	11	6	7	16	12	15	10
06-08 LST	21	14	6	7	4	11	8	8	14	25	19	20	13
09-11 LST	11	10	4	5	1	6	6	5	5	13	12	13	8
12-14 LST	5	4	3	4	4	5	4	3	3	5	6	6	4
15-17 LST	5	3	2	3	3	5	3	1	1	6	3	3	3
18-20 LST	3	3	5	4	3	2	5	2	2	4	3	7	4
21-23 LST	8	3	2	2	5	5	3	3	1	9	6	7	5
ALL HOURS	10	6	3	4	4	7	6	4	5	11	9	11	7
9. % FREQ OF CIG/VIS < 200/0.5 MI (SOURCE NO. 1):													
00-02 LST	0	0	0	0	1	1	0	0	0	3	0	0	#
03-05 LST	8	2	0	1	0	2	0	2	1	1	2	3	2
06-08 LST	8	3	1	1	#	#	2	1	1	3	6	5	3
09-11 LST	1	1	0	0	0	0	0	0	#	0	#	1	#
12-14 LST	#	1	0	0	#	1	0	0	0	#	#	0	#
15-17 LST	#	0	#	0	0	0	0	0	#	#	#	0	#
18-20 LST	0	1	0	0	1	1	0	0	0	0	1	0	#
21-23 LST	1	0	0	0	0	0	1	0	0	2	0	1	#
ALL HOURS	2	1	#	#	#	1	#	#	#	1	1	1	1

REMARKS * = DATA NOT AVAILABLE # = LESS THAN 0.5 DAY, OR 0.05 INCH, OR 0.5% MI = STAT. MILES
 \$ = % CALM > PVLG DRCTN @ = BASED ON AVAIL. DATA, I.E., < 24 HRS/DAY OR < 12 MONTHS/YEAR
 SOURCE(S) 1. USAFETAC DATSAV FOR JAN 73 - DEC 85
 2. NATIONAL INTELLIGENCE SURVEY 6-70 YEARS
 3. WORLDWIDE AIRFIELD CLIMATIC DATA SUMMARY 3-42 YEARS

STATION: HUEHUETENANGO, GUATEMALA STATION #: 786270 ICAO ID: MGHT (USAFETAC,
 LOCATION: 15°19'N, 91°30'W ELEVATION (FT.): 6134 LST = GMT: -6 1987)
 PREPARED BY: USAFETAC/ECR JAN 1985 PERIOD: VARIED (except items 6 & 7: JAN 73 - DEC 83)

SOURCE NO.		JAN	FEB	MAR	APR	MAY	JUN	JUL	AUG	SEP	OCT	NOV	DEC	ANN
1. TEMPERATURE (°F)														
EXTREME MAX	1	86	90	92	94	90	83	86	83	85	86	84	83	94
MEAN DLY MAX	1	74	76	80	81	79	74	74	75	74	73	73	73	75
MEAN	1	60	62	67	69	69	66	66	66	65	64	62	60	65
MEAN DLY MIN	1	46	46	51	53	56	58	56	56	57	57	52	47	53
EXTREME MIN	1	29	25	36	36	43	43	41	41	45	41	39	30	25
# DAYS≥90	1	0	#	1	1	1	0	0	0	0	0	0	0	3
# DAYS≤32	1	2	1	0	0	0	0	0	0	0	0	0	1	4
# DAYS≤0	1	0	0	0	0	0	0	0	0	0	0	0	0	0
2. PRECIPITATION (INCHES)														
MAXIMUM	2	0.2	0.3	0.2	1.3	3.3	7.8	12.7	10.3	14.4	10.5	2.3	0.7	43.9
MEAN	2	#	0.1	#	0.4	1.2	5.3	9.2	6.6	9.0	3.5	0.4	0.1	36.0
MINIMUM	2	0.0	0.0	0.0	0.0	0.2	3.7	4.6	4.0	4.9	1.2	0.0	0.0	27.6
MAX 24 HR		*	*	*	*	*	*	*	*	*	*	*	*	*
# DAYS≥0.01	2	1	1	#	2	4	15	13	16	19	9	2	1	82
# DAYS≥0.5		*	*	8	*	*	*	*	*	*	*	*	*	*
3. MEAN RELATIVE HUMIDITY (%) / VAPOR PRESSURE (IN Hg) / DEWPOINT (°F)														
RH (06 LST)	1	95	95	94	95	95	97	97	97	97	97	97	96	96
RH (14 LST)	1	32	29	26	27	39	55	50	50	55	54	46	38	42
VAPOR PRESS.	1	.30	.31	.33	.36	.42	.48	.44	.45	.47	.45	.39	.34	.40
DEWPOINT	1	44	45	47	49	53	57	55	55	57	55	52	47	51
4. SURFACE WINDS (16 PT/KNOTS) / 99.95% HIGHEST PRESSURE ALTITUDE (FEET)														
PVLG DRCTN	1	SE\$	E\$	E\$	E\$	E\$	SE\$	SE\$	SE\$	SE\$	SE\$	SE\$	SE\$	SE\$
MEAN SPEED	1	4	4	4	4	3	4	5	5	3	2	3	3	4
MAX (PK GST)	1	22	25	24	26	26	25	22	22	24	20	35	24	35
PRESSURE ALT		*	*	*	*	*	*	*	*	*	*	*	*	*
5. MEAN CLOUD COVER (EIGHTHS) / THUNDERSTORMS / FOG/ BLOWING SAND (BNBD)														
CLD COVER	1	3	3	3	4	5	7	6	6	7	6	5	3	5
DAYS TSTMS	1	#	1	3	6	11	12	9	8	12	6	2	1	71
DAYS FOG	1	13	11	7	9	12	5	5	5	7	6	12	16	108
DAYS BNBD		*	*	*	*	*	*	*	*	*	*	*	*	*
6. PERCENTAGE FREQUENCY OF OCCURRENCE (% FREQ) OF THUNDERSTORMS:														
	JAN	FEB	MAR	APR	MAY	JUN	JUL	AUG	SEP	OCT	NOV	DEC	ANN	
00-02 LST	0	0	0	0	5	0	1	0	0	0	0	0	1	
03-05 LST	0	0	0	0	1	0	1	0	0	0	#	0	#	
06-08 LST	0	0	0	0	0	0	0	0	#	#	0	0	#	
09-11 LST	0	0	0	0	0	0	0	0	0	0	0	0	0	
12-14 LST	0	0	#	1	5	8	4	3	4	2	1	#	2	
15-17 LST	#	1	4	9	19	17	11	10	14	10	4	1	8	
18-20 LST	0	1	2	4	9	9	8	7	9	4	1	1	5	
21-23 LST	0	0	1	1	6	5	5	6	3	1	0	#	2	
ALL HOURS	#	#	1	2	6	6	4	4	4	3	1	#	3	
7. % FREQ OF RAIN AND/OR DRIZZLE:														
00-02 LST	0	0	1	1	12	15	12	15	20	5	#	#	7	
03-05 LST	0	1	1	0	4	9	8	5	12	4	#	1	4	
06-08 LST	#	0	#	1	2	5	1	2	4	4	1	1	2	
09-11 LST	#	#	1	0	1	2	1	1	3	2	1	#	1	
12-14 LST	0	0	2	1	4	6	3	3	6	5	1	1	3	
15-17 LST	#	1	1	3	10	15	8	12	18	10	3	1	7	
18-20 LST	0	1	2	3	13	25	15	16	22	9	4	1	9	
21-23 LST	0	0	1	2	12	22	21	20	19	8	2	1	9	
ALL HOURS	#	#	1	1	6	10	5	7	11	6	2	1	4	
8. PERCENTAGE FREQUENCY OF OCCURRENCE (% FREQ) OF CEILING AND/OR VISIBILITY (CIG/VIS) < 1500/3 STATUE MILES (MI) (SOURCE NO. 1):														
00-02 LST	1	1	1	5	7	3	3	2	7	2	10	4	4	
03-05 LST	14	7	13	12	21	6	10	8	10	8	24	24	13	
06-08 LST	36	36	18	22	39	18	18	21	24	25	42	49	29	
09-11 LST	6	4	1	7	12	3	2	4	4	7	12	7	6	
12-14 LST	1	0	#	1	5	2	#	1	1	3	3	1	1	
15-17 LST	1	0	1	1	7	5	2	3	5	4	2	1	3	
18-20 LST	0	#	0	2	7	4	2	2	7	2	3	#	2	
21-23 LST	0	0	1	2	5	4	2	2	2	3	3	0	2	
ALL HOURS	9	8	5	7	14	6	5	6	8	8	13	12	8	
9. % FREQ OF CIG/VIS < 200/0.5 MI (SOURCE NO. 1)														
00-02 LST	0	0	0	1	2	0	1	0	0	0	4	#	1	
03-05 LST	7	1	6	1	4	1	5	1	3	4	9	11	5	
06-08 LST	19	13	8	3	7	4	8	4	5	7	14	26	10	
09-11 LST	1	0	#	0	0	0	0	0	0	0	1	1	#	
12-14 LST	0	0	0	0	0	0	0	0	0	#	0	#	#	
15-17 LST	0	0	#	#	#	0	#	0	#	#	#	#	#	
18-20 LST	0	0	0	#	0	0	#	1	1	0	#	0	#	
21-23 LST	0	0	0	0	0	0	0	0	0	0	#	0	#	
ALL HOURS	4	2	2	1	2	1	2	1	1	1	4	5	2	

REMARKS * = DATA NOT AVAILABLE # = LESS THAN 0.5 DAY, OR 0.05 INCH, OR 0.5% MI = STAT. MILES
 \$ = % CALM > PVLG DRCTN @ = BASED ON AVAIL DATA, I.E., < 24 HRS/DAY OR < 12 MONTHS/YEAR
 SOURCE(S) 1 USAFETAC DATSAV FOR JAN 73 - DEC 85
 2 NATIONAL INTELLIGENCE SURVEY - PRECIP DATA FOR QUEZA HENANGO 14°49'N, 91°30'W

STATION: PUERTO BARRIOS, GUATEMALA STATION #: 786370 ICAO ID: MGPB (USAFETAC, 1987)
 LOCATION: 15°44'N, 88°35'W ELEVATION (FT.): 33 LST = GMT: -6
 PREPARED BY: USAFETAC/ECR PERIOD: VARIED(except items 6 & 7 JAN 73 - DEC 83)

		SOURCE NO.	JAN	FEB	MAR	APR	MAY	JUN	JUL	AUG	SEP	OCT	NOV	DEC	ANN
1. TEMPERATURE (°F)															
EXTREME MAX	2		97	100	109	110	108	107	102	100	104	100	98	96	110
MEAN DLY MAX	2		84	86	91	93	94	93	91	92	92	89	85	84	89
MEAN	2		78	79	83	85	86	86	85	85	85	93	80	79	83
MEAN DLY MIN	2		72	71	74	77	78	79	79	78	78	76	74	73	76
EXTREME MIN	2		60	56	63	66	68	72	74	75	72	66	62	58	56
# DAYS>90			*	*	*	*	*	*	*	*	*	*	*	*	*
# DAYS<32	1		0	0	0	0	0	0	0	0	0	0	0	0	0
# DAYS<0	1		0	0	0	0	0	0	0	0	0	0	0	0	0
2. PRECIPITATION (INCHES)															
MAXIMUM	2		24.0	20.0	27.2	19.6	20.9	19.0	39.2	30.5	25.4	36.4	26.6	26.3	174.1
MEAN	2		7.1	4.2	3.0	4.1	7.8	10.8	18.7	12.1	11.5	14.6	10.6	9.2	113.7
MINIMUM	2		2.0	1.3	0.5	0.8	4.2	4.2	8.7	4.4	4.3	4.7	4.0	4.4	83.4
MAX 24 HR	2		6.8	6.6	10.1	4.7	3.6	5.5	4.9	5.2	6.6	6.2	7.8	11.2	11.2
# DAYS>0.01	2		20	11	10	12	15	23	28	25	21	20	20	21	225
# DAYS>0.5			*	*	*	*	*	*	*	*	*	*	*	*	*
3. MEAN RELATIVE HUMIDITY (%) / VAPOR PRESSURE (IN Hg) / DEWPOINT (°F)															
RH (06 LST)	1		94	94	94	93	94	93	95	94	93	94	93	93	94
RH (15 LST)	1		73	71	66	65	67	70	72	71	71	72	73	73	70
VAPOR PRESS.	1		.71	.73	.79	.83	.89	.89	.87	.88	.88	.85	.78	.76	.83
DEWPOINT	1		68	69	71	73	75	75	74	75	75	73	71	70	73
4. SURFACE WINDS (16 PT/KNOTS) / 99.95% HIGHEST PRESSURE ALTITUDE (FEET)															
PVLG DRCTN	1		N\$	N\$	N\$	N\$	N\$	N\$	N\$	N\$	N\$	N\$	W\$	N\$	N\$
MEAN SPEED	1		5	5	6	6	5	5	5	5	5	5	5	5	5
MAX (PK GST)	1		35	28	40	35	35	30	40	30	65	30	38	35	65
PRESSURE ALT	1		300	300	350	350	350	350	250	300	400	250	300	300	350
5. MEAN CLOUD COVER (EIGHTHS) / THUNDERSTORMS / FOG/ BLOWING SAND (BNBD)															
CLD COVER	1		5	5	4	4	5	7	7	7	7	6	6	5	6
DAYS TSTMS	1		1	1	1	3	9	19	23	23	20	10	4	3	117
DAYS FOG < 7	1		3	3	4	5	5	3	3	1	#	1	2	2	32
DAYS BNBD < 7			*	*	*	*	*	*	*	*	*	*	*	*	*
6. PERCENTAGE FREQUENCY OF OCCURRENCE (% FREQ) OF THUNDERSTORMS:															
		JAN	FEB	MAR	APR	MAY	JUN	JUL	AUG	SEP	OCT	NOV	DEC	ANN	
00-02 LST	1	3	0	2	10	29	37	42	36	19	1	4	15		
03-05 LST	0	2	0	2	7	20	25	28	22	11	1	1	10		
06-08 LST	1	0	#	1	5	7	8	10	6	3	2	2	4		
09-11 LST	#	1	0	0	3	3	4	4	2	2	1	1	2		
12-14 LST	#	1	#	1	3	9	13	12	11	5	2	#	5		
15-17 LST	0	1	#	2	6	18	21	18	14	5	3	1	7		
18-20 LST	1	1	0	2	5	23	30	27	11	8	3	2	9		
21-23 LST	1	2	0	2	6	25	43	45	32	19	2	4	15		
ALL HOURS	1	1	#	1	5	13	18	18	14	7	2	2	7		
7. % FREQ OF RAIN AND/OR DRIZZLE:															
00-02 LST	14	11	6	7	8	24	22	19	21	23	8	18	15		
03-05 LST	8	19	6	5	6	17	7	15	14	14	14	19	12		
06-08 LST	13	10	6	5	6	9	5	7	7	12	17	15	9		
09-11 LST	12	12	4	2	3	4	4	4	6	10	14	12	7		
12-14 LST	10	9	3	2	1	5	5	3	4	9	8	7	6		
15-17 LST	7	7	3	2	1	6	7	5	5	6	9	8	6		
18-20 LST	10	9	2	5	3	15	13	11	12	11	9	13	9		
21-23 LST	15	9	2	8	4	27	31	27	18	21	12	15	16		
ALL HOURS	11	10	4	4	3	10	9	8	9	12	11	12	9		
8. PERCENTAGE FREQUENCY OF OCCURRENCE (% FREQ) OF CEILING AND/OR VISIBILITY (CIG/VIS) < 1500/3 STATUE MILES (MI) (SOURCE NO. 1):															
00-02 LST	7	4	3	8	4	4	5	5	3	4	5	8	5		
03-05 LST	7	6	2	8	4	2	4	3	3	2	6	7	4		
06-08 LST	11	9	9	12	17	5	6	8	6	8	11	12	9		
09-11 LST	10	8	6	6	9	4	2	3	3	7	9	9	6		
12-14 LST	8	6	3	5	8	3	2	2	2	5	4	6	4		
15-17 LST	6	6	3	7	12	4	5	3	3	4	4	7	5		
18-20 LST	6	5	2	12	10	7	6	5	4	4	4	5	6		
21-23 LST	6	4	1	11	4	6	6	6	5	6	4	7	6		
ALL HOURS	8	7	4	8	10	4	4	3	5	6	8	6			
9. % FREQ OF CIG/VIS < 200/0.5 MI (SOURCE NO. 1):															
00-02 LST	0	0	0	0	0	0	0	0	0	0	0	0	0		
03-05 LST	0	0	0	0	1	0	0	0	0	0	0	0	0	#	
06-08 LST	#	0	#	#	0	#	#	0	0	#	0	1	#		
09-11 LST	#	#	#	0	0	0	#	0	0	#	#	#	#		
12-14 LST	0	#	0	0	0	#	0	0	#	#	#	#	#		
15-17 LST	0	#	#	#	0	#	#	#	#	0	#	1	#		
18-20 LST	0	0	0	#	0	#	0	0	0	0	1	0	#		
21-23 LST	0	0	0	0	0	0	#	0	0	0	0	0	#		
ALL HOURS	#	#	#	#	#	#	#	#	#	#	#	#	#		

REMARKS: * = DATA NOT AVAILABLE # = LESS THAN 0.5 DAY, OR 0.05 INCH, OR 0.5% MI = STAT. MILES
 \$ = % CALM > PVLG DRCTN @ = BASED ON AVAIL. DATA, I.E., < 24 HRS/DAY OR < 12 MONTHS/YEAR
 SOURCE(S): 1. USAFETAC DATSAV FOR JAN 73 - DEC 83
 2. NATIONAL INTELLIGENCE SURVEY FOR VARIED

STATION: CATACAMAS, HONDURAS STATION #: 787140 ICAO ID: MHCA (USAFETAC, 1987)
 LOCATION: 14°54'N, 85°56'W ELEVATION (FT.): 1450 LST = GMT: GMT -6
 PREPARED BY: USAFETAC/ECR, 1986 PERIOD: VARIED(except items 6 & 7 JAN 73 - DEC 85)

SOURCE NO.	JAN	FEB	MAR	APR	MAY	JUN	JUL	AUG	SEP	OCT	NOV	DEC	ANN
1. TEMPERATURE (°F)													
EXTREME MAX	2	97	97	99	103	104	96	93	94	92	90	90	104
MEAN DLY MAX	2	83	85	89	90	90	87	86	87	87	84	83	87
MEAN	2	72	74	77	78	79	78	77	77	78	77	73	76
MEAN DLY MIN	2	60	62	64	66	68	69	67	67	68	67	62	65
EXTREME MIN	2	39	48	49	54	52	53	56	59	54	50	46	39
# DAYS>90	2	1	5	15	21	20	12	2	5	8	4	1	#
# DAYS<32	1	0	0	0	0	0	0	0	0	0	0	0	0
# DAYS<0	1	0	0	0	0	0	0	0	0	0	0	0	0
2. PRECIPITATION (INCHES)													
MAXIMUM	2	3.9	3.5	3.5	3.2	9.8	14.0	19.4	12.0	30.1	34.0	12.4	20.4
MEAN	2	1.7	.9	.6	1.1	4.4	8.9	9.4	6.1	7.6	6.7	3.1	2.3
MINIMUM	2	.1	.1	0	0	#	6.1	3.2	2.7	4.7	1.3	1.1	.6
MAX 24 HR	2	1.2	1.6	1.2	1.3	2.1	2.4	2.3	2.0	10.0	3.5	2.6	3.5
# DAYS>0.01	2	10	6	5	6	11	19	20	20	18	17	12	8
# DAYS>0.5		*	*	*	*	*	*	*	*	*	*	*	*
3. MEAN RELATIVE HUMIDITY (%) / VAPOR PRESSURE (IN Hg) / DEWPOINT (°F)													
RH (06 LST)	1	89	83	81	82	84	89	88	89	92	91	88	88
RH (14 LST)	1	57	50	44	44	46	59	64	63	61	59	59	56
VAPOR PRESS.	1	.62	.59	.60	.62	.69	.74	.72	.74	.76	.74	.69	.65
DEWPOINT	1	64	63	63	64	67	70	69	69	70	69	68	66
4. SURFACE WINDS (16 PL/KNOTS) / 99.95% HIGHEST PRESSURE ALTITUDE (FEET)													
PVLG DRCTN	1	\$E	\$E	E	E	E	\$E	\$E	\$E	\$E	\$E	\$E	\$E
MEAN SPEED													
(PVLG DRCTN)	1	7	7	7	7	6	7	7	6	6	5	6	7
MEAN SPEED													
(ALL OBS)	1	3	4	5	5	4	4	4	3	3	3	3	4
MAX (PK GST)		*	*	*	*	*	*	*	*	*	*	*	*
PRESSURE ALT	1	1550	1550	1650	1650	1650	1600	1650	1550	1650	1600	1600	1550
5. MEAN CLOUD COVER (EIGHTHS) / THUNDERSTORMS / FOG/ BLOWING SAND (BNBD)													
CLD COVER	1	5	4	4	4	5	6	5	5	5	5	5	5
DAYS TSTMS	1	#	#	1	2	5	9	11	12	10	6	2	1
DAYS FOG < 7	1	2	1	#	1	1	2	2	3	5	5	3	4
DAYS BNBD < 7	1	0	#	0	#	0	0	0	0	0	0	0	#
6. PERCENTAGE FREQUENCY OF OCCURRENCE (% FREQ) OF THUNDERSTORMS:													
	JAN	FEB	MAR	APR	MAY	JUN	JUL	AUG	SEP	OCT	NOV	DEC	ANN
00-02 LST	*	*	*	*	*	*	*	*	*	*	*	*	*
03-05 LST	*	*	*	*	*	*	*	*	*	*	*	*	*
06-08 LST	#	0	0	0	0	0	#	#	0	0	0	0	#
09-11 LST	0	0	0	0	0	#	#	#	#	#	0	0	#
12-14 LST	0	0	#	#	1	4	7	5	2	2	#	#	2
15-17 LST	0	#	0	2	6	11	13	11	12	5	1	#	5
18-20 LST	0	0	1	2	5	7	4	5	7	4	0	0	3
21-23 LST	*	*	*	*	*	*	*	*	*	*	*	*	*
ALL HOURS	*	*	*	*	*	*	*	*	*	*	*	*	*
7. % FREQ OF RAIN AND/OR DRIZZLE:													
00-02 LST	*	*	*	*	*	*	*	*	*	*	*	*	*
03-05 LST	*	*	*	*	*	*	*	*	*	*	*	*	*
06-08 LST	5	4	2	2	2	8	8	5	2	3	3	5	6
09-11 LST	5	2	1	1	1	6	7	4	3	2	3	5	6
12-14 LST	2	1	2	1	2	7	10	9	5	6	4	5	7
15-17 LST	4	1	2	4	5	15	18	14	13	12	7	7	9
18-20 LST	5	2	3	6	7	18	13	14	16	12	9	11	10
21-23 LST	*	*	*	*	*	*	*	*	*	*	*	*	*
ALL HOURS	*	*	*	*	*	*	*	*	*	*	*	*	*
8. PERCENTAGE FREQUENCY OF OCCURRENCE (% FREQ) OF CEILING AND/OR VISIBILITY (CIG/VIS) < 1500/3 STATUE MILES (MI) (SOURCE NO. 1):													
00-02 LST	*	*	*	*	*	*	*	*	*	*	*	*	*
03-05 LST	*	*	*	*	*	*	*	*	*	*	*	*	*
06-08 LST	6	3	3	9	7	6	7	6	12	13	7	11	7
09-11 LST	4	1	1	9	4	3	4	2	5	3	3	6	4
12-14 LST	2	1	1	8	3	2	3	3	1	2	2	1	2
15-17 LST	3	1	1	12	6	5	4	4	3	3	1	2	4
18-20 LST	3	1	2	11	6	4	4	4	4	4	3	3	4
21-23 LST	*	*	*	*	*	*	*	*	*	*	*	*	*
ALL HOURS	*	*	*	*	*	*	*	*	*	*	*	*	*
9. % FREQ OF CIG/VIS < 200/0.5 MI (SOURCE NO. 1):													
00-02 LST	*	*	*	*	*	*	*	*	*	*	*	*	*
03-05 LST	*	*	*	*	*	*	*	*	*	*	*	*	*
06-08 LST	0	#	#	#	#	#	#	0	1	#	0	#	#
09-11 LST	0	0	0	#	0	#	0	0	0	#	0	#	#
12-14 LST	0	0	0	#	0	#	0	0	0	#	0	0	#
15-17 LST	#	0	0	#	0	#	0	0	#	#	0	0	#
18-20 LST	0	#	0	1	0	0	#	0	#	0	0	#	#
21-23 LST	*	*	*	*	*	*	*	*	*	*	*	*	*
ALL HOURS	*	*	*	*	*	*	*	*	*	*	*	*	*

MARKS * = DATA NOT AVAILABLE # = LESS THAN 0.5 DAY, OR 0.05 INCH, OR 0.5% MI = STAT. MILES
 \$ = % CALM > PVLG DRCTN @ = BASED ON AVAIL. DATA, 1 E., < 24 HRS/DAY OR < 12 MONTHS/YEAR
 SOURCE(S) 1 USAFETAC DATSAV FOR JAN 73 - DEC 85
 2 NATIONAL INTELLIGENCE SURVEY 12 - 18 YEARS

STATION: CHOLUTeca, HONDURAS

STATION #: 787240

ICAO ID: MHCH (USAFETAC, 1987)

LOCATION: 13°18'N, 87°11'W

ELEVATION (FEET): 164 LST = GMT: -6

PREPARED BY: USAFETAC/ECR 1985

PERIOD: VARIED(except items 6 & 7 JAN 73 - DEC 83)

SOURCE NO.	JAN	FEB	MAR	APR	MAY	JUN	JUL	AUG	SEP	OCT	NOV	DEC	ANN
1. TEMPERATURE (°F)													
EXTREME MAX	1	101	104	104	104	103	100	100	101	100	97	97	104
MEAN DLY MAX	1	92	94	96	95	92	89	91	92	89	88	90	92
MEAN	1	84	86	87	88	85	83	84	84	82	82	83	84
MEAN DLY MIN	1	76	77	79	81	79	77	77	77	75	76	76	77
EXTREME MIN	1	61	63	64	68	70	68	64	65	67	70	63	61
# DAYS ≥ 90	1	28	27	29	27	24	19	25	26	17	16	22	285
# DAYS ≤ 32	1	0	0	0	0	0	0	0	0	0	0	0	0
# DAYS ≤ 0	1	0	0	0	0	0	0	0	0	0	0	0	0
2. PRECIPITATION (INCHES)													
MAXIMUM	2	0.0	1.1	0.6	4.9	27.7	22.8	27.0	18.3	25.4	30.1	4.1	117.5
MEAN	2	0.0	0.2	0.4	1.9	11.0	13.9	7.5	9.2	16.6	13.9	1.9	76.8
MINIMUM	2	0.0	0.0	0.0	0.0	4.4	0.9	0.4	3.5	11.1	3.9	0.0	48.6
MAX 24 HR	2	0.0	0.5	0.2	2.3	5.1	4.1	2.7	3.2	3.8	3.6	1.3	5.1
# DAYS ≥ 0.01	2	0	#	1	3	12	17	12	16	23	15	3	103
# DAYS ≥ 0.5	2	*	*	*	*	*	*	*	*	*	*	*	*
3. MEAN RELATIVE HUMIDITY (%) / VAPOR PRESSURE (IN Hg) / DEWPOINT (°F)													
RH (07 LST)	1	70	66	68	71	83	84	79	78	89	87	77	77
RH (15 LST)	1	41	39	41	42	57	65	54	55	68	68	56	54
VAPOR PRESS.	1	.66	.67	.73	.77	.86	.87	.79	.82	.86	.85	.78	.78
DEWPOINT	1	66	66	69	70	74	74	71	72	74	74	71	71
4. SURFACE WINDS (16 PT/KNOTS) / 99.95% HIGHEST PRESSURE ALTITUDE (FEET)													
PVLG DRCTN	1	NNE	NNE	NNE\$	NNE\$	S\$	S\$	NNE	NNE\$	S\$	S\$	NNE\$	NNE\$
MEAN SPEED	1	8	8	6	6	3	3	5	5	3	3	5	5
MAX (PK GST)	1	38	38	30	32	24	31	30	25	30	33	30	38
PRESSURE ALT	1	450	450	500	400	400	500	350	450	500	400	400	500
5. MEAN CLOUD COVER (EIGHTHS) / THUNDERSTORMS / FOG/ BLOWING SAND (BNBD)													
CLD COVER	1	3	2	3	3	5	6	5	5	6	5	4	4
DAYS TSTMS	1	1	#	1	4	15	21	13	16	22	17	5	117
DAYS FOG < 7	1	#	1	1	1	4	5	2	5	9	7	3	39
DAYS BNBD < 7	1	*	*	*	*	*	*	*	*	*	*	*	*
6. PERCENTAGE FREQUENCY OF OCCURRENCE (% FREQ) OF THUNDERSTORMS:													
	JAN	FEB	MAR	APR	MAY	JUN	JUL	AUG	SEP	OCT	NOV	DEC	ANN
00-02 LST	0	0	1	4	22	31	6	11	22	23	3	1	10
03-05 LST	0	1	0	1	20	6	0	1	2	4	2	0	3
06-08 LST	0	#	#	0	2	1	#	#	#	0	0	0	#
09-11 LST	0	0	0	#	1	#	#	0	#	#	#	#	#
12-14 LST	#	0	0	1	5	8	2	5	10	5	2	#	3
15-17 LST	#	0	#	5	19	36	19	22	41	31	6	1	15
18-20 LST	2	0	2	4	32	47	28	36	55	41	10	1	22
21-23 LST	0	#	1	5	31	35	18	25	40	39	6	#	17
ALL HOURS	#	#	1	2	14	19	9	12	21	17	3	1	8
7. % FREQ OF RAIN AND/OR DRIZZLE:													
00-02 LST	0	0	2	2	22	15	5	6	17	24	2	2	8
03-05 LST	0	1	0	3	18	2	4	3	5	14	1	0	4
06-08 LST	0	1	1	1	4	3	1	2	5	3	2	#	2
09-11 LST	0	#	0	1	3	2	1	1	3	1	1	1	1
12-14 LST	#	0	#	#	5	5	1	4	7	4	1	#	2
15-17 LST	1	#	0	1	8	15	9	13	17	12	2	1	7
18-20 LST	1	#	2	1	18	28	13	18	31	21	5	2	12
21-23 LST	0	1	1	4	20	25	7	14	25	24	3	1	10
ALL HOURS	#	#	1	1	10	11	5	8	13	10	2	1	5
8. PERCENTAGE FREQUENCY OF OCCURRENCE (% FREQ) OF CEILING AND/OR VISIBILITY (CIG/VIS) < 1500/3 STATUE MILES (MI) (SOURCE NO. 1):													
00-02 LST	#	1	#	7	17	2	2	3	8	3	1	0	3
03-05 LST	0	0	1	4	21	2	0	5	7	3	0	0	3
06-08 LST	#	0	2	13	14	2	2	1	6	4	1	#	3
09-11 LST	0	0	#	10	13	#	0	1	4	1	#	#	2
12-14 LST	1	#	1	10	11	2	0	1	3	2	0	#	2
15-17 LST	0	#	1	10	12	5	1	3	4	3	1	#	3
18-20 LST	#	0	1	9	12	6	2	2	6	4	1	#	3
21-23 LST	#	0	1	8	12	2	1	2	6	2	1	0	3
ALL HOURS	#	#	1	10	13	3	1	2	5	3	1	#	3
9. % FREQ OF CIG/VIS < 200/0.5 MI (SOURCE NO. 1):													
00-02 LST	0	1	#	0	1	0	#	1	0	1	0	0	#
03-05 LST	0	0	1	0	0	1	0	0	0	0	0	0	#
06-08 LST	#	0	0	1	1	0	0	#	0	1	0	0	#
09-11 LST	0	0	#	0	0	0	0	#	0	#	0	0	#
12-14 LST	#	0	#	1	#	0	0	#	0	#	0	0	#
15-17 LST	0	#	0	#	0	#	#	0	#	#	0	0	#
18-20 LST	#	0	0	0	#	#	0	1	0	#	0	0	#
21-23 LST	0	0	1	0	0	0	0	#	#	#	0	0	#
ALL HOURS	#	#	#	#	#	#	#	#	#	#	0	#	#

REMARKS: * = DATA NOT AVAILABLE # = LESS THAN 0.5 DAY, OR 0.05 INCH, OR 0.5% MI = STAT MILES
 \$ = % CALM > PVLG DRCTN @ = BASED ON AVAIL. DATA, I.E., < 24 HRS/DAY OR < 12 MONTHS/YEAR
 SOURCE(S): 1 USAFETAC DATSAV FOR JAN 73 - DEC 83
 2 NATIONAL INTELLIGENCE SURVEY FOR VARIEDS

STATION: LA CEIBA, HONDURAS

STATION #: 787050

ICAO ID: MHLC (USAFETAC, 1987)

LOCATION: 15°44'N, 86°51'W

ELEVATION (FT.): 49 LST = GMT: -6

PREPARED BY: USAFETAC/ECR 1985

PERIOD: VARIED(except items 6 & 7 FEB 73 - DEC 83)

SOURCE NO.		JAN	FEB	MAR	APR	MAY	JUN	JUL	AUG	SEP	OCT	NOV	DEC	ANN
1. TEMPERATURE (°F)														
EXTREME MAX	1	92	91	99	94	95	95	94	94	94	91	90	88	99
MEAN DLY MAX	1	80	80	83	85	87	86	86	86	86	83	81	80	84
MEAN	1	76	77	80	82	84	84	83	84	82	80	77	77	81
MEAN DLY MIN	1	70	71	73	76	78	77	77	78	76	75	73	70	75
EXTREME MIN	1	61	57	59	63	68	68	66	71	64	67	63	61	57
# DAYS≥90	1	#	#	1	5	10	7	4	4	3	1	1	0	26
# DAYS≤32	1	0	0	0	0	0	0	0	0	0	0	0	0	0
# DAYS≤0	1	0	0	0	0	0	0	0	0	0	0	0	0	0
2. PRECIPITATION (INCHES)														
MAXIMUM	2	36.8	38.3	19.8	20.5	8.4	15.2	9.7	11.7	37.9	26.9	68.8	34.2	161.0
MEAN	2	13.3	8.4	4.7	4.3	3.4	4.7	5.1	5.8	8.5	15.3	22.9	16.3	112.8
MINIMUM	2	1.3	0.6	0.4	0.0	0.2	0.2	0.5	1.4	2.2	4.6	5.0	1.6	77.1
MAX 24 HR		*	*	*	*	*	*	*	*	*	*	*	*	*
# DAYS≥0.01		*	*	*	*	*	*	*	*	*	*	*	*	*
# DAYS≥0.5		*	*	*	*	*	*	*	*	*	*	*	*	*
3. MEAN RELATIVE HUMIDITY (%) / VAPOR PRESSURE (IN Hg) / DEWPOINT (°F)														
RH (07 LST)	1	92	90	73	82	78	83	85	81	81	90	91	91	84
RH (15 LST)	1	63	65	57	48	52	54	57	65	66	71	76	70	62
VAPOR PRESS.	@1	.68	.70	.62	.67	.74	.76	.79	.82	.80	.82	.81	.75	.76
DEWPOINT	@1	65	66	61	63	67	68	70	71	70	72	72	69	68
4. SURFACE WINDS (16 PT/KNOTS) / 99.95% HIGHEST PRESSURE ALTITUDE (FEET)														
PVLG DRCTN	@1	N\$	N\$	N\$	N\$	N\$	N\$	NE\$	NE\$	N\$	N\$	N\$	N\$	N\$
MEAN SPEED	@1	5	5	6	6	6	6	7	6	5	5	4	4	5
MAX (PK GST)	@1	20	25	30	33	26	25	30	28	40	20	40	35	40
PRESSURE ALT	@1	300	350	400	350	350	350	300	350	350	300	300	350	400
5. MEAN CLOUD COVER (EIGHTHS) / THUNDERSTORMS / FOG/ BLOWING SAND (BNBD)														
CLD COVER	@1	5	5	3	4	5	6	6	6	6	6	6	6	5
DAYS TSTMS	@1	#	1	#	1	4	6	6	7	7	2	1	1	38
DAYS FOG	@1	4	3	4	5	4	4	6	5	5	4	4	5	53
DAYS BNBD		*	*	*	*	*	*	*	*	*	*	*	*	*
6. PERCENTAGE FREQUENCY OF OCCURRENCE (% FREQ) OF THUNDERSTORMS:														
	JAN	FEB	MAR	APR	MAY	JUN	JUL	AUG	SEP	OCT	NOV	DEC	ANN	
00-02 LST	*	*	*	*	*	*	*	*	*	*	*	*	*	*
03-05 LST	*	*	*	*	*	*	*	*	*	*	*	*	*	*
06-08 LST	0	0	#	0	0	1	0	1	1	1	0	1	#	
09-11 LST	0	1	#	1	1	1	0	#	0	#	1	#	#	
12-14 LST	1	0	0	#	4	3	3	3	3	1	1	#	2	
15-17 LST	0	#	#	1	10	15	12	12	12	4	1	2	6	
18-20 LST	*	*	*	*	*	*	*	*	*	*	*	*	*	*
21-23 LST	*	*	*	*	*	*	*	*	*	*	*	*	*	*
ALL HOURS @	#	#	#	#	4	6	5	5	5	2	#	1	2	
7. % FREQ OF RAIN AND/OR DRIZZLE:														
00-02 LST	*	*	*	*	*	*	*	*	*	*	*	*	*	*
03-05 LST	*	*	*	*	*	*	*	*	*	*	*	*	*	*
06-08 LST	14	10	5	6	2	2	2	1	4	10	17	15	7	
09-11 LST	13	10	5	6	1	4	3	2	6	12	20	16	8	
12-14 LST	14	10	6	6	3	9	10	5	10	16	15	13	10	
15-17 LST	13	13	5	4	6	21	17	13	22	24	21	20	15	
18-20 LST	*	*	*	*	*	*	*	*	*	*	*	*	*	*
21-23 LST	*	*	*	*	*	*	*	*	*	*	*	*	*	*
ALL HOURS @	14	11	5	6	3	10	9	6	12	17	18	16	11	
8. PERCENTAGE FREQUENCY OF OCCURRENCE (% FREQ) OF CEILING AND/OR VISIBILITY (CIG/VIS) < 1500/3 STATUE MILES (MI) (SOURCE NO. 1):														
00-02 LST	*	*	*	*	*	*	*	*	*	*	*	*	*	*
03-05 LST	*	*	*	*	*	*	*	*	*	*	*	*	*	*
06-08 LST	8	4	3	4	7	3	0	1	1	3	6	8	4	
09-11 LST	6	4	3	8	9	5	0	0	2	4	7	8	4	
12-14 LST	7	5	4	7	9	6	2	1	2	4	6	7	5	
15-17 LST	5	6	4	6	9	6	2	2	3	7	6	9	5	
18-20 LST	*	*	*	*	*	*	*	*	*	*	*	*	*	*
21-23 LST	*	*	*	*	*	*	*	*	*	*	*	*	*	*
ALL HOURS @	6	5	4	7	8	5	1	1	2	5	6	8	5	
9. % FREQ OF CIG/VIS < 200/0.5 MI (SOURCE NO. 1):														
00-02 LST	*	*	*	*	*	*	*	*	*	*	*	*	*	*
03-05 LST	*	*	*	*	*	*	*	*	*	*	*	*	*	*
06-08 LST	#	#	0	0	0	#	0	#	0	0	1	1	#	
09-11 LST	0	0	0	1	0	0	0	0	0	#	#	#	#	
12-14 LST	#	0	0	1	0	0	0	0	#	#	1	1	#	
15-17 LST	#	0	0	0	#	#	#	0	#	1	0	1	#	
18-20 LST	*	*	*	*	*	*	*	*	*	*	*	*	*	*
21-23 LST	*	*	*	*	*	*	*	*	*	*	*	*	*	*
ALL HOURS @	#	#	0	#	#	#	#	#	#	#	1	1	#	

REMARKS: * = DATA NOT AVAILABLE # = LESS THAN 0.5 DAY, OR 0.05 INCH, OR 0.5% MI = STAT. MILES
 \$ = % CALM > PVLG DRCTN @ = BASED ON AVAIL. DATA, I.E., < 24 HRS/DAY OR < 12 MONTHS/YEAR
 SOURCE(S): 1. USAFETAC DATSAV POR FEB 73 - DEC 83
 2. NATIONAL INTELLIGENCE SURVEY 30-32 YEAR POR

STATION: PALMEROLA, HONDURAS STATION #: 697564 ICAO ID: MHCG (USAFETAC, 1987)
 LOCATION: 14°23'N, 87°37'W ELEVATION (FEET): 2070 LST = GMT: -6
 PREPARED BY: USAFETAC/ECR, 1986 PERIOD: SEP 83 - MAR 86

SOURCE NO.	JAN	FEB	MAR	APR	MAY	JUN	JUL	AUG	SEP	OCT	NOV	DEC	ANN
1. TEMPERATURE (°F)													
EXTREME MAX	1	93	97	100	102	100	97	95	95	95	93	91	102
MEAN DLY MAX	1	83	87	89	94	92	89	88	89	86	85	83	87
MEAN	1	72	75	76	80	80	79	78	77	76	74	74	76
MEAN DLY MIN	1	63	65	66	70	71	70	69	69	68	66	66	67
EXTREME MIN	1	52	55	55	57	63	66	66	64	63	64	54	52
# DAYS > 90	1	4	14	19	27	28	20	15	15	16	6	7	176
# DAYS < 32	1	0	0	0	0	0	0	0	0	0	0	0	0
# DAYS < 0	1	0	0	0	0	0	0	0	0	0	0	0	0
2. PRECIPITATION (INCHES)													
MAXIMUM	1	.47	.34	2.72	.69	5.07	7.03	6.18	6.01	9.37	5.02	.66	9.37
MEAN	1	*	*	*	*	*	*	*	*	*	*	*	*
MINIMUM	1	.24	.17	.14	.03	2.35	4.23	1.09	3.96	4.12	3.01	.28	.03
MAX 24 HR	1	.28	.17	2.72	.63	1.74	1.35	2.04	1.40	1.98	1.24	.29	2.72
# DAYS > 0.01	1	3	3	3	3	11	18	16	16	19	16	7	118
# DAYS > 0.5	1	*	*	*	*	*	*	*	*	*	*	*	*
3. MEAN RELATIVE HUMIDITY (%) / VAPOR PRESSURE (IN Hg) / DEWPOINT (°F)													
RH (06 LST)	1	91	83	81	81	85	90	88	91	94	91	92	88
RH (14 LST)	1	60	41	38	38	41	46	52	49	55	55	55	49
VAPOR PRESS.	1	.60	.53	.55	.63	.66	.67	.66	.67	.70	.69	.64	.63
DEWPOINT	1	63	60	60	65	66	66	66	67	68	67	65	65
4. SURFACE WINDS (16 PT/KNOTS) / 99.95% HIGHEST PRESSURE ALTITUDE (FEET)													
PVLG DRCTN	1	N	N	N	N	N	NNW	N	N	N	NNW	N	N
MEAN SPEED													
(PVLG DRCTN)	1	11	10	11	9	9	7	7	6	7	8	9	9
MEAN SPEED													
(ALL OBS)	1	9	7	8	6	6	5	6	5	5	6	7	7
MAX (PK GST)	1	41	33	35	27	35	20	30	24	30	21	28	41
PRESSURE ALT	1	2050	2200	2150	2150	2150	2100	2100	2100	2200	2150	2150	2200
5. MEAN CLOUD COVER (EIGHTHS) / THUNDERSTORMS / FOG / BLOWING SAND (BNBD)													
CLD COVER	1	4	3	3	4	5	5	5	5	4	4	4	4
DAYS TSTMS	1	0	1	1	3	14	10	10	12	13	7	1	72
DAYS FOG < 7	1	2	1	2	10	16	11	5	11	10	8	3	81
DAYS BNBD < 7	1	0	#	2	3	1	0	0	0	0	0	0	6
6. PERCENTAGE FREQUENCY OF OCCURRENCE (% FREQ) OF THUNDERSTORMS:													
	JAN	FEB	MAR	APR	MAY	JUN	JUL	AUG	SEP	OCT	NOV	DEC	ANN
00-02 LST	0	1	0	0	2	0	0	0	1	1	0	0	#
03-05 LST	0	0	0	0	1	0	0	0	2	0	0	0	#
06-08 LST	0	0	0	0	0	0	0	0	0	0	0	0	0
09-11 LST	0	0	0	0	0	0	0	0	0	0	0	0	0
12-14 LST	0	0	0	0	2	3	2	1	3	0	#	0	1
15-17 LST	0	0	1	1	12	15	10	10	10	1	#	1	5
18-20 LST	0	0	1	2	8	9	14	8	13	4	0	1	5
21-23 LST	0	1	2	3	7	2	0	2	8	5	0	0	3
ALL HOURS	0	#	1	1	4	4	3	3	5	1	#	#	2
7. % FREQ OF RAIN AND/OR DRIZZLE:													
00-02 LST	10	3	3	6	5	7	3	5	15	16	12	14	8
03-05 LST	5	3	6	5	3	4	1	1	5	4	3	7	4
06-08 LST	4	2	6	3	3	2	2	1	3	1	5	7	3
09-11 LST	#	2	2	0	1	1	1	1	3	3	3	3	2
12-14 LST	1	#	2	0	4	5	6	5	9	2	4	4	4
15-17 LST	2	1	3	2	12	18	15	16	19	7	5	4	9
18-20 LST	7	3	4	3	7	18	14	19	22	14	7	9	11
21-23 LST	12	6	5	5	10	16	16	16	28	22	9	14	13
ALL HOURS	5	3	4	3	6	9	7	8	13	9	6	8	7
8. PERCENTAGE FREQUENCY OF OCCURRENCE (% FREQ) OF CEILING AND/OR VISIBILITY													
(CIG/VIS) < 1500/3 STATUE MILES (MI) (SOURCE NO. 1):													
00-02 LST	0	0	0	0	0	0	0	2	6	8	0	0	1
03-05 LST	1	0	0	0	0	3	0	8	11	7	0	1	3
06-08 LST	1	1	0	2	0	3	3	11	11	6	3	3	4
09-11 LST	0	0	0	2	1	0	1	1	2	1	0	0	1
12-14 LST	0	0	0	2	2	0	1	1	0	0	0	0	1
15-17 LST	0	0	0	0	4	0	3	1	1	#	0	#	1
18-20 LST	0	0	0	0	2	0	0	0	0	2	0	1	#
21-23 LST	1	1	#	0	0	0	0	0	2	4	0	1	1
ALL HOURS	#	#	#	1	1	1	1	3	4	3	#	1	1
9. % FREQ OF CIG/VIS < 200/0.5 MI (SOURCE NO. 1):													
00-02 LST	0	0	0	0	0	0	0	0	1	0	0	0	#
03-05 LST	0	0	0	0	0	1	0	1	0	1	0	0	#
06-08 LST	0	#	0	0	0	1	0	0	1	1	0	2	#
09-11 LST	0	0	0	0	0	0	0	0	0	0	0	0	0
12-14 LST	0	0	0	0	0	0	0	0	0	0	0	0	0
15-17 LST	0	0	0	0	0	0	1	0	0	0	0	0	#
18-20 LST	0	0	0	0	0	0	0	0	0	0	0	0	0
21-23 LST	0	0	0	0	0	0	0	0	0	0	0	0	0
ALL HOURS	0	#	0	0	0	#	#	#	#	#	0	#	#

REMARKS * = DATA NOT AVAILABLE # = LESS THAN 0.5 DAY, OR 0.05 INCH, OR 0.5% MI = STAT MILES
 % = % CALM > PVLG DRCTN @ = BASED ON AVAIL DATA, I.E., < 24 HRS/DAY OR < 12 MONTHS/YEAR
 SOURCE(S) 1 USAFETAC DATSAV POR SEP 83 - MAR 86

STATION: SAN PEDRO SULA, HONDURAS
 LOCATION: 15°27'N, 87°56'W
 PREPARED BY: USAFETAC/ECR, 1986

STATION #: 787080 ICAO ID: MHLM (USAFETAC, 1987)
 ELEVATION (FT.): 249 LST = GMT: -6
 PERIOD: VARIED(except items 6 & 7 JAN 73 - DEC 85)

SOURCE NO.	JAN	FEB	MAR	APR	MAY	JUN	JUL	AUG	SEP	OCT	NOV	DEC	ANN
1. TEMPERATURE (°F)													
EXTREME MAX	2	95	102	104	106	106	104	97	99	99	93	91	106
MEAN DLY MAX	2	83	87	90	92	93	93	90	92	91	88	85	89
MEAN	2	74	76	79	81	82	83	81	82	81	79	77	79
MEAN DLY MIN	2	64	64	67	69	71	72	71	71	71	70	68	69
EXTREME MIN	2	51	47	52	55	54	61	66	65	65	59	55	47
# DAYS ≥ 90	2	5	10	21	27	29	26	26	28	28	16	11	231
# DAYS ≤ 32	1	0	0	0	0	0	0	0	0	0	0	0	0
# DAYS ≤ 0	1	0	0	0	0	0	0	0	0	0	0	0	0
2. PRECIPITATION (INCHES)													
MAXIMUM	2	7.3	7.5	6.3	14.6	9.8	12.0	14.9	10.1	15.2	17.9	14.9	75.0
MEAN	2	2.8	2.0	2.0	1.4	3.6	6.3	6.1	4.6	7.5	7.0	5.7	53.7
MINIMUM	2	.4	.2	0	0	.1	1.4	2.4	.7	1.4	.8	.2	14.0
MAX 24 HR	2	2.2	3.2	2.8	13.1	2.4	3.8	4.1	2.1	5.9	5.4	2.6	3.1
# DAYS ≥ 0.01	1	11	7	5	4	7	13	17	14	13	14	13	133
# DAYS ≥ 0.5	*	*	*	*	*	*	*	*	*	*	*	*	*
3. MEAN RELATIVE HUMIDITY (%) / VAPOR PRESSURE (IN Hg) / DEWPOINT (°F)													
RH (06 LST)	1	97	96	93	91	90	92	93	94	94	95	97	94
RH (14 LST)	1	70	66	58	55	57	59	62	61	61	65	67	63
VAPOR PRESS.	1	.75	.76	.80	.83	.87	.88	.86	.87	.87	.85	.86	.83
DEWPOINT	1	70	70	72	73	74	75	74	74	74	74	72	73
4. SURFACE WINDS (16 PT/KNOTS) / 99.95% HIGHEST PRESSURE ALTITUDE (FEET)													
PVLG DRCTN	1	\$N	\$N	\$N	\$N	\$N	\$N	\$N	\$N	\$N	\$N	\$N	\$N
MEAN SPEED													
(PVLG DRCTN)	1	8	8	9	9	9	8	9	8	8	8	8	8
MEAN SPEED													
(ALL OBS)	1	4	4	5	5	5	4	4	4	4	4	3	4
MAX (PK GST)		*	*	*	*	*	*	*	*	*	*	*	*
PRESSURE ALT	1	250	300	300	300	300	300	250	250	300	300	250	300
5. MEAN CLOUD COVER (EIGHTHS) / THUNDERSTORMS / FOG / BLOWING SAND (BNBD)													
CLD COVER	1	4	4	3	4	5	5	5	6	6	5	5	5
DAYS TSTMS	1	#	#	1	2	6	11	13	13	12	4	1	64
DAYS FOG < 7	1	3	3	2	4	4	2	3	2	1	3	2	31
DAYS BNBD < 7	1	0	0	0	0	0	#	#	#	0	#	0	#
6. PERCENTAGE FREQUENCY OF OCCURRENCE (% FREQ) OF THUNDERSTORMS:													
	JAN	FEB	MAR	APR	MAY	JUN	JUL	AUG	SEP	OCT	NOV	DEC	ANN
00-02 LST	0	0	#	1	6	6	3	5	8	3	3	1	3
03-05 LST	0	0	#	2	2	2	2	1	2	1	1	#	1
06-08 LST	0	0	#	1	#	#	#	0	0	0	#	0	#
09-11 LST	0	0	0	#	#	0	0	#	0	#	#	#	#
12-14 LST	#	0	#	#	#	2	2	2	2	1	#	#	1
15-17 LST	0	0	#	#	2	14	10	13	11	3	#	0	4
18-20 LST	#	0	1	0	7	17	20	17	13	4	1	1	7
21-23 LST	1	#	1	2	6	17	11	18	13	5	1	1	6
ALL HOURS	#	#	#	1	3	7	6	7	6	2	1	#	3
7. % FREQ OF RAIN AND/OR DRIZZLE:													
00-02 LST	8	8	6	5	7	8	7	5	11	8	8	11	8
03-05 LST	9	6	2	3	3	3	1	#	6	5	5	9	4
06-08 LST	9	6	3	3	2	3	1	1	2	6	9	10	5
09-11 LST	7	6	4	4	1	2	1	#	2	7	10	10	5
12-14 LST	6	3	2	2	1	1	3	3	3	8	9	10	4
15-17 LST	5	7	2	2	2	7	12	11	7	10	5	8	6
18-20 LST	8	6	2	2	4	16	17	17	12	11	10	11	10
21-23 LST	11	7	2	3	7	17	15	15	16	11	8	10	10
ALL HOURS	9	6	3	4	3	7	7	7	7	8	8	10	7
8. PERCENTAGE FREQUENCY OF OCCURRENCE (% FREQ) OF CEILING AND/OR VISIBILITY													
(CIG/VIS) < 1500/3 STATUE MILES (MI) (SOURCE NO. 1)													
00-02 LST	1	#	1	6	5	2	1	1	1	2	2	2	2
03-05 LST	4	3	2	7	7	1	1	1	1	3	2	5	3
06-08 LST	7	3	5	12	11	4	2	2	1	6	9	9	6
09-11 LST	6	5	6	12	9	2	1	#	1	5	3	5	5
12-14 LST	3	5	3	9	9	1	1	1	#	3	3	6	4
15-17 LST	4	4	3	7	10	4	1	1	1	3	2	3	4
18-20 LST	4	2	3	6	7	4	2	1	1	1	3	3	3
21-23 LST	5	2	1	7	4	3	1	1	1	1	2	2	3
ALL HOURS	4	3	3	8	9	3	1	1	1	3	3	4	4
9. % FREQ OF CIG/VIS < 200/0.5 MI (SOURCE NO. 1):													
00-02 LST	0	0	0	0	0	#	0	#	0	0	0	1	#
03-05 LST	#	0	0	0	0	0	0	0	#	0	0	#	#
06-08 LST	0	1	#	1	#	#	0	#	#	0	1	#	#
09-11 LST	#	#	#	1	0	0	0	0	0	#	#	#	#
12-14 LST	0	#	0	0	0	0	#	0	0	#	0	#	#
15-17 LST	0	#	0	0	0	#	0	#	0	0	#	#	#
18-20 LST	0	#	0	0	#	0	#	0	0	0	#	0	#
21-23 LST	1	0	0	#	0	#	0	#	0	0	0	0	#
ALL HOURS	#	#	#	#	#	#	#	#	#	#	#	#	#

REMARKS * = DATA NOT AVAILABLE # = LESS THAN 0.5 DAY, OR 0.05 INCH, OR 0.5% MI = STAT. MILES
 \$ = % CALM > PVLG DRCTN @ = BASED ON AVAIL DATA, I.E., < 24 HRS/DAY OR < 12 MONTHS/YEAR
 SOURCE(S) 1 USAFETAC DATSAV FOR JAN 73 - DEC 85
 2 NATIONAL INTELLIGENCE SURVEY, 18 -31 YEARS

STATION: SANTA ROSA DE COPAN, HOND. STATION #: 787170 ICAO ID: MHSR (USAFETAC, 1987)
 LOCATION: 14°47'N, 88°48'W ELEV. (FT.): 3530 LST = GMT: -6
 PREPARED BY: USAFETAC/ECR 1986 PERIOD: VARIED(except items 6 & 7 JAN 73 - DEC 85)

SOURCE NO.	JAN	FEB	MAR	APR	MAY	JUN	JUL	AUG	SEP	OCT	NOV	DEC	ANN
1. TEMPERATURE (°F)													
EXTREME MAX	2	89	93	93	94	95	90	90	88	85	84	85	95
MEAN DLY MAX	2	70	76	81	84	82	80	78	79	79	75	73	78
MEAN	2	62	65	68	72	71	71	70	71	71	68	66	69
MEAN DLY MIN	2	54	54	55	59	60	62	62	62	62	58	56	59
EXTREME MIN	2	39	38	37	42	40	47	52	54	55	48	44	37
# DAYS ≥ 90	2	0	#	2	5	3	#	#	0	0	0	0	10
# DAYS ≤ 32	1	0	0	0	0	0	0	0	0	0	0	0	0
# DAYS ≤ 0	1	0	0	0	0	0	0	0	0	0	0	0	0
2. PRECIPITATION (INCHES)													
MAXIMUM	2	4.3	3.2	3.1	5.2	12.3	18.7	15.9	17.3	22.2	19.2	7.0	90.5
MEAN	2	1.7	.9	1.1	1.8	5.2	12.3	10.1	7.9	12.5	6.8	3.4	66.2
MINIMUM	2	.3	0	0	0	1.3	5.6	4.9	3.1	5.1	1.8	1.0	46.5
MAX 24 HR	2	1.1	.8	1.7	2.6	4.8	5.6	3.9	3.4	3.5	3.4	1.8	5.6
# DAYS ≥ 0.01	2	12	6	5	5	11	20	22	19	22	19	16	171
# DAYS ≥ 0.5	*	*	*	*	*	*	*	*	*	*	*	*	*
3. MEAN RELATIVE HUMIDITY (%) / VAPOR PRESSURE (IN Hg) / DEWPOINT (°F)													
RH (04 LST)	1	98	97	95	92	95	96	96	98	99	98	97	96
RH (14 LST)	1	71	68	54	51	55	66	72	70	59	67	73	67
VAPOR PRESS.	1	.50	.51	.54	.58	.61	.64	.64	.64	.64	.61	.57	.60
DEWPOINT	1	60	59	61	62	64	65	65	65	65	64	62	63
4. SURFACE WINDS (16 PT/KNOTS) / 99.95% HIGHEST PRESSURE ALTITUDE (FEET)													
PVLG DRCTN	1	\$N	\$N	\$N	\$N	\$NW	\$N	\$N	\$N	\$N	\$N	\$N	\$N
MEAN SPEED													
(PVLG DRCTN)	1	6	6	7	6	6	6	6	6	5	6	6	6
MEAN SPEED													
(ALL OBS)	1	4	4	5	4	4	3	4	4	3	3	3	4
MAX (PK GST)		*	*	*	*	*	*	*	*	*	*	*	*
PRESSURE ALT	1	3500	3550	3650	3700	3600	3600	3600	3550	3600	3550	3550	3700
5. MEAN CLOUD COVER (EIGHTHS) / THUNDERSTORMS / FOG / BLOWING SAND (BNBD)													
CLD COVER	1	4	4	4	4	4	5	5	5	5	4	5	5
DAYS TSTMS	1	0	0	1	6	16	17	13	15	15	6	3	93
DAYS FOG < 7	1	19	16	18	20	20	15	17	18	15	19	16	210
DAYS BNBD < 7	1	#	0	0	#	0	0	#	0	0	0	#	#
6. PERCENTAGE FREQUENCY OF OCCURRENCE (% FREQ) OF THUNDERSTORMS:													
	JAN	FEB	MAR	APR	MAY	JUN	JUL	AUG	SEP	OCT	NOV	DEC	ANN
00-02 LST	0	0	0	1	4	2	3	2	6	1	0	0	2
03-05 LST	0	0	0	0	0	0	0	0	0	0	0	0	0
06-08 LST	0	0	0	0	0	0	0	#	1	0	0	0	#
09-11 LST	0	0	0	1	0	0	#	0	0	0	0	0	#
12-14 LST	0	0	0	0	4	6	3	4	4	1	#	0	2
15-17 LST	0	0	2	7	24	29	18	16	31	8	3	1	12
18-20 LST	0	0	2	5	25	24	23	20	27	6	5	2	12
21-23 LST	0	0	1	2	11	8	8	12	12	1	#	1	5
ALL HOURS	0	0	1	2	9	8	7	7	10	2	1	1	4
7. % FREQ OF RAIN AND/OR DRIZZLE:													
00-02 LST	12	9	1	2	3	11	16	14	22	17	14	20	12
03-05 LST	12	9	3	0	1	5	4	0	9	6	6	20	6
06-08 LST	17	10	2	3	0	2	2	1	5	9	11	15	6
09-11 LST	19	15	1	3	1	2	1	#	3	9	11	13	6
12-14 LST	9	10	3	2	7	4	2	2	5	6	8	12	6
15-17 LST	12	10	2	5	13	16	11	7	16	10	13	13	11
18-20 LST	12	9	2	4	9	26	20	16	25	17	15	18	14
21-23 LST	16	8	2	4	4	26	23	29	30	14	15	15	16
ALL HOURS	14	10	2	3	5	12	10	9	14	12	12	16	10
8. PERCENTAGE FREQUENCY OF OCCURRENCE (% FREQ) OF CEILING AND/OR VISIBILITY (CIG/VIS) < 1500/3 STATUE MILES (MI) (SOURCE NO. 1):													
00-02 LST	54	42	41	75	81	48	30	37	41	40	57	53	53
03-05 LST	74	61	61	78	92	67	36	44	70	45	68	61	64
06-08 LST	69	59	48	67	79	54	36	31	41	52	49	58	54
09-11 LST	31	19	16	43	44	6	3	1	5	16	15	21	18
12-14 LST	16	10	12	35	34	2	1	1	3	4	10	14	12
15-17 LST	18	12	13	46	51	10	6	4	7	10	12	15	17
18-20 LST	19	19	19	47	65	21	15	14	22	21	22	25	26
21-23 LST	39	33	33	58	75	38	30	30	39	27	39	31	39
ALL HOURS	40	32	30	56	65	30	20	19	29	27	23	35	34
9. % FREQ OF CIG/VIS < 200/0.5 MI (SOURCE NO. 1):													
00-02 LST	11	8	3	13	18	4	1	2	1	6	14	1	7
03-05 LST	32	14	14	28	39	18	2	12	16	16	19	16	19
06-08 LST	29	17	13	17	26	12	6	4	5	11	16	16	14
09-11 LST	9	1	2	5	9	0	#	0	0	1	2	2	3
12-14 LST	3	2	#	4	8	0	0	0	0	1	1	#	2
15-17 LST	6	3	0	5	10	#	1	#	1	#	3	2	3
18-20 LST	6	3	1	5	14	2	#	1	2	3	3	3	4
21-23 LST	11	8	2	6	21	1	1	2	2	4	5	4	6
ALL HOURS	13	7	4	12	18	5	1	3	3	5	8	6	7

REMARKS * = DATA NOT AVAILABLE # = LESS THAN 0.5 DAY, OR 0.05 INCH, OR 0.5% MI = STAT. MILES
 \$ = % CALM > PVLG DRCTN 0 = BASED ON AVAIL. DATA, I.E., < 24 HRS/DAY OR < 12 MONTHS/YEAR
 SOURCE(S) 1 USAFETAC DATSAV POR JAN 73 - DEC 85
 2 NATIONAL INTELLIGENCE SURVEY 16-29 YEARS

STATION: SWAN ISLAND, HONDURAS STATION #: 785010 ICAO ID: MHIC (USAFETAC, 1987)
 LOCATION: 17°24'N, 83°56'W ELEVATION (FT.): 40 LST = GMT: -5
 PREPARED BY: USAFETAC/ECR, 1986 PERIOD: VARIED(except items 6 & 7 JAN 73 - MAR 82)

SOURCE NO.	JAN	FEB	MAR	APR	MAY	JUN	JUL	AUG	SEP	OCT	NOV	DEC	ANN
1. TEMPERATURE (°F)													
EXTREME MAX	2	88	87	89	90	92	92	93	93	92	88	88	93
MEAN DLY MAX	1	81	81	82	84	84	85	86	85	84	83	82	84
MEAN	1	78	78	79	80	82	82	82	82	81	80	79	80
MEAN DLY MIN	1	76	75	77	78	80	80	80	80	79	78	77	78
EXTREME MIN	2	64	66	67	68	68	70	69	70	70	70	64	64
# DAYS ≥ 90	1	0	0	0	#	#	#	1	1	#	0	0	2
# DAYS ≤ 32	1	0	0	0	0	0	0	0	0	0	0	0	0
# DAYS ≤ 0	1	0	0	0	0	0	0	0	0	0	0	0	0
2. PRECIPITATION (INCHES)													
MAXIMUM		*	*	*	*	*	*	*	*	*	*	*	*
MEAN	2	3.8	1.2	.6	.9	3.4	7.4	3.8	4.1	6.2	9.7	8.9	55.7
MINIMUM		*	*	*	*	*	*	*	*	*	*	*	*
MAX 24 HR	2	4.4	2.1	2.5	3.0	3.9	5.1	4.9	7.6	4.3	10.8	9.0	10.8
# DAYS ≥ 0.01	2	13	8	6	5	7	15	12	13	13	17	16	141
# DAYS ≥ 0.5		*	*	*	*	*	*	*	*	*	*	*	*
3. MEAN RELATIVE HUMIDITY (%) / VAPOR PRESSURE (IN Hg) / DEWPOINT (°F)													
RH (07 LST)	1	77	75	78	76	78	79	80	80	82	81	79	79
RH (13 LST)	1	69	66	67	66	70	71	70	70	72	74	73	70
VAPOR PRESS.	1	.74	.71	.77	.78	.85	.87	.87	.88	.89	.87	.82	.82
DEWPOINT	1	69	68	70	71	74	74	74	75	75	74	73	72
4. SURFACE WINDS (16 PT/KNOTS) / 99.95% HIGHEST PRESSURE ALTITUDE (FEET)													
PVLG DRCTN	1	E	E	E	E	ESE	E	E	E	E	E	E	E
MEAN SPEED													
(PVLG DRCTN)	1	9	10	10	11	13	11	10	10	9	8	9	10
MEAN SPEED													
(ALL OBS)	1	10	10	12	11	12	11	10	9	10	8	10	10
MAX (PK GST)		*	*	*	*	*	*	*	*	*	*	*	*
PRESSURE ALT	1	150	100	150	200	250	200	50	200	450	300	200	450
5. MEAN CLOUD COVER (EIGHTHS) / THUNDERSTORMS / FOG/ BLOWING SAND (BNBD)													
CLD COVER	1	4	3	3	4	5	5	5	6	5	5	4	4
DAYS TSTMS	1	#	0	0	0	2	3	5	5	4	3	1	28
DAYS FOG < 7	1	0	0	0	0	0	0	0	0	0	0	0	0
DAYS BNBD < 7	1	0	0	0	0	0	0	0	0	0	0	0	0
6. PERCENTAGE FREQUENCY OF OCCURRENCE (% FREQ) OF THUNDERSTORMS:													
	JAN	FEB	MAR	APR	MAY	JUN	JUL	AUG	SEP	OCT	NOV	DEC	ANN
00-02 LST	0	0	0	0	1	0	1	3	2	1	1	0	1
03-05 LST	0	*	*	*	*	*	*	*	*	*	*	*	*
06-08 LST	0	0	0	0	1	2	1	1	2	1	0	0	1
09-11 LST	*	*	*	*	*	*	*	*	*	*	*	*	*
12-14 LST	0	0	0	0	1	1	1	1	2	1	1	0	1
15-17 LST	*	*	*	*	*	*	*	*	*	*	*	*	*
18-20 LST	#	0	0	0	1	1	0	1	3	1	1	1	1
21-23 LST	*	*	*	*	*	*	*	*	*	*	*	*	*
ALL HOURS	*	*	*	*	*	*	*	*	*	*	*	*	*
7. % FREQ OF RAIN AND/OR DRIZZLE:													
00-02 LST	2	2	1	1	1	5	1	1	11	12	3	4	4
03-05 LST	*	*	*	*	*	*	*	*	*	*	*	*	*
06-08 LST	0	3	0	2	5	7	5	4	8	12	8	5	5
09-11 LST	*	*	*	*	*	*	*	*	*	*	*	*	*
12-14 LST	3	2	1	1	5	7	5	4	8	7	9	4	5
15-17 LST	*	*	*	*	*	*	*	*	*	*	*	*	*
18-20 LST	4	3	3	3	4	6	3	9	9	13	9	5	6
21-23 LST	*	*	*	*	*	*	*	*	*	*	*	*	*
ALL HOURS	*	*	*	*	*	*	*	*	*	*	*	*	*
8. PERCENTAGE FREQUENCY OF OCCURRENCE (% FREQ) OF CEILING AND/OR VISIBILITY (CIG/VIS) < 1500/3 STATUE MILES (MI) (SOURCE NO. 1):													
00-02 LST	2	2	1	1	2	3	1	1	5	4	1	3	2
03-05 LST	*	*	*	*	*	*	*	*	*	*	*	*	*
06-08 LST	4	2	2	2	3	4	2	4	6	7	5	6	1
09-11 LST	*	*	*	*	*	*	*	*	*	*	*	*	*
12-14 LST	2	1	2	1	3	3	3	2	4	5	6	3	3
15-17 LST	*	*	*	*	*	*	*	*	*	*	*	*	*
18-20 LST	3	2	2	2	3	3	3	5	8	5	4	3	4
21-23 LST	*	*	*	*	*	*	*	*	*	*	*	*	*
ALL HOURS	*	*	*	*	*	*	*	*	*	*	*	*	*
9. % FREQ OF CIG/VIS < 200/0.5 MI (SOURCE NO. 1):													
00-02 LST	0	0	0	0	0	0	0	0	0	0	0	0	0
03-05 LST	*	*	*	*	*	*	*	*	*	*	*	*	*
06-08 LST	0	0	0	0	0	0	0	0	0	0	0	0	0
09-11 LST	*	*	*	*	*	*	*	*	*	*	*	*	*
12-14 LST	0	0	0	1	0	0	0	0	0	1	0	#	*
15-17 LST	*	*	*	*	*	*	*	*	*	*	*	*	*
18-20 LST	0	0	0	0	0	0	0	0	#	0	0	0	#
21-23 LST	*	*	*	*	*	*	*	*	*	*	*	*	*
ALL HOURS	*	*	*	*	*	*	*	*	*	*	*	*	*

REMARKS: * = DATA NOT AVAILABLE # = LESS THAN 0.5 DAY, OR 0.05 INCH, OR 0.5% MI = STAT. MILES
 \$ = % CALM > PVLG DRCTN @ = BASED ON AVAIL. DATA, I.E., < 24 HRS/DAY OR < 12 MONTHS/YEAR
 SOURCE(S) 1 USAFETAC DATSAV POR JAN 73 - MAR 82
 2 NATIONAL INTELLIGENCE SURVEY UP TO 25 YR POR

STATION: TEGUCIGALPA, HONDURAS STATION #: 787200 ICAO ID: MHTG (USAFETAC, 1987)
 LOCATION: 14°04'N, 87°13'W ELEVATION (FT.): 3304 LST = GMT: -6
 PREPARED BY: USAFETAC/ECR 1986 PERIOD: VARIED(except items 6 & 7 JAN 73 - SEP 85)

SOURCE: NO.	JAN	FEB	MAR	APR	MAY	JUN	JUL	AUG	SEP	OCT	NOV	DEC	ANN
1. TEMPERATURE (°F)													
EXTREME MAX	2	89	91	93	96	94	89	91	90	88	91	88	96
MEAN DLY MAX	2	77	80	84	86	85	81	83	83	80	78	77	81
MEAN	1	67	69	73	75	75	73	73	72	71	69	67	71
MEAN DLY MIN	2	57	57	58	62	64	65	64	63	63	60	58	61
EXTREME MIN	2	39	43	46	48	49	56	55	54	52	48	47	39
# DAYS ≥ 90	2	0	#	5	7	6	1	0	#	1	0	#	21
# DAYS ≤ 32	2	0	0	0	0	0	0	0	0	0	0	0	0
# DAYS ≤ 0	2	0	0	0	0	0	0	0	0	0	0	0	0
2. PRECIPITATION (INCHES)													
MAXIMUM	2	1.8	.4	1.9	5.6	12.2	14.0	11.8	13.3	16.1	6.0	6.6	50.3
MEAN	2	.5	.2	.4	1.1	5.7	6.3	3.5	3.9	7.2	5.4	1.7	36.4
MINIMUM	2	0	0	0	#	2.2	.1	1.2	1.4	3.0	1.1	0	27.0
MAX 24 HR	2	.8	.3	1.0	3.7	4.5	2.5	2.0	2.0	3.0	3.5	2.0	4.5
# DAYS ≥ 0.01	2	4	2	2	4	11	17	15	14	19	16	9	119
# DAYS ≥ 0.5	2	*	*	*	*	*	*	*	*	*	*	*	*
3. MEAN RELATIVE HUMIDITY (%) / VAPOR PRESSURE (IN Hg) / DEWPOINT (°F)													
RH (06 LST)	1	87	85	82	82	86	90	88	89	91	89	88	87
RH (14 LST)	1	49	42	37	38	45	55	51	50	55	56	53	49
VAPOR PRESS.	1	.47	.46	.47	.51	.58	.60	.57	.58	.60	.58	.54	.54
DEWPOINT	1	56	56	56	59	62	63	62	62	63	63	60	60
4. SURFACE WINDS (16 PT/KNOTS) / 99.95% HIGHEST PRESSURE ALTITUDE (FEET)													
PVLG DRCTN	1	NNW	N	\$N	\$N	\$N	\$N	\$N	\$N	\$N	NNW	NNW	\$N
MEAN SPEED													
(PVLG DRCTN)	1	10	9	8	8	7	6	7	7	7	8	10	8
MEAN SPEED													
(ALL OBS)	1	7	7	6	6	5	5	6	5	4	5	7	6
MAX (PK GST)		*	*	*	*	*	*	*	*	*	*	*	*
PRESSURE ALT		*	*	*	*	*	*	*	*	*	*	*	*
5. MEAN CLOUD COVER (EIGHTHS) / THUNDERSTORMS / FOG / BLOWING SAND (BNBD)													
CLD COVER	1	5	4	4	4	6	6	6	6	6	5	5	5
DAYS TSTMS	2	0	0	1	3	9	12	7	7	11	6	1	57
DAYS FOG < 7	1	5	3	6	9	10	11	8	10	14	11	9	104
DAYS BNBD < 7	1	0	0	0	0	0	0	0	0	0	0	0	0
6. PERCENTAGE FREQUENCY OF OCCURRENCE (% FREQ) OF THUNDERSTORMS:													
	JAN	FEB	MAR	APR	MAY	JUN	JUL	AUG	SEP	OCT	NOV	DEC	ANN
00-02 LST	0	0	#	1	3	2	#	#	1	#	0	0	1
03-05 LST	0	0	0	#	#	#	0	#	#	0	0	0	#
06-08 LST	0	0	0	#	#	0	#	#	#	#	0	0	#
09-11 LST	0	0	0	0	0	0	0	#	0	0	0	0	#
12-14 LST	0	0	#	1	5	5	1	4	1	1	1	0	2
15-17 LST	0	0	1	4	13	13	7	8	10	3	2	0	5
18-20 LST	0	0	1	4	13	13	8	6	14	4	1	0	5
21-23 LST	0	0	#	3	9	5	2	3	4	2	0	0	2
ALL HOURS	0	0	#	2	5	5	2	2	4	1	1	0	2
7. % FREQ OF RAIN AND/OR DRIZZLE:													
00-02 LST	7	3	2	3	13	17	9	7	16	13	7	7	9
03-05 LST	6	2	1	2	6	10	6	5	8	8	4	6	5
06-08 LST	4	3	1	2	3	4	6	4	4	5	4	5	4
09-11 LST	3	1	1	#	1	3	3	3	3	2	2	4	2
12-14 LST	2	1	1	1	5	10	5	4	7	4	3	2	4
15-17 LST	2	1	2	2	10	18	11	11	16	12	7	4	8
18-20 LST	4	2	2	3	13	26	18	17	27	21	10	6	12
21-23 LST	4	2	2	6	17	25	13	14	29	22	9	7	13
ALL HOURS	4	2	2	2	9	14	9	8	14	11	6	5	7
8. PERCENTAGE FREQUENCY OF OCCURRENCE (% FREQ) OF CEILING AND/OR VISIBILITY (CIG/VIS) < 1500/3 STATUE MILES (MI) (SOURCE NO. 1):													
00-02 LST	2	#	1	10	5	3	2	1	3	3	3	2	3
03-05 LST	2	2	1	9	5	3	3	2	5	5	4	3	4
06-08 LST	4	4	6	26	24	10	7	9	17	12	9	9	11
09-11 LST	3	1	2	19	14	2	1	2	3	2	2	3	5
12-14 LST	1	1	2	9	9	3	2	2	3	1	1	2	3
15-17 LST	1	#	1	11	9	7	3	3	5	3	3	2	4
18-20 LST	1	1	2	13	9	5	3	3	4	4	2	2	4
21-23 LST	1	1	1	8	7	2	1	1	4	2	2	1	3
ALL HOURS	2	1	2	13	10	4	3	3	6	4	3	3	5
9. % FREQ OF CIG/VIS < 200/0.5 MI (SOURCE NO. 1):													
00-02 LST	0	0	0	1	#	0	0	#	0	0	1	0	#
03-05 LST	0	0	0	#	0	#	0	0	1	#	#	0	#
06-08 LST	#	#	0	2	1	#	#	#	1	1	2	1	1
09-11 LST	0	0	0	1	1	0	#	0	#	0	0	0	#
12-14 LST	0	0	0	1	#	#	#	#	0	0	#	#	#
15-17 LST	0	#	0	#	1	#	#	#	0	0	#	0	#
18-20 LST	#	0	#	1	1	0	0	#	#	#	0	#	#
21-23 LST	0	0	0	0	#	0	#	#	#	0	#	0	#
ALL HOURS	#	#	#	1	#	#	#	#	#	1	#	#	#

REMARKS: * = DATA NOT AVAILABLE # = LESS THAN 0.5 DAY, OR 0.05 INCH, OR 0.5% MI = STAT. MILES
 \$ = % CALM > PVLG DRCTN @ = BASED ON AVAIL. DATA, I.E., < 24 HRS/DAY OR < 12 MONTHS/YEAR
 SOURCE(S): 1. USAFETAC DATSAV FOR JAN 73 - DEC 85
 2. NATIONAL INTELLIGENCE SURVEY (9 - 23 YEARS POR)

STATION: ACAJUTLA, EL SALVADOR
 LOCATION: 13°36'N, 89°50'W
 PREPARED BY: USAFETAC/ECR 1985

STATION #: 786500 ICAO ID: MSAC (USAFETAC, 1987)
 ELEVATION (FT.): 33 LST = GMT: -6
 PERIOD: VARIED(except items 6 & 7 JAN 73 - DEC 83)

SOURCE NO.		JAN	FEB	MAR	APR	MAY	JUN	JUL	AUG	SEP	OCT	NOV	DEC	ANN
1. TEMPERATURE (°F)														
EXTREME MAX	2	97	98	99	99	102	95	95	98	102	97	95	97	102
MEAN DLY MAX	2	89	89	90	90	90	88	89	89	88	89	89	89	89
MEAN	2	80	80	82	83	83	81	81	81	81	81	81	80	81
MEAN DLY MIN	2	70	71	73	75	75	74	73	73	73	73	72	70	73
EXTREME MIN	2	59	62	64	67	66	69	68	68	62	69	66	64	59
# DAYS≥90	2	16	17	29	28	25	14	23	23	17	19	23	23	256
# DAYS≤32	1	0	0	0	0	0	0	0	0	0	0	0	0	0
# DAYS≤0	1	0	0	0	0	0	0	0	0	0	0	0	0	0
2. PRECIPITATION (INCHES)														
MAXIMUM	2	0.9	1.3	1.7	9.8	15.8	29.1	21.3	19.5	27.0	28.8	15.6	1.5	92.4
MEAN	2	#	#	0.2	2.0	6.8	11.9	10.9	10.4	12.6	10.7	1.7	0.2	67.3
MINIMUM	2	0.0	0.0	0.0	0.0	0.7	4.6	2.2	3.5	2.5	1.1	0.0	0.0	38.3
MAX 24 HR	2	0.1	1.2	1.3	3.9	3.2	4.0	4.0	3.6	6.9	6.2	3.6	0.8	6.9
# DAYS>0.01	2	#	1	#	3	9	15	18	17	16	11	3	1	94
# DAYS≥0.5		*	*	*	*	*	*	*	*	*	*	*	*	*
3. MEAN RELATIVE HUMIDITY (%) / VAPOR PRESSURE (IN Hg) / DEWPOINT (°F)														
RH (02 LST)	1	74	75	79	79	87	90	88	88	90	88	82	79	83
RH (10 LST)	1	54	55	61	61	71	73	68	71	75	70	61	57	65
VAPOR PRESS.	1	.72	.72	.81	.85	.90	.88	.87	.88	.88	.86	.80	.75	.83
DEWPOINT	1	68	68	72	74	75	75	74	75	75	74	72	70	72
4. SURFACE WINDS (16 PT/KNOTS) / 99.95% HIGHEST PRESSURE ALTITUDE (FEET)														
PVLG DRCTN	1	S	S	S	S	S	S	S	N	S	N	N	N	S
MEAN SPEED	1	5	6	6	5	5	5	5	5	5	5	5	5	5
MAX (PK GST)	1	30	28	30	23	35	28	31	30	45	30	34	25	45
PRESSURE ALT	1	350	350	350	400	350	400	350	400	350	350	400	400	400
5. MEAN CLOUD COVER (EIGHTHS) / THUNDERSTORMS / FOG / BLOWING SAND (BNBD)														
CLD COVER	1	2	2	3	4	5	6	6	6	6	5	4	3	4
DAYS TSTMS	1	1	#	2	5	16	19	19	21	18	15	4	2	122
DAYS FOG	1	1	#	1	1	#	1	1	1	#	1	#	1	6
DAYS BNBD		*	*	*	*	*	*	*	*	*	*	*	*	*

6. PERCENTAGE FREQUENCY OF OCCURRENCE (% FREQ) OF THUNDERSTORMS:

	JAN	FEB	MAR	APR	MAY	JUN	JUL	AUG	SEP	OCT	NOV	DEC	ANN
00-02 LST	1	#	1	3	12	15	12	15	12	10	1	1	7
03-05 LST	0	0	0	2	6	8	4	6	4	3	1	0	3
06-08 LST	0	0	0	#	2	1	1	1	1	2	#	#	1
09-11 LST	0	0	#	0	#	1	#	0	1	#	0	0	#
12-14 LST	0	0	#	#	3	4	2	4	7	7	1	#	2
15-17 LST	0	0	#	#	3	5	7	7	7	8	2	1	3
18-20 LST	#	0	1	1	8	10	12	13	10	6	2	#	5
21-23 LST	#	0	1	4	11	15	22	22	13	9	2	1	8
ALL HOURS	#	#	#	1	5	7	7	8	7	5	1	#	3

7. % FREQ OF RAIN AND/OR DRIZZLE:

	JAN	FEB	MAR	APR	MAY	JUN	JUL	AUG	SEP	OCT	NOV	DEC	ANN
00-02 LST	1	0	1	3	13	27	22	24	25	13	2	#	11
03-05 LST	#	0	#	4	9	23	8	15	16	9	2	1	7
06-08 LST	0	0	#	1	5	11	2	6	11	4	1	#	3
09-11 LST	0	0	#	1	3	6	1	2	7	1	#	#	2
12-14 LST	#	#	1	#	2	4	1	2	7	3	#	0	2
15-17 LST	0	#	1	1	4	7	4	4	9	8	1	1	3
18-20 LST	#	0	1	2	6	12	9	12	13	8	3	1	6
21-23 LST	1	0	2	4	11	20	26	24	23	12	3	1	11
ALL HOURS	#	#	1	2	6	13	8	10	13	7	1	#	5

8. PERCENTAGE FREQUENCY OF OCCURRENCE (% FREQ) OF CEILING AND/OR VISIBILITY (CIG/VIS) < 1500/3 STATUE MILES (MI) (SOURCE NO. 1):

	JAN	FEB	MAR	APR	MAY	JUN	JUL	AUG	SEP	OCT	NOV	DEC	ANN
00-02 LST	#	#	#	6	10	4	2	3	1	1	#	0	2
03-05 LST	#	#	0	5	16	4	1	1	2	1	1	#	2
06-08 LST	#	#	1	8	6	1	#	1	1	#	0	#	2
09-11 LST	0	#	#	5	8	2	0	0	1	#	#	#	2
12-14 LST	#	#	#	3	6	1	1	0	3	#	0	#	1
15-17 LST	#	#	#	3	5	2	1	1	3	#	0	#	1
18-20 LST	1	#	#	5	5	1	1	1	2	1	#	0	2
21-23 LST	0	0	#	7	9	4	2	3	3	1	#	#	3
ALL HOURS	#	#	#	5	7	2	1	1	2	#	#	#	2

9. % FREQ OF CIG/VIS < 200/0.5 MI (SOURCE NO. 1):

	JAN	FEB	MAR	APR	MAY	JUN	JUL	AUG	SEP	OCT	NOV	DEC	ANN
00-02 LST	0	#	0	0	#	#	#	0	0	#	0	0	#
03-05 LST	0	#	0	0	0	0	1	0	0	0	0	0	#
06-08 LST	0	#	#	#	#	1	#	#	#	#	0	0	#
09-11 LST	0	0	0	0	#	#	0	0	0	0	#	#	#
12-14 LST	#	0	0	0	#	0	0	0	1	0	0	0	#
15-17 LST	0	#	#	0	0	#	#	0	#	0	0	0	#
18-20 LST	1	0	0	0	#	#	0	#	1	#	0	0	#
21-23 LST	0	0	0	0	0	#	#	0	#	#	#	0	#
ALL HOURS	#	#	#	#	#	#	#	#	#	#	#	#	#

REMARKS: * = DATA NOT AVAILABLE # = LESS THAN 0.5 DAY, OR 0.05 INCH, OR 0.5% MI = STAT MILES
 % = % CALM > PVLG DRCTN @ = BASED ON AVAIL. DATA, I.E., < 24 HRS/DAY OR < 12 MONTHS/YEAR
 SOURCE(S): 1. USAFETAC DATSAV POR JAN 73 - DEC 83
 2. NATIONAL INTELLIGENCE SURVEY POR VARIED

STATION: SAN SALVADOR, EL SALVADOR

STATION #: 786630

ICAO ID: MSSS (USAFETAC, 1987)

LOCATION: 13°43'N, 89°12'W

ELEVATION (FT.): 2020 LST = GMT: -6

PREPARED BY: USAFETAC/ECR 1986

PERIOD: VARIED(except items 6 & 7 JAN 73 - DEC 85)

SOURCE NO.	JAN	FEB	MAR	APR	MAY	JUN	JUL	AUG	SEP	OCT	NOV	DEC	ANN
1. TEMPERATURE (°F)													
EXTREME MAX	2	101	103	105	104	103	98	98	98	99	101	102	101
MEAN DLY MAX	2	90	92	94	93	91	87	89	89	87	87	87	89
MEAN	2	75	76	78	79	79	77	77	78	77	76	75	75
MEAN DLY MIN	2	60	60	62	65	67	66	65	66	66	65	63	61
EXTREME MIN	2	45	49	45	54	58	56	58	60	53	53	49	47
# DAYS ≥ 90	3	16	20	27	24	19	6	13	13	12	6	6	13
# DAYS ≤ 32	3	0	0	0	0	0	0	0	0	0	0	0	0
# DAYS ≤ 0	3	0	0	0	0	0	0	0	0	0	0	0	0
2. PRECIPITATION (INCHES)													
MAXIMUM	2	1.6	2.3	3.2	20.1	15.0	24.3	19.4	18.5	24.1	19.9	5.1	3.8
MEAN	2	.2	.2	.4	2.1	7.4	12.7	12.5	11.7	12.5	9.0	1.6	.4
MINIMUM	2	0	0	0	0	2.2	5.5	4.6	3.2	5.8	1.0	0	0
MAX 24 HR	2	.7	1.1	1.3	3.5	4.7	8.1	3.7	6.5	6.9	6.7	2.1	1.8
# DAYS ≥ 0.004	2	1	1	1	5	13	20	22	21	21	16	5	1
# DAYS ≥ 0.5													
3. MEAN RELATIVE HUMIDITY (%) / VAPOR PRESSURE (IN Hg) / DEWPOINT (°F)													
RH (06 LST)	1	84	83	85	85	93	95	93	95	95	93	88	85
RH (14 LST)	1	43	40	46	48	63	67	61	63	70	66	55	49
VAPOR PRESS.	1	.54	.53	.61	.65	.73	.73	.71	.72	.73	.71	.63	.58
DEWPOINT	1	60	60	63	65	69	69	68	69	69	68	65	62
4. SURFACE WINDS (16 PT/KNOTS) / 99.95% HIGHEST PRESSURE ALTITUDE (FEET)													
PVLG DRCTN	1	N	N	S	S	S	S	N	N	N	N	N	N
MEAN SPEED													
(PVLG DRCTN)	1	8	8	8	8	7	5	5	4	4	5	7	7
MEAN SPEED													
(ALL OBS)	1	7	7	6	6	5	4	4	4	4	5	6	6
MAX (PK GST)	1	50	50	35	40	25	30	25	35	30	30	35	40
PRESSURE ALT	1	2200	2200	2250	2350	2250	2200	2150	2200	2250	2200	2200	2250
5. MEAN CLOUD COVER (EIGHTHS) / THUNDERSTORMS / FOG/ BLOWING SAND (BNBD)													
CLD COVER	1	3	3	3	4	5	6	5	5	6	5	4	3
DAYS TSTMS	1	1	1	2	7	14	19	19	22	21	15	4	1
DAYS FOG < 7	1	1	#	1	2	5	6	4	7	8	8	3	1
DAYS BNBD < 7	1	#	1	0	#	0	0	#	#	#	0	#	#
6. PERCENTAGE FREQUENCY OF OCCURRENCE (% FREQ) OF THUNDERSTORMS:													
	JAN	FEB	MAR	APR	MAY	JUN	JUL	AUG	SEP	OCT	NOV	DEC	ANN
00-02 LST	#	0	1	1	11	14	7	15	12	8	1	0	6
03-05 LST	0	0	0	#	5	5	1	4	8	3	#	0	2
06-08 LST	0	0	0	#	1	1	#	#	1	0	0	0	#
09-11 LST	0	0	0	0	#	1	0	#	#	#	0	#	#
12-14 LST	0	#	#	1	4	6	2	5	7	5	1	0	3
15-17 LST	0	0	1	1	7	14	11	16	16	9	2	1	7
18-20 LST	1	0	1	3	9	17	24	18	13	10	3	1	8
21-23 LST	1	1	1	7	10	19	22	28	18	11	1	1	10
ALL HOURS	#	#	1	2	6	10	8	11	6	6	1	#	5
7. % FREQ OF RAIN AND/OR DRIZZLE:													
00-02 LST	2	#	3	3	14	31	16	29	28	16	3	1	12
03-05 LST	1	0	2	2	10	22	7	13	15	13	1	#	7
06-08 LST	0	1	1	1	6	8	1	3	9	3	1	#	3
09-11 LST	0	#	0	1	4	5	1	2	7	2	1	#	2
12-14 LST	#	#	1	1	5	9	3	5	12	6	1	#	4
15-17 LST	#	#	1	#	5	12	10	8	13	9	2	1	5
18-20 LST	1	0	1	3	8	16	18	18	17	14	4	1	8
21-23 LST	2	1	3	5	10	28	32	33	27	16	5	1	14
ALL HOURS	1	#	2	2	8	16	11	14	16	10	2	1	7
8. PERCENTAGE FREQUENCY OF OCCURRENCE (% FREQ) OF CEILING AND/OR VISIBILITY													
(CIG/VIS) < 1500/3 STATUTE MILES (MI) (SOURCE NO. 1):													
00-02 LST	1	0	#	4	5	8	8	7	13	10	2	#	5
03-05 LST	1	0	1	3	10	15	9	15	26	19	7	1	9
06-08 LST	5	2	3	18	17	22	15	17	27	20	8	2	13
09-11 LST	#	1	#	6	6	7	1	3	9	3	#	#	3
12-14 LST	0	#	1	4	4	4	1	2	6	2	#	#	2
15-17 LST	1	1	0	4	3	4	3	3	5	2	1	#	2
18-20 LST	0	#	0	5	5	6	4	3	5	3	1	1	3
21-23 LST	#	0	1	3	3	6	5	6	8	5	1	1	3
ALL HOURS	1	1	1	6	7	9	6	7	12	8	3	1	5
9. % IREQ OF CIG/VIS < 200/0.5 MI (SOURCE NO. 1):													
00-02 LST	0	0	#	#	1	1	1	1	2	2	1	0	1
03-05 LST	0	0	1	#	1	2	2	5	6	6	3	1	2
06-08 LST	1	0	1	2	2	6	5	4	8	5	4	1	3
09-11 LST	0	1	0	#	#	1	#	#	1	#	0	0	#
12-14 LST	0	#	#	#	0	#	0	0	#	0	0	0	#
15-17 LST	#	#	0	0	#	0	#	1	#	#	#	#	#
18-20 LST	0	0	0	0	#	0	1	#	#	#	0	1	#
21-23 LST	0	0	0	0	0	1	#	1	1	1	0	#	#
ALL HOURS	#	#	#	#	1	1	1	2	2	2	1	#	1

REMARKS: * = DATA NOT AVAILABLE # = LESS THAN 0.5 DAY, OR 0.05 INCH, OR 0.5% MI = STAT. MILES
 \$ = % CALM > PVLG DRCTN @ = BASED ON AVAIL. DATA, I.E., < 24 HRS/DAY OR < 12 MONTHS/YEAR
 SOURCE(S): 1. USAFETAC DATSAV FOR JAN 73 - DEC 85
 2. NATIONAL INTELLIGENCE SURVEY 7-49 YEARS
 3. WORLDWIDE AIRFIELD CLIMATIC DATA SUMMARY 33-39 YEARS

STATION: BLUEFIELDS, NICARAGUA STATION #: 787450 ICAO ID: MNBL (USAFETAC, 1987)
 LOCATION: 12°00'N, 83°46'W ELEVATION (FT.): 135 LST = GMT: -6
 PREPARED BY: USAFETAC/ECR 1986 PERIOD: VARIED(except items 6 & 7 JAN 73 - DEC 83)

SOURCE NO.	JAN	FEB	MAR	APR	MAY	JUN	JUL	AUG	SEP	OCT	NOV	DEC	ANN
1. TEMPERATURE (°F)													
EXTREME MAX	2	90	90	91	94	94	94	93	92	93	94	93	94
MEAN DLY MAX	2	84	85	85	86	87	86	85	86	87	87	85	85
MEAN	2	77	78	79	80	81	80	80	80	80	80	79	79
MEAN DLY MIN	2	70	71	72	74	74	74	74	74	73	72	72	73
EXTREME MIN	2	60	61	62	63	67	67	70	68	66	64	64	62
# DAYS ≥ 90	2	#	#	2	5	7	5	2	4	8	6	4	2
# DAYS ≤ 32	2	0	0	0	0	0	0	0	0	0	0	0	0
# DAYS ≤ 0	2	0	0	0	0	0	0	0	0	0	0	0	0
2. PRECIPITATION (INCHES)													
MAXIMUM	2	20.8	13.2	7.7	9.5	33.2	30.0	46.6	41.8	21.5	26.1	28.6	242.9
MEAN	2	10.5	5.1	3.2	2.9	13.6	19.8	26.2	21.5	12.3	13.6	15.3	159.7
MINIMUM	2	1.7	1.2	0.4	0.6	0.0	10.3	13.3	11.2	6.2	4.2	5.9	130.0
MAX 24 HR	2	3.7	3.4	2.5	3.7	10.2	6.9	9.5	8.2	5.8	6.2	9.1	10.2
# DAYS ≥ 0.01	2	*	*	*	*	*	*	*	*	*	*	*	*
# DAYS ≥ 0.5	2	*	*	*	*	*	*	*	*	*	*	*	*
3. MEAN RELATIVE HUMIDITY (%) / VAPOR PRESSURE (IN Hg) / DEWPOINT (°F)													
RH (07 LST)	1	95	93	90	91	91	94	93	93	95	96	95	93
RH (12 LST)	1	80	77	75	72	77	83	84	83	81	82	81	80
VAPOR PRESS.	1	.82	.82	.86	.87	.92	.93	.90	.91	.91	.90	.88	.88
DEWPOINT	1	72	73	74	74	76	76	75	76	76	75	75	75
4. SURFACE WINDS (16 PT/KNOTS) / 99.95% HIGHEST PRESSURE ALTITUDE (FEET)													
PVLG DRCTN	01	E	E	E	E	E	E	ENE	ENE	E	E	N	E
MEAN SPEED	01	7	7	7	7	5	5	7	6	4	5	6	6
MAX (PK GST)	01	24	33	25	28	40	33	30	20	35	40	30	40
PRESSURE ALT	01	350	400	400	350	350	400	300	350	350	350	300	400
5. MEAN CLOUD COVER (EIGHTHS) / THUNDERSTORMS / FOG / BLOWING SAND (BNBD)													
CLD COVER	1	6	5	5	5	6	7	7	7	7	7	7	6
DAYS TSTMS	2	0	0	0	#	1	3	5	3	3	1	#	13
DAYS FOG	1	2	1	1	1	2	2	1	2	3	3	2	21
DAYS BNBD	2	0	0	0	0	0	0	0	0	0	0	0	2
6. PERCENTAGE FREQUENCY OF OCCURRENCE (% FREQ) OF THUNDERSTORMS:													
	JAN	FEB	MAR	APR	MAY	JUN	JUL	AUG	SEP	OCT	NOV	DEC	ANN
00-02 LST	*	*	*	*	*	*	*	*	*	*	*	*	*
03-05 LST	*	*	*	*	*	*	*	*	*	*	*	*	*
06-08 LST	0	0	0	1	2	9	13	6	15	6	3	0	5
09-11 LST	0	0	0	#	3	6	11	9	10	5	1	0	4
12-14 LST	0	0	0	#	4	9	10	10	8	5	2	#	4
15-17 LST	0	0	0	#	2	6	7	6	8	3	3	0	3
18-20 LST	0	0	0	0	3	6	9	8	10	3	2	#	3
21-23 LST	*	*	*	*	*	*	*	*	*	*	*	*	*
ALL HOURS	0	0	0	#	3	7	10	8	10	5	2	#	4
7. % FREQ OF RAIN / OR DRIZZLE:													
00-02 LST	*	*	*	*	*	*	*	*	*	*	*	*	*
03-05 LST	*	*	*	*	*	*	*	*	*	*	*	*	*
06-08 LST	13	6	3	6	10	17	21	21	16	15	11	13	13
09-11 LST	10	5	3	4	7	15	21	15	15	14	11	11	11
12-14 LST	5	3	2	3	6	18	20	11	11	15	11	8	9
15-17 LST	3	5	2	3	4	15	15	14	12	14	10	11	9
18-20 LST	4	5	1	3	6	15	16	10	7	16	10	11	9
21-23 LST	*	*	*	*	*	*	*	*	*	*	*	*	*
ALL HOURS	7	5	2	4	7	16	19	14	13	15	11	11	10
8. PERCENTAGE FREQUENCY OF OCCURRENCE (% FREQ) OF CEILING AND/OR VISIBILITY (CIG/VIS) < 1500/3 STATUTE MILES (MI) (SOURCE NO. 1):													
00-02 LST	*	*	*	*	*	*	*	*	*	*	*	*	*
03-05 LST	*	*	*	*	*	*	*	*	*	*	*	*	*
06-08 LST	13	6	5	4	9	12	12	17	14	12	16	13	11
09-11 LST	10	8	6	3	10	15	20	17	16	12	14	11	12
12-14 LST	6	3	6	4	6	12	14	10	11	10	9	8	8
15-17 LST	4	4	4	3	3	11	8	11	8	7	5	8	6
18-20 LST	7	3	3	3	6	12	6	11	7	9	8	6	7
21-23 LST	*	*	*	*	*	*	*	*	*	*	*	*	*
ALL HOURS	8	5	5	3	7	12	13	14	12	10	11	9	9
9. % FREQ OF CIG/VIS < 200/0.5 MI (SOURCE NO. 1):													
00-02 LST	*	*	*	*	*	*	*	*	*	*	*	*	*
03-05 LST	*	*	*	*	*	*	*	*	*	*	*	*	*
06-08 LST	0	0	#	1	0	1	#	2	#	1	1	0	#
09-11 LST	1	#	#	#	#	1	1	1	1	1	#	#	1
12-14 LST	#	#	0	#	#	#	#	#	#	1	0	#	#
15-17 LST	0	#	#	0	0	1	#	#	#	1	0	0	#
18-20 LST	0	1	0	0	0	0	1	0	1	0	0	0	#
21-23 LST	*	*	*	*	*	*	*	*	*	*	*	*	*
ALL HOURS	#	#	#	#	#	1	1	1	#	1	#	#	#

REMARKS: * = DATA NOT AVAILABLE # = LESS THAN 0.5 DAY, OR 0.05 INCH, OR 0.5% MI = STAT. MILES
 % = % CALM > PVLG DRCTN @ = BASED ON AVAIL. DATA, I.E., < 24 HRS/DAY OR < 12 MONTHS/YEAR
 SOURCE(S): 1. USAFETAC DATSAV POR APR 73 - DEC 83
 2. NATIONAL INTELLIGENCE SURVEY POR VARIED

STATION: CHINADEGA, NICARAGUA STATION #: 787390 ICAO ID: MNCH (USAFETAC, 1987)
 LOCATION: 12°37'N, 87°09'W ELEVATION (FT.): 174 LST = GMT: -6
 PREPARED BY: USAFETAC/ECR 1986 PERIOD: VARIED(except items 6 & 7 JAN 73 - DEC 85)

		SOURCE NO.	JAN	FEB	MAR	APR	MAY	JUN	JUL	AUG	SEP	OCT	NOV	DEC	ANN
1. TEMPERATURE (°F)															
EXTREME MAX	2		95	94	97	97	96	93	96	94	91	91	92	94	97
MEAN DLY MAX	2		88	91	92	91	91	87	90	89	87	86	88	88	89
MEAN	2		80	82	83	84	84	81	83	82	81	80	81	80	82
MEAN DLY MIN	2		71	77	74	76	76	75	75	74	74	74	73	71	74
EXTREME MIN	2		65	68	70	72	71	70	72	70	70	69	68	64	64
# DAYS>90	2		13	24	26	20	18	7	18	12	5	2	6	12	163
# DAYS<32	1		0	0	0	0	0	0	0	0	0	0	0	0	0
# DAYS<0	1		0	0	0	0	0	0	0	0	0	0	0	0	0
2. PRECIPITATION (INCHES)															
MAXIMUM	2		.3	.2	.2	1.8	19.0	21.5	12.4	16.4	24.4	44.2	5.1	1.6	111.6
MEAN	2		#	.1	#	.5	3.5	12.2	7.2	8.1	14.4	15.8	3.6	.3	65.5
MINIMUM	2		0	0	0	0	.6	5.4	2.1	2.2	5.5	2.8	.4	0	44.8
MAX 24 HR	2		.2	.1	0	1.8	1.9	4.7	2.0	4.8	7.7	8.9	2.7	.8	89
# DAYS>=0.004	2		#	1	0	1	7	16	13	12	17	17	8	1	92
# DAYS>=0.5															
3. MEAN RELATIVE HUMIDITY (%) / VAPOR PRESSURE (IN Hg) / DEWPOINT (°F)															
RH (06 LST)	1		80	82	82	81	90	94	92	91	94	94	88	85	88
RH (12 LST)	1		42	40	39	42	57	64	56	58	66	68	61	48	54
VAPOR PRESS.	1		.62	.63	.66	.72	.83	.87	.81	.83	.87	.87	.80	.69	.77
DEWPOINT	1		64	65	66	68	73	74	72	73	74	74	72	67	70
4. SURFACE WINDS (16 PT/KNOTS) / 99.95% HIGHEST PRESSURE ALTITUDE (FEET)															
PVLG DRCTN	1		\$NE	\$NE	\$SW	\$SW	\$SW	\$SW	\$NE	\$NE	\$N	\$SW	\$N	\$NE	\$SW
MEAN SPEED															
(PVLG DRCTN)	1		7	9	8	7	7	5	7	6	5	5	5	6	6
MEAN SPEED															
(ALL OBS)	1		6	6	6	6	5	3	4	4	3	3	3	4	4
MAX (PK GST)			*	*	*	*	*	*	*	*	*	*	*	*	*
PRESSURE ALT	1		400	400	400	400	400	350	350	400	350	350	350	350	400
5. MEAN CLOUD COVER (EIGHTHS) / THUNDERSTORMS / FOG/ BLOWING SAND (BNBD)															
CLD COVER	1		3	4	4	4	6	6	6	6	6	6	5	4	5
DAYS TSTMS	1		#	#	1	#	7	14	10	12	14	10	3	#	71
DAYS FOG < 7	1		0	0	#	#	#	#	#	1	1	#	1	#	3
DAYS BNBD < 7	1		#	#	#	0	0	0	#	0	0	0	0	0	#
6. PERCENTAGE FREQUENCY OF OCCURRENCE (% FREQ) OF THUNDERSTORMS:															
		JAN	FEB	MAR	APR	MAY	JUN	JUL	AUG	SEP	OCT	NOV	DEC	ANN	
00-02 LST	*	*	*	*	*	*	*	*	*	*	*	*	*	*	*
03-05 LST	*	*	*	*	*	*	*	*	*	*	*	*	*	*	*
06-08 LST	0	0	0	0	2	2	1	#	1	1	0	0	1		
09-11 LST	0	0	0	#	#	1	#	#	0	#	0	0	#		
12-14 LST	#	#	#	0	5	9	2	6	8	5	2	0	3		
15-17 LST	0	0	#	#	8	20	17	20	22	12	3	#	9		
18-20 LST	1	0	1	0	10	23	21	24	26	23	3	0	11		
21-23 LST	*	*	*	*	*	*	*	*	*	*	*	*	*	*	*
ALL HOURS	*	*	*	*	*	*	*	*	*	*	*	*	*	*	*
7. % FREQ OF RAIN AND/OR DRIZZLE:															
00-02 LST	*	*	*	*	*	*	*	*	*	*	*	*	*	*	*
03-05 LST	*	*	*	*	*	*	*	*	*	*	*	*	*	*	*
06-08 LST	0	0	0	1	7	6	1	1	4	4	2	0	2		
09-11 LST	#	#	#	1	5	4	1	1	5	3	3	0	2		
12-14 LST	#	#	1	#	6	6	3	3	9	9	4	1	4		
15-17 LST	#	1	0	#	5	12	11	13	15	10	4	1	6		
18-20 LST	0	0	1	0	6	14	11	17	19	11	3	0	7		
21-23 LST	*	*	*	*	*	*	*	*	*	*	*	*	*	*	*
ALL HOURS	*	*	*	*	*	*	*	*	*	*	*	*	*	*	*
8. PERCENTAGE FREQUENCY OF OCCURRENCE (% FREQ) OF CEILING AND/OR VISIBILITY (CIG/VIS) < 1500/3 STATUE MILES (MI) (SOURCE NO. 1):															
00-02 LST	*	*	*	*	*	*	*	*	*	*	*	*	*	*	*
03-05 LST	*	*	*	*	*	*	*	*	*	*	*	*	*	*	*
06-08 LST	1	#	1	14	8	2	1	1	2	3	3	2	3		
09-11 LST	0	0	1	7	5	0	1	0	1	0	#	0	1		
12-14 LST	1	1	#	6	3	1	1	1	2	2	1	0	2		
15-17 LST	1	0	1	6	3	4	3	3	3	5	1	1	3		
18-20 LST	0	0	0	4	3	7	3	4	1	1	0	0	2		
21-23 LST	*	*	*	*	*	*	*	*	*	*	*	*	*	*	*
ALL HOURS	*	*	*	*	*	*	*	*	*	*	*	*	*	*	*
9. % FREQ OF CIG/VIS < 200/0.5 MI (SOURCE NO. 1):															
00-02 LST	*	*	*	*	*	*	*	*	*	*	*	*	*	*	*
03-05 LST	*	*	*	*	*	*	*	*	*	*	*	*	*	*	*
06-08 LST	1	0	#	0	#	0	0	#	0	#	0	1	#		
09-11 LST	0	0	0	0	0	0	#	0	0	0	0	0	#		
12-14 LST	0	0	0	0	#	1	0	#	#	#	0	0	#		
15-17 LST	0	0	0	0	#	1	#	0	#	1	0	0	#		
18-20 LST	0	0	0	0	1	1	0	0	0	0	0	0	#		
21-23 LST	*	*	*	*	*	*	*	*	*	*	*	*	*	*	*
ALL HOURS	*	*	*	*	*	*	*	*	*	*	*	*	*	*	*

REMARKS: * = DATA NOT AVAILABLE # = LESS THAN 0.5 DAY, OR 0.05 INCH, OR 0.5%
 \$ = % CALM > PVLG DRCTN @ = BASED ON AVAIL. DATA, I.E., < 24 HRS/DAY OR < 12 MONTHS/YEAR
 SOURCE(S): 1 USAFETAC DATSVA POR JAN 73 - DEC 85
 2 NATIONAL INTELLIGENCE SURVEY 7-12 YEARS

STATION: MANAGUA, NICARAGUA STATION #: 787410 ICAO ID: MNMG (USAFETAC, 1987)
 LOCATION: 12°07'N, 86°11'W ELEVATION (FT.): 150 LST = GMT: -6
 PREPARED BY: USAFETAC/ECR 1986 PERIOD: VARIED(except items 6 & 7 JAN 73 - DEC 85)

SOURCE NO.	JAN	FEB	MAR	APR	MAY	JUN	JUL	AUG	SEP	OCT	NOV	DEC	ANN
1. TEMPERATURE (°F)													
EXTREME MAX	2	95	96	100	103	102	96	94	96	98	97	96	103
MEAN DLY MAX	2	91	92	94	96	95	90	90	90	91	90	90	92
MEAN	2	81	81	83	85	85	82	82	82	82	82	82	83
MEAN DLY MIN	2	70	70	72	74	75	74	74	74	73	73	71	73
EXTREME MIN	2	62	63	64	68	71	70	71	70	69	69	66	62
# DAYS > 90	3	6	12	27	30	29	12	12	18	15	9	4	177
# DAYS < 32	1	0	0	0	0	0	0	0	0	0	0	0	0
# DAYS < 0	1	0	0	0	0	0	0	0	0	0	0	0	0
2. PRECIPITATION (INCHES)													
MAXIMUM	2	.7	1.1	2.0	3.0	19.0	21.0	9.1	11.2	19.3	23.6	4.7	70.4
MEAN	2	.1	#	#	.4	5.6	8.7	5.3	4.8	8.2	12.0	2.0	47.5
MINIMUM	2	0	0	0	0	0.2	0	1.4	1.4	1.2	.5	0	16.0
MAX 24 HR	2	.4	1.0	1.1	2.4	3.1	4.7	3.5	4.1	4.7	8.6	2.9	8.6
# DAYS > 0.01	2	2	1	1	1	7	17	19	16	18	18	7	108
# DAYS > 0.5	2	*	*	*	*	*	*	*	*	*	*	*	*
3. MEAN RELATIVE HUMIDITY (%) / VAPOR PRESSURE (IN Hg) / DEWPOINT (°F)													
RH (06 LST)	1	87	84	83	82	87	93	91	93	94	95	93	89
RH (14 LST)	1	46	42	40	40	50	63	63	63	67	65	60	54
VAPOR PRESS.	1	.65	.64	.64	.70	.79	.84	.81	.82	.83	.82	.76	.75
DEWPOINT	1	66	65	66	68	71	73	72	73	73	73	71	69
4. SURFACE WINDS (16 PT/KNOTS) / 99.95% HIGHEST PRESSURE ALTITUDE (FEET)													
PVLG DRCTN	1	\$E	E	E	E	\$E	\$E	\$E	\$E	\$E	\$E	\$E	\$E
MEAN SPEED													
(PVLG DRCTN)	1	7	7	7	7	6	6	6	6	5	4	5	6
MEAN SPEED													
(ALL OBS)	1	5	5	5	5	3	3	3	3	2	2	2	3
MAX (PK GST)		*	*	*	*	*	*	*	*	*	*	*	*
PRESSURE ALT	1	350	350	350	350	350	350	300	300	300	350	350	350
5. MEAN CLOUD COVER (EIGHTHS) / THUNDERSTORMS / FOG/ BLOWING SAND (BNBD)													
CLD COVER	1	3	3	3	3	5	5	5	5	5	5	4	4
DAYS TSTMS	1	#	1	1	2	10	15	10	13	19	17	7	95
DAYS FOG < 7	1	0	#	#	#	1	1	1	1	1	1	1	7
DAYS BNBD < 7	1	#	#	1	1	1	1	3	1	#	#	#	8
6. PERCENTAGE FREQUENCY OF OCCURRENCE (% FREQ) OF THUNDERSTORMS:													
	JAN	FEB	MAR	APR	MAY	JUN	JUL	AUG	SEP	OCT	NOV	DEC	ANN
00-02 LST	0	0	0	#	5	5	1	2	7	5	1	0	2
03-05 LST	0	0	0	1	2	2	1	1	14	1	1	0	2
06-08 LST	0	0	0	#	#	1	#	#	12	#	#	0	1
09-11 LST	0	#	#	#	1	1	#	0	8	#	#	0	1
12-14 LST	0	#	0	1	3	6	2	3	5	4	2	0	2
15-17 LST	0	#	#	1	4	9	8	9	2	9	4	#	4
18-20 LST	#	#	#	1	6	8	4	6	#	10	3	0	3
21-23 LST	0	0	#	1	5	9	3	5	#	9	1	0	3
ALL HOURS	#	#	#	1	3	5	2	4	6	5	2	#	2
7. % FREQ OF RAIN AND/OR DRIZZLE:													
00-02 LST	1	#	0	#	8	8	6	5	9	10	3	#	4
03-05 LST	1	#	#	1	4	6	5	4	6	6	3	1	3
06-08 LST	#	#	1	1	3	5	4	4	6	4	2	1	3
09-11 LST	1	1	1	1	4	5	5	4	5	2	2	2	3
12-14 LST	1	1	#	#	5	7	7	10	10	9	4	1	5
15-17 LST	1	1	#	#	5	13	12	15	15	13	5	2	7
18-20 LST	2	1	#	1	7	15	10	12	21	15	4	1	7
21-23 LST	1	#	#	#	10	12	5	6	13	11	5	1	5
ALL HOURS	1	1	#	1	6	10	7	8	11	9	4	1	5
8. PERCENTAGE FREQUENCY OF OCCURRENCE (% FREQ) OF CEILING AND/OR VISIBILITY													
(CIG/VIS) < 1500/3 STATUE MILES (MI) (SOURCE NO. 1):													
00-02 LST	0	0	#	2	2	1	1	0	1	1	#	0	1
03-05 LST	0	#	#	3	2	1	0	#	2	1	#	0	1
06-08 LST	1	#	#	2	3	1	1	1	2	1	1	#	1
09-11 LST	#	#	1	2	1	1	2	1	1	1	#	#	1
12-14 LST	#	#	#	2	3	2	3	2	3	2	1	#	2
15-17 LST	1	#	#	3	4	3	3	3	4	1	2	1	2
18-20 LST	0	0	0	4	3	2	1	1	4	2	1	#	2
21-23 LST	0	#	#	4	4	1	1	#	1	1	#	#	1
ALL HOURS	#	#	#	3	3	2	2	1	2	1	1	#	1
9. % FREQ OF CIG/VIS < 200/0.5 MI (SOURCE NO. 1):													
00-02 LST	0	0	#	#	#	#	0	0	#	0	0	0	#
03-05 LST	0	0	0	1	0	#	0	0	0	0	0	0	#
06-08 LST	1	0	0	#	1	#	#	0	0	#	#	0	#
09-11 LST	0	0	#	#	#	0	0	#	0	0	0	0	#
12-14 LST	0	0	#	#	1	#	#	1	1	#	#	0	#
15-17 LST	#	0	0	#	#	1	1	1	1	#	#	#	#
18-20 LST	0	0	0	1	#	#	1	#	1	#	#	#	#
21-23 LST	0	#	#	0	#	0	#	0	0	#	#	#	#
ALL HOURS	#	#	#	#	#	#	#	#	#	#	#	#	#

REMARKS: * = DATA NOT AVAILABLE # = LESS THAN 0.5 DAY, OR 0.05 INCH, OR 0.5%, AS APPLICABLE
 \$ = % CALM > PVLG DRCTN @ = BASED ON AVAIL. DATA, I.E., < 24 HRS/DAY OR < 12 MONTHS/YEAR
 SOURCE(S): 1. USAFETAC DATSAV POR JAN 73 - DEC 85
 2. NATIONAL INTELLIGENCE SURVEY 4-23 YEARS
 3. WORLDWIDE AIRFIELD CLIMATIC DATA 5 YEARS

STATION: PUERTO CABEZAS, NICARAGUA STATION #: 787300 ICAO ID: MNPC (USAFETAC, 1987)
 LOCATION: 14°02'N, 83°24'W ELEVATION (FT.): 49 LST = GMT: -6
 PREPARED BY: USAFETAC/ECR, 1986 PERIOD: VARIED(except items 6 & 7 JAN 73 - DEC 85)

SOURCE NO.	JAN	FEB	MAR	APR	MAY	JUN	JUL	AUG	SEP	OCT	NOV	DEC	ANN
1. TEMPERATURE (°F)													
EXTREME MAX	2	92	91	93	94	97	93	91	93	94	97	93	97
MEAN DLY MAX	2	83	84	86	87	88	86	86	87	88	87	86	86
MEAN	2	76	77	79	81	82	80	80	81	81	80	79	78
MEAN DLY MIN	2	69	70	72	74	75	74	73	74	74	73	72	72
EXTREME MIN	2	59	61	64	64	58	58	58	64	65	67	65	58
# DAYS ≥ 90	2	#	#	3	4	5	3	#	2	8	7	1	33
# DAYS ≤ 32	1	0	0	0	0	0	0	0	0	0	0	0	0
# DAYS ≤ 0	1	0	0	0	0	0	0	0	0	0	0	0	0
2. PRECIPITATION (INCHES)													
MAXIMUM	2	15.5	14.5	7.9	6.7	25.8	42.2	29.6	28.2	19.5	25.5	20.9	145.1
MEAN	1	6.5	3.3	1.5	2.0	10.4	17.0	18.8	14.4	10.9	13.2	11.0	123.0
MINIMUM	2	2.1	0.1	#	#	1.3	4.0	9.6	4.8	5.2	9.5	5.2	71.1
MAX 24 HR	2	3.5	9.0	2.3	2.8	6.7	9.8	7.6	7.4	5.5	5.7	6.3	9.8
# DAYS ≥ 0.01	2												
# DAYS ≥ 0.5		*	*	*	*	*	*	*	*	*	*	*	*
3. MEAN RELATIVE HUMIDITY (%) / VAPOR PRESSURE (IN Hg) / DEWPOINT (°F)													
RH (06 LST)	1	89	89	86	84	87	87	87	91	92	95	94	89
RH (12 LST)	1	74	73	71	70	73	78	79	78	78	77	77	75
VAPOR PRESS.	1	.79	.78	.80	.82	.89	.91	.89	.90	.90	.88	.85	.85
DEWPOINT	1	72	71	72	72	75	76	75	75	76	75	74	74
4. SURFACE WINDS (16 KT/KNOTS) / 99.95% HIGHEST PRESSURE ALTITUDE (FEET)													
PVLG DRCTN	1	ENE	E	E	E	E	E	E	ENE	E	E	N	ENE
MEAN SPEED													
(PVLG DRCTN)	1	11	10	10	10	10	11	11	11	9	9	8	10
MEAN SPEED													
(ALL OBS)	1	9	10	10	10	9	10	11	9	8	7	9	9
MAX (PK GST)		*	*	*	*	*	*	*	*	*	*	*	*
PRESSURE ALT	1	200	250	250	250	250	300	200	250	300	250	250	300
5. MEAN CLOUD COVER (EIGHTHS) / THUNDERSTORMS / FOG / BLOWING SAND (BNBD)													
CLD COVER	1	4	4	4	4	5	6	6	5	5	5	5	5
DAYS TSTMS	1	#	1	#	1	4	8	11	13	11	9	4	63
DAYS FOG < 7	1	1	#	#	1	#	#	#	#	#	1	1	5
DAYS BNBD < 7	1	#	#	#	#	#	#	#	#	#	#	#	#
6. PERCENTAGE FREQUENCY OF OCCURRENCE (% FREQ) OF THUNDERSTORMS:													
	JAN	FEB	MAR	APR	MAY	JUN	JUL	AUG	SEP	OCT	NOV	DEC	ANN
00-02 LST	*	*	*	*	*	*	*	*	*	*	*	*	*
03-05 LST	*	*	*	*	*	*	*	*	*	*	*	*	*
06-08 LST	0	0	#	#	4	10	7	11	7	7	2	1	4
09-11 LST	0	0	0	0	2	4	4	8	4	2	1	1	2
12-14 LST	#	0	0	#	3	5	6	8	7	4	2	1	3
15-17 LST	0	0	0	1	2	6	6	8	8	6	3	1	3
18-20 LST	1	1	0	1	2	12	12	3	14	8	3	1	5
21-23 LST	*	*	*	*	*	*	*	*	*	*	*	*	*
ALL HOURS	*	*	*	*	*	*	*	*	*	*	*	*	*
7. % FREQ OF RAIN AND/OR DRIZZLE:													
00-02 LST	*	*	*	*	*	*	*	*	*	*	*	*	*
03-05 LST	*	*	*	*	*	*	*	*	*	*	*	*	*
06-08 LST	7	6	4	4	10	16	13	10	11	15	13	12	10
09-11 LST	6	5	2	3	5	15	13	11	8	16	15	14	9
12-14 LST	5	4	3	3	7	13	14	12	9	12	14	9	9
15-17 LST	6	3	2	2	8	15	10	12	9	16	12	8	9
18-20 LST	3	11	3	2	9	14	12	9	11	13	14	8	9
21-23 LST	*	*	*	*	*	*	*	*	*	*	*	*	*
ALL HOURS	*	*	*	*	*	*	*	*	*	*	*	*	*
8. PERCENTAGE FREQUENCY OF OCCURRENCE (% FREQ) OF CEILING AND/OR VISIBILITY (CIG/VIS) < 1500/3 STATUE MILES (MI) (SOURCE NO. 1):													
00-02 LST	*	*	*	*	*	*	*	*	*	*	*	*	*
03-05 LST	*	*	*	*	*	*	*	*	*	*	*	*	*
06-08 LST	7	2	2	6	9	13	9	7	5	12	11	11	8
09-11 LST	4	3	#	2	4	7	7	5	4	6	6	6	5
12-14 LST	3	3	#	2	3	6	7	4	2	5	8	5	4
15-17 LST	3	2	1	2	3	7	6	5	2	6	5	4	4
18-20 LST	2	3	2	2	6	12	7	6	5	8	13	3	6
21-23 LST	*	*	*	*	*	*	*	*	*	*	*	*	*
ALL HOURS	*	*	*	*	*	*	*	*	*	*	*	*	*
9. % FREQ OF CIG/VIS < 200/0.5 MI (SOURCE NO. 1):													
00-02 LST	*	*	*	*	*	*	*	*	*	*	*	*	*
03-05 LST	*	*	*	*	*	*	*	*	*	*	*	*	*
06-08 LST	#	0	0	0	1	0	0	0	#	0	0	#	#
09-11 LST	0	0	0	0	0	0	#	#	1	0	#	#	#
12-14 LST	0	0	0	0	0	#	#	0	0	#	0	0	#
15-17 LST	0	#	#	#	0	0	0	#	#	0	#	0	#
18-20 LST	0	1	0	1	0	0	0	0	1	0	1	0	#
21-23 LST	*	*	*	*	*	*	*	*	*	*	*	*	*
ALL HOURS	*	*	*	*	*	*	*	*	*	*	*	*	*

REMARKS: * = DATA NOT AVAILABLE # = LESS THAN 0.5 DAY, OR 0.05 INCH, OR 0.5%, AS APPLICABLE
 \$ = % CALM > PVLG DRCTN @ = BASED ON AVAIL. DATA, I.E., < 24 HRS/DAY OR < 12 MONTHS/YEAR
 SOURCE(S): 1. USAFETAC DATSAV FOR JAN 73 - DEC 85
 2. NATIONAL INTELLIGENCE SURVEY 10 - 16 YEARS

STATION: LIBERIA, COSTA RICA

STATION #: 787740

ICAO ID: MRLB (USAFETAC, 1987)

LOCATION: 10°37'N, 85°26'W

ELEVATION (FT.): 262 LST = GMT: -6

PREPARED BY: USAFETAC/ECR, 1986 PERIOD: VARIED(except items 6 & 7 JAN 78 - DEC 85)

	SOURCE NO.	JAN	FEB	MAR	APR	MAY	JUN	JUL	AUG	SEP	OCT	NOV	DEC	ANN
1. TEMPERATURE (°F)														
EXTREME MAX	1	97	99	101	99	99	95	95	97	97	94	94	95	101
MEAN DLY MAX	2	91	93	96	97	95	89	89	90	88	86	89	88	91
MEAN	2	81	83	84	86	85	81	82	82	82	80	80	79	82
MEAN DLY MIN	2	71	72	72	74	74	73	75	74	73	73	71	69	73
EXTREME MIN	1	65	67	67	68	70	69	71	70	69	69	68	65	65
# DAYS ≥ 90	1	23	25	30	29	23	12	13	13	9	9	11	19	216
# DAYS ≤ 32	1	0	0	0	0	0	0	0	0	0	0	0	0	0
# DAYS ≤ 0	1	0	0	0	0	0	0	0	0	0	0	0	0	0
2. PRECIPITATION (INCHES)														
MAXIMUM	2	0	6	.1	2.5	13.3	18.7	14.6	10.8	20.3	26.1	20.2	1.6	83.1
MEAN	2	#	#	.1	.8	8.5	10.7	8.0	6.1	13.7	12.5	3.2	.4	64.1
MINIMUM	2	0	0	0	0	3	3.7	.6	1.2	8.0	5.7	.4	0	43.4
MAX 24 HR	2	0	3	.1	1.3	2.5	3.9	4.7	2.9	5.1	7.1	5.0	1.3	7.1
# DAYS ≥ 0.004	2	#	#	#	1	8	15	12	12	17	16	5	1	87
# DAYS ≥ 0.5	2	*	*	*	*	*	*	*	*	*	*	*	*	*
3. MEAN RELATIVE HUMIDITY (%) / VAPOR PRESSURE (IN Hg) / DEWPOINT (°F)														
RH (06 LST)	1	87	85	81	84	92	94	91	94	97	97	94	91	90
RH (12 LST)	1	47	44	43	44	56	66	63	66	69	70	64	53	58
VAPOR PRESS.	1	.70	.69	.71	.73	.83	.88	.84	.86	.87	.87	.83	.75	.80
DEWPOINT	1	68	68	68	69	73	75	73	74	74	74	73	70	72
4. SURFACE WINDS (16 PT/KNOTS) / 99.95% HIGHEST PRESSURE ALTITUDE (FEET)														
PVLG DRCTN	1	E	E	E	E	\$E	\$E	\$E	\$E	\$W	\$W	\$E	E	\$E
MEAN SPEED														
(PVLG DRCTN)	1	18	18	18	17	14	12	14	13	9	9	13	17	16
MEAN SPEED														
(ALL OBS)	1	12	14	13	11	6	5	7	6	4	4	6	10	8
MAX (PK GST)		*	*	*	*	*	*	*	*	*	*	*	*	*
PRESSURE ALT	1	450	350	400	350	350	350	350	400	400	400	450	450	450
5. MEAN CLOUD COVER (EIGHTHS) / THUNDERSTORMS / FOG/ BLOWING SAND (BNBD)														
CLD COVER	1	3	3	4	5	6	6	6	6	6	6	5	4	5
DAYS TSTMS	1	#	#	1	3	9	10	7	10	13	10	2	1	66
DAYS FOG < 7	1	1	1	#	#	1	2	2	2	5	6	3	1	24
DAYS BNBD < 7	1	0	#	0	0	0	0	0	0	0	0	0	0	#
6. PERCENTAGE FREQUENCY OF OCCURRENCE (% FREQ) OF THUNDERSTORMS:														
	JAN	FEB	MAR	APR	MAY	JUN	JUL	AUG	SEP	OCT	NOV	DEC	ANN	
00-02 LST	*	*	*	*	*	*	*	*	*	*	*	*	*	*
03-05 LST	*	*	*	*	*	*	*	*	*	*	*	*	*	*
06-08 LST	0	0	0	0	#	#	#	1	0	0	0	0	#	#
09-11 LST	0	0	#	0	1	1	1	0	#	0	#	0	#	#
12-14 LST	0	0	0	1	9	9	3	7	10	7	2	0	6	6
15-17 LST	#	#	1	8	15	19	16	15	22	14	3	1	9	9
18-20 LST	0	0	1	4	21	12	12	9	16	8	4	0	7	7
21-23 LST	*	*	*	*	*	*	*	*	*	*	*	*	*	*
ALL HOURS	*	*	*	*	*	*	*	*	*	*	*	*	*	*
7. % FREQ OF RAIN AND/OR DRIZZLE:														
00-02 LST	*	*	*	*	*	*	*	*	*	*	*	*	*	*
03-05 LST	*	*	*	*	*	*	*	*	*	*	*	*	*	*
06-08 LST	0	0	#	0	7	7	2	3	8	5	4	1	3	3
09-11 LST	0	0	#	0	6	4	1	4	5	5	2	1	2	2
12-14 LST	0	1	#	1	12	12	7	10	12	14	6	2	6	6
15-17 LST	0	#	1	1	15	17	12	16	25	12	10	3	9	9
18-20 LST	1	0	0	4	19	13	12	21	20	23	9	2	10	10
21-23 LST	*	*	*	*	*	*	*	*	*	*	*	*	*	*
ALL HOURS	*	*	*	*	*	*	*	*	*	*	*	*	*	*
8. PERCENTAGE FREQUENCY OF OCCURRENCE (% FREQ) OF CEILING AND/OR VISIBILITY														
(CIG/VIS) < 1500/3 STATUTE MILES (MI) (SOURCE NO. 1):														
00-02 LST	*	*	*	*	*	*	*	*	*	*	*	*	*	*
03-05 LST	*	*	*	*	*	*	*	*	*	*	*	*	*	*
06-08 LST	1	0	1	5	7	9	6	4	13	15	13	5	7	7
09-11 LST	1	0	0	1	4	3	1	0	2	1	1	1	1	1
12-14 LST	#	#	0	#	2	3	1	1	3	1	1	0	1	1
15-17 LST	1	0	0	3	2	3	2	4	4	2	2	0	2	2
18-20 LST	0	0	0	5	8	0	4	4	3	4	2	0	3	3
21-23 LST	*	*	*	*	*	*	*	*	*	*	*	*	*	*
ALL HOURS	*	*	*	*	*	*	*	*	*	*	*	*	*	*
9. % FREQ OF CIG/VIS < 200/0.5 MI (SOURCE NO. 1):														
00-02 LST	*	*	*	*	*	*	*	*	*	*	*	*	*	*
03-05 LST	*	*	*	*	*	*	*	*	*	*	*	*	*	*
06-08 LST	0	0	0	1	1	5	2	#	4	5	5	3	2	2
09-11 LST	0	0	0	0	0	1	0	0	#	0	0	0	#	#
12-14 LST	0	#	0	0	0	0	0	#	0	#	0	0	#	#
15-17 LST	1	0	0	0	1	#	0	1	#	0	0	0	#	#
18-20 LST	0	0	0	0	2	0	2	0	1	0	0	0	#	#
21-23 LST	*	*	*	*	*	*	*	*	*	*	*	*	*	*
ALL HOURS	*	*	*	*	*	*	*	*	*	*	*	*	*	*

MARKS: * = DATA NOT AVAILABLE # = LESS THAN 0.5 DAY, OR 0.05 INCH, OR 0.5%, AS APPLICABLE

\$ = % CALM > PVLG DRCTN @ = BASED ON AVAIL. DATA, I.E., < 24 HRS/DAY OR < 12 MONTHS/YEAR

SOURCE(S): 1 USAFETAC DATSAV POR JAN 73 - DEC 85

2 NATIONAL INTELLIGENCE SURVEY 3-4 YEARS

STATION: LIMON INTL, COSTA RICA STATION #: 787670 ICAO ID: MRLM (USAFETAC, 1987)
 LOCATION: 9°58'N, 83°01'W ELEVATION (FT.): 7 LST = GMT: -6
 PREPARED BY: USAFETAC/ECR, 1985 PERIOD: VARIED(except items 6 & 7 MAY 73 - DEC 83)

SOURCE NO	JAN	FEB	MAR	APR	MAY	JUN	JUL	AUG	SEP	OCT	NOV	DEC	ANN
1. TEMPERATURE (°F)													
EXTREME MAX	1	90	92	92	95	94	94	90	90	94	91	92	95
MEAN DLY MAX	1	83	83	85	85	86	85	84	85	86	85	84	85
MEAN	1	78	79	80	81	82	81	80	81	82	81	80	80
MEAN DLY MIN	1	71	71	72	73	75	75	74	74	74	74	73	73
EXTREME MIN	1	64	61	64	66	67	68	67	70	68	68	67	61
# DAYS ≥ 90	1	#	#	2	4	7	4	1	2	3	2	2	28
# DAYS ≤ 32	1	0	0	0	0	0	0	0	0	0	0	0	0
# DAYS ≤ 0	1	0	0	0	0	0	0	0	0	0	0	0	0
2. PRECIPITATION (INCHES)													
MAXIMUM	2	27.5	15.2	17.9	41.6	22.6	21.5	35.3	25.2	10.7	12.0	41.4	173.4
MEAN	2	13.5	8.6	8.3	9.2	13.5	11.1	16.0	12.1	5.1	9.0	15.5	141.1
MINIMUM	2	5.4	0.8	2.3	1.8	5.4	2.7	7.5	2.8	1.1	0.7	6.3	95.9
MAX 24 HR	2	6.5	3.8	7.1	6.3	4.7	4.8	6.4	6.2	2.7	3.8	10.3	10.3
# DAYS ≥ 0.01	2	20	14	18	17	16	16	20	20	11	12	22	206
# DAYS ≥ 0.5		*	*	*	*	*	*	*	*	*	*	*	*
3. MEAN RELATIVE HUMIDITY (%) / VAPOR PRESSURE (IN Hg) / DEWPOINT (°F)													
RH (06 LST)	1	93	93	94	93	94	94	94	95	95	94	94	94
RH (13 LST)	1	70	71	68	70	72	74	76	75	74	76	76	73
VAPOR PRESS.	@1	.80	.80	.82	.84	.90	.90	.88	.88	.88	.87	.86	.85
DEWPOINT	1	72	72	72	73	75	75	74	75	75	74	74	74
4. SURFACE WINDS (16 PT/KNOTS) / 99.95% HIGHEST PRESSURE ALTITUDE (FEET)													
PVLG DRCTN	@1	W	W	E	E	N\$	W\$	W	N\$	N\$	N\$	W\$	W\$
MEAN SPEED	@1	5	5	5	5	5	5	4	4	5	5	5	5
MAX (PK GST)	@1	27	26	34	28	40	40	39	33	28	33	34	40
PRESSURE ALT	1	200	150	250	150	200	300	350	350	300	300	300	350
5. MEAN CLOUD COVER (EIGHTHS) / THUNDERSTORMS / FOG/ BLOWING SAND (BNBD)													
CLD COVER	1	6	6	6	7	7	7	7	7	7	7	6	7
DAYS TSMS	1	#	0	#	2	6	11	10	11	10	8	4	63
DAYS FOG	1	#	#	#	#	0	#	#	#	#	#	#	2
DAYS BNBD		*	*	*	*	*	*	*	*	*	*	*	*
6. PERCENTAGE FREQUENCY OF OCCURRENCE (% FREQ) OF THUNDERSTORMS:													
	JAN	FEB	MAR	APR	MAY	JUN	JUL	AUG	SEP	OCT	NOV	DEC	ANN
00-02 LST	*	*	*	*	*	*	*	*	*	*	*	*	*
03-05 LST	*	*	*	*	*	*	*	*	*	*	*	*	*
06-08 LST	0	0	#	2	5	15	18	15	10	5	3	2	6
09-11 LST	#	0	0	#	2	4	6	6	3	2	1	#	2
12-14 LST	0	0	#	#	3	6	2	6	5	4	1	1	2
15-17 LST	0	0	0	1	4	6	4	4	5	3	2	1	3
18-20 LST	0	0	0	1	4	11	5	6	6	7	2	1	4
21-23 LST	*	*	*	*	*	*	*	*	*	*	*	*	*
ALL HOURS @	#	0	0	1	4	8	7	8	6	4	2	1	4
7. % FREQ OF RAIN AND#R DRIZZLE:													
00-02 LST	*	*	*	*	*	*	*	*	*	*	*	*	*
03-05 LST	*	*	*	*	*	*	*	*	*	*	*	*	*
06-08 LST	22	23	19	18	14	19	29	23	11	14	24	20	20
09-11 LST	18	17	13	13	11	16	27	21	14	18	20	20	17
12-14 LST	11	12	9	9	8	10	17	15	9	16	21	16	13
15-17 LST	10	9	5	9	11	10	15	12	10	14	19	15	12
18-20 LST	18	15	15	13	18	21	27	17	17	26	29	21	20
21-23 LST	*	*	*	*	*	*	*	*	*	*	*	*	*
ALL HOURS @	15	15	12	12	11	14	22	18	12	16	22	18	16
8. PERCENTAGE FREQUENCY OF OCCURRENCE (% FREQ) OF CEILING AND/OR VISIBILITY (CIG/VIS) < 1500/3 STATUE MILES (MI) (SOURCE NO. 1):													
00-02 LST	*	*	*	*	*	*	*	*	*	*	*	*	*
03-05 LST	*	*	*	*	*	*	*	*	*	*	*	*	*
06-08 LST	9	7	3	7	4	6	7	6	1	1	4	6	5
09-11 LST	6	3	4	5	2	4	7	6	3	3	4	5	4
12-14 LST	5	4	1	3	2	2	4	5	2	2	3	4	3
15-17 LST	4	3	1	2	2	3	2	3	2	3	3	4	3
18-20 LST	8	2	3	3	1	2	2	4	3	4	6	6	4
21-23 LST	*	*	*	*	*	*	*	*	*	*	*	*	*
ALL HOURS	6	4	2	4	2	4	5	5	2	2	4	5	4
9. % FREQ OF CIG/VIS < 200/0.5 MI (SOURCE NO. 1):													
00-02 LST	*	*	*	*	*	*	*	*	*	*	*	*	*
03-05 LST	*	*	*	*	*	*	*	*	*	*	*	*	*
06-08 LST	0	0	0	1	1	1	0	1	#	0	#	1	#
09-11 LST	#	0	0	1	#	#	1	1	#	0	#	0	#
12-14 LST	#	#	0	0	#	#	0	#	#	#	#	#	#
15-17 LST	#	0	0	0	1	#	0	1	#	#	#	1	#
18-20 LST	0	0	0	0	#	0	0	0	#	0	#	0	#
21-23 LST	*	*	*	*	*	*	*	*	*	*	*	*	*
ALL HOURS	#	#	0	#	#	#	#	1	#	#	#	#	#

REMARKS: * = DATA NOT AVAILABLE # = LESS THAN 0.5 DAY, OR 0.05 INCH, OR 0.5%, AS APPLICABLE
 \$ = % CALM > PVLG DRCTN @ = BASED ON AVAIL. DATA, I.E., < 24 HRS/DAY OR < 12 MONTHS/YEAR
 SOURCE(S): 1. USAFETAC DATSAV POR MAY 73 - DEC 83
 2. NATIONAL INTELLIGENCE SURVEY POR VARIED

STATION: PUNTARENAS, COSTA RICA STATION #: 787600 ICAO ID: MRPT (USAFETAC, 1987)
 LOCATION: 9°58'N, 84°50'W ELEVATION (FT.): 7 LST = GMT: -6
 PREPARED BY: USAFETAC/ECR, 1986 PERIOD: VARIED(except items 6 & 7 JAN 73 - DEC 85)

SOURCE NO.	JAN	FEB	MAR	APR	MAY	JUN	JUL	AUG	SEP	OCT	NOV	DEC	ANN
1. TEMPERATURE (°F)													
EXTREME MAX	2	107	109	108	102	102	97	100	99	94	95	104	100
MEAN DLY MAX	2	95	94	96	93	91	89	90	89	89	89	90	91
MEAN	2	85	85	86	85	84	82	82	82	82	82	83	83
MEAN DLY MIN	2	74	75	75	76	76	74	74	74	74	73	74	74
EXTREME MIN	2	68	68	68	68	66	67	66	68	69	61	69	61
# DAYS ≥ 90	1	21	23	29	27	21	13	12	14	10	8	7	13
# DAYS ≤ 32	1	0	0	0	0	0	0	0	0	0	0	0	0
# DAYS ≤ 0	1	0	0	0	0	0	0	0	0	0	0	0	0
2. PRECIPITATION (INCHES)													
MAXIMUM	2	.2	4.0	.6	3.2	7.4	15.8	3.1	11.2	14.3	22.0	7.1	22
MEAN	2	#	.7	.2	1.3	4.0	8.4	8.3	6.6	10.0	11.8	4.1	.7
MINIMUM	2	0	0	0	0	.6	3.1	5.8	3.3	4.9	6.1	1.8	0
MAX 24 HR	2	.2	1.9	.5	3.2	2.8	2.6	2.6	2.8	2.9	3.9	1.9	2.2
# DAYS ≥ 0.004	2	#	1	1	2	7	14	14	10	14	13	7	2
# DAYS ≥ 0.5	*	*	*	*	*	*	*	*	*	*	*	*	*
3. MEAN RELATIVE HUMIDITY (%) / VAPOR PRESSURE (IN Hg) / DEWPOINT (°F)													
RH (06 LST)	1	88	86	85	87	93	95	95	96	96	97	96	92
RH (12 LST)	1	54	50	51	53	67	71	70	70	71	72	70	62
VAPOR PRESS.	1	.78	.78	.82	.87	.92	.93	.91	.91	.91	.91	.89	.84
DEWPOINT	1	71	71	72	74	76	76	76	76	76	76	75	73
4. SURFACE WINDS (16 KT/KNOTS) / 99.95% HIGHEST PRESSURE ALTITUDE (FEET)													
PVLG DRCTN	1	\$S	\$W	\$S	\$S	\$S	\$S	\$S	\$S	\$S	\$S	\$S	\$S
MEAN SPEED													
(PVLG DRCTN)	1	5	6	6	6	6	5	5	5	5	5	5	5
MEAN SPEED													
(ALL OBS)	1	4	5	4	4	3	2	2	2	2	2	3	3
MAX (PK GST)		*	*	*	*	*	*	*	*	*	*	*	*
PRESSURE ALT	1	150	150	200	150	150	150	150	150	150	150	150	150
5. MEAN CLOUD COVER (EIGHTHS) / THUNDERSTORMS / FOG/ BLOWING SAND (BNBD)													
CLD COVER	1	2	2	3	4	5	6	6	6	6	5	3	5
DAYS TSTMS	1	#	0	#	2	9	11	9	12	12	9	4	1
DAYS FOG < 7	1	#	0	#	#	1	1	1	1	1	1	#	7
DAYS BNBD < 7	1	0	0	0	0	#	#	0	0	0	#	0	#
6. PERCENTAGE FREQUENCY OF OCCURRENCE (% FREQ) OF THUNDERSTORMS:													
	JAN	FEB	MAR	APR	MAY	JUN	JUL	AUG	SEP	OCT	NOV	DEC	ANN
00-02 LST	*	*	*	*	*	*	*	*	*	*	*	*	*
03-05 LST	*	*	*	*	*	*	*	*	*	*	*	*	*
06-08 LST	0	0	0	0	#	#	1	1	1	#	0	#	#
09-11 LST	0	0	0	0	#	0	0	#	#	0	#	0	#
12-14 LST	0	0	#	1	8	7	7	8	11	7	2	#	4
15-17 LST	#	0	0	4	14	17	15	15	18	15	6	1	9
18-20 LST	1	0	1	2	9	11	12	8	15	11	4	#	6
21-23 LST	*	*	*	*	*	*	*	*	*	*	*	*	*
ALL HOURS	*	*	*	*	*	*	*	*	*	*	*	*	*
7. % FREQ OF RAIN AND/OR DRIZZLE:													
00-02 LST	*	*	*	*	*	*	*	*	*	*	*	*	*
03-05 LST	*	*	*	*	*	*	*	*	*	*	*	*	*
06-08 LST	0	0	#	0	5	4	3	3	4	5	1	1	2
09-11 LST	0	0	0	0	3	3	1	1	3	3	2	1	1
12-14 LST	#	0	0	#	3	3	2	4	4	5	3	1	2
15-17 LST	1	0	#	2	12	16	17	21	23	18	10	3	9
18-20 LST	#	0	#	4	17	30	32	30	37	30	15	2	16
21-23 LST	*	*	*	*	*	*	*	*	*	*	*	*	*
ALL HOURS	*	*	*	*	*	*	*	*	*	*	*	*	*
8. PERCENTAGE FREQUENCY OF OCCURRENCE (% FREQ) OF CEILING AND/OR VISIBILITY													
(CIG/VIS) < 1500/3 STATUTE MILES (MI) (SOURCE NO. 1):													
00-02 LST	*	*	*	*	*	*	*	*	*	*	*	*	*
03-05 LST	*	*	*	*	*	*	*	*	*	*	*	*	*
06-08 LST	0	0	1	0	2	1	1	2	3	3	2	#	1
09-11 LST	0	0	0	#	2	0	#	1	1	1	1	0	1
12-14 LST	0	0	0	#	1	1	#	1	1	2	1	0	1
15-17 LST	#	0	#	#	3	3	3	3	5	5	2	1	2
18-20 LST	1	1	0	1	5	5	4	6	6	5	3	1	3
21-23 LST	*	*	*	*	*	*	*	*	*	*	*	*	*
ALL HOURS	*	*	*	*	*	*	*	*	*	*	*	*	*
9. % FREQ OF CIG/VIS < 200/0.5 MI (SOURCE NO. 1):													
00-02 LST	*	*	*	*	*	*	*	*	*	*	*	*	*
03-05 LST	*	*	*	*	*	*	*	*	*	*	*	*	*
06-08 LST	0	0	#	0	0	1	#	0	#	0	0	0	#
09-11 LST	0	0	0	0	#	0	#	0	0	#	0	0	#
12-14 LST	0	0	0	0	0	#	#	0	#	#	0	0	#
15-17 LST	0	0	0	0	1	1	#	1	1	#	0	0	#
18-20 LST	9	9	9	#	0	#	#	1	1	#	0	0	#
21-23 LST	*	*	*	*	*	*	*	*	*	*	*	*	*
ALL HOURS	*	*	*	*	*	*	*	*	*	*	*	*	*

REMARKS: * = DATA NOT AVAILABLE # = LESS THAN 0.5 DAY, OR 0.05 INCH, OR 0.5%, AS APPLICABLE
 \$ = % CALM > PVLG DRCTN @ = BASED ON AVAIL. DATA, I.E., < 24 HRS/DAY OR < 12 MONTHS/YEAR
 SOURCE(S): 1 USAFETAC DATSAV POR JAN 73 - DEC 85
 2 NATIONAL INTELLIGENCE SURVEY 6 YEARS

STATION: SAN JOSE, COSTA RICA

STATION #: 787620

ICAO ID: MROC (USAFETAC, 1987)

LOCATION: 9°59'N, 84°13'W

ELEVATION (FT.): 3080 LST = GMT: -6

PREPARED BY: USAFETAC/ECR, 1986

PERIOD: VARIED(except items 6 & 7 JAN 73 - DEC 85)

	SOURCE NO.	JAN	FEB	MAR	APR	MAY	JUN	JUL	AUG	SEP	OCT	NOV	DEC	ANN
1. TEMPERATURE (°F)														
EXTREME MAX	2	90	91	92	91	88	92	84	86	87	88	87	84	92
MEAN DLY MAX	2	75	76	79	80	80	80	78	78	80	79	76	75	78
MEAN	2	67	67	69	70	71	71	70	70	70	68	67	69	69
MEAN DLY MIN	2	58	58	59	60	61	61	61	61	60	60	60	59	60
EXTREME MIN	2	43	44	48	50	52	54	53	61	54	53	52	45	43
# DAYS ≥ 90		*	*	*	*	*	*	*	*	*	*	*	*	*
# DAYS ≤ 32		*	*	*	*	*	*	*	*	*	*	*	*	*
# DAYS ≤ 0		*	*	*	*	*	*	*	*	*	*	*	*	*
2. PRECIPITATION (INCHES)														
MAXIMUM	2	2.5	1.6	3.7	5.2	17.1	19.9	17.4	19.7	26.2	29.4	16.3	6.5	117.7
MEAN	2	.5	.2	.5	1.7	8.7	10.6	8.4	9.5	12.8	13.1	5.9	1.8	73.6
MINIMUM	2	0	0	0	0	2.0	4.6	1.5	3.0	4.1	3.3	0.1	0.2	43.1
MAX 24 HR	2	.2	.7	.9	.9	3.2	2.4	1.9	2.3	3.3	4.0	3.4	1.3	4.0
# DAYS ≥ 0.004	2	2	4	2	7	18	25	22	21	26	25	18	9	177
# DAYS ≥ 0.5		*	*	*	*	*	*	*	*	*	*	*	*	*
3. MEAN RELATIVE HUMIDITY (%) / VAPOR PRESSURE (IN Hg) / DEWPOINT (°F)														
RH (06 LST)	1	49	46	44	46	62	66	62	63	67	68	63	52	58
RH (12 LST)	1	77	75	76	77	86	87	85	85	89	89	85	78	83
VAPOR PRESS.	1	.52	.51	.53	.56	.64	.65	.62	.62	.64	.64	.61	.55	.59
DEWPOINT	1	59	59	60	61	65	66	64	64	65	65	64	61	63
4. SURFACE WINDS (16 KT/KNOTS) / 99.95% HIGHEST PRESSURE ALTITUDE (FEET)														
PVLG DRCTN	1	E	E	E	E	E	E	E	E	E	E	E	E	E
MEAN SPEED														
(PVLG DRCTN)	1	19	19	18	17	13	12	14	13	10	11	13	17	16
MEAN SPEED														
(ALL OBS)	1	17	17	16	14	9	9	10	9	8	8	10	14	11
MAX (PK GST)		*	*	*	*	*	*	*	*	*	*	*	*	*
PRESSURE ALT	1	3150	3150	3200	3200	3150	3150	3150	3150	3150	3150	3150	3150	3150
5. MEAN CLOUD COVER (EIGHTHS) / THUNDERSTORMS / FOG/ BLOWING SAND (BNBD)														
CLD COVER	1	3	2	3	4	6	6	6	6	6	6	5	4	5
DAYS TSTMS	1	1	#	1	4	10	11	7	10	12	10	4	1	71
DAYS FOG < 7	1	1	#	#	2	6	9	5	9	11	13	9	3	69
DAYS BNBD < 7	1	#	#	#	#	0	0	#	#	#	#	#	#	#
6. PERCENTAGE FREQUENCY OF OCCURRENCE (% FREQ) OF THUNDERSTORMS:														
		JAN	FEB	MAR	APR	MAY	JUN	JUL	AUG	SEP	OCT	NOV	DEC	ANN
00-02 LST		0	0	0	0	0	0	#	0	0	0	#	0	#
03-05 LST		0	0	0	0	0	#	#	1	#	0	0	0	#
06-08 LST		0	0	0	0	0	#	#	0	0	0	0	0	#
09-11 LST		0	0	0	0	#	0	0	#	#	#	0	0	#
12-14 LST		0	0	#	1	7	7	4	6	8	7	2	0	3
15-17 LST		1	#	1	3	9	9	4	6	10	7	2	#	3
18-20 LST		#	0	0	#	2	2	1	2	3	1	#	0	1
21-23 LST		0	0	0	0	#	#	#	#	#	0	0	0	#
ALL HOURS		#	#	#	1	2	2	1	2	3	2	1	#	1
7. % FREQ OF RAIN AND/OR DRIZZLE:														
00-02 LST		#	0	#	1	7	7	5	6	7	8	7	3	3
03-05 LST		#	0	1	#	4	4	5	5	5	6	5	7	4
06-08 LST		#	#	#	1	2	5	4	4	3	5	4	6	3
09-11 LST		#	#	#	#	3	4	4	5	3	5	5	3	3
12-14 LST		#	#	1	4	14	17	12	17	23	24	14	2	10
15-17 LST		2	2	3	16	39	45	33	39	50	49	28	1	26
18-20 LST		2	2	2	8	32	39	26	33	44	40	24	2	21
21-23 LST		1	1	1	3	15	14	10	15	18	15	12	2	9
ALL HOURS		1	1	1	5	15	17	13	16	20	20	13	3	10
8. PERCENTAGE FREQUENCY OF OCCURRENCE (% FREQ) OF CEILING AND/OR VISIBILITY														
(CIG/VIS) < 1500/3 STATUE MILES (MI) (SOURCE NO. 1):														
00-02 LST		2	#	2	3	19	13	8	9	14	20	14	2	9
03-05 LST		1	1	1	2	9	7	5	4	8	11	9	1	4
06-08 LST		0	#	0	1	2	4	2	3	5	6	2	1	2
09-11 LST		#	#	#	1	5	1	1	#	#	1	1	1	1
12-14 LST		#	#	#	#	3	4	2	2	4	5	3	#	2
15-17 LST		1	#	#	2	13	17	11	15	25	26	18	3	11
18-20 LST		3	2	1	4	13	21	11	17	24	28	25	9	13
21-23 LST		2	1	3	5	16	13	12	12	17	20	19	5	10
ALL HOURS		1	1	1	2	10	10	7	8	12	13	11	3	7
9. % FREQ OF CIG/VIS < 200/0.5 MI (SOURCE NO. 1):														
00-02 LST		0	0	#	#	4	3	3	4	3	6	5	1	2
03-05 LST		1	1	0	0	#	1	2	3	1	5	3	1	2
06-08 LST		0	0	0	0	2	1	0	1	1	2	#	0	1
09-11 LST		#	#	0	#	#	1	1	0	#	0	#	0	#
12-14 LST		0	0	0	#	#	#	#	#	#	1	#	0	#
15-17 LST		#	0	0	1	1	2	1	2	2	2	3	0	1
18-20 LST		#	#	0	#	1	3	2	2	3	5	5	1	2
21-23 LST		0	0	0	#	3	3	2	3	3	5	5	1	2
ALL HOURS		#	#	#	#	1	2	1	2	2	3	3	1	1

REMARKS * = DATA NOT AVAILABLE # = LESS THAN 0.5 DAY, OR 0.05 INCH, OR 0.5%, AS APPLICABLE
 % = % CALM > PVLG DRCTN % = BASED ON AVAIL. DATA, I.E., < 24 HRS/DAY OR < 12 MONTHS/YEAR
 SOURCE(S) 1 USAFETAC DATSAV FOR JAN 73 - DEC 86
 2 NATIONAL INTELLIGENCE SURVEY 6 88 YEARS

STATION: FORT SHERMAN, PANAMA STATION #: 788010 ICAO ID: MPFS (USAFETAC, 1987)
 LOCATION: 9°22'N, 79°57'W ELEVATION (FT.): 10 LST = GMT: -5
 PREPARED BY: USAFETAC/ECR, 1984 PERIOD: JAN 73 - DEC 82 (except items 6/7 - DEC 84)

SOURCE NO.	JAN	FEB	MAR	APR	MAY	JUN	JUL	AUG	SEP	OCT	NOV	DEC	ANN
1 TEMPERATURE (°F)													
EXTREME MAX	88	92	92	94	95	93	91	93	94	95	92	90	95
MEAN DLY MAX	84	85	85	86	86	86	85	85	86	86	84	85	85
MEAN	80	81	81	82	81	81	81	81	81	81	80	81	81
MEAN DLY MIN	76	76	77	77	76	76	76	76	75	75	75	76	76
EXTREME MIN	69	69	67	72	71	68	70	70	70	70	69	66	66
# DAYS ≥ 90	0	#	#	#	1	#	#	#	#	1	#	#	3
# DAYS ≤ 32	0	0	0	0	0	0	0	0	0	0	0	0	0
# DAYS ≤ 0	0	0	0	0	0	0	0	0	0	0	0	0	0
2 PRECIPITATION (INCHES)													
MAXIMUM	19.2	12.4	9.2	21.7	25.4	31.2	27.7	26.6	23.0	42.2	43.1	34.4	183.4
MEAN	3.3	1.6	1.5	4.0	12.5	13.2	15.5	15.4	12.5	15.8	22.5	12.1	129.8
MINIMUM	#	#	#	0.1	1.6	5.9	4.4	5.8	3.1	5.8	6.6	0.9	86.5
MAX 24 HR	3.4	7.9	4.2	6.7	7.5	8.5	6.8	6.9	7.5	11.0	10.4	10.3	11.0
# DAYS ≥ 0.01	16	13	11	14	21	23	25	25	23	24	25	22	242
# DAYS ≥ 0.5	*	*	*	*	*	*	*	*	*	*	*	*	*
3 MEAN RELATIVE HUMIDITY (%) / VAPOR PRESSURE (IN Hg) / DEWPOINT (°F)													
RH (06 LST)	83	81	83	83	92	94	93	95	94	96	94	88	91
RH (13 LST)	72	70	68	70	76	80	81	80	77	77	81	77	76
VAPOR PRESS. @	87	85	85	87	93	93	93	94	93	92	92	89	91
DEWPOINT @	74	74	74	74	76	76	76	77	76	76	76	75	75
4 SURFACE WINDS (16 PT/KNOTS) / 99.95% HIGHEST PRESSURE ALTITUDE (FEET)													
PVLG DRCTN @	NE	NE	NE	NE	\$NE	\$WSW	\$W	\$W	\$W	\$W	\$W	NE	\$W
MEAN SPEED @	6	5	5	5	3	3	4	3	3	3	3	4	3
MAX (PK GST)	26	27	32	24	25	22	21	30	26	30	26	26	32
PRESSURE ALT @	350	350	350	350	350	350	350	350	350	350	400	350	400
5 MEAN CLOUD COVER (EIGHTHS) / THUNDERSTORMS / FOG/ BLOWING SAND (BNBD)													
CLD COVER @	5	5	5	6	7	7	7	7	7	7	7	6	6
DAYS TSTMS	0	0	#	2	12	15	16	16	15	14	8	2	100
DAYS FOG @	0	0	0	#	#	0	#	0	#	#	0	0	1
DAYS BNBD													

6 PERCENTAGE FREQUENCY OF OCCURRENCE (% FREQ) OF THUNDERSTORMS:

	JAN	FEB	MAR	APR	MAY	JUN	JUL	AUG	SEP	OCT	NOV	DEC	ANN
00-02 LST	*	*	*	*	*	*	*	*	*	*	*	*	*
03-05 LST	*	*	*	*	*	*	*	*	*	*	*	*	*
06-08 LST	0	0	1	2	7	11	11	13	12	12	4	2	6
09-11 LST	0	0	#	4	3	7	10	9	7	7	3	1	4
12-14 LST	0	0	1	3	9	14	10	13	14	11	4	1	7
15-17 LST	0	0	2	3	12	24	25	25	19	27	6	2	12
18-20 LST	*	*	*	*	*	*	*	*	*	*	*	*	*
21-23 LST	*	*	*	*	*	*	*	*	*	*	*	*	*
ALL HOURS @	0	0	1	3	7	12	13	14	12	12	4	2	7

7 % FREQ OF RAIN AND/OR DRIZZLE:

00-02 LST	*	*	*	*	*	*	*	*	*	*	*	*	*
03-05 LST	*	*	*	*	*	*	*	*	*	*	*	*	*
06-08 LST	1	1	1	3	8	11	14	12	8	9	12	7	7
09-11 LST	2	2	2	4	8	10	12	10	6	11	13	6	7
12-14 LST	1	1	1	2	7	13	10	12	8	11	13	9	7
15-17 LST	0	3	#	3	10	15	13	19	16	23	12	8	12
18-20 LST	*	*	*	*	*	*	*	*	*	*	*	*	*
21-23 LST	*	*	*	*	*	*	*	*	*	*	*	*	*
ALL HOURS @	2	2	1	3	8	12	13	9	12	13	7	8	

8 PERCENTAGE FREQUENCY OF OCCURRENCE (% FREQ) OF CEILING AND/OR VISIBILITY

(CIG/VIS) < 1500/3 STATUTE MILES (MI) (SOURCE NO. 1):

00-02 LST	*	*	*	*	*	*	*	*	*	*	*	*	*
03-05 LST	*	*	*	*	*	*	*	*	*	*	*	*	*
06-08 LST	9	5	8	19	18	31	31	33	14	13	20	13	18
09-11 LST	6	4	8	14	17	23	23	23	10	15	16	7	14
12-14 LST	3	2	3	8	15	25	24	16	12	18	20	7	13
15-17 LST	3	4	2	9	25	38	33	30	19	24	20	11	18
18-20 LST	*	*	*	*	*	*	*	*	*	*	*	*	*
21-23 LST	*	*	*	*	*	*	*	*	*	*	*	*	*
ALL HOURS @	5	4	6	14	18	28	28	26	14	17	19	9	16

9 % FREQ OF CIG/VIS < 200/0.5 MI (SOURCE NO. 1):

00-02 LST	*	*	*	*	*	*	*	*	*	*	*	*	*
03-05 LST	*	*	*	*	*	*	*	*	*	*	*	*	*
06-08 LST	#	0	0	0	0	0	#	0	#	0	0	#	#
09-11 LST	0	0	0	0	0	0	0	0	#	0	0	0	0
12-14 LST	0	0	0	0	0	#	0	0	0	0	0	0	0
15-17 LST	0	0	0	0	0	1	0	0	0	0	0	0	#
18-20 LST	*	*	*	*	*	*	*	8	*	*	*	*	*
21-23 LST	*	*	*	*	*	*	*	*	*	*	*	*	*
ALL HOURS @	#	0	0	0	0	#	#	0	#	#	0	0	#

REMARKS * = DATA NOT AVAILABLE # = LESS THAN 0.5 DAY, OR 0.05 INCH, OR 0.5%, AS APPLICABLE
 \$ = % CALM > PVLG DRCTN @ = BASED ON AVAIL DATA, I.E., < 24 HRS/DAY OR < 12 MONTHS/YEAR
 SOURCE(S) 1 USAFETAC DATSAV
 2 NATIONAL INTELLIGENCE SURVEY (CRISTOBAL, PANAMA)

STATION: PANAMA CITY, PANAMA

LOCATION: 9°05'N, 79°22'W

PREPARED BY: USAFETAC/ECR DEC 1983

STATION #: 787920

ELEVATION (FT.): 134

PERIOD: JAN 73-DEC 82

ICAO ID: MPTO

LST = GMT: -5

(USAFETAC,

1987)

SOURCE NO.	JAN	FEB	MAR	APR	MAY	JUN	JUL	AUG	SEP	OCT	NOV	DEC	ANN
1. TEMPERATURE (°F)													
EXTREME MAX	102	95	95	95	102	95	100	97	95	102	102	93	102
MEAN DLY MAX	88	89	90	90	88	87	88	87	86	85	86	88	87
MEAN	79	80	81	81	81	80	79	79	78	78	78	79	79
MEAN DLY MIN	71	72	73	74	74	74	73	73	74	73	73	72	73
EXTREME MIN	64	64	63	69	69	70	69	69	69	70	66	64	63
# DAYS ≥ 90	4	8	13	13	6	4	6	5	2	2	2	4	69
# DAYS ≤ 32	0	0	0	0	0	0	0	0	0	0	0	0	0
# DAYS ≤ 0	0	0	0	0	0	0	0	0	0	0	0	0	0
2. PRECIPITATION (INCHES)													
MAXIMUM	*	*	*	*	*	*	*	*	*	*	*	*	*
MEAN	1.98	0.85	0.29	2.05	9.31	8.16	8.65	8.53	7.91	12.18	10.92	6.55	77.4
MINIMUM	*	*	*	*	*	*	*	*	*	*	*	*	*
MAX 24 HR	*	*	*	*	*	*	*	*	*	*	*	*	*
# DAYS ≥ 0.01	3	2	1	3	12	13	14	14	11	14	16	11	14
# DAYS ≥ 0.5	*	*	*	*	*	*	*	*	*	*	*	*	*
3. MEAN RELATIVE HUMIDITY (%) / VAPOR PRESSURE (IN Hg) / DEWPOINT (°F)													
RH (04 LST)	86	82	81	84	92	94	93	94	94	95	94	91	90
RH (13 LST)	64	60	59	64	63	78	78	78	79	80	78	70	72
VAPOR PRESS.	.75	.73	.74	.79	.87	.88	.87	.87	.87	.87	.86	.81	.83
DEWPOINT	70	69	69	71	74	75	74	74	74	74	74	72	72
4. SURFACE WINDS (16 PT/KNOTS) / 99.95% HIGHEST PRESSURE ALTITUDE (FEET)													
PVLG DRCTN	NNE	NNE	NNE	NNE	S	S	WNW	WNW	S	S	WNW	ENE	NNE
MEAN SPEED	5	6	6	6	4	3	4	4	4	4	4	4	4
MAX (PK GST)	32	22	24	30	16	20	30	20	24	20	20	32	32
PRESSURE ALT	350	400	400	400	400	350	350	350	350	350	350	350	400
5. MEAN CLOUD COVER (EIGHTHS) / THUNDERSTORMS / FOG													
CLD COVER	4	3	4	5	7	7	7	6	7	8	7	4	6
DAYS TSTMS	1	#	1	4	14	16	16	16	17	18	11	4	118
DAYS FOG	1	#	1	1	2	1	1	1	2	2	1	1	14
6. PERCENTAGE FREQUENCY OF OCCURRENCE (% FREQ) OF THUNDERSTORMS:													
	JAN	FEB	MAR	APR	MAY	JUN	JUL	AUG	SEP	OCT	NOV	DEC	ANN
00-02 LST	0	0	0	1	1	2	2	2	4	2	1	0	1
03-05 LST	0	0	0	0	1	4	4	3	2	2	1	0	1
06-08 LST	0	0	0	#	2	2	3	2	1	2	1	#	1
09-11 LST	0	#	0	#	2	2	2	2	4	2	1	#	1
12-14 LST	1	0	#	2	9	9	10	11	11	14	8	3	7
15-17 LST	#	#	1	3	13	16	17	19	18	18	9	2	10
18-20 LST	0	0	0	1	3	6	7	6	5	7	2	1	3
21-23 LST	0	0	0	#	1	2	2	2	4	5	1	#	1
ALL HOURS	#	#	#	3	4	5	6	6	6	6	3	1	3
7. % FREQ OF RAIN AND/OR DRIZZLE:													
00-02 LST	#	1	#	3	5	6	4	5	6	10	6	1	4
03-05 LST	0	#	#	2	6	7	5	5	8	6	6	3	4
06-08 LST	1	#	#	2	5	9	7	5	7	8	5	3	4
09-11 LST	#	1	1	3	7	11	9	9	10	10	7	3	6
12-14 LST	3	#	2	4	13	13	8	14	13	18	16	6	10
15-17 LST	2	1	1	6	17	17	14	19	14	22	17	6	11
18-20 LST	1	1	#	3	8	13	11	14	14	18	10	3	8
21-23 LST	1	#	#	1	4	8	4	7	6	13	7	2	4
ALL HOURS	1	1	1	3	8	10	8	10	10	13	9	3	6
8. PERCENTAGE FREQUENCY OF OCCURRENCE (% FREQ) OF CEILING AND/OR VISIBILITY (CIG/VIS) < 1500/3 STATUTE MILES (MI) (SOURCE NO. 1):													
00-02 LST	#	0	#	#	1	2	#	1	1	2	1	#	1
03-05 LST	0	0	#	1	3	2	#	1	2	1	1	1	1
06-08 LST	#	0	1	2	3	1	1	2	2	1	1	1	1
09-11 LST	#	#	#	3	3	3	2	3	4	3	2	#	2
12-14 LST	#	0	#	2	3	4	2	3	4	5	3	#	2
15-17 LST	1	0	#	3	3	3	2	3	3	4	4	1	2
18-20 LST	0	0	#	1	2	3	1	2	3	4	3	1	2
21-23 LST	#	0	0	#	1	1	#	2	#	3	3	1	1
ALL HOURS	#	0	#	1	2	2	1	2	2	3	2	1	2
9. % FREQ OF CIG/VIS < 200/0.5 MI (SOURCE NO. 1):													
00-02 LST	0	0	0	0	0	0	#	#	0	0	0	0	#
03-05 LST	0	0	#	0	#	0	#	0	#	#	#	#	#
06-08 LST	0	0	0	0	#	0	#	0	#	#	0	#	#
09-11 LST	0	0	0	0	0	0	#	0	0	#	0	0	#
12-14 LST	0	0	0	0	0	0	#	0	0	#	0	#	#
15-17 LST	0	0	0	0	0	#	0	0	0	#	0	0	#
18-20 LST	0	0	0	0	0	#	0	#	#	0	0	0	#
21-23 LST	0	0	0	0	0	0	0	#	0	0	0	0	#
ALL HOURS	0	0	#	0	#	#	#	#	#	#	0	#	#

REMARKS: * = DATA NOT AVAILABLE # = LESS THAN 0.5 DAY, OR 0.05 INCH, OR 0.5%, AS APPLICABLE

= % CALM > PVLG DRCTN @ = BASED ON AVAIL. DATA, I.E., < 24 HRS/DAY OR < 12 MONTHS/YEAR

SOURCE(S): 1 USAFETAC DATSAV POR JAN 73 - DEC 82

STATION: RIO HATO, PANAMA

LOCATION: 8°23'N, 80°07'W

PREPARED BY: USAFETAC/ECR, 1983

STATION #: 788078

ELEVATION (FT.): 98

PERIOD: JAN 73 - DEC 82

ICAO ID: MPRH

LST = GMT: -5

(USAFETAC, 1987)

SOURCE NO.	JAN	FEB	MAR	APR	MAY	JUN	JUL	AUG	SEP	OCT	NOV	DEC	ANN
1. TEMPERATURE (°F)													
EXTREME MAX	97	96	97	97	95	94	96	94	93	92	96	96	97
MEAN DLY MAX	90	91	91	91	88	87	87	87	87	86	87	88	88
MEAN	82	83	83	83	81	80	81	80	80	79	80	81	81
MEAN DLY MIN	73	74	74	75	74	73	74	73	73	72	73	73	73
EXTREME MIN	66	68	67	68	71	69	67	66	68	69	67	67	66
# DAYS ≥ 90	18	20	22	21	9	5	7	5	4	4	4	9	127
# DAYS ≤ 32	0	0	0	0	0	0	0	0	0	0	0	0	0
# DAYS ≤ 0	0	0	0	0	0	0	0	0	0	0	0	0	0
2. PRECIPITATION (INCHES)													
MAXIMUM	0.79	0.06	0.25	0.85	5.55	11.01	9.59	9.53	7.76	14.73	11.2	4.56	14.73
MEAN	0.29	0.02	0.05	0.41	3.99	5.41	4.66	4.87	4.45	7.73	6.02	2.94	40.91
MINIMUM	*	*	*	*	*	*	*	*	*	*	*	*	*
MAX 24 HR	0.69	0.06	0.15	0.69	2.15	2.14	2.40	2.25	2.88	2.80	4.89	2.36	4.89
# DAYS ≥ 0.01	2	1	1	4	13	15	15	14	13	20	20	12	128
# DAYS ≥ 0.5	#	0	0	#	3	5	4	4	3	7	5	2	33
3. MEAN RELATIVE HUMIDITY (%) / VAPOR PRESSURE (IN Hg) / DEWPOINT (°F)													
RH (04 LST)	*	*	*	*	*	*	*	*	*	*	*	*	*
RH (13 LST)	*	*	*	*	*	*	*	*	*	*	*	*	*
VAPOR PRESS.	.75	.73	.74	.79	.87	.88	.87	.87	.87	.87	.86	.81	.83
DEWPOINT	70	69	69	71	74	75	74	74	74	74	74	72	72
4. SURFACE WINDS (16 PT/KNOTS) / 99.95% HIGHEST PRESSURE ALTITUDE (FEET)													
PVLG DRCTN	NW	NW	NW	NW	ESE	SSE	SSE	SSE	SSE	SSE	WNW	NW	NW
MEAN SPEED	10	11	11	9	7	5	6	6	5	5	6	7	7
MAX (PK GST)	30	30	32	30	30	22	36	30	20	20	26	30	36
PRESSURE ALT	150	150	250	250	250	250	150	200	200	200	250	200	250
5. MEAN CLOUD COVER (EIGHTHS) / THUNDERSTORMS / FOG / BLOWING SAND (BNBD)													
CLD COVER	*	*	*	*	*	*	*	*	*	*	*	*	*
DAYS TSTMS	#	#	#	1	4	5	3	4	5	5	2	1	30
DAYS FOG	0	0	#	1	0	0	#	0	0	#	#	0	1
6. PERCENTAGE FREQUENCY OF OCCURRENCE (% FREQ) OF THUNDERSTORMS:													
JAN	FEB	MAR	APR	MAY	JUN	JUL	AUG	SEP	OCT	NOV	DEC	ANN	
00-02 LST	*	*	*	*	*	*	*	*	*	*	*	*	*
03-05 LST	*	*	*	*	*	*	*	*	*	*	*	*	*
06-08 LST	0	0	0	0	1	2	2	1	0	0	0	1	1
09-11 LST	0	0	#	#	1	1	2	1	#	0	0	1	1
12-14 LST	0	0	0	1	2	3	1	1	3	4	1	#	1
15-17 LST	#	0	0	1	3	5	3	3	4	4	3	1	2
18-20 LST	1	0	0	1	3	2	3	4	3	5	2	2	2
21-23 LST	*	*	*	*	*	*	*	*	*	*	*	*	*
ALL HOURS	#	0	#	1	2	3	2	2	2	3	1	1	1
7. % FREQ OF RAIN AND/OR DRIZZLE:													
00-02 LST	*	*	*	*	*	*	*	*	*	*	*	*	*
03-05 LST	*	*	*	*	*	*	*	*	*	*	*	*	*
06-08 LST	0	0	0	2	1	3	3	2	0	2	0	1	1
09-11 LST	0	0	#	2	1	4	3	3	2	1	2	1	2
12-14 LST	#	0	#	2	2	3	3	4	3	4	5	3	2
15-17 LST	1	0	#	2	4	5	2	3	4	6	6	2	2
18-20 LST	1	0	1	3	3	3	2	4	4	10	5	2	3
21-23 LST	*	*	*	*	*	*	*	*	*	*	*	*	*
ALL HOURS	#	0	#	2	2	4	3	3	3	4	4	2	3
8. PERCENTAGE FREQUENCY OF OCCURRENCE (% FREQ) OF CEILING AND/OR VISIBILITY (CIG/VIS) < 1500/3 STATUTE MILES (MI) (SOURCE NO. 1):													
00-02 LST	*	*	*	*	*	*	*	*	*	*	*	*	*
03-05 LST	*	*	*	*	*	*	*	*	*	*	*	*	*
06-08 LST	0	0	0	3	1	1	1	0	1	1	3	0	1
09-11 LST	0	0	0	1	#	1	1	#	1	1	1	#	1
12-14 LST	0	0	0	0	#	1	#	#	1	1	1	#	1
15-17 LST	0	0	1	1	1	1	1	1	2	2	1	1	1
18-20 LST	*	*	*	*	*	*	*	*	*	*	*	*	*
21-23 LST	*	*	*	*	*	*	*	*	*	*	*	*	*
ALL HOURS	0	0	#	1	1	1	1	#	1	1	2	#	1
9. % FREQ OF CIG/VIS < 200/0.5 MI (SOURCE NO. 1):													
00-02 LST	*	*	*	*	*	*	*	*	*	*	*	*	*
03-05 LST	*	*	*	*	*	*	*	*	*	*	*	*	*
06-08 LST	0	0	0	0	0	0	0	0	0	0	0	0	0
09-11 LST	0	0	0	0	0	0	0	0	0	0	0	0	0
12-14 LST	0	0	0	0	0	0	0	0	0	0	0	0	0
15-17 LST	0	0	#	0	0	0	0	0	0	0	0	0	0
18-20 LST	*	*	*	*	*	*	*	*	*	*	*	*	*
21-23 LST	*	*	*	*	*	*	*	*	*	*	*	*	*
ALL HOURS	0	0	#	0	0	0	0	0	0	0	0	0	0

REMARKS. * = DATA NOT AVAILABLE # = LESS THAN 0.5 DAY, OR 0.05 INCH, OR 0.5%, AS APPLICABLE

\$ = % CALM > PVLG DRCTN @ = BASED ONLY ON AVAILABLE DATA

SOURCE(S). 1. USAFETAC DATSAV

STATION: SAN ANDRES ISLAND, COLUMBIA
 LOCATION: 12°35'N, 81°42'W
 PREPARED BY: USAFETAC/ECR JUN 1986

STATION #: 800010
 ELEVATION (FT.): 7
 PERIOD: JAN 73-DEC 84

ICAO ID: MCSP (USAFETAC,
 LST = GMT: -5 1987)

SOURCE NO.	JAN	FEB	MAR	APR	MAY	JUN	JUL	AUG	SEP	OCT	NOV	DEC	ANN	
1. TEMPERATURE (°F)														
EXTREME MAX	1	101	100	100	101	104	102	104	104	100	100	102	99	104
MEAN DLY MAX	1	83	83	84	84	85	85	85	85	85	85	84	83	84
MEAN	1	80	80	81	82	83	83	82	82	82	82	82	81	82
MEAN DLY MIN	1	78	78	79	79	80	80	80	80	79	78	79	78	79
EXTREME MIN	1	69	69	69	73	68	68	69	64	65	64	63	68	63
# DAYS≥90	1	1	2	1	2	2	2	1	2	1	1	1	1	17
# DAYS≤32	1	0	0	0	0	0	0	0	0	0	0	0	0	0
# DAYS≤0	1	0	0	0	0	0	0	0	0	0	0	0	0	0
2. PRECIPITATION (INCHES)														
MAXIMUM		*	*	*	*	*	*	*	*	*	*	*	*	*
MEAN	1	12	11	9	8	12	18	20	20	18	22	21	19	190
MINIMUM		*	*	*	*	*	*	*	*	*	*	*	*	*
MAX 24 HR		*	*	*	*	*	*	*	*	*	*	*	*	*
# DAYS≥0.01		*	*	*	*	*	*	*	*	*	*	*	*	*
# DAYS≥0.5		*	*	*	*	*	*	*	*	*	*	*	*	*
3. MEAN RELATIVE HUMIDITY (%) / VAPOR PRESSURE (IN Hg) / DEWPOINT (°F)														
RH (06 LST)	1	81	82	81	80	84	86	85	85	85	84	82	83	83
RH (15 LST)	1	74	74	72	73	76	78	79	79	78	79	78	77	77
VAPOR PRESS.	1	83	82	83	86	92	94	93	94	93	92	90	86	89
DEWPOINT	1	73	73	73	74	76	77	76	77	76	76	75	74	75
4. SURFACE WINDS (16 PT/KNOTS) / 99.95% HIGHEST PRESSURE ALTITUDE (FEET)														
PVLG DRCTN	1	ENE	ENE	ENE	ENE	E	E	ENE	ENE	E	E	ENE	ENE	ENE
MEAN SPEED														
(PVLG DRCTN)	1	16	15	14	14	13	17	18	16	13	13	17	18	16
MEAN SPEED														
(ALL OBS)	1	16	15	14	13	12	15	17	14	10	11	14	18	14
MAX (PK GST)	1	*	*	*	*	*	*	*	*	*	*	*	*	*
PRESSURE ALT	1	150	200	200	200	250	350	300	200	350	250	250	250	350
5. MEAN CLOUD COVER (EIGHTHS) / THUNDERSTORMS / FOG/ BLOWING SAND (BNBD)														
CLD COVER	1	3	3	3	4	4	5	5	5	5	5	4	4	4
DAYS TSTMS	1	#	#	#	0	2	7	6	7	9	7	4	#	42
DAYS FOG < 7	1@	#	#	#	#	#	0	0	#	#	0	0	#	#
DAYS BNBD < 7	1@	0	0	0	0	0	0	0	0	0	0	0	0	0
6. PERCENTAGE FREQUENCY OF OCCURRENCE (% FREQ) OF THUNDERSTORMS:														
	JAN	FEB	MAR	APR	MAY	JUN	JUL	AUG	SEP	OCT	NOV	DEC	ANN	
00-02 LST	*	*	*	*	*	*	*	*	*	*	*	*	1	
03-05 LST	*	*	*	*	*	*	*	*	*	*	*	*	#	
06-08 LST	0	0	0	0	1	3	2	2	4	4	1	0	1	
09-11 LST	0	0	0	0	#	3	2	2	3	3	#	#	1	
12-14 LST	0	0	0	0	1	2	4	2	5	3	1	#	1	
15-17 LST	0	0	0	0	#	3	3	2	5	5	1	#	2	
18-20 LST	#	0	0	0	#	2	2	2	3	4	2	#	1	
21-23 LST	0	0	0	0	1	3	2	3	3	3	2	0	1	
ALL HOURS	#	#	#	0	#	3	3	2	4	4	1	#	1	
7. % FREQ OF RAIN AND/OR DRIZZLE:														
00-02 LST	*	*	*	*	*	*	*	*	*	*	*	*	2	
03-05 LST	*	*	*	*	*	*	*	*	*	*	*	*	1	
06-08 LST	2	2	1	1	3	8	4	6	6	10	8	5	5	
09-11 LST	2	1	1	1	3	7	5	7	9	8	7	4	5	
12-14 LST	1	1	1	1	4	7	7	5	8	14	8	4	5	
15-17 LST	2	2	1	1	3	7	6	6	9	14	8	4	5	
18-20 LST	2	1	1	1	3	7	6	4	6	8	8	6	5	
21-23 LST	2	1	#	#	1	5	4	4	3	5	8	3	3	
ALL HOURS	2	1	1	1	3	7	5	5	7	10	8	4	5	
8. PERCENTAGE FREQUENCY OF OCCURRENCE (% FREQ) OF CEILING AND/OR VISIBILITY (CIG/VIS) < 1500/3 STATUE MILES (MI) (SOURCE NO. 1):														
00-02 LST	*	*	*	*	*	*	*	*	*	*	*	*	*	
03-05 LST	*	*	*	*	*	*	*	*	*	*	*	*	*	
06-08 LST	#	1	1	#	#	1	1	#	1	#	#	#	#	
09-11 LST	0	#	0	0	#	1	#	#	1	#	#	#	#	
12-14 LST	#	#	#	#	#	#	#	1	#	#	1	#	#	
15-17 LST	0	#	#	#	#	#	1	#	#	#	1	#	#	
18-20 LST	0	1	#	1	#	#	1	1	1	#	#	0	#	
21-23 LST	#	1	#	#	#	1	1	1	#	#	0	#	#	
ALL HOURS	#	1	#	#	#	1	1	1	1	#	#	#	#	
9. % FREQ OF CIG/VIS < 200/0.5 MI (SOURCE NO. 1)														
00-02 LST	*	*	*	*	*	*	*	*	*	*	*	*	*	
03-05 LST	*	*	*	*	*	*	*	*	*	*	*	*	*	
06-08 LST	0	#	0	0	#	#	#	0	#	0	0	0	#	
09-11 LST	0	0	0	0	0	#	#	#	#	0	0	0	#	
12-14 LST	#	0	#	0	0	#	#	1	#	0	#	0	#	
15-17 LST	0	#	#	#	0	#	#	#	0	0	0	0	#	
18-20 LST	0	#	#	#	#	0	#	#	#	0	0	0	#	
21-23 LST	#	#	0	0	#	#	#	1	#	#	0	0	#	
ALL HOURS	#	#	#	#	#	#	#	#	#	#	0	#	#	

REMARKS * = DATA NOT AVAILABLE # = LESS THAN 0.5 DAY, OR 0.05 INCH, OR 0.5%, AS APPLICABLE
 \$ = % CALM > PVLG DRCTN @ = BASED ON AVAIL. DATA, I.E., < 24 HRS/DAY OR < 12 MONTHS/YEAR
 SOURCE(S) 1 USAFETAC DATSAV POR JAN 73 - DEC 84

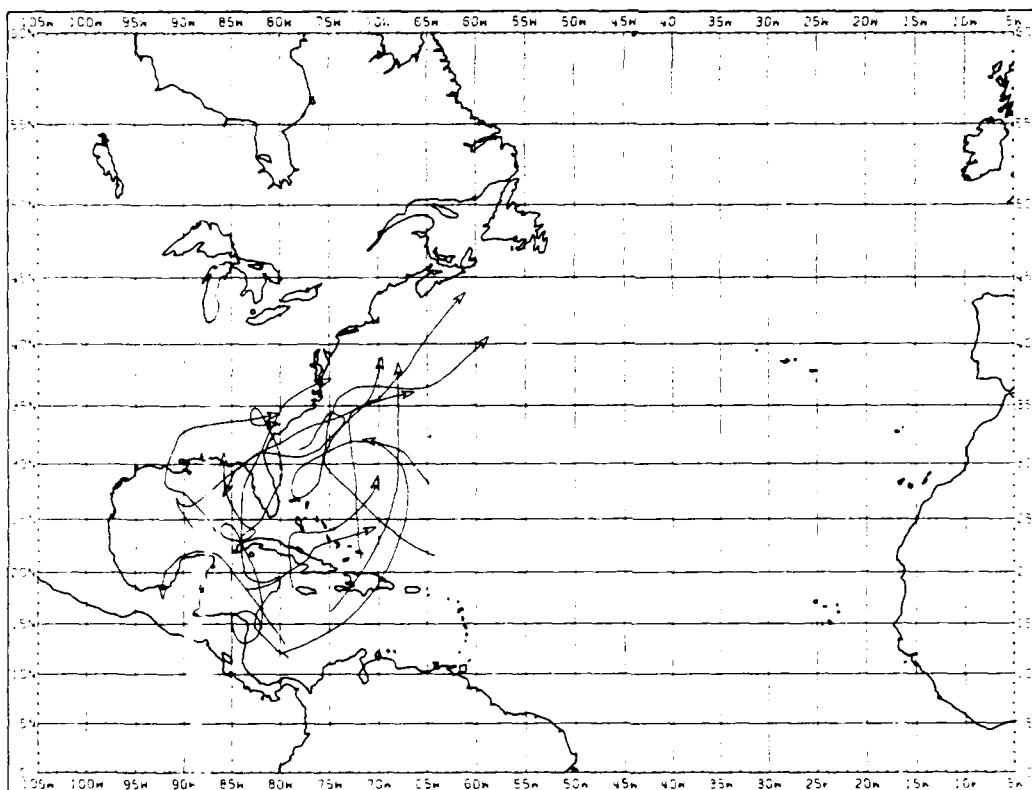
Appendix C

Tracks of North Atlantic Ocean Tropical Cyclones

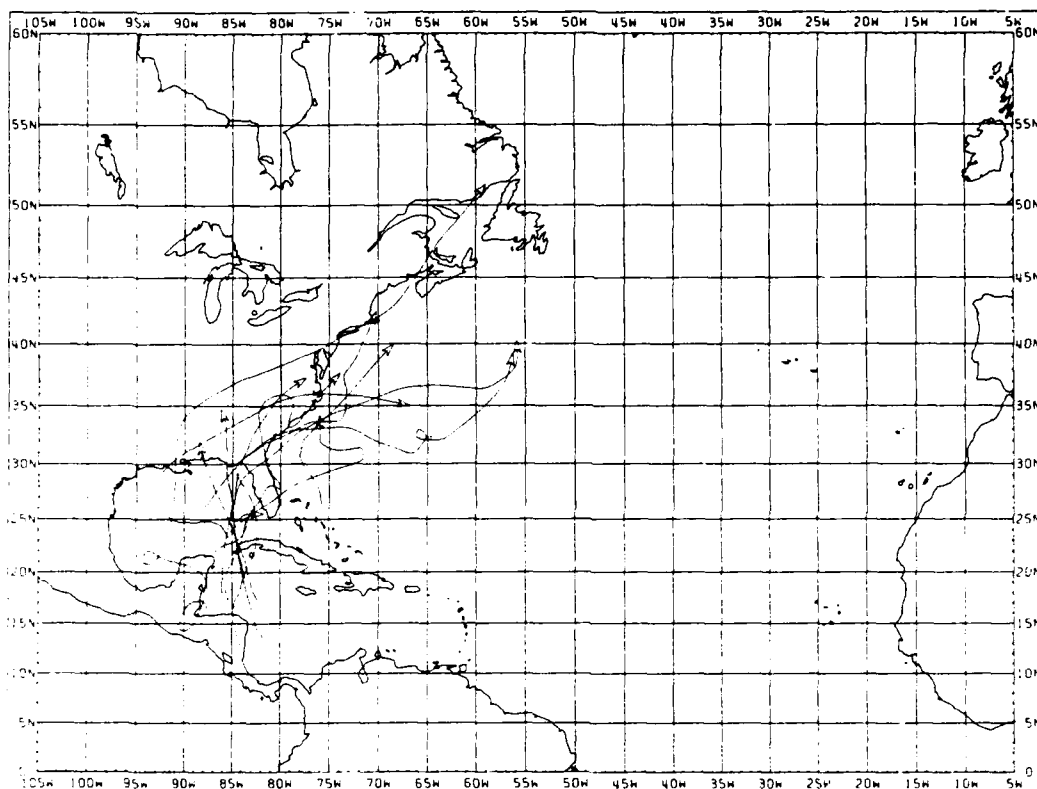
Tracks of North Atlantic Tropical Cyclones for the "official" hurricane season (1 June–30 November) are given for 10- (or 11-) day periods during the period 1886 through 1986. However, for the month preceding and the month following the "official" hurricane season, i.e., May and December, respectively, the tracks cover the entire 31 days.

The tracks of this appendix were computer drawn. The storms were assigned to the months, or to the 10- (or 11-) day periods, in which they **initially** reached tropical storm strength. The portion of their tracks during which they were either a tropical depression, a tropical storm or a hurricane is not specified. However the plotting of each track indicates that the cyclone reached tropical storm strength sometime during the specified time period.

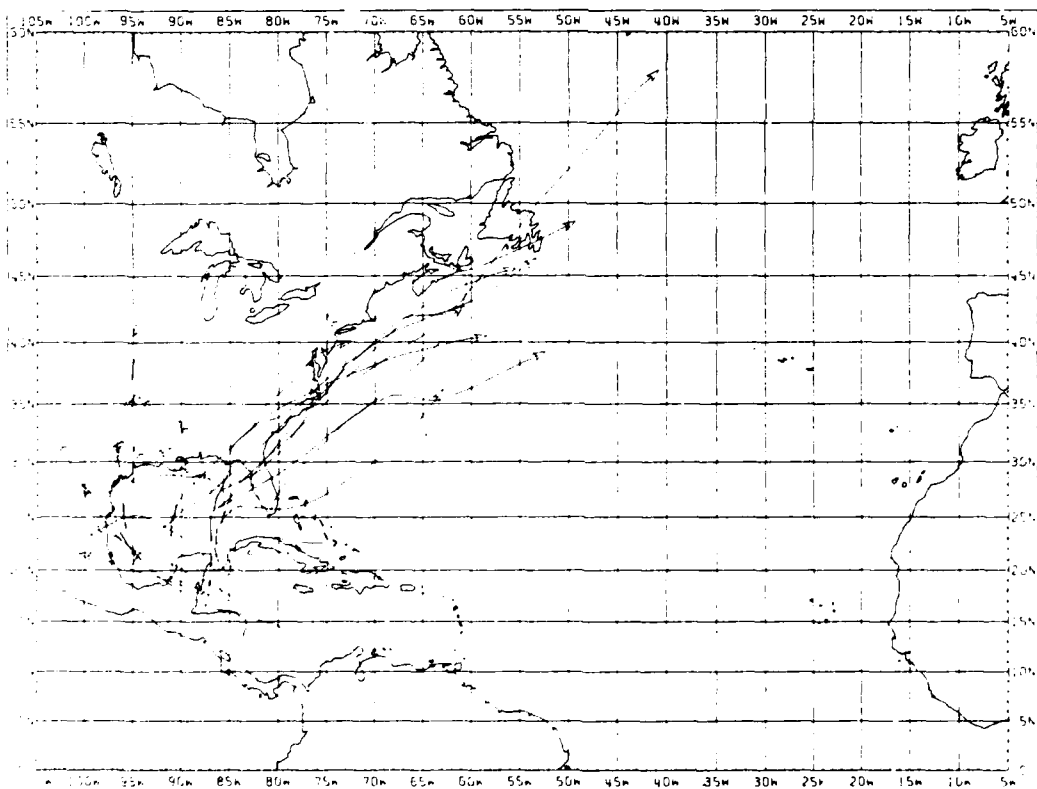
The relative frequency of storms in any given area (in any given time period) can be roughly identified by the track density. Storm positions, at 6-hourly intervals, have been specified on a computer file. While a reasonably faithful rendition of the hand-drawn tracks can be expected, there are a few cases in which the 6-hourly positions do not define tight loops and sudden changes in direction (Neumann et al., 1987).



Tropical Storm or Hurricane Tracks beginning in May, 1886-1986 (14 Storms)
See text on page C-1 for explanation (Neumann et al., 1987).

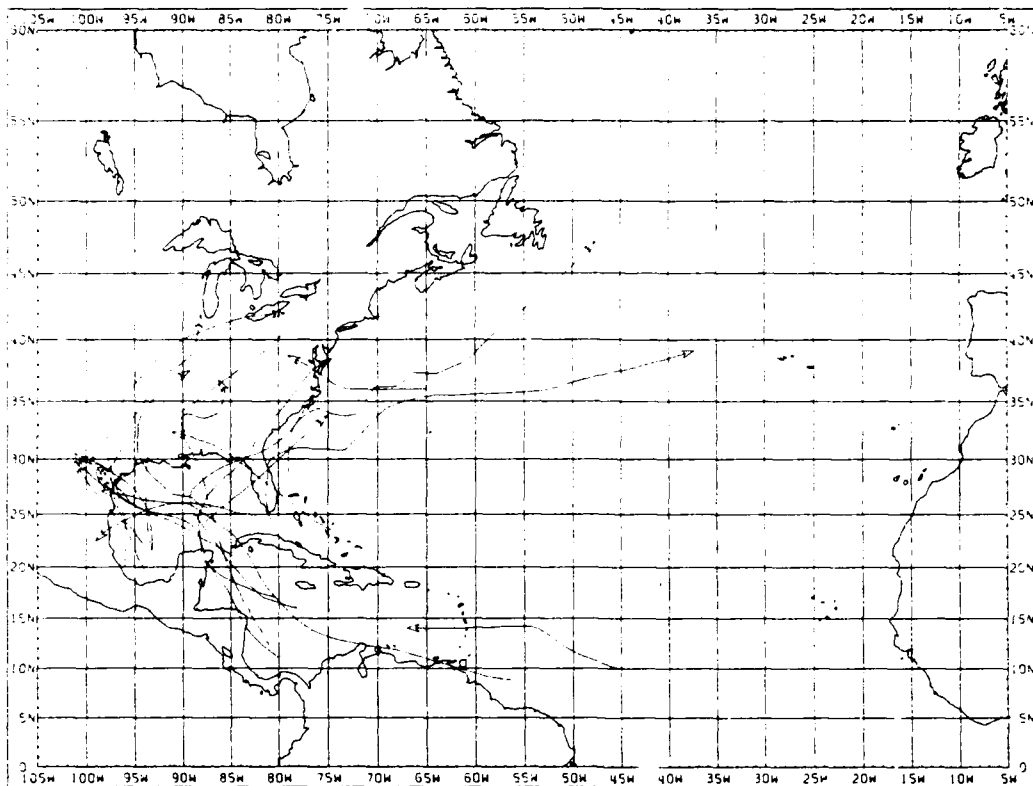


A

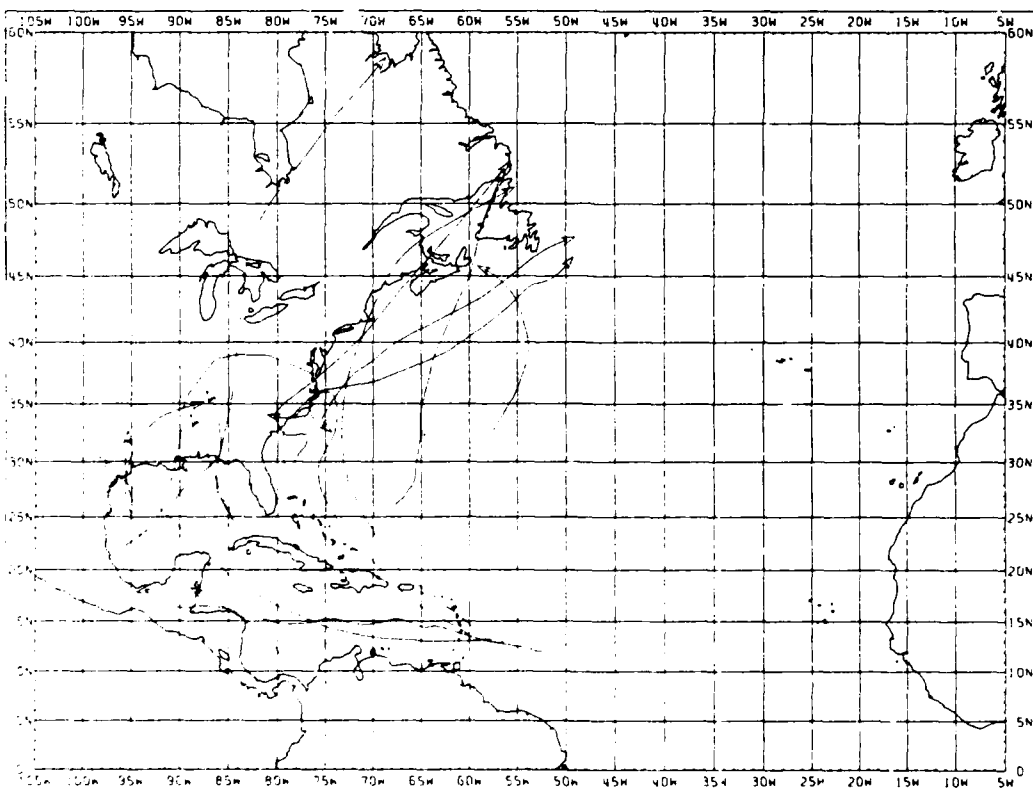


B

A. Tropical Storm or Hurricane Tracks beginning June 1-10, 1886-1986 (12 Storms)
 B. Tropical Storm or Hurricane Tracks beginning June 11-20, 1886-1986 (23 Storms)
 See text on page C-1 for explanation (Neumann et al., 1987).

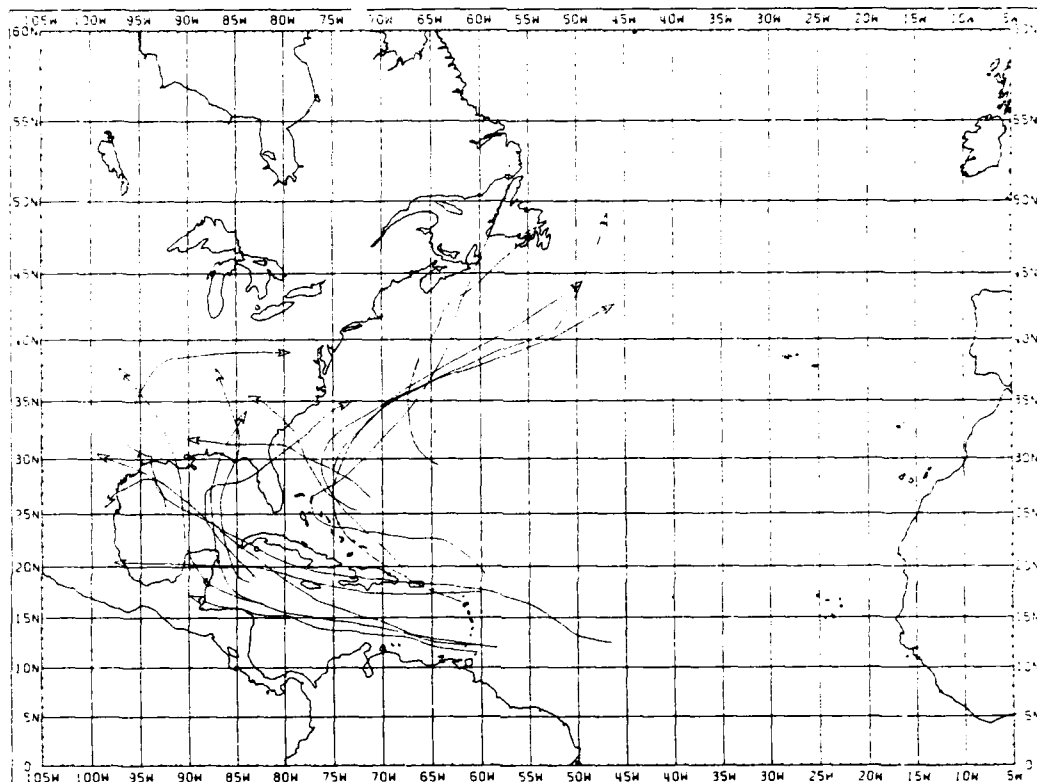


A

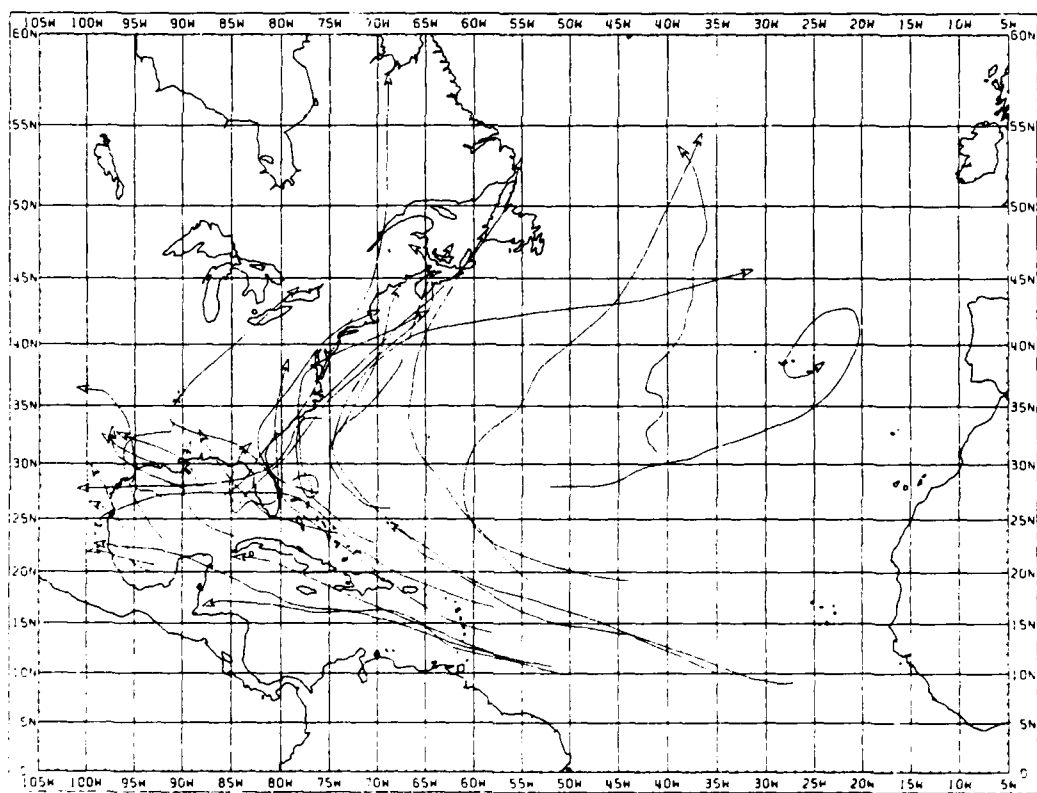


B

A. Tropical Storm or Hurricane Tracks beginning June 21-30, 1886-1986 (20 Storms)
 B. Tropical Storm or Hurricane Tracks beginning July 1-10, 1886-1986 (16 Storms)
 See text on page C-1 for explanation (Neumann et al., 1987).

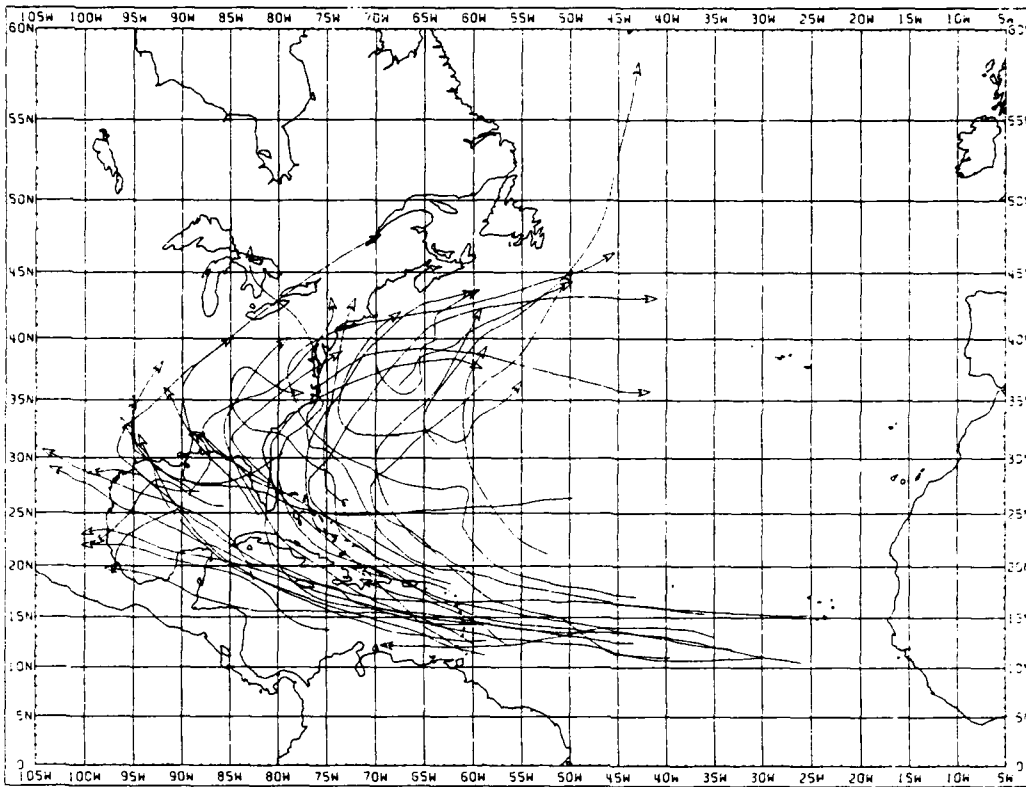


A

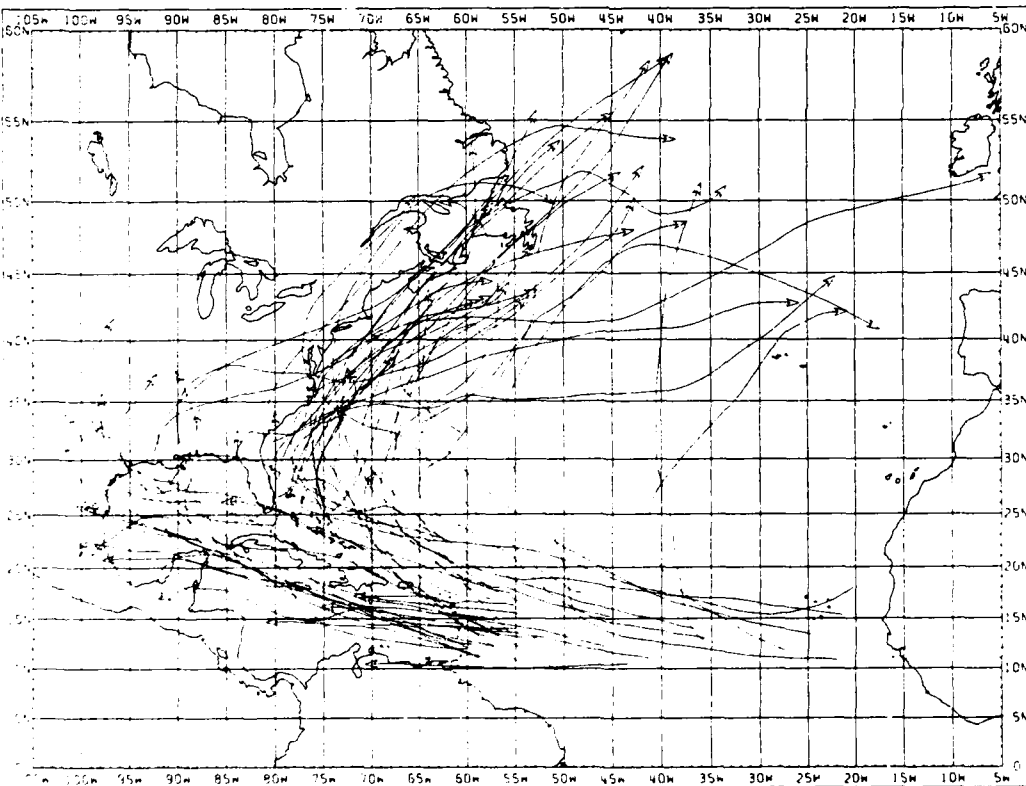


B

A. Tropical Storm or Hurricane Tracks beginning July 11-20, 1886-1986 (16 Storms)
 B. Tropical Storm or Hurricane Tracks beginning July 21-31, 1886-1986 (31 Storms)
 See text on page C-1 for explanation (Neumann et al., 1987).

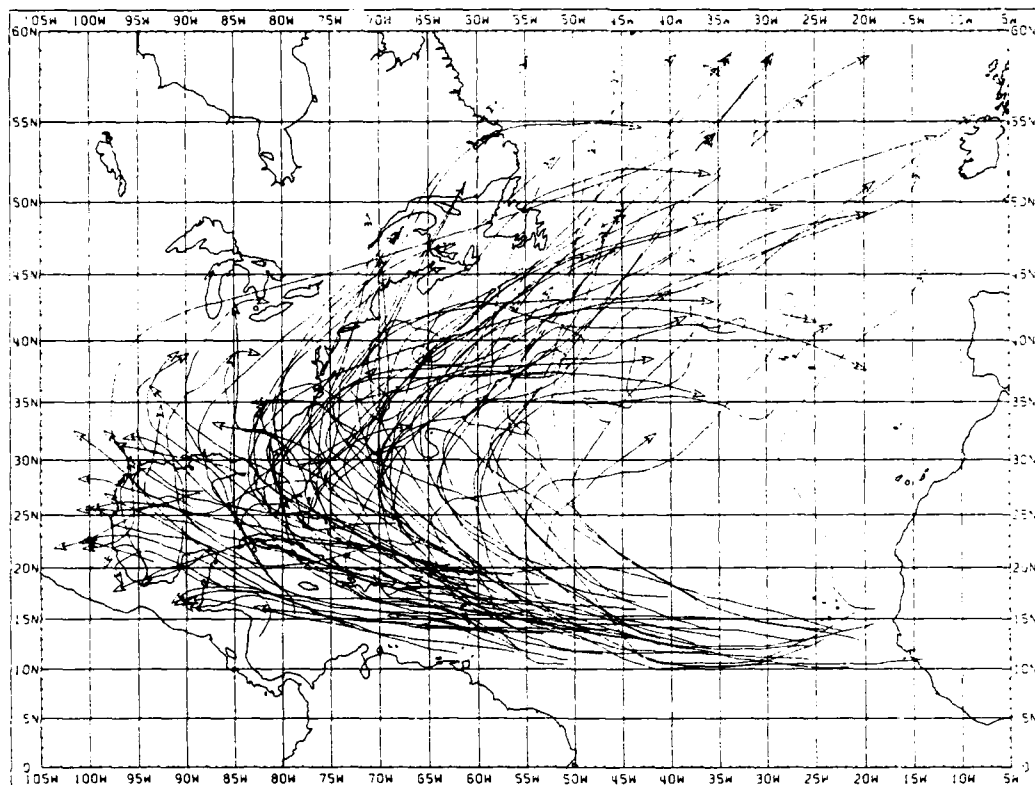


A

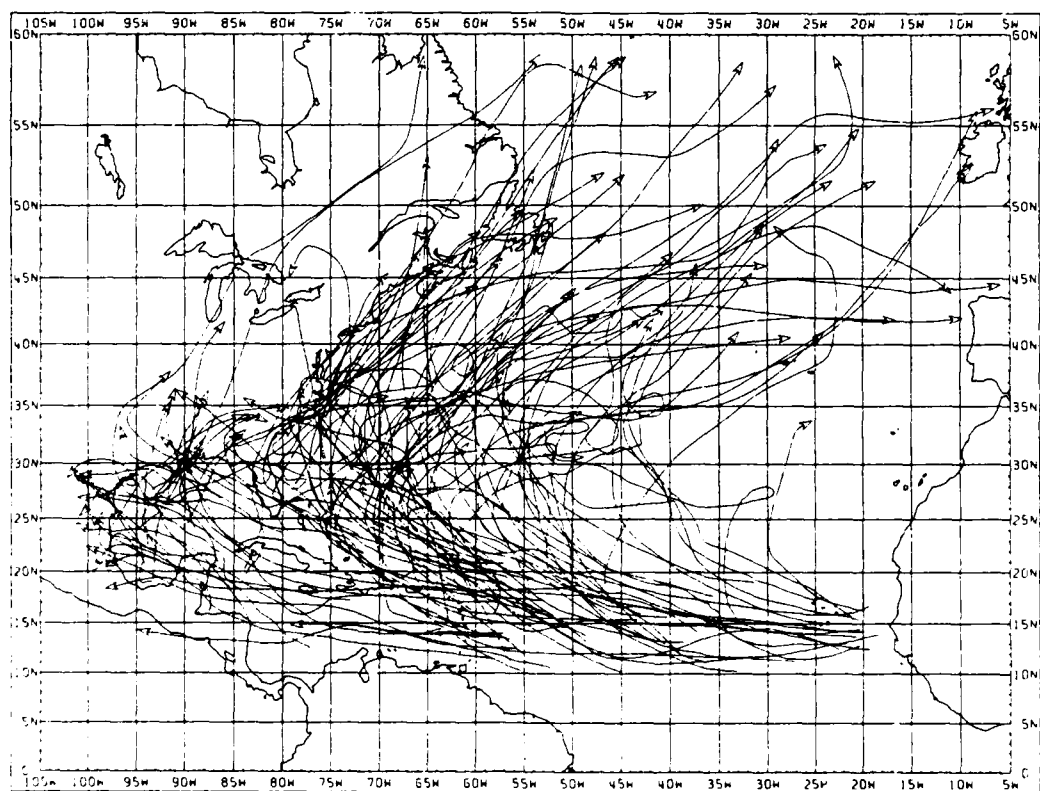


B

A. Tropical Storm or Hurricane Tracks beginning August 1-10, 1886-1986 (39 Storms)
 B. Tropical Storm or Hurricane Tracks beginning August 11-20, 1886-1986 (62 Storms)
 See text on page C-1 for explanation (Neumann et al., 1987).

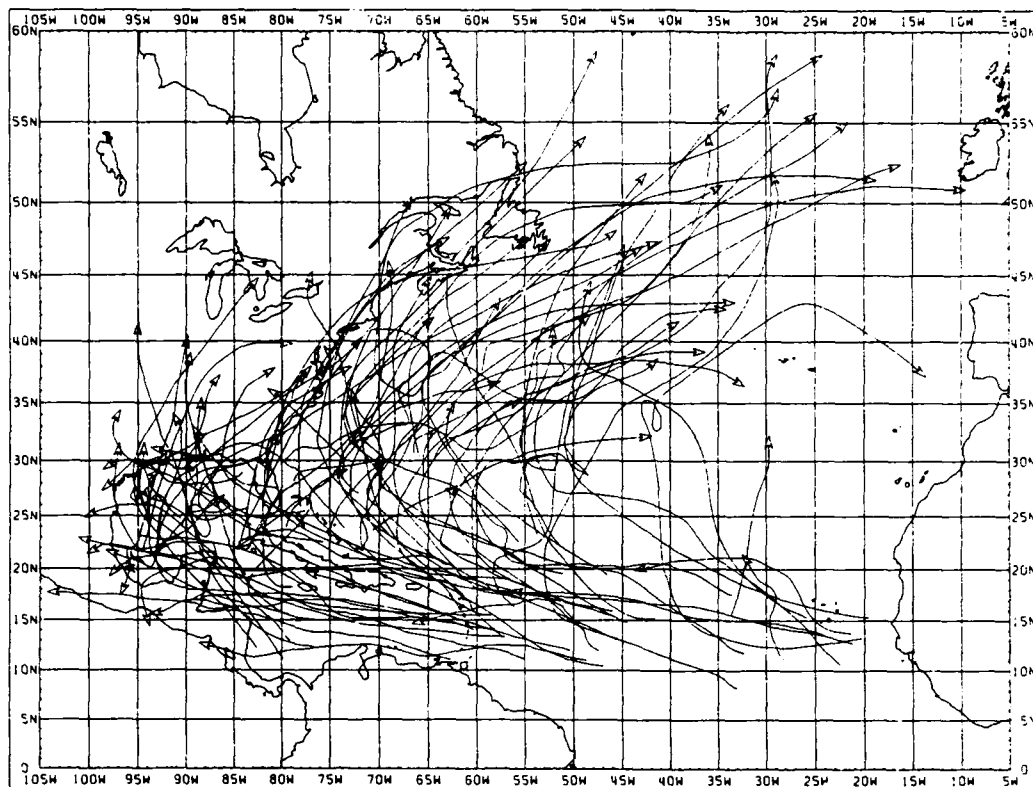


A

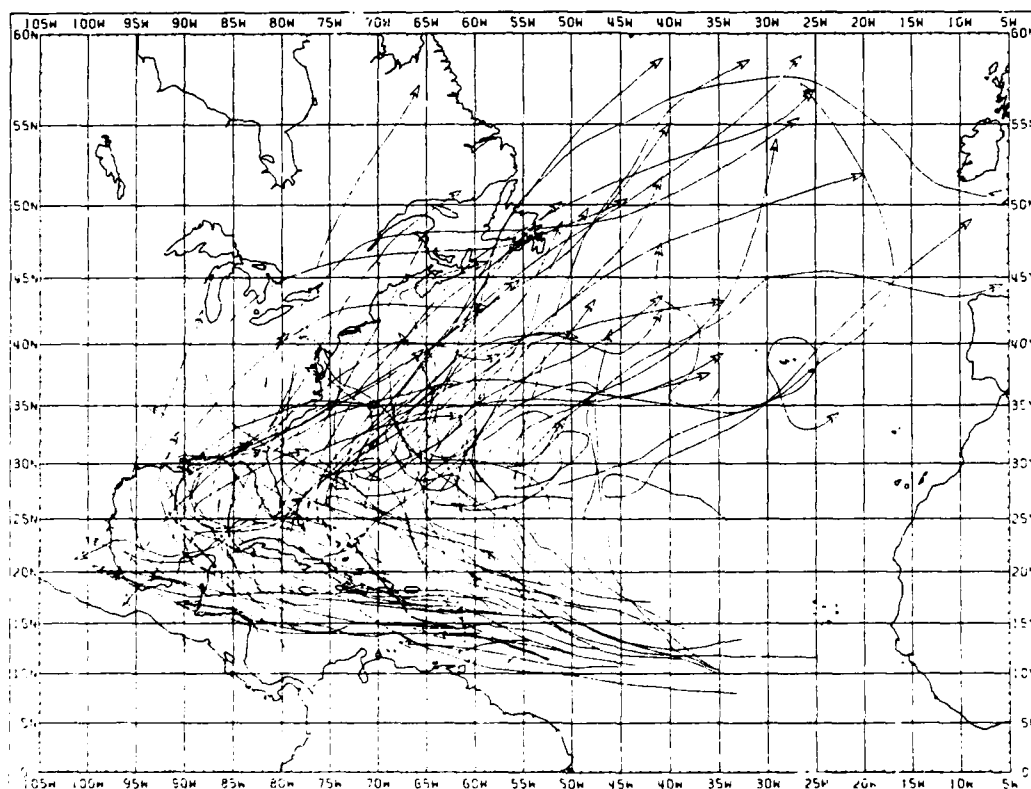


B

A. Tropical Storm or Hurricane Tracks beginning August 21-31, 1886-1986 (98 Storms)
 B. Tropical Storm or Hurricane Tracks beginning September 1-10, 1886-1986 (111 Storms)
 See text on page C-1 for explanation (Neumann et al., 1987).

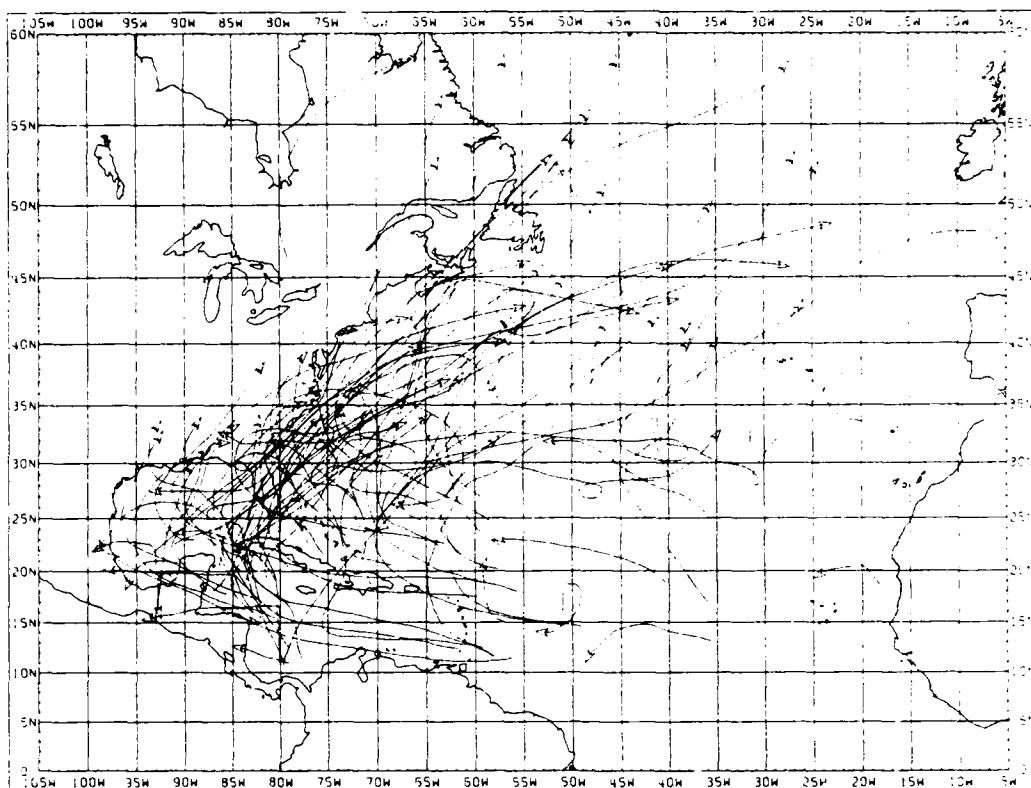


A

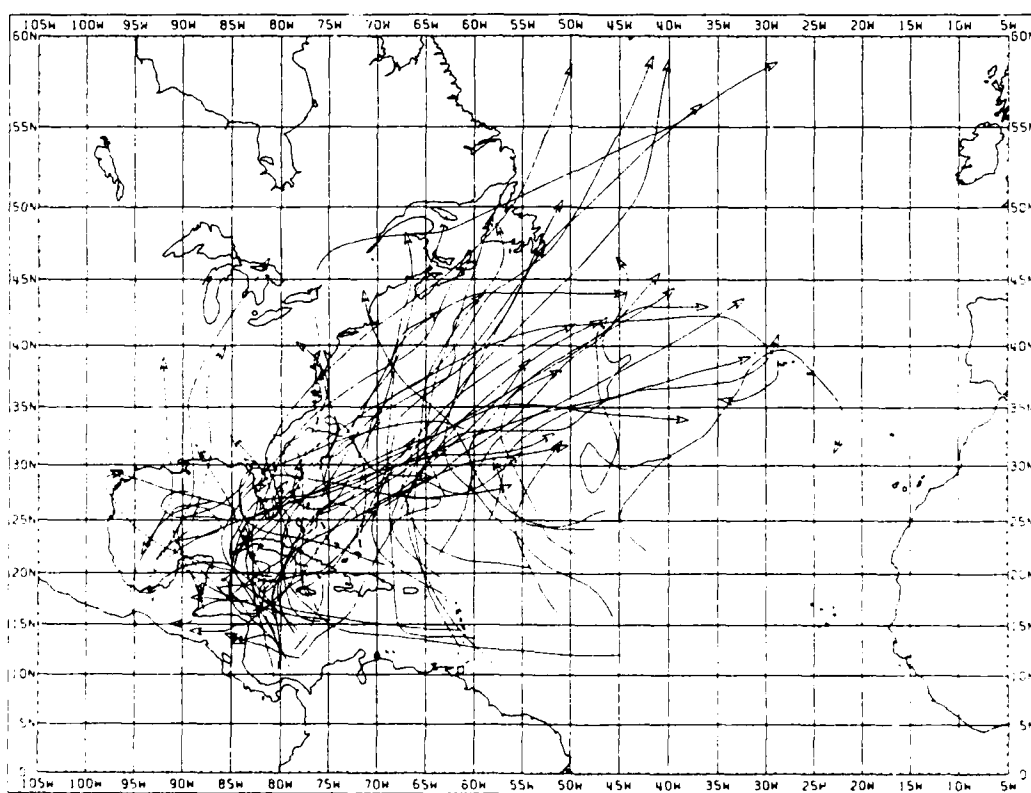


B

A. Tropical Storm or Hurricane Tracks beginning September 11-20, 1886-1986 (95 Storms)
 B. Tropical Storm or Hurricane Tracks beginning September 21-30, 1886-1986 (81 Storms)
 See text on page C-1 for explanation (Neumann et al., 1987).

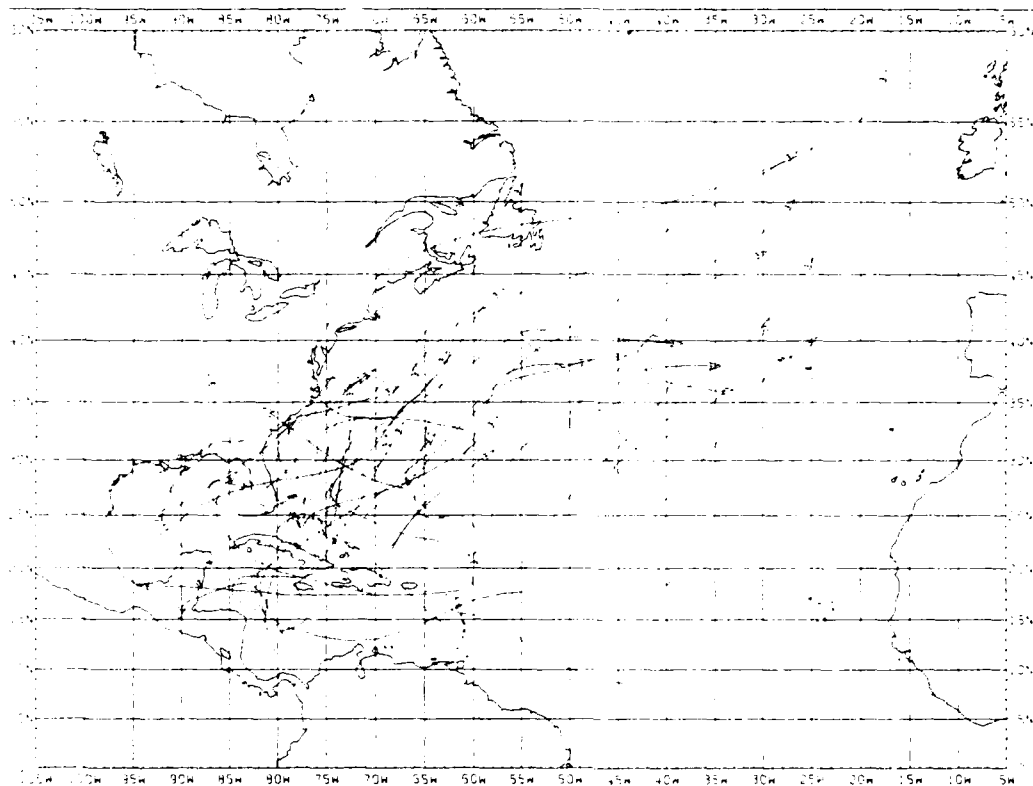


A

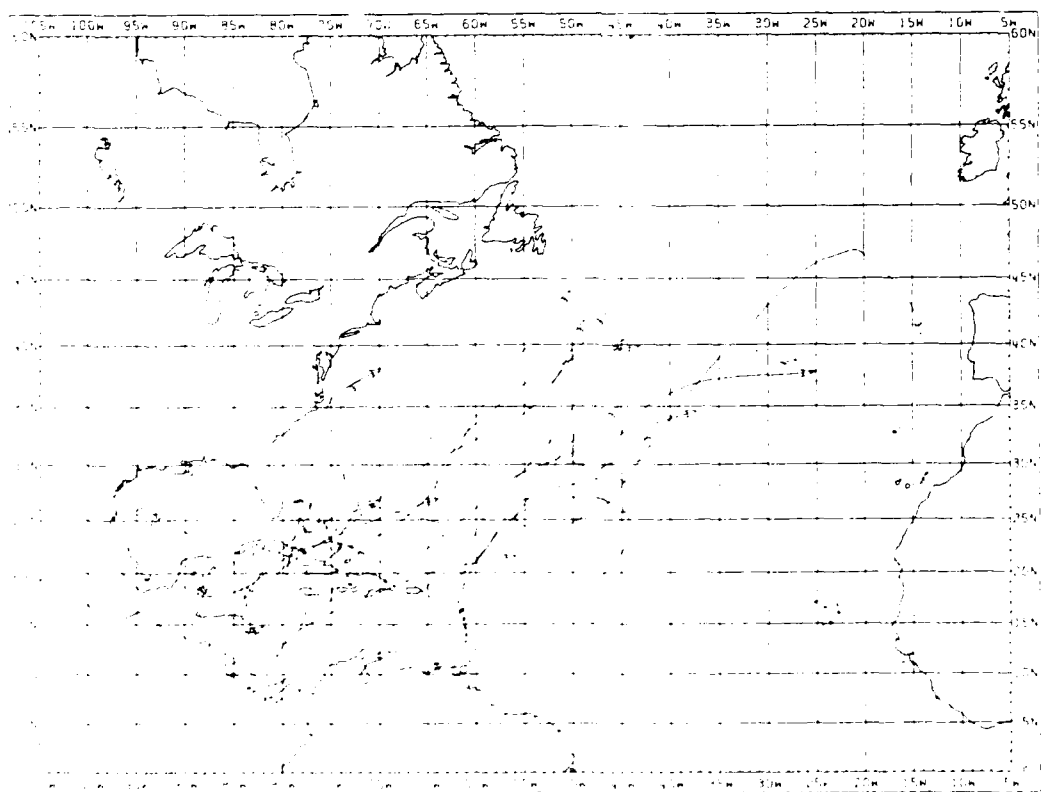


B

A. Tropical Storm or Hurricane Tracks beginning October 1-10, 1886-1986 (76 Storms)
 B. Tropical Storm or Hurricane Tracks beginning October 11-20, 1886-1986 (66 Storms)
 See text on page C-1 for explanation (Neumann et al., 1987).

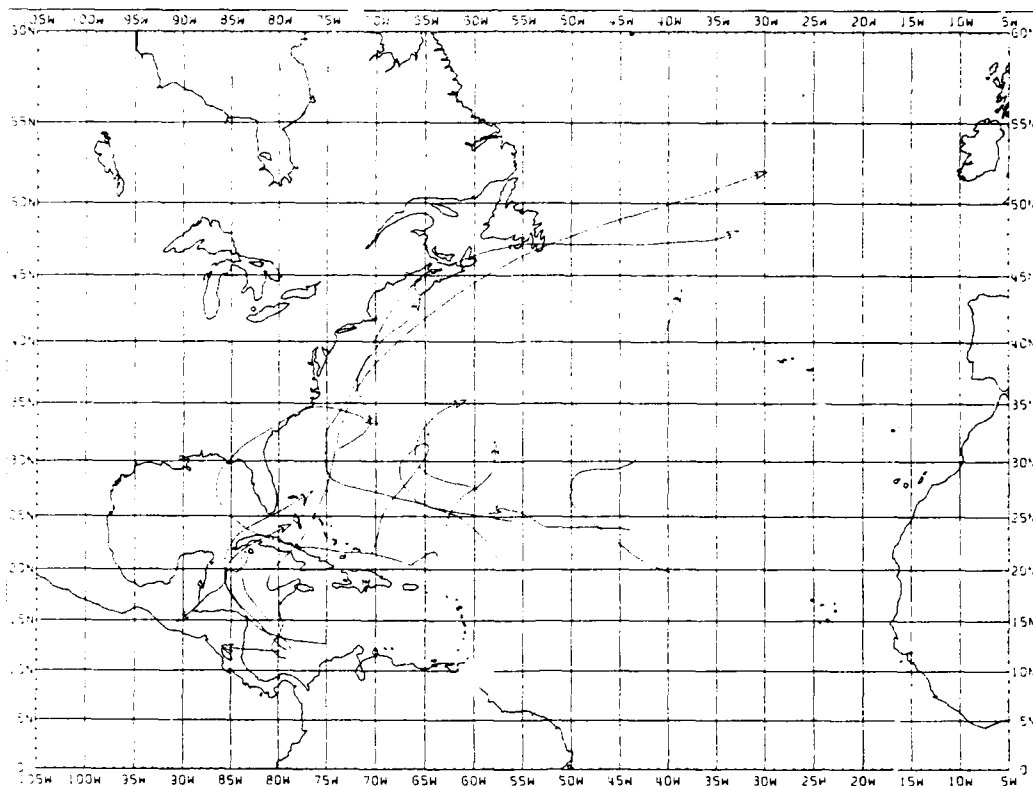


A

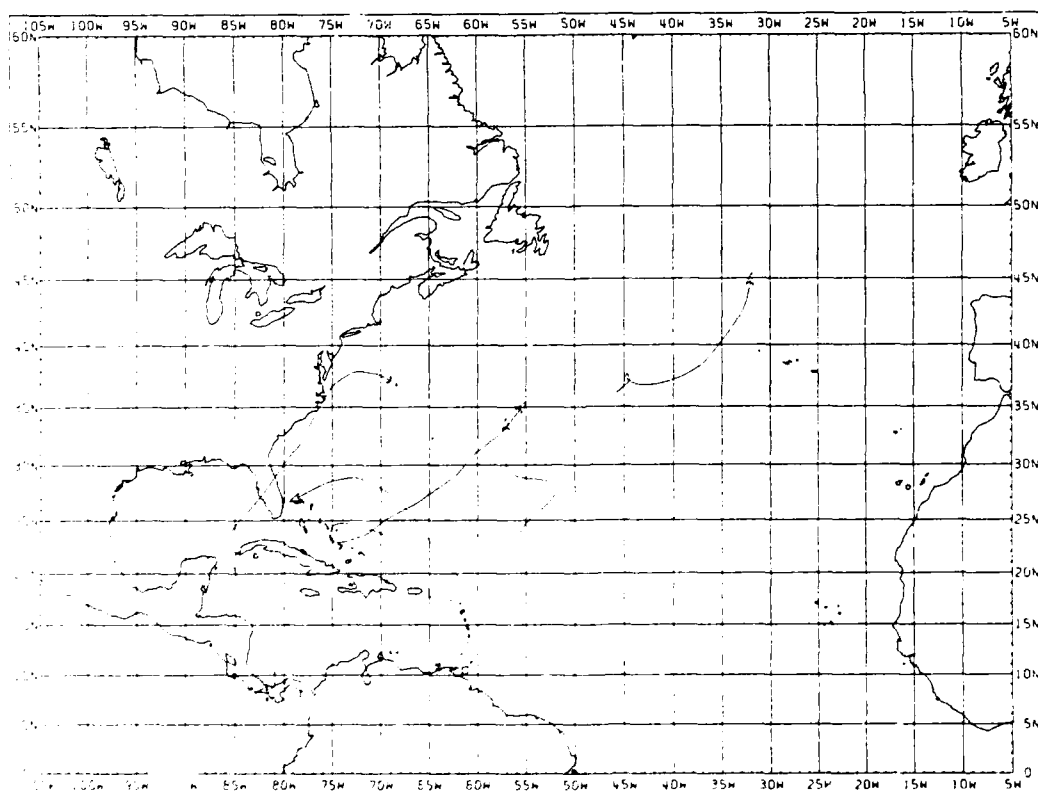


B

A. Tropical Storm or Hurricane Tracks beginning October 21-31, 1886-1986 (36 Storms)
 B. Tropical Storm or Hurricane Tracks beginning November 1-10, 1886-1986 (21 Storms)
 See text on page C-1 for explanation (Neumann et al., 1987).

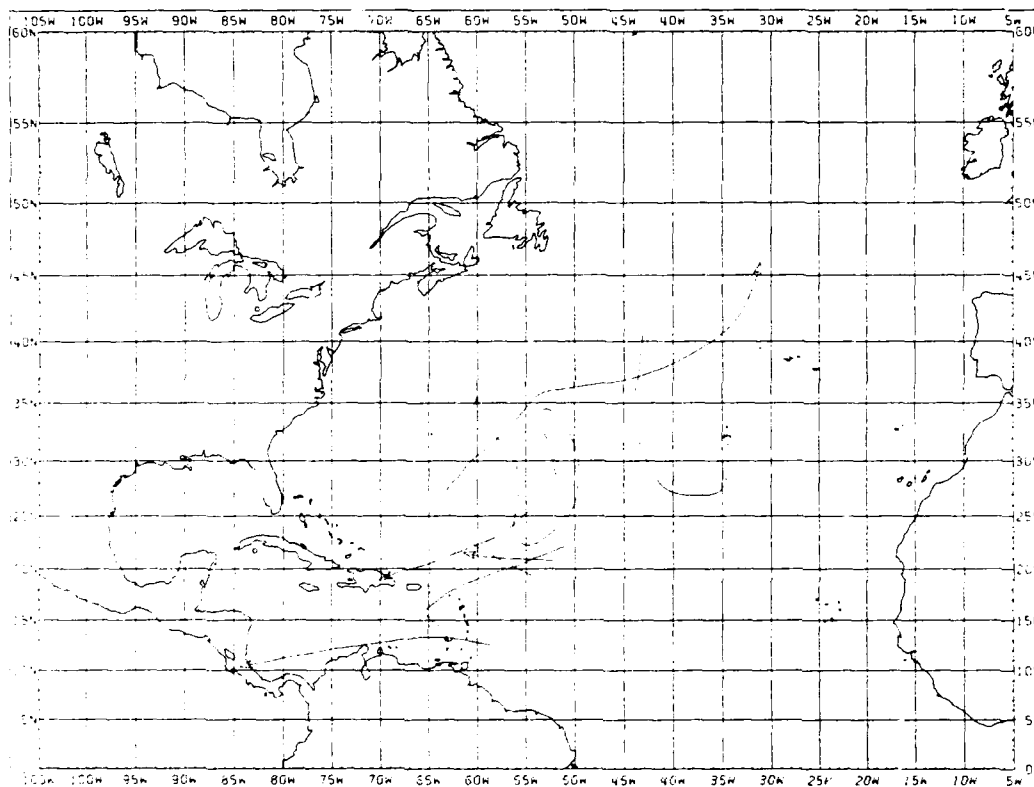


A



B

A. Tropical Storm or Hurricane Tracks beginning November 11-20, 1886-1986 (13 Storms)
 B. Tropical Storm or Hurricane Tracks beginning November 21-30, 1886-1986 (6 Storms)
 See text on page C-1 for explanation (Neumann et al., 1987).



Tropical Storm or Hurricane Tracks beginning in December, 1886-1986 (6 Storms)
See text on page C-1 for explanation (Neumann et al., 1987).

Appendix D

Mean Tracks of Eastern North Pacific Ocean Tropical Cyclones

Forecasters must always be alert to the possibility of Caribbean Sea tropical cyclones moving westward across Central America and reforming in the eastern North Pacific Ocean. However, tropical cyclones *originating* in the eastern North Pacific Ocean move—almost without exception—toward the west, or northwest. While their peripheral cloudiness affects Central America, fleet units in the eastern North Pacific Ocean must be alert to the cyclone centers which track over water. This appendix shows the mean tracks of these tropical cyclones as prepared by Miller et al. (1988).

For the eastern North Pacific Ocean (1949-1982), the data were taken from the Consolidated World-Wide Tropical Cyclone Data Base, National Climatic Data Center, Asheville, NC. The placing in service of the meteorological satellite in 1960 greatly enhanced the tracking of tropical cyclones in data-sparse areas such as the eastern North Pacific Ocean. Tropical cyclones in the western North Pacific Ocean that failed to attain at least tropical storm intensity (i.e., maximum surface wind speed >33 kt) were not considered in the study. However, since intensities were not given for tropical cyclones occurring before 1973 in the eastern North Pacific basin, *all* tropical cyclones prior to 1973 were considered in this study—despite the captions in the following figures.

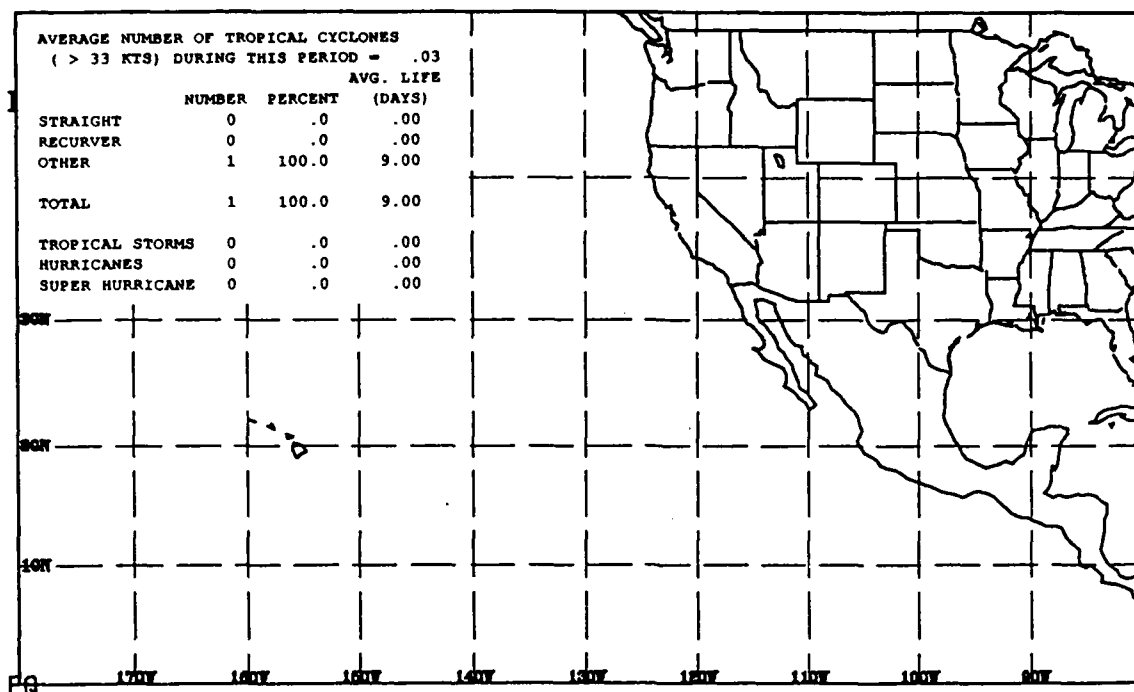
Since the study by Miller et al. (1988) plotted *three* sets of tropical cyclones (i.e., one set each for straight, recurver and “other” tracks), the need to reduce the size of this appendix dictates the presentation of only *mean tracks* of the tropical cyclones. The tropical cyclone occurrences are divided into half-month periods, with each period centered on either the 1st or 16th of the month. Thus, a period begins approximately a week before the 1st or 16th, and ends approximately a week after the 1st or 16th. *However, any tropical cyclone that occurs within 15 days of either side of the 1st or 16th day also is included in the period.* Tropical cyclones are classified into periods according to their starting dates. Therefore, each tropical cyclone belongs to two periods, and in some cases three. The starting date was chosen for classification purposes because a storm’s start date is always known. Thus, there is no confusion as to which climatological period should be used. The overlapping of periods avoids confusion about tropical cyclones whose starting dates were near the beginning or end of calendar months.

The following charts show the paths most often followed by tropical cyclones in the period. The numbers on the paths represent the percentage of tropical cyclones that follow the indicated paths during the period. *Paths that contain less than 5% of the tropical cyclones for the period are not analyzed. For a period in which 10 tropical cyclones or fewer occur, a blank chart containing only the statistics is supplied.*

NOTE: When a path branches off into multiple paths, the sum of the percentages on the branches does *not* necessarily equal the percentage indicated on the parent path. This is due to the fact that not all tropical cyclones follow a mean path, and some develop or dissipate along a path. (Miller et al., 1988)

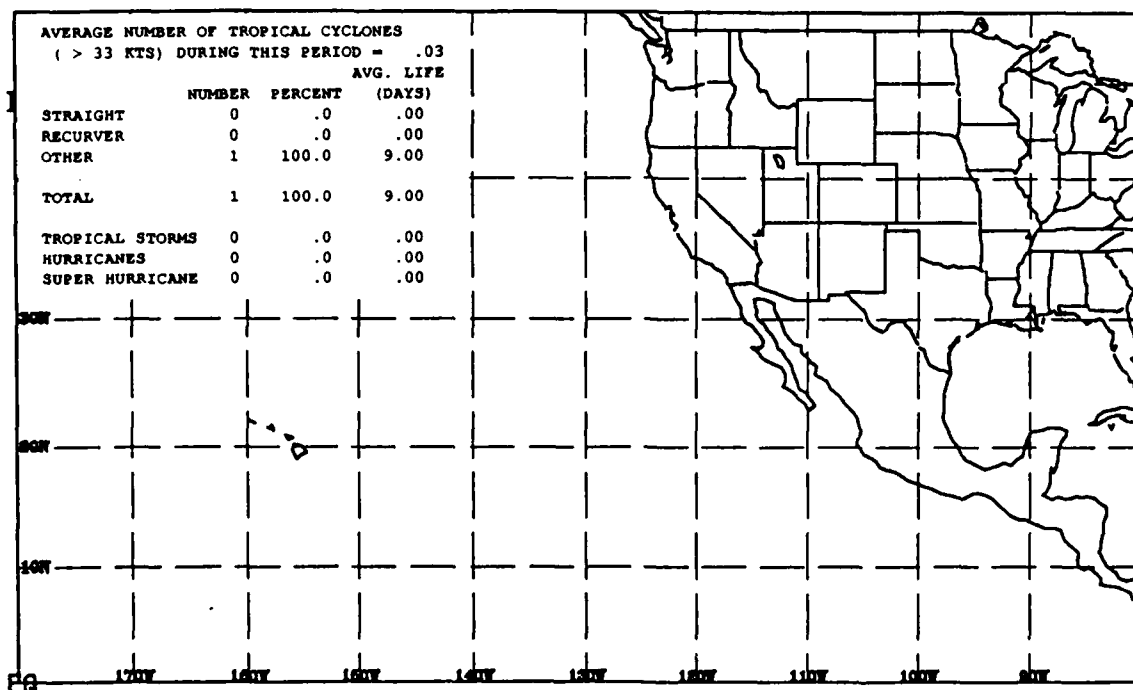
No tropical cyclones occurred in periods *before* 9 March or *after* 8 December.

MEAN PATHS FOR MAR 9 - MAR 23



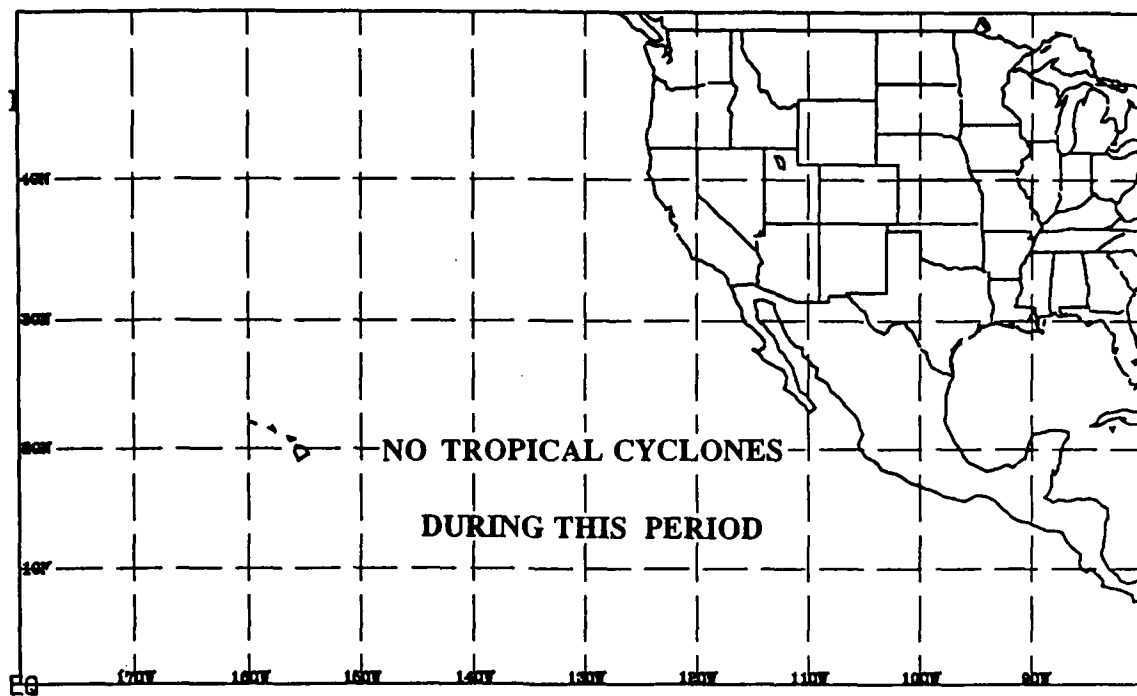
Mean tropical cyclone (> 33 kts) path. Numbers represent the percentage of tropical cyclones (> 33 kts) which followed the indicated path. These numbers may not add up to 100% since not all tropical cyclones (> 33 kts) follow a mean path and some develop/dissipate along a path. Tracks which contained less than 5% of the tropical cyclones (> 33 kts) are ignored. (Miller et al., 1988)

MEAN PATHS FOR MAR 24 - APR 8



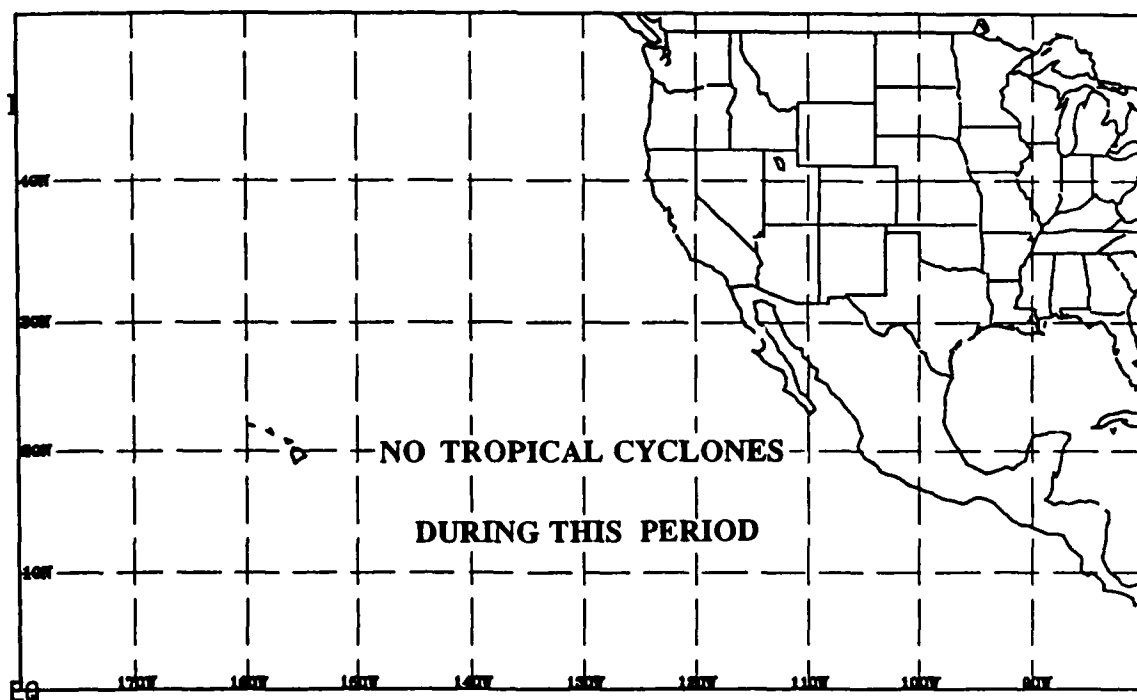
Mean tropical cyclone (> 33 kts) path. Numbers represent the percentage of tropical cyclones (> 33 kts) which followed the indicated path. These numbers may not add up to 100% since not all tropical cyclones (> 33 kts) follow a mean path and some develop/dissipate along a path. Tracks which contained less than 5% of the tropical cyclones (> 33 kts) are ignored. (Miller et al., 1988)

APR 9 - APR 23



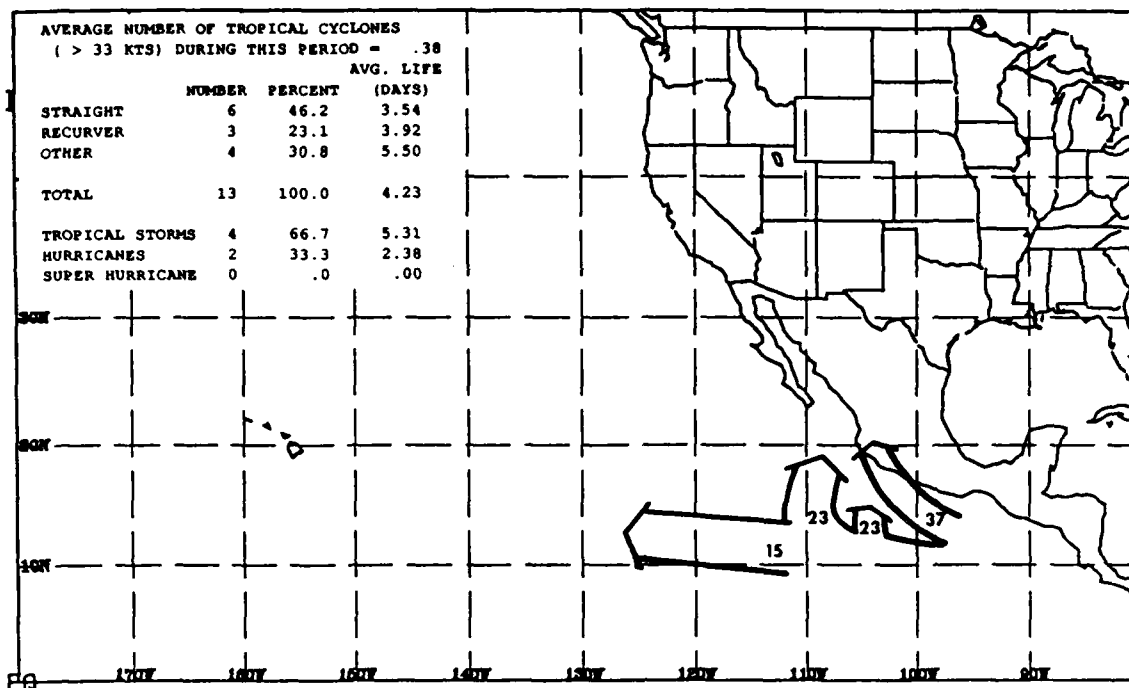
(Miller et al., 1988)

APR 24 - MAY 8



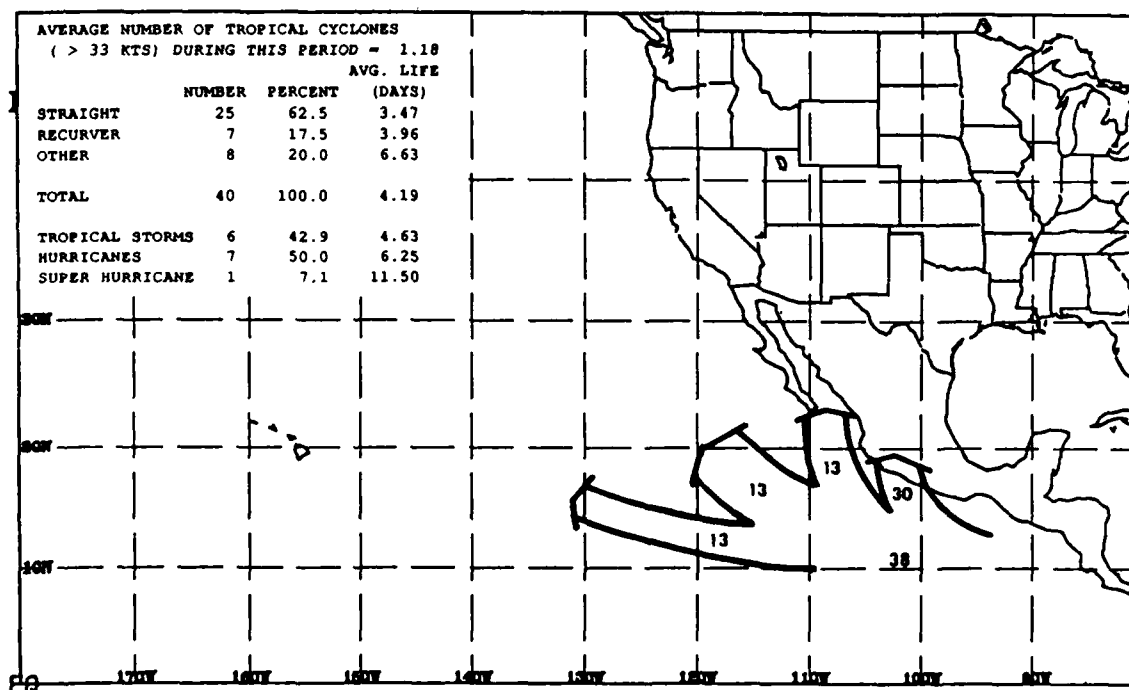
(Miller et al., 1988)

MEAN PATHS FOR MAY 9 - MAY 23



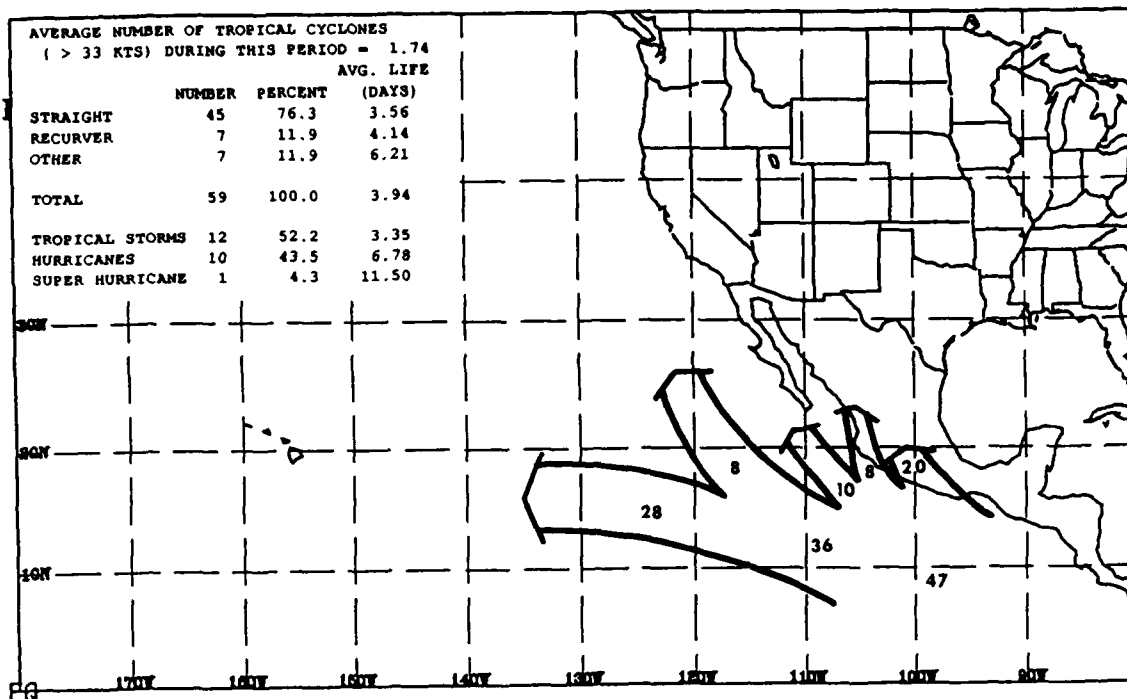
Mean tropical cyclone (> 33 kts) path. Numbers represent the percentage of tropical cyclones (> 33 kts) which followed the indicated path. These numbers may not add up to 100% since not all tropical cyclones (> 33 kts) follow a mean path and some develop/dissipate along a path. Tracks which contained less than 5% of the tropical cyclones (> 33 kts) are ignored. (Miller et al., 1988).

MEAN PATHS FOR MAY 24 - JUN 8



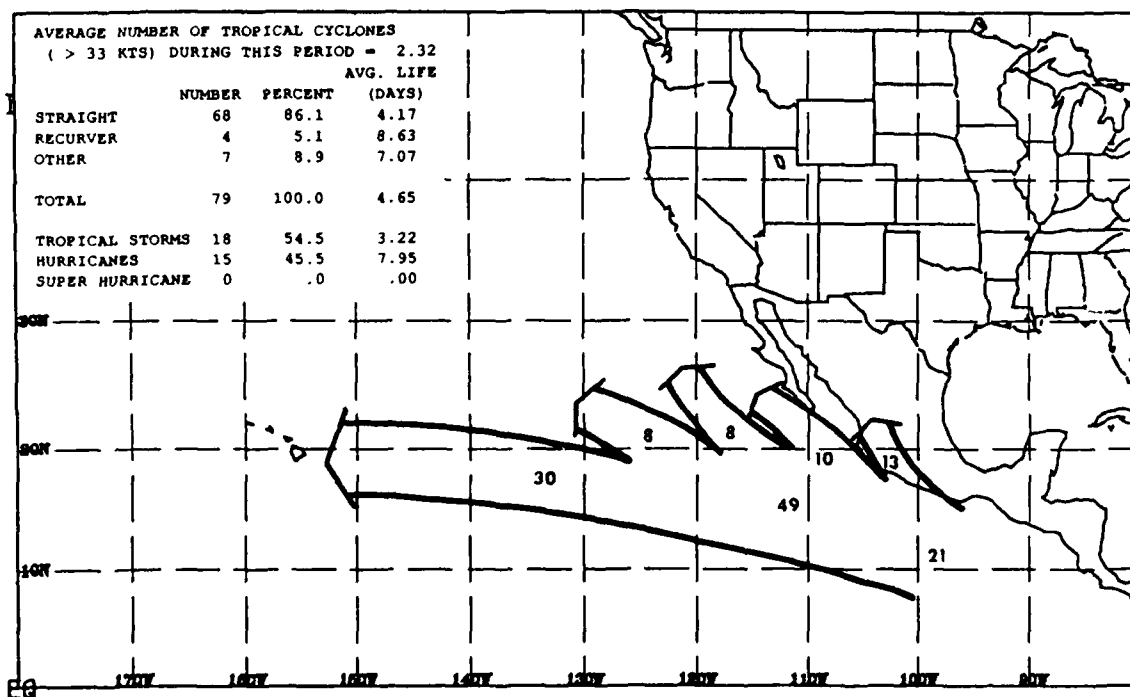
Mean tropical cyclone (> 33 kts) path. Numbers represent the percentage of tropical cyclones (> 33 kts) which followed the indicated path. These numbers may not add up to 100% since not all tropical cyclones (> 33 kts) follow a mean path and some develop/dissipate along a path. Tracks which contained less than 5% of the tropical cyclones (> 33 kts) are ignored. (Miller et al., 1988)

MEAN PATHS FOR JUN 9 - JUN 23



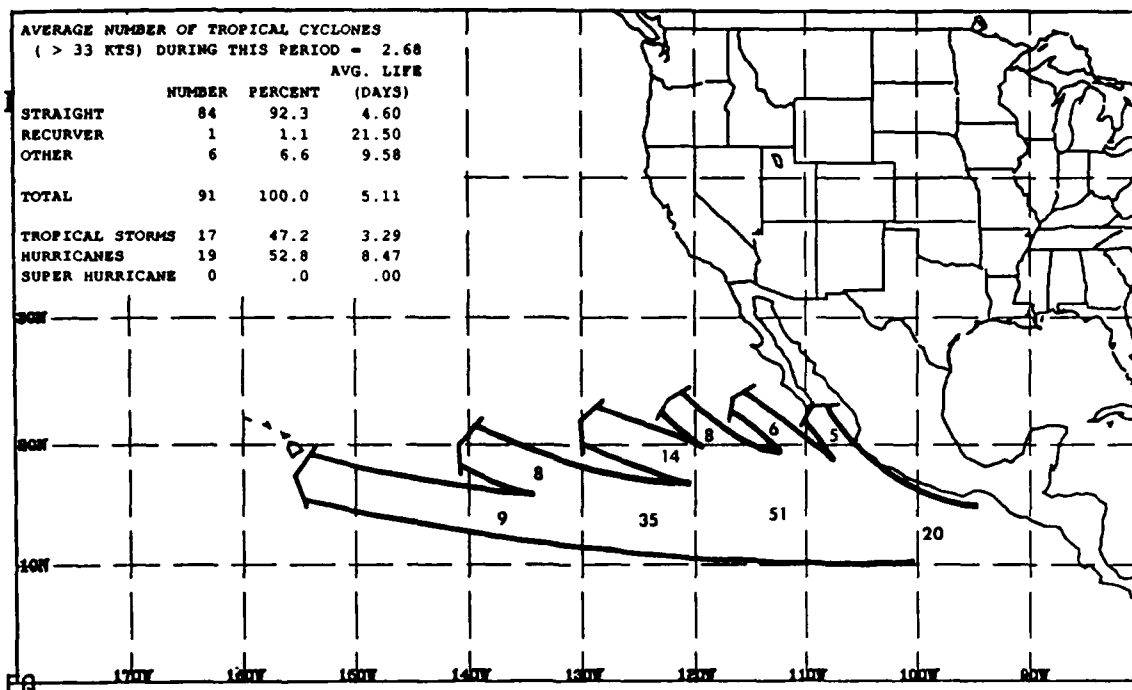
Mean tropical cyclone (> 33 kts) path. Numbers represent the percentage of tropical cyclones (> 33 kts) which followed the indicated path. These numbers may not add up to 100% since not all tropical cyclones (> 33 kts) follow a mean path and some develop/dissipate along a path. Tracks which contained less than 5% of the tropical cyclones (> 33 kts) are ignored.

MEAN PATHS FOR JUN 24 - JUL 8



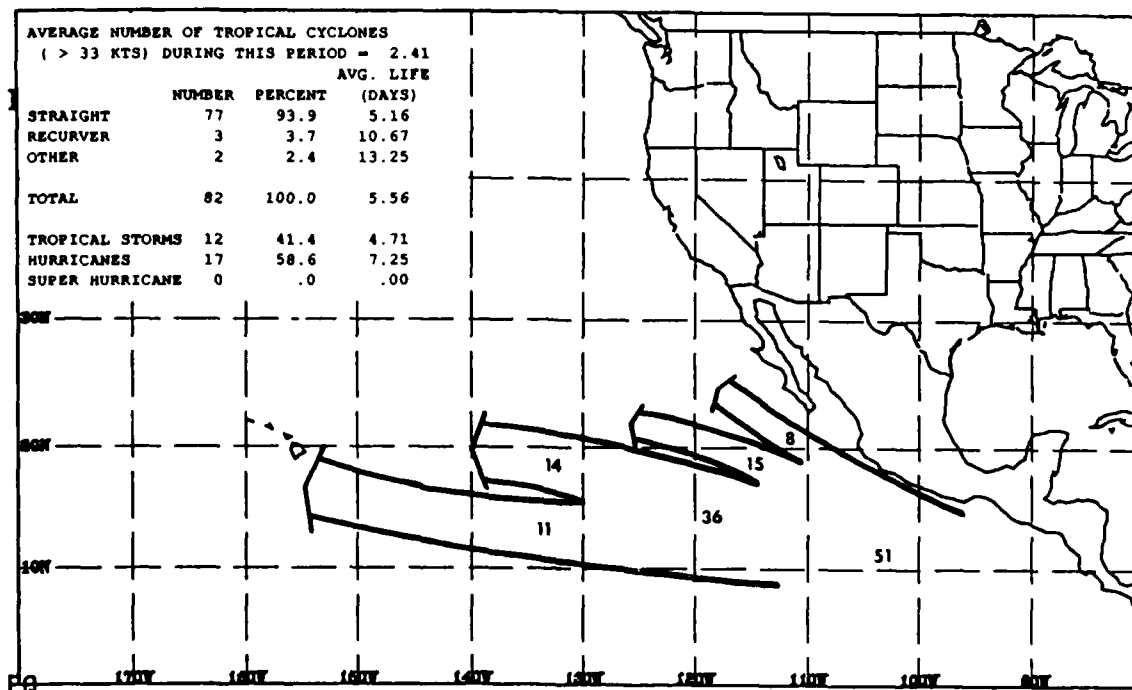
Mean tropical cyclone (> 33 kts) path. Numbers represent the percentage of tropical cyclones (> 33 kts) which followed the indicated path. These numbers may not add up to 100% since not all tropical cyclones (> 33 kts) follow a mean path and some develop/dissipate along a path. Tracks which contained less than 5% of the tropical cyclones (> 33 kts) are ignored. (Miller et al., 1988)

MEAN PATHS FOR JUL 9 - JUL 23



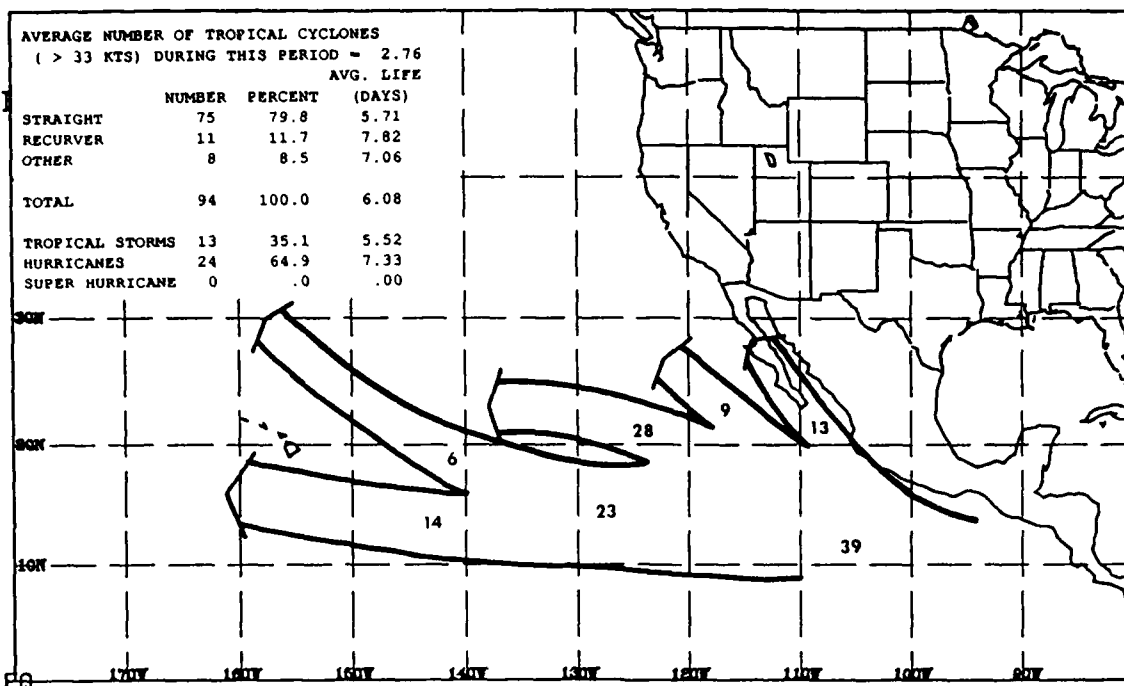
Mean tropical cyclone (> 33 kts) path. Numbers represent the percentage of tropical cyclones (> 33 kts) which followed the indicated path. These numbers may not add up to 100% since not all tropical cyclones (> 33 kts) follow a mean path and some develop/dissipate along a path. Tracks which contained less than 5% of the tropical cyclones (> 33 kts) are ignored. (Miller et al., 1988)

MEAN PATHS FOR JUL 24 - AUG 8



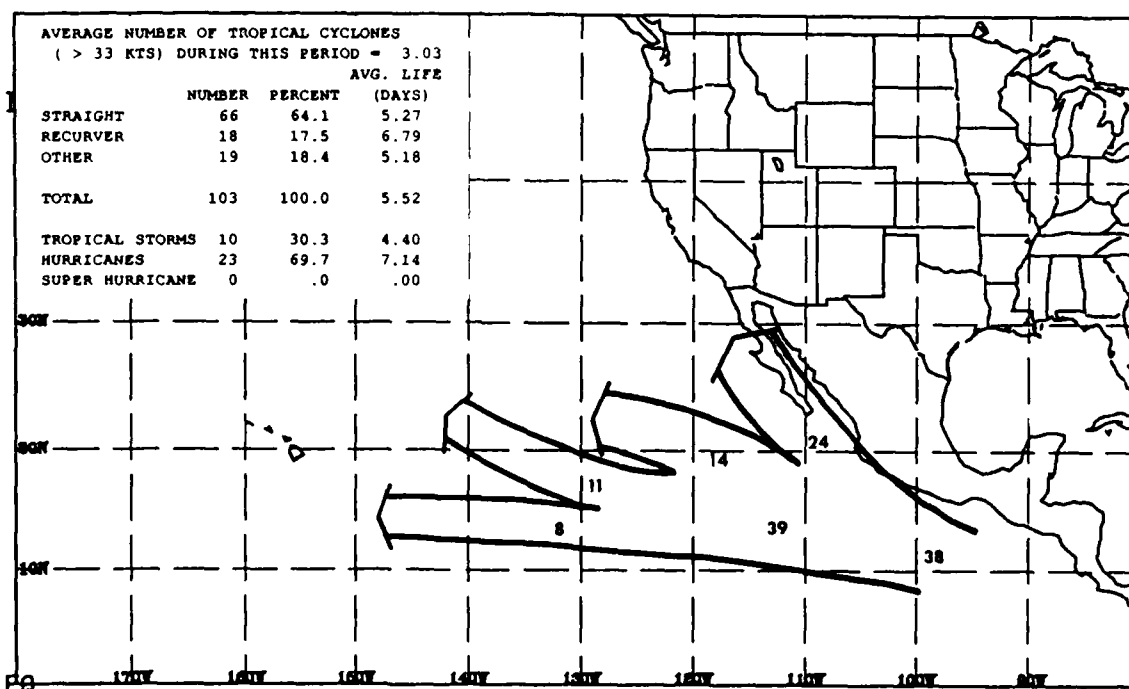
Mean tropical cyclone (> 33 kts) path. Numbers represent the percentage of tropical cyclones (> 33 kts) which followed the indicated path. These numbers may not add up to 100% since not all tropical cyclones (> 33 kts) follow a mean path and some develop/dissipate along a path. Tracks which contained less than 5% of the tropical cyclones (> 33 kts) are ignored. (Miller et al., 1988)

MEAN PATHS FOR AUG 9 - AUG 23



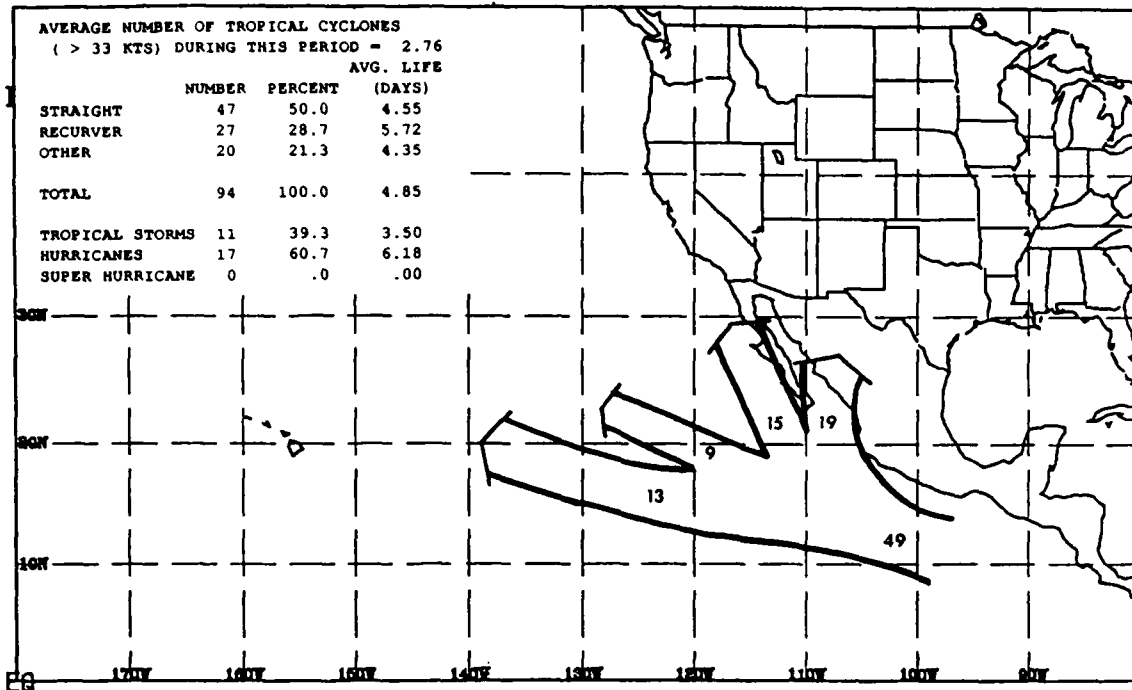
Mean tropical cyclone (> 33 kts) path. Numbers represent the percentage of tropical cyclones (> 33 kts) which followed the indicated path. These numbers may not add up to 100% since not all tropical cyclones (> 33 kts) follow a mean path and some develop/dissipate along a path. Tracks which contained less than 5% of the tropical cyclones (> 33 kts) are ignored. (Miller et al., 1988)

MEAN PATHS FOR AUG 24 - SEP 8



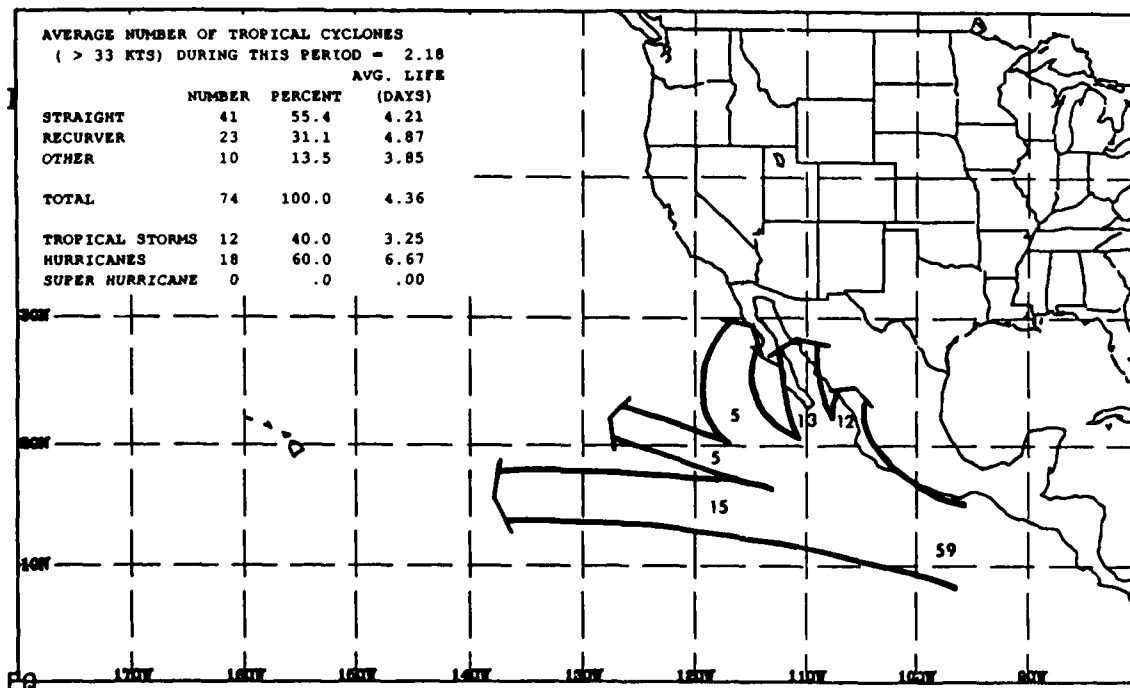
Mean tropical cyclone (> 33 kts) path. Numbers represent the percentage of tropical cyclones (> 33 kts) which followed the indicated path. These numbers may not add up to 100% since not all tropical cyclones (> 33 kts) follow a mean path and some develop/dissipate along a path. Tracks which contained less than 5% of the tropical cyclones (> 33 kts) are ignored. (Miller et al., 1988)

MEAN PATHS FOR SEP 9 - SEP 23



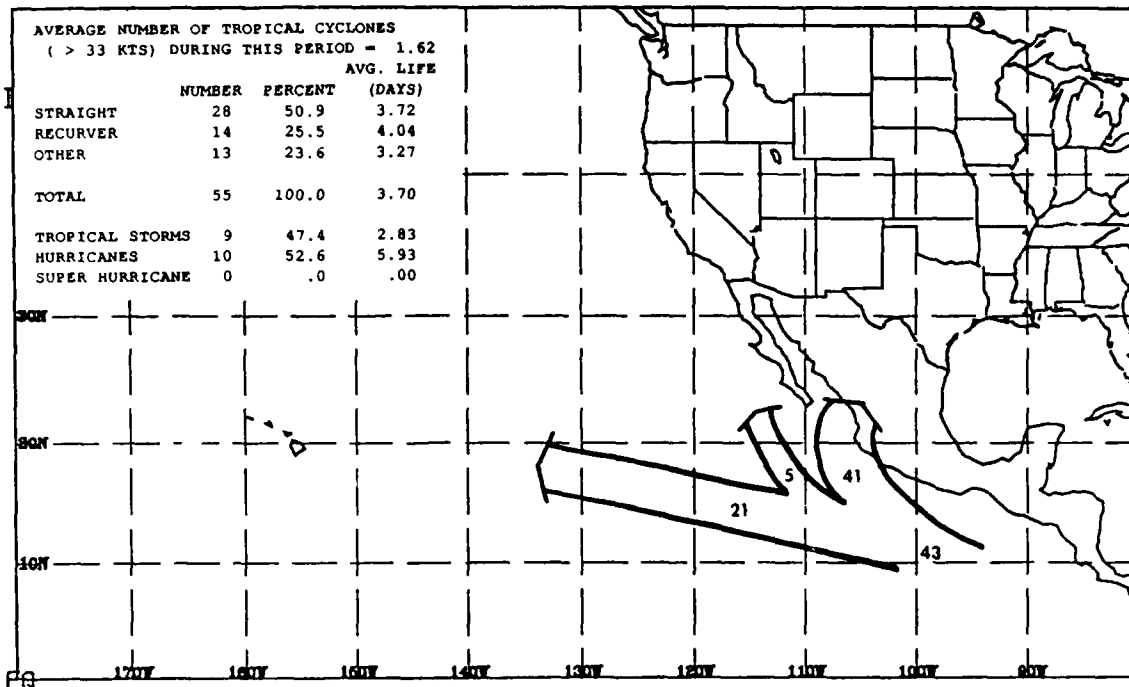
Mean tropical cyclone (> 33 kts) path. Numbers represent the percentage of tropical cyclones (> 33 kts) which followed the indicated path. These numbers may not add up to 100% since not all tropical cyclones (> 33 kts) follow a mean path and some develop/dissipate along a path. Tracks which contained less than 5% of the tropical cyclones (> 33 kts) are ignored. (Miller et al., 1988)

MEAN PATHS FOR SEP 24 - OCT 8



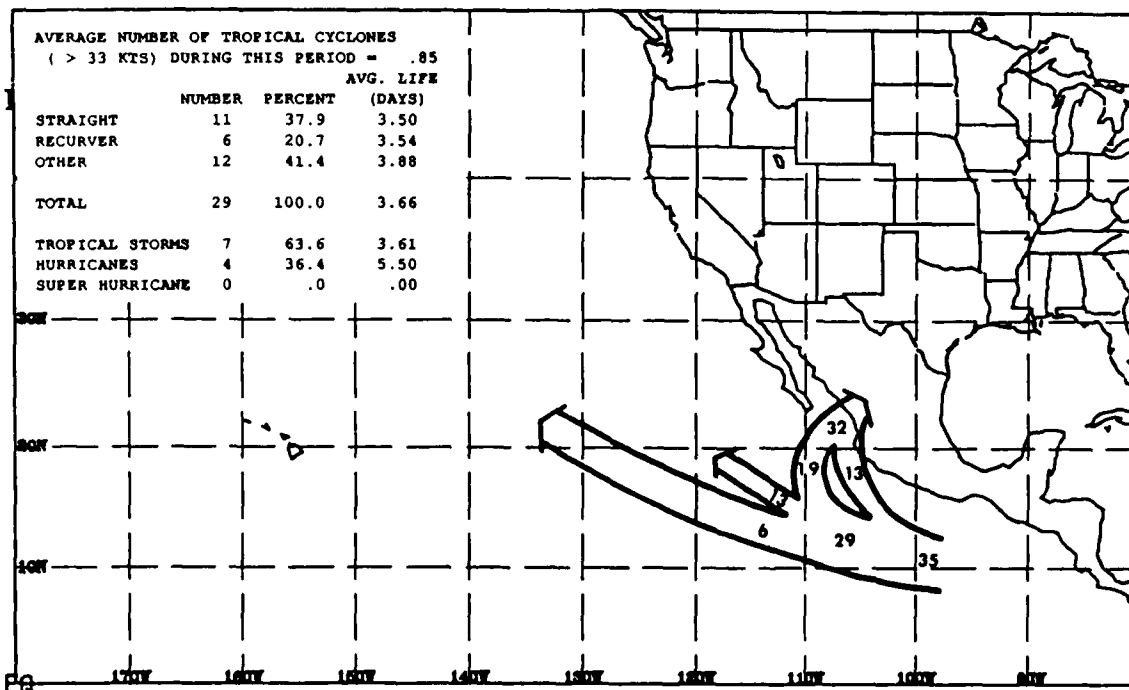
Mean tropical cyclone (> 33 kts) path. Numbers represent the percentage of tropical cyclones (> 33 kts) which followed the indicated path. These numbers may not add up to 100% since not all tropical cyclones (> 33 kts) follow a mean path and some develop/dissipate along a path. Tracks which contained less than 5% of the tropical cyclones (> 33 kts) are ignored. (Miller et al., 1988)

MEAN PATHS FOR OCT 9 - OCT 23



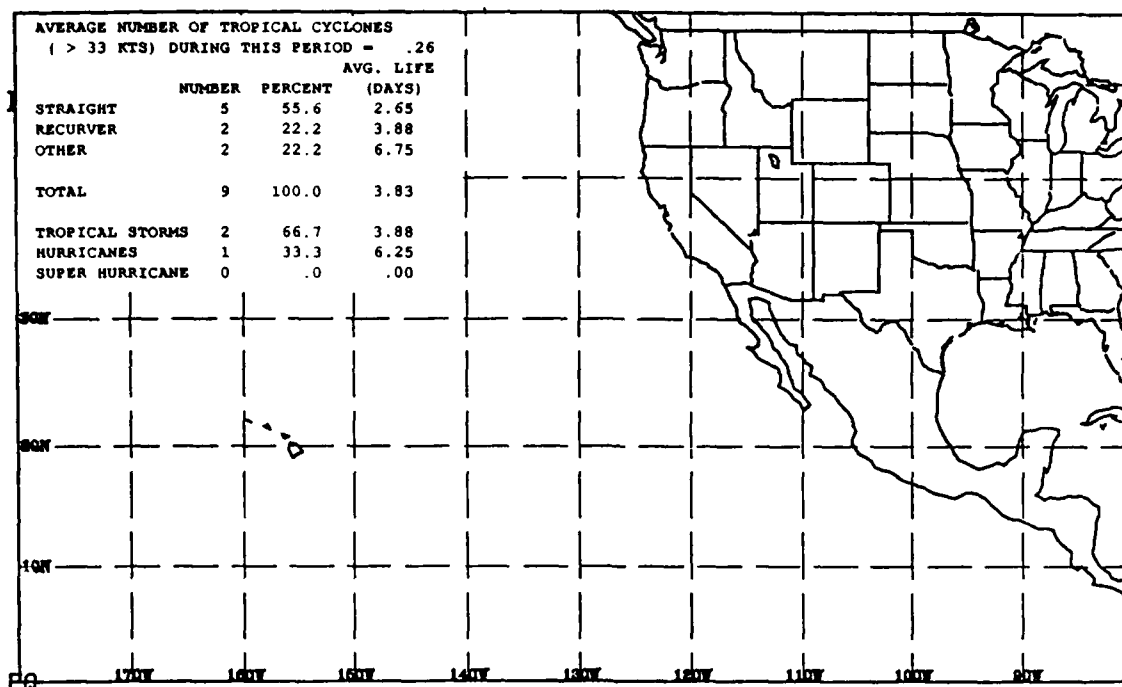
Mean tropical cyclone (> 33 kts) path. Numbers represent the percentage of tropical cyclones (> 33 kts) which followed the indicated path. These numbers may not add up to 100% since not all tropical cyclones (> 33 kts) follow a mean path and some develop/dissipate along a path. Tracks which contained less than 5% of the tropical cyclones (> 33 kts) are ignored. (Miller et al., 1988)

MEAN PATHS FOR OCT 24 - NOV 8



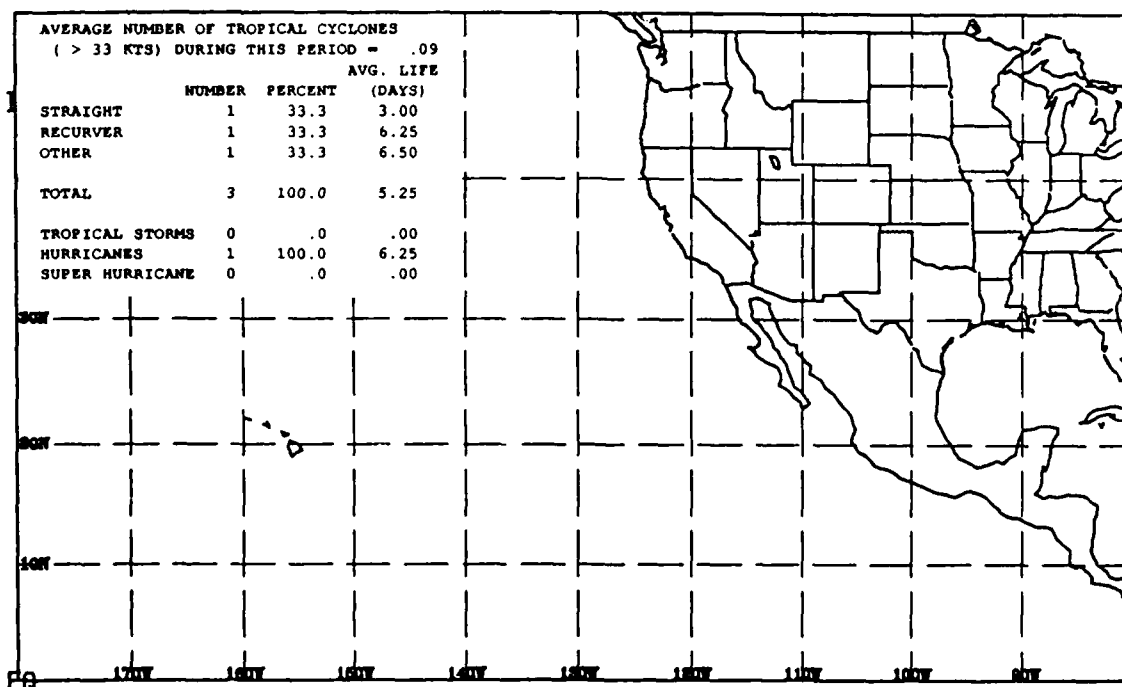
Mean tropical cyclone (> 33 kts) path. Numbers represent the percentage of tropical cyclones (> 33 kts) which followed the indicated path. These numbers may not add up to 100% since not all tropical cyclones (> 33 kts) follow a mean path and some develop/dissipate along a path. Tracks which contained less than 5% of the tropical cyclones (> 33 kts) are ignored. (Miller et al., 1988)

MEAN PATHS FOR NOV 9 - NOV 23



Mean tropical cyclone (> 33 kts) path. Numbers represent the percentage of tropical cyclones (> 33 kts) which followed the indicated path. These numbers may not add up to 100% since not all tropical cyclones (> 33 kts) follow a mean path and some develop/dissipate along a path. Tracks which contained less than 5% of the tropical cyclones (> 33 kts) are ignored. (Miller et al., 1988)

MEAN PATHS FOR NOV 24 - DEC 8



Mean tropical cyclone (> 33 kts) path. Numbers represent the percentage of tropical cyclones (> 33 kts) which followed the indicated path. These numbers may not add up to 100% since not all tropical cyclones (> 33 kts) follow a mean path and some develop/dissipate along a path. Tracks which contained less than 5% of the tropical cyclones (> 33 kts) are ignored. (Miller et al., 1988)

DISTRIBUTION LIST

FORECASTERS HANDBOOK FOR CENTRAL AMERICA AND ADJACENT WATERS

SNDL

Part I

21A1	CINCLANTFLT (Code N37 + Science Advisor)
21A2	CINCPACFLT (Code 02M + Science Advisor)
22A1	Fleet Commander Lant (Oceanographer)
22A2	Fleet Commander PAC (COMTHIRDFLT-Oceanographer + Science Advisor)
23B1	Special Force Commander LANT (USCOMSOLANT)
23B2	Special Force Commander PAC (COMNAVSPECWARCOM)
24A1	COMNAVAIRLANT (Oceanographer + Science Advisor)
24A2	COMNAVAIRPAC (Oceanographer + Science Advisor)
24D	Surface Force Commanders (Oceanographer + Science Advisor)
24J1	Fleet Marine Force Command LANT
24J2	Fleet Marine Force Command PAC
26A	Amphibious Group (Oceanographer)
28A	Carrier Group (Oceanographer)
28B	Cruiser-Destroyer Group (Oceanographer)
29B	Aircraft Carrier (CV, CVN) (OA Division)
29R	Battleships (BB) (OA Division)
31A1	Amphibious Command Ship LANT (LCC)
31H	Amphibious Assault Ship (LHA, LPH) (OA Division)
32TT	Auxiliary Aircraft Landing Training Ship (AVT) (OA Div.)
45A1	Fleet Marine Force Commands (LANT and PAC)
45A2	Marine Expeditionary Force (I MEF, II MEF)
45B	Marine Division (2ND MARDIV, 3RD MARDIV)
45CC	Topographic Platoon (2ND TOPOPLT)
46B	Aircraft Wing (1ST MAW, 2ND MAW)
46C1	Marine Aircraft Group (MAG 11)
46D2	Marine Aircraft Group (MAG 13)
46Q	Wing Support Group (17 MWSG, 27 MWSG)
46R	Marine Wing Support Squadron
50A	Unified Commands (USCINCLANT, J37), (USCINCPAC, J37), (USCINCSO, J3-W)
50C	Subordinate Unified Commands (COMUSFORCARIB, COMSOCLANT, COMSPCPAC)

Part II

A1 Immediate Office of Secretary (Codes 22, 1122, 1122AT)
A3 Chief of Naval Operations (OP-096)
B2A Special Agencies, Staffs, Boards and Committees (Joint
Staff (J-3/ESD), Joint Special Operations Command J1)
B5 U. S. Coast Guard
C40 COMNAVOCOM Shore Based Det. (Alameda, Asheville, Cecil
Field, Charleston, Corpus Christi, Guantanamo, Key West,
Kings Bay, Long Beach, Mayport, Moffett Field, Monterey,
Newport, New Orleans, Offutt AFB, Roosevelt Roads)
E3C Ocean Research and Development Activity
FA2 Fleet Intelligence Center Europe and Atlantic
FB1 FLEET Intelligence Center Pacific
FD1 Oceanography Command (Code N312)
FD2 Oceanographic Office
FD3 Fleet Numerical Oceanography Center
FD4 Oceanography Center (NEOC, NWOC)
FD6 Oceanography Command Facility (Bay St Louis, Jacksonville,
San Diego)
FF38 Naval Academy (Meteorology Dept & Oceanography Dept)
FKA1B COMSPAWARSSYSCOM (Codes 321, PMW-141)
FT1 Chief of Naval Education and Training
FT2 Chief of Naval Air Training
FT15 Unit CNET (NAVU Chanute AFB only)

Supplemental Distribution List

Commanding Officer
HQ, 1st Weather Wing
Hickam AFB, HI 96853

Commanding Officer MCAS
Weather Service Office
Kaneohe Bay, HI 96863

Commander
AWS/DNXS
Scott AFB, IL 62225

Naval Postgraduate School
Attn: Prof Renard (Code 63Rd)
Monterey, CA 93943

Naval Postgraduate School
Attn: Prof Williams (Code 63Wf)
Monterey, CA 93943

USAF ETAC
Attn: Kenneth Walters
Scott AFB, IL 62225-5483

National Hurricane Center
Attn: Mark Zimmer
Coral Gables, FL 34001

Commander
Det 25, 5th Wea Wing
APO Miami 34001

Commander
Air Force Global Wea. Cen.
Offutt AFB, NE 68113

Chief, Aerospace Science Div
5th Wea Wing/DN
Langley AFB, VA 23665-5000

U of Hawaii (Prof J Sadler)
2525 Correa road
Honolulu, HI 96822

Det 2 HQ AWS
The Pentagon
Washington, DC 20330

Defense Tech Info Center
Cameron Station
Alexandria, VA 22314

Oceanroutes, Inc
680 W. Maude Ave
Sunnyvale, CA 94086-3518

Florida State Univ
Meteorology Dept
Tallahassee, FL 32306

Federal Coordinator (OFCM)
11426 Rockville Pike Suite 300
Rockville, MD 20852

Mr. Steve Sokol (Code 28)
Johnson Space Center Met Group
Houston, TX 77058

Science Applications Int. Corp.
205 Montecito Ave
Monterey, CA 93940

Dr. William Gray
Colorado State Univ
Fort Collins, CO 80523